ASSOCIATION FOR RESEARCH IN OTOLARYNGOLOGY
FOUNDED IN 1973

43RD ANNUAL
MidWinter Meeting

January 25 - 29, 2020

San Jose McEnery Convention Center

San Jose
CALIFORNIA

ARO OFFICERS FOR 2019-2020

PRESIDENT:

Keiko Hirose, MD (19-20)
Department of Otolaryngology
Washington University School of Medicine
660 S Euclid Ave.
St. Louis, MO 63110

PRESIDENT ELECT:

Ruth Litovsky, PhD (19-20)
University of Wisconsin
Waisman Center 521
1500 Highland Avenue
Madison, WI 53705 USA

PAST PRESIDENT:

Karen P. Steel, PhD (19-20)
Kings College London
Wolfson Centre for Age Related Diseases
London, United Kingdom SE1 1UL

SECRETARY/ TREASURER:

Gabriel Corfas, PhD (17-20)
The University of Michigan, Kresge
Hearing Research Institute
1150 West Medical Center. Drive
Medical Sciences 1 Bldg; RM 5424A
Ann Arbor, MI 48109

COMMUNICATIONS OFFICER:

Donna M. Fekete, PhD (18-21)
Purdue University
829 Lagrange Street
West Lafayette, IN 47906

COUNCIL MEMBERS AT LARGE:

Lisa Cunningham, PhD (19-22)
National Institutes of Health
Porter Neuroscience Research Center
35A Convent Drive, Room 1D971
Bethesda, MD 20814

Gwenaelle S. Geleoc, PhD (17-20)
Boston Children's Hospital
3 Balckfan Circle
Boston, MA 02115

Mark Warchol, PhD (18-21)
Washington University of School of Medicine
Department of Otolaryngology, Box 8115
660 South Euclid Ave
St. Louis, MO 63110

ARO Executive Director:

Haley J. Brust
19 Mantua Road
Mt. Royal, NJ 08061

Conference Program of the 43rd Annual MidWinter Meeting

Welcome to ARO 2020 in San José! This is a transformative year for ARO with our meeting taking place at a new venue and the date being moved to January. The ARO MidWinter Meeting has traditionally met in mid-February, and our destinations have included Florida, New Orleans, Denver, Baltimore, and Southern California. This year, we will be converging on our newest location: **San José, California** from **January 25-29, 2020**. We are looking forward to experiencing the San José Convention Center and the surrounding downtown area.

This year's meeting yielded 1328 abstract submissions, resulting in nearly 300 oral presentations and 1096 posters. We are very fortunate that Matt Kelley, who has served as ARO President in the past, continues to provide leadership for ARO as the new Chair of the Program Committee. Carolina Abdala and Christopher Shera, the scientific program co-chairs, and all of the members of the Program Committee have organized a fantastic meeting! It feels as if we are embarking on an adventure as we navigate this novel environment to find familiar faces and to make new friends and colleagues. We anticipate that the outstanding science at our MidWinter Meeting will continue to lead the way.

The Presidential Symposium this year focuses on the immune system, the interaction between immunity and the nervous system, the origin and function of myeloid cells, and their contributions to disease. I am thrilled to introduce three scientists from outside of the auditory field: Jessica Williams, Gretchen Diehl, and Bahareh Ajami. We will also hear from three ARO members, Mark Warchol, Andy Griffith, and Barbara Canlon, who have studied inflammation and its contributions to the inner ear. I hope that you will find this work novel and interesting, and another important element of understanding inner ear function and disease.

This year, Lynne Werner receives the Award of Merit, the highest commendation in our society. We look forward to Dan Sanes' narrative of her brilliant career and her seminal contributions to our understanding of how hearing develops in infants and how we measure hearing in our youngest individuals. We will also present the Geraldine Dietz Fox Young Investigator Award at this event. Stay tuned to receive this announcement in a future communication. Also, we will introduce two new awards for next year: the ARO Pioneer Award in Basic Science and ARO Innovator Award in Clinical Science. These new awards have been developed to recognize researchers who are midcareer and whose body of work has contributed in a significant way to the advancement of hearing and vestibular sciences. The Awards Committee under the leadership of Ruth Anne Eatock, has identified the need to broaden the recognition of exceptional work in our field. These two new prizes will serve to increase the visibility of these important investigators and to recognize them for their remarkable contributions.

Young Investigators: be prepared for a full schedule including high impact, thought-provoking research presentations and poster sessions, opportunities to connect with mentors and future collaborators, and many spARO events designed for students, residents, fellows, and postdocs. There are many opportunities for networking, finding your next position, and learning how to succeed in funding your research.

Debara Tucci, Director of the NIDCD, will hold a Town Hall meeting on Sunday afternoon in conjunction with the ARO Business Meeting. At the conclusion of the business meeting, I will hand the gavel to our President-Elect, Ruth Litovsky, and thank our Past-President, Karen Steel, who has helped me tremendously in my role as president. I would like to thank all members of ARO Council and the ARO committees who over the past year have contributed their time and made ARO the superb research society that it is today. I would also like to extend my thanks to all of you who have contributed your science to the program: the quality of your work and your willingness to share it with us is what makes ARO truly special.

See you at ARO in San José!

Keiko Hirose
President ARO 2020

MOBILE APP

Be sure to download our mobile app to enhance your experience at the 2020 ARO MidWinter Meeting! You'll be able to plan your day by performing detailed abstract searches and can also view the schedule, browse exhibitors, sponsors, maps and general show info. *You must create an account in order to view abstracts/save talks to your itinerary.*

The app is compatible with iPhones, iPads, iPod Touches and Android devices. Download the "eventScribe" app on the App Store/Google Play and search "ARO MWM". Be sure to select the 2020 ARO MWM to access this year's app. You can also access the same information via our website version of the app through any browser on any device!

MOBILE DEVICES

As a courtesy to the speakers and your fellow attendees, please switch your mobile device(s) to silent while attending the sessions.

RECORDING POLICY

ARO does not permit audio or photographic recording of any research data presented at the meeting.

BREAKS

Complimentary coffee and tea will be available in the morning and at selected breaks.

ASSISTED LISTENING DEVICES

A limited amount of assisted listening devices are available at the AV Booth in the rear of Room 220ABC.

A SPECIAL NOTE FOR THE DISABLED

ARO wishes to take steps that are required to ensure that no individual with a disability is excluded, denied services, segregated, or otherwise treated differently than other individuals because of the absence of auxiliary aids and services. If you need any auxiliary aids or services identified in the American with Disabilities Act, or any assistance in registering for this course please contact ARO Meetings Department at meetings@aro.org; via telephone at 856-423-0041, option 2; or write to ARO Meetings Department, 19 Mantua Road, Mt. Royal, NJ 08061.

LACTATION ROOM

Please come to the ARO Registration Desk for location and access. Available hours are noted in the mobile app.

ARO Committees

PROGRAM COMMITTEE

Chair:
Matt Kelley,PhD (3/19 - 2/22)

Scientific Program Co-Chairs:
Carolina Abdala, PhD (3/17 - 2/20)
Christopher Shera, PhD (3/17 - 2/20)

Members:
Martin Basch, PhD (3/18 - 2/21)
Maria Chait, PhD (3/17 - 2/20)
Monita Chatterjee, PhD (3/17 - 2/20)
Brandon Cox, PhD (3/19 - 2/22)
Robert Froemke, PhD (3/18 - 2/21)
Gregory Frolenkov, PhD (3/18 - 2/21)
Nandini Iyer, PhD (3/17 - 2/20)
Steve Lomber, PhD (3/19 - 2/22)
Rebecca Lim, PhD (3/17 - 2/20)
Jose Antonio Lopez-Escamez, MD (3/17 - 2/20)
Teresa Nicolson, PhD (3/18 - 2/21)
Kevin Ohlemiller, PhD (3/18 - 2/21)
Sunil Puria, PhD (3/19 - 2/22)
Maria Rubio, MD, PhD (3/19 - 2/22)
Konstantina Stankovic, MD, PhD (3/17 - 2/20)
Eric Thompson, PhD (3/17 - 2/20)
Matt Winn, PhD (3/19 - 2/22)
Council Liaison: Ruth Y. Litovsky, PhD (3/17 - 2/20)
spARO Representative: Grace Soon Kim (3/19 - 2/22)

EX-OFFICIO COUNCIL MEMBER

International Committee Chair
Isabel Varela-Nieto, PhD (3/18 - 2/21)

Long Range Planning Committee Chair
Lisa Goodrich, PhD (3/17 - 2/20)

Mentoring – spARO Committee Chair
Catherine (Cat) Weisz, PhD (3/17 - 2/20)

Program Chair
Matthew W. Kelley, PhD (3/19 - 2/22)

spARO Representative Chair
Nicole Jiam (3/18 - 2/19)

BYLAW COMMITTEES

LONG RANGE PLANNING

Chair:
Lisa Goodrich, PhD (3/17 - 2/20)

Members:
Peter Barr-Gillespie, PhD (3/18 - 2/21)
Alan Cheng, MD (3/18 - 2/21)
Brandon Cox, PhD (3/8 - 2/21)
Bernd Fritzsch, PhD (3/17 - 2/20)
Matthew McGinley (3/19 - 2/22)
Chris Plack, PhD (3/18 - 2/21)
Amy Poremba, PhD, NIDCD Rep.
Yilai Shu, MD, PhD (3/18 - 2/21)
Aleta Steevens, (3/18 - 2/21)
Aaron Tward, MD, PhD (3/19 - 2/22)
Catherine Weisz, PhD (3/18 - 2/21)

Past Chair: Steven Green, PhD (3/17 - 2/20)
Council Liaison: President-Elect: Ruth Litovsky, PhD (3/19 - 2/20)
Chair, International Committee: Isabel Varela-Nieto, PhD: Spain (3/18 - 2/21)
spARO Representative: Kirupa Suthakar

NOMINATING

Chair:
Karen Steel, PhD (3/19 - 2/20)

Members:
Paul Fuchs, PhD (3/19 - 2/20)
Ronna Herzano, MD, PhD (3/19 - 2/20)
Jose Antonio Lopez-Escamez, MD, PhD (3/19 - 2/20)
Heidi Nakajima, MD, PhD (3/19 - 2/20)

STANDING COMMITTEES

AWARDS COMMITTEE

Chair:
Ruth Anne Eatock, (3/17 - 2/20)

Members:
Jutta Engel, PhD (3/18 - 2/21)
Paul Fuchs, PhD (3/17 - 2/20)
Elisabeth Glowatzki, PhD, (3/19 - 2/22)
Phil Joris (3/18 - 2/21)
Matt Kelley, PhD (3/18 - 2/21)
Anna Lysakowski, PhD (3/17 - 2/20)
Richard Rabbitt, PhD, (3/19 - 2/22)
Jenny Stone, PhD (3/18 - 2/21)
Deb Tucci, (3/18 - 2/21)
Sarah Wooley, (3/18 - 2/21)
Council Liaison: Past-President Karen Steel, PhD (3/19 - 2/20)

DIVERSITY & MINORITY AFFAIRS

Chair:
Ivan Lopez, PhD (3/18 - 2/21)

Members:
Kelsey Anbuhl (3/18 - 2/21)
Alain Dabdoub, PhD (3/18 - 2/21)
Avril Holt, PhD, (3/19 - 2/22)
Tejbeer Kaur, PhD (3/19 - 2/22)
Anil Lalwani, MD (3/19 - 2/22)
Yi Zhou, PhD (3/18 - 2/21)
Council Liaison: Lisa Cunningham, PhD (3/19 - 2/22)
spARO Representative: Karen Barrett

ARO Committees

EXTERNAL RELATIONS
Chair:
Keith Duncan, PhD (3/18 - 2/21)
Allison Coffin, PhD (3/18 - 2/21)

Members:
Yuri Agrawal, MD (3/17 - 2/20)
Dylan Chan (3/18 - 2/21)
Ronna Hertzano, MD, PhD (3/17 - 2/20)
J. Chris Holt, PhD (3/19 - 2/22)
Judith Kempfle, MD (3/19 - 2/22)
Becky Lewis (3/19 - 2/22)
Ross Maddox, (3/18 - 2/21)
Dave Raible, PhD (3/19 - 2/22)
Lavinia Sheets, PhD (3/18 - 2/21)
Aaron Tward, (3/19 - 2/22)
Council Liaison: Mark Worchol, PhD (3/18 - 2/21)
spARO Representative: Benjamin Shuster

FINANCE AND INVESTMENT
Chair:
Erick Gallun, PhD (3/17 - 2/20)

Members:
Steve Eliades (3/19 - 2/22)
Michael Roberts, PhD (3/19 - 2/22)
Anna Lysakowski, PhD (3/18 - 2/21)
Lisa Olson, PhD (3/17 - 2/20)
Ex-officio: Secretary-Treasurer Gabriel Corfas, PhD (3/17 - 2/20)

INTERNATIONAL
Chair:
Isabel Varela-Nieto, PhD (3/18 - 2/21)

Members:
Barbara Canlon, PhD: Sweden (3/19 - 2/22)
Yun-Hoon Choung, MD, PhD: Korea (3/18 - 2/21)
Lukas Landegger: Austria (3/19 - 2/22)
Yong Lu, PhD: USA (3/19 - 2/22)
Takayuki Nakagawa, MD, PhD: Japan (3/18 - 2/21)
Sonya Pyott, PhD: Netherlands (3/18 - 2/21)
Saima Riazuddin, PhD: USA (3/19 - 2/22)
Council Liaison: Gwen Geleoc, PhD (3/18 - 2/21)
spARO Representative: Patrick Atkinson, PhD

TRAVEL AWARDS
Chair:
Mike Bowl, PhD (3/17 - 2/20)

Members:
Samira Anderson (3/18 - 2/21)
Hela Azaiez, PhD (3/17 - 2/20)
Melanie Barzik (3/19 - 2/22)
Jonathan Bird, PhD (3/17 - 2/20)
JinWoong Bok, PhD (3/18 - 2/21)
Tom Coate, PhD (3/18 - 2/21)
Stephanie Eckrich (3/18 - 2/21)
Jeff Lichtenhan, PhD (3/17 - 2/20)
Manuel Malmierca, MD, PhD (3/18 - 2/21)
Jim Phillips, PhD (3/18 - 2/21)
Diana Peterson (3/18 - 2/21)
Maria Rubio, MD, PhD (3/18 - 2/21)
Ruben Stepanyan (3/19 - 2/22)
Yuri Agrawal (3/17 - 2/20)
Council Liaison: Keiko Hirose, MD (3/19 - 2/20)
spARO Representative: Cathy Sung

JARO EDITORIAL BOARD

Paul B. Manis, PhD, Editor-in-Chief (2018 - 2020)

Associate Editors:
Julie Arenberg, PhD (2015 - 2020)
Alan M. Brichta, PhD (2015 - 2020)
Catherine E. Carr, PhD (2016 - 2020)
Paul Delano (2017 - 2021)
Mark A. Eckert, PhD (2013 - 2020)
Ana Belén Elgoyhen, PhD (2013 - 2020)
W. Robert J. Funnell, PhD (2013 - 2020)
Elisabeth Glowatzki, PhD (2015 - 2020)
Nace L. Golding, PhD (2016 - 2020)
Michael G. Heinz, PhD (2016 - 2020)
Ronna Hertzano, MD, PhD (2015 - 2020)
Richard F. Lewis, MD (2015 - 2020)
Ruth Y. Litovsky, PhD (2013 - 2020)
Christian Lorenzi, PhD (2016 - 2020)
Brigitte Malgrange, PhD (2015 - 2020)
Colette M. McKay, PhD (2016 - 2020)
John C. Middlebrooks, PhD (2015 - 2020)
Heidi Nakajima, MD, PhD (2017 - 2021)
Adrian Rees, PhD (2015 - 2020)
Suhua Sha, MD (2017 - 2021)
Xiaorui Shi, MD, PhD (2013 - 2020)
George A. Spirou, PhD (2014 - 2020)
Marcel van der Heijden, PhD (2014 - 2020)
Joseph P. Walton, PhD (2016 - 2020)
Robert H. Withnell, PhD (2015 - 2020)

ISSN-0742-3152

The Abstracts of the Association for Research in Otolaryngology is published annually and consists of abstracts presented at the Annual MidWinter Research Meeting. A limited number of copies of this book and previous books of abstracts (1978-2011) are available. Please address your order or inquiry to Association for Research in Otolaryngology Headquarters by calling (856) 423-0041 or emailing headquarters@aro.org.

This book was prepared from abstracts that were entered electronically by the authors. Authors submitted abstracts over the World Wide Web using Cadmium Abstract Management System. Any mistakes in spelling and grammar in the abstracts are the responsibility of the authors. The Program Committee performed the difficult task of reviewing and organizing the abstracts into sessions. Scientific Chairs: Christopher Shera and Carolina Abdala; Program Committee Chair, Matthew W. Kelley and Program Committee constructed the final program. Cadmium and Marathon Printing electronically scheduled the abstracts and prepared Adobe Acrobat pdf files of the Program and Abstract Books. These abstracts and previous years' abstracts are available at www.aro.org.

Citation of these abstracts in publications should be as follows: **Authors, year, title, Assoc. Res. Otolaryngol. Abs.: page number.**

Table of Contents

Table of Contents

Table of Contents

Presidential Symposium: Innate Immunity in the Auditory System

Chair: Keiko Hirose

PRES SYMP 1

Innate Immunity in the Central Nervous System

Jessica Williams
Lerner Research Institute, Cleveland Clinic Foundation

Although the central nervous system (CNS) was once considered a site of immune privilege, we now know that immunity has a critical role in CNS development, pathogen clearance and also contributes to many CNS pathologies. There are resident innate immune cells that within the CNS that work to maintain proper neuronal function during homeostatic conditions as well as those that are actively recruited from the periphery, primarily during disease. During physiologic conditions, these myeloid cells that are stationed in the CNS parenchyma and at CNS-periphery borders are quiescent; however, during a pathological event, such as an infection or neurodegeneration, these cells quickly respond and become reactive. The activation of CNS myeloid cells disrupts the integrity of the blood-brain barrier and promotes the recruitment of additional activated peripheral immune cells through the expression of chemokines. While the recruitment of peripheral myeloid cells is necessary for the clearance of pathogens, a large influx of activated leukocytes can also induce by-stander damage if not properly regulated. Chemokines are a class of small molecules that have many functions in the CNS, including localization of cells during homeostasis and disease. Chemokines are ubiquitously expressed in the CNS and levels can be regulated by immune cytokines, thus a delicate balance exists between physiologic surveillance of the CNS by resident and patrolling innate immune cells and immune-mediated pathology during neurinflammation.

PRES SYMP 2

Microbiota and Development of Intestinal Immunity

Gretchen Diehl
Baylor College of Medicine

Interactions between host and its resident microbes, collectively known as the microbiota allows for proper immune responses against pathogens. These interactions are also necessary to limit inflammatory immune responses against the microbiota which, if left unchecked, will result in inflammatory conditions including inflammatory bowel disease. In our work, we seek to understand how the microbiota and dietary components regulate the immunological tone within the intestine and how this environment influences the develop of immunity against pathogens as well as the microbiota itself.

PRES SYMP 3

Homeostasis and Inflammatory Signature of Myeloid Cells in the Central Nervous System: Lost in Translation

Bahareh Ajami
Oregon Health Sciences University

A key regulator of central nervous system (CNS) inflammatory responses is a highly specialized subset of myeloid cells that reside in the CNS parenchymal and perivascular spaces known as “microglia”. Although, microglia were introduced to the scientific literature a century ago (Río- Hortega, 1919a,1919b,1919c), they remain one of the least understood cell types of the brain. The clear phenotypic similarities between microglia and other macrophage populations and lack of a reliable in vitro method that recapitulates all hallmarks of microglia led to several disagreements regarding the microglia ontogeny, their homeostasis in the adult brain and their function for several decades. Our research in recent years has focused on understanding several aspects of microglia biology in health and disease. Using chimeric mice obtained by parabiosis, we investigated the microglial origin and homeostasis in adulthood and CNS neurodegenerative diseases. In a subsequent study, using a combination of parabiosis and myeloablation, we further showed that recruited monocytes are unable to persist in the CNS and are thus unlikely to contribute to the resident microglial population. In our most recent study, using single-cell mass cytometry (CyToF), we challenged the oversimplified M1/M2 classification of microglia character. Here, we demonstrated the presence of different microglial subpopulations with different signaling and cytokine profiles among models of distinct CNS pathologies. This better understanding of microglial diversity, will tremendously help us in our understanding of microglial biological functions and the future development of better-targeted therapies.

PRES SYMP 4

Innate Immune Cells in the Inner Ear: Macrophage Interactions with Hair Cells and Afferent Neurons

Mark Warchol
Washington University School of Medicine

Immune defense in mammals is mediated by the innate and adaptive immune systems. Innate immunity is evolutionarily ancient and present in both invertebrates and vertebrates. Cells of the innate immune system can detect molecules expressed by invading pathogens and act to neutralize such invaders. However, the repertoire

of innate immunity is limited; its cells cannot learn to recognize new pathogens and it cannot form 'memories' of previously-encountered antigens. In contrast, the adaptive immune system, which is present only in vertebrates, has the ability to 'remember' proteins after an initial exposure and mount vigorous defense against targets that possess such antigens. Collectively, the cells that form both systems are known as leukocytes (i.e., white blood cells), but innate and adaptive immunity involve different types of leukocytes. Innate immunity is executed by macrophages, neutrophils and related cells, while adaptive immunity is mediated by B- and T-lymphocytes. The cochlea and vestibular organs contain resident populations of leukocytes, nearly all of which are macrophages. Additional macrophages are recruited into the ear after acoustic trauma or ototoxicity. The function of these macrophages – both in the normal ear and after injury – remains an active topic of study. In many tissues, macrophages serve as 'professional phagocytes' that engulf and remove the debris of injured or dead cells. Not surprisingly, macrophages in the ear have been shown to phagocytose dying hair cells, a task which they share with supporting cells. High numbers of macrophages are also present in the developing cochlea, particularly during the period in which epithelial and synaptic remodeling are occurring. It is not clear whether those macrophages play a vital role in otic development or whether they simply remove debris following normal programmed cell death. Macrophages are also associated with neurons of the spiral and vestibular ganglia. In the mature ear, increased numbers of macrophages are recruited to the axons and cells bodies of the spiral ganglion following acoustic trauma or ototoxic injury. This association between macrophages and afferent neuron is modulated by fractalkine, a chemokine that also regulates interactions between microglia and neurons in the CNS. Spiral ganglion cells express the fractalkine ligand and macrophages are the sole cell type within the ear that expresses the fractalkine receptor. Genetic disruption of fractalkine signaling reduces the survival of spiral ganglion neurons after loss of hair cells, suggesting that communication between neurons and macrophages has the potential to influence the progression of otic pathology.

PRES SYMP 5

NLRP3 Mutation and Cochlear Autoinflammation Cause Syndromic and Nonsyndromic Hearing Loss DFNA34 Responsive to Anakinra Therapy

Andrew Griffith
Otolaryngology Branch, National Institute on Deafness and Other Communication Disorders, National Institutes of Health

The NLRP3 inflammasome is an intracellular innate immune sensor that is expressed in immune cells, including monocytes and macrophages. Activation of the NLRP3 inflammasome leads to IL-1β secretion. Gain-of-function mutations of NLRP3 result in abnormal activation of the NLRP3 inflammasome, and cause the autosomal dominant systemic autoinflammatory disease spectrum, termed cryopyrin-associated periodic syndromes (CAPS). Here, we show that a missense mutation, p.Arg918Gln (c.2753G > A), of NLRP3 causes autosomal-dominant sensorineural hearing loss in two unrelated families. In family LMG446, hearing loss is accompanied by autoinflammatory signs and symptoms without serologic evidence of inflammation as part of an atypical CAPS phenotype and was reversed or improved by IL-1β blockade therapy. In family LMG113, hearing loss segregates without any other target-organ manifestations of CAPS. This observation led us to explore the possibility that resident macrophage/monocyte-like cells in the cochlea can mediate local autoinflammation via activation of the NLRP3 inflammasome. The NLRP3 inflammasome can indeed be activated in resident macrophage/monocyte-like cells in the mouse cochlea, resulting in secretion of IL-1β. This pathway could underlie treatable sensorineural hearing loss in DFNA34, CAPS, and possibly in a wide variety of hearing-loss disorders, such as sudden sensorineural hearing loss and Meniere's disease that are elicited by pathogens and processes that stimulate innate immune responses within the cochlea.

PRES SYMP 6 - WITHDRAWN

PRES SYMP 7

Interplay between Cochlear Inflammation, Circadian Rhythms and Noise Damage

Barbara Canlon
Karolinska Institutet

Strong links between circadian rhythms and the immune system are well established for many bodily functions but limited knowledge exists for the auditory system. A better mechanistic understanding of rhythms in the cochlea immune response will be crucial to identify new time-based interventions that could be incorporated into therapeutic practice. We discovered that recovery from noise damage in mice varies with the time of the day, with greater vulnerability at night. A circadian clock in the cochlea controls auditory recovery to noise trauma and RNAseq analyses suggest that enhanced immune responses are involved in the greater noise vulnerability at nighttime. Using cell sorting (FACS), we have found that the numbers of specific immune cells in different cochlear compartments vary depending on the time of the day. RNAseq data from whole cochleae show that chemokines and pro-inflammatory signals increase at nighttime. In the context of a noise challenge, the mRNA of TNFrsf1a, Jun, Ccl5, and IL-6 is increased after night noise trauma but

not after day noise. These preliminary findings support our hypothesis that increased vulnerability to night noise trauma may be due to inflammatory processes that could recruit immune cells and trigger their migration into the cochlea. These findings are highly relevant for the auditory field since particular types of immune cells may be involved in noise-induced hearing loss depending on the time of the day the exposure occurred.

Afferents and Efferents of the Vestibular System

PS 1

Phase Locking of Vestibular Afferent Neurons in the Oyster Toadfish

Richard D. Rabbitt; **Marta Iversen**
University of Utah

Introduction
In mammals, calyx-bearing vestibular afferent neurons respond to auditory-frequency sound and vibration by firing phase locked action potentials. Though detailed information about phase locking and auditory-frequency responses in the vestibular organs is sparse, these responses are the basis for current clinical tests of otolith function. Recent work has shown that vestibular afferents can phase lock with higher precision and up to higher frequencies than cochlear neurons [1]. These afferents receive both quantal and non-quantal synaptic transmission from type I hair cells and the unique non-quantal current has been hypothesized to be responsible for precise auditory-frequency phase locking [2]. However, fish vestibular organs lack complete calyces and type I hair cells but the primary afferent neurons are still able to phase lock to auditory-frequency stimuli. Here we report characteristics of phase locked afferent neurons in the oyster toadfish to better understand mechanisms of phase locking and auditory frequency vestibular responses.

Methods
Single-unit afferent neurons were recorded in response to auditory frequency vibration of otoliths or indentation of the membranous canal. Single unit recordings were analyzed for phase locking strength (vector strength) and timing (stimulus-triggered histograms) across a range of vibrational frequencies and amplitudes. Current was injected during intracellular recording to mimic the sustained non-quantal current in mammalian afferent neurons and recordings analyzed to investigate the effect on vector strength.

Results
Toadfish vestibular afferent neurons phase lock with high precision (>0.9 vector strength) and to high frequencies (>1000 Hz). Neurons phase locked to higher frequencies in the otolith organs than in the semicircular canals. The preferred phase angle of a single neuron tested at multiple frequencies increased as frequency increased. Some neurons exhibited “peak-splitting” similar to mammalian cochlear afferents where two or even three peaks emerged per stimulus cycle in the time histograms at high stimulus intensity levels.

Conclusion
Vestibular afferent neurons in the oyster toadfish can respond with high precision to high frequency vibration even though they lack type I hair cells. Results suggest that non-quantal synaptic input is not necessary for auditory frequency phase locking of vestibular afferents, though it may serve to improve its precision.

Funding
NIDCD R01-DC006685, R21-DC016443, NSF GRFP 1747505.

References
[1] Curthoys et al, Hear Res (2019).
[2] Eatock, Integr Comp Biol (2018).

PS 2

Resurgent Sodium Currents in Mature Vestibular Calyx Afferent Terminals

Frances Meredith; Karen Dockstader; Katherine Rennie
University of Colorado, AMC

Firing patterns of vestibular afferents vary with the position of terminal endings in vestibular neuroepithelia, but the significance of these differences to vestibular coding is unclear. We recently characterized transient Na+ currents (INaT) in zonally-identified vestibular afferent subtypes. INaT in mature calyces of crista peripheral zones (PZ) was substantially reduced by 4,9-anhydrotetrodotoxin (4,9-ah-TTX), an analog of tetrodotoxin (TTX) that selectively blocks Nav1.6 channels. However, mature calyx-only terminals located in central zones (CZ) of the crista were less sensitive to 4,9-ah-TTX, suggesting that Nav1.6 channels contribute minimally to Na+ currents in these afferents. In current clamp, evoked firing frequency was reduced by 4,9-ah-TTX in PZ afferents. In addition to INaT, Nav1.6 channels can mediate resurgent Na+ current (INaR) in a variety of cell types. This atypical current is much smaller than INaT and is associated with neurons that have the capacity for rapid spontaneous firing. We investigated the contribution of INaR to Na+ currents in afferent terminals of developing and mature cristae.

Immunohistochemistry was performed using an antibody to target Nav1.6 channels and revealed nodal and terminal staining for Nav1.6 in mature cristae. Whole cell patch clamp recordings were obtained from calyces in transverse slices of gerbil cristae in two age groups: immature (up to postnatal day (P) 8) and mature (P36 to P45). Voltage protocols were designed to characterize INaR in voltage clamp. INaR was evoked in 11 out of 21 mature calyces (10 PZ and 1 CZ) at membrane potentials between -60 mV and -10 mV following brief (10 ms) depolarizations of the calyx membrane from -90 to +20 mV. However, INaR was not observed in immature calyces (n = 12; 7 PZ, 5 CZ). Mean TTX-sensitive INaR evoked at -55 mV in mature calyces was -253 ± 122.7 pA (SD; n = 5; all PZ), which was ~ 8% of peak INaT. Mean time to peak was 3.5 ± 0.7 ms and monoexponential decay time constant was 23 ± 5.5 ms. Peak INaR was larger following 10 ms depolarizing steps to +20 mV, compared to 50 ms steps. In summary, INaR was not detected during early postnatal development, but was present in ~50% of mature calyx-bearing primary vestibular afferents. INaR has slow kinetics and is maximal after short, depolarizing voltage steps. These properties would allow INaR to depolarize the calyx immediately after an action potential and could contribute to faster firing in PZ afferents.

Supported by NIDCD DC016860

PS 3

Persistent and Resurgent Voltage-gated Sodium Currents in Mouse Vestibular Ganglion Neurons

Selina Baeza Loya; Ruth Anne Eatock
University of Chicago

The vestibular inner ear transmits head-motion information to the brain via two populations of primary vestibular ganglion neurons (VGN), which differ in the regularity of action potential (AP) timing. The two kinds of AP timing (regular and irregular) represent different encoding strategies (rate and temporal encoding, respectively) that are optimized for different kinds of sensory information. In vivo, the regularity differences may reflect differences in both synaptic inputs and intrinsic ion channel expression. Although voltage-gated sodium (NaV) currents are responsible for the rising phase of APs, their contributions to differences in VGN firing patterns are not fully understood. Rodent VGN express all NaV channel β and β subunits, including NaV1.6 which mediates NaV current in vestibular afferent terminals (Meredith and Rennie, Front. Cell. Neurosci. 12:423, 2018). In addition, NaV currents through a given β subunit can, in other neurons, take different modes: transient (inactivating current), persistent (non-inactivating current), or resurgent (current flow after relief from inactivation block). We are interested in whether differences in VGN expression of NaV channel subunits and modes influence spike timing regularity and AP waveform. Whole-cell currents were recorded from isolated cell bodies of mouse VGN. In acutely isolated immature rat VGN (P1-P8; Liu et al., J Neurophysiol 115:2536, 2016), depolarizing voltage steps activate transient NaV currents through several channel types. In the present study, VGN were cultured overnight to remove myelin, allowing us to record at older ages where AP regularity differences are better developed. Their large transient NaV currents were completely blocked by 1 μM TTX; preliminary results with a selective NaV1.6 blocker (4,9-anhydro-tetrodotoxin) indicated a substantial NaV1.6 component. In addition, we have observed both persistent NaV current, evoked by a slow voltage ramp, and resurgent NaV current, evoked by repolarization following a depolarizing step. In 68 VGN (postnatal day, (P)3-25), all had transient NaV current, 37 had persistent NaV current (P3-P25), 5 had resurgent NaV current (P17-P20), and 3 (P17-P20) had both persistent and resurgent currents. We speculate that persistent and resurgent currents, by increasing NaV channel availability in the after-spike interval, enhance the excitability of maturing regular VGNs and so help to shape sensory encoding by the vestibular inner ear.

PS 4

A Generative Model of Vestibular Afferent Discharge Reveals a Targeted Deficit of Gentamicin-Induced Hypofunction

Larry Hoffman[1]; Michael G. Paulin[2]
[1]Geffen School of Medicine at UCLA; [2]University of Otago; Dunedin, New Zealand

Generative models of neural discharge represent quantitative descriptions that may reflect fundamental biophysical processes underlying the generation of spiketrain structure. We recently showed that spontaneous discharge in vestibular semicircular canal afferent neurons can be modeled by the convolution of exponential (i.e. Poisson) and inverse Gaussian (i.e. Wald) distributions, collectively known as an exwald distribution (Paulin et al., in preparation). The exwald model captured the broad heterogeneity in interspike interval distributions recorded from horizontal canal afferent neurons in three free parameters: Poisson *tau* and Wald *mu* and *lambda*, all in units of time. While *mu* exhibited little variability over the population of afferent neurons examined, *tau* and *lambda* varied over 4 orders of magnitude, with *tau* ranging from 10μs – 100ms. Previous studies have shown that conditions of vestibular hypofunction were induced through the administration of gentamicin doses that produced virtually complete retraction of afferent calyces and only modest hair cell loss, while spontaneous discharge

was preserved (Hirvonen et al. 2005, Sultemeier and Hoffman 2017). Additionally, dynamic modulation was severely attenuated in these afferents, consistent with dramatic sensory hypofunction. Through the present study we investigated fits of the exwald model to spontaneous discharge of these afferents, testing hypotheses that 1) the exwald models consistently result in good fits to ISI distributions despite gentamicin-induced alterations; and 2) gentamicin-treatment results in changes in exwald parameters suggesting a targeted deficit(s) associated with induced hypofunction. We found that the exwald model persisted in providing good fits to spiketrains from gentamicin-treated labyrinths, suggesting that the fundamental biophysical processes underlying generation of the spiketrains were intact. Both the *mu* and *lambda* parameters of the inverse Gaussian component were similar to those resulting from exwald fits of spiketrains from untreated afferents. However, among the subpopulation of gentamicin-treated afferents values of *tau* from the exwald fits were absent of the ultralow values. We found that the Kullback-Leibler divergence measure resulting from comparing the distributions of *tau* from treated and untreated afferents could not be derived from resampling from the entire population ($p < 0.001$). This suggests that gentamicin-induced hypofunction is associated with a change in the biophysical factors resulting in the distribution of *tau*. We advocate that the distribution of Poisson *tau* reflects sensory coding characteristics among afferents in the nerve, and therefore the loss of the ultrashort *tau* values represents compromise in high-frequency stimulus coding characteristics among afferent spiketrains.

PS 5

The High Precision of Phase Locking of Guinea Pig Irregular Otolith Afferents to High Frequency Sound and Vibration

Ian S. Curthoys[1]; Wally Grant[2]; Ann M. Burgess[3]; Alan Brichta[4]; Rebecca Lim[5]
[1]University of Sydney, Australia; [2]Virginia Tech; [3]University of Sydney; [4]School of Biomedical Sciences and Pharmacy, University of Newcastle, Australia; [5]School of Biomedical Sciences and Pharmacy, Unveristy of Newcastle, Australia

Introduction

Some guinea pig primary vestibular afferents with irregular resting discharge, originating mainly from the striola of the utricular and saccular maculae, are activated by and phase-lock to sinusoidal sound and vibration up to frequencies above 2000Hz (Curthoys et al., 2016). This study reports the precision of that phase locking and compares it to the evidence of the precision of phase locking of auditory afferents in guinea pigs (Palmer and Russell, 1986).

Methods

Extracellular single primary vestibular neurons were recorded in ketamine anaesthetized guinea pigs. Vibration stimulation up to 2g peak-to-peak was delivered by a Radioear B-71 bone oscillator cemented to the skull. Sound stimulation of up to 140dB SPL was delivered by a TDH-49 headphone via a speculum.

Results

Many otolithic neurons had spontaneous activity, but a sizable number were silent at rest and were only detected because of repeated search stimulation during the electrode advance. Most otolith irregular neurons had a vigorous response to sound or vibration. When tested with high frequencies (250-2000Hz) it was found that some guinea pig primary otolithic neurons have, on average, significantly higher precision of phase locking as measured by asymptotic vector strength compared to the asymptotic vector strength of guinea pig auditory afferents (data from Palmer and Russell 1986). Furthermore the phase-locking of these otolithic afferents extends to higher frequencies than is the case for auditory afferents. Irregular canal afferents have similar high precision of phase locking to high frequency sound and vibration (after a dehiscence of the bony anterior canal).

Discussion and Conclusion

Irregular otolithic afferents make calyx synapses which envelop the type I receptors at the striola whereas cochlear afferents make small bouton terminations on inner hair cells. We suggest that the high precision phase-locking of irregular otolithic (and canal) afferents may be due to the release of potassium by the type I receptor into the calyx cleft and the potassium acts to depolarize the calyx and so effectively functions as an “ionic neurotransmitter” (Lim et al., 2011; Contini et al., 2017). The high precision of phase locking suggests that type I otolithic receptors may function as jerk detectors.

References

Contini, D. et al. J Physiology-London 2017: 595(3): 777-803.

Curthoys, I. S et al. J Neurophysiol 2019: 122: 259-276.

Lim, R., et al. Experimental Brain Research 210(3-4): 607-621.

Palmer, A. R. & Russell, I. J. (1986). Hearing Research 24(1): 1-15.

PS 6

Assessment of Utricular Nerve, Hair cell and Mechanical Function, *In Vivo.*

C Pastras[1]; S Stefani[1]; Camp A[1]; Ian S. Curthoys[2]; Daniel Brown[3]
[1]The University of Sydney; [2]University of Sydney, Australia; [3]Curtin University

Assessment of Utricular Nerve, Hair cell and Mechanical Function, In Vivo.

Pastras, C.J[1]*, Stefani, S.P1, Curthoys, I.S2, Camp, A.J1, Brown, D.J3*

1. School of Medical Sciences. The University of Sydney.
2. Vestibular Research Laboratory, The University of Sydney.
3. School of Pharmacy and Biomedical Science, Curtin University.

Objective
Vestibular reflex tests are frequently used to diagnose vestibular dysfunction in the clinic. Unfortunately, there is no way to objectively determine the origin of this loss, in the same way cochlear researchers have used in vivo measures to pinpoint hearing disorders arising from nerve, hair cell or mechanical dysfunction. This study aimed to develop and characterize analogous recordings from the utricle to differentially diagnose utricular dysfunction, in vivo.

Methods
Experiments were performed in anaesthetized guinea pigs, approved by the USYD Animal Ethics Committee. The cochlear was removed via a ventral surgical approach allowing full access to the basal surface of the utricular epithelium. A reflective microbead was placed on the macula surface and a Laser Doppler Vibrometer (LDV) was used to record the one-dimensional velocity of the bead in the dorso-ventral plane. A wire was secured into the facial nerve canal to record the Vestibular short-latency Evoked Potential (VsEP) and a micropipette was used to measure the Utricular Microphonic (UM) from the surface of the macula to Bone-Conduced Vibration (BCV) and Air-Conducted Sound (ACS).

Results
Continuous BCV and ACS evoked cyclic UM and macular velocity responses, which saturated at high drives. UMs were largest between 100-300Hz BCV and ACS, during iso-macular velocity. The phase of the UM relative to the phase of the macular velocity was different for BCV vs. ACS, suggesting a different mode of macromechanical receptor activation. Although this assumes LDV recordings provide a complete and reliable measure of the mechanical drive to the utricular hair cells, which is unlikely. VsEP input-output curves using macular motion (e.g. macular jerk) instead of ear-bar or cranial acceleration provide a more direct measure of utricular sensitivity.

Conclusion
This is the first-time hair cell and mechanical responses have been recorded from the mammalian utricle, in vivo. Experimental manipulations, such as Gentamicin, TTX, and mechanical biasing selectively altered utricular nerve, hair cell or mechanical function and provide the means to differentially diagnose peripheral utricular function. Alternative techniques are needed to reliably study the macromechanics of the utricle to BCV and ACS.

PS 7

Excitatory GABAergic Modulation of the Vestibular Nerve

Yugandhar Ramakrishna[1]; **Soroush Sadeghi**[2]
[1]California State University, Northridge; [2]University of Buffalo, NY, USA

Excitatory GABAergic Modulation of the Vestibular Nerve

Yugandhar Ramakrishna[1*] and Soroush G. Sadeghi[1,2]

[1] Center for Hearing and Deafness, Dept. of Communicative Disorders and Sciences, State University of New York at Buffalo, Buffalo, NY

[2] Neuroscience Program, State University of New York at Buffalo, Buffalo, NY

* Current address: Dept. of Communication Disorders and Sciences, California State University – Northridge, Northridge, CA

There is evidence for presence of GABA in the vestibular periphery in adult mammals in efferent fibers and supporting cells. Whether GABA could affect hair cells and afferent terminals has not been investigated. Using in vitro patch clamp recordings from calyx afferent terminals we found that membrane properties of calyx afferent terminals were modulated in the presence of metabotropic GABA-B receptor agonist baclofen. This effect was mediated by inhibition of voltage sensitive calcium channels and subsequent inhibition of calcium sensitive potassium channels. As a result, GABA-B activation exerted an excitatory effect on calyx terminals that could lead to spontaneous firing. In the absence of baclofen, calyces fired a single action potential during step depolarizations. Baclofen decreased the adaptation

and modified filtering properties of calyx membranes so that they would fire trains of spikes during current injections. Consistent with these findings, in vivo intracochlear injection of baclofen produced an increase in synchronized response of irregular fibers innervating the otolith end organs as measured by vestibular sensory evoked potentials (VsEP). Intracochlear injection of a GABA-B antagonist (CGP 35348) by itself had the opposite effect on VsEP responses, suggesting the presence of spontaneous release of GABA in the vestibular periphery. Together, these results provide evidence for an excitatory GABAergic input in the vestibular periphery, which plays an important role in regulating the resting discharge and response properties of calyx terminals and irregular afferents. Such GABAergic modifications can be used to change the tonic – phasic properties of the peripheral pathways as needed.

These studies were funded by an NIH RO3 grant and a research grant from the American Otological Society.

PS 8

Efferent CholinergicTargets in the Mammalian Utricle

Johnny J. Saldate; Felix E. Schweizer; Larry Hoffman
Geffen School of Medicine at UCLA

Efferent neurons projecting to vestibular end-organs serve as a critical feedback arm in the labyrinthine circuit. Finer evaluation of these terminal projections and their targets will undoubtedly inform hypothesis generation and experimentation regarding cholinergic contributions to the cellular physiology of sensory signaling. For example, we recently found that the density of efferent terminals was greater in the region of utricular epithelia harboring enriched calyceal KCNQ4 expression in afferent dendrites (Saldate, et al., ARO 2019). This suggests cholinergic input may modulate the activity of muscarinic receptors, potentially as a tuning mechanism of the m-current to influence sensory input from type I hair cells. However, following 3D reconstruction and volume-based colocalization of fluorescence image stacks, we did not observe a strong correlation between efferent terminals (immunopositive for vesicular acetylcholine transporter, or VAChT) and β3-tubulin-positive afferent calyces. However, we did observe efferent terminals aggregating in intraepithelial space, at and below the base of afferent calyces and near the basolateral aspects of many exposed type 2 hair cells. The present investigations aim to define the cellular targets of non-calyceal efferent projection loci via super-resolution fluorescence microscopy. This was accomplished by immunohistochemical localization and evaluation of cholinergic terminal distances from; 1) afferent calyces, 2) their parent dendrites, and 3) type II hair cells. The morphologies of postsynaptic structures were identified with antibodies for β3-tubulin (calyces and parent dendrites) and the calcium binding protein otoferlin (type II hair cells). Utricles and cristae from wild-type C57BL/6 mice were immunostained, mounted intact, and imaged with *Airyscan* confocal microscopy to identify spatial relationships between the postsynaptic components of the efferent circuit. While VAChT-positive projections terminated near type II hair cells, afferent calyces, and parent dendrites, the majority were closer to type II hair cells, including their basolateral extensions. VAChT terminals were also found to target parent dendrites below the base of the calyx. These findings support the hypothesis that the principal targets of centrifugal feedback are most likely to be type II hair cells, and potentially also signal integration sites of afferent neurons. This circuit could modulate direct inputs from type II hair cells onto afferent boutons and/or the inputs from type II hair cells onto the lateral face of the afferent calyx.

PS 9

Further Characterization of Mouse Behavioral Models for Probing Vestibular Efferent Function.

Natalie B. Dang; Anjali Sinha; Choongheon Lee; **Joseph C. Holt**
University of Rochester Medical Center, School of Medicine and Dentistry

The mammalian efferent vestibular system (EVS) begins as a modest number of bilateral, multipolar neurons in the dorsal brainstem. Contralateral and ipsilateral vestibular efferent neurons (VENs) project to the vestibular periphery where they undergo extensive branching to produce thousands of prominent varicosities on afferent terminals and hair cells. By virtue of this anatomy, VENs provide the CNS with a direct line to each side of the first synapse in vestibular transduction. Activation of mammalian VENs, at least under experimental conditions, profoundly modulates the resting discharge and sensitivity of vestibular afferents. However, the functional underpinnings for how and when the mammalian EVS gets utilized are unresolved. Recent pharmacological characterization of EVS actions in mice has identified a number of cholinergic synaptic mechanisms that contribute to the responses of vestibular afferents to efferent stimulation, including multiple muscarinic and nicotinic acetylcholine receptors. Some of the impetus for performing these studies in mice was accessibility to transgenic animals where the function of various EVS signaling components, implicated by our pharmacological data, have been disrupted. These animals may display

distinct vestibular phenotypes that can be identified in both electrophysiological and behavioral assays.

Such an approach is exemplified by a number of recent observations made in mice lacking the alpha9 nicotinic acetylcholine receptor subunit (β9nAChR-KO). The loss of functional β9nAChRs in these knockout animals is associated with changes in the timing, sensitivity and discharge regularity of vestibular afferents as well as alterations in the vestibulo-ocular reflex (VOR), vestibular sensory evoked potential (VsEP), and perhaps vestibulo-autonomic pathways. To gain additional insight into EVS function, we are developing behavioral assays that might highlight potential vestibular deficits in transgenic mice missing critical EVS signaling components. In our first attempt, we asked whether β9nAChR-KO animals, relative to controls (β9nAChR-WT), behave differently following a provocative vestibular stimulus. Postural sway and center of pressure (COP) measurements were made on a miniature force plate from β9nAChR-KO and β9nAChR-WT mice before and after 5-mins on an orbital shaker rotating at 125 RPMs. During the prestimulus period, both groups explored the confines of the force plate and displayed similar COP metrics. However, following the stimulus, β9AChR-KO animals exhibited a pronounced reduction in mobility associated with a significant compression of postural sway space as well as static freezing against the corners or walls of the plate enclosure. Initial observations suggested β9nAChR-KO mice spend less time rearing which we are working on confirming using video tracking software.

PS 10

Characterizing the Use of Intrabulla Drug Application to Target Efferent Synaptic Mechanisms in the Vestibular Periphery

Choongheon Lee; Anjali Sinha; Natalie B. Dang; Joseph C. Holt
University of Rochester Medical Center, School of Medicine and Dentistry

Electrical stimulation of cholinergic vestibular efferent neurons (VENs) in the squirrel monkey, chinchilla, and cat alters the excitability of primary vestibular afferents along several time scales suggesting multiple postsynaptic mechanisms are activated. To further characterize the cellular and synaptic mechanisms underlying efferent actions in mammals, we have recorded spontaneous discharge of primary afferents in the superior vestibular nerve of anesthetized mice, while stimulating VENs in the brainstem before and after the intraperitoneal (IP) administration of selective pharmacological agents. Comparable to previous mammalian studies, the response of mouse vestibular afferents to efferent stimulation primarily consisted of both fast and slow excitatory components, both of which were larger in irregularly-discharging afferents. Efferent-mediated inhibition of vestibular afferents was also observed in a few recordings. Emerging pharmacological evidence has suggested that the above afferent responses to efferent stimulation, at least in mice, rely on at least three distinct cholinergic mechanisms to modulate the spontaneous discharge of vestibular afferents: (1) Slow excitation - activation of muscarinic ACh receptors (mAChRs) and subsequent closure of KCNQ potassium channels, (2) Fast excitation - activation of afferent β4β2*-containing nicotinic AChRs (nAChRs), and (3) Inhibition - sequential activation of β9β10-nAChRs and SK2 potassium channels in type II hair cells.

Many of the compounds that we have administered IP to block efferent actions in the mouse peripheral vestibular system also readily access the CNS where they may interact with similar synaptic mechanisms in other neural systems beyond the ear. These off-target effects may confound our initial pharmacological observations and furthermore limit the use of these drugs in future behavioral studies designed specifically to probe vestibular efferent function. We recently developed an alternative intrabulla (IB) approach in mice that allows the direct application of these same pharmacological agents to the middle ear space on the side from which we are recording. With ipsilateral IB administration, mAChR antagonists blocked efferent-mediated slow excitation whereas selective β4β2*-nAChR antagonists selectively blocked efferent-mediated fast excitation. Efferent-mediated slow excitation was also antagonized by the KCNQ blocker XE991 but not the ERG-channel blocker E4031 suggesting a role for an M-current mechanism in the effector pathway. The onset of blockade of EVS actions with ipsilateral IB administration was faster than with IP or contralateral IB application suggesting drugs applied to the ipsilateral middle ear had direct perilymphatic access to vestibular efferent synapses. Work is continuing on characterizing candidate drugs that target these mammalian efferent mechanisms in the vestibular periphery.

Animal Models of Human Otologic Disease

PS 11

Raman Spectroscopy to Identify Changes in the Tympanic Membrane Associated With Acute Otitis Media

Anping Xia[1]; Tulio A Valdez[1]; Surya Singh[1]; Mahbuba Tusty[1]; Andrey Victorovich Malkovskiy[2]; David Zarabanda[1]; Meena Easwaran1[1]
[1]Department of Otolaryngology and Head and Neck Surgery, School of Medicine, Stanford University, Palo

Alto, CA, 94305, USA; [2]Biomaterials and Advanced Drug Delivery Laboratory, Stanford School of Medicine, Stanford, CA 94304, USA

Otitis media (OM) is one of the most commonly observed disease conditions of the middle ear and occurs mostly due to bacterial infections. It is estimated that 85% of children have witnessed an episode of OM before 5 years of age. The tympanic membrane (TM) is an integral component of the middle ear and participate mainly in the transmission of the sound waves. The backbone of the TM is mainly consists of collagen fibers, providing it with required tensile strength and rigidity Changes in the stiffness of the TM due to repeated infections is a well-known phenomenon. Long term infection in the TM can lead to a shift towards less deformation-resistant collagen type. Histopathology, immunohistochemistry, and electron microscopy are the major techniques employed for studying these changes in the TM in response to a pathological condition. However, these methods suffer from limitations in terms of time consumption, inter-observer subjectivity and destructive nature. In the present study using Raman spectroscopy (RS) we demonstrated the feasibility of identifying early changes in the TM that can serve as an indicator of acute otitis media. Bacterial lipopolysaccharides (LPS) was injected through the tympanic membrane in a murine model. Raman imaging was performed using Horiba Xplora spectrometer coupled with a 50X objective (Olympus, NA=0.80), 600 gr/mm grating and 785 nm excitation. Typical exposure time at every spot was 5 seconds and the spectra were acquired with 1 µm spatial resolution. Infiltration of cells along with the epithelial proliferation was revealed by histology. Presence of activated macrophages induced by LPS treatment was confirmed by immunostaining using antibody specific for galactopyranosyl group at their membrane surface. Successful discrimination among LPS treated and control groups suggesting spectral differences was achieved using principal component analysis. Raman mapping was performed using normalized band intensities specific for collagen and nucleic acids. LPS treated tissues had less collagen as compared to controls. Findings of the trichrome staining corroborated with this observation. Further analysis of the Raman spectrum suggests predominance of collagen IV specific signals in LPS treated samples. Overall the study demonstrated the feasibility of identifying inflammation-induced biochemical changes in the TM. Increase in collagen IV content can be considered as a potential spectroscopic marker for the diagnosis of AOM. Our future studies will focus on utilizing these markers to study otitis media progression and assessing therapeutic response or AOM reversal.

PS 12

Development of Gold Nanoclusters as Adjuvants for the Treatment of Chronic Suppurative Otitis Media

Laurent Adonis Bekale; Anping Xia; Kelly M. Khomtchouk; Peter Santa Maria
Department of Otolaryngology and Head and Neck Surgery, School of Medicine, Stanford University, Palo Alto, CA, 94305, USA

Chronic suppurative otitis media (CSOM) is characterized by a chronically discharging infected middle ear, most frequently *Pseudomonas aeruginosa* (PA). 330 million people worldwide have CSOM, and it is a leading causes of permanent hearing loss. CSOM PA exists in phenotypically variable bacterial communities known as biofilms. Ototopical fluoroquinolones (ofloxacin and ciprofloxacin) are the only available non ototoxic therapy. Unfortunately, PA biofilms contain a subpopulation of metabolically inactive and quiescent bacteria known as persister cells. As they are not susceptible to fluoroquinolones, they exhibit temporary antibiotic-resistance (also known as antibiotic tolerance), distinct from the traditionally known permanent antibiotic resistance caused by genetic mutations or horizontal gene transfer. Persister cells repopulate the biofilm niche after the antibiotic therapy is discontinued. The persister cell phenotype and biofilm endow *P. aeruginosa* with powerful mechanisms to survive fluoroquinolone treatment in CSOM. The end result is multiple rounds of surgery to debride the biofilm and a lifelong struggle with this disease. To address this unmet clinical need, our lab recently created functionalized gold nanoclusters (core size < 3 nm) (AuNCs) to augment the activity of fluoroquinolones. We show, *in vitro*, that co-administration of the AuNCs with ofloxacin dramatically enhances ofloxacin's eradication activity against *P. aeruginosa* biofilms and persister cells. *In vitro* studies have also revealed that the AuNcs have a reduced cytotoxicity compared to standard of care, ofloxacin. Our lab has also recently created and validated the first PA CSOM animal model that mimics the human condition. This model is created with bioluminescent PA allowing us to track disease progression in real time. In this model we have shown that the infection is temporarily reduced by ofloxacin before returning after cessation of therapy, just like the human condition. Now with this model in hand, we will be, for the first time, able to test this novel therapy for CSOM *in vivo*.

PS 13

Predictive Power of Antibiotic Tolerance and Preclinical Evaluation of Fluoroquinolone Treatment of Pseudomonas aeruginosa Chronic Suppurative Otitis Media

Kelly M. Khomtchouk[1]; Ali Kouhi[2]; Anping Xia[1]; Peter Santa Maria[3]
[1]Department of Otolaryngology and Head and Neck Surgery, School of Medicine, Stanford University, Palo Alto, CA, 94305, USA; [2]Tehran University of Medical Sciences; [3]Stanford University Medical Center

Chronic suppurative otitis media is a neglected pediatric disease affecting over 300 million people worldwide, for which no new drugs have been introduced for over a decade. This is a chronic biofilm infection with an incredible burden on the human population. To address this, we create and validate a robust pipeline for antimicrobial discovery targeting chronic drug tolerant biofilm infections and report a mouse model with utility in preclinical drug evaluation. This work guides therapeutic development by learning from the clinical failure of an FDA approved fluoroquinolone and proposes revisiting regulations and clinical trial designs for pan drug tolerant biofilm diseases. We question the clinical predictive value of *in vitro* antimicrobial susceptibility tests for biofilm susceptibility and determine, for drugs that freely diffuse through the biofilm matrix, these tests are irrelevant to disease outcome *in vivo*. In contrast, the *in vitro* evaluation of antibiotic tolerance with planktonic stationary phase *P. aeruginosa* predicts the failure and recurrence of CSOM post-fluoroquinolone therapy. With our novel mouse biofilm model that allows for bacteria tracking in real-time and topical administration of the standard of care, ofloxacin, we show a cohort of non-responders and a cohort resulting in temporary reduction of bacterial burden, highlighting a problem of recurrence and the need for therapeutic outcomes that assess eradication post-therapeutic endpoint. A new preclinical mouse model of long term gram-negative infection displaying the hallmark features of CSOM, chronic infection leading to inhibition of healing in a perforation of the tympanic membrane and purulent discharge in the ear (as assessed by blinded grading) supports the conclusion that persistent bacteria cells are the bottleneck for eradication in drug tolerant recurrent infections.

PS 14

Characterizing the Osteolytic and Osteoblastic Responses to Cholesteatoma and Oncolytic Virotherapy

Joseph Pinkl[1]; Ivy Schweinzger[2]; Josephine Fernandez[3]; Mark Currier[4]; Noga Lipschitz[2]; Timothy P. Cripe[4]; Ravi N. Samy[2]; Brian R. Earl[2]
[1]University of Cincinnati Department of Communication Sciences & Disorders; [2]University of Cincinnati; [3]University of Pittsburgh; [4]Nationwide Children's Hospital

Cholesteatomas (CHSTs) are benign temporal bone lesions that arise from keratinizing squamous epithelial cells and are often superinfected with Pseudomonas aeruginosa. CHSTs gradually erode the ossicles, mastoid, and skull base leading to hearing loss, facial paralysis, dizziness, and meningitis. Standard treatment involves surgical resection, although the recurrence rate may be as high as 60%. Our recent *in vitro* work with human tissue samples and *in vivo* research in a gerbil model of CHST has shown that virotherapy with an oncolytic herpes simplex virus (oHSV) can selectively eradicate CHST. This study aimed to characterize the bony erosion (osteolytic changes) and the bony growth (osteoblastic changes) within the middle ear (bulla) of gerbils with CHST over the course of oHSV treatment.

CHSTs were induced bilaterally in 10 Mongolian gerbils using a double-suture ear canal ligation approach plus inoculation with *Pseudomonas aeruginosa* as an expediter of CHST growth. The animals were treated with one, two, or three intra-bullar injections of oHSV beginning 2-6 weeks post-CHST induction. Two un-operated gerbils (n=4 ears) were used as controls. High-resolution micro-computed tomography (micro-CT) scans were obtained pre- and post-treatment to measure CHST volume as well as the perimeter of the bullae (mm) and the area of the bullae (mm^2). The bullar area-to-perimeter ratio was used to normalize the changes in bullar thickness relative to the observed regions of bullar erosion.

Osteolytic changes (e.g., thinning of and gaps in bulla, ossicular erosion) were observed in the bullae of the majority of animals prior to oHSV treatment. Osteoblastic changes (e.g., thickening of the bulla) were also observed in the majority of animals prior to treatment. Over the course of oHSV treatments, CHST volume decreased by as much as 70% relative to pre-treatment volume. In addition, the gaps in the bullar bone closed and the bullar thickness returned to normal in multiple animals in the two- and three-treatment groups. Bulla area-to-perimeter ratios were significantly higher in pre-treatment and treated animals compared with controls, while there was a downward trend observed for the ratios observed in animals receiving multiple treatments.

Both osteolytic and osteoblastic effects were observed in the gerbil model of CHST. Treatment with virotherapy appears to decrease CHST volume as well as influence the integrity of the bony middle ear cavity. Future research will assess biomarkers of the response to

oHSV treatment at both the level of immune system and the safety of oHSV within the auditory nervous system.

PS 15

An Investigative Study on Efficacy and Safety of Intratympanic Botulinum Toxin

Jung Mee Park[1]; Min Jung Kim[1]; **Jaclyn Vidal**[1]; So Young Park[2]; Shi Nae Park[1]
[1]Department of Otolaryngology-HNS, Seoul St. Mary's Hospital, College of Medicine, The Catholic University of Korea; [2]Department of Otolaryngology-HNS, Yeouido St. Mary's Hospital, College of Medicine, The Catholic University of Korea

Background
To date, management of intractable middle ear myoclonic tinnitus is limited to tenotomy of middle ear muscles (MEMs), i.e. tensor tympani and stapedius muscles. In order to avoid such invasive procedure, intratympanic injection of botulinum toxin (BTX) that may induce paralysis of MEMs could be an alternative treatment modality. This animal study was conducted to investigate the safety of BTX as well as its effect on MEMs before implementing a clinical study.

Methods
Male Sprague-Dawley rats aged 1 month were divided into 4 subgroups according to the sacrificing day after BTX injection: 3 days, 1 week, 3 weeks, and 2 months. After initial hearing tests using ABR and DPOAE, one ear was randomly assigned as the experimental ear, the other, as the control ear. Experimental ears were intratympanically injected with 0.1 ml of BTX A, whereas control ears were injected with saline. Tympanic membrane endoscopic pictures and hearing tests were conducted before sacrificing animals according to the subgroup. Collected bulla mucosa and cochleae were evaluated for morphologic changes after BTX injection. In order to analyze the efficacy of intratympanic BTX, electron microscopic study of MEMs in addition to immunofluorescent (IF) study of cleaved SNAP-25 were conducted for analysis.

Results
Tympanic membranes were completed healed without structural changes after 1 week. Light microscopic images of bulla mucosa did not show any inflammatory changes in all subgroups, indicating the safety of botulinum toxin to middle ear structures. Hearing thresholds of all experimental ears did not change ($P > 0.05$), and cochlear morphologic studies did not show significant changes in all subgroups. Electron microscopic images of MEM sections obtained from the experimental ears showed significant alterations in muscle ultrastructures compared to the control ears, and these changes were more definite in the subgroup sacrificed 2 months after BTX injection. IF study showed a high intensity of cleaved SNAP-25 up to 1 week after injection but were less evident in 2 months group.

Conclusion
Intratympanic injection of BTX does not seem to have ototoxic effects on the inner ear and middle ear. A strong IF intensity of cleaved SNAP-25 on the neuromuscular junction and muscular degenerations of MEMs showed the efficacy of intratympanic BTX as a MEM-inactivating substance. A clinical study based on these results is in progress.

PS 16

Sensorineural Hearing Loss Occurs in a Pseudomonas Aeruginosa Chronic Suppurative Otitis Media Mouse Model

Anping Xia[1]; Zhixin Cao[2]; Xiaohua Chen[3]; Laurent Adonis Bekale[1]; Peter Santa Maria[1]
[1]Department of Otolaryngology and Head and Neck Surgery, School of Medicine, Stanford University, Palo Alto, CA, 94305, USA; [2]Department of Pathology, Provincial Hospital Affiliated to Shandong First Medical University; [3]Department of Otolaryngology, The First Affiliated Hospital of Zhengzhou University

CSOM is a neglected tropical disease that afflicts 330 million people worldwide and is the most common cause of permanent hearing loss among children in the developing countries. The bacterium, *Pseudomonas aeruginosa* (PA), is the leading culprit. PA colonizes the middle ear *via* a perforated tympanic membrane and, soon thereafter, establishes itself into a biofilm community. Over the course of the disease the infection waxes and wanes as the population of bacteria within the biofilm partially respond to immune attack or topical antibiotic therapy. It is this waxing and waning of bacterial populations in the middle ear that is likely to lead to permanent inner ear hearing loss. Our lab has recently created and validated a novel PA CSOM animal model that mimics the human condition. We hypothesize that the PA CSOM leads to sensorineural hearing loss predominantly through hair cell toxicity. We extracted Perilymph from the cochlea in the living mice that 3 weeks after PA inoculation into the middle ear cavity. Mass Spectrum data determined the appearance of intracellular PA proteins, innate immune proteins and cytokines in the perilymph of CSOM compared to controls. We correlated these perilymph findings with structural damage in the cochleae that occurs at 2 weeks post inoculation with increasing PA concentrations, defined by optical density (OD). MyosinVIIa immunostaining

revealed that the outer hair cells (OHCs) were destroyed completely in the basal turn. The OHCs loss was gradually reduced from middle to apical turn. In addition, the OHCs loss depended on the PA intensity, the higher the PA intensity, the more the OHCs loss. In contrast, the inner hair cells (IHCs) loss was only found in the base with the highest PA intensity (OD 1.2) used. Based on our data, we were able to create a CSOM mouse model that resulted in SNHL due to OHC loss as the dominant phenotype in the inner ear. The future study needs to be focused on the immune response and ototoxic agents that lead to HCs death.

PS 17

Anatomical Consequences of Postnatal Zika Virus Infection on the Cochlea and Vestibular End Organs in a Mouse Model

Kathleen T. Yee[1]; Biswas Neupane[2]; Fengwei Bai[2]; Douglas E. Vetter[1]
[1]Department of Neurobiology and Anatomical Sciences, University of Mississippi Medical Center; [2]Department of Cell and Molecular Biology, University of Southern Mississippi

A significant concern for human health world-wide is the increased prevalence of Zika virus (ZIKV) infection. The primary, but not sole, vector for Zika transmission is the *Aedes aegypti* mosquito, already identified in the United States. Human transmission by sexual contact and saliva has been documented and geographic spread of the virus is enabled by the ease of world-wide travel (Hills et al., 2016). Pre- and postnatal ZIKV infection in humans can impair hearing. ZIKV infection of adults can manifest as transient hearing loss. Interestingly, there have been no reports of vestibular impairments. The underlying etiology causing postnatal hematogenous ZIKV-induced hearing dysfunction has not been thoroughly investigated. We previously reported that ZIKV can i) infect cochlear epithelial support cells and ii) alter expression of various proteins in the cochlea. We have extended our analysis and report here on other cochlear cells types infected by ZIKV and the cellular consequences of ZIKV infection on the cochlea and vestibular end organs.

Five to 6-week old *Ifnar1*$^{-/-}$ (C57BL/6J background) mice were infected and survived for 9 days. Mice were perfused (4% paraformaldehyde or 2.5% glutaraldehyde), temporal bones were isolated and embedded for cryostat or plastic sectioning. Cryostat material was sectioned (16um) and immunostained with primary antibody 4G2 to reveal ZIKV envelope protein, while plastic sections (3-4.5um) were stained with toluidine blue. Immunofluorescence was visualized using confocal microscopy and plastic sections were examined by brightfield microscopy.

At 9 days post-infection 4G2 immunofluorescence was detected in cochlear hair cells and in the stria vascularis located in the apical region of the cochlea. Examination of plastic sections revealed that ZIKV-induced damage is most severe in the cochlear epithelium of the apex. Analysis of spiral ganglion neurons revealed a diminishing apical to basal gradient of damage. Our results also show significant damage to vestibular end organs, including hair cells and support cells.

We conclude that hematogenous ZIKV infection of 5 to 6-week old *Ifnar1*$^{-/-}$ mice following a 9-day survival causes cellular damage in the cochlea and vestibular end organs. Graded damage within the cochlea and spiral ganglion neurons suggests differential viral effects and/or that some damage results from indirect effects of ZIKV. Despite our observations of vestibular damage following ZIKV infection, ZIKV-infected individuals have not reported issues of vestibular impairment. This may be due to bilateral vestibular end organ damage in humans, mirroring our mouse model.

Support: R21DC015124 (DEV), P30GM103328 (Confocal Imaging Core, UMMC)

PS 18

The Acoustic Reflex: A Comparison Between Noise-induced Hearing Loss and Selective Inner Hair Cell Loss in Carboplatin-treated Chinchillas

Andie Zang; Monica Trevino; Karen Pawlowski; Edward Lobarinas
University of Texas at Dallas

Abstract
The acoustic reflex (AR) is a diagnostic tool used to assess the auditory pathway. The AR is the result of a contraction of the stapedius muscle in response to high intensity acoustic stimuli. Reflexes remain present with mild to moderate hearing loss, but are reduced or absent with severe to profound hearing loss. These results suggest that outer hair cells (OHC) do not play a key role in the AR. Previously, we showed the AR persisted or was enhanced after selective loss of inner hair cells (IHC) in carboplatin-treated chinchillas. The purpose of this study was to evaluate and compare the persistence of the AR following noise-induced OHC loss and carboplatin-induced IHC loss.

Methods
ARs were measured in awake animals using a Tympstar middle ear analyzer before and after either a noise

exposure (89 dB SPL, OBN, centered at 4 kHz, for 24h) or carboplatin treatment (75 mg/kg). Reflexes were elicited with a 95dB HL stimulus using a 4000Hz pure tone, low bandpass noise, and high bandpass noise. AR amplitudes were compared before and after and across the noise and carboplatin conditions. Post assessments in the carboplatin condition were taken 3 weeks following treatment. Post noise exposure assessments were made 4 weeks post exposure.

Results and Conclusion
ARs in the carboplatin treated group showed either unchanged or enhanced amplitudes despite significant loss of IHC. Animals exposed to noise also showed persistence, but not enhancement of the AR. These data suggest that neither IHC nor OHC loss alone have a significant impact on the AR. Further studies are needed to determine the mechanisms driving the AR and whether these results generalize to other species.

Supported by NIH R01DC014088

PS 19

Hearing Preservation from Controlled Internal Jugular Vein Compression During Traumatic Noise Exposure

Celia D. Escabi[1]; Christina Campbell[1]; Karen S. Pawlowski[1]; Brian Sindelar[2]; Colleen Le Prell[1]; Edward Lobarinas[1]
[1]University of Texas at Dallas; [2]U.S. Army

Internal jugular vein compression (IJVC) has been suggested as a potential treatment to prevent or diminish traumatic brain injury (TBI), specifically to protect the brain against sports related impacts as well as providing protection against blast induced hearing loss. In the present study, we evaluated whether IJVC could also attenuate acoustic trauma induced by exposure to octave band noise.

In this study, 20 adult (3 – 5 months old) Sprague Dawley rats were exposed to an octave band noise (8 – 16 kHz, 109 dB SPL) for 2 hours. The experimental group (n = 10) was fit with a custom IJVC collar during noise exposure; the control group (n = 10) was exposed to the same noise without the collar. All animals underwent baseline, 24-hour post- and 2- or 3-week post-noise exposure testing that included auditory brainstem response (ABR) and distortion product otoacoustic emission (DPOAE) testing to assess auditory function. Hearing sensitivity in noise was assessed behaviorally using a pre-pulse inhibition of the acoustic startle paradigm. Following physiological and behavioral testing, the animals were sacrificed, and cochlear sensory cells and neural synaptic connections were assessed.

Statistically significant ABR threshold shift differences were observed between the collared and the control group 24 hours post-noise exposure at 16, 20, 24 and 32 kHz, with smaller temporary threshold shifts (TTS) for the collared group. At the final test time, there were statistically significant group differences at 24 kHz ($p = .04$) and 32 kHz ($p = .035$), with less permanent threshold shifts (PTS) observed in the collared rats. DPOAE amplitude was reduced at 24 hours post-noise in both groups, suggesting outer hair cell (OHC) function was temporarily compromised. At the final test time, DPOAE amplitudes generally showed complete recovery in both groups. During behavioral testing, collared rats showed a trend for enhanced responses at 20 – 24 kHz at 40 dB signal-to-noise ratio (SNR) but differences did not reach statistical significance; no differences were observed at 30 dB SNR. Cytocochleograms revealed limited sensory cell loss in both groups and counts of immunohistochemically labeled synapses did not differ between groups. The current results provide compelling evidence of protection against TTS using IJVC in the noise-exposed rat and suggest the potential for reduction of PTS as well.

Financial support provided by Q30 Innovations.

PS 20

Role of Neuroinflammation in Noise Induced Hearing Loss

Ana H. Kim; **Hunki Paek**
Columbia University Medical Center

Noise-induced hearing loss (NIHL) accounts for one-third of all hearing loss according to the World Health Organization. Dexamethasone (Dex) therapy target many different levels of apoptotic, necrotic and neuroinflammatory pathways. However, cellular mechanism underlying the Dex treatment on the retro-cochlear auditory centers such as the cochlear nucleus (CN) is largely unknown. Microglia has a critical role in neuroinflammation through the expression of surface proteins and secretion of pro-inflammatory cytokines. In addition, activated microglia displace inhibitory synapses from neurons and eventually alters synaptic activity. Using our established NIHL mouse model, we investigated the cellular alteration of microglia in NIHL by accessing *in vivo*cellular distribution, morphological changes, and examining the effect of Dex treatment on microglia activity. We also examined the role of microglia activation in neuronal cell loss and synaptic alteration in the CN. Hearing threshold assessed by auditory brainstem response (ABR) after NIHL showed

threshold recovery with Dex treatment but not with saline. Neuroinflammatory characteristics accessed by IBA1 staining showed microglia activation in the CN after noise exposure in NIHL group compared to the NIHL-Dex treated group. We observed an unexpected ~30% neuronal cell loss in the CN of NIHL animals at 30 days post noise trauma. Dex treated mice, on the contrary, showed neuron preservation compared to the saline-treated mice. Finally, imbalance of Excitatory and Inhibitory (E/I) synapses in CN after noise trauma was observed. Our results suggest that noise trauma triggers a neuroinflammatory cascade mediated by microglial cell activation, leading to neuronal cell death and to synaptic alterations with E/I deregulation, and that steroids have a neuro-otoprotective role by regulating microglial cell activation.

PS 21

Murine Complement Factor H Mutation May Share Mechanism with Sudden Hearing Loss

Kevin Ig-Izevbekhai[1]; Hangsoo Kim[2]; Jianqi Cui[3]; Rui Ma[3]; Wenchao Song[2]; Daqing Li[3]
[1]Department of Otolaryngology - Head & Neck Surgery; Perelman School of Medicine, University of Pennsylvania, Philadelphia, PA, USA; [2]Department of Systems Pharmacology and Translational Therapeutics, Perelman School of Medicine, University of Pennsylvania, Philadelphia, PA; [3]Department of Otolaryngology - Head & Neck Surgery; Perelman School of Medicine, University of Pennsylvania, Philadelphia, PA

Complement Factor H (CFH) is a glycoprotein involved in regulating the alternative complement pathway while minimizing the likelihood of autoreactivity. A point mutation in murine factor H (W1260R) has been associated with complement-mediated systemic thrombotic angiopathy, leading to cerebrovascular occlusion and neurologic deficits in mice. These systemic thrombotic processes could also involve occlusion of the labyrinthine artery, a common cause of sudden hearing loss.

The current study is, to our knowledge, the first to characterize auditory and neurologic dysfunction of CFH mutant mice. The study was conducted with 65 mice including wild type (WT), heterozygous (HTZ) and homozygous (MOZ) CFH mutants. Hearing thresholds were measured via auditory brainstem response (ABR) and compared via 2-sample t-test. Neurologic function was assessed in all mice.

A total of 57 mice, aged from 3 weeks to over 6 weeks old, were selected for ABR testing [WT (10), HTZ (17), MOZ (30)]. All WT mice had hearing thresholds within normal ranges [click frequency (20-30 dB), 4k (50-60 dB), 8k, 16k, 24k, 32kHz (20-30 dB)]. Among HTZ mice, 3 had normal hearing thresholds, while the remaining 14 had at least one elevated hearing threshold. In the MOZ group, 5 mice had hearing thresholds within normal ranges, while the remaining 25 demonstrated elevated thresholds. Among HTZ mice with hearing loss, thresholds were as follows (dB, mean ± SD): click (28 ± 10), 4kHz (57 ± 11), 8kHz (35 ± 12), 16kHz (32 ± 8), 24kHz (34± 9), 32 kHz (49 ± 13). MOZ mice with abnormal hearing exhibited the following thresholds: click (29 ± 8), 4kHz (55 ± 9), 8kHz (33 ± 11), 16kHz (31 ± 9), 24kHz (33 ± 11), 32 kHz (48 ± 10). All thresholds differed between mutant and WT mice ($P < 0.01$), but there was no difference between thresholds in HTZ and MOZ.

Among mutant mice with abnormal hearing, 4 mice developed other neurologic abnormalities; 2 showed lethargy and muscle wasting, one showed ataxia, and one showed hemiparesis. All mice with neurologic dysfunction demonstrated hearing loss. No mice with normal hearing showed neurologic dysfunction.

The incidence of hearing loss and neurologic dysfunction in CFH mutant mice suggests a shared mechanism, such as vascular thrombosis or stenosis. Concomitant neurologic dysfunction suggests cerebrovascular accident in some mice. Further histopathological studies may provide insight on a potential link, as CFH genetic mutation may be involved with sudden hearing loss or other hearing loss of vascular etiology.

PS 22

Hearing Impairment in Xeroderma Pigmentosum type A

Takeshi Fujita[1]; Tatsuya Furukawa[1]; Natsumi Uehara[1]; Hitomi Shinomiya[1]; Daisuke Yamashita[1]; Mariko Tsujimoto[2]; Akinobu Kakigi[1]; Chikako Nishigori[2]; Ken-ichi Nibu[1]
[1]Department of Otorhinolaryngology-Head and Neck Surgery, Kobe University, Graduate School of Medicine; [2]Division of Dermatology, Department of Internal Related Graduate School of Medicine, Kobe University

Xeroderma pigmentosum (XP) is an autosomal recessive hereditary disease characterized by increased susceptibility to freckle-like pigmentation and skin cancers at sun-exposed body sites. Furthermore, some patients display neurological manifestations, including hearing impairment. There are eight subtypes of XP: XP-A–XP-G and XP variant. XP occurs at a higher frequency in Japan (1:22,000) than in the United States (1:250,000). Approximately 50% of all Japanese patients

with XP are assigned to the XP-A, and most patients with XP-A exhibit severe neurological manifestations.

While its pathogenesis of skin symptoms have been well-studied, that of neurological symptoms, including sensorineural hearing loss (SNHL) remains unknown. In a recent temporal bone study of XP-A patients, diffuse and severe atrophy of the organ of Corti and spiral ganglion neurons (SGNs) was evident.

We have conducted a study to characterize the mechanisms of neurological dysfunction and hearing impairment in patients with XP through evaluation of hearing loss in *Xpa*-deficient mice. We found that these mice exhibited SNHL, with significantly higher hearing thresholds at frequencies of 4, 8, and 16 kHz, relative to those in wild type (WT) mice. We also observed lower numbers of SGNs in these mice, providing important insights into the pathogenesis of SNHL in patients with XP-A.

PS 23

Mutation of SLC7A14 Causes Syndromic Hearing Loss

Kimberlee Giffen; Huizhan Liu; David Z. He
Creighton University School of Medicine

The solute carriers (SLCs) are a large family of evolutionary conserved membrane transporters classified according to their sequence homology and transport functions. *Slc7a14,* encoding a glycosylated transporter protein with 14 transmembrane domains, has been predicted to mediate lysosomal uptake of cationic amino acids. Mutations in this gene are associated with autosomal recessive retinitis pigmentosa (RP) in humans. Deletion of *Slc7a14* in mice leads to a similar phenotype with decreased retinal thickness and abnormal electroretinography (ERG) response. Our previous transcriptomic analysis showed differential expression of *Slc7a14* in mouse inner hair cells (IHCs), compared to outer hair cells, suggesting an important role in IHC function. Through further gene and protein expression analyses, including RT-qPCR and immunofluorescence, we confirmed increasing expression of SLC7A14 during development, with strong expression observed in adult mouse IHCs. *In vitro* transport assays confirmed arginine uptake by the lysosomal membrane protein SLC7A14, suggesting an important functional role of arginine homeostasis in IHCs and retinal photoreceptors. *Slc7a14*-knockout mice showed loss of IHCs and elevated auditory brainstem response (ABR) thresholds, indicative of progressive hearing loss. Diagnosed RP patients with the homozygous SLC7A14-p.G330R missense mutation exhibited sensorineural hearing loss. *In vitro* studies showed aberrant cellular localization of mutant SLC7A14-p.G330R in the cytosol rather than in the lysosomal membrane, and subsequent loss of normal arginine transport function. We developed knock-in mice with the SLC7A14-p.G330R mutation to determine how it would affect IHC function and survival. We measured ABR and distortion product otoacoustic emission (DPOAE) to measure auditory function, and ERG to assess retinal function, to confirm the syndromic dysfunction associated with the missense mutation. Collectively, these results show that SLC7A14 is necessary for the normal function of IHCs and that SLC7A14 dysfunction will lead to syndromic hearing loss.

PS 24

The Dual AT1R/ETAR Blocker Sparsentan Prevents Hearing Loss and Renal Disease in Alport Mice

Michael Anne Gratton[1]; Dominic Cosgrove[2]; Jared J. Hartsock[1]; Grady Phllips[1]; Ruth Gill[1]; Brianna Dufek[2]; Duane Delimont[2]; Daniel Meehan[2]; Celia Jenkinson[3]; Radko Komers[3]
[1]Washington University School of Medicine, St. Louis, MO, USA; [2]Boys Town National Research Hospital, Omaha, NE, USA; [3]Retrophin, Inc., San Diego, CA, USA

Background and Design
Most emergent therapies for Alport syndrome (AS) address the renal disease but not the inner ear pathology. Endothelin-1-mediated activation of the endothelin type A receptor (ET_AR) on glomerular mesangial cells is an early triggering event in Alport glomerular disease, and activation of strial marginal cells results in strial pathology in the inner ear. Currently, angiotensin-converting enzyme inhibitors (ACEi) or angiotensin II receptor (AT_1R) blockers are the standard of care for Alport patients; however, these drugs have not been shown to improve hearing. Previously we showed that sparsentan (Spar), a dual AT_1R/ET_AR inhibitor, prevented increases in proteinuria, fibrosis, glomerulosclerosis, and glomerular basement membrane dysmorphology, and extended life-span in an AS mouse model (presentations at ASN 2018, 2019). Therefore, here we detail the comparative effects of Spar and losartan (Los) on hearing loss in the AS mouse model.

AS mice and wild type (WT) littermates were treated with vehicle (V) or Spar (120 mg/kg) by daily oral-gavage from 3-8.5 weeks (wks) of age or with Los (10 mg/kg) administered by daily oral-gavage from 3-4 wks of age and in drinking water from 4-8.5 weeks of age. Strial capillary basement membranes (SCBM) were assessed for thickness by transmission electron microscopy (TEM), and accumulation of extracellular matrix (ECM) in SCBM was determined by immunofluorescence (IF)

microscopy using antibodies to laminin β2, laminin β5, and collagen β1 IV. Hearing ability and sensitivity to noise were assessed by auditory brain response (ABR).

Results

Post-noise ABR thresholds were significantly improved in Spar-treated AS mice at 16 kHz compared to those in V-treated AS mice (*P< 0.05*, Figure 1). In contrast, no significant improvement was observed in Los-treated AS mice relative to V-treated AS mice. Spar attenuated increases in ECM expression levels by IF to a greater extent than losartan in the SCBM of AS mice. In support of the protective effect of Spar in the inner ear, Spar significantly (*P< 0.05*) prevented SCBM thickening compared to V-treated AS mice when width was analyzed using TEM (Figure 2).

Conclusions

Spar treatment significantly attenuated inner ear pathologies in Alport mice. Results from these pre-clinical studies, if successfully translated to the clinic, may present a therapeutic approach to both hearing loss and renal injury in AS.

Figure 1 Sparsentan treatment of Alport mice prevents Hearing Loss at 16KHz after Noise Exposure

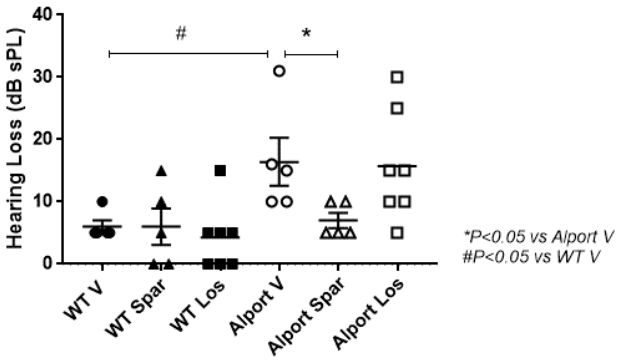

Figure 2 Sparsentan prevents increase in SCBM width in Alport mice

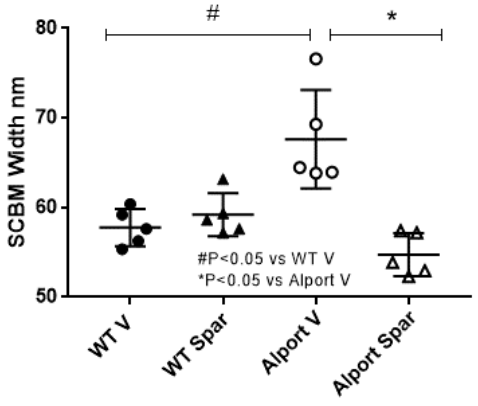

PS 25

Cdkn2a Deletion and Ototoxic Stress Synergistically Promote Abnormal Schwann Cell Proliferation in the Inner Ear

Kendra L. Stansak[1]; Johnathan D. Jones[2]; Bradley J. Walters[1]

[1]University of Mississippi Medical Center; [2]University of South Alabama

Acoustic schwannomas are the most common tumor type of the cerebellopontine angle. Though benign, these tumors can cause significant secondary symptoms including sensorineural hearing loss and facial muscle weakness. While congenital mutations in the *NF2* gene explain the vast majority of bilateral acoustic schwannoma cases, there is currently no consensus on the environmental and / or genetic parameters surrounding development of unilateral acoustic schwannomas which account for 95% of cases. Though somatic *NF2* mutations likely also contribute to a significant portion of unilateral schwannomas, nearly half of all cases are still idiopathic. Correlational epidemiological studies have suggested environmental risk factors such as exposure to heavy metals, x-rays, and ototoxic noise, however, more work is needed to determine the extent to which such environmental exposures are causative, and whether mutations in other genes may be predisposing or directly causative. Using a genetic mouse model to delete the tumor suppressor gene *Cdkn2a*, we tested the effects of aminoglycoside induced ototoxicity on cell proliferation in the inner ear. Male and female *Cdkn2a* knockout mice and their wild type counterparts were subjected to ototoxic damage by furosemide and kanamycin treatment and then provided with the thymidine analog BrdU in their drinking water for 2 weeks. Vehicle-treated *Cdkn2a* knockout mice demonstrated a modest, but significant, increase in cellular proliferation throughout the modiolus of the inner ear compared to wild type littermates. Mice injected with furosemide and kanamycin exhibited greater levels of cell proliferation compared to vehicle injected mice; and within this ototoxic condition, proliferation was significantly greater in *Cdkn2a*-null mice where neoplastic foci were commonly detected. Cells were labeled with antibodies against proliferating cell nuclear antigen (PCNA) and markers for glial cells (S-100), macrophages (CD68) and neurons (Hu-D and Tuj1). The majority of proliferating cells were S100 positive suggesting that they are glial. However, in kanamycin treated *Cdkn2a* null mice, proliferative cells expressing all 3 of the other markers, including the neuronal markers Hu-D and Tuj1 were also detected. The data show that ototoxic insult can cause increased cell proliferation in the inner ear and that a genetic background where *Cdkn2a* is ablated leads to further increases in cytogenesis and gliogenesis. These findings implicate *Cdkn2a* in the genesis of acoustic schwannomas and may provide a model for more detailed studies of environmental influence on aberrant Schwann cell proliferation in the inner ear and the 8th cranial nerve.

PS 26

A Method for Electrophysiological Evaluation of Peripheral Facial Nerve in Rats

Ji Eun Choi[1]; Nathaniel Carpena[2]; Jae-Hun Lee[3]; Gwangjin Jeong[4]; So-Young Chang[5]; Hee-Won Jeong[5]; Min Young Lee[6]; Sehwan Kim[4]; Jae Yun Jung[7]
[1]Dankook University Hospital; [2]Beckman Laser Institute Korea, College of Medicine, Dankook University, Cheonan, South Korea; [3]Beckman Laser Institute Korea, Dankook University; [4]Beckman Laser Institute Korea; [5]Dankook University; [6]Beckman Laser Institute Korea, Dankook University Hospital, Dankook University; [7]Beckman Laser Institute Korea, Dankook University, Dankook University Hospital

Compound muscle action potential (CMAP) recording via regenerated motor nerves is a critical examination to evaluate functional outcome of nerve regeneration. However, there is not much documentation on the detailed method of CMAP recording via the peripheral facial nerve (FN). Here we introduce our new CMAP recording procedure in detail as a package including surgical preparation, data acquisition, and analysis using Sprague Dawley (SD) rats. A total of 8 male SD rats (weights 200-250g) were used. There were two groups; normal FN group (n=4) and FN palsy group (n=4). In the FN palsy group, the main trunk of the left facial nerve was surgically transected and repaired with one or two 10-0 nylon epineurial sutures. CMAPs from the vibrissal muscles were recorded before injury and 14 and 28 days after injury. We compared the peak-to-peak amplitude of CMAPs between normal FN group and FN palsy group. We also examined that CMAP recordings can be practically combined with the behavioral examination using facial palsy score and histological examinations.

Acknowledgement:
This research was supported by Leading Foreign Research Institute Recruitment Program through the National Research Foundation of Korea (NRF) funded by the Ministry of Science and ICT (MSIT) (NRF-2018K1A4A3A02060572andNRF-2019R1H1A1035610)

Figure 1. The positions of electrodes in a compound muscle action potential (CMAP) recording of vibrissal muscles.

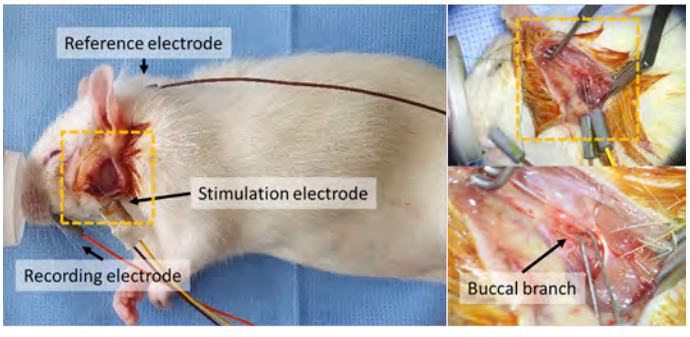

Figure 2. The waveforms of CMAP recording of vibrissal muscles with/without elevated skin flap after stimulation of the facial nerve.

(a) When stimulated the facial nerve without elevated skin flap, twitching around the right ear was observed.

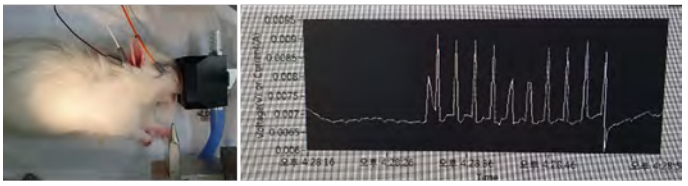

(b) When stimulated the facial nerve with elevated skin flap, twitching around the left vibrissal muscles was observed.

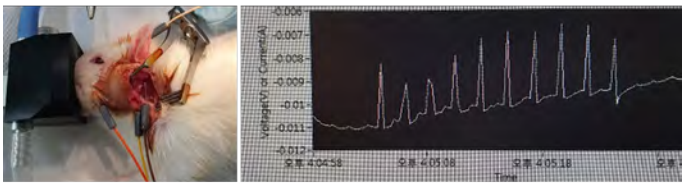

PS 27

Expression of advanced glycation end-product (AGEs) in the cultured utricles

Kazuma Sugahara; Yoshinobu Hirose; Makoto Hashimoto; Shunsuke Tarumoto; Hiroshi Yamashita
Yamaguchi University

Introduction

It is known that the prevalence of hearing loss is high in the patients with diabetes. In the last meeting, we presented that the model mice of metabolic syndrome showed the progressive hearing loss with an obesity and hyperlipidemia, high blood pressure. Advanced glycation end products (AGEs) are proteins or lipids that become glycated after exposure to sugars. AGEs are prevalent in the diabetic vasculature and contribute to the development of atherosclerosis. We have shown that the formation of AGEs in the inner ear plays an important role in the progressive hearing loss with diabetes.

We have reported that AGEs were generated in the cultured utricles after the exposure to the high concentration of glucose. In this study, we examined the optimal conditions for AGE generation in the cultured utricles.

Materials and Methods

Cultured utricles of CBA/N mice were used. The utricles were divided to 3 groups (Control group, High glucose group, High fructose group). In the high glucose group, utricles were cultured with glucose (60 mM). Five days after exposure to glucose, the cultured tissues were fixed with 4% paraformaldehyde. To evaluate the expression of AGEs, immunohistochemistry was performed using anti-AGEs antibody. The signal intensity was evaluated with the fluorescence microscope.

Results
The signal intensity of immunohistochemistry against AGEs were stronger in the high glucose group and fructose group than in the control group. The formation of AGEs was observed in the whole cultured utricles, not hair cell specific. The hair cell degeneration was not observed in both groups.

Discussiuon
The results suggested that the inner ear tissues exposed to high concentration glucose accumulate AGEs. This phenomenon has not been reported in the past. AGE is closely related to the tissue damage in the patients with diabetes. The relationship between inner ear damage and AGE formation have been unknown. However, I would like to clarify the role of AGE in inner ear disorders.

Auditory Brainstem I: Normal Hearing & Hearing Impairment

PS 28

Temporal Processing in the Cochlear Nucleus of an Autism Model Mouse

Tessa-Jonne Ropp; Michael Kasten; Paul Manis
University of North Carolina at Chapel Hill

Communication deficits play a key role in Autism Spectrum Disorders (ASD). Despite normal hearing thresholds, speech comprehension, stream-segregation and multisensory processing deficiencies have all been reported in ASD patients. It is thought that ASD is in part due to miswiring and changes in functional connectivity in the cortex, but few studies have examined whether mutations associated with ASD lead to deficits in sensory function before cortex. CNTNAP2, a gene commonly mutated in ASD produces a protein first identified as being involved in K+ channel localization in axons and associated with cortical deficits. The goal of this project was to study the functional consequences of knocking out CNTNAP2 on auditory processing in the cochlear nucleus. **Our hypothesis is that loss of CNTNAP2 disrupts auditory processing in cochlear nucleus without altering hearing thresholds.** We used click and tone ABRs (Auditory Brainstem Response) to determine errant responses in wildtype versus knockout CNTNAP2 mice. We found a shift in latencies and reduced amplitude in click ABRs, though the thresholds were preserved across animal groups. We also examined responses to auditory nerve fiber stimulation in bushy and stellate cells in cochlear nucleus slices of wildtype versus knockout CNTNAP2 mice in slice experiments. Bushy cells (principal cells in the ascending auditory pathway) exhibited apparently normal EPSCs to low frequency auditory nerve stimulation, but showed increased failures at high frequencies. Our data suggests that there is altered auditory signal encoding at the first stage in the ascending auditory pathway in this ASD mouse model, which could have detrimental effects on higher order auditory processing. This work was supported by the Auditory Hearing Research Foundation and NIDCD grant R01 DC004551.

PS 29

Induction mechanisms of activity -dependent changes in the endbulb of Held

Nicole F. Wong; Matthew A. Xu-Friedman
University at Buffalo/SUNY

Exposure to loud sound can induce long-lasting changes to neurons in the auditory system, which may result in hearing disorders such as tinnitus. One component of the auditory system subject to these changes is auditory nerve synapses in the cochlear nucleus. These synapses decrease in the probability of vesicle release (P_r) after exposure to loud, non-traumatic noise. However, the cellular mechanisms that underlie these changes are unknown. Here, we investigated how increased activity leads to a decrease in P_r by incubating slices of cochlear nucleus in a high potassium solution. This treatment drives vesicular release from the endbulb of Held and depolarizes the postsynaptic bushy cell. To assess changes in P_r, we used the paired-pulse ratio (PPR= $EPSC_2/EPSC_1$). Within four hours of incubation in the high K^+ solution, the PPR increased, similar to the effects of prolonged exposure to loud, non-traumatic noise *in vivo*. In addition, the amplitude of $EPSC_1$ decreased, consistent with a drop in P_r. These effects were stronger with a higher K^+ concentration and longer incubation times. We also tested the roles of diverse signaling pathways by applying specific antagonists during the high K^+ application. Changes to PPR and $EPSC_1$ amplitude were blocked by antagonists against PKA and nitric oxide synthase, implicating these pathways in activity-dependent changes in P_r. Further studying these pathways may help us understand the signaling mechanisms activated by loud, non-traumatic noise and give insights into treatments for hearing disorders.

PS 30

Expression and Neurotransmitter Association of Synaptic Calcium Sensor Synaptotagmin in the Avian Auditory Brain Stem

Katrina M. MacLeod[1]; Sangeeta Pandya[2]
[1]University of Maryland, College Park; [2]University of Maryland

Synaptic connections between auditory nerve axons and their neuronal targets in the cochlear nuclei define how acoustic information is processed and transmitted along

the ascending pathways. In the avian auditory brain stem, acoustic timing and intensity cues are processed in separate pathways via the two cochlear nuclei, nucleus angularis (NA) and nucleus magnocellularis (NM). Previously research has shown differences in the properties of excitatory and inhibitory synaptic inputs, such as synaptic release probability and short-term plasticity, contribute to differential processing. How these properties are differentially regulated is not well understood, but may dependent on differences in the molecular components of the presynaptic transmission. Synaptotagmins are a family of C2-domain-containing Ca^{2+}-binding proteins, and two main isoforms, Syt1 and Syt2, are thought to be the major calcium sensors for exocytosis. We investigated the distribution of Syt1 and Syt2 via immunohistochemistry and single and double immunofluorescence in the embryonic and hatchling chick brain stem (Gallus gallus). We found that anti-Syt1 and anti-Syt2 label had differential and largely complementary expression. In the timing pathway defined by NM and its target, nucleus laminaris (NL), the anti-Syt2 label was strong and the Syt1 labeling was weak, while both isoforms were intensely expressed in NA. In NM, anti-Syt2 label resembled the calyx terminals of the auditory nerve inputs, while Syt1 was more punctate. We found both isoform expression patterns were established and stable over a range of developmental ages (embryonic days E17-E18; postnatal days P0-P1; and postnatal day P7). To determine with which neurotransmitters the synaptotagmins were associated, we performed double immunofluorescence experiments. In NM, we found that the anti-Syt2 label was nearly identical in extent with anti-VGluT2 (Vesicular Glutamate Transporter 2), while the anti-Syt1 label showed only partial overlap. In contrast, neither isoform showed any significant co-label with the inhibitory neurotransmitter marker anti-VGAT (Vesicular GABA Transporter). These results suggest that synaptotagmin 2 is the major calcium binding protein underlying excitatory neurotransmission via the auditory nerve inputs in the avian brain stem, while the inhibitory terminals do not appear to associate with either Syt1 or Syt2.

PS 31

Spontaneous Action Potential Activity in Ultra Low Frequency Nucleus Magnocellularis is HCN Channel Dependent

George Ordiway; Jason Sanchez
Northwestern University

Spontaneous action potential (AP) activity in the nervous system is critical for the organization of neural circuits, including eye specific segregation in the visual system and frequency specificity in the auditory system. In the developing auditory system, spontaneous activity in peripheral structures has been well studied, but the role of spontaneous activity in central structures is less understood. Using patch-clamp electrophysiology, we recently reported the unique function of neurons located in the most caudolateral nucleus magnocellularis (NMc), a brainstem structure in birds analogous to the mammalian anteroventral cochlear nucleus. Somatic current injections of square pulse and sinusoidal stimulation revealed sustained and burst firing patterns of APs, respectively. Such firing patterns were heavily dependent on a mixture of high- and low-voltage activated potassium channels; including Kv3, Kv2 and Kv1. In addition, a special voltage-gated sodium channel worked synergistically with potassium channels through resurgent sodium current to generate rapid burst-firing patterns. Here we also report that in addition to their response to stimulation, spontaneous AP activity is seen in approximately one third of mature NMc neurons. While all neuronal activity, spontaneous or otherwise, requires expression of multiple types of ion channels, we predict that hyperpolarized cyclic nucleotide gated (HCN) channels are necessary for the generation of spontaneous activity.

To test this prediction, we bath applied ZD7288, an organic blocker of HCN channels. Drug treatment led to a profound decrease in spontaneous AP activity that was re-established during washout. HCN channel mediated current (Ih) was also significantly decreased and subsequently rescued. However, ZD7288 application did not affect AP burst rate, jitter or half width during low frequency sinusoidal stimulation. Therefore, HCN channels may not be necessary for the unique firing patterns seen in NMc. Spontaneous AP activity was also observed in early developing neurons, suggesting it might be important in circuit maturation. Response to the low frequency stimulation revealed the typical differences between immature and mature neurons: AP half width and jitter was significantly larger while AP amplitude was lower. This is due to decreased expression of sodium and potassium ion channels. There is likely decreased HCN channel expression as well, due to the rate of spontaneous spiking and significantly lower Ih current. The presence of spontaneous activity in NMc suggests an important contribution to auditory processing not yet understood, especially when observed before the onset of hearing. Future studies will look at the establishment of spontaneous activity, as well as synaptic contributions.

PS 32

Ultrastructural Changes of Murine Endbulb of Held Active Zones upon Maturation

Anika Hintze[1]; Anna Steyer[2]; Wiebke Möbius[3]; Carolin Wichmann[4]
[1]Molecular Architecture of Synapses Group, Institute for Auditory Neuroscience, InnerEarLab and Center for

Biostructural Imaging of Neurodegeneration, University Medical Center Göttingen, Germany; [2]Electron Microscopy Core Unit, Department of Neurogenetics, Max Planck Institute of Experimental Medicine, Göttingen, Germany; [3]University Medical Center Göttingen Electron Microscopy Core Unit, Department of Neurogenetics, Max Planck Institute of Experimental Medicine Göttingen; [4]1 Molecular Architecture of Synapses Group, Institute for Auditory Neuroscience & InnerEarLab, University Medical Center Göttingen

In the mammalian auditory pathway, the first central synapses are found in the cochlear nucleus (CN), where the auditory nerve fibers (ANF) project onto bushy cells (BC). Spherical BCs receive presynaptic terminals from 2-3 ANFs forming large terminals called endbulbs of Held. Globular BCs are innervated by 4-6 smaller but more numerous 'modified' endbulbs of Held (Cao and Oertel, 2010). During the maturation of the auditory system from pre-hearing to hearing, physiological changes such as the upregulation of postsynaptic potassium channels (Yang and Xu-Friedman, 2010) are accompanied by striking morphological changes on the level of presynaptic terminals and presumably also individual active zones (AZs). These changes result into synapses tuned for fast signal transmission with high temporal fidelity that is essential for their role in auditory processing tasks such as sound localization and analysis. Missing auditory input, which is usually sensed in the cochlea and transmitted via the ribbon synapses, can have striking consequences on the structure of the endbulbs. It has been shown that the lack of the hair cell specific C_2 domain protein otoferlin at inner hair cell (IHC) ribbon synapses results into an almost abolished exocytosis (Roux et al., 2006) and in changes of the number and morphology of endbulbs (Wright et al., 2014).

We use different electron microscopic techniques to investigate ultrastructural parameters at the endbulbs of Held comparing immature (postnatal day 10 (P10)) to mature (P21) synapses of C57BL/6J wild-type and otoferlin knock-out mice.

We performed high-pressure freezing and freeze-substitution (HPF/FS) followed by electron tomography of individual AZs. HPF/FS leads to a rapid immobilization of the tissue and allows us to determine the number and distribution of SVs as well as AZ sizes in a near-to-native state. A trend towards a higher number of SVs per AZ in mature synapses was observed. However, preliminary results indicate that the size of the AZs seems to decrease upon maturation. Moreover, we present focused ion beam-scanning electron microscopy (FIB-SEM) 3D reconstructions of whole BCs to show gross morphological changes that occur between P10 and P21. Our results provide first insight into morphological vesicle pool changes upon maturation at the endbulb of Held using a rapid freezing method for tissue preservation.

PS 33

Cell Types of the Dorsal Cochlear Nucleus that Receive Descending Input from the Inferior Colliculus

Timothy Balmer[1]; Laurence Trussell[2]
[1]Oregon Hearing Research Center, Vollum Institute, Oregon Health & Science University; [2]Oregon Hearing Research Center and Vollum Institute, Oregon Health and Science University, Portland, Oregon

The dorsal cochlear nucleus (DCN) integrates auditory nerve inputs with multisensory signals from non-auditory regions. In addition, the DCN integrates descending auditory signals from downstream areas of the auditory system. The inferior colliculus (IC) in particular—the main target of the DCN—sends a tonotopic projection back to the DCN. This descending projection has been proposed to have various roles in auditory processing, but without knowing the targeted cell types, and the postsynaptic responses in those cell types, the question remains how these signals are integrated into the DCN circuit and therefore what role they play in hearing. For example, descending projections to cells of the mossy fiber pathway (unipolar brush cells, granule cells and Golgi cells) could contribute to sound source localization or to suppression of self-generated sounds. Descending projections to principal projection neurons (fusiform or giant cells), or to neurons that inhibit them (cartwheel, superficial stellate or vertical cells), could sharpen tuning through feedback excitation and lateral inhibition.

We labeled neurons in the DCN that receive descending projections from the inferior colliculus using an anterograde trans-synaptic viral approach in mice. We focused on the larger descending projection to the ipsilateral DCN. Numerous cell types in the deep layer and principal cell body layer of the DCN were trans-synaptically labeled from the IC. To identify the cell types by their firing properties and to investigate the synaptic actions of these inputs, we targeted trans-synaptically labeled cells for whole-cell recording in acute brain slices that also expressed channelrhodpsin-2 (ChR2) in the descending axons. Specific activation of ChR2-expressing descending inputs showed that they were glutamatergic and were strong enough to drive action potential firing in some cells. Neurons that received monosynaptic input included principal cells, cartwheel cells and vertical cells, in addition to mossy fiber pathway cells (unipolar brush cells of both subtypes, granule cells and Golgi cells). All cell types except superficial stellate

cells, which were never labeled and would have been easily identified in the molecular layer, were verified to have direct input from the ipsilateral IC. Recorded cells were filled with biocytin and imaged along with their ChR2-expressing input to correlate synaptic morphology with their synaptic responses. The descending IC–DCN projection may have multiple roles, modulating the firing of the parallel fiber pathway, as well as sharpening tuning of the principal output neurons. Dysregulation of this excitatory pathway could lead to DCN hyperactivity and underlie tinnitus.

PS 34

Synaptic Properties of a Novel Inhibitory Neuron Type, L-Stellate Cells in the Cochlear Nucleus

Tenzin Ngodup; Laurence Trussell
Oregon Hearing Research Center and Vollum Institute, Oregon Health and Science University, Portland, Oregon

In the ventral cochlear nucleus (VCN), feedforward inhibition from glycinergic cells is important for auditory processing by principal neurons in the VCN. We used a well-characterized transgenic mouse line, GlyT2-EGFP, which labels all glycinergic neurons, to study the diversity of glycinergic cells in the VCN. With these transgenic mice, we discovered an abundance of GFP positive cells in the VCN that are distinct in somatic size, dendritic arbor and axonal projection from the well-known D-stellate cell class. We termed these cells "L-stellate" as their axons were short and terminated on local principal cells of the VCN. Our previous report indicated that these neurons receive excitatory input from auditory nerve fibers as well as from T-stellate neurons within the VCN. This latter source constitutes obligatory feedforward excitation, since the T-stellate cells are also excited by auditory nerve fibers. Here we examine how L-stellate cells respond to these dual sources of excitation. L-stellate cells were recorded in the slices made from the GlyT2-EGFP mouse line and a stimulus electrode placed on the auditory nerve root. Trains of stimuli delivered to the nerve reliably generated trains of synaptically-driven spikes in the L-stellate cells. Initially these spikes were time locked to the stimuli, but after 5 or more shocks the spikes became desynchronized and interspersed with variably timed EPSPs. Interestingly, after termination of the stimuli, EPSPs and spikes continued for ~ 100 ms. By contrast, direct current injection into the L-stellate cell never led to delayed spiking. In voltage clamp, a steady inward current slowly developed during the synaptic stimuli, while after termination of stimuli this inward current decayed slowly and was decorated by spontaneous fast EPSCs. A working hypothesis is that the asynchronous EPSCs arise from firing in the T-stellate cell, while the slow current is due to glutamate accumulation at the L-stellate cell dendrite. Both of these effects are expected to account for the development of heightened excitability of the neuron during stimulus trains. Neither of these synaptic effects were blocked by NMDA receptor antagonists. The delayed firing of the L-stellate cells could explain prolonged inhibition observed *in vivo* in VCN neurons, and may contribute to sideband inhibition observed in primary excitatory neurons, bushy cells and T-stellate cells during processing of auditory information. Therefore, future work will determine the mechanism of the increase in excitability and how that affects the dynamics of inhibitory networks in the VCN.

PS 35

Loose Coupling Between SK and P/Q-type Ca2+ Channels in Cartwheel Cells of the Dorsal Cochlear Nucleus.

Tomohiko Irie
National Institute of Health Sciences

Small-conductance Ca^{2+}-activated K^+ (SK) and large conductance, voltage- and Ca^{2+}-activated K^+ (BK) channels are Ca^{2+}-activated K^+ channels that control action potential firing diverse neurons in the brain. In cartwheel cells of the dorsal cochlear nucleus, blockade of either channel type leads to excessive production of spike bursts. In the same cells, P/Q-type Ca^{2+} channels in plasma membrane and ryanodine receptors in endoplasmic reticulum supply Ca^{2+} to BK channels through Ca^{2+} nanodomain signaling (Irie and Trussell, 2017). In order to examine the Ca^{2+} signaling pathways underlying activation of SK channels, voltage clamp experiments were performed in cartwheel cells in mouse brain slices in order to examine the Ca^{2+} signaling pathways underlying activation of SK channels. As with BK channels, SK channels required the activity of P/Q-type Ca^{2+} channels. However, this signaling occurred across Ca^{2+} micro- rather than nanodomain distances, and was independent of Ca^{2+} release from endoplasmic reticulum. These differential modes of activation may lead to distinct time courses of the two K^+ currents and therefore control excitability of auditory neurons across different time scales.

PS 36

Small Dendritic Inputs Increase Temporal Precision of Large Axosomatic Inputs in a Model of Spherical Bushy Cells

Elisabeth Koert; **Thomas Kuenzel**
Institute for Biology 2, Department of Chemosensation, RWTH Aachen University

Low frequency spherical bushy cells in the gerbil often receive only a single endbulb of Held input and still show increased temporal precision. It was suggested that small

excitatory dendritic terminals of the auditory nerve might be involved in this. It is however unknown how these small inputs interact with the giant axosomatic input.

We explored this question in both stylized and realistic 3D NEURON models of spherical bushy cells. We drove synaptic point-processes with spiking activity of independently simulated auditory fibers of identical characteristic frequencies.

Dendritic inputs caused both a tonic depolarization and a phase-locked modulation of the resting membrane potential. Surprisingly, the average effect was invariant of the number of dendritic synapses above about N=10 inputs. Both effects depended on dendritic cable properties, total conductance and the decay time-constant of dendritic synapses. In agreement with the biological situation, short and thick primary dendrites were most conducive for these effects. With increasing input frequency, tonic V_m depolarization became more pronounced and V_m modulation became smaller. Interestingly, dendritic low-threshold potassium conductance reduced the tonic depolarization without changing the modulation depth, while static leak conductance reduced both. Thus dendritic K_{LVA} conductance my play a major role in tuning dendritic integration in bushy cells.

When dendritic inputs interacted with axosomatic inputs, AP response rates increased mainly due to a smaller amount of failures at short intervals. Moreover, vector strength of phase-locking moderately increased and preferred response phase systematically shifted to the left. These effects on output spikes were frequency dependent and occurred more pronounced around and above the characteristic frequency of the simulated neuron. Endbulb events that occurred in the rising phase of the V_m modulation showed a greatly increased spike probability and had shorter EPSP-AP delay. The tonic V_m depolarization, in addition, also caused an overall reduction of endbulb threshold conductances.

In the realistic spherical bushy cell model constructed from 3D microscopy data, a higher amount of dendritic synapses and a higher total conductance was necessary to achieve similar effects. This was due to the cable properties of the more complex dendritic path.

Overall, synapses in the simulated bushy dendrite are electrotonically surprisingly close to the soma and can, when driven by phase-locked activity, indeed excert a positive effect on the temporal precision of the main auditory nerve input of spherical bushy cells.

PS 37

Muscarinic Modulation of M- and H-Currents in Gerbil Spherical Bushy Cells

Charlène Gillet; **Thomas Kuenzel**
Institute for Biology 2, Department of Chemosensation, RWTH Aachen University

Descending cholinergic fibers from multiple sources innervate the cochlear nucleus, but their role in hearing is not fully understood yet. Spherical bushy cells of the anteroventral cochlear nucleus are depolarized by cholinergic agonists on two different time scales. A fast and transient response is mediated by alpha-7 homomeric nicotinic receptors while a slow and long-lasting response is mediated by muscarinic receptors. Spherical bushy cells were shown before to express M3 receptors, but the receptor subtypes involved in the slow muscarinic response were not physiologically identified yet. Furthermore, it was not known through which conductances the muscarinic receptors influence the membrane potential.

Whole-cell patch clamp recordings combined with pharmacology and immunohistochemistry were performed to identify the muscarinic receptor subtypes and the effector currents involved. We could show that spherical bushy cells also expressed both M1 and M2 receptors. The M1 signal was stronger and mainly somatic while the M2 signal was localized in the neuropil and on the soma of bushy cells.

In voltage-clamp experiments an XE991-sensitive M-current was observed in gerbil spherical bushy cells, which was strongly inhibited by oxotremorine-M application. Surprisingly, long application of carbachol showed only a transient depolarization in current clamp recordings. On average, no clear muscarinic depolarization in long applications could be detected, although a surprising diversity of muscarinic responses was evident in our results. We however found that the membrane resistance slowly increased, which was consistent with the muscarinic effect on M-channels. We thus hypothesized that the impact on the resting membrane potential might be masked by an opposing secondary effect of muscarinic modulation.

Interestingly, ZD-7288-sensitive, hyperpolarization-activated currents were also strongly affected by oxotremorine-M application in voltage clamp experiments and this probably counteracted the effect of the inactivation of the M-current on the membrane potential in current clamp recordings.

We conclude that this double muscarinic action might allow adaptation of effects during long duration of cholinergic activation. Furthermore, the relative effectiveness of the muscarinic actions in a given cell could explain the diversity of muscarinic responses we observed. We propose that this diversity of modulatory effects may augment robust temporal coding over a wide range of natural stimulus properties and listening tasks by small, diverse populations of neighboring spherical bushy cells.

PS 38

Characterization of a Large Population of Cochlear Nucleus Small Cells

Adam Hockley; Calvin Wu; Susan E. Shore
University of Michigan

The small-cell cap of the cochlear nucleus (CN) is a major target of the low/medium spontaneous rate auditory nerve fibers, which are susceptible to synaptopathy. Small cells project to medial olivocochlear (MOC) neurons, which in turn have branched collaterals into the small-cell cap. The function of this circuit may be to counteract the suppressive effect of MOC input to the cochlea, to allow coding of true stimulus intensity in small cells.

Multichannel *in vivo* recordings of single CN units were obtained from anesthetized guinea pigs. Small cells were identified by their responses to pure tones and position along the electrode shank, with the small-cell cap located between dorsal CN and anteroventral CN. Small cell responses to tones, noise, tone-in-noise and amplitude modulated noise were characterized and compared to well-described CN cell types. Electrical stimulation of the contralateral ventral nucleus of the trapezoid body (VNTB) was used to activate MOC neurons, to assess the effect of MOC input to small cells.

Our data demonstrate that compared to all other CN cell types, small cells had wider dynamic ranges and improved tone-in-noise encoding. Small cells also displayed longer first spike latencies and lower spontaneous firing rates than ventral CN units. Phase-locked firing of small cells to amplitude modulated noise was equivalent to that of bushy cells. Electrical stimulation of the MOC pathway decreased firing of VCN stellate cells, likely due to reduction of cochlear amplification. Conversely, in bushy cells and small cells, firing rates increased, indicating a strong excitatory input from MOC neurons onto these cell types in the CN.

Hearing damage in the absence of audiometric threshold shifts – or hidden hearing loss (HHL) – especially affects the inputs to these small cells. Small cells show characteristics necessary for suprathreshold sound encoding, and therefore speech-in-noise understanding, which is a complaint often attributed to HHL. Stimulus intensity coding in small cells may be a key central change following HHL, with modulation of the MOC pathway a potential treatment for speech in noise issues.

PS 39

Variability in Synaptic Input Strength may Reduce the Cost for Synaptic Transmission of Bushy Cells in the Cochlear Nucleus

Go Ashida; Jutta Kretzberg
University of Oldenburg

Globular bushy cells (GBCs) in the anteroventral cochlear nucleus faithfully transfer acoustic information from auditory nerves (ANs) to the superior olivary complex, where binaural neurons process relevant cues for sound localization. Each GBC is innervated by about 20 AN fibers (Spirou et al., 2005), and this convergence is crucial for the improvement of phase-locking and entrainment between ANs and GBCs. In addition, GBCs are characterized by a number of physiological response properties, including low spontaneous rates, and relatively irregular firing pattern and “primary-like-with-notch” type peristimulus time histograms (PSTHs) in response to high-frequency tonal stimulation. In our recent study (presented in ARO Midwinter Meeting 2019), we simulated these physiological characteristics of GBCs using a simple model of monaural coincidence detection. By systematically varying the model parameters, we created a population of GBC models that was able to replicate known unit-to-unit response variability. In that study, we assumed that the strength of synaptic inputs was uniform in each cell. Previous anatomical studies, however, reported substantial variance in the size of synapses in GBCs (Rouiller et al, 1986; Liberman et al, 1991; Ostapoff and Morest, 1991; Gómez-Nieto and Rubio, 2009), suggesting non-uniform input strengths. Correspondingly, physiological recording results suggested that some inputs in GBCs might be considerably stronger than others (Rhode, 2008). In order to investigate possible effects of non-uniform inputs in GBCs, we expanded our previous model by incorporating the variation of synaptic strengths. We generated more than one million combinations of parameters, and tested the plausibility of each model with a set of response criteria for the spontaneous rate, phase-locking and entrainment (for low-frequency inputs), and irregular firing and PSTH shapes (for high-frequency inputs). Analyses of the resulting GBC model population indicated that the average and variance of input strength can compensate each other. Namely,

a decrease of the average input strength can be counteracted, at least partly, by an increase of the input variance, so that the output of the model still satisfies the adopted response criteria for GBCs. Because of this compensatory relation, the required average amplitude of non-uniform synaptic inputs may be reduced by up to about 20 percent, in comparison to modeled GBCs with uniform inputs. These results suggest that the anatomically observed variation in synapse sizes (and in resulting synaptic strengths) allows the GBC to reduce the cost for synaptic transmission without deteriorating its physiological functions.

PS 40

Age-dependent changes in the level of vesicular proteins and glutamate receptors in the auditory brainstem of Fmr1 knockout mice

Diego Zorio; Xiaoyu Wang; Thomas Ayzenshtat; Yuan Wang
Florida State University

The fragile X mental retardation protein (FMRP) is an RNA-binding protein that regulates the synthesis of a number of signaling and synaptic proteins. Loss of functional FMRP leads to intellectual disability, abnormal sensory processing, and difficulties in language and other aspects of social communication. In the brain, FMRP deficiency alters synaptic connectivity between auditory neurons in the brainstem and cortex. However, very few downstream effectors of FMRP, which are responsible for the development of these alterations, have been identified. In this study, we examined the developmental profile of FMRP in the auditory brainstem and characterized the time course of FMRP loss-induced protein level changes of several synaptic proteins using wildtype (WT) and *Fmr1*(gene encoding FMRP) knockout (KO) male FVB mice.

We first compared FMRP levels at postnatal day 0 (P0), P3, P5, P7, P14 (2 days after the onset of hearing), P21, and P56 (mature), using western blot. FMRP level is high within the first two postnatal weeks (P0 to P14) followed by a dramatic decline at P21 and maintained afterwards (P56). This temporal profile suggests differential influence of FMRP loss to its targets at different ages. To test this possibility, we characterized the developmental profile of three synaptic protein families in the brainstem of WT and KO mice. The first is synaptagmin 1 and 2 (Syt1 and Syt2), two primary calcium sensors on synaptic vesicles that trigger vesicle exocytosis and synchronized neurotransmitter release from presynaptic terminals. In WT mice, Syt2 starts low but detectable at P7 and then gradually upregulates at P14, P21, and P56. This upregulation is significantly delayed in KO mice so that Syt2 bands in western blot are barely detectable at P7 and P14, but at WT levels at P21 and P56. Immunocytochemistry further confirmed Syt2 reduction in the cochlear nucleus and the medial nucleus of the trapezoid body at P11 but not at P56. In contrast, Syt1 level is relatively stable in western blot across ages in WT but significantly increases in KO at P7 and P14 but not later at P21 and P56. We next examined the vesicular glutamate transporter 2 (vGluT2). vGluT2 level is increased at all four ages (P7, P14, P21, and P56) in KO as compared to WT mice. In contrast, the levels of Ras-related protein Rab3A and synapsin 1 (Syn1), two important regulators of vesicle function and validated FMRP targets in hippocampus and cortex, are comparable in the brainstem between WT and KO at all four ages. This observation demonstrates that observed changes in Syt1, Syt2, and vGluT2 are unlikely to be secondary consequences of underdeveloped synaptic vesicles. It also demonstrates that FMRP regulation of presynaptic proteins is highly selective and age-specific under mechanisms that vary across brain regions. Finally we examined the metabotropic glutamate receptor 5 (mGluR5), one of the most extensively studied FMRP effector. As expected, we detected a significant upregulation in KO mice. Surprisingly, this change is several-fold more dramatic at P7 and P14 than P21 and P56. Together, our results demonstrate that the proteome of the auditory brainstem before and around the onset of hearing is a major target of FMRP loss.

Grant Support: NIH/NIDCD R01DC13074; R21DC17267

PS 41

FMRP dependency for developmental synaptic plasticity of auditory neurons

Xiaoyan Yu; Xiaoyu Wang; Austin Burns; Diego Zorio; Yuan Wang
Florida State University

Neuronal development is a dynamic process that is influenced by afferent inputs during critical periods of development. For example, hearing loss at early ages can result in dramatic neuronal cell loss and altered synaptic connectivity in the auditory system. The underlying mechanism is not fully understood. Fragile X mental retardation protein (FMRP) is an RNA-binding protein that regulates local translation of a large number of signaling and synaptic proteins in an activity-dependent manner. While compromised developmental plasticity has been repeatedly reported in *Fmr1* (gene encoding FMRP) knockout animals, little is known about how FMRP is involved in afferent regulation of neuronal integrity and synaptic connectivity.

Here, we examined the effects of afferent deprivation on neuronal and synaptic properties of auditory brainstem nuclei using heterozygous Pou4f3$^{+/DTR}$ mice. These mice express human diphtheria toxin (DT) receptor (DTR) in hair cells, allowing hair cells to be selectively killed at any desired age by a systemic injection of DT. In addition, we examined the dependency of these afferent influences on FMRP expression by crossing Pou4f3$^{+/DTR}$ with *Fmr1* knockout mice to generate DTR mice with and without FMRP. Cellular analyses are carried out in the ventral cochlear nucleus (VCN) and the medial nucleus of the trapezoid body (MNTB). As expected, DT-induced afferent deprivation leads to neuronal cell loss and a reduction in somatic area of the remaining neurons in VCN. MNTB exhibits a similar reduction in neuronal somatic size without obvious cell loss. Interestingly, these changes are not FMRP-dependent; they are comparably identified in DTR mice without FMRP. We further examined synaptic distribution using the vesicular GABA transporter (VGAT) as an inhibitory synaptic marker. In DTR mice with normal FMRP expression, afferent deprivation results in a significant increase in the number of VGAT puncta around the cell body of MNTB neurons, implicating enhanced inhibition to MNTB. This change is diminished in DTR mice lacking FMRP, demonstrating the requirement of FMRP for this regulation.

Together, these findings indicate that FMRP is required for afferent regulation of synaptic development, but not of neuronal survival or cell size maintenance.

PS 42

Influence of Microglia on Spiral Ganglion and Cochlear Nucleus Neuron Survival Following Hair Cell Death in Mature Mice

Van A. Redila[1]; Ling Tong[1]; Robin M. Gibson[1]; Tejbeer Kaur[2]; Mark Warchol[3]; Edwin W. Rubel[1]
[1]University of Washington; [2]Creighton University; [3]Washington University School of Medicine

Background
During embryonic and neonatal development, the survival of neurons in the ventral cochlear nucleus (VCN) is dependent on synaptic input from cochlear afferents. In contrast, VCN neurons in mature animals do not require afferent activity for survival. The mechanisms that underly this 'critical period' in VCN development are not known. Transcriptional analyses suggest that increases in expression of genes associated with innate immunity may protect mature VCN neurons after the loss of afferent input. This finding implicates a role for microglia, which mediate innate immunity in the CNS. We are examining whether selective ablation of microglia in mature mice will influence survival of VCN neurons and spiral ganglion neurons after loss of afferent input.

Methods
Studies used C57Bl/6 mice that express GFP under regulation of CX3CR1 (e.g., in microglia) and express the human diphtheria toxin (DT) receptor under regulation of Pou4f3 (e.g., in hair cells). Treating these mice with DT results in rapid and complete hair cell death, coupled with complete hearing loss and loss of eighth nerve activity within 5 days. Mice in the experimental groups were fed chow that contained PLX5622, a dietary inhibitor of the colony stimulating factor-1 receptor (CSF-1R), that leads to selective depletion of microglia. Control animals were fed matching lab chow without PLX5622. After pretreatment for 10 days with either PLX5622-containing or control chow, mice received a single injection of DT. Mice were then allowed to recover for either 14 or 56 days after DT injection, and continued to receive either PLX5622 or control chow during these periods. After fixation, cochleae were sectioned and processed for immunohistochemistry, and the numbers of spiral ganglion neurons (SGNs) and associated macrophages were quantified in the same sections. Serial sections through the brainstem were processed for visualization of GFP-labeled microglia and neuronal cell bodies. Unbiased estimates of the numbers each cell type in the VCN were acquired using the MBF Stereo Investigator Optical Fractionator protocol.

Results
Mice that received PLX5622 had >60% reduction in the numbers of cochlear macrophages and VCN microglia, compared to controls. However, we observed no significant difference in the numbers of surviving SGNs or VCN neurons between these two groups, and these values were not significantly different from normal hearing mice of the same age. The data suggest that normal populations of macrophages and microglia are not required for short term survival of mature SGNs or VCN neurons after cochlear lesion.

PS 43

Stimulation of Auditory Nerve Fibers with Trains of Shocks Engages Excitatory Interconnections Between T Stellate Cells of the Ventral Cochlear Nucleus

Xiao-Jie Cao[1]; Donata Oertel[2]
[1]School of Medicine and Public Health, University of Wisconsin; [2]University of Wisconsin School of Medicine and Public Health

T Stellate cells of the ventral cochlear nucleus form an important ascending pathway from the ventral cochlear

nucleus to the ipsilateral dorsal cochlear nucleus and lateral superior olive, and to the contralateral ventral nucleus of the trapezoid body, ventral nucleus of the lateral lemniscus, inferior colliculus, and thalamus. With dual whole-cell recordings we demonstrated that T stellate cells are interconnected through excitatory synapses within an isofrequency lamina. Those interconnections become evident after they are potentiated by nitric oxide signaling when presynaptic firing is paired with postsynaptic depolarization (Cao et al., 2019). Because shocks to a small bundle of auditory nerve fibers depolarize T stellate cells within an isofrequency lamina simultaneously, we predicted that trains of shocks would potentiate interconnections. We recorded responses to shocks delivered to an adjacent fiber fascicle through a glass pipette located 0.4 – 0.6 mm from the recording pipette. T Stellate cells, identified by their responses to injected current, adjacent to the stimulated fiber fascicle responded consistently to each shock after synaptic delays of ~0.6 msec (Ferragamo et al., 1998; Cao and Oertel, 2010; Chanda and Xu-Friedman, 2010). As observed previously, trains of shocks also evoked late EPSPs after the end of the train (Ferragamo et al., 1998). The late EPSPs, but not the monosynaptic responses to shocks, were blocked by an antagonist of nitric oxide synthase, 100 µM NG-nitro-L-argenine methyl ester (L-NAME), suggesting that late EPSPs reflect the activation of interconnections between T stellate cells. These findings enable us to measure the time course with which activity of auditory nerve fibers engage the interconnections and with which those interconnections fade. Late EPSPs were evoked by trains of shocks >100 Hz for >100 msec. The frequency of late EPSPs increased with increasing rate or duration of stimulation. Their frequency faded with an exponential time course that had a time constant of ~20 sec. In octopus and bushy cells, late EPSPs were absent; these cells responded to trains of shocks with only monosynaptic EPSPs. This work is supported by a grant from NIH R01DC016861.

PS 44

Organizational Features of the Auditory Periphery shapes the Development of Tonotopically Distributed Membrane Properties in Cochlear Nucleus Neurons

Lashaka Jones[1]; Weise Chang[2]; Zoe Mann[2]; Matthew W. Kelley[3]; **Michael Burger**[1]
[1]Lehigh University; [2]NIDCD; [3]National Institute on Deafness and Other Communication Disorders, NIH

Tonotopic organization is the fundamental organizing principle of the auditory system. In birds, tonotopy arises along the basilar papilla (BP) and is defined by hair cell morphological and physiological gradients from base to apex. Tonotopic organization is preserved in central auditory neurons via precise 8th nerve innervation of the cochlear nucleus, Nucleus magnocellularis (NM). NM neurons preserve or improve the temporal precision of phase-locked discharges to sounds, a key physiological feature for sound localization. These neurons phase-lock at frequencies exceeding 2 kHz due to tonotopically distributed intrinsic membrane properties, including patterned expression of voltage-gated ion channels. Additionally, auditory nerve synapse number and size vary along this axis. One unresolved question is: How do central tonotopic properties arise during development? One hypothesis is that tonotopically distributed properties first develop in the ear which then, instructs the development of central intrinsic properties. An alternative hypothesis is that tonotopic features develop independently of afferent input instead, relying on central cues to establish tonotopic physiological patterns. We investigated this question using a novel chick model, that features an inner ear that is limited to low-frequency phenotype hair cells. Previous work by the Kelley lab showed that a gradient of Bone Morphogenic Protein 7 (BMP7) in the developing cochlear duct is a primary driver of tonotopic patterning along the BP. We monaurally overexpressed *BMP7* in the developing chick otocyst *in ovo* resulting in animals endowed with one 'normal' ear and one 'low frequency' ear. After assaying tonotopically distributed properties within NM, we found that physiological features within the high-frequency region exhibit low frequency-associated phenotypes on the treated side. For example, NM membrane excitability was increased in the 'HCF region' ipsilateral to the *BMP7* treated ear. Mechanistically, it is known that low voltage-activated potassium channels significantly influence membrane excitability in the high-frequency region (HCF) of NM. Thus, we hypothesized that our findings may be due to a reduction in Kv1.1 channel expression, and or overall Kv1 outward current magnitude. Preliminary results suggest that outward current responses to depolarizing voltage steps are significantly smaller for HCF cells within the ipsilateral NM when compared to cells in the contralateral NM. In summary, we show in a novel animal model that peripheral tonotopic patterning is required for the development and preservation of tonotopic features of central neurons in ascending pathways. This suggests that the inner ear provides an instructive signal for tonotopic refinement during development.

PS 45

Noise Exposure in Adult Mouse Induces Burst Firing and Changes in Auditory Nerve Synapses in Dorsal Cochlear Nucleus (DCN) Pyramidal Neurons.

Michael Kasten; Tessa-Jonne Ropp; Paul Manis
University of North Carolina at Chapel Hill

Pyramidal cells of the dorsal cochlear nucleus (DCN) receive auditory nerve input and fire in response to low-intensity sound. Following noise exposure, pyramidal cells *in vivo* display weakened response to sound, as expected with cochlear damage. Concurrently, pyramidal cells display increased spontaneous activity of unknown etiology. To examine effects of noise on both intrinsic firing and auditory nerve synapses to DCN pyramidal neurons, we utilized the NF107 (Colgalt2-cre) mouse line, in which male mice express Cre in spiral ganglion neurons, crossed to the ai32 mouse. Mice heterozygous for both genes express an enhanced ChR2-EYFP fusion protein in auditory nerve fibers. Focal laser scanning photo-stimulation and *in vitro* patch-clamp recording was used to determine the properties of auditory nerve input to DCN pyramidal neurons. Noise exposure consisted of a 2 hr exposure to 109 or 115 dB, 8-16 kHz bandpass noise followed by recovery of either 3 days or 2 weeks. Noise exposures were timed such that animals were harvested and transtrial slices of DCN prepared at p42-53. We observed spontaneous firing in DCN pyramidal neurons 3d after exposure consisting of brief periods of high rates of firing (up to 200 Hz for 100-500 ms). This firing was rarely seen in control animals or 2w following noise exposure. Auditory nerve EPSCs to focal laser stimulation demonstrated slower decay in DCN pyramidal neurons 3d after noise exposure. Together, these findings are consistent with homeostatic mechanisms to enhance gain following weakened auditory input after noise exposure. Supported by NIH grant DC004551.

Auditory Nerve: Anatomy & Physiology

PS 46

Pou3f4 In The Otic Mesenchyme Is Essential For Development Of Normal Spiral Ganglion Neuron Innervation Patterns In The Mammalian Cochlea

Mansa Gurjar[1]; Johnny Jung[2]; Vinodh Balendran[2]; Elizabeth Staab[2]; Thomas Coate[2]
[1]Georgetown University, Department of Biology; [2]Georgetown University

Mutations in the Pitt-Oct-Unc (POU)-domain transcription factor *Pou3f4,* located on the X-chromosome are associated with X-linked nonsyndromic hearing loss in the DFNX2 locus. Pou3f4, which is specifically expressed by otic mesenchyme cells, regulates the expression of various Ephs and Ephrin proteins that act as axon guidance cues for spiral ganglion neurons (SGNs). During development, SGNs interact with otic mesenchyme cells prior to forming synapses with hair cells. I will discuss our preliminary findings on how Pou3f4 normally inhibits *Efna1* (Ephrin-A1) and *Efna2* (Ephrin-A2) ligand expression. RNAScope assays show *Efna1* and *Efna2* mRNAs are normally expressed at low levels by otic mesenchyme cells, and that their expression increases about two-fold in *Pou3f4* knockout cochleae. These studies were carried out using mice at E15, which is the time when SGNs begin to fasciculate as they innervate hair cells. Preliminary chromatin immunoprecipitation assays have identified binding sites for Pou3f4 in *Efna1* and *Efna2* genes. Initial analyses of *Efna1* and *Efna2* double knockout cochleae show subtle differences in SGN innervation patterns compared to WT littermate controls. Both Ephrin-A1 and Ephrin-A2 attract growing SGN processes in *in vitro* assays. Hence, we hypothesize that Ephrin-A1 and Ephrin-A2 proteins on otic mesenchyme cells serve as attractive cues for SGN axons and are normally repressed by Pou3f4 to promote axon fasciculation. Additionally, I will discuss our ideas for future work to determine the Eph receptor binding partners for Ephrins-A1 and -A2 on SGNs and genetic experiments to determine whether *Efna1* and *Efna2* knockout alleles can rescue the SGN fasciculation defects observed in *Pou3f4* knockout cochlea. Determining the molecular basis for proper cochlear innervation patterns through these studies and others will help in developing therapeutics for people with sensorineural hearing loss.

PS 47

Phase Locking of Auditory-Nerve Fibers: Investigating the Origin of the Level-Dependent Exponential Transfer Function

Adam J. Peterson; **Peter Heil**
Leibniz Institute for Neurobiology Magdeburg

Phase locking of auditory-nerve-fiber (ANF) responses to the temporal fine structure of acoustic stimuli, a hallmark of the auditory system's temporal precision, is important for many aspects of hearing. Previous work has shown that phase-locked period histograms can be described by exponential transfer functions relating instantaneous spike rate to instantaneous stimulus pressure. The operating points and slopes of these functions change with stimulus level such that clipping of the histograms is avoided. The mechanism underlying this apparent gain control is unclear but it is distinct from mechanical compression, is independent of refractoriness and spike-rate adaptation, and is apparently instantaneous. Here we show, using responses of cat ANFs to tones, that the level dependence of the exponential transfer function can be accounted for by a model consisting of a static saturating Boltzmann transducer function resulting in a clipped output, followed by a lowpass filter and a static exponential transfer function. For a given ANF and stimulus frequency, one set of five model parameters can describe the period histograms obtained for all stimulus levels, without any level dependent components. The

lowpass filter accounts for the level dependence of the operating point and slope of the previous exponential transfer function, and for the level dependence of the maximum and minimum instantaneous spike rates. Notably, the estimated cutoff frequency is lower for low- than for high-spontaneous-rate ANFs, implying a synapse-specific contribution to lowpass filtering. These findings advance our understanding of ANF phase locking by highlighting the role of peripheral filtering mechanisms in shaping responses of individual ANFs.

Supported by the Deutsche Forschungsgemeinschaft (Priority Program 1608 “Ultrafast and temporally precise information processing: Normal and dysfunctional hearing”, He1721/11-2 to PH).

PS 48

Physiology and Anatomy of Glutamate Receptors at the Inner Hair Cell to Auditory Nerve Fiber Synapse Suggest GluA2-lacking, Ca2+-permeable AMPA Receptors Contribute to Transmission in the Mammalian Cochlea

Juan Goutman[1]; Shelby Payne[2]; Babak V-Ghaffari[2]; Shashank Chepurwar[3]; Adish Dani[3]; Mark Rutherford[4]
[1]INGEBI - CONICET; [2]Department of Otolaryngology - Head & Neck Surgery, Washington University School of Medicine; [3]Tata Institute for Fundamental Research (TIFR); [4]Department of Otolaryngology-Head & Neck Surgery, Washington University

Each cochlear inner hair cell provides the sole excitatory input to 10 or more auditory nerve fibers, via glutamatergic transmission dependent on post-synaptic AMPA receptors. AMPA receptors are glutamate-gated ion channels, and each post-synaptic density (PSD) contains thousands of receptors. AMPA receptors are hetero-tetrameric complexes, comprised of GluA2, GluA3, and GluA4 subunits. The absence of GluA2 from the tetrameric receptor-channel imparts several unique features which may be physiologically significant to sound encoding and excitotoxicity including inward current rectification, block by intracellular polyamines, and high permeability to Ca^{2+}. All afferent synapses between cochlear inner hair cells and auditory nerve fibers appear to include GluA2. However, individual PSDs contains thousands of AMPARs, which may differ from each other in subunit stoichiometry.

Here we show new anatomical analysis and, for the first time, physiological evidence for the presence of GluA2-lacking, Ca^{2+}-permeable AMPA receptors at cochlear afferent synapses. We measured subunit localization within synapses and relative abundance among synapses by deconvolution confocal microscopy and by Stochastic Optical Reconstruction Microscopy (STORM) of subunit immunohistofluorescence. Among synapses, we observed a broad range of relative abundances of subunits. Within synapses, we observed nano-domains that appeared to lack GluA2 alongside regions of robust GluA2 immunofluorescence, suggesting the presence of Ca^{2+}-permeable and Ca^{2+}-impermeable AMPA receptors in the same PSD. Radial distributions of subunit fluorescence suggest that GluA2 tends to be more centrally located in the PSD, relative to the center of the presynaptic ribbon, than GluA3 or GluA4 subunits which tended to be more peripheral.

With patch-clamp electrophysiology recordings on the post-synaptic terminals of auditory nerve fibers we used IEM-1460 to antagonize GluA2-lacking AMPA receptors, and found 50% block with a concentration of ~10 μM, consistent with the presence of GluA2-lacking AMPA receptors at cochlear inner hair cell afferent synapses. The addition of 100 μM spermine in the pipette produced a strong inward rectification of excitatory postsynaptic currents, consistent with the presence of GluA2-lacking AMPA receptors. Together, these results point to the presence of functional GluA2-lacking Ca^{2+}-permeable AMPA receptors at cochlear inner hair cell afferent synapses, although the permeability to Ca^{2+} has not yet been demonstrated in cochlear nerve terminals. Understanding the significance of AMPA receptor heterogeneity may be key to elucidating the differences between auditory nerve fibers that innervate the same inner hair cell, in terms of their physiology and sensitivity to noise-induced damage.

PS 49

Spatial Origins of Click-Evoked Cochlear Compound Action Potentials

Shannon Lefler[1]; Shawn Goodman[2]; Choongheon Lee[3]; John Guinan[4]; Jeffery Lichtenhan[1]
[1]Washington University School of Medicine in St Louis; [2]University of Iowa; [3]University of Rochester Medical Center; [4]Harvard Medical School

The spatial origin along the cochlear length of the click-evoked auditory-brainstem wave 1, or cochlear compound action potential (CAP), is not fully understood. It is often thought that the spatial origin of the click response is diffuse along the cochlea because of the wideband spectrum of click stimuli. On the other hand, interpretations based on single auditory-nerve-fiber responses suggest that the origin is primarily from the cochlear base where neural excitation is early and neural innervation density is greatest, while apical neural excitation is later and un-synchronized with that in the base. While much clinical and basic-science progress continues to be made

using click-evoked responses from the inner ear and central nervous system, few experiments have directly addressed questions on how click excitation along the cochlear length influences results.

We studied the spatial origin of click responses using our recently-developed perfusion technique that blocks neural excitation sequentially from low-frequency to high-frequency cochlear regions. Kainic acid, or KCl, in artificial perilymph solution was perfused into the cochlear apex of anesthetized guinea pigs and driven through the length of scala tympani toward the cochlear aqueduct in the cochlear base. Perfusion rates were varied to compensate for the changing cross-sectional area of scala tympani in order to achieve a 0.5 mm / min flow rate. In a recent publication using this technique, we found that as kainic-acid solution flowed from apex to base, CAP amplitudes to low-level tone bursts were sequentially reduced from 2 kHz to 16 kHz at a perfusion time that was consistent with their origins being centered on the characteristic frequency (CF) of each tone burst. Here we used 10 µsec electrical pulses presented to an ER-10X Probe System to yield clicks from 59 to 95 dB peSPL in 12 dB steps. The perfusion times at which the click-evoked CAP amplitudes were reduced, compared to the times that low-level tone burst responses were reduced, revealed the cochlear spatial origin of the auditory-nerve fibers that produced the CAP peak.

We found that the origin of CAPs in response to low-level clicks was primarily from the most sensitive cochlear CF place of the guinea pig. We consider how the origin of the click-evoked CAP spread in apical and basal directions as click level was increased. While a level effect was evident, it is clear that the spatial origin of the click-evoked CAP is primarily in the basal half of the cochlea.

PS 50

A Modeling Analysis of a Forward Masking Paradigm Proposed to Estimate Cochlear Compression

Gerard Encina-Llamas[1]; Jens C. Thuren Lindahl[2]; Bastian Epp[1]
[1]Hearing Systems section. Department of Health Technology. Technical University of Denmark;
[2]Department of Electrical Engineering. Technical University of Denmark

Background
The healthy human auditory system is sensitive to a large dynamic range of incoming sounds. An “active mechanism” due to outer hair cells (OHC) electromotility leads to a level-dependent amplification of basilar membrane (BM) vibration and a compressive BM input/output (I/O) function at on-frequency sites (i.e., near the characteristic frequency (CF) of the tonal stimulus). At off-frequency sites, BM grow linearly. Psychoacoustical methods using forward making have been proposed to estimate such compressive function. They assume that cochlear processing can be isolated from the perceptual response involving the overall system. In the present study, computer models of the peripheral auditory system, both for normal hearing (NH) and hearing impairment (HI), were used in combination with methods from signal detection theory (SDT) to test some of the key assumptions hold in psychoacoustical temporal masking curves (TMC).

Methods
The humanized version of the AN model by Bruce et al. (2018) was used to simulate the psychophysical TMC experiments. Masker levels from 10 to 110 dB SPL and gap lengths between 2 to 100 ms were used. Two probe frequencies (on-frequency) were considered at 1 and 4 kHz with maskers at on- and off-frequencies (0.6*on-frequency). The probe was 20 ms long and its level was kept at 10 dB SL. The simulated neuronal responses were quantified in terms of rate and synchrony. An optimal combination of d’ was considered. HI was simulated by fitting individual audiograms to the inner hair cell (IHC)-AN model. The extreme cases of only IHC or OHC dysfunction were analysed.

Results
Results showed that some degree of forward masking could be obtained when comparing the probe activity versus spontaneous activity. Simulations showed that the amount of inhibition due to the presence of the masker is limited by a flooring effect due to spontaneous rate (SR) and by a ceiling effect due to saturated rate of high-SR fibres. In addition, in the case of substantial OHC dysfunction, the range of CFs carrying probe information went beyond the on-frequency range with compressive BM growth.

Conclusions
Simulations suggested that, in the case of NH, the amount of forward masking at the level of the AN is not enough to account for the psychoacoustical TMC curves, and therefore to estimate BM compression. In the case of HI due to OHC dysfunction, probe information was also present at off-frequency CFs.

Funding
This work was supported by the Hearing Systems section at the Technical University of Denmark (DTU).

PS 51

Contribution of Auditory Nerve Nodal Structural Refinement to Postnatal Maturation of Mouse Auditory Function

Clarisse H. Panganiban[1]; Kenyaria V. Noble[2]; Carolyn M. McClaskey[3]; Kelly C. Harris[3]; Hainan Lang[3]
[1]Wolfson Centre for Age-Related Diseases, King's College London; [2]Department of Pathology and Laboratory Medicine, Medical University of South Carolina, Charleston, South Carolina 29425, United States; [3]Medical University of South Carolina

Proper passage of electrical impulses and regulation of conduction velocity through the auditory nerve (AN) fibers are necessary for normal auditory function. Myelinating glia cells ensheath type I spiral ganglion neurons (SGNs) with multiple layers of myelin. This sheathing provides electrical insulation, which helps sustain the strength of traveling action potentials along the fiber. Nodes of Ranvier, formed in part by unmyelinated gaps and the terminal ends of myelin sheaths, are necessary for the regeneration of action potentials throughout the length of the type I SGN. Our lab has previously shown that glial dysfunction resulting from dysregulation of *quaking,* a regulator of myelination, contributes to noise-induced hearing loss. We further determined that knocking out *quaking* in adult mice causes demyelination and abnormalities in nodal structures, which are associated with elevated auditory brainstem response (ABR) thresholds and delayed wave I latencies. Studies about the role of the nodal structures during the emergence of hearing function have been sparse. Here we aim to elucidate the role of nodal structural refinement in hearing onset and AN functional maturation of the developing mouse ear.

We used postnatal (P) CBA/CaJ mice ages P3-P21 and 1 month in our experiments. In our study, we identified and characterized for the first time three types of excitable nodal structures in the mouse AN, showing how these nodal structures form and refine during postnatal cochlear development around the critical period of hearing onset and hearing maturation. The two types of myelinating glial cells in the mouse AN, Schwann cells and satellite glial cells, form structurally different excitable nodal structures, which may result in differing electrical properties between the node types. To determine how nodal structural maturation contributes to the maturation of AN function, we examined the extent to which the changes in nodal lengths were associated with measurements of AN function in postnatal mice (from P14 to P21). AN function maturation was determined by quantifying neural synchrony *in vivo* with comprehensive analysis of ABR metrics such as wave I amplitude, latency, and pure-tone thresholds. Our results demonstrate that refinement of nodal structures, especially that of the nodes formed in part by the satellite glial cells, are significantly associated with maturation of the AN function. This work was supported by grants from the NIH/NIDCD.

PS 52

Optical Coding Using Photopharmacological Stimulation of Ionotropic Glutamate Receptors in Spiral Ganglion Neurons

Antoine Huet[1]; Aida Garrido[2]; Carlo Matera[2]; Pau Gorostiza[2]
[1]Institute for Auditory Neuroscience; [2]Institute for Bioengineering of Catalonia

Light stimulation of spiral ganglion neurons (SGNs) in the ear provides a future alternative to electrical stimulation used in cochlear implants. Optogenetic manipulation of neuronal activity is based on the expression of light-sensitive proteins, which requires gene therapy. An alternative to optogenetics is offered by photopharmacology which operates on endogenous receptors and does not require genetic manipulation. Among the "photoswitches", the Targeted Covalent Photoswitches (TCP) mainly reacts with the ionotropic kainate receptor GluK1. It was previously shown *in vitro* on hippocampal neurons that TCP9, the best first-generation compound, activates native GluK1 receptor upon ultraviolet light (380 nm) and a deactivates the receptor upon visible light (500 nm, Volgraf et al., 2006). In this study, we tested a new generation of blue-shifted TCP *in vivo* by applying the compound to the gerbil cochlea via the round window. Electrocochleography via a round window niche electrode showed us a preservation of the acoustically-evoked cochlear microphonic and compound action potential (CAP) amplitude, indicating that the compound and its binding to glutamate receptors does not alter cochlear function. Upon light stimulation using an optical fiber (β = 473 nm), we observed optically evoked CAPs (oCAPs). oCAPs could be evoked by light pulse radian flux as low than 3 mW, oCAP amplitudes were maximum in response to 80 µs light pulse and were sizable up to a repetition rate of 4 kHz. This performance makes this compound an interesting tool for optical SGN stimulation. Future experiments will investigate the single unit response of light evoked auditory nerve fiber and hearing restoration on a deafness model.

PS 53

Neural crest and placode contributions to congenital deafness in Waadenburg-Shah syndrome

Takako Makita
Medical University of South Carolina

Waardenburg-Shah syndrome is a congenital deafness that is associated with Hirschsprung disease. In human,

Waardenburg-Shah syndrome is an inherited condition associated with mutations in genes encoding endothelin ligand EDN3 and its G-protein coupled receptor EDNRB, and is characterized by a failure of neural crest cell migration to a variety of sites including the inner ear where they give rise to pigment cells in the stria vascularis. Their absence has been thought to result in a failure in generation of the endocochlear potential and thereby in deafness. Mouse mutations in *Edn3* and *Ednrb* genes show virtually identical phenotypes (hearing and pigmentation defects, and aganglionic colon), indicating Edn3-Ednrb signaling is essential for neural crest cell migration. Neural crest is therefore believed to contribute primarily towards deafness in Waardenburg-Shah syndrome infants.

Mechanosensory neurons of the spiral ganglia that connect mechanosensory hair cells to the auditory cortex originate from placode, however, a relevance of placode lineage to Waardenburg-Shah syndrome has never been implicated. Our mouse mutant analysis using auditory brain response (ABR) recording demonstrated that placode-specific ablation of *Ednrb* gene results in deafness while distortion product otoacoustic emissions (DPOAE) indicated that hair cell function was fully intact. We found that *Pax2Cre/Ednrb* mutant spiral ganglion neurons exhibit normal synapse formation but a significant reduction in vesicular synaptophysin staining, suggesting impaired synaptic vesicular trafficking accounts for deafness in *Pax2Cre/Ednrb* mutant mice. Neural crest-specific *Ednrb* mutant mice are also deaf as expected, although with normal presence of intermediate stria (pigment) cells. In *Wnt1Cre/Ednrb* mutant inner ear, we observed inappropriate synapse formation at the outer hair cells whereas inner hair cells synapse formation occurs normally. Our cell lineage analysis demonstrated that neural crest cells give rise to glial (satellite and Schwann) cell population of the spiral ganglia, and implies important roles of glial cells in auditory sensory axon pruning. Our study demonstrates embryonic lineage specific roles of endothelin signaling in establishment of functional hearing, and provides a new insight into the pathogenesis of sensorineural deafness in Waardenburg-Shah syndrome.

PS 54

Efferent feedback improves representation of speech envelope in auditory nerve in a stimulus-specific manner

Jason Mikiel-Hunter[1]; Heivet Hernandez-Perez[1]; David McAlpine[2]; Jessica J. M. Monaghan[1]
[1]Macquarie University; [2]Department of Linguistics, The Australian Hearing Hub, Macquarie University, Sydney, Australia

Encoding the amplitude-modulated envelope of speech is key to its comprehension (Ghitza, 2012). Evidence of enhanced envelope entrainment exists along the entire auditory pathway, from the inner ear (Nuttal *et al*., 2018) to the cortex (Riecke *et al*., 2018). One putative mechanism for increasing envelope sensitivity in the periphery is a reduction in cochlear gain by auditory efferent activity (particularly the medial olivocochlear (MOC) reflex). Although recent studies have explored this possibility, adopting precursor noise and amplitude-modulation detection paradigms (Almishaal *et al*., 2017, Marrufo-Perez *et al*., 2018; Wojtczak *et al*., 2019), there remains general disagreement about the role efferent feedback plays in determining detection thresholds let alone speech perception.

We employed model simulations to determine whether auditory efferent activity improves the entrainment of auditory nerve fibres (ANFs) to the envelope of differentially degraded speech signals (noise-vocoded speech, speech in speech-shaped noise and speech in 8-talker babble noise). By comparing these results to otoacoustic data collected under “active” and “passive” listening conditions (Hernandez-Perez *et al*., 2018), we correlate the potential benefits/disadvantages to envelope entrainment of activating MOC reflex with actual stimulus-specific reduction of cochlear gain observed experimentally.

300 word tokens were presented at 75 dB to a variant of the Meddis cochlear model incorporating biophysically-realistic efferent feedback (Meddis *et al*., 2013). Envelope coding was analysed by comparing neural spike trains of ANFs in response to degraded and natural versions of the words (Louage *et al*., 2004; Joris *et al*., 2006; Heinz and Swaminathan, 2009; Rallapalli and Heinz, 2016). The data indicate an inability of the MOC reflex to increase the signal-to-noise ratio of speech in either speech-shaped or babble noise, and demonstrate that amplitude fluctuations in noise-vocoded words were more effectively reconstructed when efferent feedback is implemented. This mirrors significant decreases in cochlear gain observed in the experimental data during “active” tasks for vocoded speech, but not for speech-shaped noise or babble maskers, highlighting the possibility that top-down modulation of efferent reflexes in the brainstem depends ultimately on the actual benefit afforded by reducing cochlear gain to the stimulus in question.

PS 55

Assessing the Effects of Kainic Acid-Induced Auditory-Nerve Damage on Envelope-Following Responses in the Budgerigar

John Wilson; Kristina Abrams; Kenneth S. Henry
University of Rochester

Sensorineural hearing loss is a prevalent medical problem that compromises interpersonal communication and can adversely affect quality of life. While the pure tone audiogram has been the traditional diagnostic tool, this method appears inadequate to detect lost synaptic connections between inner hair cells and the auditory nerve (AN), known as cochlear synaptopathy. Cochlear synaptopathy is a common pathology associated with aging and overexposure to loud sound. Synaptopathy may precede overt hearing loss detectable by audiometry and is theorized to manifest as suprathreshold difficulties hearing complex sounds in noisy backgrounds (hidden hearing loss). Previous studies used wave I of the auditory brainstem response (ABR) in attempts to quantify AN loss, but this measure is problematic in humans due to low signal to noise ratio of the response (amplitude typically < 0.5 μV). The envelope-following response (EFR) is another far-field evoked potential that can be recorded noninvasively in response to input signals with periodic envelope fluctuations. EFRs have greater amplitude than ABR wave I in humans and thus offer promise as a more sensitive way to detect cochlear synaptopathy. On the other hand, EFRs are a less direct measure of AN activity because they arise primarily from central neural generators, and may be influenced by synaptopathy-induced changes in 'central gain'. We explored the effects of moderate-to-severe AN damage on EFRs and click-evoked ABRs in budgerigars, a parakeet species with midbrain processing and modulation tuning mechanisms similar to humans. Unlike in humans, ABR wave I in budgerigars exceeds 15-20 μV and thus can provide a robust measure of AN loss following experimental manipulations. AN damage was induced using bilateral intracochlear infusions of kainic acid, a glutamate analog, which reduced ABR wave I by 40-70% while preserving hair-cell generated otoacoustic emissions. EFRs were recorded in response to sinusoidally amplitude modulated (SAM) tones and narrowband harmonic tone complexes with different fundamental frequencies and nonoverlapping frequency bands to yield responses from different tonotopic regions. Responses to modulation frequencies less than a few hundred Hz were associated with central generators based on a group delay analysis, while higher modulation frequencies evoked more peripheral (i.e., AN generated) EFR activity. EFRs and click-evoked ABRs were compared before and after kainic acid exposure to determine whether the EFR can accurately characterize AN damage following glutamate excitotoxicity. These results will help guide development of noninvasive metrics for evaluating suprathreshold hearing loss in the clinical setting.

PS 56

Noise-Induced Cochlear Synaptopathy in Guinea Pig

Monica Benson[1]; Nathaniel T. Greene[2]; John Peacock[3]; Daniel J. Tollin[4]
[1]University of Colorado Anschutz Medical Campus; [2]Department of Otolaryngology, University of Colorado School of Medicine; [3]University of Colorado; [4]Department of Physiology & Biophysics, and Department of Otolaryngology, University of Colorado School of Medicine

Hearing loss is typically characterized by permanently raised auditory thresholds due to cochlear dysfunction. However, recent animal studies have shown that brief and moderate noise exposure can cause a temporary threshold shift that recovers within a couple weeks, but a permanent loss of ribbon synapses between inner hair cells and auditory nerve fibers. Such noise-induced cochlear synaptopathy has therefore been suggested to underlie hidden hearing loss because while there is a degeneration of ribbon synapses (up to 50%), the resulting hearing dysfunction is hidden from typical clinical assays such as the audiogram.

In order to better study the hearing difficulties that result from noise induced cochlear synaptopathy we have developed a guinea pig model. Guinea pigs were chosen because their hearing range is comparable to humans and they exhibit an acoustic startle reflex, so we can measure the pre-pulse inhibition (PPI) of the acoustic startle reflex. The PPI of the acoustic startle response can be used to measure an audiogram, much like in humans.

Noise-induced cochlear synaptopathy can be reliably induced in the guinea pig and correlated with hearing abilities by measuring auditory brainstem response (ABRs), distortion product otoacoustic emissions (DPOAEs), behavioral audiometric thresholds, and immunohistochemistry. ABR and DPOAE recordings were made prior to noise exposure, 48 hours post-exposure, and 1 and 2 weeks following exposure. Behavioral audiograms were also measured through an acoustic startle response (pre-noise and 3 weeks post-noise) and a physiological audiogram through ABRs to better probe any audiometric shift caused by noise exposure. For all procedures, except behavioral audiograms, guinea pigs were anesthetized with an intraperitoneal injection

of ketamine (80mg/kg) and xylazine (8mg/kg). All experiments were performed in a double-walled sound attenuating chamber (IAC Inc., Bronx, NY).

Results show that the noise exposure (a 4-8 kHz octave band noise at 106 dB SPL for 2 hours) induces no persistent hearing loss, as measured by the behavioral audiogram, ABRs, and DPOAEs, but results in a frequently-depleted Wave I amplitude relative to control animals. Finally, cochlear synaptopathy was objectively confirmed by visualizing the loss of ribbon synapses in the cochlea. Labeling for the IHC, the presynaptic ribbon and post synaptic ribbon allowed us to visualize any permanent changes in the cochlea induced by noise.

Supported by NIH R01-DC011555

PS 57

The Effect of Chronic Electrical Stimulation on Functional and Histological Measures of Auditory Nerve Degeneration

Dyan Ramekers; Sjaak F. Klis; Huib Versnel
UMC Utrecht

Secondary to severe hair cell loss, the spiral ganglion cells (SGCs) that comprise the auditory nerve degenerate progressively. Using electrically evoked compound action potentials (eCAPs), we have previously shown that this structural degeneration is accompanied by functional changes in deafened guinea pigs (e.g., Ramekers et al., 2014, J Assoc Res Otolaryngol). In the present study we examine whether chronic electrical stimulation (CES) of the auditory nerve, as received by cochlear implant users, affects these functional changes.

Normal-hearing guinea pigs were implanted with an intracochlear electrode array. Four weeks after implantation the animals were deafened by co-administration of kanamycin and furosemide. Starting either one or five weeks after deafening, the auditory nerve was chronically electrically stimulated for two weeks. Using a MED-EL PULSAR cochlear implant, awake eCAP recordings were performed at least weekly during the entire 7-11 weeks period following implantation. In each session eCAPs were recorded in response to single biphasic current pulses of which the current level, phase duration and inter-phase gap (IPG) were systematically varied (Ramekers et al., 2014, J Assoc Res Otolaryngol). Following the final eCAP recording session the animals were sacrificed, and their cochleas were processed for histological quantification.

SGC survival was similar in the implanted right and the unimplanted left ears in control animals. Animals receiving CES showed a moderate but statistically significant increase in SGC survival in their implanted/stimulated ear compared to the contralateral ear. Most eCAP measures had stabilized during the four weeks prior to deafening, after which a decrease in both amplitude and threshold, and an increase in dynamic range was observed. A remarkable transient increase in excitability (lower threshold, steeper slope, shorter latency) was observed for all animals in the first week after deafening. The effect of CES on the eCAP was small, but appeared to result in lower amplitude and longer latency. The effect size associated with increasing IPG – previously shown to correlate well with neural health (Ramekers et al., 2015, J Neurosci) – changed as expected after deafening for all eCAP measures. CES did not affect this IPG effect.

In summary, CES slows down, but does not stop SGC degeneration. The eCAP measures reflect SGC survival in a similar fashion with CES than demonstrated previously without CES. We conclude that since changes in eCAPs after deafening are largely unaltered by CES, application of CES in animal studies is not necessary in order to mimic the clinical human situation.

PS 58

Exploring the Impact of Peripheral Myelin Disorders on Inner Ear Structure and Function Using Mouse Models of Charcot-Marie-Tooth Disease.

Luis R. Cassinotti[1]; Lingchao Ji[1]; Aditi S. Desai[1]; Adam T. Palermo[2]; Joseph C. Burns[2]; Gabriel Corfas[1]
[1]University of Michigan; [2]Decibel Therapeutics

There is increasing evidence that peripheral myelin defects can cause or contribute to hearing disorders. However, the specific aspects of myelin that are critical for normal hearing, and the diverse types of hearing deficits resulting from the different myelin alterations remain poorly understood. To gain insight into these questions, we are using mouse models to explore the functional and structural inner ear phenotypes produced by two related but different myelin peripheral neuropathies, Charcot-Marie-Tooth 1A (CMT1A) and 1E (CMT1E). CMT is a hereditary peripheral motor and sensory neuropathy that affects 1 in 2500 people in United States. CMT, which has numerous subtypes, is broadly classified as demyelinating (CMT1) and axonal neuropathy (CMT2). Two CMT1 subtypes are caused by alterations in PMP22, a gene encoding for a peripheral myelin protein expressed by Schwann cells. CMT1A, the predominant CMT1 subtype (> 50% of the cases), is caused by duplication of the PMP22 gene. In contrast, CMT1E, which is caused by point mutations in the same gene, is much rarer (< 5% of CMT1 cases). CMT1E peripheral neuropathy has earlier onset and more severe

symptoms than CMT1A. While patients with CMT1E have been reported to suffer from sensorineural hearing loss, a recent study suggested that CMT1A suffer from hidden hearing loss. We recorded auditory brainstem responses (ABRs) and distortion product otoacoustic emissions (DPOAEs) in both CMT1A and CMT1E mutant mice and their wildtype littermates at 1, 2, 3 and 4 months of age. CMT1E mice have early-onset severe 'overt' hearing loss with mild DPOAE threshold shifts, indicative of auditory neuropathy. ABR peak 1 latencies are longer, suggestive of axonal conduction defects. In contrast, CMT1A mice present with early onset 'hidden' hearing loss, i.e. normal thresholds but reduced ABR peak 1 amplitudes and increased latencies. We are using electron microscopy and immunostaining to define the structural phenotypes. Preliminary results show that nodes of Ranvier and heminodes are disrupted in 4-month old CMT1A mice. These results provide evidence that myelin defects can lead to both 'overt' and 'hidden' hearing loss, support the audiological findings in CMT1A and CMT1E patients and indicate that patients suffering from peripheral myelin disorders are likely to have hearing impairments.

This research was supported by funding from Decibel Therapeutics, Inc., a company in which Dr. Corfas holds an equity interest and serves as a consultant.

PS 59

Mild Therapeutic Hypothermia: New Insights On The Protective Mechanisms In Cochlear Implant-Induced Hearing Loss

Rachele Sangaletti[1]; Elizabeth Dugan[2]; Federica Maddalena Raciti[3]; Curtis King[4]; W. Dalton Dietrich[5]; Michael Hoffer[6]; Suhurd M. Rajguru[7]
[1]Dept. of Otolaryngology, University of Miami; [2]Department of Biomedical Engineering, University of Miami; [3]Department of Cellular Physiology and Molecular Biophysics, University of Miami Miller School of Medicine; [4]Lucent Medical Systems, Seattle,WA; [5]Department of Neurological Surgery and Biomedical Engineering,University of Miami; [6]University of Miami; [7]Dept. of Biomedical Engineering and Otolaryngology, University of Miami

Cochlear implants (CI) are a neuroprosthetic success story, having benefitted more than half a million individuals with severe to profound hearing loss. However, conservation of residual hearing function in CI recipients remains a major challenge and has become critical with the advent of combined electro-acoustic (hybrid) devices. We have recently reported that mild to moderate therapeutic hypothermia could be the new frontier in auditory field, potentially improving residual hearing outcomes in patients. Here, we detail the mechanisms underlying therapeutic efficacy of hypothermia in Brown Norway rats and highlight the safety and efficacy of mild localized hypothermia delivered post-CI. The animals were divided into one of two groups: implanted in normothermic condition or receiving hypothermia treatment following CI. Contralateral cochleae were used as controls. Cochlear hair cell and neuronal function was assessed via auditory brain stem responses (ABRs) at different time points to monitor changes in hearing. Transcriptomic and flow cytometry analysis were performed to gain insight of the molecular pathways responsible for the protection afforded by mild hypothermia after CI. The lateral wall was immunolabelled with anti-matrix metalloproteinase-2 and -9 to quantify the extent of extracellular matrix degradation. Our long-term studies have confirmed the safety of mild therapeutic hypothermia and a conservation of residual hearing at low frequencies in animals receiving mild therapeutic hypothermia. In hypothermia-treated cochleae, biological processes such as cytokine and chemokine-mediated signaling pathway, response to cytokine and tumor necrosis factor, response to hypoxia and inflammatory response, were highly enriched. The inflammatory chemokine Ccl2, Ccl7, Ccl19, Ccl21, Ccl24 interleukin-1b and -6, Cxcl1 and matrix metalloproteinase MMP-3 genes were significant down-regulated in mild hypothermia-treated cochleae when compared with normothermic-implanted cochleae. Infiltration of macrophages, lymphocytes and activated microglia were significant decreased in cochlea treated with mild therapeutic hypothermia. Furthermore, MMP-2 and MMP-9 immunoreactivity was positively reduced in CI hypothermia-treated cochleae to the levels of control cochleae. Our work suggests an important protective role of hypothermia in reducing inflammatory responses that promote sensorineural hearing loss associated with CI surgery. Current research is focused on optimizing the hypothermia protocol and translation to human clinical application.

Funding: NIH 1UL1TR000460, 1R21DC014324, 1R01DC013798, Wallace H Coulter Center for Translational Research and Cochlear Research Grant.

PS 60

Development of Middle-Ear-Muscle Reflex (MEMR) Biomarker in Mouse

Ann E. Hickox; Arun Senapati; Trang Nguyen; Lars Becker; Lillian Smith; Raja Poda; Jessica Wang; Jillian Zoglio; Qi-Ying Hu; Janeta V. Popovici-Muller; Inmaculada Silos-Santiago
Decibel Therapeutics

The middle-ear-muscle reflex (MEMR) has been employed for decades as an objective measure of

retrocochlear function. A rapid and non-invasive assay, it has recently gained additional appeal as a potential biomarker for cochlear synaptopathy: mice with noise-induced synaptopathy and normal cochlear thresholds show reduced MEMR amplitude and elevated MEMR thresholds (Valero et al. 2016, 2018); additionally, individuals with noise-exposure-related tinnitus and near-normal audiograms show dramatically reduced wideband MEMR strength (Wojtczak et al. 2017). We tested the sensitivity of this assay to synaptic loss/dysfunction in mouse within varying contexts of cochlear damage.

We established contralateral, ketamine/xylazine-anesthetized MEMR in male, CBA/CaJ mice (~6-17 wks) following Valero et al. (2016). Two custom closed-field acoustic systems (Eaton-Peabody Laboratories) were used to 1) present bandpass noise (1-2 s) stimuli to the test ear, and 2) record a continuous chirp train in the probe ear to quantify MEMR, using custom Python software interfacing with an RZ6 signal processor (Tucker-Davis Technologies). Inner ear perturbations included: synaptopathic noise overexposure (8-16 kHz, 2 hr, awake) without (97 dB SPL) or with (105 dB SPL) permanent threshold shift (PTS), and surgical delivery to round window. One group of mice was treated with Riluzole prior to noise (40 mg/kg, p.o.) to protect against synapse loss. Synaptopathy was quantified by number of CtBP2 puncta per inner hair cell.

We replicated the published observation of significantly impaired MEMR following non-PTS synaptopathic noise exposure. MEMR was more sensitive than ABR wave 1 in differentiating synaptopathic vs unexposed ears at longer post-noise intervals, in part due to greater stability of MEMR with age. MEMR was also more sensitive in differentiating noise-exposed ears with vs without synaptic protection by Riluzole. Ears with noise- or surgery-related threshold shift (by ABR or DPOAE), even mild shifts restricted to the cochlear base, showed reduced or absent MEMRs.

We corroborated MEMR's sensitivity to synaptic loss/dysfunction by 1) replicating MEMR impairment with noise-induced loss of cochlear synapses and 2) demonstrating maintenance of MEMR with protection of cochlear synapses. However, MEMR was significantly impaired or even abolished in ears with cochlear threshold shift. Although commonly held that, in man, mild-to-moderate behavioral threshold shifts do not significantly impact MEMR, we observed that in mouse MEMR is negatively affected by manipulations that produce even mild objective threshold shifts. Taken together, these findings further refine the conditions under which MEMR may be a sensitive biomarker for synaptopathy.

PS 61

Contribution of Auditory Nerve Fibers to the Auditory Nerve Neurophonic in Human

Xavier Dubernard[1]; Frederic Venail[2]; Jean-Charles Kleiber[3]; Arnaud Bazin[3]; André Chays[4]; Jean-Luc Puel[5]; Jérôme Bourien[5]
[1]INM, Inserm, Univ Montpellier and ENT Department at Robert Debré University Hospital; [2]University Hospital of Montpellier & Institute for Neurosciences of Montpellier - INSERM U1051; [3]Neurosurgery Department at Maison Blanche University Hospital, Reims, France; [4]ENT Department at Robert Debré University Hospital, Reims, France; [5]Institute for Neurosciences of Montpellier

Contribution of Auditory Nerve Fibers to the Auditory Nerve Neurophonic in Human

Xavier Dubernard[1,2,3], Frédéric Venail[1,2,4], Jean-Charles Kleiber[5], Arnaud Bazin[5], André Chays[3], Jean-Luc Puel[1,2], Jérôme Bourien[1,2]

1. Institute of Neuroscience of Montpellier - Inserm U1051, France
2. University of Montpellier, France
3. ENT Department at Robert Debré University Hospital, Reims, France
4. ENT Department at CHU Gui de Chauliac, Montpellier, France
5. Neurosurgery Department at Maison Blanche University Hospital, Reims, France

Introduction

In clinic, far field potentials evoked by acoustic clicks or tone bursts are commonly used to probe the activity within the auditory nerve. However, the contribution of auditory nerve fibers at the unit level in the far field assay is poorly understood. Here, we combine human auditory nerve recordings and computational modeling to identify the generators of the far field response.

Material and Methods

The electric response of the auditory nerve (AN neurophonic) was measured during cerebellopontine angle surgery (ClinicalTrials.gov Identifier: NCT03552224). Sound stimulations were delivered in a closed field and the auditory nerve activity was measured using a ball electrode (Ø1.6 mm) apposed directly on the nerve. The generation and acquisition of the signals was entirely processed by a NI-PXI 4461 device controlled by a LabVIEW interface (National Instrument). A computational model of human cochlea was developed to simulate the global (i.e. AN neurophonic) and unitary response of 1800 individual auditory nerve fibers distributed along the tonotopic axis.

Results

We performed electrophysiological investigations in 5 patients with normal or sub-normal audiogram (*i.e.*, auditory thresholds ≤ 20 dB HL between 500 and 4000 Hz). In response to click, the AN neurophonic exhibits a large N_1-P_1 wave followed by small oscillations that persist over 10 ms after the stimulation end. Computation model reproduces this pattern of response, and allows us to identify two different generators in the auditory nerve: *i*) the fibers from the base (2-4 kHz region) generate the N_1-P_1 wave, and ii) the fibers from the apex (below 1 kHz) give rise to the following small oscillations. In contrast, the responses evoked by tone burst departed from those elicited using clicks. Whatever the frequency, the AN neurophonic elicits by 20-ms tone bursts show the regular N_1-P_1 wave at the onset of the burst and a similar N_1-P_1 response at the stimulation offset. Computational simulation suggests that the onset response originates from a region closed to the probe frequency whereas offset response stems from regions outside the probing frequency. In response to low frequency tone bursts (below 2 kHz), the AN neurophonic also displays a frequency-following response during the tone burst, that the mathematical model identifies as a far field consequence of neural phase locking behavior of single fibers.

Conclusion

These data show that the AN neurophonic results from complex processes, even for simple *stimuli* such as clicks or tone bursts. In addition to better interpretation of electrophysiological data, mathematical model will help to better understand to more ecological sounds (*e.g.* speech), especially in patients with hearing loss.

PS 62

Hidden Hearing Loss in Human Temporal Bones: Primary Neural Degeneration in Noise Damaged Human Ears.

Peizhe Wu[1]; Leslie D. Liberman[2]; Jennifer T. O'Malley[3]; M. Charles Liberman[4]
[1]1. Eaton-Peabody Laboratories, Mass Eye & Ear; 2. Department of Otolaryngology Head & Neck Surgery, Harvard Medical School; [2]1. Eaton-Peabody Laboratories, Mass Eye & Ear; [3]1) Otopathology Laboratory, Department of Otolaryngology, Massachusetts Eye and Ear; [4]Harvard

In noise-damaged or aging ears, synapses between inner hair cells (IHCs) and auditory-nerve fibers (ANFs) are lost before hair cells degenerate. This cochlear synaptopathy does not elevate thresholds, but likely impairs performance on complex listening tasks. Age-related primary neural degeneration is seen in animals (Sergeyenko et al, J. Neurosci 2013) and humans (Wu et al. Neuroscience, 2018). However, in human, the prevalence of noise-induced synaptopathy remains unclear.

Here, we assess primary neural degeneration in aging or noise-exposed humans by counting hair cells and ANF peripheral axons in sections from the Mass. Eye and Ear temporal bone archive. We analyzed 91 cases, including 53 with a noise-exposure history (age 33 - 96, median = 76) and 38 age-matched controls. Controls had a mean audiometric PTA (0.5 - 2) of 41 dB. Mean PTA in the noise group was 34 dB, but thresholds at 4 kHz were 21 dB worse than controls. To count myelinated ANFs, we selected unstained tangential sections through the osseous spiral lamina limbus from each half turn, de-celloidinized them, stained them with Cellmask® and imaged them in the confocal. IHC and OHC counts were derived from a high-power, DIC-based re-examination of the legacy sections stained with H & E.

Stepwise multiple linear regression was used to model the relative contribution to ANF survival of IHC and OHC loss, plus cochlear location, age and noise-exposure group. After adjusting for IHC survival and cochlear location, the noise-damage group showed 31% more ANF loss than controls at 50 yrs, with the intergroup difference shrinking by 8.2% for every additional 10 years of age. Thus, noise exposure causes significant primary neural degeneration, but so does "normal" aging. After removing effects of aging, by adjusting for age, IHC and OHC loss, and cochlear location, there remains ANF loss of 7.2% attributable to noise exposure per se.

These data suggest that the noise-induced primary degeneration of cochlear nerve terminals seen in animal studies is also significant in humans. Since all the noise-exposed subjects studied here also had significant overt hearing loss, the extent of hidden hearing loss in humans with normal audiograms remains unknown.

Research supported by the NIDCD (P50 DC015857).

PS 63

Kainate- and AMPA-Induced Cochlear Synaptopathy in Gerbils

Artem Diuba[1]; Vivien Foulquier[1]; Jérôme Bourien[2]; Martin Nedelec[1]; Gilles Desmadryl[1]; Sharon G. Kujawa[3]; Jean-Luc Puel[2]
[1]INM, Inserm, Univ Montpellier; [2]Institute for Neurosciences of Montpellier; [3]Eaton-Peabody Laboratories, Massachusetts Eye and Ear and Department of Otolaryngology-Head and Neck Surgery, Harvard Medical School

Kainate- and AMPA-Induced Cochlear Synaptopathy in Gerbils

A.V. Diuba[1], V. Foulquier[1], J. Bourien[1], M. Nedelec[1], G. Desmadryl[1], S.G. Kujawa[2,3], J-L. Puel[1]
[1]Deafness, Tinnitus and Therapies, Institute for Neurosciences of Montpellier, 34096, France
[2]Department of Otolaryngology-Head and Neck Surgery, Harvard Medical School, Boston, MA 02115, USA
[3]Eaton-Peabody Laboratories, Massachusetts Eye & Ear Infirmary, Boston, MA 02114, USA

Background
Exogenous glutamate agonists, applied locally to the cochlea, produce an excitotoxic swelling of auditory nerve fiber terminals on inner hair cells (IHCs). Noise-induced cochlear synaptopathy may be similarly instigated by excess sound-evoked release of these substances. To investigate mechanisms of noise-induced synaptopathy, we mimicked excessive release of neurotransmitter by infusing artificial perilymph (AP) alone or containing kainic acid (KA) or AMPA into the round window niche of the gerbil cochlea.

Methods
KA (25 mM) or AMPA (25 mM) was infused into the round window niche of young adult gerbils for 1 hour. Cochlear function was measured 1, 3, 7, 14 and 28 days after infusion using distortion-product otoacoustic emissions (DPOAEs) and compound action potentials (CAPs) of the auditory nerve. At day 14 or 28, the cochleae were removed and immunostained against CtBP2 and GluA2 to count IHC ribbon synapses all along the tonotopic axis.

Results
KA and AMPA infusions did not affect outer hair cell function as assayed by DPOAEs. In contrast, both KA and AMPA acutely elevated CAP thresholds and reduced CAP amplitudes. Thresholds recovered to baseline. By 28 days, CAP amplitudes were partially recovered, with the degree of recovery dependent on agonist and frequency. Consistent with the amplitude data, the number of synapses/IHC in KA-perfused cochleae was reduced by ~50% as compared to AP-perfused cochleae, throughout the tonotopic axis. AMPA-induced synaptic loss was frequency-dependent, with almost full synapse repair at the apex, and loss comparable to that of KA in the basal part of the cochlea.

Conclusion:
Both KA and AMPA induce cochlear synaptopathy but differ in the extent of synaptic loss in the apex. Ongoing experiments will provide additional pharmacologic characterization of the agonist-induced synaptopathy.

Supported by Office of Naval Research Grant N00014-16-1-2867

PS 64

MHCII KO mice are protected from SGN degeneration after deafening

Muhammad Taifur Rahman[1]; Benjamin M. Gansemer[1]; Jack Parker[2]; Zhenshen Zhang[1]; Catherine Kane[2]; Steven H. Green[1]
[1]University of Iowa; [2]The University of Iowa

Background
Spiral ganglion neurons (SGNs) gradually die after destruction of hair cells, their sole afferent input. During SGN degeneration, the ganglion exhibits inflammation with upregulation of markers of MHCII mediated antigen presentation, CD4, cytokines, and markers of macrophage activation suggestive of adaptive immune response initiated by MHCII. Moreover, immunosuppressive drugs, such as dexamethasone or ibuprofen, protect SGNs after deafening. Here, we assessed the role of MHCII mediated antigen presentation in SGN degeneration in a preclinical mouse model of hair cell destruction.

Methods
To examine a possible role for MHCII mediated antigen presentation in SGN death post-deafening, we crossed a MHCII KO (B6.129S2-H2$^{dlAb1\text{-}Ea}$/J) into DTR (Pou4f3$^{huDTR/+}$) mice, in which hair cells can be selectively killed with diphtheria toxin (DTx). Mice (CBA/CaJ) were injected with DTx (1 µg/kg) on postnatal day 5 (P5). Mice were euthanized at P60, cochleae were harvested, fixed with 4% PFA, decalcified with EDTA, cryoprotected with sucrose, embedded in OCT and cryosectioned (6 µm) parallel to the midmodiolar plane. Loss of hair cells was confirmed histologically by labeling with myosin 6/7. NeuN and Tuj1 immunofluorescence was utilized to label SGNs, which were counted in every fourth near-midmodiolar section. Image analysis was done using ImageJ with custom-written macros. The outline of Rosenthal canal for each turn was manually traced to measure cross-sectional area and to calculate SGN density. Statistical significance was determined with a 2-way ANOVA with Sidak's post-hoc analysis.

Results
There was no significant difference between MHCII$^{+/+}$ vs. MHCII$^{-/-}$ in Pou4f3$^{+/+}$ mice with respect to ABR threshold and SGN density, i.e., MHCII knockout itself caused no evident change in cochlear function. Upon DTx injection, all DTR mice (but none of the non-DTR Pou4f3$^{+/+}$ mice), were deafened irrespective of MHCII genotype, evidenced by the lack of ABR to tones ≤95

dB SPL and complete loss of hair cells. This indicates that MHCII is not necessary for hair cell loss after DTx injection in DTR mice. However, our data show a significant requirement for MHCII in SGN death. SGN survival 8 weeks post-DTx is significantly reduced in DTR; MHCII$^{+/+}$ mice to ~30% of control Pou4f3$^{+/+}$ mice. In contrast, in MHCII$^{-/-}$ mice, there is no significant SGN loss and in heterozygous MHCII$^{+/-}$ mice, SGN density is at ~60% of control Pou4f3$^{+/+}$ mice. These data suggest that MHCII-mediated antigen presentation is an essential part of an immune response that results in SGN degeneration post-deafening.

PS 65

Disruption of ErbB Receptor Signaling in Schwann Cells Results in Hidden Hearing Loss.

Luis R. Cassinotti; Aditi S. Desai; David Kohrman; Beatriz C. Borges; Gabriel Corfas
University of Michigan

There is increasing evidence that auditory nerve myelin is necessary for normal hearing, but the mechanisms regulating this myelination remain poorly understood. There is ample evidence that the trophic factor Neuregulin 1 (NRG1) plays an important role in peripheral nerve myelination. NRG1 is expressed by all peripheral neurons and activates transmembrane tyrosine kinase ErbB receptors (ErbBRs) in Schwann cells, leading to myelin gene expression and increased myelin thickness (*Curr Topics Devel Biol* 116:45-64, 2016). To determine the roles of NRG1-ErbBR signaling in auditory nerve myelin and hearing, we used CNP-DN-ErbB4 mice, a transgenic line that expresses a dominant-negative ErbB4 receptor in myelinating cells. Any cell expressing DN-ErbB4 receptors becomes unresponsive to NRG1. We previously showed that these mice have delayed onset of sciatic nerve myelination in the neonate, as well as hypomyelination and decreased sciatic nerve conduction velocity in adulthood (*J Neurosci* 26:3079 –3086, 2006). Since all type I spiral ganglion neurons express NRG1 (*Brain Res Mol Brain Res* 54: 170-4, 1998; *Hearing Res* 161: 87-98, 2001; *J Neurosci* 24: 8651-61, 2004), while ErbB2 and ErbB3 receptors are expressed by all stages of the Schwann cell lineage (*Cold Spring Harb Perspect Biol* 7: a020487, 2015), we hypothesized that loss of Schwann cell ErbBR signaling will affect AN nerve myelination and function.

We found that at 3 months of age, CNP-DN-ErbB4 mice exhibit normal distortion product otoacoustic emission and auditory brainstem response thresholds, indicating normal outer hair cell function and normal hearing sensitivity. However, suprathreshold responses (ABR peak 1 amplitudes) in these mice are reduced relative to wildtype littermates, a hallmark of hidden hearing loss. We are currently evaluating myelin structure by EM and immunostaining, as well as measuring myelin gene expression to determine the morphological and molecular bases of this phenotype. This research was supported by R01 DC004820.

PS 66

In Silico Examination of Noise-Induced and Age-Related Cochlear Deafferentation in Mice

Jérôme Bourien[1]; Jean-Luc Puel[1]; Sharon G. Kujawa[2]
[1]Institute for Neurosciences of Montpellier; [2]Eaton-Peabody Laboratories, Massachusetts Eye and Ear and Department of Otolaryngology-Head and Neck Surgery, Harvard Medical School

Background
Sound-evoked auditory nerve responses can be used to detect loss of auditory nerve fibers (ANFs) or their functions; for example, after silencing by loss of synapses with sensory inner hair cells (IHCs). The AN is comprised of pools of fibers with different spontaneous firing rates (SR). Fibers with high thresholds and low SRs have been implicated as early targets in common forms of acquired sensorineural hearing loss, e.g. those occurring with age and after noise exposure. Because whole nerve responses like the cochlear nerve compound action potential (CAP) reflect synchronous activity of fibers, relative losses by SR subtype are difficult to assess. We have therefore developed a computational model of the cochlea to investigate the relationship between ANF spiking and CAP waveform and apply it to various hearing loss etiologies.

Methods
The model considers the main biophysical properties of the mouse cochlea, including the place frequency map, receptor potential of IHCs, single action potentials and single fiber tuning properties, the number of ANFs/IHC and proportion of low-, medium- and high-SR fibers along the tonotopic axis. Data input to the model were from normally-aging or noise-exposed CBA/CaJ mice. The output of the model is the CAP of the auditory nerve generated in response to tone bursts presented at various frequencies and for various simulated degrees and progressions of ANF loss. We simulated three different scenarios: i) progressive loss of fibers from low- to high-SR, ii) progressive loss from high- to low-SR, and iii) random loss, i.e., independent of SR.

Results
Simulations show that fiber loss can reach 80% with trivial effects on CAP threshold (< 8 dB shift for a progressive loss of fibers from low- to high-SR). CAP amplitude was

more sensitive to ANF fiber loss; however, it failed to predict linearly the degree of deafferentation, especially with specific deletion of high- or low-SR fibers. Simulated data from aging mice suggested progressive low- to high-SR loss, whereas simulations run using data from noise-damaged ears suggested random loss.

Conclusion
This in silico model allows us to simulate different scenarios of cochlear deafferentation that are difficult to probe in vivo. In complement to experimental studies, such models can inform understanding of the pathology underlying a neural loss phenotype with a normal audiogram (hidden hearing loss).

Supported by Office of Naval Research Grant N00014-16-1-2867

PS 67

A Convolutional Neural-Network Model of the Human Auditory Periphery for Real-time Applications and Studies of Hearing Impairment

Fotios Drakopoulos; Deepak Baby; Arthur Van Den Broucke; Sarah Verhulst
Ghent University

The interest in precise diagnosis and compensation of the different frequency-dependent combinations of hearing deficits has resulted in an increasing need for more biophysically-accurate models of the human auditory periphery. Individualized models of hearing impairment have been widely used in the design of hearing-aid fitting rules and can help to develop sensitive auditory-evoked potential (AEP) metrics that can disentangle and quantify the cochlear synaptopathy and outer-hair-cell (OHC) aspect of sensorineural hearing loss.

While auditory models have progressed to accurately capture the biophysical and nonlinear properties of human hearing, they are still slow to compute and hence unsuitable for real-time applications. Less time-consuming descriptions of cochlear processing (gammatone, DRNL, MFCC) are still used as feature extractors or as auditory front-ends even though they provide a very rough estimate of the auditory physiology. In this work, we present a hybrid approach in which convolutional neural network (CNN) techniques are combined with computational modelling to yield a real-time model of the human auditory periphery. CNNs were trained to learn the computations performed by a state-of-the-art biophysical model that can represent the cochlear mechanics and the inner-hair-cell and auditory-nerve complex in great detail. Speech corpus material was used for the training of each stage of the auditory pathway and the performance of the models was compared against human data and simulations of the biophysical model using basic stimuli (pure tones, clicks, etc.). The resulting model is based on a real-time end-to-end model for human cochlear mechanics and level-dependent cochlear filter tuning which accurately simulates human frequency selectivity and its dependence on sound intensity. This CNN-based cochlear model can be executed on a GPU yielding latencies below 10 ms, compared to state-of-the-art biophysical cochlear models that require processing times in the order of seconds to minutes.

The original biophysical model, on which this work was based, includes a transmission-line cochlear model which can simulate different degrees of frequency-specific OHC deficits as well as synaptopathy of LSR, MSR and HSR fibers. Similarly, the normal-hearing CNN-model can be adjusted to simulate frequency-specific patterns of cochlear gain loss and different degrees of synaptopathy. Because the architecture of the CNN-models is based on real-time, parallel and differentiable computations, the developed models have a wide application area in the machine-hearing and hearing-aid signal processing domains.

PS 68

Steroid sex hormones promote regeneration of cochlear synapses after excitotoxic trauma

Sepand Bafti; Ning Hu; Steven H. Green
University of Iowa

Background
Moderate noise exposure destroys cochlear afferent synapses between inner hair cells (IHCs) and spiral ganglion neurons (SGNs), even in the absence of hair cell loss or permanent threshold shifts. This cochlear “synaptopathy” is a result of excess release of the excitatory neurotransmitter glutamate from IHCs and consequent glutamate excitotoxicity. Noise-induced cochlear synaptopathy (NICS) in animal models can be detected histologically as a reduction in the number of synapses on the IHCs, and physiologically as a temporary reduction of amplitude in auditory brainstem response (ABR) wave I. A previous investigation in our lab showed that female mice are less susceptible to NICS than male mice, and their susceptibility varies through the estrous cycle with the lowest susceptibility being during the diestrous phase, when progesterone levels are highest. This implicates progesterone as playing a neuroprotective role, however our studies of cultured cochleas show that it does not protect against NICS, rather, it induces regeneration of synapses at a rapid rate. Here, we extend our in vitro studies to investigate the underlying biological mechanisms of action through

which progesterone promotes its regenerative effects in the cochlea. Previous studies from our lab have shown that the presence of endogenous neurotrophin NT-3 is necessary for synapse regeneration in the cochlea after excitotoxic trauma in vitro (Wang and Green, 2011). In the current studies, we first ask whether progesterone requires NT-3 to promote synapse regeneration or can act independently. Additionally, in a series of timecourse experiments we seek to shed light on the temporal properties of progesterone's ability to promote regeneration by determining the minimum time required to experience its full effects.

Methods

Cochlear explant cultures from postnatal day 5 rat pups were prepared as described by Wang et.al, 2011. These cultures maintain intact the middle turn of the organ of Corti, their associated SGNs, and synaptic connections. Synaptopathy is induced by addition of the glutamate agonist kainic acid (KA) for 2 hours (equivalent to the duration of noise exposure used in vivo). Exposure to 0.5 mM causes nearly complete loss of synapses. A subset of explants are not exposed to KA to serve as controls. To block NT-3 signaling, we use TrkC-IgG that we synthesize from a construct that we made and described the synthesis of previously. If NT-3 is required for synapse regeneration promoted by progesterone, then regeneration will be significantly reduced in the presence of TrkC-IgG. Following the KA treatment, the KA is washed out and the explants are incubated for either an additional 8, 16, or 24 hours in medium of the following conditions: progesterone (20 ng/ml), NT-3 (50 ng/ml), progesterone and TrkC-IgG (2 µg/mL), NT-3 and TrkC-IgG, or control culture medium that contains none of the mentioned compounds. The cultures were labeled was with anti-Ribeye (presynaptic ribbons), anti-PSD95 (postsynaptic densities), anti-Myosin 6 (IHCs), and anti-NF200 (SGNs). Synapse counts were compared among experimental conditions and controls.

Results

We show that progesterone is effective at promoting synapse regeneration after at least 16 hours in vitro following the 2 hour KA treatment. We did not observe any significant increase in the number of synapses at 24 hours compared to 16 hours. TrkC-IgG does not appear to affect progesterone's effects in promoting synapse regeneration after excitotoxic trauma, as its presence did not significantly reduce the number of synapses present at 16 or 24 hours after trauma.

Conclusions

Female mice on average are less susceptible to NICS than their male counterparts with their susceptibility varying throughout the different stages of the estrous cycle. Females are least susceptible during the diestrus phase, where progesterone levels are significantly elevated. We show that while progesterone does not protect synapses from excitotoxic trauma in vitro it does effectively promote synapse regeneration in cultured cochleas. Progesterone's ability to promote regeneration of cochlear synapses does not appear to depend on the presence of NT-3.

PS 69

A Novel Chinchilla Model of Blast-Induced Auditory Injury for Hearing Damage Prediction and Prevention Using 3D Printed "Helmet" and Earplug

Shangyuan Jiang; Kyle Smith; Junfeng Liang; Xuelin Wang; Ariana Gannon; Marcus Brown; Rong Z. Gan
University of Oklahoma

Introduction

Repeated exposures to blast result in hearing damage in Service members and Veterans. The auditory injuries are caused by two pathways of blast overpressure: structural damage in the peripheral auditory system (PAS) resulted by blast wave transmission through the ear, which has been observed in our animal model of chinchilla [1], and the injury in the central auditory system (CAS) caused by blast wave impact on the head or the traumatic brain injury (TBI). However, it is difficult to differentiate these two pathways and evaluate their contributions to the hearing damage. This gap of knowledge affects the development of effective hearing protection devices such as earplugs because the earplug can protect the PAS, but its protective function against CAS injury remains unclear. This paper reports a novel study to investigate the protective function of earplug on the CAS in addition to PAS by using the 3D printed chinchilla "helmet" as a head protection device to isolate the CAS damage from the PAS.

Methods

32 chinchillas were divided into 4 experimental groups or 4 cases (ears open, with earplug only, with both earplug and helmet, and with helmet only) and exposed to 3 blasts at the overpressure level of 15-20 psi. Hearing function tests including auditory brainstem responses (ABRs), distortion product otoacoustic emissions (DPOAEs), and middle latency responses (MLRs) were conducted pre- and post-blast on Day 1, and then, on Day 4 and Day 7 after blast exposure. The immunofluorescence staining images of chinchilla brains were also produced for analysis of the CAS injury.

Results

ABR threshold shifts and the wave I and V amplitudes, DPOAE threshold shifts, and MLR waveforms obtained

from of chinchilla ears in 4 groups after blast exposure over the 7-day experimental period indicated that the damage severity and recovery process of blast-induced injuries in CAS and PAS varied among 4 different cases. The immunofluorescence images of auditory cortex were reflecting the injury level to the function test results with differentiation between 4 cases.

Conclusion
A novel animal model of chinchilla to investigate the blast-induced damage in the PAS and CAS with the corresponding protective devices of helmet and earplug was successfully developed. The preliminary results are encouraging and advanced metrics analyses for the measurement data will be further conducted in future studies

Acknowledgment
This work was supported by DOD W81XWH-14-1-0228.

Reference
[1] T. Chen et al. *Hearing Research*, Vol. 378: 33-42, 2019.

PS 70

Comparison of Various Neurotrophic Compounds for Preservation of the Auditory Nerve in Deafened Guinea Pigs

Henk Vink; Dyan Ramekers; Glauco Cristofaro; Hans Thomeer; Huib Versnel
UMC Utrecht

The auditory nerve degenerates following severe damage to the organ of Corti including loss of hair cells. For optimal hearing performance with a cochlear implant (CI), a healthy auditory nerve is essential. Over the last two decades the protective effect of neurotrophic treatment on the nerve has been well demonstrated. Clinically applicable methods are developed for treatment in CI patients or in patients with synaptopathy. In our laboratory, using gelfoam as delivery vehicle, we seek neurotrophic compounds that yield a high survival and good electrical responsiveness of spiral ganglion cells (SGCs). Therefore, we compare various neurotrophic compounds in deafened guinea pigs using histological and electrophysiological outcome measures.

Guinea pigs were ototoxically deafened two weeks prior to neurotrophic treatment. The animals received natural neurotrophins such as brain-derived neurotrophic factor (BDNF), or synthetic compound such as the small-molecule 7,8,3'-trihydroxyflavone (THF). Gelfoam soaked in a neurotrophic solution by was placed on the perforated round window membrane of the right cochlea (Havenith et al., Otol Neurotol, 2015). Four weeks after treatment onset, electrically evoked compound action potentials (eCAPs) were recorded to assess auditory nerve responsiveness (Ramekers et al., J Neurosci, 2015). Subsequently, the cochleas were harvested and SGCs were quantified.

The highest SGC counts were found for treatment with a combination of BDNF and neurotrophin-3 (NT-3), outperforming the other treatments in the basal and middle cochlear turn. Separate treatments of compounds yielded significant SGC survival only in the basal turn. Surprisingly, the better eCAP outcomes were observed in animals treated with BDNF alone. In spite of superior pharmacokinetic properties, THF did not yield better outcomes than the natural neurotrophins.

Considering both histological and functional data we suggest that BDNF alone or in combination with NT-3 is preferable as neurotrophic compound to reduce auditory nerve degeneration.

PS 71

Immune Response Activation in the Spiral Ganglion of Aminoglycoside Deafened Rats

Benjamin M. Gansemer; Muhammad Taifur Rahman; Steven H. Green
University of Iowa

Background
Spiral ganglion neurons (SGNs) transmit information about acoustic stimuli from cochlear hair cells to the central nervous system. SGNs degenerate gradually following hair cell loss induced by aminoglycosides such as kanamycin (KM), but the reason for this degeneration is unclear. Studies from our lab and others suggest that an immune/inflammatory response may contribute to SGN death after hair cell loss. To gain a better understanding of changes that occur during the neurodegenerative process in the cochlea, we performed gene expression profiling using RNAseq on spiral ganglia from hearing and kanamycin-deafened rats. Additionally, we analyzed morphology and activation of immune cells via histological methods.

Methods
Sprague-Dawley rats were intraperitoneally injected with KM once daily from postnatal day 8 (P8) through P16 to destroy hair cells. Cochleae were collected for RNA extraction at either P32, a time at which SGN death is beginning, or P60, a time when roughly 50% of SGNs remain. The spiral ganglia were isolated from the organ of Corti and the RNA extracted and prepared for RNA

sequencing. The RNAseq data were analyzed using available computational tools and software packages. For histological analyses, cochleae were collected at P70 and cryosectioned at 25µm thickness parallel to the midmodiolar plane. Sections were labeled with antibodies to identify neurons (Tuj1), macrophages (Iba1), and CD68 (anti-CD68). Morphology of Iba1+ cells and fluorescence of CD68 were analyzed using custom-written macros in ImageJ.

Results

RNA sequencing revealed expression of ~20,000 genes in the spiral ganglion, with ~5,200 being significantly differentially expressed (adjusted p< 0.1) in deafened vs. hearing rats. Of the genes that passed the adjusted p-value threshold, 634 were upregulated >2x (log2FC >1) and 380 were downregulated < 0.5x (log2FC< -1) in ganglia from deafened rats. GSEA revealed many functional gene categories that were enriched after deafening, with the largest category containing genes associated with an immune/inflammatory response. More specifically, several genes involved in the complement cascade, chemotaxis, and/or antigen presentation were upregulated after deafening. Furthermore, histological analysis of Iba+ positive cells revealed morphological changes indicative of cell activation as well as increased expression of CD68, a marker of phagocytic activity, in deafened ganglia.

Conclusions

Many immune/inflammatory response genes are upregulated in the spiral ganglion after aminoglycoside-induced hair cell loss. This suggests infiltration and activation of immune cells occurs after deafening, the latter of which we show histologically. These findings imply that an immune/inflammatory response contributes to degeneration of SGNs after deafening.

PS 72

Activity-dependent Synaptopathy and Demyelination of Auditory Neurons following Conductive Hearing Loss in Adult Mice

Takaomi Kurioka[1]; Sachiyo Mogi[1]; Manabu Tanaka[2]; Taku Yamashita[1]
[1]Department of Otolaryngology-Head and Neck Surgery, Kitasato University; [2]Bio-imaging Center, Kitasato University School ofMedicine

Background

Cochlear insults induced by acoustic overstimulation or ototoxic drug administration cause damage to several types of cochlear cells, including hair cells (HCs), spiral ganglion neurons (SGNs), myelin of the cochlear nerve, and synapses between the HCs and SGNs as well as more central regions of the auditory pathways. This results in a decrease in auditory activity. However, it is not clear whether this decrease results in the cochlear dysfunction of auditory neurons (ANs), synapses, and myelination in adult mice. Additionally, it is unknown whether cochlear dysfunction can be fully restored if deprivation has been completely withdrawn. In our study, we investigated the functional and structural changes of the ANs after conductive hearing loss in adult mice using earplugs (EPs).

Materials and Methods

Male C57BL/6 mice at 8 weeks of age were bilaterally inserted EPs for 4 weeks (EP(+) group) and allowed to survive for a further 4 weeks following the removal of the EPs (EP(+/-) group). The control mice (EP(-) group) did not have EPs inserted and were allowed to survive until they were 12-weeks old. The auditory brainstem response (ABR) was measured to confirm the cochlear functions before and after the EPs were inserted, after the EPs had been removed, and 4 weeks following the removal of the EPs. Cochleae were examined for the survival of HCs and SGNs, synaptic and neural properties, and myelination of ANs.

Results

The ABR threshold was significantly elevated across all tested frequencies following the insertion of the EPs. After removing the occlusion, this threshold shift fully recovered. The ABR amplitude of peak1 significantly decreased and the latency was significantly prolonged at all tested frequenciesin the EP(+) mice as compared to the EP(-) mice. These changes were only partially recovered in the EP(+/-) mice. Auditory deprivation had no significant impact on the survival of HCs and auditory neurons. Contrastingly, synapses and myelin were significantly damaged, and the neuronal size of ANs was seen to significantly decrease in the EP(+) mice. These changes were also only partially recovered in the EP(+/-) mice as compared to the EP(+) mice.

Conclusions

Myelination and a number of cochlear peripheral synapses of the ANs were significantly damaged following conductive hearing loss in adult mice. Our results suggest auditory activities are required in order to maintain peripheral auditory synapses and myelination in mature animals. Therefore, an auditory deprivation model is useful for studying the mechanisms of synaptopathy and demyelination in the auditory periphery as well as for regenerative work of synapses and myelin.

PS 73

Physiological Response Properties of Auditory Nerve Fibers in Mice following Cochlear Synaptopathy

Kirupa Suthakar[1]; M. Charles Liberman[2]
[1]1. Eaton-Peabody Laboratories, Mass Eye & Ear; 2. Dept of Otolaryngology Head & Neck Surgery, Harvard Medical School; [2]Harvard

Cochlear synaptopathy, i.e. loss of ribbon synapses between inner hair cells (IHCs) and auditory nerve fibers (ANFs) can occur after exposure to noise or ototoxic drugs, and in aging. Recordings from single ANFs in noise-exposed guinea pigs, and in aging or ouabain-treated gerbils, suggest that ANFs with lower spontaneous rates (SRs) are especially vulnerable. Since low-SR fibers have higher thresholds, ABR thresholds could remain normal, while suprathreshold amplitudes are reduced, as is observed in synaptopathic ears. Prior ANF studies in guinea pig suggest that responses of ANFs surviving after synaptopathic noise are largely normal. However, synaptic recovery after noise is more complete in guinea pig than in mouse, as inferred by histopathological studies.

To further investigate the nature of synaptic damage and recovery after noise, we compared single-unit recordings from ANFs in normal and synaptopathic mice. To create permanent synaptic loss with minimal permanent threshold shift, CBA/CaJ were exposed to 8-16 kHz noise at 97.5 dB SPL for 2 hrs. After a 1 week, ABRs and DPOAEs were measured, then mice were allowed to recover for an additional week before single-ANF responses were obtained. Cochlear histopathology was assessed in a subset of animals.

As expected, thresholds and frequency tuning were normal. Surprisingly, the SR distribution in both non-synaptopathic and synaptopathic regions of exposed ears was also normal. Rate-vs-level functions to tone bursts at the characteristic frequency (CF) showed a significant increase in maximum firing rates in both high- and low-SR fibers from synaptopathic regions. Response rates to broadband maskers were also significantly increased in high-SR fibers from synaptopathic regions, but increases in noise levels required to mask the responses to tone bursts at CF presented 30 dB above threshold were not statistically significant.

These data suggest that the nature of the synaptic damage in noise-exposed mice is more complicated than originally proposed and may be different in important respects from that seen in guinea pigs or gerbils. It also appears that noise-induced hyperexcitability, well studied in the auditory CNS, can also be seen at the level of the auditory nerve.

PS 74

Targeting Alpha-Tubulin Acetylation in Spiral Ganglion Neurons for the Treatment of Hearing Loss.

Victor Wong[1]; David Goldberg[1]; Wilfredo Medllado[1]; Brett Langley[2]; Dianna Willis[1]
[1]Weill Cornell Medicine / Burke Neurological Institute; [2]University of Waikato

Deafness is the most common sensory disorder, affecting 2 out of every 1000 children and half of the population over the age of 60. Continuous wear and tear, and increasing exposure to environmental insults (e.g. noise) and aging result in hearing loss. The degeneration of these neurons' innervation of the cochlea hair cells severely compromises efforts for functional recovery of hearing. Both the success of cochlear implants and of future therapeutic approaches critically depend on the integrity of spiral ganglion neurons (SGNs), and the availability of functional neurites for direct stimulation. It was previously demonstrated that microtubule (MT) stability is regulated by post-translational modifications of β-tubulin, which can alter MT stability, intracellular transport, and neurite growth. In particular, β-tubulin acetylation is an attractive target, since β-tubulin acetylation-promoting drugs have been found to increase neurite growth in injured neurons, and promote movement of intracellular cargoes. β-Tubulin acetylation and deacetylation are mediated by β-tubulin acetyltransferase (βTAT1) and histone deacetylase 6 (HDAC6) respectively, and are attractive targets to change acetylation levels. We hypothesized that by promoting β-tubulin acetylation of MTs in SGNs will increase transport of mitochondrial and mRNA cargoes, enhancing survival and regeneration of the axons exposed to excitotoxic insult or aging, and thus improving neurological function after injury. We verified that βTAT1 and HDAC6 are expressed in SGNs *ex vivo*. Moreover, we found robust levels of acetylated β-tubulin in the mouse cochlea, as well as in dissociated cultured SGNs. We further measured the basal neurite β-tubulin acetylation, HDAC6, and βTAT1 levels. Treatment with tubastatin A, a specific HDAC6 inhibitor, in SGNs promotes neurite growth *ex vivo* under basal conditions, suggesting that this may be a relevant target to promote neurite regeneration following damage. We further found that nicotinamide riboside (NR) has pleiotropic effects by increasing β-tubulin acetylation in cortical neurons *in vitro*, and NR has been previously established to protect mice from noise-induced hearing loss. Our data demonstrated that NR treatment increases β-tubulin acetylation and SGN neurite lengths in both explanted and dissociated SGNs under basal conditions. Interestingly, the use of

an indirect βTAT1 inhibitor, 5Z-7-Oxozeaenol, in cultured SGNs shows a dose-dependent decrease in β-tubulin acetylation, and a concomitant decline in neurite outgrowth. Further studies are underway, using SGNs under pathological conditions, to examine the tantalizing possibility of restoring MT stability via β-tubulin acetylation as a means to repair SGNs after injury and aging.

Auditory Prostheses I

PS 75

Influence of Electrode to Cochlear Duct Length Ratio on Post-Operative Speech Understanding Outcomes

Shayna Cooperman[1]; Ksenia A. Aaron[2]; Emma Tran[1]; Nikolas Blevins[2]; Matthew B. Fitzgerald[2]
[1]Stanford University School of Medicine; [2]Stanford University

While cochlear implants have proven to be beneficial, there remains considerable variability in patient outcomes. One variable that may affect patient outcomes is the electrode to cochlear duct length ratio (ECDLR). The size of the cochlea has been reported to range from ~25 to ~across patients, and may even vary with ethnicity. Variance in ECDLR may be relevant because an electrode of a given length will stimulate different regions of the cochlea across individuals. This can alter the frequency-to-place relationship between the frequency table of their speech processor and their neural tonotopic map. In this study, we examine the extent to which speech understanding outcomes vary with ECDLR. We examined pre-operative CT scans of patients who received either a Med-El Flex 24 mm, 28 mm or 31 mm cochlear implant electrode at our clinic within the last 15 years (N=157). To estimate cochlear duct length (CDL), we obtained OtoPlan, a tablet-based program from Med-El and CAScination, which creates a validated measurement of the cochlea given the identification of the cochlear modiolus, basal turn, and cochlear height, as well as the location of round window and lateral wall. We then examined post-operative AzBio Quiet and CNC Words scores, taken at the time point closest, or equal, to 12 months post-implantation. Our goal is to determine how performance on these audiologic measures are influenced by the ECDLR. We are particularly interested in individuals with especially small or large cochleae, as these individuals may be at greater risk for suboptimal outcomes, and could theoretically benefit most from a customized electrode length. Our preliminary results suggest similar speech recognition scores regardless of electrode length. Our hypothesis is that the ratio of electrode length and CDL (ECDLR) will have a weak relationship to speech recognition scores, with a stronger influence in individuals with particularly small or large cochlea. These data will add to a small but growing body of work that can help surgeons and audiologists maximize positive outcomes in their patients by better accounting for anatomical variation between individuals.

PS 76

Coatings for Cochlear Implants: How Protective Properties Depend on Cross-linking

Ryan Horne[1]; Megan J. Foggia[2]; Linjing Xu[2]; Bradley Jones[3]; C. Allan Guymon[4]; Marlan R. Hansen[5]
[1]University of Iowa Carver College of Medicine; [2]University of Iowa Hospitals and Clinics, Department of Otolaryngology--Head and Neck Surgery; [3]University of Iowa Microbiology and Immunology; [4]University of Iowa Departments of Chemical and Biochemical Engineering; [5]University of Iowa Hospitals and Clinics - Department of Otolaryngology-Head & Neck Surgery

Background
A cochlear implant stimulates the inner ear via a platinum electrode housed in a silicone rubber material called poly(dimethyl siloxane) (PDMS). Following implantation, these materials trigger the immune system to create a fibrotic response, which attenuates the effectiveness of the implant and disrupts residual inner ear function. Occasionally, these materials are also the site of serious peri-operative infections. In an attempt to address these issues, our lab has developed a thin film that covalently attaches to PDMS and platinum surfaces, exhibiting reductions in fibrotic activity and bacterial adhesion. This film is called a hydrogel because of its crosslinked network of hydrophilic polymer chains. Crosslinking is provided by the monomer poly(ethylene glycol dimethacrylate) and the hydrophilic polymer chains are composed of sulfobetaine methacrylate (SBMA) or carboybetaine methacrylate (CBMA). The crosslinks provide the durability of the film, whereas the hydrophilic polymer chains imbibe the critical anti-adhesion properties. Crucial to a successful film is understanding how varying the composition of crosslinker affects the desired anti-adhesion properties.

Method
PDMS was coated by polymerizing SBMA and CBMA monomers using various concentrations of the photoinitiator benzophenone. This process resulted in zwitterionic hydrogels of various cross-link densities covalently photografted to the PDMS surface. Protein adsorption and cell adhesion were assessed to evaluate the relationship between cross-link density of zwitterionic polymers and their anti-fouling properties. Human fibrinogen was exposed to pSBMA and pCBMA coated and uncoated PDMS substrates. Epifluorescent microscopy was used to measure protein adsorption.

Results
The protein adhesion to thin hydrogel films changed dramatically as the starting crosslinker concentration was changed, particularly at the extremes of film composition. We found that pure zwitterionic monomer films alone or pure crosslinker films alone gave poor protein protection to PDMS surfaces, with protein build-up similar to PDMS alone. However, in small PEGDMA crosslinker concentrations of 2-13%, thin films reduced undesired protein adhesion 90%. In this range, PEGDMA concentration can be varied with no noticeable effect on protein adhesion. However, at moderate concentrations (13-67%) of PEGDMA crosslinker, protein adhesion gradually increases with increasing PEGDMA concentration. Interestingly bacteria adhesion seems to exhibit an opposite trend; that is, more PEGDMA in the hydrogel film leads to less bacteria adhesion.

Conclusion
A small but non-zero amount of PEGDMA crosslinker in the range of 2-13% gives excellent anti-adhesion properties to a zwitterionic hydrogel composed of the zwitterionic monomers CBMA or SBMA.

PS 77

Molecular Pathways Activations Following Insertion Trauma and Chronic Cochlear Implantation

Melissa Urbain[1]; Florence François[2]; Jean Charles Ceccato[3]; Jean-Luc Puel[4]; Frederic Venail[5]
[1]Institute for Neurosciences of Montpellier - INSERM U1051; [2]INSERM-UMR; [3]University of Montpellier & Institute for Neurosciences of Montpellier - INSERM U1051; [4]Institute for Neurosciences of Montpellier; [5]University Hospital of Montpellier & Institute for Neurosciences of Montpellier - INSERM U1051

Fibrosis is the final step of an inflammatory process caused by an extracellular matrix secretion and myofibroblasts proliferation.

Cochlear fibrosis is a common repair mechanism occurring after cochlear implantation. Overgrowth of fibrotic tissues can alter the functioning of cochlear implant, but also promote to the loss of residual hearing. To date, little is known about the molecular pathways involved during cochlear fibrosis.

In this present study, we compared the molecular activation following insertion trauma and chronic implantation with a dedicated rodent cochlear implant array.

Female Wistar rat either received an insertion trauma with a rodent specific array (Cochlear Ltd) or were chronically implanted with the same specific array under anesthesia. Cochleae were harvested 1, 4, 7, 28 and 56 days after surgery and processed either for RNA extraction (TRIzol Ambion, cDNA construction (RT2 first strand cDNA kit-Qiagen) followed by qPCR (RT2 profiler-PARNZ-120, Qiagen and Roche lightcycler 480), or immunohistochemistry after embedding in OCT and cutting using a microtome (Leica).

Cochlear implantation and insertion trauma led to a significant overexpression of several inflammatory associated protein such as CCL3 CCL 11 et CCL 12 and IL1b (fold change 9.6, 12.99, 3.46 and 2.94 at 1 month respectively for insertion trauma and fold change 15.41, 4.75, 2,14 and 6.15 respectively for cochlear implant).

Metalloproteases (MMPs) were also overexpressed under both conditions such as MMP3 (fold change 4.43 for trauma insertion and 2.18 for cochlear implant), MMP9 and MMP2 for chronic implantation only (fold change at 1day 2.82 and 2.27 respectively). The inhibitors of MMPs were also overexpressed, such as TIMP-1 in both conditions, whereas TIMP-4 was strongly underexpressed.

After chronic implantation, we observed activation of Smad-dependant pathway through the overexpression of TGFb, Smad3, Smad4, Smad6 and Smad 7 at different timepoints (fold change 3.40, 2.70, 3.00, 2.35, 2.92 respectively). Activation of Smad-independent pathways are also observed with chronic implantation via an overexpression of CTGF, PDGFa and PDGFb, VEGFa, EGF, HGf and Akt with a fold change between 2 and 3.5 at different timepoints.

The activation of TGF-Smad, MAPK/ERK and PI3K/Akt signaling pathways were not observed with an insertion trauma.

To conclude, insertion trauma and chronic implantation trigger common, but also specific pathways that could lead to fibrotic proliferation after cochlear implantation. The effect of electrical stimulation on fibrotic proliferation will be studied in a future work.

PS 78

Zwitterionic Coatings Reduce the Inflammatory Foreign Body Response to Cochlear Implant Biomaterials

Megan J. Foggia[1]; Jamison Chamberlain[2]; C. Allan Guymon[2]; Marlan R. Hansen[3]
[1]University of Iowa Hospitals and Clinics, Department of Otolaryngology--Head and Neck Surgery; [2]University of Iowa Departments of Chemical and Biochemical

Engineering; [3]University of Iowa Hospitals and Clinics - Department of Otolaryngology-Head & Neck Surgery

Introduction

Cochlear implants (CIs) have been used for auditory rehabilitation for the past 30 years. While CIs are considered biocompatible with low complication rates, it is well-known that a foreign body response (FBR) occurs after CI. Ultra-low fouling zwitterionic polymers, including sulfobetaine methacrylate (SBMA) and carboxybetaine methacrylate (CBMA), are a class of materials that show promise to eliminate the FBR. These net neutral, hydrophilic polymers recruit a layer of hydration to their surface making adsorption of any other molecules energetically unfavorable. With the application of cross-linking molecules, the zwitterionic monomers SBMA and CBMA form linear polymers that can be polymerized to implant surfaces. The concentration of the cross-linker determines the physical and surface properties of the polymer thin film; however, it is not clear to what extent the cross-link density of the thin-film influences the anti-fouling properties. Here we examine the relationship between cross-link density of zwitterionic thin films and their anti-fouling properties and durability.

Methods

To determine how cross-link density of zwitterionic thin films affects their anti-fouling properties, polydimethylsiloxane (PDMS) substrates were coated with zwitterionic polymers with a range of high to low cross-link densities. Uncoated substrates were used as controls. The substrates were cultured with bone marrow derived macrophages for 7 days or cochlear fibrocytes for 48 hours followed by immunostaining with anti-CD68 antibody and anti-vimentin antibody, respectively. Cell count was scored using epifluorescent microscopy. To determine how cross-link density affects *in vivo* durability of the coatings, SBMA-coated implants were placed subcutaneously in mice for 6 weeks and then explanted. Fibroblasts were then cultured on the explanted substrates and compared to PDMS substrates that had never been implanted. After 7 days, cell count was scored as above. Scanning electron microscope images were taken of each substrate at the varying cross-link densities to confirm the durability of the coatings. Finally, histological analysis (hematoxylin and eosin/Masson's trichrome staining) was performed on the tissue surrounding the coated and uncoated implants.

Results

Generally speaking, the anti-fouling properties of the zwitterionic thin films decreased with increasing cross-link density. The zwitterionic thin films were durable and maintained their anti-fouling properties after 6 weeks *in vivo*. Histologic analysis demonstrates that zwitterionic thin films reduce the FBR *in vivo*.

Conclusion

Zwitterionic thin films reduce the FBR to implanted biomaterials and are durable after 6 weeks *in-vivo*. The cross-link density of the thin films affects their anti-fouling properties. Zwitterionic thin films show promise in reducing the FBR in the cochlea following CI.

PS 79

The Response of Macrophages to Cochlear Implant Biomaterials

Megan J. Foggia[1]; Timon Higgins[2]; Linjing Xu[1]; C. Allan Guymon[3]; Marlan R. Hansen[4]
[1]University of Iowa Hospitals and Clinics, Department of Otolaryngology--Head and Neck Surgery; [2]University of Iowa Carver College of Medicine; [3]University of Iowa Departments of Chemical and Biochemical Engineering; [4]University of Iowa Hospitals and Clinics - Department of Otolaryngology-Head & Neck Surgery

Introduction

Cochlear implants (CIs) are composed of platinum-iridium electrodes encased in a polydimethylsiloxane (PDMS) carrier. It is well known that a foreign body response (FBR) occurs within the cochlea in response to CI. Macrophages play a significant role in the FBR within the cochlea. Although the FBR is a well-known phenomenon, the details of the response of macrophages to CI biomaterials remains unclear. Here we investigate the response of macrophages to platinum and PDMS in the inflammatory FBR.

Methods

To compare macrophage growth on platinum versus PDMS, murine bone marrow derived macrophages (BMDMs) were cultured on platinum and PDMS substrates for 7 days and then incubated with F4/80 antibody. Cell count was scored using epifluorescent microscopy. Cell proliferation was assessed by culturing BMDMs on platinum and PDMS substrates as above followed by incubation of the cells in 5-Ethynyl-2´-deoxyuridine (EdU) for 2 hours and immunostaining with F4/80 antibody. Cell proliferation was assessed by analyzing the percentage of EdU positive cells using fluorescent microscopy. Cytokine expression was then measured using cell medium from each condition and a macrophage cytokine array. To assess macrophage adhesion, BMDMs were cultured on platinum and PDMS substrates for 4 hours, then placed on a rotary shaker for 5 minutes, 15 minutes, or 25 minutes. The substrates were then incubated with anti-phosphorylated focal adhesion kinase antibody and the percent of cells that remained adhered to each surface was scored. To determine the response to CI biomaterials *in vivo*, platinum and PDMS substrates were placed subcutaneously in mice

and explanted after 6 weeks. Histological analysis was performed on the tissue surrounding the explants. Finally, platinum wire and PDMS-coated platinum wire were placed in the round window of CX3CR1$^{+/GFP}$ mice and left *in vivo* for varying time points followed by histologic analysis of CX3CR1-GFP invasion into the cochlea.

Results
Macrophage count and proliferation was significantly greater on platinum relative to PDMS. More macrophages attached to platinum than PDMS. However, macrophages were more easily displaced from the platinum substrates relative to the PDMS. There was no significant difference in cytokine expression between the two groups. Histology from the subcutaneous implants demonstrated a more robust fibrous capsule surrounding the PDMS compared to the platinum. Results of the intracochlear sections are pending.

Conclusion: Macrophage behavior differs on PDMS versus platinum, the two components of the CI. A better understanding of the response of macrophages to CI biomaterials may help mitigate the inflammatory FBR within the cochlea.

PS 80

Characterization of the Human Helicotrema: Implications for Cochlear Duct Length and Frequency Mapping

Luke Helpard[1]; Hao Li[2]; Helge Rask-Andersen[2]; Sumit Agrawal[3]; Hanif Ladak[3]
[1]Western University, School of Biomedical Engineering; [2]Uppsala University; [3]Western University

Background
Despite significant anatomical variation amongst patients, cochlear implant frequency-mapping has traditionally followed a patient-independent approach. Basilar membrane (BM) length is required for patient-specific frequency-mapping, however cochlear duct length (CDL) measurements generally extend to the apical tip of the entire cochlea or have no clearly defined end-point. By characterizing the length between the end of the BM and the apical tip of the entire cochlea (helicotrema length), current CDL models can be corrected to obtain the appropriate BM length. Synchrotron radiation phase-contrast imaging has made this analysis possible due to the soft-tissue contrast through the entire cochlear apex.

Methods
Helicotrema linear length and helicotrema angular length measurements were performed on synchrotron radiation phase-contrast imaging data of 14 cadaveric human cochleae. On a sub-set of six samples, the CDL to the apical tip of the entire cochlea (CDL_{TIP}) and the BM length (CDL_{BM}) were determined. Regression analysis was performed to assess the relationship between CDL_{TIP} and CDL_{BM}.

Results
The mean helicotrema linear length and helicotrema angular length values were 1.6±0.9 mm and 67.8±37.9 degrees, respectively. Regression analysis revealed the following relationship between CDL_{TIP} and CDL_{BM}: $CDL_{BM}=0.88(CDL_{TIP})+3.71$ ($R^2=0.995$).

Conclusion
This is the first known study to characterize the length of the helicotrema in the context of CDL measurements. It was determined that the distance between the end of the BM and the tip of the entire cochlea is clinically consequential. A relationship was determined that can predict the BM length of an individual patient based on their respective CDL measured to the apical tip of the cochlea.

PS 81

Voltage Distribution in the Facial Nerve Canal with Intracochlear Cochlear Implant Stimulation: a Human Cadaver Study

Simone R. de Rijk; Chen Jiang; Manohar Bance
Department of Clinical Neurosciences, University of Cambridge

Facial nerve stimulation (FNS) is one of the known complications of cochlear implants (CI). The reported prevalence of FNS varies between 3% and 7%. (Kelsall et al. 1997, Smullen et al. 2005, Pires et al. 2018) Several theories of the pathophysiology of FNS for CI users have been proposed, including a low resistance pathway between cochlear bone and the facial nerve due to otosclerosis or cochlear malformations. (Smullen et al. 2005, Pires et al. 2018) It is suggested that the current-induced voltage permeates directly through the cochlear bone, supported by findings of mid-array electrodes being associated with FNS. (Smullen et al. 2005) However, the exact mechanism behind FNS remains unclear. It is likely to be a combination of nerve stimulation thresholds at different parts of the facial nerve, and the voltage experienced at different segments of the facial nerve. To start understanding the mechanisms and FNS-associated risk factors, we investigated the voltage distribution at the facial nerve by directly measuring the intracochlear current-induced voltage waveforms along the facial canal in human cadaveric heads.

Fresh-frozen human cadaveric heads were implanted with clinical CI's of lateral-wall design. The cochlea

was flushed with 1.0% saline, by inserting a catheter through the round window, prior to implantation. The facial nerve was exposed, and an electrode array was placed along the facial nerve canal, reaching from the geniculate ganglion to the lower vertical segment. The CI was stimulated with pulses and the subsequent voltage waveforms were recorded along the facial canal electrode. The peak-to-peak and total voltage (PPV and TV) was analysed for all combinations of stimulating and recording electrodes.

Stimulation of basal intracochlear electrodes led to a higher PPV and TV, compared to stimulation of apical intracochlear electrodes. The location along the facial canal with the largest induced voltage was found between the cochleariform process and the short process of the incus. No difference was seen between biphasic and triphasic stimulation.

This study helps to further understand the distribution of intracochlear current-induced voltage along the facial nerve. The finding of basal intracochlear electrodes leading to the largest voltage waveform responses in the facial canal, compared to the finding of FNS being most commonly associated with stimulation of mid-array intracochlear electrodes, emphasizes the need for further research into the pathophysiology behind FNS. Future work will include mimicking pathologies associated with FNS, as well as incorporate the characteristics of the facial nerve into our measurements.

PS 82

Evaluating the Efficacy of a Novel Compound in Providing Otoprotection using an in vitro Model of Electrode Insertion Trauma

Viraj Shah; Jeenu Mittal; David Shahal; Priyanka Sinha; Erdogan Bulut; Rahul Mittal; Adrien A. Eshraghi
Department of Otolaryngology, University of Miami Miller School of Medicine

Introduction
Cochlear implants (CI) are widely used to provide auditory rehabilitation to individuals having severe to profound hearing loss. However insertion of electrode leads to inner trauma and activation of inflammatory and apoptotic signaling cascades resulting in loss of residual hearing in implanted individuals. Pharmaceutical interventions that can target these signaling cascades holds great potential to preserve residual hearing by preventing sensory cell damage. The objective of this study was to determine whether the identified compound can prevent sensory cell damage employing an *in vitro* model of electrode insertion trauma (EIT).

Materials and Methods
The organ of Corti (OC) explants were dissected from P-3 rats and placed in serum-free media. Explants were divided into control and experimental groups: 1) untreated controls 2) EIT 3) EIT+ identified compound (different concentrations). In EIT groups, a 0.28-mm diameter monofilament fishing line was introduced through the small cochleostomy located next to the round window area, allowing for an insertion of between 110° and 150°. After EIT was caused, explants were cultured in media containing different concentrations of compound. After incubation, the explants were fixed and stained with FITC-phalloidin, imaged by fluorescence microscopy, and viable hair cells (HCs) were counted.

Results
In EIT group, there was significant loss of HCs. Intriguingly, treatment with the identified compound provided significant otoprotection against HC loss in a dose dependent manner. The molecular mechanisms underlying otoprotection involved decrease in oxidative stress, lower production of proinflammatory cytokines and abrogation of generation of cleaved caspase 3.

Conclusions
The results of the present study suggests that the identified compound provides otoprotection against EIT and should be explored for developing pharmaceutical interventions for preservation of residual hearing post-CI. The availability of novel effective treatment modalities to prevent loss of residual hearing will lead to improved quality of life of many implanted patients and their families.

PS 83

Evaluating the Efficacy of New Otoprotective Drugs for Cochlear Implantation Trauma with or without Electrical Stimulation using in vitro and in vivo Models.

Adrien A. Eshraghi[1]; Jeenu Mittal[1]; Viraj Shah[1]; David Shahal[1]; Erdogan Bulut[1]; Carolyn Garnham[2]; Hannah Marwede[1]; Jorge Bohorquez[3]; Rahul Mittal[1]
[1]Department of Otolaryngology, University of Miami Miller School of Medicine; [2]MED-EL Hearing Implants, Innsbruck, Austria; [3]Department of Biomedical Engineering, University of Miami

Introduction
Cochlear implantation (CI) is widely used to provide auditory rehabilitation to hearing impaired individuals. While there is a trend to implant patients with residual hearing, CI may cause some loss of this residual hearing. The direct effect of implantation of the electrode in affecting macroscopic structures of the inner ear is well described. However, the effect of the electrical field

generated by the implant on the residual hearing and cochlear damage is not well-known. Developing *in vitro* and *in vivo* models of CI trauma with electrical stimulation, which closely mimics human clinical conditions will help in understanding the contribution of electrical stimulation in cochlear damage and loss of residual hearing.

Methods

A custom stimulator circuit that allows to study several parameters, including stimulation amplitude, pulse width, and total stimulation duration was designed. 1) For *in vitro* model, the organ of Corti explant cultures from postnatal day three (P3) rats were used and placed in microchannel slide (Ibidi, GmbH) in the incubator and exposed to stimulation or left unstimulated. Parameters (amplitude, pulsewidth and duration) were changed one at a time. The organ of Corti explants were subjected to FITC phalloidin staining to visualize hair cells using confocal microscopy. The number of surviving hair cells were counted. 2) For *in vivo*, we assessed the contribution of electrical stimulation in the loss of residual hearing and cochlear damage employing a preclinical guinea pig model of CI. Implanted guinea pigs were subjected to electrical stimulation or left unstimulated. Hearing thresholds were determined by auditory brainstem recordings (ABRs), eABRs and distortion product otoacoustic emissions (DPOAEs) at different days post-implantation. The whole cochleae harvested from stimulated and unstimulated animals were also subjected to CellROX and cleaved caspase 3 staining to determine the levels of oxidative stress and apoptosis, respectively. Three drugs were tested for their efficacy to provide otoprotection for CI trauma with and without stimulation in these models.

Result

In vitro testing suggests that the electrical stimulation may cause some damage to hair cells, mainly with higher stimulation levels and longer times of stimulation. On par with *in vitro* findings, spiral ganglion neurons and number of hair cells were decreased in guinea pig model of CI subjected to EIT and electrical stimulation compared to control and EIT alone. There were high levels of oxidative stress in EIT + electrical stimulation compared to control and EIT alone. We observed an increase in ABR threshold shifts and DPOAE amplitudes in the stimulated CI group compared to unstimulated implanted animals at all frequencies and time-periods. Our preliminary results suggest that two out of three identified otoprotective compounds provide protection against loss of hair cells in response to CI trauma and/or electrical stimulation**.**

Conclusion

The stimulator circuit we designed and constructed very closely simulates the electrical field of a cochlear implant. It has enough task flexibility to be used in *in vitro* and *in vivo* models of electrical stimulation. The *in vitro* and *in vivo* models developed in this study using electrical stimulation can be used to understand the effect of electrical field on inner ear sensory cells and to screen otoprotective drugs for the preservation of residual hearing post CI.

PS 84

Comparative Analysis of Post-Surgical Fibrosis in the Implanted Ear

Donald L. Swiderski; Deborah J. Colesa; Jenna Devare; Bryan E. Pfingst; Yehoash Raphael
Kresge Hearing Research Institute, Department of Otolaryngology-Head and Neck Surgery, University of Michigan

Bone and fibrous tissue in the scala tympani are common findings in cochlear implant (CI) patients and animal studies. Because these ectopic tissues have higher impedances than perilymph, it is possible they may alter implant function. There also is concern that the tissues contribute to hair cell loss, diminishing residual acoustic hearing, or neuron loss, diminishing implant-aided hearing. In guinea pigs, we found variation of intrascalar tissue development among animals that received implants under identical experimental conditions (deafening, neurotrophin treatment and surgical protocol), demonstrating effects of additional factors. Newly developed mouse CI protocols in our laboratory provide an opportunity to investigate genetic and molecular factors that might influence intrascalar tissue growth and to develop protocols to regulate it. In this study, we compared tissue growth in several mouse models to that observed previously in guinea pigs: (a) mice with a DTR gene insert driven by the *Pou4f3* promoter (Golub et al., 2012) deafened with a single systemic injection of DT, (b) non-deafened DTR mice, and (c) wild type mice from the same line. The mice were implanted with either a single channel or a multichannel implant and observed for up to 16 weeks. After termination, temporal bones were decalcified, embedded, and sectioned along a peri-mid-modiolar plane through the estimated location of the electrode. Tissue growth in the scala tympani of the implanted mice was compared to data from previous guinea pig studies, which included implanted-hearing ears, neomycin-deafened ears, and neomycin-deafened ears treated with neurotrophin. In mice, as in guinea pigs, different levels of tissue were observed among animals receiving identical implants under equivalent conditions. Implants completely enveloped in bone were seen in implanted-hearing (non-deafened) animals of both species, but were more common in the mice than in the guinea pigs. This difference could reflect differences between species or implants. In both species, the highest degree of intrascalar tissue growth was more

common in deafened than in non-deafened animals, which could reflect priming of the immune system by the prior trauma. These results show that implanted mice are potentially useful for investigating reactions of the inner ear to CI surgery, identifying molecular pathways leading to fibrosis and new bone formation, and testing potential means to prevent or reverse these reactions.

This study was funded by NIH NIDCD grant R01 DC015809 (BEP) and the American Academy of Otolaryngology - Head & Neck Surgery (JD).

PS 85

Long-term effects and potential limits of intratympanic dexamethasone-loaded hydrogels combined with dexamethasone-eluting cochlear electrodes in a guinea pig model

Navid Ahmadi[1]; Julia Clara Gausterer[2]; Clemens Honeder[1]; Christoph Arnoldner[1]
[1]Department of Otorhinolaryngology, Head and Neck Surgery, Medical University of Vienna, Vienna, Austria; [2]Department of Pharmaceutical Technology and Biopharmaceutics, University of Vienna, Vienna, Austria

Aim
Investigating the protective effects of a dexamethasone (Dex)-eluting electrode combined with the preoperative intratympanic application of a Dex-loaded hydrogel over a period of 4 months in a guinea pig (GP) cochlear implantation (CI) model.

Methods
40 normal hearing GPs were equally randomized into 4 groups: a control group receiving an unloaded hydrogel and a non-eluting electrode, a group treated with a Dex-loaded hydrogel and a non-eluting electrode, a group treated with an unloaded hydrogel and a Dex-eluting electrode and a group treated with both a Dex-loaded hydrogel and a Dex-eluting electrode. Residual hearing and impedances were frequently measured. Histological changes in the cochlea were analyzed.

Results
A significant protective effect of Dex treatment on residual hearing could not be observed in any of the groups. In the majority of cochleae investigated no signs of electrode insertion trauma (EIT) were observed. However, a small degree of tissue response could be detected in all animals without reaching significance between groups. A significant association between foreign body giant cells and osteogenesis could be observed. Hair cells, synapsin-1-positive cells and spiral ganglion cells were preserved in all groups. 4 months after CI, auditory nerve fibers were significantly protected by using Dex-eluting electrode alone and in combination with Dex-loaded hydrogel. Post-implantation impedances remained stable during the whole study period and did not exhibit a significant difference between the groups.

Conclusions
Auditory nerve fibers can be protected by using a Dex-eluting electrode alone and in combination with intratympanic application of a Dex-loaded hydrogel. The study has shown that -despite of the almost undetectable EIT in most of the animals- it may not be possible to completely prevent cochlear implantation-associated hearing threshold shift and tissue response by the application of Dex alone.

PS 86

Electrical Stimulation in the Cochlea: Influence of Microstructures inside the Modiolar Bone

Siwei Bai[1]; Jörg Encke[2]; Frank Böhnke[1]; Werner Hemmert[1]
[1]Technical University of Munich; [2]University of Oldenburg

Computational studies of cochlear implants have demonstrated that the structural detail of three-dimensional (3D) cochlear models exerts major influence on the current spread within the cochlea. Nevertheless, existing models still lack many important features, including the microstructures inside the modiolar bone, which in turn affects the reconstruction of the auditory nerve fibres (ANFs).

We reconstructed a 3D model of the implanted human cochlea from high-resolution micro-CT scans, in which the intricate microstructures inside the modiolar bone was meticulously captured. Using the finite element method, we calculated the electrical potential along the auditory nerve, which was elicited by cochlear implant electrodes. We then developed an algorithm to reconstruct individual ANFs running through the microstructures within the 3D cochlear model. Electrical potential along each ANF was extracted and smoothed to calculate the first and second spatial derivatives of potential along the fibres. In addition, comparison was made with a simplified model that neglected the microstructure within the cochlea.

When the stimulus was delivered from an electrode located deeper in the apex, the area of the auditory nerve influenced by a higher electric potential grew larger; at the same time, the maximal potential value at the auditory nerve also became larger. The electric potential decayed at a faster rate towards the base of the cochlea than towards the apex. Compared to the

cochlear model incorporating the microstructures in the modiolar bone, the simplified version resulted in relatively small differences in electric potential. However, in terms of the first and second spatial derivatives of electric potential along the fibres, which are relevant for the initiation of action potentials, the two models exhibited drastic differences: maxima in both derivatives with the detailed model were larger by a scale factor of 1.5 (first derivative) and 2 (second derivative). Maxima also occurred at different locations between the two models.

In conclusion, it is important to obtain a detailed-segmented cochlear model for the reconstruction of the path of the ANFs through the modiolus. Although a cochlear model with fewer details seems sufficient for analysing the current spread in the cochlear ducts, a detailed-segmented cochlear model is required for the prediction of firing thresholds and spike initiation sites.

PS 87

Modelling the human cochlear length and clinical cochlear length measurements: Consequences for CI length selection

Marcus Müller; Pia Glang; Thore Schade-Mann; Fritz Schneider; Anke Tropitzsch; Hubert Löwenheim
Tübingen Hearing Research Centre, Department of Otolaryngology-Head & Neck Surgery, Eberhard Karls University Tübingen, Germany

Matching the individual cochlear length and cochlear implant (CI) length has become more feasible with variable CI-array length today available. This allows to match the individual frequency map with the implant's stimulation map, which is an obvious approach. Electrode contact position and electrode length should be individually adapted to the cochlear anatomy which varies (literature data) between 30 and 44 mm (cochlea length along the outer lateral wall, LDC-LW). The radiologically measured A-value (longest distance between the round window and the opposite cochlear wall in the basal turn) has been suggested to be a reliable basis for cochlear length calculation. To test this, the CT and MR images of several hundred Tübingen CI-patient ears were retrospectively evaluated. The A-value was between 8 and 10 mm, a LDC-LW value of 31- 44 mm was determined by 3D reconstruction. The calculated LDC-LW derived from the A-value and the length measured by 3D reconstruction correlated significantly well. Therefore, the A-value serves the purpose described above. The course of LDC-LW was modelled using a logarithmic spiral and compared to the course determined from the 3D measurements in the radiological images. Using these models, a frequency map for the CI contacts based on literature data (Greenwood, Schuknecht and pitch-matching) is calculated.

This work was supported by the Deutsche Forschungsgemeinschaft (DFG-LO 679/3-1) and the University Tübingen (IZKF).

PS 88

Macrophage Response to Low- and High- Current Level Cochlear Electric Stimulation in CX3CR1+/GFP Mice

Rene Vielman Quevedo[1]; Alexander D. Claussen[1]; Brian Mostaert[1]; Jonathon R. Kirk[2]; Marlan R. Hansen[1]
[1]University of Iowa Hospitals and Clinics - Department of Otolaryngology-Head & Neck Surgery; [2]Cochlear Limited, Sydney, Australia

Introduction

Cochlear implants (CI) are an established tool for the treatment of hearing loss, and in cases where the patient has residual low-frequency hearing, the use of hybrid CIs can lead to successful outcomes. There is an important subset of the hybrid CI user population that experiences post-implantation loss of residual hearing (Scheperle, et al. 2017; Kopelovich, et al. 2014). These delayed changes are correlated with an increased tissue response, including inflammation, fibrosis and osteoneogenesis (Quesnel, et al. 2016) and can also affect outcomes in traditional cochlear implantation (Kamakura & Nadol, 2016). Building on past work, this study observed the effect electrical stimulation has on the inflammatory response at different current levels (CL).

Method

Normal hearing CX3CR1$^{+/GFP}$; Thy1^{YFP}/C57Bl6 adult (10-12 week old) mice were unilaterally implanted with a percutaneously connected 3-channel CI electrode array (Cochlear, Australia). Subjects received 4 hrs of monopolar stimulation per day via an implant emulator (Cochlear, Australia) coupled to a custom tethered setup from post-op day 7 (switch-on). Device programming was based on neural response telemetry (NRT) and observed behavioral response threshold; device integrity was monitored using regular impedance measurements (Custom Sound EP 4.2, Cochlear, Australia). Subjects were sacrificed at post-op day 7, 8, 11, and 14 (n=3 per time-point). An additional group had sham surgery performed, euthanized at post-op days 0, 1, 3, 7, 8, 11, and 14. Unimplanted contralateral ears served as untreated controls. Cochleae were harvested at each time-point and prepared for immunohistochemistry with confocal imaging. The images were analyzed (Imaris, Bitplane, USA) to obtain CX3CR1-GRP+ macrophage and Thy1-YFP+ neuron cell density. Results were compared to past data analyzing acute insertion, chronic implantation with no stimulation and chronic implantation with sub-threshold stimulation.

Results
All implants maintained functional NRT and impedance measures during the entire experiment. An inflammatory response was observed near the insertion site in sham surgery, acute insertion, and all chronically implanted groups. A robust inflammatory response was observed in implanted groups as early as 7 days post-operative. This included a consistent tissue response in the region of the implant and macrophage infiltration within the scala tympani. The greatest increase in cochlear macrophage density was seen in implanted groups, present in the lateral wall, implant-associated tissue response and Rosenthal's Canal.

Conclusion
In the mouse model, cochlear implantation with and without electric stimulation is associated with a heightened inflammatory response with associated macrophage infiltration throughout the cochlea. This may suggest a role for both surgical trauma and foreign body response in post-implantation intracochlear inflammation. Our model provides an opportunity for testing strategies to reduce this post-implantation response.

Auditory Prostheses II

PS 89

Short-term overstimulation elevates eCap- and eABR-thresholds in a different time frame

Dietmar Basta[1]; Susanne Schwitzer[1]; Moritz Gröschel[1]; Horst Hessel[2]; Arne Ernst[1]
[1]Dept. Of Otolaryngology at UKB, University of Berlin, Germany; [2]Cochlear Deutschland GmbH & Co. KG, Hannover, Germany

Changes in map T and C levels have been documented over time in both adults and children. These changes are possibly related to habituation to electrical stimulation and a training effect (Clark et al, 1988), which result in increased tolerance to loudness. However, a widening of eDRs and increasing C-levels are highly important for the postoperative outcome since both are associated with better speech perception scores in quiet and noise (Robinson et al., 2012). This knowledge is possibly responsible for the clinical observation that C-levels and thus, eDRs are sometimes extremely increased over time. However, it is questionable if the larger amount of electrical stimulation is tolerated by the remaining peripheral and central auditory pathway.

A short-term overstimulation could be helpful to investigate the generation of above-mentioned adaptive processes. As a first insight, the effect of a short-term overstimulation on the excitability of peripheral and central auditory structures was determined.

After mechanical deafening of 32 adult guinea pigs a special scala tympani electrode array with eight electrode contacts was inserted. Cochlear overstimulation was performed by adjusting the C-level on 0 CL, around 145 CL, 165 CL or 190 CL (n=8 for each group). All animals were stimulated with a CP810 sound processor in a standardized acoustic environment (radio play at 65 dB SPL) for eight hours under anesthesia. The eCAP and eABR measurements were performed before stimulation and after four and eight hours.

Both, the eCAP- and eABR-thresholds increased over time in the control group (insertion without stimulation) with stable electrode impedances. High overstimulation increased eCAP-thresholds after 4 and 8 h at least in the basal part of the stimulated area. eABR-thresholds were only elevated after 8 h.

The results suggest that mechanical interventions (deafening, insertion of a cochlear implant electrode) induce fast physiological reactions which lead to an eCAP- and in turn to an eABR-threshold shift. Short time overstimulation in the applied range seems to influence the response behavior only in distinct cochlear regions. The position of the electrode will be discussed as one possible explanation for these local effects.

This study was supported by Cochlear Research & Development Ltd., Addlestone, UK.

PS 90

Identifying Neural Dead Regions â€“ A Preclinical Validation Study

James Fallon[1]; Ella Trang[1]; Wolfram F. Dueck[2]; Andrew Wise[1]
[1]Bionics Institute; [2]Cochlear

The degree of neural survival within the cochlea is expected to correlate with speech outcomes; however, the evidence for a correlation is at best weak[1]. Evidence is mounting that it is the variation in neural survival along the cochlea that has a strong influence on speech understanding and that this variation can be probed using highly focused electrical stimulation[2]. So called 'dead regions', regions with relatively poorer neural survival, exhibiting elevated thresholds to focused stimulation, are thought to be the underlying cause; however, this presumption has not been verified. We developed a novel animal model of neural dead regions by noise deafening normal hearing cats (n = 4) to produce a notched hearing loss. After 5 months of degeneration, animals were acutely deafened (to eliminate all hair cell mediated responses) and implanted with the HL14 electrode array. Inferior colliculus thresholds were

determined in response to electrical stimulation using focused multipolar (FMP), tripolar (TP) and monopolar (MP) stimulation. Results showed that there was a significant correlation (Pearson correlation, p's< 0.05) between the difference between focused (FMP or TP) and unfocussed (MP) thresholds and histologically verified regions of neural loss in 7 out of 8 cochleae tested. Finally, we demonstrated that it was possible to use electrically evoked auditory brainstem response thresholds, rather than inferior colliculus thresholds, to predict neural survival, suggesting less invasive, clinically viable objective techniques may be used in the future.

1 Seyyedi, M., Viana, L.M., Nadol Jr, J.B. 2014. Within-Subject Comparison of Word Recognition and Spiral Ganglion Cell Count in Bilateral Cochlear Implant Recipients. Otol Neurotol.

2 Long, C.J., Holden, T.A., McClelland, G.H., Parkinson, W.S., Shelton, C., Kelsall, D.C., Smith, Z.M. 2014. Examining the Electro-Neural Interface of Cochlear Implant Users Using Psychophysics, CT Scans, and Speech Understanding. JARO 15, 293-304.

PS 91

Effects of Advanced Age and Duration of Deafness on Neural Responsiveness of the Electrically-Stimulated Cochlear Nerve in Adult Cochlear Implant Users

Shuman He[1]; William J. Riggs[1]; Jeffrey Skidmore[1]; Chloe Vaughan[2]
[1]The Ohio State University; [2]The Ohio State University, Eye and Ear Institute

Background
Results of histological studies using animals and human post-mortem tissue showed that advanced age and/or a long duration of deafness leads to cochlear nerve degeneration (e.g.; Makary et al., 2011; McFadden et al., 2004; Sergeyenko et al., 2013; Shepherd et al., 2004; Viana et al., 2015; Wu et al., 2019). While age-related or deafness-related decline in functional status of the CN has been evaluated in several animal studies (Nozawa et al., 1997; Sergeyenko et al., 2013; Schmiedt et al., 1996; Shepherd et al, 2004; Shepherd & Javel, 1997), it has not been established in human cochlear implant (CI) users. This study aimed to evaluate the effects of advanced age and a long duration of deafness on neural responsiveness of the CN to single biphasic pulses as well as on the sensitivity of the CN to temporal envelope cues in adult CI users.

Methods
To date, 24 postlingual deaf adult CI users have participated in this study. All participants had a Cochlear ™ Nucleus® device in the test ear. For each participant, the electrically-evoked compound action potentials (eCAP) input/output (I/O) function evoked by a single biphasic pulse were recorded at seven electrode locations across the electrode array. The slope of the eCAP I/O function was estimated using linear regression. For a subgroup of 15 subjects, the accuracy of amplitude modulation (AM) encoding in the CN was evaluated by measuring the eCAP evoked by individual pulses of an AM pulse train at four electrode locations across the electrode array. AM rates tested in this study included 20, 40, 100 and 200 Hz. Effects of advanced age and duration of deafness on the slope of the eCAP I/O function and the AM sensitivity measured at different modulation rates were assessed using Spearman correlation tests.

Results
Our preliminary data showed that advanced age had a significant negative effect on the slope of the eCAP I/O function as well as the AM sensitivities measured at all four rates. Duration of deafness did not show a significant effect on the slope of the eCAP I/O function or the CN's sensitivity to AM cues.

Conclusion
These preliminary results suggest that advanced age is the main factor affecting the functional status of the CN in adult CI users.

Acknowledgments
This work was supported by the R01 grant from NIDCD and NIGMS (1R01DC016038) and the R01 grant from NIDCD (1R01DC017846).

PS 92

Simultaneous Intra- and Extracochlear ECochG Recordings during Cochlear Implantation

Leanne Sijgers[1]; Julian Grosse[2]; Adrian Dalbert[3]; Christof Röösli[3]; Dorothe Veraguth[1]; Alexander Huber[4]; **Flurin Pfiffner**[2]
[1]University Hospital Zurich; [2]1.University of Zürich, Zürich, Switzerland. 2.Department of Otorhinolaryngology, Head and Neck Surgery, University Hospital Zürich, Zürich, Switzerland.; [3]2.Department of Otorhinolaryngology, Head and Neck Surgery, University Hospital Zürich, Zürich, Switzerland.; [4]Department of Otorhinolaryngology, Head and Neck Surgery, University Hospital Zurich, Zurich, Switzerland; University of Zurich, Zurich, Switzerland

Background
Electrocochleography (ECochG) is an objective measure, which can detect changes in cochlear function during cochlear implantation. During insertion of the electrode array, especially if recorded from the tip of the electrode array, the ECochG signal shows complex patterns with amplitude and phase changes. To date it remains controversial which of these changes of the ECochG signal are relevant for trauma or hearing preservation. The aim of this study was to validate intracochlear ECochG recordings with simultaneously recorded extracochlear ECochG recordings. As the extracochlear recording electrode is in a fixed position near the round window, changes of the signal due to movement of the recording electrode will not occur.

Methods
ECochG recordings were obtained from the tip of the CI electrode array and from an extracochlear recording electrode placed on the promontory. Recordings were performed multiple times during insertion. As acoustic stimuli, 500 Hz sinusoid tone bursts at suprathreshold intensities were used. ECochG changes were correlated with hearing preservation 4 weeks after surgery.

Results
An amplitude drop of intra- and extracochlear ECochG signals was associated with a loss of residual hearing. Slowly progressing as well as abrupt phase changes of approximately 180° occur in intracochlear ECochG recordings without a correlate in extracochlear recordings. Amplitude drops during insertion in intracochlear ECochG recordings can be recorded without associated amplitude changes in extracochlear recordings.

Conclusions
Simultaneous amplitude drops in intra- and extracochlear ECochG recordings during insertion of a CI electrode array seem to be associated with gross cochlear trauma, relevant for hearing preservation. Phase changes in intracochlear ECochG recordings may be caused by the movement of the recording electrode.

PS 93

Electrophysiological Characteristics in Children with Auditory Neuropathy Spectrum Disorder

William J. Riggs[1]; Oliver F. Adunka[1]; Shuman He[2]
[1]The Ohio State University; [2]The Ohio State University; Nationwide Children's Hospital

ANSD is a form of hearing loss known to cause deficits in neural encoding processes of temporal properties of auditory signals that are important for speech perception, listening in background noise, and sound source localization (Starr et al. 1991; Rance et al. 2004; Zeng et al. 2005). While these resultant behavioral deficits are well known, the disruptions in underlying neurophysiologic processes that are present in individual patients with ANSD, i.e. those that affect pre-synaptic regions and those that affect post-synaptic regions (Starr et al. 1996; Berlin et al. 2003), are currently unknown. Thus, the diagnosis of ANSD does not provide sufficient information about the specific site of lesion that can be used for clinical patient management. Information, such as post-synaptic injury as reflected by the nerve's inability to recover adequately following a fast rate of stimulation could be highly relevant for clinicians when selecting and optimizing CI parameters (i.e. slower rate) necessary to improve speech perception.

In this study a cohort of pediatric subjects (< 18 years) who are undergoing cochlear implantation are divided into two groups, experimental (diagnosis of ANSD) and control (idiopathic hearing loss). Intraoperative round window electrocochleography (ECochG) and post-operative electrical compound action potential (eCAP) testing are performed. Using a combined testing paradigm of acoustic and electric stimulation, two auditory nerve temporal response properties will be evaluated, adaptation and recovery from adaptation. Preliminary ECochG and eCAP response findings will be discussed. Determining the underlying site of injury and subsequent neurophysiological deficits in children with ANSD will provide clinicians with objective evidence to aid in selecting optimal intervention and habilitation strategies as well as can serve as an aid when counseling patients and families about the hearing loss. This work is supported by the Hearing Health Foundation and the NIH/NIDCD-Loan Repayment Program.

PS 94

Simulated nerve responses to cochlear implant stimulation based on three-dimensional micro-CT reconstruction of an human auditory nerve

Thomas Potrusil[1]; Amirreza Heshmat[1]; Sogand Sajedi[2]; Cornelia Wenger[2]; **Lejo Johnson Chacko**[3]; Rudolf Glueckert[4]; Anneliese Schrott-Fischer[1]; Frank Rattay[2]
[1]Medical University of Innsbruck; [2]Vienna University of Technology; [3]Anichstrasse 35; [4]Inner Ear Laboratory, Medical University Innsbruck, Innsbruck, Austria

Background
Human cochlear geometry, as well as cochlear nerve fibers arrangement, have a considerable impact on cochlear implant function. Computer simulation investigates these effects and analysis of the resulting excitation profiles reduces animal experiments. Detailed three-dimensional data of the cochlea helical structure

and the spiral neural pathways are essential to study the temporal fine structure of the transmitted neural code as well as tonotopic behavior of the electrically stimulated cochlea.

Result
A detailed anatomically Finite Element Model has been developed from two human cochlear ultra-high-resolution micro-CT images (3 µm resolution). 30 nerve fiber bundles, distributed over eight octaves (11500 – 40 Hz), were traced. From the obtained Finite Element Model, corresponding extracellular voltages of each electrode have been calculated for different points along the pathways. Finally, a compartment model of human auditory neurons has been used to analyze the excitation profiles of the traced fiber pathways.

Conclusion
Analysis of the model data lead to the following rules

I. the peripheral axon is most sensitive to cathodic stimulation (CAT)

II. in many cases, CAT evokes spikes in the peripheral terminal at threshold, but for enhanced stimulus, there is a second spike initiation site within the peripheral axon.

III. anodic stimuli (ANO) can stimulate the central axon even at threshold.

IV. electrodes located in the narrowing middle- and apical turn cause the infringement of the tonotopical principle.

V. degenerated cells which lost the peripheral axon were more sensitive to CAT when their somata are totally covered with 2 membranes of a glia cell, but they become ANO sensitive when myelin covering is reduced.

PS 95

Electrophysiological Measures of Temporal Envelope Processing in Cochlear Implant Users

Robin Gransier[1]; Robert P. Carlyon[2]; Jan Wouters[1]
[1]KU Leuven; [2]University of Cambridge

Temporal envelope modulations (TEMs) are the primary cues that cochlear implant (CI) users utilize to perceive speech intelligibly. The ability of the stimulated neural ensembles to encode TEMs is important for speech perception, especially in adverse listening situations. Electrophysiological assessment of TEM encoding ability can be assessed with the 40-Hz auditory steady-state response (ASSR). These responses can, however, be difficult to obtain due to the CI stimulation artifacts that corrupt the EEG recording. This is especially problematic when clinically relevant pulse rates are used [i.e. ≥ 900 pulses per second (pps)]. A potential alternative for the 40-Hz ASSR is the auditory change complex (ACC). The ACC is a transient cortical response evoked by a change in stimulus characteristics and can be evoked when a modulation is present in the deviant stimulus. Here we investigate the applicability of the 40-Hz ASSR and the ACC as an electrophysiological measure for TEM encoding in the auditory pathway.

We assessed the response strength of each neural measure as a function of stimulus modulation depth (MD) in adult CI users. The response strength was assessed at four different MDs ranging from 0.25 to 1. A 900-pulses-per-second, biphasic pulse train, stimulated in a monopolar configuration, was used as a carrier. Stimuli consisted of 200 blocks of a 2-s unmodulated section followed by a 2-s 40-Hz amplitude-modulated section, with different modulation depths across conditions. This paradigm evokes both an ACC (i.e. the change from the unmodulated to modulated section and *vice versa*) and an ASSR (i.e. the envelope following response to the envelope of the modulated section) and allows one to study how well each electrophysiological measure reflects TEM encoding in the auditory pathway. A high-rate-sampling EEG system recorded the responses and linear interpolation was used to remove the CI stimulation artifacts.

Initial results of five CI users show that the stimulation artifacts could effectively be removed in the majority of subjects. The presence of a 40-Hz ASSR coincided with the presence of an ACC, indicating that both measures can be used to asses TEM encoding. We will present data of a group of ~10 CI users and show the MD-dependent growth functions of both electrophysiological measures. These measures can potentially facilitate the objective selection of CI stimulation electrodes to improve speech perception.

Acknowledgements
Financial support from the Wellcome Trust Collaborative Science Award RG91976

PS 96

Modulation of Auditory Cortex Responses by The Pulse Asymmetry and Pulse Polarity in an Animal Model of Cochlear Implant

Victor Adenis[1]; Elie Partouche[1]; Dan Gnansia[2]; Pierre Stahl[2]; Jean-Marc Edeline[1]
[1]Neuro-PSI, UMR CNRS 9197; [2]Oticon Medical

Despite the fact that cochlear implant (CI) is the most successful neuroprothesis, a large field of research is still working on improving its coding strategies. The stimulation mode, the pulse shapes and grounding schemes can potentially exert moderate or drastic consequences on

the nerve excitability, electrode discriminability, spread of excitation and response strength. In a previous study (Adenis et al 2018) we showed that when stimulated with different strategies, there is a tight relationship between the eCAP amplitude and the auditory cortex neuronal response. Here, we quantified the responses from auditory cortex neurons to stimulations delivered through a CI while modifying the ratio of pulse asymmetry, the polarity of the first phase and the pulse shape. Experiments were performed in anesthetized guinea pigs (6-18months old). The tonotopic gradient of the primary auditory cortex (AI) was established by inserting an array of 16 cortical electrodes (2 rows of 8 electrodes separated by 1mm and 350µm within a row). A stimulation array (300µm) was then inserted in the cochlea (5 electrodes inserted in the 1st basal turn) and its connector was secured on the skull. The cortical electrodes were placed back in auditory cortex at the same location as before the CI insertion. The eight nerve fibers were then stimulated with 10 levels of pulse asymmetry, from 1/1 being a rectangular symmetrical pulse to 1/10 where one of the pulse phase amplitude is one tenth of the second phase (its duration was 10 times longer). The pulse shape was also modified from a current square shape to a current ramp shape. All pulses were generated at constant charge by a dedicated stimulation platform.

Whatever was the polarity of the first phase (anodic or cathodic) asymmetric pulses reduced the evoked cortical responses compared with symmetric pulses (by 15 to 20% on average). However, comparing how the different levels of asymmetry and polarity influence the spread of excitation on the cortical map a revealed more complex picture, with cases where both the evoked firing rate and the spread of excitation were increased and cases where they were decreased. These data indicate that the combination of pulse asymmetry and polarity can, at the individual level, help modulating the activation of the auditory cortex map, and thus potentially provide better frequency resolution in CI patients.

PS 97

Using the Alternating-Auditory Change Complex to Understand Changes to Modulation Sensitivity and Phase Locking with Age

Wiebke Lamping[1]; Jaime Undurraga[2]; Ben Williges[1]; Marina Salorio-Corbetto[1]; David McAlpine[3]; Deborah Vickers[1]
[1]University of Cambridge; [2]Mac quarie University; [3]Department of Linguistics, The Australian Hearing Hub, Macquarie University, Sydney, Australia

The auditory change complex (ACC) is a cortical response measured electrophysiologically. It can be elicited by a change in an ongoing stimulus and has been shown to correlate well with behavioral discrimination abilities. This study utilizes a new alternating-ACC (A-AAC) paradigm, which continuously switches between stimuli without gaps. This was used to explore the discrimination of different rates and depths of amplitude modulation to objectively explore sensitivity to these stimuli as a function of age. The A-AAC paradigm has the advantage that for the same stimuli the envelope following response (EFR) can be measured, providing information on the phase locking ability within the auditory system.

Sinusoidally modulated carriers (500 Hz) were presented via insert-headphones to eighteen normal hearing listeners, in three different age groups (18-39, 40-59, 60-79 years). Different modulation frequencies (4 vs 9 Hz; 19 vs 32 Hz; 50 vs 97 Hz), depths (50, 75, 100%), as well as presentation levels (65 and 55 dB SPL) were used to determine which rates and depths elicited the A-AAC and EFR responses. Stimuli were constantly switched at different rates (1, 2.5, or 6.5 Hz). The parameter space was explored to understand how modulation perception and phase locking change with age.

Preliminary findings suggest that for listeners tested thus far, that both A-AAC and EFR responses were present for all switching rates but that the responses with a reduction in modulation depth reduce rapidly. Further details of the exploration of the parameter set will be presented, with particular focus on the effects of age.

This work has been funded by the United Kingdom Medical Research Council (MR/S002537/1) and the Australian Government through the Australian Research Council (project number FL160100108).

PS 98

Evaluating and Comparing Behavioural and Electrophysiological Estimates of Neural Survival

Tim Brochier[1]; John M. Deeks[1]; Charlotte Garcia[1]; Manohar Bance[2]; Robert P. Carlyon[1]
[1]University of Cambridge; [2]Department of Clinical Neurosciences, University of Cambridge

Variations in neural survival along the cochlea can degrade the spectral representation of sounds conveyed by cochlear implants (CIs) and affect the transmission of temporal information by different electrodes. We evaluate and compare several methods that have been proposed as estimates of neural survival patterns. All measures are obtained from the same 12 users of the Cochlear Corporation CI.

The two behavioural measures are multipulse integration (MPI) and the polarity effect (PE), both measured on each of seven electrodes. We measure MPI as the difference between thresholds at 80-pps and 1000-pps, and PE as the difference in thresholds between cathodic- and anodic-centred quadraphasic (QP) 80-pps pulse trains. These QP pulses, as with other asymmetric pulse shapes, have been shown to produce large and reliable PEs. It has been proposed that good neural survival corresponds to a large MPI and to a large negative PE (lower thresholds for cathodic than anodic pulses).

Several methods of estimating neural survival using electrically-evoked compound action potentials (ECAPs) have been proposed. One of these is the effect of interphase gap (IPG) on ECAP amplitudes and amplitude growth functions (AGFs), both of which have been correlated with spiral ganglion nerve density in guinea pigs. We obtain both of these measures using the same subset of electrodes as for the behavioural measures. Recently, Goehring et al (2019) have proposed a method for estimating neural survival patterns and the current spread from each electrode using a measurement matrix, whereby ECAPs are obtained using the forward-masking technique, for every possible combination of masker and probe. This matrix is then subjected to a nonlinear optimization algorithm termed Panoramic ECAP (PECAP) (Cosentino et al, 2015). We obtain the measurement matrix using all electrodes of the implant and use the PECAP algorithm to estimate neural survival.

PE and MPI were uncorrelated (p=0.952), and the IPG effect on ECAP amplitude was not correlated with PE (p=0.690) or MPI (p=0.195), suggesting that these estimates of neural health reflect different characteristics of the electrode-neural interface. The neural-health estimate generated from PECAP was correlated with ECAP amplitude (p< 0.001), but was not correlated with PE (p=0.631), MPI (p=0.16), or the IPG effect (p=0.149). The long-term goal is to use these neural survival estimates to explain and potentially remedy cases of poor speech perception by CI users.

PS 99

Using the electrically-evoked compound action potential for site-selection in cochlear implant listeners

Kara C. Schvartz-Leyzac[1]; Teresa A. Zwolan[1]; Bryan E. Pfingst[2]

[1]University of Michigan; [2]Kresge Hearing Research Institute, Department of Otolaryngology-Head and Neck Surgery, University of Michigan

Background

In cochlear-implanted guinea pigs, the density of spiral ganglion neurons (SGN) accounts for about 40-50% of the variance in peak amplitude and linear slope values of the electrically-evoked compound action potential (ECAP) amplitude-growth function (AGF). Moreover, the change in the peak amplitude or linear slope of the ECAP AGF as a result of increasing the interphase gap (IPG) of the biphasic pulse (the "IPG Effect") also reflects SGN density. Studies in cochlear-implanted humans suggest that the ECAP IPG Effect is less influenced by non-neural factors and relates to speech recognition abilities in the same subjects Thus, we hypothesize that specific ECAP measures can be used to select sites for activation in a cochlear implant programming map, in order to improve perception and performance in humans.

Methods

Participants were adult human subjects with cochlear implants (Cochlear®CI24RECA, CI512, CI422, or CI532). ECAP AGFs were collected using two interphase-gap conditions (7 and 30 us IPG), and the IPG Effect was calculated for ECAP peak amplitude measures on each electrode. Two experimental maps were created, in which the five sites with the five largest (best) or the five smallest (worst) ECAP IPG Effect for peak amplitude were deactivated systematically. The deactivation strategy maintained tonotopicity with respect to the subjects' everyday program maps. Performance on sentence and consonant tests was assessed using the experimental maps and when using the subjects' everyday programs. Testing was completed using a double-blinded design.

Results

Preliminary results obtained in 12 ears showed, on average, that performance using a map in which the electrode sites with the lowest ECAP IPG values were selected resulted in significantly poorer sentence recognition in noise (6.80 dB SNR at 50% accuracy) compared to performance when listening with a map in which the electrodes with the highest ECAP IPG value are selected (5.60 dB SNR). Results using the experimental map with the best ECAP IPG values were comparable to those when using their everyday map (5.86 dB SNR). There was no significant difference between performance on the consonant recognition tests when comparing the three maps.

Conclusions

Results suggest that ECAP measures reflect underlying features of neural health that are important for sentence recognition performance in noise, and that ECAP data can be used to alter programming maps to either improve or worsen performance among adult CI recipients.

PS 100

An Evaluation on the Influence of Artifact-Reduction Paradigm on ECAP-Based Effects of Cochlear Health

Marko Takanen[1]; Stefan Strahl[1]; Konrad Schwarz[1]; Dyan Ramekers[2]
[1]MED-EL Elektromedizinische Geraete, GmbH, Research and Development; [2]Department of Otorhinolaryngology and Head & Neck Surgery, University Medical Center Utrecht, , Utrecht University

The ability of cochlear implants (CIs) to restore hearing for profoundly deaf people relies on the condition of the electrode-neuron interface inside the cochlea. This condition can be assessed by measuring electrically evoked compound action potentials (eCAPs). One popular approach to assess cochlear health is to inspect the eCAP thresholds and slopes of the eCAP amplitude-growth function (AGF) for charge-balanced pulses. ECAP thresholds are expected to decrease and slopes to become steeper when either the inter-phase gap (IPG) is prolonged or the leading/dominant polarity is changed from anodic to cathodic, with a pronounced effect for healthy cochleae (Ramekers et al., JARO, 2014; Carlyon et al., JARO, 2018; Hughes et al., Hear Res, 2018).

Analysis of eCAP-based metrics is challenged by measurement noise and stimulation artifacts that are inherently present in every eCAP measurement. Several artifact-reduction paradigms have been developed to minimize such detrimental effects. The most popular paradigms are the alternating-polarity and the (revised) forward-masking paradigms (Brown & Abbas, JASA, 1990; Miller et al., Ear Hear, 2000) – each of them having their own pros and cons for clinical practice with CI users (Miller et al., Ear Hear, 2000; Baudhuin et al., Ear Hear, 2016). However, it is not clear if and how the artifact-reduction paradigm affects assessment of IPG and polarity -effects of cochlear health.

Here, we measured eCAP AGFs on deafened guinea pigs using three artifact-reduction paradigms: alternating-polarity, revised forward-masking (Miller et al., Ear Hear, 2000) and multi-curve-fitting (Spitzer et al., Bio-Med Eng., 2006) paradigms. The two latter paradigms enabled investigation of the polarity effect. The IPG effect was investigated by repeating the measurements with 2.1 and 30 µs IPGs using both 30- and 50-µs phase durations. The preliminary results show that different polarities have an expected effect on slope of the eCAP AGF as well as to exhibit diverse influences of the facilitation phenomenon. However, the polarity effect on the eCAP thresholds seems to depend on the artifact-reduction paradigm. The IPG effect was found to be similar for all paradigms, having the expected impacts on the slopes and the thresholds. Additional signal-to-noise-ratio analysis revealed differences between the artifact-reduction paradigms, explaining some of the unexpected differences in eCAP-based metrics between them. In conclusion, we report effects of the artifact-reduction paradigms that are worthwhile considering when applying the paradigms for analyzing eCAP-based cochlear-health metrics in clinical practice.

PS 101

Estimating Neural Survival Using a New Version of the Panoramic ECAP Method

Charlotte Garcia[1]; Tobias Goehring[1]; Stefano Cosentino[1]; Richard E. Turner[1]; John M. Deeks[1]; Tim Brochier[1]; Taren Rughooputh[1]; Manohar Bance[2]; Robert P. Carlyon[1]
[1]University of Cambridge; [2]Department of Clinical Neurosciences, University of Cambridge

Ideally, the neural excitation produced by each electrode of a cochlear implant (CI) should be restricted to neurons close to that electrode. Exceptions to this optimal scenario can arise from variations in neural survival along the cochlea and from factors that influence the current spread, such as lateral electrode position. Cosentino *et al* (2015) developed an objective method for measuring neural spread of excitation and identifying those exceptions, using the forward masking method for measuring the electrically evoked compound action potential (ECAP), as described by Brown *et al* (1990). This panoramic ECAP ("PECAP") method first obtained a measurement matrix consisting of ECAPs for every possible combination of masker and probe electrode (Figure 1), and then used a nonlinear optimisation algorithm to derive excitation patterns on the assumption that each ECAP reflects the overlap between masker and probe excitation patterns. The procedure converts the estimated excitation patterns into the ECAPs that they would produce and varies those patterns to obtain the best fit between predicted ECAPs and the measurement matrix.

Here we present a new version of PECAP (PECAP2) that separately models the neural survival profiles and current spread from each electrode, and combines them to estimate the neural excitation patterns. An advantage over both PECAP1 and a similar method proposed by Biesheuvel *et al* (2016) is that changes to the neural survival parameter influence the excitation patterns from multiple adjacent electrodes in a biologically plausible way. Furthermore, knowledge of how both neural survival and current spread vary along the cochlea may

influence clinical decisions and fitting procedures. We show that PECAP2 is able to reconstruct a wide range of simulated excitation patterns, as well as identify neural dead regions simulated in human data (Figure 2). We also show that when data from DeVries *et al* (2016) are processed via PECAP2, the variations in predicted neural survival along the electrode array correlate significantly with detection thresholds obtained with focused stimulation. We are also exploring the use of Trans Impedance Matrices (also known as Electric Field Interaction; Figure 3) to constrain estimates of current spread. Finally, we evaluate other factors that might influence the measurement matrix and degrade PECAP2 accuracy, such as the reliability of each ECAP (evaluated with repeat measures), variations in refractoriness along the cochlea (evaluated by comparing ECAPs measured with the alternating polarity artefact cancellation technique to the measurement matrix obtained using forward masking), and recording electrode impedances.

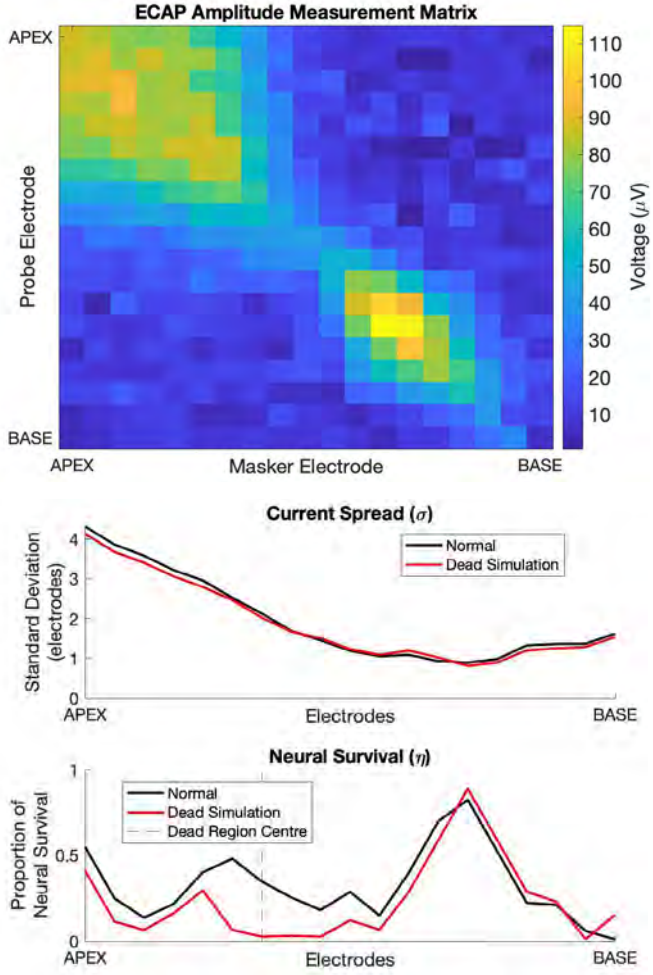

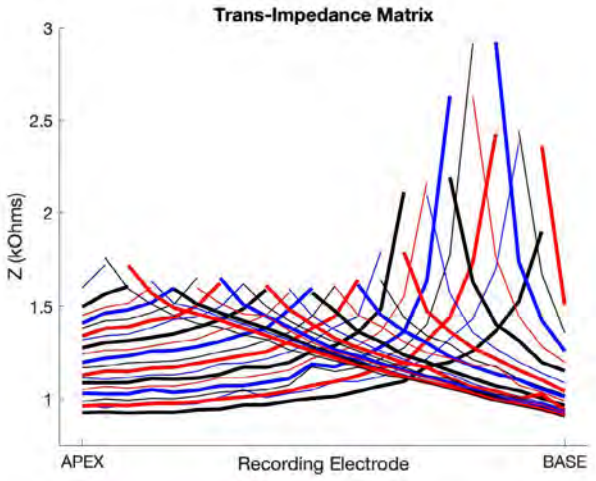

PS 102

Estimating Neural Function in Cochlear Implant Users with Stimulation Level Changes when Decreasing the Interphase Gap of a Biphasic Pulse

Jeffrey Skidmore[1]; William J. Riggs[1]; Chloe Vaughan[2]; Shuman He[3]
[1]The Ohio State University; [2]The Ohio State University, Eye and Ear Institute; [3]The Ohio State University; Nationwide Children's Hospital

Background

Directly evaluating the number and responsiveness of cochlear nerve (CN) fibers to electrical stimulation is not feasible in human listeners. Therefore, animal models have been used to find the relationship between the density of spiral gangion neurons (SGNs) and neural response properties from the electrically-evoked compound action potential (eCAP, Prado-Guitierrez et al., 2006; Ramekers et al., 2014). A significant correlation has been shown between SGN density and the change in stimulation current required to evoke equal eCAP responses when decreasing the interphase gap (IPG) of a biphasic pulse (Prado-Guitierrez et al., 2006; Ramekers et al., 2014, 2015). However, this finding has not been confirmed in human cochlear implant (CI) users. By definition, children with cochlear nerve deficiency (CND) can be considered as a human model for poor CN survival, which provides a valuable opportunity to verify this important finding in human CI users. This study compared the current level offset between children with CND and children with normal-sized CNs. It tested the hypothesis that the current level offset from stimuli with different IPGs correlates with neural function in human CI users.

Methods

Participants in this study included 30 children with CND and 30 children with normal-sized CNs. All subjects were implanted with a Cochlear™ Nucleus® device in

the test ear. For each subject, eCAPs were measured at three electrode locations across the electrode array. The stimulus was a charge-balanced, cathodic leading, biphasic pulse with a pulse-phase duration of 50 ms/phase. The current level offset was defined as the change in current required for a stimulus with a 7 ms IPG to generate an eCAP that has an equal amplitude as that evoked by a stimulus with a 42 ms IPG.

Results

The current level offset was higher for children with CND than children with normal-sized CNs at all electrode sites. The offset increased for children with CND and decreased for children with normal-sized CNs as the electrode moved from "basal" to "apical" locations, which matches patterns of neural function in these two patient populations (He et al., 2018).

Conclusions

Smaller current level offsets are associated with better neural function in human CI users. This result does not agree with the trend reported in animal studies, which highlights the importance of verifying results reported in animal models in human CI users.

Acknowledgments

This work was supported by the R01 grant from NIDCD/NIGMS (1R01DC016038) and the R01 grant from NIH/NIDCD (1R01DC017846).

PS 103

Polarity Effects in Late Electrical Compound Action Potentials as Measure of Neural Health

Wiebke S. Konerding[1]; Julie G. Arenberg[2]; Andrej Kral[3]; **Peter Baumhoff**[1]

[1]Dept. of Experimental Otology, Hannover Medical School, Germany; [2]Massachusetts Eye and Ear Infirmary, Harvard Medical School; [3]Dept. of Experimental Otology, Hannover Medical School, Germany; DFG Cluster of Excellence "Hearing 4 All"

When electrically stimulating the deaf ear with cochlear implants (CIs), the outcome may be hampered by patchy degeneration of spiral ganglion neurons (SGNs). A progressive degeneration from peripheral to central parts of the SGN could lead to regions less or nonresponsive to electrical stimulation ('hearing holes'). Our study addresses the possibility to detect local SGN degeneration via electrophysiological markers. We induced micro-lesions targeting either peripheral dendrites or somata of SGNs and recorded electrically-evoked compound action potentials (eCAPs). We propose that a polarity effect of the eCAP response (anodic minus cathodic) may be used as indicator for focal SGN lesions.

The experiments were performed in 11 normal hearing Dunkin-Hartley guinea pigs (N=17 cochleae). We used a micro-electrode to lesion the SGNs through a cochleostomy in the basal turn. The lesion target (peripheral dendrite or soma) was verified via µCT imaging and 3D autofluorescence confocal microscopy of optically cleared cochleae. The deafened cochleae (Neomycin-sulfate solution) were electrically stimulated through 6-contact CIs and eCAPs were recorded in response to charged-balanced, biphasic stimuli (50µs/phase) with alternating polarity.

Of all cases, 10 had lesions of SGN somata and 7 at the peripheral dendrites. We assessed the N1-P1 amplitude in the averaged response to 300 alternating polarity pulses. To avoid distortions by the electrical artifact in the separate analysis of the pulse polarities, we blanked the first 0.8 ms and assessed the late negative deflection N2 at around 1 ms, which presumably relates to a secondary cochlear response. The N1-P1 threshold showed the known threshold elevation at more basal contacts. N2 latency differences of ~95 µs between anodic- and cathodic-leading pulses indicated a more central location of anodic spike generation. Lesioning reduced this latency difference. The threshold increased more for anodic leading stimuli after soma lesioning (polarity effect < 0). The dendritic lesions did not lead to negative polarity effects.

We established a method to assess micro-lesions, targeting dendrites or somata of the SGNs in the guinea pig. The results revealed changes in late eCAP components based on the lesion target. Especially after soma lesions the anodic phase was less efficient in CI-stimulation. These polarity effects resemble findings in human CI patients, indicating that this measure could detect regions with reduced neuronal density. Future studies will assess polarity effects in chronically lesioned animals, with central axon degeneration, via eCAPs and auditory midbrain recordings.

Supported by Deutsche Forschungsgemeinschaft (DFG Exc. 1077) and MedEl Company (Innsbruck).

PS 104

Auditory and visual cortical activity and relationship to functional speech outcomes in post-lingual cochlear implant users: A functional near-infrared spectroscopy (fNIRS) study

Amanda Fullerton[1]; Catherine McMahon[1]; Deborah Vickers[2]; Robert Luke[1]; Heivet Hernandez-Perez[1]; Jessica Monaghan[1]

[1]Macquarie University; [2]University of Cambridge

Cortical reorganisation as a result of deafness has been proposed as a potential contributor to variability in cochlear implant (CI) outcomes. Specifically, cross-modal activity in auditory and visual cortices has been shown to correlate with auditory-only speech understanding in post-lingually deaf CI users. However, it remains unclear whether these associations are adaptive' or 'maladaptive' for functional outcome, with varied associations reported. Importantly, there has been variability across studies in the types of visual and auditory stimuli used, e.g., 'basic', such as gratings and noise, vs. 'speech-based' visual and auditory stimuli, which are likely to engage different cortical networks. This study therefore aims to 1) examine activations to both basic and speech-based visual and auditory stimuli in the same cohort of post-lingually deaf CI users, and a group of age-matched, normally-hearing controls, and 2) investigate whether a relationship exists between 'cross-modal' activation and speech recognition measures in auditory, visual-only and audiovisual conditions, and whether this changes depending on the paradigm used (basic vs. speech).

fNIRS was employed as a non-invasive technique that is not susceptible to electrical or magnetic artifacts common to other neuroimaging methods such as EEG and fMRI. Two test paradigms were administered in a block design, using 1) basic auditory and visual stimuli - modulated speech-shaped noise and morphing concentric gratings, and 2) speech stimuli - concatenated IEEE sentences presented in an auditory-only and a visual-only condition. Responses were measured via a 52-channel optode array positioned over temporal and occipital regions. Speech recognition performance on IEEE sentences were assessed in auditory-only, visual-only and audiovisual conditions.

Group-level analysis using a general linear mixed effects model indicates significant activations across both groups, paradigms and conditions. Activations are observed in temporal areas to auditory stimuli and in occipital areas to visual stimuli in both groups, for both basic and speech-based stimuli. Initial results indicate significant cross-modal activity in temporal regions at the group level in CI users, but not in normally-hearing controls.

In summary, evidence of differential activations depending on the nature of auditory and visual stimuli used is observed between CI users and normally-hearing controls. The study presents a correlational analysis, examining reported associations between cross-modal activity to both types of visual and auditory stimuli and speech recognition in auditory-only, visual-only and audiovisual conditions.

PS 105

Neurophysiological Measures of Amplitude Modulation Rate Discrimination in adults with Cochlear Implants

Ben Williges[1]; Deborah Vickers[1]; Wiebke Lamping[1]; Marina Salorio-Corbetto[1]; David McAlpine[2]; Jaime Undurraga[3]
[1]University of Cambridge; [2]Department of Linguistics, The Australian Hearing Hub, Macquarie University, Sydney, Australia; [3]Mac quarie University

Speech perception in the presence of noise can be challenging for many cochlear implant (CI) users. The main perceptual cues available to the CI user are derived from spectral place location of the electrodes within the cochlear and from the slow temporal envelope modulations. One of the main factors affecting speech perception performance with a cochlear implant is the current spread and interaction between channels that affects both the spectral and temporal information and in turn blurs the internal representation of sound.

The goal of the current research was to measure discrimination of different amplitude modulation (AM) frequencies using electro-encephalology (EEG) to measure the electrically evoked auditory change complex (eACC) in CI users. CI artefacts were reduced by the denoising source separation technique. The eACC is a response to a change in an ongoing stimulus and is thus considered a proxy for discrimination ability. The method developed to measure the eACC allows for the measurement of both transient and steady state responses, by continuously switching between the two different AM frequencies without a gap.

A group of 5 adults with CIs were tested on electrode 16 of their device using the Nucleus Implant Controller (NIC) version 3. Biphasic pulses were modulated with either 4 vs 9 Hz, 19 vs 35 Hz; 50 vs 97 Hz AM frequencies, or the nearest rates which could be discriminated, all stimuli were checked in advance to ensure that they were discriminable. Modulation depths (25, 50, 75, 100%) were used and stimuli were constantly switched between the two modulation frequencies at different rates (1, 2.5, or 6.5 Hz) either in their modulation frequency, depth, or level. This range of parameters was compared to the normal hearing abilities for the same stimuli (see poster Lamping et al).

Preliminary findings suggest that for the CI listeners that both steady state and transient responses were present for the slow switching conditions but, in contrast to normal hearing listeners, that the responses could not be measured for the faster switching rates. This

suggests adaptation in the electrically stimulated auditory system. We also observed that as the modulation depth decreased that the change in amplitude of the response was much smaller than for the normal hearing listeners. Further details on the limits of these changes in the parameter space will be presented.

This work has been funded by the United Kingdom Medical Research Council (MR/S002537/1) and the Australian Government through the Australian Research Council (project number FL160100108).

PS 106

Duration of Deafness and Adaptation of the Auditory Nerve in Cochlear Implant Subjects

William J. Riggs[1]; Jeffrey Skidmore[1]; Chloe Vaughan[2]; Shuman He[3]
[1]The Ohio State University; [2]The Ohio State University, Eye and Ear Institute; [3]The Ohio State University; Nationwide Children's Hospital

Background
Older cochlear implant (CI) users typically show speech perception deficits, especially in competing noise (Budenz et al., 2013; Lin et al., 2012), but the mechanisms underlying these deficits remain unclear. Studies suggest the importance of the functional status of the cochlear nerve (CN) for CI outcomes (e.g., Pfingst et al., 2015). Advanced age and/or long duration of deafness are associated with CN degeneration (Shepherd et al., 2004; Wu et al., 2019). What remains unknown is the effect of CN degeneration on how well the CN encodes and transmits electrical stimulation of the CI. This study aimed to evaluate effects of advanced age and duration of deafness on the amount of neural adaptation of the CN.

Methods
Currently, 13 adult CI users have participated. All had a Cochlear ™ Nucleus® device. Electrically evoked compound action potentials (eCAPs) to individual pulses of a 100-ms biphasic pulse train were recorded at four electrode locations. Duration of deafness was defined as the interval between the time when the participant's pure tone average (.5, 1, 2 kHz) initally exceeded 90 dB HL and the time point of implantation. Pulse trains were presented in monopolar-coupled stimulation mode at four carrier pulse rates: 500, 900, 1800 and 2400 pulses per second (pps). The primary dependent variable was the amount of neural adaptation as quantified using the adaptation index (AI; He et al., 2016). Effects of advanced age and duration of deafness on the AI as well as their relationship with speech perception scores (Az Bio sentences) were evaluated using Spearman correlation tests.

Results
Preliminary data showed that pulse-train eCAPs were recorded in all participants. AIs increased with the carrier rate of the pulse train, with the smallest AI (i.e., greatest amount of neural adaptation) measured at the highest pulse rate (2400 pps). The amount of neural adaptation at the CN was not significantly associated with advanced age or duration of deafness. Age at time of speech perception testing was significantly associated with AzBio sentence scores.

Conclusion
These preliminary results suggested that the amount of neural adaptation at the CN is not significantly affected by advanced age or duration of deafness. Results from more participants are needed to confirm and support this preliminary conclusion. Age at testing was significantly associated with speech perception performance, which is consistent with previous studies.

Acknowledgments
This was supported by the R01 grant from NIDCD/NIGMS (1R01DC016038) and R01 grant from NIH/NIDCD (1R01DC017846).

PS 107

The Effect of Pulse Polarity on Neural Response of the Electrically-stimulated Auditory Nerve in Children with Cochlear Nerve Deficiency and Children with Normal-sized Cochlear Nerves

Chloe Vaughan[1]; Lei Xu[2]; Jeffrey Skidmore[3]; Jianfen Luo[2]; Xiuhua Chao[2]; Rujie Wang[2]; Haibo Wang[2]; Shuman He[4]
[1]The Ohio State University, Eye and Ear Institute; [2]Department of Auditory Implantation, Shandong Provincial ENT Hospital Affiliated to Shandong University; [3]The Ohio State University; [4]The Ohio State University; Nationwide Children's Hospital

Background
Children with cochlear nerve deficiency (CND) (i.e., a small/absent cochlear nerve shown by high-resolution MRI) have been receiving cochlear implants (CI) for nearly two decades. This population generally shows poor responsiveness of the auditory system to electrical stimulation (Buchman et al., 2011; Teagle et al., 2010). Recent studies showed that responsiveness to anodic-leading stimuli was better than a cathodic-leading stimulus for typical CI users (e.g., Macherey et al., 2008). It remains unknown whether this is the case for hypoplastic CN. It has been proposed that this polarity effect is associated with neural health of the CN, with greater difference suggesting poorer CN health, though this hypothesis has not been confirmed by previous studies in typical CI

users. This study aimed to evaluate the effect of polarity on neural responsiveness of the electrically-stimulated CN in children with CND and compared the size of the polarity effect on neural responsiveness between two groups differing in neural health: children with CND and children normal-sized CNs.

Methods
31 children with CND and 31 children with normal-sized CNs participated. All children had congenital hearing loss and have a Cochlear® Nucleus™ device with full insertion. For each participant, the electrically-evoked compound action potential (eCAP) Input/Output (I/O) function was measured at three electrodes, using both anodic and cathodic-leading pulses. The dependent variables of interest were the eCAP amplitude at the maximum comfortable level measured for the anodic-leading stimulus (i.e., the anodic C-level), the eCAP threshold, the slope of the eCAP I/O function, as well as polarity effect on these variables.

Results
For children with CND, the anodic stimulus led to higher eCAP amplitudes, lower eCAP thresholds and steeper eCAP I/O functions than the cathodic. Children with CND showed larger polarity effects on the slope of the eCAP I/O function than children with normal-sized CNs. The group differences in the size of the polarity effect on the eCAP amplitude or threshold were not statistically significant.

Conclusion
The hypoplastic CN is more sensitive to anodic than the cathodic stimuli. The group difference in the size of the pulse polarity effect on slope of the eCAP I/O function is consistent with an association between the pulse polarity effect and neural health of the CN in human CI users.

Acknowledgements
Efforts of SH, JS and CV spending on this study were supported by the R01 grant from NIDCD (R01DC017846) and the R01 grant from NIDCD and NIGMS (R01DC016038).

PS 108

Residual Hair Cell Function in Electric-Acoustic Stimulation Cochlear Implant Users with Complete Loss of Acoustic Hearing Post-Implant

Viral Tejani[1]; Jeong-Seo Kim[2]; Paul Abbas[2]; Carolyn Brown[2]; Marlan R. Hansen[3]
[1]Dept of Otolaryngology - Head and Neck Surgery, University of Iowa Hospitals and Clinics; [2]Dept of Communication Sciences and Disorders, University of Iowa; [3]University of Iowa Hospitals and Clinics - Department of Otolaryngology-Head & Neck Surgery

Residual Hair Cell Function in Electric-Acoustic Stimulation Cochlear Implant Users with Complete Loss of Acoustic Hearing Post-Implant

Viral D. Tejani[1,2], Jeong-seo Kim[1,2], Paul J. Abbas[1,2], Carolyn J. Brown[1,2], Marlan R. Hansen[2,3]

[1] Department of Otolaryngology-Head and Neck Surgery, University of Iowa Hospitals and Clinics

[2] Department of Communication Sciences and Disorders, University of Iowa

[3] Department of Neurosurgery, University of Iowa Hospitals and Clinics

Changes in cochlear implant (CI) design and surgical techniques have led to preservation of residual acoustic hearing, allowing patients to utilize acoustic and electric stimulation in the implanted ear. After an initial loss of hearing post-surgery, patients utilizing the Nucleus Hybrid L24 implant maintain an average low-frequency pure tone average of 60 dB HL at 5 years of implant use, though a minority experience a total loss of hearing (Roland et al, 2016, 2018; Scheperle et al, 2017).

Electrocochleography (ECoG) enables non-invasive monitoring of peripheral auditory function, where hair cell (cochlear microphonic - CM) and neural (auditory nerve microphonic - ANN) potentials are recorded in response to acoustic stimulation (typically tone bursts). We have previously shown that longitudinal CM and ANN responses are stable for patients who maintain stable audiometric thresholds in the implanted ear, while patients with partial loss of residual acoustic hearing show decreased CM and ANN responses (Abbas et al, 2017; Kim et al, 2018; Tejani et al, 2019). In addition, our group and others have shown rises in electrode impedances for patients who lose residual acoustic hearing (Scheperle et al, 2017; Choi et al, 2017), though neural electrically evoked compound action potentials (ECAPs) are stable pre- and post-hearing loss (Scheperle et al, 2017).

This report focuses on nine patients with complete loss of residual hearing months after surgery (audiometric thresholds > 110 dB HL; average onset: 3.70 ± 2.59 months post activation of the CI). They underwent longitudinal ECoG measures several appointments before and after loss of hearing. Results indicate a significant decrease in CM amplitudes pre- and post-hearing loss ($p = 0.010$), but interestingly, all patients maintained some CM responses despite having no audiometric responses. No patients maintained an ANN response after loss of hearing ($p = 0.003$), though ANN responses in general are known to be small and close to the recording system noise floor.

These findings may indicate that loss of residual hearing could reflect synaptic changes, consistent with a previous theory that residual CM responses coupled with little to no ANN responses reflect a "disconnect" between hair cells and auditory nerve fibers (Fontenot et al, 2017). This "disconnection" may prevent proper encoding of auditory stimulation at higher auditory pathways, leading to a lack of audiometric responses, even in the presence of viable cochlear hair cells and stable ECAP neural responses.

Funding: NIH/NIDCD P50 DC 000242

Blast and Head Trauma

PS 109

Acute Hearing Threshold Shifts Following Head Impact in Mixed Martial Arts Fighters

Rory J. Lubner[1]; Michael K. Boyajian[2]; Renata M. Knoll[3]; Steven D. Rauch[4]; Jacob R. Brodsky[5]; Aaron K. Remenschneider[6]; Elliott D. Kozin[7]
[1]Massachusetts Eye and Ear Infirmary/Harvard Medical School/Warren Alpert Medical School of Brown University; [2]Warren Alpert Medical School of Brown University; [3]Massachusetts Eye and Ear Infirmary/ Harvard Medical School; [4]Massachusetts Eye and Ear, Harvard Medical School; [5]Boston Children's Hospital/ Harvard Medical School; [6]Dept. of Otolaryngology, UMass Memorial Medical Center; Massachusetts Eye and Ear; [7]Massachusetts Eye and Ear Infirmary-Harvard University

Background
Auditory symptoms, including hearing loss and tinnitus, have been recognized as a long-term consequence of sports-related head injuries. To date, no studies have investigated how hearing may acutely change following repetitive sports-related head injury, which commonly occurs during combat sports, such as mixed martial arts (MMA) and boxing. The primary aim of this study is to investigate acute hearing threshold shifts in MMA fighters.

Methods
In this prospective cohort study, twenty-nine MMA fighters volunteered to have otoscopy and air conduction pure tone audiometry completed immediately prior to and following a 45-minute sparring match. Frequencies tested included 0.5Hz, 1kHz, 2kHz, 3kHz, 4kHz, 6kHz, and 8kHz. Number of blows to the head were recorded. Groups were divided into those with (cases) and without (controls) head blows during sparring.

Results
All MMA volunteers (n=29) had normal otoscopy prior to and immediately following sparring. Cases (n=21) demonstrated post-sparring air conduction thresholds shifts (1-8kHz) ranging from 2.62 to 7.86 dB ($p< 0.05$) in the right ear. The left ear also had increased thresholds at 2 to 4 Hz, ranging from 2.62 to 6.67 dB HL ($p< 0.05$). Controls (n=8) showed no threshold shifts across all tested frequencies (p=ns). There was a positive correlation in mean change in hearing threshold and the number of blows across 1-8kHz, with the strongest correlation at 4kHz ($r=.647$, $p< .0001$).

Conclusion
This is the first study to detect acute hearing threshold shifts following repetitive head impacts following participation in a contact sport. Additional study is needed to understand the mechanism of the threshold change.

PS 110

Osmotic Challenge Alters Endolymphatic Volume in TectaC1509G/C1509G Mice

Patricia M. Quiñones[1]; Juemei Wang[1]; Frank D. Macías-Escrivá[2]; Wihan Kim[2]; Brian E. Applegate[2]; John S. Oghalai[2]
[1]USC Caruso Department of Otolaryngology - Head and Neck Surgery; [2]Caruso Department of Otolaryngology - Head and Neck Surgery, University of Southern California

Introduction
Immediately following blast-exposure, the mechanically-sensitive stereociliary bundle is damaged in CBA/CaJ mice. This leads to a build-up of endolymph in scala media (SM), known as endolymphatic hydrops. In addition, we showed that altering the osmolality of the perilymph changed the volume of endolymph in CBA/CaJ mice. Interestingly, the endolymphatic volume is larger in mouse models where the bundles are not stimulated, as is the case in the $Tecta^{C1509G/C1509G}$ mouse, where the outer hair cell stereocilia are detached from the tectorial membrane. After blast, these mice show no change in endolymphatic volume. Here, we sought to determine whether similar changes in endolymph volume occurred in $Tecta^{C1509G/C1509G}$ mice in response to osmotic challenge.

Methods
To study endolymphatic hydrops without traumatic noise exposure, we opened the middle ear bulla of mice 4-6 weeks in age (wild-type (CBA/CaJ) and $Tecta^{C1509G/C1509G}$) and imaged the cochlea using optical coherence tomography. We collected a volume stack of cross-sectional images of the cochlea and then applied a hypotonic solution (deionized water, 0 mOsm/kg, pH = 7.4) to the round window membrane and reimaged after 1 h. To quantify endolymphatic volume, we used Imaris software (Bitplane) to render 3D images from the volume stacks. We selected an identical 150-µm segment of the

scala media (SM) from each sample and the volume was measured using a built-in feature within Imaris.

Results
We found that application of hypotonic solution for 1 h in wildtype mice caused endolymphatic hydrops. We measured increases in SM volume of 4.4e5 ± 2.1e5 μm^3 (9.6 ± 4.5% increase) in wild-type mice. For $Tecta^{C1509G/C1509G}$ mice, the volume increased as well (2.7e5 ± 1.4e5 μm^3). Further studies with hypertonic solutions are ongoing.

Conclusion
Osmotic challenge via the unopened round window membrane is a reliable method for producing endolymphatic hydrops *in vivo*. Studies are ongoing to assess for changes after hypertonic challenge. This model will be useful for studying the role of endolymphatic hydrops in cochlear dysfunction.

This work was supported by NIDCD grants DC014450 (J.S.O) and DC013774 (J.S.O & B.E.A.).

PS 111

Cochlear HPA-like CRFR1 Signaling is Critical for Protection Against Elevated ABR Thresholds Following Noise Exposure and Traumatic Brain Injury

Charles C. Barnes[1]; Kathleen T. Yee[2]; Douglas E. Vetter[2]
[1]Univ. Mississippi Medical Center; [2]Department of Neurobiology and Anatomical Sciences, University of Mississippi Medical Center

The cochlea is susceptible to a myriad of challenges that can alter hearing sensitivity or even kill hair cells. Because mammalian cochlear hair cells do not regenerate, the cochlea likely possesses layers of protective signaling important for mitigating damage following insults. While much research has centered on acoustic impacts to the cochlea, other insults also represent significant threats to hearing. However, investigation of signaling systems capable of protection against a *range* of possible insults to hearing has not been previously attempted.

The cochlea expresses a signaling system molecularly identical to the systemic HPA-axis. Because the HPA-axis is critically involved in homeostatic regulation of the body in response to stressors, we hypothesize that the cochlear HPA-equivalent system represents a critical component to the cochlea's ability to protect itself from challenges that could affect hearing. We examine whether local loss of the presumptive initiation signal for cochlear HPA-like system activity results in greater susceptibility to hearing loss following both noise and non-acoustic traumatic brain injury (TBI) insults.

To assess the protective potential of cochlear HPA-like signaling, we created a conditional null CRFR1 mouse line. Tamoxifen (75mg/kg) or corn oil (vehicle) injections were provided daily for 5 days to floxed CRFR1 Sox9iCre double transgenic (fCRFR1:Sox9iCre) mice. Two separate challenges were used: 8-16kHz 100dB noise for 2 hours or a mild TBI (mTBI). mTBI was induced with the Closed Head Impact Modeling Engineered Rotational Acceleration (CHIMERA) system. ABRs were recorded up to 30 days after noise or mTBI.

Following noise exposure, 4-month old control fCRFR1:Sox9iCre mice initially exhibited a significant ABR threshold shift that almost fully resolved over 10 days. CRFR1 cKO mice expressed a more significant ABR threshold shift compared to controls and did not recover baseline thresholds after 10 days. A single mTBI impact (~0.6 Joule) in 4-5-month old control fCRFR1:Sox9iCre mice did not produce an ABR threshold shift. However, CRFR1 cKOs experienced a significant ABR threshold shift after just one mTBI insult. As with noise insults, age was a significant factor in TBI-induced ABR outcomes. Unlike the older cohort, 2-month old control mice experienced a significant ABR threshold shift. The young cKOs also showed a significant, but smaller, ABR threshold shift compared to 2-month old controls.

Our results indicate that cochlear HPA-like signaling is involved in maintaining general homeostatic balance in the cochlea following both acoustic and non-acoustic challenges to hearing.

Support: R21DC015124, Intramural Research Support Program (UMMC)

PS 112

Concussion-like Mild Head Impacts Cause Deficits in Hearing Function

Graham Casey; Mark Lewis; Bradley J. Walters
University of Mississippi Medical Center

Mild Traumatic Brain Injuries (mTBIs) and hearing loss (HL) are both exceedingly common and can adversely affect quality of life and impose significant healthcare costs on affected individuals. Despite a large body of clinical literature describing changes to hearing and balance following head injury, little is known about how concussion-like mTBIs directly affect hearing and the cochlea, particularly in cases of repeated injury. To explore the effects of mTBIs on hearing, we used a relatively new device: the Closed Head Impact Model of Engineered

Rotational Acceleration (CHIMERA). The CHIMERA can generate closed-head injuries in a manner that is both precise and consistent with the energies observed in concussions and even sub-concussive head impacts. Additionally, these head impacts permit free movement of the neck and skull, which is likely a contributing factor in the etiology of mTBI induced hearing loss (mTBI-HL). Using C57Bl/6 mice of two different ages (2-4 months old or 5-6 months old) we delivered either a single mTBI or a repeated impact paradigm (1 impact per day for 4 days). We then examined changes in hearing function and in the sensory tissues of the inner ear. Auditory brainstem responses (ABRs) and distortion product otoacoustic emissions (DPOAEs) were recorded before injury and at 1 and 7 days post injury. Additionally, we performed immunohistochemical analyses to measure hair cell survival, synaptic degeneration, and other types of tissue damage. We found that a single mTBI could induce significant increases in the wave I-III and I-IV latencies 1 day after injury, indicating disrupted communication along the auditory pathway to central auditory structures. Additionally, we observed histopathological changes within the cochlea 7 days after repeated injury, most notably the loss of cochlear outer hair cells in the 5-6 month old group. Such alterations indicate that concussion-like mTBIs significantly affect the cochlea as well auditory nuclei in the central nervous system. These findings identify multiple facets of mTBI induced hearing dysfunction and may represent unique types of injury to the auditory system. Future studies are aimed at using genetic mouse models to uncover the molecular mechanisms for this hair cell loss as well as other pathologies associated with mTBI.

PS 113

Experimental and Computational Approaches for Studying Excessive Impact-Induced Hearing Damage in Contact Sports

Shinji Hamanishi[1]; Jongwoo Lim[2]; Namkeun Kim[2]
[1]Tohoku Gakuin University; [2]Incheon National University

Kendo, Japanese fencing, is a modern martial art, which descended from swordsmanship. Each player wears a helmet and other protectors and try to hit one of the target areas on opponent's protectors with a bamboo sword to get points. However, kendo is associated with a risk of hearing loss. Many audiometric studies have shown that kendo training over many years often causes sensorineural hearing loss at 2000 Hz and/or 4000 Hz. Although the risk of permanent hearing loss by repeated head impact and trauma has long been known in other contact sports like boxing and American football (DeKlein, 1941 and Leonetti, 2018), its mechanism is still unclear.

Our hypothesis based on experiments and simulation using a skull bone model is that the cause of hearing loss by contact sports may possibly be related to accumulation of small concussions in the human head by the excessive impact-induced bone conduction. We evaluated this hypothesis by a simplified impact experiments and Finite Element (FE) simulation using a human head and kendo helmet model.

Impact experiments were performed using a dummy head and kendo helmet model. An accelerometer (NP-3211, ONO SOKKI) and an ultraminiature microphone (MB-2200M10, ONO SOKKI) were attached on impact area and ear canal of head model, respectively. Time history responses of acceleration and sound pressure to impact by a bamboo sword were measured. Impact experiments showed that effects of kendo helmet on impact reduction was significantly small. In addition, impact caused high sound pressure of more than 100 dB SPL with regardless of the helmet.

In order to reduce head trauma, we proposed an impact absorption structure made by additive manufacturing technique. This honeycomb structure have high shock absorbability and breathability, which are essential for kendo players. Impact experiments found that the newly developed kendo helmet with the absorbing structure reduced damage to head model.

We introduced a computational approach to simulate bone conduction using a newly constructed FE model consisting of the kendo helmet coupled to a human head. The head model contains the skull, brain, soft tissue, cartilage and auditory peripheries, including the middle ear, cochlea and semicircular canals. Our preliminary simulation showed good correlation with impact experiments and the proposed FE model may help us to quantify the effects of the helmet and the impact absorbing structure on reduction of head trauma.

PS 114

Examining Disparity-Driven Vergence in Chronic Symptomatic Mild Traumatic Brain Injury (mTBI)

Erin Williams[1]; **Alyssa Whinna**[2]; Neil Nayak[3]; Alex Kiderman[4]; Michael Hoffer[1]; Carey Balaban[5]
[1]University of Miami; [2]Univerity of Miami; [3]Flordia Ear and Sinus Institute; [4]Neuro-kinetics, Inc.; [5]Universtiy of Pittsburgh

Background
The coordination of vergence, or the simultaneous movement of both eyes to maintain focus, is thought to be controlled by complex neurophysiological mechanisms that can be susceptible to damage by

traumatic brain injury. Current tests of binocular disparity driven vergence examine only one frequency (0.1 Hz). While this provides some accuracy in diagnosing mTBI, accuracy could be increased with testing more frequencies.

Objectives
To examine the differences in vergence response over a set of randomly presented frequencies in subjects with symptomatic chronic mTBI as compared to an age and gender matched control group using the I-Portal IPAS goggles.

Study design
Clinical trial

Methods
Both non-TBI (n=22) and mild TBI patients (n=8) were recruited. Each patient underwent baseline calibration testing and binocular disparity vergence pursuit testing from 0.07- 0.2 Hz. The IPAS goggles presented sinusoidal binocular disparity stimuli (0.1 deg white square) over a range of frequencies from 0.07 Hz to 0.2 Hz in random fashion. Pupil area and eye position were recorded continuously. Each subject was given a medical symptom/toxicity questionnaire (MSQ) at the end of testing.

Results
Metrics of performance were assessed with MANOVA for frequency and group effects. The vergence eye movement position gains, phases and goodness of fit (R^2) did not vary significantly across the control subjects (grand means: 0.84±0.01, -6.2±3.1° and 0.82±0.02, respectively).The concurrent pupil modulation depth and phase were also constant across the range in controls. The mTBI group showed a convergence eye movement insufficiency (significantly lower gains and increased phase lags) that did not differ across frequencies (grand means: 0.77±0.03 and -18,4±5.8°, respectively), but no difference in R^2(0.83±0.02). The concurrent pupil modulation depth and phase were also constant across the range in mTBI subjects.

Conclusion
Disparity-driven vergence testing over a randomly presented set of frequencies has shown to be consistent in subjects without history of traumatic brain injury. This consistency in control subjects is a critical step in using the technology for quantitative tests of convergence insufficiency in individuals with mTBI.

PS 115

The different blast-induced cochlear damage by the different properties of the shock wave.

Eiko Kimura[1]; Kunio Mizutari[1]; Yasushi Satoh[2]; Satoko Kawauchi[3]; Shunichi Sato[3]; Akihiro Shiotani[1]
[1]Department of Otolaryngology, Head and Neck Surgery, National Defense Medical College, Japan; [2]Department of Pharmacology, National Defense Medical College, Japan; [3]Division of Bioinformation and Therapeutic Systems, National Defense Medical College, Japan

Aims/Objective
This study investigated detailed pathophysiology of blast-induced cochlear damage and the difference caused by the different property of shock wave.

Methods
This study used low-intensity blast model by shock tube and laser-induced shock wave (LISW) models. The shock tube was consisted of SUS-tubing inflated compressed nitrogen gas, and shock wave irradiated towards the diagonally front of mice head. LISW was the shock wave that was generated by irradiating a 532-nm Nd: YAG laser through a laser target. LISW irradiated to the posterior ear bone of mice.

Six-week-old male CBA/J mice were used. The auditory brainstem responses (ABRs) and the distortion product otoacoustic emissions (DPOAEs) were performed. Cochlear immunohistochemistry was performed after 28 days after shock wave exposure, using Myosin VIIA, CtBP2, and GluR2. The morphology of hair cells was investigated by scanning electron microscope (SEM) at 14 days after exposure.

Results
The permanent ABR threshold shifts about 10 - 20 dB were remained up to 28 days after exposure in both groups. The wave I amplitudes of ABR significantly decreased one day in both groups. However, the wave I amplitude was not recovered in the shock tube group, whereas it recovered at low frequencies in the LISW group. DPOAE thresholds were not elevated in the shock tube group, while elevated at high frequency in the LISW group.

The synapse ribbons of inner hair cells decreased significantly in both groups. Moreover, severer synapse degeneration was detected at basal turn than apex turn of cochlear in the LISW group, whereas the consistent degenerative changes of the synapse were observed in shock tube group. SEM study revealed the stereocilia in outer hair cells showed misalignment and absence at

the basal turn in LISW groups, whereas showed slight misalignment at apex turn in shock tube groups.

The pressure waveforms and Fast Fourier transform of each shock wave were performed to investigate the property of the shock wave. The shock tube is consistent with 25 kPa peak pressure, 400 μS duration time, and 876 Hz peak frequencies of shock wave, whereas LISW is 100 MPa peak pressure, 0.5μS duration time, and 259 kHz peak frequencies. These different peak pressure and frequency components could affect the different pathophysiological changes between both groups.

Conclusion

The primary etiology of blast-induced cochlear damage was synapse degeneration in inner hair cells and misalignment stereocilia in outer hair cells. These changes could depend on the frequency-properties of shock wave energy.

Cochlear Mechanics I

PS 116

Effects of Furosemide on Organ of Corti Vibrations

C. Elliott Strimbu; Yi Wang; Elizabeth S. Olson
Columbia University

The endocochlear potential (EP) is necessary for mechanoelectrical transduction and outer hair-cell (OHC) generated force production. Previous work has shown that IV administration of furosemide immediately reduces the EP, which mostly recovers over approximately 40 minutes. Furosemide alters the mechanical response of the basilar membrane (BM), the local cochlear microphonic (LCM) and distortion product otoacoustic emissions (DPOAEs), all of which recover over time.

Using optical coherence tomography we measured BM and organ of Corti vibrations in a region close to the OHCs in the gerbil cochlea before and after the IV administration of furosemide. The stimuli were multi-tone Zwuis complexes containing 60 frequencies presented simultaneously at 40 to 80 dB SPL. DPOAEs were measured at the same time points in response to two-tone stimuli at 50 and 70 dB SPL, and used to ascertain the successful IV administration of furosemide and monitor recovery.

As has been previously demonstrated, immediately following furosemide administration, the amplitude of BM vibrations was greatly reduced in the peak best frequency (BF) region, showed passive-like broad tuning, and scaled linearly with SPL. Following furosemide, OHC-region responses decreased and showed low-pass tuning with loss of the BF peak. However, in contrast to the BM, the vibrations of the OHC-region points retained nonlinearity across the frequency range. DPOAEs were greatly reduced following furosemide.

Over subsequent recordings, taken at approximately 10-minute intervals, the vibrations of the BM and OHC-region gradually recovered. Approximately 50 - 70 minutes post injection, BM vibrations begin to recover the BF peak and compressive nonlinearity near the BF. The OHC region BF peak recovered with a similar time course to the BM BF peak. In the best experiment, both the BM and OHC region responses showed nearly full recovery, at approximately 150 minutes.

In previous studies, local cochlear microphonic (LCM) potentials, representing OHC electrical responses, were reduced but present and nonlinear following furosemide, and the nonlinear OHC-region motion we observed is likely due to OHC motility responding to that remaining electrical response. Recovery of *cochlear amplification*, as expressed in the nonlinear BF peak in BM and OHC-region motion, appears to rely not just on OHC motility, but on an as-yet-unknown recovery process.

PS 117

Organ Of Corti Mechanical Filtering In The Guinea Pig Apex Measured By OCT: Implications For Phase Locking Auditory Receptors

Alfred L. Nuttall[1]; **George W. Burwood**[1]; Anders Fridberger[2]
[1]Oregon Health & Science University; [2]Linköping University

The apex of the mammalian cochlea is important for the perception of acoustic signals relevant to speech and music, which are carried by slowly varying sound envelopes. Envelope detection is improved by temporally sensitive receptors. Temporal sensitivity is facilitated by auditory nerve fibers, which respond in a phase locked manner to sufficiently low frequency acoustic stimuli.

Recent observations show that the filtering characteristics of the cochlear apex and base differ. Chiefly, iso-level tuning curves measured in the apex are low-pass, not band-pass. Additionally, a large number of inner hair cells are thought to contribute to signal detection at the apex of the gerbil cochlea, even at modest sound pressure levels. What is the benefit of such a distributed system, and what specialization of the apex imbues enhanced detection of physiologically relevant signals?

We have recorded the displacement and phase of the organ of Corti at separate locations within the cochlear apex of the guinea pig using spectral domain optical coherence tomography vibrometry, and employing our previously described minimally invasive preparation. We confirm that the mechanical filtering several locations in the apex of the cochlea is indeed low-pass, and that this low-pass tuning is physiologically vulnerable. We also compare the group delays of the sound evoked organ of Corti vibrations measured at different longitudinal locations, and between sensitive and insensitive cochleae. The raw group delay values compare well with published data. The relative delay between two points in the apex is almost zero despite their half turn separation. This relative delay increases post mortem, and with higher levels of stimulation. The results suggest that a mechanism exists whereby the signal to noise ratio of phase locked auditory nerve fibers is enhanced, which may aid in increasing temporal sensitivity.

PS 118

Reticular lamina and basilar membrane motion suppression in a two degrees of freedom transmission line nonlinear cochlear model

Renata Sisto[1]; Arturo Moleti[2]
[1]INAIL Research Department of Occupational and Environmental Medicine, Epidemiology and Hygiene; [2]University of Rome Tor Vergata, Department of Physics

Recent in vivo measurement of the basilar membrane (BM) and reticular lamina (RL) motion have demonstrated that RL vibration amplitudes are larger than those of the BM and that the RL response is nonlinear over a broader basal region with respect to the narrow region representing the BM activity peak. This behavior has been interpreted as the evidence of a global amplification system acting through the RL. Dewey et al. showed that although the RL response is nonlinear over a wide cochlear region, the amplification accumulates only within a narrow region roughly coincident with the BM activity peak. While the BM is directly coupled to the fluid differential pressure, the RL interacts with the BM through the cochlear amplification system, i.e. the OHC system. Looking at the details of the BM and RL motion should permit a deeper understanding of the cochlear amplification loop. In this paper the RL and BM motion is analyzed using a 2 degrees of freedom (2DOF) 1-dimensional transmission line cochlear model.

A 2DOF nonlinear transmission line cochlear model was implemented in which the BM and the RL are coupled by a local active force, nonlinearly dependent on the BM instantaneous displacement and velocity. A real-zero version of the model was chosen in which the normal modes of the system are characterized by a single oscillation and a pure damped motion. This model has some interesting physical properties such as the fact that the second mass (the RL in a realistic cochlea) shows a nonlinear behavior over much broader region than the BM activity peak.

The BM and RL response-to-tone and the two-tone-suppression curves obtained with the real-zero 2DOF cochlear model at different stimulus levels can be compared to those of the experimental studies, to highlight the relationship between the characteristics of the cochlear amplifier and of the nonlinear response of the two vibrating elements. The model seems to be able to reproduce some relevant features of the experimental data relative to the RL and BM response and their suppression curves. Caution should be put in interpreting the motion of the RL and the BM as if they were independent oscillators. As they are strongly coupled by the active feedback itself, it would not be safe to interpret the nonlinear motion of the RL as it was, independently from the BM, the only manifestation of the active loop.

PS 119

A Numerical Study of the Basilar Membrane and Organ of Corti Nonlinear Compression

Aritra Sasmal; Joshua Hajicek; Karl Grosh
University of Michigan

Measurements of cochlear nonlinear compression and amplification using optical coherence tomography and electrophysiological recordings show nonlinear compression is not exclusive to the basilar membrane (BM). In the basal turn of the guinea pig cochlea, compressive nonlinearity of BM displacement is observed over a half-octave range basal to the best frequency (BF). At frequencies less than a half-octave below the BF, BM displacement grows linearly with stimulus intensity. In contrast, nonlinear compression of outer hair cells and the reticular lamina (RL) extend more than an octave below the BF, and the input-output (I/O) curves show hyper-compressive behavior. In this study we explore the I/O growth curves using a nonlinear finite element model of the guinea pig cochlea. Displacement of the BM and the RL, as well as local endocochlear potentials are compared. The model predicts the disparity in compressive behavior between the BM and RL, consistent with *in vivo* experimental observations in the mammalian cochlea.

PS 120

Cochlear Nonlinearity and Amplification in The Guinea Pig

Elika Fallah; C. Elliott Strimbu; Elizabeth Olson
Columbia University

As two key components of cochlear transduction and frequency tuning, the electrophysiological responses of the outer hair cells (OHCs) and mechanical displacements of the Organ of Corti have previously been studied in the gerbil cochlea by us and others. To investigate the consistency of cochlear mechanics in the mammalian cochlea, we measured the responses of (1) the extracellular voltage generated by OHCs, termed local cochlear microphonic (LCM) and (2) displacements within the organ of Corti complex (OCC) to single and multi-tone stimuli in the base of the guinea pig cochlea. LCM measurements were performed through a hole in either the round window membrane or the wall of the cochlea. We found similar LCM responses in guinea pig and gerbil: Below the best frequency (BF) region, the LCM responses were mildly nonlinear in response to single tones and strongly nonlinear in response to multi-tones. In the BF region, strong nonlinearity was observed in LCM responses to both single and multi-tone stimuli. Displacement measurements were conducted through the intact round window membrane using optical coherence tomography. We observed similar cochlear displacements in guinea pig and gerbil: a strong nonlinearity in the BF region both at the basilar membrane and within the OCC. Further voltage and displacement experiments focusing on the OHC region are ongoing. Our findings so far suggest that the mechanics of cochlear amplification are similar in guinea pig and gerbil.

PS 121

Organ of Corti Vibrations in Awake Mice

Christopher G. Lui[1]; James B. Dewey[1]; Ido Badash[1]; Frank D. Macías-Escrivá[1]; Wihan Kim[1]; Matthew J. McGinley[2]; Brian E. Applegate[1]; John S. Oghalai[1]
[1]Caruso Department of Otolaryngology - Head and Neck Surgery, University of Southern California; [2]Department of Neuroscience, Baylor College of Medicine

Our understanding of cochlear mechanics has been mostly shaped by experiments with post-mortem tissues or measurements in anesthetized animals. However, anesthesia may significantly impact cochlear mechanics, as anesthesia has been shown to alter otoacoustic emissions. Here, we directly examined the effect of anesthesia on sound-induced vibrations of the organ of Corti. Using volumetric optical coherence tomography and vibrometry (VOCTV), we imaged the cochlea through the ear canal in head-fixed mice positioned on a treadmill. We noninvasively measured the radial motion of the organ of Corti in the same mice both while they were anesthetized and then again after they were fully awake and behaving. We show that organ of Corti vibrations in awake mice are larger in magnitude across all frequencies, while tuning sharpness is broadly decreased. For a 50 dB SPL stimulus, the vibratory response in the awake state was larger by 2.78 ± 1.04 dB (n = 10, p = 0.03) at the characteristic frequency (CF), and 8.8 ± 1.2 dB (n = 10, p = 0.0008) larger at ½ CF. The average Q_{10dB} value for tuning curves at 50 dB SPL was 23% (n = 10, p = 0.002) lower in awake mice. Middle ear vibrations were unaffected by state, and thus does not explain the cochlear findings. These results indicate that anesthesia alters cochlear mechanics. Here we demonstrate the utility of VOCTV to investigate cochlear mechanics in an awake animal model for the first time. Furthermore, this novel approach will allow the study of cochlear mechanics during behavioral tasks.

Supported by NIDCD grants DC014450 (J.S.O.) and DC013774 (J.S.O. & B.E.A.)

PS 122

Measuring Cochlear Impulse Responses Using Frequency Sweeps

Karolina K. Charaziak[1]; Alessandro A. Altoé[1]; John S. Oghalai[2]; Christopher A. Shera[1]
[1]University of Southern California; [2]Caruso Department of Otolaryngology - Head and Neck Surgery, University of Southern California

Linear, time-invariant systems are fully characterized by their impulse responses (i.e., by their response to an ideal pulse or Dirac delta function). Although clearly nonlinear, cochlear mechanical impulse responses have been measured using broadband acoustic clicks under the assumption of quasi-linear processing at each stimulus level. However, due to their high crest factor, click stimuli are free of measurable transducer distortion over only a limited range of click levels. Here, we employ a novel method for measuring of cochlear impulse responses that utilizes logarithmic frequency sweeps. The method, originally developed for room acoustics measurements [Farina 1995; 108th AES Convention], has two major advantages over traditional, click-derived impulse responses. First, the energy in the swept stimulus is spread out over time, resulting in considerably lower crest factors. Second, the logarithmic frequency sweep allows one to deconvolve simultaneously the linear impulse response of the system and separate responses for each order of harmonic distortion. Using optical coherence tomography, we applied this method to measure impulse responses and harmonic distortions from a mouse cochlea and compared the results to responses

measured using acoustic clicks. In the case of basilar-membrane responses, impulse responses measured with clicks and sweeps are similar, but not identical. Both exhibit compressive growth with increasing stimulus level, although sweep-derived impulse responses are shorter in duration, particularly for slower sweep rates. This difference in duration disappears post mortem, implying that it arises in active cochlear mechanics. The 2nd- and 3rd-order harmonic kernels extracted from the deconvolution display the characteristics of harmonic distortions measured previously using tonal stimuli: They are both low in level (at least 20 dB below the linear response) and dependent on the health of the preparation, at least at moderate stimulus levels. This study demonstrates the feasibility of using the swept tones for measuring cochlear impulse responses and harmonic distortions.

PS 123

Interplay between the active process and wave propagation in the mammalian cochlea

Amir Nankali[1]; Frank D. Macías-Escrivá[2]; Brian Applegate[1]; John S. Oghalai[2]
[1]University of Southern California; [2]Caruso Department of Otolaryngology - Head and Neck Surgery, University of Southern California

Sounds entering the mammalian ear produce waves that travel from the base to the apex of the cochlea. These traveling waves stimulate the microstructure of the organ of Corti (OoC). The interplay between the traveling wave and a nonlinear amplification process boosts the cochlear responses and enables sound processing over broad frequency and intensity ranges. However, the exact underlying mechanism is not well understood, mainly due to technical challenges of *in vivo* travelling wave measurements. In this study, vibration responses of the OoC were measured at multiple locations along the apical turn of the mouse cochlea using volumetric optical coherence tomography and vibrometry (VOCTV). The spatial vibration pattern varied systematically with both stimulus frequency and intensity. The wavelength and group velocity at different location and frequencies were measured and the variation with stimulus intensity was studied. Our data indicates that the spatial wavelength of the traveling wave is affected by the active process such that lower input sounds generate smaller wavelengths closer to the best place (BP) location. Moreover, the spatial and frequency domain vibration data were used to assess the scaling symmetry theorem. It is found that the accuracy of the scaling symmetry approximation is local and level dependent.

Supported by NIDCD grants R01 DC014450 and R01 DC013774

PS 124

Why is the Cochlea an Ear Horn?

Alessandro Altoè[1]; Christopher A. Shera[2]
[1]Caruso Department of Otolaryngology - Head and Neck Surgery, University of Southern California; [2]University of Southern California

The existence of approximate scaling symmetry in the cochlea greatly facilitates the interpretation and modeling of cochlear mechanical data. Strict scaling implies that basilar-membrane (BM) transfer functions measured at different locations along the spiral are everywhere identical when expressed as a function of frequency normalized by the local characteristic frequency (CF).

In 2- and 3-D models, scaling symmetry imposes contrasting requirements on cochlear geometry when the wavelength of the traveling pressure wave is long relative to the height of the scalae (i.e., in the basal, tail-region of the traveling wave) versus when the wavelength is short (i.e., in the tip region near the best place). In particular, when the wavelength is long, scaling symmetry requires a tapered horn-like geometry in which the height of the scalae decreases with distance from the stapes; when the wavelength is short, however, scaling requires that the geometry be box-like (i.e., that the height remain approximately constant along the cochlea).

In this study, we show that approximate scaling in the long-wave (tail) region of the traveling wave is both (i) necessary for pressure waves to propagate apically without substantial attenuation and (ii) consistent with anatomical and mechanical data from the basal and middle turns of the cochlea. The requirements of “long-wave” scaling induce a violation of “short-wave” scaling in the peak region of the BM transfer function, leading to a broadening of the BM tuning with a decreasing CF. The variations in tuning sharpness with location predicted by models with long-wave scaling agree qualitatively with those observed experimentally in the basal and middle turns of the cochlea.

Nevertheless, the breaking of short-wave scaling produced by long-wave scaling models is not sufficient to explain the significant broadening of cochlear tuning evident in the apical turn of various species. We note that whereas long-wave scaling appears desirable in the basal and middle turns of the cochlea (so that traveling waves can reach their tonotopic locations without significant losses), the same is not necessarily true in the most apical regions of the cochlea. In particular, minimizing reflections from the helicotrema may require that energy carried by the traveling wave be progressively dissipated in the apical turn.

PS 125

Organ of Corti Cross-sectional Area Change due to Electromotilty of the Outer Hair Cells

Mohammad Shokrian Amiri; **Jong-Hoon Nam**
University of Rochester

The organ of Corti (OoC) operates as if a sophisticated micromachine that transforms acoustical pressures into the vibrations of mechano-transducer cells. Vibration pattern of the OoC is dependent on the level of stimulation, or the extent of outer hair cell's motility. The OoC vibrations due to acoustic pressure evokes outer hair cell motility. In turn, the outer hair cell's motility modulates the OoC vibrations. The interplay between the two vibration patterns (one caused by the acoustic pressures and the other caused by the outer hair cell motility) is considered to bear the consequences in hearing—tuning and amplifying sounds. We report our observations on the vibration patterns of the OoC micro-structures in excised cochlear turns. Especially, the difference between mechanically and electrically evoked vibrations is presented in terms of the OoC cross-sectional area change.

The cochleae were isolated from young gerbil (15-30 day old). After being reduced to the middle turn, the excised cochlea was placed in a micro-chamber. The tissue in the micro-chamber was subjected to mechanical/electrical stimulations. Resulting vibrations were measured using an optical coherence tomography system (Figure). We found the following: First, the OoC fine structures vibrate in phase when mechanically stimulated, but they vibrated out-of-phase when electrically stimulated; Second, the vibration phase of OoC fine structures varied not only along the transverse direction of the OoC, but along the radial direction of the OoC; Third, the out-of-phase vibrations resulted in greater cross-sectional area change of the OoC; Finally, the area change was dependent on stimulating frequency.

Supported by NIH R01 DC014685, and NSF CMMI 1661413.

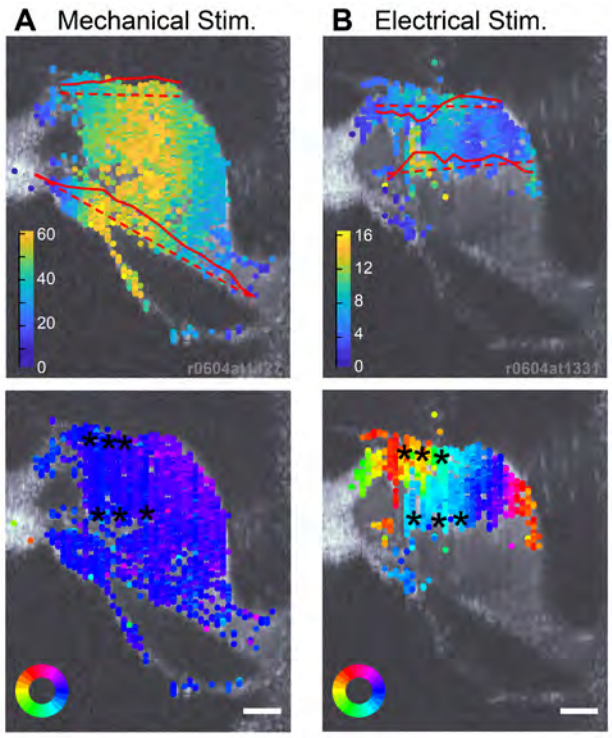

PS 126

Wave propagation on isolated tectorial membranes: radial to longitudinal mode conversion

Haiqi Wen[1]; Jonathan Sellon[2]; Amer Mansour[2]; Roozbeh Ghaffari[2]; Dennis Freeman[2]; Julien Meaud[1]
[1]Georgia Institute of Technology; [2]Massachusetts Institute of Technology

The tectorial membrane (TM) is an extracellular gel-like structure located in the organ of Corti located above the hair bundle of outer and inner hair cells. The TM contains radially oriented collagen fibrils and various non collagenous proteins including a-*tectorin* (TECTA), b-*tectorin* (TECTB) and CEACAM16. In wild-type (WT) mice, the TM is highly anisotropic and tends to show a larger stiffness in the radial than in the transverse direction due to the orientation of the collagen fibers. The TM is known to play an important role in the normal function of the mammalian cochlea. Some genetic mutations that affect the TM proteins are related to abnormal cochlear function, hearing disorders, and changes to otoacoustic emission generation.

This work aims to improve our understanding of how specific mutations affect cochlear mechanics by studying wave propagation on isolated TMs of WT and transgenic mice. A previously published wave chamber device was used to study wave propagation on isolated TMs in an artificial endolymph bath. The motion of the TMs of wild-type and transgenic (Tectb knockout and *Ceacam16*-null) mice was recorded using an optical system when

the TMs are excited in the radial direction. As previously reported, a longitudinally propagating radial (shear) wave is observed on the TMs of wild-type and transgenic mice. However, even though the excitation is primarily in the radial direction, longitudinal motion is also observed. This motion is particularly prominent in the *Ceacam16*-null and *Tectb* knockout TMs, which suggest that the mutations significant affect the properties of the TM. To improve understanding of why radial to longitudinal mode conversion is observed in the mutant TMs, a finite element model of the experiments is developed. The model includes a transversely isotropic viscoelastic model of the TM and takes into account the influence of the viscous fluid (artificial endolymph) on the wave propagation by including the added damping and mass due to the viscous boundary layer. A previously described least squares fitting method is used to determine the effective TM properties of wild-type TMs. Parametric studies are then used to evaluate the conditions for observing significant radial to longitudinal mode conversion. We found that reduction in the transverse and/or shear stiffness of the TM tends to enhance the magnitude of the longitudinal motion relative the radial motion in a manner analog to what is observed in the mutant TMs.

This work demonstrate that TM mutations affect wave propagation on isolated TMs in a complex manner. Quantifying the material properties of the wild type and mutant mice will help to elucidate how the TM properties are linked to proper function of mammalian cochlea.

Research Funding:This research is funded by NIH R01DC016114 & NIH R01-DC000238.

PS 127

Probing Force Relay in Drosophila Hearing

Thomas Effertz[1]; Philip Hehlert[2]; Dirk Beutner[1]; Martin C. Göpfert[2]
[1]Department of Otorhinolaryngology, University Medical Center Göttingen; [2]Department of Cellular Neurobiology, Institute for Zoology and Anthropology, University of Göttingen, Germany

Sensitive hearing in *Drosophila* requires the NOMPC (TRPN1) channel [1]. NOMPC is a bona fide mechano-electrical transduction (MET) channel whose amino-terminal ankyrin repeat (AR) domain consists of 29 ARs. These 29 ARs assemble into a helical structure [2], tether the channel intracellularly to microtubules [3], and are essential for mechano-gating [3]. Duplicating the NOMPC AR domain yields functional NOMPC$^{29+29ARs}$ channels [3], and we now tested how this duplication affects force transmission.

Consistent with previous reports [3], NOMPC$^{29+29ARs}$ enabled mechano-activated currents in heterologous expression systems. The mechanosensitivity of these MET currents resembled those of normal NOMPC, as did sensitive hearing when replacing NOMPC in the adult fly with NOMPC$^{29+29ARs}$. In addition, the NOMPC-dependent nonlinear gating compliance in the fly's auditory mechanics [1] was found unaffected. Hence, duplicating the NOMPC AR domain neither affects NOMPC mechanosensitivity in *in vitro* nor *in vivo*.

Our analysis suggests that the NOMPC AR domain is in series with more compliant elements whose deformation promotes mechano-gating. Genetic manipulations have narrowed down the identities of these highly compliant elements, which represent an integral component of NOMPC.

References

[1] Effertz T, et al. (2012). Direct gating and mechanical integrity of Drosophila auditory transducers require TRPN1. *Nat Neurosci.* **15**, 1198-1200.

[2] Jin, P. et al. (2017). Electron cryo-microscopy structure of the mechanotransduction channel NOMPC. *Nature* **547**, 118-122.

[3] Zhang, W. et al. (2015). Ankyrin repeats convey force to gate the NOMPC mechanotransduction channel. *Cell* **162**, 1391-1403.

Supported by DFG, SFB889, A1.

PS 128

Mechanical Contributions of the Supporting Cells in the Organ of Corti

Wenxiao Zhou; Jong-Hoon Nam
University of Rochester

The mammalian cochlea is mechanically agitated by external and internal stimulations. Externally, the vibrations of the oval window generate differential pressures across the organ of Corti (OoC), resulting in traveling waves along the cochlear coil. Internally, the outer hair cells (OHCs) can generate mechanical force, in response to the OoC vibrations, giving feedback to their external structures. The mechanical force to/from the OHCs are transmitted through structurally significant supporting cells such as the pillar cells and the Deiters' cells. The truss-like structure formed by the OoC supporting cells has been considered essential for cochlear amplification, by forming structural loop analogous to the feedback-loop in control systems (Yoon, Steele and Puria, 2011). Despite the perceived importance, the mechanical operation of the OoC supporting cells *in situ* has been challenging to observe.

We measured the relative motion/deformation of the OoC supporting cells *in situ*. Vibrations of the OoC fine structures in excised gerbil cochleas were measured using the optical coherence tomography. As the preparation secured a clearer optical path by removing the scalar bones, our imaging system could resolve fine structures such as individual OHCs. The deformations of individual OHCs, pillar cells and Deiters cells were measured when the OoC was subjected to mechanical and electrical stimulations. To better interpret experimental observations, our existing computer model of the OoC (Zhou, Nam, 2019) was modified. We present the relative stiffness of the supporting cells with respect to the OHC, and discuss how the supporting cells contribute to cochlear function.

Supported by NIH R01 DC014685,
and NSF CMMI 1661413

PS 129

Relationship between Promontory Velocity and Basilar Membrane Velocity in Bone-Conducted Hearing: Finite Element Analysis

Seongho Mo; **Jongwoo Lim**; Soyi Jung; Namkeun Kim
Incheon National University

Objectives
Investigation of the relationship between promontory velocity and basilar membrane velocity in bone-conducted hearing using a 3-D finite element model of human head including auditory periphery

Methods
The finite element model of human head (LiUHead) was modified by adding the auditory periphery consisting of middle ear and cochlea. The model was validated by comparison of mechanical point impedance, promontory velocity, and basilar membrane velocity. In the simulation, bone conduction was implemented by applying a unit sinusoidal force on the mastoid position. Three different velocities, 1) promontory velocity, 2) oval window volume velocity, and 3) basilar membrane velocity, were calculated and compared each other.

Results
The basilar membrane velocity shows similar patterns with the oval window volume velocity at all the simulated frequencies (from 60 Hz to 10,000 Hz) in both ipsilateral and contralateral cochleae. The promontory velocity shows similar patterns with the basilar membrane velocity at low frequencies below about 500 Hz and 1,000 Hz in the ipsilateral and contralateral cochleae, respectively.

Conclusion
The promontory velocity is relevant to bone-conducted hearing threshold. However, the linear relationship was valid at low frequencies below 500 Hz or 1,000 Hz depending on the cochlear position in the simulation results. Therefore, another parameter different from a promontory velocity may be in need to indicate the bone-conducted hearing ability in an experimental study.

PS 130

Bone conduction in simulation and experimental evaluation

Ivo Dobrev[1]; Tahmine Faramandi[2]; Namkeun Kim[3]; Alexander Huber[1]; Christof Röösli[4]
[1]Department of Otorhinolaryngology, Head and Neck Surgery, University Hospital Zurich, Zurich, Switzerland; University of Zurich, Zurich, Switzerland; [2]Department of ENT, Head and Neck Surgery, University Hospital Zurich, Switzerland; [3]Incheon National University; [4]2.Department of Otorhinolaryngology, Head and Neck Surgery, University Hospital Zürich, Zürich, Switzerland.

Objectives
Experimental and simulation (finite element model, FEM) investigation of bone conduction (BC) sound propagation by skull bone surface waves, intracranial pressure (ICP) pressure distribution and promontory motion.

Methods
Experiments were conducted on two sets of five Thiel embalmed whole head cadaver specimens. The electromagnetic actuators from a commercial BC hearing aid (BCHA) (Baha® Cordelle and Power) were used to provide stepped sine stimulus in the range of 0.1-10 kHz. Osseous pathways (direct bone stimulation or transcutaneous stimulation) were sequentially activated by mastoid stimulation via a percutaneously implanted screw, and a 5-Newton steel headband. The response of the skull was monitored as motions of the ipsi-, top and contra-lateral skull surface, along with the ipsi- and contralateral promontories. The surface motion was quantified by sequentially measuring ~200 points on the skull surface (~ 15-20mm pitch) via a three-dimensional laser Doppler vibrometer (3D LDV) system. Intracranial pressure (ICP) was measured in the central, anterior, posterior, ipsilateral and contralateral temporal regions of the cranial space. Experimental data were compared with corresponding predictions from a finite element model of the human head (LiUHead).

Results
The promontory and skull surface underwent spatially complex motion with similar contributions from all motion components, regardless of stimulation mode. The inferior

sections of the skull showed 5-10 higher transition frequency than the parietal sections. Spatial distribution of ICP, from both experimental and simulated data, indicated a sound propagation through the thicker bony sections first, before activating the intracranial contents.

Conclusion
Comprehensive experiments, combined with detailed numerical models, allow for detailed exploration and differentiation of the individual contributions of the various bone conduction stimulation conditions and pathways. Overall, the experimental data and FEM predictions were qualitatively comparable, however, more accurate information about the skull material properties and its spatial distribution could help improve the accuracy of the numerical predictions.

Keywords
Bone conduction pathways, 3D Laser Doppler Vibrometer, surface waves, intracranial pressure, promontory motion, cadaver head, finite element model.

Collicular/Midbrain Circuitry

PS 131

Characterization of Layer-Specific Bilateral Projections in The Mouse Corticocollicular System.

nathiya Chandrasekaran[1]; Daniel A. Llano[2]
[1]Department of Molecular and Integrative Physiology, University of Illinois at Urbana Champaign; [2]Department of Molecular and Integrative Physiology, University of Illinois at Urbana-Champaign, IL, USA

The extensive feedback from the auditory cortex (AC) to the inferior colliculus (IC) supports critical aspects of auditory learning, but has not been extensively characterized. There are widespread studies on the projections from layer 5 to the IC, the midbrain integration center of the ascending auditory system among the different species. However, the projections from the layer 6-specific projections are less clearly described, particularly with respect to the unilaterality vs. bilaterality of the projections. Here we investigate the degree to which layer 5 or layer 6 neurons project to one or both inferior colliculi. The first approach used here is to deposit fluorescent retrograde tracers to defined IC sites and then measure the numbers of retrogradely labeled cortical cells. In experiment 2, animals received matching injections to the two inferior colliculi with cholera toxin B coupled to red or green fluorophores. Data are analyzed to quantify the % of cells in each layer on the ipsi- and contralateral side as well as the proportion of double-labeled cells.

PS 132

The Distribution and Projections of Cells in the Mouse Inferior Colliculus that Express Neuropeptide Y (NPY)

Pooyan Mirjalili[1]; Nichole L. Beebe[1]; Marina A. Silveira[2]; Michael T. Roberts[3]; Brett R. Schofield[4]
[1]Northeast Ohio Medical University; [2]University of Michigan; [3]University of Michigan - Ann Arbor - Department of Otolaryngology-Head and Neck Surgery - Kresge Hearing Research Institute; [4]Northeast Ohio Medical University; Kent State University

A challenge to understanding the processing of sound in the inferior colliculus (IC) is that neuronal populations are heterogeneous, and single subtypes of neurons are not well-understood. We investigated the distribution and projections of IC cells that express Neuropeptide Y (NPY) as an initial step in evaluating this neuronal population as a functionally relevant subtype of IC neuron.

To examine neuronal distribution, we used NPY-hrGFP mice (Jackson Labs) in which NPY-expressing neurons also express hrGFP. Cells that expressed hrGFP were plotted throughout the IC in three cases. Additionally, NPY-hrGFP mice were injected unilaterally into the IC with three viruses: two that lead to the expression of Cre recombinase when co-contained in a cell that contains GFP, and one which leads to the expression of tdTomato in the presence of Cre recombinase. In these animals, tdTomato-expressing axons and boutons throughout the brain were assumed to originate from NPY expressing cells at the site of injection (the IC). In this way, we could examine the projections of NPY+ IC cells.

NPY+ cells were present in each subdivision of the IC that was examined: central nucleus (ICc), lateral and dorsal cortices (IClc and ICd) and rostral pole of the IC (ICrp), as well as the nucleus of the brachium of the IC (NBIC) and the intercollicular tegmentum (ICt). On average, NPY+ cells were most numerous in the ICd (~ 44% of NPY cells) and ICc (~40% of NPY+ cells). The IClc contained a small portion of the NPY cells (12%) and the more rostral regions contained few NPY+ neurons (< 5% total in ICrp, ICt and NBIC combined). The main targets of projections from NPY+ cells were within the ipsilateral IC, the contralateral IC, the ipsilateral NBIC, and the ipsilateral medial geniculate body.

Given their prominence in ICc and ICd and the fact that the thalamus is the major extrinsic target, we conclude that the NPY cells are likely focused on ascending auditory pathways. The relative paucity of NPY+ neurons in the lateral and rostral regions suggest a smaller or less direct role of NPY+ neurons in

multimodal (e.g., auditory/somatosensory) processing. A role in descending auditory pathways is also likely to be minimal given the absence of descending projections from the NPY+ neurons. Ongoing studies into the neurotransmitter phenotype and physiological properties of these cells should help to further elucidate their role in auditory processing. Supported by NIH R01DC004391 and R56DC016880

PS 133

Cholinergic Axons Contact Inferior Collicular Neurons that Project to Cochlear Nucleus

William A. Noftz[1]; Nichole L. Beebe[2]; Brett R. Schofield[1]
[1]Northeast Ohio Medical University; Kent State University; [2]Northeast Ohio Medical University

Acetylcholine (ACh) is associated with attention, arousal and plasticity, and alters responses to sound of many neurons in the inferior colliculus (IC). A key question is which of the numerous output pathways from the IC are directly targeted by ACh? Thus far only GABAergic cells (with unknown projections) have been identified physiologically as direct targets of cholinergic inputs (Yigit et al., 2003). We presented evidence that cholinergic axons make direct contact with GABAergic cells that project to the thalamus (Noftz et al., 2018, ARO 41:27). That same study identified putative cholinergic inputs to glutamatergic cells, some of which projected to the thalamus. Other ACh-contacted glutamatergic cells were not labeled by tracer injected into the thalamus, raising the question of whether cholinergic axons directly contact other IC output pathways. Here, we ask whether cholinergic axons contact IC cells that project to the cochlear nucleus (CN). This descending pathway is believed to be glutamatergic and is in a position to modulate auditory processing at the first stage of the central auditory pathway.

We injected fluorescent retrograde tracer into the CN of adult Long Evans rats. Following fixation, brains were immunostained for vesicular acetylcholine transporter (VAChT) to label cholinergic axons and boutons. Although the IC-CN pathway is believed to be glutamatergic, we used antibodies against glutamic acid decarboxylase (GAD) to distinguish GABAergic from non-GABAergic cells. Retrogradely-labeled cells were analyzed for GAD reactivity and for VAChT-immunopositive (VAChT+) boutons in close apposition to the labeled cells. The tracer injections labeled cells in the central nucleus (ICc), lateral cortex (IClc) and dorsal cortex of the IC (ICdc) as well as more rostral areas including the rostral pole (ICrp) and intercollicular tegmentum (ICt). Throughout the ICc, IClc, and ICdc, VAChT+ boutons appeared in close contact with somas and proximal dendrites of some of the retrogradely-labeled neurons. Nearly all of the contacted cells were GAD-negative, reflecting the predominance of GAD-negative (i.e., glutamatergic) cells in the IC-CN pathway. Retrogradely labeled cells were far fewer in the rostral areas, but cells in the ICt appeared to be contacted by VAChT+ boutons.

We conclude that cholinergic axons are likely to make direct contact with glutamatergic IC cells that project to the CN. The ACh-targeted cells were distributed across numerous IC subdivisions, suggesting roles in auditory-specific pathways (associated with the lemniscal ICc) as well as multisensory processing associated with the IClc and the ICt.

Supported by NIH R01DC004391.

PS 134

Cholinergic Innervation of the Mouse Auditory Midbrain, Lower Brainstem and Thalamus

Brett R. Schofield[1]; Pooyan Mirjalili[2]; Nichole L. Beebe[2]
[1]Northeast Ohio Medical University; Kent State University; [2]Northeast Ohio Medical University

Acetylcholine is an important neuromodulator implicated in arousal, sleep-wake cycles, and attentional processes. Previous studies used immunohistochemistry to visualize cholinergic axons and boutons, but various factors limit this technique. We used genetic manipulation to visualize cholinergic axons and boutons in subcortical auditory nuclei of the mouse. We first generated mice in which Cre recombinase is expressed in cholinergic cells, and in which the point mutation leading to early-onset hearing loss (associated with the BL6 background) has been corrected to its wild type form (ChAT-Cre^{Cdh23WT} mice). We crossbred these mice with Ai14 reporter mice. In the offspring, cholinergic cells express tdTomato and their cell bodies, axons and terminals are visible without further enhancement.

The cochlear nucleus (CN) receives cholinergic inputs to all subdivisions. Thick axons with large boutons innervate the granule cell area and parts of the core ventral CN. Thinner axons with smaller boutons occur throughout the rostro-caudal extent of the CN. In the superior olivary complex, cell bodies were labeled in a pattern that matches the medial and lateral olivocochlear cells. Labeled axons and boutons were heaviest in the lateral superior olive, ventral nucleus of the trapezoid body, and lateral nucleus of the trapezoid body. The medial nucleus of the trapezoid body and the superior paraolivary nucleus receive lighter cholinergic input.

Innervation of the nuclei of the lateral lemniscus was light, with thin axons and small boutons. In the inferior colliculus (IC), most labeled axons were thin with small boutons. Cholinergic innervation was heavier to the dorsal and lateral IC cortices than in central nucleus. Rostrally, cholinergic innervation was heavier to the rostral pole of the IC and intercollicular tegmentum than to the nucleus of the brachium of the IC. A few large cholinergic cell bodies were present in the intercollicular tegmentum medial to the IC rostral pole. Cholinergic innervation of the medial geniculate body was heavier caudally and medially, but all subdivisions received input from thin axons that gave off boutons.

We conclude that cholinergic innervation of the auditory brainstem and thalamus in mouse is widespread. Previous studies indicate that the cholinergic innervation arises from olivocochlear cells and cells of the pontomesencephalic tegmentum. Differing appearances of axons and boutons support previous findings of multiple sources of cholinergic input to subcortical auditory nuclei.

Supported by NIH R01DC004391.

PS 135

Cholinergic Inputs Contact Four Subtypes of GABAergic Cells in the Mouse Inferior Colliculus

Nichole L. Beebe[1]; Brett R. Schofield[2]
[1]Northeast Ohio Medical University; [2]Northeast Ohio Medical University; Kent State University

We have previously identified four subtypes of GABAergic cells in the inferior colliculus (IC) of guinea pigs. The subtypes are differentiated based on their association with perineuronal nets (PNs) and perisomatic rings of boutons containing vesicular glutamate transporter 2 (VGLUT2 rings). Cells can have either or both markers, or be associated with neither, and this pattern of association is correlated with soma size and distribution within the IC. It has also been demonstrated that the IC receives cholinergic innervation that contacts both GABAergic and non-GABAergic cells. Here, we asked whether the four subtypes of GABAergic cells we identified in guinea pigs are also present in the mouse, and whether some or all of the GABAergic subtypes receive cholinergic inputs.

We first generated mice in which Cre recombinase is expressed in cholinergic cells, and in which the point mutation leading to early-onset hearing loss (associated with the C57BL/6 background) has been corrected to its wild type form (ChAT-Cre^{Cdh23WT} mice). We then crossbred these mice with Ai14 reporter mice. In the offspring, cholinergic cells express tdTomato and their cell bodies, axons and terminals are typically visible without further enhancement. We identified ACh-targeted neurons by staining perfusion-fixed tissue with 1) anti-NeuN and Neuro-Chrom pan-neuronal marker to outline neuronal somas, 2) anti-GAD to identify GABAergic cells, 3) *Wisteria floribunda* agglutinin to label PNs, and 4) anti-VGLUT2 for VGLUT2 rings.

All four subtypes of GABAergic cells can be identified in the mouse IC. GAD-Only (i.e., no PN or VGLUT2 ring) or GAD-PN cells were the most common, depending on the IC subdivision. Soma area was smallest for GAD-Only cells and largest for GAD-PN-VGLUT2 ring cells, as previously shown in guinea pigs. The majority of identified neurons, including both GABAergic and non-GABAergic (i.e., glutamatergic) cells, had presumptive cholinergic contacts on the soma or proximal dendrites. On average, 61% of identified GABAergic cells had one or more presumptive contacts on the soma or proximal dendrites. Presumptive contacts occurred on all four subtypes of GABAergic cells.

We conclude that association with VGLUT2 rings and/or perineuronal nets distinguishes four subtypes of GABAergic cells in the mouse IC and that all four subtypes appear to receive direct input from cholinergic axons. The results suggest that acetylcholine has the opportunity to act on multiple subtypes of inhibitory IC cells (as well as the numerous glutamatergic cells), implying a widespread role for cholinergic effects on midbrain auditory processing.

Supported by NIH R01DC004391.

PS 136

Generation of a ChAT-Cre Mouse Line Without the Early Hearing Loss Typical of the C57BL/6 Mouse

Nichole L. Beebe[1]; Colleen S. Sowick[1]; Inga Kristaponyte[1]; Alexander V. Galazyuk[2]; **Brett R. Schofield**[2]
[1]Northeast Ohio Medical University; [2]Northeast Ohio Medical University; Kent State University

Mice with Cre recombinase expressed under the control of the promoter for choline acetyltransferase (ChAT) have allowed specific manipulation of cholinergic circuits. However, available ChAT-Cre mouse lines are based on the C57BL/6 background, which shows age-related hearing loss attributed to the *Cdh23*^{753A} allele (a.k.a., the *ahl* mutation). Mice homozygous for this mutation exhibit elevated thresholds for auditory brainstem responses (ABRs) demonstrable at 6 months of age and substantial by 9 months. Olivocochlear cells in these mice exhibit abnormalities soon after hearing onset (Sinclair et al., 2017. Hear Res 354, 28-37), indicating abnormalities at

a younger age than previously recognized. Moreover, the deficits are closely tied to brainstem cholinergic systems.

To develop ChAT-Cre mice without accelerated hearing loss, ChAT-Cre^{Cdh23WT}, we crossed the C57BL/6J ChAT-Cre mice with CBA/CaJ mice that have normal hearing. We used genotyping to obtain mice homozygous for the ChAT-Cre transgene and the wild-type allele at the *Cdh23* locus. We measured ABRs to assess hearing thresholds. We then cross-bred the animals with Ai14 reporter mice to confirm the functionality of the ChAT-Cre transgene.

In the new line, ABR thresholds were stable throughout the 3-12 month period of testing. The thresholds were ~20 dB lower than those in 9 month old C57B/6J mice at all frequencies tested (4-31.5 kHz). After crossbreeding with reporter mice, tdTomato-labeled cells were in all brainstem regions known to contain cholinergic cells. We assessed the labeled cells by staining with a neuron-specific marker, NeuN. Across several brainstem nuclei (pontomesencephalic tegmentum, trigeminal motor and facial nuclei), 100% of the tdTomato-labeled cells were double-labeled with anti-NeuN (n = 1460 cells), indicating Cre-recombinase was limited to neurons. In addition, 1457 (99.8%) of these cells were ChAT immunopositive, indicating that reporter label was expressed almost exclusively in cholinergic neurons. Across the same nuclei analyzed above, an average 87.1% of the ChAT+ cells were labeled with tdTomato, indicating that the transgene is expressed in a large proportion of the cholinergic cells in these nuclei.

We conclude that the new mouse line has normal hearing and expresses Cre recombinase almost exclusively in cholinergic neurons. This ChAT-Cre^{Cdh23WT} mouse line may provide an opportunity to manipulate cholinergic circuits without the confound of accelerated hearing loss. Furthermore, comparison with lines that do show early hearing loss may provide insight into cholinergic roles in age-related hearing loss.

Supported by NIH R01 DC004391 (to BRS) and R01 DC016918 (to AG)

PS 137

Perineuronal Nets Increase with Age on Ascending and Descending Pathways of the Inferior Colliculus in Fischer Brown Norway Rats

Lindsay N. Hofer; Amir Mafi; Matthew Russ; Jeffrey G. Mellott
Northeast Ohio Medical University

In the central nervous system, aging alters the presence of perineuronal nets (PNs), aggregates of extracellular matrix, that are routinely associated with populations of inhibitory cells, synaptic stabilization and inhibiting plasticity. We recently reported that PNs increases with age throughout the inferior colliculus (IC). We sought to determine whether the increase of PNs was specific to ascending or descending IC circuits. We assessed Fischer Brown Norway (FBN) rats in two age groups: “young” (2-6 months) and “old” (21-28 months). We injected fluorescent tracers into either the medial geniculate body (MG) or the cochlear nucleus (CN) to retrogradely label cells in the IC. Brain sections (40 µm), perfused with 4% paraformaldehyde, were immunostained for GAD67 (Millipore; MAB5406), Wisteria Floribunda Lectin (WFA; Vector; B-1355) and NeuroTrace (Molecular Probes; N-21480). Cell bodies were classified as PN-positive if ~75% of the perimeter was surrounded by WFA. A total of ~17,000 retrogradely labeled IC cells were quantified across 8 cases.

Our main finding is that the number of IC-MG and IC-CN cells surrounded by a PN increases during aging. We found that the number of IC-MG cells that were surrounded by a PN increased from 5% in the young to 12% in the old. We found a similar increase in the IC-CN pathway (7% to 15%). We also observed age-related increases of PNs in each of the three major IC subdivisions (central, lateral cortex, and dorsal cortex) of both pathways.

In the IC-MG pathway, where GABAergic cells contribute, we determined that the percentage of GAD-immunopositive IC-MG cells that had a PN increased from 20% to 26% with age. However, the age-related increase of PNs in the IC-MG pathway was not specific to GABAergic cells as we also found an increase of PNs on GAD-immunonegative IC-MG cells, 5% to 10%.

Our data lead to two main conclusions regarding the expression of PNs in the aged IC. **First,** we demonstrate that PNs are increased with age in the IC of FBN rats. **Second**, we find that the age-related increase of PNs in the IC is not specific to a singular pathway or phenotype. PNs can serve to stabilize synapses, it is possible that the upregulation of PNs is a compensatory mechanism to help maintain temporal precision as the age-related loss of inhibitory inputs in the IC occurs. This implies, given that PNs inhibit plasticity, ascending and descending IC circuits become less plastic in old age.

PS 138

Age-related loss of GABAergic Synapses is not Uniform between the Central and Lateral Nuclei of the Inferior Colliculus in Fischer Brown Norway Rats

Amir Mafi; Jeffrey G. Mellott
Northeast Ohio Medical University

It has been demonstrated that there is an age-related loss of GABAergic synapses in the central nucleus of the inferior colliculus (ICc)1. As the IC has several unique subdivisions, we sought to determine whether the age-related loss of GABAergic synapses occurs equally throughout the IC. We assessed Fischer Brown Norway rats in three age groups: 3 months, 4 months and 28 months. We used immunogold transmission electron microscopy to characterize GABAergic synapses and their post-synaptic targets in the ICc and lateral cortex of the IC (IClc). Ultrathin sections were placed on 300 Ni mesh grids, reacted for anti-GABA immunochemistry and stained with UranyLess (EMS). GABAergic synapses were identified as having pleomorphic vesicles, symmetric synaptic junctions, and GABA-positive presynaptic boutons. Postsynaptic targets comprise somas, dendrites of three calibers (>1.5 µm, between 0.5 and 1.5 µm and < 0.05 µm) and spines. Two random grid squares (3,364 µm2 each) were manually quantified at each age in both subdivisions. A total of 1,864 synapses were characterized.

Our main finding is that age-related reduction of GABAergic synaptic density was greater in the ICc than in the IClc. At 4 months each subdivision had a ~10% reduction in the density of GABAergic synapses when compared to 3 months. At 28 months the overall reduction in the ICc was 29% and only 13% in the IClc. At 3 months the majority of post-synaptic targets for GABAergic synapses in both subdivisions were dendrites with a caliber between 0.5 and 1.5 µm; ICc-61%; IClc-55%. At 28 months, in the ICc, the occurrence of GABAergic synapses on dendrites with calibers between 0.5 and 1.5 µm was considerably reduced. However, in both subdivisions at 28 months, there was an increase in the number of GABAergic synapses that targeted GABA-positive dendrites with a caliber >1.5 µm and GABAergic somas suggesting synaptic rearrangement on IC GABAergic cells as they age.

We propose two main conclusions regarding the age-related loss of GABAergic synapses in the ICc and IClc. First, there is an initial loss of GABAergic synapses in both subdivisions at 4 months with a secondary and greater loss in the aged ICc. Second, we find that GABAergic synapses more commonly target GABAergic somas and large GABAergic dendrites during aging. Taken together, the loss of presynaptic GABAergic input begins relatively early in the IC and aging may differentially affect the functions of the ICc and IClc.

PS 139

Subdivisions of the Inferior Colliculus Undergo Age-Related GABAergic Changes at Varying Degrees in Fischer Brown Norway Rats

Jeffrey G. Mellott; Lindsay N. Hofer; Amir Mafi
Northeast Ohio Medical University

Our lab has been investigating potential mechanisms underlying the age-related loss of GABA in the inferior colliculus (IC). Employed techniques include immunochemistry for the $GABA_AR$ β_1 subunit, the expression of perineuronal nets (PNs), immunogold electron microscopy, and small molecule fluorescence *in situ* hybridization (smFISH). We examined each of the major IC subdivisions (central ICc; lateral cortex, IClc; dorsal cortex, ICd). The data from each experiment revealed age-related differences between the IC subdivisions. In each experiment we assessed Fischer Brown Norway rats with multiple age groups: 2-3 months, 4-8 months, 19-24 months and 26-29 months.

We quantified the expression of the $GABA_AR$ β_1 subunit to identify IC cells that changed their postsynaptic $GABA_A$ composition by upregulating the β_1 subunit. The upregulation of this subunit has been associated with increased GABA sensitivity. We found that cells in all subdivisions upregulated the subunit with age however, the number of cells in the ICc that expressed the subunit decreased in old age while in the IClc and the ICd there was an increase.

PNs are routinely associated with inhibitory cells and synapses thus, we examined cells in the IC that had PNs during aging. It was determined that density of PNs in the ICc and ICd doubled with age. In the IClc the density of PNs did increase but it was not significant.

Immunogold electron microscopy was employed to quantify the density of GABAergic synapses in the IC. Our data show that at 4 months the ICc and IClc had a ~10% reduction in the density of GABAergic synapses when compared to 3 months. At 28 months there was an additional 19% reduction in the ICc and only 3% in the IClc.

Recently our lab has been conducting smFISH to reveal individual GAD1 (GAD67) mRNA in GABAergic IC cells. Our preliminary data shows a 45% reduction of GAD mRNA from 3 to 26 months in the ICc, 26% in the ICd and a 23% reduction in the IClc.

The data demonstrate that the IC subdivisions undergo several age-related GABAergic changes at varying magnitudes. Each experiment revealed that the greatest

degree of age-related GABAergic change occurred in the ICc. These subdivisional differences may reflect differences in the ascending GABAergic input to the IC and the targets of GABAergic IC cells. Currently, our lab is combining the above techniques with tract-tracing to determine the IC circuits likely affected by age-related losses of GABA.

Genetics: General

PS 140

Etiology of late-onset progressive hearing loss using comprehensive genetic testing: Toward future gene therapy

Hidekane Yoshimura[1]; Shin-ya Nishio[2]; Shin-ichi Usami[2]
[1]Department of Otorhinolaryngology, School of Medicine, Shinshu University; [2]Shinshu University School of Medicine

Background and Objective
Comprehensive genetic testing has emerged as the standard of care for genetic testing for patients with sensorineural hearing loss. Compared to the patients with congenital hearing loss, the overall proportion of genetic cause in patients with adult-onset hearing loss is thought to be lower. Late-onset progressive hearing loss is sometimes indistinguishable from age-related hearing loss. Therefore, we hypothesize that if presbycusis would be properly excluded, we can measure the accurate diagnostic rate in patients with late-onset progressive deafness.

Materials & methods
To assess the etiology in patients progressive hearing loss (onset; < 40yrs), 69 patients who visited at Shinshu University in 2008-2018 were studied. Genetic evaluation was performed using comprehensive genetic testing of all known deafness genes with targeted genomic enrichment and massively parallel sequencing.

Results
A genetic cause was identified in nearly half of patients with late-onset progressive hearing lossand varied significantly based on onset of hearing loss and family history of hearing loss. There were causative mutations identified in at least 15 different deafness genes with mutations in *CDH23*gene being the most common. Correlational analysis of genetic cause of deafness and phenotype is ongoing and will be presented.

Conclusion
We demonstrate the diagnostic rate in patients with late-onset progressive hearing loss except for presbycusis, whichis similar to that in patients with congenital deafness reported in some studies. Understanding genetic cause of deafness in patients will facilitate the selection of targeted genes for gene therapy studies in future.

PS 141

Rare genetic cases of non-syndromic hearing impairment in Southern Europe

Ralf Birkenhäger[1]; Maren Trabandt[1]; Carolyn Büsching[1]; Luminita Radulescu[2]
[1]University Medical Center Freiburg, Department of Oto-Rhino-Laryngology, Head and Neck Surgery, Molecular-Biology/Genetics; [2]University of Medicine and Pharmacy Grigore T. Popa

About 1-3 / 1000 newborns are affected by a profound hearing disorder at birth or in the first two years of life. About 60% of these cases are due to genetic causes. Inherited hearing disorders are divided into syndromic or non-syndromic, non-syndromic hearing disorders (NSHL) are isolated, while syndromic hearing disorders (SHL) are associated with additional organic disorders. Approximately 70% of cases of inherited hearing disorders are non-syndromic and predominantly due to sensorineural causes. Of these, around 80% of cases are autosomal recessive (DFNB) and 18% are autosomal dominant (DFNA), about 2% are X-chromosome (DFNX) or mitochondrial (MT) associated. To date, 185 gene loci and 128 genes have been identified for this type of hearing impairment. Genetic changes in the *DFNB1* gene locus, in which the genes *GJB2* (connexin-26) [MIM121011] and *GJB6* (connexin-30) [MIM604418] are localized represent the main cause (~45%) of prelingual non-syndromic hearing disorders. The aim of the project is to demonstrate, in a Romanian / Moldovan patient group, which rare genetic hearing disorders occur.

So far 236 patients have been included in our studies that have been diagnosed with severe to profound non-syndromic hearing impairment in their first two years of life and which have been shown to have no alterations and/or deletions in the *DFNB1* gene locus, in the genes *GJB2* and *GJB6*, respectively. Initially, targeted genes were analyzed, which in some few rare cases led to hearing impairment in various European populations. The detection of genetic alterations was carried out by bi-directional sequencing of the coding exons, as well as the intron transitions.

First of all, the genes *GRXCR1* [MIM613283], *ESRRB* [MIM602167], *TMIE* [MIM607237], *GIPC* [MIM608792] and *LHFPL5* [609427] were analyzed in this patient group followed by genes *CABP2* [MIM607314], *MPZL2* [604873], *TPRN* [MIM613354], *SPNS2* [612584] and *CLDN9* [MIM615799]. By DNA sequencing, 12 novel

mutations, 17 unknown polymorphisms and 24 known alterations that are already listed in the databases of international sequencing projects have been detected so far.

In the investigated patients mutations and previously unknown polymorphisms were occasionally identified in the genes *GRXCR1*, *ESRRB*, *TMIE*, *GIPC* and *LHFPL5* as well as *CABP2*, *CLDN9*, *MPZL2* and *SPNS2*, however, an accumulation of changes is not detectable. Therefore, further investigations are required for a better understanding of the etiology of prelingual hearing disorders.

PS 142

Molecular Epidemiology of Chinese Han Deaf Patients with Bi-allelic and Mono-allelic GJB2 Mutations

Xiaoyu Yu; Tao Yang; **Hao Wu**
1. Department of Otolaryngology - Head & Neck Surgery, Shanghai Ninth People's Hospital, Shanghai Jiao Tong University School of Medicine; 2. Ear Institute, Shanghai Jiao Tong University School of Medicine; 3. Shanghai Key Laboratory of Translational Medicine on Ear and Nose diseases, Shanghai, China

Recessive mutations in GJB2 is the most common cause of genetic hearing loss worldwide. In this study, we overviewed the mutation screening results of GJB2 in 1852 Chinese Han deaf patients in our laboratory. Bi-allelic GJB2 mutations was identified in 25.65% of patients, in which the c.235delC mutation is the most frequent cause for both severe-to-profound (84.93%) and mild-to-moderate hearing loss (54.05%), while the p.V37I mutation is another frequent cause for mild-to-moderate hearing loss (40.54%). Notably, in 3.89% of patients only one mutant allele can be identified in GJB2. Next generation sequencing in 44 such probands revealed digenic heterozygous mutations in GJB2/GJB6 and GJB2/GJB3 as the likely pathogenic mechanism in three probands. In 13 probands, on the other hand, pathogenic mutations in other deafness-associated genes can be identified as the independent genetic cause, suggesting that the mono-allelic GJB2 mutations in those probands is likely co-incidental. Our results demonstrated that GJB2 should be a primary target for mutation screening in Chinese Han deaf patients, and those with mono-allelic GJB2 mutations should be further screened by next generation sequencing.

PS 143

Multivariate Polygenic Risk Scores Identify Individuals At-Risk for and Protected from Hearing Loss

C. Scott Gallagher; Nicholas G. Crawford; Adam T. Palermo
Decibel Therapeutics

Hearing loss affects more than 500 million people worldwide. Here, we analyzed over 325,000 individuals from the UK Biobank to create multivariate genome-wide risk models to quantify risk for hearing loss. Future applications of these models will help inform individuals of their risk for hearing loss and may lead to new or improved mitigation strategies.

Genetic epidemiologic analyses indicate that roughly 40% of hearing loss is attributable to heritable risk factors. Genome-wide association studies (GWAS) are case-control approaches that examine genetic variation within a population to identify mutations commonly observed in individuals with a given phenotype. In collaboration with the UK Biobank, we sought to detect genetic risk variants by performing a self-reported hearing difficulty GWAS on 90,710 cases and 255,925 controls of European ancestry. We identified 40 loci as being associated with risk for hearing difficulty, including Mendelian deafness genes, and eight novel loci that exert sex-specific effects.

To ascertain and quantify risk of hearing loss within individuals, we developed multivariate Polygenic Risk Scores (PRS). PRS calculates an individual's risk by summing across an optimized set of genotypes individually weighted by the effect sizes calculated in the GWAS. We initially trained our PRS model on the association results from a subset of the initial cohort (n = 311,973) by performing high-resolution testing across distinct *p*-value thresholds to identify the most predictive set of variants. We tested predictability in a target population of 34,662 individuals. Individuals with the highest polygenic scores had significant, greater than three-fold increased odds for self-reported hearing difficulty relative to those with the lowest genetic risk. To our surprise, we observed individuals in the lowest PRS percentile to have remarkably low prevalence of hearing loss, suggesting a subset of individuals may be genetically protected. Incorporation of additional demographic and clinical variables into multivariate PRS models significantly improved predictive power.

In conclusion, we demonstrated that GWAS and multivariate PRS methods have high potential value for informing individuals of genetic risk for acquired hearing loss. Our results indicate genetic risk for hearing loss is

controlled by a defined set of genomic regions, several of which contain genes implicated in congenital deafness and several of which are sex-specific. Further, we demonstrate that results from our association analyses can be used to meaningfully predict hearing loss. More powerful predictive models could be developed in the future by refining the noise-based hearing loss phenotype and extending the analyses to non-Caucasian populations.

PS 144

Functional Characterization of Grhl2a/b in Zebrafish

Sheng-Jia Lin; Cassidy Petree; Gaurav Varshney
Oklahoma Medical Research Foundation

Approximately 360 million people worldwide are affected by some degree of hearing loss. Indeed, 1-2 in every 1000 newborns is affected by sensorineural hearing loss, making it one of the most common birth defects. Development of next-gen genomic sequencing technologies have led to the identification of the new mutations associated with human hearing loss at a rapid pace, but their functional validation is unacceptably slow. The common approach to validate a candidate disease gene is to generate a functional knockout in a model organism. Zebrafish are an ideal model organism to study hearing loss, given their external embryonic development, transparent body, accessible inner ear and the presence of lateral line neuromasts, which are functionally analogous to mechanoreceptors of the mammalian inner ear. In addition, zebrafish have been shown to effectively recapitulate disease phenotypes. As of now more than 150 loci and roughly 100 genes associated with hearing loss have been discovered, 94% of human hearing loss genes have an orthologue in zebrafish, suggesting high functional conservation. Here we developed a high-throughput mutagenesis pipeline using CRISPR/Cas9 in zebrafish and generated loss of function alleles in 90 hearing loss genes selected from the hereditaryhearingloss.org database. The loss-of function mutation of *Grainyhead-like 2* (*GRHL2*) transcription factor has implicated in non-syndromic sensorineural deafness. There are two paralogues in zebrafish *grhl2a* and *grhl2b*, and both genes has distinct and differential expression patterns during embryonic development. Previous study by *Tol2* transposon-based mutagenesis in zebrafish has shown defective otic development. To gain further insights into *grhl2* function, we generated *grhl2a*, *grhl2b* and *grhl2a/b* mutants in zebrafish using CRISPR/Cas9. The *grhl2b* mutants show the similar phenotype as described earlier, including enlarged otic lumen, small or absent otoliths and less sensitive to startle response. *Grhl2a* mutants do not show any obvious morphological defects in inner ear, however, these mutants show weak startle response. The *grhl2a/b* mutants exhibit similar phenotype to *grhl2b* mutants, suggesting that the inner ear defect is contributed by *grhl2b* mutation. Interestingly, we found the inner ear defects could be rescued by *grhl2a* only, indicating a critical function of *grhl2a* in inner ear development; this suggests a dominant role of *grhl2b*. We further identified downstream targets of Grhl2 by transcriptome profiling of these mutants. In summary, we found *grhl2a* and *grhl2b* might share same and/or distinct functions during inner ear development, and *grhl2a* is required but not sufficient in regulating the inner ear development.

PS 145

Erlong (erl) mutation in the cdh23 gene causes delayed age-related hearing loss in CBA/CAJ mice

Fangfang Zhao[1]; Tong Zhao[2]; peng ma[3]; Bo Li[2]; Tihua Zheng[4]; Renhua Xu[4]; Qingyin Zheng[1]
[1]Department of Otolaryngology- Head & Neck Surgery, Case Western Reserve University, Cleveland, Ohio, USA; [2]Hearing and Speech Rehabilitation Institute,College of Special Education, Binzhou Medical University, Yantai, China,; [3]School of Pharmacy, Binzhou Medical University, China; [4]Hearing and Speech Rehabilitation Institute, College of Special Education, Binzhou Medical University, Yantai, China

Background

We previously reported a mutation (erlong, erl) of the cadherin 23 (Cdh23) gene in a mouse model for DFNB12 characterized by progressive hearing loss beginning from postnatal day 27 and becoming deaf by 3 months of age. Genetic and sequencing analysis revealed a 208T >C transition causing an amino-acid substitution (70S-P). The genetic background of *erl* is on the C57BL/6J (B6) mice and thus is named as B6-*Cdh23*$^{erl/erl}$ (Han et al 2012). However, B6-*Cdh23*$^{erl/erl}$,mice also carry the *Cdh23*^{753A} allele causing exon 7 skipping in Cdh23 gene associated with age-related hearing loss (AHL) and the deafness modifying (*mdfw)* in many inbred strains (Noben-Trauth et al 1997 & 2003; Zheng and Johnson 2001 &2000). In contrast, CBA/CAJ mice does not carry the *Cdh23*^{753A} allele and have good hearing until very old ages.

Result

Using CRISPR-cas9, we generated the same *erl* (208T >C) mutation named *Cdh23*$^{erl2/erl2}$ on CBA/CAJ mice. Compared to C57BL/6J-*Cdh23*$^{erl/erl}$ mice, we found that CBA/CaJ-*cdh23*$^{erl2/erl2}$ mice have a later-onset hearing loss started at 5 months and progressive hair cell loss at 7 months as determined by ABR thresholds and SEM. To explore the distinct difference between this *erl* mice,

we are performing electron microscopy to look sub-cellular structure changes and molecular mechanism. We are also crossing CBA/CaJ-cdh23$^{erl2/erl2}$ X B6 to study other genetic background effects on hearing loss. Grant support: R01DC015111(QYZ).

PS 146

A Synonymous Mutation in the COL4A6 Gene Causes Congenital Hearing Loss Due to Exon Skipping

Yixi Wang[1]; Kevin T. Booth[2]; Carla J. Nishimura[1]; Kathy L. Frees[1]; Amanda O. Taylor[1]; Yuzhou Zhang[1]; Gabriella Pitcher[1]; Nicole Meyer[1]; Hela Azaiez[1]; Richard J.H. Smith[3]

[1]Molecular Otolaryngology and Renal Research Laboratories, Department of Otolaryngology—Head and Neck Surgery, Carver College of Medicine, University of Iowa; [2]Molecular Otolaryngology & Renal Research Labs, Department of Otolaryngology—Head and Neck Surgery, University of Iowa Carver College of Medicine; Department of Neurobiology, Harvard Medical School, Harvard University; [3]Molecular Otolaryngology and Renal Research Laboratories, Department of Otolaryngology—Head and Neck Surgery, Carver College of Medicine, University of Iowa; Interdepartmental PhD Program in Genetics, University of Iowa

Introduction

COL4A6 is one of 5 genes associated with X-linked non-syndromic hearing loss. To date, only one family with a pathogenic missense variant (p.Gly591Ser) in COL4A6 has been identified. In current bioinformatics pipelines, synonymous variants are removed due to the underlying assumption that they are not disease causing. Recent literature, however, has shown there are several ways that synonymous variants can cause phenotypic change, though few have been reported in relation to non-syndromic hearing loss. In this study, we confirm that a synonymous single nucleotide variant in COL4A6 causes congenital hearing loss via mis-splicing of exon 41.

Method

Comprehensive genetic testing was completed on the proband from a family segregating presumed X-linked hearing loss using a deafness-specific panel (OtoSCOPE). Bioinformatic analysis of sequencing data was carried out using a custom pipeline. Genetic variants were filtered for quality and minor allele frequency. No filtering was performed for variant type. To test the functional effect of synonymous variants on splicing efficiency, we used mini-gene assays by cloning mutant and wild-type exonic sequences.

Results

Although no pathogenic or likely pathogenic missense or truncating variants were found in the X-linked and autosomal deafness genes, an ultra-rare synonymous variant (c.4218A >G) was identified in COL4A6, which was predicted to cause mis-splicing and subsequent skipping of exon 41. In vitro splicing assays using wild-type exon produced a single 392bp band as resolved by gel electrophoresis. The mutant vector, in contrast, generated two bands, a 245bp product, identical to the empty vector backbone and a 392bp band corresponding to the wild-type sequence. Sanger sequencing confirmed exon 41 skipping in the mutant product.

Conclusion/Discussion

Herein we report a novel synonymous variant (c.4218A >G) that results in skipping of exon 41 in COL4A6 thereby leading to hearing loss. This case represents the first pathogenic synonymous variant in a gene associated with DFNX-related hearing loss and the second pathogenic variant in COL4A6. Our findings highlight the importance of retaining ultra-rare synonymous variants in bioinformatic pipelines for further analysis as warranted.

PS 147

Frame-shift mutations in OSBPL2 leads to progressive nonsyndromic hearing loss.

Young IK Koh[1]; Jinsei Jung[1]; Byunghwa Noh[2]; Sun Young Joo[3]; Choi Hye ji[4]; Kyung Seok Oh[3]; Jae Young Choi[1]; Heon Yung Gee[1]

[1]Yonsei University; [2]Yonsei university; [3]Yonsei University College of Medicine; [4]Department of Otorhinolaryngology, Brain Korea 21 PLUS Project for Medical Sciences, Yonsei University College of Medicine, Seoul 03722, Korea

OSBPL2 encodes oxysterol-binding protein related protein 2 (ORP2) belonging to oxysterol-binding protein (OSBP) family. This protein binds to some phospholipids and oxysterols, and controls neutral lipid metabolism by localizing to lipid droplet surface. Interestingly, mutations in *OSBPL2* has been reported as causing autosomal dominant progressive nonsyndromic hearing loss (DFNA67). We found two pathogenic frame-shift mutations in *OSBPL2* c.177_178delAC and c.158_159delAA by whole exome sequencing in two independent Korean families. However, it is not known mutations in OSBPL2 protein result in hearing impairment. We first measured that OSBPL2 mRNA expression level in individuals with OSBPL2 mutations using real-time PCR and found that there was no difference in mRNA level between normal siblings and patients. In addition, we compared protein stability between wild-type and mutant proteins, but there was

no significant difference in stability between them in vitro. These results suggest that truncated OSBPL2 mutant protein may exist in patients. To examine the functional effect of OSBPL2 mutations, we performed coimmunoprecipitation and found that mutant protein did not lose the ability to interact with wild-type OSBPL2 protein, suggesting that the mutant protein may act as a dominant-negative. Furthermore, proteomic approach identified 37 proteins which exclusively bound to mutant OSBPL2 protein and proteins involved in organelle organization or mRNA regulation were enriched. In addition, we carried out immunofluorescence and found that wild-type protein was evenly distributed in the cytoplasm, whereas the mutant protein formed cytoplasmic aggregate, suggesting that mutant OSBPL2 protein abrogates cellular protein homeostasis. In mice, OSBPL2 was detected on hair cells, spiral ganglion, supporting cells, stria vascularis, and spiral ligament in the inner ear, However, Osbpl2 knockout mice did not develop hearing loss phenotype up to 6 months of auditory brainstem response measurement, suggesting that DFNA67 may not result from loss of OSBPL2 function.

PS 148

Association of Polymorphisms in Grainyhead-like-2 Gene with the Susceptibility to Age-related Hearing Loss: A Systematic Review and Meta-analysis

baoai han[1]; **Haiying Sun**[2]
[1]Public Laboratory, Key Laboratory of Breast Cancer Prevention and Therapy, Ministry of Education, Tianjin Medical University Cancer Institute and Hospital, National Clinical Research Center for Cancer, Tianjin Medical University, Tianjin 30000, China.; [2]Departments of Otorhinolaryngology, Union Hospital, Tongji Medical College, Huazhong University of Science and Technology, Wuhan 430022, China.

Objective
The grainyhead-like-2 (GRHL2) genetic variants were reported in age-related hearing impairment (ARHI) susceptibility in several case-control studies. However, their conclusions are conflicting; it is difficult to precisely assess the disease risk associated with the variants. Therefore we conduct the meta-analysis to discover the association of GRHL2 polymorphisms and the risk of ARHI.

Methods
A related literature search was conducted in on-line databases, such as Wanfang database, China National Knowledge Infrastructure (CNKI), EMBASE, Web of Science and PubMed (updated to August 30, 2018). We use Review Manager 5.0 and Stata SE 12.0 software to reckon the odds radio (OR), 95% confidence interval (CI) and p value in random- or fixed-effects model according to the I2 value in the heterogeneity test.

Results
2762 cases and 2321 controls in five articles were provided data to the meta-analysis. The pooled ORs (95%CI) of the rs10955255 polymorphism were 1.26 (1.05–1.50, p=0.01), 1.33 (1.07–1.65, p=0.01) and 1.32 (1.12–1.55, p=0.0007) in the allele, homozygote and recessive model separately. Besides, a significant association was detected between rs1981361 in mixed population and the ARHI risk in the allele, heterozygote and dominant genetic model respectively. Then subgroup analyses was performed by ethnicity, for rs10955255 meaningful associations were detected for the allele model, homozygote model, dominant model and recessive model in the Caucasian population but no relations in any of the five genetic models in Asian population.

Conclusion
The meta-analysis indicated that the rs10955255 polymorphism could be an important risk factor for ARHI, especially in the Caucasians. The rs1981361 polymorphism may be a risk factor for ARHI in Asians. Larger scale researches are needed to further bring the consequences up to date.

PS 149

Spontaneous otitis media in mouse with Ptpn6 mutation

Lu Ying Liu[1]; YuKe Zheng[1]; JiangPing Zhang[1]; Christopher Mccarty[2]; HePing Yu[1]; **Qingyin Zheng**[3]
[1]Department of Otolaryngology Head & Neck Surgery, Case Western Reserve University, Cleveland, OH, USA; [2]The Jackson Laboratory, Bar Harbor, ME, USA; [3]Department of Otolaryngology- Head & Neck Surgery, Case Western Reserve University, Cleveland, Ohio, USA

Background
Otitis media (OM) is mainly an infectious disease, resulting from the interplay between genetic and environmental factors. The *viable motheaten* spontaneous mutation (*Ptpn6*$^{me\text{-}v}$) mice were found to have mutations in the gene *Ptpn6* and developed severe autoimmune disease.

Methods
In this study, *Ptpn6*$^{me\text{-}v/me\text{-}v}$ mice and their littermate controls with *Ptpn6*$^{+/me\text{-}v}$ and *Ptpn6*$^{+/+}$ (used at 1-2 months old) were observed to determine the incidence and morphology characteristics of OM. We also compared the immune status and hearing ability in *Ptpn6*$^{me\text{-}v}$ mice to their littermate controls.

Results
A high frequence (66.7%) of spontaneous OM was observed in *Ptpn6*$^{me\text{-}v/me\text{-}v}$. Inflammatory cells accumulated in the middle ear cavity, and expression of TNF-β increased in the affected middle ear. There were few mucosal mast cells, and low numbers of B and T cells in the lymph node, spleen and blood. Elevated ABR threshold indicated that the hearing loss was consistent with the severity of OM.

Conclusion
Our results showed that *Ptpn6*$^{me\text{-}v/me\text{-}v}$ mice had a high incidence of spontaneous OM. The inflammatory response and goblet cell hyperplasia likely contribute to the high incidence of OM in *Ptpn6*$^{me\text{-}v/me\text{-}v}$ mutant mice and therefore we present the *viable motheaten* mice (*Ptpn6*$^{me\text{-}v/me\text{-}v}$) as a novel model that can be used to research OM.

Grant support: R01DC015111(QYZ)

PS 150

Generation and genetic correction of USH2A point mutations in human iPSCs

Zaohua Huang[1]; Nicholas Gosstola[1]; Derek Dykxhoorn Dykxhoorn[1]; Justin Lillywhite[2]; Colin Maguire[2]; Jun Yang[3]; Zheng-Yi Chen[4]; Xue Liu[1]
[1]University of Miami Miller School of Medicine; [2]University of Utah School of Medicine; [3]Moran Eye Center, University of Utah, Salt Lake City, UT; [4]Massachusetts Eye and Ear/Harvard Medical School

Background
Usher syndrome (USH) is the leading cause of inherited combined hearing and vision loss. As an autosomal recessive trait, it affects 15,000 people in the United States alone and is responsible for 3 to 6% of early childhood deafness. Approximately 2/3 of the patients with Usher syndrome suffer from USH2, of whom, 85% have mutations in the USH2A gene. Patients affected by USH2 suffer from congenital bilateral progressive sensorineural hearing loss and retinitis pigmentosa which leads to progressive loss of vision. In order to study the molecular mechanisms of this disease, we generated induced pluripotent stem cells (iPSCs) from peripheral blood mononuclear cells (PBMCs) obtained from USH2A patients. Subsequent CRISPR genome editing experiments is in progress to correct the USH2A mutation back to a normal genotype.

Methods
Primary PBMC cells from human patients carrying three USH2A mutations were isolated and reprogramed using Cytotune 2.0 Sendai viral vector kit (ThermoFisher). To characterize and validate newly generated iPSCs, we used molecular karyotyping to screen for any chromosomal aberrations potentially caused by the reprogramming process, qPCR and immunostaining for stem-cell specific markers, and cell line authentication to genetically fingerprint these new cell lines. To correct the USH2A mutation, we will employ the homology directed repair pathway by electroporating the Cas9 protein/guide RNA complex and the 100bp donor oligonucleotide into the iPSC lines using Lonza 4D nucleofector. The homology dependent repair will be identified by PCR and Sanger sequencing before cell cloning. The repaired clones will be confirmed for the by PCR and Sanger sequencing.

Results
Nanostring molecular karyotyping revealed a normal karyotype, free of any major chromosomal additions, or deletions of the 46 human chromosomes. qPCR and immunostaining assays confirmed that blood marker (CCR7, CD3D, CD8A, CD4) are silenced, while stem-cell specific makers are markedly upregulated (SOX2, NANOG, OCT4/POU5F1, TRA-1-60, and SSEA4). A short tandem repeat (STR) analysis established and confirmed genetic fingerprint of 24 loci for these unique iPSC lines. The gene repair of these iPSCs using CRISPR technique is currently in progress.

Conclusions
We have successfully generated patient derived human USH2A mutated iPSCs which laid foundation for further studies. To examine the functional consequence of USH2A, future experiments will differentiate these patient-specific iPSC mutants and CRISPR gene edited isogenic controls into hair cells and inner ear.

PS 151

Variants in MYH1 are associated with Autosomal Recessive Syndromic Hearing Loss.

Ju Sun Yung[1]; Jinsei Jung[2]; Ji-Hyun Ma[2]; Kim Byoung Chul[3]; Choi Hye ji[4]; Jinwoong Bok[2]; Jae Young Choi[2]; Heon Yung Gee[2]
[1]Department of Pharmacology, Brain Korea 21 PLUS Project for Medical Sciences, Yonsei University College of Medicine, Seoul 03722, Korea; [2]Yonsei University; [3]Department of Nano-Bioengineering, College of Life Sciences and Bioengineering, Incheon National University, Seoul, Republic of Korea; [4]Department of Otorhinolaryngology, Brain Korea 21 PLUS Project for Medical Sciences, Yonsei University College of Medicine, Seoul 03722, Korea

Hearing loss is common sensory disorder affecting about 2.5 in 1,000 individuals around the globe. High

incidence of the disease is largely attributable to genetic factors given that 148 genes have reportedly linked to hereditary hearing loss. However, 50% of hearing loss cases are still molecularly unsolved; therefore, we applied whole exome sequencing to a cohort of individuals with hearing loss to identify additional genes required for auditory function in human. Here, we suggest MYH1 as a new candidate gene for syndromic hearing loss. MYH1 variants were identified in four independent families and segregated in an autosomal recessive manner. Out of five affected individuals, two probands were diagnosed with hearing impairment as well as developmental issues such as detectable decline in bone mineral density and craniofacial abnormality. All identified variants were missense variants and predicted to be deleterious by in silico tools. In vitro functional studies revealed that overexpression of mutant proteins (p.E194H, p. I460T and p. K744R), which harbor variants located within head domain of MYH1, resulted in reduced cellular traction force and disruption of normal cellular actomyosin ability. Myh1-knockout mice developed profound and progressive hearing loss, and were developmentally retarded. Histology of tibialis anterior (TA) muscle of knockout mice showed smaller myofibers with central nuclei and degenerated myofibers compared to their normal siblings. Taken together, our results suggest that recessive mutations in MYH1 lead to syndromic hearing loss and its function is required for the body development and auditory function.

PS 152

Hearing loss and cochlear sensory outer hair cell patterning defect in mice carrying a human mutation in Thra gene

Corentin Affortit[1]; Frédéric Flamant[2]; Jamal Nasr[1]; Carolanne Coyat[1]; Jean-Luc Puel[3]; Jing Wang[3]
[1]INSERM-UMR; [2]Institut de Génomique Fonctionnelle de Lyon, INRA; [3]Institute for Neurosciences of Montpellier

Hearing loss and cochlear sensory outer hair cell patterning defect in mice carrying a human mutation in *Thra* gene

Corentin Affortit [1,2]§, Frédéric Flamant[3], Jamal Nasr[1,2], Carolanne Coyat [1,2], Jean-Luc Puel[1,2] and Jing Wang[1,2]

[1]INSERM - UMR 1051, Institut des Neurosciences de Montpellier, 34295 Montpellier, France,

[2]Université de Montpellier, 34295 Montpellier, France,

[3] Institut de Génomique Fonctionnelle de Lyon, INRA USC 1370, Université de Lyon, Université Lyon 1, CNRS UMR 5242, Ecole Normale Supérieure de Lyon, 69364 Lyon, France

Background - Introduction
Resistance to thyroid hormone due to *THRA* mutations (RTHβ) is a recently discovered genetic disease, displaying important variability in its clinical presentation. The mutations alter the function of TRβ1, one of the two nuclear receptors for thyroid hormone. The mutation consequence is a reduced sensitivity of tissues to T3 in heterozygous patients. To probe the impact of *THRA* mutations on hearing function, we used a mouse model carrying a missense mutation (*Thra*E395fs401X) in *Thra* gene.

Methods
Mice heterozygous for a *Thra* mutation ($Thra^{S1/+}$) expressing a dominant-negative TRβ1, closely modeling the mutations found in RTHβ patients, were generated with CRISPR/Cas9 genome editing technique. Here we used $Thra^{S1/+}$and WT mice aged 1, 3, 6 and 12 months. Hearing function was assessed with auditory brainstem responses (ABRs) and distortion product otoacoustic emissions (DPOAEs). Cochlear cell morphology was analyzed using transmission (TEM) and scanning (SEM) electron microscopy. Molecular dissection of the OHC lateral wall components, mitochondrial functions and oxidative stress were assessed using immunolabeling methods, qPCR, Western blot and spectrophotometric method.

Results
Our results showed that juvenile mutant mice (1-month-old) displayed slight but significant sensorineural hearing loss as evidenced by high-to-low frequency hearing threshold shifts and reduced amplitude of DPOAEs. The hearing impairment is accompanied by an alternated sensory outer hair cell (OHC) patterning and the ectopic expression of some supernumerary OHCs organized in rows. Molecular dissection of the OHC lateral wall components revealed that the potassium channel Kcnq4 and the motor protein prestin undergo aberrant targeting into the cytoplasm of OHCs. In addition, mutant mice also exhibited increased autophagy and mitophagy associated with more severe hearing loss during aging than WT mice.

Conclusion
These results suggest a requirement for TRβ1 in OHC development and in the maintenance of hearing in adulthood.

PS 153 WITHDRAWN

Moleculargenetic Analysis of Genes Involved in the Homeostasis of the Inner Ear in Patients Suffering from M. Meniere

Nicolas Gurtler; Karl Heinimann
University Hospital Basel

Research Background
Menière's disease is characterized by attacks of vertigo, hearing loss and tinnitus. As the etiology is unknown, a specific diagnostic test is not available and likewise various therapies exist. The endolymphatic hydrops, present in Menière's patients, points to a disturbance of inner ear homeostasis. A genetic factor –among other proposed etiologies - might cause impaired function of the inner ear and is based on findings of ethnic differences and familial clustering. Identification of various genes involved in inner ear homeostasis and new techniques such as Next-Generation-Sequencing may lead to novel research paths to explore.

The aim of this study was to identify mutated genes responsible for inner ear homeostasis, which might contribute to the development of an endolymphatic hydrops leading to symptomatic M. Menière.

Methods
Single and familial patients with highly probable M. Menière according to the AAO&HNS were included. Molecular-genetic analysis was performed on the Illumina NextSeq 500-machine by a Illumina TruSight One Sequencing Panel encompassing coding sequence of 4813 genes. Following genes (23) were sequenced with a coverage of >20x with a gene-coverage of 97% (read length: 2x 150bP): SLC26A4 , WFS1, KCNQ4, CRYM, TJP2, P2RX2, TMC1, GJB2, GJB3, GJB6, ILDR1, CIB2, BSND, CABP2, S1PR2, CLIC5, TRIC, CLDN14, AQP1-4, Antiquitin. Data analysis was done by VariantStudio Data Analysis (Illumina) and NextSeq-Software (JSI), also detecting copy number variants. For variant-analysis programms such as MutationTaster, SIFT, PolyPhen2 and data-bases such as LOVD and HGMD were applied. Variants, potentially pathogenic, were verified by classic sanger-sequencing.

Results
5 sporadic and 5 familial patients were analyzed. A number of variants were found in 10 genes including one copy number variant. The mutational effect remains to be defined in about 30% of variants, in the others Minor-Allele-Frequency was > 12% indicating a benign change. Following number of variants were observed in percentage of patients : 4 in 50%, 3 in 75% and the remaining in 100%.

Conclusions
The interpretation of this analysis remains difficult. As patient number was low, a selection bias can not be excluded. About half of the genes harboured variations, some of them difficult to classify. One could still hypothesize that a single gene defect might not be sufficient for the development of M. Menière. All in all, the identification of mutated genes in Menière's disease would offer tremendous potential for improving diagnostics and therapeutic approaches.

PS 154

Elucidation of Genetic Background and Phenotypic Features in Patients with Hereditary Hearing Loss to Improve Diagnosis and Care

Tatsuo Matsunaga; Hideki Mutai; Kiyomitsu Nara; Koichiro Wasano; Shujiro Minami; Kimitaka Kaga
National Institute of Sensory Organs, National Hospital Organization Tokyo Medical Center

Genetic causes of hearing loss is highly heterogeneous, and there are still many unidentified or unconfirmed deafness genes. In addition, each deafness gene has unique phenotypes with various penetrance and expressivity. These features of deafness genes have been an obstacle to the effective genetic diagnosis and care for the patients with hereditary hearing loss. The purpose of the present study is to expand the boundary of known deafness genes and to elucidate a wide range of phenotypic features. The subjects consisted of the probands of 258 independent families with hearing loss and their parents when possible. They previously underwent at least one of the following genetic tests; 1) screening of high frequent genes or variants, 2) Sanger sequencing of predicted genes based on the clinical features, or 3) NGS of targeted deafness genes, without success to identify genetic causes. In the present study, whole exome sequencing was performed using DNA extracted from peripheral blood. Nextera Rapid Capture Exome kit or SureSelect Exome kit was used for enrichment and Hiseq 2500 or Hiseq 4000 was used for the sequencing. Candidate variants were filtered by standard processes. Genetic and phenotypic data were accumulated in the integrated database in our institute. Pathogenicity of variants were evaluated in accordance with ACMG / AMP variant interpretation guidelines. As a result, 26 known deafness genes and 9 candidate deafness genes were identified in 81 of 258 families. Analysis of genetic and phenotypic data in these families revealed that broad spectrum of known causative genes were still present after exclusion of frequent genes or predicted genes by prior genetic testing. Phenotypes of these genes showed wide range of variability that hampers diagnosis without genetic tests. Candidate deafness genes were occasionally detected, but accumulation and sharing of genetic and clinical information were considered to be indispensable to confirm the pathogenicity of most candidate deafness genes identified in a cohort of small families.

PS 155

The Hearing Loss Phenotype Associated with P2RX2 Gene Is Dependent on The Mutation Type

Xiaoya Chen; Clemer Abad; Abhiraami Kannan Sundhari; Juan I. Young; Katherina Walz; Xuezhong Liu
University of Miami

The Hearing Loss Phenotype Associated with P2RX2 Gene Is Dependent on The Mutation Type

Xiaoya Chen1, Clemer Abad2, Abhiraam Kannan Sundhari2, Juan I. Young[2,x], Katherina Walz[2,x], Xue Zhong Liu[1,2]
1. Department of Otolaryngology, University of Miami Miller School of Medicine, Miami, FL 33136, USA
2.John P. Hussman Institute for Human Genomics, University of Miami, Miami, FL 33136, USA
x.Department of Human Genetics, University of Miami Miller School of Medicine, Miami, FL 33136, USA

Introduction
The high prevalence/incidence of hearing loss (HL) in humans makes it the most common sensory defect. We previously identified p.Val60Leu mutation in P2RX2 purinergic receptor as the cause of human DFNB41 form of progressive HL, and also a likely cause for increased vulnerability to noise. Our in vitro data showed that p.Val60Leu mutation severely disrupt the ATP binding and therefore the ionic permeability of the receptor.

Goal
The characterization of mouse lines carrying different P2rx2 mutation and its effect on mouse cochlea hair cell (HC) function.

Methods
CBA/J F0 mice were generated by Crisper/Cas technology and one compound heterozygous founder carrying a P2rx2 c. 179C >G (p.V60L) in one allele and a P2rx2 c. 177T insertion allele was selected. Segregation of both alleles and colony expansion was initially accomplished by breeding the F0 with wildtype CBA/J mice. Two independent colonies, P2rx2 c. 179C >G colony and P2rx2 c. 177T insertion colony. We used auditory brainstem recordings (ABRs) and distortion product optoacoustic emissions (DPOAEs) to assess their hearing capabilities. We analyzed mouse motor coordination and activity by rotarod test, beam crossing, reaching response test and open field test. To evaluate mouse muscle strength, we did grip strength tests.

Results
Heterozygous P2rx2 c. 179C >G mice exhibited severe and progressive HL, as well as severe vestibular dysfunction. However, heterozygous P2rx2 c. 177T insertion mice exhibited no HL up to 6-months-old, but presents a phenotype suggestive of vestibular dysfunction.

Conclusions
Heterozygous P2rx2 c. 179C >G mice exhibit similar pattern of HL to that described in P2rx2 p.Val61Leu carrier patients in Chinese families, and so are ideal model for studying DFNA41 form of human deafness and for searching for therapy. Heterozygous P2rx2 c. 177T insertion mice showing putative vestibular dysfunction but no HL, suggests upregulation/compensation of other P2RX members in the hair cells.

Research Funding – The National Institutes of Health - NIDCD.

PS 156

Genetic heterogeneity of autosomal dominant hearing loss in pediatric patients

Dominika Oziβbβo; Marcin Leja; Anna Sarosiak; Henryk Skarβyβski; **Monika Ołdak**
Institute of Physiology and Pathology of Hearing

Genetic heterogeneity of autosomal dominant hearing loss in pediatric patients

Authors: Oziβbβo D.[1,2], Leja M.[1,2], Sarosiak A.[1,2], Skarβyβski H.[3], Oβdak M.[1]

Affiliation:
1. Department of Genetics, Institute of Physiology and Pathology of Hearing, Warsaw, Poland
2. Postgraduate School of Molecular Medicine, Medical University of Warsaw, Warsaw, Poland
3. Oto-Rhino-Laryngology Surgery Clinic, Institute of Physiology and Pathology of Hearing, Warsaw, Poland

Introduction
Autosomal Dominant Hearing Loss (ADHL) is the second most common form of inherited hearing loss with an onset usually after the second decade of life. Current knowledge on the genetic aspects of ADHL in Polish patients is limited, which significantly affects the diagnosis, genetic counselling and prevents prediction of disease progression.

Materials and Methods
Thirteen families with ADHL diagnosed before 18 years of age were enrolled in the study. DNA was isolated from peripheral blood or oral cavity swab samples from probands and family members. High-throughput genetic analysis using the TruSight One panel (Illumina Inc.) and

the MiSeq sequencer was carried out for the probands. To confirm the presence of identified genetic variants and their segregation with ADHL in individual families Sanger's sequencing was performed.

Results
Genetic cause of ADHL was identified in approximately 60% (8/13) of the families. The identified variants were located in *ACTG1*, *COCH*, *DIAPH1*, *EYA4*, *KCNQ4*, *PTPRQ*, *TBC1D24* and *TMC1*. Among the identified variants approximately 60% (6/8) were novel. In the remaining families the selected variants did not segregate with ADHL.

Conclusions
Our results show high genetic heterogeneity of ADHL in Polish pediatric patients. Considering frequent identification of new genetic variants, it is necessary to perform thorough clinical examination and segregation analysis of the selected variants with ADHL in the largest possible number of family members. In patients with no genetic cause identified, the study area should be extended and include all protein coding regions or whole genome.

Supported by: NCN SonataBIS6 grant no. 2016/22/E/NZ5/00470

PS 157

Genetic Counselors are Critical in Providing Comprehensive and Tailored Care for Individuals with Hearing Loss and Their Families

Amanda M. Schaefer[1]; Amanda O. Taylor[2]; Carla J. Nishimura[2]; Kathy L. Frees[1]; Diana L. Kolbe[3]; Kevin T. Booth[4]; Robert J. Marini[1]; Donghong Wang[1]; Amy E. Weaver[1]; Jori E. Hendon[1]; Colleen A. Campbell[5]; Hela Azaiez[2]; Richard J.H. Smith[6]
[1]Molecular Otolaryngology and Renal Research Laboratories, Department of Otolaryngology—Head and Neck Surgery, University of Iowa Hospitals and Clinics; [2]Molecular Otolaryngology and Renal Research Laboratories, Department of Otolaryngology—Head and Neck Surgery, Carver College of Medicine, University of Iowa; [3]Molecular Otolaryngology and Renal Research Laboratories, Department of Otolaryngology—Head and Neck Surgery, University of Iowa Hospitals and Clinic; [4]Molecular Otolaryngology & Renal Research Labs, Department of Otolaryngology—Head and Neck Surgery, University of Iowa Carver College of Medicine; Department of Neurobiology, Harvard Medical School, Harvard University; [5]Department of Internal Medicine, University of Iowa Hospitals and Clinics; [6]Molecular Otolaryngology and Renal Research Laboratories, Department of Otolaryngology—Head and Neck Surgery, Carver College of Medicine, University of Iowa; Interdepartmental PhD Program in Genetics, University of Iowa

Genetic counselors are crucial members of a multi-disciplinary healthcare team who provide comprehensive and tailored care for patients and families. Their specialized training in medical genetics and psychosocial counseling and ability to work and collaborate with a variety of medical specialties put them at the crossroad of precision medicine. Genetic counselors help people understand and adapt to the medical, psychological, and familial implications of genetic contributions to disease. They provide education about inheritance, genetic testing, and resources, and counsel patients and families to promote informed choices regarding prevention, treatment, and family planning. For disorders with significant phenotypic, genetic, and allelic heterogeneity such as hearing loss, providing genetic counseling could be challenging. Hearing loss is the most common sensory deficit worldwide and it is estimated that 70-80% of cases are due to an underlying genetic change. For newborns and children who are deaf or hard of hearing, a genetic evaluation including genetic counseling is recommended by the American Board of Medical Genetics and Genomics. If a genetic cause of hearing loss is suspected, comprehensive genetic testing is recommended.

Here, we used targeted genomic enrichment and massively parallel sequencing to screen all known genes associated with non-syndromic hearing loss and multiple common syndromes in a large multiethnic cohort. Following bioinformatics analysis evaluating single nucleotide and copy number variations, identified genetic variants were discussed in the context of the individual's medical and family history during a multidisciplinary meeting including clinicians, geneticists, scientists, bioinformaticians and a genetic counselor. Our data highlight cases in which the specialized training and knowledge of genetic counselors facilitated appropriate evaluation and pre-test counseling, provided prognosis, allowed for education about inheritance and recurrence risk in a family, explained complicated genetic etiologies, and arranged follow-up care for individuals who are deaf or hard of hearing and their families.

PS 158

A recurrent mutation in KCNQ4 in Korean families with nonsyndromic hearing loss and rescue of the channel activity by KCNQ activators

Jinsei Jung; Chan Il Song; Dong Hoon Shin; Young IK Koh; Seung Ho Shin; Young Kyun Hur; Jae Young Choi; Heon Yung Gee
Yonsei University

Mutations in potassium voltage-gated channel subfamily Q member 4 (KCNQ4) are etiologically linked to nonsyndromic hearing loss (NSHL), deafness nonsyndromic autosomal dominant 2 (DFNA2). To identify causative mutations of hearing loss in 98 Korean families, we performed whole exome sequencing. In three independent families with NSHL, we identified a cosegregating heterozygous missense mutation, c.140T >C (p.Leu47Pro), in KCNQ4. Individuals with the c.140T >C KCNQ4 mutation shared a haplotype flanking the mutated nucleotide, suggesting that this mutation may have arisen in a common ancestor in Korea. The mutant KCNQ4 protein could reach the plasma membrane and interact with wild-type (WT) KCNQ4, excluding a trafficking defect; however, it exhibited significantly decreased voltage-gated potassium channel activity and fast deactivation kinetics compared with WT KCNQ4. In addition, when co-expressed with WT KCNQ4, mutant KCNQ4 protein exerted a dominant-negative effect. Interestingly, the channel activity of the p.Leu47Pro KCNQ4 protein was rescued by the KCNQ activators MaxiPost and zinc pyrithione. The c.140T >C (p.Leu47Pro) mutation in KCNQ4 causes progressive NSHL; however, the defective channel activity of the mutant protein can be rescued using channel activators. Hence, in individuals with the c.140T >C mutation, NSHL is potentially treatable, or its progression may be delayed by KCNQ activators.

PS 159

A Genome-First Approach to EYA4-related SNHL

Shadi Ahmadmehrabi[1]; Joseph Park[2]; Douglas Epstein[2]; Jason Brant[3]; Dan Rader[2]
[1]Cleveland Clinic Lerner College of Medicine; [2]Department of Genetics, Perelman School of Medicine, University of Pennsylvania; [3]Department of Otorhinolaryngology, Hospital of the University of Pennsylvania

The heritability of age-related hearing loss has been estimated to be between 35% and 75%. This wide range in reports and “missing” heritability reflects the paucity of our understanding of the genetic architecture of hearing loss. Recently, susceptibility loci for age-related hearing loss have been identified through GWAS and family studies. EYA4 is a transcriptional co-activator which has been reported in association with both sensorineural hearing loss (SNHL) and dilated cardiomyopathy (DCM) in family studies and individual case reports. In the PennMedicine BioBank, a database of paired whole exome sequencing and EHR data for 11k+ patients, 257 variants in EYA4 were identified. 253 rare variants (minor allele frequency < 0.05) were filtered for predicted likely pathogenicity (REVEL score > 0.5). Additive rare variant analysis was performed in a genome-first approach with wild type controls matched for age, sex, and race in a 1:3 ratio. There was a significant association between EYA4 gene burden and SNHL with odds ratio = 4.5, p = 0.03. There was no significant association with DCM. In contrast to prior reports, this is the first large-scale genome-first investigation into EYA4-related SNHL. Rare variant analysis can aid the understanding of the genetic architecture of hearing, identify high-risk individuals, and guide discovery of the molecular biology of hearing.

PS 160

Genome Wide Association Study of Tinnitus in the United Kingdom Biobank Indicates Significant Genetic Heritability, Multiple Significant Loci, and Correlation with Psychiatric Traits

Royce E. Clifford; Adam E. Maihofer; Allen Ryan; Caroline E. Nievergelt
University of California, San Diego

Background
Tinnitus, defined as ringing in the ears without external sound, is the number one disability at the Veterans Administration and is clinically co-morbid with anxiety, depression, insomnia, and suicide risk. While twin studies on tinnitus suggest a genetic component, to date, no large-scale genetic analyses have been performed. Here we present first insights into the genetic basis of tinnitus based on a genome-wide association study (GWAS) in the United Kingdom Biobank (UKB).

Methods
Subjects with self-reported tinnitus and hearing loss, and controls not reporting any symptoms were identified from survey data in the UKB. GWASs were performed in subjects of European ancestry using linear regression and testing sex, age, and hearing loss as covariates. A polygenic risk score (PRS) based on the UKB GWAS was calculated for UKB subsets and external data using PRSice. Tinnitus SNP-based heritability and genetic correlations with other traits were performed using linkage disequilibrium score regression (LDSC). Mendelian randomization analyses (MR) were performed to test for causality between tinnitus and genetically correlated traits using the *TwoSampleMR* R package.

Results
Optimizing approaches for case definitions based on heritability estimates, we identified >52K cases and >120K controls in the UKB. Heritability estimates for tinnitus were ~6% and highly significant. Multiple novel genome-wide significant loci were identified, including genes which may be related to hearing loss. LDSC revealed genetic correlation between tinnitus and depression, educational attainment, hearing loss, and

insomnia, among others. MR indicates bi-directional causal associations between tinnitus and some of these other traits.

Conclusions
Results from the UKB suggest that common genetic variation contributes substantially to heritability of tinnitus, and identify several genome-wide significant loci. Correlations between tinnitus and some co-morbidities exist on a genetic level and may be causal in nature. Future directions include examining the genetic architecture of tinnitus in larger datasets and participants of other ancestries, as well as genetic correlations with hearing loss derived from audiometric data.

PS 161

Genomic Analysis of Hearing Loss and Cochlear Implant Outcomes

Ryan J. Carlson[1]; David L. Horn[2]; Mary-Claire King[1]; Jay T. Rubinstein[1]
[1]University of Washington; [2]Seattle Children's Hospital

In the U.S., hearing loss affects three out of every 1000 newborns and more than 27 million adults. For these individuals, the best treatment options are hearing aids and cochlear implants. Most patients who receive a cochlear implant can attain impressive speech recognition in quiet, but a number of patients have poorer outcomes with their implants, particularly in the presence of background noise. Future cochlear implant performance is not clinically predictable prior to implantation, so there exists a critical need to identify markers that enable meaningful prediction of implant success.

Hereditary hearing loss is genetically highly heterogeneous, with 117 different responsible genes identified so far. Given that more than 50% of childhood hearing loss in the U.S. has a genetic basis, it is plausible that some variability in cochlear implant outcomes may be due to underlying genetic variation.

We will study a cohort of more than 300 cochlear implant patients recruited from Seattle Children's Hospital over the next 2 years and combine targeted sequencing of 178 genes known to be related to hearing loss with in-depth, long-term audiometric and psychoacoustic testing to measure cochlear implant outcomes. We have designed a targeted sequencing panel that includes all genes present within commonly utilized clinical panels for hearing loss, along with several genes that were only recently identified. Genomic DNA is extracted from saliva samples collected from implanted patients or from those being evaluated for cochlear implant candidacy, and from their parents. Results from the first 20 patients yielded a 50% solve rate for mutations very likely to be causing the hearing loss of the patient. Responsible genes were *GJB2, MYO7A, GATA3, MYO15A, CHD7,* and *TBC1D24*.

Over the course of this study, we aim to correlate hearing loss severity, age of onset, progression, and other clinical characteristics with mutations in specific hearing loss genes. This will substantially augment the ability of genetic testing to predict disease severity and progression and to inform patient care. Additionally, we hope to identify genetic causes of hearing loss associated with differing cochlear implant success so as to better personalize treatments for individual patients.

PS 162

A Genetic Study for Sensorineural Tinnitus Based on Genome-wide Association & Endophenotype Study: Development of Genetic Diagnostic Kit for Precision Medicine

Jae Sang Han[1]; Minho Lee[2]; Yeun-Jun Chung[2]; Jung Mee Park[1]; Hamzah Alshaikh[1]; Shi Nae Park[1]
[1]Department of Otolaryngology-HNS, Seoul St. Mary's Hospital, College of Medicine, The Catholic University of Korea; [2]Catholic Precision Medicine Research Center, College of Medicine, The Catholic University of Korea

Background
Tinnitus is the perception of sound that does not occur from external sources which is interferes with daily life by causing insomnia, loss of concentration, and depression. It is common condition affecting between 10 and 15% of the general population. Despite its high prevalence, the genetic research of the chronic primary tinnitus is still in its early stages

Objectives
This study was performed to find genetic variation in patients with chronic sensorineural tinnitus using the genome-wide association study (GWAS) analysis method. Methods: Among those who complained of subjective or objective tinnitus, patients diagnosed with chronic sensorineural tinnitus by an expert were registered in the experimental group. We genotyped blood of 200 cases of tinnitus patients and 150 controls with Korean Biobank Array, which was optimized for the Korean population.

Results
Out of more than 800,000 single nucleotide polymorphisms (SNP), 4 loci (rs1924089, rs1039239, rs11064191, and rs9682978) were identified as significantly associated with tinnitus ($P < 10^{-5}$). Three of them were located in intergenic regions; one was located in intronic region of

a coding gene, SORBS2. Conclusion: We could not find any previous reports of the four SNPs we discovered with respect to tinnitus. Subsequent functional validation would be needed.

PS 163

Identification of a Potential Founder Effect of a Novel PDZD7 Variant Involved in Moderate-to-Severe Sensorineural Hearing Loss in Koreans

Sang-Yeon Lee[1]; Byung Yoon Choi[1]; Bong Jik Kim[2]; Seungmin Lee[1]; Doo-Yi Oh[1]
[1]Department of Otorhinolaryngology-Head and Neck Surgery, Seoul National University Bundang Hospital,; [2]Department of Otorhinolaryngology-Head and Neck Surgery, Chungnam National University Hospital,

PDZD7, a PDZ domain-containing sca old protein, is critical for the organization of Usher syndrome type 2 (USH2) interactome. Recently, biallelic PDZD7 variants have been associated with autosomal-recessive, non-syndromic hearing loss (ARNSHL). Indeed, we identified novel, likely pathogenic PDZD7 variants based on the American College of Medical Genetics and Genomics/Association for Molecular Pathology (ACMG/AMP) guidelines from Korean families manifesting putative moderate-to-severe prelingual ARNSHL; these were c.490C >T (p.Arg164Trp), c.1669delC (p.Arg557Glyfs*13), and c.1526G >A (p.Gly509Glu), with p.Arg164Trp being a predominantly recurring variant. Given the recurring missense variant (p.Arg164Trp) from our cohort, we compared the genotyping data using six short tandem-repeat (STR) markers within or flanking PDZD7 between four probands carrying p.Arg164Trp and 81 normal-hearing controls. We observed an identical haplotype across three out of six STR genotyping markers exclusively shared by two unrelated hearing impaired probands but not by any of the 81 normal-hearing controls, suggesting a potential founder effect. However, STR genotyping, based on six STR markers, revealed various p.Arg164Trp-linked haplotypes shared by all of the affected subjects. In conclusion, PDZD7 can be an important causative gene for moderate to severe ARNSHL in Koreans. Moreover, at least some, if not all, p.Arg164Trp alleles in Koreans could exert a potential founder effect and arise from diverse haplotypes as a mutational hot spot.

PS 164

Towards a Non-Invasive Differential Diagnostic Test to determine the underlying Pathology of Hearing Loss.

Neil Ingham; Karen Steel
King's College London and Wellcome Trust Sanger Institute

As we move towards treatments for people suffering from hearing loss, it will be crucial to determine the nature of the pathology causing the impairment. For example, stimulating hair cell regeneration might be of little help to a patient with a deficit in function of the stria vascularis. As knowledge of the auditory system has advanced, it has become apparent that there are many causes of hearing impairment of cochlear origin. Current clinical tools can give indications of certain broad classes of pathology such as conductive and sensorineural hearing loss. However, a reliable method to differentially diagnose dysfunction of the stria vascularis (metabolic hearing loss) has proved particularly difficult to find.

Genetic approaches using mutant mice have proved to be excellent research tools to define the underlying pathology of different patterns of hearing impairment. There are currently around 400 genes known to play a role in mammalian hearing function and a large number of these have a defined lesion producing a specific functional deficit.

Here, we combine the power of mouse mutants with known lesions with clinically available measurements (auditory brainstem responses, ABR and distortion product otoacoustic emissions, DPOAE) and use multi-parameter comparisons (based on Mills, 2006) with elliptical clustering to define spaces representative of different pathological conditions of the inner ear.

Using an *S1pr2* mutant as a model of stria vascularis dysfunction, a *Klhl18* mutant as a model of Inner Hair Cell dysfunction and an *Slc26a5* (Prestin*)* mutant as a model of Outer Hair Cell dysfunction, we have defined parameters based on ABR and DPOAE measurements in mice that suggest that it may be possible to indicate a likelihood of an individual having a specific type of cochlear pathology.

Acknowledgements
Supported by an Action on Hearing Loss International Project Grant to the authors.

References
Mills, D.M. (2006) Ear and Hearing, **27**, 508-535

PS 165

COL11A1 causes autosomal dominant non-syndromic hearing loss in the DFNA37 locus â€“ confirmation of a novel splicing variant

Thore Schade-Mann[1]; Barbara Vona[2]; Anke Tropitzsch[1]; Fritz Schneider[2]; Marcus Müller[2]; Hubert Löwenheim[3]
[11]Department of Otolaryngology, Head and Neck

Surgery, Tuebingen Hearing Research Centre, Eberhard Karls University Tuebingen, Elfriede-Aulhorn-Str. 5, 72076 Tuebingen, Germany; [2]Department of Otolaryngology, Head and Neck Surgery, Tuebingen Hearing Research Centre, Eberhard Karls University Tuebingen, Elfriede-Aulhorn-Str. 5, 72076 Tuebingen, Germany; [3]Tübingen Hearing Research Centre, Department of Otolaryngology-Head & Neck Surgery, Eberhard Karls University Tübingen, Germany

Hearing loss is a major burden for patients and it becomes of even greater importance in an aging society. Over half of hearing loss has a genetic background with different types inheritance, namely autosomal dominant, recessive, X-linked, and mitochondrial forms. Autosomal dominant non-syndromic hearing loss is the second most commonly inherited form and is present in roughly 20% of hearing impaired individuals.

The gene *COL11A1* (collagen type XI alpha 1 chain) has long been associated with Marshall syndrome and Stickler syndrome type II, which are both inherited in an autosomal dominant pattern, as well as autosomal recessive fibrochondrogenesis. The syndromes exhibit an auditory phenotype and other clinical manifestations, including vision impairment, (facial) dysmorphic features, and cheilognatho(palato) schisis. A novel splicing variant of *COL11A1* has been demonstrated to be associated with autosomal dominant non-syndromic hearing loss (DFNA37). We identified a family with autosomal non-syndromic hearing loss. The index patient presented with the major complaint of bilateral hearing loss. Pure tone audiometry confirmed moderate sensorineural hearing loss. Other syndromic features were absent. Custom-designed high-throughput sequencing panel diagnostics consisting of 160 hearing loss-associated genes revealed a heterozygous variant (c.4338+2T >C, p.?, NM_080629.2) in the gene *COL11A1*. In silico analysis predicted the 5' splice site of exon 58 (out of 68) to be abolished. Functional testing of the variant using an in vitro splice assay confirmed abnormal splicing.

We report on the second DFNA37-associated splice-altering variant, providing confirmatory evidence of *COL11A1* as a bona fide autosomal dominant non-syndromic hearing loss gene.

PS 166

Clinical next-generation sequencing database of deafness: unified management tool of clinical and genetic information.

Shin-ya Nishio; Shin-ichi Usami
Shinshu University School of Medicine

Background and Objective

Recent advances in next-generation sequencing have given rise to new challenges due to difficulties in variant pathogenicity interpretation and large dataset management. However, such big-data will be a powerful base for developing the new medical treatment including gene-therapy. Here, we report a new database development tool, named the "Clinical NGS database," for improving clinical next-generation sequencing workflow through the unified management of variant information and clinical information.

Materials & methods

We performed the next-generation sequencing analysis to screen for 68 known genetic cause of deafness in 9,500 unrelated Japanese hearing loss patients. All patient phenotypic data and genome analysis information were incorporated into the developed database.

Results

This database software offers a two-feature approach to variant pathogenicity classification. The first of these approaches is a phenotype similarity-based approach, and allows the easy comparison of the detailed phenotype of each patient with the average phenotype of the same gene mutation. The other approach is a statistical approach to variant pathogenicity classification based on the use of the odds ratio for comparisons between the case and the control comparison for each inheritance mode. In the presentation, we introduce some use case of our database.

Conclusion

We developed new database tools for unified management of variant information and clinical information of deafness patients. Based on this database software, we developed a central database system to manage the over 9,000 of target re-sequencing analysis results and clinical information associated with the Japanese nation-wide deafness gene study consortium. This dataset will be a powerful base toward the development of new medical treatment including gene-therapy.

PS 167

Clinical Features of Deafness Caused by a Novel CLDN14 Variant

Tomohiro Kitano[1]; Shin-ichiro Kitajiri[2]; Shin-ya Nishio[2]; Shin-ichi Usami[2]
[1]Department of Otorhinolaryngology, Shinshu University School of Medicine; [2]Shinshu University School of Medicine

Background

Hearing loss (HL) is the most common sensory impairment which affect two in a thousand newborns, and 60% of them account for genetic factors. Approximately one hundred genes have been reported as associated with inherited HL. The claudins are a family of proteins that play a major role in the epithelial barrier function. 24 claudins have been identified in humans thus far, of which more than 10 have been reported to express in the inner ear. Among these, one type of claudin gene, the *CLDN14*, was reported to be responsible for human hereditary hearing loss, DFNB29. To date, nine pathogenic variants have been reported, and some phenotypic features, such as details of vestibular function and outcome of cochlear implantation (CI), remain unclear. This study is intended to clarify the prevalence and clinical characteristics of DFNB29 in the Japanese population.

Methods

We conducted a study on 2,549 unrelated Japanese hearing loss patients, utilizing the massively parallel DNA sequencing on 68 target genes, to identify the genomic variations responsible for HL. Among them, we selected candidates who carried *CLDN14* probable pathogenic variants, and applied the Sanger sequencing and segregation analysis using exon-specific custom primers to confirm those variations. We also performed audiovestibular assessments for all probands.

Results

We identified a homozygous novel variant (0.04%: 1/2549) in one patient. This patient showed progressive bilateral HL, with post-lingual onset. Pure-tone audiograms indicated a high-frequency HL type, and the deterioration gradually spread to other frequencies. The patient showed normal vestibular function. CI improved her sound field threshold levels, but not the speech discrimination scores.

Conclusion

We present a patient with a novel variant in the *CLDN14* gene identified from a non-consanguineous family. This is the first report of *CLDN14*-associated HL in an east Asian population. Serial audiograms indicated high-frequency HL type, and the deterioration gradually spread to other frequencies, finally resulting in deafness. The patient showed normal vestibular function for caloric testing, cVEMPs, and oVEMPs. This is also the first report of an HL patient with *CLDN14* variant who received CI. CI improved her sound field threshold levels, but not her speech discrimination scores. This research may determine the diagnosis and treatment of *CLDN14*-associated HL.

PS 168

Copy Number Variation Detection is Essential in the Diagnosis of Hearing Loss

Paige L. Harlan[1]; Amanda O. Taylor[2]; Carla J. Nishimura[2]; Kathy L. Frees[2]; Diana L. Kolbe[3]; Kevin T. Booth[4]; Robert J. Marini[1]; Donghong Wang[1]; Amanda M. Schaefer[1]; Amy E. Weaver[1]; Jori E. Hendon[1]; Richard J.H. Smith[5]; Hela Azaiez[2]

[1]Molecular Otolaryngology and Renal Research Laboratories, Department of Otolaryngology—Head and Neck Surgery, University of Iowa Hospitals and Clinics; [2]Molecular Otolaryngology and Renal Research Laboratories, Department of Otolaryngology—Head and Neck Surgery, Carver College of Medicine, University of Iowa; [3]Molecular Otolaryngology and Renal Research Laboratories, Department of Otolaryngology—Head and Neck Surgery, University of Iowa Hospitals and Clinic; [4]Molecular Otolaryngology & Renal Research Labs, Department of Otolaryngology—Head and Neck Surgery, University of Iowa Carver College of Medicine; Department of Neurobiology, Harvard Medical School, Harvard University; [5]Molecular Otolaryngology and Renal Research Laboratories, Department of Otolaryngology—Head and Neck Surgery, Carver College of Medicine, University of Iowa; Interdepartmental PhD Program in Genetics, University of Iowa

Copy number variations (CNVs) are significant drivers of genetic diversity. Their role in human disorders has also been well established. CNVs are a major contributor to non-syndromic and syndromic forms of hearing loss as they account for up to 20% of all diagnosed cases. Their identification in more than ~40% of all known deafness-associated genes along with the diversity of their sizes and types make their screening and detection challenging.

We used targeted genomic enrichment coupled with next generation sequencing to screen all coding regions of 152 deafness-associated genes, specific intergenic regions and pseudogenes in a large cohort of individuals with hearing loss. All genes were assessed for single nucleotide variants, indels, and CNVs using a customized bioinformatics pipeline. Cases were reviewed at an interdisciplinary meeting where genetic results were interpreted in the context of clinical data.

Our results showed that genetic comprehensive screening of CNV was required to provide an accurate genetic diagnosis. For example, we identified a heterozygous deletion in *trans* with a hemizygous missense variant in *OTOF* in a 2-year-old male with profound hearing loss and auditory neuropathy. Without CNV analysis, an erroneous diagnosis of a homozygous missense variant

would have been provided which would have had serious implications for genetic counseling and carrier screening for this family. Additionally, high-resolution CNV detection capable of identifying small single exon deletions/duplications successfully elucidated the genetic etiology in many cases. A homozygous single-exon deletion in *TECTA* was identified and its exact breakpoints mapped in a 13-year-old male with congenital, moderate-to-severe hearing loss. Through the cases we will present, we will emphasize the need for a comprehensive screen of CNVs, highlight their contribution to hearing loss and their diversity and stress their impact on accurate diagnosis and implications for genetic counseling and carrier screening.

In aggregate, we assert that the inclusion of a comprehensive high-resolution CNV detection is essential in the genetic testing of persons with hearing loss.

PS 169

Contribution of mitochondrial tyrosyl-tRNA synthetase p.191Gly>Val mutation to the phenotypic manifestation of the deafness-associated mitochondrial tRNASer(UCN) 7511A>G mutation

Wenlu Fan; Min-Xin Guan
Zhejiang Unviersity

Nuclear modifier genes are proposed to modify the phenotypic expression of mitochondrial DNA mutations. In this report, we demonstrated that the p.191Gly >Val mutation in the mitochondrial tyrosyl-tRNA synthetase (YARS2) modulated the phenotypic manifestation of deafness-associated tRNASer(UCN) 7511A >G mutation. Strikingly, a Chinese family bearing both YARS2 p.191Gly >Val and m.7511A >G mutations displayed much higher penetrance of deafness than those carrying only m.7511A >G mutation. The m.7511A >G mutation changed the highly conserved A4:U69 base-pairing into G4:U69 base-pairing at the aminoacyl acceptor stem of tRNASer(UCN). The m.7511A >G mutation perturbed the structure and function of tRNASer(UCN), including the increased melting temperature, altered conformation, instability and aberrant aminoacylation of mutant molecule. YARS2 p.191Gly >Val mutation yielded the deficient aminoacylation of tRNATyr. However, mutant cell lines harboring only m.7511A >G or p.191Gly >Val mutation exhibited only mild effects on tRNASer(UCN) or tRNATyr metabolism, respectively. We found that mutant cell lines harboring both m.7511A >G and p.191Gly >Val mutations exhibited not only more severe decreases in the aminoacylation efficiencies and steady-state levels of tRNASer(UCN) and tRNATyr but also reductions in the aminoacylation and steady-state levels of other tRNAs such as tRNAThr, tRNALys, tRNALeu(UUR) and tRNASer(AGY) than those in cell lines carrying only m.7511A >G or p.191Gly >Val mutation. Furthermore, cell lines carrying both m.7511A >G and p.191Gly >Val mutations exhibited greater decreases in the levels of mitochondrial translation, respiration, mitochondrial ATP and membrane potentials as well as increasing production of reactive oxygen species. Our findings provided new insights into the pathophysiology of maternally transmitted deafness arising from the synergy between mitochondrial tRNASer(UCN) and nucleus-encoded mitochondrial tyrosyl-tRNA synthetase mutations.

PS 170

Integrating Phenotypic and Genotypic Data to Enhance Diagnosis and Clinical Care of Persons with Hearing Loss

Amanda O. Taylor[1]; Carla J. Nishimura[1]; Kathy L. Frees[1]; Diana L. Kolbe[2]; Kevin T. Booth[3]; Robert J. Marini[4]; Donghong Wang[4]; Amanda M. Schaefer[4]; Paige L. Harlan[4]; Amy E. Weaver[4]; Jori E. Hendon[4]; Hela Azaiez[1]; Richard J.H. Smith[5]
[1]Molecular Otolaryngology and Renal Research Laboratories, Department of Otolaryngology—Head and Neck Surgery, Carver College of Medicine, University of Iowa; [2]Molecular Otolaryngology and Renal Research Laboratories, Department of Otolaryngology—Head and Neck Surgery, University of Iowa Hospitals and Clinic; [3]Molecular Otolaryngology & Renal Research Labs, Department of Otolaryngology—Head and Neck Surgery, University of Iowa Carver College of Medicine; Department of Neurobiology, Harvard Medical School, Harvard University; [4]Molecular Otolaryngology and Renal Research Laboratories, Department of Otolaryngology—Head and Neck Surgery, University of Iowa Hospitals and Clinics; [5]Molecular Otolaryngology and Renal Research Laboratories, Department of Otolaryngology—Head and Neck Surgery, Carver College of Medicine, University of Iowa; Interdepartmental PhD Program in Genetics, University of Iowa

Advances in sequencing technologies have made comprehensive genetic testing for deafness the recommended diagnostic test in the evaluation of a deaf/hard-of-hearing person. However, extreme allelic, genetic and phenotypic heterogeneity can make variant interpretation challenging. Here we showcase examples of genetic and phenotypic complexity that underscore the need for a multidisciplinary approach to the interpretation of genetic and clinical data in individuals with hearing impairment.

We used targeted genomic enrichment and massively parallel sequencing to screen all genes known to

be associated with non-syndromic hearing loss and multiple common syndromes. Bioinformatic analysis was completed using a custom-built pipeline that evaluates single nucleotide and copy number variations. Genetic results were discussed at a multidisciplinary meeting in the context of the clinical history, physical exam and family history. Audioprofiles were also considered, noting any progression of hearing loss, age at diagnosis and symmetry.

We show that this approach facilitates diagnostic refinement, especially when more clinical data is provided. For example, delayed developmental milestones are consistent with Usher syndrome and not non-syndromic hearing loss in a 5-year-old male with severe-to-profound hearing loss segregating two pathogenic variants in *MYO7A*. Segregation analysis is important as it provides insight into inheritance patterns, establishes whether variants are in *cis* or in *trans*, and confirms whether a variant has arisen *de novo*.

In summary, a multidisciplinary approach that integrates the interpretation of genetic findings with clinical data facilitates diagnosis and is essential for optimal care of persons with hearing loss.

PS 171

TJP2 and Hearing Loss: Identification of a Novel Disease-Mechanism

Erika M. Renkes[1]; Kevin T. Booth[2]; Kimia Kahrizi[3]; Luke T. Hovey[1]; Hossein Najmabadi[3]; Richard J.H. Smith[4]; Hela Azaiez[5]
[1]Molecular Otolaryngology and Renal Research Laboratories, Department of Otolaryngology - Head and Neck Surgery, University of Iowa; [2]Molecular Otolaryngology & Renal Research Labs, Department of Otolaryngology—Head and Neck Surgery, University of Iowa Carver College of Medicine; Department of Neurobiology, Harvard Medical School, Harvard University; [3]Genetics Research Center, University of Social Welfare and Rehabilitation Sciences, Tehran, Iran.; [4]Molecular Otolaryngology and Renal Research Laboratories, Department of Otolaryngology—Head and Neck Surgery, Carver College of Medicine, University of Iowa; Interdepartmental PhD Program in Genetics, University of Iowa; [5]Molecular Otolaryngology and Renal Research Laboratories, Department of Otolaryngology—Head and Neck Surgery, Carver College of Medicine, University of Iowa

Tight junctions (TJs) and their associated protein complexes form intricate protein networks that allow for intracellular communication and are fundamental for a whole host of proper cellular functions. Genetic defects in TJs and/or their interacting partners have been linked to several inheritable diseases including deafness. In the inner ear, TJs are required for connecting the auditory hair cells to the surrounding supporting cells and maintaining ion homeostasis. One key protein in this complex is the Tight Junction Protein 2 (*TJP2*). A duplication in *TJP2* has been previously linked to autosomal dominant nonsyndromic hearing loss (ADNSHL) through a dosage effect mechanism. In this study, we used OtoSCOPE, a deafness-specific targeted gene panel to screen a large Iranian family segregating ADNSHL. Variants were filtered based on minor allele frequency and functional consequence through the use of a customized bioinformatics pipeline that evaluates single nucleotide and copy number variants. We have identified a variant in the canonical splice-donor site, c.2811+1G >A in *TJP2* gene that segregated with hearing loss in this family. To test the functional effect of this variant on splicing, we performed mini-gene assays in mammalian cells. We showed that the mutant *TJP2* construct affects normal splicing patterns by causing two distinct phenomena 1-exon skipping and an in-frame 80 amino acid deletion of the acidic region which is involved in actin binding and 2-partial intron retention and addition of 33 amino acids to the acidic region before encountering a stop codon. Our data suggest the c.2811+1G >A variant might hinder the wildtype protein through a gain of function/dominant-negative mechanism affecting its binding to actin. This is the first study showing that mutant *TJP2* protein acts in a dominant-negative manner on the function of the TJ complex probably by altering its binding to actin. Understanding genetic variant effects is fundamental to illuminating disease mechanisms and creating novel molecular therapies.

PS 172

In Vivo Base Editing Rescues Hearing in a Mouse Model of Recessive Deafness

Wei-Hsi Yeh[1]; **Olga Shubina-Oleinik**[2]; Jonathan Levy[3]; Bifeng Pan[4]; Gregory Newby[3]; Michael Wornow[5]; Rachel Burt[6]; Jeffrey R. Holt[7]; David Liu[8]
[1]Department of Chemistry and Chemical Biology, Harvard University/ Program in Speech and Hearing Bioscience and Technology, Harvard Medical School; [2]Department of Otolaryngology, F.M. Kirby Neurobiology Center, Boston Children's Hospital/ Harvard Medical School; [3]Merkin Institute of Transformative Technologies in Healthcare, Broad Institute of Harvard and MIT/ Department of Chemistry and Chemical Biology, Harvard University; [4]Decibel Therapeutics; [5]Merkin Institute of Transformative Technologies in Healthcare, Broad Institute of Harvard and MIT/Department of Chemistry and Chemical Biology, Harvard University; [6]Murdoch Children's Research Institute, The Royal Children's Hospital, Parkville, Victoria, Australia.;

[7]*Department of Otolaryngology, F.M. Kirby Neurobiology Center, Boston Children's Hospital and Harvard Medical School;* [8]*Merkin Institute of Transformative Technologies in Healthcare, Broad Institute of Harvard and MIT/ Department of Chemistry and Chemical Biology, Harvard University/ Howard Hughes Medical Institute*

Hearing loss (HL) is the most common neurological disorder in industrialized countries and the most prevalent sensorineural disorder, which accounts for over 250 million cases worldwide. 50%–60% of HL has a genetic etiology. Genetic mutations in *Transmembrane channel-like 1* (*TMC1*) can cause dominant or recessive hereditary HL. *TMC1* encodes a protein that forms mechanosensitive ion channels in sensory hair cells of the inner ear and is required for normal auditory function,

Recently, several successful approaches for *TMC1* gene therapy have been demonstrated: gene replacement, RNA interference and allele-specific gene disruption using Cas9/sgRNA. However, each method has some limitations, such as the size of transgene that can be delivered by AAV, duration of transgene expression (gene replacement) or possible off-target effects (RNA interferes / allele-specific gene disruption).

To circumvent these limitations we explored base editing (BE), a genome editing technology that enables the direct, irreversible conversion of a specific DNA base into another. Base editing has the potential to directly repair point mutations and may provide permanent therapeutic restoration of gene function.

We investigated the potential of BE to treat *Baringo* mice, which carry a recessive, loss-of-function point mutation in *Tmc1* (*c.A545G*, resulting in the substitution p.Y182C) which causes deafness. To repair the p.Y182C mutation we tested several optimized cytosine base editors (CBEmax variants) and guide RNAs in *Baringo* mouse embryonic fibroblasts. We packed the most promising CBE, derived from an activation-induced cytidine deaminase (AID), into dual AAV vectors using a split-intein system. The dual AID-CBEmax AAVs were injected into the inner ears of *Baringo* mice at postnatal day 1. Injected mice showed up to 51% correction of the *c.A545G* point mutation in *Tmc1* transcripts, which restored the wild-type *Tmc1* coding sequence (*c.A545A)* in sensory hair cells of the inner ear. Repair of *Tmc1 in vivo* rescued hair-cell sensory transduction, hair-cell morphology, and substantial low-frequency hearing 4 weeks post-injection.

These findings provide a foundation for a potential one-time treatment for hearing loss due to point mutations in the *Tmc1* gene and suggest future avenues for application of base editing for treatment of different forms of hereditary hearing loss caused by point mutations.

Inner Ear: Anatomy & Physiology

PS 173

Distribution of Glucocorticoid Receptors in Human Cochlea and Endolymphatic Sac - An Immunohistochemistry Study

Wei Liu; Charlotta Nordström; Niklas Danckwardt-Lilliestrom; Helge Rask-Andersen
Uppsala University

Systemic or local application of glucocorticoids are continuously reported as an effective treatment for noise-induced hearing loss, sudden hearing loss, Meniere's disease, certain forms of progressive hearing loss especially the one with autoimmune nature. Simultaneous delivery of steroid to the intra-cochlear space during cochlear implantation was acclaimed to protect inner ear from insertion trauma. Animal study on cochlear glucocorticoid receptor (GR) substantiated such practice. Study on GR distribution in human cochlea is rare, one reason being the difficulty in obtaining well-fixed human cochlear tissue. In our study, four human cochleae and three human endolymphatic sacs (ESs) were removed during surgery for treating posterior cranial fossa tumors. The specimens were fixed (4% paraformaldehyde), decalcified (0.1 M Na-EDTA) and frozen-sectioned (embedded in Tissue-Tek OCT) with shortest delay possible of each procedure. Immunohistochemistry was carried out and confocal laser scanning microscopy (CLSM) as well as super-resolution structured illumination microscopy (SR-SIM) was performed. SIM is capable of achieving a lateral (X-Y) resolution of ≈100 nm

GR appeared extensively expressed in the human cochlear tissue, but the intensity of GR immunoreactivity varied in different regions. The strongest immune staining was observed in the apical portion of the marginal cells in the stria vascularis, in the inner and outer pillar cells as well as the spiral ganglion neurons. The inner and outer hair cells were moderately stained, stronger in the apical part of the organ of Corti than in the lower turns. The labeling in spiral ganglion neurons displayed cytoplasmic granular pattern in the cell bodies but not in the nerve fibers. GR-immunostaining was also seen in the neuronal nuclei. The immunoreaction to GR antibody was also positive in the ESs especially their epithelial cells.

When GR binds to glucocorticoids, the primary mechanism of action is the regulation of gene transcription. The unbound receptor resides in the cytosol of the cell. The

activated GR complex up-regulates the expression of anti-inflammatory proteins in the nucleus or represses the expression of pro-inflammatory proteins in the cytosol by preventing the translocation of other transcription factors from the cytosol into the nucleus. Among the actions associated with the immune response and inflammation, glucocorticoids-GR complex stimulates white blood cells to release macrophage migration inhibitory factor (MIF). However, in patients with high MIF, steroids-resistance can occur, that hinders the therapeutic effects of the steroids. The mechanism of glucocorticoids action in treatment of the inner ear diseases remains unclear.

PS 174

Analyses of hearing impairment in GNE V572L point-mutant mice

Akiyoshi Yasumoto[1]; Ippei Kishimoto[1]; Kazushi Sugihara[2]; Toru Yoshihara[2]; Masahide Asano[2]; Koichi Omori[3]; Norio Yamamoto[3]
[1]Dep. Otolaryngology, Head and Neck Surgery, Graduate School of Medicine, Kyoto University, Kyoto, Japan; [2]Institute of Laboratory Animals, Graduate School of Medicine, Kyoto University, Kyoto, Japan; [3]Dept. Otolaryngology - Head and Neck Surgery, Graduate School of Medicine, Kyoto University

Background
The GNE gene encodes UDP-N-acetylglucosamine 2-epimerase/N-acetyl-mannosamine kinase (GNE). GNE is a dual-function enzyme that catalyzes the rate-limiting step in sialic acid biosynthesis. Mice with a null mutation in the GNE gene are embryonic lethal. (Schwarzkopf M et al. PNAS, 2002) Sialic acid is an acidic monosaccharide known to modify nonreducing terminal carbohydrates on glycoproteins and glycolipids, where it functions in cellular adhesions and interactions in the nervous and immune systems. Human GNE mutations result in GNE myopathy, an adult-onset, progressive, autosomal recessive muscular disorder, distal myopathy with rimmed vacuoles (DMRV). GNE V572L mutation has been reported in Japanese families affected by DMRV. (Arai et al. Ann Neurol, 2002) There were no apparent myopathic features or motor dysfunctions in the GNE V572L point-mutant (GNEpm) homozygous mice (mt-mice). However, the mt-mice had a short lifespan, massive proteinuria after birth, and abnormal kidney morphology. (Ito et al. Plos One, 2012) And observations of GNEpm mt-mice general behavior revealed that they had no startle reflex in response to acoustic stimulations. This result suggests that GNEpm mt-mice have a hearing impairment. In this study, we examined the auditory system of the GNEpm mt-mice by electrophysiological and histological analyses.

Methods
We used 4 and 12-week-old GNEpm male mice in C57BL/6 backgeound. We assessed the hearing ability of homozygous (mt) and heterozygous (ht) mouse by the auditory brainstem response (ABR) with a tone burst sound of 10, 20, 40 kHz and distortion product otoacoustic emission (DPOAE), and after that we performed histological examinations at 12 weeks.

Results
In the ht mouse, ABR showed normal hearing and DPOAE showed response at all frequencies. But in the mt mouse, ABR and DPOAE showed no response at 12 weeks. Even at 4 weeks, deterioration of ABR and DPOAE was observed. In the histological observation, the numbers of outer hair cells were reduced in the mt mouse.

Conclusions
DPOAE provides information regarding the function of outer hair cells. ABR and DPOAE results showed the hearing impairment in the mt mouse. Histological results are consistent with DPOAE results. These results suggest outer hair cell loss causes hearing impairment in GNEpm mt-mice, and outer hair cells impairment starts by 4-week-old. We will assess hearing ability and histology of cochlea in younger GNEpm mt-mice, examine when the deficit of OHCs starts, and how sialic acid affects OHC survival.

PS 175

Knockout of Mice Cochlear Connexin26 in Dose-Dependent Modes Induce Different Kinds of Hearing Loss and Pillar Cells Development Arrest Pattern.

Sen Chen; Le Xie; Kai Xu; Yue Qiu; Huimin Zhang; Xiaohui Wang; Yu Sun; Weijia Kong
Huazhong University of Science and Technology

Mutations in the GJB2 gene (which encodes Connexin26 (Cx26)) are the most common cause of non-syndromic deafness. Previous studies showed that an extensive knockout of the Gjb2 gene in cochlear epithelium can cause severe deafness, significant hair cell (HC) loss and failure of pillar cells (a type of supporting cell, PCs) to differentiate in mice. This study aimed to establish different mouse models with gradient reductions of cochlear Cx26 expression and to investigate the effect of different reduced levels of cochlear Cx26 expression on hearing and development of PCs. According to the reduction in the levels of cochlear Cx26, these models were named high knockdown (KD), middle KD and low KD group. In the low KD group, the mice showed normal hearing and well-developed PCs. In the high KD group,

up to 90 percent of supporting cells (SCs) lost Cx26 expression. These mice exhibited severe deafness, rapid hair cell degeneration and juvenile PCs. In the middle KD group, nearly half of SCs lost Cx26 expression. However, these mice showed a moderate deafness and a late-onset hair cell loss. Moreover, nearly all the PCs in mice of this group were in a partially differentiated state. These results indicated that reduction of postnatal expression of cochlear Cx26 induces hearing loss in a dose-dependent manner. Null Cx26 in a few SCs affects the developmental status of PCs and the hair cell degeneration pattern. The abnormal developmental status of PCs may be a potential cause of Gjb2-related hearing loss.

PS 176

Expression of Chemokine CXCL1 and its Receptor DARC in the Murine Inner Ear

Sasa Vasilijic; Lukas D. Landegger; Richard Seist; Konstantina M. Stankovic
Eaton Peabody Laboratories, Department of Otolaryngology, Massachusetts Eye and Ear, 243 Charles St, Boston, MA 02114, USA

CXCL1 is a chemokine with an important role in chemotaxis of inflammatory cells. In the inner ear, CXCL1 is upregulated in response to chronic otitis media, cochlear implantation, and drug- and noise-induced trauma. However, cellular sources of CXCL1 and expression of its cognate receptors in the inner ear remain unclear. Using immunohistochemistry applied to cochlear whole mounts and paraffin-embedded cochlear cross sections from 6-week old CBA/CaJ mice unexposed or exposed to noise causing permanent threshold shift (8-16 kHz for 2h at 103dB), we find the strongest CXCL1 expression in pillar cells (PCs). Three-dimensional reconstructions revealed predominant localization of CXCL1 in the apical segment of PCs. In addition to PCs, CXCL1 immunoreactivity was identified in the phalangeal processes of Deiters cells (DCs), interdental cells and Claudius cells. CXCL1 immunoreactivity was reduced in PCs in the cochlear base but not the apex 6h after noise exposure. Costaining with Iba1 revealed that Iba1-positive macrophages located within the spiral ligament and spiral limbus did not express CXCL1 irrespective of noise exposure. Immunostaining for CXCR2, a putative CXCL1 receptor, revealed no signal. However, immunostaining for the promiscuous chemokine binding protein, Duffy Antigen Receptor for Chemokines (DARC), revealed strong expression in outer PCs, HCs, a third row of DCs, and spiral ganglion neurons. DARC and CXCL1 were colocalized only in the basilar part of outer PCs. In contrast to CXCL1, DARC immunoreactivity was not noticeably affected by noise exposure. Within the peripheral vestibular system, CXCL1 immunolocalized to supporting cells of the crista ampullaris while DARC immunolocalized to a subset of HCs. Taken together, our results represent the first immunohistochemical localization of CXCL1 and its presumed receptor DARC in specific inner ear cells. The constitutive expression of CXCL1 under steady-state conditions suggests its unknown non-inflammatory role in inner ear physiology.

PS 177

Hearing Loss Associated with Diabetes: Changes of Cochlear Function in a Mouse Model of Diabetes

Ah-Ra Lyu[1]; Tae-Hwan Kim[2]; Seong-Hun Jeong[1]; Sun-Ae Shin[1]; Min Jung Park[1]; Yong-Ho Park[1]
[1]Chungnam National University; [2]Chungnam National University Hospital

Diabetes and hearing loss are two of the most widespread health concerns. Over 422 million people worldwide have diabetes, and around 466 million people worldwide have disabling hearing loss. It appears there is a lot of overlap between the two populations. Studies have shown that hearing loss is twice more common in people with diabetes than in those who don't have the disease. However, it is not well established how diabetes is related to hearing loss. Here, we investigated how hearing loss associated with diabetes causes damage to the mitochondria and microcirculation in the inner ear. B6.BKS(D)-*Lepr*^{db}/J (B6 db) male mice and age-matched wild-type (WT) mice were utilized as an animal model of diabetes. Weekly auditory brainstem response (ABR) between 4-14 weeks of age found that B6 db mice displayed a significant increase in ABR wave I amplitude starting at 6 weeks of age and ABR threshold at 10 weeks of age as compared to WT mice. Diabetic mice presented a significant inner and outer hair cell loss, spiral ganglion neuron (SGN) damage and CtBP2 decline as compared to WT. Transmission electron microscopy (TEM) images revealed a substantial impairment in mitochondrial structure and morphology in the inner and outer hair cells as well as SGNs. To evaluate how diabetes causes damage to the microcirculation in the inner ear, the cochlear blood flow was measured using a 0.1-mm-diameter laser Doppler probe placed over the lateral wall of the cochlea and TEM images were taken from the stria vascularis. Diabetic animals exerted a significantly reduced cochlear blood flow and vacuolization/gaps between the strial cells in the stria vascularis as compared to WT mice. Next, we investigated the underlying mechanisms of cochlear mitochondria in diabetic mice using qRT-PCR. B6 db mice expressed significantly increased levels of antioxidant enzymatic scavengers such as heme oxygenase (HO)-1 as compared to WT mice, indicating diabetic cochlea produces excessive superoxide radicals requiring increased ROS detoxification by the antioxidant enzymatic scavengers. These results suggest that

diabetic mice presents significantly impaired hearing function as early as 6 weeks of age, which is accompanied by damaged mitochondrial structure, decreased cochlear blood flow and increased oxidative stress response, as compared to WT. Our data imply that blood flow reduction and mitochondrial dysfunction in the inner ear contribute to hearing loss associated with diabetes.

PS 178

Re-evaluating the Histopathology of Presbycusis: Hair Cell Loss explains Audiometric Shifts in all four types

Peizhe Wu[1]; Leslie D. Liberman[2]; Jennifer T. O'Malley[3]; M. Charles Liberman[4]
[1]1. Eaton-Peabody Laboratories, Mass Eye & Ear; 2. Department of Otolaryngology Head & Neck Surgery, Harvard Medical School; [2]1. Eaton-Peabody Laboratories, Mass Eye & Ear; [3]1) Otopathology Laboratory, Department of Otolaryngology, Massachusetts Eye and Ear; [4]Harvard

Schuknecht and colleagues proposed four types of presbycusis based on cochlear histopathology in aged ears: i.e. sensory (12%), strial (35%), neural (31%) and cochlear conductive (23%). According to this view, only "sensory" cases showed hair cell loss in regions appropriate to the threshold shifts. However, the cytocochleograms in his studies were binarized: i.e. hair cells were rated as either present or absent, thus ignoring the fractional loss, which can be assessed with DIC microscopy (Wu et al, Laryngoscope, 2019).

Here, we re-analyzed Schuknecht's presbycusis exemplars (n=35), plus more recent presbycusis cases from the Mass. Eye and Ear collection (n=13), along with 29 cases with noise-induced hearing loss, and 7 normal-hearing controls. All cases have audiograms taken < 5.5 years before death and some have word-recognition scores. Blinded observer(s) used DIC and high-N.A. objectives to assess fractional hair cell loss. The cross-sectional area of the stria was also measured at 15 locations along the cochlea, and the peripheral axons of auditory nerve fibers (ANFs) were counted at 5 locations by staining myelin with Cellmask®. A statistical model for multiple regression, based on LASSO, was used to correlate hearing level with histopathology.

Throughout cochlear regions mapping to audiometric frequencies, fractional inner hair cell (IHC) and outer hair cell (OHC) loss were well correlated with hearing level (OHC, r^2 = 0.50; IHC, r^2 = 0.49). Strial survival, on the other hand, was poorly correlated with hearing level (r^2 = 0.021), and when unbiased cluster analysis was used to separate maximal vs. minimal strial-atrophy groups, mean audiograms of both clusters showed gently downsloping audiograms with < 10 dB difference between them.

All the histopathological measures were combined in a statistical model aiming to predict thresholds and word scores. Most of the variance in hearing level was explained by loss of OHCs and IHCs, along with age (r^2=0.631). Although strial atrophy and ANF degeneration were common in the aging ear, adding them to the model only increased the correlation minimally (r^2= 0.633). Although a decrease in endolymphatic potential should elevate thresholds, strial damage was apparently associated with enough OHC loss that the cochlear amplifier was already compromised. Word recognition scores were well predicted by age, IHC, OHC and ANF survival (r^2=0.578). Adding strial survival did not improve accuracy.

Our results suggest that commonly accepted ideas about strial, sensory and neural presbycusis need significant modification.

Research supported by a grant from the NIDCD (P50 DC015857)

PS 179

Neuro-immune Consequences of Noise-induced and Age-related Hearing Loss in the Mouse Cochlea

Benjamin Seicol; Ruili Xie
Department of Otolaryngology, Ohio State University

Noise-induced hearing loss (NIHL) and age-related hearing loss (AHRL) are both major causes of hearing impairment that result in chronic hearing loss in patients and researchanimals. Tissue resident macrophages and circulating monocytes respond to acute loud noise exposure leading to cochlear inflammation. Beyond NIHL, cochlear inflammation has also been shown to play a role in many other conditions that result in hearing loss, including infection, autoimmune inner ear disease, and ototoxicity. This shared pathway converges on tissue resident macrophages of the cochlea and provides an opportunity to better understand the neuro-immune interactions in peripheral sensory circuitry that contributes to traumatic forms of hearing loss. However, the timeline of macrophage recruitment and/or proliferation, the molecular mechanisms responsible for their activation and the pathophysiology of inflammation on peripheral auditory circuits following noise exposure remain to be clearly delineated. In addition, it remains unclear how cochlear inflammation occurs in ARHL as well. To address these gaps in knowledge, we have examined the time course of macrophage responses following 2 hours

of 112 dB noise exposure in young (P60) mice across acute and chronic time points. We have also measured changes in ribbon synapses and hair-cell loss associated with increased ABR thresholds. We further examined the number and activation of macrophages in mice with ARHL. Our preliminary results show significantly increased macrophage number and activation occurs acutely after noise exposure and corresponds with the initial total hearing loss for up to 24 hours post exposure (PE). Elevated ABR thresholds persist in these mice and macrophage numbers drastically decrease by 3 days PE, while the macrophages that remain exhibit a change in morphology associated with inflammation. Our preliminary results in aged mice show a more subtle increase in macrophage number and morphology consistent with low-grade, chronic inflammation. These results demonstrate that activation of immune responses occurs in the cochlea in both NIHL and ARHL and may contribute to changes in peripheral auditory circuitry. Future studies should investigate the molecular mechanisms of immune activation at critical time points following noise exposure to better understand how inflammation contributes to the pathology of hearing loss and further investigate the impact of chronic immune activation in ARHL.

PS 180

GATA3 Expression in Cochlear Tissues is Conserved across Mice, Rats, Macaques, and Humans.

Sumana Ghosh[1]; Robert Wineski[2]; Michael Pittman[3]; Bradley J. Walters[1]
[1]University of Mississippi Medical Center; [2]The University of Alabama, School of Medicine; [3]University of Richmond

GATA3 is a zinc finger transcription factor that is critical in a number of biological and disease processes, including cellular regeneration. In the inner ear, GATA3 is critical for the development and function of auditory neurons and the cochlear sensory epithelium. In the murine cochlea, GATA3 is lost from certain supporting cells and from type I spiral ganglion neurons shortly after development. The loss of GATA3 from supporting cells severely limits *Atoh1* induced hair cell regeneration, which suggests that if the pattern of GATA3 expression in human cochleae is similar to that in mice, the likelihood of *ATOH1* based gene therapies to regenerate hair cells will be limited. Furthermore, genomic sequences suggest differences between rodents and primates in key regulatory regions known to control GATA3 expression. To determine whether humans and non-human primates have similar or different patterns of GATA3 expression in the mature inner ear, we examined GATA3 distribution in adult cochleae from mice, rats, macaques, and humans using three different antibodies, each directed against highly conserved GATA3 peptide sequences or the whole protein. GATA3 immunostaining revealed nearly identical patterns of expression in the organs of Corti from all four species, where supporting cells medial and lateral to the cochlear hair cells exhibited robust nuclear labeling, but pillar and Deiters cells had little to no GATA3 immunoreactivity. In the spiral ganglia of mouse, rat, macaque, and human samples, GATA3 was expressed only in a subset of neurons, most of which were peripherin positive, consistent with previous reports in mice that suggest they are type II in nature. GATA3 immunoreactivity was not detected in the sensory epithelia nor in the ganglion cells of the vestibular system. Thus, GATA3 expression in the mature cochlea appears to be largely conserved across rodents and primates, including humans, and suggests that conserved regulatory elements such as the recently identified “otic specific enhancer” likely control expression in the inner ear, while non-conserved regulatory regions are likely more important in other tissues. The findings presented here also reinforce the notion that ATOH1 mediated hair cell regeneration in humans may be limited by a lack of GATA3 in certain supporting cells, and suggest that regenerative approaches may benefit from simultaneous targeting to upregulate GATA3.

PS 181

Long-term Histological Outcomes of Low Dose Carboplatin Administration in the Chinchilla Cochlea

Karen S. Pawlowski; Celia D. Escabi; Patricia R. Moody; Edward Lobarinas
University of Texas at Dallas

Accumulating evidence suggests that common clinical tests for assessing the condition of the auditory system, such as pure tone threshold testing, may fail to adequately detect some forms of inner ear pathology. Although, threshold testing is useful in detecting hearing deficits associated with outer hair cell (OHC) loss, emerging evidence suggests that new measures for detecting deficits associated with inner hair cell (IHC) loss and/or synapse-primary nerve (type I spiral ganglion or SG) fiber loss are needed.

In chinchillas, selective inner hair cell and spiral ganglion loss can be reliably induced by the platinum based anticancer drug, carboplatin. This species specific effect can be used to study the effects of sensory and neural cell degeneration in the inner ear and its correlates to auditory function. Here we evaluated the effects of carboplatin-induced long-term histological changes (2.5 to 6 months post carboplatin) following a relatively low dose of carboplatin (50 mg/kg, i.p.). Examination of pre and post carboplatin auditory brainstem response (ABR)

thresholds and osmium stained, whole mount organ of Corti tissue revealed small variation in threshold outcomes and 2 subpopulations in histological outcomes: One population clearly demonstrated more pathology than the other, while both subpopulations had significant IHC loss with no significant OHC loss. The SG loss varied from minimal to significant, trending similar to the IHC loss. Islands of myelinated SG fibers were often seen at the habenula perforata (HB), associated with remaining IHCs. We found no area of the HB completely void of fibers, although large areas of greatly reduced myelinated-fiber staining occurred. Results from further processing of this tissue to examine the IHC and SG will be presented in detail.

PS 182

Elucidating the Localization of Estrogen and Estrogen-related Receptors in the Inner Ear

Erika Lipford[1]; Benjamin Shuster[1]; Beatrice Milon[2]; Mark McMurray[1]; Jessica Mong[3]; Ronna Hertzano[4]
[1]Department of Otorhinolaryngology-Head and Neck Surgery, University of Maryland; [2]Department of Otorhinolaryngology-Head and Neck Surgery, University of Maryland; [3]University of Maryland School of Medicine; [4]Department of Otorhinolaryngology Head and Neck Surgery, University of Maryland School of Medicine; Institute for Genome Sciences, University of Maryland School of Medicine.

Hearing loss is the most common sensory impairment, affecting hundreds of millions of people worldwide. Although both men and women are impacted by hearing loss, the incidence rate differs considerably between the two sexes. Cross-sectional studies have reported the prevalence of bilateral high frequency hearing loss to be 2.7 times higher in males compared to females. While sex differences in hearing loss were once attributed to a disparity in occupational noise exposure and anatomical variation between males and females, recent studies have implicated estrogen as having a protective effect against high frequency noise-induced hearing loss in females. Estrogen receptors signal through canonical and non-canonical pathways, impacting the central and peripheral auditory physiology. While the localization of the estrogen receptors (ERs) within the auditory system is known, the roles of estrogen-related receptors (ERRs) in auditory function require further investigation. In mouse models, the conditional knockout of estrogen-related receptor β (Esrrβ) or estrogen-related receptor β (Esrrβ) leads to the development of hearing loss. The aim of this study is to elucidate the localization and expression of estrogen receptors β and β and estrogen-related receptors β, β, and β within the inner ear of adult B6CBAF1/J mice. Using RNAscope, a method of in situ hybridization, we are able to localize and quantify the expression of ER and ERR mRNA in the cochlea and vestibular system. Our results give insight into the molecular mechanism through which both estrogen receptors and estrogen-related receptors grant protection against hearing loss.

PS 183

Mitochondrial Calcium Uniporter in Cochlear Hair Cells is Dispensable for Hearing in Mice

Manikandan Mayakannan[1]; Carlos Antonio Padilla[1]; Aditi Deshmukh[1]; Sriya Donthi[1]; Ruben Stepanyan[2]
[1]Department of Otolaryngology–Head and Neck Surgery, University Hospitals Cleveland Medical Center, Case Western Reserve University; [2]Department of Otolaryngology, University Hospitals Cleveland Medical Center, and Department of Neurosciences, School of Medicine, Case Western Reserve University

Mitochondrial Ca^{2+} regulates a wide range of processes including morphogenesis, metabolism, excitotoxicity, and cell survival. In cochlear hair cells, mitochondrial uptake of the abundant [Ca^{2+}] inflowing through activated MET and voltage gated Ca^{2+} channels ensures cytosolic homeostasis and contributes to Ca^{2+} buffering. Rapid mitochondrial Ca^{2+} uptake occurs via a highly selective channel comprised of the pore forming subunit, the mitochondrial Ca^{2+} uniporter (MCU), and a few other regulatory proteins. Using MCU deficient ($MCU^{-/-}$) mouse model, we previously investigated Ca^{2+} homeostasis within the auditory hair cells, and cochlear function in general. In these mice, we observed an initial high frequency hearing loss at 4 weeks of age, which progressed to profound deafness by 12 weeks of age. At this time point, up to 20% of the outer hair cells (OHCs) in the mid-cochlear region of the $MCU^{-/-}$ mice were lost. Those stereociliary bundles of the OHCs still present, were showing signs of degeneration. Occasionally, the inner hair cells (IHCs) were also found to be lost. Based on these observations, we hypothesized that rapid mitochondrial Ca^{2+} uptake is necessary for hair cell preservation and hearing maintenance. Consequently, we extended our study to tissue-specific knockout mice, where the expression of $Mcu^{fl/fl}$ is disrupted in the sensory hair cells by *Atoh1-Cre* recombinase. Surprisingly, the $Mcu^{fl/fl}$, *Atoh1-Cre*$^{+}$ mice (experimental group) had hearing thresholds comparable to that of the $Mcu^{+/+}$, *Atoh1-Cre*$^{+}$ mice (control group) at 4 weeks, 12 weeks, and 24 weeks of age. Moreover, no significant difference in the wave I amplitudes was observed at all three time points between the experimental group and the control group. Exposure of these animals to broadband noise and assessment of noise-induced auditory threshold shifts at post-noise exposure day 15, revealed no significant difference between the experimental and the control group. These results suggest that MCU is dispensable in auditory hair cells with the possibility

of compensating alternative pathways handling Ca^{2+} overload. The degeneration of hair cells and hearing loss observed in whole body $MCU^{-/-}$ mice might be a consequence of the lack of MCU in other cochlear tissues and further research is needed to uncover the role of rapid mitochondrial Ca^{2+} uptake in hearing.

Supported by NIDCD grant DC015016 (R. S.) and by the Center for Clinical Research and Technology at University Hospitals Cleveland Medical Center (R. S.)

PS 184

Natural History and Disease Progression in Two Rodent Models of Monogenic Hearing Loss

Xichun Zhang; Xudong Wu; Shu-Lin Liu; Lars Becker; Arun Senapati; Nancy Paz; Bifeng Pan; Emma Alterman; Lillian Smith; Elizabeth Amaro Gonzalez; Yong Ren; Kathryn Ellis; Inmaculada Silos-Santiago; Fuxin Shi; Joseph C. Burns; Ning Pan; Adam T. Palermo; Jonathon Whitton; Martin Schwander
Decibel Therapeutics

Translation of gene therapies for monogenic hearing loss to the clinic requires demonstration of functional benefit in well-characterized model systems. Furthermore, preservation of cellular structures at ages that are amenable to treatment is essential. We have characterized the natural history of hearing loss and underlying cellular pathology in two mouse models of hearing loss due to mutations in the Otof and Strc genes.

In auditory inner hair cells, otoferlin (OTOF) functions as a calcium sensor for exocytosis during synaptic vesicle release, vesicle trafficking and replenishment. Defects in the OTOF gene lead to prelingual severe to profound hearing loss. Stereocilin (STRC) forms the horizontal top connectors and tectorial membrane (TM) attachment crown at the top of outer hair cell stereocilia. Mutations in the STRC gene are a major contributor to nonsyndromic autosomal recessive moderate-severe hearing loss.

We generated a mutant mouse line that mimics a pathogenic mutation in human OTOF. OTOF protein signal was absent in the homozygotes using an N-terminal OTOF antibody. In young adults, distortion product otoacoustic emissions (DPOAEs) were normal in the absence of auditory brainstem responses (ABR), recapitulating the phenotype of patients harboring OTOF mutations. Inner and outer hair cell counts were also normal in the mutant mice. Since patients with OTOF mutations lose outer hair cell function with age, we decided to track the DPOAE response over 9 months (40% of lifespan) and found significant DPOAE threshold shifts accompanied by morphological changes in outer hair cells starting at 8 months of age. Furthermore, the number of synaptic ribbons was reduced by 50%, and ribbons were enlarged in the mutant mice.

We also generated Strc knockout mice using CRISPR/Cas9 technology. In wild-type mice, STRC localized to the upper portion of stereocilia and the presumable stereocilia imprints on the bottom surface of the TM. STRC was undetectable in OHC stereocilia and TM of Strc knockout mice. DPOAE and ABR thresholds were elevated at three weeks. Scanning electron microscopy revealed hair bundles were slightly splayed but maintained their stereotypical “V” shape. Horizontal top connectors, the fiber net between stereocilia, and the stereocilia imprints on the TM were absent. Interestingly, hair bundles, an indication of alive hair cells, were still preserved throughout the cochlea at 4 months, suggesting that STRC mutations might be amenable to gene therapy at adult ages.

PS 185

Activating Muscarinic Acetylcholine Receptors Shapes Firing patterns By Simultaneously Closing KCNQ Channels and Activating HCN Channels in Vestibular Ganglion Neurons

Daniel Bronson; Christopher Ventura; Radha Kalluri
University of Southern California

Visual, somatosensory and vestibular systems encode different aspects of sensory information via parallel yet distinct pathways. In the vestibular system, these pathways are reflected in vestibular afferents such that irregular-spiking afferents respond to high frequency or transient head movements more rapidly than regular-spiking afferents. Spike-timing regularity of vestibular afferents is hypothesized to reflect the heterogeneity of intrinsic ion channel properties in vestibular ganglion neurons (VGNs). Several recent studies identified hyperpolarization-activated mixed cationic currents conducted by HCN channels (I_H) as a ‘pace-making’ current for driving highly-regular spiking in immature VGNs. However, we recently found that I_H becomes less ‘pace-making’ as maturing VGNs acquire potassium currents carried by KCNQ channels. Using a single-compartment model of the VGN, we demonstrated that the inhibitory influence of I_{KL} which is partially conducted by KCNQ, is enough to prevent highly-regular firing. Given that activation of muscarinic acetylcholine receptors (mAChR) closes KCNQ channels in vestibular ganglion neurons, we hypothesized that this would promote highly regular-spiking in VGNs.

To test this hypothesis, we recorded firing patterns and whole-cell currents using perforated patch-clamp

methods on isolated rat vestibular ganglion neurons ranging in age between post-natal day (P)9 and P18. We examined responses after applying the following solutions to the bath: 1) control, 2) linopiridine (10 μM), a KCNQ channel blocker, and 3) oxotremorine (10 μM), a mAChR agonist. Linopiridine and oxotremorine increased firing rates and reduced spike-train accommodation. We attribute these affects to the reduction of KCNQ-driven currents. Unexpectedly, I_H activation curves shifted to more positive potentials in oxotremorine, as indicated by depolarized $V_{1/2}$ (oxotremorine = -90.5 mV ± 2.76, n=8, control = -98.09 mV ± 1.29, n=27). Such a link between mAChR and HCN channels has not been previously reported in VGN. In contrast, linopiridine-alone had no effect on I_H ($V_{1/2}$ = -99.69 ± 2.45, n=10). Moreover, a cocktail containing both linopiridine and oxotremorine was less effective at shifting the activation range of I_H than oxotremorine alone ($V_{1/2}$ = -96.24 mV± 2.25, n=12). This suggests that the effect of mAChR on activating HCN channels occurs downstream from the G-protein cascade induced closure of KCNQ channels. These results raise the tantalizing possibility that efferent mediated activation of mAChRs both reduces the inhibitory influence of KCNQ channels and enhances the 'pace-making' capacity of HCN channels. Based on these results, we suggest that highly regular firing in vestibular afferents may involve the modulation of mAChR by the efferent system.

PS 186

Combined behavioral assays for more specifically evaluating auditory/vestibular and visual function of zebrafish larvae

Sun Peng; Zhuo Liu; Fangyi Chen
Southern University of Science and Technology

Zebrafish (Danio rerio) has been widely used to study the hearing and balance dysfunction. For the sensory neural system, functional evaluation of such a small animal has been a challenge. Although behavioral testing system has been developed to quantify the sensory functions, the accuracy and specificity of those systems were limited, which made them still a semi-quantitative tools.

Here we present two sets of behavioral assays: One for evaluating the vestibular and visual function using vestibular-ocular reflex (VOR) and optokinectic reflex (OKR); the other for auditory and visual function using acoustic and optic starlte responses. The combination of two different sensory stimulus can help exclude the interference of other, such as neuro-muscular, system to the behaviors. Specific designs, such as fish holder, were taken to facilitate performing two behavioral tests in one sample. Preliminary results demonstrated the efficacy of the combined system in identifying the sensory deficit more specifically.

PS 187

Large Animal Models for Auditory Research: a Guide to the Perplexed

Suchi Raghunathan[1]; Randolph Abutin[2]; Amanda McSweeney[2]; Misty J. Williams-Fritze[2]; Rami Tzafriri Tzafriri[3]; cyrille sage[1]
[1]CILcare; [2]CBset; [3]Cbset

Large Animal Models for Auditory Research: Guide to the Perplexed

Suchi Raghunathan[1], Randolph Abutin[2], Amanda McSweeney[2], Misty J. Williams-Fritze[2], Rami Tzafriri[3], Cyrille Sage[1].

[1]CILcare Inc., 500 Shire Way, Lexington, MA 02421

[2]CBSET, Inc., 500 Shire Way, Lexington, MA 02421

Auditory studies, including those evaluating ototoxicity and pharmacokinetics (PK), are typically performed using rodent models. Some studies, however, may require a larger species with middle and inner ear anatomy more similar to humans. Currently, there is a paucity of literature describing procedural auditory techniques, including surgical approaches, and sensitive readout for auditory changes in large animal species. Our goal was to determine if large animal species, such as swine and sheep, could be reliably used for auditory studies. Here, we report successful procedures in large animal species, such as trans-tympanic injection, a surgical approach to reach the middle ear space, recording of acoustic Auditory Brainstem Response (aABR), histology and cochleogram processes.

Using a Storz endoscope for evaluating external auditory canal (EAC) anatomy down to the tympanic membrane (TM), we found that sheep are better suited for trans-tympanic injection with an EAC/TM closer to human architecture compared to swine (EAC and TM at 90 angle) (Figure 1).

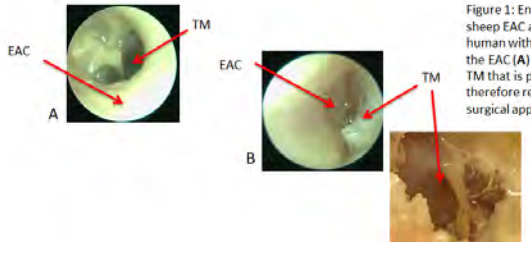

Figure 1: Endoscopy revealed that sheep EAC anatomy is closer to human with a TM perpendicular to the EAC (**A**) whereas Swine possess a TM that is parallel to the EAC (**B**) and therefore require a perpendicular surgical approach to access the TM.

Although both swine and sheep have anatomical features of the middle/inner ear similar to humans, we concluded that sheep can be used for chronic PK studies, whereas swine are only suited for non-survival PK studies. Moreover, the differences in outer ear anatomy are of direct relevance to medical device implantation (e.g. cochlear implant) and necessitated our development of

species-specific surgical procedures for accessing the middle ear space/round window membrane. Analysis of the deeper inner ear revealed that round window membrane thickness was species dependent with the sheep (~60 µm, published data) being closer to humans (60-70 µm) than swine (220 -350 µm).

We successfully recorded ABR from both swine (n=4) and sheep (n=3) under different anesthesia protocols (isofluorane by inhalation and/or propofol) using a homemade multi-channel ABR system with or without electrode brain implantation (i.e. subcutaneous sensor placement). For both species, the ABR was unaffected by the anesthesia protocol at all tested frequencies, and our system was found to be sufficiently sensitive for use with subcutaneous electrode alone.

Finally we have developed microdissection procedures that enable full cochleogram processing of both sheep and swine cochlea (Figure 2).

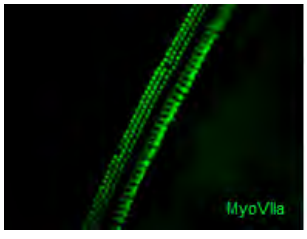

Figure 2: MyoVIIA immunostaining of a Swine base cochlea (Scale bar :40 µm)

In summary, we have developed the entire methodology needed for performing auditory studies in two new large species, sheep and swine, and characterized the specific advantages of each.

Middle Ear

PS 188

Elephant Middle Ear Anatomy and Bone Conduction Physiology

Caitlin O'Connell-Rodwell[1]; Anbuselvan Dharmarajan[2]; Rachel Chen[3]; Sunil Puria[4]
[1]Eaton-Peabody Lab., Mass. Eye & Ear; Department of Otolaryngology, Harvard Medical School; [2]Department of Otolaryngology Head and Neck Surgery, Harvard Medical School; Eaton-Peabody Laboratories, Massachusetts Eye and Ear; [3]Harvard University; [4]Department of Otolaryngology Head and Neck Surgery, Harvard Medical School; Eaton-Peabody Laboratories Massachusetts Eye and Ear

Background
Elephants rely on low frequency vocalizations for communication over long distances using either the normal air conduction (AC) pathway to the cochlea, or bone-conduction (BC) hearing, where sounds propagate through the ground and reach the cochlea through skull vibrations via the feet and body (O'Connell-Rodwell, 2007). Middle-ear bones scale with skull size, such that elephant ossicles (the largest among terrestrial mammals) are approximately seven times more massive than those of humans. Despite significant anatomical differences, humans and elephants exhibit very similar audiograms over their overlapping 20 Hz–11 kHz frequency range, although elephants can hear below 20 Hz and humans can hear above 11 kHz. Since little is known about the elephant's low frequency ear, our goal is to create computational models of the elephant middle ear physiology that can be manipulated and studied virtually.

Methods
We harvested postmortem temporal bones from both ears (ETB1,2) of an African elephant, and obtained microCT image stacks with 25.2 µm resolution (Xradia 520, Zeiss) and segmented the tympanic membrane, ossicles and their suspensory attachments, stapedius muscle, and cochlea (Simpleware, Synopsys). As a measure of input to the cochlea, 3D laser Doppler vibrometry (LDV) measurements were made of the umbo (ETB1,2) and stapes (ETB1) due to AC and BC stimulation.

Results
Compared to humans, the segmented anatomy of the elephant reveals unique anatomical differences, including a division of the middle ear cavity compartment into two by a thick membrane, with only the tip of the malleus to mid-manubrium visible. As expected, the stapedius muscle is present, while the lack of a clear tensor tympani muscle is puzzling. BC measurements below 100 Hz show that the relative stapes velocity of the elephant is greater than that of the human by up to 20 dB in the piston motion direction (y-axis) as a measure of input to the cochlea, and as much 40 dB in the x and z directions. These differences in anatomy and cochlear input at low frequencies raise questions as to what factors may contribute to enhanced BC sensitivity. The segmented anatomy will be used to develop a finite element model that will be tested and refined with 3D LDV measurements made with AC and BC stimulation. Ultimately, comparisons of elephant anatomy and physiology with humans may deepen our understanding of what factors facilitate BC hearing.

[Supported by grants K01 DC017812 and R01 DC05060 from NIDCD.]

PS 189

Skull surface motion in bone conduction stimulation depends on stimulation position and coupling

Tahmine Faramandi[1]; Ivo Dobrev[2]; Alexander Huber[2]; **Christof Röösli**[3]
[1]Department of ENT, Head and Neck Surgery, University Hospital Zurich, Switzerland; [2]Department of Otorhinolaryngology, Head and Neck Surgery, University Hospital Zurich, Zurich, Switzerland; University of Zurich, Zurich, Switzerland; [3]2.Department of Otorhinolaryngology, Head and Neck Surgery, University Hospital Zürich, Zürich, Switzerland.

Objectives: Investigation of skull bone surface wave propagation dependence on stimulation site and coupling method of the bone conduction hearing aid (BCHA). Methods: Experiments were conducted on five Thiel embalmed whole head cadaver specimens. The electromagnetic actuators from a commercial BCHA (Baha® Cordelle and Power) were used to provide stepped sine stimulus in the range of 0.1-10 kHz. Osseous pathways (direct bone stimulation or transcutaneous stimulation) were sequentially activated by mastoid stimulation via a percutaneously implanted screw, Baha® Attract transcutaneous magnet and a 5-Newton steel headband. Non-osseous pathways (only soft tissue or intra-cranial contents stimulation) were activated by stimulation on the eye, neck, and dura via a 5-Newton steel headband. The response of the skull was monitored as motions of the ipsi-, top and contra-lateral skull surface. Surface motion was quantified by sequentially measuring ~200 points on the skull surface (~ 15-20mm pitch) via a three-dimensional laser Doppler vibrometer (3D LDV) system. Results: Low frequency motion (< 1kHz) of the whole head depends on the stimulation position. Stimulation further away from the base, results in predominantly rigid-body-like motion. The stimulation area at the parietal plate undergoes deformations at lower frequencies than the whole head. The predominant motion response along the stimulation direction is only 5-10dB higher than other directions below 1 kHz, while all components contribute equality to the head motion at higher frequencies, regardless of stimulation condition. Sound propagation direction does not coincide with stimulation location at the mastoid. Potentially, because the head base remains rigid-like up to 3-5kHz and acts a large source. Conclusion: Individual sections of the skull have different sound transmission properties, which greatly affects the local, around the stimulation location, and global response of the skull depending on different stimulation locations and coupling conditions.

PS 190

A Lumped-Element Model of the Human Middle Ear for Bone Conduction

Xiying Guan[1]; Sunil Puria[2]; John Rosowski[3]; Hideko H. Nakajima[4]
[1]Eaton-Peabody Lab, Massachusetts Eye and Ear, Harvard Medical School; [2]Department of Otolaryngology Head and Neck Surgery, Harvard Medical School; Eaton-Peabody Laboratories Massachusetts Eye and Ear; [3]Eaton-Peabody Laboratory, Massachusetts Eye and Ear Infirmary,Department of Otolaryngology – Head and Neck Surgery, Harvard Medical School; [4]Dept. of Otolaryngology, Harvard Medical School & Massachusetts Eye and Ear

The middle ear plays an important role in bone-conduction (BC) hearing. When the skull is set in motion, the ossicles, which are loosely coupled to the skull, can vibrate relative to the skull due to their moment of inertia. The relative motion between the stapes footplate and the bony perimeter of the oval window contributes to hearing in a fashion similar to air conduction. It has been experimentally shown that the degree of this relative motion heavily depends on the mass and stiffness of the ossicular chain (Stenfelt et al. 2002; Huizing 1960; Tonndoff 1966). While the effects of middle-ear modifications - such as additional mass at the umbo – on BC hearing have been reported, the dynamics of the middle-ear system in BC is still not fully understood. This is partially because an analytical representation and solution of middle-ear vibrations for BC stimulation is lacking.

In the present study, we developed a BC human middle-ear model comprised of lumped mechanical components – masses, springs and dampers – to represent various middle-ear structures. The structure and parameters of those components were based on existing air-conduction human ear models in the literature (e.g., O'Connor et al. 2008; Rosowski et al. 1995). BC-elicited relative velocity of the stapes was simulated in the baseline normal condition and after performing manipulations such as adding mass at the umbo, stiffening the incudostapedial (IS) joint, separating the IS joint and stiffening the stapedial annular ligament. The model-predicted results were compared with experimental data measured with similar manipulations in human cadaveric temporal bones.

This model will help elucidate how middle-ear inertia and stiffness contribute to BC hearing. This work is supported by the NIH/NIDCD R01DC013303 and R21DC017251.

PS 191

Middle-ear Muscle Contraction Measurements Reveal No Anticipatory Activation Prior to Live Rifle Fire

Heath G. Jones[1]; Ellis R. Akins[2]; Lana S. Milam[2]; Stephen M. Tasko[3]; Madeline V. Smith[4]; William J. Murphy[5]; Gregory A. Flamme[4]; Kristy K. Deiters[4]; William A. Ahroon[1]
[1]U.S. Army Aeromedical Research Laboratory; [2]Goldbelt Frontiers, LLC; [3]Western Michigan University; [4]Stephenson and Stephenson Research Consulting; [5]The National Institute for Occupational Safety and Health

Repetitive exposure to high-level acoustic impulses, such as those from small arms fire and blast overpressure, increases the susceptibility for hearing loss. Currently, the United States Department of Defense acquisition standard (MIL-STD-1474E) mandates the U.S. Army use the Auditory Hazard Assessment Algorithm for Humans (AHAAH) for calculating impulse noise exposure limits of military systems. However, several concerns involving the appropriateness of including this model as a medical standard in an updated Damage Risk Criteria (DRC) have been raised, and thus there is still no such medical standard available in the Department of Defense. The current study addressed a concern raised about the middle-ear muscle contraction (MEMC) associated with the acoustic reflex that is assumed, and implemented, as a protective mechanism for certain instances in which a person is "warned" prior to the impulse. Accordingly, some Damage-Risk Criteria (DRC) for impulsive noise include MEMCs as a protective factor, either as acoustic reflexes or as an early MEMC engaged in anticipation of a known imminent exposure. DRC inclusion assumes that MEMCs are pervasive (> 95 % confidence of > 95% prevalence) within the population, and are of sufficient strength and duration to serve as a protective mechanism. For the purpose of a health hazard assessment, an inappropriate implementation of this assumption would result in an underestimation of auditory hazard and may incorrectly predict that some high-level exposures are safe. This assumption was addressed by attempting to condition an anticipatory MEMC in both laboratory and field environments. Five different training tasks were administered under laboratory-controlled conditions using both acoustic and non-acoustic elicitors. Results found the likelihood of observing an MEMC for short-duration acoustic stimuli was much lower than for non-acoustic stimuli, and that voluntary eye closure produced the greatest likelihood of an MEMC. Conditioned MEMC responses were far below the 0.95 criterion necessary to consider the responses pervasive. Interestingly, participant attention greatly influenced the likelihood of observing an early, conditioned MEMC. Field measurements were made in Soldiers firing military rifles for situations where they were instructed to fire and when they had no knowledge of when a second person was firing. Results indicate that MEMC do not reliably contract either in anticipation of, or in response to, an impulsive noise. Collectively, these studies indicate MEMCs should not be included as a protective factor in DRC for impulsive noise not should it be used as an acquisition standard without substantial revision.

PS 192

Tympanic Membrane Mechanics after Repeated Exposure to Loud Sound

Haimi Tang[1]; Pavel Psota[2]; John Rosowski[3]; Cosme Furlong[1]; Jeffrey Cheng[3]
[1]Center for Holographic Studies and Laser micro-mechaTronics, Worcester Polytechnic Institute; [2]Faculty of Mechatronics, Informatics and Interdisciplinary Studies, Technical University of Liberec; [3]Eaton-Peabody Laboratory, Massachusetts Eye and Ear Infirmary,Department of Otolaryngology – Head and Neck Surgery, Harvard Medical School

Intense impulsive sounds like those from blast or firearms can damage ear structures and produce both conductive and sensorineural hearing loss. Some studies have suggested that Tympanic Membrane (TM) perforation can be used as a biomarker to assess damage to the ear from blasts. However, TM mechanics after blast exposure has not been well studied. In some cases, the TM remains visually intact despite the presence of hearing loss. Although the blast-induced hearing impairment generally includes hair cell or nerve level damage, damage to the middle-ear conductive mechanism can also play a role. Several recent studies showed significant changes in the mechanical properties of the TM after exposure to blast waves, and such changes may significantly affect sound energy absorption by the TM – the first step in the hearing process. In this study, we systematically characterize TM full-field transient responses to moderate level impulsive sounds before, during and after exposing the cadaveric ear sample to a series of blasts of equivalent sound pressure greater than 150 dB SPL. Experimental modal analysis is applied to the stimulus normalized displacement at over 200,000 points that cover the entire TM surface. We compare TM mechanical indicators, such as TM shape, modal motion mode, natural frequency, and damping, before and after blast exposure to gain insight into the conductive mechanisms of hearing damage by loud sound.

PS 193

Finite-Element Modelling Based on Optical Coherence Tomography and Corresponding X-ray MicroCT Data for Two Human Middle Ears

Marzieh Golabbakhsh[1]; Xuan Wang[1]; Dan MacDougall[2]; Josh Farrell[2]; Thomas Landry[2]; robert funnell[3]; Robert Adamson[4]
[1]Department of BioMedical Engineering,McGill University, Montréal, QC, Canada; [2]School of Biomedical Engineering, Dalhousie University, Halifax, NS, Canada; [3]Department of BioMedical Engineering, Department of Otolaryngology – Head & Neck Surgery, McGill University, Montréal, QC, Canada; [4]School of Biomedical Engineering, Electrical and Computer Engineering Department, Dalhousie University, Halifax, NS, Canada

Optical coherence tomography (OCT) is an emerging imaging modality which is non-invasive and can be employed *in vivo*. There is interest in the clinical application of OCT for imaging of the middle ear because it can record both static anatomy and vibrations. We recorded vibrations at three different frequencies (500 Hz, 1 kHz and 2 kHz) for two human cadaver middle ears using OCT. X-ray microCT images were obtained from the same specimens. Two finite-element models were built based on geometries obtained from the microCT images.

The finite-element model creation was done using locally developed software (http://audilab.bme.mcgill.ca/sw/): Fie for image segmentation and for specifying material properties, boundary conditions and loads, and Tr3 for surface generation, along with Gmsh (http://gmsh.info/) for volume mesh generation. Finite-element simulations were implemented using linear transient time analysis, harmonic analysis and modal analysis. Different models of damping were tested.

The material properties and boundary conditions of the models were obtained from previously reported studies. Code_Aster was used for the finite-element simulations. The simulated vibration patterns of the middle ear in each model were compared with the corresponding experimental OCT vibration data quantitatively and qualitatively. In addition, the two finite-element models were compared with each other in terms of both geometry and function.

For both ears, OCT measurements and simulation results both showed the maximal displacement appearing in the posterior region of the tympanic membrane. There were smaller displacements on the malleus, incus and stapes. At higher frequencies, the displacement pattern of the tympanic membrane showed more complex behaviour.

Comparing the two finite-element models will help us to better understand the connection between geometry and function in the middle ear. This work will ultimately lead to patient-specific models based on *in vivo* OCT measurements and should help to improve diagnosis of abnormalities in the middle ear.

PS 194

Forward and Reverse Middle Ear Transmission in Gerbil with a Spontaneously Healed Tympanic Membrane

Xiaohui Lin[1]; Sebastiaan Meenderink[1]; Eric Duong[1]; Timothy Jung[2]; **Wei Dong**[2]
[1]VA Loma Linda Healthcare System; [2]VA Loma Linda Healthcare System & Dept. of Otolaryngology, Loma Linda University Health

The tympanic membrane's (TM) unique morphology and its physical properties determine the normal frequency-dependent pattern of vibration that is imparted to the attached malleus. TMs that healed spontaneously after perforation present abnormalities in their structural and mechanical properties, i.e., they are thickened and abnormally dense. These changes result in a deterioration of middle ear (ME) sound transmission, which is clinically presented as a conductive hearing loss (CHL). To fully understand the ME sound transmission under TM pathological conditions, a detailed description of the ME transmission is required.

To achieve this goal, we created a gerbil model with a controlled 50% pars tensa perforation, which was left to heal spontaneously for up to 4 weeks (TM perforations had fully sealed after two weeks). Over this 4-week period, the functional recovery in the MEs was monitored with auditory brainstem responses (ABRs), distortion product otoacoustic emissions (DPOAEs) and evoked potentials (EPs). After the recovery period, the ME sound transmission, both in the forward and reverse direction, was directly measured in gerbil ears with either normal or spontaneously healed TMs. Measurements were performed at the input and output of the ME system, i.e., at the TM, umbo and scala vestibuli next to the stapes, using a combination of techniques, i.e., DPOAEs, laser Doppler vibrometer, and an intracochlear micro-pressure-sensor. We found that MEs with spontaneously healed TM fully recovered for low-frequency sound transmission, while a significant loss for high-frequency sounds remained. These high-frequency losses, which we found in both forward and reverse transmission, were primarily from the "coupling" between the TM and umbo; variations along the ossicular chain were relatively

small. Also, patterns in the ABRs, DPOAEs, and EPs were similar over the 4-week time course of recovery, and their changes (re. normal) could be explained by the direct ME transmission measurements.

Our results provide detailed functional observations that explain CHL seen in clinical patients with abnormal TMs, e.g., caused by otitis media, spontaneously healed after perforation or post tympanoplasty. Besides, our results demonstrate that DPOAEs and EPs are useful to monitor ME function for certain ME pathologies.

This study was supported by VA Merit Award C2296-R (Dong) and the Department of Otolaryngology Head & Neck Surgery, at Loma Linda University Health.

PS 195

Functional Role of Ligaments in the Gerbil Middle Ear

Eileen Brister[1]; Claus-Peter Richter[2]; Mackenzie Mills[3]; Stephen Hoff[4]; Yi Shen[1]; Robert Withnell[3]
[1]Indiana University Bloomington; [2]Northwestern University, Dept Otolaryngology; [3]Indiana University; [4]Northwestern University

Ligaments of the middle ear have been described as playing a suspensory role. However, experimental studies in which ligaments are severed have not shown substantial changes in middle ear sound transmission. Resolving ambiguity regarding the contribution of ligaments to the function of the middle ear is important because advances in 3D printing technology open the possibility of new prosthetic options for middle ear reconstruction, and understanding the role of ligaments in the normal ear informs incorporation of ligament structures into new prostheses. In previous experiments, other groups have examined the anterior ligament of the malleus or the posterior ligament of the incus, but the two attachments have not been investigated in combination. In order to investigate the functional role of ligaments in the middle ear, the posterior incudal ligament and the tip of the anterior mallear process were severed in gerbil middle ears using a surgical CO_2 laser. It was hypothesized that the ligaments play a suspensory role, counteracting the force of gravity on the ossicles. Removing the ligaments was predicted to increase the effective mass reactance in the middle ear by removing the suspensory components, thus reducing high frequency sound transmission. Hearing status was measured before and after severing the attachments using compound action potential (CAP) thresholds from air-conduction and bone-conduction stimuli. Bone and air conduction thresholds were compared to make inferences about middle ear status. Results show substantial conductive hearing loss in mid- and high-frequencies after severing both the anterior mallear process and the posterior incudal ligament, but not after severing solely the anterior mallear process. Middle ear transmission change was accompanied by a positional change, with the ossicles visibly falling after both attachments are severed. This is consistent with the hypothesis that the suspensory attachments counteract the force of gravity, reducing the effective mass, and removing those suspensory attachments increases effective mass, reducing high frequency transmission.

Acknowledgements
This research used resources of the Advanced Photon Source, a U.S. Department of Energy (DOE) Office of Science User Facility operated for the DOE Office of Science by Argonne National Laboratory under Contract No. DE-AC02-06CH11357.

PS 196

Causally-Constrained Measurements of Aural Acoustic Reflectance and Reflection Functions

Douglas H. Keefe
Boys Town National Research Hospital

Causally-constrained procedures are described to measure the acoustic pressure reflectance and reflection function (RF) in the ear canal or unknown waveguide. Reflectance is the Fourier transform of RF. Reflectance calibration is reformulated to generate causal outputs, with results described for a calibration based on a reflectance waveguide equation to calculate incident pressure and source reflectance in the frequency domain or source RF in the time domain. Results are described in which incident pressure is either known from long-tube measurements or calculated as a calibration output. Calibrations based on constrained nonlinear optimizations are simpler and more accurate when incident pressure is known. Calibration outputs are more accurate when model viscothermal wall losses in tubes are slightly larger than theory predicts. Outputs measured by causally-constrained procedures differ at higher frequencies from those using standard procedures. Evanescent-mode effects formulated in the time domain and incorporated into frequency-domain calibrations are negligible for long-tube calibrations. Causal reflectance and RFs are evaluated in an adult ear canal and time- and frequency-domain results are contrasted using forward and inverse Fourier transforms. Results are promising for future applications to diagnose conductive impairments of hearing and calibrate sound stimuli in the ear canal at high frequencies.

PS 197

Controlled Comparison of Methods for Measuring Ear-Canal Reflectance

Kren Monrad Nørgaard[1]; Karolina K. Charaziak[2]; Christopher A. Shera[2]
[1]Technical University of Denmark; [2]University of Southern California

Applications of ear-canal reflectance are abundant in recent literature. Evidence supports the use of reflectance for diagnosing conductive hearing disorders and compensating for ear-canal acoustics when performing noninvasive measurements of the auditory system. However, other than the deleterious effects of leaks in ear-probe fit, little attention has been paid to assessing sources of measurement error and variability.

Variability in a representative catalog of published methods for measuring ear-canal reflectance using an insert ear probe arises chiefly from three factors: the length of the residual ear-canal space, the insertion angle of the probe, and the frequency bandwidth of the measurement. In addition to a preliminary calibration, reflectance measurements using an insert probe require an estimate of the ear canal's characteristic impedance. In this poster, we employ a uniform occluded-ear simulator as an idealized controlled setup to assess the variability of ear-canal reflectance and estimated characteristic impedance due to the three principal factors.

In addition, by measuring the sound pressure at a reference condenser microphone mounted at the termination of the occluded-ear simulator, we extend the analysis to encompass the influence of measurement variability on reflectance-based methods for calibrating ear-canal stimulus levels. Finally, we use the reference condenser microphone operating in reverse as an electrostatic speaker to assess the influence of measurement variability on estimates of the pressure emitted by the ear (i.e., otoacoustic emissions).

The various methods in the catalog differ widely in their robustness to variations in the three principal factors influencing the accuracy and variability of ear-canal reflectance. Our results provide guidelines for assessing potential measurement errors in published data and for choosing an appropriate method for measuring ear-canal reflectance.

PS 198

Quantification of Ear-Canal Cross-Sectional Area to Improve Absorbance Measurements

Katherine Fairbank[1]; Nicholas J. Horton[2]; Susan E. Voss[1]
[1]Smith College; [2]Amherst College

Background
Wideband acoustic immittance (WAI) measures offer a noninvasive objective diagnostic tool with potential to detect and identify middle-ear abnormalities. WAI measures of absorbance and reflectance require the canal's cross-sectional area at the measurement location; most published WAI data assume a constant area that is substantially smaller than presented in this work and that does not account for considerable individual variation.

Methods
Silicone molds were obtained from the ear canals of n=134 adults with normal middle-ear function. Age was roughly uniformly distributed from 18 to 75 years with similar numbers of males and females. The molds were digitized and areas measured with ShapeDesigner software (3ShapeAudio). To match the foam-tip length of Mimosa Acoustic's commercial HearID system, the first area measurement was made at a 12mm insertion depth, defined by two universal markers at the canal entrance: (1) the intertragal notch and (2) the indentation from the tragus. Additional area measurements were made in 0.6mm increments that ranged from insertion depths of 4.8mm to 13.2mm from the canal entrance. At each location, the ear-canal area was measured as the area of a cross-sectional slice normal to the canal axis.

Results
Across all ages, the mean ear-canal area was 61.6mm2 (12.9mm2 standard deviation, range 37.8 to 99.2mm2). A paired t-test showed left and right ears had similar areas (p=0.62). Subjects were grouped into six age cohorts (decade of life), with an increase in area associated with increasing age cohort (df=5, p=0.009). Minimal differences existed between male and female areas after controlling for age cohort (p=0.82). There was little evidence for an association between height and ear-canal area (p=0.48) or between weight and ear-canal area (p=0.19). Across all age cohorts, ear-canal area decreased with insertion depth from 4.8 to 13.2mm from the canal entrance.

Conclusions
The adult ear-canal areas assumed by the Mimosa Acoustics HearID system (44mm2) and the Interacoustics Titan system (50mm2): (1) are substantially smaller than

the measured mean adult area of 61.6±12.9mm2, (2) do not account for the considerable age cohort differences in area that we observed, and (3) do not capture the wide individual variability across adult ears. Absorbance and reflectance measurements would be more accurate with improved estimates of ear-canal areas.

Supported by NIH/NIDCD R15 DC014129.

PS 199

High-speed Holographic Shape and Vibration Measurement of Semi-transparent Tympanic Membrane

Haimi Tang[1]; Pavel Psota[2]; John Rosowski[3]; Cosme Furlong[1]; Jeffrey Cheng[3]
[1]Center for Holographic Studies and Laser micro-mechaTronics, Worcester Polytechnic Institute; [2]Faculty of Mechatronics, Informatics and Interdisciplinary Studies, Technical University of Liberec; [3]Eaton-Peabody Laboratory, Massachusetts Eye and Ear Infirmary,Department of Otolaryngology – Head and Neck Surgery, Harvard Medical School

Holographic interferometric methods have been used to quantify the shape and the acoustically induced vibration of the tympanic membrane (TM) to understand middle-ear mechanics. Previously, we integrated a high-speed holographic system using a 532nm wavelength laser for displacement measurement and a 770 to 789nm tunable wavelength laser for shape measurement. However, because of the semi-transparency of the TM and high recording frame rate, the tympanic membrane surface needed to be painted with a thin layer of white paint to increase reflection and allow quantifiable interference patterns. The need for painting is not practical in in-vivo patient studies. In this paper, we describe our efforts to measure the shape and motion of unpainted TMs. We adapted a multi-angle illumination shape measurement method into the existing holographic system to eliminate the need for the tunable laser source. It allows us to use the single wavelength (532nm) laser with a higher illumination intensity to perform both shape and displacement measurements on unpainted TMs. A new temporal phase unwrapping algorithm is also applied to unwrap high fringe density holograms, which challenge the spatial phase unwrapping algorithm used in our previous studies. We show results from three fresh postmortem human tympanic membranes without any paint. Our results suggest that the optical phase quality of the hologram is better when the outer skin layer of the TM remains intact, which favors its application on live ears.

PS 200

Estimating Young's Modulus of Thin Elastic Structures Using Holographic Measurements of Harmonic Vibration with an Application to Tympanic Membrane Characterization

Arash Ebrahimian[1]; Haimi Tang[2]; Jeffrey Cheng[3]; Nima Maftoon[1]
[1]University of Waterloo; [2]Center for Holographic Studies and Laser micro-mechaTronics, Worcester Polytechnic Institute; [3]Eaton-Peabody Laboratory, Massachusetts Eye and Ear Infirmary,Department of Otolaryngology – Head and Neck Surgery, Harvard Medical School

Holographic vibration measurements have been used in recent years to study vibration responses of the tympanic membrane with a high spatial resolution. We propose a method to estimate the Young's modulus of thin 2-D structures using holographic measured harmonic vibration data. As the first step in the development, we used the plate equation to express the harmonic motion of the vibrating structure and discretized it using the finite-difference method. We formulated the inverse problem for finding the Young's modulus, as an optimization process finding the minimum Euclidean distance between the measured and calculated vibration data using Bayesian optimization. To validate the proposed method, we obtained harmonic vibration patterns of structures of various geometries and boundary conditions using analytical and finite-element analyses and then used the proposed method to retrieve the known Young's moduli. The calculated error between the known and estimated Young's moduli was less than 2% for all noise-free test cases. We then applied Gaussian and non-Gaussian noise of various intensities to the vibration patterns to investigate the robustness of our proposed material characterization method to noise. The estimated Young's moduli had less than 4% error for all noisy cases. We also investigated the error caused by the uncertainty in the thickness and Poisson's ratio assumptions on the estimated Young's modulus. Practical consideration such as the effect of mesh size on the runtime was discussed as well. The proposed material characterization method was applied to harmonic vibration patterns of the tympanic membrane obtained using holography to estimate its Young's modulus and some preliminary results were obtained. The method showed promise to be integrated in holographic measurements of the tympanic membrane motion to better understand TM mechanics and to provide a new index for diagnosis.

PS 201

Optimizing Umbo Microphone for Fully Implantable Assistive Hearing Devices via Analytical and Numerical Modeling, and Electrical Shielding

Benjamin G. Cary[1]; Nicolas Verhaert[2]; Tasher Losenegger[3]; Elizabeth S. Olson[4]; Jeffrey H. Lang[1]; Hideko H. Nakajima[5]
[1]EECS, Massachusetts Institute of Technology; [2]Massachusetts Eye and Ear; KU Leuven, Dept. of Neurosciences, Research Group ExpORL, Leuven, Belgium; [3]Columbia University; [4]Columbia University, Department of Biomedial Engineering and Department of Otolaryngology; [5]Dept. of Otolaryngology, Harvard Medical School & Massachusetts Eye and Ear

Background
Current cochlear implants (CIs) are bulky, can only be worn during the day, and do not function well in noisy environments. Totally implantable CIs with implantable microphones would allow for directional and focused hearing by taking advantage of ear mechanics, and be usable in almost all environmental conditions all day and night. Current implantable microphones suffer from unstable mechanics, poor signal-to-noise ratio, and low bandwidth. We have built prototypes of piezoelectric sensors mounted between the cochlear promontory and umbo that show promise in surmounting these problems. This work builds upon these prototypes to prepare for clinical trials and encompasses maximizing high-bandwidth sensitivity, surgical viability and electrical shielding.

Methods
Our approach combines analytical models for design guidance, numerical models for design verification, and bench-test experiments for validation. Analytical modeling is driven by differential equations of plate mechanics and piezoelectricity. Numerical modeling is enabled by the COMSOL multiphysics software where we have created simulations of the piezoelectric sensor and utilize middle ear mechanical models. Our experimental tests involve imaging with holographic interferometry and optical coherence tomography (OCT), Thorlabs LSM03. The umbo sensor will 'pick-up' unwanted signal from the CI electrodes. To address this problem, experiments on shielding have been performed using a CI electrode and polyvinylidene fluoride (PVDF) sensor samples.

Results
We have derived a working analytical model which has been proven by finite-element modeling. This serves as a guide for improving the design of the umbo microphone. Optimal surgical placement of the sensor has been explored through numerical modeling and temporal bone experiments. Finally, electrical shielding with a 200 nm layer of gold reduced electrical interference from the electrode by a factor of ~70.

Conclusions
Progress has been made to advance the PVDF umbo prototype into a practical implantable microphone. We have reduced electrical interference, created a platform for system optimization, and started the iterative design process. Active shielding will be considered in future experiments. In the near future we will begin sensing circuit design which will modify the system's overall sensitivity. We will verify numerical model parameters, directly measure umbo force, develop surgical implantation methods, and generate device manufacturing processes.

Support is from NIH/NIDCD R01 DC016874; Research Foundation Flanders and University Hospitals Leuven KOOR Funding, Belgium.

PS 202

Mechanics of Total Drum Replacement Tympanoplasty Measured with Wideband Acoustic Immittance

Kristine Elisabeth Eberhard[1]; Salwa F. Masud[2]; Hamza Khalid[3]; Aaron K. Remenschneider[4]; Hideko H. Nakajima[5]
[1]Dept. of Otolaryngology, Harvard Medical School & Massachusetts Eye and Ear; Dept. of Otorhinolaryngology, Head and Neck Surgery, Copenhagen University Hospital Rigshospitalet; [2]Eaton-Peabody Laboratories, Massachusetts Eye and Ear; Graduate Program in Speech and Hearing Bioscience and Technology, Harvard Medical School; [3]Massachusetts Eye and Ear; [4]Dept. of Otolaryngology, UMass Memorial Medical Center; Massachusetts Eye and Ear; [5]Dept. of Otolaryngology, Harvard Medical School & Massachusetts Eye and Ear

Background
Total eardrum replacement is commonly performed using temporalis fascia for subtotal or total tympanic membrane (TM) perforations. Here we determined the mechanics of the reconstructed TM and compared it to normal, native TMs using wideband acoustic immittance (WAI).

Methods
Ears having undergone type 1 tympanoplasty using total eardrum replacement technique with temporalis fascia were identified. Inclusion criteria for the tympanoplasty group included healed drum graft without perforation and no evidence of ossicular pathology at the time of surgery.

Exclusion criteria included: other graft materials, previous middle ear surgery, cholesteatoma, and other mechanical middle and inner ear pathologies. WAI was measured in ears that had tympanoplasties and compared to a cohort of normal hearing ears with normal, native TMs. Pre- and postoperative audiograms were also analyzed to assess the effect of tympanoplasties on hearing.

Results

Eight ears from eight different patients were included in the tympanoplasty group. Four were male, four were female and age at surgery ranged from 28-62 years, median 47 years. Time from surgery to WAI measurements ranged from 2-122 months, median 53 months. The native TM group included 56 ears from 29 different patients, 13 males and 16 females with age ranging from 22-64 years, median 33 years. Generally, WAI measurements in the tympanoplasty group had lower absorbance from 1-4 kHz compared to ears in the native TM group. At low frequencies (< 1 kHz), WAI absorbance was similar between ears of the tympanoplasty and native TM groups. Audiometric measurements showed that tympanoplasty type 1 surgery generally improved (decreased) air-bone gap at 250 Hz whereas the improvement was generally smaller at the mid and high frequencies.

Conclusion

Our data show that the mechanics of the TM with total eardrum replacement using fascia differed from the normal native TM. In general, at low frequencies (< 1 kHz) the absorbance in ears with fascia graft is comparable to absorbance in ears with native TM. However, at high frequencies the fascia graft is mechanically different indicated by a decrease in absorbance from 1-4 kHz. Audiometric data show that the air-bone gap generally closes at low frequencies with surgery.

PS 203

Holographic Measurement of Semi-transparent Tympanic Membrane Shape by a Multiple Angle Illumination Technique

Haimi Tang[1]; Pavel Psota[2]; John Rosowski[3]; Cosme Furlong[1]; Jeffrey Cheng[3]
[1]Center for Holographic Studies and Laser micro-mechaTronics, Worcester Polytechnic Institute; [2]Faculty of Mechatronics, Informatics and Interdisciplinary Studies, Technical University of Liberec; [3]Eaton-Peabody Laboratory, Massachusetts Eye and Ear Infirmary,Department of Otolaryngology – Head and Neck Surgery, Harvard Medical School

The shape of the tympanic membrane (TM) plays an important role in sound transmission through the ear for hearing, where knowledge of the shape and the sound induced displacements of the TM are essential to understanding the mechanics of the TM. Measurements of the shape of the TM also have a diagnostic value, e.g. bulging of the TM is a sign of middle ear effusion, and an increased inward displacement is a sign of negative middle-ear pressure. Previously we developed a high-speed holographic system employing a tunable wavelength laser for rapid TM shape measurement. However, because of the semi-transparency of the TM and the short-exposure time of our camera, the illumination intensity (0.01 mW/mm^2) was insufficient for accurate measurements of the shape of the unpainted TM. Here, we describe a new multi-angle illumination technique that allows us to use a single wavelength (532nm) higher illumination intensity (0.06 mW/mm^2) laser to measure the shape of unpainted TMs. The accuracy of the new method is demonstrated by measurements of a step-wise gauge provided by the National Institute of Standards and Technology. We successfully applied the new shape measurement method to fresh postmortem human TMs without any paint. We see a potential for miniaturization of the apparatus into a holographic otoscope enabling in-vivo measurements. Key features and limits of the holographic otoscope development are discussed.

PS 204

Characterization of Quasi-Static 3-DOF-Stiffness and 3D-Morphometry of the Human Stapedial Annular Ligament

Merlin Schär[1]; Raoul Hopf[2]; Ivo Dobrev[1]; Alexander Huber[1]; Jae Hoon Sim[1]
[1]Department of Otorhinolaryngology, Head and Neck Surgery, University Hospital Zurich, Zurich, Switzerland; University of Zurich, Zurich, Switzerland; [2]Department of Mechanical and Process Engineering, Institute for Mechanical Systems, ETH Zurich, Zurich, Switzerland

The three-layered annular ligament (AL) suspends the stapes footplate in the oval window. Previous investigations indicated that the human AL features an irregular anatomy along the footplate boundary, with varying sublayer dimensions, fiber composition, and inclination relative to the footplate plane. The irregular spatial structure and resulting inhomogeneous mechanical properties of the AL influence the three-dimensional stapedial motion. This study aims to provide both the 3D-morphometry and quasi-static stiffness of the AL at micro-Newton force levels from the same sample, which are not currently available. The resulting data are key for numerical model simulations of the three-dimensional stapedial motion under physiological conditions and after reconstructive surgeries.

The oval window region with the stapes and AL was isolated from fresh-frozen human cadaveric temporal bones. For quasi-static stiffness measurements, the samples were mounted on a motorized robot arm to allow rotation around the indentation point on the stapes head. The quasi-static stiffness was measured via a commercial micromechanical testing system with a MEMS-based force sensor on three linear translation micro-stages (FemtoTools). The indentation was performed in piston mode (perpendicular to the footplate plane), and in four bending modes (positive and negative rotation about the short and long axes of the footplate). The measurements were done both before and after severing the stapedial tendon. The precise alignment of the indentation axes relative to the anatomical axes of the stapes was determined by registration of fiducial markers to a micro-CT scan of the sample. Assuming three degrees of freedom for stapedial motion, a 3x3 stiffness matrix in the anatomical reference frame of the stapes was calculated. For multiphoton microscopy, a decalcification and tissue clearing protocol was applied to the same sample to enable imaging of the complete AL from the cochlear side of the stapes. The 3D-morphometry of the AL from multiphoton imaging could be obtained from intact, unstained samples based on the autofluorescence of elastin and second harmonic generation of collagen, which are main components of the AL. The quasi-static stiffness measurements indicated a linear stiffness behavior in the tested force range for all indentation directions, with highest stiffness values for the piston mode. Severing the stapedial tendon did not influence the stiffness for indentation in the piston direction but resulted in considerably decreased stiffness values for all bending modes. The asymmetric stiffness distribution along the footplate boundary was in good agreement with the mechanical behavior expected from morphometrical data.

PS 205

Dual-Laser Measurement of Stapes Footplate Movement in Human Ears with and without Hearing Protection Device (HPD) under Blast Exposure

Rong Z. Gan; Shangyuan Jiang; Kyle Smith; Chenkai Dai
University of Oklahoma

Introduction

A series of biomechanical measurements have been conducted in our lab to investigate the blast overpressure (BOP) induced middle ear tissue damage in human cadaver ears and hearing loss in an animal model (chinchilla). However, exactly how acute exposure to blast damages the middle ear in the conductive path of blast wave into the cochlea is still unknown. Recently, a novel experimental setup was established with two laser Doppler vibrometers (LDVs) in our lab to detect the movement of the tympanic membrane (TM) under blast [1]. This innovative methodology provides the possibility to measure the movement of stapes footplate, the end part of the ossicular chain connecting to the cochlear fluid during blast exposure. This paper reports our preliminary study on the movement of the human stapes footplate under blast using dual LDVs.

Methods

Nine fresh human temporal bones (TBs) were used in this study. The facial recess surgery was performed to expose the stapes footplate (FP). A pressure sensor (P1) was inserted into the ear canal near the TM. The TB was then mounted in the “head block” with another pressure sensor (P0) placed at the ear canal entrance. The head block was exposed to blast inside the test chamber. The real-time velocities of the FP and TB specimen (as reference) were measured by two LDVs, respectively, with the P0 and P1 recorded simultaneously. The experiment protocol had two steps: the ear canal was open first and then plugged with a foam earplug. Data measured from each TB before and after insertion of earplug was compared to show the protective function of the earplug, a hearing protection device (HPD).

Results

The BOP level of P0 was around 5 psi and the P1 varied from 6 to 9 psi. The velocity or displacement waveform measured at the FP and the pressure waveform of P1 and P2 were presented over 5 ms of time duration. Results indicated that the displacement of FP ranged from 40 to 120 μm when the ear canal was open. Significantly reduced FP displacement with earplug was observed in all TBs. The reduced amount of energy entering the cochlea in protected ears was calculated.

Conclusion

This novel experimental setup provides a significant methodology in hearing research field for investigating blast-induced hearing damage and HPD’s protective function.

Acknowledgment: This work was supported by DOD W81XWH-14-1-0228.

Reference:

[1] S. Jiang et al. *Hearing Research*, Vol. 378: 43-52, 2019.

PS 206

A Comparative Study of Avian Middle Ear Morphology and Mechanics

John Peacock[1]; Garth Spellman[2]; Nathaniel T. Greene[3]; Daniel J. Tollin[4]
[1]University of Colorado; [2]Denver Museum of Nature and Science; [3]Department of Otolaryngology, University of Colorado School of Medicine; [4]Department of Physiology & Biophysics, and Department of Otolaryngology, University of Colorado School of Medicine

The middle ear mechanically transfers sound energy travelling in air to the fluid of the inner ear. In non-mammalian tetrapods this system consists of the tympanic membrane, one bone (the columella or stapes), the cartilaginous extra-columella (or extra-stapes) as well as some muscles and ligaments. The general morphology of the middle ear differs across species. How much of this variation can be attributed to phylogeny, ecology, the scaling of head size, or other considerations is not clearly described. The relationship between this variation, the mechanics of the ear, and hearing ability, has also not been well studied.

To begin to fill this knowledge gap we made measurements of middle ear morphology and mechanics in a broad range of avian taxa. We used laser vibrometry to measure the vibrations of the columella footplate in response to tones played in the ear canal, and subsequently dissected the middle ear and made general measurements of its form.

With some notable exceptions most features of the middle ear (length, mass, tympanic membrane area, footplate area) appear to scale reliably with overall head size, and some measures of middle ear soft tissue correlate well with the bony structures. This remains true for species with unusual middle ear morphology, e.g. the Coraciiformes in which the basal struts of the columella form a structure like the mammalian stapes, or those Strigiformes which have a highly bulbous footplate.

The general form of the middle ear transfer function, which describes sound transmission gain through the middle ear, is similar across species measured. The transfer function appears to closely follow the form of the avian audiogram at frequencies below the peak, but divergence is seen at higher frequencies, showing how the middle ear does not dictate the avian high frequency hearing limit. Some features of the transfer function may be predictable from the morphology of the middle ear.

Further studies of middle ear mechanics are needed to fully understand the behaviour of this system and what function the observed morphological variations in the avian ear may have. Knowledge of this relationship between form and function in extant avians could allow us to reconstruct middle ear function in extinct and fossil avian species, and may even aid development of prostheses for restorative middle ear surgery.

PS 207

Assessment of Sound Transmission Efficiency of Middle Ear Based on Direct Excitation of Ossicles by Vibration Probe

Sho Kanzaki[1]; Takuji Koike[2]; Yuuka Irie[2]; Takaaki Fujishiro[2]; Chee Sze Keat[3]; Takenobu Higo[4]; Kenji Ohoyama[4]; Masaaki Hayashi[5]; Hajime Ikegami[5]
[1]Department of Otorhinolaryngology, School of medicine,Keio University; [2]Department of Mechanical and Intelligent Systems Engineering, Graduate School of Informatics and Engineering, The University of Electro-Communications, Japan.; [3]Mechano Transformer Corp; [4]Leadence Corp.; [5]Daiichi Medical Co., Ltd.

Objective measurement of the middle-ear sound transmission efficiency (MEE) during the tympanoplasty surgery is important because the prognosis for recovery of hearing level is closely related to the MEE. The MEE can be estimated by applying sound to the external ear and measuring vibration amplitudes of the middle-ear ossicles with a laser vibrometer (LV). However, the MEE measurements have been rarely performed during the surgery because the tympanic membrane (TM) is temporarily elevated in some operative procedure and the stimulus sound cannot be applied to the middle ear through the TM. In addition, the LV system is generally expensive and space-consuming. Therefore, alternative methods have been required.

Cochlear microphonic (CM) is known to faithfully correspond to the frequency and level of sound pressure applied to the cochlea. If the CM is measured and compared before and after the treatment during middle ear surgery, the improvement of the efficiency of the middle-ear sound transmission can be evaluated, and the risk of reoperation can be decreased. However, the conventional CM measurement also requires sound stimulus through the TM.

In this study, an evaluation system for the MEE by measuring the CM during the surgery was constructed. The system consists of a vibration probe, electrodes, an amplifier, and a controller. The ossicles are vibrated by the vibration probe instead of the stimulus sound, and the CM signals evoked by the vibration are measured by the electrode placed on the round window of the cochlea.

The amplitude of CM reflects the transmission efficiency between the point where the vibration is applied and the cochlea.

The CM measurements were performed in the guinea pigs. First, the conventional CM measurement were performed by applying sound stimuli from a speaker. Next, the tip of the vibration probe was brought into contact with the stapes, and vibration was applied. The time signals of the CM obtained from the round window were transformed into frequency domain by applying FFT, and the component equal to the vibration frequency was taken as CM amplitude. These measurements were made by changing the voltage and frequency applied to the vibration probe. In most cases, the CM amplitude increased in proportion to the input voltage as is the case in sound stimulation. This result suggests that the intraoperative assessment of the MEE is possible by using the vibration

PS 208

Eustachian stent placement and tubography in Fresh-frozen Human Cadavers

Byung Chul Kang[1]; Kun Yung Kim[2]; Ho-Young Song[3]; Jung-Hoon Park[4]; Hong Ju Park[5]; Woo Seok Kang[5]
[1]Department of Otorhinolaryngology-Head and Neck Surgery, Ulsan University Hospital; [2]Department of Radiology, Chonbuk National University Hospital; [3]Department of Radiology, Asan Medical Center; [4]Department of Radiology and Research Institute of Radiology, Asan Medical Center; [5]Department of otorhinolaryngology Head and Neck Surgery, Asan Medical Center

Purpose
To evaluate the technical feasibility of Eustachian stent placement and tubography of the cartilaginous portion of the Eustachian tube (ET) in fresh-frozen human cadavers.

Material and Methods
Both ETs of 6 fresh-frozen human cadavers were utilized in this study. Eustachian tubography was performed under endoscopic guidance in 2 cadavers with positioned for submentovertical view, and under fluoroscopic guidance in the remaining 4 cadavers. Two different size stents were placed into the ETs, stents with 2.5mm in diameter for right-side ETs and 3.5mm in diameter for left-side. All stents were 28mm in length. The success rate of ET stent placement, the location of stents, and adverse effects were assessed by fluoroscopy, computed tomography, and endoscopy.

Results
The success rate of Eustachian tubography was 87.5% (7 of 8) with fluoroscopy and 100% (5 of 5) with endoscopy. All stents were successfully placed in both ETs of six cadavers . The distal end of all stents with 2.5mm diameter were located in the bony-cartilaginous isthmus of the ET. One of the six stents was protruded from the nasopharyngeal ET orifice and the remaining 5 stents were fully inserted upto the cartilaginous portion of the ET without protrusion to the nasopharynx. Two of six stents with 3.5mm diameter were fully inserted upto the bony-cartilaginous isthmus without protrusion to the nasopharynx. The distal end of the remaining 4 stents with 3.5mm diameter were inserted upto the cartilaginous portion with the other end of the stents protruded to the nasopharynx. There were no major adverse effects such as bony or cartilaginous fractures.

Conclusion
Eustachian stent placement into the cartilaginous ET is technically feasible under combined endoscopy and fluoroscopy. Accurate placement of the stent remains challenging and further studies are needed to determine the optimal length and diameter of the stents for ET.

Noise Injury

PS 209

Susceptibility to Noise Exposure in Mice Expressing Channelrhodopsin-2

Aditi Agarwal[1]; Xiaodong Tan[1]; Yingjie Zhou[2]; Alan Robinson[1]; Claus-Peter Richter[3]
[1]Northwestern University, Dept. Otolaryngology; [2]Northwestern University, Dept. Communication Sciences and Disorders; [3]Northwestern University, Dept Otolaryngology

Optogenetics is a method to genetically manipulate neurons to express exogenous proteins making the cells sensitive to stimulation with visible light. Recently it has been reported in the literature that overexpression of these proteins may damage the cell and result in apoptosis or alter the electrophysiology, thereby being a potential stressor. Channelrhodopsin-2 (ChR2) is a light sensitive chloride ion channel, which has also been introduced in auditory research. We are interested in understanding whether the exogenous ChR2 protein expression makes the cells more vulnerable to stress in the form of exposure to loud noise. We exposed mice expressing the optogenetic tool ChR2 in their neurons to noise to test whether recovery from noise exposure is similar in homozygote, heterozygote and wild type mice.

Thirteen ChR2 mice were tested for baseline cochlear function using auditory brainstem responses (ABRs).

The mice were then exposed to band limited noise (8-16 kHz) at 90 dB SPL, for 2 hours. ABRs were recorded on day 3, 7, 14 and 28 after the noise exposure. The experimenter was blinded as the mice were genotyped after recording baseline ABRs and were not revealed to the researcher until the end of the study.

ABRs were recorded with three scalp electrodes inserted under the skin at the vertex (low), the mastoid (high) and on the back of the animal (common ground). The voltage difference between the high and the low electrode was continuously measured. Recordings were filtered (0.3 to 3 kHz) and amplified 10,000 times with an ISO80 amplifier. The recordings were captured with custom-written software using a KPCI3110 computer board at a sampling rate of 250 kHz. The signal was averaged 256 times. Threshold for the ABR responses was defined as the stimulus level at which the response was visually detectible in the recorded traces.

A linear mixed model was used to analyze the data. The dependent variable was the threshold sound level for an ABR response. Predictors were noise exposure status, noise level, genotype, and sex of the animal. Grouping variable was the time after exposure.

The results show statistically significant elevated ABR thresholds at 32 kHz, 22 kHz and 16 kHz at 3 and 7 days after noise exposure. ChR2 expression is not affecting the ABR threshold after noise exposure leading to temporary ABR threshold elevations. Effects on neuronal and synaptic changes are currently analyzed.

Supported by the Hugh Knowles Foundation.

PS 210

Stress receptors in frontal brain regions impact on auditory nerve function and auditory brainstem responses

Philine Marchetta[1]; Philipp Eckert[1]; Lukas Rüttiger[1]; Wibke Singer[1]; Marlies Knipper[2]
[1]University of Tübingen, Department of Otolaryngology, Head and Neck Surgery Tübingen; [2]University of Tübingen, Department of Otolaryngology, Head and Neck Surgery Tuebingen

Systemic corticosteroids have been the mainstay of treatment for various hearing disorders for more than 30 years. Accordingly, numerous studies have described glucocorticoids (GCs) and stressors to be protective for the hearing organ during damaging situations. Conversely, stressors are also risk factors for hearing disorders, as they are known to negatively influence for instance tinnitus symptoms. How both of these contrasting stress actions are linked has remained elusive. The two different stress receptors mineralo- (MR) and glucocorticoid receptors (GR) translate the different physiologic stress responses. We induced a conditional deletion of the individual stress receptors upon tamoxifen inducible MR/GRCaMKIIβCre KO mice. This leads to selective deletion of the stress receptors in the frontal brain regions (e.g. hippocampus) within 4 weeks after tamoxifen treatment in adult mice. We analyzed the consequences of the acute deletion of MR/GR pre and post acoustic trauma using DPOAE, ASSR, ABR (with click, noise and pure tone stimuli) and analyzed suprathreshold waves. We also immunohistochemically stained cochlea and brain tissue against specific markers. We surprisingly found evidence that acute central deletion of MR/GR in frontal brain regions exhibits a top down influence in peripheral auditory fibers.

Supported by: Deutsche Forschungsgemeinschaft FOR 2060 project RU 713/3-2; GRK 2381; SPP 1608 RU 316/12-1 and KN 316/12-1

PS 211

Noise-Induced Hearing Loss and Cochlear Injury Vary Dramatically with Impulsiveness of the Exposure

Mo Chen[1]; Wei Qiu[2]; Sharon G. Kujawa[1]
[1]Eaton-Peabody Laboratories, Massachusetts Eye and Ear and Department of Otolaryngology-Head and Neck Surgery, Harvard Medical School; [2]Auditory Research Laboratories, State University of New York at Plattsburgh, Plattsburgh, NY

Background
Prior work shows that noise exposures with non-Gaussian energy distributions can yield greater threshold sensitivity and hair cell losses than energy-equivalent Gaussian noise. In recent studies, we extended these observations to include assessment of inner hair cell-afferent fiber synapses over a range of exposure levels and for exposures of varying degrees of impulsiveness, in a mouse model.

Methods
Adult CBA/CaJ mice were exposed to Gaussian or non-Gaussian noise (8-16 kHz, 2 hr) matched in overall level (100, 103 or 106 dB SPL). Non-Gaussian noises were created with impulses embedded in the continuous noise background; two values of kurtosis (k; 25, 50) defined the degrees of impulsiveness. DPOAE and ABR thresholds and amplitudes were quantified and hair cell and synaptic counts were made (5.6-64 kHz) 24 h or 2 wk post exposure and compared with controls.

Results
Threshold shifts and cochlear injury varied dramatically with temporal properties of the noise. For Gaussian exposures, DPOAE and ABR threshold shifts 24 hr post noise increased gradually with exposure level (100-106 dB SPL). Shifts were increasing functions of frequency, to ~50 dB at highest frequencies. Permanent threshold shifts quantified 2 wks post noise also were graded by exposure level and greatest at highest frequencies. There was no IHC loss at any exposure level evaluated, whereas OHC loss was graded with level and restricted to the extreme cochlear base. Loss of IHC-afferent fiber synapses occurred at frequencies above the noise band, growing to a ~50% maximum, then saturating.

For non-Gaussian noise, threshold shift and injury functions were shifted to higher levels, with maxima near the noise band. Once begun, however, they grew dramatically in magnitude and cochlear extent, with profound threshold elevations, near-total OHC loss or severe injury and large, but frequency-restricted IHC loss. Synapse losses were trivial for 100 and 103 dB non-Gaussian exposures. They were dramatic for 106 dB exposure, although quantification was uncertain given the extensive cochlear injury produced by this exposure. At lower levels, injury appeared driven by the level of the continuous noise background, which must be reduced to keep overall energy constant as high-level transients are added.

Implications
Noise damage in humans may take many forms, and consequences may differ for exposures with varying temporal properties. Results suggest that the kurtosis of noise exposure is a significant variable influencing noise risk.

Research supported by DOD (W81XWH-15-1-0103), NIH/NIDCD (1R01DC015990-01) and Office of China Postdoctoral Council.

PS 212

Reliability of Personal Noise Dosimetry

Ashley Parker; Jennifer Tufts; Erika Skoe
University of Connecticut

Increased interest in noise-induced synaptopathy and other forms of subclinical damage to the human auditory system has prompted discussions about how to accurately quantify noise exposure in human populations. Subjective self-report is a popular approach; interviews and questionnaires can provide quick, inexpensive insight into a person's exposure patterns.Yet, their reliability is contingent on a subject's memory and the validity of the specific measurement approach. Our group developed an approach for objectively measuring exposure levels using body-worn noise dosimeters, and our recent studies of the physiological and functional correlates of routine noise exposure (e.g. Tufts & Skoe, 2018; Skoe & Tufts, 2018) use a 7-day measurement period. However, questions have been raised about whether one week of dosimetry provides a representative snapshot of exposure. This concern motivated the current study, where we repeated our protocol three times in each participant (n=33). Participants wore an ER-200DW8 personal noise dosimeter (Etymotic, Inc.) for three non-consecutive weeks, spread over multiple months, with instructions to wear the dosimeter at all feasible times. Average daily noise exposure dose was calculated for each of the three weeks for each participant, with a broad range of daily noise exposure doses evident across the group. Additionally, participants completed questionnaires designed to capture their annual noise exposure via the Noise Exposure Questionnaire (NEQ; Johnson et al., 2017) and lifetime exposure via the Lifetime Exposure of Noise and Solvents Questionnaire (LENS-Q; Bramhall et al., 2017). Results suggest that average daily dose is consistent across measurement weeks, with each week of dosimetry strongly correlating with the other two weeks (Weeks 1 and 2: (r_s = .753, p < .000); Weeks 1 and 3: (r_s = .576, p < .001); Weeks 2 and 3: (r_s = .665, p < .000)). These results help to validate weeklong personal noise dosimetry as a reliable tool in capturing current noise exposure patterns. However, preliminary analyses indicate that average daily noise exposure estimated via dosimetry did not correlate with the NEQ dose (r_s = .140, p = .443) nor the LENS-Q score (r_s = -.006, p = .973), nor did the NEQ and LENS-Q metrics correlate with each other. These results suggest that the noise exposure measurement techniques under consideration (weeklong noise dosimetry, NEQ, LENS-Q) capture different dimensions of a person's noise exposure. Practical applications and limitations of the noise dosimetry approach will be discussed.

PS 213 - WITHDRAWN

PS 214

Stress-induced Expression of Galectin-3 in Cochlear Immune Cells and Supporting Cells in the Mouse Cochlea

Henry Adler[1]; Richard Salvi[2]; Qingyin Zheng[3]; Celia Zhang[1]; Gail Seigel[1]; Bo Hua Hu[1]
[1]University at Buffalo; [2]Center for Hearing and Deafness, 137 Cary Hall University at Buffalo, Buffalo, NY 14214; [3]Department of Otolaryngology- Head & Neck Surgery, Case Western Reserve University, Cleveland, Ohio, USA

Galectin 3 (Gal-3), a member of the ß-galactoside-binding protein family, has been shown to be involved in numerous biological processes such as cell adhesion, apoptosis, and immune activities. Our previous RNA-seq analysis of cochlear genes revealed a significant increase in the transcriptional expression of *Lgals3,* the gene that encodes Gal-3, after acoustic injury. To identify the location and changes in expression of this protein, we assessed Gal-3 immunolabeling in the normal, noise-exposed and aging mouse cochleae.

To evaluate noise-induced effects, C57BL/6J, B6.129P-*Cx3cr1*^{tm1Litt}/J, and *Cdh23*$^{erl/erl}$ mice were exposed to broadband noise at 120 dB SPL for one hour and their cochleae assessed at multiple times after acoustic overstimulation. To define age-related effects, we examined cochleae displaying age-related sensory cell loss and hearing dysfunction. Gal-3 expression was investigated using immunohistology along with macrophage markers (CD45, CD68, Iba1). Sensory cell integrity was evaluated using nuclear staining. Auditory function was measured using auditory brainstem responses.

Under resting conditions, young mice displayed strong Gal-3 immunoreactivity in Hensen's cells. A small group of branched cells in the lateral wall and the spiral limbus expressed both Gal-3 and immune cell markers (CD45, CD68, and Iba1) suggesting that they are tissue macrophages. This identity was further confirmed by the expression of Gal-3 in GFP-positive cells in *Cx3cr1*-GFP mice that express EGFP in monocytes and macrophages under control of the endogenous *Cx3cr1* locus. In the neural region of the osseous spiral lamina, strong Gal-3 immunoreactivity was present in a small portion of peripheral bundles of ganglion cells. After acoustic trauma, a large number of Gal-3-positive cells that co-expressed macrophage markers emerged. However, some macrophages (Iba1-positive) were Gal-3-negative, suggesting that their function may differ from Gal-3-positive macrophages. Also, Deiters cells and pillar cells showed increased Gal-3 expression in the regions of missing sensory cells. This spatial correlation was also observed in aging cochleae where higher levels of Gal-3 expression were found in supporting cells and the neural region of the osseous spiral lamina adjacent to the regions of significant sensory cell degeneration.

Our study suggests that Gal-3 upregulation may contribute to both the immune response and supporting cell response to noise-induced and age-related stress. Macrophages with diverse functional states may coexist during such stress response. The changes in Gal-3 expression could be due to the heightened role of Gal-3 in apoptosis and cell adhesion in regions of hair cell damage.

PS 215

Repair of Noise-Induced Damage in Stereocilia F-actin Cores

Elizabeth Wagner[1]; Maura I. Nakahata[1]; Terrence Imbery[1]; Jung-Bum Shin[2]
[1]University of Virginia; [2]University of VIrginia

Hair cells are exposed to mechanical stimulation throughout the life of an organism. This continuous stimulation can cause damage to hair cell structures and even lead to hair cell death. While dead hair cells are not regenerated in mammals, some minor types of damage can be repaired, such as in the case of tip link breakage. Here we present evidence that damage to the stereocilia F-actin core can also be repaired. It has previously been shown that exposure to loud noise causes damage to stereocilia cores, visualized as "gaps" in phalloidin staining of F-actin. We also see an increase in the number of these gaps in stereocilia in aging wild type mice, suggesting that damage accumulates over time and possibly contributes to age-related hearing loss. However, stereocilia core damage can likely be repaired to some extent. F-actin crosslinkers and nucleators are enriched in gaps, as well as monomeric actin, suggesting that localized F-actin remodeling is occurring. Additionally, within one week following traumatic noise exposure, we find a greater than 75% decrease in the number of gaps in auditory inner hair cell stereocilia compared to one hour post-noise. Further supporting the possibility that gaps are repaired, in noise exposed inner hair cell stereocilia, we observe discrete patches of newly synthesized GFP-labeled b-actin along the length of stereocilia with intact phalloidin staining, which are absent in non-exposed mice, where newly synthesized b-actin is restricted to stereocilia tips.

While this evidence provides support for the idea that gaps can be repaired, the mechanism for this phenomenon remains unclear. We hypothesize that XIRP2 (Xin actin binding repeat containing protein 2) plays an important role in the process. We observe an enrichment of XIRP2 immunostaining at phalloidin-negative gaps in hair cell stereocilia, similar to the previously reported enrichment of F-actin remodeling factors. In addition, *Xirp2*-null mice develop large numbers of gaps in auditory and vestibular hair cells in the absence of traumatic noise exposure. Lastly, we see an increase in *Xirp2*mRNA and protein levels following noise exposure. Together, these data suggest that XIRP2 may facilitate the repair of stereocilia F-actin damage.

PS 216

All Shook Up: Modeling Noise-Induced Damage and Repair in the Zebrafish Lateral Line

Melanie Holmgren[1]; Mike E. Ravicz[2]; Kenneth E. Hancock[3]; Mark Warchol[4]; **Lavinia Sheets**[1]
[1]Department of Otolaryngology, Washington University School of Medicine in St. Louis; [2]Eaton-Peabody Lab., Mass. Eye & Ear; Department of Otolaryngology, Harvard Medical School; [3]Eaton-Peabody Laboratories, Mass Eye & Ear; Department of Otolaryngology Head & Neck Surgery, Harvard Medical School; [4]Washington University School of Medicine

Hair cells are mechanosensory receptors required for hearing and balance. In the mammalian cochlea, excessive noise exposure can result in hair-cell death and loss of synapses, leading to permanent hearing loss. There is a need to develop protective therapies for noise-induced hearing loss, but the cellular and molecular mechanisms of damage following noise exposure are not well defined.

Hair cells in lateral-line neuromasts (NMs) of larval zebrafish are structurally and functionally similar to mammalian hair cells but are externally located, and are pharmacologically and optically accessible in vivo. We therefore developed a model for acute acoustic damage in this highly tractable system. Larval zebrafish (7 dpf) were exposed to strong water current (60 Hz; 1.04 +/- 0.01 m/s^2) in a multi-well dish rigidly mounted on an electrodynamic shaker. Larvae exposed to either a brief pulse followed by 2 hours of uninterrupted stimulation or short, repeated stimulation spanning 2 hours displayed a subset of lateral-line NMs with disrupted morphology. Mutants with impaired hair-cell mitochondrial function appeared more vulnerable to noise-induced NM disruption, supporting the notion that noise damage is exacerbated by mitochondrial stress. In disrupted NMs, we observed significant reduction in hair-cell afferent innervation. Interestingly, this neurite retraction did not correspond with a reduction in intact synapse number; instead, we occasionally observed the occurrence of “floating” synapses lacking connection to neurites in noise-exposed NMs. Additionally, larvae exposed to uninterrupted stimulation showed a significant loss of hair cells, accompanied by the recruitment of macrophages. Hair cell function, as measured by uptake of the cationic dye FM1-43, was also significantly reduced immediately following noise exposure.

Remarkably, noise-induced lateral-line damage appeared to recover within hours; hair cell morphology and number returned to normal within 4-8 hours following stimulation, corresponding to clearance of damaged hair cells by macrophages. Furthermore, exposed NMs with recovered morphology showed normal afferent innervation, suggesting neural contacts repair as well. FM1-43 uptake also completely recovered by 2 days post-exposure, indicating that MET channels were functional.

These results demonstrate the use of the zebrafish lateral line to model acute noise-induced hair-cell damage. This model system will be important for defining mechanisms of noise damage and for providing insight into repair pathways.

PS 217

The Weaker Sex: Male Rats Sustain Greater Hearing Loss and Hair Cell Loss from Gaussian and Non-Gaussian Noise Exposure

Guang-Di Chen[1]; Mo Chen[2]; Xiaopeng Liu[1]; Senthilvelan Manohar[3]; Li Li[1]; Wei Qiu[4]; Sharon G. Kujawa[2]; Richard Salvi[5]
[1]Center for Hearing and Deafness, University at Buffalo; [2]Eaton-Peabody Laboratories, Massachusetts Eye and Ear and Department of Otolaryngology-Head and Neck Surgery, Harvard Medical School; [3]Center for Hearing and Deafness,University at Buffalo; [4]Auditory Research Laboratory, SUNY Plattsburgh; [5]Center for Hearing and Deafness, 137 Cary Hall University at Buffalo, Buffalo, NY 14214

Background
Epidemiological studies suggest that males may be more susceptible to acquired sensorineural hearing loss than females. However, this apparent sex difference could be shaped by greater or different lifetime noise exposure and/or greater vulnerability to noise injury of males. Exposures having non-Gaussian (nG) amplitude distributions carry higher risk of injury than energy-equivalent Gaussian (G) exposures, and males are more likely to receive such exposures in occupational or recreational settings. To begin to clarify these influences, we exposed male and female rats to G-noise or impulsive nG-noise with the same total energy and characterized chronic consequences on cochlear structure and function.

Methods
Adult Sprague-Dawley rats were exposed to 8-16 kHz octave band noise (90 dB SPL, 5 days) with either a G or nG amplitude distribution. The kurtosis (k) value describing the degree of impulsivity of the noise was 3 for the G-noise and 60 for the nG-noise. Age- and sex-matched controls were treated identically, but were not noise-exposed. There were 10 males and 10 females in each of the exposure and control groups. Cochlear compound action potential (CAP) input/output functions (2-65 kHz) were used to assess the functional status

of the cochlea 2-weeks post-exposure. Afterwards, the cochleae were harvested for histological analysis.

Results
Overall, males were more vulnerable than females to G and nG noise exposure. Baseline CAP thresholds and suprathreshold amplitudes did not vary with sex but males showed greater post-noise deficits, particularly for nG noise and primarily at higher test frequencies (~30-60 kHz). However, G-noise exposure resulted in greater deficits in the region of the noise band (12-16 kHz). Noise-induced CAP deficits in females were smaller and largely confined to the region of the noise band frequencies, where the deficits were slightly greater for G- than nG-noise exposure. Preliminary histological assessment of the G-noise groups revealed mild outer hair cell (OHC) loss located near 12 kHz, greater in males than females. Little OHC loss was apparent in the nG group for either sex. More detailed histological analysis of afferent synapses and hair cells is underway.

Summary/Discussion
Altogether, our results indicate that male rats are more susceptible to noise-induced hearing loss and hair cell loss than females. These sex differences were most pronounced for the nG noise exposure.

***Co-1st authors: M. Chen and G-D Chen.**

Supported by grants from NIDCD: R01DC015990 (WQ), R01DC014693 (RS) and DOD: W81XWH-15-1-0103 (SGK)

PS 218

The Effects of Circadian Disruption on Threshold Shifts After Noise Exposure

Chao-Hui Yang; Chung-Feng Hwang; Ming-Yu Yang; Jiin-Haur Chuang
Kaohsiung Chang Gung Memorial Hospital and Chang Gung University College of Medicine, Kaohsiung, Taiwan

Background
Noise-induced hearing loss is one of the major causes of acquired sensorineural hearing loss in modern society. People with the lifestyle of irregular circadian rhythms are frequently the population of excessive exposure to noise. We aimed to see the effects of circadian disruption on threshold shifts after noise exposure.

Methods
We disrupted the circadian clock in the cochlea of male CBA/CaJ mice by changing the environmental light-dark cycle, and then tested the threshold shifts after low- or high- intensity noise exposure.

Results
Constant light (LL) disrupted the circadian clock significantly more than a normal light dark cycle (LD) environment, evident from a decreased amplitude of average gene expression levels in the circadian clock genes. LL did not affect the auditory brainstem response threshold of mice. After exposure to low-intensity broadband noise, mice under LL and LD had similar temporary threshold shifts initially and both returned to normal thresholds at three weeks after exposure. However, high-intensity noise led to greater elevated permanent threshold shifts in mice exposure to LL, particularly at 32 kHz.

Conclusions
These results indicate that disrupting circadian rhythm by LL does not affect basic cochlear thresholds and temporary threshold shifts after low-intensity noise, but enhances permanent threshold shifts after high-intensity noise exposure.

PS 219

Prolonged Low-Level Noise Exposure Reduces Cochlear Temporal Resolutions

Xiaopeng Liu[1]; Li Li[1]; Guang-Di Chen[2]; Richard Salvi[3]
[1]Center for Hearing and Deafness, University at Buffalo; [2]Center for Hearing and Deafness; [3]Center for Hearing and Deafness, 137 Cary Hall University at Buffalo, Buffalo, NY 14214

Background
Previously, we reported that prolonged exposure to low-level noise temporarily reduced the neural output of the cochlea and caused a small threshold shift. The noise-induced reduction in the neural output of the cochlea could potentially disrupt neural adaptation at the afferent synapse and impair temporal resolution. To investigate this issue, we evaluated the temporal response property of the cochlear compound action potential (CAP) after prolonged exposure to the low-level narrowband noise.

Methods
Rats were exposed to a narrowband noise (18-24 kHz at 85 dB SPL) for 6 weeks and CAPs were recorded at different times post noise exposure. Temporal resolution was assessed using a double-tone stimulus paradigm presented 10 times per second. The frequency and intensity of the two tone bursts (5 ms duration, 1 ms rise/fall time) were identical; however, the inter-tone interval was varied from 2 to 32 ms. The amplitude of the CAP to the second tone burst (CAP_2) was compared to the first tone (CAP_1). The CAP_2/CAP_1 amplitude ratio, expressed in percent, was plotted as a function of inter-tone interval.

Results

In normal control rats, the CAP_2/CAP_1 ratio decreased linearly from ~95% (almost no suppression) at the 32 ms inter-tone interval to ~20% at the 2 ms inter-tone interval. The decline in the CAP2/CAP1 amplitude ratio is believed to be indicative of neural adaptation occurring at the synapse between the inner hair cell and type I auditory nerve fiber. The 6-week narrowband noise (18-24 kHz at 85 dB SPL) caused a significant reduction in CAP amplitude at 24 kHz, within the noise band, but not at 6 kHz below the noise band. Immediately after the noise exposure, there was a significant reduction in the CAP_2/CAP_1 amplitude ratio, results suggestive of greater neural adaptation and slower recovery from adaptation following the noise exposure. Even though the CAP amplitudes had completely restored by 1-week post-exposure, the CAP_2/CAP_1 ratios at 1-week post-exposure were still below the control group indicating slower recovery from adaptation. However, by 4-weeks post-exposure, the CAP2/CAP1 ratio had completely recovered.

Summary and Discussion

Prolonged exposure to low-level noise reduced the CAP2/CAP1 ratios particularly at short inter-tone intervals. These changes are indicative of greater and more prolonged recovery from neural adaptation possibly at the auditory nerve afferent synapses. Such changes could contribute to noise-induced temporal processing deficits.

PS 220

Changes in microRNA expression in the cochlear nucleus and inferior colliculus after acute noise-induced hearing loss

Dong-Han Lee[1]; Sohyun Park[1]; Myung-Whan Suh[1]; Jun Ho Lee[2]; Seung-Ha Oh[1]; Moo Kyun Park[2]
[1]Department of Otorhinolaryngology-Head and Neck Surgery, Seoul National University College of Medicine, Korea; [2]Department of Otorhinolaryngology-Head and Neck Surgery, Seoul National University College of Medicine

Introduction

Noise-induced hearing loss (NIHL) can induce neural plasticity in the central auditory pathway. MicroRNAs (miRNAs) can silence complementary sequences within mRNA and regulates biological processes. This study investigated the role of miRNAs in the neural plasticity of the central auditory pathway after acute NIHL.

Methods

Four groups of 6-week-old rats (n = 12 each) were used: first and second group were assayed 1 day (1N) and 3 days (3N) after noise exposure, third and fourth were the 1-day and 3-day controls. Animals were exposed to white-band noise (2-20 kHz) at 115 dB for 2 hours. Auditory brainstem response (ABR) thresholds were measured and evaluated. Bilateral cochlear nucleus (CN) and cochleae were harvested on Days 1 and 3 after noise exposure. Morphological changes and hair cell (HC) counts were analyzed. After microarray analysis of miRNAs from the CN and IC, candidate miRNAs were validated using quantitative reverse transcription polymerase chain reaction (qRT-PCR), and putative miRNA target pathways were identified.

Results

ABR thresholds increased significantly in both 1N (4 kHz, 81.9 ± 11.6 dB; 8 kHz, 87.1 ± 3.3 dB; 16 kHz, 88.3 ± 2.4 dB) and 3N (4 kHz, 78.8 ± 11.8 dB; 8 kHz, 84.6 ± 2.9 dB; 16 kHz, 86.7 ± 3.8 dB) groups. Three days after noise exposure, animals exhibited a significantly decreased ABR threshold at 4, 8, and 16 kHz compared to animals exposed to 1 day of noise (42.7 ± 17.1 vs 65.6 ± 19.5 dB, 51.9 ± 13.7 vs 73.7 ± 10.7 dB, 63.5 ± 12.6 vs 79.4 ± 8.5 dB; $p < 0.001$). The wave II was significantly larger in the 3N group than 1N group at all frequencies ($p < 0.001$). At 4 kHz, the amplitude of wave IV was greater in the 3N group than 1N group ($p < 0.001$). The basal turn sections of organ of corti showed that the outer HCs and other non-sensory cells were lost. After validation by qRT-PCR, 5 miRNAs were retained from the CN candidates (miR-200b-3p, miR-183-5p, miR-411-3p, miR-20b-5p, and miR-377-3p) and 3 miRNAs were retained from the IC candidates (miR-92a-1-5p, miR-136-3p, and miR-26b-5p).

Conclusions

Our analyses suggest that miR-200b-3p, miR-183-5p, miR-411-3p, miR-20b-5p, miR-377-3p, miR-92a-1-5p, miR-136-3p, and miR-26b-5p may play key roles in the neuroplasticity of the central auditory pathway. 5 candidate miRNAs from the CN can be associated with the mitogen-activated protein kinase (MAPK) signaling pathway, axon guidance, and the neurotrophin signaling pathway.

PS 221

Acoustic Trauma Modulates the Cochlear Blood Flow and Vasoactive Factors in a Rodent Model of Noise-induced Hearing Loss

Sun-Ae Shin; Ah-Ra Lyu; Min Jung Park; Yong-Ho Park
Chungnam National University

The inner ear vasculature is responsible for supplying substrates for metabolic functions, transporting systemic hormones for ion homeostasis and maintaining

the endocochlear potential. Disrupted cochlear microcirculation has been considered an etiologic factor in noise-induced hearing loss (NIHL). Very few studies have identified how noise exposure alters microcirculation in the cochlea, to our knowledge, none have examined these alterations in different severity of noise trauma. In the present study, male 7-week-old C57BL/6 mice were exposed to noise trauma to induce the transient (TTS) or permanent hearing threshold shift (PTS). PTS group showed that significantly reduced the cochlear blood flow, decreased vessel diameter of the stria vascularis, and type IV fibrocytes in the spiral ligament as compared to TTS group, indicating that the cochlear blood flow and fibrocytes are differentially modulated depending on magnitude of acoustic trauma. PTS group showed a significant decrease in genes involved in vasodilation and an increase in gene involved in vasoconstriction as compared to TTS group. Moreover, PTS group also exerted higher expression levels of pro-inflammatory cytokines compared to TTS group. Collectively, these data suggest that cochlear blood flow is differently affected by the severity of noise exposure and these could be associated with the changes of vasoactive factors and inflammatory responses in the cochlea.

PS 222

Treatment with FK506 Promotes Noise Induced-Hearing Loss through Inhibition of Calcineurin and Activation of Autophagy

Zuhong He; Shan Xu; Qiaojun Fang; Su-Hua Sha
Medical University of South Carolina

Background
The contribution of calcium influx into sensory hair cells following noise exposure to the pathogenesis of hair cell loss and hearing loss has been well documented. Treatment with FK506, an inhibitor of calcineurin (CaN) attenuates noise-induced hearing loss (NIHL), supporting the notion that calcium influx activates CaN. Although FK506 is a CaN antagonist that is used clinically in humans as immunosuppressor, the detailed mechanisms of prevention of NIHL by FK506 remain unknown.

Methods
CBA/J mice at the age of 12 weeks were exposed to broadband noise (BBN) at 101 dB or 106 dB with a frequency spectrum from 2–20 kHz for 2 h to induce permanent hearing loss with loss of sensory hair cells. Auditory function was measured by auditory brainstem response (ABR). Mice were treated with FK506 by intraperitoneal injection. Immunohistochemistry and immunolabeling were used to identify changes in CaN and downstream target nuclear factor of activated T-cells (NFAT) and losses of cochlear hair cells and ribbon synapses. GFP-LC3 mice at the age of 6–7 weeks were used to estimate noise-induced autophagy levels in outer hair cells (OHCs) with and without FK506 treatment after 98-dB noise exposure. Finally, small interfering RNA against autophagy marker microtubule-associated protein light chain 3B (siLC3B) was used in CBA/J mice to assess if prevention of noise-induced hearing loss by FK506 is abolished.

Results
In agreement with a previous report, our studies using adult CBA/J mice showed that expression of CaN and NFAT are significantly increased in OHCs following noise exposure. These increases are significantly suppressed by treatment with FK506. Consequently, treatment with FK506 significantly reduces noise-induced losses of hair cells and synapses and NIHL. Furthermore, treatment with FK506 activates autophagy signaling, as assessed in GFP-LC3 mice. Importantly, prevention of NIHL by treatment with FK506 was abolished by pretreatment with siLC3B.

Conclusion
These results indicate that treatment with FK506 attenuates noise-induced OHC loss and hearing loss via inhibition of CaN and activation of autophagy.

Acknowledgements
The research project described was supported by the grant R01 DC009222 from the National Institute on Deafness and Other Communication Disorders, National Institutes of Health.

PS 223

Noise-induced Loss of Sensory Hair Cells is Triggered by ROS/p-AMPKa Pathway

Fan Wu; Su-Hua Sha
Medical University of South Carolina

Background
Accumulation of reactive oxygen species (ROS) has been well-documented in noise-induced hearing loss (NIHL). Our previous study showed that activation of AMPKβ at catalytic residue T172 (p-AMPKβ T172) is one of the key factors triggering noise-induced sensory hair cell death and hearing loss. However, the relationship between ROS and activation of AMPKβ remains unknown. Forskolin is a well-known pharmacological agent that increases intracellular cyclic adenosine monophosphate (cAMP) levels by activating the enzyme adenylate cyclase. The relationship between cAMP and ROS production are contradictory in the literature. The antioxidant activity of N-acetyl cysteine (NAC) is well

known. In this study, we addressed the link between ROS formation and activation of AMPKβ in OHCs after noise exposure.

Methods

CBA/J mice at the age of 8 weeks were used in this study. Mice were exposed to broadband noise (BBN) at 100 dB SPL with a frequency spectrum from 2–20 kHz for 2 h to induce permanent threshold shifts (PTS) with loss of hair cells. Either NAC or forskolin was administrated by intraperitoneal injection. Auditory function was assessed by auditory brainstem response (ABR) and distortion product of auto-acoustic emission (DPOAE). Immunolabeling and Western-blotting were used to detect associated molecular changes. Additionally, HEI-OC1 cells treated with hydrogen peroxide (H_2O_2) were analyzed by flow-cytometry and immunoblotting.

Results

Treatment with forskolin attenuates noise-induced losses of outer hair cells (OHCs) and synaptic ribbons as well as NIHL. Treatment with forskolin significantly increases cAMP in OHCs. Treatment with forskolin or NAC attenuates noise-induced ROS formation in OHCs, assessed by the relative levels of 4-hydroxynonenal (4-HNE) and 3-nitrotyrosine (3-NT), and decreases noise-induced activation of AMPKβ. Additionally, H_2O_2-induced HEI-OC1 cell death is prevented by administration of forskolin. HEI-OC1 cells treated with H_2O_2 confirmed that activation of AMPKβ is triggered by ROS accumulation.

Conclusions

Our data indicate that noise induced-activation of AMPKβ in OHCs is owed to accumulation of ROS, at least in part. These results suggest that noise-induced OHC death is triggered by a ROS/p-AMPKβ-dependent pathway. Forskolin may serve as a powerful compound for prevention of NIHL.

Acknowledgements

The research project described was supported by the grant R01 DC009222 from the National Institute on Deafness and Other Communication Disorders, National Institutes of Health.

PS 224

LCCL activates innate immunity in the cochlea by bacterial infection or noise stimulation

Jinsei Jung[1]; Jee Eun Yoo[2]; Byunghwa Noh[3]; Kyu Min Kim[1]; Gina Na[1]; Seung Ho Shin[1]; Dong Chul Cha[1]; Haiyue Lin[1]; Min Jin Kang[1]; Young Kyun Hur[1]; Jae Young Choi[1]

[1]Yonsei University; [2]Yonsei Univerisity; [3]Yonsei university

In the inner ear, endolymph fluid surrounds the organ of Corti, which is important for auditory function; notably, even slight environmental changes mediated by trauma or infection can have significant consequences. However, it is unclear how the immune response is modulated in these tissues. Here, we report the local immune-surveillance role of cleaved cochlin LCCL (Limulus factor C, Cochlin, and Lgl1) during Pseudomonas aeruginosa infection in the cochlea. Upon infection, the LCCL domain is cleaved from cochlin and secreted into the perilymph. This cleaved fragment sequesters infiltrating bacteria in the scala tympani and subsequently recruits resident immune cells to eliminate the bacteria. Importantly, hearing loss in a cochlin knock-out mouse model is remedied by treatment with a cochlin LCCL peptide. In addition, noise stimulation in the cochlea cleaved cochlin and induced similar immunological responses dependent on the LCCL domain. These findings suggest cleaved cochlin LCCL constitutes a critical factor in innate immunity and auditory function and may be a potential therapeutic target to treat chronic otitis media- or noise-induced hearing loss.

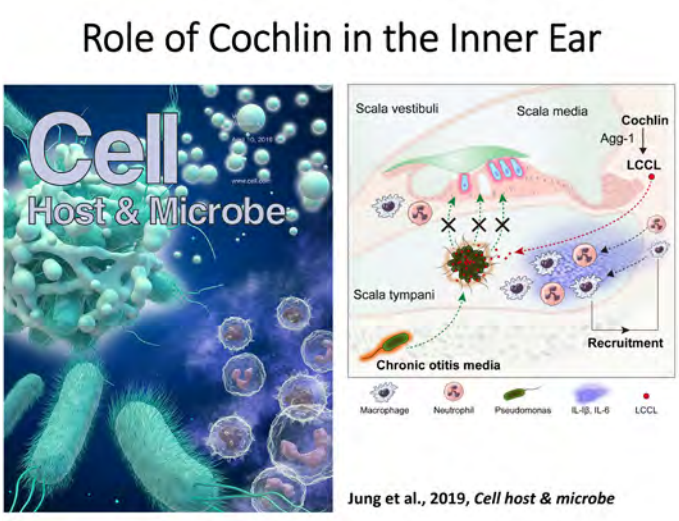

PS 225

Synergistic interaction between TRPV1 and TNF-Î± in mediating noise-induced hearing loss

Asmita Dhukhwa[1]; Sandeep Sheth[2]; Chaitanya Mamillapalli[1]; Vickram Ramkumar[1]; Debashree Mukherjea[1]

[1]SIU School of Medicine; [2]Larkin University College of Pharmacy

Noise trauma is the most common cause of hearing loss in adults. There are no known FDA approved drugs for prevention or rescue of noise-induced hearing loss (NIHL). In this study, we provide evidence that implicates stress signaling molecules (TRPV1, NOX3, and TNF-β) in NIHL. Furthermore, we provide evidence that inhibiting any one of these moieties can prevent and treat NIHL

when administered within a window period. Hearing loss induced by loud noise is associated with the generation of reactive oxygen species (ROS), increased Ca^{2+} in the endolymph and hair cells, and increased inflammation in the cochlea. Increased Ca^{2+} and ROS activity persists for several days after traumatic noise exposure (NE). Chronic increases in Ca^{2+} and ROS have been shown to increase inflammation and apoptosis in various tissue. However, the precise role of Ca^{2+} and inflammation in the noise-induced hearing loss is unknown. Here we show cochlear TRPV1 dysregulation is a key step in NIHL and that TNF-β potentiation of TRPV1-induced Ca^{2+} entry is an essential mechanism of NIHL. In Wistar rats, noise produces an acute (within 48h) and a chronic (within 21 days) increase in cochlear gene expression of *TRPV1*, *NADPH oxidase 3* (*NOX3*) and pro-inflammatory mediators such as *tumor necrosis factor-α* (*TNF-α*) and *cyclooxygenase-2* (*COX2*). Additionally, we also show that H_2O_2 (100 μM) produces a robust increase in Ca^{2+} entry in cell cultures which is enhanced by TNF-β via the TRPV1 channel and which involves ERK1/2 phosphorylation. Mitigation of NIHL could be achieved using capsaicin (agonist which desensitizes TRPV1) or by inhibition of TNF-β with Etanercept (TNF receptor antagonist), administered up to 7 days prior to noise exposure or within 24 h of noise exposure. Our results demonstrate: 1) the synergistic interaction between TNF-β and TRPV1 in the noise exposed cochlea, 2) the systemic administration of drugs that inhibit or desensitize either of these 2 targets are able to prevent and treat NIHL, indicating that prevention of dysregulation of either of these moieties is essential in NIHL. Our data provides a tangible drug treatment option as well as the window of opportunity for the treatment of NIHL.

Sensorineural Hearing Loss and Audiology

PS 226

Ototoxicity in Cystic Fibrosis Patients Following a Single Course of Intravenous Tobramycin in a Prospective Cohort Study

Angela Garinis[1]; Malcolm Gleser[2]; Alexis Johns[3]; Erik Larsen[3]; Jay Vachhani[4]
[1]Oregon Hearing Research Center; [2]Oricula Therapeutics; [3]Decibel Therapeutics; [4]National Center for Rehabilitative Auditory Research (NCRAR)

Aminoglycoside (AG) antibiotics, such as tobramycin, are known to be ototoxic but are important clinically due to their superior efficacy in treating certain bacterial infections. Patients with cystic fibrosis (CF) are particularly at risk for AG-induced ototoxicity due to necessary and repeated use of intravenous (IV)-AGs for the treatment of pulmonary exacerbations caused by P. Aeruginosa throughout the patient's lifetime. Recent studies found that up to 56% of this clinical cohort have sensorineural hearing loss (SNHL), and patients with higher cumulative lifetime IV-AG dosing were at a higher risk for developing SNHL (Garinis et al., 2017). Further, a retrospective study by Gleser & Zettner (2018) found that patients with CF exhibited AG-induced hearing loss after a single course of IV-tobramycin compared to controls with CF not receiving IV-AG treatment. This is a prospective pilot study to replicate findings of their retrospective analysis. Patients with CF, ages 15 to 64 years, were recruited from the Oregon Health & Sciences University CF centers and consented for study participation. Two groups of patients were assessed via serial audiometry (0.25 to 16 kHz) and 0.226-kHz tympanometry: Group 1] 17 patients with CF treated with a therapeutic course of IV-tobramycin (≥ 8 days) and Group 2] 8 patients with CF not receiving IV-tobramycin (controls). Test intervals for Group 1 were: baseline (pre-treatment or within 3 days of first day of dosing), and at least 30 days post-treatment. Controls were tested at similar times, and the baseline visit was chosen at random. Both groups were evaluated for changes in pure-tone hearing thresholds using the ASHA-shift criteria, and a secondary estimate of the average high frequency threshold shift (AHFTS). Findings showed 7/17 patients in the treatment group exhibited ototoxicity (primarily in the 8 to16 kHz range), compared to 0/8 in the control group. Data support Gleser & Zettner (2018) using similar analysis criteria and highlight both the significant ototoxic potential of a single-course of IV tobramycin in some patients, and the need to monitor ototoxicity in extended high frequencies (>8 kHz). Given the increased lifespan of patients with CF and the on-going need for IV-AG therapy, there remains a great need to better understand the effects of cumulative dosing on hearing after each course of treatment.

PS 227

Ototoxicity in Cancer Survivors with Chemotherapy-Induced Peripheral Neuropathy

Jennifer Henderson Sabes[1]; Christine Miaskowski[2]; Judy Mastick[2]; Grace Mausisa[2]
[1]University of the Pacific and University of California San Francisco; [2]UCSF

In the next 5 years the number of cancer survivors in the United States will reach 19 million. The most common chemotherapy-induced neurotoxicities experienced by survivors include peripheral neuropathy, hearing loss and tinnitus. While cisplatin is well-studied in the pediatric population, less is known about the effects of cisplatin in modern chemotherapy treatment regimens in the adult population. Additionally, while pain is addressed in organizational guidelines like that of the National Comprehensive Cancer Network (NCCN), there is minimal or no information on the assessment

and management of peripheral neuropathy, hearing loss, tinnitus and balance disorders in cancer survivors.

In this study, 623 participants who has cisplatin, taxane or combined chemotherapy regimens completed self-report questionnaires that evaluated trait and state anxiety, depressive symptoms, diurnal variations in fatigue and energy, sleep disturbance, changes in attentional function, tinnitus and auditory and balance function. Participants also participated in a study visit to assess neuropathy (sensation measures: temperature, pain and vibration) and balance (Timed Up and Go and Fullerton Advanced Balance Test).

Of the 623 survivors in this study, 68.4% had CIPN, 34.5% reported hearing loss, and 31.0% reported tinnitus. Survivors with these neurotoxicities were more likely to have balance problems, anxiety, depressive symptoms and morning fatigue. Additionally, increased levels of perceived stress were associated with these chemotherapy-induced neurotoxicities. Survivors with all three of these conditions experience an extremely high symptom burden and significant decrements in quality of life. Rates of reported hearing loss and tinnitus were similar to other reported studies of platinum compound-related ototoxicity, although nearly half of the survivors in this study had only a taxane compound. No between group differences were found in the types of chemotherapy regimens received or the total dose of CTX administered.

Additional research has begun to obtain more detailed objective and subjective outcomes of auditorycestibular function and tinnitus. Results from this study indicate that rates of hearing loss are higher than indicated by self-report. These studies and others are needed to evaluate the common and distinct mechanisms associated with chemotherapy-induced neurotoxicities, as well as the relative contribution of each of these neurotoxicities to balance problems, risk for falls, decrements in physical and cognitive function and quality of life.

PS 228

Hearing Loss Characterization in Younger and Older Adults: Insights from the Hearing Examinations of Southern Denmark Database

Manuella Lech Cantuaria[1]; Ellen Raben Pedersen[2]; Mette Sørensen[3]; Frans Boch Waldorff[4]; Jesper Hvass Schmidt[5]

[1]Institute of Clinical Research, Faculty of Health, University of Southern Denmark; Department of Environment and Cancer, Danish Cancer Society Research Center; [2]The Mærsk Mc-Kinney Møller Institute, Faculty of Engineering, University of Southern Denmark; [3]Department of Environment and Cancer, Danish Cancer Society Research Center; [4]Research Unit of General Practice, Department of Public Health, University of Southern Denmark; [5]Institute of Clinical Research, Faculty of Health, University of Southern Denmark; Dept. of Oto-Rhino-Laryngology Head & Neck Surgery and Audiology, Odense University Hospital; OPEN, Odense Patient data Explorative Network, Odense University Hospital

Investigating the prevalence and characteristics of hearing loss (HL) among sex and different age groups is a fundamental step for a better understanding of the risk factors and mechanisms underlying this condition. Nevertheless, the number of population-based epidemiological studies on HL characterization and audiogram configuration is scarce. The purpose of this study was to characterize HL among adults (> 18 years) in a large Danish population-based sample. All hearing examinations from the public health system of the region of Southern Denmark have been electronically recorded from 1996 and merged into a single database, named the Hearing Examinations of Southern Denmark (HESD) database. This database contains hearing information of more than 143,000 adults, totalizing 271,575 valid pure-tone audiograms (i.e. audiograms with air conduction (AC) thresholds at four octave frequencies (500-4000 Hz) or more). The following parameters were evaluated: 1) severity (i.e. mild, moderate, medium and severe) determined by the pure-tone averages; 2) asymmetry (i.e. symmetric and asymmetric HL) based on the number of interaural AC threshold differences ≥ 10 dB and 15 dB; 3) type of lesion (i.e. conductive, sensorineural and mixed); 4) audiogram configuration (i.e. flat, high frequency gently sloping (HFGS), high frequency steeply sloping (HFSS), low frequency ascending (LFA), mild frequency U-shape (MFU), mild frequency reverse U-shape (MFRU) and unspecified) based on the methods proposed by Demeester et al. (2009) and Hannula et al. (2011); and 5) speech discrimination using monosyllabic words in quiet (i.e. excellent, good, fair, poor and very poor). The results from the HL characterization indicate HFSS as the most prevalent audiogram configuration, both among men (63.1% for left ear and 60.7% for right ear) and women (33.7% for left ear and 31.6% for right ear). However, there is a substantially larger prevalence for HFGS and flat configuration for women (for left ear: 29.3% and 21%, respectively) compared to men (18.8% and 9.4%), suggesting sex differences in the configuration distribution. Furthermore, when unspecified cases were not considered, sensorineural HL was found as the most prevalent type of lesion for both men and women (for left ear: 67.2% and 61.9%, respectively), followed by mixed HL (24.8% and 24.3%). The insights hereby obtained highlight the potential of

the HESD database as a promising source of audiology-related epidemiological data, not just to evaluate hearing profiling among adults, but to further explore the effects of hearing impairment on a range of health outcomes (e.g. cognitive impairment and cardiovascular diseases).

PS 229

Reduced diameter of nervus cochlearis in long term deaf patients quantified with semiautimatic MRI ZOOMIT sequence.

Katrin Reimann[1]; Ulrike Eherenpfordt[2]; Ulrich Kloose[3]; Maximilian Schulze[3]
[1]Reduced diameter of nervus cochlearis in long term deaf patients quantified with semiautimatic MRI ZOOMIT sequence; [2]Department of Otolaryngology - Head and Neck Surgery, University of Tübingen, Germany; [3]Department of Neuroradiology, University of Tübingen, Germany

Patient with profound sensorineural hearing loss or deafness are routinely treated with cochlea implantation to restore hearing. Beside audiological testing routine preoperative evaluation includes MRI scan of the neurocranium and temporal bone. This allows the evaluation of the structures of the inner ear as well as the morphology of the nerves in the inner ear canal. Earlier studies have shown that the diameter of the cochlear nerve can be used as prognostic marker for the auditory performance after cochlear implantation in postlingual deaf patients. We have previously shown that 3 tesla MRI ZOOMIT Sequence leads to better discrimination of lateral bone anatomy and helps to identify cochlear or nerve pathologies. In this study we used 3 tesla MRI ZOOMIT Sequence together with semiautomatic analysis to determine the volume of the nerves in the inner ear canal. We therefore retrospectively analyzed 200 3 tesla MRI scans with ZOOMIT Sequence using our semiautomatic tool to measure the volume of cochlear, vestibular and facial nerve in the inner ear canal and correlated the nerve volumes with patient history and audiology testing. We could show that the volume of the cochlear nerve is decreasing the longer the patient is deaf. In patients without facial paralysis facial nerve volume remained unaltered by comparison. This tool can therefore be used prior to cochlea implantation to asess nerve diameter and possibly determine patients with nerve degeneration that will possibly not profit from cochlear implantation or vice versa.

PS 230

Correlation of ECAP and Anamnestic Parameters in Cochlear Implant Patients - Identification of Predictors for Neuronal Health Status

Verena Scheper[1]; Katharina Klötzer[1]; Thomas Lenarz[2]; Lutz Gärtner[1]
[1]Hannover Medical School; [2]Hannover Medical School, Hannover, Germany

Background
Cochlear implants (CI) are the treatment of choice in profoundly deaf patients. Measuring the electrically evoked compound action potential (ECAP) has become an important tool for verifying the vitality of the spiral ganglion neurons (SGN) which are the target cells of the CI-stimulation determining, amongst others, the success achievable with the CI. In this study we investigated possible correlations between the ECAP amplitude growth function (AGF) slope, the array length used, and the anamnestic parameters duration of deafness, age at implantation, hearing threshold, and etiology, to identify possible predictors for SGN health status and therefor for CI-outcome.

Methods
The retrospective study included 184 patients being implanted with MED-EL CIs of various array lengths. Correlation analysis was performed for the mean AGF slope of one implant (electrode 1 to 12), for separate electrodes, as well as for grouped electrodes (electrodes 1-3, 4-9, 10-12).

Results
The mean ECAP AGF slope was not correlated to the length of the CI array. It was negatively correlated to the duration of hearing loss ($p=0.002$) and age at implantation ($p< 0.001$). The ECAP AGF slope of apical electrodes was positively correlated to the etiology syndrome/hered0.2 initary ($p=0.013$).

Conclusion
Since the ECAP AGF slope, as a functional measure of neural health in the inner ear, correlates significantly negatively with age at cochlear implantation and duration of deafness, this study supports the statement that early implantation of a CI is recommended for sensorineural hearing loss.

This study was supported by the German Research Foundation, Cluster of Excellence EXC 1077/1 “Hearing4All”, Hannover, Germany

PS 231

Anatomy of vestibular aqueduct in the patients who had the edolymphatic sac surgery and its usefulness for surgery.

Takashi Sato[1]; Takao Imai[2]; Yumi Ohta[3]; Kazuo Oshima[3]; Hidenori Inohara[4]
[1]Department of Otorhinolaryngology-Head and Neck Surgery, Graduate School of Medicine, Osaka University; [2]Department of Otolaryngology – Head and Neck Surgery, Graduate School of Medicine, Osaka University; [3]Department of Otorhinolaryngology-Head and Neck Surgery, Osaka University Graduates School of Medicine; [4]Department of Otolaryngology - Head and Neck Surgery, Graduate School of Medicine, Osaka University

Endolymphatic sac surgery is one of choice for intractable Meniere's disease against a conservative medical treatment. In this surgery, it is important to identify the endolymphatic sac without injuring the neighboring structures. It is commonly thought that there is the endolymphatic sac in Meniere's disease patients on the medial side of the Donaldson line which is an extension line of the lateral semicircular duct. By the CT image, it is very difficult to confirm the exact position of endolymphatic sac. On the other hand, it is possible to find a vestibular aqueduct opening continuing to an endolymphatic sac in CT image because it is surrounded by bones.

In the operation, because a vestibular aqueduct opening toward an endolymphatic sac adheres to bone, we can easily and safely confirm the position of the endolymphatic sac by pressing an endocranium inside from bone.

We investigated anatomy of vestibular aqueduct of 49 ears with Meniere's disease, who underwent endolymphatic sac surgery by February 2019 from October, 2013.

We rebuild the sagittal section image from high resolution ear CT thin image by aqua software. We examined whether vestibular aqueduct opening located in the inside or outside of the most bulge part of posterior semicircular canal and the Donaldson line. We also checked whether there was pneumatization existed the back of the posterior semicircular canal. Vestibular aqueduct opened beyond posterior semicircular canal in 13 cases. In the operation, we summarized the careful point in each case location of vestibular aqueduct.

PS 232

Cytokine Expression in Cyst Fluid and Tumor Associated Macrophages in Cystic Vestibular Schwannomas

Eric Nisenbaum[1]; Olena Bracho[1]; Stefanie Peña[1]; Esperanza Bas[1]; Cristina Fernandez-Valle[2]; Michael Ivan[1]; Fred Telischi[1]; Xuezhong Liu[1]; Christine Dinh[1]
[1]University of Miami; [2]University of Central Florida

Background
Vestibular Schwannomas (VS) are benign intracranial nerve sheath tumors which cause hearing loss. A subset of these tumors are cystic, a trait that has been associated with worse clinical outcomes. However, little is known about the mechanisms that underly hearing loss, tumor growth, or the differentiation of tumors into solid or cystic variants. The presence of cysts in VS may be linked to M1-type (pro-inflammatory) and M2-type (tumorigenic) tumor associated macrophages and related cytokines and chemokines.

Objectives
Analyze the relationship between cytokine expression in cyst fluid obtained from cystic VS and the expression of M1 and M2-type tumor-associated macrophages.

Methods
Tumor and cyst fluid were prospectively harvested from four patients with cystic VS. Cyst fluid was analyzed using a human cytokine antibody array kit, assessing 80 cytokines and chemokines. Cytokine levels were normalized and expression levels were compared between patients. Immunofluorescence of fixed tumors was performed for CD80 and CD163 (markers for M1 and M2 macrophages, respectively). In addition, a retrospective chart review for was performed to capture clinical characteristics, hearing status, and tumor size and dimensions. Descriptive statistics was performed.

Results
The mean age of patients was 61 years (range: 52 to 58 years). Hearing ranged from mild to profound, while maximal tumor dimension ranged from 2.9cm to 5cm. Cyst fluid demonstrated tumorigenic (IGFBP-2, angiogenin, CCL2, CXCL7, and SPP1), pro-inflammatory (IL-8), and macrophage-related (CCL2, CXCL7, IL6) cytokines. In addition, proteins associated with hearing loss (TIMP-1 and TIMP-2) were also seen. M1 and M2 macrophages were present at various levels on immunofluorescence.

Conclusions
This is the first study that analyzes the molecular composition of cyst fluid in VS, which provides important information about the tumor microenvironment that may

contribute to tumorigenesis, macrophage recruitment, inflammation, and hearing loss. In order to identify potential novel targets for therapeutic intervention in cystic VS, further research is warranted to understand the role of these cytokines in hearing and tumor growth and their connection to the tumor microenvironment and native immune system.

PS 233

Test-Retest Reliability of Serum Prestin Levels in Normal Hearing Young Adults

Ashley Parker[1]; Kourosh Parham[2]; Erika Skoe[1]
[1]University of Connecticut; [2]UConn Health

At current time, there are no blood-based biomarkers clinically available to inform on the health of the inner ear. However, prestin,a motor protein uniquely expressed in the lateral membrane of the outer hair cells (OHCs), has been found to be a potential biomarker to inform on the health of the cochlea in noise exposed populations. Within minutes of OHC apoptosis, cellular contents are phagocytosed by supporting cells in the organ of Corti, with some of the cellular contents, including proteins, being releasing into blood circulation. However, even in the healthy ear, prestin levels are still expected to be measurable in the blood due to normal cyclical process by which cellular contents of OHCs are replaced. We have provided proof of concept that serum prestin levels can change after acoustic trauma and hearing loss (Parham & Dyhrfjeld-Johnsen, 2016) and that prestin levels in blood circulation show temporal fluctuations dependent on the severity of OHC injury (Parham et al., 2019). This work is in the early stages of translation to human populations. In our current study, we provide some of the first data on circulating prestin levels in healthy humans. The initial goal of the study is to evaluate the test-retest reliability of prestin, a necessary first step in evaluating its clinical potential and establishing normative values.

We collected blood samples from 33 young adults, recruited for varying noise exposure histories but with hearing thresholds in the clinically normal-normal range. Samples were taken at 5 different time points in each participant spread over multiple months. Venipuncture was performed and prestin levels were measured in the serum using the MBS167508 enzyme-linked immunosorbent assay (ELISA) kit. All participants underwent audiological evaluation at each time point that included audiometry, otoacoustic emissions, auditory brainstem responses, and speech perception in noise. A novel aspect of the protocol is the use of personal noise dosimetry (ER- 200DW8, Etymotic, Inc.), which allowed for objective measurement of noise exposure the day(s) preceding each draw. Preliminary analyses suggest stability in serum prestin levels, with no significant differences emerging across days ($F(1,22) = .564$, $p=0.497$) and very high correlations across all time points ($r > 0.9$). With the test-retest reliability of prestin established, future analyses will examine relationships between prestin levels, physiological and functional measures of inner ear function, and individual noise exposure levels.

PS 234

The Effect of Diabetes on The Prognosis of Sudden Sensorineural Hearing Loss: Propensity Score Matching Analysis

Yunjae Lee; hayoung byun; jaeho chung
Hanyang University College of Medicine

Objective
The aim of this study was to investigate the clinical implication of diabetes in the management of idiopathic sudden sensorineural hearing loss (ISSNHL).

Method
From January 2015 to December 2018, four hundred three ISSNHL patients who received inpatient management were analyzed. All patients were managed by a uniform treatment protocol of high dose steroid therapy and salvage intratympanic steroid injections. Treatment results were evaluated 3month after the start of treatment, according to Siegel's criteria. We compare the clinical parameters and treatment outcome between ISSNHL with diabetes and without diabetes. We also evaluate the influence of diabetes in prognosis of ISSNHL by propensity score matching analysis.

Results
Overall 403 ISSNHL patients, ninety-four(94/403, 23.3%) patients had diabetes and 11 patients were newly diagnosed diabetes. Patients with diabetes were significantly older than who without diabetes ($p < .001$). And the initial hearing threshold was significantly increased in patients with diabetes ($p < .001$). Diabetic patients were hospitalized for a longer period. In addition, poor hearing recovery rate was observed in diabetic ISSNHL. However, by adjusting age, sex and initial hearing level with propensity score matching analysis, diabetes patients and matched control group showed similar treatment results.

Conclusions
ISSNHL with diabetes usually present with severe hearing loss and need longer duration of hospitalization. However, diabetes itself might not influence on the prognosis of ISSNHL Proper management must be provided in SSNHL with diabetes.

TABLE 1. Demographic and Clinical Characteristics of the Study Populations

Variables	Overall ISSNHL N = 403
Sex	
Male/Female	174 (43.2%) / 229 (56.8%))
Age	54.6±14.2
Underlying Disease	
HTN	133 (33.0%)
DM	94 (23.3%)
CVD	18 (4.4%)
Affected Side	
Right / Left	189 (46.9%) / 214 (53.1%)
Associated symptoms	
Vertigo	110 (27.3%)
Tinnitus	248 (61.5%)
Ear fullness	163 (40.4%)
Onset of treatment (days)	5.3± 11.6
Initial hearing threshold (dB)	72.2± 26.3
Treatment method	
High dose oral steroid	127 (31.5%)
Oral steroid + ITDx*	276 (68.5%)
Hearing gain (dB)	24.2 ± 23.9
Hearing recovery	
Complete recovery	107 (26.6%)
Complete + partial recovery	203 (50.4%)
Complete + partial + slight improvement	287 (71.2%)
No improvement	116 (28.8%)

*ITDX : Intratympanic dexamethasone injection

TABLE 2. Difference of clinical characteristics in SSNHL regarding the presence of diabetes.

Variables	ISSNH With Diabetes N=94	ISSNH Without Diabetes N=309	P
Sex			
Male/Female	40 / 54	134 / 175	.906
Age	60.5± 10.0	52.8 ± 14.8	**< .001**
Underlying Disease			
HTN	58 (62.4%)	75 (24.3%)	**<.001**
CVD	8 (8.5%)	9 (2.9%)	0.053
Associated symptoms			
Vertigo	33 (35.1%)	77 (24.9%)	.064
Tinnitus	60 (63.8%)	188 (60.8%)	.630
Ear fullness	44 (46.8%)	119 (38.5%)	.187
Onset of treatment (days)	4.3± 9.6	5.5 ± 12.2	0.361
Initial hearing threshold (dB)	84.2 ± 24.7	68.6± 25.8	**< .001**
Treatment method			
High dose oral steroid	73 (77.7%)	203 (65.7%)	**.031**
Oral steroid + ITDx*	21 (22.3%)	106 (34.3%)	
Duration of admission (Days)	7.5± 5.8	5.9 ± 1.9	**< .001**
Hearing gain (dB)	25.5± 22.3	23.8 ± 24.3	0.554
Hearing recovery			
Complete recovery	15 (16.0%)	92 (29.8%)	**.008**
Complete + partial recovery	33 (35.1%)	170 (55.0%)	**.003**
Complete + partial + slight improvement	60 (63.8%)	227 (73.5%)	**.090**
No improvement	34(36.2%)	82 (26.5%)	
Parameters of Diabetes			
Random Glucose	226.3± 96.6		
HbA1c	7.3± 1.5		
Use of Insulin	12 (12.8%)		
Use of insulin during steroid therapy	70 (74.5%)		
Newly diagnosed diabetes	12 (12.8%)		

ISSNHL : idiopathic sudden sensorineural hearing loss
ITDX : intratympanic dexamethasone injection

TABLE 3.
Comparison of hearing recovery between diabetes group and propensity score matched control group.

Variables	With Diabetes N=94	Matched Control* N=94	P
Sex			
Male/Female	40 / 54	40/54	
Age	60.5 ± 10.0	60.9 ± 11.7	0.805
Underlying Disease			
HTN	58 (62.4%)	37	**0.001**
CVD	8 (8.5%)		
Associated symptoms			
Vertigo	33 (35.1%)	28 (29.8)	0.533
Tinnitus	60 (63.8%)	49 (52.1%)	0.139
Ear fullness	44 (46.8%)	20 (21.3%)	**< .001**
Onset of treatment (days)	4.3 ± 9.6	5.1 ± 8.3	.565
Initial hearing threshold (dB)	84.2 ± 24.7	84.2 ± 26.2	.986
Treatment method			
High dose oral steroid	73 (77.7%)	74 (78.7%)	1.000
Oral steroid + ITDx*	21 (22.3%)	20 (21.3%)	
Duration of admission (Days)	7.5 ± 5.8	6.0 ± 1.6	**.013**
Hearing gain (dB)	25.5 ± 22.3	21.7 ± 24.1	.270
Hearing recovery			
Complete recovery	15 (16.0%)	14 (14.9%)	1.000
Complete + partial recovery	33 (35.1%)	31 (33.0%)	0.878
Complete + partial + slight improvement	60 (63.8%)	56 (59.6%)	.0653
No improvement	34(36.2%)	38 (40.4%)	

*1:1 matching was done using propensity score with the parameters of age, sex and initial hearing level

PS 235

Early detection of occupational noise induced cochlear synaptopathy among young adults with normal audiograms through electrocochleogram

Qixuan Wang[1]; **Lu Yang**[2]; zhiwu huang[1]; Hao Wu[1]
[1]Department of Otolaryngology-Head and Neck Surgery, Shanghai ninth people's Hospital, Shanghai Jiao Tong University School of Medicine; Ear Institute, Shanghai JiaoTong University School of Medicine; Shanghai Key Laboratory of Translational Medicine on Ear and Nose diseases; [2]Department of Otolaryngology-Head and Neck Surgery, Shanghai ninth people's Hospital, Shanghai Jiao Tong University School of Medicine

Objective

Comparing the characteristics of electrocochleogram under different stimulus rates between pure tone normal hearing young adults with and without occupational noise exposure, to explore the early-stage change of cochlear synaptic function caused by noise exposure, which provide evidence for the cochlear pathogenesis of noise induced hidden hearing loss and basis for early diagnosis approach. Results: 87 subjects aged between 20 to 40 with normal pure tone hearing threshold (250-8000Hz) not exceeding 25dB were included, 43 subjects with occupational noise exposure(exceed 85dB A, at least one year) were defined as the noise group, while 44 subjects without any occupational noise exposure(lower than 70 dB A) were in the control group. Questionnaire information were collected, and the pure-tone audiometric testing, transient evoked otoacoustic emission (TEOAE), Mandarin hearing in noise test(M-HINT) and ECochG under different rates click stimulus were conducted. Statistical analysis was done using SPSS 24.0 version.

Results

There were 62 males (71.3%) and 25 females (28.7%) average aged 25.1±6.0 years. As the stimulus rates increased in ECochG, the amplitude of SP was basically stable in both the noise group and the control group, the amplitude of AP decreased significantly, the latency of AP gradually prolonged, and the SP/AP amplitude ratios showed an increasing trend. Under different stimulus rates, the mean amplitude of AP of the noise group was lower than that of the control group, while the mean SP/AP amplitude ratio of the noise group was increased compared with that in the control group, and the difference was statistically significant (P< 0.05). There were no statistically significant differences in pure tone threshold, TEOAE amplitude, signal-to-noise ratio of M-HINT, SP amplitude or latency of AP under different stimulus rates between the noise group and the control group (P >0.05). Conclusion: At the early

stage of occupational noise exposure, the amplitude of AP and SP/AP amplitude ratio decreased at different stimulus rates among pure tone normal hearing young adults, suggesting cochlear synaptopathy, and the electrocochleogram might be a sensitive approach to detect the noise induced hidden hearing loss.

PS 236

Predictive Factors for Hearing aid Satisfaction for Experienced and First-time Hearing aid Users: Using the International Outcome Inventory for Hearing aids

Sabina S. Houmoeller[1]; Anne Wolff[2]; Vijay Narne[3]; Gérard Loquet[4]; Dan Dupont Hougaard[5]; Dorte Hammershøi[6]; Christian Godballe[1]; Jesper Hvass Schmidt[7]
[1]Department of ORL - Head & Neck Surgery and Audiology Odense University Hospital, Odense, Denmark; Institute of Clinical Research, University of Southern Denmark, Odense, Denmark; OPEN, Odense Patient data Explorative Network, Odense University Hospital, Odense, Denmark; [2]Department of Otolaryngology, Head & Neck Surgery and Audiology, Aalborg University Hospital, Aalborg, Denmark; [3]Institute of Clinical Research, University of Southern Denmark, Odense, Denmark; [4]Institute of Clinical Medicine, Aalborg University, Aalborg, Denmark; Department of Electronic Systems, Aalborg University, Aalborg, Denmark; [5]Department of Otolaryngology, Head & Neck Surgery and Audiology, Aalborg University Hospital, Aalborg, Denmark; Institute of Clinical Medicine, Aalborg University, Aalborg, Denmark; [6]Department of Electronic Systems, Aalborg University, Aalborg, Denmark; [7]Institute of Clinical Research, Faculty of Health, University of Southern Denmark; Dept. of Oto-Rhino-Laryngology Head & Neck Surgery and Audiology, Odense University Hospital; OPEN, Odense Patient data Explorative Network, Odense University Hospital

Based on studies showing that hearing aid (HA) ownership among people with a hearing deficit is surprisingly low, it stresses the importance of improving the likelihood of achieving a successful HA treatment. The level of satisfaction with the HA treatment is assessed using the self-administered International Outcome Inventory of Hearing Aids (IOI-HA) questionnaire. The aims of the current study were to investigate the level of HA satisfaction for experienced and first-time HA users, and further to investigate which factors significantly associated with satisfaction of the HA treatment. Moreover, the study aimed to evaluate any difference between self-reported and objectively measured HA usage time (through data logging). The study population (n=1649) comprised of both experienced (n=458) and first time HA users (n=1191). The study design was a self-reported questionnaire survey and a part of the national BEAR project. Patients were enrolled from January 2017 to January 2018, and answered several questionnaires, including the IOI-HA questionnaire. The IOI-HA consists of seven items, each targeting different hearing outcome domains and scored from 1-5. A higher score indicates a better perceived outcome of the HA treatment. Data logged HA usage time was obtained at two months follow-up visits and compared to the self-reported usage time obtained from the initial IOI-HA questionnaire item. Experienced users answered the IOI-HA before and two months following HA fitting. First-time users answered two months following HA fitting. Results showed that experienced HA users reported a mean total IOI-HA score of 27.8, and first-time HA users a mean total IOI-HA score of 28.2, indicating a high level of satisfaction with the HA treatment in current clinical practice in Denmark. Total mean IOI-HA scores for experienced HA users increased significantly by 0.36 (SD=0.92) ($p< 0.001$), which indicated a higher satisfaction with the new HAs. This argues that it is meaningful to renew HAs after four years following Danish standards. Motivation was shown to be significantly associated with level of HA satisfaction among the first-time users, whereas HA usage time, monosyllabic word scores and type of hearing class were shown to be significantly associated with HA satisfaction for both groups of HA users. Data logging for experienced users showed an average HA use time of 10.4 hours (SD=5.10) and 8.35 hours (SD=1.02) of use for first time users and this difference was significant ($p< 0.001$).

PS 237 - WITHDRAWN

PS 238

The effects of an active noise control technology applied to earphones on preferred listening levels in noisy environments

Takunari Hoshina[1]; Daiki Fujiyama[2]; Takuji Koike[3]; **Katsuhisa Ikeda**[4]
[1]Juntendo University Hospital; [2]The University of Electro-Communications; [3]Department of Mechanical and Intelligent Systems Engineering, Graduate School of Informatics and Engineering, The University of Electro-Communications, Japan.; [4]Juntendo University Faculty of Medicine

Harmful effects of frequent exposure to loud sounds through portable music players (PMPs) in combination with earphones have been suggested to result in the high prevalence of recreational noise-induced hearing loss among children, adolescents, and young adults. We evaluated the effect of an active noise control applied to earphones on the preferred listening levels (PLLs) for

listening music in the presence of background noise.

Twenty-three adults ranged between 20 and 40 years with normal hearing were recruited in this study. PLLs were measured in participants' ear canal with a commercially-available PMP for four earphone/headphone configurations in quiet and noise conditions. Ear canal attenuation was measured by the open ear conditions and the earphone/headphone conditions.

The background noise of multi-talker babble significantly increased the PLL measured in the quiet conditions using any four different earphone/headphone configurations. The increases in PLL using headphones and earbuds were significantly higher than those using canal earphones with and without: (NC) in listening to both pop-rock and classical music. The increase in PLL was significantly higher in the earphone with NC than that without NC in listening to classical music, but not to pop-rock music. Ear canal attenuation in earphones was significantly reduced as compared with those in earbuds and headphones. The relationship between the increase in PLL and the ear canal attenuation was correlated.

Canal phones with NC most lessened the PLL as compared with the other three types. The increase in PLL was found to be determined by ear canal attenuation provided by earphones/headphones. To minimize recreational noise exposure at the risk of PMP use, the use of earphones with NC is recommended.

PS 239

An Early Health Economic Model on Hearing Loss: the potential added value of Novel Hearing Therapeutics

Rishi Mandavia[1]; Yvette Horstink[2]; Mirre Scholte[3]; Janneke Grutters[3]; Evie Landry[4]; Carl May[5]; Maroeka Rovers[3]; Anne G. Schilder[6]
[1]evidENT, UCL Ear Institute; [2]Operating Rooms, Radboud university medical center; [3]Operating rooms, Radboud university medical center; [4]Otolaryngology-Head & Neck Surgery, University of British Columbia; [5]London School of Hygeine and Tropical Medicine; [6]NIHR UCLH Biomedical Research Centre Hearing Theme & evidENT, UCL Ear Institute. London, UK

Background
If proven effective, novel therapeutics for hearing loss will radically change hearing services in the next decade. It is essential to start planning for novel hearing therapeutics to maximise patient access and minimise inefficiencies. Early health economic modelling can be used as a tool to help prepare healthcare systems for novel therapeutics by providing an understanding of their likely cost-effectiveness, and by informing product development and market access. We aimed to construct an early health economic model to assess the potential added value of novel hearing therapeutics, compared to the current standard of care. We used idiopathic sudden onset sensorineural hearing loss (ISSNHL) as a case example, because it is a lead indication for novel hearing therapeutics in development.

Methods
A decision analytic model was developed to assess the costs and effects of using novel hearing therapeutics for patients with ISSNHL. This was compared to the current standard of care. Input data were derived from literature searches and expert opinion. The study adopted a UK healthcare perspective. Four analyses were conducted: 1) headroom 2) scenario 3) threshold 4) sensitivity.

Results
The decision model showed that novel therapeutics for ISSNHL have potential value both in terms of improved patient outcomes and incremental net monetary benefit (iNMB). Results of the threshold and scenario analysis revealed that along with cost and degree of effectiveness, age of treatment and severity of ISSNHL are major determinants of iNMB. The most important uncertainties identified were estimates of utility and proportion of patients receiving a hearing implant in the current pathway.

Conclusions
Novel hearing therapeutics for ISSNHL can be cost-effective under current willingness to pay thresholds. The presented economic model can help guide stakeholders on parameter requirements for novel therapeutics to be cost-effective. Our team are currently leading the SeaSHeL study, a recently launched, collaborative UK prospective cohort study of adult patients presenting with SSNHL across 97 NHS hospitals. The study will map the patient pathway and collect data on the characteristics and outcomes of adult patient presenting with ISSNHL in the NHS. Data from SeaSHeL will be used to refine and validate our economic model.

PS 240

The PATH study: Preparing for the Adoption of novel Therapeutics in Hearing loss.

Rishi Mandavia[1]; Anne G. Schilder[2]; Maroeka Rovers[3]; Carl May[4]
[1]evidENT, UCL Ear Institute; [2]NIHR UCLH Biomedical Research Centre Hearing Theme & evidENT, UCL Ear Institute. London, UK; [3]Operating rooms, Radboud university medical center; [4]London School of Hygeine and Tropical Medicine

Background:
Novel drug, gene and cell therapies for hearing loss are rapidly progressing along the translational pathway to the stage of clinical testing in humans, and if proven effective are set to radically change hearing services within the next 10 years. It is essential to start planning for novel hearing therapeutics to maximise patient access and minimise inefficiencies. Crucial to planning for the implementation of these novel therapeutics, is to assess and evaluate their potential for adoption into healthcare systems. This study applies qualitative analysis to investigate adoption and implementation processes in the field of novel hearing therapeutics. Aim: To characterise and understand the interacting factors that motivate and shape the adoption of novel hearing therapeutics.

Methods
A qualitative study was performed using semi-structured interviews, informal discussions, and non-participant observation. The methodological orientation underpinning the study was abductive analysis, drawing on insights from the previously developed empirical Normalisation Process Theory (NPT). Purposive and snowball sampling were used to select a core group of key informants, knowledgeable in the field of novel hearing therapeutics. The topic guide used was theoretically informed by NPT, and comprised of a schedule of 12 questions. Field-notes were also taken throughout the study to capture informal discussions. Data were analysed using the principles of abductive analysis, using extended NPT to construct a baseline coding framework.

Results
A model of adoption is presented that enables analysis of the conditions necessary to support the introduction of novel hearing therapeutics. The model is defined by four constructs: 1) Social structural resources, 2) Social cognitive resources, 3) Capability, 4) Contribution, which represent the key mechanisms that motivate and shape the adoption of novel hearing therapeutics.

Conclusions
This conceptual model can be used by stakeholders to assess the potential for novel hearing therapeutics to become adopted into healthcare systems; and understand the interacting factors that promote or inhibit their success and failure in practice. The model will help decision makers identify which novel hearing therapeutics can be successfully implemented into existing services. It can also be used by investors to help decide which novel therapeutics to invest in; and by scientists as well as biotechnology and pharmaceutical companies to increase the likelihood of developing hearing therapeutics that can be successfully integrated into healthcare systems.

PS 241 - WITHDRAWN

PS 242

Inducing Tinnitus in Guinea Pigs Through Stimulus Timing-Dependent Plasticity

Michael Selesko; Jennifer Lampen; Rebekah Weeks; Calvin Wu; Adam Hockley; Susan E. Shore
University of Michigan

Introduction
The principal output neurons of the dorsal cochlear nucleus, fusiform cells (FCs), integrate somatosensory input on their apical dendrites and auditory input on their basal dendrites. Stimulus-timing-dependent plasticity (STDP) can be generated in FCs by paired somatosensory-sound stimulation. The order and timing of the paired stimuli determines whether long-term potentiation (LTP) or long-term depression (LTD) occurs (Koehler and Shore, J Neurosci 2013). Following noise exposure, guinea pigs with behavioral evidence of tinnitus have a higher probability for LTP-induction, while those without tinnitus demonstrate more LTD after bimodal stimulation. Thus, repeated auditory-somatosensory stimulation with bimodal intervals that induce primarily LTD can reduce the behavioral and physiological signs of tinnitus (Marks et al., Sci Transl Med 2018). In the present study, we tested the inverse hypothesis to ask whether bimodal intervals that induce primarily LTP, would *induce* tinnitus in guinea pigs without noise exposure.

Methods
Normal-hearing guinea pigs were treated with one of three stimulus conditions: LTP-inducing bimodal stimulation (auditory -preceding the somatosensory stimulation by 10 ms), unimodal somatosensory stimulation (which also induces LTP), or unimodal auditory stimulation (8 kHz tone at 40 dB SL). Somatosensory stimulation was applied through transcutaneous electrodes on the surface of the neck to stimulate the dorsal column pathway. Sound stimulation was delivered through calibrated earphones. Treatments were carried out for 40 min/day, 5 days a week for 4 weeks. Tinnitus was assessed using gap-prepulse inhibition of the acoustic startle. After treatment, animals were anesthetized and DCN single unit recordings were performed.

Results
Behavioral evidence of tinnitus was found in guinea pigs that received either the bimodal or somatosensory stimulation, both of which would be expected to induce LTP. FCs in guinea pigs with tinnitus showed BF-restricted increases in spontaneous firing rate and cross-unit synchrony.

Conclusions
These results demonstrate that tinnitus generation is possible without cochlear insult by inducing LTP in DCN FCs in normal-hearing animals.

PS 243

Bushy cells of the ventral cochlear nucleus and their relationship to tinnitus and hyperacusis

David T. Martel[1]; Susan E. Shore[2]
[1]University of Michigan, Ann Arbor; [2]University of Michigan

Introduction
Tinnitus is usually characterized as tonal or narrowband sound. Consistent with this characterization, dorsal cochlear nucleus (DCN) fusiform cells (FCs) exhibit narrowly-tuned increases in spontaneous firing rate (SFR) and synchrony in animals with behavioral evidence of tinnitus. Ventral cochlear nucleus (VCN) bushy cells (BCs) also exhibit increased SFR following cochlear damage (Bledsoe et al., 2009; Vogler et al., 2011), implicating bushy cells in neural coding of tinnitus. However, unlike FCs, following noise-overexposure, BCs show increased SFR and synchrony across a wide range of best frequencies (BF), suggesting that BC-enhanced SFR is unrelated to tinnitus. Furthermore, BCs in tinnitus animals show steepened rate-level functions (RLF) unlike FCs. BC firing patterns may be more consistent with hyperacusis, an auditory disorder characterized by enhanced loudness growth that occurs across a wide frequency range (Baguley, 2003). Tinnitus and hyperacusis are both associated with hearing-loss and can exist in the same subjects. Thus, some guinea pigs with tinnitus should also show signs of hyperacusis. Herein, we examine the role of BCs in hyperacusis and tinnitus.

Methods
Guinea pigs were exposed to unilateral noise (1/2 octave, 7 kHz, 97 dBSPL; 2 hours) twice, producing temporary threshold shifts. Tinnitus was assessed using gap/prepulse-inhibition of (pinna) acoustic startle (Turner et al., 2006; Berger et al., 2013). Startle-amplitude distributions for pre- and post-exposure were quantified. Animals were then anesthetized with ketamine/xylazine and placed into a stereotaxic frame. NeuroNexus electrodes were stereotaxically inserted into the VCN. BCs were identified by their receptive fields, peristimulus-time-histograms and locations within the VCN (Winter and Palmer, 1990). Spontaneous activity, tone-evoked and broadband-noise-evoked RLFs (0–90 dBSPL, 10 dB step-size, 50 ms, 5 ms rise/fall times) were recorded from multiple BCs. Synchrony was computed as peak normalized cross-correlation coefficients. FC data were from Wu et al. (2016).

Results
BCs in tinnitus animals showed increased SFR and synchrony across a wide best-frequency range, in contrast to FCs. Further, BCs in a subset of tinnitus animals showed enhanced BF-tone RLFs, enhanced wideband noise RLFs, and less-variable first-spike-latencies compared to those in non-tinnitus or control animals.

Conclusions
BCs exhibit neural signatures more consistent with hyperacusis than tinnitus including wideband increases in SFR and steepened RLFs. Enhanced BC RLFs are analogous to abnormal loudness growth and perceptually wide bandwidths associated with hyperacusis.

Funding
RF1-MH114244-01, R01-DC004825, T32-DC00011

PS 244

VAChT Expression in the Cochlear Nucleus of Guinea Pigs After Tinnitus Induction and Reversal

Jennifer Lampen; Karan Joseph; Susan E. Shore
University of Michigan

Introduction
Tinnitus is a disorder characterized by altered homeostatic and timing-dependent plasticity in the brain, beginning in the cochlear nucleus. In the dorsal cochlear nucleus, stimulus timing dependent plasticity (STDP) rules are inverted in animals with tinnitus (Koehler and Shore, 2013). Daily treatment for 25 days with bimodal auditory-somatosensory stimulation with bimodal intervals designed to induce long term depression can restore normal plasticity in the guinea pig cochlear nucleus (Marks et al., 2018). One mechanism that may contribute to this altered plasticity is cholinergic signaling since blocking muscarinic acetylcholine receptors alters STDP in fusiform cells (Stefanescu and Shore, 2016). In addition, spontaneous firing rates of cells in the cochlear nucleus are modulated by cholinergic synapses (Zhang and Kaltenbach, 2000; Chen et al., 1994, 1998). Vesicular acetylcholine transporter (VAChT) expression is reduced in the hippocampus of animals with tinnitus compared to noise exposed animals without tinnitus (Zhang et al., 2018). Changes in VAChT expression may also be evident in the cochlear nucleus since it receives cholinergic innervation from the superior olivary complex, pedunculopontine nucleus and the laterodorsal tegmental nucleus (Mellot et al., 2011). We thus hypothesized that cholinergic activity would be altered in the cochlear nuclei of animals after noise induced tinnitus.

Methods
Adult guinea pigs were noise exposed unilaterally twice, four weeks apart, for two hours each at 97dB with a ½ octave band noise centered at 7kHz. Gap prepulse inhibition of the acoustic startle was assessed before and 8 weeks after noise exposure for 4 weeks each to determine whether the animals developed tinnitus. A subgroup of animals with tinnitus was given a bimodal auditory-somatosensory treatment designed to reduce tinnitus. Brains from noise exposed animals with tinnitus with and without treatment, exposed animals without tinnitus, and control animals were processed using immunohistochemistry for vesicular acetylcholine transporter (VAChT). Density of VAChT labeled puncta was assessed in multiple subregions of the cochlear nucleus.

Results
Differential changes were seen in the density of VAChT puncta in the granule cell domain of animals with and without tinnitus, which returned to normal after the bimodal treatment.

Conclusions
Altered cholinergic activity in the cochlear nucleus may contribute to the altered patterns of plasticity in animals with tinnitus, and their return to normal after bimodal treatment.

PS 245

Decoding Acute Tinnitus by Classifying Dorsal Cochlear Nucleus Spiking Activity

Calvin Wu; Susan E. Shore
University of Michigan

A neural code for tinnitus is first observed in the dorsal cochlear nucleus (DCN), as increased spike synchrony and bursting of the principal neurons. Because noise-exposure does not always result in the phantom sensation of tinnitus, behavioral tests are required to differentiate animals that develop chronic tinnitus from their tinnitus-resilient littermates over the course of several weeks. In acute tinnitus that occurs immediately after noise-exposure, behavioral confirmation is not possible due to the requirement of multiple testing days. To resolve this predicament, we trained a supervised machine-learning classifier to identify an animal's tinnitus status based on features of DCN spontaneous activity with behavioral status established *a priori* by gap-prepulse-inhibition of the acoustic startle (Wu et al., J Neurosci 2016). After optimizing parameters to achieve a 97% classification accuracy, we applied the trained classifier to naive DCN single-unit data obtained in guinea pigs 0-7 hours after noise-exposure previously shown to induce tinnitus. We found that different neurons displayed a variable time-

course for tinnitus code following exposure, with the largest proportion of tinnitus-coding neurons evident 4-5 hours after exposure. Individual animals also showed high or low probability of having tinnitus based on statistics across the neural population. These results suggest that the highly-distinctive DCN neural activity can be utilized to identify animal's tinnitus status in a time scale unrealistic for behavioral testing. This technique creates the possibility in animal models to examine the development of tinnitus longitudinally from acute to chronic, enabling the examination of exciting questions previously hindered by the lack of tinnitus status.

PS 246

Comparison of three methods to detect tinnitus on a rat salicylate-induced tinnitus model

Sylvie Pucheu[1]; Camille Dejean[1]; Amandine Laboulais[2]; Veronique Baudoux[1]; Maida Cardoso[2]; Yves Cazals[1]; Arnaud Norena[3]; Christophe Goze-Bac[2]; Gaelle Naert[1]
[1]Cilcare; [2]BionanoNMRI, CNRS, University of Montpellier, France; [3]Aix-marseille University and CNRS, Marseille, France

Tinnitus, the perception of a "phantom" sound in the absence of external stimulation, is a common consequence of damage to the auditory periphery. It affects around 15% of the population and may induce intolerable discomfort. Although there are some drug candidates in the development process, currently no effective treatment exists to cure tinnitus. The biggest challenge till date is to detect tinnitus objectively in animal models, and hence carrying out new quantitative methods becomes the key step in developing new compounds for tinnitus treatment.

Aim
The objective of this study is to compare three methods on a rat salicylate-induced tinnitus model: a conditioned food reward (CFR) behavioral test, the gap pre-pulse inhibition of the acoustic startle reflex (GPIAS), and a quantitative method, Manganese Enhancement MRI in vivo imaging (MEMRI).

Material and Methods
Nine Long Evans rats were divided in two groups, a control group (n=4) and a salicylate group (n=5), where all the rats were trained for 3 months to perform a central nose poke for CFR. In order to receive the food, the rats should perform a nose poke on the correct side.

The GPIAS test measures the intensity of the startle reflex to a brief sound with high intensity. If a background acoustic signal was qualitatively similar to the rat's tinnitus, poorer detection of a silent gap would be expected.

After 3 months of training for the CFR test, the animals were presented to GPIAS & CFR baseline measurements, followed by evaluation of tinnitus 2 hours post salicylate injection (300mg/kg/day; IP).

Then rats received a trans-tympanic injection of $MnCl_2$ (0.2 mmol/kg), 24 h before brain MEMRI imaging, as a contrast agent to follow neuronal brain activity.

Conclusion
The combination of behavioral tests, and *in vivo* imaging allows to measure putative signs of tinnitus. Similar results were observed in both behavorial tests and MEMRI imaging read-outs after salicylate or vehicle administration. All animal presumed to have tinnitus showed a decrease in the % gap inhibition and proportion of correct responses in the GPIAS and CFR test respectively. Similarly, MEMRI test reported an increase of neuronal activity in the inferior colliculus in animal models with tinnitus. Taken together, these data establish a more robust tinnitus model to accelerate the development of new therapies.

PS 247

TNF-alpha mediates blast-induced tinnitus: Behavioral, electrophysiological and immunocytochemical studies

Hao Luo[1]; Xiuyuan Liang[2]; Bin Liu[1]; Edward Pace[1]; Ruishuang Geng[1]; Shaowen Bao[3]; Jinsheng Zhang[1]
[1]Wayne State University; [2]University of Science and Technology of China; [3]University of Arizona

High-pressure blast is known to induce tinnitus and hearing loss among military personnel and civilians. Recent evidence indicates that TNF-β mediates neuroinflammation and ameliorate behavioral evidence of noise-induced tinnitus in mice. In the current study, we aimed to determine how TNF-β mediates blast-induced tinnitus. Specifically, we investigated the effects of two different types of TNF-β blockers (3,6'-dithiothalidomide (dtt) and etanercept) on behavioral evidence of blast-induced tinnitus, hearing threshold shift, and on neural activity and immunohistochemical changes in the dorsal cochlear nucleus (DCN), inferior colliculus (IC), and auditory cortex (AC) of rats with or without tinnitus. Our results showed that both drugs suppressed blast-induced tinnitus and improved blast-induced hearing threshold shift at one month after blast exposure. Electrophysiologically, blocking TNF-β with dtt reduced spontaneous firing rate, bursting activity and neural-synchrony in the AC at all frequency regions, reduced

sound-driven responses in the AC, except for an enhancement of sound evoked responses in the IC and DCN. Blocking TNF-β with etanercept tended to reduce spontaneous firing rate, bursting activity in the DCN, reduce the neural-synchrony in the AC and increased neural-synchrony in the DCN, while enhancing sound evoked responses in the IC and DCN and decreasing sound evoked responses in the AC. Meanwhile, treatment with both drugs did not show significant changes in spontaneous firing rate, bursting activity and neurosynchrony in the IC. The immunocytochemical results showed that both TNF-β blockers decreased IBA-1 and TNF-β expressions in all the three brain structures compared to the vehicle control group. Taken together, although both drugs uniformly relieved blast-induced tinnitus and improved hearing, they differentially modulated neural activity in auditory brain structures, with etanercept tended to down-regulate tinnitus-related activity in the brainstem and dtt in the cortex. Such differences between the two-blockers-induced modulations may be attributed to the differences in their cellular working mechanisms. The concomitant immunocytochemical and electrophysiological changes indicate that TNF-β mediates both neural inflammation and neuroplasticity that may directly induce the therapeutic effects on behavioral evidence of tinnitus following blast trauma.

PS 248

Blocking TNF-alpha Mitigates Blast-Induced Neural Anomalies in the Auditory and Limbic Systems and Protects Hearing

Ethan Firestone[1]; Hao Luo[1]; Edward Pace[1]; Bin Liu[1]; Shane Perrine[1]; Shaowen Bao[2]; Jinsheng Zhang[1]
[1]Wayne State University; [2]University of Arizona

High-pressure shock waves are known to induce tinnitus – perception of sound in the absence of stimuli - and hearing loss. In many instances, blast-induced tinnitus is paralleled by increased neural spontaneous firing rates (SFR), bursting, among other anomalies, and it's also associated with limbic dysfunction, manifesting as anxiety, depression, and a slew of related comorbidities. However, it's unknown how the limbic and auditory systems become pathologically entangled to produce these symptoms. It has recently been shown that blocking the pro-inflammatory cytokine, TNF-alpha, can relieve behavioral evidence of tinnitus. Thus, to explore the relationship between the limbic and auditory systems following blast, we subjected mice to a single, unilateral blast (22 psi), studied limbic behavior using an elevated plus maze (EPM), and conducted electrophysiological recordings from the primary auditory cortex (AC), basolateral amygdala (AMG), and CA2 hippocampus (HPC). Our preliminary results show that the blast-exposed groups trended toward a slight increase in both entries and time spent in the open arm during EPM, and blocking TNF-alpha with Etanercept helped mitigate this risk taking behavior. Electrophysiologically, blast trauma depressed SFR in the AMG and HPC, along with bursting in the HPC, yet it elevated AC SFR. Both the TNF-alpha gene KO and drug treatment recovered the depressed SFR's in the AMG and HPC and bursting in the latter, while also elevating these two metrics in all other measurements. To elucidate the functional information flow of neural activity change, we demonstrated that blast exacerbated transfer entropy (TE) in the AC, HPC, and all connections between the three structures, and blocking inflammation reduced this pathological feature. Finally, we reiterated that blast exposure impairs hearing thresholds both acutely and chronically, and Etanercept treatment successfully preserved hearing at four-months post-blast. Taken together, our results provide direct evidence that blast exposure - a tinnitus, hearing impairment, and limbic dysfunction inducer - tends to decrease SFR and bursting in limbic structures, with the opposite effect in the AC, while enhancing information flow within and between the two systems, and blocking TNF-alpha mitigates these maladaptive changes and also protects hearing.

PS 249

Effects of Tinnitus and Hearing Loss on Spatial Release from Speech-on-speech Masking and Physiological Proxies of Cochlear Synaptopathy

Chhayakant Patro[1]; Nour El Hidek[1]; Heather A. Kreft[1]; Magdalena Wojtczak[2]
[1]University of Minnesota; [2]Department of Psychology, University of Minnesota

Previous work from our lab has shown that tinnitus is associated with reduced middle-ear-muscle reflex (MEMR) strength. The finding is consistent with the hypothesis that tinnitus in the absence of hearing loss originates from loss of synaptic connections between inner hair cells and auditory-nerve fibers (cochlear synaptopathy). Removing high-frequency components from the broadband noise elicitor did not reduce MEMR strength in individuals with normal hearing (NH) and no tinnitus. However, the effect of high-frequency hearing loss on MEMR strength has not been systematically investigated. In this study, we explored effects of high-frequency hearing loss and tinnitus on MEMR strength, and on several measures often used as proxies of cochlear synaptopathy in humans: auditory brainstem responses (ABRs), envelope-following responses (EFRs), and spatial release from masking (SRM).

Four groups of listeners were recruited: 1) NH, no tinnitus, 2) NH with tinnitus, 3) hearing-impaired (HI), no tinnitus, and 4) HI with tinnitus. Normal hearing was defined as hearing thresholds ≤ 20 dB HL at all audiometric frequencies. HI listeners had normal thresholds for frequencies up to 2 kHz and mild-to-moderate hearing loss (≤40 dB HL) at higher audiometric frequencies. MEMR strength was measured using clicks presented at 90 dB peSPL and a contralateral broadband-noise elicitor. ABRs were measured for clicks presented at 105 peak-equivalent-SPL. EFRs were measured using 2- and 4-kHz tones that were amplitude modulated at 91.4 Hz and presented in quiet and in noise. Speech recognition in two-talker babble was measured for background speakers either collocated (0-deg azimuth) or non-collocated (±15-deg azimuth) with the target. Speech stimuli were amplified for HI listeners.

Results show that MEMR strength was not affected by mild-to-moderate hearing loss (no significant difference between NH and HI with no-tinnitus groups), but MEMR strength was significantly reduced in listeners with tinnitus irrespective of whether they had high-frequency hearing loss or not. All the other measures, ABR wave I and V amplitudes, EFRs, and SRM, were significantly affected by hearing loss and the presence of tinnitus was not a significant factor.

Given the lack of association between high-frequency hearing loss and MEMR strength, the MEMR strength appears to be a good candidate for detecting diffuse cochlear synaptopathy without being confounded by mild-to-moderate hearing loss. The strong association between tinnitus and reduced MEMR strength is consistent with the hypothesis that tinnitus in the absence of hearing loss may be triggered by cochlear synaptopathy. [Supported by NIH grant R01 DC015987].

PS 250

Discriminating Tinnitus Subgroups Based on the Audiometric Profile

Eleni Genitsaridi; Theodore Kypraios; Derek Hoare; Deborah Hall
University of Nottingham

Tinnitus is a heterogeneous condition, but there is still no established framework for discriminating different types of tinnitus. Hearing function is a major factor of tinnitus heterogeneity. However, there are many uncertainties regarding how tinnitus and hearing interact, such as whether and how different types of hearing loss (HL) can define tinnitus subtypes. Unsupervised machine learning algorithms can be used to subgroup a heterogeneous population. Results, however, may depend on the assumptions of each method. This study aims to investigate the value of clustering audiometric data to subtype tinnitus. Data from 212 tinnitus participants who took part in previous studies at our center were analyzed. Audiometric thresholds from both ears (32 variables) or their first four principal components identified with Principal Component Analysis were analyzed using various clustering algorithms (e.g. k-means, PAM) for varying numbers of clusters (n=2-10). Solutions were compared regarding their ability to differentiate distributions of a set of other tinnitus-specific characteristics, using non-parametric tests for statistically significant differences. Average silhouette measures were examined for internal cluster validation. All analyses were conducted in R version 3.5.0. As expected, results differed for different configurations. In nine configurations, clusters differed significantly in at least one tinnitus-specific variable, and the silhouette measure was > 0.25. The maximum number of differences (n=4) was found when applying k-means with five clusters based on raw audiometric data (silhouette = 0.252). Two clusters were characterized by asymmetric HL and the remaining had distinguishable HL profiles. Clusters differed in age at tinnitus onset, tinnitus bandwidth, tinnitus lateralization, and head trauma at tinnitus onset. Audiometric profile has proven useful in discriminating subgroups of tinnitus patients. The value of examining both ears has been highlighted. However, our observations are limited to the available dataset. Future steps include refining the analysis by examining more metrics of cluster validation and replicating on an independent dataset.

PS 251

Evaluating Candidate Measurement Instruments for Assessing the Impact of Chronic Subjective Tinnitus on Ability to Concentrate

Maryam Shabbir; Michael Akeroyd; Deborah Hall
University of Nottingham

The Core Outcome Measures in Tinnitus (COMiT) initiative recently recommended a minimum standard of five outcomes to be included when designing a clinical trial to assess the efficacy of sound-based interventions: *ability to ignore*, *concentration*,*quality of sleep*, *sense of control*and *tinnitus intrusiveness* (doi: 10.1177/2331216518814384). The next stage is to consider which instruments might be appropriate for assessing these outcomes. Here we report our current work on the first of these five, *concentration*. A systematic review was conducted to identify existing measures of *concentration*in an adult population. Thirteen instruments, including questionnaires and performance-based tasks, were identified as candidate instruments. Some of the performance-based tasks were

cognitive batteries, therefore only subtests measuring *concentration*were selected. A feasibility survey was conductedwith sixteen tinnitus experts to assess which aspects of outcome measures are important when designing a clinical trial to investigate intervention efficacy for tinnitus. The main finding from this survey was that eight out of sixteen experts said the instrument would need to be free of charge for them to use it. From the thirteen initially identified instruments, three are free of charge. The current study aims to short-list these three instruments based on content validity and feasibility with the help of experts in cognitive psychology. A shortlisting committee meeting, including six cognitive experts, from the UK, will meet this autumn. During this meeting, the definition of *concentration*by COMiT will be provided to the experts, along with information on the candidate instruments. These experts will assess the instruments with regards to content validity and feasibility. Based on the list of short-listed instruments, a literature search will then be carried out on the measurement properties of these instruments using the COSMIN guidelines. The psychometric evidence for the short-listed candidate instruments will be presented. Findings from this study will inform future recommendations for how to measure *concentration*in clinical trials assessing intervention efficacy for tinnitus.

PS 252

Alterations in Auditory Brainstem Response Latencies in Subjects with Constant Tinnitus

Niklas Edvall[1]; Golbarg Mehraei[2]; Andra Lazar[3]; Esma Idrizbegovic[3]; Barbara Canlon[4]; Christopher Cederroth[1]
[1]Laboratory of Experimental Audiology, Department of Physiology and Pharmacology, Karolinska Institutet; [2]Decibel Therapeutics, Inc.; [3]Hörsel- och Balanskliniken, Karolinska Universitetssjukhuset; [4]Karolinska Institutet

Attempts to investigate whether auditory brainstem responses can be used as an objective measure of tinnitus in humans have yielded largely variable and contradictory outputs, likely due to differences in the classification of subtypes, methodology, and sample sizeThe goal of this project is to identify different tinnitus subtypes to better understand the causes of tinnitus and to assess potential objective biomarkers of tinnitus. Here we report an exploratory study performed on subjects from the Swedish Tinnitus Outreach Project (STOP) with and without tinnitus. Participants from the general population in Sweden answered a survey consisting of several tinnitus specific and quality of life questionnaires (N=6252). Subjects from the Stockholm region were invited for an audiological assessment consisting of otoscopy, tympanometry, DPOAE, pure-tone audiometry (including extended high frequencies), tinnitus pitch and loudness matching, residual inhibition, speech in noise, loudness discomfort levels and ABRs. Among 807 participants that were assessed, 380 had normal hearing (< 25 dB HL up to 8 kHz). A total of 160 tiptrode ABRs were obtained using the ICS EP 200 Chartr system (Otometrics). The ABR protocol consisted of 90 dB nHL alternating polarity clicks presented at a rate of 9.1/s with 50 dB nHL contralateral masking. Two thousand sweeps were collected twice on each ear. ABR Wave I, III, V amplitude and latency from control subjects (n=68) and from those with occasional (n=50) or constant (n=42) tinnitus were compared. Subjects with occasional tinnitus did not differ from non-tinnitus controls in any of the ABR parameters assessed. However, increased Wave V latency (0.14ms) and V-I interwave latency (0.10ms) were found when comparing constant tinnitus to non-tinnitus controls. A test-retest on 16 ears revealed that while all latency measures showed high reliability (ICC1 > 0.75), Wave I amplitude was below the cut-off (ICC1 = 0.43), indicating that Wave I responses are not reliably assessed with the current system. Changes in Wave V latency in the constant tinnitus group did not correlate with scores of the Tinnitus Functional Index (TFI) or the Tinnitus Handicap Inventory (THI), nor with self-reported tinnitus loudness. Our study suggests that constant tinnitus arises in the midbrain as evidenced by an increased Wave V or V-I latency, which could be potential translatable biomarkers of constant tinnitus, but not occasional tinnitus. A validation study on an independent group of subjects is required in order to confirm the reliability of the observed neural changes in subjects with constant tinnitus.

PS 253

A Pharmacogenomic Approach to Unravel the Genetic Contributors to Tinnitus

Natalia Trpchevska[1]; Yitian Zhou[1]; Kristi Krebs[2]; Lili Milani[3]; Volker Lauschke[1]; Barbara Canlon[1]; Christopher Cederroth[4]
[1]Karolinska Institutet; [2]Estonian Genome Center, University of Tartu; [3]Estonian Genome Center, University of Tartu,; [4]Laboratory of Experimental Audiology, Department of Physiology and Pharmacology, Karolinska Institutet

Tinnitus is the most frequent phantom sensation, affecting 70 million individuals in Europe with highly unmet clinical needs. While tinnitus has been thought to derive mainly from environmental factors, we evidenced a significant contribution of genetics in twins and adoptees. Here, we used a pharmacological approach in which we searched for variants in genes coding for drug targets known to cause tinnitus as a side effect. We performed an analysis of the genetic landscape of the genes encoding 22 proteins known as targets

of drugs causing tinnitus as a side-effect using freely available human sequencing data of 138,632 individuals provided by the Genome Aggregation Database (GnomAD). Variants were considered deleterious when they resulted in frameshifts, premature stop-codons, loss of the start codons or disruption of splice donor or acceptor sites. Missense variants were tested using 20 algorithms to test their likelihood of altering protein function (defined as deleterious) via ANNOVAR. Selected variants were tested for their association with clinically significant tinnitus (H93.1) using the Estonian Biobank (n=2,757 cases and 32,884 controls). Using orthogonal computational functionality predictors, we identified 42 variants with functional impact (MAF > 0.1%) in the European population. We found one missense variant associated with clinically significant tinnitus in *KCNH2* (p = 0.01) and in *SCN4A* (p = 0.04). Stratification by sex revealed an additional 3 variants in *HTR1B* and *HTR2B* associated with tinnitus in men only (p < 0.05). Our findings strongly support the notion that genetic factors impact on the development of tinnitus. We propose a molecular basis for tinnitus and provide a new understanding on the mechanism leading to this neurological disorder.

PS 254

Intracochlear Voltage Induced During Non- or Minimally-Invasive Electrical Stimulation of the Cochlea for Tinnitus Relief

Marina Salorio-Corbetto[1]; Simone R. de Rijk[2]; Chen Jiang[1]; Manohar Bance[2]
[1]University of Cambridge; [2]Department of Clinical Neurosciences, University of Cambridge

There is a pressing need to develop effective treatments for tinnitus. Cochlear implants are highly effective for tinnitus relief (Van de Heyning et al., 2008; Buechner et al., 2010; Galvin et al., 2019) but its invasive nature renders them a suitable option only if the patient has severe or profound hearing loss. For patients with normal hearing, mild/moderate hearing loss, or unilateral severe hearing loss, non- or minimally invasive electrical stimulation may be a suitable option. Stimulation is typically delivered using an ear-canal electrode (non-invasive) or a ball electrode sitting on the promontory or the round window (minimally invasive), and a second electrode located at different points on the skull or near the skull is used as ground (Zeng et al., 2019). It is currently unknown what the optimum montage of the electrodes is in order to maximise the stimulation of the cochlea. The aim of the present study is to obtain a transfer function of the intracochlear voltage from skin stimulation as a function of frequency of stimulation, current level, and electrode montage.

Ten fresh-frozen human cadaveric heads will undergo cochlear implantation. The cochlear implants, experimental versions of either Advanced Bionics HiFocus 1J lateral-wall electrode or Cochlear Corporation CI522, allow direct access to the intracochlear electrode contacts for measurement of voltage. Stimulation will be carried out using a either a TIPtrode electrode located in the ear canal of the implanted ear, or a ball electrode sitting on the promontory of the implanted ear. The site for grounding will be varied across eight locations: contralateral ear canal, ipsilateral mastoid, contralateral mastoid, ipsilateral temple, contralateral temple, forehead, vertex, and occiput. Each implanted cochlea will be flushed with saline at 1.0% using a catheter through the round window. Measurements will be taken at several cochlear locations referred to a plate electrode placed on the neck of the specimen. The effects of stimulation frequency and level, type of stimulus, electrode montage, and measurement location will be explored, as well as the individual variability across specimens. The experimental set-up has been piloted, and measures of intracochlear voltage have been successfully recorded.

Buechner A, Brendel M, Lesinski-Schiedat A, Wenzel G, Frohne-Buechner C, Jaeger B, Lenarz T (2010) Cochlear implantation in unilateral deaf subjects associated with ipsilateral tinnitus. Otol Neurotol 31:1381-1385.

Galvin JJ, III, Fu Q-J, Wilkinson EP, Mills D, Hagan SC, Lupo JE, Padilla M, Shannon RV (2019) Benefits of cochlear implantation for single-sided deafness: Data from the House Clinic-University of Southern California-University of California, Los Angeles Clinical Trial. Ear Hear 40:766-781.

Van de Heyning P, Vermeire K, Diebl M, Nopp P, Anderson I, De Ridder D (2008) Incapacitating unilateral tinnitus in single-sided deafness treated by cochlear implantation. Ann Otol Rhinol Laryngol 117:645-652.

Zeng F-G, Richardson M, Tran P, Lin H, Djalilian H (2019) Tinnitus treatment using noninvasive and minimally invasive electric stimulation: Experimental design and feasibility. Trends in Hearing 23:1-12.

PS 255

TRPC6 knockout mice exhibit lower vestibulo-ocular reflex (VOR) gain to high frequency head rotation

Jun Huang[1]; Tianwen Chen[2]; Youguo Xu[2]; Amy Pang[3]; Yang Ou[2]; Jerome Allison[2]; Zhen Wang[4]; Wu Zhou[5]; **Hong Zhu**[5]
[1]Department of Otolarynogology University of Mississippi Medical Center; [2]Department of Otolaryngology University of Mississippi Medical Center; [3]SURE Program University of Mississippi Medical Center; [4]Deapartment of Physiology Unversity of MIssissippi Medical Center; [5]University of Mississippi Medical Center

Introduction
Transient receptor potential (TRP) channels can be activated by mechanical stimuli and have been implicated in hair cell sensory transduction. Expression of a canonical subfamily of TRP channels (TRPC1-7) in vestibular hair cells and ganglion neurons has been reported (Takumida and Anniko, 2009), but their roles in vestibular function remain to be elucidated. Previous studies suggested that TRPC6 did not contribute to vestibular function because TRPC6 knockout mice were normal in swimming and trunk curly tests (Quick et al., 2012). Since these tests tend to assess general posture balance function, caution needs to be taken to interpret the test results. The goal of the present study was to re-examine the role of TRPC6 in vestibular function by measuring the vestibulo-ocular reflexes (VOR) and performing single unit recording analysis of vestibular afferents in TRPC6 knockout mice.

Methods
Seven adult TRPC6 knockout (TRPC6 KO) mice and 8 adult background control mice (B6/129S) were studied. The animals were subjected to sinusoidal head rotation (0.2~4Hz) and translation (0.2-2Hz) while their eye movements were recorded by a video-based eye tracker. Single unit activity of vestibular afferents was recorded from the TRPC6 KO and control mice under general anesthesia. A craniotomy was performed to help access to the 8th nerve. A microelectrode was inserted into the superior vestibular nerves to record spontaneous firings of single vestibular afferents and their responses to head rotation.

Results
In comparison to background control mice, TRPC6 KO mice exhibited significant decreases in angular VOR gains and increases in phase lags at frequencies higher than 2Hz. We recorded 435 vestibular afferents from the control mice and 327 vestibular afferents from the TRPC6 KO mice. There were no significant differences in spontaneous firing rates between control mice (65.7±2.2 spikes/sec) and TRPC6 KO mice (64.5±2.4 spikes/sec). However, consistent with the VOR experiments, the irregular horizontal canal afferents and anterior canal afferents of TRPC6 KO mice exhibited significantly lower sensitivities to head rotation at frequencies above 2 Hz than those of control mice.

Conclusions
The VOR tests and single unit recording studies provided convincing evidence for a specific role of TRPC6 in mediating high frequency angular VOR function. The results suggest that caution needs to be taken while assessing vestibular function using general balance tests. The VOR tests and single vestibular afferent analysis are vestibular specific and will provide insight into understanding vestibular phenotypes of genetically modified mice. Ongoing studies will further investigate the functional relationship between TRPC6 and other TRPC channel subtypes.

JH and TC: equal contribution. Supported by R01DC012060 (HZ), R21 DC017293 (HZ), R01DC014930 (WZ), R00DK113280(ZW)

PS 256

Gravity Affects VOR Adaptation to Magnetic Vestibular Stimulation

Jacob M. Pogson; Dale C. Roberts; Jorge Otero-Millan; David S. Zee; Bryan K. Ward
Johns Hopkins University

Background
Magnetic vestibular stimulation (MVS) is thought to be generated by the interaction of ionic current near the utricular macula with a strong magnetic field. This interaction creates a static magneto-hydrodynamic force in endolymph (viz. a Lorentz force), that deflects the cupula. MVS induces a sustained vestibular asymmetry. Previous studies examining the effect of head position in the pitch plane found an idiosyncratic null point around which the nystagmus direction reversed, thought to be due to an altered Lorentz force. We sought to extend investigations into roll and yaw planes, as well as the effect on the adaptation after-nystagmus.

Method
During each trial eye movements were recorded in subjects before (2 minutes), during (5 minutes) and after (4 minutes) exposure to a 7 Tesla magnetic field. Three-dimensional, binocular video-oculography (VOG) was recorded at 100 Hz. Goggle position was

synchronously recorded with a 3D accelerometer and magnetometer. Control trials were performed in Earth magnetic field only. Two experiments were conducted: head position was maintained throughout the trial (static trials), or the head position was supine during MVS then changed upon exiting the magnetic field (change trials). For *static trials,* before each trial the head was reoriented about the z-axis (supine, prone, left ear down, or right ear down positions). During *change trials* the head position was supine in the magnetic field, then upon exiting the magnetic field was reoriented about the gravity vector (sit upright, 90º roll to left ear down, or 180º whole-body rightward yaw).

Results

In subjects thus far (n=2), control trials showed slow phase velocities (SPV) typically less than 2º/s: one subject showed up-beating nystagmus in all positions and ageotropic nystagmus with each ear down, while the other showed up-beating in supine, down-beating in prone, and geotropic nystagmus with each ear down. In static trials, the greatest peak SPV and reversal peak SPV (upon exiting the magnetic field) occurred during supine position in both subjects, while prone showed the smallest peak SPV and reversal peak SPV. A greater peak SPV occurred in the magnetic field during left ear down than during right ear down, but during reversal the peak SPV for right ear down was greater. During change trials, as expected, the peak SPV and adaptation time-course was identical in the magnetic field, however in both subjects sitting upright showed the largest reversal peak SPV while roll left showed the smallest.

Conclusions

Head position with respect to gravity affects MVS adaptation. Although small changes in utricular current and Lorentz force direction may contribute, we hypothesize that central processing of canal and otolith inputs affects set point adaptation of the vestibulo-ocular reflex.

PS 257

Effect of Viewing Distance on the Vestibuloocular Reflex in Central Field Loss

Anca Velisar; Natela Shanidze
The Smith-Kettlewell Eye Research Institute

Age-related macular degeneration (AMD) can often lead to the loss of the fovea and the surrounding central visual field. This type of visual loss is extremely common (affecting nearly 7% of individuals over 40 in the United states alone (Klein et al. 2011), and are associated with an increase in vestibular complaints. In fact, two thirds of patients with central field loss (CFL) complain of dizziness and instability, and have an increased rate of falls, injury, oscillopsia, and a fear of falling. For certain tasks, individuals develop a new, eccentric fixational area – the preferred retinal locus (PRL). Data on vestibular function in this population are sparse. One study showed a potential re-referencing of the vestibuloocular reflex (VOR) to the eccentric PRL during near viewing and in darkness, with participants with AMD showing an oculomotor asymmetry in the direction of the PRL (González et al. 2018). The study also suggested that VOR gains were also significantly higher in AMD than controls, especially in the near viewing condition. In general, changes in VOR gain with viewing distance are proportional to the vergence angle, with greater vergence angle corresponding to higher VOR gains (exceeding 1 for near viewing). However, there is evidence suggesting that the relationship is not causal (Synder et al. 1992). Thus, VOR gains appropriate to the viewing distance may be preprogrammed over the life span and independent of the actual oculomotor mechanics at the time of testing. Therefore, although visual field defects are known to affect stereopsis and vergence eye movements, we hypothesized that individuals with CFL would exhibit appropriate changes in VOR gain given viewing distance.

To test this hypothesis, we examined VOR responses in 5 individuals with CFL (57-76, 3M) and compared them to 8 age-matched controls (50-77, 5M). Participants viewed a static 1° target on a large screen while volitionally moving their heads in a sinusoidal motion in the yaw plane. Movement frequency was controlled using a metronome and participants were instructed on the amplitude of the movement prior to the experiment and were allowed several practice cycles. Experiment was repeated at viewing distances of 50 (near) and 150 (far) cm. Eye and head movements were recorded using a head-mounted, infrared binocular eye tracking goggles (PupilLabs) with an inertial measurement unit (LPMS Research) rigidly attached to the frame of the eye tracking goggles. All participants were screened for history of vestibular dysfunction and had their stereoacuity tested using the Randot test. Microperimetry was performed on all CFL participants to determine size of field defect and fixational locus location.

We found that both individuals with central field loss and age-matched controls exhibited appropriate VOR gains for near and far viewing (Figure 1, compare individual points to predicted values indicated by dashed lines) with no significant difference in VOR gain between participant types ($p = 0.15$). We did find, however, a participant type-by-viewing-distance interaction, suggesting that the effect was significantly greater for control participants than those with CFL (Figure 2, p =

0.02). Our data do suggest changes in vergence angle across groups.

Our findings are consistent with our hypothesis that changes in VOR gain with viewing distance can occur in individuals with central field loss and altered oculomotor dynamics. However, we do not observe difference in VOR gain at near viewing in CFL, as reported previously. This discrepancy may be due to our aggregate analysis of leftward and rightward head movements. However, we did not observe VOR gain asymmetries, even in individuals with greatest viewing eccentricities.

Figure 1

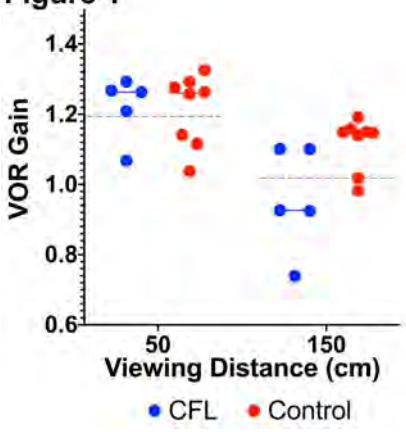

Figure 2

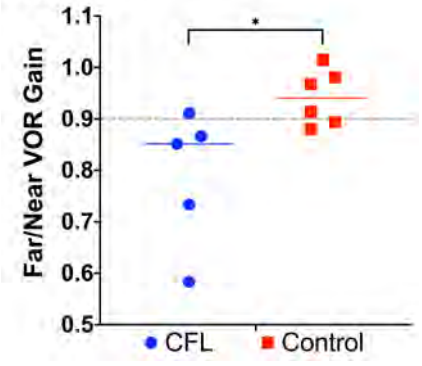

PS 258

A Novel 3D Video Oculography System for Measuring Three Dimensional Vestibulo-Ocular Reflex

Junfeng Liang; Venus Luong; Josh McCraw; Shangru Wu; Gallucci Spencer; Ke Zhang; Ryan Myers; Rong Z. Gan; Chenkai Dai
University of Oklahoma

A Novel 3D Video Oculography System for Measuring Three Dimensional Vestibulo-Ocular Reflex

Junfeng Liang[1], Venus1, Luong[1], Josh McCraw[1], Shangru Wu[1], Spencer Gallucci[1], Ke Zhang[2], Ryan Myers[1], Rong Gan[12], Chenkai Dai[12]

[1]School of Aerospace and Mechanical Engineering
[2]Stephenson School of Biomedical Engineering
University of Oklahoma, Norman OK 73019

Background

The vestibule-ocular reflex (VOR) helps humans to maintain gaze stability during head movements by generating compensatory eye movements that assist fixation on targets in space. The rotational VOR consists of 3-component: horizontal, vertical, and torsional components and precise measurement of 3D VOR is critical in balancing research and a VOR precise measurement system is essential to acquire data from animal experiments. In this study we present a video oculography (VOG) system with a hexapod with 6-degree-of-freedom (6-DOF) mobility for real-time measurements of binocular 3D eye position in rodents.

Methods

A hybrid hexapod (AI-HH-300XY, ALIO Industries) with modified programming was used to control the motion and a customized camera system was used to track the eye movement. This device allows 6-DOF complex motion with the resolution of microscopic level. The animal was secured on an animal mount that positioned on the top plate of the hexapod. The head of the animal was fixed with a head holding device (SR-AC, Tritech Research, Inc.). An array of three markers on a piece of plastic film was affixed to the cornea of both eyes of the animal. The 3D rotation matrix of the eyeball was determined by mathematical computation of the eye marker positions during the hexapod movement.

Results

Computing the rotation matrix based on the instantaneous position of the marker array relative to a reference position is mathematically feasible and allows generation of binocular three-dimensional eye position in real-time during image acquisition. The accuracy of tracking and the calculation of the 3D rotation matrix was first validated in vitro test using a fixed target with the single axis rotation (< 2% positional error). 3D VOR measurement was then performed on chinchilla and the results were comparable to literature data. The validation results demonstrate that the hybrid hexapod platform allows precise control for the animal's motion even for cross-axis rotation or translation movements.

Conclusions

The ALIO hexapod platform with high-precision control is first time integrated for VOR measurement in small animals (e.g. chinchillas). The present VOG system shows potential in measuring real-time binocular cross-axis 3D VOR and larger data will be collected in future to confirm the stability of the system.

PS 259

Development of real-time 3D video-oculography using high quality infrared video Frenzel and galvanic evoked vestibulo-ocular monitoring.

Makoto Hashimoto[1]; Yosuke Okinaka[2]; Hironori Fujii[2]; Kazuma Sugahara[1]; Yoshinobu Hirose[1]; Shunsuke Tarumoto[1]; Takuo Ikeda[3]; Hiroshi Yamashita[1]
[1]Yamaguchi University; [2]Department of Otolaryngology, Yamaguchi University Graduate School of Medicine; [3]Tsudumigaura medical center for children with disabilities

Background

It is essential to use an infrared CCD camera in clinical examination of the vestibular system. Devices are currently available that can quite accurately record human eye movements, based on the principle of video-oculography (VOG). We devised an original VOG (HI-VOG) system using a commercialized infrared CCD camera, a personal computer and public domain software program (ImageJ) for data analysis. We revised the VOG and image filing system for real-time 3D analysis of nystagmus, and developed high quality video Frenzel (yVOG-Glass).Galvanic vestibular stimulation (GVS) activates the vestibular system. Galvanic body sway test provides important information for differential diagnosis between inner ear and retro-labyrinth disorders of the vestibular system. On the other hand, interpretation of nystagmus is difficult, because precise measurement of the eye movement by electronystagmography is not feasible.

Methods

The video image from a Frenzel with high quality image camerawas captured at 60 frames per second at a resolution of 640*480 pixels. For real-time analysis of the horizontal and vertical components, the X-Y center of the pupil was calculated. For real-time analysis of torsional components, the whole iris pattern was overlaid with the same area of the next iris pattern, and the angle at which both iris patterns showed the greatest match was calculated. Galvanic evoked vestibulo-ocular response was monitored.

Results

Accurate measurements of horizontal, vertical and torsional eye movement were taken while recording the video image in real-time. For quantitative analysis, the slow phase velocity of each occurrence of nystagmus and the average value of the slow phase velocity were analyzed automatically. it was possible to carry out accurate recording and evaluation of nystagmus.

Conclusion

Using the yVOG-Glass system, it was possible to perform real-time quantitative 3D analysis of nystagmus from video images recorded with high quality video Frenzel. Recent technological developments, including the use of improved VOG, might lead to the rediscovery of GVS.

PS 260

Evaluation of Motor Function in Rats with Noise-Induced Vestibular Loss

Courtney E. Stewart; David S. Bauer; Ariane C. Kanicki; Richard A. Altschuler; W Michael King
University of Michigan, Kresge Hearing Research Institute

Introduction

The vestibular system plays a critical role in detection of head movements and is essential for normal postural control and balance. Because of their anatomical proximity to the cochlea, the otolith organs are vulnerable to sound pressure and at risk for noise-overstimulation. Reductions in vestibular short latency evoked potential (VsEP) responses in rats with a significant reduction in calretinin labeling of calyceal endings in the striolar region of the sacculus have been reported (Stewart et al., 2018). Taken together, these data suggest that noise may impair vestibular signaling in descending vestibular inputs, but the functional consequences of this impairment are unclear. It is known, however, that irregularly discharging vestibular afferents are the most sound-sensitive (Murofushi & Curthoys, 1997) and this population of afferents plays an important role in descending vestibular reflexes (Bilotto et al., 1982). The goal of the current study is to correlate changes in VsEP waveform amplitudes and jerk thresholds for evoking VsEPs with changes in rats' ability to complete a vestibular dependent motor task. We hypothesize that noise-induced reductions in vestibular nerve activity will be linked to increased task completion time and strategy.

Methods

Adult Long-Evans rats (400-450g) were exposed to intense noise (120 dB SPL, 0.5-4kHz) for six hours on a single day. Before and across time points up to 28 days after noise exposure, VsEP and motor performance were evaluated. Results: Following noise exposure, the VsEP P1N1 waveform (reflecting vestibular nerve activity) was abolished in response to weak (< 1.1/ms) jerk stimuli, and attenuated in response to larger stimuli. This attenuation persisted for up to four weeks in most animals. Additionally, there was a shift in latency for the onset of the P1 waveform in measurable responses. When pooled across all noise exposed animals, motor task completion times were not significantly different from baseline, despite significant and persistent increases in

some animals. Furthermore, the frequency at which the head moved during the task, and the intensity at which this movement occurred was significantly reduced in animals that had longer completion times, suggesting increased caution after noise-induced injury to the vestibular periphery.

Conclusions
Reduced VsEP amplitude, increased VsEP latency, and mildly impaired motor performance suggest a subtle vestibular-mediated motor impairment after noise-induced injury to the vestibular periphery. These results highlight a need for the further development of dynamic motor assessment tools to evaluate otolith function after vestibular injury.

PS 261

Instrumental and Strategic Development of the Short Latency Otolith Evoked Potential in Humans: Some Preliminary Observations

Anthony T. Cacace[1]; Sabahet T. Rizvi[1]; Faith W. Akin[2]; Paul Kileny[3]
[1]Wayne State University; [2]James H. Quillin VA Medical Center; [3]Department of Otolaryngology, University of Michigan Medical Center

Inspired by work in the area of cervical vestibular evoked myogenic potentials in humans (cVEMPs; James H. Quillin VA Medical Center, Mountain Home, Tennessee) and recent animal studies using short latency vestibular evoked potentials (VsEPs; Kresge Hearing Research Labs, University of Michigan), evidence is accumulating to suggest that otolith organs are particularly vulnerable to the deleterious effects of noise trauma (long-duration exposures, blast over pressures, and/or small-arms fire). Because the succulus is positioned directly behind the oval window, considerable force can be exerted from the stapes footplate during noise exposures; thereby increasing the vulnerability of otolith receptors to sound-induced trauma. Having a reliable and efficient electrophysiological tool, independent of muscle activity (VEMPs) to evaluate otolith function, would be especially valuable to clinicians assessing vestibular and balance systems, documenting change over time, and evaluating treatments.

Currently, the short latency otolith evoked potential in humans is being developed in our lab. This accomplishment is similar to work reported from animals with the exception that the recording montage uses a commercially available wick electrode (Lilly or Sanabel) placed on the tympanic membrane using an operating microscope; analogous to single-channel extra-tympanic electrocochleography. Stimuli were short duration 500 and 1000 Hz Blackman-windowed tone bursts presented to the skull via a plexiglass rod attached to a high-grade bone-conduction device (B&K minishaker), at a rate of 3/s and at a level of ~80 dB re: 0.2 g's force obtained via a force/load cell. Additional verification measures were made with the minishaker driving an artificial mastoid. Minishaker vibration results in a linear acceleration of the skull; predominantly in the naso-occipital and interaural axes. This approach results in the relevant input stimulus selective for otolith activation.

Data were collected from 13 normal-hearing adults (8 males; 5 females) ranging in age from 19 to 39 years (mean: 24.2 years; SD: 7.0 years).

Focusing on the 500 Hz input stimulus, reliable responses were obtained from 12/13 individuals (92%). The waveform obtained was characterized by a negative/positive (N1/P1) voltage complex with average latencies approximating 1.52 ms and 2.52 ms, respectively and N1/P1 amplitudes averaging approximately 11.2 uV. In separate recordings, ipsilateral narrowband masking noise was presented via insert earphones to minimize potential contributions from the cochlea. The narrowband maskers did *not* seem to alter the latency or amplitudes of the short latency *unmasked* bone-conduction responses.

Further data analyses, additional quantification, and our path forward will be discussed.

PS 262

Novel Evaluation Method for CVEMP

Toru Seo[1]; Izumi Koizuka[2]
[1]St Marianna University School of Medicine; [2]St. Marianna University School of Medicine

Background
Vestibular evoked cervical myogenic potential (cVEMP) has established as a functional test of the otolith-inferior vestibular nerve. Asymmetry ratio (AR) has been usually used for the evaluation of the amplitude. AR is expressed in percentage of (largest – smallest) / (largest + smallest). Therefore it is difficult to diagnose in the case with bilateral dysfunction. The aim of this study was to clarify the usefulness of normalize amplitude (NA) to diagnose bilateral vestibular dysfunction.

Subjects and methods
Subjects were 18 cases with Meniere's disease, 7 cases with vestibular neuritis and 6 cases with acoustic neurinoma. For the control, 20 normal healthy volunteers were used. All were under 65 years old. For these, the

cVEMP were and evaluated using both NA and AR. When the value was exceeded normal range (mean + 2 SD), we defined as abnormal in two evaluation methods.

Results
Abnormal results were observed in 6 cases (33%) on AR and 13 cases (72%) on NA in the cases with Meniere's disease. Those were in 4 cases (57%) on AR and 5 cases (71%) on NA in the cases with vestibular neuritis. Five cases (83%) showed abnormal results on both NA and AR in the cases with acoustic neurionoma.

Conclusion
The abnormal ratios of two methods were almost same in the cases with vestibular neuritis and acoustic neurionoma. Therefore, NA was as useful as AR in diagnosing unilateral vestibular nerve dysfunction. On the other hand, in the cases with Meniere's disease, the rate of abnormal results on NA was higher than those on AR. It was known that there are occults endolymphatic hydrops in the cases with unilateral Meniere's disease. Abnormalities of AR may have been concealed due to the reduced bilateral response. NA is useful for diagnose the dysfunction of otolith-inferior vestibular nerve in the cases with bilateral involvement.

PS 263

Effects of Sports-Related Head Impact on Otolith Function in Young adults: Preliminary Findings

Amanda Rodriguez[1]; **Sarah Schmoker**[2]; Jonathan Chiao[2]
[1]University of Nebraska-Lincoln; [2]University of Nebraska Medical Center

Background
Sports-concussions in young adults are a common injury that can cause chronic peripheral vestibular dysfunction in 25-80% of patients. Mild traumatic brain injuries (induced by blast) cause damage to the air-and-fluid-filled organs of the inner ear through rapid peak positive-negative pressurization. Specifically, the saccule has greater vulnerability to blast injury than semicircular canals (SSC), which may be due to the protected sensory epithelia of the SSC encased within the bony labyrinth. Due to the proximity of the inner-ear structures within the skull, the endolymph-filled otolith organs may also be at high risk post- blunt force. Thereby, it is suspected that sport-related head impact can similarly affect the otolith and cervical and ocular vestibular evoked myogenic potentials (c-and oVEMP) may be a useful diagnostic. However, characterization of VEMP responses are unknown in a sports population, where head impact is common. Obtaining VEMP responses provides insight on the effects of sports-related impact on the peripheral vestibular system and utility of VEMP in concussion management. Therefore, the objectives of this preliminary work were to (1) characterize c-and oVEMP responses in young adults, who are active in sports, and with and without a history of sports- concussion and (2) assess whether/what atypical otolith changes exist.

Methods
A total of 36 subjects participated (n= 15 with a sport and sports-concussion history; n= 21 without a sport or concussion history and matched on age within 2 years). Subjects completed tympanometry and audiometric screening, and case history intake. All subjects received c-and oVEMP testing at maximum stimulation using 500 Hz air-conducted tone burst stimuli.

Results
Reduced c-and oVEMP response rates in the experimental group (cVEMP= 92%; oVEMP= 80%) as compared to the control (100% c-and oVEMP) were noted. Additionally, there was a significant difference in oVEMP peak-to-peak amplitude between groups (t= 2.05; p= .040), with lower amplitudes for the experimental group (M= 14.70; SD= 2.31) as compared to controls (M= 25.77; SD= 2.59). While the mean cVEMP corrected peak-to-peak amplitudes were higher for the control group (M= 5.18) as compared to the experimental (M= 3.32), there was not a significant difference evidenced for cVEMP corrected peak-to-peak amplitude (t= 1.20; p= 0.238).

Conclusions
Preliminary trends suggest that the otolith pathways, particularly the utricle could be at risk for atypical changes following sports-related impact. Additional data collection is underway to add to these findings and improve our understanding of how otolith dysfunction contributes to vestibular symptoms post-trauma.

PS 264

Detecting Superior Semicircular Canal Dehiscence Syndrome using 2 kHz cVEMP in a Clinical Population

Kimberley Noij[1]; Aaron K. Remenschneider[2]; Barbara S. Herrmann[3]; John Guinan[4]; Steven D. Rauch[5]
[1]Massachusetts Eye and Ear; [2]Dept. of Otolaryngology, UMass Memorial Medical Center; Massachusetts Eye and Ear; [3]Massachusetts Eye and Ear Infirmary, Department of Otology and Laryngology, Harvard Medical School, Boston, Massachusetts, USA; [4]Harvard Medical School; [5]Massachusetts Eye and Ear, Harvard Medical School

Background
Superior semicircular canal dehiscence syndrome (SCD) can be challenging to diagnose. The presentation of symptoms can mimic other otologic pathologies, and not all SCD patients suffer from the same symptoms. High resolution CT imaging of the temporal bone is highly sensitive in detecting SCD, but less specific due to limitations in its resolution; CT imaging overestimates the size of the dehiscence and can misdiagnose patients with thin bone covering the superior semicircular canal as having a dehiscence in 36 - 87.5% of cases. Therefore, additional testing to confirm the diagnosis is recommended. A previous study comparing patients with SCD and healthy age-matched controls found that a cervical vestibular evoked myogenic potential (cVEMP) obtained using a 2 kHz stimulus can detect SCD with a positive predictive value (PPV) of 100% - in combination with a 96% sensitivity. The current study aims to 1) test the accuracy of this 2 kHz cVEMP testing paradigm in a "real" clinical population, meaning that all tested subjects suffer from auditory and/or vestibular symptoms, and 2) determine whether the cVEMP may reduce costs associated with SCD detection.

Methods
All adult patients who underwent 2 kHz cVEMP testing in our clinic from July 2018 to the present were screened. Patients with an available audiogram and CT scan were included. Patients with an air-bone gap (ABG) of >10 dB at any frequency were only included if they had normal tympanograms and stapedius reflexes. Exclusion criteria were: no symptoms (ear not suspected of possibly having SCD), SCD surgery prior to cVEMP testing, or presence of other vestibular pathology in addition to SCD (e.g. Meniere's disease, vestibular neuritis). At our institution the cost of a high resolution CT scan of the temporal bones, including interpretation by a radiologist is $1520. The cost of a cVEMP is $469.

Results
The PPV of the 2 kHz cVEMP remained 100% in a clinical population of 43 tested ears suspected of possibly having SCD. Three out of the 13 patients who were identified as having SCD by both cVEMP and CT scan were interested in surgical treatment. The remaining 10 have thus far not expressed an interest in surgery. Using 2 kHz cVEMP for SCD diagnosis and reserving CT only for probable surgical candidates could realize substantially decreased cost.

Conclusion
The 2k Hz cVEMP is a reliable diagnostic test for SCD detection and may reduce SCD related health care costs.

PS 265

Potential Screening Utility of 4 kHz oVEMP Responses in the Diagnosis of Superior Canal Dehiscence Syndrome

Kristen K. Steenerson[1]; Emma Tran[2]; Austin Swanson[1]; Yona Vaisbuch[1]; Matthew B. Fitzgerald[1]; Jeffrey D. Sharon[3]
[1]Stanford University; [2]Stanford University School of Medicine; [3]UCSF

Background
Superior Canal Dehiscence Syndrome (SCDS) can cause a constellation of audiovestibular symptoms including pulsatile tinnitus, sound-induced vertigo, pressure-induced vertigo, autophony and other forms of bone-conducted hyperacusis. Currently, SCDS is diagnosed with a combination of patient symptoms, audiovestibular testing and CT radiographic confirmation of the dehiscence. In particular, SCDS is associated with negative bone conduction thresholds on audiometry, reduced cervical vestibular evoked potential (cVEMPs) thresholds and enlarged ocular VEMP amplitudes from tone-burst stimulation of frequencies < 2000 Hz. In preliminary report, Manzari showed the presence of oVEMP responses at 4,000 Hz was 100% sensitive and specific for SCDS. Here we present a larger study investigating the diagnostic utility of 4K oVEMP for SCDS.

Methods
A retrospective chart review was performed on all subjects who underwent 4K oVEMP testing at our tertiary care vestibular center. Diagnosis of SCDS was based on CT scan. Sensitivity, specificity, positive predictive value, negative predictive value, and accuracy were calculated.

Results
772 subjects who underwent 4K oVEMP testing were identified. 19 subjects had positive oVEMP and SCDS. 44 had positive oVEMP and negative CT. 31 had negative oVEMP and SCDS. 678 had negative oVEMP and negative CT. Therefore, our preliminary analyses revealed sensitivity values of 38%, and specificity values of 94%, with a positive predictive value of 30%, a negative predictive value of 96%, and overall accuracy of 90%. We are presently examining whether the relatively low sensitivity of the 4 kHz oVEMP in our patient population is related to the age of the patient or their high-frequency hearing status. Moreover, we are also examining the relationship between positive 4 kHz oVEMPs and more traditional oVEMP / cVEMP testing done with lower frequency stimuli.

Conclusion
Based on our preliminary analyses, oVEMP positivity at 4K has a high specificity for predicting SCDS, but low sensitivity. This suggests that a positive 4 kHz oVEMP may be a good indicator of SCDS, but has diagnostic limitations to supplant other confirmatory tests.

Characterizing Auditory Function with Functional Near-Infrared Spectroscopy

Chairs: Antje Ihlefeld & Robert Luke

SYMP 1

Functional Near Infrared Spectroscopy: Enabling Routine Functional Brain Imaging

Maria A. Franceschini
Harvard

Functional Near-Infrared Spectroscopy (fNIRS) is an established neuroimaging methodology which enables neuroscientists to study brain activity and clinician to monitor adequate cerebral perfusion by non-invasively measuring hemodynamic changes in the cerebral cortex. In the last decade, the use of fNIRS has increased significantly with the formation of a society (fnirs.org), with an exponential growth of users and publications, and with an increasing number of available commercial instruments. fNIRS generally uses continuous wave (CW) light sources at two or more wavelengths in the red and near-infrared to continuously record oxy- and deoxy-hemoglobin concentration (HbO and HbR) changes. Our and other groups have shown that by sending light with different features we can extract more information than just changes in absorbance and improve fNIRS capabilities. In particular, with diffuse correlation spectroscopy (DCS), by using long coherence length light sources and detecting the speckle fluctuations generated by moving scatterers, we can measure functional changes of cerebral blood flow (CBF). Moreover, by operating DCS in the time domain (TD-DCS) we can double the sensitivity to the brain, and, for the first time using non-invasive diffuse optical methods, we can achieve higher sensitivity to the brain than to superficial tissues. In this presentation, I will summarize these and other recent technological advances technology developments which are going to enable routine use of NIRS for functional studies and clinical applications.

SYMP 2

A Review of the Potential for fNIRS Deployed With Audiological Intent

Hamish Innes-Brown
Eriksholm Research Centre

fNIRS offers some attractive advantages for the future of audiology. It provides a measure of cortical brain activity that can be related to sound perception. fNIRS uses small and light-weight sensors that can be safely used in all age groups and that are unaffected by electro-magnetic interference. In this presentation I will 1) identify the types of audiologically-relevant information that might be collected using fNIRS, 2) review the progress has been made in some of those areas by several groups and 3) try to identify potentially-fruitful areas for future research that consider the unique characteristics of fNIRS measurement systems.

SYMP 3

Using fNIRS to Investigate Effortful Listening in Cochlear Implant and Normal Hearing Listeners

Xin Zhou; Ruth Y. Litovsky
The University of Wisconsin–Madison

Cochlear implants (CIs) help restore functional hearing in ears with severe-to-profound hearing loss. However, due to the spectral degradation during signal processing, input through the CI can be more challenging to understand than acoustic information in normal hearing (NH) listeners. What is not well-understood is how effortful speech perception is with CIs. In this work, we use functional near-infrared spectroscopy (fNIRS) as an objective measure to shed light on this question.

fNIRS is a non-invasive method, whereby near-infrared light is used to measure neuronal activity related to changes in oxygen metabolism in the blood flow. fNIRS responses were examined in two a priori determined brain 'regions of interest' (ROIs) to test hypotheses about listening effort and speech intelligibility in CI listeners. For listening effort, we focused on the bilateral inferior frontal gyrus (IFG), because previous studies using functional magnetic resonance imaging (fMRI) and fNIRS have identified that region as being involved in effortful listening in NH adults. For speech intelligibility, we focused on the left auditory cortex as previous fMRI studies have reported that region to be sensitive to speech intelligibility.

The study design was to first test bilateral CI users with unprocessed sentences, and NH listeners with sentences processed through a vocoder (CI simulation). To increase task difficulty, two stimulus variables were manipulated in which the sentence structure and difficulty levels were varied. In addition to fNIRS responses, speech intelligibility and self-reported task difficulty levels were also measured.

Our preliminary data in both CI users and NH listeners showed that participants' speech intelligibility was

negatively correlated with their self-reported task difficulties, i.e., the harder they thought the task was, the poorer they performed on the speech tests. Corresponding with our hypothesis about speech intelligibility, fNIRS responses in the left auditory cortex were positively correlated with listeners' speech intelligibility. That is, better performance on speech tests was associated with greater fNIRS response magnitudes in the left auditory cortex. Regarding listening effort, however, mixed results were found about fNIRS responses in the bilateral lFG under different listening conditions, suggesting an interaction of listening effort and speech processing.

SYMP 4

Using Functional Near-infrared Spectroscopy to Characterize Listening Effort in Hearing-Device Users

Ian Wiggins[1]; Francisca Perea Perez[1]; Graham Naylor[2]; Adriana Zekveld[3]; Douglas Hartley[1]
[1]National Institute for Health Research Nottingham Biomedical Research Centre; [2]Hearing Sciences, Division of Clinical Neuroscience, School of Medicine, University of Nottingham; [3]Section Ear & Hearing, Department of Otolaryngology-Head and Neck Surgery, VU University Medical Center and Amsterdam Public Health Research Institute

Users of hearing aids (HAs) and cochlear implants (CIs) report greater listening effort in everyday life than their normally-hearing peers. Functional near-infrared spectroscopy (fNIRS) shows promise for examining the brain activity that underlies this elevated listening effort as it is quiet, portable, and compatible with hearing devices. We have conducted a series of studies combining fNIRS imaging with simultaneous pupillometry to quantify the cognitive demands of listening through a HA/CI. We will present the results of these studies and discuss how objective physiological markers can assist the development of novel interventions designed to make listening easier on the brain.

SYMP 5

fNIRS Applications for Clinical Management of Hearing Loss in Infants

Colette McKay[1]; Julia Wunderlich[1]; Emily Jeffries[1]; Namita Bhojani[1]; Boris Savkovic[1]; Michael Eager[1]; Virginia Olivares[1]; Hamish Innes-Brown[2]
[1]Bionics Institute, Melbourne, Australia; [2]Eriksholm Research Centre

Infants who are born with a hearing loss face the challenge of acquiring spoken language. Research has established the crucial importance of the earliest detection of the hearing loss and subsequent provision of an appropriately programmed hearing instrument. Newborn hearing screening has greatly reduced the age of diagnosis, but highlighted the need for accurate objective measures of hearing function that can be used in very young and sleeping infants to select and programme an optimal hearing instrument.

Although EEG responses are useful in assessing hearing levels in infants, these have drawbacks, such as in infants with auditory neuropathy and those being fitted with a cochlear implant. In this presentation we show data to support the use of functional infrared spectroscopy (fNIRS) for hearing assessment in infants, including patients with auditory neuropathy. Additionally, we show, utilising the cortical adaptation of repeated speech sounds, that fNIRS responses in the temporal and prefrontal regions are sensitive to the discrimination of a novel speech sound from the adapted speech sound in individual sleeping infants. This clinical information is crucial for appropriate hearing device selection and programming. fNIRS thus has the potential to greatly facilitate the early clinical management of infants with hearing impairment. At the Bionics Institute, we are developing a clinically-efficient system (EarGenieTM) for paediatric audiology clinics that uses combined fNIRS and EEG to support this early clinical management.

Supported by the Garnett Passe and Rodney Williams Memorial Foundation, BioMedTech Horizons, the Victorian Medical Research Acceleration Fund and NHMRC Development grant # 1154233. The Bionics Institute acknowledges the support it receives from the Victorian Government through its Operational Infrastructure Support Program.

SYMP 6

Using Optical Neuroimaging to Understand Cognitive Effort in Listeners with Cochlear Implants

Jonathan E. Peelle
Washington University in Saint Louis

The signal provided by cochlear implants (CIs) does not match the fidelity that can be obtained with normal biological hearing. The additional cognitive effort required to understand speech under these circumstances may contribute to individual differences in speech intelligibility among CI users. We use high-density diffuse optical tomography to study the brain systems supporting speech perception in listeners with CIs. We find increased involvement of dorsolateral prefrontal cortex when CI listeners are listening to speech relative to age- and sex-matched listeners with good hearing.

Continuing work explores individual differences in brain activity across listeners and how these relate to outcomes.

SYMP 7

Functional near Infrared Spectroscopy Can Help Predict and Monitor Cochlear Implant Outcome

Douglas Hartley[1]; Carly Anderson[2]; Rachael Lawrence[2]; Ian Wiggins[1]
[1]National Institute for Health Research Nottingham Biomedical Research Centre; [2]National Institute for Health Research (NIHR) Nottingham Biomedical Research Centre

Congenitally-deaf children typically receive their cochlear implant (CI) several years before they can complete behavioural speech tests; during this time, clinicians lack information on which to allocate rehabilitation resources or programme devices. Since speech outcomes vary considerably between children, our work aims to predict and monitor CI outcome based on cortical responses using functional near-infrared spectroscopy (fNIRS). In deaf adults, we show that fNIRS imaging before implantation predicts clinical outcome. In normally-hearing adults, we show that fNIRS responses correlate with speech intelligibility and listening effort; our paediatric testing is ongoing. We feel fNIRS can help predict and optimise CI benefit.

Gene Therapeutic Approaches for Hearing Loss

Chairs: Karen Avraham & Anne Schilder

SYMP 8

Genome Editing with and Without CRISPR

Adi Barzel
Department of Biochemistry and Molecular Biology, Faculty of Life Sciences, Tel Aviv University, Tel Aviv, Israel

Site-specific endonucleases that can induce high rates of targeted genome editing are finding increasing applications in biological discovery and gene therapy. We are using the RNA-guided nuclease CRISPR/Cas9 to design the first ever evolving cell therapy. In particular, we use CRISPR/Cas9 to integrate genes coding for broadly neutralizing anti-HIV antibodies (bNAbs) at the immunoglobulin heavy (IgH) locus of B cells. Adoptive transfer of the engineered cells into syngeneic mice allows antigen-induced activation upon immunization with HIV antigens. Importantly, mice with engineered cells generate a robust serological response that is increased further following boost immunization, implying immunological memory and affinity maturation. Uniquely, our method enables antigen-induced bNAb secretion that may be further augmented by affinity maturation, class switch recombination, and the retention of immunological memory. B cells could thus be engineered as a living and evolving drug to counteract HIV escape and obviate reliance on life-long anti-retroviral therapy. We have developed yet additional methods for genome editing in vivo, where CRISPR/Cas9 delivery may be challenging and potentially immunogenic. GeneRide is an AAV-based site-specific gene addition technology, allowing for life-long therapeutic benefits after a single injection at the neonatal phase in multiple disease models. In GeneRide, the promoterless coding sequence of a therapeutic gene is targeted by natural, error-free homologous recombination into the albumin locus, which is expressed specifically in hepatocytes. Using GeneRide, we demonstrated amelioration of diverse diseases in mice, including hemophilia B, Crigler-Najjar syndrome and methylmalonic acidemia (MMA). GeneRide obviates the need for either vector-borne promoters, promiscuously integrating vectors or the use of nucleases to induce integration. GeneRide allows for safe and efficacious gene targeting in both infants and adults by greatly diminishing off-target effects, while providing therapeutic levels of expression from integration. We will describe the first human clinical trial using GeneRide in infants with MMA, set to enroll patients by early 2020.

SYMP 9

Next Generation Gene Therapies for Genetic Hearing Loss

Jeffrey R. Holt
Boston Children's Hospital & Harvard Medical School, Boston, MA, USA

Surging interest in inner ear therapeutics has driven innovation and development of novel approaches for treating genetic hearing loss. Because hearing loss arises from many sources, our group has taken a broad perspective for selection of gene targets and therapeutic strategies. Here, I will review progress from our group and others focused on preservation and restoration of auditory function using gene replacement and gene or base editing strategies. In this rapidly evolving field, exchange of information on the latest cutting-edge techniques is critical as auditory neuroscientists collectively pursue our common goal of developing biological therapies for genetic inner ear disorders.

SYMP 10

Developing Comprehensive Patient Databases to Prepare for Gene Therapy Trials in Hearing Loss

Anne G. Schilder
NIHR UCLH Biomedical Research Centre Hearing Theme & evidENT, UCL Ear Institute. London, UK

With gene therapeutic approaches rapidly moving towards the clinical domain, there is an urgent need for developing international patient data base of systematically collected clinical hearing data, combined with biorepositories of blood samples and tissue specimens for genomic, proteomic, and metabolomic analysis. Provided patient consent-to-contact is in place, these registries allow for efficient patient identification and recruitment to clinical trials and provide an infrastructure for the collection of treatment and trial outcomes. We will highlight lessons learned from databases in other diseases areas and progress made in the hearing field.

SYMP 11

The Adeno-Associated Viral Anc80 (AAVAnc80) Vector - Precision Genetic Medicines to Address Hearing Loss

Michelle D. Valero
Akouos, Inc.

Gene therapy is a promising modality to address both genetic and acquired hearing loss, and AAVAnc80-mediated gene transfer has successfully rescued cochlear function in rodent models of genetic deafness, including those which require a dual-vector approach. Akouos's platform is designed to enable the delivery of genetic material to the sensory epithelium of the human cochlea using the AAVAnc80 vector. Here we review our platform data from rodent and non-human primate models, the approach for eventual intracochlear delivery in humans, and experimental data that support a strategy of intracochlear administration of AAVAnc80 to recover hearing in humans.

SYMP 12

Moving Gene therapies for Hearing Loss into the Clinic

Jonathan Whitton
Decibel Therapeutics

Moving gene therapies for the inner ear from proof-of-concept studies to a therapeutic for patients requires deep understanding of the construct's behavior. The intervention window must be translationally tenable, capsid and promoter performance must be understood not only in rodent disease models, but also non-rodent species, and the immune response of the inner ear to capsids and transgenes must be considered for patient selection and trial design. This presentation will describe the development platform at Decibel Therapeutics that we have put in place to address these key areas through an example from one of our gene therapy programs.

SYMP 13

Optimizing Delivery of Molecular Therapeutics to the Inner Ear

Hinrich Staecker
University of Kansas Medical Center, Kansas City, KS, USA

Our increased understanding of the underlying causes of many hearing disorders has led to the development of molecular therapeutics to address a variety of disorders. The CGF166 (Atoh1) human clinical trial has enhanced our ability to model and understand the delivery of viral vectors to the human inner ear and serves as a model for understanding the translation of a range of molecular therapeutics into clinical trials. Key issues emerging from this study are identification of appropriate models for preclinical testing development of improved testing to aid in patient selection and optimization of delivery approaches.

SYMP 14

Biohybrid Cochlear Implants: An Approach for Molecular Therapy in Cochlear Implantation?

Jennifer Schulze[1]; Eva Rohde[2]; Thomas Lenarz[1]; Hinrich Staecker[3]; Mario Gimona[2]; **Athanasia Warnecke**[1]
[1]Hannover Medical School, Hannover, Germany; [2]Paracelsus Medical University, Salzburg, Austria; [3]University of Kansas Medical Center, Kansas City, KS, USA

Sensorineural hearing loss is associated with molecular and structural changes of the inner ear. The cochlear implant as treatment of choice offers a unique opportunity to deliver cells and drugs directly to the inner ear. Cell-based approaches to deliver not only a protective cocktail to the auditory neurons but also to alter the cochlear environment are currently under investigation. Preparing the cochlea for implantation and directing immunological responses in the inner ear towards improved wound healing for the stabilization of the cochlear environment and for the prevention of insertion damage are long-term goals. We will present clinically applicable diagnostic and therapeutic approaches towards this aim.

Speech Perception

PD 1

Age-Related Changes in Phonetic Cue Usage: Contributions to Speech Understanding in Noise

Mishaela DiNino[1]; Lillian Behm[2]; Yunan Charles Wu[1]; Barbara G. Shinn-Cunningham[3]; Lori L. Holt[1]
[1]Carnegie Mellon University Department of Psychology; [2]Hamilton College; [3]Carnegie Mellon University Neuroscience Institute

Older adults, even those with normal hearing thresholds (NHTs), experience greater difficulty understanding speech in noisy environments compared to young adults. This perceptual impairment is attributed to decline in temporal processing from slower auditory neural conduction and/or age-related cochlear synaptopathy—synaptic damage observed with normal aging in animals and in human histological examinations. Poor temporal processing abilities are associated with poorer speech-in-noise understanding, but the specific mechanism by which impaired temporal encoding decreases speech-in-noise perception is unknown. This study utilized a cue-weighting paradigm to investigate age-related changes in perceptual weighting of temporal and spectral phonetic cues for speech sound categorization, which may contribute to older individuals' challenges perceiving speech in noise.

Previous research has found that young adults with NHTs rely primarily on voice onset time (VOT), the interval between stop consonant release and subsequent voicing onset, to categorize /b/ and /p/ speech sounds in quiet. In noise, the VOT dimension is masked and listeners make greater use of a secondary acoustic dimension, fundamental frequency (F0), than they do in quiet to the extent that, in some cases, F0 becomes the primary cue to /b/-/p/ category identity in noise. In a prior investigation, older adults with self-reported normal hearing relied more on F0 compared to younger adults when categorizing /b/ and /p/ in quiet, suggesting that normal aging precipitates a shift to reliance on spectral dimensions for speech categorization even in quiet listening conditions.

The current study investigated this potential influence of normal aging on VOT and F0 cue weights and whether the tendency to rely on spectral dimensions is exacerbated in noise. Adults aged 18-30 and 40-55 with NHTs performed a /bir/-/pir/ (*beer* vs. *pier*) categorization task in quiet and in speech-shaped noise. Older adults' responses were less well-predicted by acoustic content in both listening conditions. However, both younger and older listeners switched reliance from VOT to F0 to categorize speech sounds when noise was added. Further, for each group, the degree of F0 weighting in noise was significantly correlated with performance on a word-in-noise comprehension task. These results suggest that normal aging reduces one's ability to utilize both spectral and temporal acoustic dimensions for speech categorization, and support past work showing that perceptual cue weighting strategies shift to accommodate the listening situation. This study provides evidence that aging can negatively impact perceptual strategies that are advantageous for understanding speech in noise.

PD 2

Effects of Age on the Electrophysiological Correlates of Continuous-speech Processing

Juraj Mesik[1]; Lucia A. Ray[2]; Magdalena Wojtczak[3]
[1]University of Minnesota; [2]Department of Psychology, Carleton College; [3]Department of Psychology, University of Minnesota

Speech-in-noise comprehension problems are commonly reported by aging individuals, yet traditional speech tests are insensitive to this deficit, especially in the absence of clinical hearing loss. Recent electronecephalography (EEG) work on young normal-hearing adults has demonstrated that high-level features related to speech semantics elicit strong centro-parietal negativity in the EEG signal around 400 ms post-stimulus, but only in cases where participants actively attend to and comprehend the target speech [Broderick et al. (2018), Current Biology 28, 803-809]). Here we test whether this methodology is sensitive to age related effects on the neural correlates of speech-in-noise understanding, and the self-reported difficulties therewith.

Younger (18-40 years) and older (41-70 years) adult participants with normal audiometric thresholds were subdivided into groups with and without self-reported difficulty with speech-in-noise understanding.

While recording noninvasive EEG from 64 surface electrodes, participants were diotically presented with two simultaneous audiobooks (65 dB SPL each), and their task was to attend to one of them. After each ~60 sec block, audio was paused and participants responded to several comprehension questions about the target story, as well as their sense of confidence for each response, general intelligibility, and state of attentiveness.

Audiobook transcripts of both the attended and ignored stories were separately used to generate time-aligned features related to the "semantic" dissimilarity of each word relative to the preceding context. These features were then regressed against the EEG signal to estimate

the temporal response function (TRF) for both the attended and ignored stories.

Semantic dissimilarity features were related to robust TRF negativity 300-500 ms post-stimulus for the attended story only, replicating existing results by Broderick et al. (2018).

In this study we explore group differences in the attended and ignored TRFs, as well how these measures relate to behavioral data. For each experimental group we will perform correlation analyses between the TRF amplitude between 300-500 ms, and behavioral measures of speech comprehension, subjective confidence, and attentiveness. These analyses will be used to determine if the "semantic" TRFs provide a viable measure of experienced speech-understanding deficits in normal-hearing adults.

Preliminary data suggest that using high-level semantic regression features in analysis of EEG responses to narrative speech is a promising approach for isolating neural signals related to comprehension and intelligibility. If proven to be a sensitive tool, these methods may inform diagnosis of speech processing deficits within populations with clinical and sub-clinical hearing impairments. [Supported by NIH grant R01DC015462].

PD 3

Challenging Speech Perception: A Potential Role for Individual Differences in Perceptual Learning

Karen Banai; Limor Lavie
University of Haifa

Speech perception, especially under challenging conditions (e.g., when speech is rapid or in noisy environments) is characterized by substantial individual differences. Both sensory and cognitive factors contribute to this individual variation, but they do not explain it in full. Another process that contributes to speech perception is recalibration, a form of perceptual learning which allows listeners to adapt to new variations in the speech stream. A large body of work suggests that multiple aspects of speech perception are subject to perceptual learning (for review see Samuel and Kraljic, 2009), but to our knowledge, the potential contribution of this learning to individual differences in the perception of challenging speech has not been studied. To this end, we now ask whether listeners who show faster perceptual learning of one form of challenging speech (time-compressed speech, TCS), also enjoy better speech perception of other forms of challenging speech -- natural-fast speech (NFS) and speech in noise (SIN). In this talk, data from three experiments (n = 45-80 each) conducted in listeners with various ages and hearing levels will be presented. All listeners underwent an assessment of TCS learning. The perception of NFS and SIN were assessed separately. Working memory, attention and vocabulary were also assessed in some of the listeners (45 older adults with hearing loss and 55 normal-hearing young adults). Across ages and hearing levels, perceptual learning of TCS was significantly correlated with speech perception. Even after accounting for the potential correlations among different indices of speech perception, as well as for the potential contribution of working memory, attention and vocabulary, perceptual learning accounted for more than 10% of the variance in speech recognition. Learning of both SIN and NFS takes substantially longer to emerge than the duration of assessment in the current study, making it unlikely that observed performance of these tasks reflects practice effects. Therefore, we suggest that the current findings are consistent with the notion that a general perceptual learning capacity, which is partially distinct from speech perception, serves to support speech processing under adverse listening conditions.

PD 4

Understanding Different Forms of Degraded Speech as an Auditory Skill

Stephen C. Van Hedger[1]; Ingrid Johnsrude[2]
[1]Western University; [2]The Brain and Mind Institute, Western University

Background
Listeners can quickly adapt to several forms of degraded or otherwise challenging speech. This rapid learning may occur through reorienting attention to the most diagnostic features for recognition – a process that should be independent of the specific degradation and should rely on higher-order cognitive processes. Here, we tested these assumptions by assessing whether understanding diverse forms of degraded speech is a general skill related to cognitive processing.

Method
Participants transcribed 120 spoken sentences, manipulated in five ways meant to challenge recognition (noise-vocoded speech, sinewave speech, time-compressed speech, accented speech, and speech-in-babble). The manipulations were blocked, allowing listeners to adapt and learn over the course of the sentences. Participants heard 24 sentences for each manipulation, and no feedback was provided. Following the sentence transcribing task, participants completed a fluid intelligence assessment (Raven's advanced progressive matrices). In a second session, participants

completed linguistic and non-linguistic measures of working memory (n-back, reading span, and sentence repetition).

Results

Mean performance on the five types of speech was significantly intercorrelated, supporting the view that understanding degraded speech can be conceptualized as a general skill independent of the particular acoustic degradation. Performance on the different forms of degraded speech was also significantly associated with Raven's matrices and working memory measures; however, the association with the working memory measures was weaker and Raven's matrices performance mediated the relationship between n-back and degraded speech performance. Finally, while all manipulations displayed positive learning slopes (i.e., better performance on the final trials compared to the first trials), fluid intelligence and working memory were only associated with accented speech learning.

Conclusion

These results suggest that there are reliable individual differences in the ability to understand diverse acoustic degradations to the speech signal. The relationship of degraded speech understanding to cognitive functioning (fluid intelligence and working memory) presumably exists because listeners must engage in a kind active hypothesis testing of what was said, holding multiple interpretations in mind until predictions can be refined based on contextual constraints of the sentences. The absence of a relationship between cognitive measures and the learning slopes of the manipulations, with the exception of accented speech, suggests a possible dissociation of processes underlying the rapid (seconds-to-minutes) learning of degraded speech.

PD 5

Examining listener's use of cross-modal temporal cues in audiovisual speech perception

Kaylah Lalonde[1]; Destinee Halverson[2]
[1]Boys Town National Research Hospital; [2]Western Washington University

Experiments were conducted to examine the hypothesis that correlations between acoustic speech energy and visible articulatory movements of the mouth and jaw help listeners to follow the amplitude envelope of speech and predict the timing of changes in acoustic energy. Young adults with normal hearing and normal or corrected-to-normal vision participated in a series of behavioral experiments. In the first experiments, we used a moving window to measure the mean instantaneous correlation between the area of the mouth opening and the amplitude of the corresponding portion of the acoustic speech signal, over the duration of 72 syntactically correct, semantically anomalous sentences. We examined whether natural variation in the cross-modal correlations across sentences could predict stimulus differences in degree of audiovisual benefit to masked speech detection and recognition. Results failed to replicate previous findings that sentences with higher cross-modal correlations result in greater audiovisual detection benefit. However, at low signal-to-noise ratios, sentences with higher cross-modal correlations were associated with greater audiovisual recognition benefit. These results are consistent with previous neurophysiological data indicating that cross-modal correlations help the auditory cortex to track the amplitude envelope of speech. Additional experiments were undertaken to examine whether these correlations can help predict the timing of upcoming acoustic speech information. We compared speech recognition thresholds with an auditory carrier phrase to conditions with an audiovisual carrier phrase. In both conditions, the target speech was presented in an auditory-only format, eliminating any potential to use visual phonetic information. In the absence of visual phonetic information about the target speech, adults tested in a two-talker masker benefited 1.5 dB from visual information in the carrier phrase.No benefit was observed in a spectrally-matched noise masker. This result suggest that visual speech serves as a grouping cue that helps to build the auditory stream and recover from perceptual masking. In ongoing follow-up experiments, we are examining whether this benefit results from predicting the timing of the speech target. Specifically, we have disrupted the timing of the target acoustic speech by inserting a variable-duration silent segment between the carrier phrase and target. If the audiovisual carrier phrase helps by predicting the timing of the target, this manipulation is expected to eliminate the benefit of the visual speech in the carrier phrase. The results of these experiments have implications for theories of audiovisual speech perception.

PD 6

Taking Attention Away from the Auditory Modality: Behavioral and Electrophysiological Effects on Continuous Speech Processing

Zilong Xie[1]; Bharath Chandrasekaran[2]
[1]Department of Hearing and Speech Sciences, University of Maryland, College Park, MD; [2]Department of Communication Sciences and Disorders, School of Health and Rehabilitation Sciences, University of Pittsburgh

Continuous speech processing often unfolds in multisensory contexts, wherein listeners may need to

prioritize signals from sensory modalities other than audition. An example is driving a car while listening to the radio. Selective attention is thought to be a critical mechanism underlying the ability to select the sensory modality most relevant for the task at hand. To date, it remains less understood whether and how crossmodal attention affects continuous speech processing when sensory inputs from other modalities (e.g., vision) are prioritized. For studies within the auditory modality, selective attention negatively influences the processing of deprioritized continuous speech. Thus, the current study aims to determine the extent to which crossmodal attention impairs continuous speech processing when sensory inputs from *vision* are prioritized.

Young, normal-hearing adults (N = 16) performed a dual-task that involved a primary visuospatial *n*-back task of either low (0-back) or high (3-back) task demand, while a concurrently secondary listening task on audiobook narrative stories (~ 60 s). The visuospatial *n*-back tasks contained a sequence of blue squares and the goal was to compare each square with a target square for position match. The target was always the first square in the sequence for the 0-back condition and was the one 3-positions back in the sequence for the 3-back condition. Cortical electrophysiological responses were recorded while participants performed each condition. A behavioral measure on continuous speech processing was also obtained by asking multiple-choice comprehension questions related to the story content.

Our results demonstrated that participants responded to the visuospatial stimuli with lower accuracy and slower response time in the 3-back condition compared to the 0-back condition, confirming that the manipulation of visual task demand was successful. Regarding the continuous speech stimuli, behavioral speech comprehension accuracy was reduced with increasing visual task demand (3-back < 0-back). In contrast to behavioral findings, paradoxically, the neural encoding of segmental features (e.g., phonetic features) in continuous speech was enhanced with higher visual task demand (3-back > 0-back), while the neural encoding of suprasegmental features (e.g., envelope and fundamental frequency) may be *un*affected by visual task demand (3-back = 0-back)

The dissociation between the behavioral and neural findings warrants further investigations into the exact neural locus of behavioral costs on continuous speech processing in the context of crossmodal attention.

PD 7

Active Listening: A Framework for Generating and Recognizing Speech

Emma Holmes[1]; Noor Sajid[1]; David Quiroga-Martinez[2]; Thomas Parr[1]; Cathy Price[1]; Karl Friston[1]
[1]Wellcome Centre for Human Neuroimaging, UCL; [2]Center for Music in the Brain, Aarhus University

Speech recognition is a complex problem. The auditory system receives a continuous acoustic signal and, to understand the words spoken, must parse the continuous signal into discrete words ("speech segmentation"). To a naïve listener, the acoustic signal provides few cues to indicate where words begin and end. Furthermore, even when word boundaries are clear, there exists a many-to-many mapping between lexical content and the acoustic signal. This is because speech is not 'invariant'—words are always heard in a particular context. Here, we introduce active listening: a unified framework for generating and recognizing speech.

We introduce a generative model of spoken words (which can be used to generate speech) and an accompanying inversion scheme (for recognizing speech). We treat speech recognition as an active Bayesian inference problem. The scheme is based on active inference—a first principle account of perception and action that has been applied to a variety of domains in cognitive neuroscience, including active vision. In brief, it assumes that the unified goal of perception and action is to maximise the evidence for our (generative) model of the world.

Our approach considers the processes for segmenting speech and inferring the words that were spoken—which are often considered in isolation—as complementary. The generative model specifies how an acoustic signal is generated, given the causes of a spoken word: i.e., 'what' word is spoken (lexical), 'how' is it spoken (prosody), and 'who' speaks it (speaker identity)? The 'active' component is the placement of word boundaries at particular positions within the continuous acoustic signal. The placements of word boundaries are considered as internal actions, similar to (covert) saccades in visual scene analysis. For each possible word interval, the likelihoods of model parameters are evaluated—and the interval with the greatest evidence is selected (c.f., attentional selection). We demonstrate that spoken sentences can be iteratively recognised and generated under this model.

The validity of the model is established using simulations: we show that the words that the model recognizes within a spoken sentence depend on prior expectations about the

content of the words, as is the case for human listeners. Also, simulated neuronal responses resemble human electrophysiological mismatch and P300 responses.

Crucially, active listening considers speech recognition within a neurally plausible framework. It establishes plausible causes for neural responses to speech. In future work, the model will be used for simulating human conversations, voice recognition, speech-in-noise perception, and music.

PD 8

Cognitive Resources are Recruited Highly Consistently Across Individuals During Story Listening

Matthew T. Bain[1]; Björn Herrmann[1]; Ingrid Johnsrude[2]
[1]Western University; [2]The Brain and Mind Institute, Western University

Degraded speech encoding as a result of hearing loss increases the load on cognitive processes and makes listening effortful. Standard hearing assessment relying on audiometry or speech-in-noise testing does not capture this cognitive impact of hearing impairment. Moreover, speech-in-noise testing requires individuals to listen to isolated sentences that are not personally relevant and lack a broader context. Listeners may not engage well with such materials, and as a result these approaches may not tap into the mechanisms recruited in listening situations of everyday life when people are motivated to comprehend what they are hearing. Dual-task paradigms have been successfully used to characterize the cognitive load imposed by speech processing, but again have relied on artificial, isolated sentence materials. The current study explores a novel approach to capture the temporal dynamics of cognitive load during listening to real-world, engaging stories, under conditions where listening is challenging but manageable.

Sixty participants (42 female, mean age: 21.1 years) performed a dual task, in which they listened to two engaging stories, each 13.5 minutes long, and were asked comprehension questions at the end of each story. Concurrently with each story, visual letters were presented at pseudorandom points in time on a computer screen (approx. every 10 s) and participants had to categorize upper-vs lower-case letters as fast as possible with a keypress. Response times (RTs) were taken as a measure of cognitive load, with longer RTs indicating greater load. Using a subgroup sampling of data from multiple participants, response time courses with a 0.5 Hz resolution were extracted. Inter-time-course correlation and permutation analyses revealed that RT time courses were significantly correlated across participants (story 1: r = .41, p = .0113; story 2: r = .33, p = .0252), suggesting consistent cognitive load across individuals. A post-experiment questionnaire revealed that, on average, participants rated story 1 as more absorbing than story 2, possibly explaining why story 1 was a more robust driver of behavioural performance, although this difference was not significant. These results suggest that the way cognitive resources are recruited during listening to natural, engaging stories is consistent across participants. High consistency in cognitive resource recruitment among young, normal-hearing individuals opens the exciting possibility of a measure with high sensitivity to abnormality. Such a measure would have high ecological validity and could be used to detect, for example, individuals who find listening to be unusually effortful when background noise is present.

Special Session in Memory of Shigeyuki Kuwada

Chair: Laurel H. Carney

SYMP 15

Peakers, Troughers and Tweeners

Tom C. T. Yin
Dept. of Neurophysiology, University of Wisconsin-Madison

I only worked with Shig for 3 years but we bonded for life. I owe Shig a special debt as he was responsible for directing my research interests to the auditory system after I arrived in Madison. He was a driving force in the field of binaural hearing and an inspiration for generations of colleagues. My title reflects Shig's penchant for coining witty, short-hand descriptors, in this case to categorize the cells in the inferior colliculus that we studied. But it also serves as a metaphor to his own life and career, which had an unusual number of peaks and troughs. Undoubtedly, he began life in a trough: he was born in a Japanese internment camp in Canada shortly after the bombing of Pearl Harbor. His academic career also had a rocky start but he managed to get a Ph.D. in psychobiology and to find a faculty position at Antioch College where he was a popular and successful teacher. Here's where he was a tweener: he found great satisfaction and joy in teaching but felt that his destiny lay in research. So he gave up his tenured faculty position to become a post-doc at Wisconsin. Quickly his natural talent as a researcher shone through. He asked probing questions, was passionate about the research, was clever with his hands, and worked hard. From the seminal papers that Shig published in Madison, he was offered a faculty position at the University of Connecticut

where he rose to the peak of an academic career with a steady diet of NIH funding, talented students and post-docs, and study section duties.

He was a man of many different talents. He was always in good humor with a hearty belly laugh that filled every room so it was fun to do science with Shig. He was enthusiastic about every last detail of the work, even the mundane ones and was particularly skilled at coming up with a novel way to fix a problem and then go into his shop to design the perfect tool. He was full of scientific insights and new ways to look at the data. He was generous in sharing his insights and time to help others. He was a master woodworker who turned out exceptional museum-quality furniture. Some of you may also have experienced his skills at the poker table. The auditory community has suffered a great loss.

SYMP 16

The Kid, the Curmudgeon, and the Rabbit: Recollections from the Kuwada Lab's Early Days

Terrence R. Stanford
Department of Neurobiology & Anatomy; Wake Forest School of Medicine

Building your first neurophysiology laboratory from scratch is not easy. Neither is getting your first R01 or training your first graduate student. It's even tougher when your first graduate student is a 22 year old, fresh out of college, with virtually no useful research experience. Most scientists in such circumstances would be reticent to eschew a tried and true experimental model system to pioneer a new one that is likely to be viewed with suspicion by one's scientific peers. Well, as we all know, Shig Kuwada could never be confused with most scientists. And so I (the kid in the story) am here to recount goings on during some of the earliest days of Shig's lab. In the process, I'll touch on Shig's unshakable confidence in a Dutch Belted future, his ability to motivate by example (among other more subtle ways of manipulation), his uncanny ability to sense when his flagging student needed a pat on the back or a kick in the butt, and most importantly, his unwavering faith in the primacy of scientific truth. I don't know of anyone who has experienced a modicum of success in academia who doesn't recount crucial lessons learned from his/her Ph.D. thesis advisor. I'm no exception and it's hard to overstate the impact that training with Shig has had on the trajectory of my own career. Indeed as time passes and I reflect on all that's transpired in the 37 years since I crossed the threshold of Shig's lab, the line connecting the dots between then and now has never been more clear. Thank you Shig. I owe you much. You are truly missed.

SYMP 17

From Cochlear Nucleus to Cortical Evoked Potentials: Two Decades of the Neurophysiology of Monaural and Binaural Hearing with Shige San

Ranjan Batra
Dept. of Neurobiology and Anatomical Sciences; University of Mississippi Medical Center

Shigeyuki Kuwada (1942 – 2019) was a driving force in the neurophysiology of sound localization, and I had the honor of working with him for over two decades. Our collaboration yielded insights into the processing of sounds from the cochlear nucleus to the auditory cortex. The techniques we used spanned the range from evoked potentials to extracellular recording to recording intracellularly and staining the studied neurons. Along the way, we worked with other people in Farmington and elsewhere, such as Doug Fitzpatrick, Doug Oliver, Duck Kim, Tino Trahiotis, Terry Stanford, Kent Morest and Tom Yin.

Among our results were:

• A demonstration that a scalp-recorded potential, the amplitude-modulation following response, reflected hearing losses of subjects on a frequency-by-frequency basis;

• Multiple lines of evidence that responses to binaural stimuli in the inferior colliculus reflect more than the convergence of an excitatory input from one side with either an excitatory or inhibitory input from the other;

• Establishing that tuning to interaural temporal cues in envelopes of high-frequency sounds is as sharp as that to similar cues in the fine structure of low-frequency sounds in the inferior colliculus;

• Showing that spatial tuning improves along the auditory neuraxis, and that in the thalamus tuning is near-optimal for a broadly tuned system;

• Multiple demonstrations that pentobarbital anesthesia alters responses of neurons in the auditory pathway;

• Establishing that the superior olivary complex encodes interaural temporal cues for sound localization in two ways and localizing the different mechanisms to different areas; also demonstrating that both mechanisms are based on coincidence detection.

While doing top-notch science, we also shared many geeky experiences: exploding amplifiers, "Fressens" of Chinese take-out during late-night recording sessions, complete chip-swaps of functional equipment and an anticipated trip to Stockholm that fizzled.

Shige had a larger-than-life personality that will be sorely missed.

SYMP 18

You Stick'em, I'll Stain'em and how Shig's AMFR was a Blast

Douglas L. Oliver
Department of Neuroscience, University of Connecticut Health Center

Shig Kuwada was my colleague, collaborator, friend, and teacher from his arrival at the UConn Health Center in 1981 until his retirement. We were co-investigators on each other's NIH projects for 31 years. Everything I learned about auditory physiology, I learned from Shig. This knowledge allowed me to pursue new types of experiments that used auditory physiology to pose hypotheses about the circuitry of the auditory system. I would like to share some of my memories from my first and last collaborations with Shig. At the beginning, we were exploring the relationship between the morphology of the neurons in the inferior colliculus and their binaural response properties. At the end, we were using Shig's amplitude modulation following response (AMFR) method to blast mice and measure threshold shifts after exposure to impulse noises for the Navy. These collaborations illustrate the great breadth of Shig's knowledge, his creativity, and his intense passion for science.

SYMP 19

Gain Control by Local Circuits in the Inferior Colliculus: The Legacy of the Rabbit

Shobhana Sivaramakrishnan
Departments of Otolaryngology and Neuroscience, West Virginia University

Neurons in the central nucleus of the inferior colliculus (ICC) that receive and convey acoustic information between the brainstem and cortex form extensive local circuits. Beginning with recordings in awake rabbits and continuing with recordings in awake mice, we have found that local ICC circuits modify response gain and ensure that relevant features of acoustic codes emerge in the ICC. Long-range inputs to the ICC and local ICC circuits modify response gain in specific regions of an acoustic signal, and local ICC circuits fill in for regions of brainstem input that lack the range required for ICC acoustic codes. First spike latency, characteristic frequency, nonmonotonicity, the onset component of responses and the bandwidth of frequency response areas are driving components inherited from the lower brainstem. Dynamic range, peak firing rates, sustained components of firing and best frequencies are among relevant acoustic codes that emerge locally in the ICC. The strength of ascending brainstem input drives the strength of local synaptic connections between ICC neurons, effecting local gain control that is stimulus specific. The selectivity of ICC circuits is made possible by stimulus-specific temporal changes in neuronal membrane conductances and asymmetric synaptic strength between locally connected neurons. Voltage-gated calcium channels recruit ICC neurons into circuits that control the dynamic gain of responses to sound frequency and level. Topographic gradients in synaptic rise times and plasticity create temporal gradients in local circuits within and across frequency laminae and cell-type specific recurrent microcircuits facilitate or suppress spectral properties of acoustic stimuli through changes in the local excitatory-inhibitory balance.

In ongoing work, we are evaluating the factors that determine the strongest local connections. We examine local synaptic drive between nearest neighbors within the same broad topographic region, neurons separated topographically, or morphological similarity. Calcium- and voltage-sensitive dyes are used to optically image local ICC circuits activated by inputs from the cochlear nuclei. Altogether, these data show that ICC microcircuits segregate according to the requirements of acoustic codes. The extensive ramification of local axon collaterals in the ICC might be necessary to synergize different ICC regions into producing canonical correspondence between long-range and local influences to drive salient acoustic coding in the auditory midbrain.

Supported by: NIH R01 DC008120; DC008120-05 S1; R56 DC008120

SYMP 20

Transformation in ITD Processing in the Auditory Pathway: From Superior Olivary Complex to Auditory Cortex

Douglas C. Fitzpatrick
Dept. of Otolaryngology, University of North Carolina School of Medicine

The Kuwada lab primarily studied interaural time difference processing through single unit recordings at different levels of the auditory system. The preparation was the unanesthetized rabbit, chosen because the effects of anesthesia are profound and should be avoided when possible. The recordings were made throughout the auditory system, including the superior olivary complex, nuclei of the lateral lemniscus, inferior colliculus, medial geniculate body and auditory cortex. Here, I will describe some of the transformations in representation as the information ascends.

The initial sites for binaural interaction and extraction of ITD are the medial and lateral superior olives (MSO and LSO). In these nuclei the tuning to ITDs is broader than

at higher levels, so one transformation is a sharpening of the ITD tuning, which occurs relatively sequentially at each subsequent level. Still the final product is a broadly-tuned population code, because single neurons do not have the necessary sensitivity for behavioral discrimination, so pooling across neurons is required. The significance of a broadly-tuned code is that multiple sources cannot be represented simultaneously, but must be placed in memory over time as they appear as single sources from the dynamics of the sound environment. This is true even if the slopes are sharp enough to discriminate with high acuity, since one slope can provide an edge in the display, but not multiple peaks.

Another transformation between the olivary nuclei and higher levels is the degree of contralaterality of sound sources. The MSO represents primarily contralateral sources while the LSO primarily ipsilateral. At higher levels the representation in each hemisphere is primarily contralateral, although less so in the cortex than the intervening nuclei. This change from a mixed to a primarily contralateral representation is presumably produced by the crossed excitatory pathway from the LSO and uncrossed pathway from the MSO.

A further change is in temporal integration. Delays seen in slopes of phase vs. (monaural) frequency plots are less than ~5 ms in the MSO and LSO, while in the IC and above they can extend to 50 ms. Similarly, interclick intervals for 50% recovery in ITD-tuned neurons show an increase between the olives and colliculus and again between colliculus and cortex.

Finally, slopes of spike rate changes as a function of interaural correlation (IAC) are more often linear in the SOC than in the IC or cortex. Thus, higher levels show an increased sensitivity to small changes in IAC.

SYMP 21

OFF inhibition to the Inferior Colliculus: a Computational Study on its Functions in Coding Speech

Yan Gai
Department of Biomedical Engineering, St. Louis University

We previously developed a systems model for the inferior colliculus (IC) with several ascending monaural and binaural pathways to account for gap detection and forward masking. Several neuron types were captured by Hodgkin-Huxley models, with the key element being the simulation of “OFF response” (i.e., neural discharges after the termination of a sound) using a model of the superior paraolivary nucleus (SPON). The SPON model contains a hyperpolarization-activated h current and a T-type calcium current. The goal of the present study was to explore the responses of SPON neurons to speech sentences at low frequencies, and its contribution to speech encoding in the IC. Populations of auditory nerves with mixed spontaneous rates spanning the frequency range of 150 and 2000 Hz provided input to cochlear-nucleus bushy and stellate cells, which further projected to the SPON and other nuclei. Spectrograms of speech sound were compared to population responses at various stages of the model at different speech intensities. We hypothesize that, at low frequencies, SPON may create a temporal-sharpening effect in the IC response to speech. The model can reproduce several key properties exhibited by Shig’s earlier physiological work. He had helped with the initial model construction to the point I thought deserving a coauthorship, but he only wanted to be acknowledged. I believe people can nonetheless see the effort and spirit sparkling in his own work and in those he helped.

SYMP 22

Auditory Distance Coding using Amplitude Modulation Depth

Pavel Zahorik[1]; Laurel H. Carney[2]; Duck O. Kim[3]
[1]Dept. of Otolaryngology and Communicative Disorders & Dept. of Psychological and Brain Sciences, Univ. of Louisville; Heuser Hearing Institute, Louisville, KY; [2]Depts. of Biomedical Engineering and Neuroscience, University of Rochester; [3]Department of Neuroscience, University of Connecticut Health Center

This talk will describe and summarize a project designed to explore the question of how sound source distance is encoded in the auditory system. Sound intensity and the ratio of direct to reverberant sound energy (D/R) are thought to be the primary acoustic cues to perception of sound source distance. Although the encoding of intensity in the auditory system is well understood, the intensity cue is intractably confounded with acoustic power at the sound source, and thus can only be useful in conjunction with assumptions regarding source power. D/R does not suffer from this shortcoming, but it was unclear at the time how this acoustic information might be encoded in the auditory system. Our project tested the hypothesis that D/R can be encoded indirectly through analysis of the amplitude modulation (AM) characteristics at the listener’s location. In reverberant sound fields, AM depth was found to systematically very with distance, and this variation was predictable based on the modulation transfer function (MTF) between source and receiver. Under Shig’s leadership, we then tested this hypothesis from the combined perspectives of animal neurophysiology, human psychophysics, and computational modeling. This multi-pronged approach

was Shig's idea, and throughout the project he maintained frequent and enthusiastic communications with the research team members, reminding us all how science can be both rewarding and fun. Working with Shig and experiencing his creativity, ingenuity, character, and wisdom are all aspirational experiences that will never be forgotten. We consider ourselves deeply fortunate to have had the opportunities to work with him, and to see first hand the impact he has had on the field.

SYMP 23

Remembrance of Shig Kuwada

Duck O. Kim
Department of Neuroscience, University of Connecticut Health Center

It is a great privilege for me to have collaborated with Dr. Shigeyuki ("Shig") Kuwada over the past fourteen years. This was an enjoyable and productive collaboration. Until this time, each of us had pursued separate auditory research while interacting informally for decades. Our formal collaboration was a new venture for both of us involving virtual auditory space (VAS) methods. We were both excited to incorporate VAS methods into in vivo single-unit physiology, particularly in an unanesthetized mammalian preparation. For the latter, Shig is widely recognized by colleagues. Shig brought to life his inborn talents in designing and creating many elegant and efficient devices, e.g., a circular rail for positioning a point sound source around 360 degrees, a "trapeze" that held the large rabbit pinnas upright while allowing us to rotate the pinnas leftward or rightward. Shig's pragmatic instincts frequently guided our strategies. To compare the rabbit's head/ears with a rigid sphere, Shig said "of course, we should make measurements in real rigid spheres" [a racquetball and a mini-basketball]. These devices allowed us to measure head related transfer functions (HRTFs) in an anechoic chamber and binaural room transfer functions (BRTFs) in moderately- and strongly-reverberant chambers. One of Shig's sons, Clinton ("Casey"), who was an Otolaryngology Resident at University of Connecticut Health Center at that time, conducted measurement of HRTFs of human subjects (Kuwada et al., OHNS 2010). These works on rabbits and humans provide valuable information about acoustic signals in the ear canals for sound sources in various distances and directions. Shig accomplished integrating his rich insights from many years of research conducted with non-VAS binaural stimulation with the findings made in the VAS-based research. Collaborators in this research included Drs. Pavel Zahorik (Univ. Louisville) and Laurel Carney (Univ. Rochester). Shig often said to me, "if I would start my auditory research career all over again, I would start with VAS-based experiments". I always replied to him, "that makes sense." On a personal note, I witnessed how he coped with the devastating news of a stage-four pancreatic cancer. Interacting with him during the last eight or nine months of his life touched me in a way I have not experienced before in my life. Shig was at peace with himself and with people around him even in the face of his impending death. This experience is a precious gift from Shig that I deeply cherish.

Binaural Processing with Hearing Impairment

Chairs: Sean Anderson & Jonas Klug

SYMP 24

Auditory Motion Perception in Noise for Listeners with Cochlear Implants and with Normal Hearing

Michaela Warnecke[1]; Ruth Y. Litovsky[2]
[1]University of Wisconsin-Madison, Waisman Center, 1500 Highland Ave, Madison, WI, 53705, United States; [2]The University of Wisconsin–Madison

In everyday environments, listeners and objects are often in motion. Understanding the cues that affect auditory motion perception is challenging, because sound displacement co-varies with sound velocity and duration. Over the last four decades, most research on auditory motion perception has aimed to understand the effects of duration and velocity on change in location required to perceive sound source movement, i.e., the minimum audible movement angle. Notably, the majority of these studies has exclusively tested normal-hearing (NH) individuals, and very little is known about how auditory motion is perceived by listeners with hearing impairments.

To date, only one study has compared auditory motion perception in NH listeners and individuals who are deaf and fitted with bilateral cochlear implants (BiCIs). That study utilized sounds of different durations and angular displacements. Results showed that NH listeners generally outperformed BiCI users, who struggled to distinguish between stationary and moving sounds of various durations and angular displacements tested. Further, BiCI users showed bias towards classifying all sounds as moving rather than stationary (Moua, Kan and Litovsky, JASA, 145, 2498-2511, 2019).

In our natural environment, moving sounds co-occur with other events, but it is unknown whether we can detect auditory motion while attending to another sound's feature. We are interested in understanding how auditory motion perception is impacted by the presence of other concurrent sounds. NH and BiCI participants were seated in a sound proof room facing a horizontal array of loudspeakers [– 90β (left) to + 90β (right)]. Target stimuli

were band-limited noise tokens that could be either stationary or moving. Virtual auditory space stimuli were implemented to pan the sounds over a subset of the loudspeaker array. The distractor stimulus was always stationary, varied from intelligible speech to noise, and presented simultaneously with the target stimulus on half of the trials. On both distractor-present and distractor-absent trials, participants were asked to indicate the perceived target sound motion using a button-press on a small screen in a 2-AFC task. Perceptual measures of auditory motion included identifying whether a sound was stationary/moving.

This work aims to provide an improved understanding of binaural abilities using electric hearing in complex auditory environments, and has the potential to provide insight for improved engineering approaches for BiCIs.

Work supported by NIH-NIDCD (R01DC8083) and NIH-NICHD (U54 HD090256).

SYMP 25

Neurophysiological Measures of Binaural Processing – from the Lab to the Clinic

Lindsey N. Van Yper; Jaime A. Undurraga; Juan Pablo Faúndez; David McAlpine
Department of Linguistics, The Australian Hearing Hub, Macquarie University, Sydney, Australia

Binaural hearing – particularly the ability to process interaural time differences or ITDs – underpins sound source localization and speech understanding in complex acoustic environments. Accordingly, impaired binaural listening impacts real-life listening, and auditory rehabilitation programs should therefore aim at restoring binaural hearing. Identifying binaural processing difficulties, as well as optimizing binaural input in hearing-impaired listeners is challenging, not least because behavioural measures of binaural hearing are time-consuming, difficult to perform, and not standardly implemented in the clinic. A need exists for simple objective measures of binaural hearing. In this talk, I will discuss the potential of electrophysiological measures to assess binaural hearing in the clinic, and their utility in populations with various degrees of hearing impairment.

SYMP 26

Frequency Limit of ITD Sensitivity in Normal Hearing and Hearing Impaired Systems – Experimental Data and Model

Helen Heinermann; Jonas Klug; Sven Herrmann; Go Ashida; Jörg Encke; Mathias Dietz
University of Oldenburg

For young normal hearing listeners, previous studies have identified a frequency limit very close to 1400 Hz where an abrupt cliff-like increase in threshold interaural time difference (threshold ITD) is observed. Here, we report threshold ITDs as well as correct rates for a broader range of age and hearing statuses. We investigate if individual high-frequency limits much below 1400 Hz are still cliff-like or more gradual. A physiologically inspired model of the auditory pathway suggests that the duration of the excitatory input to the medial superior olive causes the steep upper frequency limit in young normal hearing listeners.

SYMP 27

Aided Loudness and Speech Perception Outcomes in Children and Adults with Extended Bandwidth Hearing Aids

Maaike Van Eeckhoutte; Danielle Glista; Paula Folkeard; Robin O'Hagan; Susan Scollie
National Centre for Audiology, University of Western Ontario, Canada

The Desired Sensation Level (DSL) algorithm prescribes age-dependent gain across frequencies and input levels for the fitting of hearing aids. The current version, DSL v5.0, was developed to provide targets between 0.2 and 8 kHz, in the interest of providing a broad audible band of speech, and prescribes targets for each ear independently. The hearing aids available at the time of development did not routinely provide audible output across the bandwidth of the targets and audibility was often achieved up to 4-5 kHz. However, modern hearing aids can provide gain above this frequency range.

The aim of this study was to investigate the effect of providing gain at such a full or extended bandwidth on several outcome measures in children and adults wearing actual, modern hearing aids. An additional interest of the study was to examine if the loudness is balanced between the ears when fitted to DSL v5.0 targets, or if listeners with asymmetric hearing loss may require different listening levels per ear.

Providing the full bandwidth resulted in audibility of peak maximum audible output frequencies exceeding 4-5 kHz. It also led to an improvement in consonant discrimination in noise scores, attributable to a better perception of /s/, /z/, and /t/ phonemes. However, aided loudness perception and preferred listening levels did not significantly change. Most listeners (79-85%) had either no subjective preference or some preference for the extended bandwidth condition. Preliminary results indicate that listeners with asymmetric hearing loss

prefer slightly less gain than currently prescribed in their worse ear than in their better ear, and that the relation depends on the asymmetry between ears.

The results suggest that providing the maximum bandwidth available with modern hearing aids can be beneficial for the tested populations.

SYMP 28

Binaural Hearing in Single-Sided Deafness with a Cochlear Implant

Sebastian Ausili
University of Miami

In single-sided deafness (SSD), a cochlear implant (CI) is applied in an attempt to restore binaural hearing. Owing to the large discrepancy in perception of sounds between one normal hearing ear and a second deaf ear with a CI, the effect of fitting a CI on spatial hearing needs to be carefully addressed. Our experiments indicate a benefit in sound localization, but also the potential disadvantage of increased listening effort. Furthermore, we discuss the pros and cons of CI over other treatments for the SSD population.

SYMP 29

Using Temporal Envelope ITD Sensitivity to Match Electric and Acoustic Hearing in Patients with Unilateral Cochlear Implants and Residual, Contralateral Acoustic Hearing: Localization and Speech Perception Outcomes

Coral Dirks[1]; Peggy Nelson[1]; Andrew J. Oxenham[2]
[1]Department of Speech-Language-Hearing Sciences, Center for Applied and Translational Sensory Sciences, UMNTC; [2]Department of Psychology, Center for Applied and Translational Sensory Sciences, UMNTC

Current cochlear implant (CI) fitting strategies aim to maximize speech perception through the CI by allocating all spectral information across the electrode array without detailed knowledge of the tonotopic placement of each electrode along the basilar membrane. For patients with considerable residual hearing in the non-implanted ear, this approach may not be optimal for binaural hearing. This study uses binaural temporal envelope beat sensitivity to estimate frequency-to-electrode matching in the CI ear. Objective and subjective outcomes will provide new information on binaural interactions in this patient population and guide methodology for frequency-matching remapping efforts. [Work supported by NIH grant F32DC016815-01.]

SYMP 30

Binaural Processing in Children with Asymmetric Hearing Who Listen with Bimodal Devices

Melissa J. Polonenko[1]; Karen A. Gordon[2]
[1]University of Rochester Medical Center, Rochester NY USA; [2]Hospital for Sick Children, Toronto ON Canada

Binaural hearing is important for listening in and navigating everyday acoustic environments. Children with asymmetric hearing loss who hear with bimodal devices (one cochlear implant and one hearing aid) benefit from bilateral input and can quickly detect changes in levels between electric and acoustic stimuli. However, bimodal users experience significant device (electro-acoustic) and hearing loss related timing delays that distort brainstem and cortical processing of timing cues and likely contribute to their poor sensitivity to interaural timing cues. Consequently, children may rely on their ability to detect level cues and perhaps other strategies to localize sound and listen in noise.

SYMP 31

Comparison of Single Cell Spike Rate and Timing in the Brainstem in Response to Cochlear Implant and Acoustic Stimulation

Michaela Müller[1]; Barbara Beiderbeck[1]; Benedikt Grothe[2]; Michael Pecka[2]
[1]Graduate School of Systemic Neurosciences, Ludwig-Maximilians-Universitaet, Munich; [2]Biocenter, Section of Neurobiology, Department Biology II, Ludwig-Maximilians-Universitaet Munich

The cochlear implant (CI) allows for the functional restoration of hearing. Unfortunately, sound localization is still severely limited in patients with bilateral CIs. Interaural time difference (ITD), the dominant cue for sound localization, is based on the integration of inputs from both ears by brainstem neurons. However, the processing differences during electrical stimulation are unknown. We obtained electrophysiological recordings from neurons in the gerbil brainstem in response to electrical and acoustical click-train stimuli. We observed significantly higher spike probability and reduced jitter for the electrically stimulated cells. These differences are likely to result in profound consequences for binaural processing.

PD 9

An Extended Model of the Characteristics of Spontaneous Otoacoustic Emissions in Lizards

Geoffrey A. Manley[1]; Pim Van Dijk[2]; Hero Wit[2]
[1]University of Oldenburg; [2]University of Groningen

Lizard ears are robust emitters of spontaneous otoacoustic emissions (SOAE). Each species produces its own spectral patterns and each ear differs in this regard. Comparing spectra across lizard families indicates that especially the tectorial membrane (TM), which varies widely between families, strongly influences the spectral patterns. The most obvious effect of a thickened, continuous TM is to reduce the number of SOAE peaks and increase their amplitudes when compared to ears that have no – or a subdivided - TM.

Previous models of hair cells as the originators of SOAE have shown that linear arrays of coupled oscillators can produce many of the patterns observed in lizard SOAE spectra. Nonetheless, the spectral peaks produced by those models were far too narrow and had uncharacteristic spacing when compared to real lizard spectral data. The work described here examines in more detail the factors responsible for the characteristic spacing of spectral peaks, for the bandwidth of these peaks, for the frequent presence of spectral “plateaus”, but also studies the origin of variability of spectra within a given species.

The model consists of a chain of oscillators linked by reactive and/or dissipative coupling. The natural frequencies applied to the oscillators were set – as in most lizard species tonotopically between 1.0 and 5.0 kHz, but the number of oscillators varied, being either 21 or 201. The striking overall effect is that to produce clustering of oscillators into isolated frequency peaks, there must be some dissipative coupling, but that the reactive coupling constant is the primary parameter that also determines how many peaks appear. Importantly, the spectral pattern does not vary with the number of oscillators; the larger array generates the same number of spectral peaks and frequency plateaus as the smaller array (Fig. 1). If we assume that these oscillator elements represent hair cells, this result could explain the fact that SOAE peak numbers and frequency spacing in lizards does not correlate with the number of hair cells. Increasing the coupling strength along the tonotopic axis can reproduce the commonly-observed increasing frequency gaps between the peaks towards higher frequencies. Varying various parameters with frequency, e.g., the effective damping, the roughness and/or the noise (Fig. 2) created more realistic peak widths and introduced more individuality in the spectra, including inducing amplitude plateaus. This model can thus explain the combinations of factors underlying the various SOAE patterns of lizard papillae.

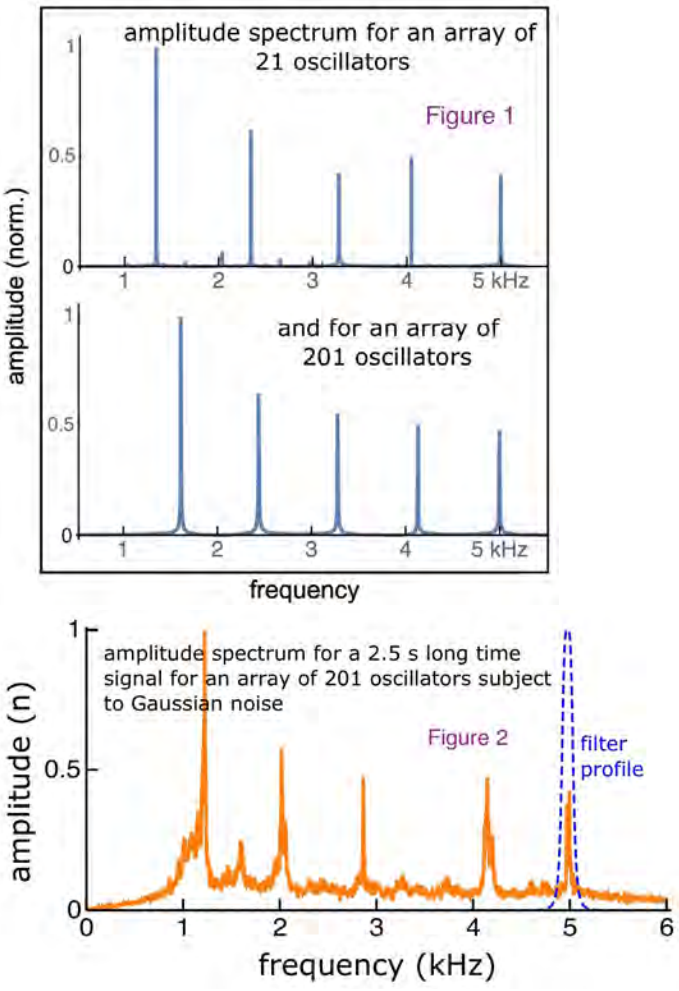

PD 10

Effects of Voltage and Membrane Cholesterol on Prestin Conformation: Insights from Molecular Dynamics Simulations

Jashan Sandhu; Richard D. Rabbitt; **Tamara C. Bidone**
University of Utah

Membrane cholesterol is known to modulate prestin-associated somatic electromotility in outer hair cells and electromechanics in the intact cochlea (1,2), implying the lipid environment is likely crucial to the function of prestin in hearing. Here, we used ns-long all-atom molecular dynamics simulations to examine how prestin and membrane lipids interplay to respond to varying levels of membrane cholesterol under excitatory electric fields. We built a 3D model of prestin, with eight transmembrane spanning segments and two helical re-entry loops, embedded in POPC lipid bilayer at 310

°K. We studied the molecular dynamics of the system by varying electric field, from 0.001 to 0.1 V/nm, and cholesterol fractional concentration 0-0.5 relative to POPC. Simulations revealed a negative correlation between concentration of membrane cholesterol and the mean square displacement of both POPC lipids and prestin residues, supporting the idea that cholesterol controls both POPC diffusion and prestin conformational fluctuations. These results are consistent with the idea that cholesterol depletion reduces prestin confinement by perturbing POPC motility. Our results also show that the presence of an electric field decreases the radius of gyration of prestin when cholesterol is present but has the opposite effect in the absence of cholesterol, demonstrating that prestin electromotility is sensitive to cholesterol levels. Cholesterol, in particular, is predicted to restrict the fluctuations of the two helical re-entry segments of prestin, while the electric field enhances the fluctuations of the inner core of the protein. Moreover, during the ns-long molecular dynamics simulations (under isometric zero net strain boundary conditions), the solvent accessible surface area of POPS increases in response to the electric field, while that of prestin decreases, supporting the idea that membrane elongation and prestin shrinking are combined molecular mechanisms in OHCs. Collectively, our results demonstrate that membrane voltage and cholesterol interplay to modulate prestin fluctuations at the molecular level by changing membrane dynamics. These mechanisms, upon first inspection, are consistent with larger conformational and physical changes at the cellular level.

Support: NIDCD R01-DC006685

References

[1] Sfondouris et al. 2008 J. Biol Chem 283: 2247-81
[2] Brownell et al. 2011 Pflugers Arch 461: 677-86

PD 11 WITHDRAWN

A Case To Re-Evaluate Baseline Shifts Of The Basilar Membrane -- 30 Years Later

Eric L. Le Page
Oaericle Australia

In the 1980s two studies of basal-turn basilar membrane (BM) displacement records were published. The first using a capacitive probe, required draining of the scala tympani to make the measurement. (LePage, JASA1987v82p139). It included records of summating potential (SP) measured simultaneously. Both dc displacement and SP showed tuned behaviour together with polarity reversals. These data did not display the classically accepted tuning behaviour and were rejected as pathological records, despite being the first data to show clear similarity between dc mechanical and dc electrical behaviours. The second study reconstructed Cook's fiber optic lever (FOL), (LePage, Hear. Res1989v38 p177). It did not require draining of scala tympani but exhibited large displacements of the BM of up to several micrometers, in response to tone bursts of varying sound levels. The raw data showed behaviour never seen from a cochlear mechanical measurement. They resembled muscle contractions. These too were inconsistent with expected enhanced vibratory tuned response of the cochlear amplifier (CA). The FOL data have recently been reprocessed to separate the dc components before each tone burst (blue curve) and with burst onset (red curve) resembling a classically tuned BM response (Figure). The peak amplitude is a rapid displacement of over 5µm at the tuned frequency. As will be shown, when computed over one cycle of each tone, the "vibration" amplitude is ca5nm, while the corresponding velocities are 100µm/s -- consistent with accepted data. Cooper and Rhode (1992) re-evaluated the dc-shift proposition under similar conditions, finding no evidence for them. A key difference between the two sets of measurements is that the FOL delivered a clean signal over a linear displacement range of 20µm whereas the laser interferometer, chosen for its high sensitivity, had a displacement range of 1% of that required here, necessitating extensive stitching and fast computation. Hence, the possibility exists that the compression mechanism is exclusively an *ac-amplifier* is a beguiling misconception. If these contractions are a mechanical analogue of the SP (summating), it predicts 1) the somatic motor (Brownell etal 1985) may act directly upon the tectorial membrane to stimulate the inner hair cells, 2) the need for an intermediary, fast, CA is a necessary consequence of the unquestioned assumption that the BM motion is always a vibration which needs to be comb-filtered at the stimulus frequency to remove high-level asynchronous noise, 3) the vulnerable tip segment may not be due to a vibration at all, explaining the phase irregularity.

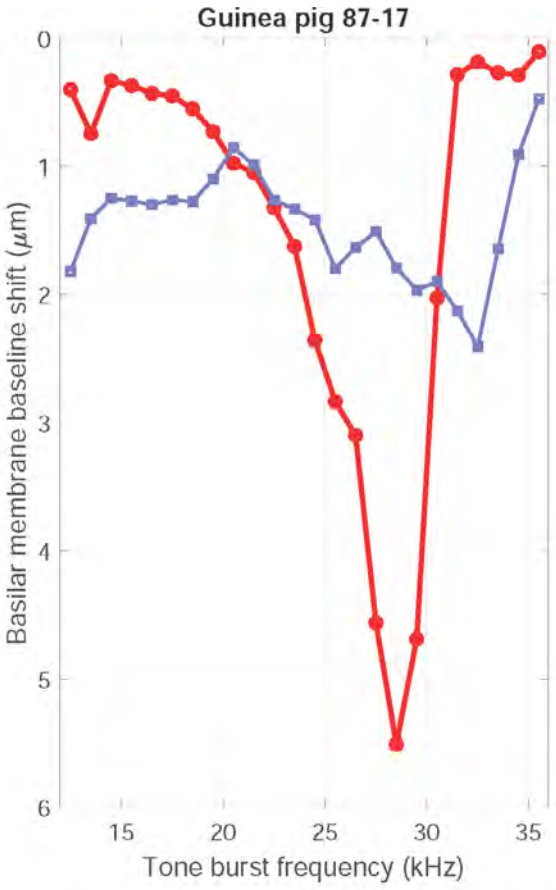

PD 12

Properties of the Traveling Wave measured with Optical Coherent Tomography (OCT)

Marcel van der Heijden; Anna Vavakou; Nigel P. Cooper
Erasmus MC, Rotterdam

Using OCT we recorded the mechanical response of the basilar membrane and the Deiters cells region to multi-tone (zwuis) stimuli in the basal turn and hook region of gerbil cochleae, with characteristic frequencies spanning 13 to 45 kHz. By recording the response to the same stimulus at multiple longitudinal locations we were able to analyze the basic properties of the traveling wave: wavelength, phase velocity, group velocity, and spatial gradients of displacement magnitude. We studied how these wave properties depend on stimulus frequency, longitudinal location and sound pressure level (SPL). For low and moderate SPLs, wavelength at the characteristic place ("peak region") varied from ~400 μm for the lowest CFs (13-16 kHz) to ~800 μm for the highest CFs (40-45 kHz). Wavelength in the peak region increased systematically with increasing SPL. High-SPL wavelength values typically exceeded low-SPL wavelength by a factor of ~1.5, suggesting a twofold reduction of effective stiffness with increasing SPL. Wavelength did not decrease indefinitely when the wave traveled beyond its peak, but instead leveled off to a value of ~65% of the wavelength at the peak. For low-SPL traveling waves, phase velocity dropped sharply at a location ~0.5 mm basal to the peak. This transition from the initial fast portion of the wave to the subsequent slow-wave portion became less abrupt at higher SPL. Group velocity basal to the peak was >20 m/s. Near the peak it dropped to 1-2 m/s for low SPLs and 2-4 m/s for high SPLs. Group velocity did not further decrease in waves traveling beyond their peak; in fact it increased slightly. The latter observation contradicts predictions of resonance based models ("critical boundary layer") in which the group velocity decreases indefinitely beyond the peak.

We discuss the functional implications of these wave properties and explore the possible mechanisms underlying them.

PD 13

Acoustic Coupling between Active Oscillators Explains Identical-Frequency Spontaneous Otoacoustic Emissions from the Two Ears

Daibhid O Maoileidigh[1]; Yuttana Roongthumskul[2]; AJ Hudspeth[3]
[1]Department of Otolaryngology - Head & Neck Surgery, Stanford University; [2]Department of Physics, Faculty of Science, Chulalongkorn University; Howard Hughes Medical Institute and Laboratory of Sensory Neuroscience, The Rockefeller University; [3]Howard Hughes Medical Institute and Laboratory of Sensory Neuroscience, The Rockefeller University

Spontaneous otoacoustic emissions (SOAEs) may be driven by active oscillators within the inner ear, but there remains debate about the mechanism of their production. In particular, it is unclear why some animals emit sounds with identical frequencies from their two ears. In most nonmammalian tetrapods, widely open Eustachian tubes connecting the middle ear to the oral cavity allow acoustic coupling between the eardrums that might influence SOAE production. We hypothesize that each ear, including the eardrum, acts as an active oscillator driven by mechanical activity in the inner ear and that identical-frequency SOAEs arise from acoustic coupling between these active oscillators.

We record SOAEs simultaneously from the two ears of the tokay gecko and find several identical-frequency SOAEs that are synchronized, synchronization rules out the possibility that their frequencies are coincidentally identical. A mathematical model describing the eardrums as active oscillators acoustically coupled by the air in the Eustachian tubes and oral cavity produces

synchronized, identical-frequency SOAEs. In agreement with our experimental observations, the model captures the frequency-dependent phase differences between ears, the complex alterations in emissions upon suppression of the contralateral ear by static pressure, the change in emission frequency as the contralateral oscillator's peak frequency is varied, the synchronization of emissions as the peak frequencies converge, and the dependence of some SOAEs on the emission strength of the contralateral ear.

The extensive agreement between our experimental observations and mathematical model implies that some SOAEs are produced by the ear's acting, as a whole, as an active oscillator. Moreover, the model predicts that the ears' activities enhance the localization of weak sound sources. The frequency response and interaural vibration-amplitude difference between the two ears depend on the location of the sound source, but these dependencies decline as the activity is reduced. The two ears of a gecko evidently function together as a single active system that is sensitive to the location of weak sound sources.

PD 14

Nonlinear Cochlear Mechanics Without Direct BM Vibration-Amplification Feedback.

Alessandro Altoè[1]; Christopher A. Shera[2]
[1]Caruso Department of Otolaryngology - Head and Neck Surgery, University of Southern California; [2]University of Southern California

The classic, "textbook" view of active cochlear mechanics postulates that the cochlear amplifier and the vibration of the basilar membrane (BM) operate in a tight, closed-loop feedback configuration. This particular arrangement generates sharply-tuned active forces, greatly enhancing the sensitivity and frequency selectivity of BM motion. However, this view of the active cochlea is hard to reconcile with cochlear mechanical data, both recent and classic, which appear to be best explained by the absence, rather than the presence of a strong BM vibration-amplification feedback loop.

One of the most striking features of the active cochlea is that whereas BM responses manifest large variations of sensitivity with sound level (and/or the health of the preparation), the corresponding response phase changes relatively little (phase-invariance). The approximate phase-invariance of BM responses imposes constraints on the level-dependent manifestation of the active forces that are not easily satisfied when assuming direct BM vibration-amplification feedback. Recent in-vivo recordings from the mammalian cochlea indicate that although the motion of the BM appears actively amplified and nonlinear over only a relatively narrow band of frequencies, the internal motions of the organ of Corti display these same features over a much wider range. The existence of broadly tuned nonlinear responses is not easily explained by sharply tuned active forces controlled by a BM vibration-amplification feedback loop.

We show that a simple, nonlinear 3-D model of the cochlea inspired by the work of Zweig (2015)—in which the direct BM vibration-amplification feedback characteristic of classic models has been "cut"—reproduces recent BM recordings from the mouse and the gerbil. The model preserves the phase invariance of the BM responses in a straightforward manner. Further, although the model BM responses are nonlinear over a relatively narrow frequency range (matching the in-vivo data), the model produces active, nonlinear forces over a much larger bandwidth, in good agreement with the picture of the cochlea now emerging from recent experimental data.

PD 15

Three-Dimensional Motion Pattern of the Human Inner Ear during Bone Conduction Stimulation

Stefan Stenfelt[1]; Mohammad Ghoncheh[2]; Patrick Maas[3]; Hannes Maier[4]
[1]Department of Clinical and Experimental Medicine, Linköping University, Linköping, Sweden; [2]Medical University Hannover, Department of Otorhinolaryngology, Hannover, Germany; [3]Oticon Medical AB; [4]Medical University Hannover, Department of Otorhinolaryngology, Hannover, Germany and Cluster of excellence Hearing4all

Bone conducted sound is vibration transmitted in the skull bone and soft tissues that interact with outer, middle and inner ear. Based on clinical findings with an interrupted or fixed ossicluar chain, sound perception from bone conduction is primarily from sound transmitted directly to the inner ear. Moreover, it has been shown that the vibration of the bone encapsulating the cochlea correlates with a hearing perception. Consequently, the vibration of the bone surrounding the inner ear is likely responsible for the sound generated inside the cochlea. However, how the bony vibration result in a sound has not been clarified. One issue is that the vibration mode and pattern of the cochlear bone has not been investigated. The aim of the current study is to investigate the vibration pattern of the bone surrounding the human inner ear during bone conduction stimulation.

The 3D vibration pattern of the human cochlear promontory bone was measured in cadaver heads. The cadaver heads' mastoid and ear canals was surgically

removed to provide a visual access to the cochlear bone. The cochlear promontory surface was smoothed resulting in an approximately 6x10 mm surface. During bone conduction stimulation, the 3D velocity of this surface was obtained at intervals of 2 mm using a Polytech CLV-3D laser Doppler vibrometer, resulting in a 3D velocity matrix of 24 points. Using these measurements, the 3D vibration pattern of the cochlear bone was extracted.

The vibration magnitude was similar for all positions in each measurement direction. The magnitude difference between directions was usually within 10 dB and the dominant vibration direction varied with frequency. When the phase was analysed, there were indications of a longitudinal wave with a wave speed close to 1000 m/s at low frequencies that decreased to around 500 m/s at frequencies above 1 kHz. The high wave speed indicate the near rigid-body behaviour at lower frequencies and a longitudinal wave transmission at higher frequencies. At some directions and at the highest frequencies measured, 5 to 10 kHz, the wave speed of the longitudinal wave decreased to merely 100 m/s.

The measurements indicate that there is very little compression and expansion of the cochlear space at low frequencies, and the primary response is caused by fluid inertial effects at these frequencies. At higher frequencies, compression and expansion of the cochlear space becomes more influential due to the decreased wavelength caused by increased frequency and decreased wave speed.

PD 16

Generation Mechanisms and Intracochlear Dynamics of Spontaneous Otoacoustic Emissions

Thomas Bowling; Haiqi Wen; **Julien Meaud**
Georgia Institute of Technology

Due to an active nonlinear feedback mechanism in the cochlea (called the cochlear amplifier), self-sustained oscillations called spontaneous otoacoustic emissions (SOAEs) can often be measured in the ear canal. While they do not play any functional role, SOAEs are a signature of the cochlear amplifier and provide insights into the fundamental biophysics of the cochlea. In mammals, two theories have been proposed to explain SOAE generation: local spontaneous oscillations of structures in the organ of Corti or a global phenomenon as predicted by the theory of coherent reflection. In that theory, the cochlea acts like a laser cavity; SOAE generation requires coherent reflection of traveling waves by inhomogeneities in the cochlear partition and amplification of the waves by the outer hair cells. While SOAEs in the ear canal provides some information about their generation in the cochlea, a more comprehensive view can be gained by examining their intracochlear response.

In this work, a physiologically motivated nonlinear computational model of the mammalian cochlea is used to study the mechanisms of SOAE generation. The model includes a one-degree of freedom middle ear model and is formulated in the time domain. Cochlear roughness is introduced in order to cause the reflection of forward traveling waves. Several methods are used to determine whether SOAE generation is a local or global phenomenon. For SOAE generation to be a global phenomenon, there must be sufficient reflection of reverse traveling waves by the stapes; the model is used to demonstrate that reduction in the magnitude of the reflectance at the stapes inhibits SOAE generation. The response of SOAEs on the basilar membrane are decomposed into forward and reverse waves to clarify how SOAEs correspond to cochlear standing waves. The effects of varying the stapes reflectance and roughness amplitude on the forward and reverse waves are examined. To test if SOAEs are generated locally, the stability of an isolated longitudinal cross-section of the organ of Corti is examined. Additionally, changes in the local properties of the organ of Corti (e.g. the viscoelasticity of the tectorial membrane) are shown to affect SOAE generation. The numerical results presented in this study support the fact that SOAEs are globally generated rather than the results of local spontaneous oscillations.

Research Funding: This research is funded by NIH grant R01DC016114.

Development: Patterning

PD 17

Characterization of Spiral Ganglion Neuron Subgroup Development Using Single Cell RNA-Seq

Tessa R. Sanders[1]; Matthew W. Kelley[2]
[1]Laboratory of Cochlear Development, National Institute on Deafness and Other Communication Disorders; [2]National Institute on Deafness and Other Communication Disorders, NIH

The afferent innervation to the cochlea is composed of spiral ganglion neurons (SGNs) which transmit mechanosensory input from the hair cells centrally to the cochlear nucleus as an electrochemical signal. Two populations of SGNs can be distinguished based on their morphology: Type 1 SGNs which constitute 90-95% of the total population, and form contacts with inner hair cells (IHCs); and Type 2 SGNs which constitute the remaining 5-10% of the total population and form contacts with outer hair cells (OHCs). Both

physiological and recent molecular studies have found that within the Type 1 population there are at least three subgroups of SGNs with distinct molecular and electrophysiological phenotypes. Given the complexity of auditory information that these neurons must encode, their phenotypic diversity is an important functional aspect of the spiral ganglion (SG). However, we know relatively little about the mechanisms which specify the different SGN subpopulations during development, or when these populations become molecularly and functionally distinct.

To profile the molecular changes in both the SGNs and their associated glial cells across the pre-hearing developmental period we undertook a high throughput single cell sequencing approach. At postnatal day 1 (P1) we have profiled 487 SGNs. 97% of the SGNs cluster into two closely related groups, defined by their expression of markers such as POU4f1 and CALB2. 3% of the profiled neurons formed a clear transcriptionally distinct cluster and likely represent the Type 2 SGN population. At embryonic day 16 (E16) we have profiled 429 SGNs. At this age the SGNs are more heterogeneous and broadly cluster into three closely related groups. Interestingly we did not identify any cluster which appeared to contain Type 2 SGNs, possibly indicating that they are not yet transcriptionally distinct from the Type 1s. In addition, we found that markers of mature Type 2 SGNs, such as Peripherin and TH were expressed by SGNs across all three transcriptional groups.

Overall this dataset provides us with wealth of information about the molecular development of SGNs. Current analyses are focusing on identifying exactly when different subgroups become molecularly distinct, and which transcription factors are involved in this specification. To aid these analyses we are currently profiling SGNs at more embryonic and postnatal timepoints. We are also analyzing the profiles of the glial cells present in the SG at these ages in order to understand how they may influence SGN development, and vice versa.

PD 18

Molecular Basis of Neuronal Diversification in the Mouse Cochlea

Brikha Shrestha[1]; Lorna Wu[2]; Lisa Goodrich[3]
[1]Dept. of Neurobiology, Harvard; [2]Dept. of Neurobiology, Harvard Medical School; [3]Harvard

Heterogeneity of Type I spiral ganglion neurons (SGNs), defined classically based on spontaneous firing rate (SR), is a fundamental feature of mammalian auditory circuits. The presence of a functionally diverse pool of SGNs is thought to be critical for sound encoding in the auditory nerve, contributing particularly to the wide dynamic range of the auditory periphery and hearing in acoustically complex environments. We recently showed that Type I SGNs are heterogeneous at the molecular level and established correspondence between molecular subtypes (Ia, Ib, Ic) and SR-based functional classes (high-SR, medium-SR and low-SR) in terms of known differences in anatomical projection and synaptic heterogeneity. We further showed that SGN subtype identities are shaped by hair cell-driven activity in SGNs. However, the molecular drivers of SGN diversification during development remain unknown. Here we report identification of the transcription factor Runx1 as a critical determinant of SGN subtype identity in mice, with important implications for efforts to reprogram SGNs.

Expression of Runx1 is detectable broadly in SGNs by E14.5, restricted to Ib and Ic SGNs by late embryonic stages, and maintained only in those subtypes thereafter. To determine if Runx1 plays a role in SGN differentiation, we generated conditional knockouts (*Runx1*^{CKO}) using an SGN-specific driver (*bhlhb5*^{Cre}/+ ; *Runx1*$^{F/F}$) and leveraged single cell RNA-sequencing (scRNA-seq) technology to assess neuronal identities. We found that loss of *Runx1* causes reduction in Type I SGN molecular diversity, resulting largely from shrinkage of Ic identity and concomitant expansion of Ia and Ib identities. Fate-mapping experiments revealed that perinatal Runx1 expression heralds Ib/Ic identity in adulthood, whereas conditional deletion of *Runx1* postnatally redirects differentiation of nascent Ib/Ic SGNs toward Ia identity. To assess how hearing is affected upon loss of *Runx1*, auditory brainstem response (ABR) recordings were performed. *Runx1*^{CKO} mice exhibited normal thresholds but larger peak 1 amplitudes at suprathreshold stimulus levels and steeper rate-level curves, consistent with expansion of the low-threshold SGN subpopulation (Ia), compared to controls. Our findings establish Runx1 as an important regulator of SGN subtype identity and position *Runx1*^{CKO} mice as a unique genetic model to study the functional and perceptual consequences of reduced SGN diversity. Additionally, molecular regulators such as Runx1 may represent effective entry points for reprogramming SGN identities as a way to restore diversity diminished by acoustic insult, pathology, or age.

PD 19

Shear forces drive precise patterning of hair cells in the mammalian inner ear

Roie Cohen[1]; Liat Amir-Zilberstein[1]; Micha Hersch[2]; Shiran Wolland[1]; Shahar Taiber[3]; Fumio Matsuzaki[4]; Svenn Bergmann[2]; Karen B. Avraham[5]; **David Sprinzak**[6]
[1]Department of Biochemistry & Molecular Biology, George S. Wise Faculty of Life Science, Tel Aviv University, Tel Aviv, Israel; [2]Department of

Computational Biology, University of Lausanne, and the Swiss Institute of Bioinformatics, Lausanne; [3]Department of Biochemistry & Molecular Biology, George S. Wise Faculty of Life Science, Tel Aviv University, Tel Aviv, Israel, Department of Human Molecular Genetics & Biochemistry, Faculty of Medicine and Sagol School of Neuroscience, Tel Aviv University, Tel Aviv, Israel; [4]Laboratory of Cell Asymmetry, RIKEN Center for Biosystems Dynamics Research, Kobe , Japan; [5]Department of Human Molecular Genetics & Biochemistry, Faculty of Medicine and Sagol School of Neuroscience, Tel Aviv University, Tel Aviv, Israel; [6]School of Neurobiology, Biochemistry and Biophysics, George S. Wise Faculty of Life Sciences, Tel Aviv University

The mammalian hearing organ, the organ of Corti, consists of a precisely organized checkerboard-like pattern of four rows of hair cells (HCs) interspersed by non-sensory supporting cells (SCs). How such precise patterning emerges during development is not well understood. Using a combination of quantitative morphological analysis and time-lapse imaging of mouse cochlear explants, we show that patterning of the organ of Corti involves dynamic reorganizations that include lateral shear motion, cell intercalations, and delaminations. A mathematical model, where tissue morphology is described in terms of the mechanical forces that act on cells and cellular junctions, suggests that global shear on HCs and local repulsion between HCs are sufficient to drive the tissue into the final checkerboard-like pattern. Our findings suggest that precise patterns can emerge during development from reorganization processes, driven by a combination of global and local forces in a process analogous to shear-induced crystallization in physics.

PD 20

The Role of LIN28B and Let-7 MiRNAs in Cochlear Tonotopic Specialization

Meenakshi Prajapati-DiNubila[1]; Angelika Doetzlhofer[2]
[1]Johns Hopkins University School of Medicine; [2]Johns Hopkins University

The inner ear cochlea is the organ responsible for the detection of sound. Its spiral-shaped sensory epithelium contains mechano-sensory hair cells (HCs) that transduce sound waves into neuronal signals. This sensory epithelium is tonotopically organized such that it detects high frequency sounds at the base of the spiral and low frequencies at the apex. Features of this tonotopic specialization include graded differences in cochlear epithelium width, in HC soma and stereocilia size, and in HC-specific gene expression. Little is known of the mechanisms that produce tonotopic specialization in the mammalian cochlea. Here, we investigate the role of the RNA binding protein LIN28B and the let-7 family of miRNAs in cochlear tonotopic specialization. The mutual antagonistic LIN28B and let-7 miRNAs are post-transcriptional regulators that control the expression levels of large numbers of genes in a dose-dependent manner. In the developing cochlea, opposing expression gradients of LIN28B and let-7s regulate the timing of cell cycle exit and HC differentiation. Interestingly, we found that these gradients persist during the maturation and specialization of HCs, with let-7s being highest expressed in basal HCs, and LIN28B being highest expressed in apical HCs. To determine the role of LIN28B and let-7 miRNAs in the tonotopic specialization of HCs, we manipulated LIN28B/ let-7 levels in the maturing cochlea using LIN28B or let-7g overexpressing transgenic mice. To determine if these manipulations disrupt frequency-specific HC function, we recorded Auditory Brainstem Responses (ABRs) from these mice. Our hypothesis predicts that LIN28B overexpression will result in a more 'apical' identity, which would disrupt the function of the basal (high frequency) region of the cochlea. Indeed, ABRs from these mice revealed a severe deficit specifically in high frequency hearing, compared to control littermates. Interestingly, these deficits worsen with age such that LIN28B overexpressing animals also develop mid frequency hearing deficits. Conversely, overexpressing let-7g during cochlear maturation show deficits specifically in low frequency hearing, compared to control littermates. HCs are mostly maintained in these mice, showing that the hearing deficits are not due to HC loss. We are currently examining whether LIN28B and/or let-7 overexpression disrupts the graded differences in gene expression and morphology along the tonotopic axis. For instance, we recently uncovered that overexpression of let-7g results in a loss of specialization of the width of the cochlear epithelium along the tonotopic axis. In summary, functional and morphological analyses suggest that the LIN28B/let-7 pathway plays a critical role in tonotopic specialization.

PD 21

Dual regulation of planar polarization by Wnt-dependent and -independent pathways in the developing mouse cochlea

Elvis Huarcaya Najarro[1]; Jennifer Huang[2]; Adrian Jacobo[3]; Lee Quiruz[4]; Nicolas Grillet[5]; Alan Cheng[1]
[1]Department of Otolaryngology-Head and Neck Surgery, Stanford University; [2]Toledo University; [3]Rockefeller University; [4]Stanford University; [5]Department of Otolaryngology – Head and Neck Surgery, Stanford University

Background

Planar cell polarity (PCP) signaling directs cell orientation within the plane of a cell sheet, leading to the

proper patterning that is fundamental to tissue assembly in multicellular organisms. PCP signaling consists of six “core” components whose asymmetric localization within a cell is a conserved molecular hallmark of planar polarization. However, little is known about the cue(s) that orient early core protein polarization. Wnt proteins have been implicated as polarizing cues in PCP, but investigating the role of Wnts in PCP has been impeded by the functional redundancy among Wnt proteins. In Wnt-producing cells, the generation of active Wnt proteins first requires lipidation by the O-acyltransferase enzyme Porcupine (Porcn). Lipidated Wnts are then transported intracellularly by the chaperone protein Wntless (Wls), prior to secretion into the extracellular space. In this study, to circumvent Wnt redundancy and uncover the role(s) of secreted Wnts in PCP in the embryonic cochlea, we genetically ablated *Porcupine* (*Porcn*) or *Wntless* (*Wls*).

Methods

Wls and *Porcn* expression analysis was carried out by immunostaining, qPCR and *in situ* hybridization (ISH). The *Emx2-Cre* and *Pax2-Cre* lines were used to ablate *Wls* and *Porcn* floxed alleles, respectively. *Wnt5a* cKO as well as *Vangl2* cKO and *Vangl2 Loop* animals were also examined. We analyzed PCP pathway by stereocilia bundle orientation and immunostaining of PCP core proteins in mutant and control animals. Wnt ligand expression analysis was performed by qPCR and ISH.

Results

Wls and *Porcn* expression was observed in the developing cochlea. In E18.5 *Emx2-Cre; Wls*$^{fl/fl}$ and *Pax2-Cre; Porcn*$^{fl/y}$ embryos, we found shortened cochlea and misrotated outer and inner HCs, both classic PCP defects. *Wls* cKO cochleae maintained the asymmetric localization of the PCP core components Vangl1/2, Celsr1, and Dvl3, but lost that of Fzd3/6 and Dvl1/2, suggesting differential dependence on Wnts. Confirming these findings, *Porcn* cKO cochlea also displayed aberrant Fzd6 and Dvl2 localization and maintained that of Vangl1/2. On the other hand, the localization of intrinsic cell polarity markers was preserved in HCs in Wnt-deficient cochleae. We identified seven candidate Wnt ligands for mediating PCP in the embryonic cochlea, and found that Wnt5a, previously shown to mediate PCP signaling, was dispensable for polarization of HCs and PCP proteins. Finally, we showed that *Vangl2* and *Wls* interact genetically to dually regulate the polarization of HCs in the cochlea.

Conclusion

Our study delineates a dual regulation by Wnt-dependent and -independent PCP signaling of HC polarization in the embryonic cochlea.

PD 22

High Resolution Imaging of Hair-Cell Ribbon Synapse Formation and Stabilization

Natalie Mosqueda[1]; Katie Kindt[2]
[1]NIDCD; [2]National Institute on Deafness and other Communication Disorders

Sensory hair cells are involved in the critical first step of transmitting sensory information to the brain. This initial relay between hair cells to afferent neurons relies on specialized ribbon synapses. In hair cells, the active zone region is dominated by ribbons, presynaptic structures that are located at the base of the cell. During development, ribbons are thought to form from cytoplasmic aggregates that coalesce at the base of the cells. In age-related and noise-induced hearing loss, the underlying pathologies are thought to be due to loss of ribbon synapses. Unfortunately, much of the work on ribbon synapse formation and loss has been performed on fixed samples. Currently, the *in vivo* dynamics of ribbons during these processes or whether ribbons are stable structures within hair cells, is not known.

To study ribbons *in vivo*, we examined synaptic ribbons in the larval zebrafish lateral line hair cells. These hair cells are advantageous because they are localized externally in clusters called neuromasts. This location, along with transparency of larval zebrafish, makes these cells accessible for *in vivo* imaging experiments. In contrast to mammalian cells where ribbon formation is thought to occur over a couple of weeks, ribbons in lateral line hair cells, form over several hours; thus, it is feasible to capture ribbon formation in its entirety. To visualize and understand the formation and stability of ribbons *in vivo*, we utilized a transgenic line *myo6b: RibeyeB-Mcherry* that labels the main protein component of the ribbon, Ribeye. For this study, we have used a diSPIM light-sheet microscope to visualize ribbon dynamics *in vivo*. This system allows us to visualize all ribbons in each neuromast with high resolution over the course of hours with minimal photobleaching.

Using this model and imaging system, we have verified the stability of ribbons in mature hair cells over minutes to hours. Over these time scales, we do not see fusion or loss of ribbons in mature hair cells. We are presently extending the time scale of our analysis of mature hair cells to days. In addition, we have begun to visualize ribbon formation during hair-cell development. In contrast to mature hair cells, we observe ribbon fusion events in developing hair cells at the base of the cell. In the future, we plan to visualize these events more closely at higher resolution using Airyscan confocal microscopy. Overall, this work will provide fundamental knowledge of ribbon synapse formation and stability.

PD 23

Early Development of Resident Macrophages in the Mouse Cochlea Depends on Yolk Sac Hematopoiesis

Takayuki Okano[1]; Ippei Kishimoto[1]; Koichi Omori[2]
[1]Dep. Otolaryngology, Head and Neck Surgery, Graduate School of Medicine, Kyoto University, Kyoto, Japan; [2]Dept. Otolaryngology - Head and Neck Surgery, Graduate School of Medicine, Kyoto University

Resident macrophages reside in all tissues throughout the body and play a central role in both tissue homeostasis and inflammation. Although the inner ear was once believed to be "immune-privileged," recent studies have shown that macrophages are distributed in the cochlea and may play important roles in the immune system thereof. Resident macrophages have heterogeneous origins among tissues and throughout developmental stages. However, the origins of embryonic cochlear macrophages remain unknown. Here, we show that the early development of resident macrophages in the mouse cochlea depends on yolk sac hematopoiesis. Accordingly, our results found that macrophages emerging around the developing otocyst at E10.5 exhibited dynamic changes in distribution and *in situ* proliferative capacity during embryonic and neonatal stages. Cochlear examination in *Csf1r*-null mice revealed a substantial decrease in the number of Iba1-positive macrophages in the spiral ganglion and spiral ligament, whereas they were still observed in the cochlear mesenchyme or on the intraluminal surface of the perilymphatic space. Our results demonstrated that two subtypes of resident macrophages are present in the embryonic cochlea, one being Csf1r-dependent macrophages that originate from the yolk sac and the other being Csf1r-independent macrophages that appear to be derived from the fetal liver via systemic circulation. We consider the present study to be a starting point for elucidating the roles of embryonic cochlear resident macrophages. Furthermore, resident macrophages in the embryonic cochlea could be a novel target for the treatment of various inner ear disorders.

PD 24

Wnt Signalling Regulates the Formation of Inner Ear Sensory Organs by Antagonizing Prosensory Signals

Magdalena Zak[1]; Vincent Plagnol[2]; Nicolas Daudet[1]
[1]UCL Ear Institute; [2]UCL Genetics Institute

The inner ear is composed of the auditory organ responsible for sound detection and the vestibular system providing the sense of balance and acceleration. The mechanisms controlling their embryonic formation in the early otocyst remain unclear. Our recent work has shown that several of the sensory organs arise by progressive segregation from a common 'pan-sensory' domain, in which Notch signalling propagates prosensory identity by lateral induction. Wnt/β-cateninsignalling is another pathway previously implicated in the development of the sensory organs, but its role in the sensory organ formation and whether it interacts with Notch in this context is unknown. Here, we show that in the developing inner ear Wnt signalling gradually expands in the dorsal part where it forms a gradient of Wnt activity. Our functional experiments in vivo revealed that Wnt signalling promotes non-sensory fate and the progression of Wnt activity coincides with the loss of neurosensory competence in the dorsal otocyst. Furthermore, Wnt antagonises Notch signalling and restricts the spatial pattern of Notch activity in the otocyst. These results suggest that Wnt signalling is part of the mechanism regulating formation and positioning of prosensory domains. RNA-Seq and bioinformatics analyses suggest that Wnt controls neurosensory specification by regulating the expression of proneural genes and inhibitors from bHLH and SRY-boxes families. Further investigation will show whether some of these genes are part of the mechanisms by which Wnt regulates prosensory organ formation in the otocyst.

A Multidisciplinary Approach to Tinnitus

Chairs: Rebecca M. Lewis & Josef P. Rauschecker

SYMP 32

The Holy Grail for Subjective Tinnitus? Seeking Standardisation amongst Heterogeneity

Deborah A. Hall
University of Nottingham Malaysia

In a recent comprehensive review of 86 studies reporting data collected from 16,381 patients, we identified 42 discrete tinnitus-related complaints which spanned physical and psychological health, quality of life and negative attributes of the tinnitus sound. This diversity in the personal experience of tinnitus makes it difficult to know what core set of complaints that should be measured consistently across clinical research studies in order to facilitate comparison of findings. This talk will update on progress achieved by the international COMiT initiative to identify minimum reporting standards using consensus-based decision making that has involved healthcare users and professionals. COMiT's approach made no assumption that a single set of measures is valid for evaluating the benefits gained by different therapies. Indeed, international health-care users with tinnitus, health-care professionals, clinical

researchers, commercial representatives, and funders identified different sets of outcomes for intervention approaches based on sound devices, psychologically informed therapies, and pharmaceutical products. Participants were highly discriminatory in their decision-making. “Tinnitus intrusiveness” was voted in for all three interventions. For sound-based interventions, the minimum set included “ability to ignore,” “concentration,” “quality of sleep,” and “sense of control.” For psychology-based interventions, the minimum set included “acceptance of tinnitus,” “mood,” “negative thoughts and beliefs,” and “sense of control.” For pharmacology-based interventions, “tinnitus loudness” was the only additional core outcome domain. This provides an important starting point for standardisation.

SYMP 33

Audiology Treatments for Tinnitus and Hyperacusis

Richard Tyler[1]; Ann Perreau[2]
[1]University of Iowa; [2]Augustana College

Tinnitus and hyperacusis can be devastating, causing emotional, hearing, sleep and concentration problems. Several counseling and sound therapies are effective to reduce the reactions. We utilize picture-based Tinnitus (and Hyperacusis) Activities Treatment. The counseling is individualized and interactive, and focuses on the primary functions affected. Sound therapy can be helpful for both tinnitus and hyperacusis patients. We recommend low levels of partial masking in most cases. Some hyperacusis patients also benefit from hearing aids that block the ear canal, attenuating and controlling the sound level getting to the cochlea.

SYMP 34

Mindfulness Based Tinnitus Stress Reduction: Tinnitus, Brain Functioning, Psychology & Mindfulness

Jennifer Gans
MindfulTinnitusRelief.com

Tinnitus within the framework of brain functioning, psychology, and current research into mindfulness is explored in this presentation. Habituation and the unblocking of the nervous system to facilitate tinnitus and hyperacusis healing is investigated within the framework of current research. Stress reduction plays a critical role in effective management of sound sensitivity disorders such as tinnitus and hyperacusis. Participants will examine the 8-week Mindfulness Based Tinnitus Stress Reduction (MBTSR) program and the online program, MindfulTinnitusRelief.com, developed and researched by the presenter at the University of California, San Francisco (UCSF).

SYMP 35

Emotional and Cognitive Impact of Tinnitus: Role of Frontostriatal Gating

Josef P. Rauschecker
Georgetown University

The opinion that tinnitus is a purely auditory disorder has long been discarded. The suffering caused by tinnitus in many patients, which ends in suicide in a large number of cases, is conveyed by brain structures outside the auditory system. Neuroimaging has provided hard evidence for an involvement of limbic structures in tinnitus, such as medial prefrontal cortex and the ventral striatum (n. accumbens). Connectivity studies have revealed changes in the connections between auditory and limbic systems in tinnitus sufferers. Conventional views consider these limbic brain changes as emotional “reactions” to tinnitus. However, given that stress and insomnia can modulate and exacerbate existing tinnitus, causality may go in the opposite direction: According to the “frontostriatal gating” theory, frontal cortex and the striatum together form a system for executive control of sensory-perceptual events. A broken frontostriatal gating system is no longer able to suppress or attenuate the tinnitus signal. If this view is correct, it opens powerful new avenues for the treatment of tinnitus.

Gene and Drug Delivery into the Inner Ear

PD 25

Gene Therapy Using RNA Interference with Concomitant Gene Replacement in a Mature Murine Model of TMC1-related Hearing Loss

Yoh-ichiro Iwasa[1]; Paul Ranum[1]; Seiji Shibata[1]; Hidekane Yoshimura[2]; Ryotaro Omichi[1]; Cody West[1]; Richard J.H. Smith[3]
[1]Department of Otolaryngology, Molecular Otolaryngology and Renal Research Laboratories; [2]Department of Otorhinolaryngology, School of Medicine, Shinshu University; [3]Molecular Otolaryngology and Renal Research Laboratories, Department of Otolaryngology—Head and Neck Surgery, Carver College of Medicine, University of Iowa; Interdepartmental PhD Program in Genetics, University of Iowa

Background
We have reported the beneficial effects of mutation-specific RNA interference (RNAi)-based gene therapy in preventing progression of hearing loss in both neonatal and mature *Tmc1*$^{Bth/+}$ mice. To generalize this methodology, we have developed a mutation-agnostic approach that uses RNAi to suppress both endogenous alleles while concomitantly providing gene replacement

with a wild-type construct engineered to resist RNAi-mediated silencing.

Methods
Heterozygous Beethoven mice (*Tmc1*$^{Bth/+}$) maintained on a C3HeB/FeJ background were used in this study. rAAV2/9 and rAAV2/2 carrying both an mU6-driven artificial miRNA construct, which was validated to suppress wild-type and mutant *Tmc1*alleles, and a CMV-driven mouse *Tmc1*construct, which was engineered to resist RNAi, were introduced into the inner ears of mice at P16-18 using the round window membrane/ canal fenestration (RWM+CF) technique we have described. Auditory function was evaluated by ABR and DPOAE, and hair cell preservation was evaluated by immunohistochemistry.

Results
Both rAAV2/9 and rAAV2/2 robustly transduced inner hair cells (~100%) although outer hair cell transduction was seen with only rAAV2/2. Hearing preservation in *Tmc1*$^{Bth/+}$mice treated with either vector was dramatic throughout the observation period (20 weeks), although results were better in rAAV2/2 treated animals. Immunohistochemistry showed absence of degeneration in virtually all inner hair cells at 20 weeks.

Conclusions
A mutation-agnostic approach using RNAi to suppress both endogenous alleles while concomitantly providing gene replacement with a wild-type construct that resists RNAi-mediated silencing is feasible and may be broadly applicable to both autosomal dominant and autosomal recessive hearing loss.

PD 26

Preclinical Testing of AAV9-PHP.B for Transgene Delivery to the Non-Human Primate Cochlea

Maryna V. Ivanchenko[1]; Killian S. Hanlon[2]; Maya K. Devine[3]; David P. Corey[1]; Casey A. Maguire[3]
[1]Harvard Medical School; [2]Harvard Medical School, Massachusetts General Hospital; [3]Massachusetts General Hospital

Hereditary hearing loss often results from mutation of genes expressed by cochlear hair cells. Gene therapy has recently made tremendous progress in animal models through adeno-associated viral vector transgene delivery to the inner ear. However, significant challenges remain before AAV-based technologies can be translated to the clinic. Recently our group reported transmastoid injection of an AAV9 capsid variant, PHP.B, via the round window membrane (RWM) in a cynomolgus monkey. PHP.B mediated efficient transgene expression of a GFP reporter in many cochlear cells including both inner and outer hair cells. However, results were inconsistent, as a second monkey injected with a lower dose showed extremely limited transduction, with no obvious transduction of hair cells. The difference might be attributed to steep dose dependency, a pre-existing immunity to the AAV vector, or the technical reproducibility of RWM injections in larger mammals.

In order to further define the transduction potential of AAV9-PHP.B we performed a dosing study and assessed GFP expression in the cynomolgus macaque inner ear after RWM injection of AAV9-PHP.B via the transmastoid route. Four animals were studied and four doses tested. Three female juvenile/adult macaques were administrated with doses of $1x10^{11}$ genome copies (gc) (n=1), $2x10^{11}$ gc (n=1), $3.5x10^{11}$ gc (n=2), and $7x10^{11}$ gc (n=2); the fourth animal served as a vehicle (PBS) control. At the higher doses ($3.5x10^{11}$ and $7x10^{11}$ gc) AAV9-PHP.B transduced nearly 100% of both IHCs and OHCs, from base to apex. GFP staining was also present in the supporting cells of the organ of Corti, the spiral ligament, the spiral limbus, spiral ganglion neurons, and Reissner's membrane from the base to the apex. No specific anti-GFP staining was observed in the uninjected ear. However, at lower doses there was a steep reduction in viral transduction. In a cochlea administrated with $2x10^{11}$ gc we observed ~50% of IHCs and ~60% of OHCs transduced, and very limited transduction in a cochlea injected with $1x10^{11}$ gc. The steep dose dependency probably explains the limited transduction previously reported with a lower dose.

In conclusion, AAV9-PHP.B efficiently transduces the IHCs and OHCs of nonhuman primates, but shows a striking dose dependency. Together, these data support a feasible path towards clinical development of gene therapy for hereditary hearing loss with AAV9-PHP.B.

PD 27

Template-free Genome Editing Profiles are Biased in Postmitotic Hair Cells

Wei Xiong; Lian Liu; Jie Li
School of Life Sciences, Tsinghua University

Donor template DNA guided genome editing precisely corrects gene mutations as designed but the efficiency is so low that the approach is not suitable for in vivo gene therapy. Emerging evidence in dividing cells has shown that, without a template DNA, the end-joining based DNA repair profiles following CRISPR-Cas9 cleavage are non-random and largely dependent on target sequence context. However, it is still an open question concerning the editing profiles in primary terminal cells, the major

target cells for in vivo gene therapy. Here we analyzed the editing profiles of 115 gRNAs targeting 43 loci that are registered for harboring human deafness mutations resulting in hair-cell dysfunctions, by utilizing gRNA injectoporation delivery, FACS, and deep sequencing on postnatal cochlear tissues in culture. We found that, with the same gRNA, the DNA repair profile was highly biased in both tissue cells and dividing cells, but there was a more complicated pattern in tissue cells. Our work suggested that the reproducible and non-stochastic editing profiles pair with the collected gRNAs in postmitotic cells, which are valuable for instructing design of in vivo gene-therapy strategies to treat genetically induced hearing loss.

PD 28

Local Delivery of Adeno-Associated Virus Vectors with Neurotrophin Gene Prevents Reduction in Synapses and ABR Amplitude in Noise Exposed Rats

Subhendu Mukherjee; Ayesha Noman; Brandon T. Paul; Andrew Dimitrijevic; Joseph Chen; Vincent Lin; Trung Le
Sunnybrook Research Institute

Introduction
The root cause of sensorineural hearing loss (SNHL), a very common sensory impairment in humans, lies in the inner ear. SNHL often occurs because of damaged hair cells or spiral ganglion neurons. One exacerbating factor in SNHL is prolonged exposure to environmental noise leading to noise-induced hearing loss (NIHL), an important health concern which is often unrecognized and undertreated. The inner ear is one of the most challenging target organs for drug delivery. Systemic drug administration is not that effective because of the blood-labyrinth barrier. While the complexity of inner ear makes it very difficult for local drug delivery. ***In this study, we used magnetic targeting of superparamagnetic iron oxide nanoparticles (SPIONs) to deliver adeno-associated virus (AAV) vectors with neurotrophin gene locally into inner ear using an external magnetic field. We examined the effectiveness of magnetic delivery of growth factors for hearing preservation after NIHL in rat.***

Methods
Long-Evans rats were exposed to white noise to induce SNHL. AAV vector was coupled with brain-derived neurotrophic factor (BDNF) expressing gene and tagged onto SPIONs. The nanoparticles were delivered to the round window niche of the left ear 72 hr after noise exposure via a post-auricular incision. The right ear was used as control. An external magnet was placed on the contralateral ear to pull the virus through the round window into the inner ear. Immunofluorescence and qPCR were used to assess the expression level of BDNF, hair cells, and synaptic markers. Audiometry was used to evaluate the hearing.

Results
There was no adverse effect of local delivery of SPION on inner ear hair cells and hearing of non-deafened rat. We found an increased expression of BDNF in the cochlea of treated ears. Noise exposure caused reversible threshold elevation without having any significant effect on hair cell survival. But we found a permanent reduction of ABR amplitude and acute loss of synapses after noise exposure. Furthermore, delivery of AAV-BDNF substantially accelerate recovery of the threshold, recovered ABR amplitude reduction, and prevent the loss of synapses at high-frequency level in deafened rat.

Conclusion
Our results indicated that magnetic targeting can deliver virus-tagged nanoparticles efficiently into the inner ear. Also, the magnetic delivery of AAV.BDNF in inner ear protect synapses effectively and reduce the degree of NIHL. This work potentially has a significant clinical implication to provide an effective approach to the local delivery of the therapeutic drug to treat inner ear disorders.

PD 29

Supraparticle-Mediated Drug Delivery Supports Retention and Biodistribution of Neurotrophin 3 in the Guinea Pig Cochlea

Niliksha Gunewardene[1]; Yutian Ma[2]; Patrick Lam[3]; Rachael Richardson[4]; Frank Caruso[2]; Andrew Wise[4]
[1]Bionics Institute, Australia; [2]The University of Melbourne, Australia; [3]Bionics Institute, Australia, Department of Medical Bionics, The University of Melbourne; [4]Bionics Institute

The neurotrophin family of growth factors have long been established as potential therapy for hearing loss, however delivery of these factors into the inner ear at therapeutic levels over a sustained period of time has remained a challenge restricting clinical translation. We recently reported that intracochlear injection of a bolus dose of exogenous neurotrophin-3 (Ntf3) in the guinea pig cochleae was rapidly cleared from the cochlea, with almost complete elimination after 3 days. We therefore explored the potential of supraparticles for Ntf3 delivery into the inner ear. Supraparticles are compact spheroid structures comprised of smaller colloidal particles that provide a platform for long-term controlled release of therapeutics. Here, a radioactive

tracer was used to determine the loading, retention and distribution of Ntf3 delivered via supraparticles. Gamma measurements taken from ^{125}INtf3 loaded supraparticles revealed high drug loading capacities with elution over months. ^{125}INtf3 loaded supraparticles were surgically delivered to the guinea pig cochlea. Whole cochlear gamma measurements from supraparticle-implanted cochleae harvested at various time points revealed detection of ^{125}INtf3 in the guinea pig cochlea over time. Autoradiography analysis of cochlear micro-sections to compare the biodistribution of Ntf3 upon implantation is currently underway. Collectively, drug delivery into the inner ear using supraparticles support sustained, long-term release of neurotrophins in the inner ear. These findings can provide valuable information useful for the development of drug treatments for hearing impairment.

PD 30

A665-conjugated Acetylcysteine target prestin of outer hair cells with peptide hydrogel delivery preventing cisplatin-induced hearing loss

Jiaqi Pang[1]; Hao Xiong[1]; Yiqing Zheng[2]
[1]Department of Otolaryngology, Sun Yat-sen Memorial Hospital, Sun Yat-sen University; [2]Sun Yat-sen Memorial Hospital, Sun Yat-sen University

Objective
The delivery of treatment agents to inner ear with drug delivery system (DDS) has been under investigation to overcome the limitations of the conventional therapeutic agents in curing or alleviating the cisplatin ototoxicity.

Methods
In the present study, a novel targeted Acetylcysteine (NAC) - loaded DDS, A665-NAC, was constructed for prevention from cisplatin-induced hearing loss. A665 peptides specifcally bind to prestin, which is limited to the outer hair cells (OHCs). HEI-OC1 and cisplatin-treated mice (3.5 mg/kg *4 days for three cycle, intraperitoneal) were used as in vitro and in vivo models for investigating the targeting and protective effciency against cisplatin.

Results
As expected, compared to random peptide-NAC (RP-NAC), A665-conjugated
Cy5.5-labeled NAC showed active targeting to OHCs. Furthermore, A665-conjugated
Cy5.5-labeled NAC could be signifcantly internalized by HEI-OC1 cells via the A665–prestin interaction. This facilitated the uptake of cells pretreated with A665-NAC, followed by the cisplatin-treated group, which led to enhanced cell viability, reduced apoptotic properties, and decreased reactive oxygen species levels as compared to cells pretreated with NAC or RP-NAC, 1 hours in advance of cisplatin treatment. In cisplatin-treated mice, pretreatment with A665-NAC with peptide hydrogel effectively preserved OHCs and showed signifcant hearing protection at 8 and 32 kHz as compared to pretreatment with saline, NAC, or RP-NAC formulation.

Conclusion
This OHC-targeting DDS provides a novel strategy for NAC application that can be potentially used to combat cisplatin ototoxicity.

PD 31

Extracellular Vesicles from HEI-OC1 Cells as Nanocarriers for Anti-inflammatory Drugs and Pro-resolving Mediators

Gilda M. Kalinec[1]; Lucy Gao[2]; Withaker Cohn[3]; Julian Whitelegge[4]; Kym Faull[4]; **Federico Kalinec**[1]
[1]Head and Neck Surgery - DGSOM-UCLA; [2]Passarow Mass Spec Lab - UCLA; [3]Pasarow Mass Spec Lab - UCLA; [4]Pasarow Mass Spectrometry Laboratory - DGSOM-UCLA

Drug- and noise-related hearing loss are intimately associated with inflammatory responses in the inner ear. We have proposed that intracochlear delivery of pro-resolving mediators, specialized proteins and lipids that accelerate the return to homeostasis by modifying the immune response rather than by inhibiting inflammation, might have a profound effect on the prevention of sensorineural hearing loss. However, intracochlear delivery of pro-resolving agents is a challenging task that requires, first, to identify a simple, reliable and effective approach to convey them, fully active, directly to cochlear cells. The present study provides evidence that extracellular vesicles from auditory HEI-OC1 cells can incorporate anti-inflammatory drugs, pro-resolving mediators and their polyunsaturated fatty acid precursors as cargo, and potentially could work as nanocarriers for their intracochlear delivery. Extracellular vesicles generated by HEI-OC1 cells were divided by size in two fractions, small (≤150 nm diameter) and large (>150 nm diameter), and loaded with aspirin, lipoxin A4, resolvin D1, and the polyunsaturated fatty acids arachidonic, eicosapentaenoic, docosahexanoic, and linoleic. Proteomic profiles obtained by LC-ESI-MS revealed a differential distribution of selected proteins between small and large vesicles. We found that only 22.1% of these proteins were present in both fractions, whereas 73.2% were unique to smaller vesicles and only 4.7% were exclusively found in the larger ones. Importantly, the pro-resolving protein mediators Annexin A1 and Galectins 1 and 3 were only detected in small vesicles. Lipidomic studies, on the other hand, showed that small vesicles contained higher levels of eicosanoids than

large ones and, although all of them incorporated the drugs and molecules investigated, small vesicles were more efficiently loaded with polyunsaturated fatty acids and the large ones with aspirin, LXA4 and resolvin D1. Importantly, our data indicates that the vesicles contain all necessary enzymatic components for the de novo generation of eicosanoids, including pro-inflammatory agents, suggesting that their cargo should be carefully tailored to avoid interference with their therapeutic purpose. Altogether, these results support the idea that both small and large extracellular vesicles from auditory HEI-OC1 cells could be used as nanocarriers for anti-inflammatory drugs and pro-resolving mediators.

PD 32

Additive Manufacturing of Fully Metallic Precision Microneedles for Round Window Membrane Perforation

Aykut Aksit[1]; Amber M. Parker[1]; Anil K. Lalwani[2]; Alan C. West[1]; Jeffrey W. Kysar[1]
[1]Columbia University in the City of New York;
[2]NewYork-Presbyterian / Columbia University in the City of New York

Microscale, ultra-sharp metallic needles with precise geometries carry vital importance for inner ear delivery and fluid sampling. Such needles are typically only a few hundred microns tall, with thicknesses less than 100µm, the thickness of a typical human hair. Metallic needles are preferable to other microneedles due to their mechanical properties: toughness, strength, and ductility. Existing methods for producing full metal microneedles inherently grant limited design freedom or result in less precise geometries. We demonstrate a novel method for precise additive manufacturing of fully metallic microneedles, using two-photon lithography and electrochemical deposition. The needles can have a wide range of geometric parameters and architectures to suit the particular needs of the ear anatomy. Furthermore, this technique allows for changing the mechanical properties throughout the needle by manipulating the microstructure of the metal during deposition. The manufactured needles have been effective in creating precise perforations on guinea pig round window membranes. The average maximum force that was exerted on the needles was 3.77 mN, force equivalent of 0.38 grams of mass. The holes were verified via confocal microscopy and were seen to agree with prior experiments: the main failure mechanism of the membrane was fiber-to-fiber decohesion. Upon examination using scanning electron microscopy after perforation, the needles were observed to sustain no structural damage. By pushing the boundaries of precision additive manufacturing of metallic microneedles, we hope to pave the way to enabling reliable inner ear delivery and sampling.

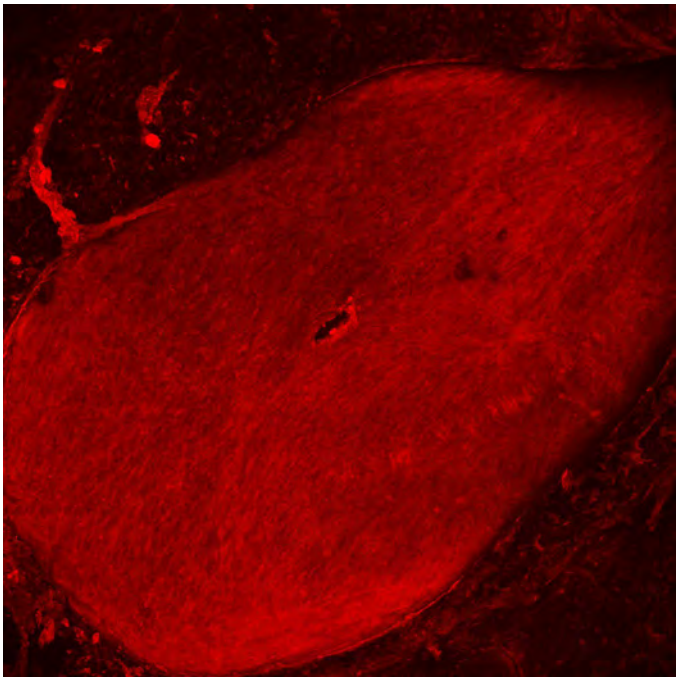

PD 33

Hearing and Proprioception Defects in Drosophila Dyb Mutants: Model for Meniere Disease

Teresa Requena Navarro[1]; Alyona Keder[2]; Joerg T. Albert[2]; Andrew Jarman[1]
[1]University of Edinburgh; [2]University College London

Background
Meniere's disease (MD) is an inner ear disorder characterized by recurrent vertigo attacks associated with sensorineural hearing loss and tinnitus. Evidence from epidemiology and Whole Exome Sequencing suggests a genetic susceptibility involving multiple genes, including DTNA. The fly's 'inner ear', called Johnston's organ (JO), is a chordotonal organ localized in the 2nd antennal segment, which mediates the sensation of hearing, gravity and wind (1). In *Drosophila*, a DTNA orthologue *Dystobrevin* (*Dyb*) is predicted to be part of the dystrophin-associated glycoprotein complex and is expressed in the support cells of the auditory/proprioceptive chordotonal sensory organs of the larvae (2).

Methods
In order to investigate whether *Dyb* causes an MD-like phenotype, we analysed *Dyb* null and RNAi knockdown flies. We collected F1 knockdown, KO and control flies. We evaluated proprioception through locomotory coordination using climbing assays in light and dark. We assessed JO auditory function in vivo using Laser Doppler Vibrometry. qPCR was performed to confirm the expression in antennae and to define the effect of the mutant allele.

Results
Dyb null mutants and RNAi knockdown flies showed normal proprioception under white light but they exhibited climbing defects when assayed in effective darkness (i.e. under red light conditions). The flies thus present a mild proprioception defect that can be compensated by visual input. In addition, *Dyb* mutant flies show a decrease in auditory active amplification in both males and females.

Conclusions
Our results support that disruption in *Dyb* mutant flies generates an MD-like phenotype. Mainly, *Dyb* null mutant flies show a climbing defect that persists over time, and a hearing loss phenotype. In addition, our results show that the flies' sense of balance integrates both mechanosensory (proprioceptive) and visual information: The proprioceptive deficits that arise from a loss of *Dyb* function can be compensated by visual cues. Preliminary analyses of *Dyb* RNAi knockdowns using neuronal specific lines suggest that *Dyb* is required in JO sensory neurons for proprioception. Further analyses need to be carried out to validate if *Dyb* is also essential for JO hearing function.

References

1. Albert JT, Gopfert MC. Hearing in Drosophila. Current opinion in neurobiology. 2015 Oct;34:79-85.

2. Dekkers LC, van der Plas MC, van Loenen PB, et al. Embryonic expression patterns of the Drosophila dystrophin-associated glycoprotein complex orthologs. Gene expression patterns. 2004 Mar;4(2):153-9.

Funding
Funded by Marie Curie Intra-European Fellowship (H2020-MSCA-IF-2017-794651) and EMBO travel fellowship (EMBO-STF_6917).

PD 34

Sox2 Maintains Type II Hair Cell Fate in Adult Mouse Vestibular Organs

Brandon C. Cox[1]; Rémy Pujol[2]; Tot B. Nguyen[3]; **Jennifer S. Stone**[3]
[1]Departments of Pharmacology & Otolaryngology, Southern Illinois University, School of Medicine; [2]University of Washington and University of Montpellier; [3]University of Washington School of Medicine

Amniotes have two types of vestibular hair cells, type I and type II, that have distinct morphology, molecular properties, and innervation. The factors that control the establishment and maintenance of these two hair cell types are not known. The SRY-box transcription factor, Sox2, is required for specification of the sensory domain in the inner ear and for the formation of hair cells during development. Sox2 is expressed in all hair cell precursors and downregulated as hair cells mature. The exception is type II hair cells in vestibular epithelia, which retain Sox2 expression throughout adulthood. We hypothesized that Sox2 maintains type II hair cell fate in adult mice. We tested this hypothesis by conditionally deleting *Sox2* from type II hair cells at 6 weeks of age using *Atoh1-CreER^{TM}:Rosa^{Tomato}:Sox2$^{f/f}$* mice, in which ~65% of type II hair cells have inducible Cre activity. At different times post-Tamoxifen (Tam), utricles were analyzed using confocal microscopy and transmission electron microscopy. *Atoh1-CreER^{TM}:Rosa^{Tomato}:Sox2$^{+/+}$* mice were processed in parallel as controls.

We confirmed loss of Sox2 protein in Tomato-expressing type II hair cells within 4 weeks after Tam injection. At

4 weeks post-Tam, most Tomato-positive (+) type II hair cells in the striola had lost immunoreactivity for calretinin, a type II-selective marker, and had gained a calyx, a type of afferent terminal that is specific to type I hair cells. The width of the striola, measured by calbindin labeling, was slightly expanded relative to control mice at 4 weeks and 4 months post-Tam. In the extrastriola, type II-to-I hair cell transdifferentiation seemed delayed relative to the striola. Tomato+ hair cells began to lose calretinin immunolabeling by 4 weeks post-Tam, and most had little calretinin left at 4 months post-Tam. By this time, many Tomato+ hair cells had gained type I features, including osteopontin expression, a basally positioned and small nucleus, a thin apical neck region, and a full or partial calyx. Between 4 and 8 months post-Tam, more Tomato+ hair cells transitioned from type II to type I-like. These findings demonstrate that *Sox2* is required to maintain type II hair cell fate, and loss of *Sox2* is sufficient to enable type II-to-I conversion in mature mice.

This work was funded by DC013771,the Kellogg Family Trust, and a Traveling Scholar Award to RP from the Virginia Merrill Bloedel Hearing Research Center.

PD 35

Dissecting the Differentiation Fates of Hair Cells in the Vestibular Sensory Epithelia during Mouse Inner Ear Development using Single Cell Transcriptomics

Soumya Negi[1]; Gabriela Pregernig[1]; Kathy So[1]; Ryan McCarthy[1]; Ning Pan[1]; Tian Yang[1]; Michael DeRan[2]; Adam T. Palermo[1]; Joseph C. Burns[1]
[1]Decibel Therapeutics; [2]Diamond Age Data Sciences

The vestibular sensory organs of the inner ear, essential for balance and spatial orientation, contain highly specialized mechanoreceptive hair cells. Utricular hair cells are classified into extra-striolar and striolar Type I, and Type II based on morphology and electrophysiology. Studies using lineage tracing and limited markers in mouse have suggested that Type I hair cells arise embryonically whereas Type II hair cells do not appear until after birth. Here, we perform a systematic characterization of transcriptional changes leading to the specification of each type of hair cell in mouse utricles using single cell RNA-seq, with a focus on understanding the drivers and molecular pathways of differentiation. Five developmental time-points between embryonic day 15.5 (E15.5) and postnatal day 12 (P12) were selected, with ~10,000 cells at each stage, including excellent representation of both hair cells and supporting cells. Cluster analysis revealed specific expression of Atoh1, an early and transient marker of hair cells, Xirp2 and Fscn2, markers of hair bundle maturation, Spp1, a marker of all Type I hair cells, Mapt, a marker of Type II hair cells, and Ocm, a marker for striolar Type I hair cells, encompassing all stages of the hair cell differentiation process. Trajectory analysis further showed distinct specification into Type I striolar and extra-striolar cells during embryonic ages, with a lower representation of Type II hair cells, that appeared only after birth. This data further supports the notion that the differentiation of Type I and II hair occurs during distinct embryonic and neonatal periods, respectively. Additionally, our analysis identified temporally expressed genes and molecular pathways that are potential drivers of subtype differentiation.

PD 36

The 3-D Spatial Orientation of the Vestibular Organs are altered in Casp3 deficient mice

Rebecca Cook; Shinji Urata; **Tomoko Makishima**
University of Texas Medical Branch

The mice have become the model animal of choice for studying the inner ear, due to ease of genetic engineering and its anatomical and functional similarity to humans. However, unlike the auditory system, the vestibular system remains under-studied due to the more complicated tests required for vestibular function evaluation and the ambiguity of the vestibular organ histology/anatomy compared to those in the cochlea. The vestibular organs are spatially oriented to each other in a functionally significant fashion. Thus, in order to evaluate the vestibular histology in mice, it is important to analyze the vestibule as a whole. Tissue clearing techniques enable whole organs to be studied without tedious manipulation. We applied tissue clearing techniques to the vestibular organs while still encapsulated in the temporal bone, in an attempt to associate with otolith organ function in caspase-3 deficient (*Casp3*$^{-/-}$) mice.

Temporal bones of wild type C57BL6J (n=5 each of males and females) and *Casp3*$^{-/-}$ (n=5 each of males and females) mice at ages 1 – 12 months were used. The temporal bones were fixed, decalcified, and co-labeled with Myosin VIIa and phalloidin to visualize the hair cells. Then the temporal bones were cleared by using a modified Sca/eS protocol. Imaging was obtained using Zeiss Lightsheet Z.1 system with 5x objective lens. Arivis software was used to obtain 3-D reconstruction of the vestibular organs. The 3-D reconstruction data was used for the analysis of the spatial orientation of the vestibular organs.

We observed significant loss of saccular hair cells, while the utricular hair cells remained preserved in the *Casp3*$^{-/-}$ mice. The utricle-saccule planar angle of the wild type

mice ranged from 69° – 92°, while it was 20° – 85° in *Casp3*$^{-/-}$ mice. Most *Casp3*$^{-/-}$ mice had unilateral saccular hair cell loss, more severe in one ear compared to the other ear.

Tissue clearing methods are compatible with fluorescent labeling, imaging and 3D reconstruction in the mouse temporal bone. Our future goal is to use these methods to determine how the inner ear organs are spatially oriented with each other, and to determine how this relationship influences the vestibular function.

PD 37

W276S/W276S mutation in KCNQ4 causes vestibular dysfunction via hair cell degeneration after acceleration stimulation

Hansol Hong[1]; Jinsei Jung[2]; Jae Young Choi[2]; Gyu Cheol Han[3]; Sung Huhn Kim[4]
[1]Yonsei University College of Medicine; [2]Yonsei University; [3]Gacheon University College of Medicine; [4]Department of Otorhinolaryngology, Yonsei University College of Medicine, Seoul, Korea

KCNQ4 mutation causes autosomal dominant progressive hearing loss. A vestibular phenotype of this kind of mutation have not been clearly identified. This study was performed to investigate if a mutation of W276S/W276S in KCNQ4 causes vestibular dysfunction in animal model and human. W276S/W276S KCNQ4 mutation mouse was created with CRSPR gene editing technique. For evaluating the contribution of KCNQ4 in maintaining vestibular function after excessive acceleration stimulation, 6G acceleration challenges were applied to each mice genotype for 24hrs. In hetero mice, 60µl (5mg/ml conc) of retigabine, a KCNQ4 activator, was injected i.p. before stimulation. After the challenges, VOR was measured by animal rotator. The difference in the value of VOR gain, time constant (Tc), and mean slow phase velocity (MSPV) during off- vertical axis rotation between the mice with retigabine injection and without injection was compared. Second, the difference the above parameters in rotation test among each mouse genotype was compared. Histological changes were observed by confocal microscopy. Human phenotype of vestibular dysfunction was investigated with vHIT and cVEMP. After the challenge, the hetero mice without retigabine injection showed lower gain and shorter Tc than those in wild type mice with retigabine injection (p=0.03). Homo mice showed significant decrease in the vestibular function (p = 0.001) at the parameters of gain (mean 0.83 ± 0.1 vs. 0.52 ± 0.03, for wild and homo, p=0.01), time constant (2.2 ± 0.4 sec vs. 1.0 ± 0.5 sec for wild and homo, p=0.02) and MSPV of nystagmus (1.6 ± 0.7 vs. 1.0 ± 0.5, p=0.005). Immunohistochemistry showed significant hair cell loss in the ampullar of each semicircular canal. In human (n=4), gain of vHIT and cVEMP loss were observed in 50% of the patients with KCNQ4 mutation. W276S/W276S KCNQ4 mutation can cause vestibular dysfunction, either after acute excessive acceleration stimulation or during daily activities.

PD 38

Evaluation of Synaptic Ribbon Architectures and Distributions in Vestibular Neuroepithelia Using Super-resolution Fluorescence Microscopy

Johnny J. Saldate; Felix E. Schweizer; Larry F. Hoffman
Geffen School of Medicine at UCLA

Vestibular neuroepithelia exhibit broad heterogeneity in synaptic ribbon size and architecture within both type I and type II hair cells [Lysakowski and Goldberg 1997, Hoffman et al., in preparation]. Ribbon archetypes are characterized by the number of protein dense ribbon cores they contain, either one or more than one, and categorized into one of two mutually exclusive classes: *simple* or *cluster*, respectively. The simple archetype is characterized by an individual ribbon core enshrouded by synaptic vesicles. Simple ribbons are often in close apposition to the hair cell presynaptic membrane. Conversely, the cluster archetype is composed of aggregated ribbon cores sharing at most a single lamina of vesicles between cores. While serial ultrastructural methods represent the gold standard for investigating ribbon architectures and morphology, they are challenging to implement efficiently in applications surveying ribbon architecture distributions and are impractical in identifying their concomitant contributions to the coding of head movement stimuli across the topology of the vestibular epithelia. However, advances in super-resolution fluorescence microscopy serve to overcome the optical diffraction limit and minimize the distortion inherent to traditional confocal microscopy. This affords novel and exciting opportunities to resolve complex synaptic ribbon architectures in a high throughput fashion, and meanwhile optically investigate their topologic distributions with substantially better spatial and temporal resolution. Specimens of utricle and crista neuroepithelia were fixed (4% paraformaldehyde) and harvested from adult C57BL/6J mice and processed via immunohistochemistry as either intact epithelia or cryosections (12-15µm). Specimens were then probed with primary antibodies specifically targeting the synaptic ribbon protein CtBP2, the postsynaptic density scaffolding protein Shank1a, and the multipurpose ß3-tubulin, in addition to a fluorophore-conjugated phalloidin. 4-channel super-resolution fluorescence imaging was then completed on either an upright Zeiss LSM 880

with Airyscan module (for intact specimens) or a Zeiss ELYRA with structured illumination (SIM) and post-processed in Zen before volume-based reconstruction and semi-automated ribbon/synapse analyses (Imaris 9.3). Identified ribbons varied in volume and morphology in both the Airyscan and SIM images, with the resolution of the latter resulting in the ability to categorize ribbons as either putative simple or cluster archetypes. Large-volume CtBP2-immunopositive structures appeared as multi-compartment aggregates, consistent with the cluster archetype. Thus, these data provide strong support for the ability to differentiate ribbon architectures via immunohistochemistry, and therefore highlights the capability of examining synaptic distributions over large regions of vestibular epithelia.

PD 39

Sensitivity of Type I hair cells to infrared radiation is conferred by intracellular TRPV4

Federica Maddalena Raciti[1]; Weitao Jiang[2]; Suhurd M. Rajguru[3]
[1]Department of Cellular Physiology and Molecular Biophysics, University of Miami Miller School of Medicine; [2]Department of Biomedical Engineering, University of Miami; [3]Dept. of Biomedical Engineering and Otolaryngology, University of Miami

Recent work has reported that vestibular neuroepithelium, especially the hair cells, are sensitive to photothermal pulsed infrared radiation (IR). It has been shown in vitro that IR induces intracellular [Ca2+] changes and calcium-induced calcium-release following the activation of temperature- dependent Transient Receptor Potential (TRP) channels localized on the endoplasmic reticulum. In the present study, we hypothesized that a similar mechanism exists within vestibular hair cells and might play a role in the observed diversity of post–synaptic responses. Infrared-evoked eye movements and afferent responses were measured as the output parameters (β=1860nm, 200µs, 200Hz, various radiant exposures) and pharmacological agents were locally perfused to define the contributions of different cell types and the mechanisms in IR stimulation. Our results suggest that IR stimulation modulates the activity of vestibular hair cells, specifically Type I. The IR–evoked responses were significantly reduced when the neurotransmission between vestibular hair cells and the afferent neurons was impaired both upstream and downstream after the local perfusion of Neomycin (100 mM) and the AMPA/kainate receptor antagonist CNQX (100 µM) respectively. Modulation of the IR – evoked eye movement was also observed following treatment with XE991 (1 mg/kg and 2.5 mg/Kg) which inhibits the activity of KCNQ4 localized on calyx – ending afferents. Furthermore, we reported the pivotal role of the endoplasmic TRPV4 in the photothermal activation of the vestibulo-ocular motor pathway. In whole mount preparations, we observed colocalization between the temperature-dependent TRPV4 and the endoplasmic reticulum which was pronounced in type-I hair cells. The IR-responses was significantly reduced when temperature of the vestibular neuroepithelium was lowered below activation threshold of TRPV4 (< 26°C) or following the perfusion of TRPV4 antagonists (GSK2193874 and HC067047). We further examined IR–induced afferent responses in vivo combined with the pharmacological treatments. Preliminary results show that local perfusion of both Neomycin (100 mM) and CNQX (100 µM) result in a significant reduction in the responses supporting the hypothesis that IR stimulation primarily affects vestibular hair cells and that the molecular mechanism responsible for IR photosensitivity of vestibular epithelium resides in the pre – synaptic element.

Funding: NIH NIDCD 1R01DC008846 and 1R01DC013798

PD 40

A Novel Cell Niche in the Cristae Ampullaris with Unprecedented Acetylcholine Evoked Calcium Transients in Mice

Holly A. Holman; Richard D. Rabbitt
University of Utah

Acetylcholine (ACh) evoked calcium transients were studied in cristae from a transgenic mouse line where Gad2-IRES-Cre was used to drive expression of the Ca^{2+} reporter GCaMP5G and co-reporter tdTomato (tdT). A novel niche of tdT expressing cells, putatively GABAergic, revealed unprecedented responses to ACh stimuli with distinct whole-cell Ca^{2+} transients. Evoked Ca^{2+} transients were reversibly blocked with atropine and 2-APB in early postnatal developmental stages and in aged mice. Based upon the anatomical location of these cells on the slope of the eminentia cruciata (EC), the predominant cell was named *clino*. Adjacent cells to clino within this niche with similar cell morphologies, but expressing tdT to a lesser extent also demonstrate ACh evoked calcium transients, and these were named *clinocytes*. Clino cells and clinocytes form a microenvironment in primarily two zones in cristae; one zone located near the center of the EC, and a second smaller zone was within the planum. Using immunohistochemical profiling we identified tdT positive Gad2 transgenic cells that express choline acetyl transferase (ChAT) and the C-terminal binding protein-2 (CtBP2) from early postnatal development to old age. A subset of these cells express the transcription factor SOX2. Age-matched wild-type mice confirmed ChAT and CtBP2 expression in this novel cell niche.

Based on their mophophysiology, clino and clinocytes comprise a previously unknown cholinergic signaling mechanism. Although the role(s) of these cells is currently not fully understood, we hypothesize that ACh signaling involving clino and clinocytes in these niches of the crista might play a role in regenerating cells of the vestibular neurosensory epithelia.

Age-Related Hearing Loss: Behavioral and Physiological Assessments

PS 266

The Effects of Ageing, Hearing Loss and Tinnitus on White Matter in the Human Auditory Pathway

Oliver Profant[1]; Antonín Škoch[2]; Jaroslav Tintβra[2]; Veronika Svobodová[3]; Diana Tothová[3]; Josef Syka[4]
[1]Department of Otorhinolaryngology, 3rd Faculty of Medicine, Charles University, Prague, Czech Republic; [2]MR Unit, Institute of Clinical and Experimental Medicine, Prague, Czech Republic; [3]Department of Otorhinolaryngology and Head and Neck Surgery, 1st Faculty of Medicine, Charles University, Prague, Czech Republic; [4]Institute of Experimental Medicine CAS, Prague, Czech Republic

The main symptoms of age related hearing loss are elevated auditory thresholds and decreased speech intelligibility, especially in noisy environments. Tinnitus is a phantom noise with a high occurrence coinciding with the onset of presbycusis. Although both are believed to originate from the auditory periphery, they also have clear central components. The aim of our study was to investigate whether ageing, hearing loss and tinnitus induce changes within the auditory and adjacent pathways.

Six groups of volunteers were used in this study: with expressed presbycusis, with mild presbycusis, young controls, with expressed presbycusis and with tinnitus, with mild presbycusis and with tinnitus and subjects with normal hearing and with tinnitus. Tractographic data were acquired using a 3 T Siemens Tim Trio system (Siemens), with a 12-channel head coil. Streamline tracking was performed on a common FOD template using the probabilistic algorithm iFOD2. Spherical masks on both inferior colliculi were defined manually. A mask of the Heschl gyrus was obtained by applying morphing of a Destrieux atlas mask of one representative subject to a FOD template. These masks were used as ROIs for targeted tracking and subsequent definition of fixel mask. Fixel based analysis was used for the detection of changes (using connectivity-based fixel enhancement, family-wise error corrected) in the following three metrics: fibre density, fibre cross-section, fibre density and cross-section.

The only observed changes of the white matter within the auditory and adjacent pathways were due to ageing. No statistically significant changes due to hearing loss were found. Tinnitus caused a borderline change in the part of the pathway from the inferior colliculus toward the amygdala.

This is most likely the first study using fixel based analysis in the auditory system. Compared to our previous report (Profant et al., 2014) that used diffusion tensor imaging, we were able to track age related changes within the auditory pathway. The presence of borderline tinnitus changes in the adjacent pathway from the inferior colliculus to the amygdala support the idea of the involvement of the limbic system in the tinnitus network.

Profant O., Škoch A., Balogová Z., Tintβra J., Hlinka J., Syka J., Neuroscience 260: 87-97, 2014

PS 267

Alzheimer's Disease (AD) Mouse Models Show Features of Hidden Hearing Loss at an Early Ag

Mincheol Kang[1]; Seojin Park[2]; Jeong Han Lee[3]; Robert Renden[2]; Ebenezer N. Yamoah[3]
[1]University of Nevada Reno; [2]University of Nevada, Reno; [3]University of Nevada,Reno

Background
Hearing loss (HL) has been proposed to be independently associated with Alzheimer's disease (AD). Moreover, cognitive tests in AD and dementia patients that use auditory stimuli should not be confounded by hearing dysfunction. Besides the correlation between HL and AD in humans, AD mouse models showed hearing dysfunction at, or before, the debut of mild cognitive impairment (MCI). What is unknown is the unequivocal mechanistic link between HL and AD, using mouse models with the appropriate genetic background to allow segregation between age-related hearing loss (ARHL) and AD-related HL.

Methods
We use cellular, molecular, imaging, and functional analyses (e.g., auditory brainstem recordings (ABR), and electrophysiological recordings) to demonstrate HL in AD.

Results
We backcrossed three AD mouse models (ADCg (stock# 34848-JAX), FAD (stock# 34840-JAX, and Tau (stock #015815)) unto CBA CaJ background for ~9 generations. Whole-genome scanning was performed to confirm strain identity and assess genetic quality between stocks. The CBA CaJ sub-strain was confirmed via

single nucleotide polymorphism (SNP)-based genome scanning (performed by Jackson Laboratories). 98% of the SNP markers evenly spaced over the 19 autosomes, and the X chromosome was identical in the CBA CaJ colony maintained at the UNR Animal Facility compared to the sub-strain maintained by Jackson Laboratories. The analyses were performed for 1-, 3-, 6-, 8-, and 10-mos old AD mouse models and wildtype (WT) littermates mice as control. WT mice yielded the characteristic ABR waveform at 1-mo of age with thresholds of 5-10 (click), 40-50 (4 – 16kHz), and 35 (32kHz) dB across different test frequencies. The hearing remained unchanged up to 10-mos old.

In contrast, AD mice exhibited a markedly reduced Peak I (PI) amplitude waveform compared to the WT at ages 3-10 mos. Analyses of the input/output (I/O) function of PI and PII amplitude and latency between WT and AD mouse models across ages showed that while PI amplitudes and latencies were markedly reduced and delayed, respectively, in response to a click stimulus, the thresholds in 1- and 3-mos old AD models were equivalent to those of the WT mice. However, by 6-mos and beyond, the AD mice exhibited significant changes in click-elicited thresholds. We also performed electrophysiological analyses of short-term plasticity at the calyx of Held, which surprisingly showed an increased ability to maintain high frequency firing, with less presynaptic depression at stimulation frequencies 100-600 Hz.

Funded by the NIDCD and NIA (DC016099; DC015135; DC006685 AG060504; AG051443).

PS 268

Age-related Changes in the Auditory Steady-State Response Measured across the Lifespan of CBA/CaJ Mice

Kendra E. Stebbins[1]; Joseph P. Walton[2]
[1]Department of Communication Sciences & Disorders, University of South Florida, Tampa, FL; Global Center for Hearing and Speech Research, University of South Florida, Tampa, FL; [2]Department of Communication Sciences & Disorders, University of South Florida, Tampa, FL; Department of Medical Engineering, University of South Florida, Tampa, FL; Global Center for Hearing and Speech Research, University of South Florida, Tampa, FL

Background

Presbycusis, or age-related hearing loss, is the most prevalent type of sensorineural hearing loss. The age-related decline in hearing that gradually progresses across the lifespan of humans also occurs in the CBA/CaJ mouse, making it a very useful animal model. Previous studies have used electrophysiological measures such as the Auditory Brainstem Response (ABR) to assess age effects on peripheral and central auditory function in various strains of mice. However, few studies have been conducted using the Auditory Steady-State Response (ASSR) as a tool for assessing temporal processing in aging animal models, and no previous studies have assessed cortical temporal processing across the lifespan. The ASSR is elicited by the phase locking of neurons to amplitude modulated (AM) stimuli in a way that follows the temporal modulation of the signal, with higher AM rates generating responses from the midbrain and lower AM rates (< 50 Hz) generating responses from the cortex. Age-related temporal processing deficits in previous studies done on humans led us to hypothesize ASSR would progressively decline with age in mice. The purpose of this study was to evaluate the use of ASSR as an effective strategy for detecting age-related changes in auditory function, as well as to further develop our understanding of the neurophysiological aspects of presbycusis.

Methods

We evaluated age-related changes of the auditory pathways by analyzing ASSR data collected from 115 CBA/CaJ mice (58 male, 57 female) grouped by age into young (111-272 days), middle-aged (273-517 days), and old (518-906 days) groups in a cross-sectional design. The ASSR was analyzed using FFT via a custom MatLab GUI which provided the magnitude (in uV) at the stimulating frequency as well as three higher harmonics. Responses of the auditory cortex and midbrain were measured using peak magnitude and signal-to-noise ratio (SNR) of the ASSR to acoustic stimuli having 400 ms durations. Modulation frequencies of 40 and 80 Hz were 100% amplitude-modulated and presented at 65 and 75 dB SPL using carrier frequencies of 8 kHz, 16 kHz, 24 kHz. Further, we evaluated the peak magnitude and SNR of the first, second, and third harmonics of the modulation frequencies. Analysis of ABR audiograms was used to assess hearing sensitivity as a function of age.

Results/ Conclusions

Results showed no significant change in the peak magnitude of the ASSR across the lifespan, indicating that as mice age, they are still able to maintain neural synchronization within the midbrain and cortex. We also found the variability in peak magnitude was greater in young mice as compared to old responding to the 40 Hz modulated stimuli, suggesting that neural coding within the auditory cortex stabilizes after about 200 days into the life cycle. Further, no significant change in SNR across the lifespan was seen, indicating that a consistent SNR

range can be expected when measuring ASSR in mice, regardless of age. Results further showed younger mice exhibiting the strongest positive correlation between the modulation frequencies, eg., midbrain to cortex suggesting that the integrity of neural locking occurring in the midbrain is associated with the integrity of neural locking occurring in the auditory cortex, especially in younger mice. Overall, ASSR proves to be a useful tool to help us further understand temporal processing in the cortex and caudal portions of the brainstem.

Work supported by NIH-NIA AG00954.

PS 269

Auditory-Frontal Channeling In Alpha And Beta Bands Is Altered by Age-Related Hearing Loss and Relates To Speech Perception In Noise

Caitlin Price; Gavin Bidelman
University of Memphis

Difficulty understanding speech-in-noise (SIN) is a pervasive problem faced by older adults particularly those with hearing loss. Previous studies have identified structural and functional changes in the brain that contribute to older adults' speech perception difficulties. Yet, many of these studies use neuroimaging techniques that evaluate only gross activation in isolated brain regions. Neural oscillations may provide further insight into the processes underlying SIN perception as well as the interaction between auditory cortex and prefrontal linguistic brain regions that mediate complex behaviors. We examined frequency-specific neural oscillations and functional connectivity of the EEG in older adults with and without hearing loss during an active SIN perception task. Brain-behavior correlations revealed listeners who were more resistant to the detrimental effects of noise also demonstrated greater modulation of a phase coherence between clean and noise-degraded speech, suggesting a desynchronization reflects release from inhibition and more flexible allocation of neural resources. Additionally, we found top-down b connectivity between prefrontal and auditory cortices strengthened with poorer hearing thresholds despite minimal behavioral differences. This is consistent with the proposal that linguistic brain areas may be recruited to compensate for impoverished auditory inputs through increased top-down predictions to assist SIN perception. Overall, these results emphasize the importance of top-down signaling in low-frequency brain rhythms that help compensate for hearing-related declines and facilitate efficient SIN processing.

PS 270

Natural Progression of Age-Related Hearing Loss in Male Wistar Rats

Mathieu Petremann; Christophe Tran Van Ba; Charlotte Romanet; Viviana Delgado-Betancourt; Pauline Liaudet; Vincent Descossy; **Jonas Dyhrfjeld-Johnsen**
Sensorion

Age-related hearing loss in male Wistar rats has recently been described using auditory brainstem response measurements in age-groups of 6-8 months, 12-14 months and 18-20 months old rats (Alvarado et al, 2014). From a therapeutic development standpoint, it is of interest to have a clearer view of the natural history of hearing loss progression. We here report monthly longitudinal progression of changes in hearing thresholds and otoacoustic emissions in a group of male Wistar rats.

Starting at 6 months of age, hearing was characterized monthly in male Wistar rats (n=7) housed under standard conditions using standard audiometry (ABR 8/16/24/32 kHz, DPOAE 4/8/16/24/32 kHz). The present report covers results up until 11 months of age. ABR thresholds, DPOAE amplitudes and ABR wave 1 amplitudes were compared over time using 1-way RM ANOVA.

ABR thresholds increased by 5.7-9.6 dB across frequencies from 6 months to 11 months of age. These changes became statistically significant at 9 months old for 24 kHz (9.64±3.2 dB, p=0.004), at 10 months old for 8 kHz (11.43±3.61 dB, p< 0.001) and at 11 months old for 32 kHz (8.93±3.17 dB, p=0.038). DPOAE amplitude changes of +0.8 to -6.9 dB were determined across frequencies, but only losses at 16 kHz from 10 months old (8.0±2.8 dB, p=0.039) and 32 kHz from 9 months old (8.0±5.1 dB, p=0.009) reached statistical significance. ABR wave 1 amplitudes varied over time in the range of +0.28 to -0.48 µV across frequencies. These ABR wave 1 amplitude changes were more variable and did not reach robust statistical significance at any frequencies, but trended towards statistical significance from 10 months old at 24 kHz (-0.36 µV, p=0.085) and for 32 kHz from 10 months old (-0.34 µV, p=0.031).

These results are in general agreement with the report published by Alvarado et al. (2014), but highlights significant decline in functional auditory measures from as early as 9 months old compared to a baseline at 6 months old on both ABR and DPOAE measures using serial audiometry, compared to the previously published pooled data from 12-14 months old male Wistar rats. While the ABR wave 1 amplitude losses were less robust at these younger ages, the trend was stronger at higher stimulus frequencies as previously reported.

Additional recording time-points and analysis will further contribute to the understanding of the natural history hearing loss progression in male Wistar rats as a model of age-related hearing loss.

PS 271

Hearing Impairment Directly Associated with Cognitive Function Decline: Results from the AGES-Reykjavik Study

Chuan-Ming Li[1]; Howard J. Hoffman[1]; Christa L. Themann[2]; Gudny Eiriksdottir[3]; Johanna E. Sverrisdottir[3]; Vilmundur Gudnason[3]; Hannes Petersen[4]
[1]Epidemiology and Statistics Program, National Institute on Deafness and Other Communication Disorders (NIDCD), National Institutes of Health (NIH); [2]Hearing Loss Prevention Team, Division of Applied Research and Technology, National Institute for Occupational Safety and Health (NIOSH), Centers for Disease Control and Prevention (CDC); [3]The Icelandic Heart Association, Kopavogur, Iceland; [4]Akureyri Hospital, Akureyri, Iceland

Background
Dementia mainly affects older adults and is a major contributor to the global burden of disease. There were 47 million people living with dementia globally in 2015 and this number is projected increase to 115 million by 2050. Hearing impairment (HI) is one of the most common chronic conditions worldwide. A meta-analysis indicated that 9% of dementia cases are linked to HI.

Objectives
Examine association between HI and cognitive function; identify factors directly associated with HI and cognitive impairment; estimate mediated indirectly effect of cognitive impairment on age-related hearing loss (ARHL).

Methods
The Age, Gene/Environment Susceptibility (AGES)–Reykjavik Study, examined a population-based cohort of 5,764 adults aged 66–96 years. Five years later, 3,411 subjects were followed-up. Better ear hearing was analyzed using the pure-tone average (PTA 0.5–1–2–4 kHz) threshold classification recommended by the Global Burden of Disease 2010 Hearing Loss Expert Group. Mild cognitive impairment (MCI) and dementia (MCI-D) were based on clinical assessment and a consensus meeting. Odds ratio (OR) and 95% confidence intervals (CIs) were calculated using multinomial logistic regression models. Bayesian Network analysis was used to identify direct risk factors associated with HI and MCI-D. The CAUSALMED procedure estimated causal mediation effects of MCI-D on ARHL.

Results
Prevalence of HI was: 40.5% (mild), 27.1% (moderate), 13.1% (moderately-severe or worse). Prevalence of dementia was 4.7% and MCI was 9.7%. Among those without HI, or with mild, moderate, moderately-severe or worse HI, prevalence of dementia increased from 1.4%, 3.6%, 5.8%, to 10.8%; prevalence of MCI increased from 3.5%, 7.3%, 13.9%, to 17.6%, respectively. After adjusting for potential confounding variables, better ear PTA (every 10 decibels) was significantly associated with increasing dementia (OR, 1.31; 95% CI, 1.18-1.46) and MCI (OR, 1.14; 95% CI, 1.05-1.24); whereas use of hearing aids was significantly associated with decreasing dementia (OR 0.53; 95% CI, 0.34-0.82). Dementia was significantly increased among those with moderately-severe or worse HI. Direct risk factors associated moderate-to-worse HI included sex, age, noise exposure, tinnitus, and cognitive impairment. Direct factors associated with MCI-D included age, depression, reduced leisure activities, lower education, and HI. Estimated 4% of ARHL was mediated through MCI-D. Sixty-three percent of MCI-D was associated moderate-to-worse HI directly and 36% was associated with aging.

Conclusions
Increased HI was associated with decreasing cognitive function. Use of hearing aids may reduce cognitive function decline. HI and MCI-D were direct risk factors for each other.

PS 272

Relating Perception of Temporal Fine Structure to Measures of Synaptopathy in the Gerbil

Henning Oetjen[1]; Sonny Bovee[1]; Friederike Steenken[1]; Christine Köppl[2]; **Georg M. Klump**[2]
[1]Department of Neuroscience, Carl von Ossietzky University Oldenburg; [2]Cluster of Excellence Hearing4all, Department of Neuroscience, Carl von Ossietzky University Oldenburg

Compromised processing of temporal fine structure and related deficits in perception have been attributed to synaptopathy. However, so far synaptopathy has not be convincingly linked to compromised perception (Bramhall et al., 2019, Hear Res 377: 88-103). Studies investigating cochlear anatomy, auditory brainstem responses (ABR) and perception in the same subjects are needed to make a strong link and probe for causality. Here we present data from such a study in Mongolian gerbils that allows to evaluate the evidence for a linkage.

Perception of temporal fine structure was investigated using the TFS1 test in five groups of gerbils: young

individuals (age < 15 months), old individuals (age >36 months), two groups of young animals treated with ouabain (40 µM, 70 µM; after Bourien et al., 2014, J Neurophysiol 112: 1024-1039) for experimentally inducing synaptopathy, and sham-treated young gerbils. The sensitivity for detecting a change of the temporal fine structure was determined for three different harmonic-complex reference stimuli (center frequency/ fundamental: 1600Hz/200Hz, 1600Hz/400Hz, and 3200Hz/400Hz), by varying the upward frequency shift of all seven stimulus components (Moore & Sek, 2009, Int J Audiology 48:161[1]171). In addition to the psychoacoustic testing, we measured the subjects' growth functions for wave 1 of the ABR. Finally, immuno-stained cochlear whole mounts of the same subjects were analyzed by manually counting functional (double-labeled) synapses on inner hair cells, at cochlear locations representing 2 and 4 kHz.

A GLMM ANOVA revealed that different treatment groups differed in their sensitivity for perceiving the frequency shift: old gerbils showed a low sensitivity while all other groups showed a similarly high sensitivity. In addition, center and fundamental frequency, as well as the frequency shift all affected the gerbils' sensitivity. We observed no correlation between the number of functional synapses (at locations corresponding to 2 and 4 kHz) with the sensitivity of the individuals to detect a frequency shift in the TFS1 test. This suggests that synapse counts as a measure of auditory neuropathy are not a good predictor of the gerbil's ability to process temporal fine structure. Alternative explanations are discussed.

Supported by the Deutsche Forschungsgemeinschaft (DFG), priority program 1608 „Ultrafast and temporally precise information processing: Normal and dysfunctional hearing"

PS 273

Age-Related Effects on the Perceptual Resolution of Attended Temporal and Spatial Acoustic Features

Kristina C. Backer[1]; Lee M. Miller[2]; Gregg H. Recanzone[2]
[1]University of California, Merced; [2]University of California, Davis

A common complaint among older adults is trouble comprehending speech, especially in noisy listening situations. This deficit may stem from age-related declines in bottom-up auditory processing (i.e., temporal and spatial processing), as well as age-related declines in certain cognitive functions, particularly selective attention. Therefore, the goal of this study was to determine how aging affects the perceptual resolution of attended temporal and spatial sound features, in the absence and presence of acoustic distraction. Young (n = 17) and older (n = 11) adult participants listened to amplitude-modulated (AM) noise combs presented in virtual acoustic space and performed a delayed match-to-sample (S1-S2) task. On Attend Location trials, participants pressed a button to report if S2 occurred to the left or right of S1. On Attend AM Rate trials, participants reported if the S2 rate was faster or slower than the S1 rate. In order to assess the effects of distraction on performance, S1 and S2 were either presented alone or simultaneously with a distractor AM noise. An adaptive procedure was implemented to obtain each participant's discrimination thresholds for location and rate changes, during the no-distractor and distractor trials. We hypothesized that compared to young adults, older adults would have worse discrimination thresholds, slower response times, and be more affected by distraction for both the Attend Rate and Attend Location trials. Linear mixed-effects models were fitted and evaluated in MATLAB, to determine the effects of Age Group and Distractor Condition on task performance for the Attend Rate and Attend Location trials. As predicted, for both Attend Rate and Attend Location conditions, the older adults had significantly slower response times compared to young adults. Furthermore, there was a significant main effect of Distractor Condition on discrimination thresholds for both the Attend Rate and Attend Location conditions. Both young and older adults' discrimination thresholds suffered in the presence of distraction. However, there was a significant interaction between Age Group and Distractor Condition for the Attend Rate condition, but not for the Attend Location condition. Specifically, on Attend Rate trials, older adults' discrimination thresholds suffered to a greater extent during distraction than did young adults' thresholds. Taken together, these results suggest that in the presence of auditory distraction, aging differentially affects the perceptual resolution of attended temporal and spatial sound features. These age-related declines in temporal processing may underlie speech-in-noise comprehension deficits to a greater extent than age-related declines in spatial processing.

PS 274

Exposure to a Temporally Modulated Augmented Acoustic Environment Improves Behavioral Gap Detection in Old CBA/CaJ Mice

Collin Park[1]; Ryan Longenecker[1]; Dimitri Brunnell[1]; Mary Reith[1]; Joseph P. Walton[2]
[1]Univ. South Florida; [2]Department of Communication Sciences & Disorders, University of South Florida, Tampa, FL; Department of Medical Engineering, University of South Florida, Tampa, FL; Global Center

for Hearing and Speech Research, University of South Florida, Tampa, FL

Background

There is growing evidence that neural plasticity can aid in the prevention or treatment of central-oriented age-related hearing loss (ARHL). Many of these studies have used auditory training or passive listening to modulate and assess neural plasticity. However, there is a paucity of published reports which have examined the effects of augmented acoustic environments on hearing function in aged animal. An augmented acoustic environment (AAE) is a paradigm first reported by Turner and Willott in which animals are exposed to a non-traumatic noise for a long period of time. In this study we use an AAE with silent gaps embedded in noise, in an attempt to improve temporal processing in aged animals.

Methods

Aged CBA/CaJ mice (age 20 months) were exposed for 2 months to an augmented acoustic environment consisting of either; 1) an 8 kHz centered, 70 dB SPL narrow-band noise containing randomly interspersed gaps of 2, 4, 8, 16, 32 or 64 msec duration presented every 250 msec for 12 hours (Gaps-AAE), or 2) a stimulus with a 20 kHz center frequency, whose envelope was amplitude modulated with frequencies of 40 Hz and 100 Hz alternating every 2s at 70dB (AM-AAE), for 12 hours during the nocturnal phase. Mice were assessed with several acoustic startle reflex paradigms: 1) input/output functions, 2) prepulse inhibition (PPI), and 3) gap detection (GPIAS). GPAIS was measured using gaps of 2, 4, 10, 20 and 50 msec, PPI used tones of 8, 16, and 32 kHz. Behavior was tested before, 1 month, and 2 months after AAE.

Results/Conclusions

Animals in both AAE groups showed statistically significant decreases in ASR input/output amplitudes following AAE exposure when compared to baseline. Gap AAE animals also exhibited increased prepulse inhibition (compared to baseline) in the GPIAS test at 1 month to 10 and 20 msec gaps, and at 2 months to 20 msec gaps. There was no effect on PPI at 8 or 32 kHz pre-pulse frequency, but there was a significant effect of time at 16 kHz, consistent with an increase in % inhibition over the two months. Animals in the AM-AEE group also displayed a main effect of time in the 16 kHz TPPI test. This study elucidates the consequences of exposure to targeted AAE in the aged auditory system and plasticity with respect to auditory perception. Later studies will determine the positive or negative perceptual consequences of AAE following presumptive neural plasticity with the central auditory system.

Work supported by NIH-NIA grant AG09524.

PS 275

Differential time course of cochlear processing deficits and GABAergic inhibition in the aging Mongolian gerbil

Mariella Kessler[1]; Mario Lukacevic[2]; Martin Mamach[3]; Jens P. Bankstahl[4]; Frank M. Bengel[5]; Tobias L. Ross[2]; Georg Berding[1]; Georg M. Klump[6]

[1]Cluster of Excellence Hearing4all, Department of Nuclear Medicine, Medical School Hannover, Hannover, Germany; [2]Medical School Hannover, Department of Nuclear Medicine; [3]Cluster of Excellence Hearing4all,Department of Medical Physics and Radiation Protection, Hannover Medical School, Hannover, Germany; [4]Department of Nuclear Medicine, Medical School Hannover, Hannover, Germany; [5]Department of Nuclear Medicine, Medical School Hannover, Hannover, Gernany; [6]Cluster of Excellence Hearing4all, Department of Neuroscience, Carl von Ossietzky University, Oldenburg, Germany

Introduction

With increasing age there are changes in cochlear processing deficits and in central GABAergic inhibition. We do not know, however, whether the time course of these changes is synchronized and whether the change in central inhibition may be functionally related to the peripheral loss in auditory sensitivity. Mongolian gerbils are a well-suited animal model to study such changes since its sensitive hearing includes the frequency range of humans. To examine the relation between peripheral loss in auditory sensitivity and GABAergic inhibition with increased age, positron emission tomography (PET) imaging using [^{18}F]flumazenil (FMZ) for the detection of $GABA_A$ receptor binding capacity and auditory brainstem response measurements (ABR) were combined.

Methods

In total 9 young (5-6 months), 10 middle-aged (27-28 months) and 13 old gerbils (39-42 months) were investigated. Dynamic PET acquisitions for sixty minutes were started simultaneously with [^{18}F]-FMZ injection via the femoral vein. Peripheral hearing was evaluated using ABR measurements with click stimuli. Non-displaceable binding potentials (BPnd) were calculated for auditory (auditory cortex, AC; inferior colliculus, IC; medial geniculate body, MGB) and non-auditory brain regions (somatosensory cortex, SC; cerebellum, CB). To evaluate the relation between BPnd and the factors age, area and the covariate ABR amplitude at 90dB, a mixed model ANOVA was conducted. The relation between ABR amplitude and age was evaluated using a one-way ANOVA. P-values of subsequent pairwise comparison with t-tests were Bonferroni corrected.

Results
The ABR amplitude at 90dB of gerbils was significantly affected by age. Young and middle-aged gerbils had similar ABR amplitudes that were on average four time larger than the ABR amplitude of old gerbils ($p< 0.0005$). BPnd was significantly related to age, area and the ABR amplitude obtained with 90db clicks. The middle-aged and old gerbils had similar BPnds, whereas the BPnd of young gerbils was significantly larger than that of the other two age groups. The BPnd of young gerbils was more than two times larger than that of the other age groups. There was a highly significant interaction of age and an ABR amplitude indicating that both factors were differently related to the BPnd. Thus, middle-aged gerbils have an ABR similar to that of young gerbils but a BPnd similar to that of old gerbil.

Conclusion
The study indicates a different time course of age-related cochlear processing deficits and changes in central GABAergic inhibition.

PS 276

Clinical feasibility of auditory processing tests in Japanese older adults: a pilot study

Shohei Fujimoto; Yukihide Maeda; Kazunori Nishizaki
Department of Otolaryngology - Head & Neck Surgery, Okayama University Graduate School of Medicine, Dentistry and Pharmaceutical Sciences

Background
Difficulty in listening comprehension is a major audiological complaint of older adults. Behavioural auditory processing tests (APTs) may evaluate it. Aims/Objectives: The aim was to assess the feasibility of administering Japanese APTs to older adults at otolaryngology clinics. Material and Methods: Using computer programs interfaced with an audiometer, APTs (dichotic listening test; fast speech test, FST; gap detection test, GDT; speech in noise test; rapidly alternating speech perception test) were administered to 20 older adults (65-84 years old; mean 75.3 years) and 20 young adults at the 40dB sensation level. Monosyllable speech perception (MSP) and the Mini Mental State Examination (MMSE) were evaluated. Results: APT results except for GDT were significantly correlated with MSP. The performance on each APT was worse in older adults than in young adults ($p< 0.01$). The older adults with good MSP≥80% (n=13) or excellent cognitive function (MMSE≥28; n=11) also did worse on APTs ($p< 0.05$). A ceiling effect was noted in the APT data, with FST showing a minimum ceiling effect and reflecting interindividual variations of data. Conclusions and Significance: It is feasible to administer APTs to older adults who visit otolaryngology clinics. Among our Japanese APTs, FST may be suitable for further large-scale clinical studies.

Table 1. Characteristics of the young adults and older adults enrolled in the study.

			mean±S.D.
Age	young adults	*n*=20	32.9±5.2 (23-41, range)
	older adults	*n*=20	75.3±6.2 (65-84, range)
Average pure tone threshold(dB HL)	young adults	*n*=20	8.7±2.1
	older adults	*n*=20	41.7±8.6
Stimulus level(dB)	young adults	*n*=20	49.8±1.1
	older adults	*n*=20	79.8±7.0
Stimulus level dB sensation level	young adults	*n*=20	41.0±2.0
	older adults	*n*=20	38.0±3.8
Monosyllable speech perception (%)	young adults	*n*=20	97.5±2.7
	older adults	*n*=20	83.6±12.6
MMSE-J	older adults	*n*=20	27.7±2.1

Table 2. Correlations of auditory processing test (APT) results with monosyllable speech perception (%) in 20 older adults.
Spearman's rank correlation $|r|$

Dichotic listening test (words)	Dichotic listening test (sentences)	Fast speech test(×1)	Fast speech test(×1.5)
0.663*	0.636*	0.629*	0.790*

Fast speech test(×2)	Gap detection test	Speech in noise test	Rapidly alternating speech perception test
0.791*	0.176	0.631*	0.804*

*p <0.01

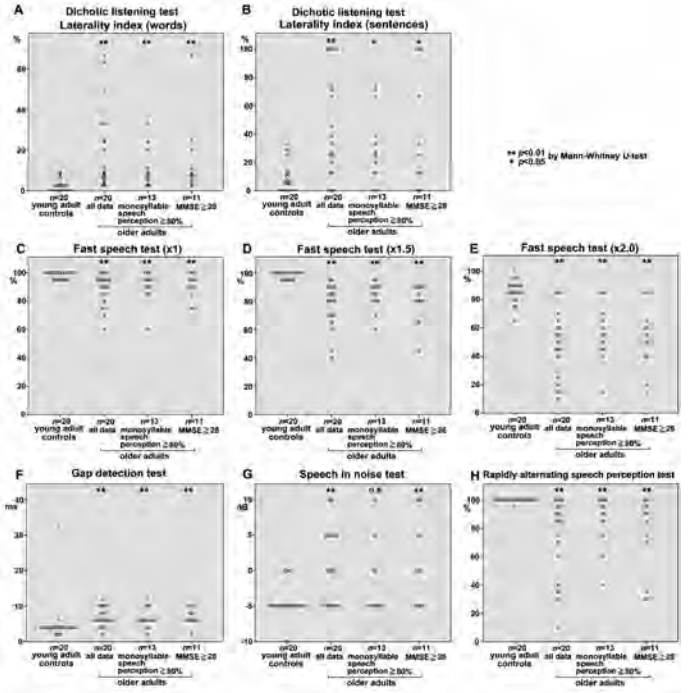

Table 3. Data of auditory processing tests in young adult controls and older adults.

(Mean±S.D.)	Young adults	All older aduls	Older adults with monosyllable speech perception≧80%	Older adults with MMSE-J≧28
	n=20	*n*=20	*n*=13	*n*=11
Dichotic listening test (words) (%)	2.1±2.7	19.5±20.2	10.7±9.4	15.0±18.5
Dichotic listening test (sentences) (%)	8.3±10.2	47.6±37.8	29.4±26.8	40.9±42.5
Fast speech test (x1) (%)	98.3±2.4	88.0±10.9	90.8±10.6	90.0±8.7
Fast speech test (x1.5) (%)	98.5±2.4	77.3±15.4	83.8±10.0	79.5±13.7
Fast speech test (x2.0) (%)	85.8±8.0	48.5±23.3	58.1±20.4	52.3±22.7
Gap detection test (ms)	5.2±6.4	6.8±2.5	6.5±2.7	6.7±2.2
Speech in noise test (dB)	-4.5±2.2	0.8±5.3	-1.3±5.3	0.9±5.8
Rapidly alternating speech perception test (%)	99.8±1.1	70.5±29.6	85.8±18.0	72.7±28.0

PS 277

Time Course of Synaptopathy and Compound Auditory-Nerve Activity in Quiet-Aged Gerbils

Friederike Steenken[1]; Rainer Beutelmann[1]; Amarins N. Heeringa[1]; Sonny Bovee[2]; Henning Oetjen[2]; Georg M. Klump[2]; Christine Koeppl[1]
[1]Cluster of Excellence Hearing4all, Department of Neuroscience, Carl von Ossietzky University Oldenburg; [2]Cluster of Excellence Hearing4all, Department of Neuroscience, Carl von Ossietzky University, Oldenburg, Germany

Quiet-aged old gerbils (> 36 months) are known to have a reduced endocochlear potential (EP) as well as a loss of synapses between inner hair cells and auditory-nerve fibers (synaptopathy). Here, we investigate the time course of synaptopathy in the aging gerbil and relate it to the neural index (NI), a frequency-specific metric sensitive to the compound activity of functional auditory-nerve fibers.

Gerbils were clustered into 5 groups: 3-10 months (young), 14-17, 23-27, 31-35 and 38-41 months (old). NI and compound action potential (CAP) thresholds to chirps were derived from a round-window electrode recording. Third-octave band noise (300 ms, 1.6-16 kHz center frequencies) was presented monaurally in stimulus pairs of opposite polarities and responses analyzed (Batrel et al., 2017, PLoS One 12(1):e0169890). Immunostained cochlear whole mounts were analyzed at seven different cochlear locations (0.5–32 kHz): functional synapses were counted manually.

Our current sample suggests that old gerbils showed an average loss of afferent synapses of 25-30%, which was largest at high-frequencies (around 40% at 8-16 kHz). The intermediate age groups showed a progressive synapse loss throughout the lifespan that likely starts at the base.

When stimulated at a fixed level of 80 dB SPL, NI was reduced in the oldest age group at all frequencies, consistent with age-related synaptopathy and lower spiking activity due to stimulation at a lower sensation level in aging animals. This reduction was, however, not clearly progressive with increasing age. Furthermore, NI showed no consistent correlation to age-related increases in CAP thresholds.

Overall, these observations suggest a mixed pathology in quiet-aging gerbils. The absence of any consistent relation between CAP thresholds and NI confirms previous findings that the loss of synapses and auditory-nerve fibers initially does not elevate thresholds. The extent of synaptopathy in aged gerbils rarely reached the degree of loss required to raise CAP-thresholds after induced synaptopathy in young gerbils (Bourien et al., 2014, J Neurophysiol 112:1024-1039). In contrast, age-related EP loss accounts for elevated thresholds (Schmiedt et al., 2002, J Neurosci 22(21):9643-9650). Interestingly, the regularly progressing synaptopathy with age was not matched by a similar regular decrease in the NI. This suggests that NI reflects not only numbers of active auditory-nerve fibers, but may also indicate age-related changes in fiber physiology. Ongoing experiments aim to correlate the relation between NI and synaptopathy in individual animals of different ages.

Supported by the DFG: PP-1608

PS 278

EEG Measures of Auditory Processing in Aging Mice

Jeffrey A. Rumschlag[1]; Jonathan W. Lovelace[2]; Khaleel A. Razak[3]
[1]Neuroscience Graduate Program, University of California, Riverside; [2]Department of Psychology, University of California, Riverside; [3]Department of Psychology and Neuroscience Program, University of California, Riverside

Background

Age-related hearing deficits, including hearing loss and temporal processing deficits, are associated with a sharp decline in cognitive function and mental health. The loss of the ability to effectively communicate eliminates a vital source of cognitive stimulation. Currently, no pharmacological treatment for age-related hearing deficits exists. Using mice as models for normal hearing and presbycusis, we have discovered age-related changes in EEG-like signals that we propose to use as outcome measures for pharmacological treatment of age-related auditory processing deficits.

Methods

We analyzed EEG signals recorded from the auditory and frontal cortices of 3-, 6-, 12-, and 20-month-old FVB (normal hearing) and C57bl/6 (model for age-related hearing loss) mice at baseline and in response to amplitude-modulated noise stimuli. The frequency content of baseline EEG signals was measured using Fourier transforms and compared across groups. Cross-frequency coupling, which describes the interactions of oscillations at different frequencies, was measured using multiple methods, including modulation index, a measure of phase-amplitude coupling. Responses to amplitude-modulated noise stimuli were transformed via complex Morlet wavelet transform into the time-frequency domain

and analyzed in terms of phase-consistency (Inter-trial phase clustering; ITPC), non-phase-locked power, and baseline-corrected total power.

Results
Baseline EEG power and cross-frequency coupling show age-related and frequency-specific differences. Responses to an amplitude-modulated noise stimulus, in which the amplitude-modulation frequency was swept linearly from 1-100 Hz over two seconds, were less consistent in older mice compared to younger mice, with the greatest differences occurring at frequencies between 20 and 50 Hz and between 70 and 100 Hz. In a time-frequency transform of event-related potentials (ERPs) evoked by noise, baseline-corrected power at long latencies (100-300 msec) showed age-related frequency-specific differences, including a decrease in low frequency power concomitant with an increase in higher frequency power in younger mice compared to older mice. During auditory steady-state responses (ASSR), a similar frequency-specific difference appears between age groups, suggesting an age-related change in synchronized cortical processing of auditory stimuli. Preliminary evidence from a novel ASSR-evoking gap-in-noise stimulus suggests that mice with hearing loss lose temporal processing acuity, even when presented with a hearing-level-matched stimulus.

Conclusions
The measures of auditory-evoked and baseline activity show interesting age-related differences in auditory and frontal cortical activity. By presenting a series of specialized auditory stimuli, we can dissociate age-related cortical auditory temporal processing changes from hearing threshold shifts.

PS 279

Aging and the Auditory Nerve â€“ Synaptic Structure, Endbulb Morphology and Peripheral Physiology

Kiera E. Grierson[1]; Satoshi Nishitani[2]; Tan Pongstaporn[3]; David Ryugo[4]
[1]Garvan Institute of Medical Research; UNSW Sydney; [2]Garvan Institute of Medical Research; St Vincent's Clinical School, UNSW Sydney; [3]Garvan Institute of Medical Research; [4]Garvan Institute of Medical Research; St Vincent's Hospital, Sydney

Background
Information about our acoustic environment is carried from the cochlea into the brain via the auditory nerve (AN). The myelinated AN fibres terminate as large, highly arborized structures with numerous axosomatic synapses. These specialised structures, the endbulbs of Held (EBs), are conserved across vertebrate species and are responsible for the transmission of high-fidelity temporal information into the brain. Their size, complexity, and synaptic structure are dependent on cochlea-driven activity. Pathological changes in the endbulb have been well characterised in animal models of induced hearing loss and congenital deafness. Our study extends previous age-related findings regarding endbulb morphology by analysing ultrastructural changes exhibited in the EB synapses.

Methods
Protocols used in this study are outlined in detail in Muniak *et al* 2018. Briefly, CBA mice were reared from newborn to 2-3 months, 6 months, 9-10 months, and 12-14 months of age. Open-field ABRs were collected to click stimuli, as well as pure tone pips at 4kHz, 8kHz, 16kHz, 24kHz, 32kHz and 40kHz from animals at their terminal age. Responses were assessed for absolute threshold, as well as normalised Wave 1 amplitudes, and the ratio of Wave 5 to Wave 1 amplitudes, an indicator of central compensation with peripheral pathology. Neurobiotin was injected into the cochlea and allowed to anterogradely fill auditory nerve fibres including EBs, which were analysed for surface area, volume and Shape Factor (SF). Selected sections were taken from animal samples and processed for EM analysis of the AN-spherical bushy cell synapse with specific attention paid to the curvature and size of the postsynaptic density.

Results
In line with results reported in Muniak *et al* 2018, ABR thresholds remained largely stable over the course of the animal's first year of life at all frequencies tested, whereas Wave 1 amplitudes decreased and Wave 5:1 amplitudes increased. EBs showed a slight reduction in complexity, as measured by shape factor. Postsynaptic densities increased in surface area and appeared to flatten.

Conclusions
These results reveal that central synaptic pathology accompanies presbycusis, perhaps as compensation for reduced activity in the auditory nerve. The conservation of high-resolution temporal information in the primary central auditory pathway facilitates sound localisation, comprehension of speech prosody and appreciation of music in humans. Any modification of synapse kinetics at the endbulb may introduce temporal jitter and even failure. Any therapeutic strategy to remedy the symptoms of age-related hearing loss must consider these issues if they are to be successful.

PS 280

Neural Envelope Coding in Middle-aged Humans with Normal Audiograms

Homeira Kafi; Alexandra Mai; Kelsey Dougherty; Anna Hagedorn; Hari Bharadwaj
Purdue University

Emerging evidence from animal models and human postmortem temporal bones suggests that cochlear synaptopathy is a primary form of age-related hearing damage. Hypothetically, cochlear synaptopathy can contribute to degraded coding of temporal information, particularly envelopes, in the ascending auditory pathway. Here, we used electroencephalography-based envelope-following responses (EFRs) to test this hypothesis in a cohort of listeners with a wide age range (18 – 60 years old) but with audiograms in the "normal" range (better than 25 dB HL up to 8 kHz). EFRs were measured in response to a broadband mixture composed of three carrier bands centered at 2, 4 and 8 kHz respectively with each band modulated at a different amplitude modulation rate. This design was based on previous work showing that separable, place-specific responses may be elicited from different cochlear sections with such stimuli. Despite audiograms being in the normal range for all subjects and accounting for residual audiometric variations across subjects using a linear model, significant age-by-frequency and age-by-modulation depth interactions were observed in the EFR magnitude (greater decline in EFR with age for shallower modulation and for higher frequency carriers), a result that is consistent with cochlear synaptopathy. In a separate study with the same cohort of subjects, auditory brainstem response wave I amplitudes and wideband middle-ear reflexes we simultaneous attenuated further corroborating this interpretation. One alternate interpretation for the EFR changes with age is that the central auditory system may be exhibiting age-related changes either independently or in response to peripheral de-afferentation. Overall, these results suggest that age-related peripheral de-afferentation may be a significant contributor to the common observation that supra-threshold temporal processing degrades with age even before symptoms of classic presbycusis are manifested. Finally, the use of the multiband stimulus to elicit place-specific EFRs as done in this study may help explain some of the inconsistencies in the previous literature exploring age effects on envelope coding.

PS 281

Peripheral Contributions to Age-Related Reductions in Phase Locking

Samira Anderson[1]; Alanna Schloss[2]; Rebecca Bieber[2]
[1]Department of Hearing and Speech Sciences, University of Maryland, College Park, MD, USA; [2]University of Maryland

Objective

Age-related deficits in the neural representation of speech and non-speech stimuli have been demonstrated across multiple studies. The mechanisms for these observed neural changes are not yet fully understood. It has been suggested that decreased afferent input and degraded auditory nerve function may lead to cascading changes throughout the auditory system. For example, a loss of auditory nerve fibers may lead to reductions in phase-locking strength, especially for responses to sustained components of auditory stimuli. This study's purpose was to evaluate the contributions of peripheral factors assessed using audiometric threshold testing, distortion-product otoacoustic emissions (DPOAEs) measurement, and auditory brainstem response (ABR) testing to reductions in phase-locking strength in normal-hearing listeners.

Method

Thirty young normal-hearing (YNH, ages 18-24) and thirty older normal-hearing (ONH, ages 55-76) adults were recruited for the study. Normal hearing was defined as audiometric thresholds ≤ 20 dB HL from 0.125 to 4 kHz and ≤ 30 dB HL from 6 kHz to 8 kHz. Thresholds were obtained for distortion-product otoacoustic emissions (DPOAEs) using input-output functions from 1 kHz to 14 kHz. Auditory brainstem responses (ABRs) were recorded to 100-μs click stimuli in quiet and in white noise (+30, +20, and +10 dB SNR). Frequency-following responses (FFRs) were recorded to two synthesized [ba] syllables that differed in steady-state vowel duration (120 ms vs. 230 ms).

Results

Though all listeners had clinically-normal hearing thresholds, expected age-related effects were found for nearly all measures. Compared to younger listeners, older listeners demonstrated elevated DPOAE thresholds, reduced Wave-I amplitudes, and delayed Wave-V latencies across conditions. FFR phase-locking strength was also reduced in the older listeners, with more pronounced effects for the sustained steady-state than the transition response regions. Regression modeling demonstrated that Wave-V latency in noise contributed to variance in phase-locking strength in the older listeners, but not in the younger listeners. Audiometric and DPOAE thresholds and Wave I amplitude did not significantly contribute to variance in either group.

Discussion

In this study, the only factor that predicted variance in phase-locking strength in older adults was Wave-V

latency in noise, while ABR measures in quiet did not significantly contribute to the variance. Wave-V's origins in the rostral brainstem support a central contribution to age-related reductions in phase-locking strength. However, the influence of low- spontaneous rate fibers on ABR latencies in noise suggests that auditory nerve contributions cannot be ruled out at this time.

Research supported by NIH/NIDCD grant R21 DC015843

PS 282

Age-Related Changes in Auditory Nerve Fiber Frequency Tuning, Temporal Coding, and Spontaneous Rate

Amarins N. Heeringa[1]; Lichun Zhang[1]; Go Ashida[2]; Rainer Beutelmann[1]; Friederike Steenken[1]; Christine Koeppl[1]
[1]Cluster of Excellence Hearing4all, Department of Neuroscience, Carl von Ossietzky University Oldenburg; [2]University of Oldenburg

Age-related hearing loss (ARHL) is a highly common and debilitating sensory disorder among elderly people. A variety of pathological changes within the cochlea is associated with ARHL, and include degeneration of the stria vascularis, hair cells, and spiral ganglion neurons and their synapses with the inner hair cell. The quiet-aged Mongolian gerbil, a commonly-used animal model to study ARHL, typically presents with strial dysfunction and synaptopathy. Studies addressing the effects of these age-related cochlear pathologies on coding of sounds in the auditory nerve at the single unit level are, however, scarce. Here, we study the effects of age on single auditory-nerve fiber frequency tuning, temporal coding, and spontaneous rates.

Single-unit auditory-nerve fiber recordings were obtained from 26 young (3-14 months), 6 middle-aged (23-33 months), and 9 old (37-42 months) gerbils. Firing rates in quiet and during stimulation with pure-tones (50ms, 3-79 dB SPL) or noise bursts (1s, 10-30 dB SL, 0.5-12 kHz bandwidth) were obtained. Frequency tuning measures included Q_{10dB}, bandwidth at half-maximum rate, and 10-dB bandwidth of the *revcor* spectrum. Temporal coding measures included vector strength to tones at best frequency, and peak amplitude of the *revcor* spectrum, DifCor, and SumCor from responses to the noise bursts. The latter two represent temporal fine structure (TFS) and envelope (ENV) coding, respectively.

Despite elevated thresholds in middle-aged and old gerbils, frequency tuning near threshold, as evaluated by various metrics, was not affected in aging gerbils. Furthermore, at comparable sensation levels, all measures of temporal coding, even when dissociating between TFS and ENV coding, were unaltered. However, spontaneous rates were significantly lower in both middle-aged and old gerbils than young gerbils.

The reduced spontaneous rate and elevated thresholds, but normal frequency tuning, of aged auditory-nerve fibers can be explained by the well-known reduction of endocochlear potential due to strial dysfunction in quiet-aged gerbils. Furthermore, these results suggest that previously reported age-related temporal coding deficits arise more centrally, possibly due to an age-related loss of active auditory-nerve fibers (starting with loss of their peripheral synapses) but not due to qualitative changes in the responses of remaining auditory nerve fibers.

This work was supported by the DFG Cluster of Excellence EXC 1077/1 "Hearing4all".

PS 283

Blockade of Corticothalamic Projections Alters Coding in Medial Geniculate Body to Less Salient Modulated Stimuli

Srinivasa Prasad Kommajosyula[1]; Edward Bartlett[2]; Rui Cai[3]; Donald Caspary[3]
[1]Southern Illinois Univ. School of Medicine; [2]Purdue University; [3]Southern Illinois University School of Medicine

Background
To disambiguate speech in cluttered acoustic environments, additional cognitive resources are engaged and top-down cortical projections sharpen the ascending auditory message. The medial geniculate body (MGB) receives extensive corticothalamic projections. These are implicated in shaping MGB neural activity, which subsequently changes cortical representation. Here we posit that decreasing the salience of a SAM stimulus would increase neural jitter and mimic decreased inhibition in aged animals resulting in increased preference coding to predictable stimuli. We also hypothesize that diminishing cognitive resources with general anesthesia or selective optogenetic blockade of corticothalamic projections would impede preference coding noticed in MGB units.

Methods
Fischer Brown Norway rats of age (4-6mos) were used. Tetrode microdrives were implanted in MGB (awake group). In the awake optogenetic group, ArchT was injected into the primary auditory cortex, targeting layer 5/6, to selectively block corticothalamic tracts in animals implanted in MGB with tetrodes including an optical probe. Tungsten electrodes were used in the

anesthetized group. Single-unit activity and/or local field potential (LFP) were recorded from the MGB of all groups. Salient and less salient SAM stimuli were generated and delivered as in Kommajosyula et al., (2019). Changes in single-unit response properties were compared across groups.

Results

Single-units (66 in the awake group; 28 in the anesthetized group; 31 in the awake optogenetic group) were recorded from rat MGB. In recordings from awake MGB units, as the salience of the SAM stimulus decreased, significant increases in MGB neuronal responses to predictable stimuli were observed. In contrast to adaptation, less salient stimuli result in increased responses to predictable/repeating stimuli. This switch toward predictable response preference was reduced by optogenetic blockade of corticothalamic inputs to MGB and was absent in anesthetized rats. These changes support our hypothesis that top-down processes alter sensitivity to repeating stimuli at MGB.

Conclusions

Here we tested the hypothesis that less salient temporal stimuli engage corticothalamic projections to switch preference coding in MGB neuronal responses. This switch was not observed in rats with selective optogenetic blockade of corticothalamic projections or in recordings from anesthetized rat MGB. These data support the contention from human studies and our previous rat studies (Cai et al., 2016) of increased use of top-down information to help disambiguate communication-like sounds in cluttered acoustic environments and the elderly.

PS 284

The Influence of Presbycusis on the Processing of Temporal Features of Sound Stimuli in the Auditory Cortex of Rats

Josef Syka; Kateryna Pysanenko; Zbynβk Bureš
Institute of Experimental Medicine CAS, Prague, Czech Republic

Age-related hearing loss is manifested primarily by a decreased sensitivity to faint sounds, that is, by elevation of the hearing thresholds. Nevertheless, even people with normal hearing thresholds often complain about deteriorated speech comprehension, particularly under difficult conditions. These difficulties are usually attributed to the age-related decline in the processing of temporal features of the sound stimulus.

To explore the precision and reliability of auditory temporal processing during ageing, stimulus-driven responses were recorded from neurons of the auditory cortex of adult and aged Fischer 344 rats anesthetized by a combination of ketamine and xylazine. First, rate-intensity functions were measured using broad-band noise (BBN) bursts and pure tones at the best frequency (BF). The aged rats had a lower proportion of strictly monotonic neurons. In response to BBN, the aged rats exhibited larger response magnitudes and also a larger variability of response magnitudes, suggesting a lower stability of the rate code. However, the responses to BF tones did not differ between adult and aged rats in either amplitude or variability. Of primary interest were the responses to temporally structured stimuli: amplitude-modulated (AM) noise, frequency-modulated (FM) tones, and click trains. In the cases of AM noise and clicks, the aged animals had a worsened ability to synchronize with the stimulus period, as indicated by lower vector strength values, and their modulation transfer function was flatter reflecting a lower specificity for different period lengths of the stimulus. Surprisingly, in the case of FM tones, synchronization with the stimulus period improved with higher age: the vector strength values and the number of phase-locking neurons were higher in the aged animals; furthermore, the van Rossum distance was smaller in the aged rats for this type of stimulus, indicating a higher reliability of the temporal code. In addition, the tuning to the FM stimulus was sharper in the aged rats.

Overall, the results show that when stimulated with wide-band sounds, such as noise or clicks, the aged auditory system exhibits a decline in the precision and reliability of both the rate code and the temporal code. However, in response to sinusoidal or nearly-sinusoidal auditory stimuli, the aged animals appear to have the same or even better processing ability.

PS 285

The Characteristics of Peripheral Cochlear Function And Central Auditory Function in Different Age Groups

Minfei Qian[1]; Hao Wu[2]; zhiwu huang[3]; Qixuan Wang[3]
[1]Department of hearing center Shanghai Ninth People's Hospital, Shanghai Jiao Tong University School of Medicine; [2]1. Department of Otolaryngology - Head & Neck Surgery, Shanghai Ninth People's Hospital, Shanghai Jiao Tong University School of Medicine; 2. Ear Institute, Shanghai Jiao Tong University School of Medicine; 3. Shanghai Key Laboratory of Translational Medicine on Ear and Nose diseases, Shanghai, China; [3]Department of Otolaryngology-Head and Neck Surgery, Shanghai ninth people's Hospital, Shanghai Jiao Tong University School of Medicine; Ear Institute, Shanghai JiaoTong University School of Medicine; Shanghai Key Laboratory of Translational Medicine on Ear and Nose diseases

Objective
To investigate the characteristics of peripheral cochlear function and central auditory function in different age groups, the decline frequency specificity of cochlear function and central auditory function, and the aging process of human's peripheral and central auditory function; to select the most sensitive examination indicators of auditory function.

Methods: Collect 149 human samples with normal audible threshold, and divide them into four age groups: 20-29, 30-39, 40-49 and 50-59 years old. Cochlear function examination methods (e.g. EcochG, TEOAE) and central auditory function testing methods (e.g. MHINT, GAP) are respectively used for the test. EcochG, TEOAE and GAP are using different stimulus frequencies.

Results
1. TEOAE CAS-, CAS+, EcochG AP, latency, MHINT and GAP have progressively declined with age, and have shown frequency characteristics. While 2K is the frequency with the slowest pace of decline. 2. TEOAE CAS- and CAS+ are two independent indicators, with no correlation as suggested by amplitude analysis. 3. Differences exist between the cochlear function and central auditory function of left and right ear. Right ear is more advantaged with its TEOAE CAS- and CAS+ both higher than that of left ear. 4. Central auditory function has higher correlation to age compared with peripheral auditory function.

Conclusion
1. Peripheral and central auditory function are both progressively declining with age; while speech frequency declines slowly with age. 2. TEOAE CAS+ is the indicator that is most relevant to age among all examination indexes of peripheral auditory function. 3. The decline of central auditory function is not secondary to that of peripheral auditory function. They are two relatively independent indicators.

Auditory Cortex - Human Studies I

PS 286

Difficulties with Speech-in-Noise Perception Related to Fundamental Grouping Processes in Auditory Cortex

Emma Holmes[1]; Karl Friston[1]; Timothy Griffiths[2]
[1]*Wellcome Centre for Human Neuroimaging, UCL;*
[2]*Institute of Neuroscience, Newcastle University*

Speech-in-noise (SIN) perception is a crucial everyday task that varies widely among people—and cannot be explained fully by the pure-tone audiogram. One factor that likely contributes to difficulty understanding SIN is the ability to separate speech from concurrent background sounds, which is not well assessed by audiometric thresholds. A basic task that assesses the ability to separate target and background sounds is auditory figure-ground perception. Here, we examined the degree to which speech-in-noise and figure-ground perception share common behavioural variance across subjects and the same neural architectures.

We recruited 97 participants with normal hearing (6-frequency average pure-tone thresholds < 20 dB HL) for a behavioural experiment. They reported sentences from the Oldenburg matrix corpus (e.g., "Alan has two old sofas"), which were presented simultaneously with multi-talker babble noise. The figure-ground stimuli were based on Teki et al. (2013, eLife), in which each 50 ms time window contains random frequency elements, and figure frequencies remained fixed over time. Performance on the figure-ground task explained significant variability in SIN performance that was unaccounted for by audiometric thresholds.

To examine the neural correlates of this shared psychophysical variance, we recruited 44 participants for a functional magnetic resonance imaging (fMRI) experiment. We used a 2 x 2 factorial design, in which each participant completed figure-ground and speech-in-noise tasks at two different target-to-masker ratios (TMRs) (calculated for each participant based on adaptive procedures that estimated 60% and 90% thresholds for each task). Using Dynamic Causal Modelling, we found common effects of greater perceptual demand in both tasks: We found strong (> 99%) evidence that the earliest stages of the auditory cortical hierarchy (left core and belt areas) are similarly disinhibited when speech-in-noise and figure-ground tasks are more challenging (i.e., at TMRs corresponding to 60% thresholds).

These results—in normally-hearing listeners—demonstrate that we can better predict SIN performance by including measures of figure-ground perception alongside audiometric thresholds. Importantly, the results support a source of variance in speech-in noise perception related to figure-ground perception that is unrelated to audiometric thresholds. The neuroimaging results suggest this shared variance reflects common processes in left core and belt areas of auditory cortex—which can be interpreted as an adaptive gain (i.e., predictive precision control) at the earliest stages of the auditory cortical hierarchy. Overall, these results highlight an important role of fundamental grouping processes, which operate centrally, on the ability to understand speech when background noise is present.

PS 287

High Frequency Cortical Processing of Continuous Speech in Younger and Older Listeners

Joshua P. Kulasingham[1]; Christian Brodbeck[1]; Alessandro Presacco[2]; Stefanie E. Kuchinsky[3]; Samira Anderson[4]; Jonathan Z. Simon[1]
[1]University of Maryland, College Park; [2]Unversity of Maryland, College Park; [3]Audiology and Speech Pathology Center, Walter Reed National Military Medical Center; [4]Department of Hearing and Speech Sciences, University of Maryland, College Park, MD, USA

The neural processing of natural sounds, such as speech, changes along the ascending auditory pathway, and is often characterized by a progressive reduction in representative frequencies. For instance, the well-known frequency-following response (FFR) of the auditory midbrain, measured with electroencephalography (EEG), is dominated by frequencies from ~100 Hz to several hundred Hz, and time-locks to acoustic features at those rates. In contrast, cortical responses to speech, whether measured by EEG or magnetoencephalography (MEG), are thought to be characterized by frequencies of a few Hz to a few tens of Hz, time locking to acoustic envelope features at those rates. However, fast (~100 Hz) MEG responses time-locked to similarly fast envelope changes in high frequency bands of speech have also been reported. In this study we show that such fast responses are dominated by early latency sources within auditory cortex, and that they are robust across age groups. Specifically, we investigate high-frequency MEG responses (70-300 Hz) to continuous speech using neural source-localized reverse correlation, whose kernels are called temporal response functions (TRFs). Continuous speech stimuli were presented to 40 subjects (17 younger, 23 older) with clinically normal hearing and their MEG responses were analyzed in the 70-300 Hz band. Consistent with the insensitivity of MEG to many subcortical structures, the spatiotemporal profile of these response components indicates a predominantly cortical origin with ~35 ms peak latency and a right hemisphere bias. TRF analysis was performed using two separate aspects of the speech stimuli: a) the 70-300 Hz band of the speech waveform itself (i.e., the carrier), and b) the 70-300 Hz envelope of the high frequency (300-4000 Hz) band of the speech stimulus. It was seen that the envelope-locked component dominated the response over that of the carrier. Age-related differences were also analyzed to investigate a reversal previously seen along the ascending auditory pathway, whereby older listeners have weaker midbrain FFR responses than younger listeners, but, paradoxically, have stronger low frequency cortical responses. In contrast to these earlier results, this study did not find consistent age-related magnitude differences in high frequency cortical responses. Together, these results suggest that the traditional EEG-measured FFR has distinct and separate contributions from both subcortical and cortical sources. Furthermore, the cortical responses at FFR-like frequencies share properties with both midbrain responses at the same frequencies and cortical responses at much lower frequencies.

PS 288

Fundamental Properties of Auditory Cortical Activity in Children as Observed from Direct Intracranial Recordings

Ariane Rhone[1]; Kirill Nourski[1]; Christopher Kovach[1]; Brian Dlouhy[1]; Mitchell Steinschneider[2]
[1]University of Iowa; [2]Albert Einstein College of Medicine

Neurosurgical interventions for remediation of medically intractable epilepsy have become a viable clinical option in pediatric patients. To investigate developmental aspects of cortical auditory processing, we studied eight children (3-19 years old) during chronic intracranial electroencephalographic (iEEG) monitoring for seizure localization. All studies were approved by the NIH and the University of Iowa Institutional Review Board. Informed consent was provided by parents or legal guardians. Verbal or written assent was obtained from the children. Depth electrodes targeting the insula were placed in all eight subjects, which permitted recordings either in or immediately adjacent to Heschl's gyrus. In three subjects (ages 9, 13, and 14), subdural grid electrodes were also placed over the lateral convexity, covering temporal, frontal, and parietal regions. Click trains with rates of 25 Hz to 200 Hz, pure tones from frequencies 250 Hz to 8 kHz, and synthetic stop consonant-vowel (CV) syllables were presented. Additionally, children engaged in a question-answer dialog based on that used previously (Nourski et al, 2016, Front Hum Neurosci 10:202) and a structured version of the children's card game "Go Fish." Analysis focused on local field potentials and event-related high gamma power (70-150 Hz).

In common with adult subjects, response latencies progressively increased and high gamma power progressively decreased from posteromedial to anterolateral portions of Heschl's gyrus. Phase locking elicited by click trains was reliably observed for rates up to 50 – 100 Hz and was maximal in posteromedial Heschl's gyrus. Phase locking to the 100 Hz fundamental frequency of CV syllables was also especially prominent in posteromedial Heschl's gyrus. On the lateral superior temporal gyrus (STG), activity elicited by sounds was maximal near the transverse temporal sulcus. High gamma activity was observed for all stimulus types, though speech generally elicited more widespread

responses than pure tones or click trains. CV syllables elicited local field potentials that differed between voiced and unvoiced consonants (5 ms and 40 ms voice onset time, respectively). Naturalistic verbal interactions were characterized by widespread high gamma activation within auditory cortex and fronto-parietal areas.

We conclude that fundamental properties of neural activity recorded from Heschl's gyrus and lateral STG are similar to those seen in adult subjects from early childhood onward. Furthermore, preliminary results provide proof of concept that naturalistic interactive tasks are feasible in children undergoing invasive monitoring for treatment of their medically intractable epilepsy and can be used to probe development of auditory cortical function using iEEG.

PS 289

Neural Processing and Perception of Speech in Children with Mild to Moderate Sensorineural Hearing Loss

Axelle Calcus[1]; Stuart Rosen[2]; Lorna Halliday[3]
[1]Ecole Normale Supérieure; [2]University College London; [3]University of Cambridge

Mild (21-40 dB HL) or moderate (41-70 dB HL) sensorineural hearing loss (MMHL) can lead to persistent changes to the cortical processing of speech sounds. This was evidenced in a study conducted on 46, 8- to 16-year old children with MMHL and 44 normally-hearing (NH) age-matched controls. While present in younger children with MMHL, there was no significant MMN in older children with MMHL. However, to date no studies have examined speech processing at the subcortical level in children with MMHL, yet this is known to be linked to speech perception in noise (SIN) in NH children. Moreover, the effects of amplification on the neural encoding of speech remain poorly understood, with previous data suggesting a benefit at the subcortical but not the cortical level.

Here, we aimed to investigate (1) the subcortical and cortical processing of speech sounds in children with MMHL, (2) the relation with SIN, and (3) the effects of amplification on the neural processing of speech, for children with MMHL. Behavioural thresholds were measured at 70 dB SPL for consonant identification in both steady and fluctuating noise. Subcortical and cortical EEG activity evoked by speech stimuli were simultaneously recorded in 18, 8- to 16-year old children with MMHL and 15 age-matched NH controls. The frequency-following-response (FFR) and MMN were used as indeces of speech processing at the subcortical and cortical levels, respectively. For the MMHL group, stimuli were presented both unamplified (70 dB SPL), and with a frequency-specific gain (without compression) based on their individual audiograms.

Behavioural thresholds were poorer for children with MMHL than NH controls, whatever the background noise. At the subcortical level, children with MMHL showed a smaller FFR than NH controls' in the unamplified condition. With simulated amplification, the FFR of the MMHL group was comparable to that of NH controls. However, the relationship between subcortical encoding of speech and SIN was not significant. At the cortical level, there was no significant MMN in children with MMHL presented with either unamplified or amplified speech.

The neural processing of unamplified speech may be impaired at both subcortical and cortical levels in children with MMHL. Moreover, amplification may benefit auditory processing at subcortical but not cortical levels in this group. We offer two alternative explanations for our findings: increasing multi-sensory integration at successive levels of the auditory system, and/or later maturation of the auditory cortex compared to the inferior colliculus.

PS 290

Fast Click Rate Evoked Auditory Brainstem Response in Children with Autism

chun liang; Jierong Chen; Binbin Sun; Yalin Liu; Chengyun Zou; Guobin Wan
Dept. of Child Psychiatry and Rehabilitation, Affiliated Shenzhen Maternity & Child Healthcare Hospital, Southern Medical University,

Objectives
Autism spectrum disorder (ASD) is a neurodevelopmental disorder and seriously affects children's life. Early detection and diagnosis is critical for ASD treatment and symptomatic improvement. Language impairments and hyperacusis are two most commonly symptoms in ASDs. Previous study demonstrated that ASDs have poor capability of auditory processing function. Fast acoustic stimulus evoked auditory brainstem responses (ABRs) is a sensitive tool for detecting and identifying fine auditory deficits. In this study, we recorded the fast click rate evoked ABR (fABR) in ASD children to examine whether it could serve as a valuable index for early ASD diagnosis.

Method
The super-threshold ABRs were evoked by clicks with two stimulus rates (19.1 clicks/s and 69.1 clicks/s). Twenty-two children with suspected ASDs and an age- and sex-

matched group of 22 children with developmental delay (DD) were recorded. All children had normal hearing threshold. The stimuli were presented monoaurally at 80dB SPL to the right ear through ER-3A insert earphones. The absolute latencies of wave I, III, V, interpeak latencies (IPLs), and the amplitude-ratio V/I of fABR with slow-rate evoked ABR (sABR) in the ASD group and the DD group were measured and compared. The difference of IPL of I to V between two presenting rates larger than 0.28ms was set as abnormal.

Results

In comparison with sABR, both groups in fABR showed prolonged wave latencies, IPLs and smaller amplitudes. However, the wave I amplitudes of fABR in the ASD group was significantly larger than that in the DD group (*t*=2.372, *df*=37, P=0.023). The ratio of V/I amplitude in the ASD group was also significantly decreased in comparison with that in the DD group (*t*=-2.466, *df*=37, P=0.018). There was no significant difference in sABR between the ASD group and the DD group. However, 82% (18 out of 22) in the ASD group and 76% (13 out of 17) in the DD group had apparent prolongation of IPLs of I to V between fABR and sABR.

Conclusions

Both ASD and DD children have abnormal fABR with prolonged interpeak latency of wave I to V. However, the amplitude-ratio of wave V/I evoked by fast click-rate in ASD children is significantly decreased in comparison with that in DD children, and could be served as a biomarker for early ASD detection.

Research Supported by FYA2018011 grant to CL, Sanming Project of Medicine in Shenzhen (SZSM201512009) and Subject Building Capacity Promotion Project of Medicine in Shenzhen (SZXJ2017043) to GBW.

PS 291

Acoustic Change Complex and the Auditory Steady State Response with Amplitude Modulated Noise in Children with Listening Difficulties

Chelsea Blankenship[1]; Lauren Petley[2]; Thu Nguyen[3]; Noah Campagna[3]; Audrey Perdew[3]; Nathan Clevenger[3]; Erin Cash[3]; Andrew Dimitrijevic[4]; David R. Moore[1]

[1]Cincinnati Children's Hospital Medical Center; [2]Clarkson University; [3]Cincinnati Children's Hospital Medical Center; [4]Sunnybrook Research Institute

Listening difficulties (LiD) are prevalent in young children and may be related to an inability to understand the acoustic environment. LiDs are the primary complaint from children visiting audiology clinics, yet around 5% of these children have conventionally defined 'normal hearing' (≤ 20 dB HL).One hypothesis is that LiD is caused by deficits in temporal processing, which is essential for speech understanding, localization, and complex listening tasks. Auditory cortical evoked potentials, including the auditory steady-state response (ASSR) and the acoustic change complex (ACC), can be used to quantify temporal processing of speech-like auditory cues objectively. Here, the ASSR examined neural synchronization to amplitude modulation (AM) with rates corresponding to syllables (4 Hz) and formants (40 Hz), and the ACC examined ability to detect changes in modulation rate and depth in an otherwise continuous signal. Children with LiD (n=44, 8-16 yrs) based on validated parent questionnaires (ECLiPS, Barry, 2015, Ear Hear.) and age-matched typically developing children (TD; n=44) were recruited from clinical services and website advertisements. Children completed a variety of behavioral and physiological tests including audiometric thresholds (0.25-16kHz), spectrotemporal resolution (PART), speech intelligibility-in-noise (LiSN-S), and behavioral AM depth detection (4 and 40 Hz; 3AFC procedure). Cortical auditory evoked responses, including the ASSR and ACC, were collected from a sub-set of participants (TD=31, LiD=19) using a 64-channel actiCHamp Brain Products recording system (BrainVision). EEG stimuli were continuous white noise with 4 and 40 Hz modulation rates and depths of 50 and 100%. Participants pressed #1 on a keyboard when they detected a change in the stimuli. All participants had normal audiometric thresholds in the standard frequency range (≤ 20dBHL; 0.25-8kHz). No significant group difference (TD vs. LiD) in AM depth threshold was found for 4 or 40 Hz ($p > 0.05$). Preliminary ACC results from 6 LiD and 6 TD participants to changes in modulation rate (4 and 40 Hz) displayed a trend of reduced P2 amplitude in LiD compared to TD participants ($p=0.05$), but no significant differences in N1 and N2 amplitude ($p > 0.05$). Results suggest that children with LiD may have compromised temporal processing supporting amplitude modulation evoked EEG as a diagnostic test for LiD. Further analyses will explore group differences in modulation rate and depth detection using ACC peak amplitude/latency and ASSR response amplitude, signal-to-noise ratio, and phase-coherence. The effect of age and correlations among cortical and behavioral measures of AM, speech-in-noise and spectrotemporal processing will be explored.

PS 292

A Brain Network of Temporo-Frontal and Hippocampal Areas Support Pattern Detection in Rapid Sound Sequences

Roberta Bianco[1]; Pavan Chaggar[1]; Rosemary Southwell[1]; Sven Bestmann[2]; Gareth Barnes[2]; Maria Chait[1]
[1]UCL Ear Institute, 332 Gray's Inn Rd, London, WC1X 8EE, United Kingdom; [2]Wellcome Centre for Human Neuroimaging, 12 Queen Square, London, WC1N 3AR, United Kingdom

To make sense of unfolding acoustic patterns, listeners must instantaneously track and maintain in memory the statistics of the sequence at hand, and use this information to evaluate the expectedness of incoming input. Recent work has showed that temporo-frontal regions, and hippocampus are recruited when human listeners detect the emergence of deterministic sequential patterns. What is the role of hippocampus, and more in general what are the dynamics of this network and the underlying mechanisms?

Here, we measured magnetoencephalography (MEG) brain signals associated with detection of patterns which are manipulated in terms of complexity (number of constituent frequencies; alphabet size) and predictability (whether tones are arranged in regular or random patterns). Rapid tone-pips sequences of 4 sec (50 ms tone duration) were built from a set of 5, 10 or 20 frequencies (alph = alphabet size of the set). These were arranged in either random order (RAN_{alph}), or in regularly repeating cycles (REG_{alph}). Novel sequences were generated on each trial. Participants were naïve to the sounds and performed a decoy visual task.

Evoked responses revealed increase in tonic activity associated with the REG as compared with RAN patterns, showing a clear effect of predictability. A weaker difference between REG and RAN patterns of 20 tones suggests that strain on memory processes, by complex acoustic patterns, overshadows the effect of predictability. Activity in primary/secondary auditory areas, inferior frontal gyrus and hippocampus was greater for REG than RAN patterns, and was also modulated by alphabet size. Connectivity analysis was used to show the dynamics underlying these network nodes.

These results highlight the role of hippocampus in a network that quickly and automatically tracks the statistics of unfolding sound sequences.

PS 293

The Developing Creative Brain: a Functional Magnetic Resonance Imaging (fMRI) Investigation of Musical Creativity in School-Aged Children

Karen C. Barrett[1]; Patpong Jiradejvong[2]; Lauren Jacobs[3]; Charles J. Limb[2]
[1]University of California, San Francisco; [2]Dept of Otolaryngology-Head and Neck Surgery, University of California, San Francisco; [3]Washington University in St. Louis

Improvisation, or the spontaneous creation of musical rhythms and melodies, is a form of musical creativity that unfolds in real-time. Over the last decade, researchers have investigated the neural correlates of musical improvisation by having participants perform control tasks involving playing pre-learned or pre-memorized music as compared to an experimental task where participants generate improvisations[1–5]. Through these experiments, knowledge has been gained about the brain areas involved in musical creativity. However, these experiments have examined adults, with an emphasis on trained musicians for whom improvisation represents a core behavior. Relatively little is known, however, about the neural substrates that underlie amateur or developing creativity in non-expert children.

In this study, children (n = 12, ages 9-11) with limited musical training performed an improvisational task on an fMRI-compatible piano using a paradigm based on the pentatonic scale. For the control task, participants played the pentatonic scale up and down repeatedly to a provided beat and backtrack. For the experimental task, participants were given the freedom to improvise, playing the notes of the pentatonic scale in whatever order they wished, although still at the same tempo and rhythm as the control task. The provided backtrack was always musically consonant with the pentatonic scale; because the music always sounded pleasant and correct, children were able to do this musical task without explicit musical training or knowledge.

Results suggest that improvisation is a distinct process from a more rote musical activity. Improvisation was associated with significant relative deactivation of neural structures: widespread deactivation was observed in limbic (posterior cingulate cortex, hippocampus) and parietal (angular gyrus, precuneus) areas. Focal deactivation in the primary motor cortex and left posterior dorsolateral prefrontal cortex (DLPFC, BA 8) was seen as well. Small areas of focal activation were identified in the right premotor cortex and left middle frontal gyrus. Although certain regions (cingulate cortex, premotor areas, DLPFC, and frontal cortices) are thought to be important for improvisation in adults, specific outcomes

vary according to study. Here, we found a similar network of regions involved during musical improvisation in children, but with less widespread deactivation of prefrontal cortex in comparison to expert musicians, potentially representing the impact of age and/or expertise on the neural substrates that underlie musical creativity. To our knowledge, this is the first neural imaging investigation of musical creativity in children, and may help us to better understand the developing creative brain.

Works Cited

Limb CJ, Braun AR. Neural substrates of spontaneous musical performance: an FMRI study of jazz improvisation. PLoS One. 2008;3(2):e1679.
Berkowitz AL, Ansari D. Expertise-related deactivation of the right temporoparietal junction during musical improvisation. Neuroimage [Internet]. 2010; Available from: http://dx.doi.org/10.1016/j.neuroimage.2009.08.042
Bengtsson SL, Csíkszentmihályi M, Ullén F. Cortical regions involved in the generation of musical structures during improvisation in pianists. J Cogn Neurosci. 2007;19(5):830–42.
Pinho AL, de Manzano Ö, Fransson P, Eriksson H, Ullén F. Connecting to create: expertise in musical improvisation is associated with increased functional connectivity between premotor and prefrontal areas. J Neurosci. 2014 Apr 30;34(18):6156–63.
Donnay GF, Rankin SK, Lopez-Gonzalez M, Jiradejvong P, Limb CJ. Neural substrates of interactive musical improvisation: an FMRI study of "trading fours" in jazz. PLoS One. 2014 Feb 19;9(2):e88665.

PS 294

Application of an Auditory Steady State Response Paradigm to Cortical Evoked Potentials

Linda J. Hood[1]; Rafael E. Delgado[2]; John D. Durrant[3]
[1]Vanderbilt University; [2]Intelligent Hearing Systems; [3]University of Pittsburgh

Background

Cortically generated late latency auditory evoked potentials provide an objective, comprehensive view of auditory pathway integrity with advantages over evoked potentials that assess function only through subcortical brainstem areas. Late Latency Responses (LLR) provide an opportunity to use more complex stimuli to evaluate both detection and discrimination of sound and are valuable in testing patients who lack neural synchrony at the brainstem level, such as patients with auditory neuropathy. Tlumak et al. (2011; IJA 50, 448-458) developed a method, which we have termed Late Latency Auditory Steady State Response (LLASSR), that integrates cortical/LLR testing into an auditory steady state paradigm. This approach applies principles of steady state response recording and facilitates incorporation of the advantages of objective response analysis and interpretation.

Methods

Data have been obtained from groups of human subjects with normal hearing, sensorineural hearing loss, and simulated conductive hearing loss. LLASSR and traditionally measured LLR were obtained for tones centered at 0.5, 1, 2, and 4 kHz and for speech syllables. Stimuli are presented at rates below 1 Hz in trains that are filtered and averaged across multiple sweeps. All single sweep recordings are automatically stored for offline and statistical analysis of signal and noise components. Responses were recorded in both LLASSR and LLR paradigms at multiple intensities descending to threshold and compared to behavioral thresholds. Preliminary data have been obtained in infants and methods of characterizing responses across multiple dimensions are being developed that include analysis of signal-to-noise and residual noise measures for fundamental and harmonic components.

Results

Comparison of responses by visual inspection of LLASSR and LLR waveforms indicate comparable response latency and amplitude characteristics for subjects with normal hearing with thresholds within 5 dB of behavioral responses. Subjects with hearing loss display results similar to the normal hearing cohort, with some responses showing closer agreement with behavioral thresholds than observed in subjects with normal hearing. Objective evaluation methods using spectral techniques analyze the significance of the contributions of the various harmonic components for response detection.

Conclusions

Incorporating a steady-state response paradigm into late latency response measurement provides a sensitive threshold detection method. A key clinical strength of this approach is the ability to determine presence of cortical responses near threshold without the need for subjective judgment. Ongoing studies are expanding stimulus sets, subject groups, and analysis methods.

[Supported by NIH-NIDCD SBIR R44DC015920, PI: Delgado]

PS 295

A pilot study to evaluate spectral resolution with Acoustic Change Complex using Ear Electroencephalography

Soojin Kang[1]; Hye Yoon H. Seol[2]; Sung Hwa Hong[3]; Il Joon Moon[4]
[1]Medical Research Institute, Sungkyunkwan University School of Medicine, Suwon, Korea; Hearing Research Laboratory, Samsung Medical Center, Seoul, South Korea; [2]Hearing Research Laboratory, Samsung Medical Center, Seoul, South Korea; [3]Department of Otorhinolaryngology-Head and Neck Surgery, Sungkyunkwan University School of Medicine, Samsung Changwon Hospital, Changwon, Korea; Hearing Research Laboratory, Samsung Medical Center, Seoul, South Korea; [4]Department of Otorhinolaryngology-Head and Neck Surgery, Sungkyunkwan University School of Medicine, Samsung Medical Center, Seoul, Korea; Hearing Research Laboratory, Samsung Medical Center, Seoul, South Korea

Sound contains frequency and temporal information. Listeners use this information for speech discrimination. Spectral resolution is an important factor for aided speech performance of listeners with hearing loss. Spectral resolution is behaviorally evaluated using the spectral ripple discrimination (SRD) test, which is a useful tool. However, certain population, such as infants, young children, uncooperative individuals who cannot provide appropriate feedback has difficulty completing the behavioral test. Therefore, an objective approach is necessary to evaluate spectral resolution. Although cortical auditory evoked potentials (CAEP) are very valuable to study central auditory processing in research, it is too complex to apply in the clinic or for real-world data acquisition. Recently, a novel approach to study neural signals using ear electroencephalogram (Ear-EEG) was introduced. The aims of this pilot study are to determine the optimal approach for Ear-EEG recording and to investigate the possibility of using Ear-EEG as a potential objective approach for spectral resolution evaluation by comparing CAEP with Ear-EEG.

Three subjects with normal hearing participated in this pilot study. We first set appropriate parameters to obtain distinct auditory evoked potential using an electrode around the ear (Ear-EEG). The electrode location, stimulus duration, and stimulus presentation side were investigated. We then compared CAEP and Ear-EEG induced by spectral ripple sound to evaluate spectral resolution.

The electrode location was decided as follows. The electrode for Ear-EEG was placed on the upper side of the ear. The reference and ground electrodes were placed contralateral and ipsilateral to the ear electrode, respectively. Cz was used to record CAEP. The stimulus presentation side was determined as the contralateral side of the ear electrode. The total stimulus duration was determined as 2s which was composed of 1.5s of standard ripple and 0.5s of inverted ripple sound. These experimental parameters were applied to the second step in this study. The results showed clear evoked potentials in response to the spectral ripple sound with Ear-EEG. Although the amplitude of Ear-EEG was smaller than that of CAEP, thresholds were obtained using the acoustic change complex evoked by the inverted ripple sound.

Findings from this study support previous literature regarding the feasibility of using Ear-EEG as an objective approach. Further studies with a greater number of participants and with hearing loss population are necessary to confirm the efficacy of this approach.

This work was supported by the National Research Foundation of Korea (NRF) grant funded by the Korea government (MSIT) (No. S-2019-0644-000-01).

PS 296

Physiology and Connectivity of the Human Superior Temporal Sulcus as Revealed by Intracortical Recordings

Mitchell Steinschneider[1]; Kirill Nourski[2]; Ariane Rhone[2]; Christopher Kovach[2]; Hiroto Kawasaki[2]; Matthew Banks[3]
[1]Albert Einstein College of Medicine; [2]University of Iowa; [3]University of Wisconsin

The superior temporal sulcus (STS) is a crucial hub in the cortical system subserving speech perception. To date, this area has been primarily examined with non-invasive functional neuroimaging (e.g. fMRI). In neurosurgical epilepsy patients, multicontact depth electrodes that target mesial temporal lobe structures such as the amygdala can traverse the upper or the lower bank of the STS. This offers a unique opportunity to study this region with high spatial and temporal resolution. The study sought to characterize fundamental electrophysiological properties of the STS using a variety of auditory stimuli presented under multiple task conditions in a large cohort of subjects (N = 29).

Stimuli were non-speech and speech sounds, presented in passive-listening, target detection and dialog-based paradigms. Electrophysiological recordings were simultaneously acquired from the STS as well as core auditory cortex in posteromedial Heschl's gyrus (HGPM),

non-core auditory cortex in anterolateral Heschl's gyrus (HGAL) and lateral superior temporal gyrus (STG). Event-related band power (ERBP) was examined between 4 and 150 Hz, with analyses focusing on gamma-band activity (30-150 Hz). Analyses of ERBP were performed using linear mixed effects model approach. Functional connectivity was examined using the weighted phase lag index metric.

Gamma activity peaked at lower frequencies in the STS compared to HGPM, HGAL and STG. Compared to auditory cortex, STS exhibited weaker responses to auditory stimuli with longer onset latencies. Responses were more robust and had shorter onset latencies in the upper bank of the STS compared to the lower bank. Comparable degrees of activity were elicited in the language-dominant and non-dominant hemispheres in a semantic classification task. In a dialog-based paradigm, sites in the anterior portion of the upper and the lower bank the STS preferentially responded to the subject's own speech over that of the interviewer's. Sites in that exhibited preferential responses to interviewer's or subject's speech were characterized by stronger functional connectivity with auditory cortical sites that displayed the same talker bias.

We conclude that human STS can be effectively probed with intracranial electrodes, providing complementary data to fMRI studies. Functional differences between the upper and the lower bank of the STS warrant their separate assessment in future studies. Multiple experimental paradigms are necessary to adequately identify its response properties and the transformations that occur from earlier processing stages in auditory cortex.

Funding: NIH R01-DC04290, UL1-RR024979.

PS 297

Informational and Energetic Masking Effects on the Acoustic Change Complex

Jared Carter[1]; Barbara Cone[2]
[1]University of Memphis; [2]University of Arizona

Introduction

Perception of speech in noise is one of the more challenging tasks in which listeners engage. Understanding how the brain processes speech in noise helps clinicians develop therapies and outcome measures to assist individuals who struggle understanding speech in noise. The purpose of this research was to evaluate the obligatory cortical auditory evoked potentials (CAEP) to vowel-consonant-vowel (VCV) tokens presented in background noise that varied along a continuum from energetic to informational. This experiment was a replication and extension of Niemczak & Vander Werff (2019). The hypothesis was that the informational masker (2-talker babble) would have a greater effect on responses evoked by speech than for tone tokens, based upon the premise that 2-talker babble has more informational content to interfere with speech understanding, than for detecting or discriminating tone tokens.

Methods

15 young adult listeners with normal hearing participated. We used VCV (/aba/, /ada/) and tone-change tokens designed to same temporal envelope characteristics as the VCVs to elicit CAEP onset and acoustic change complex responses. There were 4 test conditions: quiet (no masker), and 3 continuous noise-masker types: speech-shaped noise, 8-talker babble and 2-talker babble.

Results

The introduction of masking noise reduced the amplitude of the CAEP onset and ACC responses for both VCV and tone-change tokens, as expected. There were not statistically significant latency effects as a function of masking condition. The 2-talker babble masker had a greater effect on responses to the VCV tokens than responses to tone-change (non-speech) tokens, but these were only present in the CAEP onset response and not the ACC.

Discussion

The differential effects of informational masking on CAEPs appears to be related to its acoustic parameters. The informational masker used in this study (2-talker babble) had a 5 Hz amplitude modulation that may evoke a phase-locked response, diminishing the neural complement that would otherwise respond to the stimulus. Differences in calibration of modulated vs. unmodulated maskers may also contribute to the effects seen. In addition, the spectral-temporal characteristics of the masker relative to the stimulus (speech or non-speech) can play a role.

This study provides new knowledge about how the brain responds in a challenging listening situation when there is informational masking. The findings could contribute to developing clinical methods for diagnosis and/or prognosis of speech-in-noise problems that often drives people to seek hearing health care.

PS 298

Extracting neural representations of auditory attentional processes from fMRI using multivariate pattern analysis

winko An[1]; Abigail Noyce[2]; Alexander Pei[1]; Barbara Shinn-Cunningham[3]
[1]Electrical and Computer Engineering, Carnegie Mellon University; [2]Psychological and Brain Sciences, Boston University; [3]Carnegie Mellon Neuroscience Institute, Carnegie Mellon University

Introduction

People exploit spatial cues and/or talker-specific cues to sustain a conversation in a multi-talker scenario. There is growing interest in understanding how the human brain focuses on an auditory object when different attentional cues are being used. The current fMRI study sought to extract the neural representation of different forms of auditory attention using multivariate pattern analysis (MVPA).

Method

19 young adults participated in this study. The auditory stimuli comprised the syllables Ba/Da/Ga spoken by 5 distinguishable talkers, and played from 5 possible locations. The experiment consisted of 21 conditions that differed in the form of attention required (spatial/talker/no attention) and the talker/location of the target. fMRI data, recorded throughout the experiment, were analysed using a general linear model (GLM). MVPA was then conducted using a searchlight analysis method to capture the neural representation of auditory attention at each voxel, in the form of a representational dissimilarity matrix (RDM). The RDMs were correlated with three categorical models to depict brain areas that behave differently between each pair of attention forms (Figure 1). A one-sample t-test on the subject-level correlation coefficients was used to make group-level inferences (alpha=0.01, FDR corrected).

Results

The high values of the correlation between RDMs and Model 1/2 revealed that the brain activity in the frontal and precentral sulcus, the superior parietal lobe, the superior temporal lobe and the anterior cingulate cortex (ACC) was modulated by both spatial and talker attention (Figure 2b & 2c). The superior and inferior part of the precentral sulcus (sPCS, iPCS), the superior parietal lobule (SPL), the ACC and the superior part of the temporal gyrus (STG) showed different responses when a different form of attention (spatial vs talker) was required (Figure 2a).

Conclusions

The MVPA method can successfully extract the neural representation of auditory attention from fMRI data. It showed that the brain activity of several brain regions, forming a subset of a broader attention network, is modulated by the form of attention being used.

Funding

Office of Naval Research N00014-18-1-2069

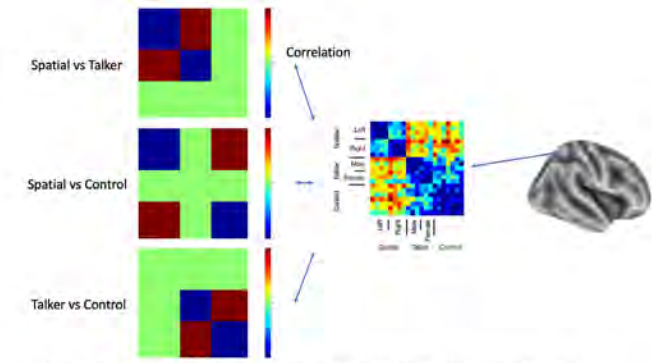

Figure 1. The three categorical models (matrices with -1s, 0s and 1s), each representing a pair-wise contrast, were correlated with the representational dissimilarity matrix (RDM) at each voxel

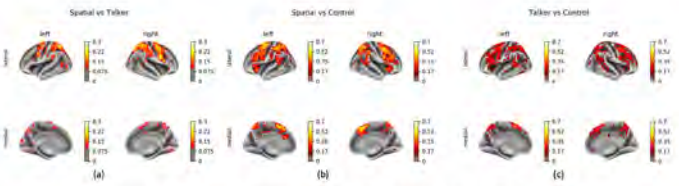

Figure 2. The volumetric maps of correlation coefficients from the 3 categorical models

PS 299

Transcranial Current Stimulation with the Speech Envelope Filtered in the Theta- but not in the Delta Band Modulates the Comprehension of Speech in Noise

Mahmoud Keshavarzi[1]; Mikolaj Kegler[1]; Shabnam Kadir[2]; Tobias Reichenbach[1]
[1]Department of Bioengineering and Centre for Neurotechnology, Imperial College London; [2]School of Engineering and Computer Science, University of Hertfordshire

Auditory cortical activity entrains to the amplitude variations of acoustic stimuli including speech. The modulation of this entrainment through neurostimulation has been found to influence the comprehension of speech in noise, evidencing a functional role of the neural entrainment for speech processing. Although the entrainment occurs mainly in two frequency bands, the delta band (1 – 4 Hz) and the theta band (4 – 8 Hz), the relative functional roles of the entrainment in the two bands to speech processing remain unclear.

To investigate this issue, we employed an experiment in which subjects were presented with speech in noise while experiencing transcranial current stimulation. The currents were obtained from the speech envelope and filtered into both the delta and the theta frequency bands. To investigate their influence on speech-in-noise comprehension, we shifted the waveform in each frequency band by six different phases. We then measured the comprehension scores of volunteers upon stimulation with the different waveforms. We found that the currents filtered in the theta band modulated speech comprehension, while the delta-band currents had no significant influence. Moreover, we found that the influence of the theta-band stimulation was consistent across subjects: the stimulation phase that yielded the highest comprehension did not differ significantly across the volunteers. Importantly, at this optimal phase, speech comprehension was significantly higher than during a sham stimulation.

Our results evidence that theta- but not delta-band entrainment to speech functionally impacts speech-in-noise comprehension. They also open a route to aiding speech comprehension in difficult listening environments.

PS 300

Low Frequency Cortical and Cochlear Oscillations during Selective Attention to Visual and Auditory Stimuli in Tinnitus

Rodrigo Donoso[1]; Alexis Leiva[2]; Constantino Dragicevic[3]; **Paul Delano**[4]
[1]Otolaryngology Department, Clinical Hospital of the University of Chile.; [2]Biomedical Neuroscience Institute, BNI. Facultad de Medicina. Universidad de Chile, Santiago, Chile.; [3]Neuroscience Department, Faculty of Medicine, University of Chile.; [4]1. Neuroscience Department, Faculty of Medicine, University of Chile. 2. Otolaryngology Department, Clinical Hospital of the University of Chile. 3. Biomedical Neuroscience Institute, BNI. Facultad de Medicina. Universidad de Chile, Santiago, Chile. 4. Centro Avanzado de Ingeniería Eléctrica y Electrónica, AC3E, Universidad Técnica Federico Santa María, Valparaíso, Chile.

Tinnitus is the perception of a phantom sound without any external physical sound source. This symptom usually arises after deafferentation of the cochlear receptor as a consequence of an acoustic trauma. The neural correlates of chronic tinnitus involve several central auditory structures, but also non-auditory brain areas, like the insula and prefrontal cortices, affecting cognitive and emotional functions. The auditory efferent system is a neural network that comprises descending projections from the auditory cortex to the cochlear receptor, reaching the outer hair cells through the medial olivocochlear fibers. The dysfunction of the auditory efferent pathways may also contribute to the generation or perpetuation of tinnitus. In this line, several studies have used contralateral acoustic stimulation to address a possible role of the medial olivocochlear brainstem reflex in tinnitus patients with contradictory results. It also remains unclear whether there is a relationship between tinnitus perception and the functioning of the corticofugal projections from the auditory cortex to the cochlear receptor. Recently, we showed that low-frequency (< 10 Hz) cortical and cochlear oscillations are modulated in amplitude and in their temporal properties during a selective attention task to visual and auditory stimuli (Dragicevic et al., PloS One, 2019). Here, we used a similar auditory and visual attention paradigm, and simultaneously recorded electroencephalogram (EEG) and distortion product otoacoustic emissions (DPOAE) in controls and tinnitus patients. We recruited 14 tinnitus patients with normal audiograms (mean age= 39.2 years) and 14 control subjects (mean age= 34.2 years). The amplitude of auditory event related potentials recorded at Cz and Fz EEG electrodes were larger in tinnitus patients (t-test, p=0.002 for Fz and p=0.017 for Cz). In addition, we found a reduction in the amplitude of DPOAE during selective visual attention in controls and tinnitus patients (-0.5 dB and -1.45 dB respectively). Regarding the frequency domain, we found that low-frequency oscillations (< 10 Hz) in cochlear (DPOAE) and cortical (EEG) channels were larger during auditory attention as compared to visual attention trials in control subjects (t-test, p=0.002), but not in tinnitus patients. These results suggest that corticofugal mechanisms of selective attention to visual and auditory stimuli from auditory cortex to the cochlear receptor are altered in tinnitus patients.

Funded by Proyecto Fondecyt 1161155, CONICYT BASAL FB008, Fundación Guillermo Puelma, and Proyecto ICM P09-015F.

PS 301

Representation of Timbre variations in Human Auditory Cortex

Prachi Patel[1]; Jose Herrero[2]; Ashesh Mehta[3]; Shihab Shamma[4]; Nima Mesgarani[1]
[1]Columbia University; [2]Hofstra-Northwell School of Medicine & Feinstein Institute for Medical Research; [3]Hofstra-Northwell School of Medicine and Feinstein Institute for Medical Research; [4]University of Maryland

Humans can easily separate sound sources of the same perceptual dimensions- same duration, pitch, spatial location, loudness and reverberant environment but different character or quality such as two different

instruments playing the same note. The timbre attribute of sound is an important perceptual dimension used by humans and animals to separate sound sources that are otherwise similar but have different character/color. While the representation of timbre has been studied using non-invasive methods in humans, there-by identifying which brain regions are crucial, how these areas represent timbre features is unclear. To answer this question, we recorded intracranially from the primary and non-primary auditory cortex of human subjects while they listened to melodies played by different instruments. We found local selectivity to timbre in the high-gamma band of neural responses resulting into a representation rich enough to enable successful decoding of different instruments. Moreover, we demonstrate how encoding of the amount of timbre information changes from primary to non-primary regions. Our findings contribute to defining the functional organization of responses in the human auditory cortex, with implications for more accurate neurophysiological models of sound processing in humans.

Auditory Cortex: Processing and Perception

PS 302

Cocktail Party Training Improves the use of Level Cues for Speech Intelligibility. Behavioral and fNIRS evidence.

Cosima Lanzilotti[1]; Guillaume Andeol[1]; Sebastien Scannella[2]
[1]IRBA; [2]ISAE-SUPAERO

To follow a conversation in a noisy environment is a real challenge that affects the listening effort and the associated cognitive workload. In a previous work (Andéol et al, 2017), a speech intelligibility task was performed while prefrontal cortex activity was recorded with a functional near infrared spectroscopy (f/NIRS) system. The experimental protocol consisted of a Target voice and a Masker voice simultaneously presented at three different target to masker ratio (TMR). The conditions of the TMR were respectively: *Adverse* (masker was louder than the target), *Intermediate* (masker and target were almost at the same level) and *Favorable* (masker was softer than the target). Participants were asked to follow only the target voice's instructions neglecting that of the Masker voice. Two behavioral performers emerged across the 16 participants, respectively the U shape performers (U) and the Non U Shape performers (NU). The performance of NU decreased monotonically when the masker level increased with no specific differences in term of cognitive workload between conditions. On the contrary, U seemed to be able to use the TMR to discriminate the two talkers even when the masker was louder with a consistent prefrontal activity in the Adverse and in the Intermediate Condition. A good performance correlated with a more important prefrontal engagement (i.e., higher Hbo concentration). In the present work, we used analogous behavioral protocol while recording cognitive workload with a larger f/NIRS head surface including temporal, parietal and occipital areas. We first replicated previous results. Once again, U and NU performers emerged across the participants. The U exhibited larger prefrontal and left IFG activity than the NU regardless of the TMR. In a second time, we aimed to evaluate the possibility to train NU to use the TMR in order to become U. Listeners were divided into two groups according to two different types of training strategies. Main results showed that both groups beneficiated from their training and became U. No more brain functional activity difference with the initial U group was observed after training of the NU groups. It seems that the ability to use the TMR does not refer to a specific individual perceptual auditory ability but it could rather be learned by training people. This study could provide insights to design more efficient communication systems useful in challenging environments.

PS 303

Comparison of Two-Tone Forward Suppression in the Auditory Thalamus and Cortex

Colin Xiong[1]; Xiuping Liu[2]; **JUN YAN**[2]
[1]University of Manitoba School of Medicine; [2]3330 Hospital Drive NW

Sounds in nature are complex in their temporal relations. Many sounds are suppressed or attenuated by the auditory system and consequently one does not hear or comprehend all the sounds that impinge upon the eardrum. Forward masking is a psychoacoustic phenomenon that describes how perception of a sound is affected by preceding ones. Neural correlate of forward masking (referring as forward suppression) has well been studied in the auditory cortex. To date, despite the determinant role of the thalamocortical (TC) system in cortical functions, it remains unclear how the thalamus and thalamocortical (TC) circuity contribute to cortical forward suppression.

To address this issue, we employed the two-tone stimulus paradigm in which preceding and succeeding tones were physically identical (at the best frequency and 20 dB above the minimum threshold of given neurons) but the succeeding tone was randomly delayed from 10 to 490 ms with 30 ms increments. The time courses of forward suppression were examined in the ventral division of the medial geniculate body (MGBv) and the primary auditory cortex (AI) as well as the local field potential in the AI (ie., TC field excitatory postsynaptic potential, TC fEPSP) of anesthetized C57 mice. We show that the preceding tone significantly suppressed the responses to the succeeding one in all three neural substrates. These forward suppressions shared two

properties. One is that early complete suppression was followed by partial suppression and the other is that the overall suppression period is ~300 ms. The complete suppression period was ~75 ms in the MGBv and ~123 ms in the AI. This period of TC fEPSP fell between those of AI and MGBv. During the partial suppression period, it was clear that the decreases in the responses to succeeding tone were significantly greater in the AI than in the MGBv. Of note, the suppression level at TC fEPSP was between the levels observed in the MGBv and AI but very close to the AI level during partial suppression.

We conclude that the early suppression in the AI must be attributed to the complete suppression in the MGBv and that the later suppression requires the TC and associated intracortical mechanisms as supplements to the MGBv partial suppression. In addition, the complete suppression in the MGBv provides the AI with a "silence" window that could potentially be important for the cortical processing and/or perception of auditory information carried by preceding sound.

PS 304

Signal-to-Noise Ratio Shapes Dip Listening in Auditory Cortex

Nima Alamatsaz[1]; Antje Ihlefeld[2]
[1]New Jersey Institute of Technology and Rutgers University; [2]New Jersey Institute of Technology

Background
When background noise fluctuates slowly over time, both humans and animals can listen in the dips of the noise envelope to detect target sound. Detection of target sound is facilitated by a central neuronal mechanism called envelope locking suppression. At both positive and negative signal-to-noise ratios (SNRs), the presence of target energy can suppress the strength by which neurons in auditory cortex track background sound, at least in anesthetized animals. However, in humans and animals, most of the perceptual advantage gained by listening in the dips of fluctuating noise emerges when a target is softer than the background sound. This raises the possibility that different mechanisms may underlie suppression of background sound at positive vs negative SNRs, a hypothesis tested here in awake behaving animals.

Methods
Normal-hearing Mongolian gerbils were placed on controlled water access. Using a Go/NoGo appetitive procedure, animals were trained to detect a target tone in the presence of modulated background sound at super-threshold SNRs of -10, 0 and +10 dB. At these SNRs, animals were able to detect the target sound with comparable behavioral sensitivity (d'=2). To record multiunit activity of neurons in core auditory cortex, two trained gerbils were then surgically implanted with chronic microelectrode probes. In a total of 9 recording sessions, neural responses at +10, 0 and -10 dB SNR were collected while animals were actively trying to hear out the target from the acoustic mixture vs listen passively to the same sounds.

Results
A total of 25 single- and 8 multi-units showed a target-evoked response in their firing rate. Pooling across NoGo trials during active and passive listening, these target-responsive units were then further classified as tonic or phasic, based on whether they significantly phase-locked to the modulation rate of the masker. In both types of units, sensory information at the population level could predict behavioral sensitivity. For phasic units at 0 and 10 dB SNR, average firing rates decreased in Go vs NoGo trials, consistent with envelope locking suppression. However, at -10 dB SNR, firing rate increased during Go trials as compared to NoGo, for both tonic and phasic units, a phenomenon not predicted by envelope locking suppression.

Conclusions
Preliminary neurophysiological data hint that the neuronal mechanisms that enable an individual to listen in the temporary dips of background sound may differ across positive vs negative SNRs.

PS 305

Characterizing Cortical Auditory Evoked Potentials in Mice

Warren M. Bakay[1]; Olivier Postal[1]; Typhaine Dupont[1]; Christine Petit[2]; Nicolas Michalski[1]; Boris Gourévitch[1]
[1]Institut Pasteur; [2]Institut Pasteur, Paris

Auditory Brainstem Responses (ABRs) are a robust and consistent response to auditory stimuli. As such, they are frequently used to measure auditory thresholds in the mammalian hearing system, and to determine deficits in the auditory periphery. However, because these measures are limited to the lower stages of the auditory pathway, they are insensitive to perceptual changes or deficits that occur in the thalamic and cortical regions. Cortical Auditory Evoked Potentials (CAEPs) capture some information from this region, but are far less frequently used as a diagnostic tool, especially in the popular rodent models, due to their inherent variability and the resulting difficulty in interpreting them.

We have aimed at developing a consistent measure of cortical responses to auditory stimuli in mice, so as to

determine the specific generators of CAEP components, and to develop diagnostic tools for cortical changes or deficits. In particular we investigated the effects on the CAEPs of several stimuli (noise, click, and tone (16kHz) bursts), several presentation rates (2/s,6/s,10/s) and with a variety of electrode placements. The recordings were examined for both the ABR components and the later CAEP components to determine the optimal presentation.

By deactivating the auditory cortex using the direct application of lidocaine we further aimed at determining the separate response components from the contralateral and ipsilateral cortices in the CAEP.

Intriguingly, CAEPs were able to provide robust and replicable cortical responses to classical stimuli, including noise bursts and gaps, suggesting a promising future for this technique as a diagnostic tool especially with follow-up protocols.

PS 306

Physiological Correlates of Masking Release

Hyojin Kim[1]; Bastian Epp[2]
[1]Hearing Systems section, Department of Health Technology, Technical University of Denmark; [2]Hearing Systems section. Department of Health Technology. Technical University of Denmark

The auditory system has the outstanding capability to enable communication in noisy environments. To do so, it utilizes various signal properties to segregate a target sound from masking sounds. Masking release is one example of auditory object segregation where the masked threshold of a target sound decreases when beneficial cues are provided. Two such cues are comodulation and interaural phase disparity (IPD). While the effect of these cues are shown in behavioral studies, little is known about the role of these cues in terms of the underlying physiological mechanisms of the sound segregation. Since behaviorally measured masked thresholds cannot be predicted solely with physical intensity of the stimulus, we postulated an “internal signal-to-noise- ratio (iSNR)”, describing the neuronal representation of the stimulus at the level of the auditory cortex. As the proxy of iSNR, we investigated late auditory evoked potentials (LAEPs). A stimulus paradigm was designed to account for the effect of cues on masking release in both behavioral and electrophysiological experiments. We additionally investigated how their effects change depending on temporal contexts. To achieve this, eight different conditions were applied where each condition has varied combinations of comodulation, IPD and onset asynchrony. Behaviorally measured masked thresholds indicate that comodulation and interaural phase disparity show a superposition of masking release. While onset asynchrony has a negative effect on masking release induced by comodulation (CMR), it does not affect masking release by interaural phase disparity (BMLD). The P2 component of the vertex LAEPs was suggested to be an objective measure of iSNR. The results of this study will provide us with information about neuronal processing along the auditory pathway responsible for masking release in the presence of comodulation, IPD and onset asynchrony. Specifically, it shows how temporal contexts affect to CMR and BMLD as perceptual links from top-down processing or play a role as part of bottom-up processing.

PS 307

Dynamic encoding of sensory features, perceptual category and behavioural choice in ferret A1

Rupesh K. Chillale[1]; Shihab Shamma[2]; Srdjan Ostojic[3]; Yves Boubenec[4]
[1]Ecole Normale Superieure; [2]University of Maryland; [3]Laboratoire de Neurosciences Cognitives INSERM U960; [4]Laboratoire des Systèmes Perceptifs, CNRS UMR 8248

In a goal-directed task, sensory features of the stimulus are transformed into abstract perceptual representation for appropriate behavioural decisions. This process is classically believed to be implemented by hierarchical processing through a series of cortical areas within which primary sensory areas are the first step and supposed to encode only sensory features associated with the stimuli. Recent studies have however challenged that picture and argued that primary sensory areas may already be extracting the task-dependent, behavioral meaning of stimuli.

To further determine to which extent auditory cortex represents task-dependent vs sensory properties, here we examine the population representations in primary auditory cortex (A1) during a delayed categorization task. We trained ferrets to classify regular click trains into Target/Reference categories (low and high rates) during an appetitive Go/No-Go task. After training, we chronically recorded from primary auditory cortex (A1) while ferrets were either passively listening or actively discriminating the stimuli. Using population-level analyses, we exploit the structure of the task to contrast the representation of stimuli features (click-rates), perceptual categories (Target/Reference) and behavioural choice (Go/No-Go choices).

We found that A1 population responses encode mostly sensory features during passive listening, while categorical signal is enhanced during active discrimination. Target stimuli elicited a behavior-dependent sustained activity during the delay period after stimulus offset. A1 population decoding reveals that stimulus representation

dynamically evolves between the different trial epochs, with mixed (sensory and categorical) encoding during stimulus presentation and purely categorical encoding during the delay period before response window. We used linear regression to disentangle sensory features, categorical encoding and behavioural choice. Our results suggest a picture in which these task-related variables are represented along different directions in the high-dimensional neural state space, so that the overlaps between these directions at different trial epochs represent the transformation of sensory information into categorical percepts and finally behavioural output.

PS 308

Functional and Structural Analysis of Cortical Profiles in Feline Primary Auditory Cortex – Effect of Auditory Deprivation

Peter Hubka[1]; Lea Sollmann[1]; Kwame S. Kutten[2]; J. Tilak Ratnanather[2]; Andrej Kral[3]
[1]Hannover Medical School; [2]Johns Hopkins University; [3]Dept. of Experimental Otology, Hannover Medical School, Germany; DFG Cluster of Excellence "Hearing 4 All"

The structure and function of neuronal tissues are closely connected at subcellular and cellular level. It is, however, not clear if and how are the neuronal network structure and function related at the meso- and macroscopic level. Here we propose an analytical framework for studying this relation. We tested the framework on an example of consequences of the congenital auditory deprivation on structural and functional changes in the auditory cortex.

For the structural analysis, two pipelines for analyzing and parametrizing 3D equivolumetric normal coordinate systems for comprehensive structural analysis on meso- and macroscopic level were developed. In the magnetic resonance imaging pipeline, 3D auditory cortical representations of cat brains were acquired. In the histological pipeline, brains were axially cut through the auditory cortex at 0.25 mm intervals and stained using Nissl method and SMI-32 antibody. While the Nissl staining provides an overall overview of the neuronal cell body distribution in the cerebral cortex, the SMI-32 stains neurofilament H contained mainly in the excitatory pyramidal neurons and provides information about an arrangement of individual cortical layers. The cortical depth and cortical depth profiles of the normalized staining intensity were evaluated.

The functional signals were recorded using multichannel intracortical electrode arrays (Neuronexus, 16-channel linear arrays) inserted perpendicularly into the primary auditory cortex. The position of the recording probes were reconstructed from the histological sections showing probe traces stained by DiI. Local field potentials, corresponding current source density, and multi-unit activity were analyzed and activation parameters (strength, latency and duration of activation) were evaluated. Depth profiles of the activation parameters were constructed and correlated with histological depth profiles.

The staining intensity depth profiles as well as functional parameters depth profiles of the primary auditory cortex could reliably recognize cortical layer IV, and supra- and infra-cortical layers. Both structural and functional cortical profiles in hearing and congenitally deaf animals showed similar changes in supra and infra-granular layers with more pronounced effect of deafness in infragranular layers. We have proposed a framework for statistical comparison of the strength in the structure-function relation at meso- and macroscopic level. This approach enables a complex assessment of the function-structure dependence in a pathological situation. A comprehensive mapping can result in identification of novel structural biomarkers, which will enhance interpretation and informative value of noninvasive imaging techniques used in clinics.

PS 309

Temporal Integration of Sequences in Secondary Auditory Region of the Zebra Finch Forebrain

Adam R. Fishbein[1]; Kai Lu[2]; Wanyi Liu[3]; William J. Idsardi[4]; Jonathan B. Fritz[5]; Shihab A. Shamma[3]; Robert J. Dooling[1]
[1]Neuroscience and Cognitive Science Program and Department of Psychology, University of Maryland, College Park; [2]Institute for Systems Research, University of Maryland, College Park; Now at Department of Biology, Emory University; [3]Institute for Systems Research, University of Maryland, College Park; [4]Department of Linguistics, University of Maryland, College Park; [5]Institute for Systems Research, University of Maryland, College Park; Now at Center for Neural Science, New York University

Human speech perception relies on central auditory processing of sequential information contained in words, phrases, and sentences. Indeed, psychophysical studies have shown that human subjects can perceive sequence differences for strings of elements ranging from at least 5 ms – 5 s. Songbirds, such as zebra finches (*Taeniopygia guttata*), are popular models for human speech as the birds learn to produce song elements in sequential patterns. Past neurophysiological studies have shown that the caudomedial nidopallium (NCM), a secondary auditory region in the zebra finch forebrain, is sensitive to changes in both synthetic and natural song sequences, but the temporal range of that sensitivity has not been previously tested. Here, we examine the temporal integration of sequences in zebra finch NCM.

We compare these results to those of zebra finches tested on the same stimuli in a psychophysical paradigm.

For neurophysiological experiments, a 24-channel silicon probe (Plexon) was inserted into NCM of awake head-fixed birds. Birds were passively exposed to sequences of synthetic song elements varying from 80 – 200 ms per element (around the range of natural song elements). After a block of 20 repetitions, birds were exposed to blocks of the same sounds but in different sequences. NCM neurons are known to habituate in spike rate to repeated stimuli and dishabituate to novel stimuli. Here, we measured the change in spike rate after a change in sequence, using dishabituation as an index for sequence sensitivity. For behavioral experiments, birds were trained through operant conditioning to perform a psychophysical discrimination task where they listened to a synthetic song sequence and were asked to detect changes in the order of the elements.

We present the results of the responses of >250 neurons in NCM to changes in sequence. We show significant sequence sensitivity for shorter (80 ms) and longer (160, 200 ms) elements. In contrast, behavioral experiments show that zebra finches are largely insensitive to sequence changes for both shorter and longer elements.

These results show that the temporal integration of sequential elements in the zebra finch central auditory system is within the range of natural song elements. Yet the physiological sensitivity to sequence in NCM is not evident in the behavioral discrimination responses, highlighting potential differences in avian and human representation of acoustic sequences.

PS 310

Differential Neural Representation of Identical Acoustic Stimuli in the Context of Different Behavioral Paradigms in Frontal Cortex of the Ferret

Wanyi Liu[1]; Kai Lu[2]; Pingbo Yin[3]; Shihab A. Shamma[1]; Jonathan B. Fritz[4]; **Stephen V. David**[5]
[1]Institute for Systems Research, University of Maryland, College Park; [2]Emory University; [3]University of Maryland, College Park; [4]Institute for Systems Research, University of Maryland, College Park; Now at Center for Neural Science, New York University; [5]Oregon Health and Science University

This study explores how the representation of sensory stimuli in frontal cortex is shaped by task demands and reward structure. In a previous study, ferrets were trained to distinguish target pure tones from distractor broadband noise, using an aversive, conditioned avoidance Go-NoGo (CA-GNG) paradigm (Fritz et al., 2010). In that paradigm, animals learned to briefly refrain from licking a water spout after presentation of target stimuli to avoid a mild shock. Responses in frontal cortex were highly selective for target tones (NoGo) during active behavior, and showed no response to the noise (Go) stimuli. In order to clarify whether this highly selective, gated response to target tones was dependent upon the design and reward structure of the behavioral paradigm, we trained additional ferrets on the same acoustic discrimination, but now using two other behavioral paradigms. Three ferrets were trained on a positive, appetitive version (POS-GNG) of the Go-NoGo paradigm (David et al., 2012), and three additional ferrets were trained on a 2-alternative forced choice (2AFC) appetitive task, to lick an upward water spout for tones, and a downward spout for noise stimuli. Although there was some variation in task acquisition, all ferrets learned the different tasks to behavioral criterion.

We recorded neuronal activity in dorsal frontal cortex of head-fixed ferrets during passive listening to the acoustic stimuli, and also during task-engaged conditions for all three behavioral paradigms. We measured single unit responses to tones and noise in CA-GNG (n=474), POS-GNG (n=250) and 2AFC (n=180). We observed striking differences in the neural representation in frontal cortex in the three behavioral paradigm conditions. Unlike the highly selective response to target stimuli observed for the CA-GNG task, there were responses to either or both tonal targets and noisy distractors in POS-GNG. Furthermore, we observed no post-passive responses (during passive listening to task stimuli immediately after task performance) in POS-GNG, unlike previous results described in CA-GNG. The same pattern of selective responses to either target or noise stimuli, and the presence of some cells that responded to both tones and noise with different dynamics, was observed in the 2AFC paradigm.

These results reveal the highly paradigm-dependent representation of sensory stimuli in frontal cortex and help us better understand the way in which task-engagement and attention, task design and motor responses, and reward valence, all contribute to shaping neural responses and representation of sound in frontal cortex.

PS 311

Auditory Learning Improves a Natural Social Behavior in Mice

Cristina Besosa; Alex G. Dunlap; Brenda Belwood; Dorottya Kacsoh; Robert C. Liu
Emory University Biology

Learning the meaning of new sounds can be vital to a species' survival in many natural contexts, including in social situations. However, the degree of flexibility and neuroplasticity involved in auditory learning in natural

social behaviors is still not well understood. Our lab uses a maternal model of social behavior to investigate how the auditory cortex helps learn the meaning of new, behaviorally relevant sounds that are associated with social responses. Pup ultrasonic vocalizations elicit retrieval behavior in adult mice, but the functional significance of auditory cortical processing and plasticity when learning this association still remains unclear. Using a T-maze paradigm to pair a synthetic, amplitude-modulated noise stimulus with the retrieval behavior lets us study a newly formed sensory association that can give insight into how auditory learning in a pro-social context is encoded in the brain. Over a period of 7 training days, we use the mouse's inherently rewarding retrieval behavior as motivation to learn to approach the arm of the maze from which sound is being played in order to receive a pup reward. We found that in this paradigm, mice have an innate strategy where they return to the last arm from which they previously received a pup, but after pairing they learn to use a more efficient search strategy guided by the stimulus. Hence, animals shift from using spatial cues to navigate to using the sound stimulus to guide their choice with an increase in performance accuracy from chance to an average of 91% (n=6) on day 7. Additional experiments suggest that animals have formed a long-term sensory memory for the sound. Animals trained in the T-maze perform better than chance from the moment they hear the sound in a new context (Y-maze) to guide retrieval, unlike those without initial T-maze training (p=0.037, n=3). Moreover, even weeks after the end of the initial training, re-tested animals continue to accurately follow the sound into the arm that allows them to retrieve a pup. By establishing a newly-formed sensory association using a natural maternal behavioral response, this work lays a solid foundation for studies into the neurochemical and circuit mechanisms that mediate auditory learning in natural social contexts. This work is supported by NIH R01DC008343.

PS 312

Functional UltraSound imaging of Ferret Auditory Cortex Reveals a Unique Neural Signature of Human Speech and Music Perception

Agnes Landemard[1]; Celian Bimbard[1]; Sam Norman-Haigneré[2]; **Yves Boubenec**[1]
[1]École Normale Supérieure; [2]Columbia University

How have speech and music shaped the human brain? Many signatures of speech and music processing have been observed in non-human animals, raising the question of whether there exist uniquely human mechanisms for processing speech and music. Humans have non-primary neural populations that respond selectively to speech and music compared with both other natural sounds and with synthetic sounds that have matched spectrotemporal modulation statistics ('modulation-matched' sounds), suggesting selectivity for higher-order structure (Norman-Haigneré, 2015/2018). Using functional ultrasound imaging, a cutting-edge high-resolution neuroimaging technique, we tested if similar regions are present in ferrets.

We measured responses from the auditory cortex of passively listening head-fixed ferrets to natural and modulation sounds tested previously in humans. Ferret cortical responses recapitulated many of the response patterns observed in humans. Interestingly, we observed speech selective regions in the ferret auditory cortex. However, and contrary to the real speech- and music-selective response components observed in human non-primary regions, ferret auditory cortex did not show selective responses to natural vs. modulation-matched sounds. These findings suggest that human cortical organization has diverged from other species in non-primary auditory cortex due to the need to represent higher-order structure in speech and music.

Because speech and music are not ecologically relevant sounds for ferrets, we wanted to test whether ferret auditory cortex could discriminate between ferret pup vocalizations and their corresponding model-matched versions. We observed differences in animal motor activity for original vocalizations compared to model-matched stimuli, indicating that the animal is able to perceptually discriminate these two classes of sounds. We are currently investigating the neural correlates of this capability in auditory cortex responses.

PS 313

Representation of Perceptual Integration Time Downstream of Auditory Cortex

Justin D. Yao; Justin Gimoto; Dan H. Sanes
New York University

The central representations of environmental signals are transformed at each locus of an ascending sensory pathway. One characteristic of this hierarchical processing is that the time required to fully encode a sensory cue (i.e., integration time) increases at ascending levels of the nervous system. Here, we sought to determine how auditory information is transformed downstream from gerbil core auditory cortex (ACx), at a location thought to support sensory decisions, the parietal cortex (PC). We first obtained behavioral measures of integration time, using an appetitive alternative forced-choice (AFC) procedure. Specifically, gerbils were trained to discriminate between amplitude modulated (AM) noise at 4 versus 10 Hz, and tested across a range of

stimulus durations (100-2000 ms). Integration times were measured from psychometric functions, plotting behavioral sensitivity (proportion of correct trials) as a function of stimulus duration. Task performance was poor at short stimulus durations (< 300 ms) and asymptotic at ~600 ms. Average threshold (integration time to reach 0.76 proportion of correct trials) was 354 ms (± 127 SD). To determine the anatomical pathway from ACx to PC, antero- and retrograde viral tracing experiments were performed. The data revealed a disynaptic pathway from ACx to dorsal auditory cortex (AuD) to PC. Therefore, we asked whether this pathway contributed to the integration time using DREADDs to modulate the gain of excitatory neuronal input from AuD to PC during task performance. Bilateral injections of a viral vector with a neuron-specific promotor (CaMKII) that expresses hM4D were made into AuD, and cannulae were implanted above each PC. After two weeks of expression, we infused compound 21 (C21), a chemogenetic actuator of hM4D, through each cannula prior to task performance to target projection-specific axon terminals from AuD to PC. Across 6 test days, infusion sessions of C21 were interleaved with saline to serve as within-subject comparisons (3 sessions per C21 and saline). C21 led to an increase of integration times. To confirm whether a general reduction of PC activity impaired behavioral integration times, bilateral PC infusions of muscimol were performed prior to task performance and compared with interleaved sessions of saline. While animals continued to perform the task following muscimol infusion, the effect of muscimol inactivation was more pronounced: integration times were increased and performance at even the longest stimulus durations was poorer, as compared to saline infusion sessions. Collectively, these experiments indicate that auditory integration times emerge within the disynaptic pathway from ACx to PC.

PS 1039 *(Late Addition)*

Spectral Combination-sensitivity and FM Direction Preference Contribute Equally to Maximizing Responses of Cortical Neurons: A Possible Mechanism for Binding Acoustic Features

Stuart D. Washington[1]; Georgios A. Keliris[2]; Jagmeet S. Kanwal[3]
[1]Georgetown University; [2]University of Antwerp

Mustached bats, *Pteronotus parnellii*, use an acoustically diverse and rich variety of social calls for communication. The presence of harmonics and parameters of frequency modulations (FMs) within conspecific vocalizations can be used to differentiate different call types. Auditory neurons may decode the information within calls by being tuned for both spectral (e.g., spectral combination-sensitivity) and temporal (e.g., temporal ordering of frequencies within an FM) parameters. Spectrally combination-sensitive neurons are responsive to two or more sounds that traverse separate frequency bands, and these facilitated responses are greater than the sum of neural responses to the same sounds presented individually. Temporal order is the sequence of frequencies occurring in a sound, a simple form of which is linear FM direction (upward vs. downward). Here, we demonstrate that FM direction contributes to the spectral combination-sensitivity of Doppler-shifted constant frequency (DSCF) neurons in the primary auditory cortex of the mustached bat. Specifically, we presented linear FMs within the 57-60 kHz frequency range (BF_{high}) and obtained extracellular recordings from single neurons. We optimized the rates, bandwidths, central frequencies, amplitudes, and modulation direction based on the tuning to the respective parameters for each neuron. We paired each FM sound at onset with a tone in the 23-27 kHz range (BF_{low}) to spectrally facilitate neural responses. In this way, we achieved maximal excitation using "best-FMs" paired at onset with a tone at BF_{low} for each neuron. We also presented the best-FM alone, reversed the best-FM and paired it with the tone at BF_{low}, and presented the reversed best-FM alone. Uncoupling the tone at BF_{low} from the best-FM typically reduced peak response magnitude by ~50%. However, pairing the reversed best-FMs with a tone at BF_{low} or presenting the reversed best-FM alone reduced peak response magnitude by 65% and 77%, respectively. Thus, despite spectral equivalence between upward and downward FMs, spectral combination-sensitivity and FM direction had equivalent influence on DSCF neural response magnitude. We propose that this selectivity for sound features represents a mechanism for binding feature-specific acoustic information for the perception of and discrimination between different types of social calls.

Auditory Prostheses III

PS 314

The Effect of Tactile Stimulation on Pitch Perception in Normal Hearing and Cochlear Implant Users

Susan R. Bissmeyer; Juri Hwang; Raymond L. Goldsworthy
University of Southern California

In healthy hearing, frequency is encoded into the spatial and temporal response properties of the auditory nerve. Cochlear implants (CIs) excite both spatial and temporal properties of the auditory nerve response, but with limited resolution. There is evidence that tactile stimulation can be used to provide a degree of frequency resolution for low-frequency sounds (less than 200 Hz), with best discrimination thresholds around 10%. The present

study considers augmenting pitch perception with tactile stimulation for normal hearing and cochlear implant users. Auditory frequency discrimination and tactile stimulation discrimination thresholds were measured. The auditory stimulus for normal hearing listeners is a 1000 Hz tone sinusoidally amplitude modulated with fundamental frequencies of 55 and 110 Hz, and the stimulus for CI users is an electric pulse train with stimulation rates of 55 and 110 pulses per second. The tactile stimulus was a low-pass filtered harmonic complex with fundamental frequencies of 55 and 110 Hz delivered through a tactile device to the index finger. The six conditions were auditory, tactile, and combined stimulation for the two frequencies. Preliminary results suggest that tactile stimulation will supplement pitch perception in cochlear implant users. More conclusive results will be presented from this experiment designed to test how well CI users can combine pitch cues provided by stimulation rate and tactile stimulation.

PS 315

Understanding the Causes and Effects of Temporal Pitch Distortion in Cochlear Implant Users.

Barry D. Jacobson
MIT

Cochlear Implants (CIs) have done a wealth of good for the profoundly deaf. In quiet environments, they allow for good speech perception and enable normal conversation, which significantly improves quality of life. However, in more complex environments, such as with significant background noise, or on pitch and music perception tasks, users often experience great difficulty, as numerous studies have shown. We argue that a common design practice may contribute to these problems. By taking a step-by-step tour through the block diagram of a prototypical CI processor, properly accounting for the input and output frequency components at each stage, we will uncover some surprising results that may explain the difficulties users have. These include frequency transformations, flattening of pitch contours, generation of output components that were non-existent at the input, and other problems that degrade the musical experience, such as inharmonicity and dissonance. A major culprit is the envelope processing scheme which has been widely adopted in some form or another by almost all contemporary manufacturers. We recommend that alternatives be sought that do not suffer from these issues. We endeavor to avoid any complex statistical models or particular assumptions that might engender controversy, but rather to stick to standard signal-processing theorems and straightforward, back-of-the-envelope calculations for utmost clarity. The results fully conform to our own experience as a CI user, and we believe are consistent with the many behavioral studies that have previously been published. Along the way, we will attempt to provide historical context as to current design philosophy, and to contrast temporal and spatial pitch, and the difficulties in making each of them effectively available to users.

PS 316

Pulse Symmetry and Channel Interactions in Cochlear Implants

Gunnar L. Quass[1]; Peter Baumhoff[1]; Dan Gnansia[2]; Pierre Stahl[2]; Andrej Kral[3]
[1]Dept. of Experimental Otology, Hannover Medical School, Germany; [2]Oticon Medical; [3]Dept. of Experimental Otology, Hannover Medical School, Germany; DFG Cluster of Excellence "Hearing 4 All"

Conventional loudness coding with CIs has the disadvantage that increasing the stimulation current increases the spread of excitation in the auditory nerve (Kral et al., 1998, Hear Res). The result are channel interaction effects, which limit the number of effective channels a CI user can resolve. Loudness can alternatively be coded by changing pulse duration (Zeng et al., 1998, Neuroreport). Pseudomonophasic pulses have been shown to reduce spread of excitation in humans compared to biphasic pulses (van Wieringen, 2008, Hear Res). Coupling pseudomonophasic pulses with duration loudness coding could thus reduce the current spread, while still providing a coding of stimulus intensity, alleviating channel interaction effects.

We implanted 6-channel CIs (Oticon) in 12 acutely deafened guinea pigs and recorded neural responses along the tonotopic gradient of the IC while stimulating on the CI with either of 2 different cathodic-leading pulse shapes: symmetric, biphasic, charge-balanced increasing in amplitude (50 µs phase duration and a 1:1 phase duration ratio), or asymmetric, biphasic, charge-balanced either increasing in phase duration or phase amplitude (50 µs first-phase duration with a 1:5 phase duration ratio). All stimuli at equal levels thus delivered the same charge. Stimuli were presented at channels 2 and 5 on the CI, and the overlap of the activated neuronal populations was compared. There was significant overlap of the activated neuronal populations for both stimulus shapes. However, pseudomonophasic pulses produced a reduced overlap as well as 1 dB better median thresholds (MAD 1.2 (ch2) and 1.7 (ch5), $p < 0.001$). There was no difference in dynamic range between the stimuli.

We further analyzed the stimulus locking by presenting interleaved pulse trains of different frequencies and extracting the vector strength. Stimulus locking in the IC to rates of 19 and 37 pps was strong and similar with

different stimuli when a single stimulus was presented at suprathreshold intensity on the implant. When the two symmetric stimuli of different frequencies were simultaneously presented, the median stimulus locking decreased by 73 (ch2) and 51% (ch5, $p < 0.001$). Pseudomonophasic, phase-duration coded pulses could mitigate this drop by 4-5%, down to 62 (ch2) and 47% (ch5, $p < 0.001$), demonstrating that channel interaction effects are reduced using this stimulation strategy.

The results show that the brain's ability to resolve individual streams of overlapping information at a subcortical level slightly improves when asymmetric stimuli combined with phase duration coding are used instead of symmetric, amplitude-coded stimuli.

Supported by the Oticon Foundation

PS 317

Exploring Polyphonic Pitch Perception in Cochlear Implant Users

Andres Camarena; Raymond L. Goldsworthy
University of Southern California

A cochlear implant (CI) restores hearing to individuals with profound sensorineural loss through electrical stimulation of the auditory nerve. These devices take advantage of the tonotopic organization of the auditory nerve and provides reasonable speech recognition in quiet. When there are competing sound sources, CI users struggle to group and separate noise from their desired target. Studies examining the inferior colliculus and comodulation masking release suggest that two sources are likely to be perceived as separate if they are characterized by different modulation frequencies — or periodicities. If the spectral periodicity aids in source separation, then enhancing modulation encoding electrically at the auditory nerve will improve source separation in CI users. To this end, this study examines the effect on source separation when the modulation of two competing signals are characterized either by sinusoidal amplitude- modulated (SAM) pulse trains or single pulses given at the peak of the periodic signal (dynamic). This study uses a demanding polyphonic pitch-trajectory task in which neither the beat frequency nor a shifting of a perceptually fused stimulus correlate with success. Participants with Cochlear Americas CI devices will perform a hierarchy of tasks that separately probe pitch ranking ability and polyphonic pitch detection. Additionally, these tasks serve as a source of training for the more demanding psychoacoustic task which combines pitch ranking and polyphonic detection. In this polyphonic pitch-trajectory task, two streams (low and high pitch) are presented simultaneously. Participants perform a 2-interval-4-alternative forced-choice procedure to identify which stream had its modulation frequency shift in frequency and whether it went higher or lower in pitch (low-pitch-lower / low-pitch-higher / high-pitch-lower / high-pitch-higher). Both streams are either SAM or dynamic pulse trains with the low-frequency stream presented to the most apical electrode and the high-stream to varying electrodes with electrode separations of 0, 2, 4, and 8 examined. A standard interval will be followed by a target interval which will shift one of the streams up or down an octave with the endpoint adaptively controlled based on correct answers. Preliminary results suggest that CI users perform better on the electrode psychophysical tasks than on acoustic variations of the task, suggesting a loss of envelope information when transmitted through the clinical processor. Additionally, polyphonic pitch detection improves with increasing temporal resolution. These preliminary results suggest that CI users can perceive polyphonic pitch, but that resolution is limited by how temporal information is conveyed by clinical devices.

PS 318

A Coding Strategy to Remove Temporally Masked Pulses and its Effect on Speech Perception by Cochlear Implant Listeners

Wiebke Lamping[1]; Tobias Goehring[1]; Jeremy Marozeau[2]; Robert P. Carlyon[1]
[1]University of Cambridge; [2]Hearing Systems Section, Department of Health Technology, Technical University of Denmark

Speech recognition in noisy environments remains a challenge for cochlear implant (CI) recipients. Unwanted charge interactions between current pulses in the same and across different electrode channels are likely to impair performance. Here we investigate the effect of reducing the number of current pulses on speech perception. This was achieved by implementing a psychoacoustic temporal-masking model where current pulses in each channel were passed through a temporal integrator to identify and remove pulses that were less likely to be perceived by the recipient. The decision criterion of the temporal integrator was varied to control the percentage of pulses removed in each condition. In experiment 1, speech in quiet was processed with a standard Continuous Interleaved Sampling (CIS) strategy and with 25, 50 and 75% of pulses removed. In experiment 2, performance was measured for speech in noise with the CIS reference and with 50 and 75% of pulses removed. Speech intelligibility in quiet revealed no significant difference between reference and test conditions. For speech in noise, results showed a significant improvement of 2.4 dB when removing 50%

of pulses. Performance both in quiet and in noise was not significantly different between the reference and when 75% of pulses were removed. Further, by reducing the overall amount of current pulses by 25, 50, and 75% but accounting for the increase in charge necessary to compensate for the decrease in loudness, estimated average power savings of 20.5, 36, and 49.5%, respectively, could be possible for this set of listeners. In conclusion, removing temporally masked pulses may improve speech perception in noise and result in substantial power savings. Measurements for different masker types are currently in the making. This work was supported by the Oticon Centre of Excellence for Hearing and Speech Sciences (CHeSS) as well as by award MR/S002537/1from the U.K. Medical Research Council (MRC) to author WL, by award RG91365 from the U.K. MRC to author RC, and by Action on Hearing Loss (Grant 82) to author TG.

PS 319

Evaluating the Effect of Focussed Stimulation on Excitation Patterns in Humans and Cats: Linking Psychophysics and EEG Measurements

Francois Guerit[1]; Andrew J. Harland[1]; John C. Middlebrooks[2]; Robin Gransier[3]; Matthew L Richardson[2]; Jan Wouters[3]; Robert P. Carlyon[1]
[1]University of Cambridge; [2]University of California; [3]KU Leuven

The spread of current along the cochlea is one of the main factors limiting speech understanding for Cochlear Implant (CI) users. Animal physiological recordings suggest that tripolar stimulation can reduce this spread. However, attempts to use tripolar stimulation in human CI users have not shown such a clear and consistent advantage. This might be due to anatomical differences, but also differences in methods, since some paradigms are not easily comparable across species. We therefore develop a paradigm to measure tripolar and monopolar excitation patterns in both humans and cats, for use with both psychophysics and EEG. The aim is to identify which factors are important for a large benefit of tripolar stimulation to be observed.

We investigate the psychophysical excitation patterns of three different maskers: monopolar, partial-tripolar and a three-electrode “ralopirt” masker in which the current on the flanking and central electrodes have the same polarity, thereby potentially broadening the excitation pattern (“Ralopirt” stands for tripolar read backwards). For both the partial-tripolar and ralopirt maskers, we include conditions with 0 (tripolar+0, ralopirt+0) and 2 electrodes between the central and flanking electrodes (tripolar+2, ralopirt+2). The masker is always a continuous pulse train at 400 pps presented on a given electrode X. The probe is a 50-ms, 400-pps partial-tripolar pulse train, shifted in time by 1.25 ms and presented on electrodes X-2, X and X+2 700 ms after masker onset. First, all maskers are loudness-balanced to the monopolar masker at a comfortable level, and we measure detection thresholds for the probe at electrode X (on-site) in masked and unmasked conditions. Next, we adjust the level of the maskers to yield equivalent on-site amount of masking, and measure detection thresholds with the probe on electrodes X-2 and X+2. This manipulation effectively allows the comparison of shapes of excitation patterns elicited by the different maskers.

Pilot results (N = 6) indicate a significant effect of changing the masker on the obtained excitation patterns. The only significant contrasts are that excitation patterns for the ralopirt+2 masker are broader than for the other conditions, although some individuals show slightly narrower excitation patterns for partial-tripolar compared to monopolar maskers. These effects are small when compared to the large differences the same maskers create in the cochlea, as measured with Electrical Field Imaging. We will investigate if these results are consistent with EEG recordings (cortical onset responses) in the same participants.

Acknowledgement
Wellcome Trust Collaborative Science Award RG91976.

PS 320

How Temporal is Temporal Modulation Detection? The Relationship between Modulation Sensitivity and Spectral Resolution in Cochlear Implant Users

Ning Zhou; Lixue Dong; Susannah Dixon; Baylee Engelhardt
East Carolina University

Temporal modulation sensitivity, a strong predictor for speech recognition performance in cochlear implant (CI) users, is thought be mediated by temporal processes. Recent findings from our laboratory [Zhou et al. JARO, 2018] suggested that CI users’ ability to detect phase duration modulation depends on spatial excitation patterns of the neurons, i.e., electrodes with sharper spatial tuning showed better modulation detection thresholds (MDTs). The current study extended these findings to examine the relationship between MDT and spectral resolution of the entire electrode array. Subjects’ spectral resolution of the whole array was assessed by measuring the spectral ripple detection thresholds. MDT was measured first for each functioning electrode via direct stimulation and averaged across

the whole array, and then via subjects' processor using acoustically modulated stimuli. Fourteen subjects using the Cochlear© devices participated in the study. All psychophysical testing used monopolar (MP 1+2) stimulation. Modulation rate was 4 Hz for both the direct and acoustic stimulation. Results showed that MDTs measured via processor and via direct stimulation were both strongly correlated with the subjects' spectral ripple detection thresholds. None of these measures correlated with subjects' duration of deafness. These results provided further evidence that CI subjects' modulation sensitivity depends on how the neurons that code the modulation are spatially excited. A more spatially selective excitation pattern driving the excited neurons to a higher point on their dynamic ranges would produce less variances in their responses, which may lead to a more robust coding of the modulation. The correlations may not necessarily indicate better neural survival in subjects who did well on both tasks, because it is known that spectral resolution can be affected by factors that are not physiological, such as electrode placement. The fact that duration of deafness did not predict either measure also supports the notion that neural survival is not the only common factor. The current results suggest that for CI users, temporal modulation sensitivity may not entirely depend on the temporal factors, but also strongly correlate with the implanted ear's spectral resolution. The results also suggest that customized strategies that aim to improve CI users' spectral resolution may improve the ears' modulation sensitivity as well.

PS 321

Rapid Simultaneous-Masked Spatial Tuning Curves in Cochlear-Implant Users

Jordan A. Beim[1]; Heather A. Kreft[1]; Julie G. Arenberg[2]; Andrew J. Oxenham[3]
[1]University of Minnesota; [2]Massachusetts Eye and Ear Infirmary, Harvard Medical School; [3]Department of Psychology, Center for Applied and Translational Sensory Sciences, UMNTC

Rapid sweep-based methods have been shown to provide efficient estimates of absolute threshold across the electrode array in cochlear-implant (CI) users. However, the same method resulted in less reliable estimates when used for spatial tuning curves (STCs) under forward masking, such that any benefit of speed was lost through increased variability. This may be because listeners typically find forward-masking tasks challenging without extensive psychoacoustic training. Forward masking has been used for STCs in normal-hearing listeners to avoid potentially artifactual effects that can occur with simultaneous masking, such acoustic beats between the target and masker, as well as cochlear suppression, but the same constraints do not apply for electrical stimulation. Here we tested a sweep-based threshold estimation technique for STCs using simultaneous masking, in an attempt to make the task easier and more reliable for untrained participants. The goal is to develop a method of estimating electrode interactions that is sufficiently fast and reliable for potential clinical use.

Participants listened for 100-ms monopolar pulse trains embedded in a sweeping quasi-continuous masker. Masker and probe pulses were interleaved so that electrical stimulation was never strictly simultaneous. The masker pulses were swept across the cochlear array using a steered quadrupolar stimulation strategy that resulted in 10 discrete stimulation steps between each electrode. A 2-interval 2-alternative forced-choice (AFC) procedure was also used as a comparison to the new Bekesy method.

Preliminary results indicate that the simultaneous-masking procedure substantially increased the reliability of the results as compared to the previously reported forward-masking procedure, while retaining a factor of 3 increase in measurement speed over the AFC procedure. The overall patterns of results were similar between the Bekesy and AFC procedures. The shapes and bandwidths of the simultaneous-masked STCs were compared with previously measured forward-masked STCs in the same participants.

The results of the study show that a Bekesy tracking procedure utilizing simultaneous masking can reduce the measurement time of STCs in CI users without sacrificing reliability, thus providing a rapid and efficient way to estimate electrode interactions.

Work supported NIH grant R01 DC012262.

PS 322

Revisiting Loudness Growth with Increasing Pulse Amplitude or Phase Duration in Cochlear Implant Users

Ning Zhou[1]; Lixue Dong[1]; John Galvin III[2]
[1]East Carolina University; [2]UCLA

Previous studies have shown that when manipulating pulse amplitude (PA) or pulse phase duration (PPD) in cochlear implant (CI) users, equal charge does not result in equal loudness. It is possible that newer electrode designs and higher stimulation rates, as well as relaxed CI indications, may modify the loudness relationship between PA and PPD. In this study, loudness growth functions were measured in CI users as the PA or PPD was increased from a fixed anchor. Ten CI ears (3 bilateral

and 4 unilateral subjects) were tested. All subjects (except for prelingually deaf, late-implanted bilateral subject S16) were adult, post-lingual, users of Cochlear© devices. Loudness growth functions were measured for a "PA stimulus" in which the PA was increased for a fixed PPD, and for a "PPD stimulus" in which the PPD was increased for fixed PA. First the dynamic range (DR) was measured for the PA stimulus with fixed PPD (25 ms/ph) and for the PPD stimulus with fixed PA (same as the threshold for the PA stimulus above). Loudness ratings were obtained for the PA and PPD stimuli at 10, 20, 30, 40, 50, 60, 70, 80, and 90% DR (in linear steps). PA stimuli were also loudness-balanced to PPD stimuli presented at 30, 50, and 70% DR. In terms of percent DR, loudness grew more quickly with increasing PPD than PA. In terms of charge, loudness grew more slowly with increasing PPD than PA, requiring on average a 50% greater increase in charge to achieve DR. The exponents of power functions fit to the loudness growth data were significantly smaller for the PPD than the PA stimuli. Significantly greater charge was required for the PPD than for the PA stimulus to maintain a target loudness, but only for the upper portion of the DR. This difference was especially evident for prelingually deaf subject S16. The patterns of results were similar with the loudness rating and loudness-balancing methods. The present data are in agreement with previous studies that show loudness coding with PPD requires greater charge than with PA. The difference in excitatory efficiency between the PA and PPD stimuli may indicate neuronal demyelination associated with long-term and/or early deafness. Therefore, comparing PA and PPD DRs (in terms of charge) may be useful in characterizing differences in charge integration and neural health across patients and stimulation sites.

PS 323

Effects of Instrument Timbre on Musical Emotion Recognition by Cochlear Implant Users

Brendon Warner[1]; Xin Luo[2]
[1]*University of Arizona College of Medicine - Phoenix;*
[2]*College of Health Solutions, Arizona State University*

Background
Emotions (e.g., happy and sad) can be effectively conveyed via musical melodies with different modes (e.g., major and minor) and tempi (e.g., fast and slow). Compared to normal-hearing listeners, cochlear implant (CI) users rely more heavily on the tempo cues to recognize musical emotions, due to their poor access to pitch cues. Musical pitch perception with CIs has been shown to be the best with organ but the worst with piano among a group of instruments. However, it is unknown how instrument timbre may affect the use of mode and tempo cues in musical emotion recognition by CI users.

Methods
To answer this question, post-lingually deafened adult CI users were tested with clinical CI processors in a musical emotion recognition test. The original-melody condition used ten happy melodies (in major modes and with fast tempi) and ten sad melodies (in minor modes and with slow tempi) played with piano, violin, trumpet, and organ (which represented different instrument families). In the tempo-normalized condition, all the melodies were played with the same intermediate tempo to limit the use of tempo cues in musical emotion recognition. In each cue condition, melodies played with different instruments were tested in separate blocks in random order. After listening to each melody, subjects were asked to identify the target emotion of the melody.

Results
The results showed that both the cue condition and instrument timbre significantly affected musical emotion recognition by CI users. The two factors also significantly interacted with each other. Post-hoc Bonferroni t-tests showed that in the original-melody condition, CI users had significantly better musical emotion recognition with piano and trumpet than with violin and organ. However, similar musical emotion recognition was found with the four instruments in the tempo-normalized condition. Tempo normalization significantly degraded musical emotion recognition with piano and trumpet but not with violin and organ.

Conclusions
Effects of instrument timbre on musical emotion recognition by CI users in this study differed from those on musical pitch perception in previous studies and suggested that compared to violin and organ, piano and trumpet generated better musical emotion recognition for CI users by providing better access to tempo cues. This was possibly due to the sharp temporal onsets of piano and trumpet notes. Future studies will test whether sharpening the temporal onsets of violin and organ notes can enhance CI users' musical emotion recognition with the two instruments.

PS 324

Impact of Flat Panel CT-Based Cochlear Implant Fittings on Speech, Timbre, and Pitch Perception

Melanie L. Gilbert[1]; Nicole T. Jiam[1]; Patpong Jiradejvong[1]; Daniel L. Cooke[2]; Charles J. Limb[1]
[1]*Dept of Otolaryngology-Head and Neck Surgery, University of California, San Francisco;*
[2]*Neurointerventional Radiology, University of California, San Francisco*

Music perception remains the most difficult listening endeavor for many cochlear implant (CI) recipients,

due in part to the frequency mismatch between the cochlear neural interface and the frequencies allocated by the programming. Due to individual differences in CI users' ear anatomy, electrode array length, and surgical insertion, great variability exists in CI users' implants, but these differences are not typically accounted for by current CI programming techniques. Flat panel computed tomography (FPCT) technology has been used to visualize the location of the electrodes within the cochlea to improve pitch perception accuracy.

To assess the impact of FPCT-based CI fittings using custom frequency allocations, we scanned 10 CI recipients (4 bilateral, 6 unilateral) and administered a test battery of speech and music perception tests. Speech metrics included words (CNC), vowels (hVd), and consonants (aCa); music assessments, developed by our lab, examined instrument timbre discrimination and puretone pitch scaling.

Subjects used 3 different FPCT-based fittings for a chronic period of 1 month each, and the test battery was administered at the beginning and end of each chronic trial. Our first fitting methodology involved assigning the center frequency of channels to that of the characteristic frequency (CF) of the corresponding electrodes. During this iteration of the multiphase study, we chose to deactivate electrodes located at CFs >16 kHz, and logarithmically distribute the channels for electrodes with CFs from 2 to 16 kHz. The second and third fitting methodologies preserved the CT-based activation/deactivation status for electrodes and employed a logarithmic frequency allocation across all channels, but varied the total bandwidth.

Preliminary results show no significant change with acute use of experimental fittings; however, both speech and music test score averages improved for the group in almost every category following chronic use of the first and second FPCT-based fitting methodologies. Further data collection and enrollment is ongoing.

Image-guided fitting is a promising tool, although additional research is necessary to identify optimum use of its findings. While the results are preliminary, this study may have significant implications for all CI recipients, and be especially relevant for young children and special populations. This project and previous work suggests that an image-based approach to CI mapping may improve pitch perception outcomes by reducing pitch-place mismatch. Future studies in pediatric and newly-implanted CI recipients are needed to assess the full potential of personalized image-guided CI fitting strategies.

Acknowledgments: This study was supported by a grant from MED-EL Corporation.

Auditory Prostheses IV

PS 325

Decoding Selective Attention in Cochlear Implant Users and its Relation to Speech Performance

Waldo Nogueira[1]; Hanna Dolhopiatenko[2]; Irina Schierholz[2]
[1]Hannover Medical School, Hannover, Germany; Cluster of Excellence, Hearing4all, Germany; [2]Medical University Hannover and Cluster of Excellence Hearing4all

Electroencephalography (EEG) data can be used to decode an attended speech source in normal-hearing (NH) listeners and cochlear implant (CI) users using high-density EEG caps. The technology may be used for 1) The identification of the target speaker in a cocktail party like scenario and the steering of speech enhancement algorithms in CIs; as well as for 2) The prediction of CI user's speech performance by means of the decoding accuracy in a selective attention paradigm. This work investigates if selective attention can predict speech performance in CI users.

NH-listeners and CI-users listened to target sentences in the presence of competing non-target sentences, whereby all sentences were presented on the same ear. Target sentences could be uttered by a male or female voice, whereby non-target sentences were always uttered by a voice of opposite sex. The speech material consisted of sentences of the HSM sentence test and the signal to interference ratio (SIR) between the target and the non-target speech was varied from -20 dB SIR to +20 dB SIR. In the first part of the experiment, NH-listeners and CI-users were asked to repeat the sentences. In the second part of the experiment, participants were instructed to attend to one of the two speech streams while a 96-channel EEG was recorded. Speech envelope reconstruction from the EEG data was obtained by training decoders using a regularized least square estimation method. Decoding accuracy was defined as the percentage of accurately reconstructed trials for each subject. For NH-listeners, the experiment was repeated using noise-vocoded sounds.

The results showed a decoding accuracy of 80.9% using the original sound files in NH-listeners. The performance dropped to 73.3% in the vocoder condition. Preliminary results in two CI users show a decoding accuracy of 71.2%. In sum, although the accuracy drops when the spectral resolution becomes worse, the results show the feasibility to decode the attended sound source in NH-listeners with a vocoder simulation, when competing talkers were presented on the same ear. Furthermore, the study confirms that it is possible to decode

selective attention in CI users despite the introduced electrical artifact. Results on the single-subject level showed that in several NH listeners selective attention decoding accuracy significantly correlated with speech performance, which holds potential for its use to predict speech performance in CI users.

PS 326

F0 Discrimination, Speech recognition, and Emotion Recognition in Younger and Elderly Adults Listening to Noise-Vocoded Harmonic Complexes

Lendra M. Friesen; Robert Morse
University of Connecticut

Temporal-envelope based voice-pitch coding is important for listeners with hearing impairment, especially listeners with cochlear implants (CIs), as spectral resolution is not sufficient to provide a spectrally based voice-pitch cue. More specifically, the encoding of fundamental frequency (F0) information is critical to communicating in such environments. Voiced speech can be approximated by a harmonic complex, with the perceived pitch of listeners' voices roughly corresponding to the F0 of the harmonic complex. Voiced pitch information has also been used in other types of processing such as speech intonation recognition, lexical tone recognition, and talker-gender identification, but also to separate competing sound sources and to determine speaker authenticity and voice emotion.

Differences in F0 discrimination between young and elderly normal hearing individuals has been shown, with elderly individuals performing more poorly. This difference has also been shown to occur in young and elderly individuals listening through CI vocoders with different numbers of spectral channels. However, it is still somewhat unknown as to how this encoding relates to more real-life listening situations such as speech understanding in quiet and noise and emotion recognition.

The objectives of this study were to compare results between younger and elderly individuals with normal hearing (at least up to 2000 Hz) and measure noise-vocoded listening by measuring: 1) F0 discrimination using 8 and 24 channel vocoders, with a 2000 and 4000 Hz cut-off, 2) 8-channel sentence recognition in quiet and in +5 SNR babble, and 3) emotion recognition with the 8-channel vocoder. Results so far reveal an age-related effect on all tasks.

PS 327

Cochlear Implants Users have Larger Visual Evoked Potentials and Delayed Alpha Oscillations in a Visual Working Memory Task

Priyanka Yogarajah[1]; Brandon T. Paul[2]; Andrew Dimitrijevic[2]
[1]Sunnybrook Health Sciences Centre, Otolaryngology Head and Neck Surgery, University of Toronto;
[2]Sunnybrook Research Institute

Speech perception in noise involves the use of multiple cognitive resources such as working memory and attention. People with hearing loss often draw upon a pool of cognitive resources while trying to decode a degraded auditory input. The goal of this study was to quantify the neural processes associated with working memory in people with cochlear implants (CI) and relate this metric to CI outcome. Fourteen age-matched individuals with CIs and normal hearing (NH) were recruited to perform a working memory task while 64 channel EEG was recorded. For the task, seven characters were sequentially presented and after a 4 second retention interval, a probe character was presented for which they indicated if it was in the list of previously presented seven characters. Participants also rated the difficulty of the task from 0-10 and the amount of effort they put into the task from 0-10. Results from the time-frequency analysis in the CI group showed an alpha synchronization during the working memory retention period that was both delayed and consisted purely of alpha (8-10 Hz) compared to the NH group's oscillatory activity where it occurred earlier and consisted of high alpha (10-12 Hz) and low beta (13-16 Hz). Brain source analysis revealed that the alpha synchronization in the CI group originated in the left occipital and left parietal regions whereas the high alpha in the NH group occurs in the right temporal and right frontal regions. Although trends existed, correlations between source activity and behavioural performance and effort were not significant. In the NH group, left frontal alpha was negatively correlated with performance and positively correlated with effort while the right frontal alpha was positively correlated with both; occipital and parietal sources were negatively correlated with effort and performance. In the CI group, temporal alpha was positively correlated with performance and negatively correlated with effort. The visual evoked response (P1 and N1) to the character onset were significantly greater in the CI group compared to the NH group. These results suggest that oscillatory neural networks for working memory are different between NH and CI users. Larger evoked responses in the CI users suggest that hearing loss may strengthen visual processing.

PS 328

The Effects of Reverberation on Speech Understanding in MED-EL Cochlear Implant Recipients

Sandra Prentiss
Sandra Prentiss, PhD

Reverberant environments negatively affect speech understanding[1] and the decline further progresses with increased reverberation times[2]. The negative affects of reverberation are even greater in cochlear implant users[3,4]. Understanding in reverberant environments requires the ability to process fine structure cues[2,4]. Med-El's unique FS4-p coding strategy incorporates fine-structure processing and envelope cues, which may lead to improved understanding in reverberant situations. The benefits of fine structure processing were investigated in simulated reverberant conditions.

Med-EL adult recipients implanted with either the Flex 24 or Flex 28 electrodes were included for this study. The modified Speech Perception in Noise-Revised (SPIN-R) test was used to simulate 4 reverberant listening situations: 1) Unprocessed 2) Reverberation time of 600 ms (similar to a furnished living room space), 3) reverberation time for 1200 ms (similar to lecture hall) and 4) reverberation time of 3600 ms (similar to an auditorium). Speech perception in reverberant environments (2-4) was assessed in the 1) fine structure processing strategy condition and 2) HDCIS processing strategy condition. One sentence list from each condition was presented via loudspeaker with the subject seated at 0° azimuth. Subjects repeated the last word of each sentence. Scores were based on number of words repeated correctly.

Unprocessed sentences revealed significantly better performance than any of the reverberant conditions. An increase in reverberation time resulted in a decrease in performance. No significant differences were observed between the FS4-p strategy and the HDCIS coding strategy.

A significant decline in performance was observed in the least difficult condition suggesting that performance in current standard testing metrics do not reflect realistic listening conditions. Reverberation is present in almost every listening situation and must be considered when analyzing outcomes as well as patient report.

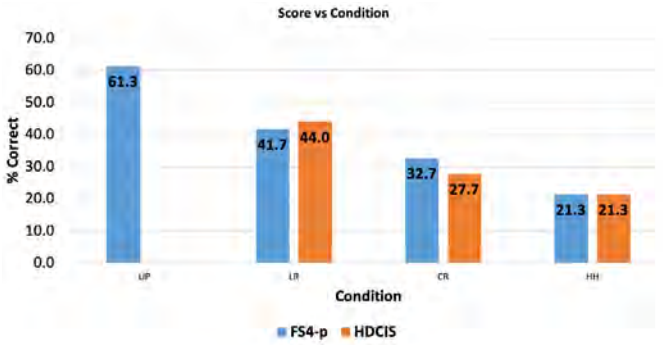

PS 329

Contribution of the Functional Status of the Cochlear Nerve to Speech Recognition Outcomes in Adult Cochlear Implant Users

Jeffrey Skidmore[1]; William J. Riggs[1]; Chloe Vaughan[2]; Shuman He[3]
[1]The Ohio State University; [2]The Ohio State University, Eye and Ear Institute; [3]The Ohio State University; Nationwide Children's Hospital

Background

Substantial variations in patient outcomes for cochlear implant (CI) users creates a challenge in treating and counseling these patients (Lazard et al., 2012; Holden et al., 2013; Moberly et al., 2016). Many factors have been shown to contribute to the observed variability in CI patient outcomes (Lazard et al., 2012; Moberly et al., 2016). For example, speech recognition scores are negatively correlated with the duration of severe to profound hearing loss before CI implantation (Kelly et al., 2005; Green et al., 2007; Lazard et al., 2012) and positively correlated with longer CI experience (Lazard et al., 2012). However, there is still a lack of adequate predictors to explain the observed variability in CI patient outcomes. Because the number and function of cochlear nerve (CN) fibers (i.e. CN functional status) are theoretically important for patient outcomes, an estimate of CN functional status should be important for understanding inter-patient variations. This study tested the hypothesis that the functional status of the CN is correlated to speech recognition outcomes in CI patients.

Methods

To date, 15 deaf adults have participated in this study. All subjects were implanted with a Cochlear™ Nucleus® device in the test ear. For each participant, electrically-evoked compound action potentials (eCAPs) were measured at multiple electrode locations across the electrode array. This data was used in a recently developed predictive model (Skidmore et al., 2019) to generate an index for the functional status of the CN (i.e. CN index)

for each participant. Correlation analysis was performed with four variables of interest: CN index, CI experience, duration of severe to profound hearing loss before implantation, and AzBio sentence recognition scores.

Results
Our preliminary results showed that AzBio sentence recognition scores were correlated with CN index (r=0.37), CI experience (r=0.38), and duration of severe to profound hearing loss before implantation (r=-0.37). CN index and CI experience were not correlated (r=0.03, p=0.90) and accounted for 32% of the variance in AzBio scores when performing multiple regression (r^2 = 0.32, p=.10).

Conclusions
Based on our preliminary results, the functional status of the CN seemed to be an important factor for speech perception performance for adult CI users. These preliminary results suggest that CN index, especially in combination with other predictor variables, provides valuable information for explaining and/or predicting variability in CI outcomes.

Acknowledgments
This work was supported by the R01 grant from NIDCD/NIGMS (1R01DC016038) and the R01 grant from NIH/NIDCD (1R01DC017846).

PS 330

Improved Neural Responses in Cochlear Implants Using a Physiologically Based Stimulation Strategy: Preliminary Results

Andres F. Llico; Thomas M. Talavage
Purdue University

Introduction
Cochlear implants (CI) are implantable devices capable of partially restoring hearing loss by electrically stimulating the auditory nerve to mimic normal-hearing conditions. Resulting speech perception varies among CI users, depending mostly on their deafness and surrounding noise conditions. Current electrical-stimulation strategies are often developed following phenomenologically based approaches instead of being derived from known physiological functions of the auditory system. The framework developed in this study seeks to provide an optimized electrical-stimulation strategy by maximizing the similarity between simulated neural patterns elicited in the auditory nerve by acoustic and electrical means. Preliminary results show increased correlation and reduced mean square error between acoustic and electric stimulation when the proposed optimized strategy is used instead of a commonly used CI strategy that stimulates electrodes based on spectral energy content.

Materials and Methods
A 100-ms segment of the utterance 'had' spoken by a male speaker was used as input to a computational model of normal hearing (NH) (Zilany et al., 2014) and a CI pulse generator followed by an electrical-stimulation model of the auditory nerve (Bruce et al., 1999), yielding two neural activity patterns (NAPs) for each speech sample. NAPs are compared using an objective function to maximize the correlation between them and select the electrical sequence that best matches the output from the normal hearing model. An implementation of the advanced combination encoder (ACE) strategy (Seligman & McDermott, 1995) was used as a reference to evaluate performance of the proposed optimized strategy through cross correlation and mean square error metrics.

Results and Discussion
Cross correlation and mean square error metrics were computed between the output NAP for normal-hearing and each of the output NAPs for the proposed and ACE strategies. Preliminary results yielded a 1.7% increase in cross-correlation and a 2.4% reduction in mean square error, both in favor of the proposed optimized strategy over the ACE strategy.

Conclusion
Preliminary results suggest that optimized CI stimulation patterns may provide neural responses more similar to NH than a commonly used CI strategy. This is supported by previous work in which this framework led to increased speech perception in background noise conditions, as well as provided more consistent performance in quiet conditions. (Llico et al., BMES 2017) Further research is necessary to evaluate alternative objective functions that could better represent in NAPs perceptual differences.

PS 331

Evaluating a mixed-rate cochlear implant strategy on speech understanding in noise

Tanvi Thakkar[1]; Thibaud Leclere[2]; Alan Kan[3]; Ruth Y. Litovsky[4]
[1]University of Wisconsin-Madison; [2]Waisman Center, University or Wisconsin-Madison; [3]School of Engineering, Macquarie University; [4]The University of Wisconsin–Madison

Listeners with bilateral cochlear implants (BiCIs) exhibit benefits in speech understanding and sound localization in quiet compared to unilateral listeners, but still experience difficulties in noise compared to normal hearing (NH) listeners. One reason for this outcome is that NH listeners can utilize small interaural time differences (ITDs) to spatially separate target from noise. However, BiCI listeners have poor access to ITDs when using

clinical processors. This is because acoustic fine-timing information is replaced with high-rate pulsatile stimulation during processing. High stimulation rates are needed for achieving good speech understanding, but low stimulation rates are needed for ITD sensitivity. A potential solution is to use a unique strategy combining high and low stimulation rates at different electrodes. Previous work in our lab has found that ITD sensitivity with mixed rates is comparable to that with all low rate stimulation, particularly when low stimulation rates were introduced toward the basal end of the electrode array in a mixed rate strategy. Here we investigated speech recognition in noise with various mixed-rate strategies. We hypothesized that, if BiCI listeners can utilize the ITD in a mixed-rate strategy to spatially separate the sources, a greater improvement in speech recognition will be achieved compared to using uniform rates across all electrodes.

Using synchronized research processors, listeners were presented with a CIS-like strategy where stimulation occurred on eleven electrodes. Uniform rates were tested, with all electrodes at each patient's clinical rate ("All High") or at 10% of the clinical rate ("All Low"). Mixed rate configurations were: (a) 5 low-rate electrodes near the base with the remainder at the clinical rate; (b) 6 low-rate electrodes near the apex with the remainder at the clinical rate; (c) interleaved low-and high-rates. Stimuli were CNC words mixed with speech-shaped noise. Stimuli were presented with SNRs that changed adaptively at 3 dB steps using a 2-down 1-up procedure. An ITD of either 0 μs or + 800 μs was applied to the target. A binaural benefit was calculated as a difference in performance between the 0 μs and 800 μs ITD conditions.

Results suggest that speech recognition in noise could be achieved with mixed rate stimulation, though the binaural benefits obtained in listeners varied with the mixed rate configuration tested. These data suggest that mixed rates have the potential to convey ITDs for spatial separation of speech from noise.

PS 332

Age-related Temporal Processing Deficits for Word Segments in Adult Cochlear-Implant Users: Perceptual and Electrophysiological Evidence

Zilong Xie[1]; Samira Anderson[2]; Sandra Gordon-Salant[1]; Matthew Goupell[1]
[1]Department of Hearing and Speech Sciences, University of Maryland, College Park, MD; [2]Department of Hearing and Speech Sciences, University of Maryland, College Park, MD, USA

Introduction
Increasing numbers of older adults use cochlear implants (CIs) to restore hearing ability. Many older listeners gain substantial benefits to speech understanding from CIs; however, their performance may still be worse than that of younger CI users. To date, factors contributing to age-related differences in speech understanding of CI users remain unclear. Successful speech understanding in CI users is heavily reliant on the processing of temporal cues because CI sound processors convey primarily temporal envelope information. In acoustic-hearing listeners, temporal processing abilities tend to decline with advancing age, and these declines relate to similar declines in speech understanding with aging. Thus, the current study aims to identify age-related temporal processing deficits in CI listeners and to determine the extent to which such aging effects contribute to speech understanding deficits in older CI users.

Methods
Temporal processing was quantified as the ability to identify words based on manipulation of a single temporal cue. The words dish and ditch, which differ primarily in the duration of a silent interval preceding the final fricative, were chosen for this study. A seven-step continuum of the dish-ditch contrast was created with silence duration cues varying from 0 to 60 ms. Listeners tend to perceive 'dish' for words with shorter silence durations and perceive 'ditch' for words with longer silence durations. Younger, middle-aged, and older CI users were asked to perform a perceptual categorization task on the word contrast continuum. Cortical auditory-evoked potentials were also elicited to words from the continuum endpoints. Participants completed both the perceptual and electrophysiological tasks across three presentation levels: most comfortable level (MCL), or 10 dB below or above MCL.

Results
Preliminary results from older CI listeners revealed that while CI listeners could identify the words dish and ditch, they needed longer silence durations to discriminate the word contrast at lower presentation levels compared to higher levels. Data collection will continue to determine the extent to which aging affects both the perceptual ability to utilize temporal cues for word identification and the neural representation of temporal cues in speech. Regression analyses will be conducted to determine the contribution of central (cortical) processing to perceptual performance.

Discussion
The current study has implications for understanding how auditory temporal processing limits speech understanding of older CI listeners and the associated neural mechanisms.

[This research was supported by the National Institute on Aging of the National Institutes of Health under Award

Number R01AG051603.]

PS 333

Compared to Normally Hearing Listeners, Cochlear Implant Users Rely More on Lexical-Semantic Cues than on Prosodic Cues for Speech Emotion Identification

Margaret Richter[1]; **Monita Chatterjee**[2]
[1]Division of Speech and Hearing Sciences, University of North Carolina; [2]Boys Town National Research Hospital

Emotions in speech are conveyed with both prosodic cues (how it was said) and with lexical-semantic information (what was said). Of the two, prosody (including voice pitch, speaking rate, loudness, and spectral envelope) dominates our perceptions of the talker's emotion. In this study, we tested the hypothesis that when the primary cue for prosody, voice pitch, is degraded (as in noise-vocoding or in listening with cochlear implants (CIs)), listeners shift their perceptual emphasis to lexical-semantic cues for emotion identification.

Participants included 17 listeners with normal hearing (NH) and 8 listeners with CIs. Stimuli were sentences conveying five kinds of lexical-semantic emotion: angry, happy, sad, neutral, and scared. Each of these sentences was then recorded in five kinds of prosodic emotion (also angry, happy, sad, neutral and scared) by two female talkers. During the test, participants heard one recording at a time and indicated which emotion they thought it was associated with. Stimuli were blocked by talker and presented in random order within a block. NH listeners heard both original and noise-vocoded versions of the stimuli, while CI users heard only the original stimuli. Participants were instructed to keep in mind that emotions are conveyed using both kinds of cues, and to consider both the words and the manner of speaking to decide on the talker's intended emotion.

Results showed that in the conditions where prosodic and semantic cues to emotion matched (congruent condition), NH listeners scored near ceiling, while CI users' scores were significantly poorer. When prosodic and semantic cues were incongruent, NH listeners relied more strongly on the prosodic cues than CI users, who relied more on lexical-semantic cues. When stimuli were noise-vocoded, NH listeners showed a pattern more closely resembling the CI users: they relied significantly less on prosodic cues and more on lexical-semantic cues.

In everyday life, incongruent cues to emotion are most often encountered when the talker is conveying sarcasm or irony. In these cases, the tone of voice often indicates the true emotional meaning of the utterance (e.g., *I just had the best day ever* spoken in an angry tone), and facial expressions are often neutral. If CI users are less able to decipher the prosodic cue, they might miss the entire point of the communication. Thus, these findings have implications for the perception of both emotion and sarcasm by CI users.

[Work supported by NIH grants R01 DC014233, T35 DC008757, P20 GM109023]

PS 334

The Role of Semantic Context and Talker Variability in Speech Perception for Cochlear-Implant Users and Normal-Hearing Listeners under Vocoded Conditions

Erin R. O'Neill[1]; Heather A. Kreft[1]; Andrew J. Oxenham[2]
[1]University of Minnesota; [2]Department of Psychology, Center for Applied and Translational Sensory Sciences, UMNTC

Background
Much variability exists in the speech perception abilities of cochlear-implant (CI) users that cannot be explained by clinical or anatomical factors. In this study, our aim was to assess the impact of semantic context and talker variability on speech perception for CI users and compare the variance in performance across conditions with normal-hearing (NH) listeners under vocoded conditions.

Methods
Post-lingually deafened adult CI users were tested on word intelligibility in sentences with and without semantic context, presented in quiet and noise, recorded by four different talkers. Age-matched and younger NH adults also participated, listening via tone-excited vocoders, adjusted to produce mean performance for speech in noise comparable to that of the CI group. Overall performance between groups and variance within groups were compared.

Results
Preliminary data suggest that both semantic context and talker variability influence speech perception in CI users, with differences in the speech production of individual talkers sometimes having a greater impact on overall performance. The within-group variance in speech understanding for the NH groups was similar in magnitude to that of the CI groups for many of the conditions tested.

Conclusions
Overall, these data highlight the potential importance of central factors, not unique to the CI population, in

explaining individual differences in hearing outcomes of CI users.

Acknowledgements
This work is supported by NIH grant R01 DC012262 and NSF training grant NRT-UtB-1734815.

PS 335

Age at Cochlear Implantation and Frequency-to-Place Mismatch Influence Early Speech Recognition Outcomes

Michael W. Canfarotta[1]; Brendan P. O'Connell[1]; Emily Buss[2]; Kevin D. Brown[1]; Margaret T. Dillon[1]
[1]University of North Carolina at Chapel Hill; [2]UNC

Background
Default electric frequency filters of cochlear implant (CI) devices assign frequency information irrespective of intracochlear position, resulting in varying degrees of frequency-to-place mismatch. Substantial mismatch negatively influences speech recognition in postlingually deafened CI recipients, and acclimatization may be particularly challenging for older adults due to effects of aging on the auditory pathway.

Objective
The objective of this study was to investigate the influence of mismatch and age at implantation on speech recognition within the initial 6 months of CI use.

Methods
Forty-eight postlingually deafened adult CI recipients of lateral wall electrode arrays underwent postoperative computed tomography to determine angular insertion depth of each electrode contact. Each subject had a complete electrode array insertion (defined as all contacts being intracochlear on review of imaging) and listened exclusively to default electric frequency filter assignments during the initial 6 months of device use. The absolute semitone deviation from the average spiral ganglion map (Stakhovskaya et al. 2007) was determined at 1500 Hz (approximately 267 degrees), which has been shown to be an important region for frequency alignment in vocoder simulations (Baskent & Shannon 2007). Consonant-nucleus-consonant (CNC) scores in the CI-alone condition at 1, 3, and 6 months post-activation were subsequently compared to the degree of mismatch at 1500 Hz and age at implantation.

Results
Younger adult CI recipients experienced more rapid growth in speech recognition during the initial 6 months of CI use. Greater degrees of frequency-to-place mismatch were associated with poorer speech recognition, yet older listeners were not particularly susceptible mismatches.

Conclusion
While older adults are not necessarily more sensitive to detrimental effects of frequency-to-place mismatch, other potential factors – such as cognitive decline – appear to limit early benefit with a CI. These results suggest that minimizing mismatch could optimize outcomes in adult CI recipients across the lifespan, but this consideration may particularly important for elderly patients.

PS 336

Behavioral Assessment of Selective Attention with Competing Speech Stimuli in Hearing Aid Users

Sébastien Santurette; Martha Larsen; Lu Xia; Jens-Christian Britze Kijne; Josefine Juul Jensen
Oticon A/S

Focusing and sustaining auditory attention are essential abilities to successfully communicate with another person in the presence of other speech and noise sources that one wishes to ignore. For hearing-impaired (HI) listeners, such situations can be very challenging, while normal-hearing (NH) listeners typically easily navigate through complex auditory scenes. In a task requiring young NH and HI listeners to repeat a target digit stream in the presence of simultaneous, spatially-separated masker digit streams, Best et al. (2018, Trends in Hearing 22) showed that a buildup of auditory streaming was observable in both NH and HI listeners using speech stimuli. HI listeners obtained lower scores than NH listeners, a difference that was driven by more confusions between target and masker digits in the HI group, suggesting a role of selective attention.

We investigated whether such a buildup of speech intelligibility could be observed in older hearing aid (HA) users using a similar task in a loudspeaker setup, and whether the task was sensitive to differences in HA signal processing strategies. Twelve older experienced HA users, seated in the center of a loudspeaker array with HAs on, were asked to repeat sequences of four target digits randomly located at either -45, 0, or +45 degrees azimuth, while competing digit sequences were simultaneously presented from the two other locations. The digit streams were spoken by different female talkers. In half of the trials, background speech-shaped noise was added from loudspeakers located at -112.5, 180, and +112.5 degrees. The task was performed with two adaptive HA compression strategies in the speech-only conditions and with and without the activation of HA noise reduction in the speech-plus-noise conditions.

All listeners were able to perform the task above chance level after a short training session. Mean recognition scores increased with digit position and this marginally significant effect (p=0.050) indicated that a buildup of speech intelligibility was observable in this group of older HA users. This effect was mainly due to a decrease in masker errors with digit position, while random errors remained stable. Background noise negatively affected recognition scores with noise reduction turned off. The activation of noise reduction yielded similar scores to the quiet conditions. The significant effect of condition (p=0.049) suggested that such a task may, with some adjustments, be sensitive to compare HA processing strategies. Overall, a competing digits task may be suitable to behaviorally assess selective attention abilities in older HA users.

Binaural Hearing and Speech Perception

PS 337

Effects of Binaural Fusion on Benefits from Voice Pitch Differences and Spatial Separation in a 'Cocktail Party' Environment

Yonghee Oh[1]; Curtis Hartiling[2]; Nirmal Kumar Srinivasan[3]; Morgan Eddolls[4]; Anna Diedesch[5]; Frederick J. Gallun[6]; Lina Reiss[4]
[1]University of Florida; [2]Portland State University; [3]Towson University; [4]Oregon Health and Science University; [5]Western Washington University; [6]VA RR&D NCRAR

Voice pitch differences and spatial separation are important cues for auditory object segregation. Recently, we showed that the ability to segregate and identify speech based on voice pitch differences is highly correlated with the breadth of binaural pitch fusion, the fusion of dichotic stimuli that evoke different pitches across ears in bimodal cochlear implant listeners (Oh et al., ASA 2018). The goal of this study was to investigate the relationship between binaural pitch fusion and the ability to use these cues in normal-hearing (NH) and hearing aid (HA) listeners. We also investigated whether benefit from voice pitch differences in monaural listening conditions is correlated with the breadth of binaural fusion, in order to rule out that the correlation of binaural fusion with voice pitch benefit is not due to both being correlated with monaural abilities. We also investigated the relationship of spatial benefit to localization ability.

Twelve bilateral HA users (age: 30-75 years) and nine NH listeners (age: 36-67 years) were tested in the following experiments. First, speech on speech masking performance was measured as the threshold target-to-masker ratio (TMR) needed to understand a target talker in the presence of either same- or different-gender masker talkers. These target-masker gender combinations were tested with two spatial configurations (maskers co-located or 60° symmetrically spatially separated from the target) in both monaural and binaural listening conditions. Second, binaural pitch fusion range measurements were conducted using harmonic tone complexes around a 200-Hz fundamental frequency. Third, absolute localization ability was measured using broadband (250-8000Hz) noise and one-third octave noise bands centered at 500 and 3000 Hz.

Voice pitch differences between target and maskers improved TMR for both listener groups in both monaural and binaural listening conditions, with greater benefit in co-located than spatially separated conditions. Voice pitch benefit was correlated with the breadth of binaural pitch fusion in the binaural, but not monaural, listening condition, ruling out a role of monaural abilities in the relationship between binaural fusion and voice pitch benefits. Spatial separation in the binaural listening condition improved performance more for NH listeners than for HA users, indicating a decreased ability of HA hearing-impaired users to benefit from spatial release from masking. Spatial separation benefit was correlated with absolute localization ability. These findings suggest that both sharp binaural pitch fusion and accurate localization ability are necessary for maximal speech perception in multi-talker environments.

Funding: Supported by NIH-NIDCD grant R01 DC013307 and F32 DC016193.

PS 338

Binaural-Temporal Integration of Speech Reflections in Hearing-Impaired Listeners

Jan Rennies[1]; Anna Warzybok[2]; Thomas Brand[2]; Birger Kollmeier[2]
[1]Fraunhofer Institute for Digital Media Technology IDMT and Cluster of Excellence Hearing4all, Oldenburg, Germany; [2]Medical Physics Group, Department of Medical Physics and Acoustics and Cluster of Excellence Hearing4all, University of Oldenburg, Germany

In reverberant rooms, speech reflections overlap with the direct sound when they arrive at the listener's ears. To what degree these reflections can be integrated with the direct sound depends on different factors such as reflection delay and direction as well as on the spatial configuration of interfering noise sources. In a previous study [Rennies et al., Trends Hear. 23, 1–22, 2019], we investigated the capability of normal-hearing (NH) listeners to integrate speech reflections that were systematically manipulated in their delay and interaural phase difference (IPD). Speech recognition thresholds (SRTs) were measured in

stationary speech-shaped noise. The data showed that direct sound and one or several early speech reflections could be perfectly integrated when they had the same IPD. Remarkably, when amplitude or IPD favored late RIR components, which are commonly considered detrimental for speech intelligibility, NH listeners were capable to focus on these late components rather than on the precedent direct sound. This indicated a previously unknown degree of flexibility in temporal integration of speech information in the normal auditory system.

The present contribution extended the previous study by measuring SRTs in listeners with sensorineural hearing impairment (HI). Listeners received individual linear amplification to reduce the influence of audibility. Baseline measurements showed that all listeners had a benefit from IPD differences between speech target and noise in conditions that did not require temporal integration of speech reflections, although this benefit was smaller than for NH subjects. In conditions requiring temporal integration of speech reflections but no IPD processing, the negative impact of increasing the reflection delay was generally much greater in HI than in NH subjects. Large interindividual variability was observed in conditions in which NH listeners had been able to focus on a late reflection if this reflection carried binaurally advantageous information. Some HI listeners also showed this remarkable capability, while others were incapable of exploiting IPD information. An even larger interindividual variability occurred when speech information was distributed across direct sound and multiple reflections spread across a period of up to 200 ms after the direct sound. Some listeners even were incapable of measuring SRTs with the present procedure because they did not recognize more than 50% of the target words at SNRs as high as 20 dB, while other showed close-to-normal performance. The new data indicate that measuring spatio-temporal integration may provide useful insights into individual hearing loss.

PS 339

The Effect of Asymmetric Dynamic Range on Speech Intelligibility and Binaural Unmasking in Normal Hearing Individuals Listening to Vocoded Speech

Emily A. Burg[1]; Tanvi Thakkar[1]; Sean R. Anderson[1]; Matthew B. Winn[2]; Ruth Y. Litovsky[3]
[1]University of Wisconsin-Madison; [2]University of Minnesota; [3]The University of Wisconsin–Madison

Cochlear implants (CI) can restore speech perception in children and adults with severe-to-profound sensorineural hearing loss. Many CI listeners are able to achieve excellent speech intelligibility. However, there is substantial variability both across- and within-listeners. Within a listener, bilateral users can exhibit large performance asymmetries across ears. Electric dynamic range, which is substantially smaller than acoustic dynamic range, can vary across ears and likely contributes to some of this variability. This work aimed to investigate whether interaural differences in dynamic range could contribute to asymmetric speech performance. Additionally, we were interested in how across-ear differences in dynamic range influence how well bilateral CI listeners are able to utilize their implants together and function in complex listening environments. We simulated these effects in normal hearing (NH) individuals by reducing the dynamic range of vocoded speech, which has limited spectral information similar to a CI. Target stimuli consisted of female-talker IEEE sentences and masker stimuli consisted of female-talker AzBio sentences. All stimuli were processed using a 16-channel sine wave vocoder and presented over headphones at 65dB-A. We investigated the effect of reduced dynamic range on speech intelligibility in quiet, and used a binaural unmasking paradigm to examine how symmetric and asymmetric reduced dynamic range affected listeners' ability to integrate signals across ears. In one listening configuration, target speech was presented in quiet. In a second configuration, target and masker speech were presented to one ear. In a third configuration, a copy of the masker was also presented to the contralateral ear, which enables the listener to perceive the target and masker at different intracranial locations and obtain binaural unmasking. We predicted that speech intelligibility in quiet and in noise would decrease monotonically with decreasing dynamic range. Further, we predicted that binaural unmasking would decrease as asymmetry in dynamic range increased, and that asymmetries would negatively affect binaural unmasking more than symmetrical reductions across ears. In line with our first prediction, data show that speech intelligibility decreased with reduced dynamic range. Additionally, binaural unmasking decreased with increasing asymmetry, however, preliminary data suggest that asymmetry has a smaller impact on unmasking than the absolute magnitude of (symmetrical) reductions in dynamic range. These results are in line with previous findings that report dynamic range as a relevant factor for speech perception in CI listeners and may motivate future studies to further examine the impact of interaural asymmetries on binaural outcomes.

PS 340

Spectro-Temporal Weighting of Interaural Time Differences in Speech

Lucas Baltzell; Jayaganesh Swaminathan; Virginia Best
Boston University

Recent studies have suggested that the perceptual

weighting of interaural time differences (ITDs) is non-uniform in time and frequency, leading to two main hypotheses: (1) ITDs are preferentially extracted during acoustic onsets and (2) ITDs are preferentially extracted in a frequency region centered at around 600 Hz. The extent to which these two hypotheses extend to speech, with its complex spectro-temporal structure, is unclear. To begin to answer this question, the present study aimed to characterize spectro-temporal weighting of ITDs in spoken words. In order to dissociate the effect of phoneme type and temporal position, weights were derived for a CV ("two") and a VC ("eight") word token. Each word token was divided into eight frequency bins (between 80 and 8000 Hz) and two time bins (separated at the phoneme boundary). ITDs drawn from a random distribution centered on 0 µs were independently assigned to each spectro-temporal bin, and listeners were asked to indicate whether they heard the word token on the right or the left side of their head. Lateralization judgments were regressed on ITD values in each bin to yield spectro-temporal weights. Results suggest that more weight was given to phonemes in the first position and to frequencies around 600 Hz, consistent with both "onset dominance" and the "dominance region" hypotheses.

PS 341

The Effect of different Head-Related Transfer Functions on the Spatial Release from Masking in Children with Auditory Processing Disorder

Katharina Zenke; Stuart Rosen
University College London

Auditory Processing Disorder (APD) is a developmental disorder characterized by difficulties in listening to speech in noise despite normal audiometric thresholds. It is still poorly understood and much disputed and there is need for better diagnostic and intervention tools for young children, not least because of suspicions that APD leads to learning difficulties in language and literacy, and hence to poor school performance. One promising avenue of research is the claim that around 20% of children referred for APD assessment are found to have a reduced spatial release from masking (SRM). Current clinical tests measure the SRM in virtual auditory environments generated with head-related transfer functions (HRTFs) from a standardized adult head. Adults and children, however, can be very different in head dimensions and mismatched HRTFs are known to affect localization accuracy. HRTFs in children have not been systematically measured so far and it is unclear whether HRTF mismatch also impacts speech perception, especially for children with APD due to their problems with processing auditory information. In our current study, we measured individual HRTFs in children with diagnosed APD and typically-developing children aged 7 to 12 years. The SRM was measured for target sentences and two symmetric speech maskers in virtual auditory environments generated from these individualized HRTFs or HRTFs of an artificial adult head as well as in a real anechoic environment. In order to assess the influence of spectral pinna cues, we also measured speech reception thresholds for HRTFs gained from a spherical head model that only contains interaural time and level differences. Preliminary findings suggest differences in speech reception thresholds between listening conditions and slightly better overall performance of typically-developing children but similar amounts of SRM for all conditions. Both groups of children obtained significantly worse speech reception thresholds and smaller SRM as normal-hearing adults in our previous study.

We hope our results will help to determine the relevance of individualized spatial cues for SRM and further clarify the nature of spatial processing difficulties in children with APD.

PS 342

Central Auditory Mechanisms Revealed by Dichotic Listening in Noise

Carrie Clancy[1]; Jillian Bushor[1]; Maggie Schefer[1]; Alyssa Everett[1]; Barrett St. George[2]; Frank Musiek[1]
[1]University of Arizona; [2]The University of Arizona

The Dichotic Digits Test (DDT) is utilized to evaluate central auditory nervous system (CANS) dysfunction. It is a popular test with good sensitivity and specificity and has been used in clinics worldwide for over 30 years. On the downside, the DDT has a ceiling effect which mitigates its effectiveness in some situations.

It was hypothesized that one way to decrease the ceiling effect would be to add competing noise to the DDT. In addition, adding noise to the DDT would create a new paradigm that would herald a novel investigation into the effect of noise on dichotic listening—a process about which little is currently known.

To create dichotic listening in noise, editing software was utilized to add speech spectrum noise to the standard DDT at two different signal-to-noise ratios (SNRs). First, speech spectrum noise was added at equivalent RMS-amplitudes to the presentation of the digits, creating a 0 dB SNR. Then, the noise in the 0 dB SNR tracks was amplified to create a set of identical tracks with a -2 dB SNR. Noise and digit-presentation track files were combined into single-track presentations with

noise onset/offset synchronized to the presentation of the digits. Four test conditions at each of the two SNRs were created: standard (no added noise), bilateral noise, monaural right noise, and monaural left noise, which were presented in random order to all 20 normal hearing subjects at an intensity of 50 dB sensation level (re: SRT).

Results for the no-noise condition were consistent with published norms for each ear on the standard DDT. Adding binaural noise showed much smaller effects, on both combined and individual ear scores, than did adding monaural noise to either ear, which demonstrated a clear binaural advantage for listening in noise. Interestingly, while preliminary results did not demonstrate a clear right ear advantage in the no-noise condition, the -2 dB SNR binaural noise-added condition did show distinctly higher right ear scores, indicating a right ear advantage for speech in binaural noise. On the other hand, -2 dB SNR monaural noise conditions showed the right ear to be more susceptible to monaural noise than the left. Finally, as expected, adding -2 dB SNR noise reduced the standard DDT ceiling effect, with combined scores dropping from 98% in the no-noise condition to 91% in the -2 dB SNR binaural noise condition, and even lower for both -2 dB SNR monaural noise conditions.

PS 343

On the Relation Between Binaural Temporal Processing and Speech Understanding in Noise.

Jaime A. Undurraga[1]; Jeremie Lienart[2]; David McAlpine[1]
[1]*Department of Linguistics, The Australian Hearing Hub, Macquarie University, Sydney, Australia;*
[2]*University of Montpellier*

It is well established that hearing capabilities decline with ageing and/or following noise exposure. Clinically, hearing abilities are assessed by pure-tone audiometry thresholds. However, some normal hearing (NH) listeners report great difficulties in understanding speech, particularly, in environments with background noise despite having normal audiometric thresholds, and so their problem remains untreated - Hidden Hearing Loss (HHL). One factor deemed to be associated with HHL is selective damage to high-threshold auditory nerve fibres which can reduce the ability to encode the fine temporal fluctuations conveyed by sounds, and so the ability to understand speech in the presence of noise. Here we investigate the relation between neural coding of temporal processing using objective (Electroencephalogram (EEG)) and behavioural (speech-in-noise listening) binaural measures in 23 NH listeners. Speech reception thresholds (SRTs) were obtained using a 2-down 1-up adaptive staircase task in which participants were presented with digits in background speech-shaped noise. The noise was presented at 65 dBA and it was always diotic. Digits were presented with an interaural time difference (ITD) spanning 0 to 800 µs. SRTs were also obtained by presenting the inverted version of the digit's waveform at one ear—the antiphasic condition. For each run, the speech level was adapted using step sizes of 6, 3, and 2 dB. The SRT of a single run was estimated as the average of the last 6 reversal points. The final SRT was obtained as the average of three runs. EEG measures of binaural processing were obtained by presenting bandpass noise (100-1000 Hz) at 65 dBA. The noise was presented using the same conditions as in the behavioural task. To evoke neural responses, the ITD of the stimulus was periodically modulated between 0 and a given ITD at a rate of 6.7 Hz. This modulation evoked a steady-state following response to the ITD modulation—the interaural time difference following response (ITD-FR).

Results demonstrated that both ITD-FR amplitudes and SRTs improved with increasing ITD and were maximum for the antiphasic condition (SRT ~ 6 dB and ITD-FR ~ 15 dB improvement). Statistical analyses revealed that 19 out of 23 individual correlations between SRT and ITD-FR were significant. The group correlation was also highly significant ($r = 0.98$, $p < 0.001$). Our results demonstrate that ITD-FRs may be a reliable tool to assess temporal processing in human listeners and could be a potential clinical tool for screening.

Binaural Hearing: Cochlear Implants, Bone Conduction, and Hearing Aids

PS 344 **WITHDRAWN**

Binaural Hearing Benefits of Bone Conduction Devices in Individuals with Conductive Hearing Loss

Hillary Snapp; Brianna Kuzbyt; Alyssa Whinna; Seba Ausili
University of Miami, Miller School of Medicine

In individuals with conductive hearing loss (CHL), bone conduction hearing devices (BCDs) can bypass the conductive component to stimulate the intact cochlea. Yet, in unilateral CHL, adoption and acceptance of BCDs is low, and in bilateral CHL most patients only use a single device. This is of interest, as stimulation by BCDs in unilateral CHL and bilateral stimulation in bilateral CHL should provide access to binaural cues, which patients are bereft of in the unilateral hearing condition. Studies of simulated CHL in normal hearing listeners demonstrated no improvement in localization performance when unilaterally plugged and aided, and that the unilateral

aided condition significantly impaired performance for bilaterally plugged listeners. These findings may not directly translate to impaired listeners who have adapted over time to both their hearing condition and listening with the BCD. Here we study these effects in hearing impaired listeners using both passive and direct drive stimulation with a BCD implant. The current study aims to quantify the binaural hearing benefits of CHL patients with BCD implants using measures of speech perception in noise and localization as behavioral markers binaural hearing.

Speech perception, head-shadow, binaural summation, and localization performance of individuals with CHL was evaluated in direct drive and passive BCD listening conditions. Speech perception was assessed using an adaptive listening in noise test and all test stimuli were presented in a sound attenuated room. Localization stimuli consisted of broadband, high-pass, and low-pass noise bursts, 150-ms in duration at 55 dB SPL and roved +/- 10dB. Localization stimuli were presented at random in azimuth. Preliminary results suggest a primary benefit of audibility for soft inputs and in the head-shadow condition. Mean absolute error (MAE) deviates significantly from normal hearing for both passive and direct drive BCD stimulation. MAE For unilateral CHL demonstrated a relatively low degree of error in the aided condition, although this does not significantly deviation from unaided or between the passive and direct drive aided conditions. Localization performance is improved in the bilateral BCD listening condition. The largest errors are observed when bilateral CHL participants are unilaterally aided, with significant bias towards the aided side.

PS 345

Horizontal Sound Localization of Bonebridge Implant in Patients with Single-Sided Deafness

Chunli Zhao; Jinsong Yang; Yujie Liu; Shouqin Zhao
Department of Otolaryngology Head and Neck Surgery, Beijing Tongren Hospital, Capital Medical University

Bonebridge® (BB, Med-EL, Innsbruck, Austria), a semi-implantable transcutaneous device, was a bone conduction hearing aid for patients with Single-sided deafness(SSD). The purpose of present study was to evaluate the sound source localization performance of BB implanted in SSD patients. It contained four patients with BB used of different durations (range 7-12 months). The average age of all subjects was 23 years (rang 13-50yr). Localization ability was measured using seven loudspeakers presented in a sound-proof room. The broadband (BB, 0.5-20 kHz) filtered noise of 150ms duration was given at different sound levels (65,70,75 dB SPL). Subjects were asked to face the middle loudspeaker in an arc from -90° to +90° azimuth (30°interval) in horizontal plane. To evaluate the performance of sound localization, we quantified the mean absolute error (MAE) in degrees under two conditions (BB-off and BB-on). Compared with the results in BB unaided condition, the performance of sound localization was no significant improvement at 6-month follow-up period in BB aided condition($P > 0.05$). Sound localization ability at three sound levels was highly variable in each subject. The improvement of MAE among individual subjects was increased at large sound level. However, the level of MAE in BB-on condition was similar to that measured in BB-off condition($P > 0.05$). Our results suggest localization performance listening with BB was neither improved nor deteriorated compared to listening without BB. The processing of binaural cues may be not provided by this BB device in the short term.

PS 346

Sound Localization in Patients with a Unilateral Hearing Aid: Discordance Between Right and Left Ear

Hun Yi Park[1]; Hantai Kim[2]
[1]Dept. of Otolaryngology, Ajou University School of Medicine; [2]Department of Otolaryngology, Ajou University School of Medicine

Introduction
Function of sound direction is determined by several factors, including the time of arrival of the sound, its intensity, and the shape of the spectrum. Patients with unilateral hearing loss have difficulty in recognizing the direction of sound. Previous studies have shown that the use of hearing aids in hearing loss can improve directional perception of sound. In this study, we analyzed the results of the sound localization test in patients using a unilateral hearing aid.

Materials and methods
All patients with unilateral hearing loss who had performed sound localization tests since 2018 were included in this study. All patients underwent sound localization tests, functional gain test with a hearing aid, and speech audiometry. The tests were followed up for 6 months after the use of HA.

Results
Of the 48 patients, right hearing loss was 20 and left hearing loss was 28. Before wearing the hearing aid, there were no significant differences in the aided speech dicrimination score (SDS) and sound localization tests according to the left and right ears. In the test performed 6 months after wearing the hearing aid, the patients with right hearing loss scored significantly higher in sound localization test.

Conclusion
After use of hearing aids, aided SDS results seemed to improve on both sides. However, the side of hearing loss could make a substantial effect on sound localization in unilateral hearing loss patients with a hearing aid. Therefore, it is necessary to pay attention to the interpretation of the sound localization test results in unilateral hearing loss patients.

PS 347

Cochlear Implant for Congenitally Deaf Children with Single-sided Deafness

Susan Arndt; Hassepass Frederike; Antje Aschendorff; Thomas Wesarg; Iva Speck; Rainer Beck
Department of Otorhinolaryngology - Head and Neck Surgery, Medical Center - University of Freiburg, Faculty of Medicine, University of Freiburg, Germany

Introduction
Cochlear implantation in unilateral deafness and asymmetrical hearing loss has become increasingly important as an established therapeutic option in adults. However, the recommendation of cochlear implantation in children with congenital single-sided deafness (SSD) has been still discussed controversially since the first implantations. The aim of this investigation is to determine the optimal time interval for cochlear implantation of children who are congenitally deaf on one side.

Methods
Out of 58 unilaterally deaf children who presented themselves for cochlear implant (CI) pre-operative evaluation, 11 children were supplied with a CI. The age of the children was between 1.8 and 13.8 years at the time of implantation. Depending on the level of development, age-adapted speech tests were performed pre-operatively, one year as well as in median 35 months after implantation. The subjective assessment of hearing with and without CI was obtained with the adapted version of the speech, spatial, and quality scale (SSQ) for children and adults. Furthermore, the pattern of speech processor use was examined.

Results
The post-implantation test results of children with congenital SSD showed a large variance depending on the age of implantation and the ability to fulfill the tests. The 12-month- and long term data was available from 11 children. We found clear indications that children implanted up to an age of four years showed more favorable outcome. With higher age, the risk of non-usage of the CI increased and the test results showed a higher variability due to insufficient or diminished hearing with the implant. The subjective results of the SSQ questionnaire reflected the determined objective results.

Conclusions
Children with a shorter duration of SSD, implanted under the age of 3 years tend to evolve higher benefit with the CI than children with a longer duration of deafness (implanted over the age of 5 years). This should be considered when counseling parents and patients on possible treatment options for congenital unilateral deafness.

PS 348

Objective and Subjective Long-term CI Usage Evaluation of Patients with Single-sided Deafness and Asymmetric Hearing Loss

Susan Arndt; Pascal Challier; Hassepass Frederike; Ann-Kathrin Rauch; Thomas Wesarg; Iva Speck
Department of Otorhinolaryngology - Head and Neck Surgery, Medical Center - University of Freiburg, Faculty of Medicine, University of Freiburg, Germany

Introduction
For the first time, we were able to examine a large number of cochlear implant (CI) recipients with AHL and SSD (n=78) in a long-term setting. Long-term users were defined as patients with more than three years after initial CI fitting. The usage (user vs. non-user), wearing behavior as well as the subjective benefit of the CI and auditory hearing rehabilitation were investigated.

Methods
Validated questionnaires were used to determine the daily wearing behavior (IIEH), the subjective benefit with the CI (SSQ), the subjective quality of life (HUI Mark 2/3), and subjective evaluation of tinnitus (visual scale). In addition, speech recognition in noise and localization ability were determined. The results of the above mentioned examinations and questionnaires were collected, evaluated and compared at different points in time (pre-operative examination, 12 months and > three years after implantation). Additionally, the objective usage time was detected using data logs from SCAN, an automated auditory scene classifier, which categorizes auditory input into six listening environments.

Results
More than 85% of the included 78 CI recipients with SSD and AHL wore their CI for a daily average of six to 10 hours. The objective results of the data logging supported the reported usage time (7.73h/d). Four SSD CI recipients were non-users One AHL patient deceased during evaluation period. For nine percent of the patients the wearing behavior is unknown. Daily wearing behavior for CI users was stable throughout the period surveyed. In addition, there was a significant positive correlation between the results in the subsections speech intelligibility, the quality of speech in the SSQ, and the wearing behavior in the IIEH. In the course of CI use, there was a significant improvement in subjective speech intelligibility and spatial resolution in the SSQ. Furthermore, speech recognition in noise (SssdNnh) and localization improved after 12 months and long-term usage compared to the pre-operative examination results, respectively.

Conclusions
The aim of the present study was to investigate the long-term benefits of cochlea implants (CI) in single-sided deaf (SSD) and asymmetric hearing impaired (AHL) patients. The majority of participants have been wearing their CI regularly over three years after implantation. In addition, the presented long-term study proves that SSD and AHL patients benefit from their CI in subjective speech intelligibility and spatial resolution as well as speech recognition in noise and localization consistently for more than three years.

PS 349

Lateralization of Competing Interaural Envelope Cues Measured with the CCi-Mobile Research Platform

Stephen R. Dennison[1]; Alan Kan[2]; Tanvi Thakkar[3]; Ruth Y. Litovsky[4]
[1]Waisman Center, University of Wisconsin-Madison; [2]School of Engineering, Macquarie University; [3]University of Wisconsin-Madison; [4]The University of Wisconsin–Madison

Listeners with bilateral cochlear implants (BiCI) experience greater spatial hearing benefits compared to unilateral listeners but are unable to perform as well as normal-hearing (NH) listeners. NH listeners rely on binaural cues, namely interaural time differences (ITDs) and interaural level differences (ILDs), to localize accurately. Cochlear implant processing discards the fine-timing cues that NH listeners use for good sound localization but retains the slow-varying envelope modulations that have the potential to convey ITD (ENV-ITD) cues to BiCI listeners. Previous work in our lab has found that BiCI listeners are able to lateralize ENV-ITDs when an acoustic transposed-tone stimulus is presented through clinical processors. However, ILDs are also available for spatial hearing. To date, the role of each cue has been studied in isolation, and the extent to which ENV-ITDs contribute to localization performance in the presence of ILDs is unknown.

This study investigated the impact of co-varied and competing ENV-ITDs and ILDs in order to determine the relative influence each cue has on perceived lateralization of an auditory percept. BiCI listeners completed a

lateralization task with stimuli containing "complementary" and "competing" cues. The stimulus was a single-electrode pulse train with raised-cosine on-ramps. Electrode pairs and modulation rates were selected for each subject to maximize sensitivity to ENV-ITDs. Stimuli were imposed with complementary interaural cues generated from an 8-cm radius spherical head model. Competing cue pairs were created by applying a shift to the complementary interaural cues in either the ENV-ITD or ILD domain. Stimuli were delivered using the CCi-Mobile research platform developed at the University of Texas at Dallas, which allows for synchronized delivery of envelope cues across the two implants. The acoustic stimuli are processed by the Advanced Combination Encoder (ACE) strategy before presentation.

Cue weights were estimated for ENV-ITDs and ILDs to determine each cue's contribution to overall perceived lateralization. Preliminary data suggests that ENV-ITD cues received a small weighting, while ILD cues received a large weighting. These results are consistent with findings from previous free-field studies suggesting that BiCI listeners mainly use ILDs for localization.

This work was supported by NIH-NIDCD R01DC016839 and NIH-NIDCD R01DC03083 to RYL, NIH-NIDCD R03DC015321 to AK, and NIH-NICHD U54HD090256 to the Waisman Center.

PS 350

Aiding the Fitting of Bilateral Cochlear Implants Using a Tool for Loudness Balancing

Marina Salorio-Corbetto[1]; Deborah Vickers[1]; Lorenzo Picinali[2]
[1]University of Cambridge; [2]Imperial College London

Spatial listening performance with bilateral cochlear implants may be limited by surgical, technical, and pathological factors (Kan and Litovsky, 2015), but also due to lack of optimisation of bilateral fittings. This may contribute to poor communication in everyday environments, which negatively impact on the speech and language development, education, and social wellbeing of bilateral cochlear implantees. Loudness balance across ears, although not the only factor underlying the deficits in spatial listening (Fitzgerald et al., 2015; Kan and Litovsky, 2015), is optimised in the fitting process. An app was created to assist audiologists in achieving this aim. In a first stage of development, ten normal-hearing participants were presented with sounds via headphones. Participants controlled the sound level balance across ears using a wheel so that the sound was perceived in a central position. The feasibility of the task, the occurrence of learning or fatigue effects, and the outcomes expected for normal-hearing listeners were determined. The task was feasible and the average RMS error across sounds was small (2.51 dB across participants). Occasionally spurious results occurred due to procedural interface-related aspects. There were no effects of level, type of sound, or number of run, although there was a trend for the RMS errors to be higher for the first and the last runs (run 10), and just before the break (run 5). Reliable outcomes can be obtained by averaging two runs after allowing a practice run. The critical difference between runs 2 and 3 was 6.55 dB on average across sounds, and can inform any decisions about discarding/repeating runs. Changes to the app were made in order to avoid spurious readings. The second stage of the study is currently under development. In this phase, ten additional normal-hearing participants will perform the task in conditions of simulated asymmetric hearing in order to determine the sensitivity of the app. The frequency bands at which attenuation will be applied and the level of such attenuation will be systematically varied. Once optimised for use, the App will be trialled with bilateral cochlear-implant users and outcomes of a spatial speech-in-noise test will be compared before and after using the App for loudness balancing.

Acknowledgments
Marina Salorio-Corbetto is funded by Imperial Confidence in Concept (ICiC). Deborah Vickers and Marina Salorio-Corbetto are funded by the Medical Research Council (MRC) UK, Grant code MR/S002537/1.

References

Fitzgerald MB, Kan A, Goupell MJ (2015) Bilateral Loudness Balancing and Distorted Spatial Perception in Recipients of Bilateral Cochlear Implants. Ear Hear 36:e225-e236.

Kan A, Litovsky RY (2015) Binaural hearing with electrical stimulation. Hear Res 322:127-137.

PS 351

Robust Spatial Unmasking of Speech in Children with Bilateral Cochlear Implants by Harnessing Interaural Time and Level Cues with Large Angular Separation between Target and Maskers

Z. Ellen Peng[1]; Ruth Y. Litovsky[2]
[1]Waisman Center, UW-Madison; [2]The University of Wisconsin–Madison

The ability to use auditory spatial cues to segregate speech from noise is crucial for effective communication; past studies typically found worse performance in children with bilateral cochlear implants (BiCIs) than normal hearing (NH) children. Various factors potentially contribute to the limitation, including lack of access to binaural cues when

stimuli are delivered in free-field. This study focused on understanding the contribution of different auditory cues to spatial unmasking in children with BiCIs.

Spatial unmasking is the ability to gain speech intelligibility benefits from target-masker spatial separation (e.g., spatial release from masking, SRM) and from listening with two ears (e.g., binaural summation and squelch). We implemented new approaches to overcome two potential limitations in previous paradigms. First, prior work may have underestimated SRM by limiting target-masker segregation to 90°. Second, when sounds were presented in free-field, all auditory cues co-occurred and their relative contributions to spatial unmasking cannot be parsed. Thus, we implemented a virtual auditory space (VAS) paradigm for teasing apart the contributions of head shadow, binaural summation and interaural differences (i.e., interaural time and level differences). VAS was created using individual head-related transfer functions measured behind the ears of each child, convolved with speech materials, and played back to the audio input ports of the speech processors during testing. Target speech consisted of short sentences, while maskers consisted of two continuous, unrelated stories. SRTs were measured in 4 conditions: 2 *spatial configurations* (target-masker co-located vs. separated by 180°) X 2 *ear conditions* (unilateral vs. bilateral). The new spatial configurations were as follows: Targets were located at virtual location of 90° on the side of the better ear. Maskers were located at either the same location as the target or at 90° on the side of the opposite ear. Intelligibility benefit for head shadow, binaural summation, interaural differences, SRM, and binaural squelch was computed by comparing SRTs across the four test conditions.

Novel results show that, with the larger target-masker separation of 180°, children with BiCIs showed a benefit between -2 and 6 dB (half showed > 1 dB) when only interaural difference cues were available. While head shadow provided an intelligibility benefit between 3-8 dB, binaural summation had very small magnitudes from -1 to 3 dB. All children showed larger than typical SRM between 4-9 dB and binaural squelch between 0-7 dB. Together, children with BiCI received intelligibility benefit through spatial unmasking between 6-10 dB.

Work supported by NIH-NIDCD (R01DC003083 & R01DC008365 to RL) and in part by NIH-NICHD (U54HD090256) to the Waisman Center.

PS 352

Onset Weighting of Temporal Spatial Cues with Cochlear Implant Stimulation in Early Onset Deafness

Alexa Buck[1]; Nicole Rosskothen-Kuhl[2]; Lakshay Khurana[3]; Stella Mayer[3]; Kongyan Li[1]; Jan W. Schnupp[4]
[1]Department of Biomedical Sciences, City University of Hong Kong, Hong Kong (SAR China); [2]Neurobiological Research Laboratory, Section for Clinical and Experimental Otology, University Medical Center Freiburg, Freiburg, Germany; [3]University Medical Center Freiburg; [4]City University of Hong Kong

Cochlear implants (CIs) are undeniably useful, but the perceptual performance they permit in complex, real-life environments still falls short. One particular shortcoming is the inability to provide CI users with adequate temporal spatial cues, interaural time differences (ITDs). Early deaf users of current CIs are entirely insensitive to ITD cues over the physiological range. However, we have previously shown that neonatally deafened (ND) rats are capable of discriminating ITDs as small as 50 µs, no worse than normal hearing (NH) rats (Rosskothen-Kuhl et al., 2019). Better ITD sensitivity may therefore be achievable with better devices, and rats may be a great model to develop improved technology. We therefore determined whether rats show similar onset weighting for ITDs as humans (Brown and Stecker 2010), and whether that onset weighting is similar in NH and ND CI animals.

ND-CI rats were prepared by neonatal injection of kanamycin, followed by bilateral implantation as young adults. Age matched NH litter mates were also tested. Animals learned a two-alternative forced choice task to lateralize pulse trains consisting of eight binaural pulses (for ND rats: biphasic electric stimuli delivered via CIs; for NH rats: acoustic clicks delivered over tube phones). ITD values for individual pulses varied independently and uniformly across the rat's physiological range (+/-130 µs). Pulse rates were 50, 300 or 900 Hz. Two types of trials were presented for each session: Honesty trials comprised either all left- or all right-ear leading pulses, while for probe trials pulse ITDs were unconstrained. Temporal Weighting Functions (TWFs) were calculated using multiple regression analysis to determine the perceptual weight of each pulse in the train in shaping the behavioral response to probe trials.

NH animals showed TWFs across all frequencies that were comparable with the TWFs of human listeners. At lower pulse rates (≤300 Hz), CI rats also showed TWFs with strong onset responses. However, this up-weighting was not as pronounced as in NH listeners, and was lost for higher stimulation rates (900 Hz).

Rat TWFs are fundamentally very similar to those found in humans, illustrating the suitability of rats as a model for human binaural hearing. The pulse rate dependence of onset ITD processing we observed in CI rats may also help explain the poor ITD perception of early deafened CI users, given that current clinical CI processors are running at ≥900 pps.

PS 353

Spatial Hearing with Two CIs: Pulse Rate and Envelope Shape Affect Interaural Time Difference Sensitivity of Hearing Inexperienced Rats

Nicole Rosskothen-Kuhl[1]; Alexa N. Buck[2]; Stella Mayer[1]; Lakshay Khurana[1]; Jan W. Schnupp[2]
[1]University Medical Center Freiburg; [2]City University of Hong Kong

To date, sound localization is one of the major challenges for bilateral cochlear implant (CI) users. Their ability to use binaural cues, especially interaural time differences (ITDs), falls far below that of their normal hearing peers. While it is widely suspected that the issue lies in the lack of sensory input during early development, our recent study on neonatally deafened, CI implanted rats has shown that, at least at low pulse rates (pps), very good ITD sensitivity can be developed even in the absence of early sensory input if the bilateral CIs are synchronized. Here, as a follow up to our prior study, we investigate how pulse rates and envelope shapes affect ITD sensitivity of early deafened CI users.

Rats were deafened neonatally by kanamycin injection. Profound hearing loss was confirmed by measuring auditory brainstem responses while presenting click stimuli. In young adulthood (~p60), CI electrodes were chronically implanted bilaterally. Sensitivity to onset and ongoing ITD of binaural, biphasic pulse trains at pulse rates of 50, 300, 900, and 1800 pps was studied by training CI rats on a two-alternative forced choice lateralization task.

All neonatally deafened CI rats showed sensitivity to the ITD of the CI pulse trains with thresholds of ~50 microseconds or better after a few days of training. For rectangular envelope pulse trains, good ITD sensitivity was observed from 50 to 900 pps, followed by a significant drop in performance at 1800 pps. For Hanning envelope pulse trains, CI rats were still able to discriminate sub-millisecond ITDs at lower rates of 50 and 300 pps but had a significant fall in performance for 900 and 1800 pps. Overall, ITD sensitivity tended to be slightly better for stimuli with sharper onsets, but this only reached significance at 300 pps.

In conclusion, clinical stimulation rates of 900 pps should not prevent the development of ITD discrimination, but the highest ITD sensitivity was found at lower pulse rates. Furthermore, CI pulse trains with gentle rising slopes can provide usable ITD information for low pulse rates but stronger onset cues are required to perceive microsecond ITDs presented at clinically relevant pulse rates.

PS 354

Impact of Synchronized Automatic Gain Controls on Perception of Stereo Spatialization in Bilateral Cochlear Implant Users

Stephanie B. Purnell[1]; Charles J. Limb[2]; Patpong Jiradejvong[2]; Karen C. Barrett[1]
[1]University of California, San Francisco; [2]Dept of Otolaryngology-Head and Neck Surgery, University of California, San Francisco

Complex sound processing, such as music perception, auditory stream segregation, and spatial localization remain difficult for cochlear implant (CI) users. In an effort to improve the listening experience and capabilities of CI users, bilateral implantation has become an increasingly common practice. However, the exact degree of restoration of advantage conferred by bilateral implantation remains unclear, especially relative to spatial sound localization (Litovsky et al, 2006). Currently processors utilize Automatic Gain Controls (AGC) which deliver a degree of gain relative to incoming sound sources and levels. However, current AGC designs typically work independently even when there are two devices, potentially delivering non-uniform gain (i.e. uncoordinated between the two ears) and degrading binaural cues important for sound source localization.

The present study investigates the impact of a synchronized AGC platform on perception of stereo spatialization in CI users. Stereophonic sounds and musical excerpts with a broad range of stereo spatialization were manipulated in three ways in order to increase or decrease stereo spatialization: (1) Experimental Interaural Time Differences were created by delaying left- or right-channel onsets of the stimulus by a range of 50-250ms. (2) Experimental Interaural Level Differences were created by manipulating the gain of left- or right-channels by a range of 5-10dB. (3) Degree of Stereo Separation was manipulated by narrowing the width of the stereo soundfield in varying degrees ranging from 100% stereo to 0% stereo (monophonic). These manipulated stimuli were then tested for their impact on sound quality using several novel adaptations of the CI-MUSHRA, an assessment allowing CI users to rate sound quality of presented stimuli in comparison to an unaltered reference stimulus (Roy et al, 2012). The poster presentation

will discuss the methodology used to manipulate musical samples and share results of CI-MUSHRA pilot testing in normal hearing adults. Preliminary pilot data suggests higher ratings for unaltered reference stimuli in comparison to stimuli that are highly degraded along parameters of stereo separation, interaural timing differences, and interaural level differences, suggesting that these manipulations do impact perceived sound quality. Followup studies in bilateral CI users using synchronized AGCs are currently underway. This strategy may represent an important advancement for the ability of bilateral CI users to perceive stereo sound, with potential subsequent benefits of binaural hearing.

References

Roy A. T., Jiradejvong P., Carver C., Limb C. J. (2012). Assessment of sound quality perception in cochlear implant users during music listening. Otology & Neurotology, 33(3), 319-327

Litovsky, R., Parkinson, A., Arcaroli, J., & Sammeth, C. (2006). Simultaneous bilateral cochlear implantation in adults: a multicenter clinical study. *Ear and hearing*, *27*(6), 714–731. doi:10.1097/01.aud.0000246816.50820.42

PS 355

Binaural Hearing Benefits in Aging Bilateral Cochlear Implant Recipients

Sandra Prentiss[1]; Hillary Snapp[2]
[1]Sandra Prentiss, PhD; [2]University of Miami, Miller School of Medicine

Normal hearing listeners rely on interaural timing and level cues for spatial hearing and processing of sound in complex listening environments. Bilateral cochlear implantation (CI) provides auditory input to each ear; however, in order to process interaural cues, the brain must integrate the signals arriving at each ear, which are highly degraded in CI stimulation. Improvements in speech perception in noise and localization have been shown in bilateral implantation[1,2]; however, performance in bilateral CI recipients does not reach that of their normal hearing peers. This is further complicated in the aging population, with poorer overall outcomes[3,4]. It is unclear if the ability to integrate the signals required for binaural processing of complex auditory stimuli can be realized in the aging brain.

Post lingually deafened adults with sequential bilateral cochlear implants were enrolled for study. Behavioral measures of binaural hearing included adaptive speech perception in noise and at a fixed SNR of +5 dB. Localization abilities were assessed in azimuth using a 189-ms broadband stimuli band-passed 100-8000 Hz and narrowband stimuli centered at 4000 and 500 Hz. Testing was performed in the “best-ear”, as determined by monosyllabic word scores, and in the bilateral hearing CI aided condition. A subjective questionnaire was administered to determine benefit of the second implant.

A significant, negative correlation between age and speech performance in noise was observed. Further, the benefit of the second implant on behavioral measures were significantly poorer in the older population than the younger population. Localization accuracy was poorer in the older population compared to the younger cohort

While significant gains in speech perception are observed in postlingually deafened adults who receive bilateral implants, performance variability increases as a function of age and overall performance is poorer in the aging adult.

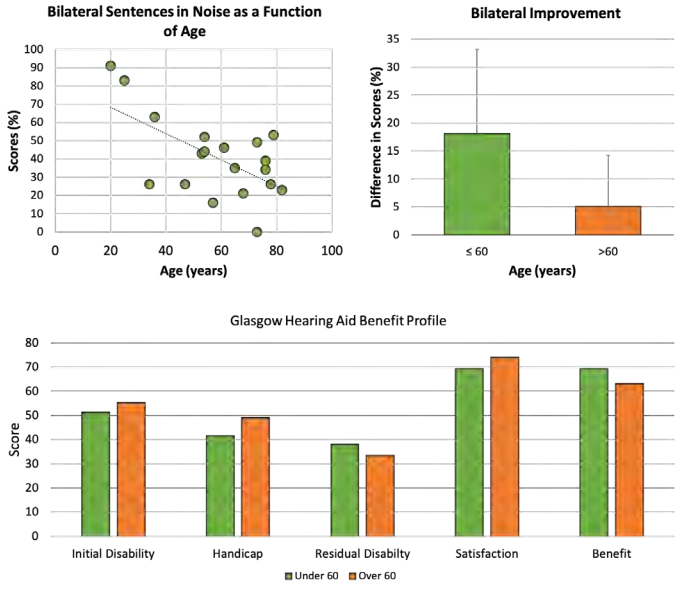

Clinical Vestibular Disorders

PS 356

Human Schwann Cells are Less Susceptible to Radiation Injury than Merlin-Deficient Schwann Cells through Expression of RAD51 DNA Repair

Stefanie Peña[1]; Erin Cohen[2]; Stefania Goncalves[1]; Olena Bracho[1]; Brian Marples[3]; Nagy Elsayyad[3]; Michael Ivan[1]; Paul Monje[4]; Cristina Fernandez-Valle[5]; Fred Telischi[1]; Xuezhong Liu[1]; Christine Dinh[1]
[1]University of Miami; [2]University of Miami Dept. of Otolaryngology; [3]University of Miami Dept. of Radiation Oncology; [4]University of Indianapolis Dept. of Neurological Surgery,; [5]University of Central Florida

Background

Vestibular schwannomas are Schwann cell-derived intracranial tumors that arise from the cochleovestibular

nerve. Vestibular schwannomas develop from NF2 mutations leading to merlin dysfunction and/or loss. Although tumor control rates with stereotactic radiosurgery are ~85% at 10 years, hearing preservation rates approach a dismal 25%. Understanding the radiobiology of normal Schwann cells and merlin-deficient Schwann cells is the first step toward optimizing radiation protocols and identifying novel therapies to improve tumor control and hearing preservation rates.

Methods
Human primary Schwann and merlin-deficient Schwann cells were exposed to either 0 or 12 Gray (Gy) of radiation. A cell-based viability assay was performed at 96 hours to determine effects of radiation on cell lines. Western blot was performed for gamma-H2AX (marker of double-stranded DNA breaks) and RAD51 (DNA repair enzyme) expression at 60 minutes post-irradiation, and expression levels were quantified using ImageJ software. In addition, immunofluorescence was performed for both proteins post-irradiation, representative images were taken using a confocal microscope, and the number of cells with positive nuclear staining were measured. Statistical analysis was performed with Wilcoxon rank sum test.

Results
Merlin-deficient Schwann cells demonstrated significantly lower levels of viability after 12 Gy irradiation compared to normal Schwann cells. There was also differential expression of gamma-H2AX and RAD51 proteins on western blot and immunofluorescence imaging between both cell lines, supporting findings demonstrated on viability assays.

Conclusion
Normal Schwann cells exposed to 12 Gy of radiation are more resistant to radiation injury than merlin-deficient Schwann cells, in part through differential expression of double strand DNA breaks and DNA repair mechanisms. Further research is warranted using different dosages of single fraction radiation, appropriate hypofractionated protocols, as well as a primary human vestibular schwannoma cells. Understanding the radiobiology of vestibular schwannomas and normal Schwann cells is imperative in improving radiation protocols and determining novel therapies to maximize tumor control while preserving hearing.

PS 357

Vibration-induced nystagmus in patients with vestibular schwannoma: Characteristics and clinical implications

Jeon Mi Lee[1]; Hyun Jin Lee[2]; Sung Huhn Kim[3]
[1]Department of Otorhinolaryngology, Ilsan Paik Hospital, Inje University College of Medicine, Goyang, Korea; [2]Department of Otorhinolaryngology, Incheon St. Mary's Hospital, College of Medicine, The Catholic University of Korea, Seoul; [3]Department of Otorhinolaryngology, Yonsei University College of Medicine, Seoul, Korea

Objective
To investigate the clinical significance of vibration-induced nystagmus (VIN) in unilateral vestibular asymmetry and vestibular schwannoma.

Methods
Thirteen patients with vestibular schwannoma underwent the VIN test, in which stimulation was applied to the mastoid processes and sternocleidomastoid (SCM) muscles on the ipsilateral and contralateral sides of lesions. Preoperative VIN was measured, and changes in VIN were followed up for 6 months after tumor removal. Significance of VIN was determined by evaluation of its sensitivity, correlation with vestibular function tests and tumor volume, and postoperative changes.

Results
The overall pre and postoperative sensitivities of VIN were 92.3% and 100%, respectively, considering stimulation at all four sites. Maximum slow-phase velocity (MSPV) of VIN was linearly correlated with caloric weakness and tumor volume, especially when stimulation was applied to the SCM muscle. Postoperative MSPV of VIN exhibited stronger linear correlation with postoperative changes in canal paresis value and inverse correlation with tumor size upon stimulation of the ipsilateral SCM muscle than upon stimulation of other sites. During the 6-month follow-up period, persistence of VIN without changes in MSPV was observed even after vestibular compensation.

Conclusions
Evoking VIN by stimulation of the mastoid processes and SCM muscles is effective for detecting vestibular asymmetry. It could also help determine the degree of vestibular asymmetry and volume of vestibular schwannoma if stimulation is applied to the SCM muscle.

PS 358

Identification of A Genetic Mutation Underlying Familial Cases of Recurrent Benign Paroxysmal Positional Vertigo

Yinfang Xu[1]; Yan Zhang[2]; Ivan Lopez[3]; Shelley Smith[4]; Akira Ishiyama[5]; Xuezhong Liu[6]; **Yesha (Yunxia) Lundberg**[1]
[1]Boys Town National Research Hospital; [2]Creighton University; [3]University of California Los Angeles; [4]University of Nebraska Medical Center; [5]Deparment

of Head and Neck Surgery, David Geffen School of Medicine; [6]University of Miami

Benign paroxysmal positional vertigo (BPPV) is the most common cause of vertigo in humans, yet the molecular etiology is completely unknown. Evidence suggests that genetic factors may play an important role in some cases of BPPV, particularly in familial cases, but the responsible gene variations/mutations have not been identified. In this study, we performed whole exome sequencing (including UTR regions) of 12 families and Sanger sequencing of additional 29 families with recurrent BPPV in non-Hispanic whites from the US Midwest region, to identify the genetic variations/mutations responsible for heightened susceptibility to BPPV. *In silico* and experimental analyses of candidate variants ranked an insertion mutation rs113784532 (frameshift causing truncation) in the neural cadherin gene *PCDHGA10* (protocadherin-gamma 10) as an exceedingly strong candidate ($p=1.1x10^{-4}$ vs. sample controls; $p=1.5x10^{-100}$ vs. ExAC data). In mouse inner ear tissues, the expression of *Pcdhga10* is only in the ganglia and increases with age. The protein forms aggregates in the vestibular ganglia of BPPV patients, which worsens with age. In summary, the data show that mutation in the *PCDHGA10* gene may cause some familial cases of recurrent BPPV, and suggest that the most significant mutation may lead to vestibular ganglia deficits or degeneration, which is a novel finding in BPPV etiology.

PS 359

Improvement in Postural Control and Quality of Life after Stapedotomy

Andrea Viziano[1]; Alessandro Micarelli[2]; Marco Alessandrini[3]
[1]Department of Clinical Sciences and Translational Medicine, 'Tor Vergata' University, Rome, Italy; [2](1) Department of Clinical Sciences and Translational Medicine, 'Tor Vergata' University, Rome, Italy (2) ITER Center for Balance and Rehabilitation Research (ICBRR); Rome, Italy; [3]Department of Clinical Sciences and Translational Medicine, Otolaryngology, 'Tor Vergata' University, Rome, Italy

Vestibular symptoms may occur in patients with otosclerosis, both before and after surgery, as up to 30% of cases are accompanied by complaints such as dizziness or recurrent attacks of vertigo. Previous studies aimed at delineating the extent of vestibular peripheral impairment in otosclerosis focused on functional tests such as vestibular-evoked myogenic potentials and caloric testing; results showed various degrees of abnormalities, but did not explore the relationship between objective findings and balance-related quality of life aspects reported by the patients. Static posturography – especially when implemented with power spectra analysis - has been described as an useful method of assessing the impact of different sensory domains on postural dysfunction; to our knowledge, an evaluation of postural sway coupled with its impact on daily functioning has never been performed in patients with otosclerosis.

In our study, otoneurological function and balance-related quality of life, before and six weeks after surgical treatment, were assessed in thirty-tree patients affected by otosclerosis. Subjects underwent a thorough clinical examination, Video Head Impulse Testing (vHIT), and static posturography. Quality of life and dizziness-related handicap were screened by means of validated questionnaires such as Dizziness Handicap Inventory (DHI), Activities-Specific Balance Confidence scale (ABC) and Dynamic Gait Index (DGI). Correlation analysis was performed in order to discover possible relations with audiological pre- and post-operative parameters.

Results showed significant post-operative improvement in posturographic scores, with respect to classical parameters such as surface and length, and spectral oscillations in the low-frequency range. It is noteworthy that only low-frequency power spectra values reported significant modifications after surgery, as these oscillations are mainly under vestibular control, strengthening the hypothesis of neural streams involving vestibular signaling being responsible of the improvement in balance observed in this study. Moreover, a negative correlation between pre-operative bone conduction auditory threshold and both vHIT scores and postural performance improvement was found. Such correlations with pre-operative auditory levels may reflect lesser chance for balance restoration in cases with worse sensorineural function. Finally, a positive correlation was also found between improvements in posturographic parameters and changes in quality of life questionnaire scores (ΔABC).

Taken together, our results confirm the usefulness of posturography as a monitoring tool for postural function, due to consistent and reliable correlations with other objective measures, and suggest possible implications for overall quality of life in light of improved self-report questionnaire results after surgery.

PS 360

Noisy Galvanic Vestibular Stimulation Has a Greater Ameliorating Effect on Postural Stability in Unstable Subjects.

Chisato Fujimoto; Makoto Kinoshita; Teru Kamogashira; Tatsuya Yamasoba; Shinichi Iwasaki

Department of Otolaryngology and Head and Neck Surgery, Graduate School of Medicine, The University of Tokyo

Objective
Ameliorating effect of noisy galvanic vestibular stimulation (nGVS) on postural stability varies among subjects. We investigated the association between original postural instability and the ameliorating effect of nGVS on postural stability.

Methods
Thirty healthy elderly subjects were recruited. Two nGVS sessions (30 min or 3 h) were performed in a randomized order. The optimal intensity of nGVS, the most effective intensity for improving posture, was determined before each session. Postural stability was measured for 30 s during and after nGVS in the eyes-closed/foam rubber condition.

Results
The velocity, envelopment area, and root mean square of the center of pressure movement without nGVS were significantly larger in the group with an optimal intensity than those in the group without an optimal intensity. There was a significant positive correlation between these values and the long-term ameliorating effects. The eyes-closed foam ratio, the ratio of the values in the eyes-closed/foam rubber condition to those in the eyes-open condition, was significantly larger in the group with an optimal intensity, and had a significant correlation with the long-term ameliorating effects.

Conclusions
The ameliorating effects of nGVS are greater in subjects who were originally unstable and in those whose postural stability was relatively independent of vestibular input.

PS 361

Vestibular Implantation and the Feasibility of Fluoroscopy-guided Electrode Insertion

Raymond Van de Berg[1]; Joost Stultiens[2]; Herman Kingma[3]; AA Postma[4]; Nils Guinand[5]; Angélica Perez-Fornos[6]
[1]Maastricht University Medical Center, Tomsk State University; [2]Resident ENT, MUMC+; [3]Professor of Clinical Vestibulology, Maastricht University Medical Centre+; [4]Radiologist, Maastricht University Medical Centre+; [5]Geneva University Hospital; [6]Department of Clinical Neurosciences, University of Geneva

Background
Recent research has shown promising results for the development of a clinically feasible vestibular implant in the near future. However, correct intralabyrinthine electrode placement remains a challenge. Fluoroscopy can provide real-time visual feedback and thus might guide electrode insertion. Objective: To determine the feasibility of fluoroscopy-guidance to correctly place three vestibular implant electrodes in the semicircular canals. Methods: Six ears of three human heads were sequentially implanted with electrodes in the semicircular canals using real-time fluoroscopic guidance, and underwent CT scanning with and without the electrodes implanted. In the CT scans without implanted electrodes, the centers of the ampullae were determined. In the CT scans with implanted electrodes, the locations of the electrodes were determined. After fusing both CT images (with and without implanted electrodes), distances from the electrode tips to the corresponding centers of the ampullae were calculated. A distance < 1.5mm was considered correct electrode placement. Differences with previous data from “blind” electrode insertion (n=12 electrodes) were calculated. Results: Semicircular canal ampullae could be visualized using fluoroscopy. Median distances from the electrodes to the target were 0.60mm, 0.85mm and 0.65mm for the superior, lateral and posterior semicircular canal, respectively. The mean distances were significantly lower compared to “blind” insertion (P=0.01). Overall, 17 of the 18 electrodes (94%) were implanted correctly. Conclusion: Fluoroscopy can provide the surgeon with direct feedback on the location of the vestibular implant electrodes, and may consequently improve correct electrode placement.

PS 362

Multimodality Electrode Interactions in a Combined Vestibular and Cochlear Implant.

James Phillips; Leo Ling; Amy Nowack; Jay T. Rubinstein
University of Washington

Introduction
A combined vestibular and cochlear prosthesis may restore hearing and vestibular sensation. For this to be optimally realized, parametric stimulation of an electrode site should produce consistent behavioral effects, independent of stimulation from other sites. For example, auditory percepts from cochlear stimulation should be unaffected by vestibular stimulation, and eye movements elicited by vestibular stimulation should be unaffected by cochlear stimulation. In this study, we examined interleaved stimulation of multiple sites of a cochlear/vestibular implant to understand such interactions if they were present.

Methods
3 human subjects with hearing and vestibular loss were

implanted with a combined cochlear and vestibular prosthesis. The devices had 3 semicircular canal arrays and one Hybrid-L cochlear array, which were implanted into a single ear. The devices were mapped to determine the threshold and comfortable sound levels for cochlear stimulation. The pulse rate and pulse current amplitude of stimulation in each canal was parametrically varied to produce slow phase eye movements of varying velocity to map the vestibular arrays. Perceived loudness and pitch were assessed with a Likert scale for each cochlear site. To assess interactions, interleaved stimulation was performed with cochlear and vestibular sites activated in a variety of combinations. Differences in sound percepts, and differences in slow phase eye velocity, between single site and interleaved stimulation were studied.

Results
Stimulation of individual vestibular electrode sites failed to produce sound percepts at even the highest stimulation currents. Stimulation of the individual cochlear sites failed to elicit slow phase eye movements. However, interleaved stimulation of the cochlear and vestibular sites tended to raise the perceived pitch and loudness of a percept elicited by single cochlear site stimulation, and also significantly altered slow phase eye velocities produced by single vestibular site stimulation alone. The interactions were greatest for the basal electrode of the cochlear array and the lateral canal of the vestibular array. The effect was not consistent across subjects.

Conclusions
Interactions exist during interleaved single site pulse stimulation with a combined vestibular and cochlear prosthesis. Such interactions mirror the interactions seen when individual sites of a vestibular implant are activated with interleaved stimulation to produce natural vestibular stimulation in response to off canal axis motion. While these interactions appears suboptimal, it is possible that the central nervous system can correct for any unwanted interactions through adaptation to long term combined stimulation, or that multipolar stimulation strategies or can reduce or eliminate them.

PS 363

Prevalence of Vestibular and Balance Disorders in Asymptomatic Controls and HIV+ Adults

Helen S. Cohen[1]; Michael W. Plankey[2]; Susan P. Willilams[1]; Haleh Sangi-Haghpeykar[1]
[1]Baylor College of Medicine; [2]Georgetown University

Background
The prevalence of vestibular and balance disorders in otherwise asymptomatic adults and adults with HIV disease is unknown. Previous studies of the general population have been mostly surveys. Few studies have tested actual performance. Previous studies of the HIV population have been mostly done with older antiretroviral regimens than are used currently. In the current study we tested balance on standard clinical screening tests and tested vestibular function with clinical objective diagnostic tests.

Methods
Subjects were tested on tandem walking with eyes closed and Romberg on foam with eyes closed and head either still or moving at 0.3 Hz. They were given cervical vestibular evoked myogenic potentials, bi-thermal caloric tests, Dix-Hallpike maneuvers and, where available, low frequency tests of the vestibulo-ocular reflex in darkness in the rotatory chair.

Results
Looking at the non-HIV+ population by decades, the prevalence at ages 20 to 39 is approximately 20%, at ages 40 to 59 is approximately 31%, at ages 60 to 89 approximately 40, but those data should be viewed with caution as the prevalence in the oldest subjects may be different. In the HIV+ group, who were all middle-aged, the prevalence is 15% but 28% in age-matched controls.

Conclusions
The increased prevalences with age are not surprising and are probably due to age-related changes in the vestibular system. The lower prevalence in the HIV+ group is surprising but may be due to a protective effect of anti-retroviral medication.

Supported by NIH grant 2R01-DC009031.

PS 364

Bilateral vestibulopathy, age and walking speed increase drop-out rate when testing Dynamic Visual Acuity during walking

Raymond Van de Berg[1]; Herman Kingma[2]; Floor Lucieer[3]; Marlou Snelders[4]; Dmitrii Starkov[3]; Maksim Pleshkov[5]; Vincent Van Rompaey[6]; Nils Guinand[7]; Angélica Perez-Fornos[8]
[1]Maastricht University Medical Center, Tomsk State University; [2]Professor of Clinical Vestibulology, Maastricht University Medical Centre+; [3]Division of Balance Disorders, Department of Otorhinolaryngology and Head and Neck Surgery, Maastricht University Medical Centre, Maastricht, Netherlands.; [4]1Division of Balance Disorders, Department of Otorhinolaryngology and Head and Neck Surgery, Maastricht University Medical Centre, Maastricht, Netherlands.; [5]Division of Balance Disorders, Department of Otorhinolaryngology

and Head and Neck Surgery, Maastricht University Medical Centre, Maastricht, Netherlands; [6]University of Antwerp, Antwerp University Hospital; [7]Geneva University Hospital; [8]Department of Clinical Neurosciences, University of Geneva

Introduction

It has recently been shown that the vestibular implant can be feasible as a therapeutic option for patients with bilateral vestibulopathy. However, the right outcome measures for vestibular implantation should still be determined. One of these outcome measures might be the dynamic visual acuity (DVA) tested on a treadmill. This test is able to quantify the loss of dynamic visual acuity, as a result of oscillopsia that occurs during walking due to bilateral vestibulopathy. However, next to bilateral vestibulopathy, age might also influence DVA and the possibility to complete the test at all walking speeds. Objective of this study was therefore to investigate whether DVA tested during walking, and drop-out rate (not being able to complete the test) are significantly influenced by age in BV-patients and healthy subjects.

Methods

Forty-seven bilateral vestibulopathy patients (22 male, mean age 59 years, range 21-79 years) and 63 healthy subjects (27 male, mean age 46 years, range 19-83 years) performed the DVA test on a treadmill at 0, 2, 4, 6 km/h. A Sloan optotype chart was used to test visual acuity in both static and dynamic conditions. Drop-out rate and DVA were measured at all walking speeds. The drop-out rate and DVA were compared between bilateral vestibulopathy patients and healthy subjects, walking speeds, and age groups.

Results

Age, bilateral vestibulopathy and walking speed significantly increased drop-out rate up to >75% ($p< 0.012$). A significant higher visual acuity loss at all speeds was found in BV-patients compared to healthy subjects ($p< 0.001$), while age showed no effect. In BV-patients increasing walking speeds resulted in higher visual acuity losses ($p< 0.001$).

Conclusion

Bilateral vestibulopathy, age and walking speed significantly increase drop-out rate when testing Dynamic Visual Acuity during walking. It would therefore be recommended to use age-matched controls at all walking speeds, when testing DVA. However taking the high drop-out rate and the higher age of most bilateral vestibulopathy patients into account, testing DVA on a treadmill might not be the preferred outcome measure for vestibular implantation in the setting of a clinical trial.

PS 365

Understanding Extremely Elevated Dizziness Handicap Inventory Scores: An Analysis of Predictive Factors

Emily C. Wong[1]; Whitney Chiao[2]; Katrina Luong[1]; Lauren Pasquesi[1]; Jeffrey D. Sharon[1]
[1]UCSF; [2]University of Minnesota

Introduction
The Dizziness Handicap Inventory (DHI) is a 25-item assessment that evaluates self-perceived impairment in quality of life due to dizziness on a scale of 0-100, with higher scores indicating greater impairment. Studies have suggested that age, psychiatric history, and sex are associated with higher DHI scores (DHI >60), but these results have been inconsistent. Furthermore, no studies to date have examined associations with extremely elevated DHI scores (eeDHI). In this study, we aimed to identify characteristics associated with eeDHI scores.

Methods
We conducted retrospective chart reviews of 217 patients who were seen by one provider at the UCSF Balance and Falls Center between October 2016–April 2019. Patients were considered to have eeDHI scores if their scores were greater than 1 standard deviation higher than the mean of our sample. Univariate and logistic regression analyses were performed to generate odds ratios (OR) and 95% confidence intervals (CI) for having an eeDHI score based on demographic information, dizziness symptoms and duration, medical and psychiatric history, physical exam findings, audiometric test results, MRI and CT imaging, and vestibular testing results.

Results
The mean DHI score for our study was 45.2 (SD 25.8). The cut-off for eeDHI scores was set at 71. In total, 43 patients in our sample (19.8%) had eeDHI scores. We conducted a multivariate logistic regression model, identifying four independent predictors for eeDHI scores: a history of falls (OR=6.95, 95% CI 2.68–18.05), numbness in the face or body during episodes of dizziness (OR=5.04, 95% CI 1.55–16.46), caloric asymmetry or bilateral weakness on videonystagmography (VNG) (OR=2.53, 95% CI 1.11–5.81), and total number of associated symptoms occurring during episodes of dizziness (OR=1.39, 95% CI 1.19–1.63). The model had a pseudo r squared of 0.27 ($p < 0.0001$). Other metrics, including sex, age, dizziness characteristics and time course, history of migraines, psychiatric history, physical exam findings, audiometric results, imaging, vestibular testing other than VNG caloric testing, and clinical diagnosis were not significantly associated with eeDHI in our model.

Conclusions
eeDHI is associated with a history of falls, numbness in the face or body associated with dizziness episodes, abnormal VNG caloric testing, and increased number of symptoms associated with dizziness. These findings suggest that patient reported symptoms, rather than specific physical exam or imaging findings, are the primary predictors of eeDHI scores. By understanding the drivers of high DHI scores, we may be better able to alleviate disease related suffering for vestibular disorders.

Development I

PS 366

The Notch Ligand Jagged1 is Required for Normal Cochlear Function and Inner Hair Cell Stereocilia Integrity in the Postnatal Organ of Corti

Felicia A. Gilels[1]; Jun Wang[2]; Anwen Bullen[3]; Patricia M. White[1]; Amy E. Kiernan[4]
[1]University of Rochester Medical Center; [2]University of Rochester Medical School; [3]University College London; [4]University of Rochester

The Notch signaling pathway plays various roles that are crucial for proper sensory development in the inner ear. Embryonically, JAG1-Notch signaling is first used to establish the prosensory progenitors that give rise to hair cells and supporting cells. Later, during the process of lateral inhibition, DLL1/JAG2-Notch signaling mediates the decision in the sensory precursors to become either a hair cell or supporting cell. Despite these important early roles, there is a limited understanding of the function of Notch signaling postnatally in the cochlea. Interestingly, the Notch ligand JAG1 is the only Notch ligand reported to be expressed postnatally and into adulthood where it is localized to supporting cells. Here, to understand the role of JAG1-Notch signaling in the postnatal cochlea, JAG1 was conditionally deleted in mice carrying both an inducible Cre allele ($Sox2^{CreER}$) and a floxed (fl) *Jag1* allele ($Jag1^{fl/fl}$) by delivering tamoxifen via intraperitoneal injection at postnatal days (P)0 and P1. To determine the effects of JAG1 removal on cochlear function, we performed measures of auditory brainstem responses (ABR) and distortion product otoacoustic emissions (DPOAE). We found that conditional deletion of *Jag1* in supporting cells ($Sox2^{CreER}Jag1^{fl/fl}$) resulted in significantly elevated ABR thresholds at all frequencies. By contrast, DPOAE thresholds of these mice were relatively normal, indicating auditory neuropathy. Interestingly, morphological analyses including hair cell counts, synaptic analysis and plastic sections failed to reveal any defects that could account for the hearing loss observed in $Sox2^{CreER}Jag1^{fl/fl}$ mice. To further investigate the molecular basis of $Sox2^{CreER}Jag1^{fl/fl}$- induced hearing loss, RNA-seq analysis was performed on control and $Sox2^{CreER}Jag1^{fl/fl}$ cochleae. Pathway

analysis of *Sox2^{CreER}Jag1$^{fl/fl}$* inner ears identified *Diaph3*, a gene previously implicated in auditory neuropathy and hair cell stereocilia integrity, as significantly upregulated. Interestingly, scanning electron microscopy (SEM) of the sensory regions in *Sox2^{CreER}Jag1$^{fl/fl}$* mice revealed similar stereocilia defects as those observed in *Diaph3* gain-of-function mouse models. Our results demonstrate that JAG1 is essential postnatally for normal cochlear function and indicates a novel role for JAG1-Notch signaling in stereocilia integrity.

PS 367

Wnt Signaling Impacts Central Pathfinding of Spiral Ganglion Neurons

Zach A. Stoner[1]; Elizabeth Ketchum[1]; Karen Elliott[2]; Jeremy S. Duncan[1]
[1]Western Michigan University; [2]The University of Iowa

Auditory perception begins in the cochlea where mechanosensory hair cells (HCs) transform sound into electrical impulses. These electrical impulses are relayed to the central nervous system by afferent spiral ganglion neurons (SGNs). During development directed navigation of growing SGN axons to their proper peripheral and central synaptic targets is essential for the generation of a tonotopic sensory map. The molecular mechanisms driving central pathfinding of SGNs to, and within, the cochlear nucleus (CN) are poorly understood. Wnt signaling may be a promising avenue for revealing some of these molecular drivers. Previous work has implicated that central guidance of SGNs as well as segregation of axons within the CN requires wnt signaling components. Several *Frizzled* (*Fzd)* receptors, which bind wnt ligands, are expressed within developing SGNs and may be reacting to a diffusible gradient of wnt ligands released from the hindbrain. Specifically, *Wnt5a,* which is expressed within the CN, may be acting as a molecular cue for SGN central projections. Here we demonstrate that both *Wnt5a* and *Fzd3* are necessary for SGNs to make proper wiring decisions within the cochlear nucleus. Further, we show that *Fzd3* expression within a specific cell type is necessary for these neurons to branch properly within the cochlear nucleus.

PS 368

A Novel Wnt/G-Protein/PI3K Signaling Pathway Regulates Planar Polarity In The Cochlea

Andre Landin Malt[1]; Arielle K. Hogan[2]; Connor D. Smith[2]; Maxwell Madani[2]; Xiaowei Lu[1]
[1]University of Virginia Health System; [2]University of Virginia

During development, sensory hair cells in the cochlea develop a planar polarized apical cytoskeleton, including the V-shaped stereociliary hair bundle with a kinocilium tethered at its vertex. Concurrently, hair cells align their kinocilium and hair bundle along the medial-lateral axis of the cochlear duct. Previous work has demonstrated that tissue-wide alignment of hair cell orientation is mediated by the non-canonical Wnt/Planar Cell Polarity (PCP) pathway, while planar polarization of the hair cell cytoskeleton is regulated by the concerted action of several planar polarized cell-intrinsic PCP signaling modules and microtubule motors. However, the mechanisms by which cell-intrinsic and tissue-level PCP signaling are coordinated and the precise functions of secreted Wnt ligands in this process are poorly understood.

To address these questions, we blocked Wnt secretion by conditional inactivation of *Wntless* (*Wls*) in the embryonic cochlear epithelium. *Wls* encodes a transmembrane protein required for secretion of all Wnt ligands. *Wls* conditional knockout (*Wls^{cKO}*) mutants had a shortened cochlear duct with a reduced number of hair cells, and misoriented and misshapen hair bundles associated with kinocilium positioning defects. These phenotypes indicate that epithelial Wnts regulate both tissue-level and cell-intrinsic PCP signaling.

To elucidate the underlying mechanisms, we analyzed the asymmetric localization of known “core” PCP proteins and cell-intrinsic polarity proteins. Interestingly, asymmetric junctional localization of the core PCP proteins Fzd6 and Dvl2, but not Vangl2, was abolished in *Wls^{cKO}* cochleae. Thus, Wnts differentially regulate asymmetric junctional localization of core PCP proteins.

Among the cell-intrinsic polarity proteins examined, only Daple localization was disrupted in *Wls^{cKO}* cochleae. Daple interacts with Dishevelled and acts as a guanine nucleotide exchange factor (GEF) for Gαi proteins in cultured cells. We therefore tested whether Wnts regulate Gαi activity in the cochlea. Immunostaining using an antibody specific for Gαi-GTP revealed that Gαi activity was greatly reduced in *Wls^{cKO}* cochleae. These findings suggest that Wnts activate G-protein signaling via Daple in the cochlea.

We next tested whether Wnt/G-protein signaling activates phosphoinositide 3-kinase (PI3K), similar to observations in cell culture. Immunostaining of phospho-AKT, a target of PI3K, showed that PI3K activity was greatly reduced in *Wls^{cKO}* cochleae. Furthermore, transgenic expression of constitutively active PI3K rescued most of the PCP defects in *Wls^{cKO}* cochleae, including hair bundle orientation, kinocilium positioning, cochlear length, and hair cell numbers. Taken together, these findings identify a novel Wnt/G-protein/PI3K

pathway that regulates hair cell apical cytoskeleton and core PCP protein localization, thereby coordinating cell-intrinsic and tissue-level PCP.

PS 369

Deficient and Excessive Retinoic Acid Signaling Inhibits Morphogenesis of Stem Cell-Derived Otic Vesicles into Inner Ear Organoids

Liqian Liu; **R. Keith Duncan**
Kresge Hearing Research Institute, Department of Otolaryngology-Head and Neck Surgery, University of Michigan

The derivation of inner ear organoids from pluripotent stem cells relies on chemical cues to mimic otic development. Although retinoic acid (RA) is an essential morphogen in normal otocyst development, the role of RA signaling in organoid production is unclear since culture protocols do not explicitly control RA activity. *In vivo*, exposure to excess RA as well as inhibition of RA signaling results in dysmorphogenesis of the otic vesicle (OV) and often arrest of inner ear development. Recently, using whole-transcriptome RNASeq, we identified differences in native and stem cell-derived OVs related to anterior-posterior patterning, possibly due to aberrant RA signaling in the organoid cultures. Thus, we sought to elucidate the role of RA signaling in organoid production. Toward that end, we developed mouse embryonic stem cells carrying a lacZ transgene under the control of a RA response element (RARE-lacZ). Mice carrying the transgene exhibited normal auditory brainstem response thresholds and normal cochlear morphology. RARE-lacZ stem cell lines were able to reproduce major milestones in organoid development including the generation of Pax2+/Sox2+ OVs and protruding organoid cysts containing MyoVIIa+ sensory hair cells with phalloidin+ hair bundles. Whole aggregates and frozen sections were stained with X-gal to localize RA activity. At day-9, RA activity was highest in the core of the aggregates associated with mesoderm/neuroectoderm and possibly pre-placodal epithelia. Over the next few days, RA activity decreased substantially before intensifying again on day-13 in a portion of OVs. These data revealed spatiotemporal dynamics in RA signaling consistent with activity around the time of placode/otic-cup formation, but the heterogeneity in RA activity among late-stage vesicles could point to heterogeneity in vesicle-to-organoid maturation. To test whether the stem cell-derived tissues were sensitive to changes in RA signaling, we treated cultures with exogenous all-trans RA or inhibitors to RA receptors or synthesis and then examined the effects of treatment on day-12 OVs and day-20 organoids. Excess RA did not alter the number or size of OVs, but increased expression of Pax2 and decreased expression of Sox2; excess RA also eliminated organoid production. Inhibition of RA receptors resulted in normal OV number, shape, and marker expression but, as with excess RA, receptor inhibition severely decreased organoid production. Likewise, inhibition of RA synthesis reduced organoid production. Gaining more control over RA signaling in organoid cultures could increase efficiency, allow manipulation of anterior-posterior patterning *in vitro*, and uncover RA-responsive genes involved in otic development.

PS 370

Defining the Role of Gata3 During Cellular Differentiation

Paige Blinkiewicz; Jeremy S. Duncan
Western Michigan University

Mammalian HDR syndrome is characterized by hyperparathyroidism, deafness, and renal dysplasia and is caused by *Gata3* haploinsufficiency. We have previously shown that early deletion of *Gata3* in the inner ear of mice results in abnormal development of inner ear neurosensory epithelia. When *Gata3* is knocked out before E9.5, there are no hair cells or supporting cells in the region where the organ of Corti (OC) should be. Additionally, when *Gata3* is deleted after E9.5, the hair cells and supporting cells that do develop are patchy throughout the OC and do not demonstrate the typical arrangement in three rows of outer hair cells and one row of inner hair cells. However, *Gata3* expression begins in the otic placode and spans from early embryogenesis through adulthood at varying levels in the organ of Corti. Although *Gata3* expression in the otic placode is high in early embryogenesis it decreases into adulthood and, importantly this low, continuous level does not lead to regeneration of hair cells. Furthermore, the later function of *Gata3* during cellular differentiation has been minimally investigated. In order to determine the later roles of *Gata3* we utilized conditional knock outs using Atoh1-cre, Fgf8-cre, $Sox2^{ERT2}$-cre, and $Fgf10^{ERT2}$-cre to better understand the requirement of *Gata3* at later time points and in different cell types. We have found that absence of *Gata3* at the time of differentiation results in a disorganized arrangement and number of cells, as well as altered gene expression within differentiated cells.

PS 371

Endothelin Expression Suggests Multiple Roles in Inner Ear Development

Justine M. Renauld[1]; William Davis[2]; Martín L. Basch[2]
[1]CWRU; [2]Case Western Reserve University

Mammals are able to hear due to sensory cells present in the cochlea which convert sound vibrations into nerve impulses. These cells require a special environment called the endolymph which is rich in potassium and

creates an endocochlear potential. This endolymph is generated by the Stria Vascularis, which is a specialized epithelial structure located in the lateral wall of the cochlea. The Stria Vascularis is composed of three different cell types of distinct embryonic origin: marginal cells derived from otic epithelium, melanocyte-like intermediate cells derived from neural crest cells and basal cells of a mesenchymal origin. Intermediate cells of the Stria Vascularis are melanocyte-like cells. They originate from the same precursor cells and synthesize melanin. In this study, we looked at the transcriptome of P0 Intermediate cells compared the other cells of the Stria Vascularis by RNA-seq. We identified high levels of expression of endothelin receptor B (EdnrB) in intermediate cells. This result was interesting, because although EdnrB expression is necessary for melanocyte precursor migration, it is sharply downregulated in melanocytes once they reach the dermis. We then analyzed the spatio-temporal expression of the endothelin family of receptors and ligands by *in-situ* hybridization in the developing cochlea. Our data indicates a specific expression of the Endothelin family in the Stria Vascularis, with a specificity of the Endothelin Receptor B for the intermediate cells. We finally quantified the expression of Endothelin Receptor B between the melanocyte-like intermediate cells and the melanocytes of the skin at different stage of development using RNAscope. Our semi-quantitative analysis of the Endothelin Receptor B expression in the melanocytes of the skin and the intermediate cells of the ear showed a high level of expression during migration and differentiation of the neural crest cells, with a gradual decrease of expression in the mature Intermediate cells which is not seen in melanocytes. In conclusion, our data suggest multiple roles of Endothelin in the migration and differentiation of the intermediate cells of the Stria Vascularis.

PS 372

Retinoic Acid Synthesis via Retinol Dehydrogenase 10 and Aldehyde Dehydrogenase 1a3 Enzymes Mediate Formation of Peripheral versus Central Region of Vestibular Sensory Organs

Kazuya Ono; Doris Wu
NIDCD

Each of the five vestibular sensory organs of the inner ear comprises of a specialized central region known as the striola in the macula and the central zone in the cristae. These regions differ from the peripheral regions in anatomical and functional properties, attributing to the central regions being more suitable for encoding acute changes in acceleration. Retinoic acid (RA) is a Vitamin A (retinol) derivative and upon binding to its receptors, they function as a transcription factor by binding to promoters and regulate transcription of downstream genes. RA is synthesized de novo from retinol via two enzymatic reactions. First, alcohol dehydrogenase (Adh) or retinol dehydrogenase (Rdh) family of proteins including Adh1, 3, 4, and Rdh1, 10 convert retinol into retinaldehyde. Retinaldehydes are further oxidized into RA by a family of aldehyde dehydrogenase 1a enzymes (Aldh1a1, a2, and a3). Synthesized RA can also be eliminated by RA degradation enzymes, Cyp26a1, b1, or c1. We have found that *Aldh1a3* is strongly expressed in the extrastriola/peripheral zone of the respective macula and crista, and formation of the striola/central zone is regulated by degradation of RA, mediated by *Cyp26b1*expressed in the prospective striola/central zones. Mice lacking *Cyp26b1* exhibit a reduction in the striola/central zones, whereas *Aldh1a3* knockouts show an expansion of the striola, but the central zone in the cristae is unchanged. These results suggest that Aldh1a3 is essential for RA synthesis in the maculae but not the cristae and other Aldh1a enzymes could be involved. Furthermore, it is not known which Adh or Rdh enzyme(s) generates the substrate retinaldehyde required for RA synthesis in the vestibular end-organs.

Here, we show that *Rdh10* conditional knockout mice exhibit an expansion of the striola, based on the expression pattern of two striolar markers, oncomodulin (Ocm) and b-tectorin. In addition, the conditional mutants exhibit utricle-saccule fusion and loss of the otoconia, phenotypes that are reminiscent of those described for *Aldh1a3* knockouts. However, unlike *Aldh1a3* knockouts, *Rdh10* conditional knockouts show increased Ocm expression in the cristae. These results suggest that other Aldh1a enzyme(s) besides Aldh1a3 is required either alone or in combination with Aldh1a3 in the regional patterning of the cristae. The complementary phenotypes obtained between *Rdh10* and *Cyp26b1* mutants strongly suggest that formation of both maculae and cristae are regulated by RA signaling. In summary, our results indicate that Rdh10 is a key enzyme for providing the retinaldehyde required for RA synthesis and formation of the vestibular organs.

PS 373

GATA3 and NEUROD1 Regulate the Projection of Spiral Ganglion Neurons from the Cochlea to the Cochlear Nucleus

Elizabeth Ketchum; Jeremy S. Duncan
Western Michigan University

Hearing aids and cochlear implants are utilized by individuals who have lost some or all of the hair cells of the organ of Corti (OC). Both treatment options require that spiral ganglion neurons (SGNs) are intact in order for these devices to work. Despite the necessity

to understand how to preserve functioning SGNs or regenerate new ones, there is still much to be learned regarding the proper formation and projection of SGNs from the cochlea to the cochlear nucleus. There is some indication that *Gata3*, a zinc finger factor protein, and *Neurod1*, a basic helix-loop-helix transcription factor, may play a role in the proper development of SGN peripheral projections. Previous studies have looked at the elimination of these genes from the entire neurosensory portion of the inner ear, but have had limited assessment of SGN central processes. In addition, a potential relationship between the two transcription factors has not been discerned. By utilizing the Cre-lox system in mice, we have combined a *Neurod1-cre* line with floxed lines that specifically eliminate *Gata3* or *Neurod1* from SGNs to study whether their roles are cell-intrinsic or cell-extrinsic. Using a combination of immunohistochemistry and lipophilic dye tracing, we have examined the phenotypes of mice in which *Gata3* or *Neurod1* have been conditionally knocked out of SGNs. In addition, we have used *in situ hybridization* and qPCR to examine changes in expression of other genes in response to elimination of *Gata3* or *Neurod1* from SGNs. Our preliminary data indicates that these conditional knockout models result in SGNs with aberrant central and peripheral projections. In addition, there are changes in expression levels of other genes, which may be indicative that these genes are working downstream of *Gata3* and/or *Neurod1*. Based upon our preliminary findings, we hope to uncover the relationship between the major transcription factors involved in SGN development and the possible pathway(s) in which these transcription factors function for proper SGN formation.

PS 374

Multiple Roles of the Notch Ligand Jagged1 during Sensory Development of the Cochlea

Courtney Kellogg[1]; Amy E. Kiernan[2]
[1]University of Rochester Medical Center; [2]University of Rochester

Hearing loss is a common health issue that affects millions of individuals worldwide. Most hearing loss is the result of damage to the organ of Corti, the sensory region of the cochlea. Unfortunately, once damage occurs to critical cell types within the organ of Corti, including hair cells (HC), supporting cells (SC), and spiral ganglion neurons, there are no natural repair or replacement mechanisms within the mammalian cochlea. Understanding the genetic and molecular factors involved in the development of these critical cell types will aid future treatments in the repair or regeneration of these important cells. Studies have shown that the Notch ligand, Jagged1 (JAG1), is critical for sensory formation in the ear. However, the expression pattern of JAG1 changes dramatically during development, indicating it may have several roles during sensory development. Here, we investigated two possible roles of JAG1: an early role in sensory progenitor development (~E9.5 & E12.5) and a later role in boundary formation (E14.5). During early otic development (~E9.5, E12.5), JAG1 is widely expressed in the sensory region of the organ of Corti. Later in development (E14.5), JAG1 becomes localized to the boundary between the inner hair cell (IHC) and outer hair cell (OHC) regions. To dissect the potential roles of JAG1 during cochlear development, we conditionally knocked-out *Jag1* at several developmental time points via the *Foxg1*$^{+/Cre}$ (~E9.5), and the inducible Cre, *Sox2*$^{+/CreER}$ (E12.5 & E14.5) to determine how and when JAG1 is required for sensory development using marker analysis on frozen sections and wholemounts. Our results showed that when *Jag1* is conditionally removed during early sensory development (~E9.5, E12.5), there was an overall loss of sensory cells, particularly OHCs, but there were also regions of the cochlea that showed excess IHCs. By contrast, when *Jag1* is conditionally knockout out at E14.5, there was no loss of sensory cells but the excess IHCs were still observed. These data indicate that the increase in IHCs was due to deletion of JAG1 at later time points whereas the loss of sensory cells was caused by the earlier deletion of JAG1. We hypothesize that the increase in IHCs may be due to a loss of boundary formation at E14.5, whereas the loss of sensory cells is likely caused by a disruption of the early prosensory role of JAG1. These data show that there are multiple roles of JAG1 that are separated in time during cochlear development.

PS 375

Insulin-Like Growth Factor-1 Controls Autophagic Flux in Differentiating Otic Cells

Sara Pulido[1]; Angela Garcia-Mato[1]; Lourdes Rodriguez de la Rosa[2]; Marta Magariños[3]; **Isabel Varela-Nieto**[4]
[1]"Alberto Sols" Biomedical Research Institute (CSIC-UAM); CIBERER Unit 761, CIBER, Institute of Health Carlos III; [2]"Alberto Sols" Biomedical Research Institute (CSIC-UAM); CIBERER Unit 761, CIBER, Institute of Health Carlos III; IdiPAZ, La Paz Hospital Institute for Health Research; [3]"Alberto Sols" Biomedical Research Institute (CSIC-UAM); CIBERER Unit 761, CIBER, Institute of Health Carlos III; Department of Biology, Autonomous University of Madrid; [4]"Alberto Sols" Biomedical Research Institute (CSIC-UAM); CIBERER Unit 761, CIBER, Institute of Health Carlos III; IdiPAZ, La Paz Hospital Institute for Health Research, Madrid, Spain

Embryonic development is an energy demanding state resolved at the cellular level by balancing *de novo* synthesis and recycling of intracellular components.

Autophagy is the cellular program that supplies energy by degrading and recycling these components. Depending on the developmental time, autophagy is required to preserve cell homeostasis or to facilitate cell remodeling. During inner ear development, autophagy has been reported to participate in neuroblasts migration, as well as being essential for the clearance of cells entering programmed apoptosis. Insulin-like growth factor 1 (IGF-1) is an anabolic hormone that promotes survival and proliferation of otic progenitor cells. Depending on the cellular context, IGF-1 has been reported to either increase or decrease autophagic flux.

We have studied if IGF-1 modulates autophagy during early otic development and in the differentiation of progenitors to hair cells by using organotypic chicken otocyst cultures and mouse HEI-OC1 auditory cells. IGF-1 downstream signaling pathways were studied by western blotting. Cell proliferation and apoptosis were studied by measuring EdU incorporation and TUNEL labelling, respectively. Autophagic flux was analyzed by western blotting of LC3 and p62 and by using *in vivo* cell imaging with the mCherry-GFP-LC3 reporter plasmid.

Here we show that IGF-1 stimulated anabolism and otic cell survival and, alongside, reduced autophagy, in both the otocyst and HEI-OC1 progenitor cells. In contrast, IGF-1 promoted anabolism and survival of differentiating HEI-OC1 but the autophagic flux was unaltered. Our results suggest that final differentiation requires constructive metabolism and autophagy to achieve cellular remodelling.

This work was supported by FEDER/SAF2017-86107-R-HEARCODE. SP holds an FPI predoctoral fellowship (BES-2015-071311; European Social Fund/MINECO). AGM holds a MECD FPU fellowship (FPU16/03308). LR-R holds a contract supported by CIBERER (Institute of Health Carlos III) co-financed with FEDER funds.

PS 376

Signaling by Ndp through its Receptor Fzd4 in Cochlear Hair Cells is Critical for Hair Cell Function and is Disrupted in Norrie Disease

Yushi Hayashi[1]; Artur Indzhykulian[1]; Albert Edge[2]
[1]Department of Otolaryngology, Harvard Medical School; [2]Harvard

Norrie disease is an X-linked recessive neurological syndrome whose symptoms include bilateral blindness with a prominent intraocular mass (pseudoglioma) and avascularity of the retina, mental retardation, and progressive sensorineural hearing loss beginning in adolescence. The disease is caused by mutations in the *Ndp* gene, which codes for the secreted Ndp protein. Frizzled 4 (Fzd4) has been identified as the receptor for Ndp. *Ndp* or *Fzd4* mutations result in vascular defects in the retina and cochlea, including enlarged vessels in the stria vascularis with vascular degeneration. Studies in both the retina and the cochlea have concluded that the neurological deficits associated with the disease are caused by this underlying vascular defect.

To understand whether the disease affects the organ of Corti directly, we assessed cochlear expression of Ndp and its receptor Frz4 and analyzed the phenotype of *Ndp* KO mice. Fzd4 was prominently expressed in hair cells, and Ndp was expressed in supporting cells. In the absence of *Ndp*, the ABR and DPOAE exhibited progressive hearing loss. Immunohistochemistry for hair cell and supporting cell markers showed hair cell death and surprisingly many Myo7a-negative hair cells in the KO cochlea, which was consistent with the shift of DPOAE thresholds in the KO mice. Immunostaining for hair cell markers such as prestin and espin in the KO cochlea did not show obvious differences compared to the WT cochlea.

To elucidate the downstream molecules of the Ndp/Fzd4 signaling pathway in hair cells, we sorted hair cells from the *Ndp* KO cochlea by crossing with Atoh1-GFP mice and extracting total RNA. Hair cells from the KO cochlea exhibited down-regulation of not only *Myo7a* but also *Pou4f3* and *Gfi1*, factors for hair cell maturation and survival.

We concluded that Ndp expressed in and secreted from supporting cells acted through Fzd4 receptors on hair cells in the WT cochlea. Moreover, *Myo7a*, *Pou4f3* and *Gfi1* were effector molecules of the Ndp/Fzd4 signaling pathway. Since these genes, which are required for normal cochlear function, were downstream of *Ndp*, their decreased expression in the *Ndp* KO is likely to explain the hearing loss phenotype.

PS 377

Development of Ossification in the Neonatal Gerbil Middle Ear

Eileen Brister[1]; Christoph Rau[2]; Robert Withnell[3]; Yi Shen[1]; Stephen Hoff[4]; Claus-Peter Richter[5]
[1]Indiana University Bloomington; [2]Diamond Light Source; [3]Indiana University; [4]Northwestern University; [5]Northwestern University, Dept Otolaryngology

Gerbils are born with an immature auditory system, with onset of hearing not occurring until around 10 days after birth. After onset of hearing, the auditory system continues to develop both at the cochlear and middle ear levels. At 20 days after birth, middle ear transmission

is not yet adultlike, with stapes vibration sensitivity being reduced in a frequency-dependent manner. Understanding of how development of middle ear structures leads improved sound transmission is limited by our incomplete understanding of the development of the gerbil middle ear. Changes to ossicular length and mass during development have been reported, but bone formation is not well described. In this study, synchrotron-based microtomography was applied to the gerbil middle ear to investigate the development of ossification during for gerbils aged 0-21 days. Ears were imaged using phase-contrast, synchrotron-based microtomography at Diamond Light Source. Tomographic images were visually analyzed and 3D-rendered using a semi-automated segmentation method. Images showed ossification beginning first in the body of the malleus and the body of the incus, then in the footplate of the stapes. In each ossicle, ossification spread from the initial point of ossification. By 21 days, the exterior structure and the dimensions of the ossicles are adultlike, but the interior of the ossicles contains many large, unossified spaces. This is comparable to studies of ossification in the human middle ear, where the internal ossicular structure does not become adultlike until several months after birth.

Acknowledgments
We acknowledge Diamond Light Source for time on the Diamond-Manchester Branchline at the I13 Imaging and Coherence beamline under proposal number MG21066.

PS 378

FGF8 expression specifically marks differentiating type I vestibular hair cells shortly after mitosis

Evan Ratzan[1]; Michael Deans[2]
[1]University of Utah; [2]Dept. of Surgery, Div. of Otolaryngology, Dept. of Neurobiology and Anatomy

: Under the appropriate conditions, perinatal vestibular hair cells retain the ability to regenerate following ototoxic damage. In theory, successful therapeutic adaptation of this phenomenon requires that regenerated hair cells are also directed towards the appropriate type 1 or type 2 hair cell fate. However, these two classes cannot be distinguished until later stages of development when they become morphologically distinct, or when type 1 hair cells lose expression of Sox2. Moreover, signaling pathways directing nascent hair cells towards one or the other type are not known. We have identified FGF8 as a specific marker of type1 hair cells that can be used to identify this population at the earliest stages of their development and has the potential to be a useful tool for regeneration studies. Examination of FGF8 expression by conventional and fluorescent ISH, and CreER-mediated lineage tracing reveals unique, restricted patterns of expression in different prosensory cells at different developmental stages. Early lineage tracing prior to hair cell differentiation (E9) shows FGF8 expression in vestibular ganglion neurons. As hair cell differentiation begins (E10-E13), FGF8 becomes restricted to type I vestibular hair cells. Induction of FGF8 expression begins shortly after mitosis (E10) and lineage tracing only marks type I vestibular hair cells without labeling type II hair cells or supporting cells. FGF8 remains restricted to type I vestibular hair cells at subsequent stages of embryonic development (E16-P0). Separate, lineage tracing in the cochlea reveals early expression in spiral ganglion neurons (E10-E13) and confirms previously observed restriction of FGF8 expression to inner hair cells at later stages (E16-P0). Importantly, specific and sustained expression in type 1 vestibular hair cells suggests FGF8 might contribute to cell specific differentiation. To assess the role of FGF8 in type I hair cell differentiation, we compared morphologic criteria and afferent neuron calyx formation in FGF8 conditional knockouts and littermate controls. However, FGF8 gene deletion by Pax2-Cre or Atoh1-Cre was not sufficient to perturb type I hair cell differentiation or number, morphologic development, stereociliary bundle polarity or innervation. Based upon these results we conclude that Fgf8 is a specific and early marker of type I vestibular hair cells but is not necessary for their differentiation likely due to redundancy in FGF signaling pathways.

PS 379

Expression of Semaphorins and Their Receptors in Developing Chicken Auditory Ganglion and Cochlear Nucleus

Xiaoyu Wang[1]; M. Katie Scott[2]; Donna Fekete[2]; Yuan Wang[1]
[1]Florida State University; [2]Purdue University

Auditory ganglion (AG) neurons connect the ear to the brain via auditory nerve fibers (ANFs). Molecular mechanisms that guide the development of ANF projections within the cochlear nucleus are not fully understood. We have recently found that AG neurons express a high level of fragile X mental retardation protein (FMRP), a mRNA binding protein that regulates local translation of its targets in dendrites and axons. In chickens (*Gallus gallus*), ANFs reach and start terminating on neurons in the nucleus magnocellularis (NM), the avian analogue of the mammalian anteroventral cochlear nucleus, at embryonic day 8 to 10 (E8-10). Genetically knocking down FMRP expression in a subset of AG neurons at E8 results in abnormal projection of their axons away from their normal target in NM. In mammalian brains, a number of Semaphorins (Sema) and their receptors are predicted FMRP targets and FMRP regulates Sema-induced axonal protein translation of cultured hippocampal neurons. We

hypothesize that FMRP interacts with Sema signals in developing ANF axons and that this interaction plays a substantial role in mediating connections at the first synaptic station in the ascending auditory pathway.

Recent *in situ*hybridization studies in the Fekete lab reveal that the class III Semaphorins and their receptors are expressed in the chicken inner ear including the AG, giving rise to the possibility that Sema pathways are employed in ANF pathfinding and targeting. In this study, we examined the spatiotemporal expression profiles of transcripts for Sema3D, Sema3F and their receptors plexin A1 (PlxnA1) and neuropilin (Nrp) in NM. At E8 and E10,*in situ*hybridization reveals robust expression of *PlxnA1*, but not *Nrp2*, in both AG and NM neurons. Notably,*Sema3D*is highly expressed by AG neurons at these ages, providing a potential ligand for activating PlxnA1 in NM. On the other hand, both *Sema3D* and*Sema3F* show modest expression in NM, which may potentially interact with PlxnA1 on ANF terminals. Although relative contributions of these potential bi-directional interactions are yet to be determined, one possible model is that presynaptic FMRP deficiency leads to increased Sema (or PlxnA1) in ANF axons, which prevents them from terminating on PlxnA1 (or Sema)-expressing NM neurons through a repulsive interaction, thus resulting in axonal misprojection. An alternative possibility is that FMRP does not regulate Sema-PlxnA1 binding so directly, but instead influences how axons respond to this binding by modulating protein pathways downstream of PlxnA1 activation. Our ongoing studies are investigating whether and how FMRP regulates expression and localization of *Sema3D* and*PlxnA1* in ANF axons and whether this regulation contributes to FMRP-mediated axonal targeting.

Grant Support: NIH/NIDCD R01DC13074; F31DC015946; R01DC002756

PS 380

Absence of Integrin Alpha8 Apical Expression Results in Abnormal Hair Cell Morphology and Hearing Loss

Marisa Zallocchi[1]; Jian Zuo[2]; Huizhan Liu[1]; Duane Delimont[3]; Linda Goodman[1]; David Z. He[1]
[1]Creighton University School of Medicine; [2]Department of Biomedical Science, Creighton University; [3]Boys Town National Research Hospital, Omaha, NE, USA

An organism's perception of its surrounding environment depends on sensory function. Neurosensory cells from the inner ear are involved in key biological processes associated with hearing and balance. To be able to achieve their function these cells depend on a complex array of membrane receptors, ion channels and signaling molecules that are concentrated at extremely sophisticated structures positioned at the apical (hair cell stereocilia and kinocilium) and basal (ribbon synapses) poles. Disruption of this network results in morphological and functional abnormalities and forms the bases of many human genetic disorders. Our previous work demonstrated a functional interaction between protocadherin-15 (Pcdh15) and integrin alpha8 (Itga8) in hair cells from the zebrafish lateral line. Based on these results, we decided to address whether a similar interaction exists in mammalian hair cells. Proximity ligation assay and co-immunoprecipitation studies suggest Itga8 interacts with specific Pcdh15 isoforms and that they are forming a complex at the hair cell bundle level. To determine the importance of Itga8 during hair cell development, we crossed the transgenic mouse Math1-CreER^{T2} with the LoxP-Itga8 mouse, in which Cre-mediated excision of the loxP cassette resulted in loss of Itga8 expression. CreER^{T2} was activated by tamoxifen administration at gestation day 14 and the organ of Corti and utricle were isolated at post-natal day 1 (P1). Absence of Itga8 resulted in a disarrangement of the sub-apical cytoskeleton network that results in hair bundle misorientation. Auditory brainstem responses and distortion otoacoustic emissions measured at P60, demonstrated these animals have a hearing deficit more likely associated with outer hair cell dysfunction. In vitro studies in wild type and knock down UB-OC1 cells suggest that absence of complex formation results in a reduction in RhoA signaling cascade but not focal adhesion kinase activation; the two major signaling cascades activated by integrin beta1 heterodimers. More importantly, absence of the complex leads to a decrease in actin polymerization, determined by differential centrifugation of filamentous *versus* globular actin. Collectively, these studies point to a functional role for Pcdh15-Itga8 complex in hair cell maturation, introducing for the first time a direct functional link between Usher syndrome and an integrin-downstream signaling cascade. Moreover, the formation and localization of this functional complex are conserved between fish and mammals suggesting it may be playing a key evolutionarily role in sensory cells.

Support: NIH 5P20RR018788, 5R01DC015010-04 and Bellucci Donation Fund.

PS 381

Canonical Wnt signaling modulation using CHIR vs non-canonical signaling with photobiomodulation on the development of inner ear organoids

Nathaniel Carpena[1]; So-Young Chang[2]; Jae Yun Jung[3]; Phil-Sang Chung[3]; Min Young Lee[4]
[1]Beckman Laser Institute Korea, College of Medicine, Dankook University, Cheonan, South Korea; [2]Dankook University; [3]Beckman Laser Institute Korea, Dankook

University, Dankook University Hospital; [4]Beckman Laser Institute Korea, Dankook University Hospital, Dankook University

Background
Organoid technology has recently exploded and being showcased be able to represent the development of various organs and tissues. Meanwhile, the Wnt signaling pathway has become the core in determining the cell fate specification of different tissue developments. Wnt signaling has been shown to function in the inner ear development through both canonical and non-canonical pathways. CHIR99021 is a pharmacological activator of the canonical Wnt signaling by inhibiting GSK3 and promoting nuclear accumulation of beta-catenin leading to the activation of Wnt-target genes. On the other hand, intracellular calcium has been implicated as the important second messenger in all the beta-catenin independent Wnt pathway. Photobiomodulation (PBM) using low power light sources (laser or LED) can increase intracellular calcium levels through the activation of the light sensitive calcium channels.

Objectives
In this study, we investigated the effects of Wnt signaling modulation using the canonical pathway with CHIR and non-canonical pathway with PBM on the development of inner ear organoids.

Materials and Methods
We recently demonstrated the optimal conditions for differentiating mouse mouse embryonic stem cells (ESCs) in a self-organizing 3D culture into otic organoids via hanging drop technique followed by ectodermal differentiation with the addition of growth factors. Wnt signaling activity was induced either by the addition of CHIR99021 or exposure to PBM to the embryonic bodies and culture until day 21.

Results
The resulting EBs after Wnt activation has higher success in forming otic-like vesicles and a higher number of vesicles per EB than the PBM treated EBs. However, the CHIR treated EBs also generated other organoids with different morphology including beating organoids while the PBM treated EBs did not. Immunofluorescence staining also showed the expression of cardiac and neural markers in the CHIR treated EBs. Despite the lower number of otic organoid formation in PBM treated EBs, expression of otic organoid related genes are higher compared to CHIR treated EBs.

Conclusion
The present study suggests that Wnt signaling enhances the development of otic organoids. However, unlike the localized regulation of Wnt signaling during embryo development, the differentiation of other cells within the EBs towards different lineages can also be affected with the addition of the Wnt agonist CHIR while PBM delivers a more specific effect in inducing otic progenitor cells capable of giving rise to inner ear organoids.

Acknowledgement:
This research was supported by The National Research Foundation of Korea (NRF - 2019M3D1A1078943, 2019R1F1A1058485) grants funded by the Korean government.

PS 382

Differentiation of Inner Ear Progenitors with Defective CHD7 in Chimeric Human Inner Ear Organoids

Yoshitomo Ueda; Jing Nie; Eri Hashino
Indiana University School of Medicine

CHARGE syndrome, caused primarily by mutations in the *CHD7* gene, leads to outer, middle and inner ear anomalies, resulting in mixed conductive and sensorineural hearing loss in over 90% of cases. While malformations of ear structures have been well characterized in human patients and mouse models, it is still unclear how *CHD7* mutations affect the proper development of otic progenitors and their progenies, such as mechanosensitive hair cells and sensory neurons. To investigate the inner ear phenotypes of CHARGE syndrome in an *in vitro* model, we engineered wild type (WT) and *CHD7* mutant human embryonic stem cell (hESC) lines with CRISPR and differentiated them towards an inner ear lineage in the inner ear organoid culture system we recently established. Specifically, we generated *CHD7* mono-allelic knockout hESC lines on a *PAX2*-2A-nGFP (*PAX2* ^{nG}) reporter background, which labels nuclei of PAX2-positive otic progenitors with green fluorescence. Another *PAX2* ^{nG} reporter that is WT at the *CHD7* allele was further fluorescently labeled with AAVS1-CMV-membrane-bound tdTomato (AAVS1 ^{mT}) for a constitutive red membrane marker expression in all cell types. For direct comparison of WT and mutant tissues in the same organoids, the mT positive WT hESCs were mixed with mT negative *CHD7*+/- cells, and these two cell populations were aggregated chimerically into 3D spheres. During *in vitro* differentiation, *PAX2* ^{nG}+ otic vesicles were successfully derived in the chimeric aggregates. Over 90% of *PAX2* ^{nG}+ cells expressed PAX8 on differentiation day 20 (d20) and d40. The ratio of SOX2+ cells in otic vesicles decreased from 70% on d20 to 40% on d40. Over 60% of cells in *PAX2* ^{nG}+ otic vesicles expressed SOX10 on d20 and d40. However, the percentage of PAX8-, SOX2- or SOX10-positive cells in otic vesicles was not statistically different

between WT and *CHD7*+/- populations on d20 and d40. Moreover, MYO7A+ SOX2+ cells bearing hair bundles arose from both WT and *CHD7*+/- populations on d60 of differentiation. Collectively, these data suggest that mono-allelic *CHD7* knockout does not critically affect the differentiation of otic progenitors and hair cells. Further analysis is currently underway using *CHD7* bi-allelic knockout cells in chimeric organoids.

PS 383

Patterning the Radial Axis of the Cochlea: Exploring the Role of Fgfs downstream of Wnt Signaling

Elizabeth R. Wehren; M. Katie Scott; Rachel M. Maibach; **Donna Fekete**
Purdue University

The hearing organs of amniotes are segregated into two functional compartments across the radial axis. In mammals, inner hair cells on the neural (medial) side connect to large, myelinated afferent fibers that convey auditory information to the brain, while outer hair cells on the abneural (lateral) side receive robust efferent input, display electromotility, and synapse with thin unmyelinated afferent fibers that convey pain sensation following damage to the sensory organ. Understanding how these neural-abneural specializations arise during development is an active area of investigation in both birds and mammals. Genetic or pharmacological perturbation of Notch, Wnt, Fgf or Bmp signaling prior to cell fate specification can alter the number and/or types of sensory cells across the radial axis. The current study explores whether and how Fgf signaling may function downstream of Wnt signaling to influence this radial axis patterning in the chicken embryo.

Previously our lab showed that retrovirus-mediated overexpression (OE) of Wnt9a in the developing basilar papilla enhances cell proliferation and disrupts radial patterning by embryonic day 6 (E6), which is 3 days after virus injection into the chick otocyst. Positional identities are altered at this time, as evidenced by a loss of abneural-side genes and an expansion of neural-side genes. Afferents respond by spreading across the entire radial axis, instead of remaining confined mostly to the neural side. By E18, Wnt9a-OE cochleas contain only tall hair cells with excess numbers of presynaptic puncta, while short hair cells are missing. RNAseq performed on E6 identifies *Fgf3* and *Fgf19* among the early genes upregulated in response to Wnt9a-OE. In the present study, in situ hybridization confirms their upregulation and further shows that this effect is spatially restricted within the cochlear duct to the prosensory domain; Wnt9a-infected cells in the non-sensory domains of the cochlea do not ectopically express these two *Fgf* transcripts. We are focusing on Fgf19 because our lab previously showed that Fgf19 enhances neurite outgrowth when added to cultured E4 statoacoustic ganglia. This leads us to hypothesize that Fgf19-OE may phenocopy the Wnt9a-OE effect of excessive afferent projections. To test this idea, we have generated a retroviral vector that encodes both GFP and Fgf19 and we are injecting it into E3 chicken otocysts. We will examine cochlear innervation, hair cell phenotypes, cell proliferation and gene expression patterns to determine whether Fgf19 functions as a downstream effector of Wnt9a in any of these aspects of radial patterning.

PS 384

Slc26a9P2ACre, a New Pan-Otic Cre Driver for Conditional Manipulation of Inner Ear Gene Expression

Lisa Urness[1]; Xiaofen Wang[1]; Chaoying Li[1]; Rolen Quadros[2]; Channabasavaiah Gurumurthy[2]; **Suzanne Mansour**[1]
[1]University of Utah; [2]University of Nebraska Medical Center

Tg(*Pax2-Cre*) and *Foxg1*^{Cre} are frequently used as pan-otic drivers for conditional knockout (CKO) studies in mice, but postnatal analyses are often limited due to overlap of CRE activity and the gene-of-interest in non-otic tissues where it is required for viability. Furthermore, both CREs also recombine conditional alleles in auditory and vestibular nuclei in the brain, making it difficult to unambiguously ascribe auditory or vestibular CKO phenotypes to the inner ear. To circumvent these limitations, we sought to develop an alternative CRE driver that is active in the otic placode lineage, but with fewer sites of activity outside the inner ear epithelium and ganglion, especially in the brain, and that does not disrupt an essential gene. We noticed that *Slc26a9*, a gene we identified as an otic placode-expressed target of FGF3/FGF10 signaling, appeared otic placode specific as assessed by in situ hybridization of whole E8.5 embryos. *Slc26a9* is located on chromosome 1 and encodes a protein expressed in adult stomach and lung epithelia where it functions as a Cl^--HCO_3^- exchanger, a Cl^- channel and a Na^+-coupled transporter. Null mutants are viable and fertile with a defect in gastric acid secretion. We show here that *Slc26a9* is specific for the otic placode, cup and vesicle from E8.5-E10.5, but is not required for audition. We used *Easi*-CRISPR to insert *P2ACre* before the *Slc26a9* stop codon, producing a correctly targeted allele designed to express CRE in the same lineages as *Slc26a9* without disrupting its function. Reporter analyses of the embryonic and early postnatal *Slc26a9*^{P2ACre} lineages show that recombination in the inner ear starts at E9.5, one day later than Tg(*Pax2-cre*), but nevertheless, encompasses the entire otic epithelium and is extensive in cochlear and vestibular neurons.

There was very little recombination in the brain, but CRE activity could be detected pre- and perinatally in a variety of endoderm-derived epithelia that require *Fgf10* for their development. In contrast to *Fgf10* or *Fgf8* Tg(*Pax2-Cre*) CKO mutants, *Fgf10* or *Fgf8 Slc26a9*^{P2ACre} CKO mutants survived postnatally. ABR thresholds were elevated in both CKOs. We also used *Slc26a9*^{P2ACre} to drive activation of a dominant-negative FGFR2b ligand trap from E17.5-P3, thereby briefly inhibiting both FGF3 and FGF10 function, and observed partially penetrant hearing loss correlating with a reduction in the outer sulcus. These data indicate that *Slc26a9*^{P2ACre} mice provide a useful alternative to Tg(*Pax2-Cre*) and *Foxg1*^{Cre}, particularly for postnatal analyses.

PS 385

Generation and Characterization of PAX2-CreERT2 Reporter Cell Lines for Lineage Tracing in Human Inner Ear Organoids

Takashi Nakamura; Jing Nie; Eri Hashino
Indiana University School of Medicine

During inner ear development, PAX2+ otic progenitors give rise to all essential cell types for hearing and balance function, including hair cells, supporting cells, and sensory neurons. However, little is known about how otic progenitors differentiate into various sensory cell types in the inner ear. More specifically, we have limited understanding as to whether there are distinct subtypes in PAX2+ otic progenitors that are destined to become different cell types in the inner ear and at what degree otic progenitors possess the potential to switch cell fates. To address these unmet questions, we generated inducible PAX2 reporter human embryonic stem cell (hESC) lines that allow for permanent labeling of PAX2+ cells and unequivocal identification of progenies of these otic progenitors. Using CRISPR/Cas9, we first knocked-in a dual-fluorescence cassette comprising a membrane-bound tdTomato (mT) followed by a membrane-bound eGFP (mG) into the “genetic safe harbor” AAVS1 locus (AAVS1-mT/mG) in hESCs. The mT gene is expressed under the control of a ubiquitous CAG promoter, and is flanked by two LoxP sites followed by the un-floxed mG sequence. Upon Cre recombinase excision, the LoxP sites-flanked mT sub-cassette is removed, allowing mG to be expressed from the CAG promoter instead, thus converting the cell membrane fluorescence signal from red to green. To generate the cell line, wild-type hESCs were transfected with an AAVS1-targeting high-fidelity Cas9 ribonucleoprotein (HiFi Cas9 RNP) and an AAVS1-mT/mG donor vector. AAVS1-mT/mG hESC lines were clonally isolated from single cells, and the established cell lines were tested with Cre transfection. Cre transfected hESCs successfully converted their membrane fluorescence from red to green, validating the correct insertion of the donor vector. Using this AAVS1-mT/mG reporter line as the parental line, we subsequently knocked-in the tamoxifen inducible Cre recombinase (CreERT2) just prior to the stop codon of *PAX2*. The resultant *PAX2*-CreERT2; AAVS1-mT/mG hESCs were differentiated into inner ear organoids and treated with 4-hydroxytamoxifen (4-OHT) at different time points. These hESC-derived organoids constitutively expressed membrane-bound tdTomato, but upon 4-OHT treatment, a subpopulation of PAX2+ cells switched their color to eGFP in a dose-dependent manner. Investigation is currently underway to determine the trajectory of PAX2+ otic progenitor differentiation in human inner ear organoids.

PS 386

Evaluating the Role of the Basic Helix-Loop-Helix Family Member E40 (Bhlhe40) Transcription factor in Inner Ear Development and Function.

Braulio Peguero[1]; Sarah Allen[2]; Talah Wafa[3]; Rafal Olszewski[4]; Michael Hoa[4]; Tracy S. Fitzgerald[5]; Matthew W. Kelley[6]
[1]Laboratory of Cochlear Development, National Institute on Deafness and Other Communication Disorders; [2]Neuroscience Program, Colgate University / National Institute on Deafness and Other Communication Disorders; [3]Mouse Auditory Testing Core Facility, National Institute on Deafness and Other Communication Disorders; [4]Auditory Development and Restoration, National Institute on Deafness and Other Communication Disorders, NIH; [5]Mouse Auditory Testing Core Facility, National Institute on Deafness and Other Communication Disorders, NIH, Bethesda, Maryland, USA; [6]National Institute on Deafness and Other Communication Disorders, NIH

The cochlear and the vestibular sensory organs of the inner ear are comprised of complex cellular structures that are crucial for the sensations of sound and balance. All inner ear sensory structures contain specialized hair cells and supporting cells that are arranged into unique cellular mosaics. How these cell types are specified and patterned is an ongoing topic of research. To identify genes that might be involved in the specification of unique hair cell types, our laboratory conducted a single-cell RNA sequencing (scRNA-seq) experiment of developing cochleae and utricles. Our results identified several genes that are uniquely expressed in subsets of hair cell types. Here, we focus our investigation to the Basic Helix-Loop-Helix Family Member E40 (*Bhlhe40*) transcription factor which was predominantly expressed in the outer hair cells (OHC) of the cochlea and the type I hair cells of the utricle in early postnatal ages. Based on these findings we hypothesized that *Bhlhe40* expression may be necessary for different aspects of normal auditory and/or vestibular function.

To examine the potential role(s) of *Bhlhe40*, we first used single molecule RNA fluorescent *in situ* hybridization (smFISH) and quantitative PCR (qPCR) to validate the expression of *Bhlhe40* in the proposed cell types. Next, to elucidate the role of the *Bhlhe40* gene in auditory and vestibular function we recorded auditory brainstem response (ABR), distortion product otoacoustic emission (DPOAE), *vestibular sensory-evoked potential* (VsEP), and endocochlear potential (EP) measurements in adult *Bhlhe40* knock out (KO) mice. Finally, we used immunohistochemical (IHC) assays to visualize potential changes in the anatomical morphology of the cochlea and utricle in the absence of the *Bhlhe40* gene.

Our results validate the findings of the scRNA-seq experiment showing expression of the *Bhlhe40* transcription factor in OHCs and type I utricular hair cells in neonates; this expression is maintained in older ages as well. Phenotypically, *Bhlhe40* knockout mice show little indication of a functional or morphological deficit through early adulthood. Additional work is underway to determine whether *Bhlhe40* mutant mice may show increased susceptibility to age related hearing loss and to determine if possible functional compensation by the related transcription factor *Bhlhe41* may account for the limited effects of deletion of *Bhlhe40*.

PS 387

Live Imaging of Cochlear Organotypic Explants – a Tool for Studying Development, Pathology, and Regeneration

Shahar Taiber[1]; Shiran Wolland[2]; Roie Cohen[2]; Liat Amir-Zilberstein[2]; Olga Lonza[2]; Karen B. Avraham[3]; David Sprinzak[4]
[1]Department of Biochemistry & Molecular Biology, George S. Wise Faculty of Life Science, Tel Aviv University, Tel Aviv, Israel, Department of Human Molecular Genetics & Biochemistry, Faculty of Medicine and Sagol School of Neuroscience, Tel Aviv University, Tel Aviv, Israel; [2]Department of Biochemistry & Molecular Biology, George S. Wise Faculty of Life Science, Tel Aviv University, Tel Aviv, Israel; [3]Department of Human Molecular Genetics & Biochemistry, Faculty of Medicine and Sagol School of Neuroscience, Tel Aviv University, Tel Aviv, Israel; [4]School of Neurobiology, Biochemistry and Biophysics, George S. Wise Faculty of Life Sciences, Tel Aviv University

The organ of Corti is a strikingly complex organ that undergoes dramatic morphological and regulatory changes during early development, as well as in later stages, in response to ototoxic drugs and aging. Understanding these dynamic processes in mouse model systems can improve our ability to develop new strategies for hearing preservation and restoration. Current techniques, however, are predominantly based on analysis of fixed samples, only providing snapshots of the state of the cells at each time point. Here, we report the development of a method for high resolution live imaging of cochlear organotypic explants using transgenic mice expressing the ZO1-GFP reporter that allows both short term (seconds to minutes) and long term (hours and days) tracking of cellular morphological changes and organization processes at different developmental stages. Time-lapse movies generated are analyzed using a custom-made image analysis platform, allowing for quantitative analysis of cellular morphologies. The imaging platform also allows for probing the role of different signaling pathways in the development of the organ of Corti by adding pharmacological inhibitors to the explants during imaging. Finally, the response of the tissue to local ablation of cells can be studied using a laser ablation system integrated into the microscopy system. As a demonstration of the systems' capabilities, we show the morphological effect of ablating a hair cell on surrounding supporting cells, and the effect of Blebbistatin, a non-muscle myosin II inhibitor, on tissue morphology. Overall this approach can be used to better understand developmental and pathological processes, as well as proliferation and trans-differentiation, in order to devise therapeutic strategies for hearing loss and regeneration.

PS 388

Early determinants of cell fate in 3D inner ear organoids

Pei-Ciao Tang; Emily R. Verbrugge; Rick F. Nelson
Dept. Otolaryngology-HNS, IUSM

Stem cell-derived 3D inner ear organoids contain heterogeneous cell populations that recapitulate mammalian inner ear sensory epithelia. The system has shown increasing promise in development and disease modeling, regenerative medicine, and drug screening. However, due to the complexity of cell types and the process of the self-organization, a high degree of variability in protocol reproducibility has been documented in organoid systems. During the derivation of inner ear organoids, all ectodermal lineages arise; as time progresses, off-target cell types (e.g., skin, hair follicles, and cartilage) emerge in addition to the target inner ear sensory epithelia. Understanding the development of otic placodes in the pre-placodal region (PPR), then, will not only be critical for advancing our knowledge of the development of sensory organs, but it will be essential in establishing protocols that lead to more efficient and more highly reproducible inner ear organoid induction. The PPR is located in the anterior neural border, which also features neural crest cells (NCC); both the PPR and NCC play important roles in sensory organ biology, yet the cell fate commitment of neither region is well characterized, especially in mammals. In this study, we

showed that moderate activation of the Wnt signaling pathway during the early induction prompts cells to commit to the posterior PPR fate, ultimately giving rise to otic vesicles. In contrast, inhibition of Wnt significantly decreases the expression of *Pax8* gene, a marker of posterior PPR. With such modification, ~90% of our aggregates now regularly contain inner ear organoids, and single cell RNA-sequencing data revealed the progression of cell lineages during organoid induction. Collectively, this system could be used to study molecular mechanisms underlying the development of the neural border, and, more generally, sensory organs.

Endolymph & Ménière's Disease

PS 389

The Modulation of the Sensitivity of the Mammalian Utricle by Low Frequency Hydrostatic Bias.

C Pastras[1]; S Stefani[1]; Ian S. Curthoys[2]; Camp A[1]; Daniel Brown[3]
[1]The University of Sydney; [2]University of Sydney, Australia; [3]Curtin University

Background
Auditory hair cell function is altered by nanometre displacements of the organ of Corti. This can be observed by measuring cochlear hair cell or nerve responses at various phases of a low-frequency (LF) bias, which cyclically displaces the organ of Corti. This approach is useful for studying cochlear transduction and associated auditory pathologies, such as, the effect of endolymphatic hydrops on hearing sensitivity. By contrast, the effect of mechanical bias and endolymphatic hydrops on vestibular function is not well established. Interestingly, recent clinical evidence reveals an enhanced vestibular reflex response at the time of a vertigo attack in early Meniere's patients. Although, several explanations have been proposed such as increased hydrostatic pressure of the labyrinth, it remains to be seen how endolymphatic hydrops and mechanical modulation alters vestibular sensitivity at the time of a vertigo attack.

Objective
To investigate the effect of a LF hydrostatic bias of the mammalian utricle on utricular nerve, hair cell, and mechanical function, as a means to investigate balance dysfunction associated with endolymphatic hydrops.

Methods
Experiments were undertaken in anaesthetized guinea pigs, approved by the USYD Animal Ethics Committee. Functional and mechanical utricular hair cell responses (in the Utricular Microphonic and macular velocity), were recorded from the surface of the utricle via a ventral surgical approach, alongside gross utricular nerve responses (in the VsEP) recorded from the facial nerve canal. The macular epithelium was cyclically modulated via a LF hydrostatic bias delivered via a fluid-filled pipette in the horizontal semi-circular canal or from an intense Air-Conducted Sound (ACS) tone delivered to the ear canal. A dorsal surgical approach was also used to investigate the effect of LF hydrostatic bias on vestibular nerve (VsEP) function, with the cochlear intact. Here cochlear function was chemically ablated using 0.2M KCl, and thereafter vestibular nerve function was monitored at various phases of the LF hydrostatic bias, across various levels.

Results
The amplitude of utricular hair cell and nerve responses varied with macular displacement, similar to cochlear response modulation by a low-frequency tone. At certain displacements there was an increase in the amplitude of the responses, above the non-displaced baseline amplitude.

Conclusion
Displacement of the utricular macula alters its sensitivity and can make it hyper-sensitive to bone-conduction. This may explain the enlarged vestibular reflex responses observed in some Meniere's disease sufferers during vertigo attacks.

PS 390

Effect of Intratympanic Vasopressin on Inner Ear in Mouse

Minbum Kim; So Yeon Yoon
Department of Otorhinolaryngology-Head & Neck Surgery Catholic Kwandong University International St. Mary's Hospital

Objective: The purpose of this study is to investigate the effect of intra-tympanic vasopressin on AQP2 and inner ear function in mouse. Methods: We used the C57BL/6 mouse. After exposure of round window via transbullar approach, intratympanic application of Desmopressin (Arg-vasopressin) was performed at the right ear. One hour after injection, temporal bone was harvested with cardiac perfusion. Histologic sections parallel to the modiolar axis were made. Confocal immunohistochemistry of the inner ear was performed using antibodies for AQP-2 and DAPI. Auditory brainstem response (ABR) test were performed before and after VP, respectively. Both behavioral observation using a video camera and rotator test were done for the evaluation of vestibular function . Results: In the confocal image, AQP-2 was exclusively stained on the basal membrane of the basal cell at the stria vascularis after intra-tympanic injection of vasopressin (IT-VP). ABR threshold was increased after IT-VP compared to contralateral ear (42.85±9.06

vs. 23.57±3.77, p< 0.01). After IT-VP, rotational behavior was observed bidirectionally in some animals after IT-VP, and symmetric score of rotator test (SHA) increased (32.79±19.71%). Conclusion: IT-VP can transiently induce acute imbalance of inner ear homeostasis via the membrane trafficking of AQP-2 at the stria vascularis. Using IT-VP, it is possible to induce the transient water shift in the mouse model for endolymphatic hydrops. Furthermore, it might give some clues to explain the mechanism in the acute stage of endolymphatic hydrops.

PS 391

Rat Model of Acute Attack of Ménière's Disease: Direction-changing Spontaneous Nystagmus and Hearing Fluctuations Induced by Intratympanic Injection of Potassium Chloride

Takefumi Kamakura[1]; Tadashi Kitahara[2]; Makoto Kondo[1]; Arata Horii[3]; Yukiko Hanada[4]; Yasumitsu Takimoto[5]; Yusuke Ishida[6]; Yukiko Nakamura[1]; Takao Imai[7]; Hidenori Inohara[5]; Shoichi Shimada[1]
[1]Department of Neuroscience and Cell Biology, Graduate School of Medicine, Osaka University; [2]Department of Otolaryngology – Head and Neck Surgery, Nara Medical University; [3]Department of Otolaryngology Head and Neck Surgery, Niigata University Graduate School of Medical and Dental Sciences; [4]Department of Otorhinolaryngology, National Hospital Organization Osaka National Hospital; [5]Department of Otolaryngology - Head and Neck Surgery, Graduate School of Medicine, Osaka University; [6]Division of Anatomy and Cell Biology, Tohoku Medical and Pharmaceutical University; [7]Department of Otolaryngology – Head and Neck Surgery, Graduate School of Medicine, Osaka University

The major symptoms of Ménière's disease are episodic vertigo, fluctuating hearing loss, and tinnitus. Direction-changing spontaneous nystagmus is one of characteristic vestibular findings in Ménière's disease. In the acute stage, spontaneous nystagmus beating to the affected side (irritative nystagmus) is often observed, while paralytic nystagmus beating to the healthy side is found in the chronic stage. This direction-changing nystagmus can be reproduced in guinea pigs by increasing the potassium ion concentration in the perilymph. The objectives of the present study are to examine the effects of increasing the potassium ion concentration of the rat perilymph on hearing and nystagmus. Thirty 8-week-old Wister rats were studied in the present study. Under isoflurane anesthesia, twenty-two rats received intratympanic injection of different concentrations of potassium chloride (KCl) solution or distilled water: Groups 1, 2, 3, and 4 (8, 8, 3, and 3 rats, respectively) received saturated (3.4 M) KCl solution, 2 M KCl, 1 M KCl, and distilled water, respectively. The nystagmus direction and number per 15 s were monitored for 150 min. In the other eight rats, hearing was monitored 30 min and 20 h after intratympanic injection of 2 M KCl (Group 5, 5 rats) or distilled water (Group 6, 3 rats) using the auditory brainstem responses (ABR) under isoflurane anesthesia. The KCl solution and distilled water were kept at 37 °C to avoid caloric effect. Rats in Groups 1 and 2 showed spontaneous irritative nystagmus beating to the affected ear followed by paralytic nystagmus beating to the healthy side. In Group 3, irritative nystagmus occurred but paralytic nystagmus was rarely observed. Rats in Group 4 showed no nystagmus. Rats in Group 5 showed significant hearing impairment 30 min after KCl injection that recovered 20 h later. Control animals in Group 6 showed no significant hearing changes. The reversible hearing impairment with direction-changing spontaneous nystagmus induced by intratympanic potassium injection in rats was quite similar to that observed in acute Ménière's attacks. This rat model could be used for basic research investigating the pathophysiological mechanisms underlying acute Ménière's attacks.

PS 392

Roles of Macrophages/Microglia in Endolymphatic Sac Pathologies Associated with Meniere's Disease

David Bächinger[1]; Joseph B. Nadol[2]; Joe C. Adams[3]; Andreas H. Eckhard[1]
[1]Department of Otorhinolaryngology, Head and Neck Surgery, University Hospital Zurich, Zurich, Switzerland; [2]1) Otopathology Laboratory, Department of Otolaryngology, Massachusetts Eye and Ear 2) Department of Otolaryngology, Harvard Medical School; [3]Massachusetts Eye and Ear Infirmary

Background

In approximately 75% of patients with Meniere's disease (MD), the presumed disease-causing inner ear pathology is degeneration of the endolymphatic sac (ES) epithelium. The cause of ES degeneration in MD is yet unknown. Cell-mediated inflammatory responses in the area of the ES are one potential mechanism that could cause irreversible damage to the ES epithelium. Here, we investigated the tissue distribution patterns of macrophages/microglia (M/M) in the normal mouse and human ES, as well as in the ES region in cases with MD. We studied lymphatic routes of M/M migration towards the ES and the molecular mechanisms of M/M recruitment and activation.

Material and Methods

To investigate the origin and distribution patterns of M/M in the ES, tissue sections of the normal murine and human ES were immunolabeled using M/M-specific antibodies against Iba1 and TMEM119. Possible circulatory routes of M/M to the ES were studied by immunolabeling whole-

mount specimens of the murine ES using markers for blood vessels (Concanavalin A, ConA) and lymphatics (LYVE1). To assess epithelial interleukin production in the ES epithelium, murine tissue sections were immunolabeled against IL-1β. Lastly, in tissue sections from MD patients with degenerative ES pathology, the M/M population was quantified using immunohistochemistry.

Results

The normal murine and human ES are surrounded by a dense Iba1$^+$ TMEM119$^-$ M/M population interacting with the ES epithelium. Negative immunostaining for TMEM119 suggests that these M/M are monocyte-derived macrophages, which are ontogenetically and functionally distinct from microglia. Assessing possible supply routes for M/M and other immune cells to the ES, a prominent LYVE1$^+$ lymph trunk as well as a confluence of ConA$^+$ blood vessels was found in the ES region. Further, IL-1β immunolocalized to the ES epithelium suggesting epithelial interleukin production in the ES. In MD, ES degeneration is associated with a loss of the local Iba1$^+$ M/M population.

Conclusion

The ES is densely populated by peripherally derived macrophages, but not by resident microglia. Macrophages presumably reach the ES via its dense lymphatic and blood vessel supply. Epithelial secretion of IL-1β may activate macrophages to exert tissue homeostatic functions, or drive inflammatory responses in the ES. In MD, the absence of macrophages in the degenerated ES may be either a primary pathological event, or secondary to the epithelial loss. In conclusion, we identified in the ES a large population of macrophages, a prominent lymphatic supply, as well as epithelial IL-1β secretion, which may play an important role in ES degeneration as seen in MD.

PS 393

Quantitative 3D Volume Measurement of Endolymphatic Hydrops is Different form the Conventional 2D Area Measurement in Meniere's Disease

Tae-Soo Noh[1]; In Chan Song[2]; Ji Hoon Kim[2]; Doo Hee Kim[1]; Moo Kyun Park[1]; Jun Ho Lee[3]; Seung-Ha Oh[4]; Myung-Whan Suh[4]

[1]Department of Otorhinolaryngology-Head and Neck Surgery, Seoul National University College of Medicine, Korea; [2]Department of Radiology, Seoul National University Hospital; [3]Department of Otorhinolaryngology-Head and Neck Surgery, Seoul National University College of Medicine; [4]Department of Otorhinolaryngology-Head and Neck Surgery, Seoul National University College of Medicine, Korea

Background

Recently, the diagnosis of endolymphatic hydrops (EH) by MR imaging has become possible. However, the previous 2D analysis method on a single section can produce several errors. In order to reduce errors in the analysis, a 3D analysis method has been tried. This study was performed to quantitatively evaluate the 3D volume of endolymphatic hydrops by gadolinium-enhanced MR in Meniere's disease (MD). We also aimed to compare the degree of qualitative 3D EHI with the qualitative 2D EHI.

Methods

HYDROPS2-Mi2 EHI image was acquired in 17 unilateral definite MD patients (17 ipsi-lesional MD ear and 17 contra-lesional non-MD ears). Clear demarcation between the perilymph and endolymph was possible in all the 34 ears. The quantitative volume ratio of (endolymph)/(endo+perilymph) was calculated by an automated 3D image analysis software(EH%). The 2D image was analyzed by drawing endolymphatic area ROI on the cross section of cochlea and vestibule according to the method proposed by Naganawa et al. 2014. For the cochlear ROI, the slice with the largest cochlear modiolus was selected. For the vestibular ROI, the lowest slice where the lateral semicircular canal ring is visible more than 240° was selected. The 3D outcome and 2D outcome were compared.

Result

The gender(M:F = 8:9), age(48.0±8.7 yrs), and duration of illness(52.0±43.9 mo) of the MD patients were similar to the previous reports. The vestibule 3D EH% was always larger in the ipsi-MD ears (49.6±16.0%) when compared to that of the non-MD ears (40.3±15.5%). Except for two patients (11.76%), the EH% was always larger in the ipsi-MD ear with a mean difference of 9.3±10.5% (p=0.018). Also, the vestibule 2D EH% was larger in the ipsi-MD ears (62.3±29.0%) when compared to that of the non-MD ears (31.6±21.7%). Except for five exception (29.4%), the EH% was larger in the ipsi-MD ear with a mean difference of 30.7±36.9% (p=0.004). The vestibule and cochlear 3D EH% showed a significant correlation with that of the 2D EH% of the ipsi-MD ear, respectively (vestibule, p=0.001; cochlea, p=0.001).

Conclusion

Quantitative 3D volume and 2D image measurement of the hydrops MRI can provide valuable information of MD. But since the cochlea is spiral structure, it seems that the 2D analysis of the mid-modiolar section cannot accurately represent the EH which is found in the whole cochlea. On the contrary, EH is usually most sever only in the vestibule which can be represented as a single slice of image.

PS 394

Vestibulo-ocular Reflex Gain of the Video Head Impulse Test (vHIT) with Re-fixation Saccades on Patients with Meniere's Disease

Shreyas Bharadwaj[1]; Michelle Petrak[2]; Cammy Bahner[2]; Laurin Moodie[3]; Sara Claycomb[3]; Akihiro Matsuoka[1]
[1]Northwestern University; [2]Interacoustics; [3]Northwestern Medicine

Meniere's disease is a condition characterized by sensorineural hearing loss, recurrent rotational vertigo, fullness in the ear, and tinnitus. Although the definite pathophysiology of Meniere's disease is still unknown, several studies point to a relationship between Meniere's disease and endolymphatic hydrops. Recently, the video Head Impulse Test (vHIT) has been used clinically to test the horizontal semicircular canal of patients. This test has shown some clinical significance. The video camera of the vHIT overcomes many of the limitations of the human eye when performing a clinical Head Impulse Test (HIT). The goal of this study is to identify significant diagnostic parameters for evaluating Meniere's disease.

Subjects between the ages of 18-85 were recruited for the study. Forty subjects without Meniere's disease were recruited for the healthy population, and forty subjects with Meniere's disease were recruited for the second population. Subjects must not have had an Meniere's disease flare-up within the last 6 months. EyeSeeCam® is a light-weight goggle with a video oculography camera integrated for tracking head movement that is tightly fixed with a headband. The vHIT results were defined as normal if they were within the calculated gain-reference range, mean was normal ±2 standard deviation, and no re-fixation saccades occurred. We collected data on the velocity regression gains (VRGs), number of saccades (overt and covert), average peak velocities of saccades, and caloric asymmetry. The data were statistically analyzed using t-test and ANOVA.

The mean gains for the right ear and left ear of the normal population were both 1.00. The mean right ear gain for the subjects with Meniere's disease was 0.87, and the mean left ear gain was 0.90. Although the differences of the gains between the two populations are statistically significant, both are within the normal range. In normal subjects, no re-fixation saccades were recorded. In subjects with Meniere's disease, 27 subjects had covert saccades recorded and 26 subjects had overt saccades recorded.

In conclusions, gains have been used as diagnostic parameters for Meniere's disease. However, our data show that re-fixation saccades can also be used as diagnostic parameters for Meniere's disease. Further data on average peak velocities of saccades and caloric asymmetry will be analyzed and presented.

Gene Expression and Regulation

PS 395

Comparison of Different Sample Preparation Methods for sNuc-RNASeq of the Adult Stria Vascularis

Shoujun Gu[1]; Rafal Olszewski[1]; Ian Taukulis[1]; Madeline Pyle[1]; Zheng Wei[2]; Daniel Martin Izquierdo[2]; Robert Morell[3]; Michael Hoa[1]
[1]Auditory Development and Restoration, National Institute on Deafness and Other Communication Disorders, NIH; [2]Biomedical Research Informatics Office, National Institute of Dental and Craniofacial Research, NIH; [3]Genomics and Computational Biology Core, National Institute on Deafness and Other Communication Disorders, NIH

The stria vascularis (SV) is located on the lateral wall of the cochlear duct and consists of three main layers, composed predominantly by marginal, intermediate and basal cells, respectively. The SV generates the endocochlear potential (EP) that is necessary for hair cell mechanotransduction. Recently, single cell (sc) and single nucleus (sn) RNA sequencing methods have been shown to be powerful tools for identifying transcriptional heterogeneity between cell types. However, the accuracy of single cell/nucleus RNA sequencing data largely depends on the effectiveness of initial sample preparation steps. In this study, based on our prior knowledge about SV cell type-specific transcriptional profiles, we analyzed the effects of methanol fixation and RNALater on SV cell type profiles using snRNA-Seq from the adult mouse SV. Samples were sequenced using the 10x Genomics Chromium platform, and reads were mapped to GRCm38 (mm10) mouse reference genome. Downstream data analysis was performed using the Scanpy (v1.4) single cell analysis platform. To our knowledge, this is the first study to systematically compare the effects of different sample preparation techniques on snRNA sequencing results. These data will provide guidance for translation of single cell techniques to human tissues, particularly in the auditory system, that may require optimized sample preparation.

PS 396

The ATP-Dependent Chromatin Remodeler CHD7 is Critical for Neuronal Lineage Differentiation by Changing Chromatin Accessibility and Nascent RNA

D Ford Hannum[1]; Hui Yao[2]; Sophie F. Hill[3]; Ricardo D. Albanus[4]; Wenjia Lou[2]; Jennifer M. Skidmore[2]; Gilson J. Sanchez[2]; Alina R. Saiakhova[5]; Stephanie L. Bielas[3]; Peter C. Scacheri[5]; Mats Ljungman[6]; Stephen CJ Parker[7]; **Donna M. Martin**[8]

[1]Department of Computational Medicine and Bioinformatics; Department of Pediatrics;University of Michigan; [2]Department of Pediatrics; University of Michigan; [3]Department of Human Genetics; University of Michigan; [4]Department of Computational Medicine and Bioinformatics; University of Michigan; [5]Department of Genetics and Genome Sciences;Case Western Reserve University; [6]Department of Radiation Oncology; University of Michigan; [7]Department of Computational Medicine and Bioinformatics; Department of Human Genetics; University of Michigan; [8]Department of Pediatrics; Department of Human Genetics; University of Michigan

Background

CHARGE syndrome, a rare congenital multiple anomaly condition, is caused mainly by haploinsufficiency of the ATP-dependent chromatin remodeling enzyme Chromodomain Helicase DNA binding protein 7 (*Chd7*). Brain abnormalities and intellectual disability are commonly observed in CHARGE patients. n addition, neuronal differentiation is reduced in CHARGE patient-derived iPSCs and in conditional knockout mouse brains. However, the underlying mechanisms of *Chd7* function in nervous system development is not well understood.

Methods

Chd7$^{+/+}$ and *Chd7*$^{Gt/Gt}$ (null) embryonic stem cells (ESCs) were derived from sibling blastocysts. Using a previously described protocol, ESCs were differentiated to neural progenitor cells (NPCs) and then further differentiated to neurons and glial cells. Quantitative RT-PCR, cell growth assays, immunostaining, ATAC-sequencing and Bru-sequencing were performed on ESCs and NPCs.

Results

Chd7 expression increased during ESC to NPC and neuronal differentiation, suggesting important roles for *Chd7* in NPCs and neuronal differentiation. Interestingly, loss of *Chd7* did not affect ESC or NPC identity or proliferation, but significantly reduced TUJ1^{+} neurons ($P = 9.7 \times 10^{-4}$) and GFAP^{+} glial cells ($P = 5.8 \times 10^{-9}$) ATAC- and Bru-seq experiments identified transcription factors (*Pax3*, *Tbx3*, *Nkx6-1*, and *Zic5*) with differentially accessible promoter regions and expression in *Chd7*$^{Gt/Gt}$ vs wildtype NPCs. These transcription factors are known to play roles in central nervous system development and neural/glial differentiation.

Conclusion

Chd7 loss does not adversely affect ESCs and NPCs but results in a decrease of differentiated neurons and glial cells. CHD7 has a profound effect on the chromatin landscape in NPCs and genome-wide studies indicate mis-regulated transcription factors in *Chd7*$^{Gt/Gt}$ NPCs. These studies suggest that *Chd7* acts preferentially during the transition of NPCs to neurons and glial cells to promote one or more aspects of differentiation and lineage differentiation.

Supported by NIH R01 DC009410

The Donita B. Sullivan M.D. Research professorship in pediatrics and Communicable Diseases (DMM)

A. Alfred Taubman Medical Research Institute (DMM)

PS 397

"Passenger Gene" Problem in Transgenic C57BL/6 Mice Used in Hearing Research

Jun Suzuki[1]; Hitoshi Inada[2]; Chul Han[3]; Mi-Jung Kim[3]; Ryuichi Kimura[2]; Yusuke Takata[4]; Yohei Honkura[5]; Yuji Owada[6]; Tetsuaki Kawase[7]; Yukio Katori[5]; Shinichi Someya[3]; Noriko Osumi[2]

[1]Department of Otolaryngology-Head & Neck Surgery, Tohoku University Graduate School of Medicine; [2]Department of Developmental Neuroscience, Centers for Neuroscience, Tohoku University Graduate School of Medicine; [3]Departments of Aging and Geriatric Research, University of Florida; [4]Department of Otolaryngology, Tokyo Women's Medical University Medical Center East; [5]Department of Otolaryngology-Head and Neck Surgery, Tohoku University Graduate School of Medicine; [6]Department of Organ Anatomy, Tohoku University Graduate School of Medicine; [7]Laboratory of Rehabilitative Auditory Science, Tohoku University Graduate School of Biomedical Engineering

Despite recent advances in genome engineering technologies, traditional transgenic mice generated on a mixed genetic background of C57BL/6 and 129/Sv mice remain widely used in age-related hearing loss (AHL) research, since C57BL/6 mice exhibit early onset and progression of AHL due to a mutation in cadherin 23-encoding gene (*Cdh23*$^{753G>A}$). In these transgenic mice, backcrossing for more than 10 generations results in replacement of the donor background (129/Sv) with that of the recipient (C57BL/6), so that approximately 99.9% of genes are C57BL/6-derived and are

considered congenic. However, the regions flanking the target gene may still be of 129/Sv origin, creating a so-called "passenger gene problem" where the normal 129/Sv-derived *Cdh23*^{753G} allele can travel with the target gene. This problem is very important to consider because it can lead to misinterpretation of the functional effect of the target gene, which in fact may be caused by passenger genes of the 129/Sv origin. In this study, we initially intended to investigate the role of fatty acid-binding protein 7 (Fabp7), which is important for cellular uptake and intracellular trafficking of fatty acids in the cochlea, using traditional *Fabp7* knockout (KO) mice on the C57BL/6 background. We found that, although *Fabp7* KO mice showed delayed AHL progression and milder cochlear degeneration, the genotype of the *Cdh23* region flanking *Fabp7* was still of 129/Sv origin (*Cdh23*^{753GG}). Our study indicates that researchers should be aware of the passenger gene problem when using traditional transgenic mice generated on the C57BL/6 background with 129/Sv-derived ES cells, because the 129/Sv-derived normal *Cdh23*^{753GG} gene could travel with the target gene in the mice considered as congenic after thorough backcrossing. Therefore, there is a risk that phenotypes attributed to the target gene can actually be caused by tightly-linked flanking loci or even by unlinked loci located in different chromosomes derived from 129/Sv cells.

PS 398

Characterisation of Fibroblasts Derived From an Usher Syndrome Patient with USH2A Gene Mutations and the Subsequent Generation of Induced Pluripotent Stem Cell Lines

Abbie Francis[1]; Sam McLenachan[2]; Sharon Redmond[1]; Fred Chan[2]; Marcus Atlas[1]; Rodney Dilley[1]; **Elaine Y.M. Wong**[1]
[1]Ear Science Institute Australia; [2]Lions eyes institute

A Francis[1], S McLenachan[2,3], ZY Ng[1], SL Redmond[1], FK Chen[2,3,4], MD Atlas[1,3], RJ Dilley[1,3], **EYM Wong***[1,3,5]

1. Ear Science Institute Australia, Nedlands, Western Australia
2. Lions Eye Institute Australia, Nedlands, Western Australia
3. University of Western Australia, Crawley, Western Australia
4. Royal Perth Hospital, Perth, Western Australia
5. Curtin University, Bentley, Western Australia

Background
Mutations in USH2A can cause Usher syndrome type 2A, characterised by congenital hearing loss and progressive vision loss due to retinitis pigmentosa.

Aims
Characterise fibroblast lines derived from patient samples containing USH2A c.949C >A and c.1256 G >T mutations, and healthy controls. Next, generate and characterise iPSC lines.

Methods
Fibroblasts were characterised using viability assays and immunocytochemistry; and reprogrammed to pluripotency using Oct4, Sox2, Lin28, Klf4, and L-Myc with episomal vectors. On Day 25, colonies were selected for clonal expansion and USH2A mutations confirmed using Sanger sequencing. iPSC gene expression was measured using qRT-PCR; protein expression was analysed using immunocytochemistry.

Results
Fibroblast lines had typical elongated morphology, and normal cells had faster growth than patient cells. All iPSC displayed typical growth characteristics and morphologies of pluripotent stem cell colonies. Pluripotency proteins (OCT4, NANOG, SOX2 and SSEA-4) and genes (OCT4, NANOG, SOX2 and KLF4) were expressed similarly in all lines. Trilineage genes (PAX6, DCX, TBXT, AFP, and SOX7) had minimal expression in undifferentiated iPSC and increased expression in embryoid bodies derived from these iPSC.

Conclusion
Development and characterisation of iPSC lines from patients with Usher syndrome represents a unique opportunity to study differences in inner ear development from those of healthy controls.

PS 399

Generation and Correction of P2RX2 c.178G>T mutation in Human and Mouse iPSCs

Aida Nourbakhsh[1]; Zheng-Yi Chen[2]; Zaohua Huang[1]; Nicholas Gosstola[1]; Derek Dykxhoorn Dykxhoorn[1]; Xuezhong Liu[3]
[1]University of Miami Miller School of Medicine; [2]Massachusetts Eye and Ear/Harvard Medical School; [3]University of Miami

Background
Hearing loss affects more than 10% of the human population and over half of the hearing loss is genetically related. Currently, there are no FDA approved pharmacologic therapies for the genetic etiology of human hearing loss and it continues to be well accepted that the ultimate direction of treatment is based on gene and/or cell therapy. The goal of our study is to create a gene therapeutic mechanism using the CRISPR-Cas9 technology in our P2RX2 mouse and

induced pluripotent stem cell (iPSC) model of genetic hearing loss. The P2RX2 gene, encodes a purinergic receptor, an ion channel gated by extracellular ATP and is involved in a variety of cellular functions; including excitatory postsynaptic response in sensory neurons, neuromuscular junction formation, and hearing. In the inner ear, P2RX2, plays a role in regulation of sound transduction, auditory neurotransmission, outer hair cell electromotility, inner ear gap junctions, and K+ recycling. Human P2RX2 mutation follows a dominant pattern of genetic disease of hearing loss.

Methods
The primary mouse fibroblasts carrying P2RX2 mutation were isolated and transduced by four stem cell transcription factors. The iPSC line was then confirmed by stem cell markers: SOX2, Nanog, TRA-1-60, OCT4 and SSEA4. The mutation was further confirmed by sequencing. We also generated human iPSCs hosting P2X2 mutation via normal human iPSCs. The P2RX2 mutation correction was conducted by CRISPR-Cas9 genome editing technology. In brief, Cas9 and guide RNA complex were co-introduced into mouse iPSCs with the homology dependent repair template using electroporation. The correction of mutation was confirmed, before cell cloning, using sequencing.

Results
We successfully isolated primary cells from P2RX2 mutant mouse tail tip and we generated mouse iPS cells using four transcription factors. The established mouse iPSC

showed strong expression of OCT4, SOX2, SSEA4, TRA-1-60, confirming their stem cell characteristic. In addition, we generated a human iPSC line carrying the same mutation. Sequencing confirmed mutations in both types of iPSCs. Finally, we attempted to correct the mutation using CRISPR genome editing technique. Our sequencing results demonstrated that the mutation was rescued using this genome editing technique.

Conclusions
Our results demonstrate that we successfully generated mouse and human iPSCs cell lines that carry P2RX2 mutation and we were able to correct the mutation using CRISPR genome editing technique. This work will provide the foundational platform for future in vivo therapeutic application in both mouse and human models for hearing loss.

PS 400

Conditional Deletion of the RNA-Binding Protein Caprin-1 Leads to Progressive Hearing Loss in Mice.

Lisa S. Nolan[1]; Jing Chen[2]; Ana Cláudia Gonçalves[3]; Emily Towers[4]; Naila Haq[4]; Karen Steel[5]; Jonathan Gale*[6]; Sally Dawson*[7]
*[1]University College London; Current address: King's College London; [2]King's College London; [3]Univeristy College London; [4]University College London; [5]King's College London and Wellcome Trust Sanger Institute; [6]University College London; *equal contributon; [7]University College London; *equal contribution*

Caprin-1 (Cell Cycle Associated Protein 1) is a multifaceted protein. It is an important component of stress granules where it plays a role in the cellular response to stress, and of neuronal RNA granules where it regulates synaptic plasticity and long term memory formation. More recently, it has also been associated with neurodegenerative diseases e.g. Amyotrophic lateral sclerosis. Caprin-1 is a direct target of POU4F3, a POU domain transcription factor which underlies a form of autosomal dominant non-syndromic hearing loss in humans, DFNA15 (Towers et al 2010). Furthermore, Caprin-1-containing stress granules form in OC-2 cells and in *ex-vivo* cochlear explants following various types of cellular stress (e.g. heat-shock and sodium arsenite treatment) and form in hair cells *in-vivo* in response to aminoglycoside treatment.

Stress granules are dynamic, cytoplasmic granules which assemble very early during cellular stress and are thought to act as a checkpoint for untranslated mRNAs; mRNA is silenced or degraded and/or stored for rapid re-initiation of translation once the stress has ended. In this manner, stress granules are considered pivotal in coordinating the cell's resources towards translation of mRNAs that contribute to cellular homeostasis. Our recent work has shown that pharmacological manipulation of stress granules can protect hair cells from aminoglycoside ototoxicity (Gonçalves et al 2019).

In order to understand the role of Caprin-1 in the cochlea we have undertaken a conditional knockout approach in the inner ear. Mice carrying a floxed Caprin-1 allele were crossed with mice carrying SOX10 driving Cre recombinase to generate Caprin1^{tm3d};SOX10-Cre mice. Caprin1^{tm3d};SOX10-Cre mutant mice exhibit elevated auditory brainstem response hearing thresholds at P28 in response to click stimuli and tone pips (3-42kHz) compared to littermate controls. The greatest elevation in auditory thresholds was observed in the mid-high frequency range (24-30kHz). The hearing loss continued

to progress with age; by P210 it included the low-mid frequency range (6-12kHz), with thresholds significantly elevated compared to littermate controls. Additional data showing that the targeted deletion of Caprin-1 also affects the cochlea's response to acoustic trauma will be presented. Taken together, these data suggest that Caprin-1 plays a critical role in cochlear function and homeostasis.

PS 401

Genomic Analysis of Enhancer Identity and Function in Hair Cell Regeneration

Erin Jimenez; Claire Slevin; Shawn Burgess
NHGRI

Millions of Americans experience a hearing or balance disorder due to hair cell damage or loss which negatively impacts quality of life. The hair cells are mechanosensory cells used in the auditory and vestibular organs of all vertebrates and in the lateral line systems of aquatic vertebrates. Hair cells in zebrafish and other non-mammalian vertebrates turn over during homeostasis and regenerate completely after being destroyed or damaged by acoustic or chemical exposure, while in mammals, destroying or damaging hair cells results in permanent impairments to hearing or balance.

Transcriptional profiling experiments on adult zebrafish inner ears following injury have identified ~2,200 genes that are implicated in hair cell regeneration. We have followed up on 254 candidate genes for roles in hair cell regeneration in zebrafish using CRISPR/Cas9 mutagenesis to generate mutants for genes transcriptionally responsive to regeneration. Surprisingly, we found 10 genes responsible for hair cell regeneration. We hypothesize that there are differences in the DNA sequences that regulate how those genes respond during injury/regeneration.

The principle regulatory element of the genome that orchestrates cell type specific gene expression is the enhancer. Studies implicate enhancers in response to tissue damage, raising the possibility that enhancer elements may exist in the zebrafish inner ear in response to hair cell death. Thus, our goal is to identify in vivo the enhancers that are involved in repairing a functional vertebrate inner ear. We are undertaking a three-pronged approach to identify enhancers in the inner ear and in response to hair cell damage. Because physical accessibility of genomic DNA defines the "active" genome, we seek to identify open chromatin locations using the Assay for Transposase Accessible Chromatin with high-throughput sequencing (ATAC-seq), a method for mapping chromatin accessibility genome-wide. Enhancer transcription correlates with outputs from downstream coding genes and may represent the earliest event in gene activation. Therefore, our second approach is to identify genes transcriptionally responsive to regeneration using RNA-seq. Finally, to functionally characterize identified enhancers that are required for regeneration we will employ a genetic screen using CRISPR/Cas9 mutagenesis to generate mutants for identified enhancers. Results from these approaches will a have an important positive impact on our understanding of hair cell regeneration mechanisms and suggest potential therapeutic strategies to stimulate a regenerative response in the mammalian inner ear.

PS 402

The expression of human TMPRSS3 gene in zebrafish

Shunsuke Tarumoto; Youichi Asaoka; Kazuma Sugahara; Yoshinobu Hirose; Makoto Hashimoto; Makoto Seiki; Hiroshi Yamashita
Yamaguchi University

The *TMPRSS3* gene is a member of the Type 2 Transmembrane Serine Protease family and is expressed in inner hair cells, outer hair cells, spiral ganglia and vascular streak. It has been reported that TMPRSS3 is involved in the processing of epithelial sodium channel(ENaC) and potassium ion channels. Clinically, it is a progressive deafness in the form of autosomal recessive inheritance, with DFNB10 showing congenital severe deafness and high-frequency deafness after 10 years of language acquisition. DFNB8, which is supposed to lead to hearing loss, has been reported. We examine the expression site of the gene causing deafness in zebrafish, and creates a knockout zebrafish causing the deafness. We report that the expression of the human *TMPRSS3* gene in zebrafish . The subject was a zebrafish on the fifth days of life, and the method was examined using the *in situ* hybridization method. Human *TMPRSS3* gene is orthologue of *TMPRSS3a* gene and *TMPRSS3b* gene in zebrafish. The primers of *TMPRSS3a* gene and *TMPRSS3b* gene were designed with the first exon respectively. The cDNA of the same gene was amplified by PCR, and it was conformed by electrophoresis that the cDNA was amplified. Then, the cDNA was inserted into the plasmid vector to prepare a sense RNA probe and a antisense RNA probe. The RNA probe incorporated Digoxygenin(DIG), which was recognized by alkaline phosphatase-labeled anti-DIG antibody and detected by color development reaction of alkaline phosphatase substrate with MP purple. A sense RNA probe was used as a control. *In situ* hybridization was performed using the prepared probe on zebrafish on the fifth days after birth. In *TMPRSS3a* gene and *TMPRSS3b* gene, the zebrafish inner ear was stained

with the antisense RNA probe, and the inner ear was not stained with the sense RNA probe. As a result, it was clarified that both *TMPRSS3a* gene and *TMPRSS3b* gene were expressed in the inner ear.

PS 403

The Expression of GDPD3 and its Response to Noise in the Cochlea

Holly J. Beaulac[1]; Patricia M. White[2]
[1]University of Rochester; [2]University of Rochester Medical Center

The prevalence of noise-induced hearing loss (NIHL) continues to increase globally with limited therapeutic options available. By studying the underlying genetic mechanisms of NIHL, our goal is to identify and target genes altered in noise that can be screened to identify and protect individuals with acoustic sensitivities. GDPD3 (Glycerophosphodiester Phosphodiesterase Domain Containing 3) is a protein coding gene with the ability to hydrolyze lysoglycerophospholipids in the creation of lysophosphatidic acid (LPA). GDPD3's activity is calcium-dependent and LPA treatment has previously been shown to attenuate noise damage (Han et al. 2015). It remains unclear whether or not GDPD3 upregulation is important in protection from noise or if its LPA product and subsequent receptor activity are the main drivers for this result. Given its possible role as an acoustic protective factor, we are interested in identifying GDPD3's developmental expression in the cochlea and how it responds to normal levels of noise in our FVB mouse line.

Methods
To establish the time course of GDPD3 cochlear expression, we performed immunohistochemistry at postnatal days 0 (P0), P6, P14, P28, and P60 in Lfng-eGFP/FVB mice. These mice express enhanced GFP in their Pillar and Deiter Cells. Cochleae were sectioned and stained with fluorescent probes to determine GDPD3 colocalization in the subcellular compartments of supporting cells, afferents, efferents, and spiral ganglion neurons (SGNs).

Results
At P0, GDPD3 appeared most prominent in the SGNs, efferents, afferents, and synaptic terminals. By P60, the Pillar and Deiter Cells contained high levels of anti-GDPD3 antibody that colocalized with their actin filaments.

Methods
To determine GDPD3's response to noise in our Lfng-eGFP/FVB mouse strain, we evaluated its expression levels in P28 mice exposed to different acoustic environments. Both males and females underwent testing for ABRs and DPOAEs prior to and following noise exposure. The control group was divided into single-housed cages in an environment with an average loudness of 55-70 dB. The experimental group was single-housed and exposed to noise at 85 dB for 1 hour over five days. The left cochleae were extracted for immunohistochemistry and the right cochleae for qPCR following the fifth day of exposure.

Results
Analysis of GDPD3 levels is ongoing though we expect to see an elevation in the noise-exposed group in agreement with the differential expression levels seen previously in noise-exposed B6 and 129 mouse strains (Gratton et al. 2011).

PS 404

Connexin 26 in Mature Ears Influences Survival of Hair Cells and Neurons

Xiaobo Ma[1]; Jennifer M. Skidmore[2]; Jelka Cimerman[2]; Lisa A. Beyer[3]; Donald L. Swiderski[1]; Lisa Kabara[1]; David F. Dolan[1]; Donna M. Martin[4]; **Yehoash Raphael**[1]
[1]Kresge Hearing Research Institute, Department of Otolaryngology-Head and Neck Surgery, University of Michigan; [2]Department of Pediatrics; University of Michigan; [3]Kresge Hearing Research Institute, Department of Otolaryngology - Head and Neck Surgery, Michigan Medicine, Ann Arbor, MI, USA; [4]Department of Pediatrics; Department of Human Genetics; University of Michigan

The most common form of autosomal recessive hereditary deafness is caused by bi-allelic pathogenic variants in *GJB2*, the gene encoding Connexin 26 (Cx26) protein. Mice with reduced Cx26 show early and extremely severe hearing loss associated with loss of hair cells, supporting cells, and spiral ganglion neurons. In contrast to these mouse phenotypes, humans with *GJB2*-related hearing loss exhibit relatively normal inner ear morphology. These differences in mouse vs. human phenotypes have made it challenging to model human *GJB2*-related deafness in mice. Here, we sought to generate and analyze mice with phenotypes that more closely resemble humans with loss of *GJB2*, in order to elucidate disease mechanisms and develop therapies. Toward that goal, we generated *Sox10CreERT2*;*Gjb2*$^{flox/flox}$ mice in which conditional deletion of *Gjb2* can be induced in non-sensory cells at specific time points. The ability to delete *Gjb2* during development or in the postnatal period permits analysis of its roles at different time points. We report on long term effects of *Gjb2* deletion at postnatal day 14. In these animals, hair cells

survive and appear normal throughout the cochlea until 2 months of age. At 4 months of age, these mice exhibit partial hair cell degeneration involving both inner and outer hair cells, with a base-to-apex gradient. Spiral ganglion neurons are similarly affected, appearing normal at 2 months of age and degenerating in a base-to-apex gradient at 4 months. At 8 months of age, the mice exhibit severe loss of both hair cells and spiral ganglion neurons. We conclude that deletion of *Gjb2* at postnatal day 14 in near-mature ears uncovers important roles for Cx26 in maintenance of the cochlea. These studies help define a critical time period for developing phenotypic rescue approaches.

Supported by NIH-NIDCD grants R01-DC014832, R01-DC010412, R01-DC009410, R01-DC014456 and P30-DC005188. We thank Leda Dimou for the *Sox10iCreERT2* mice.

PS 405

Screened AAV Variants Permit Efficient Transduction Access to Inner Ear Cells for Gene therapy

Yilai Shu[1]; Jinghan Wang[1]; Xinde Hu[2]; Yuanyuan Xue[1]; Hui Yang[2]; Huawei Li[1]
[1]ENT Institute and Otorhinolaryngology Department of the Affiliated Eye and ENT Hospital, State Key Laboratory of Medical Neurobiology, Fudan University; [2]Institute of Neuroscience, State Key Laboratory of Neuroscience, Key Laboratory of Primate Neurobiology, Shanghai Institutes for Biological Sciences, Chinese Academy of Sciences

Objective
Lack of efficient delivery system into mammalian inner ear remains a major barrier for gene therapy. Adeno-associated viral (AAV) vectors have become the significant vector of choice for gene delivery. We report the screen of pseudoserotype vectors including AAV-PHP.eB, AAV-DJ and AAV-8, AAV-9 delivery into mammalian inner ear *in vivo*.

Methods
We packaged different AAVs (AAV-8, AAV-9, AAV-DJ and AAV-PHP.eB, AAV-DJ) that expressing tdTomato and injected them in mice. Three weeks after injection, we performed immunofluorescence analysis in the inner ear. Auditory brainstem response (ABR) thresholds of the inner ear were measured.

Results
We found that AAV-PHP.eB, AAV-8 and AAV-9 achieved infection efficiencies at 100.00%, 98.94% and 98.41% in the apical turn of IHCs respectively. In the middle and basal turn of IHCs, AAV-PHP.eB also achieved very high efficiency (99.07% and 100.00%), while AAV-8 and AAV-9 achieved relatively low efficiencies. Infection efficiencies of OHCs using AAV-8 and AAV-DJ serotypes were minimal. By contrast, AAV-PHP.eB and AAV-9 infected OHCs at 97.48% and 33.62%, respectively. Interestingly, we found that AAV-DJ showed much higher efficiency (52.51%) of SC infection. We also found that both IHCs and OHCs were infected efficiently with only a dose of 3×10^9 vg AAV- PHP.eB and SCs were infected at up to 50% with a dose of 1×10^{10} vg. In addition, tdTomato expression in diverse inner ear cell types including spiral ganglion, spiral ligaments, stria vascularis, spiral limbus in cross-sections study. Hearing was preserved well after infection.

Conclusion
AAV-PHP.B showed the extremely high transduction efficacy on HCs. AAV-DJ demonstrated a high ratio to infect SCs. They are potent viral vectors to achieve genetic agent delivery, holding a great promise for gene therapy approaches to deafness.

PS 406

DYNC1LI1 is required for auditory hair cell development in mice

yuan zhang[1]; renjie chai[2]
[1]Key Laboratory for Developmental Genes and Human Disease,Ministry of Education,Institute of Life Sciences,Southeast University, NanJing, China.; [2]Key Laboratory for Developmental Genes and Human Disease, Ministry of Education, Institute of Life Sciences,Southeast University, NanJing, China

Cytoplasmic Dynein 1 is important for intracellular transport, such as membrane trafficking, organelle positioning, and microtubule organization. DYNC1LI1 is a critical binding subunit of cytoplasmic Dynein 1. However, studies on DYNC1LI1 in mammals are currently limited. In this study, we investigated the possible roles of DYNC1LI1 in the cochlea of mice. We first studied the expression pattern of DYNC1LI1 at different development stages of wild type mice cochlea. We found that high DYNC1LI1 expression in hair cell which indicates its important roles in hair cell. Then we used DYNC1LI1 gene knockout mice to investigate its effects on hearing of mice. The results showed that ablation of DYNC1LI1 results in early-onset progressive hair cell and hearing loss of mice. Besides, loss of DYNC1LI1 led to reduced intracellular transportation and impairs the clearance of autophagosome which in turn led to hair cell apoptosis. Further study reveals that loss of DYNC1LI1 may destabilize dynein complex and alters the normal subcellular function of dynein in hair

cells. Our studies demonstrate that DYNC1LI1 plays an important role in the autophagosome clearance process and is required for hair cell development and survival.

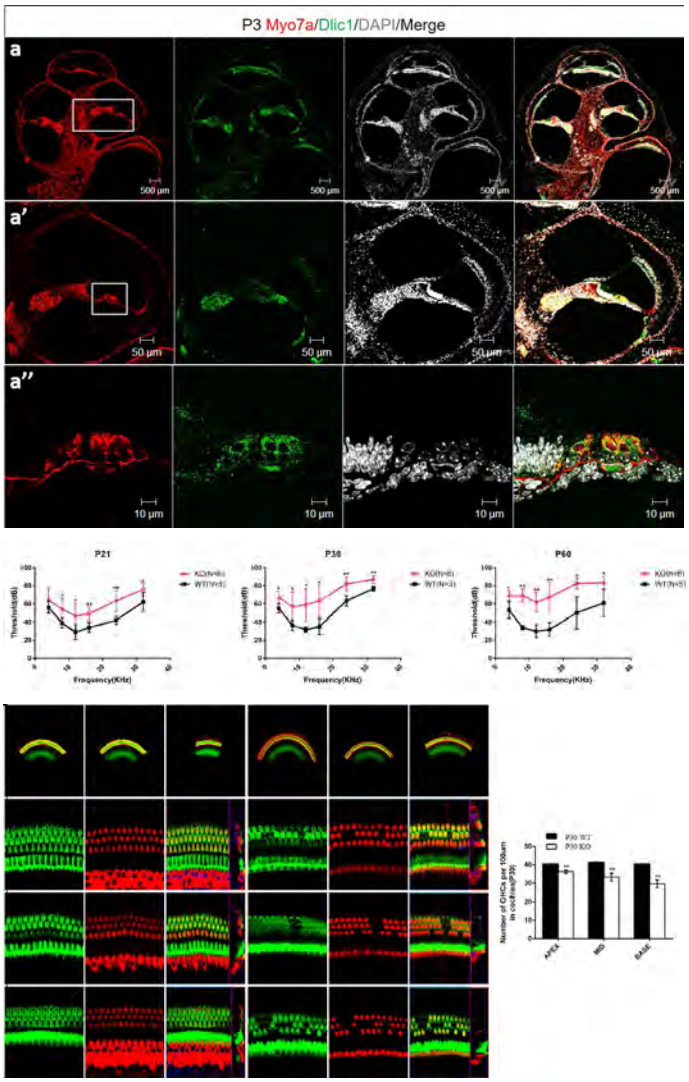

PS 407

The Genetics of Variation of The Wave 1 Amplitude of The Mouse Auditory Brainstem Response

Ely Cheikh Boussaty[1]; Danielle Gillard[1]; Joel Lavinsky[2]; Pezhman Salehi[3]; Juemei Wang[4]; Amanda L Crow[5]; Aline Mendonça[2]; Hooman Allayee[5]; Uri Manor[6]; Rick A Friedman[1]

[1]University of California, San Diego; [2]Federal University of Rio Grande do Sul; [3]Creighton University, School of Medicine; [4]USC Caruso Department of Otolaryngology - Head and Neck Surgery; [5]University of Southern California; [6]Salk Institute for Biological Studies

Introduction

This is the first genome-wide association study with the Hybrid Mouse Diversity Panel (HDMP) to define the genetic landscape of the variation in the suprathreshold wave 1 amplitude of the auditory brainstem response (ABR) both pre- and post-noise exposure. This measure is correlated with the density of the auditory neurons (AN) and/or the compliment of synaptic ribbons within the inner hair cells of the mouse cochlea.

Methods

We analyzed suprathreshold ABR for 635 mice from 102 HMDP strains pre- and post-noise exposure (108 dB 10 kHz octave band noise exposure for two hours) using auditory brainstem response (ABR) wave 1 suprathreshold amplitudes as part of a large survey. Genome-wide significance levels for pre- and post-exposure wave 1 amplitude across the HMDP was performed using FaST-LMM. Synaptic ribbon counts (Ctbp2 and mGluR2) were analyzed for the extreme strains within the HMDP.

Results

ABR wave 1 amplitude varied across all strains of the HMDP with differences ranging between 2.42 and 3.82-fold pre-exposure and between 2.43 and 7.5-fold post-exposure with several tone burst stimuli (4 kHz, 8 kHz, 12 kHz, 16 kHz, 24 kHz, and 32 kHz). Immunolabeling of paired synaptic ribbons and glutamate receptors of strains with the highest and lowest wave 1 values pre- and post-exposure revealed significant differences in functional synaptic ribbon counts. Genome-wide association analysis identified genome-wide significant threshold associations on chromosomes 3 (24 kHz; JAX00105429; p< 1.12E-06) and 16 (16 kHz; JAX00424604; p< 9.02E-07)prior to noise exposure and significant associations on chromosomes 2 (32 kHz; JAX00497967; p< 3.68E-08)and 13 (8 kHz; JAX00049416; 1.07E-06) after noise exposure. In order to prioritize candidate genes we generated cis-eQTLs from microarray profiling of RNA isolated from whole cochleae in 64 of the tested strains.

Conclusions

This is the first report of a genome-wide association analysis, controlled for population structure, to explore the genetic landscape of suprathreshold wave 1 amplitude measurements of the mouse ABR. We have defined two genomic regions associated with wave 1 amplitude variation prior to noise exposure and an additional two associated with variation after noise exposure.

Keywords: GWAS; HMDP; NIHL; eQTL;

PS 408

Investigating the effects of exonic and intronic variants of NF2 on pre-mRNA splicing

Masaru Noguchi[1]; Masato Fujioka[2]; Naoki Oishi[3]; Hideki Mutai[4]; Kiyomitsu Nara[4]; Tatsuo Matsunaga[4]; Kaoru Ogawa[2]; **Koichiro Wasano**[4]

[1]Hino Municipal Hospital; [2]Department of Otolaryngology, Head and Neck Surgery, School

of Medicine, Keio University; [3]Department of Otolaryngology-Head and Neck Surgery, Keio University School of Medicine; [4]National Institute of Sensory Organs, National Hospital Organization Tokyo Medical Center

Neurofibromatosis type II (NF2; MIM# 607379) is caused by dominantly inherited mutations of *NF2*, mapped on chromosome 22q12, which encodes a cytoskeletal protein neurofibromin-2 (also called merlin or schwannomin). It is generally understood that truncated *NF2* variants are often associated with severe NF2, whereas non-truncated variants are associated with the milder form of NF2. Our recent genetic screen found that two *NF2* variants, c.357_359del, and c. 516+1G >A, are associated with mild NF2 with bilateral acoustic neurinoma. The c.357_359del variant causes an in-frame deletion within exon 3, which may affect an exonic splicing regulatory element that regulates splicing of pre-mRNA (Human splicing finder ver.3.1). The c. 516+1G >A variant disrupts the donor site of exon 5, and thus is predicted to induce mis-splicing after exon 5 (inclusion of the intronic mRNA after exon 5) (Human Splicing Finder, ver.3.1). Therefore, these *NF2* variants may truncate neurofibronmin-2 despite their association with the mild form of NF2.

In order to determine if these *NF2* variants indeed truncate neurofibronmin-2 by disrupting splicing of pre-mRNA splicing, we performed in vitro splicing assay. Briefly, mini-gene constructs containing an exon 3 (123-bp) or exon 5 (69-bp) of NF2 were created in a pET01 vector for wild-type (WT), c.357_359del, and c. 516+1G >A, and introduced to HEK293T cells. After 40-48 hrs post transfection, the transcripts were extracted, reverse transcribed, and amplified by PCR to see if the exons are correctly spliced.

Contrary to the in silico predictions, we found that exon 3 harboring c.357_359del is normally spliced, and that c. 516+1G >A results in skipping of the entire exon 5. Since the exonic deletions induced by c.357_359del, and c. 516+1G >A are in-frame deletions of 3-bp and 69-bp, respectively, these *NF2* variants would not truncate neurofibronmin-2. These results are in line with the preceding observation that non-truncated *NF2* variants are often associated with mild NF2. This study underscores the importance of experimentally characterizing the functional consequences of disease-associated genetic variants.

PS 409

Serum activity of MMP9 and functional polymorphism of MMP9 and BDNF as potential biomarkers of neuroplasticity in prelingual deafness treatment with cochlear implantation

Monika Matusiak[1]; Anita Obrycka[1]; Emilia Rejmak-Kozicka[2]; Leszek Kaczmarek[2]; Henyk Skarzynski[1]
[1]Institute of Physiology and Pathology of Hearing; [2]Nencki Institute of Experimental Biology

Treatment of congenital deafness with neural prostheses allows for effective acquisition of language skills, however considerable interindividual differences among implantees exist. To date, very little or nothing is known about determinants of linguistic proficiency development, other than the age of implantation, in children without comorbidities. Genetic biomarkers of neuroplasticity in prelingually deaf children treated with cochlear implantation could facilitate their clinical management, especially rehabilitation, giving higher chances for development of robust proficiency of the spoken language. We investigated whether the carrying of certain variants of genes encoding matrix metalloproteinase MMP-9 and BDNF and serum level of MMP9 at CI activation is a prognostic marker of auditory skills acquisition outcome.

Method
We performed a prospective analysis of serum activities of MMP9 at activation, 1, 5, 8, 18 and 24 months follow up in the group of 70 children, diagnosed with bilateral profound sensory-neural non-syndromic hearing loss, aged below 2, treated with unilateral cochlear implantation. The analysis of functional variants of MMP9 (RS 3918242, -1562 C/T, known to affect MMP-9 gene expression levels) and rs6265 of BDNF (Val/Met, known to affect the protein function) was performed. We studied associations between serum activities of MMP9 in the aforementioned intervals and auditory development of implanted children and associations between the carrying of relevant variants of MMP9 and BDNF and their auditory development. Language acquisition was assessed with Little Ears Questionnaire in the same follow up intervals.

Findings
Multiple regression model shows that carriers of C/C of rs 3918242, score on average 3,6 points higher in LEAQ than carriers of C/T when implanted above 1 yo. We haven't found any statistically significant relation for variants of rs6265 of BDNF. Correlation analysis shows that there is a statistically significant relationship between the level of serum activity of MMP9 and LEAQ score in 18 months follow up (rho=-0.69, p= 0,060)

Conclusion
C/C of MMP9 predisposes their deaf carriers to better response to a sensory stimulation up to 24 months post-CI activation than carriers of the other variant of MMP9. A low serum level of MMP9 activity at CI activation predisposes deaf children to better response to a sensory stimulation in the first 24 months after CI activation. Further studies should address certain variant potential biomarker value of those genetic variants as well as, the possible functional role of MMP9 and BDNF in neuroplasticity evoked by cochlear implantation.

Funding: National Centre of Science grant NCN UMO 2013/14/D/NZ5/03337

PS 410

Investigating the effects of exonic single nucleotide variants of SLC26A4 on pre-mRNA splicing

Koichiro Wasano[1]; Takashi Kojima[2]; Satoe Takahashi[2]; Hideki Mutai[1]; Tatsuo Matsunaga[1]; Kazuaki Homma[2]
[1]National Institute of Sensory Organs, National Hospital Organization Tokyo Medical Center; [2]Northwestern University, Feinberg School of Medicine

SLC26A4 encodes an anion transporter, pendrin, which is essential for normal inner ear function. Currently, over 500 *SLC26A4* variants are reported to be associated with Pendred syndrome (PDS, OMIM 274600) or nonsyndromic hereditary sensorineural hearing loss with enlarged vestibular aqueduct (DFNB4, OMIM 600791). Most of these variants are exonic and classified as missense variants. Thus, functional consequences of these variants are typically examined using full-length recombinant *SLC26A4* proteins harboring the missense changes. However, it is possible that these exonic variants can disrupt posttranscriptional gene regulation, which represent a distinct pathological mechanism that requires different mode of intervention.

In this study, we performed in vitro splicing assay to examine whether exonic single nucleotide variants in *SLC26A4* affects pre-mRNA splicing. To do so, mini-gene constructs containing one or two human pendrin exons were created in a pET01 vector for wild-type (WT) and 33 exonic single nucleotide variants and introduced to HEK293T cells. After 40-48 hrs post transfection, the transcripts were extracted, reverse transcribed, and amplified by PCR to see if the exons are correctly spliced. As a positive control, c.919-2A >G intronic *SLC26A4* variant with known pathogenic effect on splicing was included. We also performed the splicing assay for the c.601-1G >A and c.1707+5G >A intronic *SLC26A4* variants, which are predicted to be pathogenic. We found exon skipping for the c.919-2A >G variant, confirming the ability of this in vitro assay to detect abnormal splicing. We also found splicing defects for c.601-1G >A and c.1707+5G >A, suggesting that these two intronic variants are pathogenic as well. Among 33 exonic *SLC26A4* variants, p.G131V (c.392G >T) and p.G334V (c.1001G >T) were found to disrupt normal splicing. Interestingly, p.G334V variant exhibited WT-like transport activity, while aberrant splicing would result in a truncated product, which is likely a functional null.

Taken together, our results underscore the importance of experimentally determining the effects of exonic single nucleotide variants on pre-mRNA splicing to determine their pathogenicity, especially for functional and/or synonymous variants. Combined with functional analyses of the protein products, our comprehensive approach will help guiding future therapeutic approaches for individual cases of *SLC26A4* variants.

PS 411

Constructing and Exploring Regulatory Networks of miR-96 in the Inner Ear

Morag Lewis[1]; Maria Lachgar[2]; Miguel Angel Moreno Pelayo[2]; Karen Steel[1]
[1]King's College London and Wellcome Trust Sanger Institute; [2]Hospital Universitario Ramón y Cajal and IRYCIS and CIBERER

Progressive hearing loss is a very common sensory deficit among the global human population, and has a strong genetic component, but although many of the genes underlying hearing have been identified, many more remain unknown and, crucially, so do the molecular interactions in which those genes are involved. It is not only important to discover new genes involved in deafness, it is also critical that we improve our understanding of the transcription and interaction networks associated with pathology, both in order to better understand the inner ear and to find generic therapeutic targets which may serve to prevent hearing loss.

The microRNA miR-96 is a transcriptional regulator which controls hair cell maturation. Mice and humans carrying mutations in *Mir96* all develop hearing loss, but different mutations result in different physiological, structural and transcriptional phenotypes. We have studied mice with four different *Mir96* mutant alleles; one ENU-induced point mutation, one null allele, and two point mutations which were first identified as underlying progressive hearing loss in humans. Here we present transcriptome analyses from the organs of Corti of mice carrying these alleles. Many genes are misregulated in

more than one mutant, but identifying the regulatory links between these genes and miR-96 is not straightforward. We have chosen several complementary approaches to construct and explore networks controlled by miR-96 using these transcriptional datasets, including literature-based regulatory networks, protein-protein interaction networks and gene set enrichment analysis. The resulting networks offer multiple hypotheses, some of which we have tested using methods such as immunohistochemistry and qPCR.

Through building and exploring the regulatory networks controlled by miR-96, we aim to determine the critical genes and pathways underlying hearing impairment due to *Mir96* mutations, to discover novel deafness genes, and ultimately to identify candidate therapeutic targets.

PS 412

CACHD1-Deficient Mice Exhibit Hearing and Balance Deficits Associated with a Disruption of Calcium Homeostasis in the Inner Ear

Cong Tian[1]; Jaclynn M. Lett[2]; Robert Voss[2]; Alec N. Salt[2]; Jared J. Hartsock[3]; Kevin Ohlemiller[4]; Kenneth R. Johnson[5]
[1]Creighton University; [2]Washington University in St. Louis; [3]Washington University School of Medicine, St. Louis, MO, USA; [4]Washington University School of Medicine; [5]The Jackson Laboratory

CACHD1 recently was shown to be an β2β-like subunit that can modulate the activity of some types of voltage-gated calcium channels, including the low-voltage activated, T-type Ca_V3 channels. CACHD1 is widely expressed in the central nervous system but its biological functions and relationship to disease states are unknown. Here, we report that mice with deleterious *Cachd1* mutations are hearing impaired and have balance defects, demonstrating that CACHD1 is functionally important in the peripheral auditory and vestibular organs of the inner ear. The vestibular dysfunction of *Cachd1* mutant mice, exhibited by leaning and head tilting behaviors, is related to a deficiency of calcium carbonate crystals (otoconia) in the saccule and utricle. The auditory dysfunction, shown by ABR threshold elevations and reduced DPOAEs, is associated with reduced endocochlear potentials and increased endolymph calcium concentrations. Paintfills of mutant inner ears from prenatal and newborn mice revealed dilation of the membranous labyrinth caused by an enlarged volume of endolymph. These pathologies all can be related to a disturbance of calcium homeostasis in the endolymph of the inner ear, presumably caused by the loss of CACHD1 regulatory effects on voltage-gated calcium channel activity. *Cachd1* expression in the cochlea appears stronger in late embryonic stages than in adults, suggesting an early role in establishing endolymph calcium concentrations. Our findings provide new insights into CACHD1 function and suggest the involvement of voltage-gated calcium channels in endolymph homeostasis, essential for normal auditory and vestibular function.

PS 413

The Shared Genetic Program of the Peripheral and Central Auditory Systems Using Transcriptomics

Mor Bordeynik-Cohen[1]; Constanze Krohs[2]; Naama Messika Gold[1]; Ran Elkon[1]; Hans Gerd Nothwang[2]; Karen B. Avraham[3]
[1]Tel Aviv University; [2]Carl von Ossietzky University; [3]Department of Human Molecular Genetics & Biochemistry, Faculty of Medicine and Sagol School of Neuroscience, Tel Aviv University, Tel Aviv, Israel

The auditory system is comprised of the peripheral and the central auditory subsystems. The former receives the sound signals and transforms them into mechanical movements and afterwards into electrical signals. The latter is in charge of processing the signals and sound perception. The main component of the peripheral subsystem is the organ of Corti, containing the sensory cells of hearing, the hair cells. The superior olivary complex (SOC) in the brainstem is involved in primary assessment of the sound, including sound localization. We suggest that the same genetic mechanisms will affect both parts of the auditory system. Support for this hypothesis can be found in thirteen peripheral deafness genes that are implicated in central auditory processing, and in SOC temporal gene expression analysis, which revealed enrichment of known deafness-associated genes (Ehmann et al, *J Biol Chem* 2013). We have now compared the differential expression between tissues of the peripheral and central hearing subsystems at different developmental stages. Twelve microRNAs (miRNA) previously identified in the organ of Corti, were also shown to be expressed in the SOC and both auditory and non-auditory cortex at E16, P0, and P30 using TaqMan microRNA assays. To further characterize and compare the transcriptomes of the organ of Corti and the SOC at E16, P0 and P16, we are using high-throughput sequencing to capture mRNAs, long non-coding RNAs (lncRNA) and miRNA. Thus far, bioinformatics analysis for the SOC demonstrates that out of approximately 3500 genes, about 1600 are differentially expressed between P0 and E16 and about 2400 are differentially expressed between P0 and P16 (using Limma-voom, FDR = 0.0001, |FC| > 2). Genes were divided between patterns of changed expression, most of which show continuous changes of expression, towards up or down regulation during development. Functional gene ontology (GO) analysis demonstrates

enrichment of different ion transport, lipid metabolism and myelination in the continuous 'up' gene group, while in the continuous 'down' gene group, processes of DNA arrangement, cell cycle and division are enriched. The analysis demonstrates the power of high-throughput and unbiased expression profiling to reveal relevant biological processes. Understanding common genetic pathways may provide a key for customized precision medical treatment of hearing loss in the future.

PS 414

Characterization of a Prestin Mouse Model Carrying the p.R130S Missense Variant

Satoe Takahashi[1]; Yingjie Zhou[2]; Mary Ann Cheatham[3]; Kazuaki Homma[1]
[1]Northwestern University, Feinberg School of Medicine; [2]Northwestern University, Dept. Communication Sciences and Disorders; [3]Northwestern University

SLC26A5 (prestin) is an outer hair cell (OHC)-specific membrane protein that confers voltage-dependent somatic electromotility. Despite its importance for the sensitivity and frequency selectivity of mammalian hearing, only a few deafness-associated SLC26A5 variants have been reported. Of those, p.R130S (c.390A >C) and p.W70X (c.209G >A) SLC26A5 variants werefound in two compound heterozygous Japanese patients with moderate to severe hearing loss (Mutai et al., 2013). While the W70X nonsense variant is most likely a functional null, our previous in vitro examination of R130S-prestin revealed its potentially pathogenic effects on membrane targeting, motor kinetics, and transport activity (Takahashi et al., 2016). These observations warranted further investigation in vivo to definitively assess the pathogenicity of R130S-prestin. To this end, we generated an R130S-prestin knock-in mouse model using CRISPR/Cas9. After several rounds of backcrossing to wild-type (WT) FVB mice, we measured distortion product otoacoustic emissions (DPOAEs) of littermates from heterologous breeding pairs to evaluate their hearing at f2 frequencies ranging from 2 to 47 kHz. Auditory brainstem responses (ABRs) were also acquired. By one month of age, R130S-prestin homozygous mice exhibited significantly elevated ABR and DPOAE thresholds across frequency, while their heterozygous littermates did not. Immunofluorescence using a custom prestin antibody (Zheng et al., 2005) confirmed lateral membrane localization of R130S-prestin in homozygotes with minimal OHC loss at P42. Electromotility and its electrical signature, nonlinear capacitance (NLC), were clearly detectable in OHCs isolated from R130S-prestin homozygotes although their magnitudes were reduced compared to WT littermates. In order to recapitulate the R130S/W70X compound heterozygosity of the two patients, we crossed the R130S-prestin mice with a prestin-knockout (KO) (Liberman et al., 2002). The R130S/KO compound heterozygous (cHet) mice also showed significantly elevated DPOAE thresholds across the mouse audiogram at onemonth of age. Although R130S-prestin was detected in the lateral membranes of OHCs in cHet mice, the OHCs appeared shorter in length and showed fragility reminiscent of OHCs lacking prestin protein (prestin-KO). OHC loss was also found at P42 in cHet mice, but only in the high-frequency region of the cochlea. Although NLC and electromotility were observed, both were diminished in OHCs harvested from cHet mice.

Our results demonstrate that the R130S missense variant is indeed a disease-causing allele of SLC26A5. Further study will provide insights into how prestin contributes to mammalian cochlear amplification.

This work is supported by DC017482 (NIDCD) and the Knowles Hearing Center.

PS 415

KCNQ4 variants lacking the C-terminal cytosolic domain are cytotoxic

Takashi Kojima[1]; Koichiro Wasano[2]; Satoe Takahashi[1]; Kazuaki Homma[1]
[1]Northwestern University, Feinberg School of Medicine; [2]National Institute of Sensory Organs, National Hospital Organization Tokyo Medical Center

KCNQ4 (Kv7.4) is a homotetrameric voltage-gated potassium channel abundantly expressed in the basal membrane of the outer hair cells (OHCs). Sound-induced depolarization of OHCs activates KCNQ4, which plays a major role in subsequent repolarization and effusion of potassium ions to maintain ionic homeostasis of OHCs. Currently, over forty KCNQ4 variants associated with a progressive form of nonsyndromic sensorineural hearing loss (DFNA2) have been identified. Since tetramerization is essential for the function of KCNQ4, dominant-negative effect is often considered to explain the dominant inheritance of most KCNQ4 variants. Three truncated KCNQ4 variants, p.Q71fs (c.211delC), p.W242X (c.725G >A), and p.A349fs (c.1044_1051del8), lack the entire C-terminal cytosolic domain that mediates tetramerization. Since they should not be able to impose dominant negative effect on the wild-type (WT) KCNQ4 subunit, less severe hearing phenotype owing to haploinsufficiency would be anticipated in patients with these variants. In fact, hearing loss found in patients with heterozygous p.Q71fs (c.211delC) is moderate. However, patients with heterozygous p.W242X (c.725G >A) suffer

severe hearing loss. Furthermore, hearing is normal in patients with heterozygous p.A349fs (c.1044_1051del8), i.e., this variant is recessively inherited unlike the other KCNQ4 variants. Due to these perplexing observations, we sought to investigate an alternative pathological mechanism not based on dominant negative effect or haploinsufficiency, and hypothesized that mere expression of these truncated KCNQ4 variants may impair the viability of OHCs. In order to explore this possibility, we established HEK293T-based stable cell lines that express WT-, p.Q71fs-, p.W242X-, or p.A349fs-KCNQ4 in a doxycycline-dependent manner. The cytotoxicity of these KCNQ4 constructs was assessed using CellToxTM Green Cytotoxicity Assay kit (Promega) in Synergy Neo2 plate reader (BioTek). We found that all three truncated KCNQ4 variants, but not WT KCNQ4, indeed show cytotoxicity in varying degrees, which positively correlates with the severity of hearing loss found in patients with these KCNQ4 variants. We also confirmed that none of these truncated KCNQ4 variants binds to WT KCNQ4 subunit using stable cell lines co-expressing RFP-tagged WT-KCNQ4 and GFP-tagged truncated KCNQ4 variants. The recessive inheritance of p.A349fs and its inability to form a functional channel by itself or with the WT subunit suggest that just one copy of WT KCNQ4 allele is sufficient for maintaining normal inner ear function. Taken together, our results underscore the importance of assessing cytotoxicity for other KCNQ4 variants, and suggest that targeted silencing of a mutated KCNQ4 allele may generally be applicable for DFNA2 treatment. This work is supported by DC017482 (NIDCD).

PS 416

The Genetic Background of Mice Plays a Role in the Severity of TECTA-Related Hearing Loss

A. Monique Weaver[1]; Kevin T. Booth[2]; Hela Azaiez[3]; Richard J.H. Smith[4]
[1]Molecular Otolaryngology & Renal Research Labs, Department of Otolaryngology—Head and Neck Surgery, University of Iowa Carver College of Medicine; Interdisciplinary Graduate Program in Genetics; [2]Molecular Otolaryngology & Renal Research Labs, Department of Otolaryngology—Head and Neck Surgery, University of Iowa Carver College of Medicine; Department of Neurobiology, Harvard Medical School, Harvard University; [3]Molecular Otolaryngology and Renal Research Laboratories, Department of Otolaryngology—Head and Neck Surgery, Carver College of Medicine, University of Iowa; [4]Molecular Otolaryngology and Renal Research Laboratories, Department of Otolaryngology—Head and Neck Surgery, Carver College of Medicine, University of Iowa; Interdepartmental PhD Program in Genetics, University of Iowa

Mutations in the gene *TECTA* have been shown to cause both autosomal dominant and autosomal recessive non-syndromic hearing loss (ADNSHL or ARNSHL). *TECTA* encodes for alpha-tectorin, the major non-collagenous component of the tectorial membrane (TM) in the inner ear. Preliminary data in our lab have shown ethnically-based differences in audioprofiles from patients with mutations in *TECTA* suggesting that either genetic or environmental factors may modify the expected hearing loss. To assess the contribution of genetic modifiers, we compared mutant mice with missense mutations in *TECTA* across different genetic backgrounds. Four strains of mice, *Tecta*^{C1619S} on FVB/NJ and CBA/J backgrounds and *Tecta*^{C1837G} on FVB/NJ and C57BL/6 backgrounds were used. Auditory brainstem response (ABR) measurements were recorded in wild type and heterozygous animals from all four strains at four weeks of age. Results showed a significant difference in hearing thresholds for different mutations across different backgrounds. We also observed significant hearing thresholds differences between *Tecta*^{C1837G} and *Tecta*^{C1619S} variants suggesting domain specific effects on hearing threshold. Identifying genetic modifiers of recognized deafness-associated genes will help in designing personalized molecular therapies relevant to specific genetic backgrounds.

PS 417

Single Nucleus Sequencing of the Mouse Cochlea with Cisplatin Treatment

Erica C. Sadler[1]; Soumya Korrapati[2]; Ian Taukulis[3]; Madeline Pyle[2]; Rafal Olszewski[3]; Katharine Fernandez[1]; Zheng Wei[4]; Erich Boger[5]; Robert Morell[6]; Michael Hoa[3]; Lisa L. Cunningham[1]
[1]Laboratory of Sensory Cell Biology, NIDCD, NIH; [2]Auditory Development and Restoration Program, NIDCD, NIH; [3]Auditory Development and Restoration, National Institute on Deafness and Other Communication Disorders, NIH; [4]Biomedical Research Informatics Office, National Institute of Dental and Craniofacial Research, NIH; [5]Genomics and Computational Biology Core, NIDCD, NIH; [6]Genomics and Computational Biology Core, National Institute on Deafness and Other Communication Disorders, NIH

Background

The anti-cancer drug cisplatin is ototoxic and causes hearing loss in many treated patients. Our lab has developed a mouse model of cisplatin-induced hearing loss that utilizes three cycles of cisplatin treatment. We have previously shown that this model results in hearing loss that is similar to cisplatin-induced hearing loss observed clinically. We used single-nucleus RNA sequencing (snRNA-Seq) to analyze gene expression in cells of the adult mouse cochlea after the first cycle of cisplatin treatment. This timepoint allowed us to observe

the transcriptional responses of hair cells prior to the onset of hair cell death.

Method

We performed snRNA-Seq on the 10x Genomics Chromium platform to obtain gene expression data from cochlear cells before and after cisplatin treatment. We prepared nuclei from both whole cochleae and microdissected cochleae in which the organ of Corti was dissected away from the surrounding tissue. A single cycle of cisplatin treatment consisted of four days of cisplatin administration at 3mg/kg, and cochleae were collected one day after completion of treatment. All experiments utilized CBA/J mice aged P30-P32 at the time of cochleae collection. Sequencing data were analyzed and clustered using R packages including Seurat and DoubletDecon. Multiple trials of the same condition were integrated following computational removal of cell doublet transcriptome profiles. Gene regulatory networks were examined using the SCENIC package.

Results

Control cochleae revealed a distinct hair cell cluster, expressing known hair cell markers, including Ptprq, Ano4, and Dnm3, significantly more than other clusters of nuclei. Inner and outer hair cells clustered together rather than forming unique clusters. Strial and immune cell markers were present in multiple clusters, suggesting our analysis separated distinct strial and immune cell types. Preliminary data from cisplatin-treated mice reveal hair cell, stria vascularis, and immune cell markers suggesting the presence of these same cell types.

Conclusions

Our data suggest that cochlear hair cells can be successfully captured, sequenced, and clustered from P30 mice using 10X Genomics single-nucleus sequencing methods. Integration of multiple experiments including hair cell captures enables identification of hair cell clusters using known hair cell gene expression. Future directions include analysis of gene regulatory networks, additional cisplatin-treated sequencing experiments, and cluster validation using RNAScope.

This work was supported by the NIDCD Division of Intramural Research.

PS 418

Partial Vestibular Deficit after Cx26 Deletion in Mice

Xiaobo Ma[1]; Jennifer M. Skidmore[2]; Donald L. Swiderski[1]; Donna M. Martin[2]; **Yehoash Raphael**[1]
[1]Kresge Hearing Research Institute, Department of Otolaryngology-Head and Neck Surgery, University of Michigan; [2]Departments of Pediatrics and Human Genetics, University of Michigan

Many deafness mutations also affect vestibular function because the same genes play key roles in the development or function of auditory and vestibular epithelia. A prominent exception is the *GJB2* gene that encodes the gap junction protein connexin26 (Cx26): patients with *GJB2* mutations often have profound hearing loss with little or no vestibular deficiency. To provide a model for human patients with *GJB2* mutations, we generated mice with tamoxifen inducible *Sox10iCre*-mediated loss of *Gjb2* (*Sox10iCreERT2;Gjb2*$^{flox/flox}$). Tamoxifen inducible constructs provide control over the timing of gene deletion, allowing investigation of temporal changes in the role of a gene. We used this approach to investigate the role of *Gjb2* in maintenance of function after completion of development. Tamoxifen was administered at post-natal day (p) 21 to induce *Gjb2* deletion after development of the inner ear was complete. Consequences of the loss of gene function were evaluated by comparing mice with the deletion to age matched controls. Vestibular function was quantitatively assessed using the rotarod test at 1 and 2 months after tamoxifen injection, then the organ of Corti and the vestibular sensory epithelia were stained to visualize Cx26 and hair cells (HCs). Some *Sox10iCreERT2;Gjb2*$^{flox/flox}$ mice treated with tamoxifen at p21 had measurable reduction of vestibular function at 1 month after deletion (shorter times in the rotarod test) and all had measurable reduction of function two months after deletion, even though the functional impairment was not visually apparent during free movement. Histological examination revealed that Cx26 was usually reduced but was not completely eliminated in both auditory and vestibular epithelia, and some mice showed no apparent reduction of Cx26. Similarly, there was variable HC loss in the organ of Corti and in the vestibular organs. These results suggest that Cx26 production is necessary for maintenance of vestibular function in adult animals, but that it may not be as important for vestibular function as it is for hearing. The contrasting effects of *Gjb2* deletion on the vestibular and auditory systems may reflect differences between them in the compensatory roles of other connexins or other mechanisms of intercellular communication.

Supported by NIH-NIDCD grants R01-DC014456 and P30-DC005188, The Donita B. Sullivan M.D. Research Professorship in Pediatrics and Communicable Diseases (DMM) and The R. Jamison and Betty Williams Professorship (YR). We thank Leda Dimou for the *Sox10iCreERT2* mice.

PS 419

Long-Term Expression Stability of Anc80L65-Containing Virus Infected Hair Cells in the USH1C Mouse Model

Weinan Du[1]; Gwenaelle S. Geleoc[2]; Aizhen Zhang[1]; Tianwen Chen[3]; Jun Huang[4]; Hong Zhu[5]; Wu Zhou[5]; Qingyin Zheng[1]
[1]Department of Otolaryngology- Head & Neck Surgery, Case Western Reserve University, Cleveland, Ohio, USA; [2]Boston Children's Hospital & Harvard Medical School; [3]Department of Otolaryngology University of Mississippi Medical Center; [4]Department of Otolarynogology University of Mississippi Medical Center; [5]University of Mississippi Medical Center

Usher syndrome type 1C (USH1C) is characterized by profound sensorineural deafness, vestibular dysfunction and childhood onset of retinitis pigmentosa. We generated an Anc80L65::Harmonin B1 virus to introduce a fully functional harmonin B1 protein into the hair cells in the USH1C knockout mice to restore the function.

To investigate the long-term expression stability of this virus in the hair cells, virus was injected into the USH1C (-/-) model mice at postnatal p2-5. The hearing function was evaluated by auditory brainstem response (ABR) measurement; general motor and balance function were evaluated by swim test and circling count and open field test. The mice were assessed up to 16 months of ages.

The USH1C (-/-) mice with Anc80L65::Harmonin B1 virus gene therapy exhibited a stable but slightly decreased hearing, while rescue in circling behavior and swimming capability was stable. Since rescue in balance function was more permanent than that in hearing function, expression of the Harmonin B1 in vestibular hair cells likely does not decrease over time in the vestibular hair cells comparing to the cochlear hair cells.

We also found the female USH1C Knockout mice are fertile but couldn't breed them. After gene therapy, however, the infected USH1C female mice were able to breed pups. There were more survived pups from the gene therapy treated mice than the untreated counterparts.

These results demonstrated the potential of a gene therapy approach that restores the loss of vestibular function in the mouse model of Usher Syndrome, which was likely due to stable expression of Harmonin B1 in the hair cells up to 16 months. Future studies will quantitatively examine effects of gene therapy on vestibular function by subjecting animals to sinusoidal head rotation (0.2~4Hz) and translation (0.2-2Hz) while their eye movements are recorded by a video-based eye tracker. Single unit activity of the vestibular afferents will also be recorded.

Grant support: R01DC015111(QYZ), R01DC012060 (HZ), R21 DC017293 (HZ), R01DC014930 (WZ)

PS 420

Differential Effects of Immune Modulation on Cochlear Responses to Acute and Chronic Degeneration in of Cdh23-erl/erl Mice

Qingyin Zheng[1]; Aizhen Zhang[1]; Weinan Du[1]; Bo Hua Hu[2]; Fangfang Zhao[1]
[1]Department of Otolaryngology- Head & Neck Surgery, Case Western Reserve University, Cleveland, Ohio, USA; [2]University at Buffalo

Background. Age-related and noise-induced cochlear degenerations are common causes of acquired hearing loss in the adult population. While the biological and molecular mechanisms of these auditory dysfunctions are not well known, our recent studies have implicated the immune and inflammatory activities in cochlear responses to these disease conditions. The current study aims at a better understanding of the role of immune activity in the development of auditory dysfunction caused by age-related or noise-induced cochlear dysfunction. Methods. Cdh23erl/erl mutant mice were used in the current study. These mice, due to a point mutation at 208(G >A) in CDH23 gene have an early onset and rapid development of auditory dysfunction as age increases. To induce acoustic stress, we exposed erl mice to broadband noise at 117 dB SPL for 2 hrs. To modulate immune activities, we orally applied Cyclosporine-A(CsA), an immunosuppressant drug, at the dosage of 40mg/kg/day. To investigate the immune modulation in age-related degeneration, we gave the drug treatment for 40 days, beginning at postnatal day 41. To investigate the effect of immune modulation on acute acoustic stress, we started the drug treatment 2 days before the noise exposure, and the treatment continued until 16 days post-noise exposure. The thresholds of auditory brainstem responses were measured before and after the treatments .Age-matched mice without corresponding treatments were used as controls Results. The analyses of ABR threshold revealed that the effect of the CsA treatment was dependent on the type of stress. For the age-related cochlear degeneration, we found that both the CsA-treated and untreated littermate erl mice displayed a increase in ABR thresholds. However, the drug-treated ears exhibited greater threshold shifts, suggesting that the inhibition of immune function potentiates age-related cochlear dysfunction. For noise-induced cochlear damage, we found that the the CsA-treatment reduced the level of the ABR threshold shifts compared to the

untreated littermate mice at the young age (5 weeks). This observation suggests that immune suppression is beneficial to the ears sustained acute acoustic stress at a younger age. However, the protective effect became insignificant at the age of 2 months when age-related sensory cell degeneration had started due to erl mutation. In Summary. CsA-induced immune modulation has differential effects on acute and chronic cochlear pathogenesis. Grant support: R01DC015111(QYZ)

PS 421

Investigating the Role of the Epigenetic Reader Brd4 in Hearing and Development of the Inner Ear

Abhiraami Kannan Sundhari; Clemer Abad; Marie Maloof; Nagi Ayad; Juan Young; Susan Blanton; Katherina Walz; Xuezhong Liu
University of Miami

Hearing loss (HL) is the most common sensorineural disorder among the human population with profound congenital HL presenting itself at the rate of one in 500 births. In mammals, Sensorineural Hearing Loss (SNHL) arises from irreversible damage to the sensory hair cells (HC) in the cochlea. Investigation of the transcriptional regulation is necessary to understand the mechanisms involved in sensory HCs development, function and maintenance. Recently, genes involved in DNA methylation, histone modification, and chromatin remodeling has been associated with hereditary HL. In this study, we investigate the role of *Brd4*, a chromatin reader protein that recognizes and binds acetylated histones which plays a relevant in transcription regulation**.** To generate the conditional knock-out model we crossed *Brd4*$^{tm1a(EUCOMM)Wtsi}$ heterozygous with B6.Cg-Tg (ACTFLPe)9205Dym/J and bred them to homozygosity. These were then crossed to B6.Cg-Tg (Atoh1-cre)1Bfri/J mice to obtain conditional expression of Cre in the inner ear to eventually generate *Brd4*$^{fl/fl;Atoh1\text{-}cre+/-}$, *Brd4*$^{fl/fl;Atoh1\text{-}cre-/-}$ *and Brd4*$^{wt/wt}$ littermates. To evaluate the effect of *Brd4* inactivation in *Brd4*$^{fl/fl;\ Atoh1\text{-}cre+/-}$ mice, they were anesthetized intraperitoneally (IP) and auditory brainstem response (ABRs) were recorded and compared to $^{Brd4fl/fl;\ Atoh1\text{-}cre-/-}$ and *Brd4*$^{wt/wt}$ mice as controls using a Smart EP Universal Smart Box (Intelligent Hearing Systems, Miami, FL). ABR stimuli were induced as 0.1 ms broadband clicks and 0.1 ms pure-tone pips at frequencies 8, 16 and 24 kHz through 20-100dB intensities. To test the mechanical activity of outer hair cells (OHCs) in the cochlea, distortion product acoustic emission (DPOAEs) were recorded in the mutant mice and compared to controls. At P21, the ABR thresholds for click response in *Brd4*$^{wt/wt}$ mice were ~ 65dB SPL, ~67 dB SPL in *Brd4*$^{fl/fl;(Atoh1\text{-}cre)-/-}$, and ~100 dB SPL in *Brd4*$^{fl/fl;(Atoh1\text{-}cre)-/-}$. Similarly for the pure-tone frequencies, mutant mice had significantly elevated ABR thresholds at P21 (~100dB SPL) compared with control mice . The DPOAE recordings produced by OHCs in the mutants had reduced amplitudes in 8-16 KHz compared to both control groups but had a similar profiles at 24 KHz. Thus, the *Brd4*$^{fl/fl;\ Atoh1\text{-}cre+/-}$ mice were profoundly deaf, indicating a relevant role of *Brd4* in the postnatal development of HCs. This study has been supported by R01 DC005575 and R01 DC012115 from the National Institutes of Health/National Institute on Deafness and Other Communication Disorders to Xue Zhong Liu.

PS 422

Characterizing a Mouse Model of Non-Syndromic Deafness Caused by TMPRSS3 Mutation

Ksenia A. Aaron[1]; Ina A. Lee[1]; Katja Pekrun[1]; Elvis Huarcaya Najarro[2]; Yasmin Eltawil[1]; Wuxing Dong[1]; Mark A. Kay[1]; Alan Cheng[2]
[1]Stanford University; [2]Department of Otolaryngology-Head and Neck Surgery, Stanford University

Background

More than 70% of all hereditary hearing loss is attributed to mutations of autosomal recessive non-syndromic deafness (ARNSD) genes. Transmembrane protease/serine3 (TMPRSS3) mutations cause up to 10% of all ARNSD cases, exhibiting a variable onset of hearing loss in affected individuals. Previous studies show that TMPRSS3 is expressed in multiple sensory and non-sensory cell types in the cochlea. Thus, hearing loss may result from degeneration and dysfunction of multiple cell types, making this a unique and challenging model to study the potential application of gene therapy on a multicellular level. We set out to first define the histological changes seen in Tmprss3^{tm1Lex} mutant mice, with the goal of testing the potential role of gene rescue.

Methods

Tmprss3^{tm1Lex} mutant mice, as well as wild type and heterozygous littermates, were used in this study. Temporal bones were harvested for histological analysis from postnatal day (P) 5-120. To assess auditory function, we evaluated auditory brainstem responses and distortion product otoacoustic emissions at P14 and P21. To rescue the phenotype of Tmprss3 mutation, we will test AAV-DJ and a novel chimeric capsid delivered via a posterior semicircular canalostomy approach.

Results

At P5, *in situ* hybridization shows TMPRSS3 mRNA expression in the Organ of Corti including hair cells, supporting cells, epithelial cells spanning the lateral sulcus and stria vascularis, and in the modiolus. At P12, there was no obvious loss of TMPRSS3-expressing cells in the cochlea from the homozygous

and heterozygous Tmprss3^{tm1Lex}mice. At P14 and P21, homozygous Tmprss3^{tm1Lex}mice have elevated auditory thresholds, with their cochlea demonstrating extensive inner and outer hair cell loss in the Organ of Corti while spiral ganglia neuron counts were comparable to wild type controls. When examined at P120, the mutant mouse has a significant decrease in spiral ganglion neuron counts. Preliminary data of the novel chimeric TdTommato-tagged capsid demonstrated very high transduction on a multicellular level of the Organ of Corti of wild type mice as compared to AAV-DJ. We have ongoing experiments confirming the preliminary results and testing viral transduction of inner ear tissues of Tmprss3^{tm1Lex}mutant mice using AAV-DJ and a novel chimeric tdTomato-tagged capsid.

Conclusions
TMPRSS3 is widely expressed in the developing/maturing cochlea. Its mutation causes primarily early hair cell loss with elevated auditory brainstem responses, and a delayed spiral ganglion neuron loss. TMPRSS3^{tm1Lex}mouse model is hence a unique model to study the potential efficacy of gene therapy on a multicellular level using a novel chimeric capsid.

PS 423

Overexpression of mitochondrial histidyl-tRNA synthetase restored mitochondrial dysfunction caused by a deafness-associated tRNAHis mutation

Shasha Gong[1]; Min-Xin Guan[2]
[1]Zhejiang University; [2]Zhejiang Unviersity

Mitochondrial tRNA mutations are associated with deafness. The deafness-associated tRNAHis 12201T >C mutation abolished the highly conserved A5-U68 base-pairing into of accepted stem of tRNAHis. Using molecular dynamics simulations, we showed that the m.12201T >C mutation caused unstable tRNAHis structure, supported by decreased melting temperature and faster electrophoretic mobility of mutated tRNA. The primary defect in this mutation was the aberrant aminoacylation and instability of tRNAHis. We investigated whether the overexpression of human mitochondrial histidyl-tRNA synthetase (HARS2) in the cytoplasmic hybrid (cybrid) cells carrying the m.12201T >C mutation restored mitochondrial dysfunctions. Human HARS2 localizes exclusively to mitochondria. The transfer of HARS2 into the cybrids carrying the m.12201T >C mutation raised the levels of aminoacylated tRNAHis from 56.3% to 75.0% but did not change the aminoacylation of other tRNAs. Strikingly, the overexpression of HARS2 increased the steady state levels of tRNAHis and non-cognate tRNAs including tRNAAla, tRNAGln, tRNAGlu, tRNALeu(UUR), tRNALys, tRNAMet in cells bearing the m.12201T >C mutation. This suggested that overexpression of HARS2 improved function of tRNA or prevented unstably mutant tRNAHis from degradation. The improved tRNA metabolism elevated the efficiency of mitochondrial translation, activity of oxidative phosphorylation complexes and respiration capacity. Furthermore, overexpression of HARS2 yielded marked increases in mitochondrial ATP production and membrane potential, reduced production of reactive oxygen species in cells carrying m.12201T >C mutation. These data demonstrated that the overexpression of HARS2 corrected the mitochondrial dysfunction caused by a tRNA mutation. These findings may provide new insights into the pathophysiology of mitochondrial disease and a step toward therapeutic interventions for mitochondrial disorders.

PS 424

DFNA5 ablishment augments noise induced hearing loss by inhibition synapse regeneration

Yong Tao[1]; zhuoer Sun[2]; Xingle Zhao[2]; Hao Wu[2]
[1]Massachusetts Eye and Ear/Harvard Medical School; [2]Shanghai Ninth People's Hospital, Shanghai Jiaotong University School of Medicine

Background
DFNA5 (Deafness Autosomal Dominant Nonsyndromic Sensorineural 5) is an autosomal dominant gene that causes non-syndromic hearing loss. Although DFNA5 has been cloned, the biological function and mechanism of hearing loss remain unclear. Exon 8 of DFNA5 deletion by homologous recombination, results in a frameshift of the open reading frame which leads to the dysfunctional translation of DFNA5. The results of auditory brainstem response (ABR) showed that the DFNA5 KO mouse does not suffer deafness. At present, there is no conclusion about the hearing study of DFNA5 KO mouse. Studying the hearing function and inner ear morphology of DFNA5 knockout mice is helpful to explore the mechanism of DFNA5 gene in deafness.

Methods
DFNA5 KO mice and C57BL/6J mice aged 4-6 weeks and 8-10 weeks of both genders were selected for ABR detection. 1 day later, the mice were continuously exposed to 106 dB SPL noise ranged from 8 to 16 kHz for 2 hours. ABR were detected respectively on day 1, 3, 7, and 14 after noise exposure, and immunofluorescence staining was performed after ABR test. The number of hair cells, synapses and nerve connections were counted as well.

Results
There was no difference in the ABR threshold of 4-6 week-old and 8-10 week-old DFNA5 KO mice and the C57BL/6J of the same age. After noise, the ABR

thresholds of DFNA5 KO mice aged 4-6 weeks and 8-10 weeks were all up-shifted. Especially on day 1 and day 3 after noise, at 22 kHz and above, the ABR threshold shift of DFNA5 KO mice was statistically greater than that of C57BL/6J. No ABR thresholds shift was detected in DFNA5 KO mice after noise. The cochlear histology of DFNA5 KO after noise presented normal nerve connection and hair cell, but less synapses.

Conclusions

This study confirmed that the ABR thresholds DFNA5 KO mice were the same as those of the C57BL/6J mice, but the ABR threshold shift after noise was higher than that of C57BL/6J mice, especially at the high frequencies. The hearing of C57BL/6J mice was able to recover partially after noise, but no significant hearing recovery was found in DFNA5 KO mice.Hair cells and neural connections did not change significantly after noise of both DFNA5 KO mice and the C57BL/6J mice, but hair cell afferent synapses of the DFNA5 KO mice decreased significantly after noise. All evidences demonstrated DFNA5 KO mice is susceptible to noise, and DNFA5 gene plays role in synapse regeneration.

PS 425

HOMER2 is Involved in Actin Dynamics in Hair-Cell Stereocilia

Heather Widmayer[1]; Kevin T. Booth[2]; Ana Sierra[3]; Hela Azaiez[1]; Richard J.H. Smith[4]
[1]Molecular Otolaryngology and Renal Research Laboratories, Department of Otolaryngology—Head and Neck Surgery, Carver College of Medicine, University of Iowa; [2]Harvard University; [3]University of Iowa; [4]Molecular Otolaryngology and Renal Research Laboratories, Department of Otolaryngology—Head and Neck Surgery, Carver College of Medicine, University of Iowa; Interdepartmental PhD Program in Genetics, University of Iowa

HOMER2, a stereociliary scaffolding protein involved in intracellular calcium homeostasis and cytoskeletal organization, is required for normal hearing in humans and mice. Mutations in HOMER2 cause autosomal dominant non-syndromic hearing loss through a dominant-negative mechanism. We have previously shown that Homer2 knockout mice (Homer2$^{-/-}$) exhibit early-onset progressive high-frequency hearing loss that progresses to encompass all frequencies. However, HOMER2's exact function in the ear remains unclear. Two hypotheses were proposed: 1) HOMER2 is involved in hair cell bundle function, formation, development or maintenance through its interaction with CDC42, or 2) it is required for intracellular calcium homeostasis. We hypothesized that HOMER2 regulates actin in stereocilia by interacting with CDC42, a highly conserved small GTPase of the RHO family that is implicated in actin dynamics and is localized to stereocilia membranes in the cochlea. We used scanning electron microscopy (SEM) to fully characterize the ultrastructural morphological changes of hair cells in the Homer2 knockout mice at P15, P30 and P60. At P15, hair bundle formation and morphology were already altered. Stereocilia of outer hair cells appeared elongated and disorganized with loss of their precise staircase pattern. There was no degeneration of hair cells up to P60. These results suggest the implication of HOMER2 in regulating actin dynamics in the inner ear. Whether this involvement is carried through its interaction with CDC42 remains to be elucidated via additional functional assays. Our data provide novel insights into the interactome required for maintaining structural integrity of hair bundles in the organ of Corti.

PS 426

Big Data to Therapy: Precision Medicine for the Deaf in the Diverse Jewish Population

Zippora Brownstein[1]; Shahar Taiber[2]; Mor Bordeynick-Cohen[1]; Hana Bibi[3]; Daniella Beller[3]; Gabriel Chodick[3]; Varda Shalev[3]; Karen B. Avraham[1]
[1]Department of Human Molecular Genetics & Biochemistry, Faculty of Medicine and Sagol School of Neuroscience, Tel Aviv University, Tel Aviv, Israel; [2]Department of Biochemistry & Molecular Biology, George S. Wise Faculty of Life Science, Tel Aviv University, Tel Aviv, Israel, Department of Human Molecular Genetics & Biochemistry, Faculty of Medicine and Sagol School of Neuroscience, Tel Aviv University, Tel Aviv, Israel; [3]Maccabitech, Maccabi Healthcare Services, Tel Aviv, Israel

Precision medicine is critical for providing medical care for individuals based on their unique variants and phenotypes. Given the advances for deafness in gene discovery and correlations of audiological phenotypes with variants in specific populations, the field of hearing loss is in an optimal position to integrate precision medicine into care for patients. Moreover, with the availability of electronic medical records (EMR) for hearing impaired individuals, datasets of large numbers of patients is available for analysis regarding genotype-phenotype correlations and can be used to create and improve personalized treatment. Over 100 genes are involved in deafness worldwide, with specific genes in distinct populations. However, about half of inherited deafness likely remains unsolved. The same is true for the Israeli Jewish population, which includes multiple ethnic groups, turning Israel into a microcosm of genetic diversity that harbors mutations in many deafness genes. This population mixture presents

a challenge to determining the cause of deafness in unsolved cases, and next-generation sequencing (NGS) has proven an efficient tool for tackling this task. We have begun a large-scale study of the hearing-impaired population in Israel, utilizing the Maccabi Tipa Biobank of approximately 100,000 samples. An initial search of 56,000 samples yielded 6,000 individuals suffering from hearing loss. Inclusion in the study will be determined by fulfilling strict criteria with regards to the hearing loss phenotype. NGS will be performed on all probands, followed by bioinformatics analysis, variant validation and determination of genotype-phenotype-ethnicity correlations. Novel variants will be immediately applied in the genetics and audiology clinics, setting a guideline for precision medicine for hearing loss in Israel. In parallel, novel variants, including in genes and in regulatory domains, will be functionally investigated, beginning from basic characterization and progressing to advanced experiments of epigenomics, CRISPR-Cas9 gene editing, and gene therapy. Solving the etiology of deafness in the diverse Israeli Jewish population in a large-scale study is the key for precision medicine for hearing loss, including diagnosis, prevention and treatment. The research is supported by the Israel Precision Medicine Partnership Program.

Hair Cells to Vestibular Nuclei

PS 427

Cellular Origins and Response to Atoh1 Overexpression in the Vestibular Flat Epithelium of Mice

Lu He[1]; Jing-Ying Guo[1]; Teng-Fei Qu[1]; Wei Wei[2]; Ke Liu[1]; Zhe Peng[1]; Guo-Peng Wang[1]; Shu-Sheng Gong[1]
[1]Department of Otolaryngology-Head and Neck Surgery, Beijing Friendship Hospital, Capital Medical University; [2]Department of Otolaryngology-Head and Neck Surgery, Shengjing Hospital, China Medical University

Vestibular flat epithelium (FE) has been found in the vestibular end organs of humans and mice with severe vestibular dysfunction. However, the pathogenesis of FE remains unclear and inducing hair cell (HC) regeneration is challenging, as both HCs and supporting cells (SCs) are damaged in the vestibular FE. To determine the cellular origins of vestibular FE and examine the response to *Atoh1*overexpression, we fate mapped vestibular epithelial cells in three transgenic mouse lines (*vGlut3-iCreER^{T2}:ROSA26^{tdTomato}*, *GLAST-CreER^{T2}:Rosa26^{tdtomato}*, and *Plp-CreER^{T2}:Rosa26^{tdtomato}*) after inducingsevere lesions. *Aoth1*overexpression in vestibular FE was mediated by the adeno-associated virus serotype 8 (AAV8) vector. Suberoylanilide hydroxamic acid (SAHA),a histone deacetylase inhibitor, was administered with AAV8 to enhance the level of *Atoh1*overexpression.The transduction efficiency and population of myosin VIIa-positive cells were analyzed. The data demonstrated the presence of a small number of HCs in vestibular FE, which included regenerated cells and those that survived the lesion. SCs and cells in the transitional epithelium region were both significant cellular sources of the vestibular FE. SAHA dramatically enhanced AAV8-mediated exogenous gene overexpression, and enhanced overexpression of *Atoh1*induced transdifferentiation of vestibular flat cells into myosin VIIa-positive cells in vestibular FE. Our study provides insights into FE formation and introduces a promising therapeutic approach for HC regeneration in vestibular FE.

PS 428

The Role of Pou4f3 in Vestibular Hair Cell Survival and Function

Betty Y. Chen[1]; Nnenna Ezeilo[1]; Kaley A. Graves[2]; Tianwen Chen[3]; Jun Huang[4]; Hong Zhu[5]; Wu Zhou[5]; Bradley J. Walters[5]; Brandon C. Cox[6]
[1]Department of Otolaryngology, Southern Illinois University School of Medicine; [2]Department of Pharmacology, Southern Illinois University School of Medicine; [3]Department of Otolaryngology University of Mississippi Medical Center; [4]Department of Otolarynogology University of Mississippi Medical Center; [5]University of Mississippi Medical Center; [6]Departments of Pharmacology & Otolaryngology, Southern Illinois University, School of Medicine

It is critical to understand the factors that promote hair cell [HC] survival during inner ear development, with aging, and in response to ototoxic insults. Similar to the cochlea, vestibular end organs have specialized HCs that transduce mechanical forces into neural signals. Vestibular HCs are stimulated by head movement and act to mediate gaze stabilization and balance. HCs in the otolith organs of the utricle and saccule detect linear accelerations, while HCs in the ampullae of the semicircular canals detect rotational accelerations. Vestibular HC loss occurs with aging and after exposure to ototoxic agents, resulting in vestibular deficits. Therefore, characterizing pathways that regulate vestibular HC survival is important to develop protective strategies. Previous studies have shown that the transcription factor *Pou4f3*, which is exclusively expressed in both nascent and adult HCs of the cochlear and vestibular systems, is critical for HC maturation and survival during development. Mice with germline deletion of *Pou4f3* have significant functional defects caused by incomplete HC differentiation and impaired HC survival. While the developmental role of *Pou4f3* is well characterized, the extent to which *Pou4f3* continues to be necessary for

HC survival as mice age remains an open question. We investigated the role of *Pou4f3* in vestibular HC survival and function at four different stages of HC maturation by using the CreER/loxP system to delete *Pou4f3* from vestibular HCs at specific postnatal ages. We bred *Atoh1-CreER*$^{TM/+}$ mice, which express CreER specifically in HCs, with *Pou4f3*$^{loxP/loxP}$ mice to delete *Pou4f3* after injection of tamoxifen in neonates, juveniles, and two different ages of adults. Temporal bones were collected at 2, 4, and 6 weeks after tamoxifen injection and the number of HCs in the utricle were quantified, noting the presence or absence of *Pou4f3.* To assess vestibular function, linear and angular vestibulo-ocular reflexes (VORs) were tested. Preliminary results show decreased *Pou4f3* expression in utricular striolar and extrastriolar HCs, as well as in type I and type II HCs relative to controls, yet there was no significant HC loss in mice lacking *Pou4f3*. Compared to control littermates, mice with *Pou4f3* deletion had largely intact linear VOR function, but exhibited decreased angular VOR function. These results suggest that *Pou4f3* may not be required for HC survival in the utricle after gestation. However, further testing in other vestibular end organs, such as the ampullae and saccule, are warranted.

PS 429

Single-cell RNA-seq Reveals Novel Cell Subtypes and Gene Expression Patterns in the Mouse Crista Ampullaris

Brent A. Wilkerson[1]; Alex D. Chitsazan[2]; Heather L. Zebroski[1]; Olivia Bermingham-McDonogh[1]
[1]University of Washington; [2]CEDAR, OHSU Knight Cancer Institute, School of Medicine

Cristae, which are critical for vestibular function, have not yet been characterized by single cell RNA-seq. We performed RNA-seq in single cells dissociated from ampullae microdissected from E18, P3 and P7 mice, then validated cell type-specific markers *in situ*. Cluster analysis identified the hair cells, support cells, dark cells, and glia of the crista as well as the fibroblasts, vascular cells and epithelial cells of the ampulla roof and wall. Cluster-specific expression predicted spatially restricted domains of gene expression in the crista and ampulla not previously described. For example, expression of one cluster-specific transcript is spatially restricted to a subset of the Sox2+ support cells bordering the crista sensory epithelium. Moreover, cluster specific-expression corresponds to restricted patterns of gene expression in spatially distinct populations of fibroblasts in the mesenchyme surrounding the ampulla. Trajectory analysis revealed the transcriptomic profile of immature hair cells as well as new transcriptomic dynamics associated with hair cell maturation in the crista. The new cell subtypes and states revealed by single cell RNA-seq could be important for crista function and the markers identified in this study will enable the study of their dynamics during development and disease.

PS 430

Hypergravity stimulation deteriorates vestibular function in mouse with selective ablation of p2rx2

Sang Hyun Kwak[1]; Hansol Hong[2]; Jae Young Choi[3]; Gyu Cheol Han[4]; Sung Huhn Kim[5]
[1]Yonsei university college of medicine; [2]Yonsei University College of Medicine; [3]Yonsei University; [4]Gacheon University College of Medicine; [5]Department of Otorhinolaryngology, Yonsei University College of Medicine, Seoul, Korea

p2rx2 is a subtype of purinergic receptors. It is a non-selective cation channel and regulates intracellular ion concentration by purines which secreted from surrounding cellular structures. In the cochlea, p2rx2 is distributed at supporting cells and outer sulcus cells. It protects hair cells by providing cation shunt during noise stimulation, which reduces cation burden to hair cells. Although p2rx2 is distributed at supporting cell and transitional cell of vestibular labyrinth, little has been known about its role in the vestibular system. In this study, we investigated if ATP is secreted to vestibular labyrinth by mechanical stimulation and if p2rx2 stimulated by ATP plays a role in the protection of vestibular hair cell during excessive mechanical stimulation. ATP concentration and site of secretion in the membranous vestibular labyrinth after mechanical stimulation was determined by luciferin-luciferase assay and quinacrine staining. 4G and 6G Hypergravity stimulation was performed in p2xr2+/+ and p2rx2-/- mouse with animal eccentric rotator for 24 and 48 hrs. After the stimulation, vestibulo-ocular reflex (VOR) was measured using animal rotator and infra-red camera for eye movement recording. The number of hair cell loss after the stimulation was counted after confocal microscopy using ZEN and FIJI software in each genotype. ATP secretion after mechanical stimulation was most significant in ampullary and utricular area of vetibular labyrinth. The main sites for ATP secretion were macula, crista ampullaris, and dark cell area. VOR was more significantly decreased in p2rx2-/- mouse than p2xr2+/+ mouse as time- and stimulation gravity-dependent manner. After hypergravity stimulation of 6G 48 hrs, gain and time constant of p2rx2-/- mouse were significantly decreased when compared to those of p2xr2+/+ mouse ($p < 0.05$). Hair cell loss after the hypergravity stimulation was more prominent in p2rx2-/- mouse than that in p2rx2-/- mouse ($p < 0.05$). ATP-stimulated p2rx2 function plays an important role in the protection of vestibular hair cells during excessive mechanical stimulation by providing cation shunt to reduce the cation burden to hair cells.

PS 431

Evidences of vestibular synaptopathy induced by aminoglycoside exposure

Hee-Won Jeong[1]; Jae-Hun Lee[1]; Han-Seung Nam[2]; Hyeongbeom Kim[1]; Ilyong Park[1]; Nathaniel Carpena[3]; So-Young Chang[1]; Ji Eun Choi[4]; Min Young Lee[5]; Phil-Sang Chung[6]; Jae Yun Jung[6]
[1]Dankook University; [2]Dankook Unviersity; [3]Beckman Laser Institute Korea, College of Medicine, Dankook University, Cheonan, South Korea; [4]Dankook University Hospital; [5]Beckman Laser Institute Korea, Dankook University Hospital, Dankook University; [6]Beckman Laser Institute Korea, Dankook University, Dankook University Hospital

Background
Disturbance of balance or vertigo is thought to be related to the damage of vestibular organ such as utricle, saccule, and ampullae of semicircular canals. Hair cell loss of these organs is thought to be responsible for the vestibular dysfunction. However, variable degree of clinical symptoms suggests that pathophysiology without obvious hair cell loss such as 'synaptopathy' which describes loss of synaptic connection between morphologically normal hair cells and nerve fibers may take place in vestibular organ which is recently well recognized in cochlea. Synaptopathy can be induced by overstimulation and ototoxic drug application in cochlea, and results in decreased peak 1 amplitude of auditory brainstem response (ABR) and reduced number of synaptic puncta between inner hair cell and nerve fiber.

Objectives
We aimed to establish optimal ototoxic rat model which shows compatible vestibular dysfunction and histologic finding for vestibular synaptopathy.

Material and Methods
7 weeks old SD rats were used for this experiment. For vestibular sensory-evoked potential (VsEP) measurement, head bolt was implanted and fixed under general anesthesia before a week of baseline VsEP measurement. To induce vestibular synaptopathy, Gentamicin (100 mg/kg) was injected intraperitoneally. VsEP was measured 3 and 7 days after Gentamicin injection. The latencies and amplitudes of VsEP components were analyzed. After the last VsEP recording, rats were sacrificed and utricle or whole cochlear was harvested for histological analysis.

Results
In the VsEP results, there was no difference in the VsEP threshold until 7 days after GM treatment. The latencies of P1, N1, P2, N2 were not changed, while inter-peak amplitude of P1-N1 decreased significantly at 7 days after GM injection. Histological analysis showed the reduced number of the utricular ribbon synapses without obvious hair cell loss.

Conclusions
In this study, we demonstrated decreased peak 1 amplitude in VsEP and reduced number of synaptic puncta between utricular hair cell and nerve fiber After ototoxic damage. This result shows evidence of vestibular synaptopathy induced by ototoxic drug which is possible reason for relatively mild symptomatic balance problem in clinics.

Acknowledgements
We thank Micheal King (University of Michigan) for assistance to build VsEP system. This research was supported by Leading Foreign Research Institute Recruitment Program through the National Research Foundation of Korea (NRF) funded by the Ministry of Science and ICT (MSIT) (NRF-2018K1A4A3A02060572).

PS 432

Electrical Response Evoked by Pulsed Infrared Stimulation on Mouse Peripheral Vestibular System

Weitao Jiang; Fangyi Chen; Dingxuan Zeng
Southern University of Science and Technology

Introduction
Though Electrocochleography (EcochG) has been widely used in auditory system study, the Electrovestibulography (EVestG), is rarely used in vestibular system study. Limited spatial selectivity and co-stimulation of cochlea prevent EVestG from accurately evaluating vestibular function. As a spatial selective stimulation selective methods, Infrared Neuron Stimulation(INS) has been widely used in inner ear study. To validate the efficacy of INS as a selective stimulating method for EVestG, we used pulsed infrared laser to stimulate the mouse vestibular system through oval window and recorded the optical evoked electrical responses.

Method
C57B/J mice(4-8 weeks, n=5) were used in the study. After anesthetization, the right bulla of the animal was exposed and opened approximately 1.5×2 mm with a motorized drill. Infrared pulses(@1870nm,100μs, 20-260μJ/pulse and repetition rate of 20Hz) were delivered to the oval window using a optical fiber with core diameters of 200 μm. A sliver wire were placed at round window for electrical responses recording. Two electrodes were placed at the contralateral facial nerve and body of the animals as reference and ground. The electrodes were connected to an customized amplifier, of which the amplification was set at 20,000. The high-

and low-pass of the amplifier was set at 300 Hz and 3 kHz, respectively. All the signals were averaged by 200–500 repeated responses, with the sampling rate set at 300 kHz. After stimulation, the tip of the fiber was fixed inside the bulla using dental acrylic and fixed 24h in 4% PFA. Then the bulla was imaged by Mico-CT imaging to show the site of stimulation.

Result

In round window recordings, IR evoked electrical responses showed similar waveforms as compound action potential(CAP). Multiple peaks representing neural activity from different locations along the vestibular pathway can be seen. The latency and the amplitude of response increased with the increase of pulse energy. The threshold radiant energy of IR evoked electrical responses was 15μJ/pulse. The micro-CT imaging results shows that the end of fiber was pointing towards the utricular macula, horizontal canal and anterior canal of the animal.

Conclusion

We showed that pulsed IR could evoke electrical response of vestibular system. This suggests the feasibility of INS as a potential stimulating method for IR based VestG. Future experiments will focus on optimizing the parameters of infrared neural stimulation and improved surgical approach.

PS 433

Bilateral Round Window Ouabain Application as a Model for Vestibular Hypofunction

Matthew Farr[1]; Leila Abbas[1]; Jaydip Ray[2]; Marcelo N. Rivolta[1]
[1]University of Sheffield; [2]Royal Hallamshire Hospital

Input from the vestibular system is a key component of the signals that facilitate maintenance of equilibrium in space in humans and other animals. Whilst both unilateral and bilateral vestibular dysfunction can have a large impact on patient wellbeing, the economic cost and falls risk is greatest when both of the paired vestibular organs are affected. The patients most commonly encountered with bilateral vestibular hypofunction acquired the complaint as older adults. At present there is a dearth of treatments available to restore vestibular input after it has been lost. If these are to be developed, it will be useful to model bilateral vestibular hypofunction in an adult mammal. Here we aim to do so as a result of damage to the neurons of Scarpa's ganglion.

In order to produce a model of vestibular neuronal damage we investigated the effects of ouabain serially applied to the round window niche of C57BL/6 mice during a single surgical procedure. Study groups included non-surgical controls, unilateral labyrinthectomy, bilateral saline, unilateral ouabain and bilateral ouabain application subjects. All groups underwent weekly behavioural testing and had pre and post procedure auditory brainstem response testing. Behavioural testing included rotarod, balance beam and swim testing. We demonstrate a persistent, quantifiable impact of bilateral ouabain application on behaviour and correlate this with histological patterns of inner ear damage. This effect persists after controlling for the impact of the surgical approach with bilateral round window saline application.

Ouabain-induced selective damage to the neurons of Scarpa's ganglion with preservation of the membranous labyrinth would be an ideal model to investigate the potential therapeutic effect of otic neural progenitors transplanted directly into the internal auditory meatus. A middle ear approach allows such transplants to be performed without damage to the membranous labyrinth or the need for intracranial access. Behavioural outcome metrics provide non-invasive, clinically relevant markers for the assessment of vestibular function.

PS 434

The Starliner Zebrafish Mutant Has Central Deficits in Hearing and Balance

Yan Gao[1]; Eliot Smith[1]; Itallia Pacentine[2]; Timothy Erickson[3]; Alex Nechiporuk[2]; Teresa Nicolson[1]
[1]Stanford School of Medicine, Department of Otolaryngology; [2]Oregon Health & Science University; [3]East Carolina University

Central defects in the auditory/vestibular system remain largely unexplored. Few genes have been implicated in central processing of auditory and vestibular input by the brain. In a mutagenesis screen for balance and hearing defects, the *starliner* mutant was identified based on its abnormal posture of resting on its side, reduced sensitivity to tapping on the petri dish and uninflated swim bladder. When spontaneous or evoked swimming occurred, the bursting swim pattern was comparable to wild-type siblings but the distances travelled were variable, suggesting some impairment of the regulation of locomotion. Despite the abnormal resting position, *starliner* mutants have robust vestibular-induced eye movements, suggesting that utricular hair cells and the neural circuitry of the vestibulo-ocular reflex (VOR) and otolith tilting reflex (OTR) are normal. In contrast, vestibulospinal reflexes in response to rotation of the head are absent, indicating that transmission of vestibular information at central synapses of this circuitry are defective in *starliner* mutants. Testing acoustically evoked behavior responses (AEBR) revealed that this

reflex is also greatly diminished or absent. Collectively these results point to a defect in central brain regions that eliminate the execution of startle reflexes. In addition, we will explore potential defects in saccular hair cells in *starliner* mutants.

We identified a nonsense mutation in the *split ends*(*spen*) gene using RNAseq analysis of *starliner* mutant transcripts. In *Drosophila*, *spen* has been previously implicated in axonal outgrowth and fasciculation. In zebrafish, we found that *spen* is highly expressed in the central nervous system. Spen (also known as SHARP, MINT) is a transcription factor and analysis of differential expression between mutants and siblings demonstrated striking changes in many genes, particularly *smc1a*. This gene is highly downregulated in *starliner/spen* mutants and encodes a component of DNA cohesin rings. Mutations in *SMC1A* in humans are associated with Cornelia de Lange syndrome, a rare disease that includes delayed developmental milestones such as walking and deafness as symptoms. Efforts are underway to validate the putative transcriptional changes in the *starliner/spen* mutant and to understand the cellular basis of the defects.

PS 435

Central Defects in the raumschiff Zebrafish Mutant

Anna Shipman[1]; Matthew Hill[2]; Eliot Smith[1]; Timothy Erickson[3]; Teresa Nicolson[1]
[1]Stanford School of Medicine, Department of Otolaryngology; [2]Oregon Health & Science University; [3]East Carolina University

In the 2001-2004 NHANES survey, 35% of adults in the US age 40 and older showed signs of vestibular dysfunction. As the aging population in the US continues to grow, it is vital to deepen our understanding of vestibular disorders and identify new therapies to treat them. The zebrafish is an excellent model organism to study vestibular function and disease due to the high genetic homology between zebrafish and humans, the transparency of larvae, and the ability to quantify vestibular function. Through the use of an ENU mutagenesis screen, we generated *raumschiff* mutants, which display a balance phenotype. However, *raumschiff* mutant larvae have a normal vestibulo-ocular reflex (VOR), indicating that the mutation may act at the level of the central nervous system (CNS) rather than in the inner ear. Our current research focuses on identifying the mutation responsible for the *raumschiff* phenotype, and characterizing the defects in molecular mechanisms that result in vestibular dysfunction. Analysis of differential expression generated from RNA Sequencing data has revealed that several genes are potentially misregulated in the *raumschiff* mutant, including those involved in Fos-Jun signaling. Whole-mount *in situ* hybridization was used to validate changes in gene expression. In accordance with the normal VOR, we found striking changes in the expression patterns of target genes in the brain. On-going efforts include Whole Genome Sequencing to identify the causative mutation. Our future work will aim to further explore the differences in signaling pathways in the CNS of *raumschiff* mutants and how the defects lead to changes in how the brain processes vestibular information.

PS 436

Systemic Injection of CGRP Prolongs a Nausea-like State in Mice

Benjamin Liang[1]; Catherine Hauser[1]; Stefanie Faucher[1]; Raajan Jonnala[1]; Shafaqat Rahman[1]; **Anne E. Luebke**[2]
[1]University of Rochester; [2]University of Rochester Medical Center

Nausea is a prominent symptom and major cause of complaint for patients with migraine and specifically vestibular migraine (VM). As a readout of a nausea-like statepresent in migraine and VM, we will assessed hypothermic responses to provocative motion. Recent studies have demonstrated that provocative motion causes robust and prominent hypothermic responses in rats, humans, house musk shrews, and mice that there is a clear parallel in hypothermic responses between animals and humans in underlying physiological mechanism - cutaneous vasodilatation that favors heat loss. Additionally, because systemic CGRP injection has been shown to cause light-aversion (photosensitivity) in mice, we wondered what effect systemic CGRP injection would have on these nausea-like states in wildtype mice.

We carried out these studies on 20 wildtype C57BL/6J (JAX 664) mice (10F/10M). Head and tail temperatures were measured using an FLIR E60 IR camera before, during, and after a 20 min orbital rotation (0.75 Hz to 4 cm displacement). One week later, the same mice were injected systemically with 0.1 mg/kg rat α-CGRP (Sigma), and were retested.

We confirmed in both female and male C57BL/6J mice during provocative motion there is a decrease in head temperature (hypothermia) of ~1.5 degree C which recovers and is associated with a short-lasting tail-skin vasodilation (tail skin temperature increase of ~4 degrees C). Interestingly, systemic CGRP injection caused a similar reduction in head temperature, yet the hypothermia did not recover. Moreover, there was no associated tail-skin vasodilation in CGRP-injected mice.

In conclusion, provocative motion in wildtype mice is accompanied by hypothermia that involves both

autonomic and thermo-effector mechanisms. Moreover, a systemic CGRP injection prolongs the hypothermia and eliminates the tail-skin vasodilation. Experiments are underway to determine what effects CGRP antagonists and triptans may have on these physiological correlates of nausea.

Research supported by NIH R01 DC017261 (AL) and grants from the Kearns Center (UR) and Discovery grants (UR)

PS 437

Systemic Injection of CGRP Increases Postural Sway and Auditory Sensitivity in Mice

Benjamin Liang[1]; Catherine Hauser[1]; Stefanie Faucher[1]; Raajan Jonnala[1]; Shafaqat Rahman[1]; **Anne E. Luebke**[2]
[1]University of Rochester; [2]University of Rochester Medical Center

About 42% of people with migraine have a vestibular component causing balance problems and dizziness. This form of migraine, termed vestibular migraine (VM), has been recently defined as having at least five episodes of moderate or severe vertigo lasting 5 min-72 hours, history of migraine, either phonophobia, photophobia, or visual aura, and vertigo that cannot be caused by other ear or brain pathologies. In fact, VM is a major cause of vertigo in dizziness clinics and is estimated to affect 1% of the overall population. As migraine increases light, and sound sensitivities, it also increases sensitivities to movement or perceived movement in VM. The most common symptoms of VM were unsteadiness, balance disturbances, and "light headedness". When balance disturbances were quantified, VM patients swayed more than migraine-only or healthy controls when challenged with optic flow, and after optokinetic (OKN) stimulation (with eyes closed) than did either healthy controls or migraine-only patients. In addition postural sway or center of pressure (CoP) testing can be used in mouse models as this test has been used successfully to detect fine tremors in mouse models. In addition, patients with migraine, and especially VM, exhibit a heightened sense of sound, or phonophobia. Phonophobia is also related to hyperacusis (extreme sensitivity to sound). Behavioral evidence of hyperacusis and phonophobia in mice can be inferred using the acoustic startle reflex (ASR) and pre-pulse inhibition (PPI) of startle testing.

We studied 40 wildtype C57BL/6J (JAX 664) mice (20F/20 M). Twenty mice were used for the postural sway testing and twenty mice were used for ASR and PPI testing. For postural sway or center of pressure (CoP) testing, mice were placed on force plate (AMTI Biomechanics) and after acclimatization with the mouse resting still with all feet on platform, we recorded forces and moments for 1 sec, with measurements repeated 10-12 times/ mouse. We also obtained CoP measurements after a brief 30-sec vestibular rotation (125 rpm), and repeated the process. For ASR/PPI testing, we determined target reception thresholds in dB (that gives A'=. 75 or 50% inhibition) for each animal. Each animal is only tested for 45 min/day (one series of acoustic startle/day; i.e., 1) acoustic startle series in quiet and in noise, and 2) PPI in quiet with noise burst (NB) targets of varying loudness. One week after initial testing, the same mice were injected IP with 0.1 mg/kg rat β-CGRP (Sigma), and after 20 min, were subjected to the same postural sway and ASR/PPI procedures.

We determined that female mice swayed more than male mice after a vestibular rotation as well as after a systemic CGRP injection (2-fold increase in CoP area). In addition, both male and female mice were more sensitive to sounds (5 dB SPL) after a single systemic CGRP injection.

In conclusion, systemic CGRP injection increased both motion sensitivity (as measured by postural sway) and sound sensitivity (as measured by ASR/ PPI). Experiments are underway to determine what effects systemic-delivered CGRP antagonists and triptans may have on these CGRP-induced sensitivities.

Research supported by NIH R01 DC017261 and grants from the Kearns Center

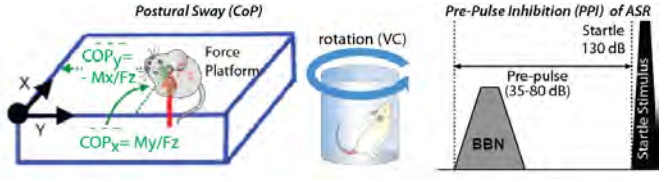

PS 438

Vestibulo-Sympathetic Projections: Synaptic Proteins Associated with Vestibular Axonal Varicosities in the Rostral and Caudal Ventrolateral Medullary Regions of the Rat

Amelia H. Gagliuso; Giorgio P. Martinelli; Gay R. Holstein
Icahn School of Medicine at Mount Sinai

Cells in the caudal vestibular nuclei project directly to regions of the caudal medulla that participate in central autonomic control. These pathways convey vestibular information about changes in head position and movement to autonomic areas controlling heart rate, blood pressure, respiration and some aspects of gastrointestinal (GI) function. Axons comprising these pathways have unique morphology amongst vestibular nuclear efferents: the axonal processes are fine, poorly myelinated, and highly varicose. The varicosities provide an opportunity for widespread innervation of target regions from a small population of cells. Moreover, the presence of multiple varicosities along single axons innervating a target neuron could result in a significant postsynaptic effect exerted by individual afferents. Both possibilities, however, require that the vestibular axonal varicosities form synaptic contacts with the postsynaptic cells. The present study was conducted determine whether these synaptic contacts are formed, based on the localization of SNARE proteins associated with vestibular axonal varicosities in the rostral and caudal ventrolateral medullary regions (RVLM and CVLM, respectively).

Unilateral iontophoretic injections of the anterograde tracer *Phaseolus vulgaris leucoagglutinin* (PhaL) were placed in the caudal vestibular nuclei of male Long-Evans rats. The animals were euthanized 10 days later by cardiac perfusion with aldehydes and the harvested brainstems were vibratome-sectioned. Identification and then mapping of the PhaL injection sites was accomplished using PhaL-diaminobenzidine immunohistochemistry. Additional brainstem sections from rats with optimally-placed tracer injections were used for double and triple label immunofluorescence identification of PhaL with SNARE-related proteins including VAMP, MUNC and syntaxin, as well as PSD-95. This labeling initially verified our previous observations that vestibular axons are more prevalent in RVLM than CVLM but in both regions are sinuous, unmyelinated and highly varicose. In addition, vestibular axonal varicosities appear to form a chain of contacts with the cell bodies and dendrites of target neurons. SNARE protein immunofluorescence indicates that these contacts are synaptic.

Our results indicate that vestibular innervation of neurons in RVLM and CVLM occurs through a series of *en passant* synapses formed by axonal process varicosities. This synaptology suggests that there is an extensive vestibular influence on caudal medullary neurons controlling sympathetic autonomic outflow, including those involved in heart rate, blood pressure, respiration and GI activity. It is conceivable that this vestibulo-sympathetic innervation is responsible for the rapid changes in heart rate and blood pressure that occur with sudden shifts in posture.

PS 439

Stochastic Noise Differentially Effects Neuronal Subtypes within the Medial Vestibular Nucleus In Vitro

S Stefani[1]; C Pastras[1]; P Breen[2]; J Serrador[3]; M Schubert[4]; Camp A[1]
[1]The University of Sydney; [2]Western Sydney University; [3]Rutgers New Jersey Medical School; [4]John Hopkins University

Stefani S[1], Pastras C[1], Breen P[2], Serrador JM[3], Schubert M[4] and Camp A[1]

1. Department of Physiology and the Bosch Institute, University of Sydney.
2. Marcs Institute, Western Sydney University.
3. Department of Pharmacology and Physiology, Rutgers New Jersey Medical School.
4. Department of Otolaryngology, Johns Hopkins Medicine.

Stochastic resonance is a phenomenon whereby sensitivity to sub-threshold signals is modified via low-level noise application. Application of stochastic noise has been shown to improve visual, auditory, vestibular and autonomic functions within humans. A key feature of stochastic noise is the low frequency and amplitude of the stimulus - that is, it remains imperceptible to the user. This means that rather than eliciting a profound habituation or hyperstimulation, stochastic noise presumably exerts its effect by subtly altering neuronal sensitivity to incoming signals. Here we aim to determine how stochastic noise effects the gain and phase dynamics of individual medial vestibular nucleus neurons.

All experimental materials and procedures were approved by the University of Sydney Animal Ethics Committee (protocol 2018/1308). All experiments were performed in 3 - 5 week-old male and female C57BL/6 mice. Whole-cell current-clamp recordings of individual neurons in the medial vestibular nucleus (MVN) were made at 25ºC from 200 µm tissue slices. Recordings were made in response to a suite of depolarising current steps (6 steps, 10 pA/step) with stochastic, sinusoidal or stochastic+sinusoidal noise or without noise (control). Spike rate vs current plots were produced and the slope of the line of best fit used to

quantify neuronal gain. Neuronal type was characterised based on their afterhyperpolarisation. Phase dynamics of neuronal firing was determined by analysing the timing of action potentials in accordance with the positive peaks of the sinusoidal stimulus.

In 25/45 MVN neurons stochastic noise produced a significant alteration in neuronal gain when compared with the no noise control condition. In 12 of these neurons this difference was expressed as an increase in neuronal gain and in 13 of the cells, neuronal gain was reduced. Type A MVN neurons most strongly increased in gain, whilst type B and C neurons were equally effected. However, neuronal type had no effect on shifts in phase dynamics.

These results indicate that the sensitivity of MVN neurons can be influenced by the application of stochastic noise. Importantly this data suggests that the impact of stochastic noise is variable - that is, in some neurons the impact is an increase in gain while in others it is a reduction with neuronal subtype playing a role. These differential effects may provide a 'normalisation' mechanism to modulate the overall sensitivity of the vestibular system and as such may be useful in the development of therapeutic devices to treat those suffering from balance dysfunction.

Human Temporal Bone Studies, Head and Neck Disease

PS 440

Middle-Ear-Muscle Forces Could Aid the Diagnosis of Otosclerosis with Wideband Tympanometry (WBT)

Anbuselvan Dharmarajan[1]; Mike E. Ravicz[2]; Kevin N. O'Connor[2] ; Sunil Puria[3]
[1]Department of Otolaryngology Head and Neck Surgery, Harvard Medical School; Eaton-Peabody Laboratories, Massachusetts Eye and Ear; [2]Eaton-Peabody Lab., Mass. Eye & Ear; Department of Otolaryngology, Harvard Medical School; [3]Department of Otolaryngology Head and Neck Surgery, Harvard Medical School; Eaton-Peabody Laboratories Massachusetts Eye and Ear

Background
Techniques for non-invasively diagnosing otosclerosis are of clinical significance, as otosclerosis is typically only detected during invasive surgical procedures. Standard tympanometry, a measure of middle-ear (ME) impedance at one frequency as a function of ear-canal (EC) static pressure, cannot provide specific information about otosclerosis. Wideband tympanometry (WBT), a measure of EC power absorbance (PA) over a wide range of frequencies and EC static pressures, shows promise for screening, but still lacks enough sensitivity and specificity to detect otosclerosis (e.g., Wang et al., 2019). This is partly due to the inherently high variability among PA responses, regardless of whether the ears are normal or otosclerotic. We demonstrate that ME-muscle tension changes ME sound transmission in ways that are detectable with WBT. We hypothesize that (1) by counteracting the effects of negative EC static pressure during WBT measurements, ME-muscle pulls can alter PA in ways that differ depending on whether the ear is normal or otosclerotic; and (2) perturbing the ME through evoked ME-muscle pulls can increase the sensitivity of WBT for detecting otosclerosis by allowing each individual ear to be compared against itself rather than against a highly variable population.

Methods
In human-cadaver temporal bones, we performed a mastoidectomy and (1) opened the facial recess to expose the stapes footplate and stapedius muscle (STM) and (2) gained access to the tensor-tympani muscle (TTM) and cochleariform process through an anterior approach. Forceps on calibrated load cells produced and measured static STM and TTM tensions up to 80 and 150 gram-force, respectively. We measured 3D stapes velocity and performed WBT with the Interacoustics Titan research platform for various muscle tensions, before and after fixing the stapes footplate to simulate otosclerosis.

Results
PA is generally lower at many frequencies below about 1.5 kHz for positive and negative EC static pressures, consistent with previous results. Applying tension to the STM or TTM has no effect on PA at positive EC pressures, but tends to counteract some of the effects of negative EC pressures. TTM tension has a greater effect than STM tension. When the stapes footplate is fixed (confirmed by > 20 dB reduction in stapes velocity), the interaction between ME-muscle tension and EC pressure is different than in the unfixed case, especially for TTM tension. The combination of WBT with ME-muscle pulls shows promise for the noninvasive diagnosis of otosclerosis. [Work supported by grant R01 DC05960 from the NIDCD of NIH].

PS 441

Improving Anatomical Understanding of the Human Tympanic Membrane Through Histologic Processing and Imaging

Jennifer S. Zhu[1]; Nicole Black[1]; Dhrumi Gandhi[2]; Aaron K. Remenschneider[3]
[1]John A. Paulson School of Engineering and Applied Sciences, Harvard University; [2]Massachusetts Eye and Ear Infirmary- Harvard University; [3]Dept. of Otolaryngology, UMass Memorial Medical Center; Massachusetts Eye and Ear

Background
While the human tympanic membrane (TM) has the capacity to self-heal following injury and infection, a subset of patients will develop chronic TM perforations. The structural and cellular changes that occur in chronically perforated TMs are poorly described. Herein we histologically process and describe perforated TM specimens from human patients undergoing tympanoplasty.

Method (Histology)
Perforated TM samples are collected from patients undergoing middle ear surgery and are stored in formaldehyde until ready for processing. They are decalcified in EDTA, dehydrated and rehydrated through ethanol solution, and embedded into paraffin blocks. These blocks are sliced into ribbons where every tenth slide is stained with hematoxylin and eosin (H&E) for evaluation. Slides chosen for imaging are captured at 1.25x, 2x, 4x, and 10x magnification to analyze TM anatomy at different locations of each specimen.

Method (TM Holder)
Currently, TMs extracted from surgery lose their three-dimensional conical shape during processing. To address this, we 3D-printed a custom holder using stereolithography (EnvisionTEC Aureus) to mimic the natural size and conical shape of the human TM, allotting space for variation in patient structure. A solid perimeter with lips allows the holder to align and to hold the TM in place, while a porous interior (Meshmixer) allows formaldehyde to seep through the holder and into the TM during fixation and staining.

Results
A TM holder was printed successfully and was able to clamp human TMs in their native shape. It withstood formalin soaking without degradation. Processed human TM specimens demonstrate loss of lamina propria in areas adjacent to the perforation, as well as calcific deposition and thickening of the TM in specimens with a history of trauma. Specimens from patients with chronic otitis media demonstrate chronic inflammation throughout the entire lamina propria, obliterating normal architecture. Specimens from revision surgical cases demonstrate previously implanted graft materials (cartilage and fascia) with preserved architecture of extracellular matrix, indicating a lack of structural remodeling over time.

Conclusion
Surgically explanted human TM tissue represents an important source of data for the study of TM mechanics and healing following injury. Further analysis includes the use of immunostaining to identify and localize progenitor cells, collagen content and potential pathogens.

PS 442

Intra-Operative Assessment of Ossicular Mobility: Measurements in Cadavers and Numerical Analysis

Takuji Koike[1]; Sho Kanzaki[2]; Sinyoung Lee[1]; Yuuka Irie[1]; Takaaki Fujishiro[1]; Chee Sze Keat[3]; Takenobu Higo[4]; Kenji Ohoyama[4]; Masaaki Hayashi[5]; Hajime Ikegami[5]
[1]Department of Mechanical and Intelligent Systems Engineering, Graduate School of Informatics and Engineering, The University of Electro-Communications, Japan.; [2]Department of Otorhinolaryngology, School of medicine,Keio University; [3]Mechano Transformer Corp; [4]Leadence Corp.; [5]Daiichi Medical Co., Ltd.

Assessment of ossicular mobility during ossiculoplasty is absolutely essential because the mobility of each ossicle is an important factor in determining surgical procedure and prognosis for recovery of hearing level. The assessments are made by palpation in most cases. However, the palpation is inherently subjective and may not always be reliable, especially in milder degrees of ossicular fixation and in the case of complex fixation. Objective and quantitative measurements therefore have been required.

We have been developing a measurement system for ossicular mobility. The measurement system consists of a hand-held probe and control devices. The probe is composed of an ear pick, which is usually used in ear surgery, a force censor, and an actuator. When the tip of the ear pick contacts an object (each ossicle), the actuator vibrates the ear pick at constant amplitude and frequency (40 microns and 20 Hz). At the same time, the reaction force from the object is detected by the force sensor. The ossicular mobility is evaluated by the ratio of the vibration amplitude to the reaction force (i.e., compliance).

The measurements were performed in fresh cadavers. The tympanic cavity was opened, and the ossicles were confirmed to be normal by visual observation. Measurement points were set at the head of the malleus, the long leg of the incus, and the posterior crus of the stapes. The compliance was obtained at each point, and the effects of the measurement direction on the compliance was also checked at the several points. In addition, these measurements were simulated using a finite-element model of human middle ear, and the compliance at each ossicle and the effects of the measurement direction were numerically evaluated.

The measurement results showed that the compliance was different for each ossicle and depends on the measurement direction. These results were similar to

those obtained by the numerical analysis. Therefore, we believe that our measurement system can provide surgeons with quantitative information about the ossicular mobility. On the other hand, some variation were shown in each measurement result, suggesting that a certain level of measurement skill is required for accurate measurements.

PS 443

Soft Tissue Stimulation Result in Hearing by Skull Bone Vibration

Stefan Stenfelt[1]; Srdan Prodanovic[2]
[1]Department of Clinical and Experimental Medicine, Linköping University, Linköping, Sweden; [2]Linköping University

Several studies have reported hearing perception with vibratory stimulation on soft tissues such as the neck, eye, or direct to the dura, and claimed it to be different from ordinary bone conducted sound. It has been hypothesized that the perception from such stimulation is through a direct fluid pathway and not through skull bone vibration. Here, the induced skull bone vibrations with stimulations at the eye, neck and dura are estimated in a model and compared with skull bone vibrations obtained with ordinary mastoid stimulation.

The evaluations were conducted on the LiUHead, a finite element model of a human head developed for simulations of bone conducted sound. All simulations were done with a circular interface of 15 mm in diameter, simulating the excitation from a B71 transducer. In addition, a computational model of the B71 transducer was used to estimate the output force at each stimulation position. The vibration of the cochlear promontory was evaluated for equal voltage provided to the B71 transducer.

The magnitudes of the load impedances at the soft tissue stimulation positions were significantly lower at frequencies below 2 kHz compared to the mastoid position which lowered the stimulation output from the B71 transducer at low frequencies at these positions. Compared to mastoid stimulation, a stimulation at the neck is predicted to give hearing thresholds that worsen with frequency at 20 dB/decade, which is also reported in the literature. Similar, a stimulation on the eye is predicted to give 10 to 20 dB worse hearing thresholds than at the mastoid, which is also reported in the literature. A stimulation on the dura should give 20 to 40 dB worse hearing thresholds than at the mastoid, which is also in the range reported in the literature.

The simulation indicate that the promontory vibration is a good predictor of the hearing perception when the stimulation is at a soft tissue position. Consequently, soft tissue stimulation is transformed to skull bone vibration that excite the inner ear as with ordinary bone conduction sound.

PS 444

3D X-ray Microscopy Quantification of Intracochlear Tissue Response and Trauma Following Cochlear Implantation in Multiple Species

Alexander D. Claussen; Christopher Kaufmann; Rene Vielman Quevedo; Brian Mostaert; Marlan R. Hansen
University of Iowa Hospitals and Clinics - Department of Otolaryngology-Head & Neck Surgery

Introduction
A cochlear implant (CI) associated tissue response within the scala tympani composed of neo-ossification and soft-tissue is described in animal models and human temporal bones. The tissue response may result from insertional trauma and a foreign body response and is hypothesized to hamper CI performance by raising electrode impedance and contributing to delayed residual acoustic hearing loss following Hybrid CI. Techniques to examine the intracochlear tissue response and grade insertional CI trauma rely on destructive histology techniques and 2D sections. 3D X-ray Microscopy (3DXRM) is a novel approach for enabling 3D volume segmentation and quantification of the intracochlear soft-tissue response and neo-ossification. Improved visualization with 3DXRM allows refinement of pre-existing CI insertion trauma grading scales. Here we present updated intracochlear volumetric quantification and CI trauma grading techniques across multiple species using 3DXRM.

Methods
Samples included fixed human, mouse, and sheep temporal bones with CIs left in-situ. Samples were imaged using a Xradia 520 Versa 3D X-ray Microscope (Zeiss, USA). 3D reconstructions and artifact rejection were implemented within Scout and Scan Control System and XM Reconstructor-Cone Beam 10 software (Zeiss, USA). 3D segmentation, visualization, and trauma grading were performed within Dragonfly 4.1 (ORS, Canada).

Results
3DXRM scans of mouse cochleae with CI in-situ provided high resolution detail (2μm voxel size) of the intracochlear tissue response. 3D segmentation allowed volumetric quantification and improved localization of the scala tympani tissue response with reference to the electrode bearing portions of the CI. There was no significant difference in the total volume of soft-tissue or neo-ossification within the scala tympani between

electrically stimulated and non-stimulated mice. Neo-ossification was centered around electrode bearing surfaces of the CI in both groups. Human and sheep temporal bone scans showed high resolution detail (6µm-12µm voxel size) of soft-tissue and bony elements within the scala, modiolus and lateral wall. 3D reconstruction enabled analysis of scalar implant positioning and traumatic events along the entire insertion depth.

Conclusion
We demonstrate the utility of 3DXRM to study CI related intracochlear trauma and tissue response in multiple species. 3DXRM volumetric quantification of the tissue response and 3D assisted trauma grading provides analysis not subject to the sampling error and sectioning artifact seen with traditional histologic methods. Consistent volumetric quantification of the entire intracochlear tissue response with 3DXRM will enable study of factors contributing to the tissue response and the effect the volume, composition and location of the tissue response has on CI performance.

PS 445

Fetuin A – A Potential Biomarker of Hearing Loss

Wei Liu[1]; Goran Laurell[2]; Jesper Edvardsson-rasmussen[2]; Per-Olof Eriksson[2]
[1]Uppsala University; [2]Dept of Surgical Sciences, Otorhinolaryngology, Uppsala University

Background
Vestibular schwannoma (VS) is an intracranial benign tumor arising from the eigth cranial nerve and has in most cases an effect on inner ear pathology. The primary symptoms of VS are sensorineural hearing loss, tinnitus and vertigo. During surgical treatment of a VS the surgeon has a unique possibility to sample perilymph from the cochlea. We have in a homogenous cohort of VS patients found that the level of the protein Fetuin-A in perilymph correlates with tumor-associated hearing loss. Here we use immunohistochemistry to localize Fetuin-A in the human cochlea.

Methods
Fetuin-A immunoreactivity was detected in a human cochlea, harvested during transcochlear meningioma surgery. The specimen was fixed in paraformaldehyde, decalcified in Na-EDTA and eight µm frozen-sections were prepared. Fetuin-A-immunohistochemistry was carried out using a monoclonal Fetuin-A antibody as the primary antibody. Anti-laminin antibody was used to locate the basement membrane of the glial cells, basilar membrane and blood vessels. Finally, DAPI nuclei staining was performed. Confocal laser scanning microscopy was used to investigate the results.

Results
Fetuin-A-immunoreactivity appeared in human spiral ganglion neurons, inner hair cells, pillar cells and epithelial cells in the Reissner's membrane. The staining was seen in the cytoplasm. Cells in stria vascularis appeared negative for Fetuin-A-immunostaining.

Conclusion
We have in a previous clinical study shown that Fetuin-A is a potential biomarker of sensorineural hearing loss in patients with VS. The present morphological study confirms that Fetuin-A is present in the human inner ear.

PS 446

Are thickened subneuroepithelial extracellular deposits of the cristae ampullares in the human associated with vestibular diseases?

Tadao Okayasu[1]; Jennifer T. O'Malley[2]; Joseph B. Nadol[3]
[1]1) Otopathology Laboratory, Department of Otolaryngology, Massachusetts Eye and Ear 2) Department of Otolaryngology, Harvard Medical School 3)Nara Medical University; [2]1) Otopathology Laboratory, Department of Otolaryngology, Massachusetts Eye and Ear; [3]1) Otopathology Laboratory, Department of Otolaryngology, Massachusetts Eye and Ear 2) Department of Otolaryngology, Harvard Medical School

Background
We previously reported a unique pattern of degeneration of the neuroepithelium of the cristae ampullares with a thickened subepithelial extracellular deposit in three human subjects. In the three cristae of normal controls, the thickness of deposits was positively correlated with age. Our results suggested that age may be associated with the thickness of the sub-neuroepithelial deposits in this unique pattern of degeneration. However, other causative factors associated with the thickness of these deposits are proposed because the thickness of the deposits in three diseased cases was significantly greater than that of age-matched controls. These three human subjects suffered vestibular diseases during life and the neuroepithelium had degenerated to a monolayer of cell at the summit of the cristae ampullares. Therefore, we compared the thickness of the subepithelial extracellular deposits the thickness in cases which had vestibular disease and non-focal degeneration of the neuroepithelium of the cristae ampullares.

Objective
The purpose of this otopathologic study was to compare the thickness of the subepithelial deposits, and to evaluate the effect of vestibular disease on the thickness of those deposits.

Methods

The subepithelial deposits of the vestibular end organs of the three subject cases and controls (unilateral Ménière's disease (n=9), vestibular neuritis (n=7), cupulolithiasis (n=9), severe nonfocal degeneration of the vestibular neuroepithelium (n=14), and Alport syndrome (n=8)) were studied using H&E stained sections. The deposit thickness as measured by light microscopy was compared to control ears without vestibular disease.

Results

The thickness of the subepithelial deposits in three study cases was significantly greater than that of all controls. A comparison of thickness between the diseased ears and the opposite unaffected ears in Ménière's disease, vestibular neuritis and cupulolithiasis found no significant difference in the thickness of the subepithelial deposit with the exception of the lateral semicircular canal where the thickness was significantly greater on the unaffected side in Ménière's cases. The thickness of the subepithelial deposit in the severe non-focal degeneration of the vestibular neuroepithelium was significantly greater than two cristae ampullares and two maculae of the age-matched controls. The thickness of the subepithelial deposit in Alport syndrome was significantly greater for two maculae compared to age-matched controls.

Conclusion

Our results demonstrated that the severe non-focal degeneration of the vestibular neuroepithelium may be associated with the thickness of subepithelial deposits in the cristae ampullares of humans.

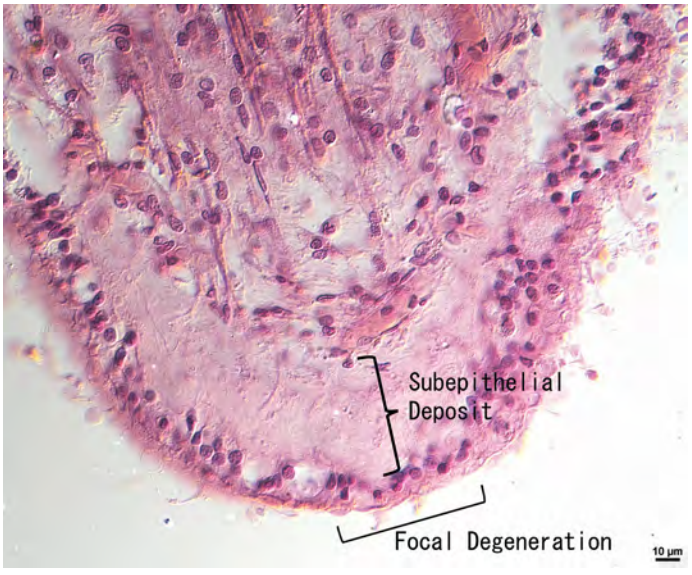

PS 447

Otopathologic Findings in Patients with Alzheimer's Disease

Renata M. Knoll[1]; Nicholas Koen[2]; Rory J. Lubner[2]; Victor E. Alvarez[3]; David H. Jung[4]; Aaron K. Remenschneider[5]; Elliott D. Kozin[6]

[1]Massachusetts Eye and Ear Infirmary/Harvard Medical School; [2]Massachusetts Eye and Ear Infirmary/Harvard Medical School/Warren Alpert Medical School of Brown University; [3]Boston University School of Medicine/ Department of Veterans Affairs Medical Center; [4]Department of Otolaryngology, Massachusetts Eye and Ear Infirmary, Harvard Medical School, Boston, MA, USA; [5]Dept. of Otolaryngology, UMass Memorial Medical Center; Massachusetts Eye and Ear; [6]Massachusetts Eye and Ear Infirmary- Harvard University

Background

Alzheimer's disease is a neurodegenerative disorder characterized by progressive intellectual decline associated with senile plaques, neurofibrillary tangles, and amyloid angiopathy as the main pathological hallmarks. Hearing loss has been associated with Alzheimer's disease and other incident cognitive impairments in older adults.However, the exact mechanism underlying hearing loss in patients with cognitive impairment is still unknown. Herein, we aim to use human otopathologic techniques to analyze the histopathology of the peripheral auditory system in patients with a history of Alzheimer's disease.

Methods

Specimens from the National Temporal Bone Pathology Registry with history Alzheimer's disease confirmed by neuropathologic examination of brain tissue were included. Were excluded cases with a history of other otologic disorders and/or ear surgery. Inner ear anatomy, including counts of spiral ganglion neurons (SGN), was evaluated. SGN counts were compared to historical age-matched controls.

Results

Five temporal bones (TBs) from 3 male patients with history of Alzheimer's disease were identified, and the average of death was 73 years (range, 67 to 81). The interval between the first reports of cognitive decline and death ranged from 10 to 17 years. The number of total SGN was decreased, with an average of 84% loss (range, 64% to 99%) compared to historical age-matched controls. All cases presented with greater SGN loss in the Segment I of the cochlea (mean, 74%).

Conclusions

Otopathological analysis in patients with history of Alzheimer's disease demonstrated reduction of SGN

population. Further studies are necessary to better understand the peripheral auditory system involvement in Alzheimer's disease.

PS 448

Effect of Intermittent Hypoxia on Respiratory Allergic Reaction

Do-Yang Park; Dong Young Kim; Jung Jun Lee; Hun Yi Park; Hyun Jun Kim; Chul-Ho Kim
Dept. of Otolaryngology, Ajou University School of Medicine

Obstructive sleep apnea (OSA) is a highly prevalent disease that induces low oxygen saturation due to repeated complete or partial obstruction of the upper respiratory tract. Most OSA patients present with upper-airway symptoms, and clinical reports have recently reported an association between OSA and allergies. In general, although narrowing of the upper respiratory tract upon allergic reaction is thought to affect the occurrence and severity of OSA, previous studies have shown that hypoxic conditions resulting from OSA may affect the allergy process. Therefore, we hypothesized that OSA may affect the incidence and severity of allergies, and that immune cells involved in this process play an important role. We constructed and verified an OSA mouse model that reflects the characteristics of the disease. This model was then subjected to allergic conditions; we investigated the differentiation of immune cells in OSA and/or allergy mouse models. After OSA and/or allergic conditions for 4 weeks, allergy symptoms, and levels of total Ig E, specific Ig E, and allergic cytokines were only elevated in allergic condition-applied groups compared with those in the control group. The OSA and allergy models showed decreased $CD4^+CD25^+Foxp3^+$ regulatory T cell levels, increased Th17 cell levels, and increased HIF1 levels compared with the control group. We therefore conclude that intermittent hypoxia resulting from OSA affects the development of regulatory T cells through HIF, which may also affect allergy development.

PS 449

Determining Neck Lymph Node Level Patterns in Different Subtypes of Head and Neck Cancer

Brianna Hope[1]; Rahul Varman[2]; Joehassin Cordero[2]
[1]Texas Tech University Health Sciences Center School of Medicine; [2]Texas Tech University Health Sciences Center

Neck dissections have been a consistent treatment option in the management of head and neck cancers, yet they pose very high risks to patients. Performing a neck dissection can cause damage to vital structures in the neck, resulting in significant bleeding, infection, and damage to nerves that could lead to numbness and weakness of the face and neck as well as problems with the vocal cords. Additionally, when more lymph nodes are unnecessarily removed lymphatic drainage is significantly impaired. There is currently an underwhelming amount of data regarding the specific lymph node levels that are most commonly involved with different subtypes of head and neck cancers and the pattern of spread based on their stage and grade. The majority of current recommendations involve either operating on multiple lymph node levels or a very large area of the neck, such as the entire lateral neck or the entire central neck. If specific patterns of spread exist between a specific type of cancer at different stages and the lymph node levels involved, neck dissections could be performed more efficiently and pose fewer risks to the patient. This study aims to identify to which lymph node levels that different subtypes of head and neck cancer preferentially spread. A retrospective cohort study will be performed on head and neck cancer patients at a local facility to identify which neck lymph node levels contained positive lymph nodes after neck dissections. Factors that will be evaluated include grade and stage of the cancer, site of cancer, location of positive lymph nodes, lymph node density in those locations, and whether or not chemotherapy and radiation have been initiated prior to surgery. Based on the results of this study, recommendations for neck dissections could be made based on the subtype of cancer being treated.

Inner Ear Therapeutics I

PS 450

Mitochondrial-ROS Induced Cochlear Hair Cell Death in IDH2 Deficiency Can be Prevented by Mitochondria-Targeted Antioxidant MitoQ

Myung Hoon Yoo[1]; Ye-Ri Kim[2]; Min-A Kim[2]; Un-Kyung Kim[2]; Kyu-Yup Lee[1]
[1]Department of Otorhinolaryngology-Head and Neck Surgery, School of Medicine, Kyungpook National University; [2]Department of Biology, College of Natural Sciences, Kyungpook National University

Mitochondrial $NADP^+$-dependent isocitrate dehydrogenase 2 (IDH2) is a major NADPH-producing enzyme which is essential for maintaining the mitochondrial redox balance in cells. We sought to determine whether IDH2 deficiency induces mitochondrial dysfunction and modulates auditory function, and investigated the protective potential of an antioxidant agent against reactive oxygen species (ROS)-induced cochlear damage in Idh2 knockout ($Idh2^{-/-}$) mice. Idh2 deficiency leads to damages to hair cells and spiral ganglion neurons (SGNs) in the cochlea and ultimately to apoptotic cell death and progressive sensorineural hearing loss in $Idh2^{-/-}$ mice. Loss of IDH2 activity led

to decreased levels of NADPH and glutathione causing abnormal ROS accumulation and oxidative damage, which might trigger apoptosis signal in hair cells and SGNs in Idh2$^{-/-}$ mice. We performed ex vivo experiments to determine whether administration of mitochondria-targeted antioxidants might protect or induce recovery of cells from ROS-induced apoptosis in Idh2-deficient mouse cochlea. MitoQ almost completely neutralized the H2O2-induced ototoxicity, as the survival rate of Idh2$^{-/-}$ hair cells were restored to normal levels. In addition, the lack of IDH2 led to the accumulation of mitochondrial ROS and the depolarization of $\Delta\Psi_m$, resulting in hair cell loss. In the present study, we identified that IDH2 is indispensable for the functional maintenance and survival of hair cells and SGNs. Moreover, the hair cell degeneration caused by IDH2 deficiency can be prevented by MitoQ, which suggests that Idh2$^{-/-}$ mice could be a valuable animal model for evaluating the therapeutic effects of various antioxidant candidates to overcome ROS-induced hearing loss.

PS 451

Quinoxaline protects hair cells from noise-induced damage

Marisa Zallocchi[1]; Jian Zuo[2]; Santanu Hati[1]; Sonia Rocha-Sanchez[3]; Umesh Pyakurel[3]; Shikha Tarang[3]
[1]Creighton University School of Medicine; [2]Department of Biomedical Science, Creighton University; [3]Creighton University School of Dentistry

Hair cell death is the leading cause of hearing and balance disorders in humans. It can be caused by multiple insults, including noise, aging, and treatment with certain therapeutic drugs. As society becomes more technologically advanced, the source of noise pollution and availability of ototoxic drugs are rapidly increasing, posing a threat to our hearing health. While this knowledge has fueled the scientific enthusiasm towards the development of pharmacological interventions, establishing therapeutic measures that slow the progression of hearing loss and protect hearing is still a major clinical challenge. Previous findings from our laboratory have underscored the therapeutic potential of quinoxaline (Qx) and some of its derivatives, to protect the inner ear from cisplatin and aminoglycoside ototoxicity and potentially treat hearing loss. The present study was designed to further expand our current knowledge on the otoprotective effects of Qx and its mechanism of action in hair cells. For this purpose, mice were treated with saline solution or a single intraperitoneal dose of Qx and 24 hours later exposed to an 8-16 kHz octave band noise for 1 hour at 103 dB SPL. Auditory brainstem responses (ABRs) were measured before Qx administration, immediate after noise-exposure or 7 days after noise treatment. While animals treated with saline solution showed threshold shifts of 20 dB or more after 7 days post-noise, ABRs from mice pre-treated with Qx did not show any differences compare to non-noise exposed animals. These results suggest that Qx not only can protect hair cells from drug-induced ototoxicity but also can prevent noise-induce hearing loss. Elsewhere in the body, Qx is known to block NF-kB signaling by inhibiting IKKb and preventing NF-kB nuclear translocation, thereby deterring inflammation and apoptosis. We decided to address whether Qx is targeting the same signaling cascade in hair cells. For this purpose, experiments were performed in HEI-OC1 cells and in transgenic zebrafish lines as well as zebrafish morphants. Results from these experiments suggest that NF-kB pathway is the main target for Qx therapeutic effect. Collectively, the results presented here demonstrated the potential beneficial effect of Qx against noise induced damage, through the regulation of NF-kB and other associated pathways.

Support: NIH 5P20RR018788, R21OD019745-01A1 and 5R01DC015010-04

PS 452

Drug-Induced Hearing Loss Prevention through Clinical Data Driven Drug Re-purposing

Dong Xu; Shaikh Emdadur Rahman; Yuying Huang
Idaho State University

Platinum-based antineoplastic drug and aminoglycoside antibiotics cause irreversible hearing damage or hearing loss. In-vitro studies showed that certain antidepressant agents, HMG-CoA reductase inhibitors (aka statins), and proton pump inhibitors may have protective effects against drug-induced hearing loss (DIHL). A cross-sectional observational study was conducted to evaluate the effect of combinational use of antidepressants with ototoxic drugs using de-identified clinical data obtained from FDA Adverse Events Reporting System. MedDRA PT terms related to DIHL were used to identify the ototoxic events. Among these events, individuals taking any of the 10 ototoxic drugs were considered as the exposed group, while individuals taking any drug from the 32 antidepressants concomitantly with 1 ototoxic drug were put into the outcome group. By calculating the adjusted odds ratio of each drug combination, our study suggests that fluoxetine significantly reduce the ototoxicity of carboplatin (combination aOR 0.03, CI 0.01-0.05, $p < 0.05$, vs Carboplatin aOR 0.80, CI 0.65-0.97, $p < 0.005$). citalopram is found to reduce tobramycin induced ototoxicity significantly (aOR 0.08, CI 0.03-0.17, $p < 0.05$, vs tobramycin aOR 0.198152, CI 0.24-0.16, $p < 0.05$). Atorvastatin shows strong evidence of preventing ototoxic effects. The unadjusted odds ratio

for carboplatin and atorvastatin is 0.55 whereas cisplatin alone is 1.32. Additionally, lansoprazole and omeprazole also show mitigating effects on ototoxicity resulting from cisplatin (OR 0.58, CI 0.08 - 4.13 and OR 0.45, CI 0.11 - 1.8, respectively). Using cross-sectional clinical data, our study identified FDA-approved drugs that can be potentially repurposed to prevent DIHL. Further validation of these results using large longitudinal clinical data is underway.

PS 453

Reducing Cisplatin-Induced Hearing Loss by Manipulating the Blood Labyrinth Barrier

Ayesha Noman; Subhendu Mukherjee; Trung Le
Sunnybrook Research Institute

Introduction
Cisplatin is a chemotherapeutic medication used to treat many types of cancers. It has been shown to remain in the cochlea indefinitely, causing permanent bilateral hearing loss. Mannitol, a diuretic medication, can alter the permeability of the blood-labyrinth barrier (BLB). We hypothesized that administering mannitol during cisplatin chemotherapy will increase the permeability of the BLB, allow cisplatin to egress from the inner ear, and provide otoprotective properties against cisplatin induced hearing loss.

Method
We investigated whether mannitol increases the efflux of cisplatin from the inner ear by injecting rats with either cisplatin and mannitol or cisplatin alone. Perilymph of injected rats was surgically collected at different time points to generate a pharmacokinetic curve. The perilymph was processed using an optimized derivatization protocol that extracts cisplatin-platinum from bodily fluids. The cisplatin-platinum concentrations were detected using Liquid Chromatography MS/MS. We further investigated whether mannitol has otoprotective properties by injecting rats with cisplatin alone, cisplatin with mannitol or cisplatin with mannitol injections 6 hours later. The rats were subjected to a clinically relevant cisplatin regime comprising of 3 cycles. Each cycle consisted of 4 days of injections followed by a 10-day recovery period. Auditory experiments were performed at 30 and 60 days after the start of the trial. Auditory Brainstem Response (ABR) and Distortion Product Otoacoustic Emission (DPOAE) was measured to monitor changes in hearing threshold and amplitude.

Results
The results indicated that 3 cycles of cisplatin injections are necessary to induced long term bilateral hearing loss. Mannitol injections when given with and 6 hours after cisplatin injections had beneficial effects in reducing hearing loss noted with a lower hearing threshold and an improved amplitude for each frequency. Mannitol injections 6 hours post cisplatin injections had an additional protective effect at a higher frequency range.

Conclusions
Here our results demonstrated the role of mannitol in the manipulation of the blood labyrinth barrier and preventing long-term retention of cisplatin in the cochlea. Mannitol can reduce cisplatin ototoxicity in susceptible tissues of the inner ear. This will provide an important therapeutic strategy to prevent cisplatin ototoxicity, a direct implication in hearing rehabilitation in cisplatin chemotherapy. To further this research, we hope to test whether mannitol injections with antioxidant will have an additive effect in preventing cisplatin-induced hearing loss. Mannitol may increase the influx of antioxidants into the inner ear therefore enhancing their efficacy.

PS 454

Screening Hair Cell Protection in Autophagy Library using the zebrafish lateral line

Yoshinobu Hirose; Kazuma Sugahara; Makoto Hashimoto; Shunsuke Tarumoto; Hiroshi Yamashita
Yamaguchi University

Zebrafish lateral line hair cells are physiologically and morphologically similar to inner ear hair cells. As the zebrafish lateral line is located on the body surface, damage to the hair cells can be rapidly assessed. Therefore, the zebrafish lateral line is an effective system for the evaluation of drugs that damage or protect hair cells. We have been used to screen protective effect of supplement and herbal medicines drugs, and damage effect of anti-cancer drugs.

Autophagy is one of the mechanisms of cells to break down intracellular proteins. It is a mechanism found in eukaryotic organisms from yeast to humans, preventing the accumulation of abnormal protein in the cell, recycling proteins when protein synthesis is excessive or when the nutrient environment deteriorates. It is involved in maintenance of homeostasis of living organisms by eliminating pathogenic microorganisms invaded into the cytoplasm. In addition, it is known to be involved in programmed cell death in the process of ontogeny, occurrence of diseases such as Huntington's disease, and inhibition of canceration of cells.

There will be a possibility that autophagyplays an important role in the inner ear. In this research, we have used the zebrafish lateral line to screen a library of 94 Autophagy drugs (Cancer Research Institute of Kanazawa University Drugs Set) that induce or inhibit autophagy for hair cell protection.

5 dpf Zebrafish embryos of the AB wild-type strain were produced by paired mating of adult fish. Zebrafish larvae were exposed to the drug library at concentrations of 0, 1, 10, 100, and 1000 mM for 1 h prior to neomycin exposure. After fixation in 4% paraformaldehyde, zebrafish were incubated with anti- parvalbumin antibody at 4º C overnight. Hair cells from the SO1, SO2, O1, and OC1 neuromasts were counted. Ten fish per dose were counted. Results were calculated as the mean hair cell survival as a percentage of the control.

Screening identified some protective drugs against neomycin. Especially, Rapamycin, Timosaponin A-III showed a strong protection, and both related to mTOR inhabitation.

This study suggested thatautophagy play an important rolein hair cells protection.

PS 455

Drug Repurposing by Transcriptomic Analysis Identifies Potential Otoprotective Agent for Noise-induced Hearing Loss

Parinaz Dabestani[1]; Joseph DiGuiseppi[1]; Cassidy Nguyen[1]; Jian Zuo[2]; Sarath Vijayakumar[3]
[1]Creighton University; [2]Department of Biomedical Science, Creighton University; [3]Creighton University School of Medicine

Noise-induced hearing loss (NIHL) via occupational, residential and recreational activities is the second most prevalent form of acquired sensorineural hearing loss and is a major health problem worldwide. Development of therapeutic approaches for NIHL has been challenging because of the diverse cellular and molecular mechanisms underlying NIHL. Drug repurposing is a faster and relatively cheaper alternative to the lengthy and expensive de novo drug discovery and development. As such, we have elected to follow drug repurposing protocols. In the present study, we performed functional enrichment and pathway analyses using cochlear transcriptome from acoustic overstimulation mouse models. L1000 CDS^2 search engine tool was used to probe library of integrated network-based cellular signatures (LINCS) small molecule expression profile dataset. We identified 16 novel drugs/compounds that can either mimic or reverse the gene signature associated with mouse models of NIHL. We selected 4 drugs from our drug candidates for further study. Toxicity screens done in HEI-OC1 cell line and cochlear explants showed median toxic dose (TD_{50}) of ~0.5mM for the tested drugs. We are currently evaluating the efficacy of these drugs in protection against NIHL through morphological and functional studies in mouse models of acoustic trauma. We anticipate that the drug(s) will prevent NIHL when administered concurrently with acoustic trauma.

This study was supported in part by NIHR01DC015010, NIHR01DC015444, ONR-N00014-18-1-2507, USAMRMC-RH170030, and LB692/Creighton to JZ and Bellucci Funds to SV.

PS 456

Identification of Exosome Associated Factors that Protect Against Aminoglycoside Induced Hair Cell Death

Tucker Q. Costain[1]; Lizhen Wang[1]; Andrew M. Breglio[1]; Lindsey A. May[1]; Nora C. Welsh[1]; D. Eric Anderson[2]; Melanie Barzik[3]; Lisa L. Cunningham[3]
[1]NIDCD, National Institutes of Health; [2]NIDDK, National Institutes of Health; [3]Laboratory of Sensory Cell Biology, NIDCD, NIH

Exosomes are cell-derived extracellular vesicles that facilitate cell-cell communication. They range from 50-150 nm in size, possess a lipid bilayer, and contain a distinct combination of proteins, lipids, and nucleic acids. Exosomes can induce functional changes in target cell behavior, either through interaction with cell surface receptors or fusion with the plasma membrane.

We have recently shown that exosomes play a role in intercellular communication in the inner ear. Exosomes derived from heat-shocked utricles protect hair cells from aminoglycoside-induced ototoxicity and exosome-associated heat shock 70 kDa protein (HSP70) is required for this pro-survival effect. Given the small yield of exosomes from mouse utricles, we are expanding our studies to include cell line-derived exosomes. Here, we are further investigating the protective role of HSP70 as well as the functions of other exosome-associated proteins involved in exosome targeting and delivery, such as integrins.

Whole-organ cultures of utricles from adult mice were used as a model system, and multiple cell lines were analyzed for exosome secretion. Exosomes were isolated via centrifugal ultrafiltration, quantified by nanoparticle tracking analysis, and applied to utricles to investigate their ability to inhibit neomycin-induced hair cell death. Tandem mass spectrometry and Western blot analysis were used to identify and compare exosome content from inner ear tissue and cell lines.

Native exosomes derived from an epithelial cancer cell line (CT26) protected hair cells from neomycin-induced hair cell death in a concentration-dependent manner. Both heat shock and exogenous expression of HSP70 increased the amount of HSP70 in CT26 exosomes.

Comparative mass spectrometry analyses showed that CT26-derived exosomes contain multiple members of the HSP70 protein family. Exosomes derived from utricles and CT26 cells contain similar repertoires of integrin family members, which may play a role in targeting exosomes to inner ear cell types.

The identification of otoprotective exosomes derived from cell lines enables the development of precision-engineered exosome therapeutics. Compared to inner ear tissue, cell lines can yield large quantities of exosomes and can be subjected to biological manipulation aimed at optimizing exosome content. In addition, analysis of exosome cargo established an inventory of factors that may be required for the pro-survival effect in the inner ear. Using this information, we intend to engineer cell line-derived exosomes to systematically investigate which exosome-associated factors are necessary and sufficient to protect hair cells.

PS 457

Too much of a good thing: High doses of antioxidant can damage P3 cochlear cultures

Haiyan Jiang[1]; Dalian Ding[1]; Richard Salvi[2]
[1]Center for Hearing and Deafness; [2]Center for Hearing and Deafness, 137 Cary Hall University at Buffalo, Buffalo, NY 14214

Excessive oxidative stress is believed to contribute hearing loss when the cochlea's antioxidant defense systems are overwhelmed intense noise and high doses of ototoxic drugs. Therefore, there have been many attempts to reduce the risk of noise- and drug-induced hearing loss with a variety of compounds with antioxidant properties. However, high doses of these antioxidant can become toxic if they disrupt the endogenous oxidant vs. antioxidant balance. In current study, we evaluated antioxidant-induced stress in P3 rat cochlear organotypic cultures treated with 50 μM of M40403, a superoxide dismutase mimetic, 50 μM coenzyme Q-10, or 50 μM d-methionine for 48 h. We compared the condition of the hair cells and neurons in control cochlear cultures maintained under normal culture conditions versus cochlear explants culture with M40403, coenzyme Q-10 and d-methionine. The hair cells and neurons in the control cultures appeared normal after 48 h in cultures. In contrast, many cochlear hair cells were destroyed and slight damage was evident to the auditory nerve fibers in the cochlear explants treated with M40403 or coenzyme Q-10. More extensive damage was observed with d-methiodine which severely damaged the surface structure of the hair cells and completely destroyed the spiral ganglion neurons and their auditory nerve fibers. These results indicate excessive amounts of antioxidants can become toxic when the disrupt the endogenous oxidative-antioxidant balance. This results illustrate the importance of carrying out a full dose-response range with antioxidant therapeutics to not only identify the most effective therapeutic dose, but also dose that increase the risk hearing loss and cochlear damage.

PS 458

Protective Effects of Synthesized Berbamine Analogs Against Aminoglycoside-Induced Hair Cell Death

Alexandria Hudson[1]; Gavin Lockard[2]; Bruce Blough[3]; Peter Steyger[4]; Allison Coffin[1]
[1]Washington State University, Vancouver; [2]Washington State University, Spokane; [3]Research Triangle Institute; [4]Creighton University

Aminoglycosides are used globally due to their potent antibacterial properties and low cost, surpassing expensive antibiotics with fewer harmful side effects. However, their use is often coupled with permanent hearing loss that affects 20% of patients requiring these life-sustaining antibiotics. To date, there are no FDA-approved drugs that prevent hearing damage from aminoglycosides. Our goal is to develop a drug that prevents aminoglycoside-induced hearing loss. A previous study by our lab identified four compounds that share a modified quinoline scaffold and strongly protect zebrafish lateral line hair cells by attenuating aminoglycoside uptake, likely via partial block of the mechanotransduction (MET) channel. The present study builds on previous work, investigating analogs of berbamine, our most protective compound, to determine the core protective structure and the specific molecular targets that are responsible for protection. Recent findings suggest that co-treatment of our analogs with aminoglycosides robustly protect hair cells from ototoxic damage at higher potencies than the parent compounds. Some analogs were found to be particularly efficacious and blocked uptake of aminoglycosides, implying those structures likely mitigate damage via a transient block of the MET channel. Additional experiments further demonstrate that some analogs may attenuate aminoglycoside hair cell damage via intracellular mechanisms in addition to transiently blocking the MET channel. Hair cell protection also varied depending on the combination of analog and aminoglycoside. Certain analogs protected hair cells from multiple aminoglycosides while others only prevented neomycin damage. These data suggest multiple pathways of protection and are consistent with the literature on aminoglycosides activating different mechanisms of damage. Future studies will further explore the derivative chemical structure to refine the functional groups for optimization as an otoprotectant for aminoglycoside toxicity.

PS 459

Evaluation of various therapeutic classes in protection against cisplatin-induced hearing loss (Preclinical models)

Natalia Tsivkovskaia; Rayne Fernandez; Claudia Fernandez; Bonnie E. Jacques; Fabrice Piu
Otonomy Inc

Background
Cisplatin is a potent chemotherapeutic agent that is widely used to treat a variety of cancers in adults and children. Each year, in the U.S. alone, approximately 500,000 patients receive platinum-based chemotherapy. However, the administration of cisplatin is commonly associated with severe adverse effects including nephrotoxicity, peripheral neuropathy and ototoxicity. Cisplatin-induced ototoxicity, commonly referred to as cisplatin-induced hearing loss (CIHL), has a high prevalence and manifests as sensorineural hearing loss and tinnitus, with the hearing loss being progressive, bilateral and irreversible. To date, there are no FDA approved treatments for cisplatin-induced ototoxicity. In an effort to compare different pharmacological approaches against cisplatin ototoxicity, a variety of pharmacological tools (targeting cisplatin binding, drug transport, oxidative stress, apoptosis / cell death) were evaluated in preclinical rat models of acute and chronic cisplatin administration.

Methods
Adult rats (Sprague-Dawley) served as subjects in these experiments.

Acute paradigm: animals received a single intraperitoneal infusion (over 30 min) of cisplatin at a dose of 11-12 mg/kg and were monitored for 3 days. Pharmacological intervention was conducted as a single intratympanic administration, given 30 min prior to cisplatin.

Chronic paradigm: animals were submitted to 4-6 cycles of cisplatin injections at 3 mg/kg given intraperitoneally. Each cycle consisted of a single injection of cisplatin followed by a 4- to 5-day recovery period. Pharmacological intervention was conducted at every other cycle via intratympanic administrations given 30 min prior to cisplatin.

During the course of the studies, animal health, body weight and mortality were monitored and recorded. Hearing function was measured using ABR (auditory brainstem response) at various frequencies for the duration of the studies. Hair cell integrity was determined at termination via cytocochleograms.

Results
There were notable differences in the relative otoprotective effects of various therapeutics evaluated when given intratympanically. Almost complete protection was achieved with certain therapeutic classes, as determined both functionally and histologically, whereas only partial protection was evident with others.

Conclusions
Preclinical models of acute and chronic cisplatin-induced hearing loss were developed and used to characterize the relative otoprotective properties of various therapeutics targeting multiple aspects of cisplatin ototoxicity. The differential profiles of otoprotective agents evaluated in these studies may be helpful in selecting molecules and mechanisms that have a greater potential of clinical success.

PS 460

Otoprotective Effect of Selegiline in Noise-Induced Hearing Loss in BALB/c Mice

Judit Szepesy[1]; Viktória Humli[2]; Ágnes Szirmai[3]; Gábor Polony[3]; Anita Gáborján[3]; László Tamás[3]; Tibor Zelles[2]
[1]Department of Pharmacology and Pharmacotherapy and Department of Otorhinolaryngology, Head and Neck Surgery; Semmelweis Universiy; [2]Department of Pharmacology and Pharmacotherapy; Semmelweis Universiy; [3]Department of Otorhinolaryngology, Head and Neck Surgery; Semmelweis Universiy

Noise-induced hearing loss (NIHL) is one of the most common form of SNHLs with increasing prevalance as a consequence of change in our music listening habits. Acute noise exposure can cause temporary threshold shift (TTS) what frequently becomes permanent (PTS). Even though NIHL imposes a realistic threat to the modern society, there is no efficient drug therapy. Excitotoxicity and increased level of reactive oxygen species (ROS) are presumed to play a role in the pathomechanism. Selegiline is a selective monoamine oxidase type B (MAO-B) inhibitor, used for increasing DA-ergic neurotransmission in Parkinson's disease. It can also decrease the generation of ROS and shows neuroprotective actions. We expected that its mixed activity is beneficial in the prevention of NIHL.

To test the effect of selegiline against permanent NIHL, we have deployed a one-time noise exposure mouse model. We developed a noise box with spatially homogeneous sound field and exposed BALB/c mice to 8-16 kHz white noise with different sound pressure level and duration time. TTS and PTS were determined by ABR. Thresholds were measured using both click and tone burst (4-32 kHz) stimuli before and after (1 day, 4 days, 15 days and 1 month) noise exposure. Based on our measurements, the 30 min, 98 dB noise exposure

was chosen for further experiments. N-Acetylcysteine, a compound shown to be protective against NIHL, was used to validate the model. Both drugs were administered parenterally for 5 consecutive days, starting one day before noise exposure.

Although NIHL was attenuated by NAC one day after exposure, this protection proved to be temporary. In contrast, the slight but significant protective effect of selegiline remained even a month later, providing protection against PTS.

In summary, we have set up a mouse model for testing protective action of drugs against hearing loss induced by overexposure to acute noise and used it successfully to show the otoprotective effect of selegiline. The complex, multifactorial pathomechanism of NIHL, most likely requires drugs acting on multiple targets. By inhibiting MAO, selegiline probably increases the release of dopamine (DA) from lateral olivocochlear (LOC) efferents in the cochlea. LOC system provides endogenous protection against excitotoxicity, thereby, plays a role in the protective effect of selegiline. Selegiline with combined antioxidant, antiapoptotic, neuroprotective action might be a good candidate for small-molecule-based pharmacotherapy in NIHL.

PS 461

Role of Mitochondrial Deacetylase SIRT3 in Hearing Protection

Xiaodong Tan[1]; Yingjie Zhou[2]; Aditi Agarwal[1]; Alan Robinson[1]; David Gius[3]; Claus-Peter Richter[4]
[1]Northwestern University, Dept. Otolaryngology; [2]Northwestern University, Dept. Communication Sciences and Disorders; [3]Northwestern University, Dept. Radiation Oncology; [4]Northwestern University, Dept Otolaryngology

Background
Sirtuin 3 (SIRT3) is the primary NAD+-dependent deacetylase in mitochondria. SIRT3-mediated protein deacetylation through Manganese Superoxide Dismutase and isocitrate dehydrogenase 2 activation are essential for reactive oxygen species detoxification and cell protection from oxidative damage. It has been suggested that SIRT3 activation prevents from noise/drug-induced and age-related hearing loss. While different compounds and treatments have been tested for SIRT3 activation, their clinical use faces challenges. For example, the dose of nicotinamide riboside (2000 mg/kg/day) used for SIRT3 activation given for hearing protection in noise is too high for clinical application. Adjudin, which protects against gentamycin ototoxicity, is a male contraceptive. Despite all studies claim that elevated SIRT3 leads to hearing protection, none of them provided convincing evidence of increased SIRT3 expression in the cochlea.

In this study, we demonstrate for the first time the role of honokiol induced elevated SIRT3 expression and protection from cisplatin-induced cochlear damage.

Methods
For cell culture, House Ear Institute-Organ of Corti 1 (HEI-OC1) cells were cultured with the co-application of cisplatin (50 μM) and HNK (0, 10, 25 μM, respectively). Expression levels of SIRT3, SIRT2, caspase 3, anti-cleaved poly ADP ribose polymerase, and acetylation level were examined with western blot. For in vivo studies, honokiol (10-20 mg/kg) was injected intraperitoneally 1 hour prior to cisplatin injections (15-20 mg/kg) or noise exposure (8-16 kHz band noise, 90 dB SPL for 2 hours) in adult C57BL/6J mice. Honokiol was also given to another experimental group twice per week starting from 3 months to 6 months. Auditory brainstem responses (ABRs) were measured pre- and post-treatment to determine cochlear damage by the elevation of ABR thresholds. After euthanasia and fixation, immunostaining and confocal microscopy of cochlear whole mounts were performed to count missing outer hair cells, number of synaptic endings at the inner hair cells, and the levels of SIRT3 expression. SIRT3 knock out (*SIRT3*$^{-/-}$) mice were used as a negative control.

Results
Honokiol increased the expression of SIRT3 but not SIRT2. The expression of apoptosis-related gene and cellular acetylation level decreased. Honokiol treatment significantly reduced the threshold elevation and improved animal health during cisplatin treatment. Confocal imaging showed that honokiol increased OHC survival in cisplatin treated mice. SIRT3 expression was detected in wild type animals, increased by honokiol treatment, and was not expressed in *SIRT3*$^{-/-}$ mice.

Funding
Supported by grants from the Hearing Health Foundation and the American Hearing Research Foundation to XT.

PS 462

Transcriptome Analysis to Identify Drugs Against Cisplatin-Induced Ototoxicity

Pezhman Salehi[1]; Marisa Zallocchi[2]; Madeleine Urbanek[1]; Molly Kubesh[1]; Zhuo Li[1]; Kimberlee Giffen[2]; Tal Teitz[3]; Jian Zuo[4]
[1]Creighton University, School of Medicine; [2]Creighton University School of Medicine; [3]Deaprtment of Pharmacology and Neuroscience; [4]Department of Biomedical Science, Creighton University

Cisplatin is one of the most effective platinum-based compounds in the treatment of solid tumors. Despite its efficacy, ototoxicity, neurotoxicity, and nephrotoxicity stand out as the top three dose-limiting side effects in patients receiving chemotherapy. Ototoxicity refers to drug or chemical-related damage to the inner ear sensory cells and neurons, resulting in permanent, irreversible hearing loss. Elevation of hearing thresholds have been reported in most patients treated with cisplatin. To date, there are no FDA-approved drugs for the treatment of cisplatin-induced hearing loss, creating an imperative need for new treatments to diminish ototoxicity in patients receiving cisplatin for cancer treatment.

This study aims to prevent cisplatin-induced damage to the cochlear cells by investigating drug candidates which could potentially activate multiple pathways involved in mechanisms of cisplatin cytotoxicity. Using recent advances in developing bioinformatic web-based tools, The Library of Integrated Network-Based Cellular Signatures (LINCS), we have analyzed 15 gene expression databases available on NCBI GEO and identified 18 candidate drug candidates for prevention of cisplatin-induced hearing loss. Following testing candidate compound on cells and zebrafish, the 6 final top drugs candidates were selected based on their ability to grant at least 40% protection in either cell or zebrafish models.

The results of this study will provide the key proof of principle to develop novel therapeutic strategies against cisplatin-induced ototoxicity in patients receiving cancer chemotherapy.

PS 463

DB-020 Protects Cells from Cisplatin Cytotoxicity in vitro and Hair Cells in a Guinea Pig Model of Cisplatin Induced Ototoxicity

Yong Ren[1]; Changsuk Moon[1]; Ryan McCarthy[1]; Yuan Xu[2]; Brendan Arsenault[1]; Qi-Ying Hu[1]; Ruiben Feng[2]; Janeta V. Popovici-Muller[1]; John Lee[1]; John Soglia[1]; Inmaculada Silos-Santiago[1]; **Fuxin Shi**[1]
[1]Decibel Therapeutics; [2]Chempartner

Cisplatin is widely used and effective chemotherapy in the treatment of adult and pediatric solid tumors.[1] While cisplatin is effective in killing tumor cells, it can also kill other cells in the body leading to side effects such as neurotoxicity, nephrotoxicity and ototoxicity.[2]

We are developing a small molecule compound, DB-020, to protect hearing in patients undergoing cisplatin-based chemotherapy. DB-020 is a nucleophile, binds, and inactivates cisplatin. In in vitro and ex vivo studies, we demonstrated that DB-020 protected cisplatin-induced cell death in both differentiated UB/OC2 cells and neonatal mouse cochlear explant model in a concentration-dependent manner. Importantly, DB-020 was shown to completely protect UB/OC2 cells and outer hair cells from cisplatin-induced cell death using clinically relevant cisplatin incubation concentrations. We showed that DB-020 markedly reduced both cell- and DNA-associated platinum levels assessed by ICP-MS in differentiated UB/OC2 cells. These results suggested that DB-020 protects cells from cisplatin toxicity by preventing cisplatin from cell entry and preventing DNA-platinum adduct formation.

We hypothesized DB-020 administered locally to the middle ear leads to a high level of exposure in the cochlea and selectively protects hair cells without significantly increasing systemic levels of DB-020. A guinea pig model of cisplatin-induced ototoxicity was developed that produces consistent, bilateral hearing loss and hair cell damage at high frequency ranges of 24 and 32 kHz following a single IV injection of cisplatin. A single dose of DB-020 administered by intratympanic injection, before or after cisplatin dosing, prevented cisplatin-induced hearing loss and hair cell death in a dose-dependent manner. Hearing loss protection was maintained for at least 90 days (the last time point assessed) after a single DB-020 administration.

Therefore, DB-020 has the potential to provide maximum protection from cisplatin ototoxicity, without negatively impacting cisplatin anti-tumor efficacy. DB-020 is currently being tested in a phase 1 trial for safety, tolerability, and systemic pharmacokinetics.

1. Paken J, Govender CD, Pillay M, et al. Cisplatin-Associated Ototoxicity: A Review for the Health Professional. J Toxicol. 2016;2016:article ID 1809394.
2. Callejo A, Sedo-Cabezon L, Juan ID, et al. Cisplatin-Induced Ototoxicity: Effects, Mechanisms and Protection Strategies. Toxics. 2015;3(3):268-93.

PS 464

Ex Vivo Evaluation of the Therapeutic Potential of Several Drug Classes to Prevent Cisplatin Mediated Ototoxicity in the Rat Cochlea

Pranav D. Mathur[1]; Phillip Uribe[2]; Stephanie Szobota[3]; Anne Harrop-Jones[1]; Sairey Siegel[3]; Oliver Silerio[3]; Fabrice Piu[2]; Bonnie E. Jacques[2]; Alan C. Foster[3]
[1]Otonomy, Inc.; [2]Otonomy Inc; [3]Otonomy Inc.

Background
Cisplatin is a first line drug used in the treatment of a variety of cancers. One of the major side effects of

cisplatin therapy is hearing loss, which can be particularly severe in children and elderly patients. In the inner ear, hair cells (HCs), spiral ganglion neurons (SGNs) and the cells of stria vascularis (SV) have been reported to be the primary targets of cisplatin ototoxicity. Upon entering a cell, cisplatin binds to nuclear and mitochondrial DNA, forming adducts that cause cell cycle arrest, increased levels of reactive oxygen species (ROS), and activation of several apoptotic pathways that ultimately lead to cell death. Potential agents to prevent cisplatin-induced ototoxicity include anti-apoptotic molecules, antioxidants and molecules that can bind to and sequester cisplatin. Here we compared the otoprotective profiles of these classes of molecules in ex-vivo models of cisplatin-induced ototoxicity in rats.

Methods

Cochlear explants from P2-P3 Sprague-Dawley rats were established, allowed to acclimate overnight, and pre-treated for 1.5 hours with various concentrations of test compounds prior to co-incubation with cisplatin for 72 hours. After incubation, explants were fixed and stained with HC and SGN specific markers to quantify otoprotection. To evaluate protection of the SV cells, dissociated strial cells were cultured for 48-72 hours to achieve ~85-90% confluency, pre-incubated with the otoprotectants, followed by co-incubation with cisplatin for 22 hrs. SV cultures were tested for caspase3/9 activation, markers of apoptosis. Reverse phase-HPLC was used to assess the cisplatin binding potential of the test compounds.

Results

We observed antioxidant molecules with varying degrees of cisplatin-binding ability. Interestingly, our results indicate that, in general, antioxidants and cisplatin-binding molecules demonstrate preferential protection of HCs and SV cells compared to anti-apoptotic molecules, whereas anti-apoptotic molecules display consistent protection of SGNs in a dose-dependent manner.

Conclusions

Evaluation of different therapeutic classes of compounds identified dose-dependent protection of the key cell types of the inner ear targeted by cisplatin ototoxicity. Compounds that have cisplatin-binding properties in addition to acting on other pathways may provide greater otoprotection relative to compounds with a single mechanism of action. Our data also revealed differing toxicity profiles across cell types within the cochlea in response to cisplatin suggesting that different cell types may respond differently to otoprotective agents.

PS 465

Cellular Senescence Caused by a Low Concentration of Hydrogen Peroxide is Alleviated by a NAC Treatment in a HEI-OC1 Cell Line

Tae-Hwan Kim[1]; Min Jung Park[2]; Yong-Ho Park[2]
[1]Chungnam National University Hospital; [2]Chungnam National University

Cellular senescence is defined as irreversible growth arrest that can be induced prematurely in actively dividing cells through application of various stimuli. Hydrogen peroxide (H_2O_2) was used to induce cellular senescence in the House Ear Institute-Organ of Corti 1 (HEI-OC1), one of the few mouse auditory cell line. HEI-OC1 cells were cultured under permissive conditions (33°C, 10% CO_2) in high-glucose Dulbecco's Modified Eagle Medium (DMEM) containing 10% fetal bovine serum (FBS) without antibiotics. HEI-OC1 cells were treated with 50 μM or 75 μM H_2O_2 in the growth medium for 2 h. Culture media was replaced with fresh DMEM with 10% FBS. Cells were then maintained in culture for 3 days to establish senescence. Biomarkers of cellular senescence, including senescence-associated β-galactosidase (SA β-gal) staining and DNA foci, was apparent in 50 μM and 75 μM hydrogen peroxide-treated HEI-OC1 cells at 48h and 72h after hydrogen peroxide removal as compared to control treatment (0 μM H_2O_2). Importantly, real-time quantitative live-cell imaging and analysis system (IncuCyte® Live-Cell Analysis System, Satorius, France) revealed that HEI-OC1 cells treated with 50 μM and 75 μM hydrogen peroxide showed growth arrest and a significant increase in mitochondrial ROS production in a dose-dependent manner. The most abundant ROS production was found during the first 6 h after hydrogen peroxide treatment. To investigate the cellular senescence-associated mechanisms, N-acetylcysteine (NAC) was administered 24h prior to (pre-treatment), simultaneously (co-treatment) or 24h post (post-treatment) hydrogen peroxide administration. Both pre- and co-treatment of NAC significantly diminished markers of cellular senescence, SA β-gal staining and DNA foci, accompanied by decreased mitochondrial ROS production as compared to hydrogen peroxide-treated cells. Interestingly, no significant changes were found in SA β-gal staining and DNA foci by post-treatment of NAC. Taken together, the results of the study suggest that low concentration of hydrogen peroxide induces cellular senescence in HEI-OC1 mouse auditory cell line accompanied by mitochondrial ROS production. The hydrogen peroxide-induced cellular senescence was attenuated by pre- and simultaneous (co-) treatment of NAC, but not by post-treatment, indicating scavenging early-releasing ROS ("critical time period") is an important factor in alleviating hydrogen peroxide-induced cellular senescence.

PS 466

Electrical Stimulation and Exogenous BDNF and NT-3 in Murine Cochlea Explant Cultures: Only a Neural Survival Factor or also Promoting Axonal Outgrowth?

Dominik Schmidbauer[1]; Stefan Fink[2]; Francis Rousset[3]; Marcus Müller[2]; Pascal Senn[3]; Rudolf Glueckert[1]
[1]Inner Ear Laboratory, Medical University Innsbruck, Innsbruck, Austria; [2]Tübingen Hearing Research Centre, Department of Otolaryngology-Head & Neck Surgery, Eberhard Karls University Tübingen, Germany; [3]Department of Clinical Neurosciences, Service of Otorhinolaryngology, Head and Neck Surgery, University Hospital of Geneva

Cochlear implants (CI) are very well-established devices to replace hair cell function. Despite their success, only little progress in speech recognition, especially in monosyllabic words, could be achieved for decades. The main obstacle for further advancement is a lack in specificity of electrical stimulation. The gap between the CI's electrodes and the stimulation target, the spiral ganglion neurons (SGN), results in current spread and an unspecific stimulation of the tonotopically organized SGNs. This impedes frequency discrimination and deteriorates speech recognition. A proposed solution to overcome this gap could be directed regrowth of SGNs towards the electrodes' surface.

In this study, we tested the influence of two neurotrophins and electrical stimulation on regrowth and branching behavior in murine SGN explants from apical, medial and basal turns in vitro. Therefore, a new insert for 24 well plates was developed to apply currents from cochlea implants via platinum/iridium electrodes. Cochleae were extracted from p6-7 C57/B6N mice and dissected into two spiral ganglion pieces per turn and then cultured for four days. The culture medium was supplemented by different concentrations of BDNF and NT-3. Additionally, biphasic electrical pulses with different parameters were applied to unsupplemented and supplemented specimens. Subsequently, the explants were fixed, immunohistochemically stained for beta-3-tubulin and analyzed in Matlab. In order to obtain more information about branching, axonal density and other properties, the resulting images were skeletonized and converted to graphs.

BDNF and NT-3 do not have an influence on the mean length of neurites. Compared to unsupplemented controls, no increase could be observed even at concentrations as high as 200 ng/ml. Regardless of the neurotrophin concentration, the mean length of neurites is more dependent on the number of outgrowing neurites indicating an influence of mutual support of neurites. However, total length and therefore the number of resprouting SGNs increased with higher concentrations of BDNF and NT-3. Also, the explant size had a small effect on the number of outgrown neurites. There were no noteworthy differences in outgrowth performance within the three turns evident. Effects of electrical stimulation will also be reported. Results considerably varied among single explants, which is probably caused by variances during dissection.

This study sheds more light on the effects of BDNF and NT-3 on murine SGN explants and suggests that their main beneficial effect is an increased number of surviving and resprouting SGNs rather than promoting elongation of axons.

PS 467

Single-Cell Fluorescence Analysis of Pseudotemporal Ordered Cells Provides Protein Expression Dynamics for Neuronal Differentiation

Zhichao Song; Alejandra Laureano; Kishan Patel; Sylvia Yip; Azadeh Jadali; **Kelvin Y. Kwan**
Rutgers University

Stem cell replacement therapy is a potential method for repopulating loss spiral ganglion neurons (SGNs) in the inner ear. Efficacy of cell replacement relies on proper differentiation. Defining the dynamic expression of different transcription factors essential for neuronal differentiation allows us to monitor the progress and determine when proteins function in differentiating stem cell cultures. Using immortalized multipotent otic progenitors (iMOPs) as a cellular system for SGN differentiation, a method for determining dynamic protein expression from heterogeneous cultures was developed. iMOP-derived neurons were identified and ordered by increasing neurite lengths to create a pseudotime course that reflects the differentiation trajectory. The fluorescence intensities of transcription factors SOX2 and NEUROD1 from individual pseudotemporally ordered cells were measured. Individual cells were grouped by K-means clustering and the mean fluorescence intensity for each cluster determined. Curve fit of the mean fluorescence represented the protein expression dynamics in differentiating cells. The method provides information about protein expression dynamics in differentiating stem cell cultures.

PS 468

Directional Growth and Development of Spiral Ganglion Neurons Regulated by Superparamagnetic Iron Oxide Nanoparticles and Magnetic Field

Menghui Liao[1]; renjie chai[2]
[1]Key Laboratory of Developmental Genes and Human Disease, Institute of Life Sciences, Southeast University, Nanjing, Jiangsu; [2]Key Laboratory for Developmental Genes and Human Disease, Ministry of Education, Institute of Life Sciences,Southeast University, NanJing, China

Magnetic iron oxide nanoparticles (SPIO) have the characteristics of small particle size, good biocompatibility and superparamagnetic. It has been widely reported to promote the repair and regeneration of nerve cells in the fields of magnetic heat of tumors, drug delivery and other biomedical fields. Magnetic field (MF) is a recognized complementary medical tool, which can improve the body's life activities by regulating the metabolism of individual cells. It can also promote bone regeneration and regulate cell growth and differentiation. Spiral ganglion neurons (SGN), a bipolar neuron cell, are the first neuron in auditory signal transduction pathway, which connects to the hair cells and plays an important role in auditory transmission. Ototoxic drugs, aging, noise pollution, heredity and other factors can easily trigger the secondary degeneration between spiral ganglion neurons and cochlear hair cells or the connection barrier between spiral ganglion neurons and hair cells, which could initiate sensory nerve deafness. Importantly, injured spiral neurons have limited self-repairing ability. How to promote the development of SGN morphology structure and regulate the directional growth of SGN neurites are still facing severe challenges. In this study, we investigated the effects of different magnetic fields and SPIO on the morphological structure and function of SGN neurites. The main experimental methods include preparation of SPIO, characterization of SPIO and surface coating modification, extraction and culture of spiral ganglion neurons, trypan blue staining, apoptosis experiment, Prussian blue staining, inductively coupled plasma mass spectrometry (ICP-MS), SPIO labeling rhodamine, transmission electron microscopy observation of subcellular horizontal localization of SPIO complex, immunofluorescence, scratch test, results statistics and analysis. We found that the SPIO prepared by co-precipitation based magneto-endothermic method has better superparamagnetic, shape, hydrodynamic distribution. Meanwhile, SPIO can effectively label SGN without affecting the cell activity of SGN, and obviously promote the growth of SGN neurites while achieving the tracing effect. In addition, the SGN labeled with SPIO can respond positively to the magnetic field and grow preferentially along the direction of the magnetic field, and further promote the growth and development of SGN. In conclusion, we found that SPIO and MF can promote the growth and development of SGN and induce the directional growth of SGN. Our study provides a theoretical and experimental basis for clinical application of SPIO and magnetic field to promote SGN regeneration to treat inductive deafness.

PS 469

A novel bisphosphonate-NT-3 small molecule derivative for regeneration of spiral ganglion synapses

Judith Kempfle[1]; Andrea Zhang[1]; Marlon Duro[2]; Carolina Amador[2]; Boris Kashemirov[2]; Charles McKenna[2]; David H. Jung[1]
[1]Department of Otolaryngology, Massachusetts Eye and Ear Infirmary, Harvard Medical School, Boston, MA, USA; [2]Uiversity of Southern California, Department of Chemistry, Los Angeles, CA, USA

Background

Improving spiral ganglion neuron (SGN) survival, neurite outgrowth, and synaptogenesis may lead to significant gains for deaf and hearing-impaired patients. Local treatment with the two major neurotrophic factors in the cochlea, brain-derived neurotrophic factor (BDNF) and neurotrophic factor 3 (NT-3), has demonstrated promising results in regards to promotion of both survival of SGNs and re-wiring of hair cells by surviving SGNs. We have previously shown that Ris-DHF, a small bisphosphonate hybrid molecule that mimics activity of brain-derived neurotrophic factor (BDNF), allowed for long-term binding of cochlear bone with sustained neurotrophic activity, leading to improvement of neurite outgrowth and synapse regeneration *in vitro.*

We describe here 1Aa, a small molecule that specifically mimics NT-3 activity. We have anchored 1Aa to the bisphosphonate risedronate to create Ris-1Aa. By analogy to our prior work, we assessed the neurotrophic properties of the Ris-1Aa hybrid molecule to promote SGN neurite outgrowth and synaptogenesis.

Methods

Dissected SGNs or explants of neonatal cochleas (CBA, p4) were plated and treated in vitro with Ris-1Aa or control small molecules (400nM). Explants underwent kainic acid treatment (glutamatergic synaptotoxicity) beforehand. Tissue was fixed for immunohistochemistry using neural and synaptic markers. After imaging with confocal microscopy, neurite outgrowth was measured with ImageJ and synaptogenesis in explants was quantified with AMIRA.

Results
The Ris-1Aa hybrid molecule demonstrated sustained ability to stimulate neurite outgrowth in SGN cultures. Both Ris-1Aa and native 1Aa stimulated neurite outgrowth significantly better than control molecules alone. Furthermore, in organotypic organ of Corti explant cultures with attached spiral ganglion neurons, Ris-1Aa stimulated synaptic regeneration following synaptotoxic kainic acid treatment.

Conclusions:
A novel bisphosphonate-1Aa hybrid molecule mimics NT-3 activity and retains neurotrophic properties as measured by neurite outgrowth length and synaptic regeneration in vitro.

PS 470

A 3D Finite Element Model of the Diffusion Profile of BDNF in the Murine Inner Ear: Biological Validation

Shreyas Bharadwaj; Kevin Nella; Sajel Peters; Christian Roque; Rachel Heuer; Jose Fernandez; Andy Oleksijew; Kyle Coots; Akihiro Matsuoka
Northwestern University

Sensorineural hearing loss is the most common type of hearing impairment. One potential treatment for this form of hearing loss is by using transplanted human stem cell-derived spiral ganglion neurons (SGNs) to regenerate synaptic connections with extant SGNs. One of the important growth factors for this regeneration is brain-derived neurotrophic factor (BDNF), which helps direct the growth of SGN neurites towards one another. BDNF is delivered to the cochlea through the Polyhedrin Delivery System (PODS). One important note is that we want the concentration of BDNF to remain sufficiently high for neurite growth across several weeks. Thus, we need to determine an appropriate number of BDNF-containing PODS to insert inside the murine cochlea so that a sufficient concentration is maintained. We chose to develop a finite element model to estimate the diffusion profile of BDNF throughout the scala tympani.

Using COMSOL Multiphysics, we are able to run experiments through a 3D surface of a murine scala tympani reconstructed from microCT slices (taken from Argonne National Laboratory). We also gathered data of the reaction kinetics of BDNF from the PODS and its subsequent degradation. A curve-fitting algorithm was used to fit the concentration-time data and obtain constants for the model. A simulated study was run for 14 days on COMSOL with varying initial parameters, and BDNF diffusion profiles were obtained. The model predicts that 50 million PODS should lead to a concentration sufficient for neurite growth that is sustained for 14 days.

We then also conducted empirical experiments by performing in-vivo studies to insert PODS containing BDNF into the inner ear of deafened mice. We then used immunohistochemistry as a measurement tool to check for neurite growth in the mice. With the results of the empirical experiments, we can compare with the parameters and coefficients of the mathematical model for further insights and improved iterations. Optimization of this model that contains physiologically relevant parameters will inform studies that use stem cell-derived otic neuronal progenitors in vivo.

Otitis Externa, Otitis Media and Eustachian Tube Pathology

PS 471

Single Application Thixotropic Drug Delivery Systems for Otitis Externa

Bogdan Serban[1]; Jeremy Alverson[2]; Nigel Priestley[2]; **Monica Serban**[3]
[1]Department of Biomedical and Pharmaceutical Sciences, University of Montana; [2]Department of Chemistry and Biochemistry, University of Montana; [3]Department of Biomedical and Pharmaceutical Sciences and Department of Chemistry and Biochemistry, University of Montana

In the United States, according to a comprehensive 5-year report published by the Centers of Disease Control and Prevention, annually, approximately 2.4 million health care visits are diagnosed with outer ear infections (otitis externa or OE). Both the pediatric and adult population are affected by OE, with a higher prevalence recorded in adults (approximately 53% of cases). OEaffects the external auditory canal, which connects the outside of the ear to the eardrum. The most common cause accounting for approximately 98% of all ear infections is bacterial infection typically attributable to *Pseudomonas aeruginosa* or *Staphylococcus aureus.*Treatment of OE involves patient or caregiver administered topical antibiotic drops for 7-14 days with multiple daily applications. Incorrect application or non-compliance with the administration schedule of antibiotics often translates to ineffective drug doses at the infection site and leads to infection persistence, recurrence and development of antibiotic resistant bacterial strains. In this context, we seek to develop a point-of-care single application product that would eliminate the current risks associated with treatment regimen non-compliance.

We have formulated several drug delivery systems that have thixotropic properties and can transition between

liquid-gel states in response to shear stress. We used a hybrid rheometer/dynamic mechanical analyzer to characterize the viscoelastic and swelling properties of these materials as well as their temperature dependence. We used validated skin irritation and skin corrosion assays to assess the formulation's biocompatibility. Finally, we evaluated the ability of these thixogels to release incorporated antibiotics and efficiently inhibit bacterial growth via broth micro-dilution assays.

Our tests demonstrate that our materials are thixotropic (Figure 1), their swelling under physiological conditions is negligible and have superior temperature resistance. In addition, they are non-irritant (Figure 2) and non-corrosive (Figure 3 and Figure 4). In antibacterial assays, we show that the gels do not affect the release and efficacy of the loaded antibiotics.

Overall, our data show the feasibility of our approach and that thixotropic drug delivery systems loaded with drugs can be efficiently used against bacterial strains commonly associated with outer ear infections. Future studies will address drug release kinetics from the thixogels, and the safety and efficacy evaluations of these formulations in preclinical models.

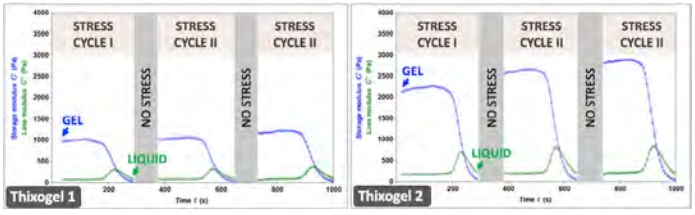

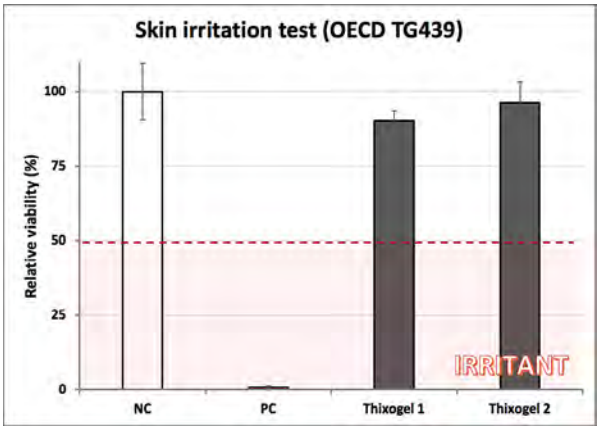

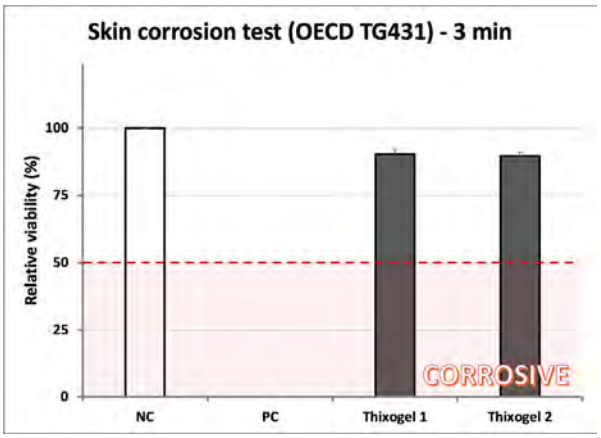

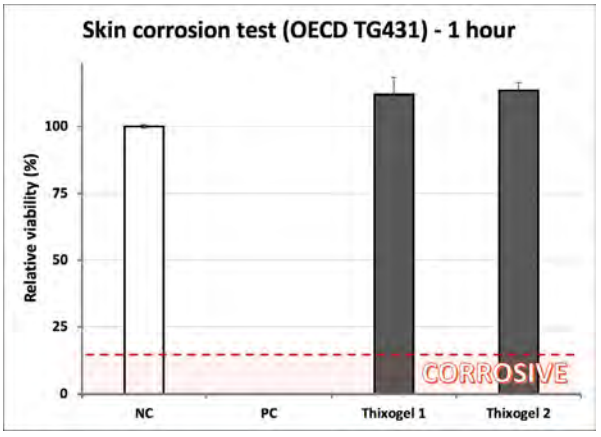

PS 472

Deep Learning in Automated Region Proposal and Diagnosis of Chronic Otitis Media Based on Computed Tomography

Yan-Mei Yang[1]; **Yi-Ke Li**[2]; Yu-Shu Cheng[1]; Zi-Yu He[1]; Juan-Mei Yang[1]; Jiang-Hong Xu[1]; Zhang-Cai Chi[1]; Fang-Lu Chi[1]; Dongdong Ren[1]
[1]Affiliated Eye and ENT Hospital, Fudan University; [2]Department of Otolaryngology, Vanderbilt University Medical Center

Objectives

The purpose of this study was to develop a deep learning framework for diagnosis of chronic otitis media (COM) based on temporal bone CT scans.

Design

A total of 562 COM patients with 672 temporal bone CT scans of both ears were included. The final dataset consisted of 1147 ears, and each of them was assigned with a ground truth label from one of the 3 conditions: normal, chronic suppurative otitis media (CSOM), and cholesteatoma. A random selection of 85% dataset (n = 975) was used for training and validation. The framework contained two deep-learning networks with distinct functions: a region proposal network for extracting regions of interest from 2-dimensional CT slices; and a

classification network for diagnosis of COM based on the extracted regions. The performance of this framework was evaluated on the remaining 15% dataset (n = 172) and compared to that of 6 clinical experts who read the same CT images only. The panel included 2 otologists, 3 otolaryngologists and 1 radiologist.

Results
The area under the ROC curve of the AI model in classifying COM versus normal was 0.92, with sensitivity (83.3%) and specificity (91.4%) exceeding the averages of clinical experts (81.1% and 88.8%, respectively). In a 3-class classification task, this network had higher overall accuracy (76.7% vs 73.8 %), higher recall rates in identifying CSOM (75% vs 70%) and cholesteatoma (76% vs 53%) cases, and superior consistency in duplicated cases (100% vs 81%) compared to clinical experts.

Conclusions
This paper presented a deep learning framework that automatically extracted the region of interest from 2-dimensional temporal bone CT slices and made diagnosis of COM. The performance of this model was comparable and, in some cases, superior to that of clinical experts. These results implied a promising prospect for clinical application of AI in diagnosis of COM based on CT images.

Key words
Chronic otitis media; diagnosis; computed tomography; artificial intelligence.

PS 473

A System for High-throughput Clinical Optical Coherence Tomography and Vibrometry

Robert Adamson[1]; Dan MacDougall[2]; Josh Farrell[3]; Christine Morrison[4]; Matthew Jahns[2]; Matthew Farrell[5]; Drew Hubley[5]; David Morris[2]; Nael Shoman[2]
[1]School of Biomedical Engineering, Electrical and Computer Engineering Department, Dalhousie University, Halifax, NS, Canada; [2]Dalhousie University; [3]School of Biomedical Engineering, Dalhousie University, Halifax, NS, Canada; [4]Nova Scotia Health Authority; [5]Audioptics Medical

Optical coherence tomography (OCT) is an important emerging tool for middle ear diagnostics owing to its ability to safely and non-invasively image both the structure and mobility of middle ear anatomy. We report on our efforts to develop an easy-to-use, turnkey clinical system for middle ear optical coherence tomography that allows a single operator to perform an imaging and vibrometry examination in less than two minutes. We quantify the system's reliability, repeatability and reproducibility at measuring middle ear vibration amplitude and phase and present on clinical imaging results in patients using 2D structural, 3D structural, 1D Doppler, 3D Doppler, variance imaging and M-mode imaging to obtain diagnostic information in a range of diagnostic scenarios.

The imaging system is a self-contained and portable unit consisting of a console and tethered handpiece similar to a large otoscope. It is designed for use by a single operator who holds the handpiece in the patient ear with one hand while controlling a user interface with a controller in the second hand. The system supports several different imaging modes that can be used for specific assessments. All data acquisition, image processing and rendering occurs in real time, allowing immediate feedback to the clinician and the ability to observe changes during patient maneuvers such as swallowing and Valsalva.

The ability of the system to produce reliable vibration measurements was assessed by analyzing Doppler vibrometry measurements made by three operators across five healthy subjects at three frequencies. Results are assessed graphically and using intraclass correlation (ICC) and relative absolute difference (RAD) measures.

Clinical imaging scenarios were identified in consultation with clinicians and ranked for the frequency with which they would be encountered in a typical clinical practice and the estimated value that OCT can bring to clinical decision-making. For each of these scenarios, a representative patient was imaged and a case report was generated that includes the imaging session outputs and a clinical analysis of the adjunctive value of the OCT imaging relative to standard of care diagnostics.

OCT appears to hold the most promise for evaluating tympanic membrane perforations, assessing the state of the middle ear following traumatic head injury, confirming the presence of ossicular fixations, and discontinuities, assessing middle ear implant stability post-surgery and for pre-surgical screening in middle ear exploration and reconstruction surgeries to rule out situations that would contraindicate for surgery.

PS 474

A New Detection Scheme for Detection of Otitis Media with Effusion

Junfeng Liang; Warid Islam; Ke Zhang; Chen Wang; Sarah Crooks; Rong Z. Gan; Qinggong Tang; Bin Zheng; **Chenkai Dai**
University of Oklahoma

A New Detection Scheme for Detection of Otitis Media with Effusion

Junfeng Liang[1], Warid Islam[3], Ke Zhang[2], Chen Wang[2], Sarah Crooks[2], Rong Gan[12], Qinggong Tang[2], Bin Zheng[3], Chenkai Dai[12] [1]School of Aerospace and Mechanical Engineering [2]Stephenson School of Biomedical Engineering [3]School of Electrical and Computer Engineering University of Oklahoma, Norman OK 73019

Background
Otitis media with effusion (OME) is the most commonly diagnosed middle ear inflammation in young children. While numerous research studies of OME have been conducted, biomechanical abnormalities occurring across OME's entire time course, from dysfunction onset to restoration of normal hearing, are incompletely described at best. This critical knowledge gap has limited development of new approaches to quantify time course related biomechanical pathologies in middle ears and justify the stage of the middle ear inflammation. Therefore, accurately assessing severity and prognosis of OME is difficult and depends on physicians' experience and subjective rating. In order to address this clinical challenge, we developed a new detection scheme using optical coherence tomography (OCT) and a scanning laser Doppler Vibrometry (SLDV) plus computational modeling to identify the effusion amount and effusion viscosity at different stage of OME development.

Methods
OME was simulated in six human cadaver ears by injecting various volume of fluid with different viscosities into the middle ear cavity. OCT and SLDV were used to collect the images data and a new Computer-aided detection (CAD) scheme was developed to explore and compute the feature related to effusion volume and viscosity. A finite element (FE) model was created to simulate the middle ear inflammation and analyze the motion change at various stages of OME and the FE model was validated with experimental data.

Results
This study tested a new method of using the dedicated SLDV and OCT devices to non-invasively acquire OME video images and a new CAD scheme to automatically detect and segment fluid volume and regions, compute region size and fluid density. The preliminary results indicate that the computed density distribution features and fluid volume values correlate well with the pre-designed fluid extension and density in human ears.

Conclusions
This preliminary study demonstrates feasibility of developing and applying a novel method integrated with two imaging devices of OCT and SLDV and a CAD scheme to reliably detect and identify the effusion volume and viscosity in human cadaver ears. It has potential to provide health professionals a quantitative decision-making supporting tool to improve accuracy in detecting and diagnosing OME at different stages of the disease

PS 475

High-energy Visible Light Inactivation of Bacteria Found in Otitis Media

Shae D. Morgan; Deborah Yoder-Himes; John Naber; Thomas J. Roussel; Douglas Jackson; Rachel Berry
University of Louisville

High-energy visible light has been used in other fields (e.g., dermatology) for the inactivation of harmful bacteria. A recent study has shown that certain doses of the light at specific frequencies can be lethal to one bacteria found in acute otitis media (i.e., *streptococcus pneumoniae*). This presentation will show the effects of different light characteristics on the survival rates of three bacteria commonly found in acute otitis media (i.e., *Streptococcus pneumoniae*, *Moraxella catarrhalis*, and *Haemophilus influenzae*). Mechanisms of bacterial cell death will be proposed and described. Effects of light intensity, wavelength, and duration of exposure will be considered. Clinical considerations such as heat, risk to healthy tissue, and comparison to current treatment methods will be discussed. Finally, we will describe the future considerations and implications of using light as a preventative and/or therapeutic treatment option for otitis media.

PS 476

Hearing Loss and Audiologic Features in Children with Down Syndrome

Siran Liu[1]; Fangfang Zhao[2]; Robin Tellez[1]; Alberto Costa[3]; Sarah Mowry[2]; **Qingyin Zheng**[2]
[1]Hearing and Balance Clinic, Reeves Rehabilitation Center, University Health System, San Antonio, Texas; [2]Department of Otolaryngology- Head & Neck Surgery, Case Western Reserve University, Cleveland, Ohio, USA; [3]Departments of Pediatrics and Psychiatry, Case Western Reserve University School of Medicine, Cleveland, Ohio, USA

Objective
Evaluate hearing loss and other audiological features in children with Down Syndrome (DS).

Method
The subjects were selected based on internal referrals of "DS" or "Trisomy 21" over a six-month period within University Health System at San Antonio, Texas.

Audiological results were collected for analyzing hearing loss type, severity, laterality, and threshold changes over time.

Results
Nineteen subjects (total of 35 ears) had at least one audiologic assessment and showed abnormal finding. 16 subjects (84.2%) had bilateral hearing loss, 3 subjects (15.8%) had unilateral hearing loss. During the initial hearing evaluation, 10 ears had pure conductive hearing loss (28.6%) and 26 ears had undefined hearing loss (71.4%). During the second hearing evaluation, 7 ears (24.1%) had pure conductive hearing loss, 2 ears (6.9%) had pure sensorineural hearing loss, and 18 ears (62.1%) had undefined hearing loss. Majority of the ears (68.6%, n=24) had Type B tympanograms during the initial hearing evaluation. Combing the first and second hearing evaluation results, 19 ears (54.3%) had mild hearing loss. Most of the subjects (73.7%, n=14) eventually met the criteria for tympanostomy tube placement. Most of the subjects also had a history of congenital cardiac malformations (63.2%, n=12) and speech disorders (78.9%, n=15).

Discussion
Conductive hearing loss resulting from chronic otitis media with effusion or recurrent acute otitis media is more prevalent among children with DS. Accurate behavior audiometric results were often hard to obtain. Tympanometry result is often easier to obtain and can be used to determine middle ear status when audiometric result is unavailable.

Grant support: R01DC015111(QYZ)

PS 477

High Frequency Hearing Following Middle Ear Surgery

Marc Polanik[1]; Danielle Trakimas[2]; Jeffrey Cheng[3]; Elliott D. Kozin[4]; Aaron K. Remenschneider[5]
[1]Massachusetts Eye and Ear Infirmary-Harvard University; [2]Johns Hopkins University School of Medicine; [3]Eaton-Peabody Laboratory, Massachusetts Eye and Ear Infirmary,Department of Otolaryngology – Head and Neck Surgery, Harvard Medical School; [4]Massachusetts Eye and Ear Infirmary- Harvard University; [5]Dept. of Otolaryngology, UMass Memorial Medical Center; Massachusetts Eye and Ear

Objectives
Conductive hearing outcomes following middle ear surgery are conventionally reported as a single air-bone-gap (ABG) average representing multiple frequencies, typically biased towards low frequencies: 500, 1000, 2000, and 4000Hz. This method of outcome reporting may overlook high frequency conductive hearing loss. Herein, we evaluate high frequency ABG in patients undergoing either type 1 tympanoplasty or ossiculoplasty.

Subjects
Retrospective review of patients from a tertiary care center undergoing middle ear surgery. Inclusion criteria included two groups: 1) patients undergoing type 1 tympanoplasty via total drum replacement technique or 2) patients undergoing ossiculoplasty. Exclusion criteria included: patients without perforation closure, canal wall down mastoidectomy, stapedotomy, and/or absence of pre- or postoperative audiograms.

Methods
Patients were sorted into one of two groups: type 1 tympanoplasty or ossiculoplasty. Low frequency ABG was calculated as the mean ABG at 250, 500, and 1000Hz. High frequency ABG was calculated at 4000Hz. Pre- and postoperative ABGs were compared.

Results
Type 1 Tympanoplasty: Twenty-three patients were included (Figure 1). Mean time from surgery to postoperative audiogram was 6.7 months, range of 2.1 to 28.4 months. Postoperatively, the mean low frequency ABG was significantly reduced ($P < 0.001$) while the mean high frequency ABG insignificantly changed ($P=0.450$), see Figure 2a. Mean postoperative high frequency ABG was 18.9 +/- 12.4 dB.

Ossiculoplasty: Thirty-five patients were included (Figure 1). Average time from surgery to postoperative audiogram was 4.0 months, range of 1.4 to 16.2 months. Postoperatively, there was a significant reduction in both the mean low frequency ABG ($P < 0.001$) and mean high frequency ABG ($P=0.017$); however, the magnitude of improvement was significantly larger at low frequencies ($P=0.018$), see Figure 2b. Air conduction was significantly improved at 2000 Hz ($P < 0.001$) and 4000 Hz ($P=0.004$) but not 8000 Hz ($P=0.538$). The type of reconstruction material used had no impact on low or high frequency ABG reduction ($P=0.238$ and $P=0.275$, respectively).

Conclusion
In a series of patients undergoing middle ear surgery, high frequency ABG is unresolved postoperatively. Following a temporalis fascia total drum replacement, low frequency ABG improves but high frequency conductive hearing is unchanged. Following ossicular reconstruction, ABG improves at all frequencies but the most substantial benefits are observed at low frequencies. Additional study of the mechanisms of high

frequency sound conduction in reconstructed middle ears is needed to improve postoperative high frequency hearing outcomes.

Figure 1. Patient Demographics

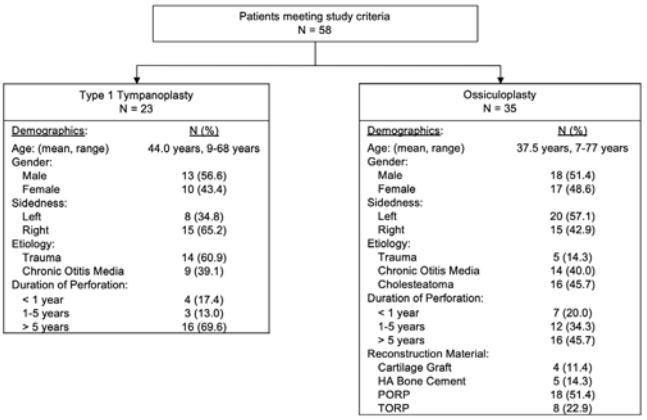

Figure 2. Audiometric Outcomes

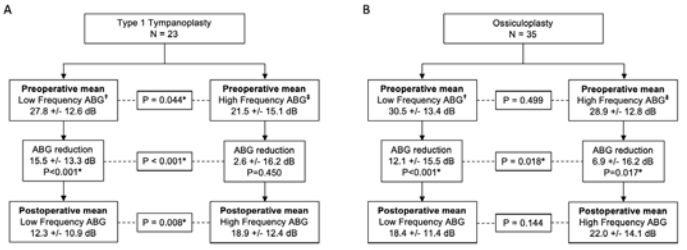

* Denotes statistical significance between the two means (P<0.05)
† Low frequency air-bone-gap (ABG) is the three-tone average of 250, 500, and 1000 Hz
‡ High frequency air-bone-gap (ABG) is measured at 4000 Hz

PS 478

Assessment of Eustachian tube with optical coherence tomography

Jae Ho Chung[1]; Yeon Hoon Kim[2]; Hayoung Byun[1]; Yunjae Lee[1]; Hongki Yoo,[2]
[1]Department of Otolaryngology, College of Medicine, Hanyang University; [2]Dept.of Mechanical Engineering, KAIST

Introduction
The Eustachian tube is a long tubular structure connecting the nasopharynx and the middle ear cavity. Optical Coherence Tomography (OCT), a high-resolution medical imaging technique based on optical interference, provides microstructural imaging inside living tissues. The aim of the study was to assess anatomical structure and change of Eustachian tube using a fiber-based OCT probe with a diameter of less than 1mm.

Methods
The Eustachian tubes of swine was harvested and used for the image test and histological analysis. To obtain microstructural tomographic images of the Eustachian tubes, we used a swept-source OCT System with a center wavelength of 1310 nm. The OCT imaging catheter made of ball lens probe has an outer diameter of 0.96 mm for insertion into the Eustachian tube without damaging the tissue. Three-dimensional imaging was obtained by helical scanning of the imaging probe at a rotational speed of 50 rps and a translation speed of 1 mm/s with OCT. In addition, OCT image was acquired after ballooning of Eustachan tube with balloon tipped catheter (OD 5mm). Histological images of the corresponding Eustachian tubes were compared to images obtained by the OCT System.

Result
OCT image catheter was successfully inserted in the lumen of Eustachian tube. The cross-sectional images of Eustachian tube were obtained, and anatomical structures can be distinguished. After ballooning of the Eustachian tube, the expansion of the cross-section area was identified.

Conclusion
We developed the OCT catheter with an outer diameter of only 0.96 mm which is suitable for imaging Eustachian tube. The application of OCT in the visualization of Eustachian tube limen might be feasible and potentially have diagnostic value.

PS 479

Cone Beam CT with Different Prototypes of a Eustachian Tube Stent

Robert Schuon[1]; Tamara Wilfling[1]; Philipp Krueger[2]; Tobias Stein[2]; Kerstin Schuemann[3]; Niels Grabow[3]; Thomas Lenarz[4]; Gerrit Paasche[1]
[1]Hannover Medical School; [2]bess; [3]IBMT, University of Rostock; [4]Hannover Medical School, Hannover, Germany

Stenting the Eustachian tube (ET) might provide a new approach to treat obstructive ET dysfunction. Stents have to be positioned properly in the cartilaginous part of the ET. To control position of the stent after insertion, cone beam CT (CBCT) seems to be appropriate. The aim of the current study was to evaluate different prototypes of ET stents by CBCT.

In a human cadaver study, 17 donors were bilaterally implanted with either coronary stents or prototypes of ET stents. Stents were positioned by using different generations of application tools. Before and after stenting, CBCT scans were performed. Resulting DICOM images were evaluated for position and dimension of the stents using OsiriX.

All metal stents could be directly visualized and polymer stents can only be evaluated indirectly due to the lumen that is generated. Whether a stent was correctly positioned and expanded could be proven. Visualization

depended on the design of the stent and the dimensions of the struts. Especially stents from a Ni-Ti alloy were able to adapt better to the paisley-shaped cross section of the ET.

CBCT is suitable as imaging technique for stents in the ET. Evaluation of the position and expansion provided important information on requirements for further development of the ET stent.

PS 480

Mid-term Results of Fluoroscopy-guided Balloon Dilation using a Flexible Guide Wire to Treat Obstructive Eustachian tube Dysfunction

Yehree Kim[1]; Kun Yung Kim[2]; Jung-Hoon Park[3]; Sung Hwan Yoon[3]; Jae Yong Jeon[4]; Ho-Young Song[5]; Hong Ju Park[1]; Woo Seok Kang[1]
[1]Department of otorhinolaryngology Head and Neck Surgery, Asan Medical Center; [2]Department of Radiology, Chonbuk National University Hospital; [3]Department of Radiology and Research Institute of Radiology, Asan Medical Center; [4]Department of Rehabilitation, Asan Medical Center; [5]Department of Radiology, Asan Medical Center

Purpose
To prospectively evaluate the mid-term outcomes of fluoroscopic Eustachian tube (E-tube) balloon dilation using a flexible guide wire in patients with obstructive E-tube dysfunction.

Materials and Methods
From October 2016 to September 2017, we prospectively enrolled adult outpatients with persistent otitis media who were unable to perform the Valsalva maneuver. Participants underwent fluoroscopic E-tube balloon dilation with a 0.035-in. flexible guide wire and a 6 mm by 20 mm balloon catheter. Clinical examinations to check for ability to perform the Valsalva maneuver and otomicroscopy were conducted 1 week, 1 month, 3 months, 12 months, 18 months, and 24 months after the procedure.

Results
The analysis included 32 E-tubes from 31 patients (18 women, 13 men; mean age 47 years, range 25-72 years). Balloon dilation was technically successful in all E-tubes. The mean time required for the procedure was 6.9 minutes (range, 5.8-10.3 minutes). The Valsalva maneuver was possible for 25 of 32 of E-tubes (78.1%) 3 months after balloon dilation. During the median follow-up of 15.9 months, aggravation of Valsalva maneuver occurred in 4 of 25 improved E-tubes (16%), yielding a 2-year patency rate of 84%.

Conclusion
The mid-term fluoroscopic balloon dilation results were encouraging, and using a flexible guide wire for E-tube balloon dilation helped the balloon catheter pass smoothly into the E-tube preventing the creation of a false passage.

PS 481

Serial Histopathologic Changes after Repeated Eustachian Tube Balloon Dilation in Rats

Yehree Kim[1]; Zhe Wang[2]; Jun Min Kang[3]; Ho-Young Song[4]; Hong Ju Park[1]; Woo Seok Kang[1]
[1]Department of otorhinolaryngology Head and Neck Surgery, Asan Medical Center; [2]Department of Radiology, Tianjin Medical University General Hospital; [3]Department of Radiology and Research, Institute of Radiology, Asan Medical Center; [4]Department of Radiology, Asan Medical Center

Purpose
To evaluate the serial histopathologic changes of the Eustachian tube (ET) after repeated balloon dilation in a rat model.

Materials and Methods
Forty male Wistar rats were used. The left side ET was dilated once for group A (n=20) with a balloon catheter of 1mm in diameter and 5mm in length, and twice for group B (n=20) with an interval of 4 weeks between dilations. Five rats from each group were sacrificed immediately after the last balloon dilation, 5 after 1week, 5 after 4weeks and 5 after 12weeks. Histopathologic evaluation included presence of dilation in ET, quality of epithelium and cilia, basal layer integrity, degree of fibrotic change, and encircling cartilage destruction at the nasopharyngeal, middle and tympanic segment of the ET.

Results
We found no histologic changes of the nasopharyngeal orifice of the ET after dilation except for 1 rat in group B. Immediately after the last dilation, we found more mucosal breaks in group B which extended to the encircling cartilage at the middle segment and the tympanic segment. At 1 week, the epithelium and basal layer integrity recovered, and migrating fibroblasts were observed in the matrix and the cartilage in both groups. At 4 weeks, fibrotic changes were observed in both group A and B, however the changes were more extensive in group B. One rat from group B which was sacrificed at 1 week showed far more extensive fibrotic changes which in turn caused paradoxical narrowing of the lumen.

Conclusion
Repeated balloon dilation induced multiple fissures in the mucosa leading to multiple foci of fibrosis which resulted in successful dilation of the ET. The epithelium and cilia damage were observed immediately after the dilation. They, however, were regenerated at 1 week, which may suggest that mucociliary clearance of ET is preserved after balloon dilation.

PS 482

Complications After Eustachian Tube Dilatation

Ingo Todt; Holger Sudhoff
Bielefeld University, Department of Otolaryngology, Head and Neck Surgery

Background
Eustachian tube function is of central importance for the aereation of the middle ear. A dysfunction can be associated with ototonus, chronic otitis media and cholesteatoma. Eustachian tube dilatation is a treatment option to solve this problems. Although widely performed little is known about the occurence rate of complications associated with the eustachian tube dilatation. Aim of the present study was to observe the rate of complications after eustachian tube dysfunction

Material and Methods
We evaluated 1840 cases of eustachian tube dilatation performed in a single center between 2015 and 2019 with the Spiggle and Theis eustachian tube dilatation system for complications.

Results
We observed seven cases of hearing loss, four cases of emphysema and one disruption of the balloon. In two cases of hearing loss a simultanous tympanoplasty was performed. The overall complication rate was 0,6 %.

Conclusion
The eustachian tube dilatation procedure has a low complication rate. Micro lesions of the tubal epithelium and middle ear pressure changes are assumed to be causative for emphysema and hearing loss.

PS 483

A Novel Technique for Patulous Eustachian Tube Surgery

Holger Sudhoff[1]; Ingo Todt[2]
[1]Bielefeld University, Department of Otolaryngology, Head and Neck Surgery; [2]Department of Otorhinolaryngology, Head and Neck Surgery

To investigate the effectiveness of a soft-tissue bulking agent comparing transnasal-transpalatinatal surgical procedure in local and general anesthesia versus a transnasal–transoral endoscopic surgical procedures in general anesthesia for eliminating symptoms of unilateral patulous Eustachian tube dysfunction (PETD). Patients suffering from PETD underwent one of the following procedures: i) transnasal-transpalatinatal soft-tissue bulking agent in local anesthesia ii) transnasal-transpalatinatal soft-tissue bulking agent in general anesthesia, or iii) transnasal-transoral soft-tissue bulking agent in general anesthesia. The necessity to repeat the procedure due to recurrence of any PETD related symptoms was recorded. The frailty model, an extension of the Cox proportional hazards model, was used for the survival analysis. A total of 41 procedures were performed in 41 patients. Median duration of symptom relief after surgery was 5.0 months (interquartile range [IQR]: 1.1–15.5 months) and varied by procedure type, ranging from 3.0 months (IQR: 0.7–7.0 months) for calcium hydroxyapatite injection to 20.6 months (3.4–35.9 months) for obliteration. Compared to shim insertion, the risk of 12-month failure was significantly higher for calcium hydroxyapatite injection (hazard ratio [HR] = 2.18; 95% confidence interval [CI] 1.29, 3.67; P = 0.004) and patulous ET reconstruction (HR = 1.62; 95% CI 1.04, 2.52; P = 0.035). Patients undergoing shim insertion (52.2%) and obliteration (81.8%) were likely to require pressure equalization tubes or to have had otitis media with effusion. Although all procedures different approaches resulted in an improvement of PETD symptoms resolution, the transnasal-transpalatinatal ET augmentation in local was more likely to accomplish a complete resolution of PETD related symptoms.

PS 484

Development of Eustachian Tube Dysfunction in a Rat Model

Yehree Kim[1]; Zhe Wang[2]; Jung-Hoon Park[3]; Sung Hwan Yoon[3]; Jae Yong Jeon[4]; Ho-Young Song[5]; Hong Ju Park[1]; Woo Seok Kang[1]
[1]Department of otorhinolaryngology Head and Neck Surgery, Asan Medical Center; [2]Department of Radiology, Tianjin Medical University General Hospital; [3]Department of Radiology and Research Institute of Radiology, Asan Medical Center; [4]Department of Rehabilitation, Asan Medical Center; [5]Department of Radiology, Asan Medical Center

Objectives
To describe the clinical and histological progression of a rat model of Eustachian tube (E-tube) dysfunction using different embolic materials with and without Lipopolysaccharide (LPS) introduction.

Materials and Methods

A total of 36 Wistar rats with the age of 16 weeks were used in our current study. All left ears of the rats underwent the exposure of tympanic bulla by surgery, making a hole at the surface of bulla, and then microcatheter insertion to the tympanic end of the E-tube through the hole. After that, they were randomly assigned to 6 groups (from Group A to Group F) according to the perfusion of different embolic agents through the catheter. Group A (n=6) only received saline injection. Group B (n=6) received LPS perfusion in the tympanic cavity (TC). Group C (n=6) received 300-μm polyvinyl alcohol (PVA) injection at the E-tube. Group D (n=6) received PVA injection in the E-tube and LPS perfusion in the TC. Group E (n=6) received tissue adhesive glue (TAG) injection at the E-tube. Group F (n=6) received TAG injection in the E-tube and LPS perfusion in the TC. All left ears were evaluated by weekly otomicroscopy. All rats were sacrificed 12 weeks after surgery, and the E-tube samples were obtained for histological observation.

Results

5 rats died of procedure-related complications. During the first three weeks, most of the rats in groups B to F showed various degree of bulging of tympanic membrane. In Groups E and F, the surgical ear had tympanic membrane retraction and mucous effusion over the next few weeks. Whereas, in groups B to D, the tympanic membranes gradually recovered to the normal state. Histology analysis showed a chronic inflammatory reaction of middle ear in Groups E and F. Also, we can find the width of epithelium and submucosa layer were larger in Groups E and F. In the submucosa layer, more dilated vessels can be detected in Groups E and F.

Conclusion

The application of new procedure combined with tissue adhesive glue injection in rats may create a Eustachian tube dysfunction animal model. This new model could be reliable in creating a persistent and long-lasting otitis media with effusion (OME). It is valuable to investigate the pathogenesis, course and treatment of OME in future studies.

Otoacoustic Emissions I

PS 485

Comparing Spontaneous and Stimulus Frequency Otoacoustic Emissions in Mice with Tectorial Membrane Defects

Mary Ann Cheatham[1]; Yingjie Zhou[2]; Peter Dallos[1]
[1]Northwestern University; [2]Northwestern University, Dept. Communication Sciences and Disorders

Zweig and Shera (1995) and Shera (2003) proposed the global standing wave model for generation of spontaneous otoacoustic emissions (SOAEs), which suggests that they are amplitude-stabilized standing waves. This theory predicts that the spacing between SOAEs corresponds to the interval over which the phase changes by one cycle as determined from the phase-gradient delays of stimulus frequency otoacoustic emissions (SFOAEs). Because data characterizing the relationship between spontaneous and evoked emissions in nonhuman mammals is limited, we examined SOAEs and SFOAEs in various tectorial membrane (TM) mutants and their controls.

Since the spacing between adjacent SOAEs tends to increase with emission frequency, Shera introduced a dimensionless representation, N_{soae}, which is computed by taking the geometric mean frequency of adjacent SOAEs and dividing by the absolute value of their difference. In humans, constant values of N_{soae} correspond to constant fractions of an octave with a spacing of ~1/10 of an octave, i.e., the SOAE spacing (N_{soae}) was ~15 for SOAE frequencies around 1500 Hz. We also examined the spacing of SOAEs (N_{soae}) in mice to learn if SFOAE phase-gradient (or group) delays in periods of the stimulus frequency (referred to as N_{sfoae}), predicted the characteristic minimum spacing between SOAEs in this species. In mice, SOAEs are higher in frequency and show a wider spacing, consistent with shorter group delays in the very short mouse cochlea. Computations indicated that the spacing between adjacent SOAEs (N_{soae}) was predicted by the SFOAE phase-gradient delays (N_{sfoae}) for wildtype mice, and for TM mutant mice lacking CEACAM16 that retain near-normal hearing when young. The spacings also tended to correspond to ~1/10th of an octave. We then examined *Tecta*$^{Y1870C+/-}$ heterozygous mice since several animals generated clusters of SOAEs where higher-frequency SOAEs appeared to be integer multiples of lower-frequency "primary" partners. Although the spacing of primary SOAEs in *Tecta*$^{Y1870C+/-}$ mice was generally consistent with SFOAE predictions, that for harmonically-related SOAEs in the higher-frequency clusters was not. However, if N_{soae} values for second (third) harmonic SOAEs were divided by 2 (3), they corresponded to N_{sfoae} predictions. In addition, the average frequency separation between SOAEs was ~1.1 kHz for *all* SOAEs, i.e., SOAE spacing corresponded to ~1/10th of an octave, including those in the higher-frequency clusters, but only when the latter were assumed to originate from the more apical, primary location. Further comparisons between SOAEs and SFOAEs may help us to better understand the origins of these phenomena.

PS 486

The Effects of the Mouse Middle Ear on Otoacoustic Emissions

Hamid Motallebzadeh[1]; Sunil Puria[2]
[1]Havard Medical School; [2]Department of Otolaryngology Head and Neck Surgery, Harvard Medical School; Eaton-Peabody Laboratories Massachusetts Eye and Ear

Introduction

Sounds in the ear canal (EC) are transmitted to the cochlea through the middle ear (ME). The resulting hydrodynamic pressure inside the cochlea in turn generates low-amplitude sounds by means of complex electro-mechanical processes within the organ of Corti (OoC). These sounds travel backward through the ME, are measured in the EC, and are called otoacoustic emissions (OAEs). However, our understanding of how the ME affects OAEs generated by the mouse cochlea is limited. While the motions of the mouse ossicular chain have been reported for forward EC-pressure drive (Dong *et al.*, 2013), a more thorough empirical characterization of the effects of forward and reverse ME transmission on OAEs has been lacking.

Methods

In this study we develop a finite-element model of the mouse EC, ME, and ME cavity, coupled to each other and to a cochlear model capable of generating stimulus-frequency OAEs (SFOAEs). SFOAE generation in the cochlear model is achieved by introducing random perturbations (Shera and Zweig, 1993 and 1995; Shera and Guinan, 1999) to the gain produced by the outer hair cells in the OoC. The model is tested against EC-sound-driven *in-vivo* measurements of: (1) ossicular motion with the pars-flaccida region of the eardrum removed (Dong *et al.*, 2013); (2) umbo motion with an intact ME (Rosowski *et al.*, 2003); and (3) SFOAEs measured with an intact ME (Cheatham *et al.*, 2014).

Results

After validating the model against the available data, a number of additional responses of the mouse ME are calculated. These include the cochlear input impedance, stapes-footplate reflection, the EC to cochlear pressure gain in the forward, and cochlea to EC pressure gain in the reverse direction. We demonstrate via a sensitivity analysis that SFOAE transmission through the ME is substantially affected by the following ME parameters: (1) stiffness of the stapes annular ligament; (2) stiffness of the eardrum; and (3) ossicular mass. The results show that conventional ME pressure-gain functions cannot fully capture the variations observed in SFOAEs resulting from ME parameter variations because they typically use the total pressure consisting of the sum of incident and reflected pressures. However, by modifying the EC input pressure in the forward direction and the cochlear pressure at the stapes footplate in the reverse direction, to account for the reflected pressures, the SFOAE variations due to the ME parameters are well characterized. [Work supported by grants R01 DC05960 and DC07910 from the NIDCD of NIH].

PS 487

An Otoacoustic Emissions Screen to Identify Hearing Loss Mutations in the Rhesus Macaque Colony at the Oregon National Primate Research Center

J. Beth Kempton[1]; Edward V. Porsov[1]; Samuel M. Peterson[2]; Benjamin N. Bimber[2]; Betsy Ferguson[2]; John V. Brigande[1]
[1]Oregon Hearing Research Center; [2]Oregon National Primate Research Center

The rhesus macaque is a compelling model system for the study of human hearing due to similarities in inner ear development, anatomy, and physiology. Our immediate goal is to identify genetic mutations that model human hearing loss in the 4,300 member pedigreed rhesus macaque breeding colony at the Oregon National Primate Research Center (ONPRC). Our long term goals are to validate gene therapy strategies that rescue sensory function in rhesus models of hearing loss and then translate these strategies to the clinic. We are deploying two approaches to meet our short term goal. The Macaque Genotype and Phenotype (mGAP) Resource (Version 1.8) includes ~30 million DNA single nucleotide variants (SNV) discovered by whole genome sequence analysis of 739 rhesus macaques. mGAP contains direct links to extensive, human-based annotations and individual animal genotypes. We hypothesize that Combined Annotation-Dependent Depletion-based bioinformatic analysis of the mGAP SNVs will reveal hearing loss mutations as our database of sequenced individuals continually expands. Here we report on the complimentary phenotype-to-genotype approach. We hypothesize that a simple audiological test will identify individuals with severe to profound hearing loss during the rhesus semi-annual health checks. Our approach was constrained by the superficiality of anesthesia; the brevity of the testing window; the cacophony of the test environment; and the ease of adoption by others. We designed a distortion product otoacoustic emissions (DPOAE) test paradigm using the Madsen Capella[2], an OAE system designed for human patients. The DPOAE testing was conducted at high frequency and higher intensity levels to negate the effects of the noisy test environment. DPOAE input/output functions were collected at f_2 equal to 10 kHz (f_1=f_2/1.2). f_1 was

presented at 65, 70, and 75 dB SPL with corresponding f_2 levels reduced by 10 dB SPL. A DP-gram at 75 dB SPL was also performed on 200/330 subjects at 4, 6, 8, and 10 kHz. We present a normative data set for rhesus DPOAE responses from 1-21 years of age. Remarkably, animals through 21 years largely retained sensitive OAE responses. Two primates out of 330 failed to produce distortion products bilaterally and are scheduled for confirmatory audiological testing in a sound booth. The mGAP and DPOAE analyses are expected to enable identification of spontaneous mutations in rhesus that model human hearing loss.

NIH Funding: R24 OD021324 (BF); R01 DC014160 and R21 DC018126 (JB); P51 OD011092 (Peter Barr-Gillespie); P51 Pilot Research Program (JB and BF).

PS 488

Loading the Basilar Membrane: Effects of Heavy Beads on Reflection-Source OAEs in Gerbil

Sebastiaan Meenderink[1]; Xiaohui Lin[1]; Wei Dong[2]
[1]VA Loma Linda Healthcare System; [2]VA Loma Linda Healthcare System & Dept. of Otolaryngology, Loma Linda University Health

Otoacoustic emissions (OAEs) are sounds emitted from the inner ear. It is currently believed that there are two types of OAEs, 'distortion-source emissions' and 'reflection-source emissions.' The difference between them is in the mechanism by which the intracochlear apex-to-base (i.e. backward) traveling waves arise. For the latter type of emissions, the backward-traveling waves are hypothesized to result from linear reflection of forward-traveling waves from (not yet identified) pre-existing perturbations or irregularities in the local impedances within the inner ear. Both stimulus-frequency otoacoustic emissions (SFOAEs) and upper-sideband distortion product otoacoustic emissions (DPOAEs; i.e., $2f_2$-f_1) are thought to be reflection-source OAEs as they show frequency-dependent amplitude fine structure and quickly varying phase.

We attempted to locally change the mechanical properties of the basilar membrane (BM) in gerbil by loading it with one or more heavy beads (HBs; Barium Titanate coated glass beads, 45–53 μm with a density of 4.26 g/ml; equivalent to effective mass used in gerbil cochlear models) and study its effect on SFOAEs and $2f_2$-f_1 DPOAEs. Presumably, these HBs change the local mass and/or stiffness (i.e. impedance) and therefor affect the creation of backward-traveling emission wavelets (via reflection) and the motion of the BM. We simultaneously measured SFOAEs and $2f_2$-f_1 DPOAEs using two-tone stimuli with narrow frequency spacing (f_2=f_1+0.1 kHz), both in the ear canal (using a microphone) and on the BM (using laser Doppler vibrometry) before and after loading the BM with the HBs in the vicinity of the intracochlear recording location. The introduction of a single HB did not change the intracochlear tuning at the nearby measurement location, indicating that the loading-effect is local indeed. As for the reflection-source emissions, $2f_2$-f_1 DPOAEs and SFOAEs showed near-identical fine structure (although the DPOAE amplitudes were smaller) before the introduction of the beads. After HB placement, amplitudes of these OAEs and their intracochlear counterparts reduced, but their presence did not change in the OAE fine structure, nor its phase. Results show that intracochlear wave propagation in both forward and reverse direction were little affected by a localized change in the (real part) of the impedance at the level of the BM.

This study was supported by NIDCD R01DC011506 (Dong), and the Department of Otolaryngology Head & Neck Surgery, at Loma Linda University Health.

PS 489

Acoustic Communication is Not Compromised by Dysmorphic Features in Cururu Toads

Ariadna Cobo-Cuan[1]; Luís Felipe Toledo[2]; Peter M. Narins[1]
[1]Department of Integrative Biology & Physiology, UCLA; [2]Departamento de Biologia Animal, Instituto de Biologia

Introduction

Amphibian malformations occur naturally in wild populations. On the Brazilian archipelago of Fernando de Noronha, the introduced population of Cururu toads (*Rhinella jimi*, Anura: Bufonidae) exhibits one of the highest rates of amphibian malformation on Earth. The causes underlying this high deformity rate are still unknown, but malformed toads have made up 50% of this population for at least 10 years. Considering that acoustic communication plays an essential role in amphibian reproductive behavior, the stability of this population implies that malformed individuals are able to produce normal calls, attract females, and reproduce as effectively as normal toads.

Methods

Toads were examined for visible external malformations and were assigned to two groups: malformed (with clear anatomical deformities) and normal (with no external deformities). We investigated the spectro-temporal characteristics of the advertisement calls and the release calls produced by male Cururu toads. Distortion-product otoacoustic emissions (DPOAEs) were used to assess

the hearing sensitivity of both normal and malformed toads, and to compare the peak auditory sensitivity of each group to their call characteristics.

Results
Malformed toads transmit their sexual receptivity with a vocal repertoire similar to that of their normal conspecifics. Hearing evaluation of Cururu toads demonstrated that despite significant physical deformations, malformed males maintain a close match between the spectral features of their calls and the frequency tuning of their inner ears, as much as the males in the normal population. No DPOAEs were recorded when the deformities affected the tympanum, thus suggesting that the hearing is compromised.

Conclusions
Our results suggest that whatever is causing the physical deformations in this species has spared auditory frequency tuning-call matching, and thus malformed toads are able to communicate as normal toads do. Most anatomical deformities in the Cururu toads, except dysmorphic tympana, do not interfere with their acoustic communication either as senders or as receivers and, consequently, are not likely to limit their chances of finding a mate and reproducing.

PS 490

Otoacoustic Emissions Show Hearing Impairment as an Early non-Motor Feature of Parkinson's Disease

Andrea Viziano[1]; Arturo Moleti[2]; Rocco Cerroni[3]; Elena Garasto[3]; Mariangela Pierantozzi[3]; Renata Sisto[4]; Alessandro Stefani[3]
[1]Department of Clinical Sciences and Translational Medicine, 'Tor Vergata' University, Rome, Italy; [2]Department of Physics, University of Rome 'Tor Vergata', Rome, Italy.; [3]Parkinson's Center, Department of Systems Medicine, University of Rome 'Tor Vergata', Rome, Italy; [4]INAIL Research Department of Occupational and Environmental Medicine, Epidemiology and Hygiene

Several studies have hypothesized a connection between Parkinson's disease (PD) and hearing impairment. Auditory dysfunction in PD has been linked to the degeneration of dopaminergic and nondopaminergic neurons located outside of the substantia nigra. Animal studies have demonstrated the presence of dopaminergic signaling in the auditory pathway, mainly in the lateral olivocochlear efferent system (LOC), related to suppression of cochlear nerve activity and implicated in noise-induced excitotoxicity. Moreover, previous studies have found alterations in distortion-product otoacoustic emissions (DPOAE) in PD patients, postulating outer hair cell (OHC) impairment, possibly due to medial olivocochlear efferent (MOC) involvement.

Hearing levels and OHC function were evaluated, by means of pure tone audiometry (PTA) and DPOAE, in a cohort of 86 PD patients (45 M; 41 F, mean age 65±18) compared to age- and gender-matched healthy controls (n=49, 26 M; 23 F, mean age 63±17). DPOAE spectra were recorded, with high frequency resolution and time-frequency analysis to unmix the distortion and reflection components. Ear-canal calibration of the forward pressure and of the OAE signal was performed. Statistical analysis using a multivariate linear model was performed. PTA and DPOAE testing showed an impairment in auditory function in PD patients, with respect to healthy subjects.

In our study cohort, PTA impairment encompassed frequency bands ranging from 1 to 8 kHz, indicating widespread hearing dysfunction, while previous works showed variability in the extent of frequency involvement, possibly due to smaller sample sizes. It has been speculated that LOC function is to modulate auditory nerve discharge; in this scenario, dopaminergic activation seems to have a net inhibitory effect, as a depletion in dopamine levels has shown to decrease auditory function, possibly due to an increase in excitotoxicity. It is unclear whether such alterations may influence OHC function, as previous animal experiments involving DPOAE measurements hypothesized a mutual influence between the two efferent systems, either due to the presence of MOC-LOC synapses or to possible paracrine effects of dopamine on OHC. Our findings are in accordance with previous works indicating DPOAE to be impaired in PD subjects.

Taken together, our findings further confirm evidences pointing at hearing loss being a non-motor feature of PD, with important implications, as non-motor symptoms appear to be pivotal in quality of life impairment. From a technical standpoint, the consistent correlation between audiological measurements in our dataset confirms DPOAE to represent a reliable, objective diagnostic tool for auditory dysfunction.

PS 491

Longitudinal Monitoring of Medial Olivocochlear Reflex Inhibition in Patients with Cystic Fibrosis Receiving Intravenous Aminoglycoside Treatments

Angela Garinis[1]; Patrick Feeney[2]; Douglas Keefe[3]; Dawn Konrad-Martin[4]; Garnett McMillan[4]; Jay Vachhani[4]
[1]Oregon Hearing Research Center; [2]National Center for Rehabilitative Auditory Research; [3]Boys Town National Research Hospital; [4]National Center for Rehabilitative Auditory Research (NCRAR)

The medial olivocochlear (MOC) system is an efferent-mediated reflex thought to control cochlear gain by modifying or inhibiting outer hair cell activity in frequency ranges important for processing speech. Preclinical research shows that aminoglycosides (AGs) cause dose-dependent reductions of otoacoustic emission (OAE) levels, but the effects of AG-dosing on MOC reflex inhibition remain unclear. The purpose of this study was to establish the clinical utility of physiological measurements of MOC reflex inhibition in combination with OAEs for identifying early indicators of ototoxicity. The novel aspects of this study are to utilize the MOC response to provide new knowledge about how ototoxic drugs affect the pathophysiology of the cochlea, and determine if monitoring MOC reflex inhibition provides a more sensitive measure of ototoxic damage than OAEs alone. A longitudinal study design was used to measure transient-evoked (TE)OAEs in quiet, and with contralateral acoustic stimulation (CAS) to activate MOC reflex inhibition. Two groups of patients with cystic fibrosis (CF), ages 15 years or older, were evaluated: [Group 1] 29 patients with CF treated with a therapeutic course of IV-tobramycin and [Group 2] 19 patients with CF not receiving IV-tobramycin. Test intervals for Group 1 were: baseline (pre-treatment or within 3 days of first day of dosing), mid-treatment (7-10 days) and at least 30 days post-treatment. Group 2 patients were tested at similar times, and the baseline visit was chosen at random. Data from both groups were compared to controls without CF or a history of AGs (Group 3; N= 7). Tests at each visit included serial audiometry (0.25 to 16 kHz), 0.226-kHz tympanometry, wideband absorbance, broadband acoustic reflex thresholds and MOC reflex inhibition via TEOAEs. Preliminary group data revealed reduced MOC inhibition amplitudes for both CF groups, when compared to non-CF control subjects. Specifically, controls without CF exhibited 1-1.5 dB of MOC inhibition in the 1.5-2.2 kHz region, compared to < 0.5 dB of MOC inhibition for both CF groups. Results also revealed that patterns of TEOAE changes were not reflective of MOC inhibition changes across visits for any group. Findings will be discussed in relation to middle-ear effects and cumulative IV-AG dosing history for patients in the CF groups.

PS 492

Utilizing Cochlear Place-Specific Properties in Distortion Product Otoacoustic Emission Stimuli for the Identification of Hearing Loss

Samantha Stiepan; Sumitrajit Dhar
Northwestern University

Hearing loss is a major healthcare issue because of the sheer number of people afflicted, as well as the known cognitive, emotional, social, behavioral, and socioeconomic consequences. In order to combat these negative outcomes, it is necessary to identify hearing loss or pathology at the earliest possible opportunity. Therefore, a sensitive and accessible tool for early and accurate identification of the most common forms of hearing loss is a critical national healthcare need.

One of the most common forms of adult-onset hearing loss originate at the cochlear base, where high frequency information is encoded, affecting cochlear outer hair cell (OHC) function. The OHCs provide sharp frequency selectivity, wide dynamic range, and acute sensitivity that is characteristic of a normal auditory system. Identifying cochlear pathologies using distortion product otoacoustic emissions (DPOAEs) holds promise as they are objective, noninvasive, and directly evaluate the vulnerable OHCs. Furthermore, DPOAEs are already a well-established tool in both clinical and research settings. However, timely and accurate detection of cochlear pathology remains suboptimal as current protocols: 1) do not assess frequencies that span up to the highest frequencies of human hearing and 2) do not consider local cochlear mechanical properties when setting DPOAE stimulus parameters. Recent advances in calibration techniques and hardware have allowed for delivery and recording of accurate emission levels up to the highest frequencies of human hearing.

The purpose of this study was to tackle a remaining important step: **developing clinical DPOAE protocols guided by cochlear mechanical properties to derive physiologically motivated, locally appropriate, stimulus parameters.** To do this, we investigated the DPOAE stimulus parametric space in humans in order to identify the most appropriatestimulus frequency ratio and level combinations for frequencies up to 19kHz. DPOAEs were recorded using f_2/f_1 ratios and L_1 and L_2 levels that produced robust emission levels and signal-to-noise ratios in audiometrically normal-hearing, young adults. Preliminary analysis revealed a systematic decrease in the optimal stimulus frequency ratio across the cochlear length with wider ratios needed at the cochlear apex and narrower ratios at the base. Receiver operating characteristic curves were then used to illustrate if these optimal ratios improved accuracy in differentiating between normal-hearing and hearing-impaired ears, compared to a standard clinical protocol. These optimizations are expected to aid in early and accurate detection of cochlear decline by improving DPOAE test performance.

PS 493

Developing a Combined SFOAE+DPOAE Diagnostic Profile

Carolina Abdala; Chandan Suresh; Ping Luo; Christopher A. Shera
University of Southern California

Over the last decades we have learned much about the intracochlear generation of otoacoustic emissions (OAEs). It is now accepted that OAEs arise from one (or a combination) of two basic mechanisms within the cochlea: nonlinear *distortion* and coherent *reflection*. Past work has also confirmed that distortion- and reflection-source OAEs can be impacted independently by various manipulations; hence, the two OAE classes appear to provide distinct information about cochlear function and dysfunction. While our understanding of OAEs has progressed, their application in the audiology clinic remains rudimentary and neglects their potential for the differential diagnosis of sensory hearing loss.

Here, we measure both classes of emissions in a group of normal-hearing adults (and in a small number of mild-to-moderately hearing-impaired individuals) and conduct *relational* analyses to exploit the unique generation mechanisms of each OAE. The $2f_1$-f_2 distortion-product OAE (DPOAE) was unmixed to isolate its distortion-component while the stimulus-frequency OAE (SFOAE) was recorded as a gauge of cochlear reflection. We presented rapid swept-tone stimuli to evoke DPOAEs and SFOAEs over a 5-octave frequency range (0.5-16 kHz) at 10-12 stimulus levels. Relational OAE metrics characterizing the peak strength, compressive properties, level, and SNR of both OAEs together were calculated using improved fitting and analysis methods.

Preliminary results show that in healthy young-adult ears (1) SFOAEs have greater peak strength than DPOAEs (and higher amplitudes overall) when compared at equivalent stimulus levels; (2) SFOAE input/output functions produce a “compression knee” (i.e., amplitude plateau) at slightly higher stimulus levels than do DPOAEs; (3) the SNR is higher for the SFOAE through approximately 4-5 kHz while the DPOAE has higher SNR from 4-8 kHz, suggesting that together, SFOAEs and DPOAEs achieve optimal frequency coverage; and (4) hearing-impaired ears often fall outside of the normative distributions although they are not affected by hearing loss in a uniform way. The short-term objective of this study was to generate a normative profile; however, our overarching goal is its eventual application to ears with varied hearing loss. Both promising experimental work and theory suggest that a combined SFOAE-DPOAE profile will better distinguish among hearing losses that look the same by audiogram but have different etiologies, underlying pathology, and perceptual difficulties.

PS 494

Diagnostic Accuracy of Clinical DPOAEs and High-Frequency Chirp TEOAEs to Identify Aminoglycoside Ototoxicity and Detect Significant Changes in Hearing in Individuals with Cystic Fibrosis

Chelsea Blankenship[1]; Lisa Hunter[1]; Lindsey Bittinger[1]; Jordan Caylor[1]; Douglas H. Keefe[2]; Patrick Feeney[3]; Denis Fitzpatrick[2]
[1]Cincinnati Children’s Hospital Medical Center; [2]Boys Town National Research Hospital; [3]National Center for Rehabilitative Auditory Research

Individuals with cystic fibrosis (CF) commonly receive intravenous aminoglycoside antibiotics (IV-AGs; tobramycin, vancomycin, amikacin) to treat drug-resistant chronic lung infections. While IV-AGs are essential for treatment, they are ototoxic and result in permanent sensorineural hearing loss that originates in the high frequencies and progresses to the standard frequency range. DPOAEs are commonly included in ototoxicity monitoring protocols to evaluate cochlear function and include both reflection and distortion sources. The ability to detect changes in the reflection source of the basal portion of the cochlea (>10 kHz), where ototoxicity first occurs, is of clinical importance. High-frequency double-evoked TEOAEs with chirp stimuli allow measurement of the reflection component up to 14.7 kHz. The goal of this study was to compare the sensitivity and specificity of DPOAE and TEOAEs to identify hearing loss and detect significant changes in hearing. Individuals with CF (n=57; 6-21 years) and age-matched typically developing individuals without CF (NCF; n=61, 7-18 years) were recruited for the study. Audiometric thresholds (0.25-16 kHz), clinical DPOAEs (Interacoustics Titan; 2-10 kHz), and double-evoked TEOAEs using chirps (0.71-14.7 kHz) were measured at each visit. Chirp TEOAEs were recorded with a custom designed software (Keefe et al., 2019). CF participants were tested every 3 to 6 months with repeated IV-AG treatment. Hearing status was classified as normal (≤ 15 dB HL) or impaired (≥ 20 dB HL). Significant changes were defined as a decrease of 10 dB at two frequencies or a decrease of 20 dB at one frequency compared to the initial study visit. CF participants had significantly poorer hearing across all audiometric test frequencies (0.25-16 kHz; $p < 0.001$), with thresholds in the CF group ranging up to 55-75 dB HL in the 8-16 kHz region. CF individuals with hearing loss displayed lower DPOAE SNRs compared to NCF and CF individuals with normal hearing. For TEOAEs, CF and NCF individuals with normal hearing displayed equivalent SNRs across all test frequencies ($p > 0.05$;

1-14.7 kHz). However, CF individuals with hearing loss displayed lower TEOAE SNRs from 8-14.7 kHz ($p < 0.001$). Further analyses include canonical correlations to determine whether DPOAEs or TEOAEs have a higher correlation with audiometric thresholds. Receiver operating characteristic analyses will be presented with multiple cut-off criteria to optimize DPOAE and TEOAE classification of hearing loss and detect significant changes in hearing.

Psychoacoustic Studies on Humans and Animals

PS 495

The Effects of Blasts on Hearing in CBA/CaJ Mice

Kali Burke[1]; Senthilvelan Manohar[1]; Laurel Screven[2]; Amanda M. Lauer[2]; Richard Salvi[3]; Micheal L. Dent[1]
[1]University at Buffalo, SUNY; [2]Johns Hopkins School of Medicine; [3]Center for Hearing and Deafness, 137 Cary Hall University at Buffalo, Buffalo, NY 14214

Laboratory mice (*Mus musculus*) are frequently used in studies on hearing and communication disorders because of similarities in the cochleae and dynamic vocal repertoire between them and humans. The characterization of the auditory effects of blast trauma in humans has largely relied upon heterogeneous injury outcomes with no baseline pre-blast measurements. Conductive hearing loss, tinnitus development, and difficulty communicating in noisy/reverberant environments are common long-term symptoms of acute blast exposure in humans. The auditory system is especially susceptible to acoustic trauma initiated by high intensity improvised explosive devices (IED) that generate intense overpressure blast waves. We used a custom blast wave generator to produce consistent and controllable blast waves and investigated the co-morbidity of auditory damage and traumatic brain injury (TBI) in CBA/CaJ mice. We evaluated auditory perception of simple and complex stimuli before and up to 90 days following blast exposure using operant conditioning and a detection task. Absolute thresholds for a pure tone (8, 16, 24, or 42 kHz) or an ultrasonic vocalization (complex, downsweep, jump, or upsweep) were measured in 48 adult CBA/CaJ mice (24 M and 24 F). Absolute thresholds from each subject before the blast were compared to daily absolute thresholds after the blast. Changes in threshold stability before and after blast exposure suggests that clinical measurements at an acute time point, such as those taken on humans or in labs that study auditory brainstem responses, may not accurately reflect systemic functioning. Shifts in detection thresholds for all stimuli were observed in post-exposure mice, indicating the blasts likely lead to cochlear damage. Following the 90th day of testing, brains and cochleae were collected and stained to examine inner and outer hair cell loss, damage to ribbon synapses, and degeneration. Supported by R01DC016641 to MLD.

PS 496

Effects of Noise Level Statistics and Instantaneous Compression on Adaptation to Noise in Word Recognition

Enrique A. Lopez-Poveda; Miriam I. Marrufo-Pérez; Dora Sturla; Almudena Eustaquio-Martin
University of Salamanca

The recognition of isolated words in noise is easier when words are presented later rather than earlier in the noise. This phenomenon has been referred to as noise adaptation and is probably due to the leading noise shifting (adapting) the dynamic range of auditory neurons, which can improve the neural encoding of spectral and/or temporal (envelope) cues in speech. At least two mechanisms can produce the shifts in question: (1) activation of the medial olivocochlear efferent reflex (MOCR) by the leading noise (MOCR adaptation); and/or (2) adaptation of the neural synapses to mean sound level in the leading noise ("statistical" adaptation). However, noise adaptation is more likely due to "statistical" than to MOCR adaptation because cochlear-implant (CI) users show noise adaptation despite lacking MOCR effects. Here, we further investigated the importance of "statistical" adaptation for noise adaptation. We compared speech reception thresholds (SRTs) (defined as the signal-to-noise ratio at 50%-word recognition) for words delayed 50 ms (early condition) or 1500 ms (late condition) from the onset of a simultaneous speech-shaped noise. In the late condition, the level of the leading noise was either constant (65 dB SPL) or was changing every 50 ms such that 80% or 20% of the 50-ms segments were at 65 dB SPL. Noise adaptation was quantified as the SRT improvement in the late condition with respect to the early condition. Noise adaptation was largest (1.8 dB) for the constant-level noise, 0.8 dB for the mildly fluctuating (80%) noise, and smallest (0.4 dB) for the highly fluctuating (20%) noise. Instantaneous compression of the stimulus degraded recognition (increased SRTs) but produced as much adaptation in the highly fluctuating noise as in the constant-level noise. Altogether, the results support the notion that noise adaptation in speech recognition is due to "statistical" adaptation rather than to MOCR adaptation. Further, they suggest that instantaneous compression, such as that applied by the basilar membrane, facilitates adaptation in fluctuating noise by reducing the amplitude fluctuations in the noise. This also suggests that hearing-impaired listeners show less noise adaptation than do normal-hearing listeners possibly because they have reduced cochlear compression. Lastly, our results suggest that the strong compression used in CIs

facilitate noise adaptation. [Work supported by grant BFU2015-65376-P from the Spanish MINECO].

PS 497

Gap Detection Tests Reveal Central Auditory Deficits in Adults with Well Controlled Human Immunodeficiency Virus Infection

Jay Buckey[1]; Christopher Cox[2]; Gayle Springer[2]; Abigail Fellows[1]; Peter Torre[3]; Howard J. Hoffman[4]; Michael Plankey[5]

[1]Geisel School of Medicine at Dartmouth; [2]Johns Hopkins University Bloomberg School of Public Health; [3]San Diego State University; [4]Epidemiology and Statistics Program, National Institute on Deafness and Other Communication Disorders (NIDCD), National Institutes of Health (NIH); [5]Georgetown University Medical Center

Background

Human immunodeficiency virus (HIV) infection can affect the brain, which may result in poorer performance on central auditory tests. The ability to detect gaps in background noise can reflect difficulties with sound processing in the brainstem and cortex. We hypothesized that HIV+ adults would have impaired gap detection abilities, not related to measures of peripheral auditory function as measured by audiometry and auditory brainstem responses (ABR).

Methods

45 HIV+ (mean age 59 years, 65% male) and 39 HIV- (mean age 65 years, 92.3% female) adults from the Multicenter AIDS Cohort Study (MACS) and the Women's Interagency HIV Study (WIHS) participated. ABRs and audiometric thresholds were measured using standard clinical techniques in a sound treated room. The adaptive gap detection test presented a 4.5 second burst of white noise with a gap placed randomly within the middle 2.5 seconds. The test started at a gap duration of 20 msec and was reduced progressively to find the participant's threshold. For each participant, at each gap length, the percentage of time the participant correctly identified the gap was measured. The dependence of correct identification rate on gap length was sigmoidal, showing a threshold below which no gaps were detected, a rapid rise in detection percentage as gap length increases, and then a plateau. The sigmoidal response curves between the HIV+ and HIV- group were analyzed using a non-linear mixed model to account for repeated measures, and the two model parameters between groups were compared using a likelihood ratio test.

Results

The HIV+ group showed worse gap detection ability despite being younger (59 vs. 65 yrs) and having no difference in pure tone averages (13.5 dB vs. 16.0 dB) compared to the HIV- group (Table 1, Figure 1). The likelihood ratio statistic comparing the model with the HIV effects to the null model assuming one curve for both groups was 19.94 ($p < 0.001$). No differences in wave I latencies or amplitudes were seen, suggesting no differences in cochlear output.

Conclusions

Gap detection ability was worse in the HIV+ group despite good immunological and viral control and similar audiometric and ABR findings to the HIV- group. These data suggest differences in central nervous system processing of sound in the HIV+ group, which may be a consequence of HIV infection or treatment that could potentially be tracked using gap detection testing.

Table 1. Overall characteristics of the groups

Variable	All (n=84)	HIV+ (n=45)	HIV- (n=39)
Age years mean (std)	61.5 (8.8)	58.9 (8.0)	64.6 (8.9)
Male number (%)	67 (79.8%)	31 (68.9%)	36 (92.3%)
PTA dB HL mean (std)	14.7 (7.3)	13.5 (6.4)	16.0 (8.1)
Wave I latency ms mean (std)	2.4 (0.2)	2.4 (0.1)	2.3 (0.2)
Wave I amplitude μv mean (std)	0.2 (0.1)	0.2 (0.1)	0.2 (0.1)
Wave V latency ms mean (std)	6.8 (0.4)	6.8 (0.4)	6.8 (0.4)
Wave V amplitude μv mean (std)	0.3 (0.1)	0.3 (0.2)	0.2 (0.1)
Undetectable HIV RNA number (%)		39 (86.7%)	
CD4 count mean (std)		733 (328.9)	
Years on anti-retroviral therapy mean (std)		31.9 (13.2)	

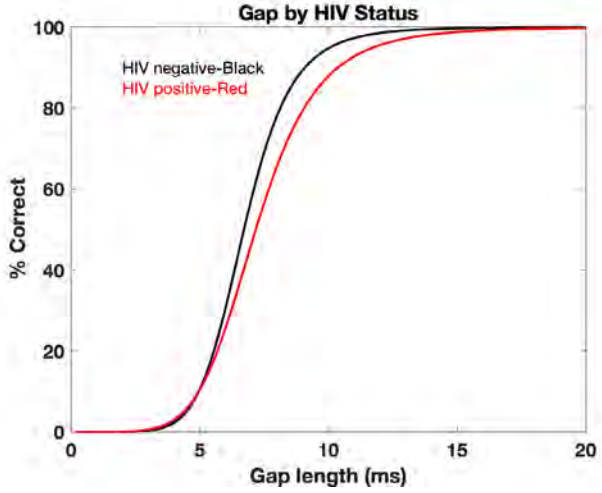

PS 498

A 6 dB Increase in Trauma Level reduces ABR Wave 1 Amplitude without Alteration of Behavioral Thresholds

Katja Bleckmann[1]; Sonja J. Pyott[2]; Georg M. Klump[1]
[1]Cluster of Excellence Hearing4all, Department of Neuroscience, Carl von Ossietzky University, Oldenburg, Germany; [2]University of Groningen, University Medical Center Groningen, Groningen, Department of Otorhinolaryngology and Head/Neck surgery, The Netherlands

Background
The effects associated with noise-induced hearing loss (NIHL) are of profound interest for understanding the etiology of hearing disorders. Acoustic trauma in anesthetized or awake animals is commonly applied to induce NIHL. We evaluated the effects of two different trauma levels on auditory thresholds and auditory brainstem response (ABR) wave 1 amplitudes in anesthetized C57BL/6.CAST-*Cdh23*$^{Ahl+}$ (WT) mice and mice with a glutathione peroxidase 1 knock-out (Gpx1-KO) with C57BL/6.CAST-*Cdh23*$^{Ahl+}$ background.

Methods
To elicit threshold shifts by acoustic trauma, ketamine-anesthetized animals were exposed to an octave band noise (8-16 kHz) for 2 h with a level of 98 dB SPL or 104 dB SPL. ABR wave 1 amplitudes were measured under ketamine anesthesia using pure tones of 5, 10 and 20 kHz (0.5 ms) and clicks (20 µs) at the start and at the end of the behavioral experiments, i.e., before and after acoustic trauma.

We also compared absolute auditory thresholds in quiet and masked threshold in background noise (spectrum level 20 dB/Hz, frequency range 2-50 kHz) before and after acoustic trauma. Absolute and masked thresholds were assessed applying a reward-based Go/NoGo procedure. Based on hit and false alarm rates, thresholds were obtained for a sensitivity d' of 1.8.

Finally, we counted the number of functional inner hair cell-spiral ganglion neuron synapses using immunofluorescence and confocal microscopy at the end of the behavioral tests.

Results and Conclusions
Data from the ongoing study show that post-trauma ABR amplitudes of wave 1 appear unchanged after 98 dB SPL trauma, suggesting that either ketamine-xylazine anesthesia or strain differences reduce the effects of trauma on ABR thresholds described previously in CBA/CaJ mice (Shaheen and Liberman, 2018). Mice exposed to 104 dB SPL, however, showed decreased wave 1 amplitudes. Interestingly, independent of the trauma level pre- and post-trauma auditory thresholds were not significantly different. These results are discussed with respect to the synapse counts in the two strains.

Funded by the DFG, **EXC 2177**

PS 499

Effect of the Distribution of Tone Frequency in Tone Cloud Scene on the Discrimination of Notched Noise

Shunsuke Kidani
Japan Advanced Institute of Science and Technology

Background
Human perception of sound varies with the context. The auditory attention for focusing target sound is increased by the context as presenting information about the target sound. In a rat study, the ability to discriminate between tones increases with exposure to the tone cloud during growth [P. Znamenskiy & A. M. Zador, 2013]. The study suggests that the frequency distribution within the tone cloud affects the discrimination by increasing attention to the target frequency. This study determines whether humans are able to pay attention to a particular frequency under a stochastically presented tone. The question posed by this study is as follows: "Are humans able to focus on the particular frequency from a random sequence that comprises tones from several frequencies?"

Methods
The hypothesis of this study was that the ability to discriminate between noises increases by focusing on a particular frequency. This experiment was conducted in the presence of tone cloud stimuli. The tone cloud stimuli were used to focus the attention on a particular frequency and comprised sinusoidal tones in a random frequency sequence. Each tone was generated from a normal probability distribution (the µ as the average was 1000, 2000, 3000, or 4000 Hz for focusing frequency, and the β as the dispersion was 250 Hz) and had a duration of 100 ms. The tone sequence was presented at intervals of 50 ms. The discrimination task was to judge whether there was a frequency notch in wideband noise (250–4750 Hz). There were nine notch conditions and the width of each was 500 Hz. The experiments investigated whether the "*d'*"s of the discrimination task varied with the central frequency of the normal distribution within the tone sequence. Participants of the experiments did not know the focusing frequency.

Results and conclusions
According to reports of self-observation, the tone sequence helped participants focus on the particular

frequency (). The *d'* increased when the notch frequency was the same as the particular frequency. These results suggest that humans can extract a particular frequency from a random sequence that comprises tones from the normal probability distribution. Conversely, the *d'* also increased when the notch frequencies were at lower and higher conditions. This result is thought to be the effects of tone height of the noise.

PS 500

Masking of Amplitude-Modulation Detection by Low-Frequency Temporal Fine Structure in Listeners with Normal Hearing and Sensorineural Hearing Loss

Charles Babb; Kenneth S. Henry
University of Rochester

Individuals with sensorineural hearing loss (SNHL) can show dramatic differences in speech intelligibility despite having similar audiometric thresholds on standard clinical tests of hearing function. Proposed mechanisms for deficits in speech understanding include changes in cochlear innervation density, central processing/ cognition, and underlying pathophysiologic differences in the etiology of SNHL (e.g., noise induced vs metabolic related to reduced endocochlear potential). Prior studies in chinchilla models of noise-induced and metabolic hearing loss have shown differences in auditory-nerve encoding of envelope (ENV) fluctuations and temporal fine structure (TFS). Specifically, in response to a white-noise stimulus, these studies found abnormally strong encoding of TFS at frequencies well below the characteristic frequency of individual auditory-nerve fibers. Abnormal TFS encoding was more pronounced with noise-induced than metabolic hearing loss, and appears likely to impair processing of ENV fluctuations though no previous studies have tested this possibility in human subjects. In this study, we sought to determine whether abnormally strong encoding of low-frequency TFS in human subjects with SNHL adversely impacts ENV perception by measuring the effect of low-frequency TFS maskers on the ability to detect 200-Hz amplitude modulation in the temporal envelope of a 4-kHz probe. Two-down, one-up adaptive tracking procedures and a single-interval, two-alternative task were used to quantify subjects' detection thresholds for the target modulation. TFS maskers were narrowband signals with center frequencies near the target modulation frequency of the probe. Additionally, the same TFS masker waveforms were applied directly to the ENV of the probe in a modulation masking experiment for comparison of masking patterns. Behavioral results were compared between subjects with normal hearing and those with SNHL. Decision variable analyses were then used to evaluate whether a model of pathophysiological encoding of low-frequency TFS better explains trial-by-trial behavioral responses in listeners with SNHL compared to those with normal hearing. These results will help advance our understanding of perceptual changes that occur with hearing loss and hopefully guide development of novel treatment strategies and improvements in amplification technology. Furthermore, low-frequency TFS maskers may be useful for distinguishing noise-induced and metabolic hearing losses.

PS 501

Spectrotemporal Modulation Discrimination in Normal Hearing School-Aged Children and Adults: Effects of Age and Vocoding.

Anisha R. Noble[1]; Jesse M. Resnick[1]; Jay T. Rubinstein[1]; Lynne A. Werner[2]; Mariette S. Broncheau[2]; David L. Horn[3]
[1]University of Washington; [2]Department of Speech and Hearing Sciences at the University of Washington; [3]Seattle Children's Hospital

Background
Acoustic spectral resolution – the ability to perceive peaks and troughs of energy across frequency – is essential for speech perception. Spectral resolution has been proposed as a proxy measure of device efficacy in cochlear implant users and relies on both spectral frequency resolution (FR) and across-spectrum intensity modulation sensitivity (SMS). Spectral resolution develops through adolescence in normal hearing and implanted children; it remains unclear whether prolonged maturation of FR and/or SMS is responsible for this finding. Furthermore, the relatively poor spectral resolution of CI listeners might be due to degraded FR, SMS or both. A test of spectral resolution was used to study two main hypotheses: First, that school-aged children would show immature SMS but mature FR relative to adults. Second, that testing with vocoded stimuli would yield reduced FR but not SMS.

Methods
Participants included thirteen 5-12 year old children and ten adults. The psychoacoustic task was based on the "spectral-temporally modulated ripple test" (SMRT, Aronoff & Landsberger, 2013). Stimuli were 1s pure-tone-complex carriers with spectrotemporally modulated envelopes using a fixed 5Hz temporal modulation ripple rate and spectral ripple densities from 0.125 – 20RPO. Vocoded stimuli were created by filtering with an 8-channel vocoder with analysis / carrier filter range 200-7000Hz and filter slope 24dB/octave. An adaptive, 2-up, 1-down, 3-interval 3-alternative forced choice procedure was used to measure highest ripple density discriminable from 20RPO. Listeners were tested at four ripple depths

in vocoded and unfiltered conditions in random order. SMRT thresholds were used to fit logarithmic functions for each condition. Function slope and x-intercept were taken as measures of FR and SMS, respectively, based on the model of Supin et al. (1999).

Results

Mean SMRT threshold was significantly better in the unfiltered condition than the vocoded condition and better for adults than children. Mean log function x-intercept was significantly poorer in children than in adults, but no age effect was found for slope. Mean slope was significantly lower (flatter) in the vocoded than in the unfiltered condition for both age groups. Effects of vocoding were not different between children and adults.

Conclusions

Findings support the hypothesis that undeveloped spectral resolution in school-age children is largely due to immature SMS. Although spectral degradation with vocoding had a marked effect on FR, this was similar in children and adults. These findings suggest that performance of CI children on tests of spectral resolution may not just reflect degraded frequency resolution but also immature across-spectrum intensity modulation sensitivity.

PS 502

Informational Masking in the Modulation Domain

Christopher Conroy; Gerald Kidd
Department of Speech, Language & Hearing Sciences and Hearing Research Center, Boston University

Informational masking (IM) in the spectral domain, or *spectral IM*, implies a breakdown in frequency selectivity (i.e., a failure of segregation and/or selective attention) under conditions of uncertainty. In this study, we sought to determine whether an analogous breakdown would be evident in the modulation frequency domain. We employed the "multitone masking" paradigm devised by Neff and Green [Perception & Psychophysics, **41**, 409-415 (1987)]—a paradigm typical of studies of spectral IM—but adapted it for testing the effects of uncertainty in the modulation frequency domain. A one interval, two-alternative forced-choice paradigm was used. The task was to detect a fixed and known 32-Hz target modulation frequency (the *target*) imposed on a broadband noise carrier. In addition to the target, a masker modulation frequency (the *masker*) also was added to the same noise carrier. Six maskers were tested, spanning the range 8- to 128-Hz in half-octave steps. Maskers that fell within a two-octave "protected zone" centered on the target were excluded. Target modulation detection thresholds were measured in two conditions: a *fixed* condition, in which the masker was held constant throughout a block of trials, and a *roved* condition, in which the masker was selected at random on each trial from the set of six. Psychometric functions (*d'* vs. target modulation depth) were constructed for each individual masker in both conditions, yielding 12 psychometric functions overall (six fixed, six roved). A comparison between the fixed and roved functions revealed the effects of masker modulation frequency uncertainty. Preliminary results showed poorer performance for the condition in which the masker modulation frequency was uncertain. The magnitude of this effect, however, depended on both the masker and the observer. Our conclusion was that, when manifest, such a performance decrement was evidence for IM in the modulation frequency domain, or *modulation IM*. Bias also was measured, which shed additional light on how decision processes changed under conditions of uncertainty. The results will be discussed with respect to the modulation filterbank concept, the role of selective attention in the modulation frequency domain, and in the context of a broader theoretical interpretation of IM, i.e., one that incorporates modulation IM.

PS 503

Investigating the role of harmonic cancellation in masked speech intelligibility

Luna Prud'homme[1]; Mathieu Lavandier[1]; Virginia Best[2]
[1]LGCB, Universite de Lyon; [2]Boston University

Previous studies (e.g., de Cheveigné et al., 1995; Deroche and Culling, 2011) suggested that harmonic cancellation might play a role in the segregation of harmonic sounds based on fundamental frequency (F0), but its utility for sounds with non-stationary F0s is unclear. A behavioral experiment was designed to understand if and when harmonic cancellation is important for understanding speech masked by competing speech. The focus was on energetic aspects of masking, and thus informational masking was deliberately minimized. Speech reception thresholds (SRTs) were measured in normal-hearing listeners using seven maskers: speech-shaped noise, noise-vocoded speech, monotonized and intonated harmonic complexes, monotonized speech, reversed speech and natural speech. The noise-based maskers were chosen as reference stimuli with no harmonic structure, with and without amplitude modulation. The harmonic complexes provided a comparison of stationary and non-stationary F0s, while the monotonized and natural speech extended this comparison to speech which also contains unvoiced portions. Reversed speech served as a control condition to reveal any residual informational masking. The role of harmonic cancellation was estimated based on a comparison of SRTs across masking conditions and on predictions from a speech

intelligibility model that has been modified to include harmonic cancellation. Of particular interest is the contribution of harmonic cancellation for natural speech maskers, which provides an indication of the potential role of F0 segregation in cocktail party scenarios.

PS 504

The Effect of Harmonic Number and Pitch Salience on the Ability to Understand Speech-on-speech Based on Differences in Fundamental Frequency

Sara M. K. Madsen[1]; Andrew J. Oxenham[2]; Torsten Dau[3]
[1]University of Minnesota; [2]Department of Psychology, Center for Applied and Translational Sensory Sciences, UMNTC; [3]Department of Health Technology

Differences in fundamental frequency (F0) between competing voices facilitate the ability to segregate a target voice from interferers, thereby enhancing speech intelligibility. Although lower-numbered harmonics produce greater pitch salience than higher-numbered harmonics, it remains unclear whether differences in harmonic ranks, and therefore pitch salience, affects the benefit of pitch differences. An earlier study (Oxenham & Simonson, 2009)tested conditions with either only high or low harmonic ranks present and did not find an effect of harmonic rank. However, that study only tested conditions where the difference in long-term average F0 (∆F0) between the two competing voices was fairly large (4 and 8 semitones, ST) and it is possible that the effect of pitch salience would be greater in more challenging conditions, i.e. in conditions with a smaller ∆F0. This study tested speech intelligibility in conditions with one speech masker for ∆F0s of 0,2, and 4 ST. The speech was presented in a broadband condition or was highpass or lowpass filtered. Results show similar performance in the highpass- and lowpass-filtered conditions for all ∆F0s, suggesting little or no effect of harmonic rank in the ability to use F0 to segregate voices, even with smaller ∆F0s between competing voices.

[Work supported by the Wilhelm Demant Foundation and NIH grant R01 DC005216.]

PS 505

Sensitivity to Temporal Fine Structure Predicts Language Skills in Children with Sensorineural Hearing Loss

Lorna Halliday[1]; Laurianne Cabrera[2]
[1]University of Cambridge; [2]Université Paris Descarte

Children with mild to moderate sensorineural hearing loss (MMHL) tend to be rehabilitated with hearing aids, and yet there is considerable variability in the language outcomes seen in this group. Previous research has shown that adult hearing-aid users show positive correlations between measures of temporal fine structure (TFS) processing and speech perception in both quiet and noise. However, sensitivity to envelope (E) cues has not been found to correlate with the speech discrimination abilities of adults with MMHL either in quiet or noise. The current study examined the hypothesis that sensitivity to TFS cues might predict language abilities in children with MMHL, over and above E cues, and the information contained within the audiogram.

Psychophysical measures designed to assess sensitivity to TFS (frequency discrimination for a 1-kHz sinusoid and discrimination of modulations in the F0 of a complex sound) and E (envelope onset discrimination and amplitude modulation detection) were obtained for 46, 8- to 16-year-old children with MMHL. Thresholds on the tasks were averaged to create TFS and E composite scores. Children who wore hearing aids (n = 43) were tested both while they were wearing their hearing aids (aided condition) and while they were not (unaided condition). Language abilities were assessed using standardised measures of receptive vocabulary and repetition of nonsense words. A series of multilevel linear models was used to determine whether TFS or E composite thresholds significantly contributed to the variance in vocabulary, or nonword repetition, after controlling for other known predictors (i.e. better ear pure tone average (BEPTA) thresholds, age, nonverbal intelligence, maternal education levels, and family history of language difficulties). Changes to the Log Likelihood (-2LL) were used to establish whether the addition of TFS, E, or both, significantly improved the model fit. Models were run separately for unaided and aided conditions.

Results showed that, for vocabulary, TFS scores made a significant contribution to the model, for both the aided and unaided conditions, whereas E scores did not. For nonword repetition, TFS scores significantly improved the model fit for the unaided condition. However, for the aided condition, both TFS and E scores predicted nonword repetition abilities. These findings suggest that sensitivity to TFS may contribute to individual differences in language abilities for children with MMHL, over and above audiometric thresholds.

PS 506

Factors Underlying the Relationships Between Performance on Different Psychoacoustic Tasks During Adolescence

Julia J. Huyck[1]; Beverly A. Wright[2]
[1]Kent State University; [2]Northwestern University

There is wide individual variation in performance across psychoacoustic tasks, especially during development. Many factors likely contribute to these individual differences, including the age or maturity of the listener, the extent to which different tasks require the same basic acoustic encoding (e.g., temporal processing), and the top-down engagement required to do each task. In one group of developing listeners (n=28; age 8-17 years, mean = 12.7 years), thresholds for signal tone detection was highly correlated ($R^2 \geq 0.34$, $p \leq 0.02$) across four non-simultaneous masking conditions (three backward masking conditions and one forward masking condition) after controlling for log-transformed age. Thresholds also correlated ($R^2 \geq 0.14$, $p = 0.05$) between two simultaneous-masking conditions (the signal either shared an onset with the bandpass masker or was presented 200-ms after the masker onset). However, thresholds did not correlate ($p \geq 0.67$) between the non-simultaneous and simultaneous masking conditions after controlling for log-transformed age, consistent with previous research indicating that different types of temporal masking involve different underlying mechanisms. In another group of developing listeners (n = 60; age 8-15 years, mean = 11.8 years), regression modeling indicated that performance on a backward masking condition was predicted (R^2 = 0.49, $p < 0.001$) by a combination of log-transformed age, performance on forward masking and temporal interval discrimination conditions, and auditory working memory scores. In contrast, performance on the forward masking condition was predicted (R^2=0.35, $p < 0.001$) by performance on the backward masking condition, years of musical experience (normalized for age) and performance on a speech-in-noise task. Finally, performance on the temporal-interval discrimination condition (R^2 = 0.34, $p < 0.001$) was predicted by log-transformed age, performance on the backward masking condition, sex (better performance in males), and speech-in-noise scores. Thus, even when performance correlates across listening conditions, cognitive (e.g., memory), biological (e.g., sex), and environmental (e.g., musical experience) factors may differentially contribute to performance on different psychoacoustic conditions during adolescence.

PS 507

Modeling Pitch Perception of Concurrent High-Frequency Complex Tones with Auditory Nerve Simulations

Daniel R. Guest[1]; Andrew J. Oxenham[2]
[1]University of Minnesota; [2]Department of Psychology, Center for Applied and Translational Sensory Sciences, UMNTC

Previous studies have shown that accurate pitch perception is possible for harmonic complex tones with fundamental frequencies (F0s) in the musical range (1.4 kHz) but with all their harmonics beyond the putative limits of phase locking (i.e., above 8 kHz). These findings are consistent with a place code for pitch at high frequencies. However, it is unknown whether such a code can support accurate pitch perception of more complex stimuli, such as mixtures of complex tones. To address this question, we studied pitch perception using mixtures of complex tones with low F0s (around 280 Hz) and high F0s (around 1400 Hz), comprising a target complex tone and one or more masker complex tones. The masker tones were always presented concurrently and spectrally overlapping with the target. The target tones were filtered to ensure that in the high-frequency case only harmonics beyond the putative limits of phase locking were present. First, F0DLs were measured for target tones in isolation and for target tones with a single masker tone. Although pitch perception was generally poorer at high frequencies than at low frequencies, listeners retained accurate F0DLs (i.e., < 6%) at both low and high frequencies in the presence of the single masker tone. Next, percent correct at 0 dB target-to-masker ratio (TMR) and the TMR required to achieve 79% correct were measured for target tones in the presence of two masker tones. Listeners performed better at low frequencies than at high frequencies in 0 dB TMR but were above chance in both cases, and listeners needed better TMRs to achieve 79% correct at high frequencies relative to low frequencies. Ideal-observer analysis of auditory-nerve simulations of the stimuli were used predict the behavioral results. Preliminary analyses suggest that neither a model based on spike rate and timing information (all-information model) nor a model based only spike rate information (rate-place model) could account for the key trends in our data. However, with the additional assumption of poorer decoding efficiency at high frequencies relative to low frequencies, the rate-place model provided the best fit to the data so far. Collectively, our preliminary results are consistent with the idea that a unitary rate-place mechanism underlies complex pitch perception at both high and low frequencies, but that some unknown non-peripheral factor limits the accuracy of pitch perception at higher frequencies [Grant support: R01 DC005216 and NSF NRT-UtB1734815].

PS 508

The Discriminability of Temporal and Frequency Modulations in Budgerigars – Natural Vocalizations

Huaizhen Cai
SUNY at Buffalo

Animal vocalizations like budgerigar warble sounds are complex signals with enriched amplitude fluctuations in the frequency and temporal domains. Birds rely on these characteristics for acoustic communication, making them a particularly interesting model to study

auditory processing. Birds show superior temporal resolution acuity when discriminating synthetic sounds with different temporal fine structures. Physiological studies indicate that birds' HVc neurons respond to synthetic vocalizations best when synthetic vocalizations mimic the amplitude modulations embedded in natural vocalizations. However, few studies have investigated the ability of birds to behaviorally discriminate frequency or temporal modulations in ecologically relevant vocalizations. The present study aims to investigate the behavioral thresholds and the 'core bands' of temporal and frequency modulations in natural vocalizations with an operant conditioning procedure. Budgerigars were trained to discriminate a modified contact call or an unmodified natural call (a different contact call, alarm call, long harmonic, or noisy call) from an unmodified contact call. The modified contact calls in phase 1 were low pass filtered with different cutoff frequencies, and the higher frequency components of either the frequency modulations or the temporal modulations were eliminated separately by the filters. The discriminability of the temporal or frequency modulation was investigated by recording the hit rates for calls modified by filters with different cutoff frequencies. In phase 2, the frequency or temporal modulations in contact calls were band stopped by notch filters to investigate the 'core bands' of modulations for birds to discriminate in natural vocalizations. The notch filters eliminated the frequency components of either the frequency or the temporal modulation within a range. The hit rate and response latency for each type of call modification were recorded in both phases 1 and 2. Birds showed better performance discriminating calls between categories than within the same category. In phase 1, birds indicated an increased discriminability for calls modified by filters with lower cutoff frequencies in both temporal and frequency modulations when the majority of frequency and temporal modulations in the vocalization were eliminated. In phase 2, the birds showed better discriminability when the notch filters eliminated frequency and temporal modulations at the lower frequency ranges. The perceptual sensitivity of temporal and frequency modulations obtained behaviorally with natural vocalizations were better than those obtained physiologically with synthetic vocalizations. Budgerigars rely on the frequency and temporal modulation features in natural vocalizations for call discrimination.

PS 509

Multiple Integration Windows in Auditory Perception

Richard McWalter; Josh H. McDermott
Department of Brain and Cognitive Sciences, MIT

Sound textures, as arise from swarming insects or falling rain, are believed to be represented with time-averaged statistics measured from early auditory representations [McDermott et al. 2013]. Texture statistics show signs of being averaged over a multi-second temporal integration window [McWalter and McDermott, 2018]. However, many different statistics are needed to account for texture perception. It remains unclear whether there is a single global integration window for all statistics, or whether integration windows vary across statistics.

We investigated the extent of time-averaging for individual classes of statistics from the auditory texture model of McDermott and Simoncelli (2011). We divided the statistics into seven classes: (i) envelope mean, (ii) envelope variance, (iii-vi) 4 bands of amplitude modulation power from slow (< 4Hz) to fast (>36Hz) and (vii) pair-wise envelope correlations. These statistics differ in the sample size required for robust estimation, and we hypothesized that the averaging window might reflect these differences.

We conducted an experiment in which listeners judged which of two synthetic sound textures was most similar to a reference texture [McWalter & McDermott, 2018]. The duration of the two textures varied across trials, from 50ms to 5s. The two textures on a trial were generated from statistics that differed in one of the seven classes of statistics, being drawn from a continuum between the statistics of a real-world sound texture (the reference) and Gaussian noise for the selected statistics class. Texture discrimination performance increased with stimulus duration and then asymptoted, presumably when the duration of the sound texture exceeded the time-averaging window used to estimate the statistics [McWalter & McDermott, 2018]. We found that the performance asymptote occurred at different durations for different statistics, ranging from roughly 150 milliseconds for the envelope mean (capturing the spectrum) to several hundred milliseconds for the envelope correlation, to a second for the envelope variance. The performance asymptote for the modulation power depended on the modulation band rate, ranging from several hundred milliseconds for fast modulations to a few seconds for slow modulations. The results suggest the extent of time-averaging varies across texture statistic classes, revealing a continuum of integration windows in auditory perception.

PS 510

Extending the GammaChirp Model of Notched-Noise Masking to Include Absolute Threshold: Exploring Improvements in the Fit Provided by Assuming an Internal, Level-Dependent, Cochlear Noise Floor

Kenji Yokota[1]; Toshio Irino[1]; Roy D. Patterson[2]
[1]Faculty of Systems Engineering, Wakayama

University; [2]Department of Physiology, Development and Neuroscience, University of Cambridge

This paper shows how sets of notched-noise (NN) thresholds with a large range of masker-noise levels (40, 30, 20, 10, 0, and -10 dB at 1000 Hz) and notch widths (0.0, 0.1, 0.2, 0.4, 0.6, and 0.8 times the signal frequency) can be used to refine our understanding of the internal, level-dependent, cochlear noise floor suggested by earlier versions of the GammaChirp (GC) model. The NN thresholds and absolute thresholds of 8 normal-hearing (NH) listeners were gathered at two signal frequencies (1000 Hz and 2000 Hz) and three subsets of these thresholds were compared: a Full 36 set; an Upper 18 set, in which the external masker level was high relative to absolute threshold (40, 30, or 20 dB); and a Lower 18 set (10, 0, or -10 dB) where the internal, cochlear noise floor was assumed to interacted with the external masker in the determination of NN threshold.

The data were fitted by the extended GC model (Eqs. 1 – 7) which included terms for the level-dependent noise floor, N_c(LD) (Eq. 4), and the noise floor in quiet, N_c(Q) (Eq. 5). The NN threshold, Ps_hat, was estimated (Eq. 1) from the sum of the external NN component, Pext_hat (Eq. 2) and the internal, level-dependent component, Pint_hat (Eq. 3). Absolute threshold, Pabs_hat, was estimated from N_c(Q) (Eq. 6). A least-square method was used to estimate the GC and internal noise parameters (Eqs. 7 and 8).

The model with the level-dependent noise floor, N_c(LD), was compared to the traditional model with threshold-limit, P_0. Table 1 shows the estimation errors averaged over signal frequency since the pattern of values for 1000 and 2000 Hz was very similar. The grand mean NN rms error of the N_c(LD) model (averaged over threshold set) was just under 1 dB, while that of the P_0 model was 1.66 dB. The grand mean absolute-threshold error for the N_c(LD) model was just over half a dB, while that of the P_0 model was 5 dB! The filter shapes, bandwidths, and input-output functions of the N_c(LD) and P_0 models were broadly similar; however, the high frequency skirt of the filter was typically steeper when estimated with the N_c(LD) model. The steeper skirt is more consistent with physiological observations. In conclusion, GC filter estimation can be improved simply by introducing a level-dependent, cochlear noise floor, without any modification of the parameters of the GC model itself.

$$\hat{P}_s = \tilde{K} + 10\log_{10}\{10^{\hat{P}_{ext}/10} + 10^{\hat{P}_{int}/10}\}. \quad (1)$$

$$\hat{P}_{ext} = \tilde{N}_0 + 10\log_{10}\Big[\int_{f_{l_{min}}}^{f_{l_{max}}} |T(f)G_c(f)|^2 df + \int_{f_{u_{min}}}^{f_{u_{max}}} |T(f)G_c(f)|^2 df\Big]. \quad (2)$$

$$\hat{P}_{int} = 10\log_{10}\Big[\int_{f_{a_{min}}}^{f_{a_{max}}} |N_c^{(LD)}(f)\cdot G_c(f)|^2 df\Big], \quad (3)$$

$$\text{where } \tilde{N}_c^{(LD)}(f) = \tilde{N}_c^{(Q)}(f) + n_{LD}(\tilde{N}_0 - \tilde{N}_{0_{min}}) + \tilde{N}_b \quad (4)$$

$$\text{and } N_c^{(Q)}(f) = N_c^{(Q)}(f_{ref})\cdot H_{L0}(f)/H_{L0}(f_{ref}). \quad (5)$$

$$\hat{P}_{abs} = \tilde{K} + 10\log_{10}\Big[\int_{f_{a_{min}}}^{f_{a_{max}}} |N_c^{(Q)}(f)\cdot G_c(f)|^2 df\Big]. \quad (6)$$

$G_c(f)$: gammachirp, $T(f)$: transfer function from field to cochlea.

$H_{L0}(f)$: 0−dB HL function. Paremeter with tilde($\sim$) represents the level in a dB scale.

$$\mathbf{c_{gc}} = \underset{\mathbf{c_{gc}}}{\text{argmin}}\{\frac{1}{N}\sum_{i=1}^{N}(P_{s_i} - \hat{P}_{s_i})^2 + (P_{abs} - \hat{P}_{abs})^2\}, \quad (7)$$

$$\text{where } \mathbf{c_{gc}} := \{b_1, c_1, f_{rat}^{(0)}, f_{rat}^{(1)}, b_2, c_2, \tilde{K}, \tilde{N}_c^{(Q)}(f_{ref}), n_{LD}, \tilde{N}_b\}. \quad (8)$$

Table 1: Estimation error. Bold and italic fonts represent smaller error.

		NN rms error (dB)				Absolute thresh. error (dB)			
		Full36	Upper18	Lower18	Mean	Full36	Upper18	Lower18	Mean
1 kHz	$N_c^{(LD)}$	*0.93*	*0.66*	1.13	*0.90*	*0.02*	*0.11*	*0.33*	*0.16*
	P_0	1.65	1.20	*1.04*	1.30	2.56	7.36	2.48	4.13
2 kHz	$N_c^{(LD)}$	*1.16*	*1.07*	*0.91*	*1.05*	*1.41*	*0.47*	*0.71*	*0.87*
	P_0	2.15	1.68	2.23	2.02	4.75	8.63	4.24	5.87
Mean	$N_c^{(LD)}$	**1.05**	**0.86**	**1.02**	**0.98**	**0.72**	**0.29**	**0.52**	**0.51**
	P_0	1.90	1.44	1.64	1.66	3.65	8.00	3.36	5.00

PS 511

Internal Noise in AM and FM Detection

Sarah Attia[1]; Andrew King[2]; Leo Varnet[3]; Christian Lorenzi[4]

[1]PhD Student; [2]Reseacher; [3]Researcher; [4]Full Professor

Frequency modulation (FM) has often been assumed to be detected as amplitude modulation (AM) by human listeners because FM is converted into temporal-envelope fluctuations at the output of cochlear filters. The validity of this assumption has been challenged in numerous studies over the last decades. Surprisingly, little effort has been made to characterize internal noise (i.e., sources of variability such as the stochastic nature of neuronal firing, the internal state of the listener or fluctuations in attention) in AM and FM processing. According to the “FM-to-AM” conversion hypothesis, the same source of internal noise should constrain AM and FM detection.

The purpose of this research was to challenge the validity of the above hypothesis by testing whether a single computational model of temporal-envelope processing based on the modulation-filterbank concept could reproduce the consistency of auditory judgments (an aspect of behavior depending on internal noise) of real listeners in AM and FM detection tasks using a double-pass paradigm. The only model parameter adjusted to the data collected on human listeners was the variance of the Gaussian internal noise added to the output of modulation filters.

The psychophysical measures were conducted in 15 young normal-hearing (NHy) listeners. A 2-interval, 2-alternative forced choice task and a constant-stimuli

paradigm were used to measure the ability to detect a sine AM or FM at two rates (2 and 20 Hz). A 500-Hz sine carrier was used and a bandpass (0.5-80 Hz) modulation noise with a fixed standard deviation was applied to all stimuli. This masking modulation noise had either a low or a high standard deviation. The AM or FM targets were presented at a sensitivity (d') level of 0.5,1 or 1.5 as initially measured for each listener using an adaptive task. All stimuli used during the first session (the first "pass") were stored and presented again in a different order during a second session (the second "pass") after about 5mn. Percent agreement (PA) between responses was calculated for corresponding trials in the first and the second pass.

Simulation results show that the predictions the modulation filterbank model are accurate for slow and fast AM but not for FM. This finding is inconsistent with the "FM-to-AM" conversion hypothesis.

PS 512

Sensitivity to Periodicity: Potential Discrepancies between Frequency-Following Response and Psychophysics

Yi Shen; Ryan Anderson; William P. Shofner
Indiana University Bloomington

Neural encoding of stimulus periodicity is important for pitch perception. Frequency-following response (FFR) provides a non-invasive tool to assess periodicity coding at the level of auditory brainstem in humans, however, a quantitative link between FFR and pitch perception has not been fully established. Previous studies suggest that periodicity cues in different spectral regions may contribute to pitch perception differently, which may not be accurately reflected in FFR. In the current study, the stimuli were iterated rippled noises with different numbers of iterations (IRN iterations of 2, 4, 8, 16, and 32). Higher IRN iterations were associated with greater periodicity in the stimuli. The noises spanned a six-octave range from 177 to 11314 Hz. The fundamental frequency (F0) for the iterated rippled noise was 100 Hz. A harmonic complex of the same fundamental frequency was also included as a reference stimulus. Further, additional filtering conditions were included to limit the periodicity cues to regions above cutoff frequencies of 354, 707, 1414, 2828, and 5657 Hz. In Experiment 1, the FFRs to the stimuli were collected from a group of 10 normal-hearing adults. In Experiment 2, the fundamental frequency difference limens were measured for the same stimuli behaviorally from another group of 10 normal-hearing adults. Both the FFR and psychophysical data exhibited band-pass characteristics, indicating the limited involvement of periodicity cues in low- (< 0.5 kHz) or high-frequency regions (> 4 kHz). Comparing F0 discrimination to FFR, it seems that some of the listeners were able to utilize extended high-frequency regions for F0 discrimination, but similar high-frequency contributions were not observed in FFR.

Acknowledgments
This work was supported by the PhD student research grant from the Department of Speech and Hearing Sciences at Indiana University (awarded to R. Anderson) and NIH grant R21 DC013406 (Co-PIs: V. M. Richards and Y. Shen).

PS 513

Characterizing Comodulation Masking Release in Hearing-Impaired Listeners

Jonathan Regev; Paolo A. Mesiano; Johannes Zaar; Torsten Dau
Hearing Systems Section, Technical University of Denmark

Tone-in noise detection thresholds have been demonstrated to be lower in conditions with low-frequency modulations in the masker (i.e., in comodulated noise) than in conditions with unmodulated noise. This phenomenon has been termed comodulation masking release (CMR). Several studies showed that CMR is reduced in hearing-impaired (HI) listeners compared to normal-hearing (NH) listeners. However, a recent investigation found that some HI listeners still exhibit CMR comparable with that of NH listeners (Mesiano et al., 2019). Furthermore, audibility and frequency selectivity were found to be good predictors of CMR, but not sufficient to account for the differences across listeners when using a suitably-adapted computational model.

In the present study, it was hypothesized that tone detection in unmodulated noise is correlated with intensity discrimination sensitivity, while tone detection in comodulated noise is correlated with the sensitivity to discriminate amplitude modulation depth. In an effort to explain the differences in CMR across HI listeners, the study investigated the supra-threshold processes in these two domains. Multiple psychoacoustic measurements were conducted using a 3-alternative-forced-choice paradigm to estimate intensity discrimination and modulation depth discrimination difference limens (DL), as well as amplitude modulation detection thresholds. These measurements, combined with a hearing profile of the listeners including pure-tone thresholds, auditory-filter bandwidth estimates and CMR results, were analyzed both at the group level and at the level of individual listeners through statistical and linear regression analyses, respectively.

The general trends in the collected data supported the initial hypothesis, as HI listeners with near-normal- and reduced CMR showed different discrimination DLs in specific experimental conditions. However, these trends were not statistically significant or conclusive in regression analyses. Overall, the measures related to the loss of outer hair cells (OHCs) were found to be the dominating predictors of CMR, possibly indicating a dominant effect of loudness recruitment on CMR. To verify these observations, additional data with a new panel of listeners were collected using a subset of the mentioned experiments and including an alternative estimate of OHC loss. The results are discussed with respect to the mechanisms hypothesized to underlie CMR in HI listeners.

PS 514

Connecting a Biophysical Auditory Periphery Model to Perceptual Back-ends for Psychoacoustic Performance Prediction across Tasks

Alejandro Osses Vecchi; Sarah Verhulst
Ghent University

Biophysical models of the human auditory periphery can simulate objective markers of peripheral hearing such as otoacoustic emissions, auditory brainstem responses (ABRs), and envelope-following responses (EFRs), and can be used to simulate how sensorineural hearing loss affects these responses. Given their physiological detail, it would be interesting to extend these models to include a perceptual back-end and allow a prediction of behavioral detection thresholds. In the most basic approach, simulated neural responses to reference and target stimuli in a three-alternative forced-choice (3-AFC) psychoacoustic tasks can be compared to each other to yield a detection cue. The detection cue degradation as a function of outer-hair-cell deficits or synaptopathy can inform how these hearing deficits impact detection thresholds. This basic approach also predicts less accurate responses and degraded thresholds when the external stimulus variability increases.

In this work, we compare different psychoacoustic back-ends to evaluate which approach more accurately captures behavioral thresholds of normal and hearing-impaired listeners across a range of detection tasks in quiet or background noise. We simulated an amplitude-modulation detection task with tonal and noise carriers (fc=4000 Hz) which were either presented in quiet, or in a broadband or narrowband noise masker. The considered psychoacoustic back-ends included a within-trial RMS detector, a classical template-based optimal detector, and a template-based RMS detector.

In our analysis, we compared simulated and experimental thresholds across N=21 listeners with normal or high-frequency sloping audiograms. Simulated detection cues were analyzed across the different cochlear characteristic frequencies and we discuss how simulated detection thresholds are impacted by (1) different sensorineural hearing loss profiles, and (2) different inherent properties of the background noises (external variability). Although within-trial model back-ends are more directly related to the task, we observed a higher robustness of template-based approaches to external stimulus variability. This supports the view that listeners are able to “internalize” both target and reference sounds over the course of a task and speaks for the inclusion of basic top-down approaches in auditory perception models.

PS 515

The Effect of Broadband Elicitor Duration on Transient-Evoked Otoacoustic Emissions and a Behavioral Measure of Gain Reduction

William B. Salloom[1]; Kristen Wade[1]; Hari Bharadwaj[2]; Elizabeth A. Strickland[1]
[1]Purdue University; [2]Speech, Language, & Hearing Sciences, and Weldon School of Biomedical Engineering, Purdue University

Background
Physiological and psychoacoustic studies of the medial olivocochlear reflex (MOCR) in humans have often relied on long elicitors (> 100 ms). This is largely due to previous research using otoacoustic emissions (OAEs) that found MOCR time constants in the 100’s of milliseconds when elicited by broadband noise. However, Roverud & Strickland (2014), using a psychoacoustic measure of gain reduction, found differential effects of duration for on- and off-frequency tonal elicitors. For the on-frequency elicitor, thresholds increased with increasing on-frequency duration up to about 50 msec, and then plateaued. In contrast, thresholds with off-frequency elicitors continued to increase with elicitor duration. These results are consistent with cochlear gain reduction, possibly by the MOCR, in which the on-frequency elicitor is affected by gain reduction at the signal frequency place, but the off-frequency elicitor is not. The effect of the duration of broadband noise elicitors on similar psychoacoustic tasks is currently unknown. Additionally, the relationship between gain reduction measured psychoacoustically and physiologically with OAEs in the same subjects as a function of elicitor duration are unknown. This study measured the effects of ipsilateral broadband noise elicitor duration on transient-evoked OAEs (TEOAEs) and psychoacoustic gain reduction estimated from a forward-masking paradigm.

Methods
The effects of an ipsilateral pink broadband noise precursor (0.2 - 10 kHz) on TEOAEs and behavioral thresholds were measured as a function of precursor duration in normal-hearing humans. For all experiments, the precursor was fixed at a level below MEMR threshold (50-60 dB SPL). TEOAEs were measured to estimate MOCR strength (magnitude and phase) at precursor durations of 50, 100, 200, and 400 msec. For the same subjects, a psychoacoustic forward-masking paradigm was used to measure the effects of precursor duration (50, 65, 100, 200, 400, and 800 msec) on masking by on- and off-frequency maskers at a 4 kHz signal frequency. Gain reduction is indicated by a relatively larger shift for the off-frequency masked threshold than for the on-frequency one.

Results/conclusions
The effects of the precursor on TEOAEs and behavioral thresholds will be compared as a function of precursor duration. The goal is to determine how duration of a broadband MOCR elicitor affects cochlear gain physiologically and perceptually, and if there is a relationship between these measures.

Acknowledgements
Supported by NIH R01 DC008327 (EAS), and NIH R01 DC015989 (HMB).

PS 516

Effects of Tone Duration on Three Psychophysical Measures: Evidence of Temporal Integration in Rhesus Macaques

Chase Mackey[1]; Alejandro Tarabillo[2]; Ramnarayan Ramachandran[2]
[1]Vanderbilt University; [2]Vanderbilt University Medical Center

The effect of tone duration on detection threshold has long been thought to reflect the process of temporal integration, with particular emphasis placed on the rate of integration inferred from these data. Animal models represent an opportunity to establish neurophysiological correlates of this behavior, and explore its dysfunction after controlled cochlear insults. The macaque model of noise-induced hearing loss is one such example. However, the available data in macaques and other species suggest much slower rates of temporal integration when compared to humans. This could pose problems for animal models of human hearing loss, in which loss of temporal processing ability is a key dysfunction.

We re-evaluated the effects of tone duration on detection in macaques using a reaction-time Go/No-Go tone detection task in quiet and in 76 dB SPL broadband noise (BBN). Monkeys detected tone frequencies between 0.5 kHz and 32 kHz. Tone durations were 3.25-200 ms, with appropriately ramped rise/fall times. Signal detection theoretic methods were used to calculate behavioral accuracy (probability correct) and create psychometric functions at each duration tested in five young macaques. From these psychometric functions, we calculated detection threshold (tone level at probability correct = 0.76), reaction time (RT, time between tone onset and time of lever release), and dynamic range of the psychometric function (DR) to provide estimates of sensitivity, processing speed and performance variability, respectively.

Psychometric functions were shifted to higher levels and with reduced slopes as durations decreased below 50 ms. Thresholds, DR and RTs decreased as tone duration increased. Threshold, RT, and DR were well described by exponential functions of tone duration. The time constant of the exponential fit (rate of threshold change, ~20 ms) suggests similar rates of temporal integration between macaques and humans. The decrease in macaque RT with increases in tone duration is similar to human data, but is contrasted by animal literature that reports a lack of effect of duration on RT. The time constant of the DR was significantly changed by BBN background, which contrasted the other measures, suggesting that DR is uniquely sensitive to masking or other effects on temporal integration. Together, these behavioral measures provide converging evidence of temporal integration, suggesting macaques may serve as a good model of human temporal sensitivity. These results will serve as baseline data for ongoing studies of the perceptual effects of noise-induced cochlear synaptopathy, and for future investigations of neural correlates of perceptual abilities.

Synaptopathy

PS 517

Persistence of the Acoustic Reflex After Selective Inner Hair Cell Loss and its Relation to Auditory Tasks in Carboplatin-treated Chinchillas

Monica Trevino; Celia D. Escabi; Karen Pawlowski; Edward Lobarinas
University of Texas at Dallas

Abstract
The acoustic reflex (AR) is an involuntary contraction of the middle ear stapedius muscle to moderately loud sound. This response results in a measurable decrease in the admittance of the ossicular chain that reduces acoustic input to the inner ear. The AR threshold and amplitude are widely used in diagnostic hearing assessments and

are part of standard hearing test batteries to evaluate retrocochlear pathways, corroborate hearing thresholds, and detect nonorganic hearing loss. Robust reflexes can be obtained in patients with mild to moderate sensorineural hearing losses associated with loss of outer hair cells (OHC), but are substantially diminished or abolished by severe to profound hearing loss. Previously, we found that AR amplitudes were either unchanged or increased as a result of carboplatin-induced selective inner hair cell (IHC) loss in chinchillas. To investigate this phenomenon further, we correlated AR amplitude with performance on various auditory perception tasks in chinchillas before and after carboplatin, a treatment that reliably and selectively destroys IHC.

Methods

This study used young adult chinchillas (2-4 years-of-age), that were housed in enriched environments and allowed to free-feed. Ipsilateral ARs were obtained in awake animals using a Tympstar middle ear clinical analyzer. Stimuli were presented at a fixed level of 95 dB HL (91-100 dB SPL) using a 4 kHz tonal stimulus, low bandpass noise, and high bandpass noise. To control for potential OHC dysfunction, distortion product otoacoustic emissions (DPOAEs) were measured using a commercially available system. Animals were trained over a period of weeks to respond to auditory stimuli using shock avoidance conditioning. Pure tone thresholds were assessed in quiet and in a competing narrowband noise condition. Detection of gaps in octave band noise was also evaluated. Following baseline measures, animals were treated with 75 mg/kg of carboplatin (i.p.), a dose shown to produce 50-80% selective IHC loss. Post-carboplatin assessments were performed three weeks post-treatment.

Results and Conclusions

As expected, carboplatin treatment eliminated 50-80% of IHC, but had no effect on DPOAEs, suggesting OHC survival and function. No significant relationship was established between AR amplitude response and pure tone thresholds in quiet. Although post-carboplatin results showed poorer hearing in noise and gap-detection thresholds, robust ARs were still present. These results suggest that the AR is insensitive to significant inner ear pathology and is unlikely to be an effective assay of synaptopathy or IHC loss.

Supported by NIH R01DC014088

PS 518

SENS-401 Significantly Reduces ABR Wave 1 Amplitude Loss after Chronic Noise Exposure in a Rat Model

Mathieu Petremann; Christophe Tran Van Ba; Viviana Delgado-Betancourt; Charlotte Romanet; Vincent Descossy; Pauline Liaudet; **Jonas Dyhrfjeld-Johnsen**
Sensorion

Since the publication of the landmark paper on noise-induced synaptic loss and delayed spiral ganglion neuron degeneration despite recovery of auditory thresholds (Kujawa & Liberman, 2009), cochlear synaptopathy has been widely investigated as a substrate for “hidden hearing loss” with a role in different hearing pathologies, implicated in auditory perceptive deficits, tinnitus and hyperacusis. We here report a significant reduction of ABR wave 1 amplitude loss, a measure of cochlear synaptopathy, by oral administration of the clinical stage otoprotectant SENS-401 (arazasetron) in a rat model of chronic noise exposure.

Following baseline audiometry (ABR 8/16/24/32 kHz, DPOAE 4/8/16/24/32 kHz), 7 week old male Wistar rats were exposed to 100 dB SPL, 3-12 kHz noise for 2 hours daily for 14 days followed by audiometry on D15. During noise exposure, animals were randomized to receive (n=8 per group) placebo vehicle, 6.6 mg/kg or 13.2 mg/kg SENS-401 treatments p.o. all twice daily starting ahead of noise exposure on the first day.

After ended noise exposure on D15, animals exhibited ABR threshold shifts of 2.19-26.25 dB across frequencies with no statistically significant difference between groups and negligible changes in DPOAE amplitudes. When comparing mean ABR wave 1 amplitude changes at 90 dB SPL stimulus intensity across frequencies from baseline to D15, SENS-401 treated animals exhibited statistically significantly reduced amplitude loss compared to placebo ($p=0.033$ and $p=0.027$; 0.43 µV loss for placebo vs 0.14-0.17 µV loss for SENS-401 treated groups). There was no statistically significant difference between SENS-401 doses, which respectively lead to mean ABR wave 1 loss reductions of 67% and 60%.

These results demonstrate for the first time the potential of SENS-401 to significantly reduce loss of ABR wave 1 amplitude in a model of mild NIHL from chronic noise exposure, which suggests functional preservation of cochlear synapses in addition to the established hearing preservation with enhanced outer hair cell survival in more severe hearing loss models (Petremann et al., 2017 & 2019). The lack of effect on the ABR threshold shifts immediately after end of noise exposure is consistent

with recently published results in a model of severe, acute acoustic trauma, where significant treatment effects on ABR threshold shifts and DPOAE amplitude losses became evident after 28 days of twice daily treatment following hearing loss induction (Petremann et al., 2019). SENS-401 is currently being investigated for the treatment of sudden sensorineural hearing loss (SSNHL) in an international, multi-centric clinical trial (AUDIBLE-S, NCT03603314).

PS 519

Relationship Among Selective Inner Hair Cell Loss, Auditory Brainstem Response Amplitudes and Acoustic Reflexes in Carboplatin Treated Chinchillas

Celia D. Escabi; Monica Trevino; Christina Campbell; Karen Pawlowski; Edward Lobarinas
University of Texas at Dallas

Background
The relationship between anatomical damage and hearing deficits is complex, and pure tone threshold testing does not adequately detect some forms of inner ear pathology, such as the loss of afferent synapses or inner hair cells (IHC). Thus far, evidence from animal studies have shown that reductions in auditory brainstem response (ABR) Wave I amplitudes are correlated with synaptopathic loss. Acoustic reflex (AR) thresholds and amplitudes are also thought to be potential measures for detecting synaptopathy. In contrast, we have found that AR amplitudes are unchanged or increased following carboplatin-induced selective IHC loss in chinchillas. Here we present data aimed at evaluating the relationship among the AR, ABR Wave I amplitude, and IHC loss.

Methods
ABR thresholds, AR amplitudes and distortion product otoacoustic emissions (DPOAEs) were evaluated in adult chinchillas (1-3 years of age) before and after carboplatin treatment. Ipsilateral ARs were obtained in awake animals using a Tympstar middle ear analyzer. ARs were elicited by a 4 kHz tonal stimulus, low bandpass noise, and high bandpass noise presented at 95 dB HL (91-100 dB SPL). Following baseline measures, animals were treated with 75 mg/kg carboplatin (i.p.); a dose reliably shown to produce 50-80% IHC loss with little to no outer hair cell (OHC) loss. Post-carboplatin assessments and histology were performed three weeks following treatment.

Results and Conclusions
Carboplatin treatment produced significant IHC loss, leaving OHCs largely intact and no effect on DPOAEs. ABRs were characterized by relatively low thresholds, reduced Wave I amplitudes and overall poorer wave morphology. However, AR amplitudes remained unchanged or showed increased amplitudes. These results suggest that severe IHC loss, as evidenced by histology and reduced ABR Wave I amplitudes, has no effect on the AR and that this clinical measure may have limited use in detecting synaptopathy or selective IHC loss.

Supported by NIH R01DC014088

PS 520

The Role of Sex in the Pathophysiology and Treatment of Cochlear Synaptopathy

Stephanie Rouse; Ian Matthews; Dylan Chan
UCSF

The role of sex as a biological variable is critical when studying the pathophysiology and treatment of hearing loss. Whereas sex is known to affect noise-induced hearing loss (NIHL) in humans and animals, very little is known about its effect on cochlear synaptopathy, characterized physiologically in mice as a decrease in the amplitude of wave I of the auditory brainstem response (ABR). In humans, women exhibit larger wave I amplitudes, despite similar auditory thresholds, compared to men. In this study, we sought to investigate the role of sex in cochlear synaptopathy and its treatment in mice.

For our model system, we exposed 8-week-old male and female CBA/J mice to 2-hour, 8-16-kHz, 97.8 dB SPL noise with or without pre-treatment with ISRIB (Integrated Stress Response InhiBitor, 10 mg/kg), a modulator of the unfolded protein response (UPR), which we have shown to protect against NIHL. Multiple drugs targeting the UPR promote synaptic plasticity, suggesting that ISRIB may be effective against cochlear synaptopathy. Finally, like NIHL, many neurodegenerative diseases in which the UPR is implicated exhibit significant sex differences in their pathophysiology and treatment.

ABR thresholds and intensity functions (10-90 dB SPL) were recorded in response to 4-45.2 kHz tone pips in mice 1, 7, 14, and 21 days after noise exposure. Amplitudes of suprathreshold ABR Wave I peaks were measured and synapses quantified by immunohistochemistry against CtBP2 and GluA2.

Baseline ABR thresholds were identical between male (n=69) and female (n=62) mice, but wave I amplitude was significantly greater in female mice ($p < 0.0001$, two-way ANOVA). We then analyzed male (n=21) and female (n=16) mice 21 days after noise exposure and

drug treatment. Among vehicle-treated mice, females exhibited larger noise-induced wave-I amplitude shift compared to males (p = 0.0002), but no difference in threshold shift. 3-way ANOVA revealed significant frequency-independent interaction between sex and drug (p = 0.0002): whereas male mice treated with ISRIB had significantly higher wave-I amplitudes compared to vehicle-treated mice (p = 0.019), female mice showed no significant drug effect.

In conclusion, we found significantly higher baseline wave I amplitudes in female mice, consistent with what has been reported in the literature in humans. Additionally, our results suggest that sex has an impact on both the post-noise-exposure wave-I amplitude shift and the efficacy of ISRIB in preventing synaptopathy. As such, sex warrants examination and consideration in the study of the pathophysiology and treatment of cochlear synaptopathy.

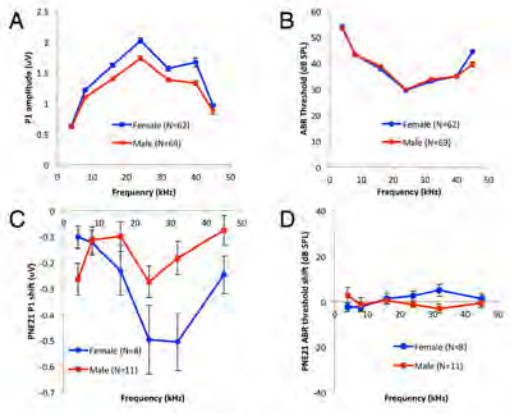

Figure 1. ABR P1 amplitude (A) and thresholds (B) were recorded at baseline and 21 days after exposure to 97.8 dB SPL 8-16 kHz octave-band noise in male (red) and female (blue) mice. Female mice exhibited higher baseline P1 amplitude (A, $p < 0.0001$), greater noise-induced wave-I amplitude shift (C, $p = 0.0002$), and no difference in threshold or threshold shift (B, D).

PS 521

Endolymphatic Hydrops is a Marker of Synaptopathy Following Traumatic Noise Exposure

Ido Badash[1]; Patricia M. Quiñones[2]; Juemei Wang[2]; Christopher G. Lui[2]; Frank D. Macías-Escrivá[1]; Brian E. Applegate[1]; John S. Oghalai[1]
[1]Caruso Department of Otolaryngology - Head and Neck Surgery, University of Southern California; [2]USC Caruso Department of Otolaryngology - Head and Neck Surgery

Background
After traumatic noise exposure, there can be large losses of synapses between inner hair cells (IHCs) and auditory neurons. Currently, there is no reliable diagnostic test for detecting cochlear synaptopathy *in vivo* nor a reliable treatment for this injury. We have previously studied mice with blast-induced cochlear synaptopathy and found they develop an excess build-up of endolymph, termed endolymphatic hydrops. The purpose of this study was to determine whether a similar relationship exists between endolymphatic hydrops and cochlear synaptopathy following high-level noise delivered over several hours. If correlated, we hypothesized that round window application of hypertonic saline would reduce endolymphatic hydrops and prevent cochlear synaptopathy.

Methods
4- to 6-wk old CBA/CaJ mice were exposed to 8-16 kHz noise of varying intensities for 2 hours. We used optical coherence tomography to measure endolymphatic volume in live mice. To test the effects of osmotic stabilization on endolymphatic hydrops, we opened the middle ear bulla and applied test solutions onto the round window membrane. In mice used for immunolabeling experiments, a test solution was applied to the round window through an intratympanic injection immediately after noise exposure. One week later, we counted IHCs and synaptic ribbons.

Results
Seven hours after noise exposure, mice exposed to 100 dB SPL noise had significantly greater endolymph volume than those exposed to 80 ($p < 0.001$), 90 ($p < 0.001$), 95 dB SPL ($p < 0.001$), or controls ($p < 0.001$). With this increase in endolymph volume, synapses per IHC were significantly decreased in the base of the cochlea in mice exposed to 100 dB SPL noise compared to controls and those exposed to lower noise intensity levels. Round window application of hypertonic saline reduced endolymphatic hydrops 7 hours after 100 dB SPL noise exposure by 44.8% compared with ears treated with normotonic saline ($p=0.002$). Hypertonic saline also prevented 42.7% of the IHC synaptic ribbon loss in the cochlear base compared with normotonic saline ($p < 0.001$).

Conclusion
Similar noise intensity thresholds exist for the development of endolymphatic hydrops and IHC synaptic ribbon loss, suggesting that endolymphatic hydrops may be a surrogate marker for cochlear synaptopathy following acoustic trauma. Round window application of hypertonic saline can reduce the degree of noise-induced endolymphatic hydrops and partially rescue synaptic ribbon loss in the cochlear base. These findings may have translational potential in humans for detecting and treating synaptopathy and associated hearing impairments.

Supported by NIDCD grants DC014450 (J.S.O) and DC013774 (J.S.O & B.E.A.).

PS 522

Effect of IGF1 Receptor Antagonist on Presynaptic Ribbons in Inner Hair Cells in Mouse Cochlear Explants

Li Gao[1]; Tomoko Kita[2]; Tatsuya Katsuno[3]; Koichi Omori[4]; Takayuki Nakagawa[4]
[1]Department of Otolaryngology, Head and Neck Surgery, Graduate School of Medicine, Kyoto University; [2]Kyoto University; [3]Department of Otolaryngology - Head and Neck Surgery, Kyoto University Graduate School of Medicine, Kyoto City, Kyoto, Japan; [4]Dept. Otolaryngology - Head and Neck Surgery, Graduate School of Medicine, Kyoto University

Insulin-like growth factor 1 (IGF1) is essential for control cell proliferation, differentiation, and apoptosis in various tissues and organs. IGF1 plays critical roles in the development and maintenance of cochleae. Previous study has demonstrated that IGF1 protects cochlear hair cells from various insults and induces the regeneration of inner hair cell (IHC) - spiral ganglion neuron (SGN) synapses in cochlear explant cultures of postnatal day 2 mice. In this study, we examined the roles of IGF1 for the maintenance of presynaptic ribbons in IHCs in cochlear explants of postnatal day 4 mice. We cultured cochlear explants with an IGF1 receptor (IGF1R) antagonist JB1that is an IGFI peptide analog. As CtBP2 is the main component of ribbon synapses, CtBP2 puncta number was counted as pre-synapse number to define the effect of JB1 on presynaptic ribbon. We tested the concentration and exposure period of JB1 to cause the loss of CtBP2 puncta but not IHC loss. We found that in each turn, JB1 exposure caused CtBP2 puncta number decreased, along with the extending of exposure time and increasing of JB1 concentration. Our data showed that 25 μg/ml JB1 exposure for 24 h is suitable, which caused a significant loss of CtBP2 puncta without inducing IHC loss. Then we performed an additional 24-h culture without the presence of JB1 to verify the capacity of spontaneous recovery, which might be induced by endogenous IGF1 paracrine in explants. As a result, in the apical and middle turns, an increase of CtBP2 puncta was observed in comparison with those before an additional culture. Our data indicated that IGF1 could be involved in the maintenance of presynaptic ribbons in IHCs.

PS 523

Circadian impact of Cisplatin-induced Ototoxicity on Synaptic Ribbons.

Evangelia Tserga[1]; Heela Sarlus[1]; Rocio Moreno-Paublete[1]; Erik Björn[2]; Barbara Canlon[1]; Christopher Cederroth[3]
[1]Karolinska Institutet; [2]Umeå University; [3]Laboratory of Experimental Audiology, Department of Physiology and Pharmacology, Karolinska Institutet

Around 75% of cancer patients treated with chemotherapeutic agent cisplatin, present hearing deficits. It is generally known that cisplatin ototoxicity has 3 major targets, hair cells, spiral ganglion neurons and the stria vascularis. Our laboratory found that mice deficient for the glutamate aspartate transporter GLAST exhibited 20-25 dB greater loss of ABR thresholds in comparison to WT mice when treated with salicylate, despite equally affected OHC function. These findings indicate that ototoxic agents may target the IHC/afferent synapse when defective in its glutamate buffering capacity. Moreover, our laboratory reported that the cochlea has a circadian clock, which increases the vulnerability to noise at night-time. Here, we hypothesized that the IHC/afferent synapse of GLAST KO mice might be more vulnerable to cisplatin at specific times of the day. At baseline, GLAST KO mice displayed dramatically reduced ABR Wave 1 amplitudes when compared to WT littermates, however with normal ribbon counts. When treated with cisplatin for 4 consecutive days, KO mice displayed higher hearing threshold shifts (20-25 dB) at 24 kHz compared to WT after night but not after day treatment. Consistent with a greater damage occuring after night cisplatin administration, a greater loss of synaptic ribbons and post-synaptic pairing was found in GLAST KO mice when compared to WT. Such differences did not occur in day treated animals. A pharmacokinetic analysis of cisplatin bioavailability in the cochlea after day or night administration was performed by Inductively Coupled Plasma Mass Spectrometry (ICP-MS) and showed that the greater damage after night administration was not related to greater bioavailability of platinum compounds in the cochlea. To evaluate whether cisplatin impacted on cochlear clock rhythms, we exposed cochlear explants froom PER2::LUC reporter mice to 20 uM cisplatin after forskolin synchronization and found no alterations in amplitude, period and phase of PER2 rhythms. Overall, these findings suggest that the impact of cisplatin on the cochlea is not mediated by changes on the cochlear clock, rather it's the clock status of the cochlea at night-time that increases its vulnerability to ototoxic challenges. XPC is a DNA repair protein that is recruited after DNA damage and which has been involved in human cisplatin-mediated ototoxicity. Recent RNAseq

data identify XPC as a circadian transcript in the mouse cochlea and whose expression is greater at night-time. It is thus possible that DNA repair mechanisms are compromised during the active phase of the animal, rendering it more vulnerable to cisplatin ototoxicity.

PS 524

Characterization of OTO-413, an intratympanic sustained-exposure formulation of the neurotrophic factor BDNF, in preclinical models of cochlear synaptopathy

Natalia Tsivkovskaia; Xiaobo Wang; Claudia Fernandez; Jeremy Barden; Rayne Fernandez; Phillip Uribe; Bonnie E. Jacques; **Fabrice Piu**
Otonomy Inc

Background
Recent evidence from both preclinical and clinical studies indicates that a loss or dysfunction of the synapses that connect inner hair cells in the cochlea with spiral ganglion neurons (SGNs), whose axons form the cochlear nerve, contributes to hearing impairment. This synaptopathy is proposed as an underlying pathology in age-related and noise-induced hearing dysfunctions and has been hypothesized to explain speech-in-noise hearing difficulties that occur despite normal audiometric thresholds. The application of exogenous neurotrophins, such as Brain-Derived Neurotrophic Factor (BDNF), has been investigated as a therapeutic approach based on their ability to provide trophic support to spiral ganglion neurons in the cochlea. Previously, we reported on the efficacy of OTO-413, a thermo-reversible sustained-exposure formulation of BDNF developed for intratympanic round window delivery, in a rat model of noise-induced cochlear synaptopathy. Here we further characterize the otoprotective effects of OTO-413 in models of noise-induced cochlear synaptopathy after delayed administration.

Methods
Adult rats (Sprague-Dawley) served as subjects in the noise-induced cochlear synaptopathy model. Specifically, animals were acutely exposed to noise (105 dB, 8-16 kHz, 1h) then received a single intratympanic injection of OTO-413 at different times following the acoustic trauma, ranging from 1 to 14 days, and were followed up to 28 days. In all experimental settings, hearing function was monitored (ABR, Wave 1 amplitude) throughout the course of the studies. At termination, evidence of cochlear synaptopathy was determined histologically by quantifying the number of synaptic puncta associated with the inner hair cells.

Results
A sustained-exposure formulation of BDNF, OTO-413, was effective in alleviating noise-induced cochlear synaptopathy when administered intratympanically in a delayed manner, both at the functional and histological levels.

Conclusions
Along with previously reported findings, these studies support the potential of OTO-413 as an attractive and novel therapeutic approach for the treatment of cochlear synaptopathy-associated hearing difficulties. OTO-413 will be evaluated in a Phase 1/2 clinical trial in patients with hearing impairments.

PS 525

Post-Exposure Recovery of Synaptic Counts and Ribbon Gradients in Noise-Exposed Guinea Pigs

Tyler T. Hickman[1]; Ken Hashimoto[2]; M. Charles Liberman[3]
[1]1. Eaton-Peabody Laboratories, Mass Eye & Ear; 2. Department of Otolaryngology Head & Neck Surgery, Harvard Medical School; [2]1. Eaton-Peabody Laboratories, Mass Eye & Ear; 2. Department of Otolaryngology Head & Neck Surgery, Harvard Medical School; 3. Department of Otorhinolaryngology-Head and Neck Surgery, Tohoku University Graduate School of Medicine; [3]Harvard

Noise exposure in mice can destroy 50% of the synapses between inner hair cells (IHCs) and auditory nerve fibers (ANFs), even when threshold shift is temporary and hair cell loss is minimal. With increasing post-exposure time, spiral ganglion cells slowly degenerate, also reaching ~50% loss after ~2 yrs (Kujawa and Liberman, J. Neuroscience 2009 29: 14077). Although permanent noise-induced synaptopathy has been reported in rats, chinchillas and monkeys, guinea pig studies suggested significant post-exposure regeneration (Shi et al., Acta Otolaryngologica 2015;135(11):1093). Given that immunostaining intensity of synaptic puncta is reduced immediately post-exposure in mice, we wondered whether the observations in guinea pig represented regeneration or recovery of protein expression.

Here, we studied guinea pig cochleas at 1 day, 1 wk and 1, 2 or 6 months (≥ 6 ears per time point) after exposure to noise (4-8 kHz at 106 dB for 2 hrs), designed to produce minimal permanent threshold shift and maximal synaptopathy. Cochlear function was assessed before sacrifice via CAPs and DPOAEs, then cochleas were immunostained for ribbons (CtBP2), glutamate receptors (GluA2), hair cells (myosin VIIA) and nerve terminals (neurofilament). Confocal z-stacks were acquired from

~25 adjacent IHCs at each of 11 cochlear locations in each ear.

We observed minimal hair cell loss in all ears. IHC synaptic counts showed massive initial reduction and dramatic post-exposure recovery. For females, at 1 day post exposure, counts were < 20% of normal throughout much of the basal turn, but recovered to 40% at 1 wk and 80% at 1 month. By 6 months, mean counts were 90% in some affected regions, and essentially 100% in some individuals. Males were only studied at 1 month post exposure, at which point synaptic counts were similar to females. Analysis of ribbon size showed the expected gradient (modiolar > pillar) in controls. Immediately after exposure, the gradient was abolished and many remaining ribbons were enlarged and closer to the cuticular plates than normal. As pre- and post-synaptic puncta reappeared, a more normal size gradient was reestablished, but ANF terminals and synapses remained higher on the IHC than normal.

Thus, the fall and rise in synaptic counts reflects more than just reduction and recovery of synaptic protein expression. The spontaneous post-noise recovery of cochlear synaptic architecture in guinea pig is clearly greater than in mouse. The molecular basis for this dramatic difference is important to uncover.

Research supported by a grant from the NIDCD (R01 DC 00188) and a generous donation from Tom and Helene Lauer.

PS 526

Multiple Outcome Parameters of Auditory Evoked Potential for measuring Noise-induced Cochlear Synaptopathy and its Postnoise Time Course

Ning Hu; Zhenshen Zhang; Steven H. Green
University of Iowa

Noise exposure, even without inducing hair cell (HC) loss, can cause significant cochlear synapse loss, so-called noise-induced cochlear synaptopathy (NICS). In animal models, NICS can be noninvasively detected by auditory brainstem response (ABR), as reduced ABR Wave I (W1) amplitude, and, histologically, by examination of synapses. NICS does not necessarily include elevation of DPOAE or ABR threshold. However, W1 in human is small and variable; other outcome parameters, such as SP, SP/W1 (i.e. SP/AP) ratio, latency, have been proposed to measure cochlear synaptopathy. In animal models, NICS can be clearly identified by postnoise day 14 (PND14). Here we evaluate multiple outcome parameters of auditory evoked potentials used for identifying NICS and demonstrate the postnoise time course of NICS up to PND14.

12 to14 week-old CBA/CaJ male mice were exposed to 100 dB SPL 8-16 kHz octave band noise for 2 hours to generate NICS. ABRs were measured at 8, 16 and 32 kHz prior to noise exposure, postnoise day one, three, seven (PND1,3,7) and PND14 to obtain measures of baseline, temporary threshold shift (TTS), threshold recovery and other outcome parameters in a within-subject design. The parameters include W1 and SP amplitude and latency, SP/W1 ratio, and SP-W1 interval. Mice were euthanized after final ABR measure to confirm synaptopathy without HC loss. Ribbons, postsynaptic densities and HCs were immunohistologically examined for quantitation of synapses/IHC in organ of Corti wholemounts at 8, 16 and 32 kHz locations.

ABR thresholds recovered to the prenoise baseline and W1 amplitudes were significantly reduced in all assessed ears by PND14. W1 latencies were similar to prenoise values at high stimulus levels but became slightly longer at low stimulus levels. SP amplitudes were slightly reduced without a consistent trend of changes in latency. SP/W1 amplitude ratios significantly increased, but changes in SP-W1 intervals were not consistent. ABR thresholds and W1 amplitudes both reached the maximal recovery level by PND3 and there was insignificant further change from PND3 to PND14. Changes prior to PND3 could not be determined because of postnoise TTS. Measure of SP/W1 amplitude ratios demonstrated a similar trend to W1 amplitudes but more variable.

We confirmed the previous reports that SP/W1 amplitude ratios strongly correlate with synapse loss or synaptopathy and can be alternatively used in clinic application. The postnoise time course suggests that acute NICS can be identified electrophysiologically as early as PND3.

(Support from NIH DC02961, DoD W81XWH-14-1-0494, and an AHRF grant.)

PS 527

Lack of Macrophages Impair Spontaneous Repair of Ribbon Synapses After Synaptopathic Acoustic Trauma in C57BL/6 Mice

Anna C. Clayman[1]; Kevin Ohlemiller[1]; Mark Warchol[1]; **Tejbeer Kaur**[2]
[1]Washington University School of Medicine; [2]Creighton University School of Medicine

Background
Inner hair cell (IHC)-ribbon synapses are vulnerable to degeneration following acoustic trauma. Such synaptopathy can occur without any hair cell loss and trigger slow, progressive degeneration of spiral ganglion

neurons (Kujawa and Liberman 2009), possibly leading to difficulty in speech recognition and listening in noisy environments. Cochlear macrophages migrate towards and directly contact the IHC-synaptic region immediately after synaptopathic acoustic trauma (Kaur et al., 2019). However, the functional consequences of these contacts remain unknown. The aim of this study was to determine the contribution of macrophages towards degeneration and repair of ribbon synapses after synaptopathic acoustic trauma.

Methods

Adult (5 weeks of age, both sexes) CX_3CR1-GFP mice on C57BL/6 background were employed. Macrophages were depleted by subjecting mice to a constant diet of colony stimulating factor 1 receptor (CSF1R) inhibitor PLX5622 (Plexxikon). After 10 days on chow, mice were exposed for 2 hours to an octave band (8-16 kHz) noise at 93 dB SPL. ABR thresholds and wave I amplitudes were characterized prior to PLX5622 treatment, 10 days after PLX5622 treatment (pre-noise exposure), immediately after noise exposure, and at two weeks recovery. Isolated temporal bones were fixed and processed for immunohistochemistry to label hair cells, macrophages, and synapses. Control or PLX5622 chow fed mice exposed to ambient noise levels served as controls.

Results

PLX5622 treatment led to robust reduction (~95%) in macrophage numbers in unexposed mice and was also efficient to keep macrophages depleted after acoustic trauma compared to mice fed on control chow. Lack of macrophages did not influence hearing thresholds and hair cell density after exposure. Synaptic immunolabeling revealed that PLX5622 treatment alone did not affect IHC-synapse density. Acoustic trauma resulted in a rapid ~50% degeneration of synaptic ribbons across the mid-basal frequency regions of the cochlea that was comparable between control and PLX5622 treated mice. At two weeks after exposure, the damaged synapses spontaneously repaired (nearly complete) in mice fed on control chow. However, PLX5622 treated mice displayed enhanced synaptic degeneration (~30-50%) that correlated with attenuated (64%) suprathreshold neural responses at higher frequencies.

Conclusions

The data demonstrate that PLX5622-mediated macrophage elimination does not affect noise-induced degeneration of IHC-ribbon synapses but impairs the spontaneous repair of damaged synapses. This implies that macrophages may promote synaptic repair after acoustic trauma. We have identified a novel biological pathway for synaptic repair that could be developed into therapies for hidden-hearing loss.

PS 528

Photobiomodulation protects noise induced cochlear synaptopathy by affecting synaptogenesis

Jae-Hun Lee[1]; Jun-Sang Bae[1]; Nathaniel Carpena[2]; Hee-Won Jeong[3]; So-Young Chang[1]; Ji Eun Choi[4]; Min Young Lee[5]; Phil-Sang Chung[6]; Jae Yun Jung[6]
[1]Beckman Laser Institute Korea, Dankook University; [2]Beckman Laser Institute Korea, College of Medicine, Dankook University, Cheonan, South Korea; [3]Dankook University; [4]Dankook University Hospital; [5]Beckman Laser Institute Korea, Dankook University Hospital, Dankook University; [6]Beckman Laser Institute Korea, Dankook University, Dankook University Hospital

Background

Photobiomodulation (PBM) is considered a therapeutic approach using light emitting diodes (LED) or LASER. The neuroprotective effect of PBM has been studied in various areas such as diverse kinds of peripheral nerve injuries, especially with the use of red or near infrared light (NIR) wavelengths. In our previous studies, we proved the neuroprotective effect of PBM in the pre and post synaptic receptor, auditory nerve fiber, and spiral ganglion neuron after neurotoxic damage.

Objectives

In this study, we investigated whether PBM could modulate synaptogenesis after excitotoxic damage in the cochlea.

Materials and Methods

SD rats were exposed to narrow band noise (16 kHz center, 1 kHz bandwidth) for two hours and PBM was irradiated at 24 and 48 hours after noise exposure. Protein and mRNA expressions related with neural regeneration were measured at various time points after PBM treatment.

Results

The results showed that BDNF protein expression was significantly increased at 24 hours after noise exposure with PBM treatment as compared to the noise only group but decreased at 48 hours after noise exposure. In case of Synpasin 1, both groups showed an increase at 24 hours and PBM treatment group showed additional increment while it decreased in noise only group at 48 hours after noise exposure. The protein level of NT3 was only increased in the PBM treatment group 24 hour after noise exposure. The mRNA levels of *BDNF* and *Synapsin 1* were significantly increased right after noise exposure and gradually decreased until 4 hours after noise exposure in PBM treatment group. However, there was no changes in mRNA level of *NT3*.

Conclusions
These results shows that PBM after noise exposure can preserves the number of hair cell synapse by increasing neuro-regeneration related proteins and mRNAs.

Acknowledgement
This research was supported by The National Research Foundation of Korea (NRF) grant funded by the Korea government (MSIT)(2017R1D1A1B03033219).

PS 529

Temporary versus permanent synaptic loss from repeated noise exposure in Guinea pigs and C57 mice

Jian Wang[1]; Zhen Zhang[2]; Liqiang Fan[3]
[1]Dalhousie University; [2]Otolaryngology Research Institute, Shanghai Jiao Tong University Affiliated Sixth People's Hospital, Shanghai China; [3]1. Otolaryngology Research Institute, Shanghai Jiao Tong University Affiliated Sixth People's Hospital, Shanghai China

A single brief noise exposure can cause a significant loss of cochlear afferent synapses without causing permanent threshold shift (PTS). Previously we reported that the initial noise-induced loss is partially reversible in Guinea pigs. This indicates that synaptic loss can be categorized as either temporary or permanent. Since synapse loss is biased to those innervating auditory nerve fibers (ANFs) with low spontaneous spike rates (SSR), and this group of ANFs is critical for coding in background noise, coding-in-noise deficits (CIND) have been predicted to be a consequence of noise-induced synaptic damage. However, our recent study investigating noise masking of amplitude-modulation (AM) evoked compound action potentials (CAP), did not find evidence for such deficits in either mice or Guinea pigs. In the present study, we sought to determine the effects of repeated noise exposure on temporary versus permanent synapse loss in Guinea pigs and C57 mice, and whether such effects were additive. We also sought evidence of CIND following repeated noise exposure in Guinea pigs. In the Guinea pigs, the 2nd noise exposure caused much less temporary synaptic loss and no permanent loss. In the C57 mice, however, the 2nd noise exposure resulted in a large amount of permanent loss in addition to a small recovery from the temporary loss, although the permanent loss was not significantly additive. In Guinea pigs, evidence for CIND after repeated noise exposure was found in increased masking of the AM CAP.

PS 530

Measures of Synaptopathy Linked with Tinnitus and Hyperacusis

Naomi F. Bramhall; Sarah M. Theodoroff; Sean D. Kampel
VA RR&D NCRAR

Cochlear synaptopathy, the loss of the synaptic connections between the inner hair cells and their auditory nerve fiber targets, has been demonstrated in a number of animal models in response to noise trauma, ototoxic drugs, and aging, and can precede changes to auditory thresholds. However, because synaptopathy cannot be confirmed in humans without post-mortem temporal bone analysis, the perceptual consequences remain unclear. Nonetheless, non-invasive physiological measures, such as the amplitude of wave I of the auditory brainstem response (ABR) and wideband acoustic reflexes, have been shown to be sensitive to synaptic loss in animal models and can also be obtained in human subjects. We have previously demonstrated decreased ABR wave I amplitude in young Veterans with high levels of noise exposure, non-Veterans with a history of firearm use, and Veterans reporting tinnitus, despite normal audiograms and otoacoustic emissions. These findings suggest that noise-induced synaptopathy occurs in humans and may lead to tinnitus. Both tinnitus and hyperacusis can occur in the absence of conventional hearing loss and are associated with noise exposure. Therefore, it is important to further explore whether tinnitus and hyperacusis are perceptual consequences of noise-induced synaptopathy.

In this study, a number of behavioral and physiological measures of auditory function, including extended high frequency audiometric thresholds, loudness growth functions, contralateral wideband acoustic reflexes, and auditory evoked potentials (ABR, middle latency response (MLR), late latency response (LLR)), were obtained in a sample of over 85 young (19-35 years) Veterans and non-Veterans with clinically normal audiograms (.25-8 kHz) and robust distortion product otoacoustic emissions. This sample was divided into four groups based on Veteran status and self-reported perception of tinnitus and/or hyperacusis: (1) Non-Veteran control, (2) Veteran no tinnitus/hyperacusis, (3) Veteran tinnitus-only, and (4) Veteran tinnitus+hyperacusis.

Compared to controls, the Veteran tinnitus-only and Veteran tinnitus+hyperacusis groups showed indirect evidence of synaptopathy-related auditory dysfunction. However, these two groups differed considerably on many of the test measures, with patterns suggestive of pre-neural hyperactivity in the Veteran tinnitus+hyperacusis

group. Our findings strongly suggest that synaptopathy can be measured indirectly in humans using auditory physiological metrics and further indicate that noise-induced synaptopathy may lead to perceptual consequences including tinnitus and hyperacusis. In addition, the observed physiological differences between the Veteran tinnitus-only and Veteran tinnitus+hyperacusis groups highlight the importance of screening for tinnitus and hyperacusis when performing and interpreting physiological measures of synaptopathy.

PS 531

Modulating the Cochlear Proteostasis Network to Prevent Hidden Hearing Loss

Jeffrey N. Savas; Nopporn Jongkamonwiwat; Miguel A. Ramirez
Northwestern University Feinberg School of Medicine

The long-term goal of this project is to develop a new therapeutic strategy to prevent noise induced hearing loss (NIHL). We will focus on a recently described and mysterious form of NIHL called “hidden hearing loss (HHL).” HHL occurs when excess noise damages peripheral synapses without reducing the hair cell population or causing hearing threshold shifts. Auditory nerve fiber swelling and subsequent ribbon synapse deterioration represent key steps in HHL. We already know that excess noise represents a blunt and potent auditory stimulant that affects many cochlear cells and structures. To investigate how the cochlear proteome is remodeled after noise causing temporary and permanent hearing loss and we performed multiplexed quantitative mass spectrometry-based proteomics.

Our analyses confirmed that noise represents a broad dose-depended stressor that drives changes in the level of many cochlear proteins in several common pathways. We analyzed the cochlear proteome acutely after noise exposure and during the recovery period two-weeks after exposure. Interesting we found that auditory overstimulation causes a rapid increase in the level of many proteins. Unexpectedly, we found that the majority of proteins with increased levels immediately after noise exposure showed normal or reduced levels after two weeks of recovery. We used bioinformatics to mine our datasets and found noise exposure triggered acute protein synthesis of proteins involved with metabolism and proteostasis. With these datasets in hand, the objective of the current research is to confirm these findings and test the possibility that therapeutic modulation of these protein targets protect mice from HHL.

The proposed research is based on our discovery-based findings that are supported by the published literature the central nervous system but have not yet been deeply investigated in the auditory system. We are testing the hypothesis that therapeutic modulation of cochlear protein networks with altered levels after noise exposure using commercially available molecules may provide a new opportunity to prevent cochlear synaptopathy. To test this hypothesis, we will determine if these drugs prevent NIHL or accelerate recovery. Our goal is to focus on those therapeutic targets that can be engaged with noninvasive strategies in the short term. Thus, we are testing if repurposed FDA approved drugs or commercially available supplements can potentially provide therapeutic relief on a short time frame. Taken all together, our research aims to rapidly translate basic science discovery-based proteomic results in rodent models to non-invasive intervention strategies to prevent or treat noise induced hearing loss.

Auditory Brainstem and Midbrain Implants: Advances in Basic and Translational Research

Chairs: Mahan Azadpour & Andreas Bahmer

SYMP 36

Investigating Perceptual Limitations in ABI and AMI Devices

Colette McKay[1]; Karl-Heinz Dyballa[2]; Waldo Nogueira[2]; Hubert H. Lim[3]; Thomas Lenarz[4]
[1]Bionics Institute, Melbourne, Australia; [2]Hannover Medical School, Hannover, Germany; Cluster of Excellence, Hearing4all, Germany; [3]University of Minnesota, Minneapolis, USA; [4]Hannover Medical School, Hannover, Germany

Auditory brainstem and midbrain implants (ABIs and AMIs) aim to provide access to sound in patients for whom cochlear implants (CI) are not feasible. ABIs stimulate the auditory pathway via a paddle electrode array placed on the surface of the cochlear nucleus (CN), whereas AMIs use one or two penetrating shanks of electrodes to stimulate the inferior colliculus (IC). Studies with ABI users have highlighted the poor access to tonotopic frequency information and the poor temporal resolution experienced by the majority of ABI users, which underlie their poor ability to understand speech. The AMI was developed with the aim of overcoming the factors that limit speech understanding with ABIs, based on the assumptions that the IC offers improved access to tonotopic frequency regions compared to the CN, and that damage to the CN by tumors and/or the surgery to remove them underlie the poor temporal resolution experienced with the ABI. In this presentation, we will first summarize the published work that aimed to understand the deficits experienced by ABI and AMI users, and

explain how the work led to the development of the first AMI, and then to a second (current) AMI design that uses two electrode shanks (instead of one) to enable activation of the IC across iso-frequency laminae. The latter innovation was based on studies that suggested that temporal resolution could be improved by utilizing multiple pulses within the same laminae. We will then report on the preliminary results of ongoing perceptual studies with participants using the second AMI design, in which we are assessing the effects of stimulation across two sites versus one site across the IC with varying temporal patterns. These findings will be incorporated into new stimulation strategies for improving temporal coding performance with central auditory implants.

The current work with AMI patients is funded by NIH grant U01 DC013030 as well as support from Cochlear Limited and the Deutsche Forschungsgemeinschaft (DFG, German Research Foundation) under Germany's Excellence Strategy EXC 2177/1—Project ID 390895286. The Bionics Institute acknowledges the support it receives from the Victorian Government through its Operational Infrastructure Support Program.

SYMP 37

How the Auditory Brainstem Implant Advances Auditory Neuroscience

Robert V. Shannon
Caruso Department of Otolaryngology-HNS, University of Southern California, Los Angeles, CA

When Auditory Brainstem Implants (ABI) and Auditory Midbrain Implants (AMI) were first introduced many researchers (including myself) were highly skeptical that such devices could provide useful sound sensations. People were initially skeptical of Cochlear Implants (CI) as well, but CIs have become the most successful neural prosthesis, restoring speech recognition to most patients. Even some ABI patients can converse by telephone. Understanding how these prostheses work so well can tell us much about the sensory and physiological factors important for complex pattern recognition. The CI at least stimulates neurons in a tonotopic pattern, with electrodes that carry low-frequency information stimulating neurons from the apical cochlear region. But the ABI and AMI activate complex patterns of higher-order neurons in the cochlear nucleus and inferior colliculus in uncertain tonotopic order. These brainstem and midbrain regions contain some neurons that have highly specialized functions. Indeed, the ABI and AMI outcomes are poor compared to the CI outcomes, in most patients. However, recently as many as 30% of ABI patients in some clinics have demonstrated CI-like speech recognition, and some AMI patients have demonstrated some word recognition. In this talk I will compare psychophysical and speech recognition performance across normally hearing, CI, ABI, and AMI listeners. The pattern of results suggests that many psychophysical tasks are similar across locations of stimulation, once equalized for loudness. The fact that stimulation of the cochlear nucleus (ABI) can produce good speech recognition shows that the fine spectral and temporal detail of the cochlea are not required for speech. Speech can be understood with only diffuse patterns of activation modulated at low rates. One factor that stands out in these comparisons is that fine spectral resolution is the key factor in complex pitch and music, as well as in the emotional and qualitative components of speech. The brain's ability to recognize speech, even in such highly degraded conditions, shows the gradations of processing that are required for different auditory tasks. Good speech recognition is possible with surprisingly little spectro-temporal resolution. More fine-grained information is required when the auditory patterns are more complex, and in more difficult listening conditions. Further studies of the differences in perception between prosthetic devices can give us insight into the relation between details of neural processing and auditory capabilities.

SYMP 38

New Directions in Central Auditory Prostheses: Development of an Auditory Midbrain Implant and an Auditory Nerve Implant

Hubert H. Lim[1]; Thomas Lenarz[2]
[1]University of Minnesota, Minneapolis, USA; [2]Hannover Medical School, Hannover, Germany

Two new central auditory implant technologies are currently being developed and evaluated in pre-clinical and clinical research supported by the National Institutes of Health. One device is the auditory midbrain implant (AMI) developed with Cochlear Limited and consists of two linear electrode arrays (11 sites each) for placement into the three-dimensional inferior colliculus in deaf patients who do not have a functional auditory nerve (i.e., those with neurofibromatosis type 2 patients whose nerves have been damaged from removal of acoustic neuromas). After a series of pre-clinical safety and functional studies in animals and cadaver specimens as well as technology development and validation, a clinical trial was initiated in 2016 in Germany after ethics/regulatory approvals. By 2019, five patients have been implanted and an overview of their progress, surgical outcomes, and performance will be presented. The other central auditory prosthesis technology is an auditory nerve implant (ANI) consisting of a high-density electrode array (e.g., 6x9 penetrating shanks) developed by Blackrock Microsystems that can be inserted into the auditory nerve using either a retrosigmoid or translabyrinthine

approach that are being investigated in human cadaver experiments. This array technology has already been used in humans for motor/somatosensory implants in the cortex and peripheral nerves, and is being modified for use in the auditory nerve. This array will be connected with the MED-EL Synchrony implant and these components will be extensively tested for reliability, biocompatibility, functionality and safety through benchtop testing and chronic animal experiments (in cats and non-human primates) before transitioning into human patients. The 5-year NIH BRAIN Initiative project involves pre-clinical research (2019-2022) followed by a pilot clinical trial to implant and evaluate up to three deaf patients (2023-2024). Initially, the ANI will be implanted in deaf patients who cannot be successfully implanted or sufficiently benefit from a CI due to anatomical distortions/obstruction of the cochlea or facial side effects. The long-term vision is for the ANI to achieve more focused activation and greater transmission of auditory information to the brain compared to the cochlear implant since it more directly interfaces with the cochlear nerve pathway. The success of both the AMI and ANI will not only open up new directions for auditory prosthetics and alternative hearing options for those who cannot sufficiently benefit from cochlear implants, but will also provide improved neural technologies for other clinical applications relevant to the BRAIN community.

SYMP 39

Revisiting the Design of the Auditory Brainstem Implants Using Microtechnology

Nicolas Vachicouras[1]; Osama Tarabichi[2]; Vivek V. Kanumuri[2]; M. Christian Brown[2]; Daniel J. Lee[2]; **Stéphanie Lacour**[1]
[1]Institute of Bioengineering, Centre for Neuroprosthetics, École Polytechnique Fédérale de Lausanne (EPFL), Lausanne, Switzerland; [2]Massachusetts Eye and Ear Infirmary, Department of Otology and Laryngology, Harvard Medical School, Boston, Massachusetts, USA

The auditory brainstem implant (ABI) was first developed in the 1970s as an implantable neuroprosthetic system that provides sound awareness to deaf individuals who are not candidates for the cochlear implant. The ABI system is a modified cochlear implant that delivers stream of electrical pulses to the surface of the cochlear nucleus (CN) in the brainstem rather than the cochlea. The complex anatomy and physiology of the CN together with the poor spatial selectivity of electrical stimulation and inherent stiffness of contemporary implants lead to only modest auditory outcomes in ABI users. We hypothesize that improving the biomechanical interface of the array to the curved CN surface may improve the position and stability of the device and result in higher selectivity of electrical stimulation. In this talk, we will review our design approach to a soft and microfabricated ABI. Over the past 6 years, our team has designed and developed a soft conformable multichannel ABI array and tested it in rodent models and in cadavers. We have scaled the implant to conform to the CN, from mouse (~ 500 x 500 μm2) to human (~2 x 2 mm2) dimensions. We have further optimized the surgical approach to stabilize the soft ABI array on the CN. Animal studies demonstrate these soft electrodes can reliably activate auditory pathways. Furthermore, the soft ABIs display improved electrochemical performance compared to current clinical devices.

This soft neurotechnology is an exciting opportunity for advancing the treatment of deafness in a specialized group of patients who are not candidates for the cochlear implant.

SYMP 40

New Insights Into Array Position and Perception in Adult Auditory Brainstem Implant Patients

Dana Egra-Dagan; Isabeau van Beurden; Barbara S. Herrmann; Mary E. Cunnane; Samuel R. Barber; M. Christian Brown; Daniel J. Lee
Massachusetts Eye and Ear Infirmary, Department of Otology and Laryngology, Harvard Medical School, Boston, Massachusetts, USA

Background: The auditory brainstem implant (ABI) provides sound detection and speech pattern perception that aids lip reading in the majority of patients. A few ABI users, however, are able to achieve open-set speech perception through audition alone. The underlying factors contributing to ABI outcome variability are not well understood. The goal of this study is to compare three-dimensional (3D) ABI electrode array position with perceptual data. We hypothesize that differences in ABI array position may explain some of the variance in perceptual outcomes. Methods: Retrospective review of adult ABI subjects with Neurofibromatosis type 2 (NF2) and non-NF2 etiologies with postoperative head computed tomography (CT) and perceptual data. Using the imaging methods of Barber, S. et al. (2017, Ear and Hear. 38(6):e343-e351), three-dimensional (3D) electrode array position was classified based on angles from the horizontal using posterior and lateral views and on distances between the proximal array tip superiorly from the basion (D1) and laterally from the midline (D2). Perceptual data included the number of electrodes that provided auditory sensation, threshold level (T) for each electrode and the speech perception outcome (from no sound to open-set word recognition of monosyllables). Results: CT data were analyzed from 24 NF2 and non-NF2 adult ABI subjects. Although three-dimensional

(3D) orientation of the ABI array exhibited a variety of angles, most arrays were posteriorly tilted in the lateral view and most were medially tilted in the posterior view. ABI positions relative to the basion and midline showed mean D1 distances of 1.77±0.4 cm and 1.10±0.35 cm, and mean D2 distances of 1.33±0.4 cm. The number of electrodes that provided auditory sensations ranged from 4 to 19 (out of a total of 21). Speech perception outcomes ranged from no sound detection to open-set recognition of monosyllabic words. Of the four subjects with open-set recognition of monosyllabic words, 2 had arrays that when viewed from posterior were oriented superiorly, one had a medial tilt and one array (of a non-NF2 subject) was tilted inferiorly. Conclusion: ABI users with the best speech perception skills have a) electrodes with low current thresholds, b) high numbers of active electrodes (10 and more), and c) arrays that are tilted superiorly and located in an area closer to the midline when viewed from the posterior.

SYMP 41

Computational Modeling of Auditory Brainstem and Midbrain Networks for Improving Central Auditory Prostheses

Andreas Bahmer
University Clinic Wuerzburg

In contrast to Cochlear implants (CI), the hearing performance with auditory brainstem implants (ABI) and auditory midbrain implants (AMI) is limited not only because target structures (Cochlear Nucleus, CN, and inferior colliculus, IC) are highly complex but also because stimulation patterns are not adapted to the characteristics of the corresponding neuronal structures and functions.

To explain temporal processing in the CN and the IC, the model from Langner and Bahmer (Bahmer and Langner 2006 I, II, 2018) accounts for network characteristics of neurons in these nuclei. Chopper neurons in the CN are the main projecting cells in the ascending auditory system from the CN to the IC and are therefore the target of ABI stimulation. Certain features of chopper neurons like preferences for interspike intervals and high dynamic range in amplitude modulation encoding can be explained by the microcircuits of these neurons.

We have proposed a new stimulation paradigm which accounts for certain features of chopper neurons (Patents Bahmer 2014 WO2014070553A1, Bahmer and Schleich 2014 US9398382). This new stimulation paradigm adapts the auditory prostheses stimulation rate to a multiple of the intrinsic oscillation in the CN. In addition, multi-channel stimulation accounts for the broad frequency integration of onset neurons. The broad frequency integration enables the coding of AM with a high dynamic range.

By utilizing a potential resonance of chopper neurons, which are located in the ventral CN, the rather far field stimulation from the electrode on the surface of the dorsal CN may be circumvented. This kind of resonance can be observed in electrophysiological brainstem responses recorded in the operation room while the electrode is positioned during the surgery.

Similarly, for the AMI, certain features of the IC are relevant for electrical stimulation. E.g. a periodotopic map was found (orthogonal to the tonotopic map). This map may be utilized by penetrating AMI because encoding of periodicity is the basis of speaker separation in difficult listening situations.

SYMP 42

Temporal Processing and Hearing Performance with Auditory Brainstem Implants

Mahan Azadpour; William H. Shapiro; Mario A. Svirsky
Department of Otolaryngology, New York University School of Medicine

Auditory brainstem implants (ABI) are used clinically to restore hearing to patients who cannot be treated with a cochlear implant (CI), mainly due to abnormal or damaged auditory nerve or cochlea. ABIs bypass the auditory nerve and stimulate the brainstem directly via electrodes placed on the cochlear nucleus. Speech perception outcomes are much poorer with ABIs than with CIs. Only a small percentage of ABI users achieve a level of speech understanding comparable to that of the average CI user. In addition, there are often non-auditory side effects associated with stimulation delivered by ABI electrodes. These two points suggest that the stimulated brainstem networks in most ABI patients may not correctly transmit some important speech cues provided by the current ABI devices.

The current ABI devices use the same coding strategies as those developed for CIs. These strategies typically divide the incoming signal into different frequency bands, with the output of each band being used to modulate the amplitude of electrical pulses delivered by a stimulating electrode. We hypothesized that amplitude modulation cues may not be well transmitted when stimulation is delivered to the cochlear nucleus with an ABI electrode. The cochlear nucleus is complex and consists of different neuron types that have specialized functions in the normal hearing system. Most cochlear nucleus neurons respond sparsely during an ongoing acoustic stimulus,

with some responding to sound onset or offset only. It is conceivable that temporal cues would not be correctly transmitted in those ABI users in whom the stimulated cochlear nucleus neurons do not capture rapid stimulus variations, or do not project that information to the midbrain and the auditory cortex.

In this talk, we will address the hypothesis that processing of temporal cues is impaired in ABI users. We will compare different behavioral and electrophysiological measures of temporal processing performance obtained in ABI and CI users. The obtained measures will also be used to infer some auditory processing properties in the cochlear nucleus and the auditory nerve, as well as the more central auditory system. The relation between temporal processing and hearing performance with the ABI device will be discussed.

On the Form and Functions of Type II Spiral-Ganglion Neurons

Chairs: Tom Coate & Michaels Deans

SYMP 43

Introduction to Type II SGNs and Eph/Ephrin Signaling in Type II SGN Development

Thomas Coate; Juliet Mejia; Mansa Gurjar
Georgetown University, Department of Biology

Spiral ganglion neurons (SGNs) are afferent neurons that relay auditory information from the cochlea to the cochlear nuclei. Type I SGNs are the most numerous SGNs, are myelinated, and respond to glutamate released from inner hair cells as part of the conventional "hearing" circuit. By contrast, type II SGNs represent the minority of SGNs, are unmyelinated, form synapses with only outer hair cells, and may constitute an inner ear nociceptive circuit. Classic physiological studies showed type II SGNs respond to glutamate as a result of outer hair cell depolarization, but more recent studies suggest they also respond to hair cell damage in a manner dependent on extracellular ATP. Additionally, type II SGNs develop quite differently than type I SGNs: they bypass the inner hair cells, make a 90 degree turn toward the cochlear base, then form synapses with multiple outer hair cells. In this symposium, presenters will discuss type II SGN development, diversity, function, and regulation, as well as related aspects of pain circuitry.

Ephrins are cell-surface ligands that bind to Eph receptors to control numerous aspects of nervous system growth, differentiation, and plasticity. In the cochlea, Ephrins and Eph receptors control several important aspects of spiral ganglion neuron (SGN) development. As examples, inner hair cell innervation is controlled by Ephrin-A5, and radial bundle fasciculation patterns are controlled by both EphA4 and EphA7. Here, we present results from genetic and in vitro studies (using mouse) that support a model in which Ephrin-A ligands interact with EphA7 to promote the turning of type II SGNs toward the cochlear base. In mouse, EphA7 is expressed by both type I and II SGNs at the time of hair cell innervation and loss of Epha7 leads to type II SGN turning defects. Interestingly, type II SGN turning defects are also present in mice that lack the Prospero Homeobox-1 (Prox1) gene, and Epha7 gene regulatory regions contain multiple candidate Prox1 binding sites. Thus, we are also investigating the extent to which Epha7 expression in the cochlea is regulated directly by Prox1.

SYMP 44

Seq-ing Insights into Molecular Heterogeneity of Spiral Ganglion Neurons

Brikha Shrestha[1]; Lisa Goodrich[2]
[1]Dept. of Neurobiology, Harvard; [2]Harvard

Spiral ganglion neurons (SGNs) have long been known to comprise a functionally diverse population, but their molecular correlates have remained largely elusive until recently.

Leveraging single cell RNA sequencing (scRNA-seq), we identified three broad subtypes of Type I SGNs in addition to gene expression programs distinguishing Type I from Type II SGNs. Gene ontology analyses revealed that the major axes of differences between Type I and II SGNs involve connectivity, glutamate responsiveness, neurotransmitter release and neuronal excitability. These data offer valuable molecular insights and genetic access for investigation of Type II SGN development, connectivity and function at greater depth. Emerging evidence suggest that Type II SGNs also comprise a heterogeneous population. The advantages and challenges of scRNA-seq-based approaches for elucidating Type II SGN diversity will be discussed.

SYMP 45

Staying in or Going Out: Neurotropic and Neurotrophic Signals in Spiral Ganglion Peripheral Process Navigation

Bernd Fritzsch[1]; **Karen Elliott Thompson**[2]; Jennifer Kersigo[2]
[1]University of Iowa, Dept. of Biology and Dept. of Otolaryngology; [2]University of Iowa, Dept. of Biology

The organ of Corti (OC) consists of two sections separated by the tunnel of Corti. Each shows distinct innervation:

inner spiral ganglion neurons (iSGNs/Type I) to inner hair cells (IHCs) and outer spiral ganglion neurons (oSGNs/Type II) to outer hair cells (OHCs) (Fritzsch and Elliott, 2018). The overall reduced SGN viability in mutants for the neurotrophins, BDNF and Ntf3 (aka NT3), and their high affinity receptors, Ntrk2 (aka TrkB) and Ntrk3 (aka TrkC), showed reasonable numerical match to oSGNs and iSGNs. It was thus suggested (Ernfors et al., 1995) that these two neurotrophins have complimentary roles and both attract and support the respective processes of neurite growth and maintenance in each section of the OC. However, while follow up work confirmed the numerical effect, it did not support the hypothesis. Neither misexpression of Ntf3 under BDNF control (Tessarollo et al., 2004) nor of BDNF under Ntf3 control (Agerman et al., 2003) showed specific loss or gain of IHC or OHC innervation beyond rerouting of vestibular fibers into the cochlea that may be related to changes in neurotrophin expression levels over time (Fritzsch et al., 2016). Furthermore, there is no evidence of a differential distribution of receptors based on recent RNAscope data (Kersigo et al., 2018).

Here we ask what happens to IHC innervation if some OHCs turn into IHCs, if most IHCs degenerate, or if a specific neurotrophin (or both) are lost in some or all hair cells. Our data show that unusually placed IHCs can attract nerve fibers with a different pattern of innervation (Jahan et al., 2018). Many, but not all, iSGNs project to OHCs if there are no IHCs left and the simple presence of IHCs does not suffice to keep all iSGN fibers near neurotrophin-depleted IHCs. Combined, these data reveal a hierarchy of choices that mostly reflect availability of neurotrophin concentrations. We provide evidence suggesting that neurotrophin receptor level and distribution in the two types of SGNs might play a subtle and incompletely understood bias to help sort out the two types of afferents to the two sections of the OC.

B Fritzsch, KL Elliott (2018) Front Neuroanat 12:99
P Ernfors et al (1995) Neuron 14:1153
J Kersigo et al (2018) CTR 374:251
L Tessarollo et al (2004) J Neurosci 24: 2575.
K Agerman et al (2003) Development 130: 1479
B Fritzsch et al (2016) in: A Dabdoub et al (eds) The Primary Auditory Neurons, 49-84.

SYMP 46

PCP Signaling and Axon Pathfinding: Molecular Trail Blazes that Guide Growth Cone Navigation

Michael Deans
Dept. of Surgery, Div. of Otolaryngology, Dept. of Neurobiology and Anatomy

Type II spiral ganglion neurons (SGN) are anatomically distinct from other classes of SGN because they extend a peripheral axon beyond the inner hair cells that subsequently makes a distinct 90 degree turn towards the cochlear base. As a result, patterns of outer hair cell innervation are coordinated with the tonotopic organization of the cochlea, and the neuron is able to contact multiple OHCs. We show that Planar Cell Polarity (PCP) signaling is required to maintain the fidelity of axon turning and that disrupted PCP results in misdirected axons that project incorrectly towards the cochlear apex. While our previous studies implicated the transmembrane protein VANGL2 in this process, we demonstrate here that the Frizzled (FZD) receptors FZD3 and FZD6 similarly direct axon turning, are functionally redundant with each other, and genetically interact with Vangl2. Unexpectedly, VANGL2, FZD3 and FZD6 are not required in the growth cone itself, and instead function non-autonomously by providing directional cues from organ of Corti support cells. We further demonstrate that FZD3 and FZD6 are asymmetrically distributed along the basolateral walls of cochlear supporting cells, and are required to promote or maintain the asymmetric distribution of VANGL2 and CELSR1. These data indicate that intact PCP complexes formed between cochlear supporting cells contribute to the non-autonomous regulation of axon pathfinding during cochlear innervation. As a result, every growth cone receives identical modular cues which ensures that similar patterns of Type II SGN connectivity occur throughout the cochlear length. Additional analyses of Porcn mutant mice in which WNT secretion is reduced suggest that non-canonical WNT signaling establishes or maintains PCP signaling in this context. A deeper understanding of these mechanisms is necessary for repairing auditory circuits following acoustic trauma or promoting cochlear re-innervation for the success of regeneration-based deafness therapies.

SYMP 47

Peripheral Sensory Neurons that Participate in the Perception Pain

Rebecca Seal
Departments of Neurobiology and Otolaryngology, Pittsburgh Center for Pain Research, University of Pittsburgh

Dorsal root and trigeminal ganglia are the principal neural detectors for touch, temperature, itch, pain and proprioception. Subsets tuned to detect acute noxious mechanical, thermal or chemical stimuli are termed nociceptors. These neurons are critical for conveying acute noxious insults, which are protective as well as in maladaptive circuits that support chronic pain. In this talk, our current understanding of how primary sensory neurons participate in both forms of pain will

be presented. Spiral ganglion neurons as analogous contributors to auditory pain also will be discussed.

SYMP 48

The Not-so-hidden 'Hearing Loss' of Type II Cochlear Afferents

Paul Fuchs
the Center for Hearing and Balance, Johns Hopkins University School of Medicine

Type II afferents contact many OHCs. Despite that convergence, the summed synaptic drive of those many OHCs is far less effective than the single IHC ribbon synapse presynaptic to each type I afferent dendrite. Intracellular recording from type II afferents in excised cochlear tissue of young rats (Weisz et al., 2012 J Neurosci. Jul 11;32(28):9528-36) showed that individual outer hair cells release single vesicles upon strong depolarization, and do so with low probability. Synaptic ultrastructure viewed with transmission electron microscopy echoes this debility (Figure). The ribbon synapses of OHCs have fewer, disorganized vesicles compared to those of IHCs. In addition, half the type II boutons are not associated with presynaptic ribbons. This proportionality also can be observed using confocal microscopy to examine immunolabeled cochlear whole-mounts. While all afferent boutons appear to label for postsynaptic density markers, only those opposite ribbons show immunolabel for GluA2 receptor subunits (Martinez-Monedero et al. 2016, eNeuro. 12; 3 (2)). Synaptic structure and function support the finding that type II afferents are poorly sensitive to sound. Ongoing studies ask whether the synaptic organization of type II afferents is activity-dependent.

Figure legend: Ribbon synapses in mouse cochlear hair cells. Those in IHCs have more, better -organized and similarly sized vesicles. Ribbons of OHCs have fewer, scattered and variously sized vesicles. Scale bar 500 nm.

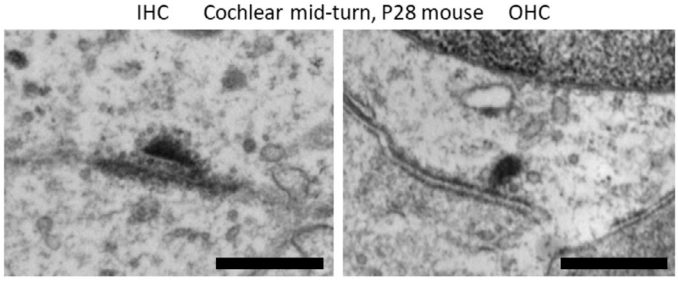

SYMP 49

Efferent Inhibition of Type II Cochlear Afferents

Catherine Weisz
National Institute on Deafness and Other Communication Disorders

In the canonical outer spiral bundle circuitry, medial olivocochlear (MOC) efferent neurons form cholinergic synapses onto outer hair cells (OHC), while OHC in turn form glutamatergic synapses onto type II spiral ganglion afferent neurons to signal to the brain. MOC neurons inhibit OHC function through coupling of the post-synaptic acetylcholine receptor to SK or BK potassium channels; a mechanism of cochlear gain control. The role of the ascending synapse from OHCs to type II afferent neurons is unknown, but may signal loud, damaging sounds, or act to integrate acoustic information over time. Furthermore, histological evidence exists for additional synaptic contacts between MOC efferents, OHCs, type II afferents, and supporting cells. Electron microscopy studies have suggested synaptic contacts between MOC neurons and type II afferents. Moreover, MOC axon terminals stain for markers of GABA, but OHCs do not respond to GABA, suggesting an alternate target for GABA release from MOC neurons. Therefore, GABA is a potential neurotransmitter at putative MOC efferent to type II afferent synapses. We used patch-clamp electrophysiological recordings from dendrites of type II spiral ganglion afferent neurons in mice paired with immunohistochemistry and optical stimulation techniques to probe GABAergic MOC synapses onto type II neurons. Exogenous GABA application evoked currents in type II dendrites that are sensitive to the GABA-A receptor blocker gabazine. The amplitude of GABAergic currents decreases over the first post-natal week suggesting a developmental down-regulation of GABA responses. However, GABA receptor currents persist past the onset of hearing, suggesting a potential role in the mature hearing circuit. Immunolabeling experiments confirm that MOC terminals have the necessary components for synaptic release of GABA, apposed to post-synaptic GABA-A receptor labeling in type II spiral ganglion dendrites. The role of MOC-type II synapses in hearing is unknown, but this work suggests complex patterns of signaling within the outer spiral bundle.

Plasticity Following Hearing Loss or Restoration

PD 41

Hearing loss is associated with modified brain oscillations during non-auditory verbal working memory

Brandon T. Paul[1]; Arunan Srikanthanathan[2]; Andrew Dimitrijevic[1]
[1]Sunnybrook Research Institute; [2]University of Toronto

Hearing loss (HL) is a risk factor for dementia and mild cognitive impairment. The reason for this risk is unknown, but one explanation could be that HL accelerates the decline of cognitive function known to occur with

neurodegenerative disease. Working memory, or the ability to temporarily hold items (e.g., stimuli) in a "mental workspace", is a cognitive ability known be affected by mild cognitive impairment and dementia. HL is also known to affect working memory when using auditory stimulation. However, the effects of HL on non-auditory memory are less understood, which could reveal a more general effect of HL on cognition. The objective of this study was to identify if HL is associated with changes in neural signatures underlying visual-based, verbal working memory.

Twenty-four adults (12 females, age range 18-74), without any neurological condition and with normal to sloping audiograms, participated in a modified Sternberg task. Five-word sentences from the Matrix Sentence Test were presented as white text on black background. Words were presented individually and sequentially over six seconds. After, participants held the sentences in memory for 2 seconds (i.e., the memory maintenance period). Then, a target word was presented, and participants reported if the target word was in the presented sentence. The 64-channel electroencephalogram (EEG) was recorded throughout. Beamforming was used to estimate neural sources of oscillations during the memory maintenance period. Specifically, beta oscillations (14-25 Hz EEG rhythms) during the maintenance period are known to be affected in individuals with dementia, and here were correlated to the degree of HL at high frequencies while partialling out the effect of age.

The power of beta oscillations during the memory maintenance period was significantly and negatively correlated to HL, even after partialling out the effect of age ($r = -0.77$, corrected $p = 0.03$). The effect suggested that individuals with more HL had a larger desynchronization of beta when holding items in memory. These correlations localized to right frontal brain regions and peaked in right middle frontal gyrus, a region strongly associated with working memory function. Performance on the task was near ceiling for all participants. Results overall suggest that independent of age, those with more HL at high-frequencies may have to "work harder" to perform the task. Findings imply that HL may have an effect on general cognitive function, and clarify how HL may accelerate symptoms of dementia or cognitive impairment.

PD 42

Neural Acclimatization to Hearing Aids

Hanin Karawani[1]; Samira Anderson[2]
[1]Department of Communication Sciences and Disorders, University of Haifa, Haifa, Israel; [2]Department of Hearing and Speech Sciences, University of Maryland, College Park, MD, USA

Objective
The purpose of this study was to determine the time course of neural acclimatization to hearing aids and to determine whether objective measures can be used to provide information regarding potential hearing aid outcomes.

Design
Nineteen older-adults with mild to moderate age-related hearing loss with no history of hearing aid use were fit with bilateral hearing aids and were tested during a period of six months. Participants underwent six testing sessions within this six-month period. Cortical auditory-evoked potentials to the speech syllable /ga/ in quiet and in 6-talker babble noise conditions were recorded during these testing sessions.

Results
Cortical plasticity was demonstrated in N1 and P2 peak amplitudes over the course of six months. N1 amplitudes increased as early as two weeks following the hearing aid fitting, whereas increases in P2 amplitudes were observed after twelve weeks of hearing aid use. N1 amplitude in the first testing session predicted the degree of change that occurred after six months of hearing aid use.

Conclusions
This study demonstrated rapid cortical acclimatization to amplified sound. The earliest changes were observed for N1 amplitude changes, suggesting that the auditory system quickly adapts to processing auditory stimuli that were previously diminished in audibility. However, a longer period of hearing aid use is required to demonstrate changes in P2, the component that corresponds to auditory object representation.

Funding source
Hearing Health Foundation and Widex USA

PD 43

Effects of Auditory Hair Cell Ablation on Spatial Learning/Memory

Z. Jason Qian[1]; Anthony Ricci[2]
[1]Department of Otolaryngology-Head & Neck Surgery, Stanford University School of Medicine; [2]Department of Otolaryngology and Department of Molecular and Cellular Physiology, Stanford University

Background
Current clinical interest lies in the relationship between hearing loss and cognitive impairment. Previous work demonstrated that noise exposure, a common cause of sensorineural hearing loss (SNHL), leads to cognitive

impairments in mice. However, it is difficult to distinguish if this effect is due to the oxidant stress of the noise trauma on the cognitive brain versus the subsequent SNHL. Here, we investigate the effects of isolated SNHL on cognitive function.

Methods

Cochlear hair cells were conditionally and selectively ablated in transgenic mice where the human *diphtheria toxin receptor (DTR)* gene was inserted behind the *Pou4f3* promoter, which encodes a hair cell-specific transcription factor. Administration of a low dose of diphtheria toxin (DT) in these mice caused profound SNHL within 4 days without vestibular dysfunction while having no effect on wild type littermates. Cognitive performance was compared between three conditions: early-onset SNHL (DT on P30), late-onset SNHL (DT on P60), and wild type littermates (DT on P30). Daily cognitive testing began on P120 using an 8-arm radial maze (RAM). The testing period was divided into two phases: fully-baited RAM training and partially-baited RAM training. Results were recorded as the number of working memory (WM) errors per day during both training phases and number of reference memory (RM) errors per day during partially-baited RAM training (Figure 1).

Results

Normal hearing mice performed better than both early and late SNHL groups on measures of WM and RM. For WM, the early SNHL group performed better than the late SNHL group. When the RAM was converted from fully-baited to partially-baited, the normal hearing and early SNHL groups had similar increases in WM errors, which were appropriate for the paradigm shift. However, the late SNHL group had an attenuated increase in WM errors, suggesting poorer task acquisition. WM performance plateaued at different levels for all groups, with normal hearing mice having the fewest WM errors and late SNHL mice having the most. For RM, early and late SNHL groups had similar performance, which plateaued at greater error levels than the normal hearing group.

Discussion

SNHL impairs performance on a spatial learning/memory task. Late-onset SNHL had more adverse effects on task acquisition and WM performance compared to early-onset SNHL. This may be due to decreased neural plasticity after SNHL with age. Future work will be needed to identify the neural circuits involved and if the loss is an activity-driven process.

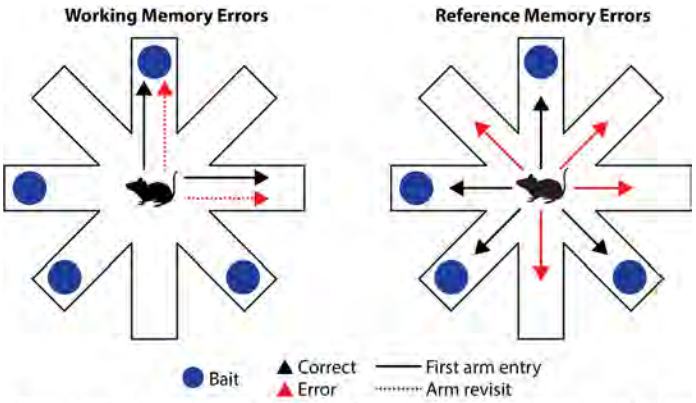

Figure 1. Schematic for recording spatial working and reference memory errors in an 8-arm radial maze. Working memory errors are scored each time a previously visited arm is re-visited, regardless of if the arm is always-baited or never-baited (working memory, which is short-term and trial-dependent, provides information on which arms have already been visited in a given trial). Reference memory errors are scored for first entries into never-baited arms (reference memory, which is long-term and trial-independent, provides information on which arms are always baited between seperate trials).

PD 44

Deep Neural Networks With Simulated Hearing Impairment Replicate Behavioral Deficits of Hearing Impaired Listeners

Mark R. Saddler; Jenelle Feather; Andrew Francl; Ray Gonzalez; Josh H. McDermott
Department of Brain and Cognitive Sciences, MIT

Recent work has shown that artificial neural networks optimized to perform auditory recognition tasks from simulated cochlear input replicate aspects of human auditory behavior. Here, we extend this approach to investigate whether changes in peripheral auditory processing believed to accompany hearing impairment can account for the deficits experienced by hearing-impaired listeners when recognizing speech in noise. We optimized deep convolutional neural networks to recognize words from simulated cochlear representations of noisy speech signals. We then measured how network performance on simulated psychophysical experiments depended on parameters of the cochlear model. Specifically, we simulated outer hair cell (OHC) loss in our peripheral model by broadening the cochlear filter bandwidths and by decreasing nonlinear compression. Networks trained with a healthy peripheral model and tested with an impaired peripheral model (broader cochlear filters and reduced compression) replicated aspects of hearing-impaired human auditory behavior. These “mismatched” networks model an auditory system with zero ability to adapt to peripheral damage. Like hearing-impaired humans, the mismatched networks exhibited impaired word recognition at low SNRs and a reduced benefit from fluctuating maskers. However, networks trained and tested with the impaired peripheral model exhibited remarkably unimpaired auditory behavior. These networks, which model an auditory system with perfect ability to adapt to peripheral damage, showed relatively normal word-in-noise recognition and

benefitted from fluctuating maskers relative to stationary noise. These results suggest that the behavioral deficits of hearing-impaired listeners are not necessarily an inevitable consequence of OHC loss, and could instead reflect a lack of plasticity in the auditory system following alterations to the cochlea.

PD 45

Developmental sensory deprivation weakens interareal coupling in the auditory connectome

Prasandhya Yusuf[1]; Peter Hubka[2]; Jochen Tillein[3]; Martin Vinck[4]; **Andrej Kral**[5]
[1]Faculty of Medicine University of Indonesia, Department of Medical Physics / Medical Technology Core Cluster IMERI, Jakarta, Indonesia; [2]Dept. of Experimental Otology, ENT Clinics, Medical University Hannvoer, Germany; [3]J.W. Goethe University, Department of Otorhinolaryngology, Frankfurt am Main, Germany; [4]Ernst Strüngmann Institut (ESI) for Neuroscience in Cooperation with Max Planck Society, Frankfurt, Germany; [5]Dept. of Experimental Otology, Hannover Medical School, Germany; DFG Cluster of Excellence "Hearing 4 All"

Absence of sensory input from birth affects cortical development required to form a functional sensory system. A previous study demonstrated that congenital deafness leads to near loss of induced cortical oscillations that are considered a fingerprint of corticocortical interactions (Yusuf et al., 2017, Brain). Here we aimed at directly quantifying the functional and effective connectivity between a primary and a secondary auditory fields.

Adult congenitally deaf cats (n=5), acutely deafened hearing animals (n=6) and hearing, acoustically stimulated animals (n=6) were used for the present study. Deaf and deafened animals (by intrascalar neomycine application) were stimulated with feline cochlear implants (6 intracochlear implants) in wide bipolar configuration. Hearing animals were stimulated acoustically using callibrated loudspeakers. The electrical stimuli consisted of a train of three charge-balanced biphasic pulses (200 µs/phase) at a repetition rate of 500 pps., the corresponding acoustic stimuli consisted of three condensation clicks at 500 pps (click duration 50 µs). All animals were artificially ventilated and anaesthetized using isoflorane in O_2/N_2O. Cortex was exposed by a wide trephination and was stabilized by a modified Davies chamber for recording. Cortical activity was registered using two 16-channel multielectrode arrays (Neuronexus) in primary auditory cortex (field A1) and posterior auditory field (PAF). Local field potentials (filtered to 1 Hz – 9000 Hz, amplification 5000 x) were analyzed. To eliminate the influence of the reference electrode, bipolar derivation was used in field A1. Interareal coupling strength and directionality were analyzed to investigate the effects of developmental experience (hearing vs. deaf) and stimulation mode (acoustic vs. electric) on cortical coupling. Three measures of effective connectivity were used: pairwise phase consistency, weighted phase lag index and Granger causality.

All measures consistently demonstrated a decoupling between the primary and the higher order field in the congenitally deaf animals during (electrical) auditory stimulation, particularly in the alpha- and the beta-band. Granger causality demonstrated that the observed effect was predominantly due to top-down decoupling. Consequently, early hearing experience is essential for development of functional interareal couplings during sensory processing, particularly important for the top-down interaction related to stimulus prediction.

Supported by Deutsche Forschungsgemeinschaft (Cluster of Excellence Hearing4all and Kr 3370/1-3) and MedEl Comp., Innsbruck, Austria.

PD 46

Auditory Sequence Learning with Linguistic and Environmental Stimuli in Cochlear Implant Users as Compared to Normal Hearing Listeners

Liat Kishon-Rabin[1]; Shira Cohen[1]; Ronen Perez[2]
[1]Department of Communication Disorders, Steyer School of Health Professions, Sackler Faculty of Medicine, Tel-Aviv University; [2]Department of Otolaryngology, Head and Neck Surgery, Shaare Zedek Medical Center affiliated with the Hebrew University Faculty of Medicine

Background
Spoken language development has been shown to depend on auditory processing mechanisms that extract structural regularities present in the auditory linguistic input. To date, the few studies that attempted to assess the extraction of regularities (by statistical or rule learning) in cochlear implant (CI) users have done so in the *visual* modality and showed mixed results. We argue that because the primary mode for speech and language development is via hearing, such learning should be assessed in the *auditory* modality. Thus, the purpose of the present study was to assess auditory rule learning (ARL) in normal hearing (NH) and in CI users using linguistic and non-linguistic stimuli.

Method
Participants included 16 NH adults and 11 prelingually hearing-impaired adult CI users who varied in their years of implantation (1.5-18 years). A similar double- condition

rule was applied to two sets of natural auditory stimuli: environmental sounds (dog barking, bird singing, door knocking and bell ringing) and linguistic sounds (/sa/, /ta/, /si/ and /ti/). ARL for each type of stimuli consisted of three sessions. In each session, participants listened to 16 sequences according to the rule. After each sequence, participant keyed what they heard to induce active learning. Assessment of learning included judgement (correct/incorrect) and completion of the last sound in a sequence of trained and novel stimuli. Measures included correct responses (in %) and reaction time (in msec).

Results

(1) CI users showed difficulty in ARL compared to NH for both types of stimuli. This difficulty, however, could not be explained by general speed of processing because both groups had similar reaction times when repeating the heard sequences; (2) For CI, ARL was similar for both types of stimuli with an advantage to the environmental sounds. In contrast, an advantage for ARL to speech sequences was reported for NH; and (3) All NH showed significant ARL by the end of training, while only the CI who had progressive hearing loss through childhood showed similar performance.

Conclusions

The data provide novel insight to the ramifications of a period of early auditory deprivation on implicit learning in the auditory modality. These may explain some of the difficulties CI users have in performing under difficult listening conditions as well as in demonstrating poor high-level linguistic skills where encoding, processing and learning of rules from the stream of speech sounds are necessary.

PD 47

Neuromodulation Enhances Plasticity in a Rodent Model of Cochlear Implant Use

Erin G. Glennon[1]; Mario A. Svirsky[2]; Robert C. Froemke[2]
[1]New York University; [2]NYU School of Medicine

Rates of auditory perceptual learning and asymptotic speech perception performance with cochlear implants are highly variable across patients. Adaptation to cochlear implants is believed to require neuroplasticity within the central auditory system. However, mechanisms by which behavioral training enables plasticity and improves outcomes are poorly understood. Here we investigate the hypothesis that neural mechanisms that promote plasticity in the rodent auditory system are key to optimizing cochlear implant usage, and might be especially helpful in cases of poor performance. We focus on noradrenergic modulation of rat auditory cortex by the locus coeruleus, which can enable robust and long-lasting neural and behavioral changes.

We developed a surgical approach for cochlear implantation in adult rats. Our approach allows insertion of an 8-channel electrode array covering up to 360 degrees in the cochlea and allows rats to freely behave while using the implant to perform auditory tasks (King et al. J Neurophysiol 2016). Rats are trained on a go/no-go task, and self-initiate trials to respond to a target tone. Previously, we showed in normal hearing animals that this task requires auditory cortex and is enhanced by cortical neuromodulation and plasticity.

Here we examined the effect of pairing locus coeruleus stimulation with an auditory stimulus on auditory learning when the animal has to relearn a tone identification task using a cochlear implant. Initial training was done using acoustic stimuli in normal hearing animals. Animals were then bilaterally deafened, unilaterally cochlear-implanted, and retrained on the auditory task with the new target delivered by intracochlear electrical stimulation. Prior to daily behavioral training sessions, rats underwent 5-10 min pairing sessions either with optogenetic locus coeruleus or sham stimulation. Pairing accelerated learning with cochlear implants compared to animals that did not receive it as measured by days to criteria (sham: n=10, 5.5±1.5 days; paired: n=9, 2.0±0.2 days; p=0.02). We then conducted multi-unit recordings in the auditory cortex to assess responses to the cochlear implant. Animals that had been trained with the cochlear implant had increased activation of the cortex, and those that underwent pairing had a sharper representation of the target cochlear implant channel. We used fiber photometry to monitor activity of noradrenergic locus coeruleus neurons. During auditory learning, normal hearing animals display dynamic locus coeruleus activity, specifically during the acquisition of the new meaning of reward relevant tones. These studies indicate that neuromodulation can play a powerful role in shaping outcomes with cochlear implant use and training.

PD 48

Tinnitus Induced Hyperexcitability in View of Deafness and Cochlear Implants?

Marlies Knipper[1]; Pim van Dijk[2]; David Baguley[3]; Lukas Rüttiger[4]
[1]University of Tübingen, Department of Otolaryngology, Head and Neck Surgery Tuebingen; [2]University Medical Center Groningen, Department of Otorhinolaryngology/ Head and Neck Surgery; [3]University of Nottingham, Division of Clinical Neuroscience,Hearing Sciences; [4]University of Tübingen, Department of Otolaryngology, Head and Neck Surgery Tübingen

Subjective tinnitus is the conscious perception of sound heard in the absence of physical sound sources. Most tinnitus literature argues for increased central spontaneous firing rates or central hyper-excitability following peripheral deafferentation leading to tinnitus percept through a homeostatic response (or central neural gain). In alternative views, tinnitus is linked to elevated cortical synchronicity, to disrupted interaction of frontostriatal with auditory-sensory regions or to a reinforcement of a `tinnitus precursor` through attention or fear. We here suggest that elevated hyper-excitability in tinnitus is the result of an incapacity to generate homeostatic adjustments due to loss of signals in noise. This alternative view of origin of elevated hyper-excitability in tinnitus results from reflecting excitability stages between (i) congenital deafness that describe a low prevalence of tinnitus (ii) acquired deafness that describe a high prevalence of tinnitus and (iii) cochlear implant electrodes (used to restore hearing) that can to some degree reduce tinnitus.

Supported by DFG KN316/13-1; RU 713/6-1; KL1093/12-1

Pulling the Threads of Hair Cell Fate with an Omic Tug

Chairs: Ronna Hertzano & Mike Bowl

SYMP 50

Functional Characterization and Therapeutic Targeting of Gene Regulatory Elements

Nadav Ahituv
Department of Bioengineering and Therapeutic Sciences, University of California San Francisco, San Francisco, California, USA; Institute for Human Genetics, University of California San Francisco, San Francisco, California, USA

Nucleotide variation in gene regulatory elements (GREs) is a major cause of human disease. Despite continual progress in the cataloging of these elements, little is known about the code and grammatical rules that govern their function. As such, we are using massively parallel reporter assays (MPRAs) to simultaneously test the activity of thousands of GREs in order to learn the 'regulatory grammar' and how mutations alter their function. Regulatory elements can also serve as therapeutic targets. To highlight this role, we used CRISPRa of regulatory elements to rescue haploinsufficient (having only one functional gene copy) diseases in vivo.

SYMP 51

"First came Atoh1…..: Epigenetic Mechanisms Guiding Hair Cell Gene Regulatory Networks During Development and Transdifferentiation."

Neil Segil
Keck Medical School of the University of Southern California

In the inner ear, sensory hair cell differentiation initiates embryonically through the expression of Atoh1, a bHLH transcription factor that lies at the top of a complex regulatory cascade of hair cell-specific gene expression. Using techniques adapted to analyze chromatin structure, epigenetics, and transcription factor binding in the small cell numbers available from the inner ear, we have begun dissecting the molecular events that follow Atoh1 up-regulation in the nascent hair cells, as well as during supporting cell transdifferentiation. My talk will focus on new knowledge of the transcriptional and epigenetic mechanisms that govern the process of hair cell differentiation.

SYMP 52

The Role of GFI1 in Hair Cell Development: Further Hints From RiboTag Analyses

Maggie Matern
University of Maryland School of Medicine, Baltimore

The GFI1 transcriptional repressor is essential for the development and function of cochlear and vestibular hair cells. However, the field maintains a limited knowledge of the downstream targets of GFI1 during development. Utilizing a model for Gfi1 knockout paired with RiboTag immunoprecipitation methods to study hair cell-specific differences in gene expression, we identify a key role for GFI1 in repressing a neuronal transcriptional program that is normally active in early cochlear hair cell development. Discussion of GFI1 function in other systems further supports a role in neuronal gene repression, suggesting that this is a critical step also in hair cell development.

SYMP 53

Outer vs Inner Hair Cell Fate Consolidation by Zinc Finger Transcription Factor INSM1

Jaime Garcia-Añoveros
Departments of Anesthesiology, Physiology and Neurology, Knowles Hearing Center, Northwestern University

Embryonic OHCs but not IHCs transiently express INSM1. In the absence of INSM1, OHCs born in their expected location (the outer compartment) and expressing early

OHC markers switch fates and transdifferentiate into IHCs. Although transdifferentiated cells acquire all IHC features, only about half OHCs transdifferentiate, and their distribution reveals a gradient suggestive of an IHC-inducing morphogen. Transcriptomics of differentiating IHCs vs OHCs and of OHCs with and without INSM1 reveal that INSM1 represses in OHCs a core set of genes characteristic of embryonic IHCs. It appears that INSM1 transiently represses these genes in embryonic OHCs to prevent their responding to an IHC-inducing gradient, thus consolidating the OHC fate.

SYMP 54

RFX Transcription factors – Key Regulators of Hair Cell Terminal Differentiation

Ronna Hertzano
Department of Otorhinolaryngology Head and Neck Surgery, University of Maryland School of Medicine; Institute for Genome Sciences, University of Maryland School of Medicine.

Once hair cell differentiation is initiated, these cells undergo numerous additional transcriptional changes, culminating in their mature function and ability to withstand the metabolic stress of mechanoelectrical transduction. We have previously identified the RFX transcription factors as key regulators of hair cell-expressed genes in the early post-natal period and specifically RFX1 and 3 as critical for outer hair cell survival at the onset of hearing. Here we extend our studies to define their critical period for action and, through a variety of omic-based approaches, provide insights into the pathways they regulate in hair cell terminal differentiation.

SYMP 55

Helios, Helping Illuminate Our Understanding of Outer Hair Cell Maturation

Michael Bowl
Mammalian Genetics Unit, MRC Harwell Institute

Given the age-related vulnerability of OHCs, identifying factors that specify OHC fate and maintenance is crucial as we work towards therapies for presbycusis. Utilizing two independent, unbiased gene discovery approaches, we demonstrate that Ikzf2/helios is a critical determinant of hearing through regulating the postnatal OHC transcriptome. Moreover, we show that virally-induced, ectopic expression of Ikzf2/helios in early postnatal IHCs is sufficient to cause a systematic change in cell fate towards an OHC-like transcriptome, including: reduced expression of canonical IHC genes; expression of OHCspecific genes; and, electromotility. Thus, Ikzf2/helios represents a novel regulatory pathway essential for the maturation of OHCs.

SYMP 56

Transcription Factors and Hair Cell Fate; Where Do We Go From Here?

Matthew W. Kelley
National Institute on Deafness and Other Communication Disorders, NIH

The specification of precursor cells as mechanosensory hair cells is a key step during inner ear development and is also required as part of any regenerative response. While the formation of any cell type requires the actions of myriad genes and pathways, many studies have focused on transcription factors that can represent the tips of “signaling icebergs”. Over the course of the last 20 years, significant progress has been made in the identification of a group of transcription factors, including Atoh1, Pou4f3, and Gfi1, that play key roles in the early development of hair cells across vertebrate species and organ systems. The broad expression of these transcription factors emphasizes their importance for hair cell formation but also suggests that hair cell diversity is probably mediated through additional pathways. The development of single cell molecular profiling techniques should provide powerful new methods for characterizing and comparing unique hair cell types. As a first step, we used single cell RNA sequencing to examine transcriptional differences between inner and outer hair cells in the cochlea and Type I and Type II hair cells in the utricle. Comparisons of common and novel transcriptional pathways expressed in each cell type will provide insights regarding the specification of hair cell diversity.

Stereocilia Dynamics: Insights into Cytoskeleton and Membrane Organization

Chairs: A. Catalina Velez-Ortega & Ben Perrin

SYMP 57

New Tools for a Dynamic View of GPSM2-GNAI Function in Stereocilia

Anil Akturk; Amandine Jarysta; **Basile Tarchini**
The Jackson Laboratory, Bar Harbor ME

The hair bundle, the transduction compartment of sensory hair cells in the inner ear, is a highly organized array of stereocilia that adopt graded heights during development. In the mouse, postnatal stereocilia elongation is promoted by a protein complex brought to stereocilia tips by MYO15A that is thought to enhance monomeric actin incorporation into filaments there. Recently, we and others identified two new members of the “elongation complex”: the scaffolding protein GPSM2 and the inhibitory subunit of the heterotrimeric G protein,

GNAI (Gβi) (Tarchini et al, Development 2016; Mauriac et al., Nat. Commun. 2017; Tadenev et al., Curr. Biol. 2019). Interestingly, while GPSM2-GNAI depends on MYO15A for trafficking to stereocilia tips, these proteins show a unique distribution. They are first planar polarized at the apical membrane and label the expanding bare zone, a region devoid of protrusions that emerges before the bundle is formed. They then form a new module (along with WHRN), that is added to pre-existing MYO15A-EPS8 tip complexes, but only in the first row of stereocilia abutting the bare zone. Based on molecular and morphological evidence, we proposed that GPSM2-GNAI confers to the first row its unique tallest and non-transducing identity. To gain a better understanding of the dynamics of GPSM2-GNAI function, we generated HaloTag-Gpsm2 and Gnai3-Egfp knock-in mouse models. Preliminary evidence suggest that both fusion proteins recapitulate the dual subcellular localization observed with immunolabeling, and that these tags do not interfere with stereocilia elongation or hearing ability in young adults. While GNAI3-EGFP is produced endogeneously, HaloTag can self-conjugate to a variety of cell-permeable ligands. We anticipate that live imaging of inner ear explants using these complementary models will help clarify how GPSM2-GNAI regulate dynamic alterations of the cytoskeleton and apical membrane during hair bundle morphogenesis.

SYMP 58

Characterization of the Molecular Impact of Deafness Mutations in MYO3A

Laura K. Gunther; Joseph A. Cirilo; Christopher M. Yengo
Department of Cellular and Molecular Physiology, College of Medicine, Pennsylvania State University

Class III myosins are actin-based motors proposed to transport cargo to the stereocilia tips in inner ear hair cells and/or to participate in stereocilia length regulation, especially during development. MYO3A mutations are associated DFNB30, an autosomal recessive form of delayed onset deafness. Two dominant mutations in the MYO3A motor domain have been characterized in the literature, G488E and L697W. Biochemical and biophysical studies of purified MYO3A containing G488E suggest that this mutation may reduce the ability of MYO3A to localize to the stereocilia tips where length regulation is crucial. However, L697W localizes to actin protrusions more efficiently than WT MYO3A suggesting a completely different mechanism of impairment of stereocilia length regulation. We found that the L697W mutant slows in vitro motility 2-fold while it decreases ATPase more than 4-fold and increases actin affinity 2-fold. Thus, we hypothesize that the L697W mutation increases the MYO3A motor duty ratio, fraction of ATPase cycle myosin is bound to actin, which allows it to increase its residence time at the stereocilia tips and out complete its WT counterpart. Since L697W is a slower motor its presence impairs stereocilia length regulation. We examined the ADP release rate constant of L697W MYO3A and found that it was reduced 2-fold, which is consistent with the motility experiments and duty ratio hypothesis. We also found similar values for the maximum rate of ATP-induced dissociation from actomyosin monitored by light scattering. We are currently examining the residence time at the filopodia tips of COS7 cells using fluorescence recovery after photobleaching (FRAP). We have performed measurements of filopodia extension in L697W MYO3A containing filopodia and found that the extension rate is 2-fold slower than WT. Our overall hypothesis is that dominant mutations can impair stereocilia length regulation in two main ways, by enhancing stereocilia tip localization of an impaired MYO3A motor or reducing MYO3A associated cargo transport.

SYMP 59

Molecular Mechanisms that Shape the Stereocilia Actin Cytoskeleton

Jonathan E. Bird
Department of Pharmacology and Therapeutics, University of Florida, Gainesville, FL, USA

The architecture, mechanical strength and longevity of the hair bundle is directly set by the actin cytoskeleton, which forms a rigid structural foundation within individual stereocilia. Emerging evidence indicates that the stereocilia actin core is highly plastic, not only during development, but also in response to mechano-transduction. How stereocilia actin polymerization is regulated in these contexts is unknown, but a molecular “toolbox” of key proteins has been identified. Here we show that myosin 15, a component of this toolbox, directly controls actin polymerization and further demonstrate how this fundamental activity is regulated to drive hair bundle development and maintenance.

SYMP 60

Role of Myosin XV Isoforms in the Mechanotransduction-dependent Remodeling of the Stereocilia Cytoskeleton

Ana I. López-Porras; Gregory Frolenkov; **A. Catalina Vélez-Ortega**
Department of Physiology, University of Kentucky

Stereocilia, the inner ear sensory organelles, are modified microvilli with mechanotransduction channels located at their tips. In normal conditions, only the tips of auditory hair cell stereocilia exhibit actin remodeling.

However, changes to the resting influx of calcium through mechano-electrical transduction (MET) channels can significantly impact the shape and height of transducing stereocilia, indicating the presence of activity-dependent plasticity in the stereocilium actin core. Given that myosin XV is crucial for the normal growth and maintenance of stereocilia, we explored its role in the MET-dependent remodeling of the stereocilia cytoskeleton. We found that, in the absence of one or all isoforms of myosin XV, the stability of the stereocilia actin cytoskeleton still requires a resting MET current. Shaker-2 mice have a missense mutation in the motor domain of myosin XV which prevents all isoforms from reaching and elongating the stereocilia bundles. However, cells from shaker-2 mice do exhibit MET currents during their early postnatal development. We found that the blockage of the MET channels in cochlear explants from shaker-2 mice leads to the thinning and shortening of stereocilia in the auditory hair cells. Myo15ΔN mice lack the long isoform of myosin XV yet develop auditory hair cells with MET currents and stereocilia bundles of normal heights and staircase arrangements. However, after MET channel blockage or an increase in intracellular calcium buffering, auditory hair cells from Myo15ΔN mice exhibit faster rates of stereocilia shortening than heterozygous or wild type controls. These results indicate that the molecular machinery involved in the calcium-dependent stability of the stereocilia cytoskeleton does not rely solely on myosin XV. However, the molecular mechanisms that lead to stereocilia cytoskeleton instability after changes in intra-stereocilia calcium concentrations in the absence of myosin XV remain to be explored.

Supported by NIDCD/NIH (R01DC014658 and R21DC017247).

SYMP 61

Mechanotransduction-dependent Control of Stereocilia Dimensions and Row Identity in Inner Hair Cells

Jocelyn F. Krey[1]; Paroma Chatterjee[1]; Rachel A. Dumont[1]; Dongseok Choi[2]; Jonathan E. Bird[3]; Peter G. Barr-Gillespie[1]
[1]Oregon Hearing Research Center & Vollum Institute, Oregon Health & Science University, Portland, Oregon, USA; [2]OHSU-PSU School of Public Health, Oregon Health & Science University, Portland, Oregon, USA; Graduate School of Dentistry, Kyung Hee University, Seoul, Korea; [3]Department of Pharmacology and Therapeutics, University of Florida, Gainesville, FL, USA

Actin-rich structures like stereocilia and microvilli are assembled with precise control of length, diameter, and relative spacing. We found that developmental widening of the second-tallest stereocilia rank (row 2) of mouse inner hair cells correlated with the appearance of mechanotransduction. Correspondingly, Tmc1KO/KO;Tmc2KO/KO or TmieKO/KO hair cells, which lack transduction, have significantly altered stereocilia lengths and diameters. EPS8 and the short splice isoform of MYO15A, identity markers for row 1 (tallest), lost their row exclusivity in transduction mutants, a result that was mimicked by block of transduction channels. Likewise, the heterodimeric capping protein subunit CAPZB and its partner TWF2 lost their row 2 tip localization in mutants, and GNAI3 failed to accumulate at row 1 tips. Redistribution of marker proteins was accompanied by increased variability in stereocilia height. Transduction channels thus specify and maintain row identity and control addition of new actin filaments to increase stereocilia diameter.

SYMP 62

Refining Stereocilia Shape by Severing Actin Filaments

Jamis McGrath; **Benjamin Perrin**
Indiana University - Purdue University Indianapolis

While the majority of actin in the stereocilia core is highly stable, a population at stereocilia tips is continuously turned over. The balance of assembly and disassembly dictates stereocilia size and seems to depend on protein complexes that are specific to the tallest or shorter rows of the bundle, as well as mechanotransduction and tip link integrity. We found the actin severing proteins ADF and cofilin localize to the tips of shorter rows and are required to control stereocilia length, width, and tip shape. Disrupting mechanotransdution changes ADF/cofilin localization and activity, identifying actin severing as a downstream mechanism for controlling actin dynamics.

SYMP 63

Voltage and Calcium Modulate Stereocilia Membrane Fluidity: Implications Regarding Hair Cell Mechanotransduction

Shefin George[1]; Charles Steel[2]; Anthony Ricci[3]
[1]Department of Otolaryngology – Head and Neck Surgery, Stanford University; [2]Department of Mechanical Engineering, Stanford University; [3]Department of Otolaryngology and Department of Molecular and Cellular Physiology, Stanford University

Voltage and calcium modulation of mechanically-gated (MET) ion channel open probability (Popen) in mammalian cochlear hair cells is postulated to involve the lipid bilayer (Peng et al. 2016). We combined whole-cell patch-clamp with two-photon FRAP (fluorescence recovery after photobleaching) in rat inner hair cells to investigate the

role of calcium and voltage on stereocilia membrane mechanics. Two-photon FRAP confined photo-bleaching to within 2 µm of the stereocilia tip. Diffusivity of membrane dye Di-3-ANEPPDHQ was determined by fitting the fluorescent recovery time course to a one-dimensional diffusion model of the cylindrical stereocilia.

Intracellular Ca2+ buffering (10 mM BAPTA vs 0.1 mM BAPTA) and low extracellular Ca2+ (20 µM vs 2 mM) resulted in slower membrane diffusivity and an increase in resting Popen, suggesting a mechanism in which Popen modulation occurs through the membrane lipid. These data support the conclusion that reducing lipid diffusivity increases MET channel open probability. Prolonged depolarization resulted in faster diffusivity, suggesting that the gradual decrease in resting Popen during prolonged depolarization could be through a lipid-based mechanism, which reduces the force applied to MET channels. Mechanisms regulating diffusivity are presently under investigation.

This work is supported by NIDCD RO1 DC003896 and NIDCD RO1 DC014658 to AJR. Our thanks for core support from the Stanford Initiative to Cure Hearing Loss through generous gifts from the Bill and Susan Oberndorf Foundation.

SYMP 64

LOXHD1 is required for Mechanotransduction and Lipid Dynamics in Mature Hair Cells

Alix Trouillet[1]; Shefin George[1]; Katharine Miller[1]; Noor Ali[1]; Charles Steel[2]; Anthony Ricci[3]; **Nicolas Grillet**[1]
[1]Department of Otolaryngology – Head and Neck Surgery, Stanford University; [2]Department of Mechanical Engineering, Stanford University; [3]Department of Otolaryngology and Department of Molecular and Cellular Physiology, Stanford University

Background
Here we investigated the molecular function of the LOXHD1 gene that we previously linked to an autosomal-recessive form of hearing loss in mice and human (Grillet N., AJHG, 2009). LOXHD1 encodes a protein made of 15 PLAT (Polycystin/Lipoxygenase/Alpha-Toxin) domains, known in other proteins to bind lipid and proteins. LOXHD1 is detected with an antibody against PLAT11/12 in hair cells at a high level only after the first postnatal week. The LOXHD1 protein localizes in the stereocilia, at the interface between the membrane and the actin-cytoskeleton. The molecular function of LOXHD1 is unknown. We hypothesize that LOXHD1 is necessary for the hair bundle functionality by forming a physical link between the membrane and the actin-core of the stereocilia.

Methods
To test this hypothesis, we studied two mouse strains carrying mutations in the LOXHD1-PLAT10. We analyzed the auditory phenotype (ABR, DPOAE, CM), the stereocilia structure (SEM), the IHC mechanosensitivity (patch-clamp), and the stereocilia membrane dynamics (FRAP).

Results
We found that, while IHC MET of Loxhd1-mutants animals is comparable to control at P7, the amplitude of the MET current is drastically reduced by P11. Despite this strong MET phenotype, the hair bundle organization is not affected, and the number of tip-links not decreased. As LOXHD1 localizes below the stereocilia surface, we asked if the stereocilia membrane dynamics were affected by LOXHD1 expression. For this purpose, we measured lipid diffusivity in single stereocilia.

In control, we found the lipid diffusivity to be stable between P7 and P11 in both the taller and middle rows. However in both Loxhd1 mutants, the lipid diffusivity was drastically increased between P7 and P11, in particular in the tallest row.

Conclusions
Here, we identify a protein required for hair cell MET, which is localized at a distance from the mechanotransduction complex. LOXHD1 is the first stereocilia protein identified as affecting the stereociliary-membrane dynamics. We propose that LOXHD1 acts from or next to the membrane of mature hair cell stereocilia to modulate coupling channel gating to stereocilia displacement.

Our results identify a novel MET-regulatory pathway occurring at a distance from the MET machinery, and which underlies the hearing loss of LOXHD1/DFNB77 patients.

Acknowledgements
The work was funded by NIDCD grant RO1 DC016409-01A1 for N.G., and NIDCD RO1 0003896 for A.J.R. Our thanks also for core support from the Stanford Initiative to Cure Hearing Loss, through generous gifts from the Bill and Susan Oberndorf Foundation and the Eberts family.

Traditional Psychophysics and Sound Perception

PD 49

Speech in Noise Perception in Childhood: Role of Modulation Filtering and Processing Efficiency

Irene Lorenzini[1]; Christian Lorenzi[2]; **Laurianne Cabrera**[1]
[1]CNRS- Université Paris Descartes; [2]Full Professor

The present study explored the relationship between the capacity to detect amplitude modulation (AM) and speech-in-noise (SIN) identification during childhood. Auditory models suggest that AM detection is not only constrained by the filtering properties of sensory mechanisms in the modulation domain, but also by "processing efficiency", the ability to make optimal use of the available sensory information. Behavioral tasks were designed to assess the development of modulation filtering and processing efficiency of AM cues and its relationship with SIN between 6 and 8 years of age.

Eighty-two children first completed a 2-alternative-forced choice task (AFC) using an adaptive procedure estimating AM detection thresholds for an 8-Hz sinusoidal AM. In this task, the AM carrier was varied in 2 conditions to assess: i) AM sensitivity using a 500-Hz sine tone (No Masking), and ii) AM masking using a 4-Hz wide narrowband noise centered at 500 Hz with small envelope fluctuations (Masking). Second, a "double-pass technique" evaluated the consistency of children's responses for AM detection using a constant-stimuli procedure. Then, AM detection performance in the Masking condition was measured at threshold for 200 trials repeated twice (2 passes) using a 2-AFC task. Percentage of Correct AM detection in each pass (PC) and Percentage of Agreement between the 2 passes (PA) were used to estimate within-listener consistency, a proxy of AM processing efficiency related to internal noise. Finally, children completed an XAB adaptive task measuring consonant identification thresholds in noise using fricatives and stops contrasting over three phonetic features (voicing, place, and manner). Additionally, children completed two standardized tests assessing receptive vocabulary and non-verbal reasoning.

Results showed that AM detection thresholds obtained with both carriers did not significantly improve from 6 to 8 years (ps > .37) and all children were similarly affected by AM masking (p < .001). When children were tested at threshold, both PC and PA increased with age (ps = .03). Thus, AM filtering is not affected by age, but aspects of processing efficiency are. Regarding SIN, thresholds significantly improved with age (p = .02) and were affected by phonetic feature (p < .001). Backward regression analyses showed that AM masking associated with vocabulary scores significantly predicted data for Manner (8.9%), PC and PA predicted to a small extent SIN data for Voicing (adjusted R^2 = 5.8%) and vocabulary predicted data for Place (5.1%). Overall, processing efficiency, modulation filtering and linguistic level determine SIN identification in childhood.

PD 50

The Roles of Long-Term Envelope Regularity and Efferent Activation in the Simultaneous Masker Phase Effect

Hisaaki Tabuchi[1]; Bernhard Laback[2]
[1]University of Innsbruck, Department of Psychology; [2]Austrian Academy of Sciences, Acoustics Research Institute

Simultaneous masking of a target tone by a harmonic multi-tone masker depends on the masker's phase curvature, known as the masker phase effect (MPE). The masker's phase curvature is thought to determine the amount of peakedness (modulation) of the masker representation at the output of cochlear filters where multiple masker components interact. Both listening in the temporal dips of an internally modulated masker and fast cochlear compression, causing the masker excitation level to be lower for a modulated *re* shallow masker, have been suggested as underlying mechanisms. In this study, the contributions of these mechanisms and the potential influence of long-term analysis of the stimulus envelope regularity were explored.

In experiment 1, the duration of a wideband masker and target tone were covaried and presented without or with an on-frequency precursor tone intended to reduce compression by efferent activation. Without the precursor, simultaneous MPEs increased with increasing stimulus duration, suggesting multiple-looks like temporal integration of target information across masker dips, and not supporting an explanation based on efferent control of compression. The presence of a precursor decreased the MPE and prevented the duration effect. This suggests either the reduction of compression due to efferent activation or the disturbance of long-term envelope regularity analysis given the unmodulated envelope of the precursor.

In experiment 2, a short target was presented towards the beginning, the end, throughout, or following a long fixed-duration harmonic-complex masker with phase curvatures causing either a modulated or shallow internal envelope. All of these temporal configurations were tested without a precursor for two masker levels and bandwidths. The MPE was constant across the temporal configurations, and depended on the masker level, again not consistent with a role of efferent compression control.

Experiment 3 used a short target-and-masker stimulus and studied the effects of different types of precursor or postcursor. Postcursors or precursors were an on-frequency pure tone or a wideband harmonic complex with

phase curvatures causing either a modulated or shallow internal envelope. Compared to a reference condition without pre/postcursor, the MPE largely decreased with the presence of either a precursor or a postcursor if it was a pure tone or shallow-envelope harmonic complex. In contrast, a modulated harmonic-complex precursor produced some enhancement of the MPE.

Overall, the three experiments suggest a role of fast compression, probably no important role of its efferent control, and the influence of long-time temporal regularity analysis in simultaneous masking by modulated maskers.

[Austrian Science Fund (FWF), P24183-N24]

PD 51

Are a Sound and the Background in Which It Is Presented Perceived Simultaneously?

Beverly A. Wright[1]; Ruijing Ning[1]; Victoria Smith[1]; Julia R. Curato[1]; Matthew B. Fitzgerald[2]
[1]Northwestern University; [2]Stanford University

Are a sound and the background in which it is presented perceived simultaneously? To address this question, we presented a brief clearly audible probe at random times before, during, or after a longer-duration noise and asked normal-hearing adults to judge whether that probe was presented in noise or in silence. The task was either to mark the perceived presentation time of the probe on a schematic diagram that depicted the noise and the silence preceding and following it, or to judge whether the probe occurred inside (during) or outside (before or after) the noise. If the probe and the background (noise or silence) are perceived simultaneously--as a probe-in-noise or a probe-in-silence—all of the judgments should be correct. In contrast, listeners frequently misperceived the background in which the probe was presented. Brief (20-ms) probes presented ~50 ms before the noise were perceived to have occurred in the noise on 50% of trials, regardless of the noise duration (150 to 750 ms). Probes presented ~50-200 ms before the end of the noise were perceived to have occurred in the silence after the noise on 50% of trials, with the magnitude of the effect increasing with increasing noise duration. Similar results were obtained with a range of probe durations (20 to 200 ms) and with various combinations of probe and masker spectra. Overall, listeners perceived the probes as having occurred later than they actually had, and frequently misperceived them as having occurred in the background (noise or silence) that was presented after, rather than during, the probe. These misperceptions suggest that the percepts of the probe and the background are not processed simultaneously, but rather are processed separately and sequentially, and that these separate percepts are then ultimately recombined. By this account, the lag in the perceived temporal position of the probe reflects, in part, the time it takes to process the probe and then to switch to the processing of the background, and the final percept of the probe in the background reflects the combination of the memory of the recently identified probe and the newly identified background. These results are consistent with the idea that listeners cannot attend to two auditory objects simultaneously. They add to that idea the possibility that this limitation in attention can distort the perceived temporal relationship between those objects.

PD 52

Probing Spectrotemporal Modulation Processing to Better Understand Supra-Threshold Hearing Deficits

Emmanuel Ponsot; Peter Neri
École Normale Supérieure, Paris, France

The origins of the variability between individuals with similar audiograms for understanding speech in noisy environments still remain poorly understood. Solving this problem requires being able to disentangle the respective contributions of the supra-threshold mechanisms recruited along the auditory pathway to process complex signals. Interestingly, recent works have shown that the ability of listeners with hearing loss to detect a spectrotemporal modulation (STM) signal – a noise whose envelope is jointly modulated in time and frequency like in speech - correlates with their SPiN understanding scores even after accounting for their differences in audibility. STMs thus provide an integrated model to assess the supra-threshold mechanisms underlying SPiN deficits. Yet, at present, it remains unknown how STMs are processed by the human auditory system, and how this processing varies between individuals. In order to provide a clear computational understanding of STM processing in both normal-hearing (NH) and hearing-impaired (HI) listeners, we developed a novel methodological framework that combines psychophysical reverse-correlation deployed in the modulation domain with modeling. We first deployed this framework in a STM detection task, where listeners had to detect a specific STM target embedded in other masking STMs. Using system identification tools, we found that NH and HI individuals relied on average on a similar linear-non-linear processing strategy, monitoring the output of non-directional band-pass filters deployed in the STM space by a MAX operation. However, contrary to the NH group showing fine-tuning to the STM target parameters, the filters of the HI group were erroneously biased toward temporal modulations. Simulations revealed that a modulation filter-bank

model could readily account for NH listeners' strategy, and that the overall shift toward temporal modulations observed in the HI group could be accounted for by an increase in cochlear filters' bandwidths. However, beyond these group-level observations, there was a significant variability among individuals within each group. This variability was even further enhanced in a STM discrimination task, where listeners had to discriminate between upward and downward STMs embedded in masking STMs (surrounded by additional interfering modulations in some trials). Critically, this variability imposes computational constraints that could be used in the development and tuning of supra-threshold auditory models. By connecting interindividual differences returned from such measurements with SPiN understanding scores, we anticipate that this joint experimental-modeling approach will be helpful to identify the peripheral and central components underlying supra-threshold hearing deficits.

PD 53

A Population of Adults with Normal Hearing Sensitivity but Significant Noise Exposure and/or Tinnitus exhibit Speech Recognition Deficits at High Levels and Weak Middle-Ear-Muscle-Reflexes

James Shehorn[1]; Olaf Strelcyk[2]; Pavel Zahorik[3]
[1]Heuser Hearing Research Center; [2]Sonova; [3]Dept. of Otolaryngology and Communicative Disorders & Dept. of Psychological and Brain Sciences, Univ. of Louisville; Heuser Hearing Institute, Louisville, KY

Although it has been hypothesized that cochlear synaptopathy in humans may result in deficits for speech perception in complex listening environments, there is currently little evidence to support this claim. Previous studies have typically measured speech recognition in noise at conversational levels. However, there is evidence that noise exposure may selectively degrade the encoding of high-level sounds due to the susceptibility of low-spontaneous rate auditory nerve fibers to noise damage. Here we demonstrate decreasing speech recognition as a function of level (from 75 to 105 dB SPL) and reduced middle-ear muscle reflexes (MEMR) in listeners with normal audiograms who report noise exposure history or tinnitus and self-reported difficulties. We also show that contralateral MEMR magnitude is related to speech recognition specifically for participants with noise exposure history. These methods and results show promise for the detection in humans of cochlear synaptopathy and functional deficits due to noise exposure.

PD 54

Effects of Age on Behavioral and Electrophysiological Measures of Cochlear Synaptopathy in Humans

Samuele Carcagno[1]; **Christopher J. Plack**[2]
[1]Lancaster University; [2]The University of Manchester

Background

Histological studies indicate that in rodents and humans cochlear synaptopathy (CS) occurs as a result of aging. CS is thought to affect mainly low-spontaneous rate (SR) fibers and may result in auditory deficits at high stimulus levels. Hence, comparing auditory function at low and high levels should provide a differential measure of the effects of CS.

Methods

One hundred and two listeners (age range: 19-74) with audiometric thresholds within 40 dB HL up to 4 kHz were tested. Behavioral tasks focused on auditory temporal coding, and included amplitude modulation (AM) detection, frequency/F0 discrimination, and interaural phase-difference detection. Stimuli were presented at 40 and at 80 dB SPL. Cognitive performance was also assessed. Click-evoked auditory brainstem responses (ABRs) at 80 and 105 dB ppeSPL were collected in quiet, or with highpass-filtered noise (3.5-kHz cutoff). Frequency-following responses (FFRs) were recorded to 0.6 and 2 kHz, 75 dB SPL, pure tones, amplitude modulated at 100 Hz with modulation depths of 70% and 100%, in the presence of a highpass-filtered noise (3-kHz cutoff). For both ABRs and FFRs the highpass noise level was selected to completely mask basal cochlear contributions to the response, thus minimizing the effects of age-related audiometric losses above 4 kHz.

Results

Performance on several behavioral temporal coding tasks declined with age, even after controlling for absolute threshold, and cognitive ability. However, only 50-Hz AM detection showed a significant high vs. low level performance difference consistent with CS. The ratio of wave I amplitude in the high-level condition to that in the low-level condition showed a significant age-related decline in quiet but not in the presence of highpass masking noise. FFR amplitude at the modulation frequency for the low-frequency carrier showed marked age-related declines for both modulation depths. If CS affects mostly low-SR fibers, the slope of FFR level as a function of modulation depth should become steeper with age. However, no significant age-related differences were found for this differential measure at either carrier frequency.

Conclusions
For several conditions, performance on temporal coding tasks, and ABRs and FFRs, showed robust age-related declines even after controlling for audibility and other relevant covariates. However, overall there was only weak evidence for a differential decline at high levels as predicted by the low-SR CS hypothesis.

Support
This work was supported by the Biotechnology and Biological Sciences Research Council (BB/M007243/1). Author CP is supported by the NIHR Manchester Biomedical Research Centre.

PD 55

Sound-Offset Sensitivity in Individuals with Speech-in-Noise Perception Difficulties

Fatima Ali[1]; Stuart Rosen[2]; Doris E. Bamiou[3]; **Jennifer F. Linden**[4]
[1]Ear Institute, University College London; [2]University College London; [3]The Ear Institute, University College London; Department of Neuro-otology, University College London Hospitals; NIHR UCLH BRC Deafness and Hearing Problems Theme, London, UK;; [4]Ear Institute, University College London; Department of Neuroscience, Physiology and Pharmacology, University College London; UCLH-NIHR BRC Deafness and Hearing Problems

Difficulty perceiving speech in noisy backgrounds is a common symptom of developmental disorders in humans, and often occurs without any apparent loss of peripheral hearing. Recent studies in a mouse model of human developmental disorders reported an auditory brain abnormality specific to the processing of sound offsets (Anderson & Linden, 2016). Sound offsets provide information relevant to auditory scene analysis and speech discrimination, and therefore may play an important role in speech-in-noise perception. However, there are no validated psychoacoustical tests for assessing sensitivity to sound offsets in human subjects. We designed a psychoacoustical test battery to assess performance on tasks thought to depend on sound-offset sensitivity, including gap detection, duration discrimination, forward masking, and discrimination of vowel-consonant-vowel (VCV) stimuli in noise. Here, we report results of these psychophysical tests in participants with and without speech-in-noise perception difficulties. All participants had normal peripheral hearing sensitivity on standard audiometric tests. We recruited participants with speech-in-noise difficulties from an Auditory Processing Disorder support group and used a Speech, Spatial and Qualities of Hearing Scale (SSQ; Gatehouse & Noble, 2004) questionnaire to confirm self-reported difficulty with speech perception in noisy situations. We then tested: (a) gap-detection thresholds; (b) duration discrimination thresholds for 'filled' versus 'empty' intervals (i.e., time elapsed between onset and offset of a noise or between two successive clicks); and (c) detection thresholds for a click following a noise at various delays between the end of the noise and the click. We also tested discrimination of VCV stimuli using 16 consonants in 3 vowel environments and 5 varying levels of background multi-talker babble noise. In participants with self-reported speech-in-noise perception difficulties, we found significant impairments in consonant discrimination in noise, and differences compared to controls in the putative psychophysical measures of sound-offset sensitivity. We discuss the variation of offset sensitivity in normal and abnormal temporal processing. Our findings suggest that people with speech-in-noise perception difficulties may also have abnormal sensitivity to sound offsets.

Acknowledgements
This research was co-funded by EPSRC (1644123), MRC (MR/P006221/1), Action on Hearing Loss (G77), and the NIHR UCLH BRC Deafness and Hearing Problems Theme.

References
Anderson, L.A. & Linden, J.F. (2016) Mind the gap: two dissociable mechanisms of temporal processing in the auditory system. *Journal of Neuroscience*, 36 (6), 1977-95.

Gatehouse, S. & Noble, W. (2004) The Speech, Spatial and Qualities of Hearing Scale (SSQ). *International Journal of Audiology*, 43, 85–99.

PD 56

Selective Sensory Gating of Behaviorally Significant Sounds during Sleep

Philipp van Kronenberg[1]; Linus Milinski[2]; Livia de Hoz[1]
[1]Charité - Universitätsmedizin Berlin; [2]University of Oxford

Sleep is essential for the maintenance of physiological processes. At the same time, it poses a risk as a result of the associated immobility and partial sensory disconnection. The auditory system remains an important link with the surrounding environment during sleep such that a well-balanced sensory gating of auditory stimuli is essential for survival. Here we propose a model to investigate sensory gating of auditory stimuli during sleep. We conditioned mice to a frequency-modulated sound, by associating it with a loud noise together with an air puff, both of which the mice could avoid by leaving the conditioned corner. Recordings of the EEG and EMG patterns on the days before and during conditioning allowed us to distinguish

between wakefulness, non-rapid eye movement (NREM) sleep, and REM sleep. On the days before conditioning, mice were exposed to a control sound during sleep, to assess the general effect that sound has on sleep. In subsequent days, on sleep sessions that followed conditioning we presented the conditioning sound or a second control sound. We used the power of the EEG signal at the characteristic frequency band for each sleep state (NREM: 1-4 Hz; REM: 6-10 Hz) as our main readout of sleep modulation. The first control sound did not elicit any changes in the EEG patterns, suggesting that sounds without any behavioral relevance do not modulate sleep. The conditioning sound elicited the strongest changes during NREM sleep and was the only sound that elicited significant changes during REM sleep. This suggests that behaviorally relevant sounds are selectively gated during all sleep stages. The second control sound elicited significant but weaker EEG pattern changes during NREM sleep than the conditioned sound, implying certain sound generalization during NREM. A small fraction of mice did not learn the conditioning paradigm and showed a lack of EEG pattern changes to all presented sounds, indicating that learning the meaning of the sound plays a causal role in the development of selective sensory gating. Overall, the results suggest that mice can discriminate behaviorally relevant sounds during sleep and the paradigm offers a great opportunity to study auditory sensory gating.

Coming to Our Senses: Vestibular Research- From Molecules to Systems- Commonalities and Differences with the Auditory System

Chairs: Gwenaelle S. Geleoc & Hong Zhu

SYMP 65

Introduction: What Binds and Distinguishes Vestibular and Auditory Research?

Ruth Anne Eatock
University of Chicago

Research at the level of inner ear transduction and development exploits both sides of the vestibular-auditory boundary. Systems-level studies, in contrast, are siloed, reflecting the distance between the occult impact of head motion on behavior and the highly social sense of hearing. Here we introduce the symposium by reviewing some common and distinct questions motivating vestibular and auditory research.

SYMP 66

Genetic of Audio-Vestibular Disorders

Jose Antonio Lopez-Escamez[1]; Alvaro Gallego-Martinez[2]; Pablo Roman-Naranjo[2]; Teresa Requena[3]
[1]Otology and Neurotology Group CTS495 at the Center for Genomics and Oncology Research (GENyO) at the University of Granada; [2]Otology & Neurotology Group CTS495, Department of Genomic Medicine, GENYO - Centre for Genomics and Oncological Research – Pfizer/University of Granada/ Junta de Andalucía, Spain; [3]Centre for Discovery Brain Sciences, Edinburgh Medical School: Biomedical Sciences, University of Edinburgh, Edinburgh, UK

The genetic underpinnings of audio-vestibular disorders are starting to be deciphered. A growing number of non-syndromic monogenic sensorineural hearing loss (SNHL) disorders are expanding the cochlear phenotype to a cochlea-vestibular phenotype in humans. Meniere's disease (MD) is now considered a set of rare disorders with an overlapping audio-vestibular phenotype and additional comorbidities such as migraine or autoimmune disorders. Despite of this extended phenotype in MD, a burden of rare missense variants in certain SNHL genes including GJB2, USH1G, SLC26A4, ESRRB, and CLDN14 has been found in sporadic and familial cases that suggest a multiallelic model of common and rare variants interacting that will explain incomplete penetrance and variable expressivity in familial MD. Moreover, we have found an enrichment of damaging missense variants in the NTN4 gene supporting axonal guidance signaling as a novel pathway involved in sporadic MD.

Funding
JALE is partially funded by Segovia Arana Grant INT18/00031 from ISCIII.

References

1. Gallego-Martinez A, Requena T, Roman-Naranjo P, Lopez-Escamez JA. Excess of Rare Missense Variants in Hearing Loss Genes in Sporadic Meniere Disease. Front Genet. 2019;10:76.

2. Gallego-Martinez A, Requena T, Roman-Naranjo P, May P, Lopez-Escamez JA. Enrichment of damaging missense variants in genes related with axonal guidance signaling in sporadic Meniere Disease. J Med Genet 2019 (in press)

SYMP 67

How Mammalian Vestibular Hair Cells Differ From Auditory Hair Cells

Katie Rennie
University of Colorado

In mammals, specialized outer and inner hair cells in the cochlea and type I and type II hair cells in the vestibular organs transform mechanical signals into electrical potentials using unique mechanisms. Hair cell properties are tonotopic within the cochlea and emerging

data support topographic differences in hair cells across vestibular epithelia. During embryonic development, hair cells arise from progenitor cells and acquire clear-cut hair bundle configurations and mechanotransduction channels tailored to sensory function. A variety of basolateral voltage- and ligand-gated ion channels and synaptic proteins are added to distinct hair cell populations conferring zonal-specific filtering properties to achieve hearing and balance sensation.

SYMP 68

Role of Tmc1 and Tmc2 Channels in Hair Cells of the Vestibular Organs

John Lee; Gwenaelle S. Geleoc
Boston Children's Hospital & Harvard Medical School

Transmembrane channel-like Tmc1 and Tmc2 are expressed in auditory and vestibular hair cells of the inner ear where they form the pore of the mechanotransduction channel. While Tmc2 is only transiently expressed in the developing cochlea, its expression persists in vestibular hair cells. To determine the role played by Tmc2 in developing and mature vestibular organs, we performed hair cell and neuronal physiology assays along with behavior assessment of mice lacking Tmc2. Our data reveal specific contributions of Tmc2 to vestibular hair cells and balance function.

SYMP 69

The Unusual Hair Cell – Calyx Terminal Synapse in the Vestibular Periphery

Soroush Sadeghi[1]; Elisabeth Glowatzki[2]
[1]University of Buffalo, NY, USA; [2]Johns Hopkins School of Medicine, Baltimore, MD, USA

Vestibular sensors in the inner ear of amniotes contain a unique afferent terminal – the calyx – that completely covers the basolateral walls of type I hair cells. Accumulation of glutamate, potassium ions, and hydrogen ions in this closed synaptic space results in a non-quantal synaptic transmission mechanism that is used for fast signal transmission. Traditional quantal synaptic events are also present, with unusually slow kinetics due to glutamate accumulation and spillover. These properties are in contrast to the fast and large synaptic events that are required for precise timing of information transmission by auditory afferents. Such differences will be discussed considering differences in the function of the two systems.

SYMP 70

The New Vestibular Stimuli: Sound and Vibration

Ian S. Curthoys[1]; J. Wally Grant[2]; Alan Brichta[3]; Rebecca Lim[4]
[1]University of Sydney, Australia; [2]Department of Engineering Science and Mechanics, Virginia Tech, Virginia, USA; [3]School of Biomedical Sciences and Pharmacy, University of Newcastle, Australia; [4]School of Biomedical Sciences and Pharmacy, Unveristy of Newcastle, Australia

Sound and vibration test vestibular as well as auditory function. Irregular otolithic afferents show activation with highly precise phase locking to narrow phase bands of high frequency (>1000Hz) sound and vibration. The hair bundles of type I receptors on which these afferents synapse at the striola are tenuously attached to the otoconial membrane, so fluid displacement can deflect the hair bundles. The synaptic cleft between type I receptors and the calyx ending is unique in being rich in potassium which may be responsible for the high precision, high frequency phase locking, allowing fast responses to the onset of vestibular stimuli.

SYMP 71

Single afferent recording of vestibular responses to acoustic stimuli

Hong Zhu; Wu Zhou
University of Mississippi Medical Center

Sound-evoked vestibular myogenic potentials recorded from the sternocleidomastoid muscles (the cervical vestibular-evoked myogenic potential or cVEMP) and the extraocular muscles (the ocular VEMP or oVEMP) have been widely used in clinical assessment of vestibular function. To provide the neural basis for developing discriminative VEMP testing protocols, we employed single vestibular afferent recording technique to examine the extent to which air-conducted tone bursts differentially activate the five vestibular end organs. Our results demonstrated that both semicircular canals and otoliths can be activated by sound. However, specific combinations of sound parameters can be used to achieve selective assessment of otolith and canal functions.

Gene Expression and Regulation

PD 57

Comparing Mouse and Human Fetal Cochlear Development with Single Cell Analysis

Kevin Shengyang Yu; Stacey Frumm; Jason Park; Katharine Lee; Daniel Wong; Lauren Byrnes; Sarah Knox; Julie Sneddon; **Aaron Tward**
UCSF

Cochlear development requires complex interactions of multiple cell types throughout key developmental time points. Mice and other animal models have been critical in understanding cochlear development, however knowledge of human cochlear development is much more rudimentary. In this study, we aim to compare the cochlear gene expression profiles of mouse development to human development. We dissociated mouse cochlea from 5 developmental time points (E12.5, E14.5, E16.5, E18.5 and P2) and 5 time points from fetal human cochlea (gestational age 15, 17, 18, 23, and 24 weeks) and performed single cell RNA-sequencing through the 10x Genomics platform. Using the CellFindR clustering algorithm, we identified distinct populations of cells from each time point and from each organism. The gene expression of these groups such as the hair cells, supporting epithelium, fibrocytes, melanocytes and Schwann cells were compared across the time points and across mouse versus human. For groups such as hair cells, the developmental trajectories in the human cochlea were remarkably similar to mouse hair cell maturation, albeit on a different time scale. Following marker genes for hair cells, epithelial cells and fibrocytes, we extrapolate the 15 week fetal human development is most similar to past the E16.5 mouse data while most of the human data beyond 17 weeks is past our latest P2 mouse timepoint. We did observe, however, that the timing of maturation of different lineages within the cochlea was not synchronous between mice and humans. This emphasizes that even at the molecular level, most critical steps in the development of the human cochlea occur in utero compared to the development of the mouse cochlea that continues after its birth. Overall, this work serves as a roadmap for understanding human the molecular events governing human cochlear development.

PD 58

RNA-seq Profiling and Co-expression Network Analysis of lncRNAs and mRNAs Reveal Novel Pathogenesis of Noise-induced Hidden Hearing Loss

Wei Wei[1]; Xi Shi[2]; Wei Xiong[2]; Lu He[3]; Shusheng Gong[2]; Ke Liu[3]; Xiulan Ma[4]

[1]Department of Otolaryngology-Head and Neck Surgery, Shengjing Hospital, China Medical University; [2]Department of Otolaryngology-Head and Neck, Beijing Friendship Hospital, Capital Medical University; [3]Department of Otolaryngology-Head and Neck Surgery, Beijing Friendship Hospital, Capital Medical University; [4]Department of Otolaryngology-Head and Neck, Shengjing Hospital, China Medical University

Long noncoding RNAs (lnRNAs) mediate essential epigenetic regulation in a wide range of biological processes and diseases. In this study, we explored the dynamic changes in lncRNA and mRNA expression in mice cochlear tissues in the first time of noise exposure (NE-1st) group, i.e. noise-induced hidden hearing loss (NIHHL) model, the second time of noise exposure (NE-2nd) group, i.e. noise-induced hearing loss (NIHL) model and control group using high throughput screening technology and co-expression network analysis. We identified 71 lncRNAs and 290 mRNAs were specifically expressed in the NE-1st Group, i.e. NIHHL model and co-expression network was built using co-expression of these lncRNAs and mRNAs. Followed by a further KEGG analysis showed that adrenergic signaling pathway including mRNA *GNAS*, mRNA *Atf2* and its upstream lncRNA *Sept7,* lncRNA *Skt39* was the key pathway in the process of NIHHL and they were also validated. Our findings give us a fresh insight into the novel pathogenesis of NIHHL which might provide potential therapeutic targets.

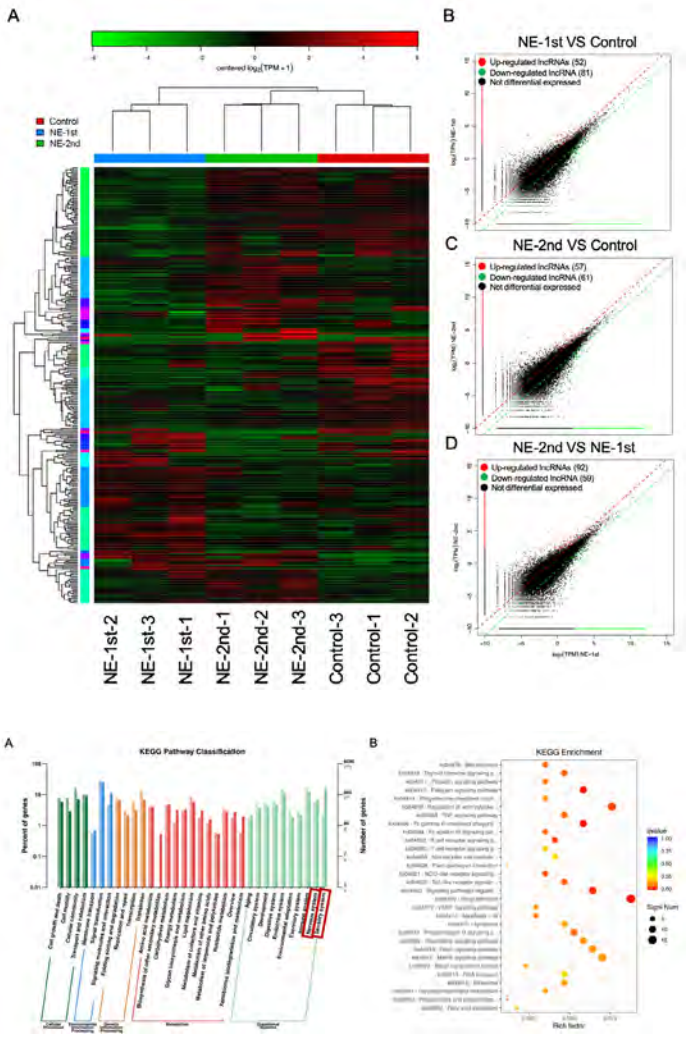

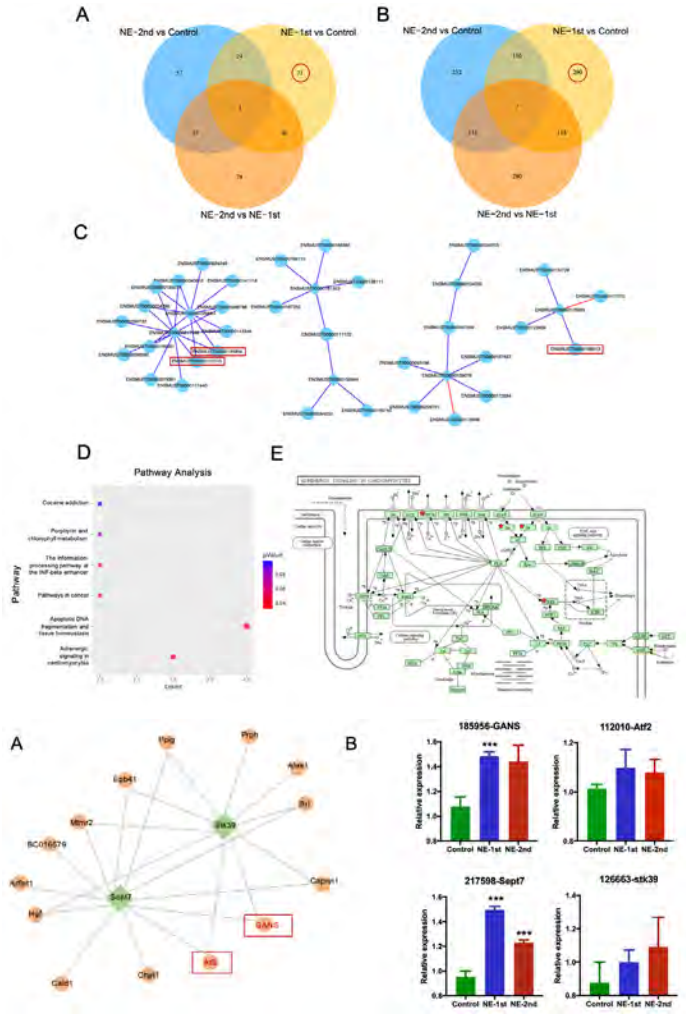

PD 59

Co-regulation of multiple genes promote inner ear progenitors to regenerate hair cells via AAV mediated gene therapy

Renjie Chai
Key Laboratory for Developmental Genes and Human Disease, Ministry of Education, Institute of Life Sciences,Southeast University, NanJing, China

Hearing loss is the most common sensory disorder world-wide, affecting over 6.8% of the world's population. Damage to hair cells in adult mammals causes permanent hearing impairment because these cells cannot regenerate. By contrast, newborn mammals possess limited regenerative capacity because of the active participation of various signaling pathways. Gene therapy has recently emerged as a promising strategy for the treatment of inherited diseases like hearing loss. Adeno-associated viral (AAV) vector-mediated gene therapy has been approved in the US for treating patients with a rare inherited eye disease. However, for hearing loss, it remains constrained by a lack of safe and efficient vectors that can target the diverse types of inner ear cells. Here, we identify the rationally designed AAV-inner ear (AAV-ie) vector for gene delivery in mouse inner ear cochlea. Our results show that AAV-ie transduces SCs with high efficiency *in vivo*, representing a vast improvement over conventional AAV serotypes. Furthermore, we find that after AAV-ie-mediated transfer of Atoh1 gene, which plays a key role in HC fate determination, many SCs trans-differentiated into new hair cells *in vivo*. Pou4f3 and Gfi1, are orderly expressed in the process of HC differentiation and maturation. The Pou4f3 gene is an essential gene for HC formation in the cochlear development, and also is a target of Atoh1 in HCs. Gfi1 is a target of the Pou4f3 gene, and is essential for the survival of cochlear HC. Considering the possible roles of these genes in mammalian hair cell regeneration and maturation, we co-regulated these genes simultaneously in postnatal cochlear supporting cells via AAV mediated gene therapy, and explored the roles of these genes in SC-to-HC conversion and maturation of new HCs.

PD 60

Functional Evaluation of Hair Cell Specific Promoter Variants for Gene Therapy in the Inner Ear

Sarah Cancelarich[1]; Ning Pan[2]; Lars Becker[2]; Janell Smith[1]; Danielle Velez[1]; Daniela Di Battista Miani[1]; Max Beyman[1]; Kathryn Ellis[2]; Martin Schwander[2]; Jonathon Whitton[2]; Adam T. Palermo[2]; Christos Kyratsous[1]; Leah Sabin[1]; **Meghan C. Drummond**[1]
[1]Regeneron Pharmaceuticals; [2]Decibel Therapeutics

Several ubiquitous promoters have been engineered for gene therapy applications to be minimal in size and to drive desired levels of transgene expression in target cells. For successful gene therapy in the inner ear, restricting transgene expression to specific cell types and controlling the level of transgene expression in transduced cells may be critical for the safety and efficacy of AAV-based therapies. We previously identified a murine hair cell specific promoter that restricts expression of a GFP reporter to hair cells. In this study, we dissected this hair cell specific promotor to isolate the critical functional elements and identified putative orthologous elements in other species. To understand the behavior of these promoter variants, we first confirmed that the newly engineered promoters retained hair cell specificity, and then quantified expression levels of the GFP reporter in infected cochleae. Our results identified conserved DNA elements responsible for restricting expression to hair cells. Using this approach to dissect the functional components of a mammalian hair cell promoter, we now have a toolbox of hair cell specific promoter variants capable of driving varying levels of transgene expression that are small enough for use in AAV-mediated gene delivery. These resources will be invaluable for supporting future gene therapies targeting hair cell function.

PD 61

Single-cell Transcriptional Profiling of Mature Cochlear Inner and Outer Hair Cells

Giovanni Diaz[1]; Joerg Waldhaus[2]; Daniel Ellwanger[1]; Mirko Scheibinger[1]; Amanda Janesick[1]; Stefan Heller[1]
[1]Department of Otolaryngology–HNS, Stanford University; [2]University of Michigan

Background

Molecular and biochemical studies of the mammalian cochlea have experienced limitations compared to other organs due to the paucity of cell numbers and the inaccessibility of the organ embedded in dense bone. The increasing feasibility of single-cell technologies and bioinformatic methodology is rapidly changing this impediment. This technological advance is accompanied by the availability of transgenic reporter mice and cell sorting methods to isolate viable individual cells from the mature cochlea. Here, we present differential gene expression analysis of single-cell RNA-Seq data of flow cytometrically isolated mature cochlear hair cells, and provide validation of our bioinformatic predictions, via *in situ* hybridization.

Methods

Single-cell RNA-seq was performed on postnatal day 28 (P28) hair cells isolated using fluorescently activated cell sorting (FACS). We utilized transgenic Myosin15aCre/Ai14-tdTomato mice that express red fluorescent tdTomato within hair cells. Data was aligned and annotated using STAR and RSEM algorithms and analyzed in R. *In situ* hybridization was conducted with digoxigenin-labeled antisense RNA.

Results

Our bioinformatic analysis revealed distinct groups of putative inner hair cells (IHC), outer hair cells (OHC), and contaminant cells. Differential gene expression analysis allowed us to identify distinct marker genes that are associated with each group of cells. *In situ* hybridization validated the differentially expressed genes between IHC and OHC in cryosections of the P2, P7, and P28 cochlea.

Discussion

Our results are comparable to recent single-cell RNA-seq analysis of hand-picked HCs (Ranum et al., 2019), based on comparison of top differentially expressed genes and overlap of putative IHC/OHC clusters in our bioinformatic comparison studies using published data. We show that *Ccer2* is a novel and abundant transcript in adult cochlear HCs. Intriguingly, this gene is associated with Moyamoya disease, which presents with sensorineural hearing loss. The hair cell marker, *Fcrlb* was previously identified by RNA-seq, however, we have validated its spatial expression in mature hair cells *in situ*. The presented work increases our understanding of the transcriptomic landscape of auditory hair cells and has the potential to identify new molecular targets to be used for the development of diagnostic strategies, and perhaps for therapeutic intervention to prevent hearing loss.

PD 62

Mice with Targeted Deletion of the Estrogen-Related Receptor Gamma (ESRRG) Gene exhibit a Low Frequency Hearing Loss.

Lisa S. Nolan
University College London; Current address: King's College London

The estrogen-related receptor gamma (*ESRRG*) gene encodes a transcription factor central to a complex network of endocrine and metabolic pathways. It is an orphan nuclear receptor and one of three closely related paralogues that form the NR3B subgroup of the nuclear receptor superfamily. In tissues with a high metabolic demand, like the cochlea, *ESRRG* mediates metabolic homeostasis primarily through transcriptional regulation of genes involved in mitochondrial function (oxidative phosphorylation, fatty acid oxidation), contractile functions and homeostasis of potassium ions.

Previously, by following up a genome-wide association study into adult hearing conducted on 3,900 participants of the 1958 British Birth Cohort, we showed that the single nucleotide polymorphism (SNP) rs2818964 at the *ESRRG* locus is associated with poorer hearing thresholds at 4kHz[1]. Subsequently, we showed that the minor allele of *ESRRG* SNP rs2818964 is associated with age-related hearing loss (ARHL) in women, but not men, in two independent genetic cohorts[1]. In the first, an ARHL case-control cohort from London U.K., the strongest evidence of association was identified in women with a family history of ARHL. In the second, a cohort from isolated populations of Italy and Silk Road Countries, quantitative measures of hearing function showed that the association was strongest in the low-mid frequencies[1]. In the cochlea, *ESRRG* is expressed in discrete cell types essential for the maintenance of hearing[1]. However, the function of the *ESRRG* gene in the cochlea and the molecular mechanism by which *ESRRG* mediates any sex-specific effect on the maintenance of hearing is not known.

Mice carrying a germline knockout for the *Esrrg* gene exhibit postnatal lethality[1]. Therefore, in order to understand the role of the *ESRRG* gene in the cochlea, I have undertaken a conditional knockout approach. Mice

carrying a floxed allele, *Esrrg*^{tm1c}, were crossed with mice carrying the *Sox10-Cre* transgene [*Tg(Sox10-Cre)1Wdr*; MGI ref: 3586900] to generate *Esrrg*^{tm1d}/*Sox10-Cre* mice with targeted deletion of *Esrrg* in the inner ear.

Auditory brainstem response (ABR) recordings show that *Esrrg*^{tm1d}/*Sox10-Cre* mutant mice exhibit a low frequency hearing loss that is significantly different to wildtype controls at 2 months of age (Fig.1). Subsequent longitudinal ABRs with ageing show little progression in low frequency hearing thresholds by 7 months of age. Work is now in progress to characterize the nature of this functional defect including any sex-specific effect of loss of Esrrg protein on auditory function.

Funding
King's College London Prize Fellowship; Action on Hearing Loss Pauline Ashley Grant and Flexi Grant.

6. Nolan, L.S. et al. Estrogen-related receptor gamma and hearing function: evidence of a role in humans and mice. Neurobiol Aging 34, 2077 e1-9 (2013).

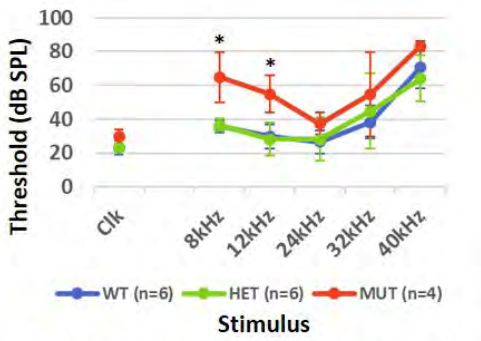

Fig.1. Mean auditory brainstem response thresholds for click and tone pip stimuli are shown for *Esrrg*^{tm1d}/*Sox10-Cre* Wildtype (blue), Heterozygous (green) and Mutant (red) mice at 2 months of age. Error bars: St.Dev; *p<0.005, unpaired t-test comparing mutant versus wildtype.

PD 63

Gom1 mice as a model of otitis media

Qingyin Zheng[1]; Wenyi Huang[2]; HePing Yu[3]; Lu Lu[4]; YuKe Zheng[3]; Christopher Mccarty[5]; JiangPing Zhang[3]; Bo Hua Hu[6]
[1]Department of Otolaryngology- Head & Neck Surgery, Case Western Reserve University, Cleveland, Ohio, USA; [2]Case Western Reserve University; [3]Department of Otolaryngology Head & Neck Surgery, Case Western Reserve University, Cleveland, OH, USA; [4]University of Tennessee Health Science Center (UTHSC); [5]The Jackson Laboratory, Bar Harbor, ME, USA; [6]University at Buffalo

Background
Otitis media (OM) is a common cause of hearing loss in children, and this disease is often associated with middle ear infection. At present, our understanding of molecular mechanisms leading to the development of OM is limited because of a lack of animal models of OM, particularly the otitis media with effusion (OME). Here, we report that *nmf391* N-ethyl-N-nitrosourea (ENU) mutant mice are prone to OM. Thus, we name this novel mouse model *Genetic Otitis Media One (gom1).* These mice demonstrate many common features of OM, such as middle ear effusion and hearing impairment.

Methods
We evaluated the middle ear function using tympanometry and hearing function using the thresholds of auditory-evoked brainstem response (ABR) and the cochlear microphonic (CM) response in *gom1* mice. The middle ear inflammation and pathogenesis were assessed using pathological and histological examinations of middle ear structures. To assess gross malformation of the skull, we measured skull dimensions. To determine the sensory cell integrity, we quantified the number of inner hair cells and outer hair cells.

Results
We found an increase in ABR thresholds and CM thresholds in all examined *gom1* mice in at least one ear. Tympanometry revealed a type B or type C curve in the ears with hearing loss. While individual ears had diverse levels of effusion and inflammatory cells in the middle ear cavity, these ears commonly displayed a thicken middle ear epithelium compared to that in wild-type control mice. The mutant mice also displayed craniofacial abnormalities, which could be a contributing factor to the development of OME in the *gom1* mouse model. Moreover, the mutant mice exhibited various levels of outer and inner hair cell loss, which could be a consequence of middle ear infection.

Conclusion
The study suggests that *gom1* mice are susceptible to middle ear infection and could be valuable for investigating genetic contribution to the development of middle ear disease caused by middle ear infection.

Grant support: R01DC015111(QYZ)

PD 64

The CDHR3 c.1586G>A (p.Cys529Tyr) Variant is Protective against Otitis Media in Children

Scott Hirsch, MD[1]; Tori C. Bootpetch Roberts, BS[1]; Norman R. Friedman, MD[1]; Todd M. Wine, MD[1]; Sven-Olrik Streubel, MD[1]; Jeremy D. Prager, MBA, MD[1];

Patricia J. Yoon, MD[1]; Kenny H. Chan, MD[1]; Melissa A. Scholes, MD[1]; Daniel N. Frank, PhD[2]; Regie Lyn P. Santos-Cortez[1]
[1]Department of Otolaryngology, University of Colorado School of Medicine; [2]Division of Infectious Disease, University of Colorado School of Medicine

Background
Human genome-wide association studies (GWAS) have identified variants for otitis media (OM) susceptibility, including variants in linkage disequilibrium (LD) with common, coding variants within CDHR3, FUT2 and PLG. The FUT2 c.461G >A (p.Trp154*) variant was associated with OM in European-American children and middle ear microbiota shifts. A mouse Plg-knockout developed chronic OM at age 18 weeks. Additionally a PLG c.1414G >A (p.Asp472Asn) variant was associated with susceptibility to fungal infection in mice. Lastly an intronic CDHR3 variant identified in OM GWAS is in LD with CDHR3 c.1586G >A (p.Cys529Tyr); the latter is a susceptibility variant for asthma. In this study, we determined whether these genetic variants play a role in OM susceptibility after taking into account other known environmental risk factors for OM.

Methods
Ninety-one children who underwent otologic surgery provided clinical data, salivary DNA samples and middle ear samples for 16S rRNA profiling. Sanger sequencing of the CDHR3, FUT2 and PLG variants was performed using DNA samples. Presence of OM at surgery was used as the outcome variable. Bivariate analyses were performed using Fisher exact and Mann-Whitney-Wilcoxon tests to determine association between OM and these variables: genetic variants, age, gestational age at birth, sex, ethnicity, allergic rhinitis, sinusitis, antibiotic use, breastfeeding, daycare attendance, tobacco exposure, and alpha-diversity indices for nasopharyngeal and middle ear microbiota. Logistic regression was performed while including significant variables from bivariate analyses.

Results
Of 91 children, 51 (63%) had OM at surgery. The following carried variants: 27 (35.1%) for CDHR3, 59 (77.6%) for FUT2, and 27 (39.1%) for PLG. OM was associated with young age (p=0.02), daycare attendance (p=0.009), and wildtype genotype for the CDHR3 variant (OR=0.3, 95%CI:0.09-0.85, p=0.01). Carriage of the CDHR3 variant was also associated with less antibiotic use (p=0.006). The FUT2 variant was associated with lower rate of previous OM surgery (p=0.03), while the PLG variant was not associated with OM. The CDHR3 variant was associated with greater evenness (Shannon H p=0.02) and complexity (Shannon E p=0.03) of the nasopharyngeal microbiota. In the regression model, only the CDHR3 variant remained significantly associated with OM. Our RNA-sequencing analyses showed that CDHR3 was expressed in human middle ear mucosa and down-regulated in cholesteatoma (p=0.004).

Conclusions
The CDHR3 c.1586G >A (p.Cys529Tyr) variant is protective against OM, potentially through changes in the nasopharyngeal microbiota. We identified a novel association between a CDHR3 variant and OM, which is further supported by middle ear expression studies.

Hair Bundles and Mechanotransduction

PD 65

Viscoelastic Coupling of Stereocilia Coordinates Whole Bundle Motion in Mammalian Auditory Inner Hair Cells

Alexandra L. Scharr[1]; Daibhid O Maoileidigh[2]; Anthony Ricci[3]
[1]Stanford University; [2]Department of Otolaryngology - Head & Neck Surgery, Stanford University; [3]Department of Otolaryngology and Department of Molecular and Cellular Physiology, Stanford University

The site of the mechanoelectrical transduction process underlying hearing in all modern vertebrates is the auditory hair cell bundle. Yet bundle morphology, stimulating structures, and auditory systems vary greatly between species. The primary sensory cell of hearing in the mammal, the inner hair cell (IHC), has unique bundle properties such as few rows of free standing stereocilia that can move semi-independently. These properties are significant because the mechanics of bundle deflection shape the receptor potential of the cell. The mechanics of the IHC bundle have yet to be fully characterized, and what advantage these mechanics might confer to mammalian hearing is unknown.

To characterize the mechanics of the IHC bundle and predict how they contribute to the specializations of mammalian hearing, we stimulated IHC bundles from acutely dissected cochlea of p9-10 Sprague Dawley rats with step displacements using small piezoelectric-driven glass probes (~1 µm diameter) while simultaneously recording mechanoelectrical transduction responses using whole cell patch clamp electrophysiology, and recording individual stereocilia motion with high speed (25 – 50K fps) imaging. Stimulating the bundle using a small probe limited the number of stereocilia in contact with the probe. Therefore non-contacted stereocilia moved only due to the connections linking the stereocilia. By analyzing the motion of non-contacted stereocilia, we

could determine if the connections between stereocilia were rigid, slack, elastic, or viscoelastic.

Stereocilia directly contacting the probe moved farthest in the direction of stimulation, whereas stereocilia not directly contacting the probe moved exponentially less with increasing distance from the stimulus, excluding the possibility that the connections between stereocilia were rigid. However, all stereocilia moved almost simultaneously, regardless of distance from the probe, indicating no slack in the connections between stereocilia. During sufficiently large step displacements, most stereocilia not contacting the probe showed a reverse motion, moving backwards towards their starting position by ~20 nm with a time constant of ~0.5 ms.

A mathematical model quantitatively reproduced many experimental observations including exponential decrease in displacement with distance from the stimulus, almost-simultaneous movements, and reverse motion of non-contacted stereocilia. Fitting experimental data to analytical expressions for stereociliary motions showed that links were weaker than stereociliary anchors.

The lack of cohesiveness of the IHC bundle, combined with the limited number of rows, may help specialize mammalian hearing by facilitating rapid channel opening in response to high frequency sound.

Funding: Stanford Neurosciences NIH Training Grant, NSF GRFP, NIDCD R01 DC003896

PD 66

TRIOBP-5 is Required to Establish and Maintain Stereocilia Rootlet Architecture: Implications for Presbycusis and Gene Therapy

Inna A. Belyantseva[1]; Tatsuya Katsuno[2]; Alexander X. Cartagena-Rivera[3]; Keisuke Ohta[4]; Ronald S. Petralia[5]; Kazuya Ono[6]; Risa Tona[1]; Ayesha Imtiaz[1]; Atteeq Rehman[1]; Hiroshi Kiyonari[7]; Tracy S. Fitzgerald[8]; Takaya Abe[7]; Makoto Ikeya[9]; Cristina Fenollar-Ferrer[10]; Kohei Segawa[2]; Koichi Omori[11]; Juichi Ito[12]; Gregory I. Frolenkov[13]; Shin-ichiro Kitajiri[2]; Thomas B. Friedman[1]
[1]Laboratory of Molecular Genetics, National Institute on Deafness and Other Communication Disorders, NIH, Bethesda, Maryland, USA; [2]Department of Otolaryngology - Head and Neck Surgery, Kyoto University Graduate School of Medicine, Kyoto City, Kyoto, Japan; [3]Section on Auditory Mechanics, National Institute on Deafness and Other Communication Disorders, NIH, Bethesda, Maryland, USA; [4]Advanced Imaging Research Center, Kurume University School of Medicine, Kurume, Japan; [5]Advanced Imaging Core, National Institute on Deafness and Other Communication Disorders, NIH, Bethesda, Maryland, USA; [6]NIDCD; [7]Animal Resource Development Unit and Genetic Engineering Team, Riken Center for Life Science Technologies, Japan; [8]Mouse Auditory Testing Core Facility, National Institute on Deafness and Other Communication Disorders, NIH, Bethesda, Maryland, USA; [9]Department of Life Science Frontiers, Center for iPS Cell Research and Application, Japan; [10]Molecular Biology and Genetics Section, National Institute on Deafness and Other Communication Disorders, National Institutes of Health, Bethesda, MD 20892, USA., Laboratory of Molecular Genetics, National Institute on Deafness and Other Communication Disorders, NIH, Bethesda, Maryland, USA; [11]Dept. Otolaryngology - Head and Neck Surgery, Graduate School of Medicine, Kyoto University; [12]Shiga Medical Center Research Institute; [13]Department of Physiology, University of Kentucky, Lexington, USA

TRIOBP-5 is one of three major alternative mRNA isoform classes of the *TRIOBP* gene. TRIOBP-5 protein encompasses sequences of both TRIOBP-1 and TRIOBP-4 and an additional stretch of unique amino acids. In human, variants of *TRIOBP-5* cause moderate hearing loss (Wesdorp et al., 2017; Pollak et al., 2017) and are associated with age related hearing loss in a GWAS study (Hoffmann et al., 2016). These observations underscore the medical importance of understanding TRIOBP-5 functions in the auditory system, which has implications for future gene therapy efforts for TRIOBP-5-related progressive deafness. We previously reported that in human and mouse, mutations that eliminate both TRIOBP-4 and TRIOBP-5 isoforms cause profound deafness due to failure of stereocilia to form rootlets, subsequently leading to hair cell degeneration (Kitajiri et al, 2010). However, the unique role of TRIOBP-5 in stereocilia rootlet development and function was unknown. We developed two new TRIOBP-5-specific deficient mouse models and a GFP-TRIOBP-4 transgenic mouse to decipher TRIOBP-5 unique contributions to stereocilia rootlet formation. We found that endogenous GFP-TRIOBP-4 is localized predominantly to the stereocilia rootlet segment above the cuticular plate and diffusely distributed within the cuticular plate. Consistent with the preferential localization of TRIOBP-5 in the segment of the rootlet penetrating the cuticular plate, FIB-SEM examination shows that mouse TRIOBP-5 deficiency causes thinning of rootlets within the cuticular plate, but, surprisingly, induces their extensive expansion within the stereocilia core. These rootlet dysmorphologies lead to progressive deafness recapitulating the human phenotype. Hence, TRIOBP-5 is essential for thickening F-actin bundles of rootlets within the cuticular plate and regulating their mature architecture. Interestingly, a deletion of only the

C-terminal coiled-coil domains of TRIOBP-5 results in splayed or bent rootlets without rootlet-thinning within the cuticular plate, arguing for the importance of these domains for reinforcement and maintenance of rootlet actin bundles for life-long hearing. In addition, supporting Deiters' cells lacking TRIOBP-5 showed decreased apical stiffness as measured by Atomic Force Microscopy, pointing to yet another critical function of TRIOBP-5 for reinforcing supporting cells of the auditory sensory epithelium. This study advances our knowledge of individual TRIOBP isoform contributions not only to the mechanisms of stereocilia rootlet formation and profound or progressive hearing loss, but also to supporting cell function, which is crucial when considering gene therapy for TRIOBPopathies.

PD 67

ANKRD24 is Required for Hair Bundle Organization and Hearing Function in the Mouse Cochlea.

Jocelyn F. Krey[1]; Julia Halford[2]; Rachel A. Dumont[2]; Michael Bateschell[2]; Bo Zhao[3]; Peter G. Barr-Gillespie[2]
[1]Oregon Hearing Research Center & Vollum Institute, Oregon Health & Science University, Portland, Oregon, USA; [2]Oregon Hearing Research Center & Vollum Institute, Oregon Health & Science University; [3]Department of Otolaryngology-Head and Neck Surgery, Indiana University School of Medicine

The ankyrin repeat domain (ANKRD) is one of the most common repeat domains in mammalian proteomes and ANKRD containing proteins participate in diverse cellular functions, including cell-cell signaling, transcriptional regulation and cytoskeleton organization. ANKRD proteins are thought to act as scaffolds mediating specific protein-protein interactions, however the majority of proteins in the ANKRD family have not been genetically or biochemically characterized. Using proteomic analysis, we observed that ANKRD24 was enriched in purified hair bundles from mouse and chick utricles; in addition, ANKRD24 specifically co-immunoprecipitated with MYO7A from chick inner ear lysates. To characterize the function of ANKRD24 in hair cells, we generated an *Ankrd24* knockout (KO) mouse using CRISPR/Cas9-mediated genome-editing, creating a large deletion between exons 6 and 17 of the *Ankrd24* gene, producing a frameshift for the remainder of the sequence. *Ankrd24* KO mice had near-complete high-frequency hearing loss, elevated hearing thresholds at moderate frequencies, and no change at low frequencies. In wild-type mice, ANKRD24 was expressed in inner and outer hair cells throughout the entire cochlea and was absent in *Ankrd24* KO mice. ANKRD24 was present in hair cells of the utricle but no significant vestibular dysfunction was detected in the *Ankrd24* KO mice. In *Ankrd24* KO mice, cochlear bundles were structurally altered in both inner and outer hair cells. While rows of stereocilia with graded heights were still present, bundles of inner and outer hair cells lost their characteristic U- and V- shapes, respectively, shifting to variable curled shapes. The shape of the cuticular plate was also altered in the *Ankrd24* KO mice as was the density of F-actin in the rootlet region.

Using super-resolution immunofluorescence microscopy, we found that ANKRD24 was specifically enriched at the base of each stereocilium in all hair cell types, extending from the lower portion of the taper region down into the rootlet. In cross sections, ANKRD24 expression marked the footprint of the hair bundle, filling in gaps in the cuticular plate F-actin where the stereocilia enter the cuticular plate. ANKRD24 staining partially colocalizes with GRXCR2, MYO7A, SPTBN1, and TRIOBP. Immunoprecipitation analysis demonstrated an interaction between GRXCR2 and ANKRD24 and GRXCR2 was mislocalized in the *Ankrd24* KO hair bundles. Together, the ANKRD24 expression pattern and phenotype of *Ankrd24* KO mice suggest that ANKRD24 may link the base and rootlet of each stereocilium to the cuticular plate, therefore playing a crucial role in hair bundle organization and function.

PD 68

Structuring Inner-Ear Mechanotransduction

Deepanshu Choudhary[1]; Yoshie Narui[1]; Brandon L. Neel[1]; Sanket Walujkar[1]; Jeffrey M. Lotthammer[1]; Joseph C. Sudar[1]; Collin Nisler[1]; Lahiru N. Wimalasena[1]; Carissa F. Klanseck[1]; Pedro De-la-Torre[1]; Conghui Chen[1]; Raul Araya-Secchi[2]; Elakkiya Tamilselvan[1]; **Marcos Sotomayor**[1]
[1]The Ohio State University; [2]Niels Bohr Institute, University of Copenhagen

Inner-ear sensory perception begins when "tip links", fine protein filaments essential for hearing and balance, gate TMC ion channels to elicit transduction currents. Tip links are 150 to 180 nm long, their integrity is calcium-dependent, and they are made of protocadherin-15 (PCDH15) and cadherin-23 (CDH23), two enormous proteins involved in hereditary deafness. Here we report X-ray crystal structures of a PCDH15 + CDH23 heterotetrameric complex and of various PCDH15 fragments used to build high-resolution models of the complete lower-end of the tip-link. Simulations suggest conditions in which a structurally diverse and multimodal PCDH15 ectodomain can act as a stiff or soft gating spring. In addition, we present simulations of PCDH15's transmembrane domain coupled to TMHS, a transmembrane protein involved in mechanotransduction, and of TMEM16-based TMC1

homology models in the presence of applied voltage. These simulations suggest mechanisms by which TMHS could amplify membrane stretching and provide insight into TMC1 ion conduction pathways and gating mechanisms. Overall, our structures and simulations provide a detailed view of the first molecular steps in inner-ear sensory transduction and support the putative role of TMC channels as pore-forming subunits of the inner-ear transduction apparatus.

PD 69

Novel Myosin VIIa Isoforms And Their Significance For Shaping Hair Cell Mechanotransduction And Hearing Function.

Sihan Li[1]; Andrew Mecca[2]; Jeewoo Kim[1]; Elizabeth Wagner[1]; Tingting Du[1]; Guisy Caprara[2]; Runjia Cui[3]; Ivan Rebustini[3]; Bechara Kachar[3]; Anthony Peng[2]; Jung-Bum Shin[4]
[1]University of Virginia; [2]University of Colorado; [3]NIH/ NIDCD; [4]University of VIrginia

In the hair cell mechanotransduction (MET) complex, the upper end of the tip link is believed to house a tension-generating element that biases the transduction channels to be at an optimally sensitive open probability. This mechanism is essential for the extraordinary sensitivity of the auditory system, but is insufficiently understood. Recent localization studies have advanced the unconventional myosin VIIa (MYO7A) as the likely candidate, but functional evidence implicating MYO7A in this role is missing. Also, the broad subcellular localization of MYO7A suggests that it is important for additional hair cell functions.

By using 5'RACE, we discovered that multiple isoforms of MYO7A with alternative start sites are expressed in the inner ear. To investigate the different isoforms, we generated mouse models in which each isoform is specifically deleted. In the *Myo7a-ΔC* mouse that lacks the canonical isoform (MYO7A-C), MYO7A expression was severely diminished in inner hair cells (IHCs), but only mildly affected in outer hair cells (OHCs), suggesting that MYO7A-C is preferentially expressed in IHCs, while the alternative isoforms are predominantly expressed in OHCs. Ultrastructural analyses suggest that IHCs in *Myo7a-ΔC* mice, despite a severe reduction in MYO7A levels, undergo normal development. Electrophysiological analysis of MET currents demonstrated that mutant IHCs exhibit markedly reduced resting open probability, a shift in the activation curve and a slower current onset, consistent with a role of MYO7A in establishing tip link tension. Auditory brainstem response thresholds in *Myo7a-ΔC* mice are only mildly affected initially, but worsen over time, culminating in profound hearing loss by 9 weeks of age. Distortion product otoacoustic emissions (DPOAEs), a measure for OHC function, were not affected. Mirroring a gradual decline in MET and hearing function, the transducing rows of IHC stereocilia degenerate over time, as shown by ultrastructural analysis.

Furthermore, genetic deletion of an alternative MYO7A isoform did not affect IHCs, but led to a severe reduction in MYO7A levels in OHCs, with a tonotopic gradient. Based on our findings, we hypothesize that IHCs mainly express the canonical MYO7A isoform, while the OHCs express one or more alternative isoforms with a tonotopic gradient in expression level. The differential expression of isoforms of MYO7A, a candidate for the tip link tensioning motor, has the potential to explain the previously reported differences in MET properties in IHCs and OHCs, as well as tonotopic gradients tip link tension reported in OHCs.

PD 70

Exploring the Functional Implications of the Structural Relationship Between TMC1 and TMEM16 proteins.

Angela Ballesteros; Kenton J. Swartz
NINDS

The biophysical properties of the mechanotransduction (MET) channel essential for hearing have been extensively characterized, yet its molecular identity and structure have remained elusive. Increasing evidence has made the transmembrane-like channel 1 (TMC1) the most likely candidate; Mutations in the transmembrane-like channel 1 (TMC1) alter the MET channel properties and cause deafness. In addition, TMC1 localizes to the site of the MET channel and interacts with the tip-link responsible for mechanical gating. Furthermore, bioinformatic analyses proposed an evolutionary relationship between TMC1 and the TMEM16 proteins, a family of calcium-activated chloride channels and lipid scramblases. Based on this relationship, we generated a structural model of TMC1 that revealed the presence of a large cavity near the protein-lipid interface. This cavity harbors the two TMC1 mutations (p.M418K and p.D572N/H) known to cause autosomal dominant hearing loss (DFNA36), and selective modification of cysteine mutants for residues in the cavity alter MET channel properties, indicating that it could function as the permeation pathway of the MET channel. The localization and the large size of this cavity led us to hypothesize that TMC1 may also share the lipid scrambling activity of the TMEM16 proteins. We have begun to explore the possibility that TMC proteins may function as lipid scramblases. Interestingly, we

found that blockade of the MET channel triggered the externalization of phosphatidylserine in the stereocilia membrane, suggesting a potential role of the MET channel in lipid scrambling. We are currently exploring the implication of the TMC proteins in lipid scrambling, and the role of the plasma membrane in MET channel permeation and hair cell survival.

PD 71

Tmie and TMC1/2 Cooperate to Form Mechanotransduction Channels in Cochlear Hair Cells

Christopher L. Cunningham[1]; Xufeng Qiu[1]; Zizhen Wu[1]; Bo Zhao[2]; Ye-Hyun Kim[3]; Amanda M. Lauer[3]; Ulrich Mueller[1]
[1]Johns Hopkins University; [2]Department of Otolaryngology-Head and Neck Surgery, Indiana University School of Medicine; [3]Johns Hopkins School of Medicine

The hair cell mechanotransduction channel that is activated by sound stimuli localizes to the tips of stereocilia. Several proteins are essential for proper channel function. These proteins include the transmembrane proteins TMIE, TMC1/2 and LHFPL5. Using mouse genetics, biochemistry, immunofluorescence, and electrophysiology, we have investigated the functional contributions of TMIE and TMC1/2 to channel function. By utilizing CRISPR/CAS9, we have generated epitope-tagged knock-in alleles of TMC1, TMC2 and TMIE, as well as mice carrying specific point mutations in these proteins. Although TMC1/2 have recently been proposed to act as pore-forming subunits of the channel, we demonstrate that TMC1/2 cannot form a mechanotransduction channel in hair cells without TMIE. Similarly, TMIE cannot form a functional mechanotransduction channel without TMC1/2. Using mutational analysis we have identified protein domains in TMIE that mediate its function in mechanotransduction, and we have investigated the mechanisms by which point mutations in TMIE that are linked to deafness cause disease. Our results are consistent with a model where TMIE and TMC1/2, and likely other proteins, are assembled into an ion channel complex, where TMIE affects channel pore and gating properties.

PD 72

Unconventional Secretory Pathway Activation Restores Hair Cell Mechanotransduction in an Usher Syndrome type IIIA Model

Suhasini Gopal[1]; Yvonne Lee[1]; Ruben Stepanyan[2]; Brian McDermott[3]; **Kumar Alagramam**[4]
[1]Department of Otolaryngology–Head and Neck Surgery, University Hospitals Cleveland Medical Center, Case Western Reserve University; [2]Department of Otolaryngology, University Hospitals Cleveland Medical Center, and Department of Neurosciences, School of Medicine, Case Western Reserve University; [3]Department of Otolaryngology–Head and Neck Surgery, University Hospitals Cleveland Medical Center, Department of Neurosciences, Department of Genetics and Genome Sciences and Department of Biology, Case Western Reserve University; [4]Department of Otolaryngology–Head and Neck Surgery, University Hospitals Cleveland Medical Center, Department of Neurosciences, and Department of Genetics and Genome Sciences, Case Western Reserve University

Clarin-1 (CLRN1) belongs to a superfamily of four-transmembrane proteins that includes the tetraspanin and claudin families. The pathogenic variant c.144T >G (p. N48K) in *CLRN1* results in progressive loss of vision and hearing in Usher syndrome type IIIA (USH3A) patients. CLRN1 is an essential hair cell protein. When expressed in animal models, CLRN1 localizes to membrane of the soma and hair bundle, whereas glycosylation-deficient $CLRN1^{N48K}$ aggregates in the endoplasmic reticulum, with only a fraction sorting to the bundle. We hypothesized that the small amount of $CLRN1^{N48K}$ that reaches the hair bundle does so via an unconventional secretory pathway and that activation of this pathway could be therapeutic. Using genetic and pharmacological approaches, we find that clarin1 knockout ($clrn1^{KO/KO}$) zebrafish that express the $CLRN1^{c.144T>G}$ pathogenic variant display progressive hair cell dysfunction, and that $CLRN1^{N48K}$ is trafficked to the hair bundle via the GRASP55 cargo-dependent unconventional secretory pathway (GCUSP). On expression of GRASP55 mRNA, or on exposure to the antimalarial drug artemisinin (which activates GCUSP), the localization of $CLRN1^{N48K}$ to the hair bundles was enhanced. Artemisinin treatment also effectively restored hair cell mechanotransduction and attenuated progressive hair cell dysfunction in $clrn1^{KO/KO}$ larvae that express $CLRN1^{c.144T>G}$, highlighting the potential of artemisinin to prevent sensory loss in $CLRN1^{c.144T>G}$ patients.

Auditory Cortex - Human Studies II

PS 532

Switches in Perception During Auditory Streaming of Bistable Stimuli Enhances BOLD Activity in Auditory Cortex

Nathan C. Higgins[1]; Alexandra Scurry[2]; Fang Jiang[2]; David F. Little[3]; Mounya Elhilali[3]; Claude Alain[4]; Joel S. Snyder[5]
[1]University of Nevada, Las Vegas; [2]University of Nevada Reno; [3]Johns Hopkins University; [4]University of Toronto; [5]Unversity of Nevada Las Vegas

Repeated presentation of tones set in a low-high-low (ABA) configuration at an appropriate frequency and rate elicit competing percepts of 1- or 2-auditory streams that spontaneously alternate between those two percepts. These bistable stimuli provide a valuable tool for studying the neural mechanisms underlying conscious perception by evoking distinct percepts without manipulation of the physical properties of the stimulus. In this experiment, we used an intermittent-response paradigm to measure the neural dynamics of perceptual switching reflected in the BOLD (Blood Oxygenation Level Dependent) signal using fMRI. Participants were presented five blocks of 152 trials (approximately 6.5 minutes), each trial consisting of three ABA triplets (2.6 s duration) followed by 650 ms of intermittent silence during which they indicated their perception (1- or 2-streams) with a button press. Behavioral results, in agreement with prior work, demonstrated that participants perceived both percepts in roughly equal proportions, and generally exhibited behavioral characteristics of bistability, despite the intermittent nature of the stimuli. Perceptual phase durations were logarithmically distributed, with the average duration approximately 8 trials prior to a switch. Following standard fMRI preprocessing routines, sound-responsive voxels were extracted for regions of interest (ROIs) encompassing auditory cortex (Heschl's gyrus and surrounding areas in the superior temporal lobe) and the parietal lobe. Response magnitudes were calculated for each trial, and comparisons were made for 1-stream versus 2-streams (excluding switch trials), and switch versus no-switch trials. In the inferior parietal lobe ROI, significant enhancements were observed for 2-stream compared to than 1-stream perception, but no difference between switch versus no-switch trials. Conversely, voxels in the anterior superior temporal gyrus (STG) exhibited greater responses during switch compared to no-switch trials, but minimal difference between 1- and 2-stream percepts. The pattern of results suggests differential mechanisms underly the representation of the contents of perception compared to the modulation of conscious perception. Regions anterior to primary auditory cortex such as anterior STG, have previously been implicated as part of the "what" pathway in the auditory domain, comparable to the ventral pathway in the visual system. Switch related activity observed in anterior STG, could therefore be related to the process of auditory object identification.

PS 533

Central Auditory Tests Show Differences Between Drug Treatment Regimens in Human Immunodeficiency Virus Affected Adults

Fengxiang Song[1]; Yi Zhan[2]; Hongzhou Lu[1]; Guochao Chen[1]; Abigail Fellows[3]; Sigfrid Soli[4]; Odile Clavier[5]; **Jay Buckey**[3]; Yuxin Shi[1]

[1]Shanghai Public Health Clinical Center; [2]Huashan Hospital; [3]Geisel School of Medicine at Dartmouth; [4]University of British Columbia; [5]Creare LLC

Background

We have shown that tests probing central auditory function (such as the hearing-in-noise (HINT) and gaps-in-noise (GAP) tests) reflect cognitive difficulties in human immunodeficiency virus (HIV) infected patients. This suggests central auditory tests could assess central nervous system (CNS) effects of HIV treatment. The non-nucleoside reverse-transcriptase inhibitor (NNRTI) efavirenz (EFV) has been associated with neurological and neuropsychiatric effects in treated patients and might cause or worsen HIV-associated neurocognitive disorder. We hypothesized that HIV+ adults who had taken EFV would have impaired gap detection abilities and worse thresholds on the HINT test compared to those who had not.

Methods

321 HIV+ (mean age 36 years, 94% male) adults performed the HINT and 282 (mean age 35 years, 92% male) completed gap detection testing at the Shanghai Public Health Clinical Center. Drug regimen data were collected from the medical record. The adaptive gap detection test presented a 4.5 second burst of white noise with a gap placed randomly within the middle 2.5 seconds. The test started at a 20 msec gap duration, which was reduced progressively to find the participant's threshold. The Mandarin HINT test presented 20 sentences in random order in the presence of reference noise fixed at 65 dBA. The test instrument adjusted the level of each sentence adaptively to find the speech reception threshold (SRT) for the test condition.

Results

HINT SRTs were significantly better in those who had ever taken EFV (n=205, -6.3 dB), compared to those who had no record of taking the drug (n=116, -5.7 dB, $p< 0.01$ one-way ANOVA). Using logistic regression, ever taking EFV was significantly associated with both better SRT thresholds and shorter HIV durations. Also, gap detection thresholds did not differ between groups (n=174, 4.9 ms EFV vs. n=108, 5.2 ms no EFV, p=0.19). In those taking another commonly-used NNRTI nevirapine (NVP) SRT tended to be worse in those who had ever taken NVP (n=36, -5.5 dB) compared to those who had not (n=285, -6.2 dB, p=0.05 one-way ANOVA). Gap thresholds also tended to be worse in the NVP group (n=33, 5.5 ms NVP vs. n=249 4.9 ms, p=0.08 one-way ANOVA).

Conclusions

The data show no adverse central auditory consequences among those who took efavirenz, although this group

also had shorter HIV durations on average. HINT performance was worse among those who had taken nevirapine. These data suggest central auditory tests may be useful for tracking CNS effects in HIV care.

PS 534

Tinnitus and Auditory Cortex; Using Adapted Functional Near-Infrared-Spectroscopy to Expand Brain Imaging in Humans

Angela Ash-Rafzadeh[1]; Tianqu Tian Zhai[2]; Xiao-Su Hu[3]; Jessica Kim[3]; Juan San Juan[1]; Mohammed Islam[2]; Ioulia Kovelman[3]; **Gregory Basura**[4]
[1]University of Michigan; [2]University of Michigan; Department of Electrical Engineering; [3]University of Michigan; Center for Human Growth and Development; [4]University of Michigan; Department of Otolaryngology-Head and Neck Surgery; Center for Human Growth and Development

Tinnitus, phantom sound perception in the absence of a sound stimulus, arises from aberrant brain activity within central auditory pathways. Auditory cortex neurons in tinnitus animal models show increased spontaneous firing and neural synchrony. Functional near infrared-spectroscopy (fNIRS) can translate similar brain changes in human tinnitus as we showed for the first-time increased hemodynamic activity and brain connectivity between auditory and non-auditory cortices. This suggested that these changes may serve as potential objective correlates of human tinnitus readily measurable with fNIRS. A limitation of current fNIRS technology is the restricted depth of IR penetration through skin and skull bone using “cap/scalp” recording configurations. These approaches restrict IR penetration (3cm) to outer cerebral cortex. To improve IR penetration to deeper brain structures for measurement of putative tinnitus correlates we adapted fNIRS probes to fit in the external auditory canal to physically be placed deeper into the skull to record never-before reached portions of the brain. Twenty age-matched normal/near-normal hearing adults with subjective bilateral tinnitus and 20 non-tinnitus controls were selected for this proof of concept. Region of interest (ROI) included the auditory cortex and surrounding auditory belt regions. Using this highly innovative approach we measured hemodynamic activity and resting state functional connectivity (RSFC) to auditory stimulation (with broadband noise; BBN) and silence using a block paradigm. Using separately adapted ear canal probes serving as IR-sources and detectors with concurrent scalp detectors, controls showed increased hemodynamic activity to BBN versus silence, while the tinnitus group showed increased hemodynamic activity under conditions of rest as compared to stimulation with BBN. Furthermore, the ROI in tinnitus showed a trend toward increased RSFC to itself and to adjacent non-ROI cortices. The ROI of controls showed no evidence of increased RSFC. Overall, these data using highly innovative adapted fNIRS technology to the human ear canal, essentially replicated our previously published work using traditional cap/scalp probes. This proof of concept substantiates our published data in human tinnitus and concurrently validates the use of this innovative adaptive technology going forward to ideally expand brain surveillance in tinnitus and other brain diseases.

PS 535

Electrophysiological Measurement of Working Memory in Veterans with APD: Effects of Sensory Modality on the N-back test

Melissa A. Papesh; Melissa T. Frederick; Curtis J. Billings; Frederick J. Gallun
VA RR&D NCRAR

Military Veterans are at increased risk of developing auditory processing disorders (APD) due to military risk factors including high-intensity blast wave exposure and traumatic brain injuries (TBI). However, the results of behavioral diagnostic test measures for APD may be confounded by cognitive deficits which are also common among those who have suffered neurological insults. In the current study, we hypothesize that Veterans who have failed a behavioral APD assessment battery will also demonstrate reduced working memory capacity affecting multiple sensory modalities. To test this hypothesis, we will compare electrophysiological and behavioral responses to the N-back test among participants with and without behaviorally established symptoms of APD. The N-back is a well-established measure of working memory on which cognitive load can be adjusted to examine performance at different levels of difficulty. Study participants include those who have a history of TBI or blast exposure who have failed a behavioral APD test battery (experimental group), and age- and sex-matched participants with neither previous neurological injuries nor behavioral symptoms of APD (control group). Consonant vowel (CV) stimuli are presented in both the visual and auditory modality in response to three levels of difficulty (0-back, 1-back, and 2-back conditions). Behavioral responses will be evaluated based upon classification accuracy (targets versus non-targets) and response time for each condition in each stimulus modality. Electrophysiological responses will be evaluated in the time domain where we will measure the amplitude and latency of P300 responses time-locked to target stimuli, and in the spectral domain where we will quantify the power in theta (4 to 8 Hz) and alpha (8 to 13 Hz) regions. Compared to control participants, we predict that experimental participants will demonstrate poorer working memory capacity in the following ways: (1)

Poorer classification accuracy, particularly on the 2-back conditions, (2) larger response times indicating need for more processing time, (3) smaller P300 amplitudes in response to target stimuli, and (4) lower power in alpha bands and greater power in theta bands, particularly for the more difficult conditions. We anticipate that these effects will be found in response to both auditory and visual stimulus presentations, confirming that working memory is impaired regardless of stimulus modality. The results of this work will reveal insight into the neural basis of auditory processing deficits among Veterans with previous blast exposure and TBI.

PS 536

Cortical Processing of Location and Feature Changes of Sounds in Normal Hearing Listeners

Fawen Zhang[1]; Kelli McGuire[1]; Gabrielle Firestone[1]; Qian-jie Fu[2]
[1]University of Cincinnati; [2]UCLA

Research Background
Sounds we hear in our daily life contain changes in the acoustic features (e.g., frequency, intensity, and duration) and/or changes in location. The auditory system needs to automatically process these changes before selectively attending to the "what" and "where" information of the sounds in order to perceive target sounds in complex listening situations such as parties and restaurants. This study aims to examine the cortical auditory evoked potentials (CAEPs) to the change in frequency and location of the sound in normal hearing listeners. The data will be used to compare those from patients with abnormal hearing in order to identify the nature of abnormality in these patients.

Methods
Ten right-handed young normal hearing listeners participated in the electroencephalographic (EEG) recordings. The acoustic stimuli were pure tones (base frequency at 250 Hz) of 1 sec, with a perceivable change either in frequency (F), location (L), or both frequency + location (F+L) in the middle of the tone. The two sound segments before and after the change occurred were equalized in terms of the root mean square energy. Additionally, the 250 Hz tone of 1 sec without any change was used as a reference. The stimuli were presented using loudspeakers at a loud but comfortable level. The reference tone was presented from the left speaker (90^{o} in azimuth); for the tone containing the F change, the whole stimulus was presented from the left speaker (90^{o} in azimuth); for the tones containing the L and the F+L change, the first segments of the tones were presented from the left speaker (90^{o} in azimuth) and the second from the right speaker (270^{o} in azimuth). The participants were asked to listen passively to the stimuli and not to move the head during the testing.

Results
Compared to the reference tone, to which only the onset-CAEP was elicited, the tones containing changes (F, L, or F+L) elicited both onset-CAEP and the change-CAEP. The change-CAEP for the L change is substantially different from that for the F or F+L change. The change-CAEP and the onset-CAEP present different features. The ongoing source localization analysis will further reveal differences and commonalities in the brain activation for different types of sound changes.

Conclusions
The results provide evidence that separate brain mechanisms are involved for processing the "what" and "where" information of the sound in normal hearing listeners.

PS 537

Isolating Neural Correlates of Streaming and Attention to Components within Complex Tones

Hao Lu[1]; Andrew J. Oxenham[2]
[1]University of Minnesota; [2]Department of Psychology, Center for Applied and Translational Sensory Sciences, UMNTC

Alternating sequences of harmonic complex tones can form separate auditory streams, based on differences in fundamental frequency (F0) between the two tones. Attention can enhance the cortical representation of the attended stream, relative to the unattended stream, as measured via EEG. However, it is not known whether such enhancement can be observed at the level of individual components within complex tones. In particular, it is unclear whether or how a frequency component that is common to both tones is modulated by attention. To study this question, we used amplitude modulation (AM) around 40 Hz to generate auditory steady-state responses (ASSRs) that were used to tag certain frequency components within the complex tones of the attended or unattended stream.

EEG data were collected while normal-hearing young participants performed an auditory task. In each trial, 150-ms harmonic complex tones with F0s of 700 Hz and 1050 Hz were played in an alternating sequence lasting 6 s to generate the perception of two streams. Participants were instructed to selectively listen to either the low (700-Hz) or high (1050-Hz) stream and to report the number of level oddballs in the attended stream at the end of each trial. Some of the frequency components in each complex were AM-tagged. EEG responses were

measured and quantified to each tagged component using the multi-channel phase-locking value (PLV).

Analysis on entire epoch without windowing showed that PLVs at all AM frequencies were significant, suggesting stable distinct ASSRs evoked by AM-tagged frequency components. PLVs calculated with windowed EEG also matched the tagging frequency for components in either stream. Therefore, our paradigm successfully tracked the response to various frequency components in each stream. An effect of attention was observed, based on the event-related potential (ERP) to the onset of tones in the attended stream. However, no significant attentional modulation of the PLV was observed.

The proposed paradigm provides a tool to simultaneously measure responses to multiple frequency components within complex tones that are presented in an alternating sequence. The lack of attentional modulation of the ASSR on individual components may be due to the early cortical origins of the ASSR or the short duration of the tones, and suggests that other approaches may be needed to elucidate the effect of attention on individual components or features within auditory streams.

PS 538

[18F]FDG PET Imaging to visualize Asymmetry of the Inferior Colliculi and Primary Auditory Cortex in Asymmetric Hearing Loss

Iva Speck[1]; Susan Arndt[1]; Johannes Thurow[2]; Antje Aschendorff[1]; Ganna Blazhenets[2]; Philipp T. Meyer[2]; Lars Frings[2]
[1]Department of Otorhinolaryngology - Head and Neck Surgery, Medical Center - University of Freiburg, Faculty of Medicine, University of Freiburg, Germany; [2]Department of Nuclear Medicine, Medical Center - University of Freiburg, Faculty of Medicine, University of Freiburg, Germany

The purpose of the present ^{18}F-Fluordesoxyglucose ([^{18}F]FDG) positron-emission tomography (PET) study was to evaluate regional cerebral glucose metabolism as a marker of neural activity of the auditory pathway, especially the inferior colliculi and the primary auditory cortices, in asymmetric hearing-impaired subjects. The newest generation of fully-digital clinical PET/CT systems provides an improved spatial resolution that permits identification also of small brainstem nuclei. Regional glucose metabolism of two auditory regions of interest (ROI), the inferior colliculi and primary auditory cortices, was assessed in 13 subjects with asymmetric hearing impairment. By ROI analyses of the inferior colliculi and the primary auditory cortices, differences between ipsi- and contralateral normalized [^{18}F]FDG uptake was analyzed in reference to the cerebellum. In addition, we investigated the associations between duration of hearing impairment and normalized [^{18}F]FDG uptake. Regional metabolism of the inferior colliculus and primary auditory cortex was significantly reduced contralateral to the most impaired ear compared to the ipsilateral side ($p < 0.01$ and $p < 0.005$, respectively). The hypometabolism of the primary auditory cortex was attenuated with prolonged hearing impairment ($r^2 = 0.33$, $p = 0.04$). Regional metabolism of the contralateral inferior colliculus predicted the metabolism of the contralateral primary auditory cortex only when adjusting for the duration of hearing impairment ($r^2 = 0.61$, $p < 0.03$). The use of newest-generation, fully-digital clinical PET scanners permits imaging and quantitative assessment of small brainstem nuclei such as the inferior colliculi. Asymmetric hearing loss and duration of deafness (possible indication of multimodal plasticity) have a significant impact on the regional neuronal activity of parts of the auditory pathway. This might be of important clinical relevance with respect to the prediction of the performance outcome of patients after cochlear implantation.

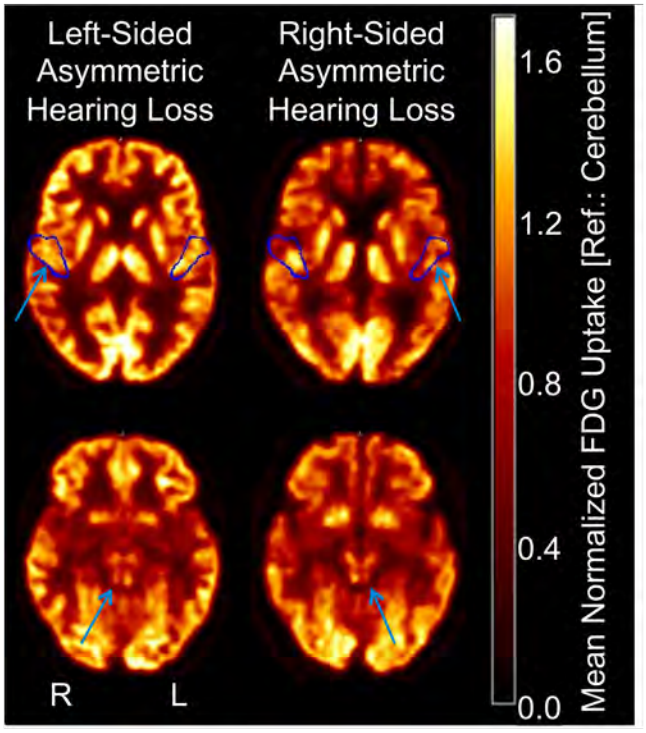

PS 539

Neural Mechanisms underlying Speech Perception in Listeners with Cochlear Implants Mapped using High-density Diffuse Optical Tomography

Arefeh Sherafati[1]; Mahlega S. Hassanpour[2]; Noel Dwyer[1]; Adam T. Eggebrecht[1]; Joseph P. Culver[1]; Jill B. Firszt[1]; Jonathan E. Peelle[1]
[1]Washington University in St. Louis; [2]University of Utah

Speech processing is variable in people with cochlear implants (CI) due to factors such as the degraded quality of sounds, the length, age of deafness, and the time since receiving the implant [1]. One hypothesis is that similar to effortful listening in normal-hearing individuals, people with CI might engage higher-order neural mechanisms as a result of enhanced attention during listening [2, 3].

Our goal is to map the neural systems supporting speech perception in listeners with CIs using High-density Diffuse Optical Tomography (HD-DOT), an optical neuroimaging technique with a spatial resolution comparable to that of fMRI [4]. HD-DOT is ideal for studying people with implanted medical devices because it poses no safety risk, and artifacts in the measured signal are minimal [5]

We recorded the brain's hemodynamic response to the presentation of single words and during passive movie watching in both listeners with CIs and normal-hearing age- and sex-matched control participants using a previously described HD-DOT system (Fig. 1a-d) [4, 6]. During each hearing words run, participants listened to a total of 180 words during twelve trials. Each trial contained 15 words, followed by 15 seconds of silence. During each movie task, participants watched a 10 min clip from the "The good, the bad, and the ugly" [6]. We studied twelve control subjects (31-72 years) and fourteen participants with a right-side unilateral CI. We used a General Linear Model (GLM) by extracting the speech feature from the movie stimulus to find the cortical activity involved in processing speech.

Our results demonstrate bilateral superior temporal gyri (STG) activation in response to the hearing words task for both control participants and CI receivers, as well as left dorsolateral prefrontal cortex (DLPFC) activation for CI listeners. In response to the speech in movies, we found more extended activations around the left and right STG in both controls and CI recipients as well as left and right DLPFC activation observed only in CI recipients (Fig. 1e-f)

DLPFC is a region that is known to play an important role in executive functions such as working memory and abstract reasoning. DLPFC is one of the nodes of the frontoparietal attention network it is playing a key role when we pay more attention to the meaning of the degraded sound [2, 3]. This frontal activation is consistent with a need to rely on executive resources to compensate for a degraded acoustic signal.

References

[1] J. B. Firszt, et al. Recognition of speech presented at soft to loud levels by adult cochlear implant recipients of three cochlear implant systems. Ear Hear 25:375-387 (2004)

[2] C. J. Wild, et al. Effortful listening: the processing of degraded speech depends critically on attention. Journal of Neuroscience. Journal of Neuroscience. 2012 Oct 3;32(40):14010-21

[3] Peelle JE (2018) Listening effort: How the cognitive consequences of acoustic challenge are reflected in brain and behavior. Ear Hear 39:204-214

[4] A. T. Eggebrecht, et. al. Mapping distributed brain function and networks with diffuse optical tomography, Nature Photonics 8, 448–454 (2014)

[5] M. S. Hassanpour. Developing Diffuse Optical Tomography (DOT) for Neuroimaging of Speech Perception in People with Cochlear Implants, Arts & Sciences Electronic Thesis and Dissertations, 652 (2015)

[6] A. K. Fishell, et. al. Mapping brain function during naturalistic viewing using high-density diffuse optical tomography. Scientific Reports, volume 9, Article number: 11115 (2019)

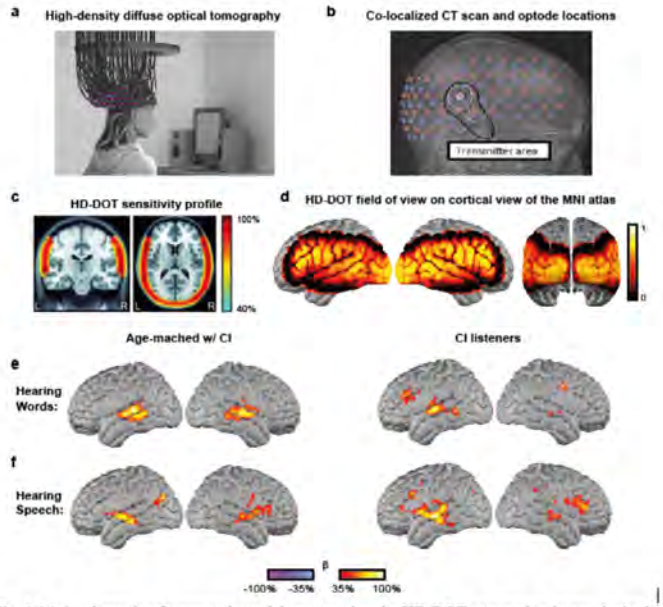

Fig. 1 (a) A schematic of a research participant wearing the HD-DOT cap used to image the brain in this study. **(b)** HD-DOT head model co-registered to a CI recipient's CT scan. **(c)** HD-DOT sensitivity profile. **(d)** HD-DOT field of view spatially registered on the cortical view of the MNI atlas. **(e)** Response to words, **(f)** response to the movie speech, in age-matched controls and CI recipients.

PS 540

Concurrent EEG and Pupillometry Measures of Listening Effort while Listening to Speech in Noise.

Emily Graber[1]; Emmanuel Chan[1]; Brandon T. Paul[2]; Andrew Dimitrijevic[2]
[1]Sunnybrook Health Sciences Centre, Otolaryngology Head and Neck Surgery, University of Toronto; [2]Sunnybrook Research Institute

Listening to speech in noisy environments is often effortful for individuals with hearing impairments, yet clinical tests and procedures to detect and reduce listening effort are lacking. Pupil diameter is a promising measure that has recently been related to listening effort ratings and EEG alpha across normal hearing participants in difficult listening conditions. Studies have also shown that single-trial alpha power relates to listening effort ratings. Thus, a within-subject relationship between listening effort ratings and pupil diameter on a trial-by-trial basis is expected. Here we explore whether pupil diameter mirrors trial-by-trial effort ratings and EEG alpha activity within individuals.

64-channel EEG and pupillometry were recorded in 12 normal hearing participants listening to short sentences embedded in multi-speaker babble. The babble was presented at 60 dB for all trials while the sentence level varied over three signal-to-noise ratios (SNRs) to make easy, medium and hard trials. The SNRs for the three conditions were obtained in a short behavioral session just prior to the EEG session. In the EEG session after each stimulus, the participants verbally repeated the sentence and gave a rating of their listening effort on a 1-9 scale.

Pupil diameters as a function of time and condition were examined for individuals. EEG in the alpha range (8-12 Hz) was beamformed into time series as well using LCMV. Preliminary findings suggest that changes in alpha sources and pupil diameter correspond, but multiple types of relationships exist between reported listening effort and the objective measures, EEG alpha and pupil diameter, despite equated behavioral performance.

Future work will characterize how trial-by-trial pupil diameter relate to listening effort ratings and EEG alpha. These results may aid in the development of clinical tests that reveal listening effort, though further investigation is required.

PS 541

Neural modulation to direction and speaker in spatial multi-talker speech perception

Prachi Patel[1]; Jose Herrero[2]; Ashesh Mehta[3]; Nima Mesgarani[1]
[1]Columbia University; [2]Hofstra-Northwell School of Medicine & Feinstein Institute for Medical Research; [3]Hofstra-Northwell School of Medicine and Feinstein Institute for Medical Research

Humans can attend to speech of a talker in an acoustically complex, spatial separated multi-talker environment. How the human auditory cortex encodes speech of simultaneous spatially separated talkers and how attention to the location of a talker modulates the neural response is unknown. Here, we record intracranially from the auditory cortex of subjects engaged in a listening task with two simultaneous spatially separated talkers, and each spatial talker stand alone. We demonstrate that the location of speech played in quiet has little effect on its encoding in the human auditory cortex, however, irrespective of attention, in the presence of spatial interfering talker the neuronal tuning narrows to the speech of contralateral talker for the majority of electrodes. Moreover, we show what aspects of the neural response are modulated by attention to the direction of speech and by attention to the talker. Our results demonstrate how the neuronal tuning changes in presence of spatially competing talkers and how the spatial auditory attention modulates the neuronal response.

PS 542

Neural Correlates of Auditory Enhancement

Anahita H. Mehta[1]; Lei Feng[1]; Andrew J. Oxenham[2]
[1]University of Minnesota; [2]Department of Psychology, Center for Applied and Translational Sensory Sciences, UMNTC

Introduction

Auditory enhancement is a phenomenon where a target tone in a simultaneous masker complex becomes perceptually more salient if a copy of the masker, termed the precursor, is presented first. This effect reflects the general principle of contrast enhancement, and may help in the detection of new acoustic events and in the perceptual constancy of speech under varying and noisy acoustic conditions. The physiological mechanisms underlying auditory enhancement are still unknown. In this study, we used auditory steady-state response (ASSR) with a double-modulation paradigm to test the hypothesis of the enhancement of the neural response to the target tone when the precursor is present. Four EEG experiments were carried out with different

stimulus parameters designed to dissociate cortical and subcortical contributions to this phenomenon.

Methods
Four passive-listening EEG experiments were conducted, each with 16-18 normal-hearing (NH) listeners. There were two main conditions in all experiments: a simultaneous masking condition (MSK) and an enhancement condition (ENH). For the MSK condition, each trial consisted of a five-component inharmonic complex, including one target and four masker tones. The frequencies of the complex were roved from trial to trial. In the ENH condition, the masker-plus-target complex was preceded by a precursor with the four maskers alone. In three of the experiments, the level of the target was tested at three target-to-masker ratios (TMRs) to estimate the level function in both conditions. The target and masker components were differentially amplitude modulated by frequencies around 40, 100, and 200 Hz in various combinations to tag the subcortical (100 and 200 Hz) and cortical (40 Hz) representations. The neural response to the tagged components was quantified using the phase locking values (PLVs). The amount of enhancement for all stimuli was also measured behaviorally for all experiments, in terms of TMR at detection threshold.

Results
Behaviorally, all the stimuli showed comparable amounts of enhancement of 15-20 dB. The EEG data across three experiments showed robust enhancement of the ASSR around 40 Hz, as indicated by an absolute increase in the target PLV in the presence of a precursor across TMRs. Additionally, some enhancement of the neural responses to the target was observed at subcortical levels via the PLV at both 100 and 200 Hz.

Conclusions
The data indicate that the double-modulation paradigm can be used to reveal the neural correlates of auditory enhancement at both cortical and subcortical levels simultaneously.

Supported by NIH grant R01DC012262.

PS 543

Signatures of Regularity in Low- and High-Frequency Activity Recorded from Human Primary and Non-Primary Auditory Cortex

Alexander Billig[1]; Phillip Gander[2]; Christopher Kovach[2]; Hiroto Kawasaki[2]; Timothy Griffiths[3]; Ingrid Johnsrude[4]; Matthew Howard[2]; Maria Chait[5]
[1]UCL Ear Institute; [2]University of Iowa; [3]Institute of Neuroscience, Newcastle University; [4]The Brain and Mind Institute, Western University; [5]UCL Ear Institute, 332 Gray's Inn Rd, London, WC1X 8EE, United Kingdom

Making sense of the auditory environment is facilitated by the identification of repeating acoustic structure. The human auditory system rapidly and automatically detects regular patterns in tone sequences, as evidenced by distinct signatures in neural activity at the time of their emergence, over the course of repetition, and after the sequence ends (Barascud et al., PNAS, 2016; Southwell & Chait, Cortex, 2018). The contribution of different fields within auditory cortex to each of these signatures has not been firmly established, but may shed light on different stages of processing of regularities in sound. We recorded intracranially from seven human subjects who were undergoing monitoring to identify epileptic seizure foci. Electrode coverage included primary and non-primary auditory cortical fields on the superior temporal plane and superior temporal gyrus. We presented 4.5-s sequences of 50-ms tone pips, each sequence consisting of consecutive sets of the same 5 or 10 frequencies ordered either consistently ("regular") or inconsistently ("random") from set to set, while subjects listened without performing any task. Clear spectral peaks at the *tone* repetition rate (20 Hz) were present at contacts in primary auditory cortex (posteromedial Heschl's gyrus), and these were significantly greater for regular compared to random sequences in a subset of subjects. In one case, patterns of length 5 were associated with greater power at the *pattern* repetition rate (4 Hz) in primary cortex, during regular compared to random sequences. In contrast, high gamma power – a proxy for neural spiking activity – was modulated to a greater extent for *random* compared to *regular* sequences at the tone repetition rate, indicating a dissociation of high and low frequency neural activity with respect to regularity processing. A broader set of non-primary sites, including in anterolateral Heschl's gyrus, planum polare, and superior temporal gyrus, displayed effects of regularity and alphabet size, either at the time of pattern emergence or following sequence offset. These effects varied in latency and direction across sites and subjects. Ongoing work will further characterise this variability, with a view to better establishing the contribution of distinct neural sources to auditory regularity processing.

PS 544

Task Effects on Cortical Responses to Auditory Novelty: An Intracranial Electrophysiology Study

Kirill Nourski[1]; Mitchell Steinschneider[2]; Ariane Rhone[3]; Hiroto Kawasaki[3]; Matthew Banks[4]
[1]The University of Iowa; [2]Albert Einstein College of Medicine; [3]University of Iowa; [4]University of Wisconsin

Elucidating changes in predictive coding across attentional and arousal states is a major focus in neuroscience. The local/global deviant paradigm (Bekinschtein et al, PNAS 2009 106:1672-7) engages auditory predictive coding over short (local deviance, LD) and long (global deviance, GD) time scales. It has been used to assay disruption of predictive coding upon loss of consciousness. Our previous work (Nourski et al, J Neurosci 2018 38:8441-52) examined effects of general anesthesia on short- and long-term novelty detection. GD effects were suppressed at subhypnotic doses of propofol, suggesting that they may be more related to attention than consciousness per se. This study addressed this hypothesis by comparing cortical responses to auditory novelty between passive and active task conditions in awake listeners.

Subjects were 7 adult neurosurgical patients undergoing chronic invasive monitoring for medically intractable epilepsy. Sequences of five 100 ms vowels separated by 50 ms silent intervals were presented to subjects as they attended to a silent TV program (passive task) or responded to GD stimuli by pressing a button (active task). Intracranial recordings were made from multiple brain regions, including core and non-core auditory, temporo-parietal auditory-related, prefrontal and sensorimotor cortex. Task performance was measured as sensitivity, hit rate and reaction times. Cortical activity was measured as averaged auditory evoked potentials (AEPs) and event-related band power.

Vowel stimuli and LD elicited robust AEPs in all studied brain areas in both passive and active experiments. The active task led to an increase in the fraction of sites in prefrontal cortex responding to vowels and exhibiting an AEP LD effect. High gamma (70-150 Hz) responses to stimulus onset and LD were localized predominantly to the auditory cortex in the superior temporal plane and had a comparable spatial extent between the two conditions. In contrast, high gamma GD effects were greatly enhanced during the active task in auditory cortex on the lateral superior temporal gyrus, auditory-related, prefrontal and sensorimotor cortex. The active task was associated with an increase in the magnitude of LD and GD effects on individual sites, particularly outside canonical auditory cortex. The prominence of GD effects was associated with subjects' task performance.

The data demonstrate distinct task-related effects on auditory novelty responses across the cortical hierarchy. The results motivate a closer examination of connectivity underlying attentional modulation of cortical sensory responses, and serve as a foundation for examining changes in sensory processing associated with general anesthesia, sleep and disorders of consciousness.

PS 545

Using Functional Near-Infrared Spectroscopy to Assess Auditory Responses in Auditory and Lateral Frontal Cortex

Min Zhang; Antje Ihlefeld
New Jersey Institute of Technology

Background

In situations with background sound, speech intelligibility is often low for most cochlear implant (CI) users. Using functional near infrared spectroscopy (fNIRS), we previously confirmed that lateral frontal cortex (LFC) engages more strongly when normal-hearing listeners actively attend to speech in the presence of a speech background vs listen passively (Zhang et al. 2018). To elucidate how the types of perceptual cues delivered by CI devices shape cortical responses in situations with background sound, we here extend this prior work and test normal-hearing listeners with simulations of the types of perceptual cues available to CI users.

Methods

We presented two competing talkers, a target and a masker, consisting of streams of key- and distractor-words. The listeners' task was to detect when the target talker uttered one of four key-words. Utterances were either unprocessed speech or vocoded with 8, 16 or 32 bands. Infrared optodes from a continuous-wave diffuse-optical NIRS system (CW6; TechEn Inc., Milford, MA) were embedded in a custom-made head-cap and placed directly above each of four ROIs (bilateral LFC, bilateral auditory cortex). 3D-location tracking verified optode position via the Montreal Neurological Institute ICBM-152 brain atlas. 14 normal-hearing listeners (aged 21-40, 4 females) initially performed a controlled breathing task, followed by auditory testing. Using HOMER2, we extracted oxy- and deoxy-hemoglobin traces (HbO and HbR), combining them to a total fNIRS trace (HbT). All traces from the auditory task conditions were normalized by recruitment strength during controlled breathing. To calculate activation levels, we then used canonical hemodynamic response functions to fit four general linear models (GLM) to the normalized trace, one GLM for each ROI.

Results

Behavioral performance was best in the unprocessed and worst in the 8-band vocoded conditions, as expected. Task-driven HbT responses in all four ROIs were significantly different from zero. Moreover, HbT responses were significantly correlated with task performance in right AC ($R^2 = 0.4$, $p = 0.01$).

Conclusions
In right AC, fNIRS recordings are sensitive to intelligibility of masked vocoded speech.

Reference
Zhang, M., Mary Ying, Y.L. and Ihlefeld, A., 2018. Spatial Release From Informational Masking: Evidence From Functional Near Infrared Spectroscopy. Trends in hearing, 22, p.2331216518817464.

PS 546

Effects of Linguistic and Non-Linguistic Interference on Speech Categorization and Neural Encoding

Jared Carter; Gavin Bidelman
University of Memphis

Speech perception requires the grouping of acoustic information into meaningful phonetic units though the process of categorical perception. Environmental masking also influences speech recognition. However, it remains unknown at which stage of processing (encoding, decision, or both) masking affects listeners' identification of speech signals. The purpose of this study was to determine whether semantic interference influences the early acoustic-phonetic conversion process inherent to CP. To this end, we recorded EEGs as listeners rapidly categorized speech sounds along a /da/ to /ga/ continuum presented in three listening conditions: quiet, and in the presence of forward (informational masker) and time reversed (energetic masker) 2-talker babble noise. Maskers were matched in overall SNR to vary only in their degree of linguistic interference (i.e., information masking). We hypothesized informational masking would have a differential effect on categorization compared to energetic masking with the same spectro-temporal features. Psychometric identification functions were expectedly shallower in noise overall. However, we found an interesting gradient effect dependent on masker type, with steeper categorization slopes in time-reversed compared to forward babble. Response times showed a similar gradient in listeners' speed of speech labeling (i.e., $RT_{quiet} < RT_{REV} < RT_{FOR}$). These psychometric changes suggest the neural representations and perceptual access to phonetic speech categories are more susceptible to acoustic interference when competing noise carries lexical-semantic information. Moreover, our data reveal informational masking has a larger effect on listeners' ability to identify speech sounds than energetic masking with the same fine-structure acoustic properties, suggesting top-down modulation of early categorical processing.

Auditory Learning

PS 547

Rapid Perceptual Learning and Individual Differences in the Recognition of Rapid Speech in Younger and Older Adults

Tali Rotman; Limor Lavie; Karen Banai
University of Haifa

Perceptual learning operates across the lifespan, but its role in speech and language beyond infancy is not well understood. The goal of the current study was to determine whether rapid perceptual learning can explain unique variance in the recognition of natural fast speech once the contribution of other variables is accounted for. We tested the recognition of very fast speech (221 words/min) in young adults (YA, n = 55) and in older adults with age-related hearing loss (OA, n = 45). Perceptual learning was estimated using time-compressed speech. To get an estimate of learning clean of the potential effects of age and hearing on speech recognition, different rates of time-compressed speech were used for the two groups (226 and 339 words/min in older and younger adults, respectively). Hearing, verbal memory and attention capacity were also assessed. Older adults recognized fast speech less accurately than YA (95% CI: 31-43% vs. 84-88%). Rapid perceptual learning was also reduced in older adults. Nevertheless, in both groups, learning accounted for unique variance in FS recognition. Rapid perceptual learning was the only significant predictor in young adults (R^2 >15%). In older adults, both rapid perceptual learning and vocabulary scores accounted for significant unique variance in recognition. These findings suggest that perceptual learning may support the recognition of perceptually difficult speech and that age/hearing related declines in learning may partially explain why older adults are disproportionally affected by rapid speech rates.

PS 548

Rats Discriminate the Salience of Deviant Stimuli in an Oddball Paradigm

Camilo J. Morado-Díaz[1]; Gonzalo Terreros[2]; Cristian Aedo-Sánchez[1]; Daniel Duque[3]; Manuel S. Malmierca[1]
[1]University of Salamanca; [2]Universidad de O'Higgins; [3]Institut d'Investigacions Biomèdiques August Pi i Sunyer

We have previously used the oddball paradigm to study stimulus-specific adaptation (SSA), deviance detection and assess neuronal responses to expected and unexpected stimuli in the auditory midbrain, thalamus and cortex. However, it remains unknown how the brain resolves the conflict between what is likely to happen and

what is behaviourally relevant (attention). Thus, in order to evaluate the modulation of SSA during an attentional task, we trained rats to discriminate deviant tones in an oddball paradigm. We designed and progressively implemented three levels of stimulus complexity with food rewards. First, animals learnt to respond to a sound activating a nose-poke in an operational chamber, then they learnt to recognize a deviant tone presented in between periods of silence, and finally they learnt to distinguish a deviant tone embedded in an oddball paradigm. Once training was completed, data were collected after three oddball paradigms options: 1) the classical, high probability standard tones (90%) randomly interrupted by low probability deviant tones (10%) and 0.5 octaves in frequency contrast, 2) a similar paradigm, but in this case, the frequency contrast between standard/deviant tones varied in 3, 0.25 octaves steps, and 3) a many deviants sequence made of several blocks of the classical oddball paradigm as in 1, where every 10 stimuli, the sound frequency of the a deviant tone is randomly changed from 9 possibilities of different tones, and the standard sound is maintained throughout the entire sequence. To quantify the ability discrimination of the rat to the deviant sound at each stage, we calculated the conventional *d'* index. We implemented options 2 and 3 to test the animals' responses to irregularity. We also compared the results with those obtained in not-trained animals. Results so far (n=19) show that trained animals were able to complete this target-detection tasks with 70.1±14.6% of correct detections, 8.6±4.8% of false alarms, and a *d'* value of 2.1±0.6 (mean ± std). Thus, our data demonstrate that rats can successfully discriminate the salience of deviant stimuli. This behavioural study will be useful in future neurophysiological studies in the behaving animal, as it will be the key resource to understand the neuronal link between expectation and attention.

Supported by the Spanish MINECO (SAF2016-75803-P) to MSM, (FJCI-2016-27897) to CJMD, (IJCI-2016-29358) to DD; and Fondo de Movilidad Institucional Univ. O´Higgings and Beca iberoamericana Santander Universidades to GT.

PS 549

Observational Learning Exploits the Available Physical and Social Cues

Nihaad Paraouty; Joey A. Charbonneau; Dan H. Sanes
New York University

The ability to acquire a new behavior can be facilitated by witnessing the performance of a conspecific demonstrator. This observational learning (OL) typically depends on both sensory and social cues. However, in natural environments where parents or siblings may serve as demonstrators, OL is likely to occur under a range of conditions. For example, many species, including the Mongolian gerbil, are most active in underground burrows or at night when visual cues are limited. Here, we tested the idea that OL can benefit from the available sensory or social cues, thereby permitting task acquisition in different environments. The ability of naïve male and female observer gerbils to learn a sound discrimination task through observation of a performing demonstrator was tested in the presence or absence of visual cues. The results show that observers acquired the task at a significantly faster rate under either condition, as compared to controls with no previous experience. Furthermore, when observer gerbils watched a demonstrator performing a visual discrimination task, they were subsequently able to acquire the auditory task significantly faster than controls. Taken together, these results suggest that either visual or non-visual information is sufficient for task acquisition. To determine whether sensory cues alone could support OL, observers were exposed to experimenter-triggered trials instead of a performing demonstrator. The rate of task acquisition was delayed compared to observers exposed to a performing demonstrator, but faster than the controls, suggesting a discrete contribution of non-social cues.

PS 550

Auditory Categorical Learning is Shaped by Inherent Musical Listening Skills

Kelsey Mankel; Gavin Bidelman
University of Memphis

Humans organize diverse, continuous stimuli in the environment into categories that share perceptual similarities, including speech and music sounds. The neural mechanisms underlying categorical learning, including when and where in the brain categories are formed, remains undetermined. Additionally, while music expertise enhances speech perception and sound-to-meaning learning, it is unclear whether innate musicality (in the absence of formal music training) influences categorical learning of unfamiliar sounds. To address these questions, we trained nonmusicians to identify musical pitch intervals (minor and major 3rd dyads) in a short-term learning task (15-20 min). A separate continuum (minor to major 6ths) served as a control set to assess perceptual learning and transfer effects. Identification training was highly effective as most individuals scored >80-90% on interval labeling by post-test. Psychometric curves for the trained continuum were steeper post-training relative to the untrained stimulus set, indicative of stronger categorization performance. Although smaller, post-training gains for the untrained intervals suggested subtle transfer in perceptual learning.

These findings demonstrate that feedback training was more critical for establishing perceptual categories than mere exposure. Category learning was then compared with performance on a test of receptive musicality (Profile of Music Perception Skills; PROMS). Individuals who possessed naturally higher musicality (better PROMS scores) showed enhanced tone categorization by higher accuracy and faster response times compared to those with lower musicality. Our results have implications for understanding individual differences in categorical perception and learning by demonstrating certain listeners with inherently superior auditory skills are better primed to map sounds to meaning.

Auditory Prostheses V

PS 551

Electric Stimulation Thresholds Are Correlated with Acoustic Hearing Changes in an Aged Guinea Pig Cochlear Implant Model

Lina Reiss[1]; Melissa Lawrence[2]; Irina Omelchenko[2]; Wenxuan He[2]; Michael Reiss[2]; Jonathon R. Kirk[3]; Douglas Fitzpatrick[4]
[1]Oregon Health and Science University; [2]Oregon Health & Science University; [3]Cochlear Limited, Sydney, Australia; [4]University of North Carolina at Chapel Hill

The electro-acoustic stimulation (EAS) or Hybrid cochlear implant (CI) combines electric stimulation with residual low frequency acoustic hearing, with benefits for voice recognition, music appreciation, and speech perception in noise. However, 30-55% of hybrid CI users lose residual hearing days to months after implantation and CI activation, reducing this benefit. Further, recent studies showed that outcomes with the CI alone are better with hearing preservation, suggesting a link between hearing preservation and electrical stimulation efficacy (Carlson et al., 2011; Fitzpatrick et al. 2013). The objective of this study was to determine the relationship between measures of electrical stimulation efficacy to acoustic hearing changes after implantation and EAS in a guinea pig CI model.

Two groups of guinea pigs, aged 9-21 months, were implanted with a CI in the left ear, and allowed to recover for 4 weeks. The EAS group (n=5) received chronic EAS (amplitude-modulated noise, 1-20 kHz, acoustic: 72-75 dB SPL, electric: 1800 pps, C level) at 40 hours/week for 20 weeks. The non-stimulated group (NS; n=6) received no EAS over the same timeframe. Auditory brainstem responses (ABRs) and electrically-evoked ABRs (EABRs) were recorded monthly over the course of the experiment to assess changes in acoustic and electric thresholds, as well as amplitude growth functions. Following the completion of the experiment, all animals were perfused and cochlear tissue was harvested for histological evaluation.

Cochlear implantation led to an immediate increase in ABR thresholds peaking between 3-5 weeks after surgery and then recovering and stabilizing by 5-8 weeks. EABR thresholds also similarly peaked over this time period, with greater recovery in NS animals. These older animals also exhibited larger ABR threshold shifts at 3-5 weeks compared to younger animals tested in previous studies. By the end of the 20-week period, EAS animals had greater long-term low frequency ABR threshold shifts compared to NS animals, consistent with previous findings (Tanaka et al., 2014; Reiss et al., 2015).

For all animals pooled together, higher EABR thresholds were positively correlated with greater ABR threshold shifts at 8 and 16 kHz, but not lower frequencies. Similarly, EABR amplitude growth function slopes were negatively correlated with 8 and 16 kHz ABR threshold shifts. The correlations between acoustic threshold shifts and electric stimulation measures suggest that surgical trauma may disrupt both acoustic hearing and electric stimulation via the neural pathway. This work was funded by a contract with Cochlear and by NIH/NIDCD grant R56 DC016308.

PS 552

Relationship between Peripheral Spread of Excitation and Binaural Fusion in Bilateral Cochlear Implant Users

Logan Remington[1]; Holden Sanders[2]; Morgan Eddolls[2]; Lina Reiss[2]
[1]Oregon Health & Science University; [2]Oregon Health and Science University

Binaural fusion is the fusion of auditory stimuli across the ears into a single auditory object. Many individuals with hearing aids and/or cochlear implants (CIs) experience abnormally broad binaural pitch fusion, fusing sounds that differ greatly in pitch across ears (Reiss et al., 2014, 2016, 2018). However, there is significant variability with some experiencing narrow fusion and others experiencing broad fusion. The objective of this study was to determine if the variation in peripheral spread of excitation (SOE) can explain the variation in binaural fusion in bilateral CI users.

The electrically-evoked compound action potential (ECAP) is an objective measure that can be used to record the population auditory nerve response to electric stimulation. The amount of forward masking

of the ECAP response to a probe electrode by various preceding masker electrodes provides an objective estimate of the SOE. In this study, we recruited six bilateral CI recipients, with Cochlear Nucleus CI24RE or later. ECAP SOEs were recorded for each even-numbered probe electrode in the comparison ear and for probe electrodes 6, 12, and 18 in the reference ear. SOEs were recorded with the probe and all maskers at the same comfort level (6,7, or 8 on a scale of 0-9).

Binaural pitch fusion was measured behaviorally using a single interval procedure. Both reference and dichotic comparison electrodes were stimulated simultaneously for 1500-ms, with the reference electrode was held constant in one ear and the comparison electrode in the contralateral ear varied with pseudorandom order across trials. At each trial, subjects were asked to indicate whether they heard a single fused sound or two different sounds in each ear. Binaural fusion functions were generated by the average of the responses.

A mathematical model was used to predict binaural fusion from the overlap between the SOEs from the two ears. For instance, the SOE for reference electrode 12 in the reference ear was multiplied by the SOE for electrode 2 in the comparison ear and summed to generate a prediction for binaural fusion between these two electrodes, and so on for other electrodes in the comparison ear. Preliminary results from three subjects show that binaural SOEs can predict binaural fusion functions for some, but not all subjects and electrodes. The findings suggest that abnormally broad binaural fusion may not be explained solely by peripheral auditory resolution.

This work was funded by NIH/NIDCD grant R01 DC013307.

PS 553

Acoustically Evoked Compound Action Potentials (CAPs) Recorded from Electro-Acoustic Stimulation (EAS) Cochlear Implant Users: A Preliminary Study

Jeong-Seo Kim[1]; Viral Tejani[2]; Carolyn Brown[1]; Paul Abbas[1]; Inyong Choi[1]
[1]Dept of Communication Sciences and Disorders, University of Iowa; [2]Dept of Otolaryngology - Head and Neck Surgery, University of Iowa Hospitals and Clinics

Introduction

Shorter electrode arrays and soft surgical techniques allow for preservation of acoustic hearing in many cochlear implant (CI) users. For these electro-acoustic stimulation (EAS) CI users, the Neural Response Telemetry system can be used to record acoustically evoked responses from an intracochlear electrode (Abbas et al., 2017), including hair cell responses (cochlear microphonic (CM)) and phase-locked neural responses (auditory nerve neurophonic (ANN)). Unfortunately, ANN responses are considerably smaller in amplitudes and complete segregation of the CM from the ANN has proven difficult (Forgues et al., 2014). The compound action potential (CAP) is a measure of the synchronous response of multiple auditory neurons and may provide an alternative to the ANN where the status of the auditory nerve is of primary interest. In this study, we recorded chirp-evoked CAPs, presuming that enhanced neural synchrony offered by chirp stimuli would lead to better CAP responses compared to standard clicks or tone bursts (TB) (Fobel and Dau, 2004; Chertoff et al., 2010). This study describes within-subject comparisons of CAPs recorded using low-frequency tone bursts, clicks, and chirps.

Methods

Ten adult Nucleus L24 Hybrid CI users with residual low-frequency hearing participated. CAP growth functions were recorded from the most apical intracochlear electrode using 500 Hz tone bursts, clicks, and chirps presented via an insert phone to the implanted ear. In addition, nine chirps with varied cochlear group delays were generated and CAP responses to each stimulus were measured with the goal of determining the optimal chirp for this population of CI users. Response morphology, threshold, latency- and amplitude-intensity functions were compared.

Results

Click- and chirp-evoked CAPs were more reliably measurable than TB-evoked CAPs. The general morphology of chirp-evoked CAPs was more consistent than clicks. However, click-evoked CAPs had slightly lower thresholds than chirp-evoked CAPs and peak amplitudes were comparably similar. The cochlear group delay used to construct the optimal chirp was found to vary across subjects. For some subjects, enhanced CAP morphology and larger peak amplitudes were obtained when shorter group delay values for chirp stimuli were used.

Conclusions

Preliminary results suggest that CAPs can be measured more effectively using either click or chirp stimuli than low-frequency tone bursts in EAS CI users. The advantage of using a chirp relative to standard click may prove to be dependent on the cochlear group delay used to generate the chirp and potentially also audiometric configuration. This work is supported by NIH/NIDCD grant P50 DC 000242.

PS 554

Perceptual Integration of Speech Information Across Ears with Bilateral Cochlear Implants and Simulations in Normal-Hearing

Sean R. Anderson[1]; Frederick J. Gallun[2]; Ruth Y. Litovsky[3]
[1]University of Wisconsin-Madison; [2]VA RR&D NCRAR; [3]The University of Wisconsin–Madison

Speech information in the better ear interferes with the poorer ear in patients with bilateral cochlear implants (BiCIs) that have large asymmetries in speech intelligibility between ears (Goupell et al., 2016; 2018). The goal of the present study was to assess how each ear impacts, and whether one dominates, speech perception. We hypothesized that if abnormal integration of speech information occurs for listeners with BiCIs that have asymmetrical speech understanding, then listeners with BiCIs and simulations in NH would demonstrate an atypical preference to report speech in the better ear when speech was presented simultaneously to both ears.

We presented one or two words to each ear and listeners reported the word(s) they perceived. Studies in normal-hearing (NH; Cutting, 1976) showed that when a word beginning with a stop consonant (e.g., “pay”) and another beginning with a liquid (e.g., “lay”) were presented to opposite ears, listeners integrated information and reported a combined percept (e.g., “play”). Here we tested three conditions: (1) same word in both ears, (2) two different words to the two ears beginning with stop and liquid consonants, or (3) two different words to the two ears that shared no phonemes.

In listeners with BiCIs, stimuli were presented via direct connection to the auxiliary port of their device or via circumaural headphones at a comfortable level using their clinical MAPs. In NH listeners, vocoded stimuli were presented via circumaural headphones at 65 dB(A). Vocoding was completed by filtering stimuli into logarithmically spaced bands between 150-8000 Hz using noise or sine-tone carriers.

Both groups heard one word approximately 30% of the time when the words in each ear differed by only their first phoneme, consistent with Cutting (1976). This rate increased when stimuli were vocoded compared to unprocessed for listeners with NH. The word perceived by listeners with BiCIs was related to the speech recognition in either ear, and most often corresponded to the right (better) ear. However, in some cases a word corresponding to neither ear was reported, suggesting that the worse ear interfered with speech perception. Together, these results suggest that degradations of speech representation, related to speech understanding asymmetries in listeners with BiCIs or simulations in NH, limit the auditory system’s ability to accurately represent speech sounds. Abnormal binaural speech perception has important implications for patient counseling and training post-bilateral implantation.

Work supported by NIH-NIDCD R01-DC003083 to RL and NIH-NICHD U54HD090256 to the Waisman Center.

PS 555

Within-Ear Balancing of Response Strength Between Acoustic and Electric Stimulation Improves Interaural Time Difference Coding in an Animal Model of Single-Sided Deafness

Maike Vollmer[1]; Merle Berents[1]; Andrew Curran[1]; Armin Wiegner[2]
[1]Department of Otorhinolaryngology-HNS, University Hospital Magdeburg; [2]Comprehensive Hearing Center, University Hospital Würzburg

Unilateral cochlear implants (CIs) have emerged as a treatment option for subjects with single-sided deafness (SSD), allowing combined electric stimulation of one ear and acoustic stimulation of the other ear. Although such bimodal stimulation enables binaural hearing in these subjects (‘SSD-CI users’), their speech perception in noise and directional hearing is typically poorer than in normal-hearing listeners. Moreover, improvements in directional hearing in SSD-CI users are mainly based on interaural level differences, not on interaural time differences (ITDs). Possible explanations for these deficits in SSD-CI users include deafness-induced degradations in neural ITD sensitivity or between-ear mismatches in the sites of activation or in the relative stimulation level of either mode.

Here, we characterized the responses of single neurons in the inferior colliculus to ITDs in normal-hearing gerbils that had been unilaterally implanted with a round window electrode to enable electric stimulation of auditory-nerve fibers while maintaining acoustic sensitivity of the implanted ear. This approach excluded the possibility of deafness-induced degradations as a contributing factor in ITD processing, and allowed us to directly compare ITD coding to transient, broadband bimodal and unimodal-acoustic stimulation (low-rate biphasic electric pulses and acoustic clicks) in the same neuron.

The incidence of ITD-sensitive neurons was similar for bimodal and unimodal-acoustic stimulation. Also, ITD-dependent modulations in spike rate occurred within similar ITD ranges after adjusting for peripheral delay

differences between acoustic and electric stimulation in the implanted ear. However, within given neurons, the shapes of rate-ITD functions for bimodal stimulation often differed from those for unimodal-acoustic stimulation and were highly level dependent. To balance the response strength between stimulus modes, we adjusted the electric stimulus level in the implanted ear to match the spike rate of the same ear in response to acoustic stimulation. This in turn balanced the binaural level cues between the two ears and increased the shape similarity of rate-ITD functions to bimodal and unimodal-acoustic stimulation obtained from the same neuron. Moreover, matched-pair comparisons in the same sample of neurons showed no differences in the degree of ITD sensitivity or in neural discrimination thresholds between bimodal and unimodal-acoustic stimulation.

Our results in the normal-hearing system reveal widespread similarities of neural ITD coding to bimodal and unimodal-acoustic stimulation. Nevertheless, the results also suggest that balancing the relative delay and binaural level cues between the two modes of stimulation is important to improve the binaural benefit from bimodal hearing in SSD-CI users.

Supported by DFG VO 640/2-2.

PS 556

Unilateral Hearing Loss During Development and Adulthood Differently Disrupts Binaural Integration in the Auditory Midbrain

Andrew Curran; Maike Vollmer
Department of Otorhinolaryngology-HNS, University Hospital Magdeburg

Subjects with single-sided deafness (SSD) increasingly undergo cochlear implant surgery (SSD-CI users) to obtain binaural hearing benefits, such as directional hearing. However, asymmetric hearing may disrupt the hemispheric balance of central auditory circuits that support spatial hearing. In an animal model of unilateral deafness, we test whether binaural integration of auditory midbrain neurons is differently impacted by unilateral hearing loss during development or during adulthood.

Single unit responses were recorded in the inferior colliculus of Mongolian gerbils. First, basic response parameters to unilateral and bilateral acoustic stimuli (pure tones and clicks) were characterized in normal hearing (NH) juveniles (postnatal days P15-23) to identify critical periods for binaural integration. Second, juvenile (P15, P19, P23) and adult (~P65) animals were unilaterally deafened. After 15 days of deafness, animals received bilateral round window electrodes, and responses to monaural and binaural biphasic electric pulses were recorded. NH adult gerbils served as controls. Parameters of binaural integration included: interaural frequency receptive field alignment, interaural response strength dominance, and interaural time difference (ITD) coding.

In hearing animals, responsiveness to transient acoustic stimuli (clicks) matured around P19. Although adult-like neural ITD discrimination thresholds were observed at P21, the overall incidence of ITD sensitive neurons did not reach adult-like levels until P23. However, interaural receptive field alignments were still immature at this age.

In SSD animals, deafness-onset before the closure of the critical period for ITD coding (~P23), resulted in a lower incidence of ITD sensitive neurons, a reduced degree of neural ITD sensitivity, and an increase in ITD discrimination thresholds. These degradations were independent of the hemisphere relative to the deafened ear. In contrast, SSD-onset later in life led to asymmetric degradations in ITD sensitivity and ITD discrimination thresholds that were particularly pronounced in the hemisphere contralateral to the deafened ear.

Results show that neural ITD coding is vulnerable to asymmetric hearing loss both during development and during adulthood. Nevertheless, deficits in ITD coding were clearly dependent on the age at deafness onset. SSD-onset during early development resulted in symmetric degradations in ITD coding, whereas SSD-onset after the closure of the critical period for ITD coding was associated with hemisphere-specific degradations. These results suggest that differential therapeutic strategies are required to optimize directional hearing in juvenile and adult SSD-CI users.

Supported by DFG Vo 640/2-2.

PS 557

Effects of Amplitude Modulation on Binaural Pitch Fusion in Cochlear Implant Users

Yonghee Oh[1]; Lina Reiss[2]
[1]University of Florida; [2]Oregon Health and Science University

Binaural pitch fusion, the fusion of dichotically presented stimuli that evoke different pitches, was recently shown to be affected by temporal envelope modulation in normal-hearing (NH) listeners and hearing aid (HA) users (Oh and Reiss, 2018, Trends in Hearing, 22, 1-12). The goal of this study was to determine whether amplitude modulation (AM) similarly affects binaural fusion in cochlear implant (CI) users.

Fourteen CI users (seven bimodal CI users with a HA in the contralateral ear and seven bilateral CI users) were tested using a dichotic pitch fusion measurement procedure. Both reference and dichotic comparison stimuli were presented simultaneously in a 1500-ms single interval. The reference stimulus was held constant in one ear and the comparison stimulus was presented in the contralateral ear with pseudorandom order across trials. In the unmodulated (control) condition, both reference and comparison stimuli had a constant envelope. In the coherent AM condition, both reference and comparison stimuli were co-modulated at a 4-Hz modulation rate with the modulation depth ranging from 20% to 100% in 20% steps. Two incoherent AM conditions, interaural AM phase differences (0, 45, 90, 135, and 180°) and interaural AM rate differences (4 Hz vs 3, 5, and 7 Hz) with randomized starting phases were also tested with 60% AM depth. Subjects were asked to indicate whether they heard a single fused sound or two different sounds in each ear.

The group-averaged results show that coherent AM increases binaural pitch fusion ranges, the frequency/electrode ranges over which binaural pitch fusion occurs, to about 1.5 to 2 times wider than those in the unmodulated condition in both bimodal CI and bilateral CI subjects. Even small temporal envelope fluctuations (i.e., the 20% AM depth) significantly increased fusion ranges. Incoherent AM introduced through interaural differences in AM phase or AM rate led to narrower binaural pitch fusion ranges than those observed with coherent AM or in the case of 7 Hz, narrower binaural pitch fusion than in the unmodulated condition.

The effects of temporal envelope cues, specifically AM cues, in binaural pitch fusion are similar in CI users to those observed previously in HA users. These effects suggest that binaural fusion is not determined solely by peripheral processes that govern spectral resolution. Instead, the effects of AM suggest that binaural pitch fusion is mediated at least in part by central processes involved in auditory grouping.

Funding: Supported by NIH-NIDCD grant R01 DC013307 and F32 DC016193.

PS 558

Comparison of Acoustic and Electrical Functional Changes Over Time after Cochlear Implant Surgery

Deborah J. Colesa; Laila A. Al-Jerdi; Donald L. Swiderski; Yehoash Raphael; Bryan E. Pfingst
Kresge Hearing Research Institute, Department of Otolaryngology-Head and Neck Surgery, University of Michigan

Introduction
Functional responses to acoustic and electrical stimulation often change over time after cochlear implant insertion. Large negative and positive changes in electrical hearing during the first months after implantation have been described previously. Loss of acoustic hearing after hearing preservation surgery has also been reported. Here we compare changes in functional responses to electrical stimulation with changes in responses to acoustic stimulation over time after implant insertion into non-deafened ears in mature guinea pigs.

Methods
Electrical hearing was assessed using electrically-evoked compound action potential (ECAP) amplitude growth functions (AGFs) and psychophysical detection thresholds. Previous studies have shown that these and/or closely related measures are indicative of the condition of the auditory nerve array in animals and are related to speech recognition in humans. Acoustic hearing was assessed using psychophysical detection thresholds for pure-tones. Simple impedances were also assessed. These measures were followed over time from implantation until the animals were euthanized for histological examination of the implanted cochleae.

Results
Slopes of ECAP AGFs and electrical detection thresholds typically showed large changes during the first months after implantation but then stabilized showing much smaller variation up to the end of functional data collection, 6 to 22 months or more after implantation. In contrast, psychophysical detection thresholds for acoustic pure tone stimulation in the tonotopic region where the implant was located (8 kHz to 24 kHz), showed a variety of patterns over time after implantation including (a) minor to large threshold elevations soon after implantation that then remained stable over time, (b) steady increases in thresholds throughout the post-implantation period, and (c) steady increases after several months of stable thresholds post-implantation. The patterns of acoustic thresholds over time were usually not matched by the patterns of ECAP AGF slopes, electrical detection thresholds, or impedances. In several cases, acoustic thresholds increased steadily over time during the period when ECAP AGF slopes and electrical detection thresholds were stable.

Conclusions
These observations suggest that the loss of acoustic sensitivity after implantation is the result of mechanisms that do not directly affect the long-term stability of functional responses to electrical stimulation.

Acknowledgements
This work was primarily supported by NIH NIDCD grants R01 DC015809, and P30 DC005188. Electrodes were obtained from Cochlear Corp. and MED-El; ECAP software and hardware were provided by MED-EL.

PS 559

Comparing Complementary Usage of Information with Better-Ear-Listening in Bimodal and Single-Sided Deaf Cochlear Implant Users

Ben Williges[1]; Ladan Zamanindezhad[2]; Tim Jürgens[3]
[1]Department of Clinical Neurosciences, University of Cambridge; [2]Medical Physics and Cluster of Excellence "Hearing4all", Carl-von-Ossietzky University Oldenburg; [3]Institute of Acoustics, University of Applied Sciences Lübeck

A growing number of cochlear implant (CI) users show usable acoustic hearing supported by a hearing aid (bimodal CI users) or even normal hearing in the contralateral ear (CI-Single-sided deaf, CI-SSD). The combination of electric and acoustic hearing leads to improved speech intelligibility, better localization abilities and an improved quality of life. The underlying mechanism of this acoustic and electric combination is not fully understood, and it is very likely subject-specific and task-dependent. This study investigates possible mechanisms of this combination in spatial speech perception using a model-based approach.

An ongoing debate is, how much of the bimodal or CI-SSD users' performance can be explained by using each listening mode alone and how much of the performance is due to the combination of complementary information across ears. Here we compare measured data from actual CI subjects with data predicted using two different versions of a detailed physiologically-inspired speech intelligibility prediction model based on an automatic speech recognition approach: One model version uses only the better of the two monaurally predicted SRTs (better-ear-listening mode) for speech reception thresholds (SRTs) in the combined stimulation mode. The other model version consists of a concatenation of the acoustic and electric internal representations, thus enabling the speech recognizer to take advantage of both acoustic and electric information, i.e., using of complementary information.

Reference data for simple, but realistic anechoic acoustic scenes were beforehand collected in stationary speech-shaped noise in eight bimodal CI and in eight CI-SSD listeners (Williges et al., 2019). The models were fitted to reproduce monaural S0N0 thresholds of either listening with CI only or without any hearing loss assumed in the acoustic ear. Aided acoustic hearing was simulated with a software hearing aid fitted to the group median hearing loss. Thus, only the audibility threshold was taken into account, no supra-threshold effect of hearing impairment were assumed.

Both model versions showed a satisfactory fit to the measured data (RMS-Error: 2.7 dB). The complementary information model showed a bimodal benefit (3 dB for bimodal CI, 2 dB for CI SSD), surprisingly only for lateral noise incident, but not for frontal sound incident. Simulations were performed on the HPC Cluster CARL funded by the DFG under INST 184/157-1 FUGG. Author BW also received support by the NHS grant RRAG/121.

Williges, B., Wesarg, T., Jung, L., Geven, L. I., Radeloff, A., & Jürgens, T. (2019). Spatial Speech-in-Noise Performance in Bimodal and Single-Sided Deaf Cochlear Implant Users. *Trends in Hearing*, *23*, 233121651985831. https://doi.org/10.1177/2331216519858311

PS 560

A Computational Model of Electric-Acoustic Stimulation in Cochlear Implant Subjects with Residual Hearing

Daniel Alrutz[1]; **Waldo Nogueira**[2]
[1]Medical University Hannover and Cluster of Excellence Hearing4all; [2]Hannover Medical School, Hannover, Germany; Cluster of Excellence, Hearing4all, Germany

Thanks to recent improvements in the cochlear implant (CI) surgical technique and the electrode design, it is now often possible to preserve residual acoustic hearing in the low frequencies during the insertion of a CI in the same ear. CI users with preserved low frequency hearing receive combined electric-acoustic stimulation (EAS) and show improved speech performance scores especially in noisy situations when compared to CI users without preserved residual hearing.

However, it has been shown that simultaneous acoustic and electric stimulation causes interactions between both modalities. One form of interaction is masking. Masking between electric and acoustic stimulation has been observed in auditory nerve fiber (ANF) spike trains in animals (Miller et al., 2009; Tillein et al., 2015) as well as in electrocochleographic (ECochG) responses (Koka and Litvak, 2017) and psychophysical experiments in humans (Lin et al., 2011; Krüger et al., 2017; Imsiecke et al., 2018). To date, it remains unclear at which stage of the auditory pathway these masking effects arise (i.e. at the level of hair cells, the auditory nerve or more centrally).

In this work we use a computational model to better understand the underlying interaction mechanisms in

EAS users. Existing models simulate ANF spiking for sole acoustic or electric stimulation. We present a new model of the spiking activity in a single ANF, where we coupled a model of acoustically evoked spiking (Bruce et al., 2018) with a model of electrically induced spikes (Joshi et al., 2017). In our implementation, an action potential occurring in one of the two models triggers adaption processes in both models, leading to an inhibitory interaction between both modalities. The model shows appropriate spiking responses to acoustic stimulation of remaining hair cells as well as direct electroneural stimulation of the ANF.

Acknowledgments
This work was supported by the DFG Cluster of Excellence EXC 2177/1 Hearing4all and funded by the German Research Foundation (DFG) - Project number: 396932747 (PI: Waldo Nogueira)

PS 561

Influence of Cochlear Place Frequency on Initial Low-frequency Pitch Matches in Cochlear Implant Recipients with Normal Hearing in the Contralateral Ear

Brendan P. O'Connell[1]; Michael W. Canfarotta[1]; Emily Buss[2]; Kevin D. Brown[1]; Margaret T. Dillon[1]
[1]University of North Carolina at Chapel Hill; [2]UNC

Current cochlear implant (CI) mapping procedures present the full spectrum of speech information distributed across available electrodes, taking advantage of the tonotopic organization of the cochlea. The presence of normal hearing contralateral to the CI provides an opportunity to assess the relationship between place of stimulation and perceived pitch. This report investigated the relationship between cochlear place frequency and pitch perception in 12 adult CI recipients with unilateral hearing loss. Subjects were implanted with a long electrode array, mapped with default frequency filter assignments, and listened with a coding strategy presenting temporal fine structure (TFS) cues and envelope information. Cochlear place frequency was derived using angular insertion depth of electrode contacts determined by plain film imaging and a custom MATLAB script. Comparisons were made between spiral ganglion (SG) and organ of corti (OC) frequency-to-place functions. Low-frequency pitch perception was assessed at 1, 3, 6, and 12-months after CI activation on electrodes E1-E5 with an adaptive pitch-matching task. Individual electrodes were continuously stimulated at 80% of the dynamic range in 300-ms bursts, with a 700-ms gap between bursts. Comparison stimuli in the normal-hearing ear were either bandpass filtered clicks or pure tones, presented via an insert. Subjects indicated whether the comparison stimulus in the normal-hearing ear was higher or lower in pitch than the stimulus delivered to the CI using a two-alternative forced choice procedure. The frequency of the acoustic stimulus was adjusted to estimate a pitch match for each electrode. Pitch matches at the 12-month interval were compared between the familiar coding strategy and an envelope-only strategy.At the 1-month interval, behavioral pitch matches were consistent with place frequency using the average SG function for E1 and E2, and to a lesser extent E3-E5. By 3 months, pitch matches on E1 and E2 shifted toward the electrode center frequency, irrespective of cochlear place; a similar shift was not observed for E3-E5. The presence of TFS cues reduced the perceived pitch on E1, with some subjects demonstrating greater pitch discrimination between E1 and E2 with TFS cues compared to the envelope-only strategy. These findings support the following conclusions: 1) place of stimulation is important for pitch perception, 2) the average SG map reliably predicts place pitch for recipients of deeply inserted lateral wall arrays, and 3) the presence of TFS cues facilitates acclimatization to pitch mismatches on the apical most electrode contacts, particularly early in the post-activation period.

PS 562

Spatial Disadvantage in the Listening of Spatialized Noise by Bilateral and Bimodal Cochlear Implant Patients

Qian-jie Fu; Shelby Willis; Kevin Xu; Quinton Gopen; Akira Ishiyama
UCLA

Bilateral and bimodal cochlear implant (CI) patients can benefit from the binaural input in several spatial hearing tasks. However, CI patients may be less able to take advantage of binaural cues that normal-hearing (NH) listeners use for spatial hearing, thus less able to segregate spatial and temporal properties of speech from target speakers from other competing talkers. The present study measured speech recognition performance in the presence of competing talkers using the listening in spatialized noise by bilateral CI patients, bimodal CI patients, and NH controls. Both target speech and competing speech maskers used five-word sentences. Speech recognition thresholds (SRTs) of the target sentence were measured in the presence of two competing sentences. The target sentence came from directly in front of the listener (0°), whereas the two speech maskers were varied according to either their spatial locations (both maskers from the front: 0°/0° or one masker from the right ear and the other from the left ear: 90°/270°), the vocal identities of the maskers (same voice gender as, or different voice gender from, the speaker of the target sentence), or both. Based on the vocal identities and spatial locations of the two speech maskers, SRTs were measured in four listening conditions: same-gender voices at 0°/0° (low-cue SRTs),

different-gender voices at 0°/0°, same-gender voices at 90°/270°, and different-gender voices at 90°/270° (high-cue). Performance was evaluated on the low-cue SRTs and on three "advantage" measures. These advantage measures represent the benefit in dB gained when either voice pitch (talker advantage), spatial (spatial advantage), or both voice pitch and spatial cues (total advantage) are incorporated in the maskers. The results showed that NH controls performed the worst in the low-cue condition while performed the best in the high-cue condition. The mean SRTs were 1.2 dB for the low-cue and the mean advantages were 9.0 dB, 12.9 dB, and 13.2 dB for the talker, spatial, and total effects. For CI patients, the mean SRTs were 4.7 dB for the low-cue condition. The mean advantage were 2.8 dB and 2.6 dB for the talker and total effects. However, CI patients perform significantly worse (-1.2 dB) with spatially separated target and competing speech (same-gender). These results suggested that bilateral and bimodal CI patients could benefit from the talker cues but demonstrated a significant spatial disadvantage in the presence of competing speech. Such spatial disadvantage is likely introduced by the spectral mismatch across two ears.

Auditory Prostheses VI

PS 563

Auditory Profiling and Profile-based Hearing-aid Processing Strategies

Raul H. Sanchez-Lopez[1]; Michal Fereczkowski[2]; Sébastien Santurette[3]; Tobias Neher[2]; Torsten Dau[4]
[1]Hearing Systems Section, Department of Health Technology, Technical University of Denmark, Kgs. Lyngby, Denmark; [2]Institute of Clinical Research, University of Southern Denmark, 5230 Odense M, Denmark; [3]Oticon A/S; [4]Hearing Systems Section, Technical University of Denmark

Currently, clinical characterization of hearing deficits for hearing-aid fitting is based on the pure-tone audiogram only. Implicitly, this assumes that the audiogram can predict performance on complex, supra-threshold tasks. Sanchez-Lopez et al. (Trends in Hearing, Vol. 22, 2018) hypothesized that the hearing deficits of a given listener, both at threshold and supra-threshold levels, result from two independent types of auditory distortion. In their study, a data-driven method for classifying the listeners into four auditory profiles was proposed and validated. However, the definition of the two types of distortion was challenged by differences between the two datasets in terms of the tests and listeners used. In the current study, a refined method and definition of the auditory profiles is proposed. A new dataset was generated with the aim of overcoming the limitations of the previous study. A heterogeneous group of listeners was tested across three locations using a test-battery designed to tap into different aspects of hearing, including speech perception in quiet and noise, loudness perception, binaural processing abilities, and spectro-temporal resolution. The collected data were analyzed using the data-driven analysis developed by Sanchez-Lopez et al. (2018). Furthermore, a profile-based hearing-aid fitting differing in terms of gain prescription and signal-to-noise ratio improvement was proposed and tested with listeners belonging to the four proposed auditory profiles. Using a hearing-aid simulator, the listeners' subjective preference for the proposed hearing-aid processing strategies was assessed in various realistic sound scenarios. The results suggested that the different auditory profiles are associated with different preferences in terms of amplification, compression and signal-to-noise ratio improvement. Altogether, the developed method for profile-based HA fitting shows promise with respect to individualizing HA signal processing. Future work will be concerned with testing it in a large field study with wearable devices. Moreover, profile-based hearing-aid fitting may be extended to new paradigms of hearing loss compensation and advanced signal processing.

Collaboration and support by Innovation Fund Denmark (Grand Solutions 5164-00011B), Oticon, GN Resound, Widex and other partners (University of Southern Denmark, Aalborg University, the Technical University of Denmark, Force, and Aalborg, Odense and Copenhagen University Hospitals) is sincerely acknowledged.

PS 564

Computational Optimization of Total Ossicular Replacement Prosthesis Shape

Mario Milazzo[1]; Pieter G. G. Muyshondt[2]; Josephine V. Carstensen[1]; Joris J. J. Dirckx[2]; Serena Danti[3]; Markus J. Buehler[1]
[1]Dept. of Civil and Environmental Engineering, Massachusetts Institute of Technology; [2]Laboratory of Biophysics and Biomedical Physics, University of Antwerp; [3]Dept. of Civil and Industrial Engineering, University of Pisa

Conductive hearing loss, due to traumas or pathologies of the middle ear, affects more than 5% of the population worldwide and more than 15% of the elderly. Current middle-ear prostheses, shaped for partially or totally replacing the ossicular chain, are made of synthetic, biological materials, or homo/allografts, with topologies strictly dependent on traditional fabrication technologies. Despite their high success rate, some problems still occur: significant rejections in the mid/long term and sub-optimal acoustic behavior, especially at high frequencies.

This work provides a study on total ossicular replacements, to achieve the best topology for enhancing middle-ear sound transmission without specific manufacturing constraints, in view of a fabrication based on additive manufacturing or ultraprecision milling.

We define initial bulk volumes with lengths from 5 to 7 mm, with different geometries at the umbo plate: bulk (Case 1); big holes (Case 2); small holes, with non-symmetric (Case 3) and symmetric (Case 4) position on the umbo plate (Fig. 1). The optimization study aims at maximizing the overall stiffness of the prostheses under static loading, required for the otologic application, and minimizing the volume while ensuring material continuity. To simplify the model optimization problem, we fix the transversal displacements at the prostheses' end surfaces, and apply static longitudinal displacements with amplitudes over the auditory frequency range available from literature.

We assess the prostheses' acoustic performance upon dynamic loads with a finite-element model that includes the eardrum and cochlear load.

As it is a linear study, we depict in Fig. 2 only the results for the four cases using titanium as constitutive material. By increasing the prosthesis' length, the final topologies present thin branches at the umbo plate (Case 1 and 2 for L = 6–7 mm, and Case 4 for L = 7 mm). From the acoustic assessment with the 5-mm prostheses of different materials (titanium, cortical bone, silk, and collagen-HA), the new designs appear to retrace the native middle-ear behavior well, with a slight, almost constant positive shift. Only for silk and collagen-HA, we observe a significant mismatch down to -10 dB above 7 kHz (Fig. 3).

This study opens a new perspective for middle-ear prostheses to be manufactured via additive manufacturing or ultraprecision machining with materials that, besides titanium, may show a better biocompatibility in the mid/long term.

This work was supported by the European Union's Horizon 2020 research and innovation program under the Marie Skβodowska-Curie grant agreement COLLHEAR No 794614.

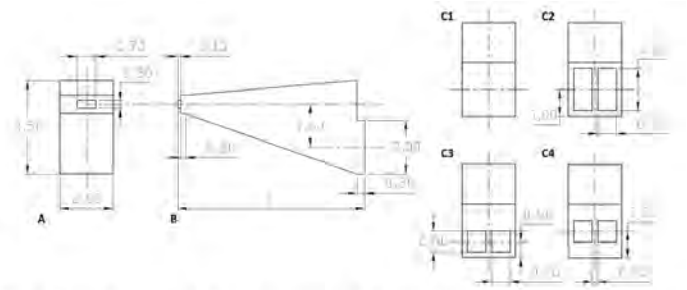

Fig. 1. Main dimensions, loads, and constraints of the body used as baseline for the topology optimization. A. Lateral view with the interface for the oval window. B. Frontal view. Due to specific clinical needs, the length of the prosthesis (L) was set to 5 mm, 6 mm and 7 mm. C1-C4. Depiction of the four different umbo plate topologies: bulk (Case 1 – C1), big holes with borders of 0.2-mm thickness (Case 2 – C2), holes of half the height, asymmetrically positioned with the umbo plate (Case 3 – C3), and symmetrically positioned (Case 4 – C4).

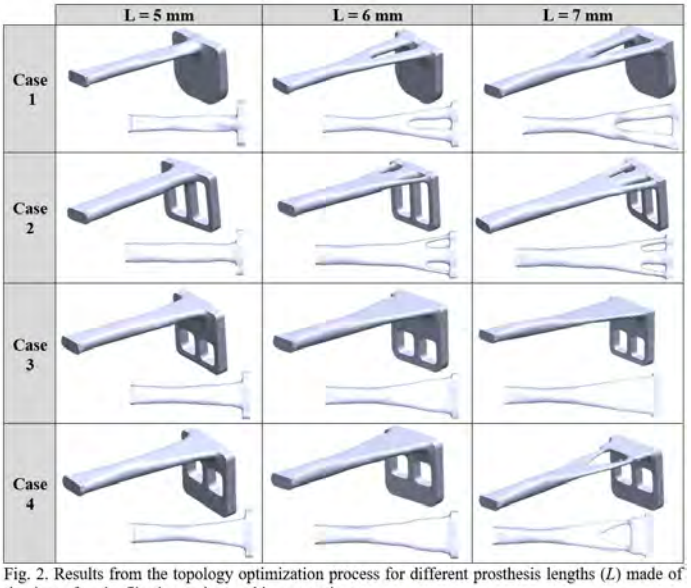

Fig. 2. Results from the topology optimization process for different prosthesis lengths (L) made of titanium after the filtering and smoothing operations.

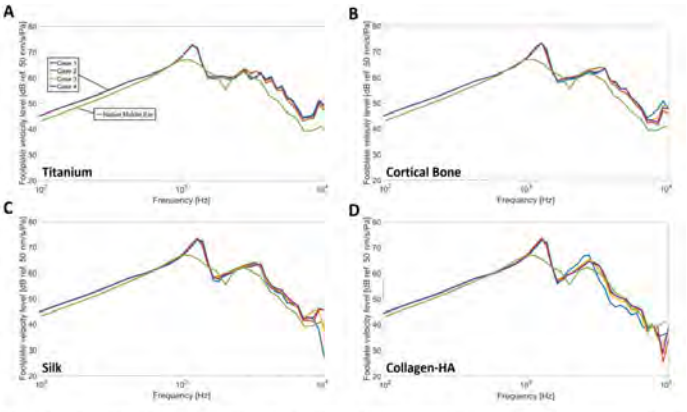

Fig. 3. Semi-logarithmic plots showing the footplate velocity level as a function of frequency for the native ossicular chain (green curve) compared with the performance evaluated for the four 5-mm prostheses (colored curves) made of titanium (Panel A), cortical bone (Panel B), silk (Panel C), and Collagen-HA (Panel D).

PS 565

Comparison of Perception Characteristics of Distantly-presented Bone-conducted Sounds between Ultrasonic and Low-frequency Ranges

Riki Ogino; Koichiro Doi; Sho Otsuka; Seiji Nakagawa
Chiba University

High-frequency sound above 20 kHz can be heard clearly via bone conduction (Bone-conducted ultrasound: BCU). Additionally, BCU is perceived even when presented to body parts distant from the head. In the previous studies, we measured hearing thresholds and vibrations in the ear canal when a 30-kHz stimulus was presented to the neck, upper limb, and trunk in normal hearing participants. The results showed that BCU presented to the distal parts can be perceived whereas the hearing thresholds increased and the vibrations attenuated depending on the distance from the head. However, details of mechanisms of propagation and perception of the distantly-presented bone-conduction remain unclear. We have used a 30-kHz stimulus, however, comparison among other frequencies, especially lower “audible” frequencies may be useful to verify the mechanisms of bone conduction in the human body. In this study, we measured the hearing thresholds for the ultrasonic and low-frequency sounds presented to the distal parts of the body via bone-conduction. A 30-kHz tone-burst was used as the BCU stimulus. Additionally, as the low-frequency stimuli, 250, 500, 750, 1000, 1500, 2000, 3000, and 4000 Hz tone-burst were used. These stimuli were presented to the mastoid process of the temporal bone, the muscle of the neck, and the middle part of the back bone. Ears of the participants were plugged by silicone ear plugs not to perceive air-conducted sounds radiated from the vibrators. Hearing thresholds were measured using a 2 up-1 down three-alternative forced-choice (3AFC) in normal hearing 6 participants. All participants were able to perceive both 30-kHz and low-frequency bone-conducted tones at each location. Significant effects of the stimulus location ($p < 0.01$) and the stimulus frequency ($p < 0.05$) were obtained. The increase of hearing threshold was less than 20 dB for the 30-kHz stimulus. On the other hand, within the low-frequency range, the increase hearing threshold tended to increase depending on frequency increase, and the increases were much larger and ranged from 25 to 60 dB. The results obtained indicated that (1) bone-conducted sounds can be clearly perceived at distal parts of the body even in lower-frequency ranges, (2) distance attenuation of bone-conducted sound in the human body depends on frequency, especially the attenuation at 30 kHz were extremely small. These results provide useful information to elucidate mechanisms of the distantly-presented bone-conduction.

PS 566

Benefits of a new hearing device termed as cartilage conduction hearing aids in the ears with aural atresia

Tadashi Nishimura[1]; Hiroshi Hosoi[2]; Osamu Saito[2]; Tadao Okayasu[3]; Chihiro Morimoto[4]; Toshiaki Yamanaka[2]; Tadashi Kitahara[5]
[1]Otolaryngology-Head and Neck surgery, Nara Medical University; [2]Nara Medical University; [3]1) Otopathology Laboratory, Department of Otolaryngology, Massachusetts Eye and Ear 2) Department of Otolaryngology, Harvard Medical School 3)Nara Medical University; [4]Nara Medical Universtiy; [5]Department of Otolaryngology – Head and Neck Surgery, Nara Medical University

Background

A clear sound can be heard when a vibration signal is delivered to the aural cartilage. This new form of sound transmission was referred to as cartilage conduction (CC). A hearing aid utilizing CC is lightweight and compact, and comfortable for wearing. It is effective even in the ear with aural atresia. In this study, we measured the benefits of this new hearing aid in the ears with severe conduction hearing loss, particularity with aural atresia, and evaluated its potential for practical use.

Methods

Forty-one subjects (21 with bilateral aural atresia; 15 with unilateral aural atresia; and 5 others) participated in this study. Fitting and gain adjustments of the CC hearing aids were performed to the ear(s) with conduction hearing loss. The function gains were measured. Evaluation of the measurements of speech performance-intensity functions, speech recognition scores, tolerance of environmental noise, and subject questionnaires were also performed, and judged according to the “Guidelines for the evaluation of hearing aid fitting” established by the Japan Audiological Society.

Results

The thresholds were significantly improved by CC hearing aids. The functional gains for CC hearing aids were nearly equivalent to that for their previously used hearing aids. Most of the assessment results were judged to be sufficient. Before the trial, bone conduction hearing aids had been used most frequently by bilateral aural atresia subjects. However, after the trial, most subjects continued to use CC hearing aids instead of reverting back to their original device. Overall, 39 subjects continued use of the CC hearing aids. No severe adverse effects were noted in the trial.

Conclusion
Cartilage conduction hearing aids could be an additional and beneficial option for severe conduction hearing loss from aural atresia.

PS 567

Perceptual characteristics of bone-conducted ultrasound presented to the neck, trunk, and arms — Effect of self-demodulation in the human body

Koichiro Doi; Riki Ogino; Sho Otsuka; Seiji Nakagawa
Chiba University

High-frequency sound above 20 kHz presented via bone-conduction (bone-conducted ultrasound: BCU) can be heard clearly. Moreover, BCU can transmit speech information using amplitude-modulation (AM).

In typical bone-conduction, a vibrator is pressed onto osseous sites of the head, such as the mastoid process. On the other hand, BCU can be perceived even when the vibrator is presented to the body parts distant from the head, like the neck, arm, and trunk. Therefore, it can be applied to a novel interface that can transmit sound information selectively to the specific persons who touch the device. However, there is room for improvement on sound quality of distantly-presented BCU.

In AM-BCU, users perceive two sounds. One is the high-pitch tone due to the ultrasonic carrier. The other is the modulator represented as the envelope of the modulated wave. Normal-hearing people may perceive the latter one as a low-pitch tone due to self-demodulation generated by the nonlinearity in the human body and it is thought that the demodulated sound contributes to improve sound quality of BCU. When BCU is presented to distal parts, vibration propagates through various tissues in the body including the cartilage that have strong non-linearity, therefore, more demodulation may occur. However, mechanisms of the demodulation in the human body remains unclear.

First, to elucidate the psychoacoustic characteristics of distantly-presented BCU hearing, difference limens for frequency (DLFs) of AM-BCU was measured with/without low-pass masking sounds that mask demodulated-components. The stimuli presented to the neck, clavicle, upper-limb, backbone (Fig. 1). No significant differences were observed between the mastoid and the distal parts, however, DLFs rose above 1 kHz under the higher-level masker.

Second, to elucidate demodulation characteristics in the propagation process, the vibration at the external-auditory meatus was measured when AM-BCU was presented to the distal parts. The result showed that the peak level corresponding to the carrier-frequency tended to decrease depending on the distance between stimulation and measurement sites, however, the peak of the modulator did not change by the distance.

And third, vibrations around the cartilages of the auricle, tragus, and articulations, which shows strong nonlinearity, were measured. The demodulation components were larger for the auricle and tragus than the peripheral articulations.

These results indicated that the demodulation component has certain contribution for transmission of the frequency information. Also, it was suggested that even in the BCUs presented to the distal parts, the demodulation mainly occurs at the cartilages of the pinna.

Fig. 1 Locations of the BCU stimuli

PS 568

Which patients with a unilateral hearing aid for symmetric sensorineural hearing loss have auditory deprivation?

Hyun Jin Lee[1]; Gina Na[2]; Jinsei Jung[3]
[1]Department of Otorhinolaryngology, Incheon St. Mary's Hospital, College of Medicine, The Catholic University of Korea, Seoul; [2]Department of Otorhinolaryngology, Yonsei University College of Medicine, Seoul, Republic of Korea; [3]Yonsei University

Purpose
The aim of study is to find conditions that aggravate auditory deprivation in patients with symmetric hearing loss after unilateral digital, non-linear hearing aid (HA).

Methods
Retrospective case-comparison study. We assessed 23 patients with symmetric sensorineural hearing loss (SNHL), wearing unilateral conventional HAs.

Audiological outcomes were assessed > 1 year after HA fitting (mean duration, 42.7 months). Pure-tone audiometry in HA-aided and HA-unaided conditions was performed over time. Word recognition scores (WRS) was evaluated at the most comfortable listening level.

Results

The initial average of thresholds at 500, 1000, 2000, and 4000 Hz (PTA_4) did not show a difference of > 5 dB HL between HA-aided and HA-unaided ears. WRS progressively decreased for both HA-aided and HA-unaided ears, although the extent of decrease was significantly greater for HA-unaided (10.8%) than for HA-aided ears (6.2%) ($p < 0.05$). Notably, auditory deprivation in HA-unaided ears was significantly greater in patients with an initial PTA4 ≥ 53 dB HL.

Conclusion

Bilateral HAs are strongly recommended, particularly for patients with moderate-to-severe SNHL, to prevent auditory deprivation in the contralateral ear.

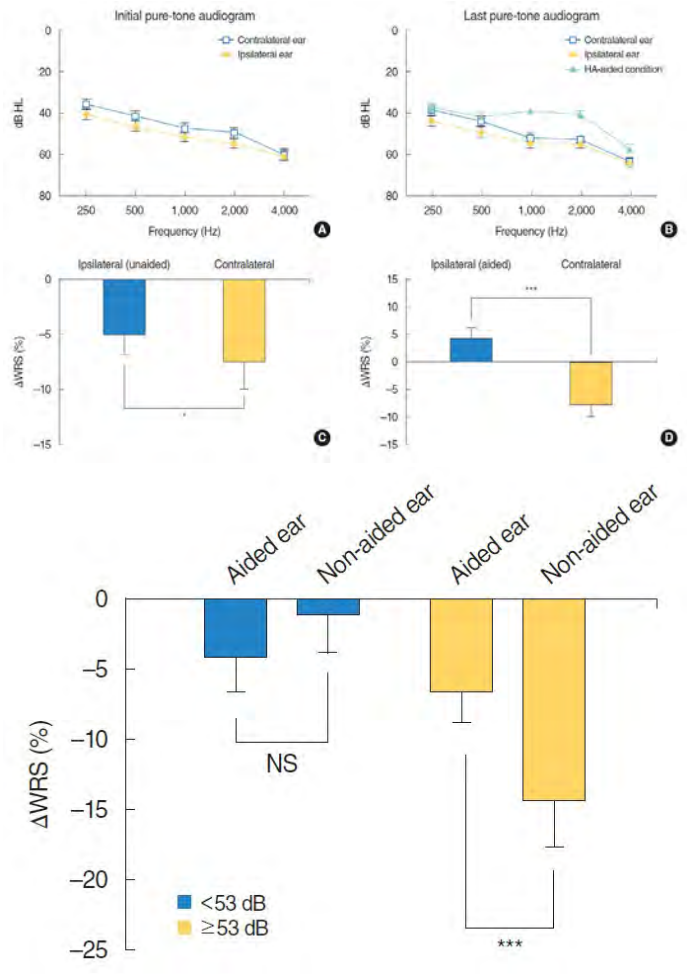

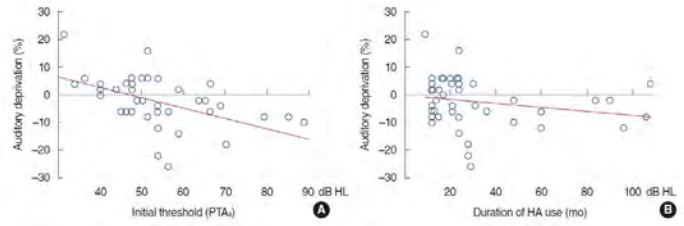

PS 569

Development of the novel hearing device as a substitute for the bone conduction hearing aid

Ichiro Furuta[1]; Hideaki Ogita[2]; Fukuichiro Iguchi[3]; Takayuki Okano[1]; Kohei Yamahara[4]; Tatsuya Namatsu[5]; Shinsuke Shichi[5]; Kazuya Nakatera[5]; Yoshihiro Iwasaki[5]; Shuichi Kawata[5]; Koichi Omori[6]; Norio Yamamoto[6]

[1]Dep. Otolaryngology, Head and Neck Surgery, Graduate School of Medicine, Kyoto University, Kyoto, Japan; [2]Shiga Medical Center Research Institute, Shiga, Japan; [3]Iguchi ENT Clinic, Kyoto, Japan; [4]Shizuoka City Shizuoka Hospital; [5]Murata Manufacturing Co., Ltd., Kyoto, Japan; [6]Dept. Otolaryngology - Head and Neck Surgery, Graduate School of Medicine, Kyoto University

Active middle ear implants (AMEI), bone anchored hearing aids (BAHA), or conventional bone conduction (BC) hearing aids are used for the complex conductive hearing loss, including external auditory canal (EAC) atresia and severe congenital middle ear anomaly. However, AMEI and BAHA require surgery to implant them into the body. Although conventional BC hearing aids are very effective, they require the hard contact of the transducer against the head skin, causing skin erosion and pain on the head. To overcome this, Hosoi et al. (Laryngoscope, 2014) developed cartilage conduction device. They attached the transducer to cartilaginous tissue softly to conduct sound to the inner ear. As a different approach to achieve efficient BC conduction without pressure to the skin, we decided to use a novel piezoelectric diaphragm as a transducer. Conventional piezoelectric diaphragms are usually composed of the piezoelectric material and two electrodes on the both sides of the material and adding voltage through the electrodes causes the vibration of the piezoelectric materials. Our novel piezoelectric transducer has only one electrode attached to the piezoelectric material. The other electrode attaches to the skin so that the sounds are conducted only when the material attaches to the skin.

To elucidate the pathway that our novel piezoelectric diaphragm conducts the sound to the cochlea, we objectively measured the response of the cochlea to the sound generated by a speaker, a conventional

piezoelectric diaphragm, or our novel piezoelectric transducer. Due to the fine electrical current within the body caused by novel piezoelectric transducer, we used compound action potential (CAP) rather than ABR as the objective measurement.

We used male guinea pigs. The right cochlea was destroyed before measurement to avoid cross hearing. Pure tone sound with various frequencies (2, 4, 8 and 16 kHz) was applied. To evaluate the sound transmission pathway with the novel piezoelectric transducer, we measured CAP in three conditions, before treatment, after incus removal, and after EAC cartilage removal.

The CAP threshold shifts after incus removal is significantly less in novel piezoelectric transducer than a speaker and a conventional piezoelectric diaphragm. Removal of EAC cartilage did not affect the threshold in the novel piezoelectric transducer.

These results suggest that our novel piezoelectric transducer conducted most of the sound though BC and the novel piezoelectric transducer can be used as a novel BC device without hard conduct to the skin and substitute AMEI, BAHA, and a conventional BC hearing aid.

PS 570

New stapes-head (SH) coupler for Vibrant Soundbridge (VSB) system

Birthe Warnholtz[1]; Merlin Schär[2]; Pascale Cuny[1]; Kathrin Sonntag[3]; Ivo Dobrev[2]; Flurin Pfiffner[4]; Christof Röösli[5]; Alexander Huber[2]; **Jae Hoon Sim**[2]
[1]University Hospital Zurich; [2]Department of Otorhinolaryngology, Head and Neck Surgery, University Hospital Zurich, Zurich, Switzerland; University of Zurich, Zurich, Switzerland; [3]MED-EL Medical Electronics; [4]1.University of Zürich, Zürich, Switzerland. 2.Department of Otorhinolaryngology, Head and Neck Surgery, University Hospital Zürich, Zürich, Switzerland.; [5]2.Department of Otorhinolaryngology, Head and Neck Surgery, University Hospital Zürich, Zürich, Switzerland.

The Vibrant Soundbridge (VSB; MED-EL Medical Electronics, Austria) is an active middle-ear implant with a floating mass transducer (FMT), for patients with conductive and mixed hearing loss. Though the FMT of the VSB can be attached to various locations of the middle-ear structures depending on status of the middle ear, coupling of the FMT on the stapes head is known to produce larger stimuli to the cochlea than other coupling locations. While the FMT is mounted to the top of the stapes head with the current Vibroplasty Clip coupler, the new design of the stapes-head (SH) coupler prosthesis (MED-EL Medical Electronics, Austria) was developed to mount the FMT on the inferior side of the stapes, with the purpose to use the middle-ear space more efficiently with firmer fixation. In this study, the expected surgical outcomes with the new SH coupler were assessed in 11 human cadaveric temporal bones, in comparison with the current Vibroplasty Clip coupler. Placement of the couplers onto the stapes were examined, and effective stimuli to the cochlea were evaluated by measuring piston-like motion of the stapes footplate with a current of 1 mA on the FMT. The results showed that the new SH coupler generally establishes a stable and firm coupling. With the new SH coupler, a small gap between the stapes head and the plate of the stapes coupler part is sometimes (2 out of 11 in this study) unavoidable in order to prevent the FMT from touching the promontory. However, even with the gap, attenuation of effective stimuli to the cochlea by vibrational motion of the stapes was not observed. Effective stimuli to the cochlear with the new SH coupler were reduced at high frequencies above 3 kHz compared to the effective stimuli with the current Vibroplasty Clip coupler, but the relative attenuation over all the 11 cadaveric temporal bones was less than 10 dB. Considering the results, the new designs of the stapes-head (SH) coupler can be used as an alternative of the current Vibroplasty Clip coupler, to overcome anatomical variation of the human middle ear without considerable attenuation of effective stimuli to the cochlea.

PS 571

Clinical Performance of a New Implant System for Bone Conduction Hearing

Susan Arndt[1]; Emmanuel Mylanus[2]; Rob Briggs[3]; Piotr Skarzynski[4]; Steven Telian[5]
[1]Department of Otorhinolaryngology - Head and Neck Surgery, Medical Center - University of Freiburg, Faculty of Medicine, University of Freiburg, Germany; [2]Radboud University Medical Centre; [3]The Royal Victorian Eye and Ear Hospital RVEEH; [4]World Hearing Center Institute of Physiology and Pathology of Hearing; [5]University of Michigan

Introduction

The Investigational Device, Osia System (Osseointegrated Steady State Implant System), is developed to provide the benefits of a non-skin-penetrating system combined with the benefits of a skin-penetrating system. The OSIA Device is a bone-conduction hearing device that allows direct bone-conduction through an implanted actuator on the osseointegrated BI300 Implant.

Methods

We report about an open, two-armed prospective, multicentre clinical investigation with 3-month investigation (primary analysis). Primary safety analysis

was evaluated at 6 months. Fifty-three (53) subjects were enrolled in the investigation across the five investigational sites. Fifty-one (51) subjects underwent the surgical intervention and received the Investigational Device. Two (2) subjects did not undergo surgery and were withdrawn from the investigation following the preoperative baseline visit. The hearing performance with a BP110 Power Sound Processor on a Baha softband were compared to postoperative results with the OSIA system using thresholds audiometry, free-field [PTA4], speech in quiet [% correctly perceived words at 50dB, 65dB and 80dB SPL], adaptive speech in noise [speech-to-noise ratio, 50% speech understanding] and BC Direct.

Validated questionnaires were used to determine the health status measured with the generic quality of life scale Health Utilities Index (HUI3), the self-reported assessment of hearing aid outcome using Abbreviated Profile of Hearing Aid Benefit (APHAB), the subjective benefit with the Speech, Spatial and Quality (SSQ), and the subjective comfort was measured by a visual analogue scale.

Results

Free field threshold audiometry showed that the OSIA provides significant improvement compared to the unaided situation in terms of the primary parameter PTA4. Speech tests in quiet showed statistically significant improvements at all tested speech presentation levels. Also in adaptive speech tests in noise significant improvement in signal to noise ratio (SNR) was recorded with the OSIA compared to preoperative unaided hearing. All patient questionnaires (HUI, APHAB, SSQ) showed significant improvements in subjective outcomes.

Conclusions

The OSIA provides significantly improved objective and subjective audiology outcomes and health-related quality of life in subjects with a conductive or mixed hearing loss or single-sided sensorineural deafness already 3 months after surgery.

PS 572

Predicting the Utility of Hearing-Aid Noise Reduction based on Spectro-Temporal Modulation Detection

Johannes Zaar[1]; Lisbeth Simonsen[2]; Thomas Behrens[3]; Torsten Dau[1]; Søren Laugesen[2]
[1]Hearing Systems Section, Technical University of Denmark; [2]Interacoustics Research Unit; [3]Oticon A/S

Hearing-aid amplification is typically tailored to the individual listener's hearing loss based on the pure-tone audiogram to restore audibility. However, some listeners experience severe supra-threshold difficulties with speech understanding in adverse conditions despite audibility compensation. For those, additional help may be provided using recent approaches that combine classical single-channel noise reduction with minimum variance distortionless response beamforming (MVDR-NR). MVDR-NR, especially when aggressively parametrized, typically improves speech intelligibility substantially. However, it may also impair the perceived naturalness of the sound scene and its acceptance may therefore be highly listener-specific. To use its full potential, MVDR-NR thus needs to be carefully tailored to the individual, such that "aggressive" settings are only prescribed to those listeners who need and therefore tolerate them. To this end, a clinically viable measure that represents supra-threshold speech processing is required to identify listeners with severe supra-threshold deficits. Here, it was investigated whether spectro-temporal modulation detection (STMD) sensitivity, which has been shown to be associated with speech-in-noise perception in hearing-impaired (HI) listeners, could be useful in this context.

The present study tested 30 HI participants (70 years on average), all of whom were native speakers of Danish and regular hearing-aid users. All participants underwent standard audiological screening. Furthermore, a measure of working memory was obtained using the reverse digit span (RDS) test. STMD thresholds were adaptively measured using bilateral headphone-based presentation with linear amplification to ensure at least 15 dB sensation level. The participants were provided with hearing aids, which were individually fitted based on the audiogram. Speech reception thresholds (SRTs) were adaptively measured using the Danish HINT (Nielsen and Dau, 2011) in a spatial multi-talker set up with MVDR-NR (i) turned off, (ii) set to a moderate "Default" setting, and (iii) set to a highly aggressive "FullThrottle" setting. Furthermore, the listeners' preference for Default or FullThrottle MVDR-NR was assessed by means of a field study using evaluation questionnaires.

The results indicate that STMD thresholds were strongly associated with SRTs (measured without MVDR-NR), as well as with the SRT benefit induced by FullThrottle MVDR-NR (as compared to Default). The individual listeners' MVDR-NR preference was also associated with STMD thresholds. However, the relationship was mediated by the RDS scores, indicating that STMD thresholds were affected by working memory capacity, whereas MVDR-NR preference was not. Overall, a clinical test that assesses STMD sensitivity may be useful for prescribing MVDR-NR settings in hearing-aid fitting, thus complementing the audiogram.

PS 573

Validation of a Fitting Method for Over-The-Counter Hearing Aids: A Clinical Trial

Soumya Venkitakrishnan; Dana Urbanski; Yu-Hsiang Wu
University of Iowa

Age-related hearing loss (HL) or presbycusis, is the third most prevalent chronic condition in older Americans after hypertension and arthritis. Although hearing aid amplification is the primary management option, only approximately 30-percent of older Americans with HL use hearing aids, with over 75-percent identifying financial factors as a barrier. Thus, less expensive over-the-counter (OTC) amplification devices that utilize direct-to-consumer service delivery models have infiltrated the market. However, many of these devices are inappropriate for sloping-age-related HL because of their emphasis on low-frequencies. This could lead to less satisfaction and poorer outcomes with OTC hearing aids. To address this limitation, we optimized gain-frequency responses for these devices so that they provide appropriate amplification for older adults with age-related HL. We developed a set of 4 gain frequency responses (presets) suitable for pre-configured OTC hearing aids. These 4 presets could fit 67.9% of older adults with mild-moderate HL found in the National Health and Nutrition Examination Survey database.

The aim of the current clinical trial was to compare the effectiveness of the presets developed (PRO) with that of an existing OTC hearing aid (TWK) and traditional audiologist-fitted hearing aid (AUD). Thirty-seven participants (18 females, mean age =70.5 years) participated in laboratory testing and field trials in a single-blinded, randomized, cross-over design. Linear mixed models and follow-up testing with Tukey test with correction for multiple comparisons was used to compare speech perception scores (Figure 1) and real-world hearing aid performance (Figure 2). For both these measures, no significant difference was found between the scores for AUD and PRO model, but AUD was significantly better than TWK. The participants were also asked to indicate their hearing aid preference at the end of the study. Out of the total 37 subjects, 20 preferred PRO, 12 preferred AUD, and 5 preferred TWK hearing aids. Cochran's Q test with follow-up testing by Dunn test showed that among these subjective preferences, preference for PRO over TWK was statistically significant; and though more users preferred PRO over AUD, this difference was not significant. Our results, thus, provide evidence that our presets are preferred by hearing aid users more than an existing OTC hearing aid, and their speech performance with PRO is comparable to AUD model. If such presets can be preconfigured in OTC devices, these may result in better outcomes and more cost-effective amplification devices, leading to increased access to lower-cost hearing healthcare for older adults with HL.

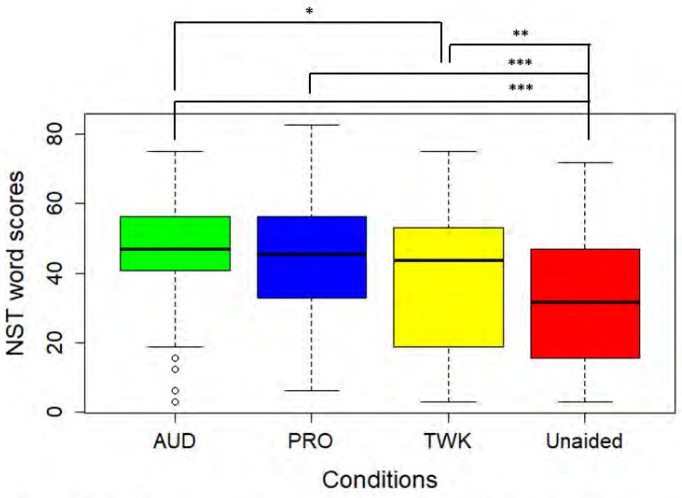

Figure 1: Speech perception results for Nonsense Syllable Test (NST) in quiet for different conditions and unaided.

*p-value: * <0.05, ** <0.01, ***<0.001*

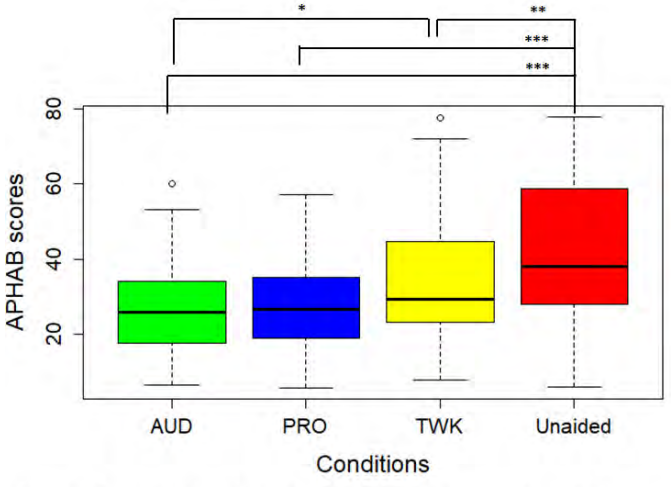

Figure 2: Real-world hearing aid performance was assessed using Abbreviated Profile of Hearing Aid Benefit (APHAB). These scores are displayed for different conditions (higher scores denote more handicap).

*p-value: * <0.05, ** <0.01, ***<0.001*

PS 574

Diaphanoscopy of the Tympanic Membrane

Madeleine Goblet[1]; Farnaz Matin[1]; Thomas Lenarz[2]; **Gerrit Paasche**[1]
[1]Hannover Medical School; [2]Hannover Medical School, Hannover, Germany

Implant associated infections can lead to formation of biofilm, are one of the main reasons for complications after implantation and can lead to explantation of the affected device. Treatment is often conducted by

systemic or local application of drugs. In case of biofilm formation drugs are relatively ineffective. To address these challenges, antibacterial photodynamic therapy has been developed where the antibacterial properties of a special coating of the implant can be "switched on" by illumination with light. To transfer this approach to the ear, the wavelength dependent optical density of the tympanic membrane has to be determined.

Tympanic membranes were prepared from newborn rats such that the membrane remained attached to the surrounding bony ring and placed under a plate reader. An area scan was performed to find the least optical density surrounded by a ring like structure of higher optical density. Then the position with highest transmission was chosen for scanning wavelengths between 300 nm and 900 nm.

To avoid movement artifacts during the procedure, samples could not be wetted by additional fluid. Retests of the samples showed that measured values were not influenced by any drying artifacts for at least 2 hours. Optical density was highest at the shortest and lowest at longest wavelengths with an additional isolated peak between 420 nm and 440 nm.

Longer wavelengths seem to be more promising for a transfer of this approach to the ear. Success will strongly depend on the necessary light intensity to induce the antibacterial effect.

PS 575

Effects of Body-Coupled Ultrasound Stimulation on the Auditory System for a New Hearing Technology

Gerardo Rodriguez[1]; John Basile[1]; Hubert H. Lim[2]
[1]University of Minnesota; [2]University of Minnesota, Minneapolis, USA

Our lab has shown that ultrasound (US) coupled to the head of guinea pigs activates the peripheral auditory system through vibration of the cerebrospinal and cochlear fluids (Guo et al., Neuron, 2018). This discovery of a noninvasive, fluid-driven cochlear activation pathway opens up the possibility of a new type of hearing technology, which can bypass outer and middle ear regions as well as avoid acoustic feedback issues. We previously demonstrated that frequency specific activation of the auditory system is possible with amplitude modulated US stimuli. We further investigated how different carrier and modulating frequencies influence the response of the auditory system. We also investigated how the US signal propagates and distorts at the inner ear.

We positioned two-shank electrode arrays into the right central nucleus of the inferior colliculus (ICC) of ketamine-anesthetized guinea pigs. We collected frequency response maps in response to amplitude-modulated US (1-40 kHz, 10-400 kPa) with varying carrier frequencies (0.10, 0.22, or 1 MHz), as well as air-conducted pure tone stimuli. We placed the transducer either on the skull or on the exposed brain, as well as varied the location proximal or distal to the left ear, coupled with degassed agarose. We presented long and short pulses of US (>100 us) to investigate threshold responses. To investigate how the US propagates into the cochlea, we placed a hydrophone (Onda Corporation) into the inner ear of a deceased guinea pig. We filled the space with degassed agarose to couple the hydrophone and perform similar stimulation paradigms as described above.

Our results show reliable activation patterns in the ICC with different amplitude-modulated US stimuli. The modulating frequency has a large influence in the pattern of activation in a frequency-specific manner, while the carrier frequency affects the response thresholds and amount of distortion at the inner ear. We have also observed how varying the location of the transducer influences the auditory response, in which thresholds were lower when the transducer was closer to the target ear, further supporting a fluid rather than a bone conduction mechanism.

US applied to the head reliably activates the auditory midbrain in a frequency-specific pattern that depends on the carrier and modulating frequencies, and placement of the US transducer closer to the target ear can reduce activation thresholds. The unilateral specificity and minimization of acoustic feedback issues of US are potential advantages compared to air or bone conduction hearing aid devices.

Auditory Prostheses VII

PS 576

The Optical Cochlear Implant

Claus-Peter Richter
Northwestern University, Dept Otolaryngology

Our goal is to develop a cochlear implant (CI) that uses photons to stimulate surviving auditory neurons. The benefit of optical stimulation is its spatial selectivity with the potential to create significantly more independent channels to encode acoustic information and likely enhances the CI users' performance in challenging listening environments. We have explored the mechanism and parameter space for neural stimulation with infrared light and have shown the spatial selectivity

of optical stimulation. The challenges for infrared neural stimulation (INS) include the potential heating of the tissue. For wavelengths around β=1550 nm, laser tissue interactions are comparable to those at β=1860 nm and INS is possible. Since radiation at β=1260 nm to β=1675 nm is used in the communication industry small optical sources and waveguides are well developed and can readily be used for a human opto-electrical hybrid cochlear implant.

First, opto-electrical hybrid electrodes have been fabricated. To fabricate the optrode, 25 µm diameter platinum wires were connected to the cathode and anode of the optical sources using conductive silver epoxy (EPO-TEK H20E, Epoxy Technology Inc., Billerica, MA). The separation of the optical sources was about 1 mm. The function of each light source was tested prior to embedding and after the assembly of the optrode. For the embedding, the optrode was placed in a custom fabricated mold, which was filled with Silastic® (MDX4-4210, Medical Grade Elastomer, base and curing agent (LOT 0006932899, Dow Corning Corp., USA). The silicone was cured overnight at 60°C. After the silicone solidified the electrode was removed from the mold and electrical contacts with their wires were placed between the optical sources. The entire electrode was then placed in a second, slightly larger mold and were embedded in Silastic®. The wires of the optrode and electrical contacts were connected to a transcutaneous connector or to our custom designed implantable optical implant.

Length and diameter of all electrodes was measured and documented at each of its optical and electrical sources. The electrodes' bending stiffness, the force during the insertion into a life-sized, matrix printed acrylic model, and during insertion into cadaveric temporal bones was measured. Values compared to gold standards obtained with contemporary electrodes for electrical alone stimulation. Another subset functional electrodes, which did not undergo physical stress for testing, was submersed in a 40°C saline solution. The radiant energy was measured daily until one of the optical sources started failing.

Funded by the NIH, R56DC017492

PS 577

Hearing Colors: Evaluation of Frequency Representation in Optogenetic Midbrain Implants

Meike Rogalla[1]; Adina Seibert[2]; K. Jannis Hildebrandt[1]
[1]Cluster of Excellence Hearing4all, Neurobiology of Hearing Group, Department for Neuroscience, School of Medicine and Health Sciences, University of Oldenburg; [2]Neurobiology of Hearing Group, Department for Neuroscience, School of Medicine and Health Sciences, University of Oldenburg

Auditory implants (cochlea or brainstem) already partially restore auditory function in patients with disabling hearing impairments very successfully. However, the current electric stimulation approaches for such implants suffer from the drawback of limited temporal and spectral resolution. Electrical field spread is dictated by the relatively high impedance of the surrounding tissue, impeding spatially focused electrical stimulation in the nervous system. To overcome these technical limitations, optogenetic stimulation could be used in such prosthesis to achieve a more focal and precise stimulation with enhanced resolution. This method may allow for more precise and specific stimulation of nearby sites at a particular stage of the auditory pathway. Previous experiments have provided proof-of-principle of detection of excitation at a single outlet in the inferior colliculus (IC) in a rodent model. However, the feasibility of discrimination of stimulation at different sites remains to be shown and will be the next steps towards a differential stimulation of the tonotopic axis.

In this study, we aimed to perform behavioral tests of the ability of mice to a) generally detect optogenetic stimulation in a reward based Go/No Go paradigm and b) to discriminate stimulation at two different points within the IC. To this end, we devised an optogenetic midbrain-implant, which stimulates two points within different tonotopic layers of the IC. We aimed to provide a proof-of-principle for stimulation of neural populations that represent different acoustic frequencies. Pre-surgery, animals were trained in a frequency oddball task in which they had to indicate a change in frequency within a continuous sequence of tone pips. We then implanted two well-separate excitatory outlets at two sites in the IC (unilateral) with a distance of 700µm in depth after injection of rAAV5-CAG-ChR2-GFP. Post-surgery, auditory stimuli were converted into an optical oddball paradigm: the mouse had to report a switch of the site of continuous pulses from one outlet to the respective other. Discrimination performance was highly significant for both acoustic and optogenetic stimulation. Results from behavioral tests and from modeling of light spread and neural activation indicate that distances of the outlets < 100µm should be well discriminable, thus establishing the first steps towards continuous frequency stimulation in auditory brain implants.

PS 578

Combined Optogenetic and Electrical Stimulation of Auditory Neurons

Alex Thompson[1]; Andrew Wise[1]; William Hart[2]; Karina Needham[3]; James Fallon[1]; Paul Stoddart[2]; **Rachael Richardson**[1]
[1]Bionics Institute; [2]Swinburne University of Technology; [3]University of Melbourne, Department of Otolaryngology

Electrical stimulation has long been the gold standard for evoking neural activity and has been used with great success in the cochlear implant to restore hearing. Despite its success in contemporary devices, electrical stimulation activates a broad region of the cochlea with limited precision due to the spread of electrical current. Optical stimulation has the potential to provide highly focused stimuli, but falls short of the speed and efficiency of electrical stimulation. This work explores whether high spatial and temporal precision can be obtained by combining optical and electrical stimuli. Transgenic mice expressing the H134R variant of channelrhodopsin-2 in spiral ganglion neurons (SGNs) were acutely deafened. Multiunit activity of inferior colliculus (IC) neurons were recorded in response to 488 nm optical, electrical or combined stimuli presented in the base or apex of the cochlea via a single channel optical fibre and platinum electrode hybrid device. Stimuli were systematically varied in strength, pulse width, frequency and delay between the optical and electrical stimuli. *In vitro* electrophysiological recordings from isolated SGNs were also obtained to study interactions between optical and electrical modalities at the membrane level. Responses to optical, electrical and co-stimulation were detected in the IC in a cochleotopic manner, such that responses to stimuli applied to the cochlear base were recorded at deeper sites within the IC and those applied to the cochlear apex were recorded more superficially. Multiunit IC activity was detected when using combined stimuli that were individually sub-threshold. This 'summation effect' was particularly evident when the electrical stimulus was delayed with respect to the optical pulse and was maintained up to 60 ms after the end of the optical pulse when recorded from isolated spiral ganglion neurons. Co-stimulation did not affect the spread of the spatial tuning curve at d'=1 above threshold compared to optical stimulation alone *in vivo* but did enable SGNs to entrain to a higher stimulation rate compared to optical stimulation alone. A hybrid optical/electrical device may exploit the advantages of both modalities during and after the optical pulse. Using the light stimulus to 'prime' the neurons to a sub-threshold level of excitability enables activation with low electrical currents and an increased rate of stimulation that cannot be achieved with optical stimulation alone.

PS 579

Comparison of Responses to DCN or VCN Electrode Placements in a Mouse Model of the Auditory Brainstem Implant (ABI)

Stephen McInturff[1]; Nicolas Vachicouras[2]; Stéphanie Lacour[3]; Daniel J. Lee[4]; Christian Brown[1]
[1]Harvard Medical School; [2]École Polytechnique Fédérale de Lausanne; [3]Institute of Bioengineering, Centre for Neuroprosthetics, École Polytechnique Fédérale de Lausanne (EPFL), Lausanne, Switzerland; [4]Massachusetts Eye and Ear Infirmary, Department of Otology and Laryngology, Harvard Medical School, Boston, Massachusetts, USA

Introduction

The auditory brainstem implant (ABI) is indicated for deaf patients with damaged or absent cochlear nerves and electrically stimulates the cochlear nucleus (CN). Most ABI users have modest performance as measured by speech comprehension. The reasons for these poor outcomes are not fully understood but has been thought to arise in part from the variability of ABI electrode array placement (Barber et al., 2017, Ear and Hearing 38:e343-e351). In this study, we compared electrophysiological responses following stimulation of the dorsal (D)CN vs. ventral (V)CN using surface stimulating electrodes in a mouse model of the ABI. Specifically, we examine location dependent changes in latency and amplitude of responses and tonotopic specificity before and after lesioning of output pathways of the CN.

Methods

In anesthetized CBA/CaJ mice, surface ABI arrays are placed either on DCN or VCN following posterior craniotomy. DCN placement was done visually whereas VCN placement was by insertion in the cleft between the lateral most CN and the temporal bone. Electrical stimulation was biphasic and bipolar pulse trains of varying rates. Electrically evoked auditory brainstem responses (eABR) were recorded with needle electrodes in the skin, and multi-unit neural activity was recorded with a 16-channel recording probe (NeuroNexus) placed in the central nucleus of the contralateral inferior colliculus (IC). Surgical cuts of two output pathways of the CN, the dorsal and/or ventral acoustic striae, were made with a scalpel and confirmed in Nissl-stained transverse sections by comparing sections to our previous database of labeled axons.

Results/Conclusion

We observed similarities and important differences in the two types of responses. Overall latencies were similar, with DCN or VCN placements each producing a bimodal

response consisting of early and late components. Cuts to the dorsal acoustic stria (DAS) attenuated early responses in both DCN or VCN stimulation, whereas eABRs were little affected. DCN placements had a pattern in which early responses had lower thresholds than late responses while VCN placements had the opposite pattern. In preliminary data, DCN stimulation had a higher synchrony index than VCN stimulation at pulse rates greater than ~50Hz. In the future, differences between DCN and VCN stimulation may be used to identify which subdivision is being stimulated in human ABI subjects.

PS 580

A Penetrating Auditory-Nerve Electrode for Improved Transmission of Temporal Fine Structure

John C. Middlebrooks[1]; Bing Xu[2]; Matthew L Richardson[3]; Harrison W Lin[1]
[1]UC Irvine; [2]Advanced Bionics, LLC; [3]University of California

Present-day cochlear implants stimulate primarily the basal cochlea, with essentially no selective stimulation of the apical cochlea. Also, human implant users show relatively poor sensitivity to temporal fine structure. In short-term experiments in cats, we find that electrical stimulation with a penetrating auditory-nerve electrode can selectively activate pathways from the apical cochlea. Moreover, electrical stimulation of those apical pathways can transmit temporal fine structure at higher rates compared to pathways from the basal cochlea (Middlebrooks and Snyder, *J. Neurosci*, 2010). Now, we are developing a penetrating electrode that is suitable for long-term implantation and that, eventually, could translate to human application.

The electrode is similar to one shank of the multi-shank penetrating auditory brainstem implant, which was approved by the FDA for clinical trials (Otto et al., *Otol and Neurotol*, 2008). Our electrode, made by Advanced Bionics, consists of a sharpened parylene-insulated iridium shank. The tip is exposed and activated to increase the charge capacity and, thereby, mitigate electrochemical toxicity of neural tissue.

Initially, we have tested the electrode in short-term experiments in anesthetized cats. We monitor activation of auditory pathways by recording at 32 depths along the frequency-representation axis of the inferior colliculus (IC). As the electrode is advanced into the auditory nerve, the tip first encounters fibers from the cochlear base, stimulation of which activates deep, high-frequency IC neurons. Further advances bring the electrode tip in contact with fibers from the cochlear apex, permitting selective stimulation of superficial, low-frequency IC neurons.

We evaluated transmission of temporal fine structure by presenting electrical pulse trains at varying rates and recording phase-locking of IC neurons. In our first tests, phase locking to stimulation of basal fibers was limited to rates ≤200 pulses per second. In contrast, stimulation of apical fibers showed phase locking to rates ≥400 pulses per second.

We soon will begin implanting the penetrating electrode in cats for long-term trials. We will evaluate safety of long-term implantation and stability of temporal transmission over the course of ~6 months of deafness or of chronic electrical stimulation. Our goal is to augment the cochlear implant with a penetrating electrode that could improve sensitivity to temporal fine structure, thereby enhancing perception of temporal pitch and of temporal cues for spatial hearing, both of which could improve hearing in the presence of competing sounds.

Funded by NIDCD R01 DC017182 and T32 DC010775-09. The penetrating electrode was provided by Advanced Bionics, LLC.

PS 581

Development and Translation of an Intracranial Auditory Nerve Implant

Hubert H. Lim[1]; Abigail Heiller[2]; Meredith Adams[2]; Loren Rieth[3]; Moritz Leber[4]; Karl-Heinz Dyballa[5]; Waldo Nogueira[6]; Geoffrey Ghose[2]; Luke Johnson[2]; Amir Samii[7]; Rob Franklin[4]; David Warren[8]; Bo Connelly[2]; Florian Solzbacher[8]; Andrew J. Oxenham[9]; Thomas Lenarz[10]
[1]University of Minnesota, Minneapolis, USA; [2]University of Minnesota; [3]Feinstein Institute for Medical Research; [4]Blackrock Microsystems; [5]Hannover Medical School; [6]Hannover Medical School, Hannover, Germany; Cluster of Excellence, Hearing4all, Germany; [7]International Neuroscience Institute; [8]University of Utah; [9]Department of Psychology, Center for Applied and Translational Sensory Sciences, UMNTC; [10]Hannover Medical School, Hannover, Germany

Sensory restoration with implantable neural technologies has been around for over 50 years. In particular, the cochlear implant (CI) is considered one of the most successful applications of neural implants. However, performance levels are still far from natural hearing. With recent advances in neural technologies and neurotological surgical approaches, there are greater opportunities for pursuing an intracranial auditory prosthesis that targets the auditory nerve between the cochlea and the brainstem (auditory nerve implant, ANI) to potentially improve hearing performance over current hearing treatment options. The ANI can be directly

implanted into the auditory nerve with the aim to achieve more focused activation and greater transmission of auditory information to the brain compared to the CI, which is positioned into the cochlea and transmits current across the bony wall to access the auditory nerve fibers. Initially, the ANI can be implanted in deaf patients who cannot be successfully implanted or sufficiently benefit from a CI due to anatomical distortions/obstruction of the cochlea or facial side effects. A 5-year NIH BRAIN Initiative grant has been awarded across five institutions and two medical device companies (MED-EL and Blackrock Microsystems) to develop and translate a new ANI through pre-clinical studies (Years 1-3), and then implant the ANI in up to 3 deaf patients through a pilot clinical trial (Years 4-5). Over the past year, we have modified for use in the auditory nerve the well-known Utah electrode array developed by Blackrock Microsystems that is currently used in humans for motor/somatosensory implants in the cortex and peripheral nerves. Different dimensions and configurations of the array have been evaluated in human cadaver experiments, in which both retrosigmoid and translabyrinthine approaches are under consideration for implantation, to achieve proper cable anchoring and array insertion with a custom surgical inserter. The electrode array and cabling will interface with the MED-EL Synchrony implant and these components will be extensively tested for reliability, biocompatibility, functionality and safety through benchtop testing and chronic animal experiments (in cats and non-human primates). Additionally, perceptual testing protocols and novel stimulation algorithms relevant for the ANI patients are being developed through simulations in normal hearing subjects and will be evaluated in CI patients to permit comparison with the performance observed in the actual ANI patients. The success of this project will not only open new directions for auditory prosthetics, but also provide improved neural technologies for other clinical applications relevant to the BRAIN community.

PS 582

Pre-Clinical Validation of Silicon-Based Auditory Brainstem Prostheses

Nicholas Nolta; Pejman Ghelich; **Martin Han**
University of Connecticut

Patients with damaged auditory nerves may not benefit from cochlear implants. They include neurofibromatosis type 2 patients and a subset of cochlear implant users. Extensive animal study has been conducted to validate chronically-implanted arrays of penetrating 3D microelectrodes in the cat's cochlear nucleus as a brainstem prosthesis. While these silicon-based multisite devices have been effective to selectively stimulate along the tonotopic organization of the cochlear nucleus and to evoke neural responses in the inferior colliculus, additional pre-clinical device validation is needed to enable human clinical trials. We explored three major improvements to our penetrating silicon-based 3D microelectrode arrays. First, we developed a technique for recessing (burying) the traces that connect the electrode sites to the bond pads. The technique used a dry etch to create a trench, then the metal for the traces is deposited so that it fills the trench exactly to the level of the wafer surface. This prevents the next layer, the insulating dielectrics, from having to cover raised topographies, which normally create weak points for cracking and corrosion. Second, we compared two techniques to deposit silicon dioxide on the vertical sidewalls of the silicon shanks. This is important because silicon is known to be etched slowly in the *in vivo* environment. In previous designs, we protected the sidewalls by conformally depositing Parylene C and then individually de-insulating electrode sites with a deep-UV laser. This process was effective, but time consuming, and had unwanted side effects on the electrode sites. These issues have been avoided by our new silicon dioxide batch process with conformal coating. Finally, while previous designs had electroplated iridium oxide film (EIROF) electrode sites, we have begun optimizing deposition parameters for sputtered iridium oxide films (SIROFs). SIROF is the current state-of-the-art electrode material as it is batch-processed and provides a higher charge injection capability than EIROF. In combination, these three innovations push us closer to our ultimate goal of producing high-performance, failure-free neural microelectrodes that may be suitable for human implantation as a cochlear nucleus prosthesis.

Acknowledgments
This work was supported by NIH grant R01DC014044 (MH).

PS 583

Light-induced Protein Synthesis in Human Mesenchymal Stem Cells for Cochlea Implants

Nina L. Wichert[1]; Andy Martinez[2]; Martin Witt[1]; Rebecca Jonczyk[1]; Malte Sgodda[3]; Lani Torres[4]; Marc Wahalla[5]; Alexander Heisterkamp[4]; Tobias Cantz[3]; Holger Blume[6]; Cornelia Blume[1]
[1]Leibniz Universität Hannover - Institut für Technische Chemie; [2]Northeastern University Boston; [3]Medizinische Hochschule Hannover; [4]Leibniz Universität Hannover - Institut für Quantenoptik; [5]Leibniz Universität Hannover - Institut für Mikroelektrische Systeme; [6]Leibniz Universität Hannover - Institut für Mikroelektrische Systeme

The aim of this project is the regulation of gene expression in mammalian cells, especially human mesenchymal stem cells (hMSCs), via light induction in a temporally

and spatially focused manner. This optogenetic approach shall be used to enable light induced protein biosynthesis of neuroprotective factors such as the brain-derived neuroprotection factor (BDNF), which promotes cochlear spiral ganglion cell survival and function. These optogenetically activatable stem cells should be placed on the cochlear implant during implantation for improved cochlea implant performance. In order to regulate gene expression via light induction, two plasmids are co-transfected into the cells. The first plasmid carries the optogenetic toggle switch gene sequences including the photo-activator and the second plasmid carries the gene sequence for *bdnf* (see figure 2). After co-transfection, target gene expression can be activated and deactivated via light induction (660 rsp. 740 nm) in the presence of the chromophore phycocyanobilin (PCB) (see figure 1). For transient transfection of CHO-K1 cells, PEI (polyetherimine) was used, while hMSCs were electroporated. Using a third generation lenti-virus, hMSCs will be stably transfected (see figure 3). For the lenti-viral transfection, the optogenetic toggle switch and the target gene are cloned on the same vector with a defined promotor activity and predictable stoichiometric ratio. The lenti-viral system used is authorized for human stem cells. The induction of gene expression by LED and laser-light induction has been established and optimized in CHO-K1 cells with the optogenetic switch for EGFP synthesis (see figure 4 and 5). The transfection efficiency was determined by pixel analysis with ImageJ using 10 representative fluorescence microscopic images per sample. In order to transfer the system to hMSCs derived from adipogenic tissue, a new transfection method is established, because chemical transfection and some lenti-viral systems can influence the cell biology of hMSCs. After optimization, a transfection efficiency of 11 % could be verified by flow cytometer analysis after electroporation (see figure 6). The induction of gene expression by LED- and laser-light induction has been established successfully in CHO-K1 cells after PEI-transfection, and a protocol for electroporation for gene transfer in hMSCs was verified reaching a transfection efficiency of 11% up to now. Currently, MSCs are gene transfected using a third-generation lenti-viral system. In further experiments, synthesized BDNF has to be quantified and co-culture experiments with cochlear spiral ganglion cells have to be performed to document the neuron supporting effect.

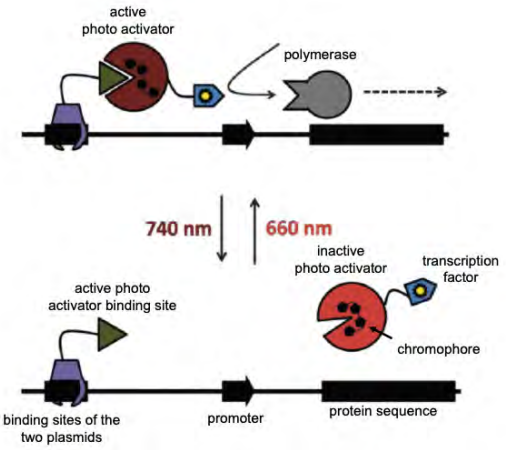

Figure 1: *Principle of the optogenetic switch using red light and far red light[8]: After light induced conformational change of the photo-activator, phyB and pif6 bind, and this newly composited transcription factor activates the promotor for target gene transcription.*

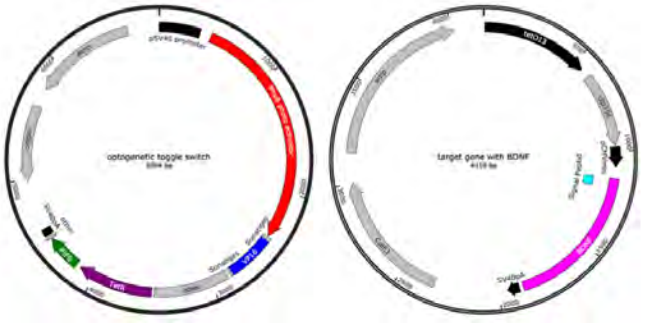

Figure 2: Plasmid maps of the optogenetic toggle switch with PhyB photo activator=phyB, PIF6 and VP16 as parts of the transcription factor, the target gene sequence bdnf, the pCMV min promotor.

Figure 3: Plasmid map of the lentivirus with the optogenetic toggle switch genes (phyB, PIF6, VP16) and bdnf (CAG promotor).

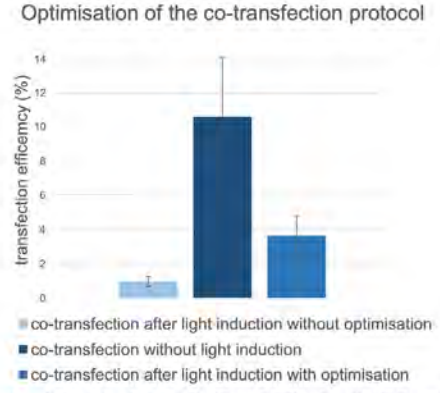

Figure 4: Optimisation of the co-transfection[8] with PEI in CHO-K1 cells with LED-illumination: As compared to the first approach, DNA amount was increased by 1/3, PEI concentration was increased by 50% and the cell count was decreased by 1/6 and transfected cells were screened as late as 72 h after transfection.

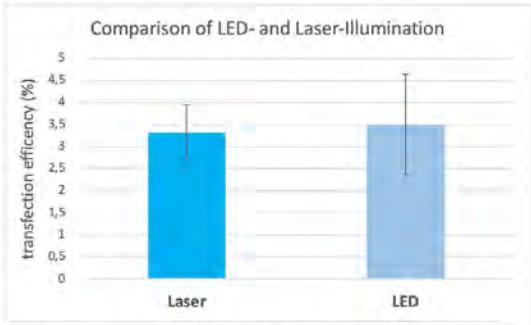

Figure 5: Comparison of transfection efficiencies after LED- or Laser-Illumination in CHO-K1 cells after co-transfection with PEI.

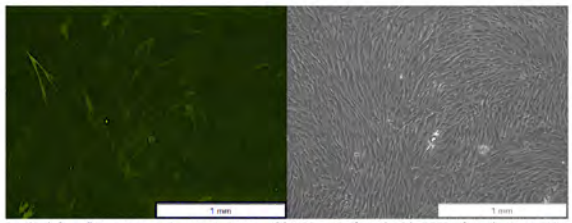

Figure 6: On the left, a fluorescence microscopic image of hMSCs transfected with EGFP after electroporation is shown; on the right, a phase contrast microscopic image of hMSCs transfected with EGFP after electroporation is shown.

PS 584

Robotic Insertion of New Cochlea Implants

Hideaki Ogita[1]; Koji Nishimura[2]; Takayuki Nakagawa[2]; Juichi Ito[3]; Tetsuro Tsuji[4]; Satoyuki Kawano[4]; Hidetoshi Kotera[5]; Takeshi Nizuka[6]; Masanori Enrin[6]; Hisakazu Ninomiya[6]

[1]Shiga Medical Center Research Institute, Shiga, Japan; [2]Department of Otolaryngology-Head and Neck Surgery, Graduate School of Medicine, Kyoto University; [3]Shiga Medical Center Research Institute; [4]Graduate School of Engineering Science, Osaka University; [5]Institute of Physical and Chemical Research (RIKEN); [6]Kyocera Corporation

We are developing a new type of cochlea implant (CI) named 'HIBIKI'. This new CI was designed to operate without battery and totally implantable. The width of this device is about 1.5mm and the length is about 1mm. There is some difficulty in implanting the device into the cochlea manually. To implant the device more easily and stably, we are developing an apparatus for inserting the new CIs into the cochlea. This apparatus consists of a robotic arm and other attachments.

The insertion apparatus consists of three parts. The main part is a robotic arm. The second part is a gripper. The third part is a tweezer slider. We used commercial robotic arm 'UR3' (Universal Robots, Denmark). This robotic arm has a gripper (Robotiq, Canada). This gripper open and close tweezers. The tweezer hold a CI and insert it into the cochlea. The tweezer holder has a slider. The slider has a holding plate. With a sliding gripper and a holding plate, it is possible to avoid to slip out CIs. At the base of the gripper, a force sensor is equipped. This force sensor can measure the force on the tweezer. By monitoring the force, we know that the tip of a CI touches the cochlea modiolus. Because we have to change the direction of insertion of the CI, after the CI touches the modiolus.

This apparatus is also equipped a small endoscope. Before CIs enter the bulla, it is possible to see the position of CIs with a microscope. But after CIs enter the bulla, it is not possible to see the tip the tweezers and CIs with a microscope. Because the tips of the tweezers were hidden by the robotic arm. The diameter of the endoscope was very small (1.4mm) to avoid the interference with tweezers.

With this apparatus, we inserted the CI device into guinea pigs cochlea. We used Hartley guinea pigs. After making a posterior auricular incision, we make a small hole on the bulla. Then we made a cochleostomy. CIs were held with tweezers and inserted into the cochlea. After the insertion of CIs, we slided out the tweezers. Then we slided out the holding plate. This insertion apparatus composed of a robotic arm is useful for inserting the new CIs stably.

PS 585

Safety of Transcranial Ultrasound for Neuromodulation and a Novel Hearing Technology

John Basile[1]; Gerardo Rodriguez[1]; James Kerber[1]; Hubert H. Lim[2]

[1]University of Minnesota; [2]University of Minnesota, Minneapolis, USA

Ultrasound (US) research has grown rapidly in the past decade for noninvasively activating or modulating brain regions with high spatial resolution. Studies have also quickly moved into humans citing diagnostic US imaging safety ranges in a FDA guidance document (Docket: FDA-2017-D-5372); however, the parameter settings between imaging and neuromodulation can be quite different. Therefore, safety of sonicated tissue with neuromodulation parameters needs to be studied. Additionally, while studying US neuromodulation, our lab discovered that US applied to the head readily activates the auditory system through vibrations of cerebrospinal fluid that then directly vibrate fluids within the cochlea (Guo et al., Neuron, 2018). This discovery has opened up an opportunity for using ultrasound energy as a new type of hearing technology. Recently, our lab has shown that frequency specific activation of the auditory system in animals is possible with amplitude-modulated US stimuli. To move this US technology into humans for hearing and neuromodulation applications, tissue and hearing safety studies are required. In anesthetized

guinea pigs, we recorded auditory brainstem responses (ABRs) and electrocochleography (ECochG) in response to amplitude-modulated US (carriers: 100 and 220 kHz) presented on top of the skull, as well as to air-conducted acoustic pure tones and broadband noise. We presented chronic US to these animals for 5 hours each day for 5 days and for 8 hours per day for 10 days with different pressures (100-800kPa), duty cycles (5-80%), and sonication durations (.05-9.6 s), spanning parameters relevant for both hearing and neuromodulation applications. We assessed ABR and ECochG thresholds, amplitudes, and latencies over time to identify potential hearing damage. We performed histology using Hematoxylin and Eosin to assess brain tissue damage. The neural responses to US stimuli closely resembled those to air-conducted stimuli. Most parameters maintained consistent thresholds, amplitudes, and latencies over time. However, threshold shifts occurred at the higher intensities, those of which are likely beyond what are necessary for hearing applications, but are used for neuromodulation studies. No noticeable brain damage was observed for all tested parameters. Overall, US stimulation appears to be safe for hearing applications but caution is needed when applying higher intensities for neuromodulation applications since hearing damage may be possible even though tissue damage is not observed. Currently, a wearable US device that can be potentially used for neuromodulation and hearing applications in humans is being developed with our lab and a start-up company (SecondWave) funded by DARPA.

Binaural Hearing in Animals: Neural Recordings

PS 586

Hidden Island Navigation Task (HINT): A Novel Paradigm to Study Auditory Processing During Goal-Oriented Behavior in Freely Moving Animals

Dardo N. Ferreiro[1]; Diana Amaro[1]; Lucile Belliveau[1]; Michael Pecka[2]
[1]Division of Neurobiology, Ludwig-Maximilians-University Munich; [2]Biocenter, Section of Neurobiology, Department Biology II, Ludwig-Maximilians-Universitaet Munich

Experimental methods to study sensory processing in model animals have been increasing in number and complexity, especially in the last decade. Ethologically driven paradigms (including behavioral observations in natural habitats) have largely been replaced by highly controlled experiments in head-fixed or even anesthetized animals. While such preparations are crucial for the dissection of specific mechanisms, they are prone to overlook ethologically fundamental aspects of sensory biology. Specifically, sensory systems evolved to gather information about dynamic interactions with the environment during locomotion, which requires the continuous update of the 'framework' within which the organism interprets its sensory inputs. Accordingly, a number of studies recently showcased the importance of movement during neuronal processing in a variety of sensory modalities, including in barrel cortex (Kerekes et al., 2017), visual cortex (Dadarlat and Stryker, 2017), and auditory cortex (Schneider et al., 2018; for a review see Schneider and Mooney 2018). Moreover, this informational framework is combined across sensory systems in highly context-dependent manner (Deneux et al., 2019) and is crucial for inference and sensory object formation (Atilgan et al., 2018). Despite the fundamental role of these contextual factors for natural behavior in complex sensory scenes, investigation of sensory neurophysiology in freely moving animals performing goal-oriented behavior is sparse (Krakauer et al., 2017). To fully capture ethologically relevant sensory processing, active engagement in a context-dependent decision-making task with unrestricted movement and corresponding closed-looped multi-sensory modulation is required. Here, building upon seminal studies in rats and mice (Polley et al., 2004; Whitton et al., 2014), we present a novel free-navigation experimental paradigm with simultaneous neural recordings in which gerbils forage for an auditory target. To navigate the arena the animals rely on the changes of acoustic stimulation, which is controlled in real-time via closed-loop video tracking. They are trained to find a particular area in the arena ("hidden target island") for which the target stimulus is presented. The location of the target island is randomized across trials, making the studied stimulus property the only informative cue for task completion. Animals report detection of the target island by remaining within the it for a defined time period. Multiple "distractor" islands and multimodal cueing can be incorporated to test discrimination and identification performance. Here we showcase HINT for studying frequency detection and identification, as well as sound source localization. Paired with chronic recordings, HINT also facilitates investigating neuronal auditory object formation and goal-oriented behavior.

PS 587

Age-Related Changes to Binary Hearing and the Auditory Brainstem in the Mongolian Gerbil

Elizabeth McCullagh[1]; Alexandra Lucas[2]; Shani Poleg[2]; Nathaniel T. Greene[3]; John Peacock[4]; Melinda Anderson[2]; Daniel J. Tollin[5]; Achim Klug[2]
[1]Oklahoma State University; [2]University of Colorado School of Medicine; [3]Department of Otolaryngology, University of Colorado School of Medicine; [4]University of Colorado; [5]Department of Physiology & Biophysics,

and Department of Otolaryngology, University of Colorado School of Medicine

One of the most common medical conditions in any aging society is presbycusis, or age-related hearing loss, with approximately one third of American adults diagnosed with the disorder. One of the mechanisms of presbycusis happens in the central nervous system and is termed *central hearing loss*. Older adults with central hearing loss may have normal or near normal audiograms yet experience listening difficulties in complex environments - e.g., situations with multiple sound sources, such as restaurants, workplaces, or any situation where background noises are active. In these environments, affected individuals have trouble perceptually isolating sound sources of interest (e.g., the voice of the speaker they want to listen to) effectively from other sources. We hypothesize that these difficulties arise in part because the brainstem neural circuits that perform the initial computation of spatial information, and thus the separation of sources, are less effective. To begin to understand how aging affects these circuits and also binaural hearing we used prepulse inhibition (PPI) of the acoustic reflex (ASR) to measure gap detection as well as spatial hearing ability including the minimum audible angle and spatial release from masking in aged gerbils (average age 1147 days for old group, 87 days for young group). Older gerbils showed deficits in minimum audible angle detection, but no difficulties in gap detection or spatial release from masking compared to younger animals. To assess brainstem function, we measured auditory brainstem responses (ABRs) to study hearing thresholds and the binaural interaction component (BIC) of ABRs to study neural binaural circuit function. Old gerbils had slightly increased ABR thresholds (not significant) compared to young animals. However, old gerbils did have lower amplitude wave 3 and decreased BIC compared to younger animals. Lastly, we measured anatomical changes to the auditory brainstem including Western blots and immunohistochemistry for gephyrin, glycine receptor alpha1 and glycine transporter 2. Older gerbils had decreased gephyrin and a trend towards decreased glycine receptor alpha1 as measured by Western blotting. We found that the older animals showed more variable amounts of hearing loss as measured by PPI and ABR, with some animals showing no changes to ABR or PPI while others had what appeared to be hearing loss. In addition, it appears that there are likely changes to inhibition in the auditory brainstem which may underly some of the changes in auditory spatial acuity observed in behavioral/physiological responses.

PS 588

In Vivo Physiological and Functional Investigation of Cholinergic Modulation in the MNTB of Adult Gerbil

Chao Zhang[1]; Nichole L. Beebe[2]; Michael Pecka[3]; Brett R. Schofield[4]; Michael Burger[1]
[1]Lehigh University; [2]Northeast Ohio Medical University; [3]Ludwig Maximilian University of Munich; [4]Northeast Ohio Medical University; Kent State University

The superior olivary complex (SOC) is a vital component of auditory circuitry devoted to localization of sound sources. Within SOC, principal neurons of the medial nucleus of the trapezoid body (MNTB) reliably convert contralaterally derived monaural excitation to inhibition that is distributed to several postsynaptic targets, thus conveying precisely timed inhibition to nuclei involved in computation of sound location. Secure synaptic transmission is essential to maintain temporal precision for accurate sound localization. The Calyx of Held synapse in MNTB appears specialized for reliable transmission. However, this reliability is challenged in some species including gerbils when confronted by intense sound stimulation (Kopp-Scheinpflug *et al.*, 2003a; Hermann *et al*., 2007). Maintaining computational stability requires mechanisms that dynamically modulate neurons' responses, however, the underlying modulatory mechanisms have yet to be illuminated. One candidate mechanism is the cholinergic system, which influences neural signaling throughout the brain. Happe and Morley (1998) first demonstrated high expression of nicotinic acetylcholine receptors (nAChRs) in SOC, suggesting a role for cholinergic modulation. This finding is further substantiated by our current anatomical data showing that the cholinergic inputs to MNTB derived from sound driven nuclei, pontomesencephalic tegmentum (PMT) and ventral nucleus of trapezoid body (VNTB). Despite this evidence, no physiological investigation of cholinergic function has been reported for MNTB neurons.

In order to investigate the role of endogenous cholinergic input to the MNTB, we made *in vivo* extracellular recordings from anesthetized gerbil MNTB, using piggyback multi-barrel electrodes which allowed us to pharmacologically block cholinergic inputs with iontophoresis of antagonists of nAChRs. Our results reveal that tone-evoked firing rates in MNTB are reduced during drug application, suggesting a potent modulatory role of ACh in maintaining MNTBs' ability to fire action potentials in response to acoustic input. Furthermore, a decreased encoding efficiency in rate-level functions of MNTB neurons after blocking nAChRs suggests that ACh confers modulation that increases synaptic gain for near-threshold stimuli. Decreased synaptic gain leads to loss of acoustic information transmitted

through Calyx of Held / MNTB synapse. This reduced synaptic efficacy may diminish MNTB neurons' ability to differentiate sounds in noise. To study the functional impact of this modulation, we embedded pure-tone stimuli in wide band noise to test whether nAChR antagonists hamper MNTBs' ability to detect signal in noise. Our results suggest that endogenous cholinergic input to MNTB is sound-evoked and functions to improve signal detection.

PS 589

Neuronal Encodings of Upper Spatial Hemifield Across the Ascending Auditory Pathway of awake mouse (mus musculus)

Paul LC Feyen; Alfonso Junior Apicella
University of Texas at San Antonio

In everyday life listeners are continuously bombarded with a barrage of auditory information. The ability to disentangle the spatial source of these signals is a reliable means of tracking prey and predator, navigating, and facilitating communication. Here we characterize how information pertaining to the spatial location of an auditory stimulus is encoded in neuronal firing patterns along the ascending auditory pathway. Specifically, we look at the collicular-thalamo-cortical pathway using multielectrode recordings of a head restrained mouse that is centered in a hemispherical speaker array to produce frontal, rear, lateral, and vertical sources of auditory stimuli. We characterize neuronal response types and investigate how the temporal dynamics of firing rates contribute to a representation of a signal's spatial source. This allows us to quantify the distributions of spatial acuity levels and tuning orientation across the ascending auditory pathway. Past studies have shown that increasing stimulus duration improves performance on a sound localization tasks in freely moving subjects; an effect thought to be mediated by the subject's ability to reorient and re-asses sound characteristics at different proximities and incidence angles. In contrast we will assess how inherent transfer functions shape neural representations at the single neuron and multi-unit network scales as a function of stimulus time. Overall, this study will elucidate the extent of egocentric representations of acoustic space across the distributed auditory pathway.

PS 590

Loss of Neural Sensitivity to Interaural Time Difference Following Noise-Induced Hearing Loss

Hariprakash Haragopal; Ryan Dorkoski; Gareth A. Whaley; Timothy R. Wohl; Noelle C. Stroud; Mitchell L. Day
Ohio University

Sensorineural hearing loss degrades the ability to localize the direction of sound sources in the horizontal plane (i.e., azimuth), but the physiological mechanisms underlying this degradation are unknown. To investigate the causes of reduced localization ability with hearing loss, we recorded from single-units in the inferior colliculus (IC) of unanesthetized, Dutch-belted rabbits with noise-induced hearing loss (NIHL) and compared responses to those of unexposed, normal-hearing (NH) rabbits. NIHL was induced under anesthesia using octave-band noise centered at 750 Hz and presented at 133 dB SPL for 90 min. Click-evoked auditory brainstem response thresholds measured before and two weeks after exposure shifted by approximately 50 dB. The sensitivity of a neuron's response to changes in the azimuth of a broadband noise stimulus was quantified as the mutual information (MI) between firing rate and azimuth. At a sound level of 0 dB re: "sensation level" (the click-evoked ABR threshold for each individual rabbit), the distribution of MI across neurons was similar between NIHL and NH rabbits, suggesting similar amounts of information about sound source direction. However, at 70 dB SPL the distribution of MI for NIHL rabbits was weighted towards zero, largely because of stimuli being below the level threshold of neurons. In order to determine which binaural cue dominated neural sensitivity to azimuth, sounds presented through earphones in virtual acoustic space were manipulated to independently vary interaural time and level differences (ITDs and ILDs), or present stimuli to only the contralateral ear. Using these cue manipulations, we deduced that azimuth sensitivity in NIHL rabbits was solely due to sensitivity to ILD or sometimes monaural sensitivity, whereas that in NH rabbits was due to sensitivity to ITD, ILD, or both. We additionally measured responses to noise stimuli presented at ITDs between β1,000 and +1,000 μs (i.e., outside of the physiological range). For NIHL rabbits, the MI between neural firing rate and ITD was always near zero, indicating a lack of neural sensitivity to ITD. To determine if loss of neural ITD sensitivity could be explained by dysfunction at the periphery, we computed a shuffled cross-correlogram of the left and right spike trains of an auditory nerve model. Reducing the number of functioning cochlear inner and outer hair cells in the model did not eliminate ITD sensitivity. Therefore, loss of ITD sensitivity in IC neurons may be due to a dysfunction of central mechanisms.

Supported by NIDCD-NIH award numbers R15DC017616 and R03DC013388.

PS 591

The Effect of Anticipated Cue Reliability on the Barn Owl's Discriminability of Sound Location

Keanu Shadron[1]; Roland Ferger[1]; Andrea J. Bae[1]; Brian J. Fischer[2]; José L. Peña[1]

[1]*Dominick P. Purpura Department of Neuroscience - Albert Einstein College of Medicine, NY, USA;* [2]*Department of Mathematics - Seattle University, Seattle, WA, USA*

To create an efficient representation of the world, the brain has to encode informative stimuli while ignoring stimuli of little value. This is found in the barn owl's midbrain, which uses interaural time difference (ITD) to compute sound location in azimuth. Previous work found that space-specific neurons in the midbrain are tuned to the frequency range that is most reliable at each preferred location. This effect is predicted by the acoustical properties of the head, causing higher frequencies to convey ITD more reliably in frontal space and lower frequencies in the periphery in the presence of concurrent sound. We hypothesized that this frequency tuning has an effect on sound location discriminability when the sound is expected to be unreliable.

We first tested this behaviorally using the pupillary dilation response, an orienting response that adapts upon repetition of a stimulus and readily recovers when novel stimuli are presented. A bandpass noise at one ITD was repeatedly presented to an awake barn owl through earphones. A deviant in ITD was presented to assess if the owl is able to discriminate the two locations. Presentation through earphones allowed us to assess discrimination when the actual reliability does not change with frequency. We found that spatial discrimination is worse when the anticipated reliability is low. To determine the neural basis of this behavioral feature, we performed multi-electrode array recordings of the optic tectum. Stimuli were again presented through earphones at different ITDs and frequency ranges. We then constructed a decoder based on a population vector readout of the optic tectum. We found that when there was a mismatch between ITD and frequency tuning, the decoder performed worse and was biased away from the presented ITD.

PS 592

Pushing the envelope: understanding responses of low-frequency MSO neurons through their sensitivity to the stimulus envelope

Jason Mikiel-Hunter[1]; Barbara Biederbeck[2]; Michael Pecka[2]; David McAlpine[3]
[1]*Macquarie University;* [2]*Ludwig Maximilian University of Munich;* [3]*Department of Linguistics, The Australian Hearing Hub, Macquarie University, Sydney, Australia*

In vivo recordings were made from the medial superior olive (MSO) of the gerbil to assess the extent to which the cochlear-filtered envelopes of broadband sounds modulated neural firing patterns. Despite its energy being distributed over a wide frequency spectrum, individual MSO neurons effectively receive a narrow band-pass filtered version of broadband sounds (Joris, 2003; Louage *et* al., 2005; Fontaine *et al*., 2014). Whilst the amplitude-modulated envelopes that arise from cochlear filtering are considered the main substrate for coincidence detection in MSO neurons of high characteristic frequency (CF), sensitivity to stimulus envelopes has also been demonstrated in binaural neurons with low CFs, and generates asymmetries in interaural time difference (ITD) tuning functions (Agapiou and McAlpine, 2008). More recently, *in vivo* recordings from low CF MSO neurons have demonstrated the emphasis of neural responses towards the onset of amplitude-modulated stimuli's envelopes (Dietz *et al*., 2014), raising the question whether envelope fluctuations generated by cochlear filtering of BBNs could also influence the spiking time course of MSO neurons. Single-neuron recordings were made from the MSO of anaesthetised gerbils. Ten noise tokens were presented binaurally, and responses recorded from MSO neurons with CFs ranging from 267Hz to 1500Hz. ITDs, ranging from -1800μs and +1800 μs (in 50μs steps) were presented to generate ITD tuning functions. Spike-triggered averaging using gammatone-filtered versions of the noise token was performed to observe the prominence of cochlear-filtered envelopes in determining neural firing. Other factors such as spike latency, intrinsic filtering and potential differences in synaptic inputs were also considered with the ultimate goal to be able to correlate an MSO neuron's envelope sensitivity with the diverse noise delay functions observed for different tokens.

Cochlear Mechanics II

PS 593

Localization of Harmonic Distortion inside the Cochlear Partition in Sensitive Gerbil Cochleae

Tianying Ren; Wenxuan He
Oregon Health & Science University

The wide dynamic range of mammalian hearing depends on the compressive nonlinearity of the cochlear partition vibration. The cochlear nonlinearity also generates different distortions, which have been measured for studying cochlear mechanics and for diagnosing auditory disorders. Mechanical harmonic distortion has been shown in the basilar membrane vibration and in intra-cochlear fluid pressure near the cochlear partition. Motile outer hair cells are thought to play an essential role in the generation of harmonic distortion. To test this hypothesis, the cochlear partition vibrations at fundamental and harmonic

frequencies were measured in sensitive gerbil cochleae. Young Mongolian gerbils of either sex with normal hearing were used in this study. After the bulla was widely opened, the cochlear partition was visualized through a microscope. When the object beam of a heterodyne low-coherence interferometer was focused on the basilar membrane, the best frequency was determined by the peak frequency of the magnitude spectrum measured at a low sound level. When a best-frequency tone is presented continuously, the magnitude and phase of the vibration were measured as a function of the radial and transverse location at fundamental and harmonic frequencies and at different sound levels.

Harmonic distortion was detected inside the cochlear partition in all sensitive preparations. At the low and intermediate sound level, the second and third harmonic dominate the vibrations at the outer hair cell region including the reticular lamina on the cross section of the cochlear partition, which shows a pattern similar to that at the fundamental frequency. Although the vibration pattern at the fundamental frequency becomes broader expanding from the outer hair cell region to the location of the basilar membrane at high sound levels, the pattern of the second harmonic remains unchanged. In contrast, the vibration pattern of the third harmonic spreads to the basilar membrane area at high sound levels. The preliminary data also reveals a significant baseline shift (bias or DC shift) of the vibration at the outer hair cell region.

The current preliminary result suggests that the mechanical harmonic distortion is generated mainly by motile outer hair cells although the basilar membrane vibration is involved.

Supported by NIH-NIDCD grant R01 DC004554.

PS 594

Even-order Distortion Products in the Organ of Corti at the Base of the Gerbil Cochlea

Anna Vavakou; Nigel P. Cooper; Marcel van der Heijden
Erasmus MC, Rotterdam

When the mammalian ear is presented with a multitone stimulus, distortion products (DPs) are generated in the cochlea. DPs have been studied in psychophysical experiments, auditory nerve recordings, and recordings of cochlear microphonic potentials, otoacoustic emissions and cochlear-mechanical vibrations. The psychophysical work by Zwicker (1955, 1979) already discussed the markedly different behavior of even-order and odd-order DPs. Odd-order DPs such as the cubic difference tone at 2f1-f2 have been extensively used in physiological experiments, otoacoustic emission studies, clinical hearing tests and modeling studies. They have also been extensively reported in cochlear-mechanical studies of the basilar membrane (BM). On the other hand, even-order DPs are less well understood because they are absent on the BM except near their own characteristic place. Technical limitations of laser vibrometry have restricted the measurement site to the BM.

Optical Coherence Tomography (OCT) allows for vibration measurements in depth in the organ of Corti. OCT data reveal even-order distortion products inside the organ of Corti (Nuttall et al. Nature Commun. 9:4175, 2018). In a recent study we reported an abundance of even-order distortion products inside the OoC that are generated by below-CF stimuli presented at sound levels as low as 25 dB SPL (Vavakou et. al, eLife in press, 2019).

The aim of the current study is to describe the propagation properties of the even-order distortion products inside the organ of Corti. For that purpose we employed a zwuis tone complex, a stimulus designed to produce a rich even-order DP spectrum upon rectification (van der Heijden and Joris, J. Neurosci. 23:9194, 2003). Rectifying an N-component zwuis stimulus generates N^2 distinct second-order DP components at frequencies $f_k \pm f_m$, each of which can be traced back to a "parent" pair of interacting primary frequencies (f_k,f_m).

We recorded from adjacent locations, separated by 45 μm, in the organ of Corti of Mongolian gerbils. We compared the propagation of even-order DPs, the primaries, and acoustic references across different frequencies. Our results show that distortion products traveling near their characteristic place accumulate phase similarly to the phase of an acoustic reference having the same frequency. For DPs more basal to their characteristic place, the phase rather matches the prediction from the parent primaries within ~0.05 cycle.

Our findings show that even-order DPs are abundant inside the organ of Corti over a wide range of frequencies. In contrast, on the BM they are found only when the DP frequency matches the characteristic frequency of that region. Additionally, even-order DPs are widely generated and propagating in the OoC. These results may improve our understanding of the contrasting behavior of odd and even DPs and the corresponding otoacoustic emissions, with applications in clinical research and modeling studies.

PS 595

Frequency Dependence of Harmonic Distortions in Vibrations of the Mouse Organ of Corti

James B. Dewey; Alessandro Altoè; Christopher A. Shera; Brian E. Applegate; John S. Oghalai
Caruso Department of Otolaryngology - Head and Neck Surgery, University of Southern California

Mammalian hearing sensitivity and frequency tuning depend on active force-generation by cochlear outer hair cells (OHCs). Mechanical amplification by OHCs is largely attributed to their somatic electromotility, which is mediated by the voltage-sensitive motor protein, prestin. Isolated OHCs have been shown to produce constant electromotile force in response to transmembrane potential changes at frequencies approaching 100 kHz *ex vivo*. However, it remains unclear whether OHCs can provide such wideband, cycle-by-cycle force generation in response to acoustic stimulation *in vivo*. To examine whether there are any obvious frequency limitations to *in vivo* OHC force generation, we used optical coherence tomography to study harmonic distortions in the vibrations measured from the ~9 kHz region of the mouse cochlea. Vibratory harmonic distortions are thought to originate from nonlinearities in OHC mechanotransduction, which introduce distortion into the receptor potential and thus lead to the generation of force at harmonic frequencies. Consistent with these origins, we found that harmonics were strongest in vibrations measured from the center of the organ of Corti, near the OHC region. Harmonics were measurable up to at least 50 kHz and appeared with a negligible delay relative to the stimulus response over a wide range of frequencies. This is consistent with the harmonics arising via local, cycle-by-cycle force generation. To understand the nonlinearity underlying the measured responses, we derived a Boltzmann function that could replicate the level-dependent growth of the harmonic displacements. However, compared to the output of the Boltzmann function, the measured harmonic displacements declined at a rate of ~6-12 dB/octave. Whether this implies low-pass filtering in the OHC's electromotile response depends on the impedance seen by the OHCs. If the impedance is mass dominated, a plausible conclusion is that there is no such low-pass filtering, and that *in vivo* OHC force generation is not strongly limited at frequencies extending several octaves above the local characteristic frequency.

Supported by NIDCD/NIH grants F32 DC016211 (to J.B.D.), R01 DC014450 and DC013774 (to J.S.O.), and R01 DC003687 (to C.A.S.).

PS 596

Two-tone Acoustic Suppression in the Ear Canal Mirrors Organ of Corti but not Basilar Membrane Suppression

Jonathan H. Siegel
Northwestern University; Dept of Communication Sciences and Disorders

Two-tone nonlinear interactions in the ear canal sound pressure appear to originate in a region that extends considerably basal to the frequency range of nonlinear interaction near the peak of the basilar membrane traveling wave (Martin, et al, Hearing Res; 1999, Charaziak and Siegel, 2015). Recent measurements from inside the organ of Corti exhibit two-tone nonlinear interactions that appear consistent with the ear canal acoustic phenomenon (e.g, Dewey et al, J. Neurosci; 2019). At the same location the basilar membrane motion shows no evidence of significant nonlinearity.

The suppression of the acoustic response to a fixed low-level probe tone by a suppressor tone varied in frequency from near that of the probe to two or more octaves higher was investigated in anesthetized chinchillas. The magnitude of suppression (the residual) is averaged over the full range of suppressor frequencies or subdivided into the effects of suppressors within one octave of the probe frequency and for suppressors greater than one octave above the probe. Suppressors limited to one octave or less above the probe frequency are expected to reduce the gain and nonlinearity of the basilar membrane at its peak displacement. Higher-frequency suppressors are expected to interact in a cochlear region where the basilar membrane has been repeatedly shown to be linear. The measurements were repeated with probe frequencies ranging from 0.5 to 12 kHz.

These measures of suppression of the probe response were generally uncorrelated with the average CAP threshold from 0.5 to 18 kHz, but were strongly correlated with the average distortion-product otoacoustic emission (DPOAE) levels in the same animal. The average magnitude of suppression of the probe pressure for suppressor frequencies within one octave of the probe frequency was also strongly correlated with suppression for higher-frequency suppressors.

There does not appear to be any basis in these data to distinguish between what have been referred to as "reflection emissions" (i.e, stimulus-frequency otoacoustic emissions (SFOAEs)) from emissions previously classified as "distortion emissions" (i.e., DOPAEs) (Shera and Guinan, 1999). All OAEs co-vary in a given animal with little relation to average neural

thresholds. These results also suggest that intracochlear mechanical nonlinearity is coupled directly between the organ of Corti and the ear canal without propagation along the basilar membrane. Direct demonstration that altering the nonlinear interaction within the organ of Corti is linked to altered nonlinear interaction in the ear canal pressure has yet to be shown.

PS 597

Does the "Reticular Lamina nonlinearity" contribute to the basal DPOAE source?

Renata Sisto[1]; Arturo Moleti[2]
[1]INAIL Research Department of Occupational and Environmental Medicine, Epidemiology and Hygiene; [2]University of Rome Tor Vergata, Department of Physics

Recent experiments on animals showed nonlinear response of the RL motion over a large cochlear region, basal to the resonant place. This observation might suggest that the RL nonlinear response could be “responsible” for the generation of a basal DPOAE component.

Nonlinear cochlear models solved in the time domain allow one to monitor the generation of an intracochlear traveling wave at the distortion product frequency, propagating along the BM and RL, as well as the associated DPOAE response in the ear canal.

We used a two degrees of freedom (2DOF) nonlinear 1d transmission line cochlear model, in which two oscillators, the BM and the RL, are coupled by an internal nonlinear force representing the action of the OHC amplification system. A real-zero version of the model was used in which the normal modes of the system are characterized by a single oscillation and a pure damped motion. This model has some interesting physical properties, such as the fact that the second mass shows a nonlinear behavior over a frequency range much wider than the width of the activity peak of the basilar membrane.

The simulations show indeed that the DP intracochlear wave along the RL extends itself over a large basal region, contributing to the total DPOAE measured in the ear canal.

PS 598

Effects of Rotation of the Stereociliary Bundles of Outer Hair Cells on the Cochlear Amplification

Michio Murakoshi[1]; Hiroshi Wada[2]
[1]Kanazawa University; [2]Tohoku Bunka Gakuen University

The stereociliary bundles of the outer hair cells (OHCs) are normally arranged in a uniform pattern with specific orientations, i.e., the open side of V-shaped bundle faces the central axis of the cochlea. Rotation of the bundles in the plane of the cuticular plate has been observed in the cochleae of normal guinea pigs. These abnormal OHC bundles have various degrees of rotation. Since the displacement pattern of the stereociliary bundles is thought to be responsible for mechanoelectrical transduction of the OHCs, alterations in the bundle organization are likely to affect such transduction, leading to changes in the cochlear dynamics. However, the relationship between the rotational conditions of the OHC stereociliary bundles and the cochlear dynamics have not yet been fully understood. In the present study, therefore, a finite element model of the organ of Corti, including the OHCs, in the cochlea was constructed and changes in the displacement amplitude of the basilar membrane (BM) due to such stereocilia abnormality were analyzed.

In our model, it was assumed that the maximum force generated by the OHC decreases with an increase in the degree of rotation of the stereociliary bundle and that the OHC loses its function totally when the bundle rotates more than 90 degrees (Fig. 1).

As shown in Fig. 2, the BM displacement decreased with an increase in the degree of bundle rotation. When the abnormality was considered in the innermost row (i.e., close to the modiolus) of OHCs, it decreased by 6.2 dB at a rotation angle of 90 degrees. This result is consistent with a previously reported experimental observation; that is, the compound action potential (CAP) threshold in animals with abnormality in the innermost row of OHCs was elevated by 5-10 dB compared with normal controls. When the rotation angle was assumed to be 45 degrees, the BM displacement decreased only 1.8 dB. On the other hand, when the outermost row (i.e., close to the cochlear wall) of OHCs was subjected to the abnormality, it decreased by 12.7 dB and 5.2 dB at rotation angles of 90 and 45 degrees, respectively These results suggest that OHCs located at the outer row are likely to have a larger effect on cochlear amplification than those located at the inner row. Even if the stereociliary bundles of two rows of OHCs were assumed to be rotated, the tendency was similar to that described above.

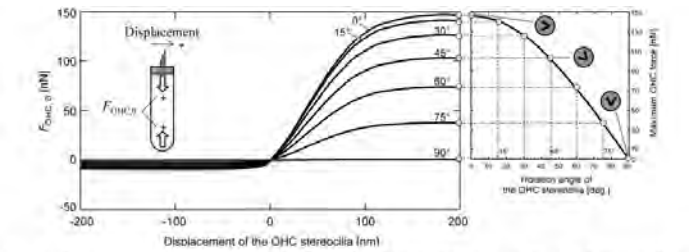

Fig. 1. The maximum force generated by the outer hair cells (OHCs). The relationship between OHC force and displacement of the stereocilia (left). The relationship between OHC maximum force and rotation angle of the stereocilia (right).

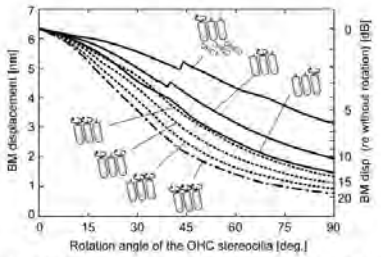

Fig. 2. Basilar membrane (BM) displacement against the rotation angle of the stereocilia. One row (solid line), two rows (dotted line) and three rows (dashed-dotted line) of OHCs were assumed to be rotated.

PS 599

Resonance in Outer Hair Cells is Essential for Human Auditory System

Yasushi Horii[1]; Wenjia Hong[1]; Airi Tamaki[1]; Toshiaki Kitamura[1]; Koichiro Wasano[2]
[1]Kansai University; [2]National Institute of Sensory Organs, National Hospital Organization Tokyo Medical Center

According to Bekesy's traveling wave theory, basilar membrane (BM) plays an important role to analyze sound spectrum by using dispersive BM characteristics. However, some facts deny his theory. (1) In TE-OAE, two kinds of waves are observed; one is the wave which simply returns quickly, and the other is the continuous wave lasting for a few 10ms. The second one implies that acoustic resonance exists somewhere in cochlea. (2) Large sound is exposed to healthy ears of test animals to make their outer hair cells (OHC) damaged. This preparation process suggests that the OHC, not the BM, has an energy storable mechanism based on resonance. (3) The CF/FM bats have the similar auditory system to human's. The difference is that the bats' OHCs and BM changes very slightly in the mid-area of cochlea for echo-location. If they used their BM for echo-location, the BM should be extremely dispersive to improve frequency resolution. (4) If the small BM displacement caused by sound stimuli was amplified by Prestin, the output would affect the BM again. Resultantly, positive feedback circuit would be formed and catastrophic oscillation would be occurred. Because of these facts, we believe that the BM does not have any function to analyze sound spectrum. Rather, we should focus on resonance in OHCs. Looking at the OHC structure, we notice that the OHC has rootlets penetrating cuticle layer, whose tube-like architecture makes sound-phase delayed by 90 degrees, while, the cell membrane advances the sound-phase by 90 degrees. These responses are quite similar to those of inductors and capacitors in electric circuit. This fact indicates that the OHC works as a series LC resonant circuit against sound waves.

To demonstrate the hypothesis, a micron-sized OHC model is designed by using a FEM-based commercial software COMSOL Multiphysics. Transmission properties are evaluated when the OHC is placed in an acoustic tube and one end of the tube is excited by plane wave. The results indicate that resonance is clearly observed at audible frequency and it is tunable in a wide frequency range by changing the OHC structural parameters slightly. The LC resonance in OHC is quite important to explain (a) how we detect sounds in cochlea and (b) why we hear sounds outside the body, but cannot hear sounds inside the body.

Funding
Kansai University Outlay Support for Establishing Research Centers 2018.

PS 600

Output Evaluation of a Transcutaneous and a Percutaneaous Bone Conduction Device using LDV and Intracochlear Pressure measurements

Mohammad Ghoncheh[1]; Stefan Stenfelt[2]; Patrick Maas[3]; Hannes Maier[4]
[1]Medical University Hannover, Department of Otorhinolaryngology, Hannover, Germany; [2]Department of Clinical and Experimental Medicine, Linköping University, Linköping, Sweden; [3]Oticon Medical AB; [4]Medical University Hannover, Department of Otorhinolaryngology, Hannover, Germany and Cluster of excellence Hearing4all

Bone conduction hearing devices are used to treat patients with conductive or combined hearing loss. The vibration measurements using single axis laser Doppler vibrometry (LDV) on the promontory can be used to characterize the performance of bone conduction devices only on one direction. The purpose of this study was to compare the output performance of a new transcutaneous bone conduction implant (Sentio, Oticon Medical, Askim, Sweden) with an established percutaneous bone conduction device (Ponto 3, Oticon Medical, Askim, Sweden) using LDV measurements. In addition, we investigated the feasibility of intracochlear pressure measurement as a method to predict the performance of a bone conduction device.

The percutaneous Ponto and transcutaneous Sentio were implanted at the usual position for percutaneous devices and alternative sites in human cadaveric heads. The promontory vibration was measured using LDV in response to both bone conduction devices and the results were compared. The intracochlear pressure in scala vestibuli (SV) and scala tympani (ST) was also measured in response to the bone conduction stimuli (Ponto) using FISO FOP-M260 pressure sensors. Additionally, SV and ST pressures were measured in response to the acoustic stimuli in the external auditory canal as reference.

The vibration amplitude of the cochlear promontory showed the output performance of the new transcutaneous bone conduction implant system (Sentio) in comparison to the established percutaneous device at the same position. The results showed lower velocity levels of the active transcutaneous device when compared to the percutaneous device in its common retro-auricular position. However, comparison of output levels for different stimulation sites showed an increase for positions closer to the ear canal. This indicates a beneficial effect of transcutaneous devices where the actuator can be placed closer to the ear canal separately from the outer component with the processor and the microphone. It was also feasible to measure intracochlear pressures in response to the acoustic and bone conduction stimuli.

Our preliminary results indicate that the vibration response of the new bone conduction implant Sentio is lower than the percutaneous Ponto 3. However, more flexible placement of the active bone vibrator can be used to compensate for the reduced output at least partially.

PS 601

Influence on Intracochlear Sound Pressure Variations due to Round Window Reinforcement: A Human Temporal Bone Sstudy

Nuwan Liyanage[1]; Julian Grosse[2]; Lukas Prochazka[3]; Adrian Dalbert[4]; Michail Chatzimichalis[5]; Christof Röösli[4]; Tobias Kleinjung[2]; Alexander Huber[6]; Flurin Pfiffner[2]
[1]1. University of Zürich, Zürich, Switzerland. 2. Department of Otorhinolaryngology, Head and Neck Surgery, University Hospital Zürich, Zürich, Switzerland.; [2]1.University of Zürich, Zürich, Switzerland. 2.Department of Otorhinolaryngology, Head and Neck Surgery, University Hospital Zürich, Zürich, Switzerland.; [3]2.Department of Otorhinolaryngology, Head and Neck Surgery, University Hospital Zürich, Zürich, Switzerland.; [4]2.Department of Otorhinolaryngology, Head and Neck Surgery, University Hospital Zürich, Zürich, Switzerland.; [5]3.Dorset County Hospital, Dorchester, United Kingdom; [6]Department of Otorhinolaryngology, Head and Neck Surgery, University Hospital Zurich, Zurich, Switzerland; University of Zurich, Zurich, Switzerland

Round window (RW) is a membranous structure, which acts as the pressure-relieving mechanism for the cochlea. Changes in stiffness of the RW are imposed in treatment of Superior Semicircular Canal Dehiscence (SSCD) or cochlear implant surgery through the RW. This study aims to investigate the pressure variations in the cochlea when the RW is reinforced. Twelve cadaveric human temporal bones (HTBs), which extracted within 48 hours of the death of the donor were used in this study. Six out of twelve HTBs were analyzed while others helped to improve the experimental methodology. Primarily the HTBs were tested for a functional middle ear, according to the ASTM standards and for the absence of air bubbles inside the cochlea. A surgeon performed a cochleostomy procedure in each scala at the basal part of the cochlea. Intracochlear sound pressure (ICSP) sensors were inserted through the cochleostomy and tightly sealed with soft tissue after insertion. A stepped-sine stimulus between 80 dB SPL – 120 dB SPL within the frequency spectrum of 200 Hz – 15 kHz was fed through an artificial ear canal to the tympanic membrane. The RW was reinforced with three different clinically used materials; soft tissue, cartilage, and medical-grade silicone. The stiffness between the materials is assumed to be different. Simultaneous ICSP measurements in both scalae were recorded using ICSP sensors before and after the RW was reinforced. Below 1 kHz, an increased intracochlear sound pressure (up to 26 dB / in mean 13 dB) in the Scala Tympani (ST) was measured for the reinforced cases relative to the baseline. The ICSP in Scala Vestibuli (SV) only showed a minor pressure change with reinforcement (below 1 kHz, up to 10 dB/ in mean 4 dB). To summarize, the results indicate that a reinforced RW with an increased stiffness value increases the pressure in ST in the low frequencies, hence affecting the cochlea fluid dynamics. The next steps aim to investigate the effects of RW reinforcement with novel materials that allow controllable stiffness coefficients that can then be incorporated into a lumped element model of the RW.

PS 602

Transport of Prestin-dependent Fructose in the Outer Hair Cell Electromotil Responses

Metin BUDAK[1]; Zuleyha Dilek GULMEZ[2]; **Erdogan BULUT**[3]; Rahul Mittal[4]; Adrien A. Eshraghi[4]
[1]Trakya University; [2]Istanbul-Cerrahpasa University; [3]University of Miami Ear Institute, Department of Otolaryngology; [4]Department of Otolaryngology, University of Miami Miller School of Medicine

Background
Glucose transporter 5 (Glut5) is a fructose transporter in the OHC lateral membrane. A transmembrane motor protein called prestin has been described in the lateral wall of OHCs. Fructose transport hasn't been explained exactly in the OHC lateral membrane. The aim of this study was to investigate the transport of Prestin-dependent fructose with salicylate administration and to determine the epigenetic modifications in the promoter of the Glut5 gene.

Materials and Methods
Twelve guinea pigs (24 ears) underwent electrophysiological evaluation including 1 kHz tympanometry and distortion product otoacoustic emission (DPOAE) test. The animals were randomly divided into three groups. Group 1 (6 ears) received no injection. Groups 2 (6 ears) and 3 (12 ears) were injected with intramuscular saline (%0.9 NaCl) and sodium salicylate (200 mg/kg), respectively twice daily for 2 weeks. DPOAE measurements were performed at baseline; after 1and 2h (acute effect); after 8h and 2 weeks (chronic effect). After electrophysiological measurements, the animals were sacrificed for DNA isolation and it was evaluated potential epigenetic modifications in the promoter of the Glut5 gene by means of methylation-specific polymerase chain reaction (MSP).

Results
According to baseline measurements (Figure 1) there was no difference in terms of chronic effect (Figure 2) while a significant decrease ($p < 0.01$) was found in terms of acute effect (Figure 2) in all frequencies in DPOAE responses in Group 3. DNA methylation increased during the acute phase (Figure 3) of salicylate administration, whereas it returned to initial levels during the chronic phase (Figure 4).

Conclusion
Changes in DPOAE responses and DNA methylation because of salicylate may explain that fructose transport in the outer hair cell lateral membrane is dependent on Prestin

Keywords
Glucose transporter-5; Hair Cells, Auditory, Outer; Distortion Product Otoacoustic Emission; Sodium salicylate; DNA methylation; Prestin

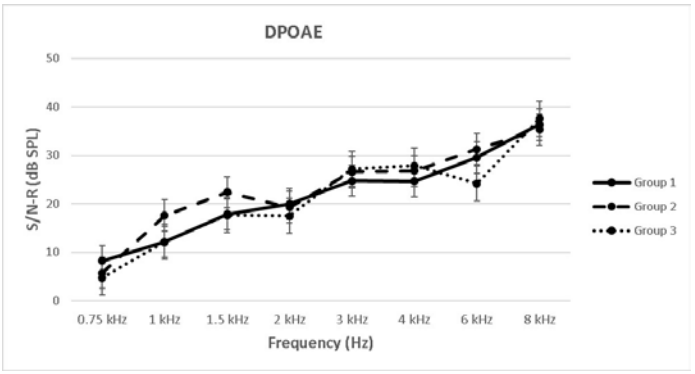

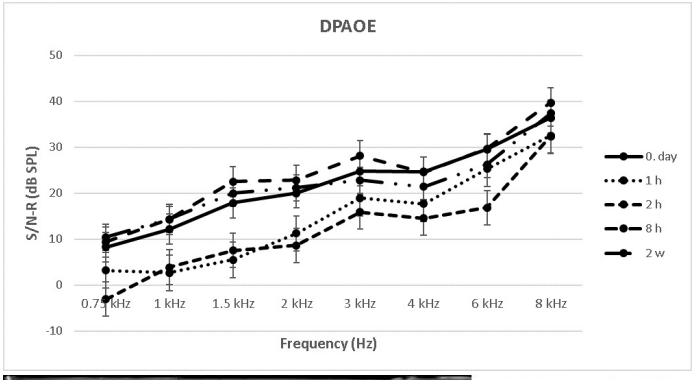

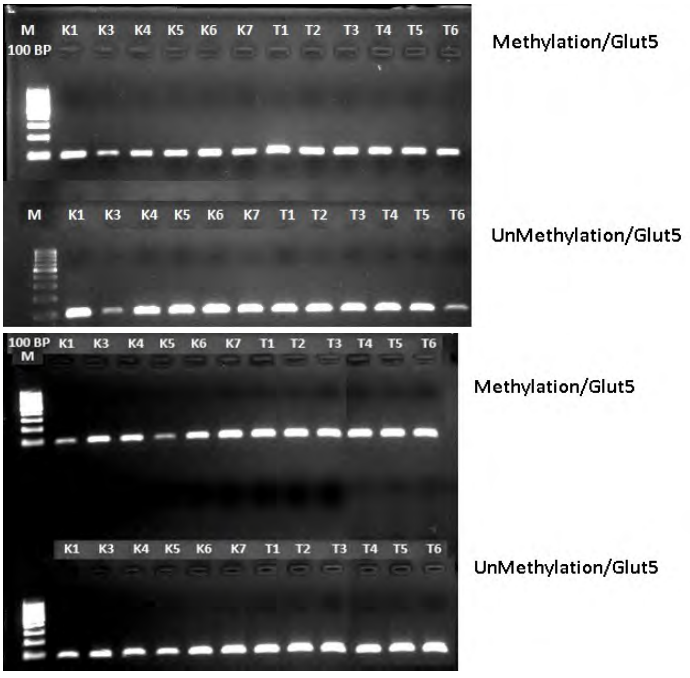

PS 603

Building a Structural Model of the Tip-Link Cadherin-23 Protein

Pedro De-la-Torre[1]; Jasanvir Sandhu[2]; Joseph Sudar[1]; Deepanshu Choudhary[1]; Marissa Boyer[1]; Florencia Velez-Cortes[1]; Jeshua K. Avila[1]; Collin Nisler[1]; Michael Leake[1]; Marcos Sotomayor[1]
[1]The Ohio State University; [2]the ohio state university

Cadherin-23 (CDH23) is a large atypical member of the cadherin superfamily of adhesion proteins involved

in calcium-dependent cell-cell adhesion. In the inner ear, CDH23 forms the upper end of the tip link, a fine protein filament that gates transduction channels to initiate sensory perception. Absence of CDH23 results in deafness and progressive blindness in humans (Usher syndrome), while single missense mutations typically cause deafness, balance disorders, and retinitis pigmentosa in humans and mice. CDH23 has 27 extracellular cadherin (EC) repeats that are similar but not identical in sequence and fold. As part of a systematic effort to understand inner-ear mechanotransduction at the molecular level, we solved high-resolution structures of 18 CDH23 EC repeats showing 13 out of 26 EC linker regions (Jaiganesh et al., Structure 2018). Here we present biochemical experiments that suggest putative parallel dimerization sites along CDH23 and new structures of various CDH23 fragments revealing the location of missense mutations causing inherited deafness. These results provide insights into the structural determinants of tip-link elasticity and into the molecular basis of inherited deafness.

PS 604

LATS1 Deficiency Cause Congenital Hearing Loss Associated with Mouse Cochlea Abnormally

Takanori Nishiyama[1]; Masato Fujioka[2]; Makoto Hosoya[3]; Naoki Oishi[1]; Tatsuhiko Harada[4]; Kaoru Ogawa[2]
[1]Department of Otolaryngology-Head and Neck Surgery, Keio University School of Medicine;
[2]Department of Otolaryngology, Head and Neck Surgery, School of Medicine, Keio University;
[3]Department of Otolaryngology-Head and Neck Surgery, School of Medicine, Keio University;
[4]Department of Otolaryngology, International University of Health and Welfare

Introduction

LATS1 belongs to the family of AGC kinases and participates in Hippo signaling pathway. LATS1 phosphorylates transcriptional coactivators YAP and TAZ and thereby inhibits their activity. YAP and TAZ are critical effectors of the Hippo pathway, which regulates organ size, self-renewal of stem cells, and cell differentiation. Likewise, Cyclin dependent kinases inhibitors (CKIs) are a mediator of the cell cycle. It is also known that some of the CKIs, such as Cip1 and Ink4d, are necessary to maintain the structure of inner ear, and consequently, those deficiency causes hearing loss. Here we investigated the roles of LATS1 in the mouse cochlea. We examined expression pattern of LATS1 and LATS2 in the mouse cochlea, particularly in the organ of Corti. Because we only found LATS1 expression in the organ of Corti, we next investigated Lats1 deficiency mice.

Materials and Methods

Lats1$^{-/-}$mice were derived from embryonic stem cells of the 129/sv strain by replacement of exon 4 of *Lats1* with a neomycin resistant cassette. The mice were backcrossed to C57BL/6 more than seven times. Hearing function was measured by Auditory Brainstem Response (ABR) and Distortion Product Otoacoustic Emission (DPOAE) under general anesthesia with ketamine and xylazine at P28 or later. Superstructure of the organ of Corti was observed using Scanning Electron Microscope (SEM). Newborn to adult mice cochlea were demonstrated by surface preparation for immunostaining with primary antibodies to LATS1, Myosin7a and acetylated tubulin. Nuclei were counterstained with DAPI. F-Actin was stained with Alexa Fluor conjugated phalloidin. *Lats1*$^{-/-}$ mice were compared with those littermates.

Results and Discussion

LATS1 deficiency caused congenital hearing loss with abnormal polarity and stereocilia bundles in both inner and outer hair cells, and also manifested abnormal migration of kinocilium at hair cell development. The result suggests that LATS1 has a role in keeping the appropriate planar cell polarity (PCP) of inner and outer hair cells. In the mouse hair cells, PCP is maintained by essential signal interactions such as Frizzled, Vangl, Celsr, Par3 and Wnts. In the prostate glands, for example, Par3 deficiency disrupts the interaction of Par3/Lats1/LGN and causes abnormal angle of luminal cells, then consequently generates a malignant tumor. In the cochlea, Par3 is known essential for the establishment of PCP. We speculate that LATS1 deficiency may affect Par3 related PCP cascade. For more understanding of LATS1 function, we are currently investigating these signals in the mutants at different embryonic stages.

PS 605

Identification of Hearing-Loss Associated Mutations in MYO6 and In Vitro Functional Analysis

Timothy F. Day; Shin-ichiro Oka; Shin-ichiro Kitajiri; Hideaki Moteki; Shin-ya Nishio; Shin-ichi Usami
Shinshu University School of Medicine

Mutations in the *MYO6* gene cause hereditary hearing loss, but their pathologies have not yet been clearly revealed. *MYO6* encodes myosin VI, a motor protein localized at the base of stereocilia. In this study, we identified novel human mutations and performed functional analysis of these mutations using LLC-PK1-CL4 epithelial cells.

We performed massively parallel DNA sequencing on 8,074 Japanese families and found 27 *MYO6* mutations in 34 families, 23 of which are novel. Most patients showed juvenile onset progressive hearing loss. Of

the 1366 families in this study who had an autosomal dominant mode of inheritance, 2.40% were found to be caused by *MYO6* mutations.

As mutations in *MYO6* are associated with abnormalities of the stereocilia of inner and outer hair cells in the cochlea, we next investigated the functional effects of selected novel mutations by using LLC-PK1-CL4 cells. In LLC-PK1-CL4 cells, when espin-1 (an actin bundler in stereocilia) is transfected, elongated broad microvilli form and may be used as an *in vitro* structure to analyze protein function. Patient-identified mutations were introduced to *MYO6* cDNA by site-directed mutagenesis. Site specific primers with variations were constructed and PCR performed for 9 mutations; c.374C >A, c.604A >G, c.614G >A, c.647A >T, c.1376G >A, c.1455T >A, c.2111G >A, c.2438G >C, and c.3746T >C. PCR products were then re-circularized, amplified, and confirmed for targeted mutations by Sanger sequencing. Wild-type and mutant *MYO6* cDNA were co-transfected with *GFP-espin1* into LLC-PK1-CL4 cells. Immunocytochemistry was performed after visual confirmation of microvilli formation by epifluorescent microscopy. The wild-type myosin VI did not disrupt the elongation of microvilli by espin-1, evidently accumulating at the base of elongated microvilli. However, cells expressing mutant myosin VI exhibited significantly shortened microvilli.

Our data suggest that human *MYO6* mutations are more common than expected, and patients with mutations may have resultant hair cell stereocilia malformations.

PS 606

Generation of Schwann Cells from unaffected and NF2-mutated human iPSCs

Nicholas Gosstola[1]; Zaohua Huang[1]; Eric Nisenbaum[2]; Christine Dinh[2]; Fred Telischi[2]; Derek Dykxhoorn Dykxhoorn[1]; Xue Liu[1]; Cristina Fernandez-Valle[3]
[1]*University of Miami Miller School of Medicine;* [2]*University of Miami;* [3]*University of Central Florida*

Background
Neurofibromatosis type 2 (NF2) is an autosomal dominant disorder that predisposes individuals to develop multiple intracranial and intraspinal tumors, in particular bilateral vestibular schwannomas that can lead to deafness. This syndrome is caused by mutations in the neurofibromin 2 tumor suppressor gene, which codes for merlin protein. Two-hit inactivation of the NF2 gene in Schwann cells of the cochleovestibular nerve can lead to VS formation. By understanding the molecular mechanisms involved with tumorigenesis, tumor growth, and hearing loss in individual NF2 patients, we can identify new and effective therapies for NF2. Here we established an in vitro differentiation model of Schwann cells from human induced pluripotent stem cells (iPSC) that were either wild type or bear mutations in the NF2 gene with the aim of facilitating the study of NF2-related diseases.

Methods
We differentiated Schwann cells from human iPSCs through the stages of neural rosettes, Schwann cell progenitors, and finally Schwann cells. The differentiation was confirmed by RT-PCR and immunocytochemistry. In addition, we are using CRISPR-Cas9 genome editing to introduce the NF2 mutations, c.191T >C or c.1613A >T, into normal human iPSCs and we are cloning each mutation. Schwann cells are derived from these isogenic, mutation bearing and parental control, iPSC lines. Similarly, peripheral blood mononuclear cells (PBMCs) from NF2 patients that have mutations in the NF2 gene were collected, and reprogramming into iPSCs is currently in progress. Pluripotency of these iPSC lines will be confirmed by qRT-PCR and immunocytochemistry for stem cell markers. All of the NF2 mutations will also be confirmed by Sanger sequencing before and after the iPSCs generation.

Results
After completion of a 60-day hiPSC differentiation into Schwann cell, we observed the up regulation of Schwann cell markers S100β and NGFR5 by immunocytochemistry and the loss of the expression of the pluripotency marker Nanog. In addition, we observed expression of the Schwann cell markers MPZ, EGR2, and S100 by RT-PCR. Morphological analyses were consistent with the cells adopting a classic Schwann cell morphology. Furthermore, we are in process to generate human iPSC from patient PBMCs.

Conclusions
We have established a protocol for the differentiation of Schwann cells from normal hiPSCs. We can use this protocol to further understand the mechanisms of NF2 disorders using patient derived iPSCs and CRISPR mutated iPSCs for Schwann cell development. All these human iPSCs provide an excellent platform for further mechanistic studies of NF2-related diseases.

Complex Sounds in Complex Environments

PS 607

Minimal oscillator model of auditory streaming

Andrea Ferrario; James Rankin
University of Exeter

In the auditory streaming paradigm (van Noorden 1975) a repeating sequence of A and B tones leads to the

perception of a single integrated ABAB stream or of two segregated streams A-A and -B-B. Perception depends on tone frequency difference (DF) and presentation rate (PR): low DF values give integration and high DF and PR give segregation. At intermediate DF values both interpretations are possible (bistability). Recent work suggests that auditory-motor neural interactions and learning play a crucial role in auditory perception (Large etal 2015) and show that oscillations in motor cortex synchronize with auditory stimuli in the typical range of PR values without overt movement (Will & Berg 2017).

We propose a minimal model with three differential equations. Two equations describe the oscillatory activity of excitatory and inhibitory populations in motor cortex receiving input from A1. Inputs match neural responses at the A-tone tonotopic location in macaques over a range of DF and PR values (Fishman etal 2004). A third equation describes a Hebbian learning rule (Righetti etal 2006) enabling input frequencies to be learned.

The oscillator's frequency can converge to one of the main input frequency components: PR or PR/2. For PR the oscillator responds to every A and B tone - integration. For PR/2 it responds only to every A tone - segregation. Fig 1A shows the stability regions for these states, qualitatively matching van Noorden's experiments where transitions were initiated for DF slowly increasing or decreasing. Fig 1B shows a simulation where segregation is initially stable and, as DF dynamically decreases, the oscillator's frequency remains at PR/2 before switching to PR, which marks the transition to integration (see Fig 1C for increasing DF). When the input is turned off the learned frequency remains close to PR.

With our model we propose that coordinated auditory-motor neural oscillations and learning may contribute to the emergence of auditory streaming. Unlike previous models, ours (1) considers the role of oscillations, (2) is equipped with a learning rule (adaptable for any PR) and (3) considers the effect of dynamically changing stimuli (as in van Noorden's experiments). Moreover, its simplicity allows for a detailed description of its dynamical states and their stability (Fig 1A). Our model predicts that motocortical oscillations with integrated (PR) or segregated frequencies (PR/2) might continue after the stimulus offset, which would bias the perception of subsequent stimuli.

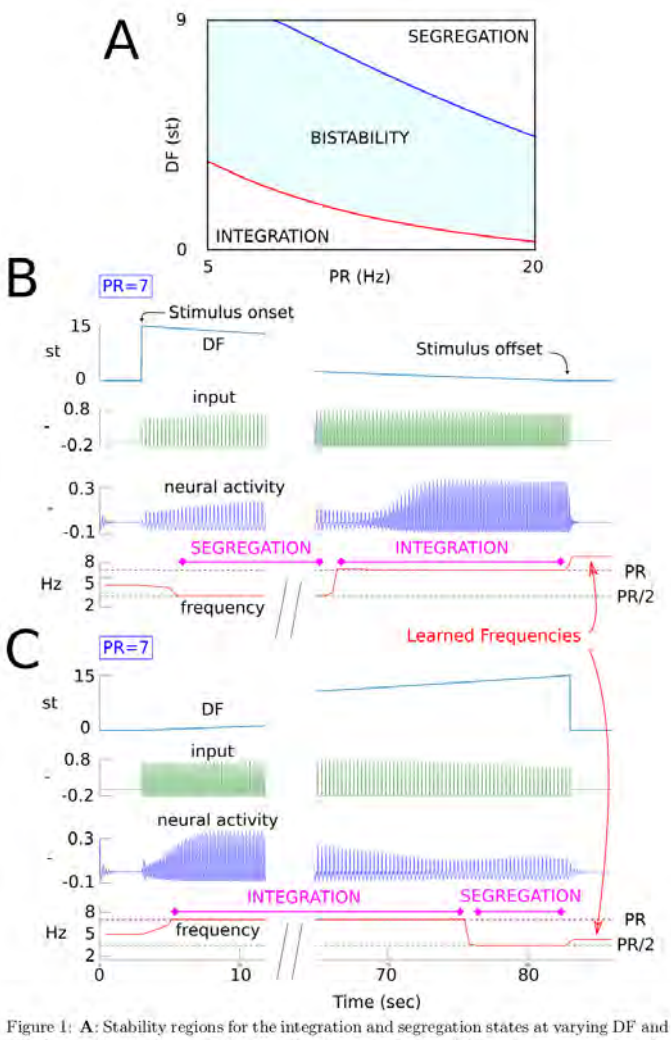

Figure 1: **A**: Stability regions for the integration and segregation states at varying DF and PR that qualitatively match the van Noorden organisation (although we may expect the integration-bistability boundary to be more horizontal). **B–C**. Model simulations showing the dynamic transition between segregation and integration states at fixed PR=7Hz. From top to bottom each panel shows the DF modulation (1st row), the A1 stimulus (2nd row), the activity of the motor cortex excitatory population (3rd row) and the computed oscillator frequency (4th row). Panel B shows the transition from segregation to integration, while panel C shows the transition from integration to segregation. In each case the initial frequency is at 5 Hz and the integration (PR) or segregation (PR/2) frequency is learned within a few seconds. As DF is ramped up/down a sudden switch in perception occurs after 65–75 s.

PS 608

Pupil Response to Rapid Predictable Auditory Sequences

Alice E. Milne; Christina Tampakaki; Sijia Zhao; Maria Chait
University College London

The brain is highly sensitive to auditory regularities. We exploit the predictable order of sounds in many scenarios, from parsing complex auditory scenes to the acquisition of language. However, it remains difficult to study incidental auditory sequence learning.

Pupillometry can be used across populations (e.g. infants and adults) and species (e.g. human and non-human primates); therefore, offering a potential technique to

implicitly study sequence processing across different subject groups. However, it remains unclear exactly how sequence processing will be reflected in the pupil response.

Abrupt changes to the sequential structure of auditory sounds elicit a phasic pupil dilation response that is thought to reflect an arousal-based spike in norepinephrine. However, slower changes to pupil dilation (tonic response) are also observed. These tonic changes have been linked to the release of acetylcholine and hypothesized to be associated with learning processes.

Here we assessed whether the predictability of a rapid stream of auditory tone pips modulates pupil diameter. Stimuli were 9-second-long sequences of 50ms tones presented in either a structured or random order. Pupil diameter was tracked while subjects completed an auditory task unrelated to the sequence structure, thus probing implicit auditory sequence learning.

In Experiment 1, 'structured' sequences were created by selecting a number (5, 10 or 15) of random frequencies from a set pool of 20 tones and repeating that order to create a regularly repeating pattern (anew on each trial). Matched 'random' sequences were created by using the same frequencies but in a random order. We found that structured sound sequences consistently resulted in a smaller tonic pupil dilation response than their corresponding random sequences.

In Experiment 2, we used sequences with more variable predictability using probabilistic relationships commonly studied in the field of statistical learning (Saffran et al., 1996, *Science)*. Following exposure to the probabilistic sequences we contrasted sequences containing the previously heard regularities to random sequences generated from the same set of tones. We show that following habituation probabilistic sound sequences also result in smaller tonic pupil dilation response than sequences of the same tones presented in a random order.

Overall, across multiple experiments we demonstrate that predictability of an auditory sequence modulates changes in pupil diameter and thus show the potential of this technique for implicitly studying auditory regularities across cognition. It paves the way for future work to probe the underlying neurochemical drivers and cognitive processes implicated in auditory sequence processing.

PS 609

Segregation from Noise as Outlier Detection

Jarrod M. Hicks[1]; Josh H. McDermott[2]
[1]*Department of Brain & Cognitive Sciences, MIT;*
[2]*Department of Brain and Cognitive Sciences, MIT*

Because sound events often occur amid the clutter of background noise, the auditory system must segregate foreground events from noise in order to make sense of the everyday acoustic environment. We explored whether listeners might identify foreground sound events by estimating distributions over environmental background sounds and registering outliers of these distributions as new events. To test this, we assessed listeners' ability to detect brief (0.5 s) foreground sounds embedded in real-world background noise (3 s excerpts of sound textures). Critically, learning the background distribution in an online manner requires accumulating enough data samples to adequately estimate the distribution parameters. Thus, we predicted that foreground detection performance should increase with exposure to the background and level off once the background has been accurately estimated. Our results support this hypothesis, with foreground detection performance increasing over the first one-second exposure to the background. In addition, the peak foreground detection performance occurred later when background sounds were less homogenous (as measured by variability in their statistics over time), suggesting listeners collect a larger sample when more data is required to accurately estimate parameters of the background. These results are consistent with the idea that listeners estimate the distribution of ongoing background noise and segregate sound events that are outliers from this distribution.

PS 610

Is Auditory Salience Just About the Acoustic Structure of Natural Scenes?

Sandeep Reddy Kothinti; Mounya Elhilali
Johns Hopkins University

Studies of salience have been shedding light on what makes a sound attention-grabbing against other competing sounds. Understanding what influences salience has basic science as well as practical implications as sound technologies are increasingly aiming to deliver a complete experience to a user that takes into account their full acoustic soundscape. Unlike hand-crafted sound tokens, using natural scenes in the study of salience offer the possibility to examine multiple dimensions of sound that shape our perception of its acoustic and semantic salience.

In recent studies, we have shown that salience of certain sound events can be mostly explained by changes in a range of acoustic dimensions such as loudness, pitch, harmonicity, etc., But the extent to which the semantic context affects salience is still unknown. In the current work, we employ psychoacoustic studies on Amazon Mechanical Turks to explore the effect of semantics on salience in a wide variety of natural scenes.

PS 611

Resetting of Auditory and Visual Segregation Occurs Only After Transient Stimuli of the Same Modality

Ambar G. Monjaras[1]; Nathan C. Higgins[2]; Breanne D. Yerkes[1]; David F. Little[3]; Jessica E. Nave-Blodgett[1]; Mounya Elhilali[3]; Joel S. Snyder[4]
[1]University of Nevada Las Vegas; [2]University of Nevada, Las Vegas; [3]Johns Hopkins University; [4]Unversity of Nevada Las Vegas

Sensory systems are often faced with organizing and resolving competing neural representations for external stimuli, with the goal of bringing the most relevant interpretation to the forefront of conscious perception. Bistable stimuli capable of eliciting mutually exclusive percepts without manipulating the physical parameters therefore provide a valuable tool for understanding the neural mechanisms that control conscious perception. Whether there are common processes that control perception independent of sensory modality remains unknown. To test the extent of modality independence in perceptual resetting, two experiments were performed, one using an auditory streaming paradigm and the other using a visual stimulus based on the ambiguous moving plaid paradigm. In the auditory streaming paradigm, repeating triplets of low-high-low pure tones were used to create bistable perception of integrated or segregated sound streams. In the ambiguous moving plaid paradigm, a circular aperture containing gratings angled at 120 degrees were used to elicit perception of integrated or segregated moving patterns. Participants responded continuously via button press to indicate their perception. For each experiment, transient auditory and visual distractor stimuli were presented in separate blocks, such that the distractors did not overlap in frequency or space with the streaming or plaid stimuli, respectively, thus preventing peripheral interference. The auditory distractor was a 500 ms iterated ripple noise (centered at 1, 2, or 3 kHz), and the visual distractor was a 500 ms flash of red, green, or blue on the screen. Participants' button presses were used to quantify switch rate following the onset of a distractor, and distractor modality and initial percept were used as independent variables. When a distractor was presented in the opposite modality as the bistable stimulus (visual distractors during auditory streaming or auditory distractors during visual streaming), the rate of percept switching was not significantly different than when no distractor was presented. Conversely, significant differences in switch rate were observed following within-modality distractors, but only when the pre-distractor percept was segregated. Due to the modality-specificity of the distractor-induced resetting, the results suggest that conscious perception is at least partially controlled by modality-specific processing. The fact that the distractors did not have peripheral overlap with the bistable stimuli suggests that the resetting is a result of interference at a locus in which stimuli of different frequencies and spatial locations interact with each other.

PS 612

Auditory Sustained Attention Fluctuates Similarly to Visual Sustained Attention

Hiroki Terashima[1]; Ken Kihara[2]; Jun I. Kawahara[3]; Hirohito M. Kondo[4]
[1]NTT Communication Science Laboratories; [2]National Institute of Advanced Industrial Science and Technology; [3]Hokkaido University; [4]Chukyo University

In our daily activities, we often need to maintain our attention but it can spontaneously fluctuate and sometimes be lost in spite of our efforts to maintain it. Attentional fluctuations have been studied by using continuous performance tasks (CPTs) in auditory and visual modalities. However, it is still unclear how the mechanisms of attentional fluctuations overlap between auditory and visual modalities, mainly due to the effect of sudden stimulus onsets in CPTs. There is also a lack of a method for analysis of fluctuation dynamics as CPTs typically use only temporally-averaged statistics to characterize sustained attention.

To reduce the onset effect and compare dynamics in both modalities, we developed a new gradual-onset CPT (gradCPT) in the auditory domain. Combining this with a gradCPT in the visual domain (Esterman et al., 2013), we investigated the dynamic fluctuations of auditory and visual attention and evaluated their relationships to personality traits. In our auditory gradCPT, participants were presented with a stream of excerpts from human narration instead of natural images without sudden onsets. We evaluated the fluctuation of sustained attention by using the stability of reaction times (RTs) in accordance with the visual gradCPT (Esterman et al., 2013). When RTs are stable, participants are considered to be "concentrating" (or "in the zone"); otherwise, they are "distracted" (or "out of the zone"). To measure the basic personality traits of participants, we used the Big Five Inventory (BFI) obtained by a questionnaire.

Our within-individual comparison revealed that auditory and visual attention are similar in terms of performance and dynamic properties. The false alarm rates were significantly correlated between the auditory and visual gradCPTs. A Fourier analysis revealed that the fluctuation frequencies were also significantly correlated. The time scales of the fluctuation in both modalities were in a similar range, despite different stimulus onset asynchronies. Personality traits did not affect behavioural performance regardless of sensory modalities.

The results suggest that fluctuations of auditory and visual sustained attention are underpinned by common principles and open a way to study modality-specific and -unspecific properties of sustained attention.

PS 613

Loudness Discomfort Level as a Test for Hyperacusis: Test – Retest Reliability and its Clinical Value

Jaclyn Vidal; Jung Mee Park; Jae Sang Han; Hamzah Alshaikh; Shi Nae Park
Department of Otolaryngology-HNS, Seoul St. Mary's Hospital, College of Medicine, The Catholic University of Korea

Background
To investigate the test-retest reliability of loudness discomfort levels (LDLs) and to evaluate its clinical value as a test method for hyperacusis.

Methods
For the test-retest reliability of LDLs (study 1), a total of 68 patients who had tinnitus with or without hyperacusis were enrolled and subgrouped into 3 groups; patients with tinnitus (group 1), patients with tinnitus and hearing loss (group 2), and patients with hyperacusis (group 3). Their LDLs measured with pure tone and white band noise were compared with normal controls to suggest the cut-off point for hyperacusis. Inter-hour and inter-day test-retest reliability using different stimuli were also investigated. For study 2, the clinical value of the LDLs using pure tone stimuli were analyzed by comparing the changes before and after sound generator use in 42 patients with hyperacusis.

Results
For study 1, group 3 patients showed significantly lower LDLs compared to the other groups. High test-retest reliability of LDL tests has also been demonstrated, regardless of the type of stimulus used for the test. The cut-off values for screening the patients with hyperacusis were 90 dBHL for the pure tone stimuli and 62dBHL for white band noise stimuli. For study 2, significantly increased LDLs correlated with improved hyperacusis symptoms were observed after sound generator use, indicating that LDLs may be a valuable test to screen and reflect the condition of hyperacusis during the course of therapy.

Conclusion
Measurement of LDLs seems to be clinically valuable for screening hyperacusis as well as reflecting the changes in hyperacusis, considering its high test-retest reliability and correlation with subjective symptoms.

PS 614

Modulation Transfer Functions Measured with Broad- and Narrow-band Noise Carriers in a Deep Neural Network Trained for Natural Sound Recognition

Takuya Koumura; Hiroki Terashima; Shigeto Furukawa
NTT Communication Science Laboratories

Auditory processing of amplitude modulation (AM) is often characterized by a modulation transfer function (MTF). In psychophysical studies, an MTF is usually defined as the dependence of AM detection threshold on the AM rate. Generally, the form of an MTF depends on the type of carrier. An MTF with a broadband noise carrier takes the form of a low-pass filter in the domain of AM rate, for example, whereas an MTF with a narrow band noise carrier is like a high-pass filter. Earlier studies have attempted with some success to account for the psychophysical MTF characteristics by constructing a sophisticated functional model that involves peripheral processes and hypothetical modulation processing mechanisms, such as a modulation filter bank.

This study took a different approach to understand the underlying mechanisms of the human MTF. We previously demonstrated that AM tuning in a cascade of layers in a deep neural network (DNN) trained for natural sound recognition exhibits similar characteristics to that in the cascade of brain regions in the auditory system. Regarding the DNN as a computational model of auditory processing, this study explored whether psychophysical MTFs could be accounted for by the activities in the model units. It is important to note that no prior hypothesis on AM processing was assumed to form the properties of the model. AM detection performance by a layer in the DNN was calculated by dβ on the basis of the representations of modulated and unmodulated noises projected onto one-dimensional space with maximum AM detectability. The AM detection threshold was defined as the minimum AM depth that yielded a certain value of dβ.

We calculated MTFs with several types of noise carriers and found human-like characteristics in some of the lower and middle layers of the trained DNN. Generally, the dβ was larger for deeper AM and in the higher layers. With broadband noise carriers, low-pass-type MTFs were observed in the middle layers, with their forms being similar to those in humans. For noise carriers with a 3-Hz bandwidth centered at 5 kHz, high-pass-type MTFs were observed in the lower layers, with the threshold sharply increasing from 2 Hz to 8 Hz as in human MTFs. In contrast, with carriers with a 31-Hz bandwidth, no human-like MTFs were observed. We expect that exploring the causes of the similarity and inconsistency between the model and humans will provide useful insights into human AM processing.

PS 615

Comparison of Cartilage-conduction and Conventional Bone-conduction Hearings on Fundamental Perception Characteristics: Temporal and Frequency Resolution

Gaik Sean Yap; Sho Otsuka; Seiji Nakagawa
Chiba University

Usually, sound that we perceive are initially entered in the form of air particle vibrations into our auditory canal, and thus it is often referred as air-conduction. On the other hand, sound transmit using vibrations of bone structures (including skin and muscle tissues) into our ear is called the bone-conduction (BC). Generally, BC is presented by attaching a sound transducer to the mastoid process of the skull, and it is said to be transmitting using 4 components: (1) the osseotympanic component, which involves sound radiated into the auditory canal; (2) the inertial osteogenic component, which is based on the relative motion between middle ear ossicles and temporal bone; (3) the compressed osteogenic component, which results from compression and expansion of cochlear shell; and lastly (4) the air-conducted component. BC has been applied to devices such as headphones and hearing aids, but problems such as the cause of pain and discomfort and the difficulty of securing the transducer in place have hindered its widespread application. Therefore, as a solution, “cartilage-conduction” (CC) has been proposed and applied to devices such as hearing aids and smartphones. Unlike BC, CC uses ear cartilage tissues as the main transmission medium by bringing a transducer into contact with the cartilage region of outer ear and transmits using components (1) ~ (4) of different quantity due to its placement method. Despite of its practical use, CC has limited number of studies and the effect from nonlinearity of cartilage tissues is unclear. In this study, the perceptual characteristics of CC hearing were evaluated using hearing threshold, temporal resolution and frequency resolution, and compared with conventional BC hearings. Three experimental sessions were conducted: 3 forced-alternative-choice of 2 down-1 up method in estimating hearing thresholds, Temporal Modulation Transfer Function tracing for temporal resolution and Frequency Difference Limens test for frequency resolution characteristic; with all sessions conducted in two conditions: (a) BC – transducer attached to mastoid process, (b) CC – similar transducer attached to ear pinna. As result, CC showed lower hearing thresholds but poorer temporal and frequential sensitivity compared to BC. Because ear pinna is much lighter than the skull, CC is assumed to require much lower energy than BC in transmitting vibrations, however, at the same presentation energy level, BC appeared to have better resolution than CC and these findings may have reflected certain deterioration of sound components travel through the ear cartilage tissues in CC.

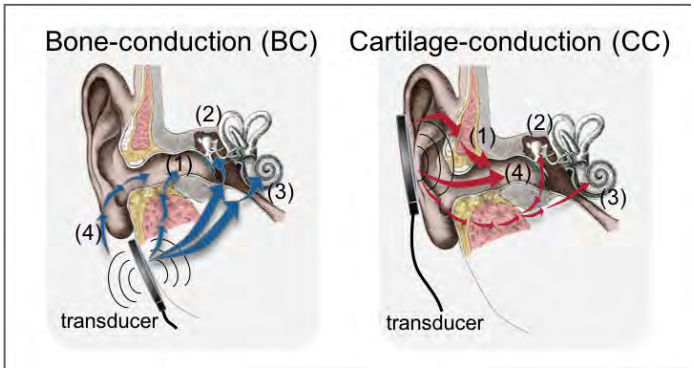

PS 616

Effect of the vibrator placement on perception and propagation of bone-conducted sound during earplugging

Taishi Shinobu[1]; Sho Otsuka[2]; Seiji Nakagawa[2]
[1]Student; [2]Chiba University

Workers sometimes need to wear earplugs under strong noises. However, earplugs usually inhibit speech communication and listening environment sounds. Meanwhile, bone-conducted sound can be heard easily even during earplugging. Therefore, developments of noise-robust communication-aids using bone-conduction are anticipated.

In typical bone-conduction, vibrators are pressed onto the mastoid process using steel-headbands, however, it often brings pain and beauty problems. Further, the vibrator is easily moves from the optimal location. These problems can be solved by building the vibrators into working-headgears such as helmets.

Bone-conducted sound can be heard even from the scalp locations, like the vertex, frontal or occipital regions. Some studies have been conducted on

hearing threshold of bone-conducted sound presented to the scalp, however, none of them focused on sound propagation in the head and its relations to perception. In this study, both perception and propagation of bone-conducted sounds from various placements on the head during earplugging were investigated.

First, hearing thresholds were measured in 7 normal-hearing subjects by a 3AFC procedure. The bone-conduction vibrator (RadioEar, B71) was placed on 5 locations (ipsilateral mastoid and condyle, Fpz, Cz, and Oz; the latter three were decided by the international 10-20 system in EEG) and tone-busts (300-ms duration) were presented in 7 frequencies (125 , 250, 500 , 1000, 2000, 4000, and 8000 Hz). An Generally, the scalp location showed higher threshold in lower-frequency (125-500 Hz) than the mastoid and condyle.

Second, ear-canal sound pressure (ECSP) and vibration of the head are measured simultaneously in 6 normal-hearing subjects. ECSP were recorded by a probe microphone fixed in the left ear-canal, and the head vibration were measured by a accelerations sensor at the same frequencies as the threshold measurement. ECSP is measured for 7 stimulus locations (left/right mastoid and condyle, Fpz, Cz, and Oz) and the head vibration is measured for the same except the right mastoid. No significant differences were observed among the stimulus location except the left mastoid/condyle, despite the scalp locations have longer distance from the right ear canal/mastoid than other locations.

These results indicated that (1) bone-conducted sounds can be clearly perceived even from the scalp locations (the vertex, frontal and occipital regions), whereas the hearing thresholds in the scalp location increased for the lower-frequencies, and (2) ECSP and the head vibration for the scalp location did not show significant decreases despite of their distance from the ear.

PS 617

The Discussion on The Influence of Different Materials of Earplugs in Bone Conduction Measurements.

Xiuyuan Qin; Sho Otsuka; Seiji Nakagawa
Chiba University

In experiments of bone conduction (BC), the results are easily affected by an air-conducted sound radiated from a BC transducer. For preventing from the influence of air conduction (AC), one of the methods is to wear earplugs during the experiments, but simultaneously the earplugs will cause the occlusion effect. Nowadays, earplugs made by polyurethane (PU) foam are used in most BC measurements, and they usually have enough capability of insulating AC sound. On the other hand, earplugs made by silicone are increasingly used in people's daily life because of its waterproof ability and the deformable shape to fit any size of ears. Since they can cover the ear canal thoroughly, they are expected to have a good performance on noise insulation. Nevertheless, the influence of different types of earplugs in BC measurements has not been discussed enough.

In this study, ear-canal sound pressures (ECSPs) were measured by using PU foam earplugs (Silencia Regular from Silencia Company) and silicone earplugs (Insta-putty from Insta-Mold Products Inc.). By comparing the results of Silencia and Insta-Putty, the influence of materials of earplugs used in BC measurements were discussed.

Six subjects with normal hearing ability participated in the measurements. The ECSPs were measured by a probe microphone (ER-7C, Etymotic). Three conditions were set to be measured, an open-canal condition, an occluded-canal condition with Silencia, and an occluded-canal condition with Insta-Putty. Each subject was equipped with a headband for fixing the bone-conducted vibrator Radioear B71 on the mastoid and the static force was controlled to about 2.5 N. ECSPs to six tone bursts from 0.25 kHz to 8 kHz were measured at each frequency.

The results show higher ECSPs were obtained when Insta-putty was used, and the differences between the two types of earplugs are larger at low frequency than they are at high frequency. The sound radiated into the ear canal is blocked by the earplug and reflected to the tympanic membrane, making an increase of sound level, which is called occlusion effect. The PU foam may absorb the signal in the ear canal to some extent, but the silicone earplug has less ability of absorption, causing more obvious occlusion effect.

In conclusion, higher ECSPs were obtained with Insta-Putty in BC measurements, showing the possibility of better BC hearing perception, but it will also cause serious occlusion effect which may affect the further discussion of BC transmission.

PS 618

Sound Descriptions of Musicianship: Relationships between Pitch Discrimination, Audiometric Measures of Hearing Sensitivity and Musical Skill.

Justin Cha; Kevin Ng; Devin Inabinet; Jan de la Cruz; Patricia Tan; Gabriella Musacchia
University of the Pacific

Pitch perception is related to sound periodicity and provides important information for musical and vocal communication. Our previous data show that musicians have better diotic and dichotic frequency discrimination limen (DLF) thresholds compared to non-musicians, and that DLF is related to musical ability and self-evaluation of musical competence. These data not only suggest that musical training impacts peripheral and central mechanisms of sound perception, but also that discrimination thresholds can be related to both objective and subjective measures of musical competence. This gives rise to the notion that that musicianship impacts perception in three realms: sound discrimination, musical skill and self-evaluation of musical competence. However, it is unclear whether the positive impact of musical training on sound perception is restricted to pitch discrimination thresholds, or if it extends to more basic audiometric measures such as absolute threshold of pure tones. The current study aims to answer this question by examining putative relationships between DLFs, music competency measures and standard audiometric results (e.g. pure-tone thresholds, ultra-high frequency thresholds, QuickSIN scores, DPOAE measurements). Previous data suggest that ultra-high frequency thresholds, QuickSIN scores and musical skill will be interrelated. However, there are conflicting reports regarding the degree to which musicianship impacts certain measures of hearing sensitivity, such as speech-in-noise. Based on these data, our hypothesis is that hearing sensitivity plays a role in pitch perception to a different degree in musicians and non-musicians. The results of study shed light on the relationships between music training, psychoacoustics and audiometric measures of sound and inform the defining characteristics of musicianship.

PS 619

Musician Advantage for F0 Coding

Kelly Whiteford[1]; Angela Sim[1]; Kara Stevens[1]; Andrew J. Oxenham[2]
[1]University of Minnesota; [2]Department of Psychology, Center for Applied and Translational Sensory Sciences, UMNTC

It is well established that musicians have enhanced pitch perception relative to naïve non-musicians, but the mechanisms underlying this benefit remain unclear. One possibility is that enhanced pitch perception in musicians is a result of better fidelity in the temporal coding of periodicity at early stages of the auditory system. Another possibility is that the musician advantage is unrelated to temporal coding but reflects enhanced F0 processing at more central stages of the auditory system. To test this hypothesis, frequency and F0 coding were assessed in musicians and non-musicians for stimuli with F0s within (< 5 kHz) and outside (> 8 kHz) the range of musical pitch using methods that either required participants to label the frequency contour ("Which sequence was rising?") or detect a pitch change in a tone sequence ("Which sequence was changing?"). The limits of frequency coding were assessed for low (280 Hz) and high-frequency (12600 Hz) pure-tones in quiet and for low (F0=280 Hz) and high F0 (F0=1400 Hz) complex tones embedded in broadband threshold equalizing noise. Only harmonics 6-9 of the complex tones were present, so that both F0 conditions contained resolved harmonics, but the high-F0 condition contained spectral content well outside the range of musical pitch. In addition, frequency modulation detection was assessed for a low-frequency carrier (f_c = 280 Hz) at slow (f_m = 2 Hz) and fast (f_m = 20 Hz) modulation rates, and amplitude modulation detection was measured at the same carrier and rates as a control. Preliminary results show the musician advantage extends across tasks, but the magnitude of this benefit is greatest for F0s within the range of musical pitch and for tasks that rely on labeling frequency contours. These early results suggest that the pitch advantage in musicians is present even when temporal cues are unavailable. [Supported by NIH grant R01 DC005216.]

PS 620

Exploring the Relationship between Statistical Surprisal and Music Engagement

Sandeep Reddy Kothinti[1]; Benjamin Skerritt-Davis[1]; Aditya G. Nair[2]; Alain de Cheveigné[3]; Mounya Elhilali[1]
[1]Johns Hopkins University; [2]University of Washington; [3]CNRS / ENS / Université Paris Descartes / University College London

Music is often described as a series of moments of tension and release, where music builds powerful expectations over time that create tension when they are violated and release when they are met. This makes music a useful stimulus for studying predictive processing in the human brain. Previous work has explored how the statistical properties of music relate to behavioral and physiological responses from listeners, especially with regards to deviance responses to local violations of musical expectations. However, the relationship between broader statistical properties of musical pieces and listener experience is less well-studied. In this work we explore the relationship between surprising moments and listener engagement. In particular, we ask the question: Do more surprising musical pieces lead to more engagement? Our approach utilizes the D-REX model for statistical predictive coding to modify existing musical pieces to increase their unpredictable moments. We investigate the feasibility of synthesizing maximally surprising melodies and the effect of these manipulations on the listener's experience.

PS 621

Harmonicity Aids Detection of Sounds in Noise

Malinda McPherson[1]; River Grace[2]; Josh H. McDermott[2]
[1]Speech and Hearing Bioscience and Technology Program, Harvard University; [2]Department of Brain and Cognitive Sciences, MIT

Hearing in noise is a core problem in audition, and a challenge for hearing impaired listeners, yet the underlying mechanisms are poorly understood. We explored whether harmonic frequency relations, one of the primary cues used to segregate concurrent sound sources, also aids hearing in noise. We measured detection thresholds for harmonic and inharmonic tones in noise. Harmonic tones were consistently easier to detect than otherwise identical inharmonic signals. Harmonicity also improved pitch discrimination in noise. However, even though musicians outperformed non-musicians at segregating tones from other tones via harmonicity, they did not show a larger harmonic advantage for detecting tones in noise. These results suggest that harmonicity is critical for detecting and discriminating signals in noise, regardless of musical training, demonstrating its relevance to auditory scene analysis.

PS 622

Effects of Modified Auditory Feedback Simulating Age-Related Hearing Loss on Piano Performances

Minoru Tsuzaki[1]; Noriko Maegawa[2]; Chie Ohsawa[3]; Hideki Banno[4]; Toshio Irino[5]
[1]Kyoto City University of Arts; [2]JATO Co. Ltd.; [3]Mukogawa Womens' University; [4]Meijo University; [5]Faculty of Systems Engineering, Wakayama University

The dependence on auditory feedbacks would be significant when one plays a musical instrument to achieve fine performances. One of the aging effects on hearing is a reduction of the cochlear amplification by the outer hair cells. This deterioration makes the response of our auditory system more linear, leading to raised absolute thresholds and reduced dynamic ranges. The characteristics of this deterioration are complicated, and some changes in hearing are tended to be ignored as far as people can hear the target sounds. The purpose of this study was to investigate any effect of modified auditory feedbacks simulating age-related hearing loss on piano performances. We implemented a real-time signal processing which could apply two types of frequency equalization to mimic the responses of the average 60-years-old's audiogram. One type could apply a dynamic, non-linear equalization which counteracted the non-linear amplification by the healthy cochlear. The other type was a simple linear equalization to trace the frequency-dependent elevations of the threshold. In addition, a control condition was prepared by bypassing the signal processing. Twenty undergraduate/graduate students of the piano course at Japanese conservatory level institutes participated in the experiment. They were required to play a MIDI piano with auditory feedbacks via headphones which were subject to the two types of hearing loss simulations. In addition to the hearing loss factor, two levels of the amplification were tested. Recorded data was: (a) the unprocessed line output of the MIDI piano (P); (b) the MIDI velocity data (V). The temporal correspondence of each note between each of the experimental conditions and its reference was specified and the level differences were calculated for each of the recorded data, P and V, respectively, which provided ΔP and ΔV. The results of two way ANOVAs with the hearing loss type and the amplification level as the factors showed significant differences by the amplification factor for both ΔP and ΔV. On the other hand, the type of the hearing loss was not significant as a main factor. For ΔP, however, a significant interaction between the two main factors was observed. The sound outcomes of the participants' performance tended to be stronger for the non-linear equalization compared to the linear equalization under the low amplification condition, but that they were almost comparable between the two hearing loss types under the high amplification. Further analyses on the dynamic characteristics taking the note context into account will be executed.

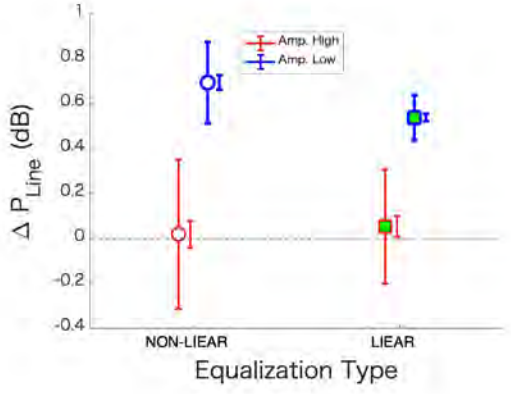

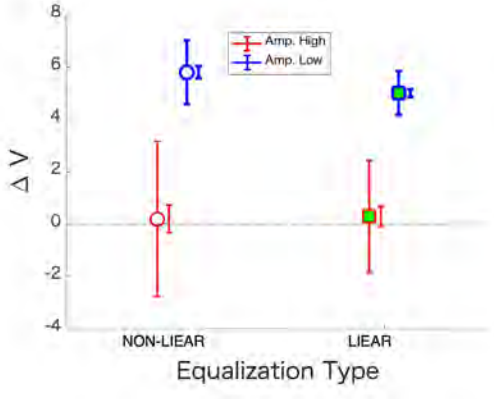

PS 623

Simultaneous Measures of Auditory Brainstem Frequency Following Response, Pupillary Response, and Microsaccade during Auditory Selective Attention Task

Shimpei Yamagishi; Shigeto Furukawa
NTT Communication Science Laboratories

The effect of auditory selective attention on subcortical activity remains controversial (Varghese et al., 2015; Riecke et al., 2018). A possible cause of this controversy is the significant variation of the internal state over time within or across a large number of recording blocks required to compute the average subcortical event-related potentials. The instantaneous and spontaneous change in attentional states can be obscured to observe the effect of attentional conditions.

Eye-metrical measurements can be candidate markers for monitoring time-varying attentional states. The pupil size and microsaccades (involuntary tiny saccades) have been reported to reflect arousal level during a cognitive task (Gilzenrat et al., 2010) and covert spatial attention (Engbert and Kliegl, 2003; Rolfs et al., 2005), respectively, not only in visual but also in auditory tasks.

In this study, we simultaneously measured auditory brainstem frequency following response (FFR), pupil size, and microsaccades during a dichotic oddball detection task. Nineteen human listeners participated in experiments in which a sound sequence (standard and oddball) was presented as stimuli under five conditions that differed in terms of the ear of stimulus presentation and task: (1) presented to the left ear only and the listener was instructed to respond to oddballs; (2) same as (1) but presented to right ear only; (3) presented to both ears, instructed to respond to left-ear oddballs: (4) same as (3) but instructed to respond to right-ear oddballs; and (5) same as (3) but no response is required (i.e., passive listening). The sound sequence for the dichotic task consisted of 500 repetitions of sounds. Out of the 500 sounds, 96% were standard sounds (harmonic complex tones with 315-Hz F0 for the left ear and 395-Hz F0 for the right ear), and 4% were oddball sounds (white noise). The oddball sounds were divided and presented equally to each ear. Except for condition (5), each participant was asked to respond by pressing a button as soon as possible when an oddball was detected.

We found no correspondence between spatial attention and spectral amplitude (associated with the ear of presentation) of FFR averaged within each condition. However, there were indications that the instantaneous FFR amplitude correlated with the direction of co-occurring microsaccades and pupil size at the corresponding time interval. These results indicate a possibility that auditory sub-cortical activities vary with the instantaneous fluctuation of attentional states (i.e., the direction of spatial attention or drowsiness/arousal level), which may not be captured by a whole trial average.

PS 624

Sensitivity of Eye-Metrical Responses to Sound Salience: Contributions of Detectability, Signal-to-Noise Ratio, and Spectral Consistency of Acoustic Context

Yung-Hao Yang; Hsin-I Liao; Shigeto Furukawa
NTT Communication Science Laboratories

Previous studies have shown that salient sound evokes stronger microsaccade inhibition (Rolfs, Kliegl, & Engbert, 2008) and larger pupillary dilation response (PDR) (Wang, Boehnke, Itti, & Munoz, 2014). The loudness of the sound is a potentially major factor that influences eye-metrical responses (Liao, Kidani, Yoneya, Kashino, & Furukawa, 2016). However, it is unclear whether the high detectability and/or signal-to-noise ratio (SNR) contributes to the salient sound that evokes these eye responses. We addressed this issue by adopting an experimental paradigm regarding information-masking (Neff & Green, 1987). Participants were requested to detect a 1000-Hz target tone embedded in a masker in a two-interval-forced-choice task, while her/his pupil size and eye movements were continuously monitored. The masker consisted of either 20 frequency components (20CM condition) or 500 frequency components (500CM condition). The frequency components were selected randomly for each trial (consisting of two intervals) from a range of frequencies except for a “protected” band around the signal frequency. Since the frequency components distributed more sparsely in the 20CM condition than in the 500CM condition, trial-by-trial variability of the masker spectrum was greater for the 20CM condition. On the basis of the results of a pilot measurement, three target levels (SNRs) were used, corresponding to roughly 50% (not detectable), 70.7% (barely detectable), and 99.99% (easily detectable) of correct responses for each participant and masker condition. As expected from the masker uncertainty, the adopted SNRs were generally higher in the 20CM condition than in the 500CM condition even though the detectability was comparable. We found stronger microsaccade inhibition for the interval with the masker including the target than with the masker alone when the SNRs were at the easily detectable level, regardless of 20CM or 500CM condition. This implies that microsaccade inhibition reflects the subjective detectability in general. On the other hand, a reliable PDR was found only in the 500CM condition at the easily

detectable level. The absence of PDR for the target in the 20CM condition indicates that a target-related PDR could not be accounted for the target detectability (since the target was equally detectable in the two frequency component conditions with comparable SNRs) or the target SNR (the target SNR was even higher in the 20CM condition) alone. Considering the higher spectral variability across the trials in the 20CM condition, we speculate that the spectral consistency of background acoustic context plays a significant role in determining target-related PDR.

PS 625

Phasic arousal suppresses suboptimal auditory decision biases in mice and humans

Jan Willem de Gee[1]; Konstantinos Tsetsos[2]; David McCormick[3]; Tobias Donner[2]; Matthew J. McGinley[4]
[1]Baylor College of Medicine, Department of Neuroscience; [2]Department of Neurophysiology and Pathophysiology, University Medical Center Hamburg-Eppendorf; [3]Department of Biology, University of Oregon; [4]Department of Neuroscience, Baylor College of Medicine

Decisions under uncertainty entail an accumulation of ambiguous evidence supporting different choice alternatives. The brain's arousal systems are rapidly recruited during such decisions. But how do the rapid ("phasic") arousal boosts affect decision-making? We here established a principle of the function of phasic arousal in decision-making, which generalizes across species (humans and mice) and bases rates of sound presentation: suppressing maladaptive biases in the accumulation of acoustic evidence leading up to choice.

We exploited that pupil dilation indexes cortical arousal state as well as response of the noradrenergic locus coeruleus in humans, monkeys and mice. We recorded the pupil diameter of 20 humans and 5 mice during a difficult auditory go/no-go detection task. Humans responded with a button press, mice by licking for sugar water reward. In addition, fifteen human subjects performed a forced-choice decision task based on identical stimuli under systematic manipulations of target probabilities, 54 human subjects performed a memory-based decision task, and 37 human subjects performed a basic laboratory task model of value-based stock market decisions.

In mice and humans, task-evoked pupil responses occurred early during decision formation, even on trials without any motor response, and predicted a suppression of a suboptimal conservative choice bias. Drift diffusion modeling revealed that the bias reduction was due to a selective interaction with the evidence accumulation process, rather than a shift in starting point. We showed that, within the same subjects, phasic arousal flexibly reduces both conservative and liberal accumulation biases in a context-dependent manner. Our findings point to a precise role for global arousal state of the brain in auditory decision making in the face of uncertainty.

PS 626

Automated Classification of Acoustic Startle Reflex Measurements in Young CBA/CaJ Mice using Machine Learning

Timothy Fawcett[1]; Chad Cooper[2]; Ryan Longenecker[1]; Joseph P. Walton[3]
[1]Univ South Florida; [2]Univ. South Florida; [3]Department of Communication Sciences & Disorders, University of South Florida, Tampa, FL; Department of Medical Engineering, University of South Florida, Tampa, FL; Global Center for Hearing and Speech Research, University of South Florida, Tampa, FL

Introduction
The acoustic startle response (ASR) is a simple reflex that results in a motoric response after most animals hear a brief loud sound and has been used in many behavioral disciplines for evaluating hearing and hearing disorders, such as tinnitus. Unfortunately, a method of how to record, measure, process, and analyze ASRs has yet to be standardized, which leads to high variability within and between laboratories using this assessment tool. The goal of this study is to develop an automated, supervised machine learning approach to classify and separate ASR waveforms across various stimulus protocols and levels, eliciting ASRs of various magnitudes and shapes.

Method
Young adult (2 – 6 months old) CBA/CaJ mice were individually tested in wire mesh cages resting on a custom-built platform connected to piezoelectric transducers, located inside one of eight identical sound attenuated chambers. Each animal received three testing sessions, every other day, over the course of one week, which included startle input-output using noise bursts (startle I/O) and tonal pre-pulses (TPP). A total of 9,624 ASR measurements and manually classified as startle (5,486) or non-startle (4,138) by two experienced scientists. Each ASR waveform was centered and scaled with many waveform based features were extracted including features from power spectral density estimates (PSD) and continuous wavelet transforms (CWT) of the normalized waveforms. The features were then partitioned into two sets (training and test/validation) in which repeated k-fold cross validation was also employed.

Machine learning methods from different families of algorithms were used to combine startle-related features into robust predictive models to predict whether an ASR waveform is a startle or not a startle. The machine learning algorithms employed include linear classification methods such as logistic regression and linear discriminant analysis (LDA), bagged classification methods such as bagged tree and random forests, boosted classification methods such as extreme gradient boosted and C5.0, and discriminative classification methods such as support vector machines (SVM) using various kernels. In addition to evaluating models using each of these machine learning methods, multiple models were also stacked together into an ensemble method in an effort to produce an extremely robust model.

Results/Conclusions

The mean Receiver Operating Characteristics (ROC) of the machine learning methods investigated were all over 0.95 (as seen in the table below) with Random Forests demonstrating the greatest performance with an ROC of 0.979, area under the ROC (AUC) of 0.978, and a validation accuracy of 0.9266. The linear ensemble model performed similarly to Random Forests with similar ROC and AUC characteristics but with a slightly higher validation accuracy of 0.9301, which is expected given the Random Forests models carries the highest weight in the linear ensemble model. Results of this study indicate that a machine learning algorithm can be adapted to nearly any ASR paradigm to accurately process, sort, and classify startle waveforms.

Work supported by NIH-NIA AG00954.

PS 627

Psychoacoustical assessment of thermal impression of HVAC sounds

Seiji Nakagawa[1]; Takuya Hotehama[2]
[1]Chiba University; [2]National Institute of Advanced Industrial Science and Technology (AIST)

Background

Noise induced by a heating, ventilation and air conditioning (HVAC) system in a vehicle is an important factor that affects the comfort of the interior of a car cabin. Much effort has been devoted to reduce noise levels, however, there is a need for a new sound design that addresses the noise problem from a different point of view. In this study, two subjective assessments were performed focusing on the auditory impression of automotive HVAC noise concerning coolness and warmness.

Test for subjective auditory impression concerning coolness and warmness

First, paired comparison tests were carried out under various conditions of room temperature. Five stimuli were synthesized by stretching the spectral envelopes of recorded automotive HVAC noise to assess the effect of the spectral centroid. Normal-hearing subjects were asked to rate the auditory impression of the stimuli for each pair on a seven-point scale according to how much the latter is warmer (for the winter tests) or cooler (for the summer tests) than the former. Results show that the spectral centroid significantly affects the auditory impression concerning coolness and warmness; a higher spectral centroid induces a cooler auditory impression regardless of the room temperature (Fig. 1).

Test for sensation of coolness and warmness

Second, effects of HVAC noises on the subjects' sensation of coolness and warmness were evaluated by using a method of continuous judgment by category. Room temperature were controlled to increase/decrease linearly, and HVAC noise, having warm/cool auditory impressions, were presented alternately. Subjects were requested to evaluate their thermal sensation, satisfaction level for air-conditioning and, comfort level every 30 seconds. Results showed that transition of sensation of coolness/warmness can be affected by HVAC noises with warm/cool impressions, especially just after switch of these sounds. The maximum thermal effect of these HVAC noises was 0.42°C (Fig. 2).

Conclusions

The results obtained indicated that the auditory impressions of HVAC noises can be controlled by changing the spectrum centroid of the noise. It was also suggested that HVAC noises with warm/cool auditory impressions can have some significant effect on the sensation of coolness/warmness.

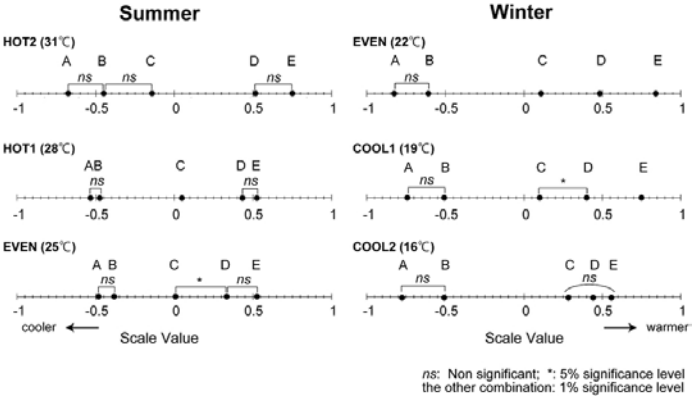

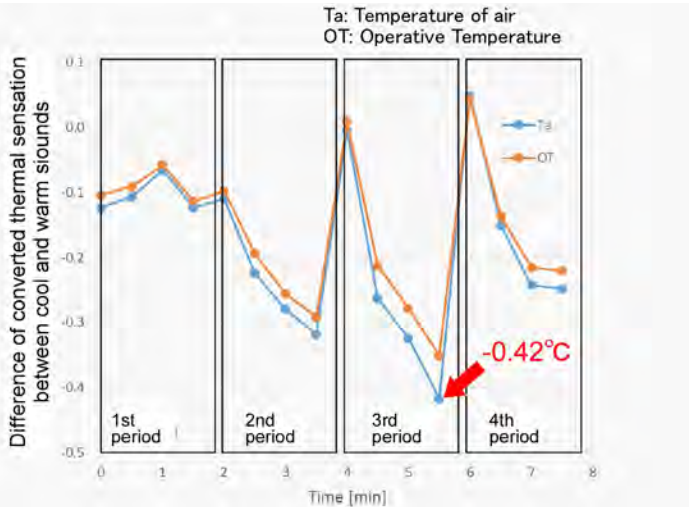

Electrophysiology of Binaural Hearing

PS 628

Effect of Interaural Frequency Mismatch on Lateralization Threshold and the Binaural Interaction Component of the Auditory Brainstem Response in Human Subjects

Carol A. Sammeth[1]; Nathaniel T. Greene[2]; Andrew D. Brown[3]; Daniel J. Tollin[4]
[1]Department of Physiology & Biophysics, University of Colorado School of Medicine; [2]Department of Otolaryngology, University of Colorado School of Medicine; [3]Department of Speech & Hearing Sciences, University of Washington; [4]Department of Physiology & Biophysics, and Department of Otolaryngology, University of Colorado School of Medicine

The auditory brainstem response (ABR) indexes a cascade of neural events elicited by sound. Here, we evaluated the influence of sound frequency on the derived binaural interaction component (BIC) of the ABR. Specifically, we evaluated the effect of acoustic interaural (between-ear) frequency mismatch on BIC amplitude and on perceptual ITD discrimination thresholds. Goals were to (1) increase understanding of sound features influencing the BIC and (2) gain insight on persistence of the BIC with interaural *electrode* mismatch in bilateral cochlear implant users – presently a limitation on its prospective utility in audiologic settings.

Subjects were normal hearing young adults who had previously shown reliable BIC responses and good ITD discrimination thresholds for click stimuli. ABRs were recorded from electrodes at high forehead (Fz) referenced to the nape of the neck with a nasion (Fpz) ground. Alternating-polarity tone pips of 5-ms duration with 1-ms linear rise/fall were presented at 14 Hz (jittered) via ER-2 insert earphones at 75 dB SL (sensation level relative to hearing threshold, or ~95-105 dB peSPL). During each measurement, 2000+ right monaural, left monaural, and binaural stimuli were presented in random order. Four measurements were averaged, yielding 8000+ stimuli/condition in total. Left ear frequency was fixed at 4000 Hz; right ear frequency was varied ±0, 0.5, or 1.0 octaves re: 4000 Hz. The BIC appeared as a small negative trough ("DN1") near the latency of wave V. BIC amplitude tended to decrease with increasing frequency mismatch, suggesting reduced binaural interaction.

Separately, subjects performed an ITD discrimination task at 75, 55, 35 and 15 dB SL with ±0, 0.33, 0.5, or 1.0 octaves of mismatch across ears (left ear again fixed at 4000 Hz). ITD discrimination thresholds tended to increase with increased interaural frequency mismatch, particularly at lower presentation levels. Results were simulated using established models of the brainstem pathway thought to underlie the BIC.

Though BIC measurement is challenging in many subjects, the results of this study, together with existing evidence, suggest that the BIC can be used in a research setting to interrogate sound features affecting human binaural brainstem processing. Results also lend support to current efforts to use electrically evoked BIC to optimize interaural electrode matching in bilateral cochlear implant patients.

Supported by NIH R01-DC011555 [DJT], NIH R21-DC017213 [ADB]

PS 629

Cortical Electrophysiology Indices of Fixed vs. Moving Stimuli

Barrett St. George[1]; Barbara Cone[2]
[1]The University of Arizona; [2]University of Arizona

How do obligatory cortical auditory evoked responses reflect the perception of fixed vs. moving sound sources? In the present study, we evaluate psychoacoustic and cortical auditory evoked potential (CAEP) metrics of sound lateralization for fixed and moving auditory stimuli, when interaural time differences (ILD) and interaural time differences (ITD) are varied.

Methods

20 normal hearing young adults participated. Stimuli were pulse trains in which the first 1000 ms were diotic, and the next 655 ms were dichotic, reflecting either a discrete ("fixed") change in ITD and/or ILD, or a dynamic ("moving") change in ITD and/or ILD. ITD and ILD cues were systematically varied in magnitude in both leftward and rightward directions. Perceptual laterality ratings and CAEPs were obtained for all stimulus conditions.

Results
The independent variables of fixed vs. moving, magnitude of ILD, magnitude of ITD, and type of cue (single ITD or ILD vs. combined ITD-ILD) had significant effects on the perception of laterality, but direction of change (right vs. left) did not. The magnitude of the laterality rating was smaller for moving compared to fixed targets, for single ITD or ILD cues vs. combined cues, and for the smaller ITD and ILD magnitudes.

Fixed-type spatial changes evoked the CAEP Acoustic Change Complex (ACC) whereas moving-type spatial changes did not. ACC amplitudes for fixed type stimuli exhibited a clear relationship with with psychoacoustic ratings of laterality, with r^2= 0.85. Although the tokens with sound movement cues did not evoke an ACC, the stimulus offset CAEPs exhibited greater negativity for moving compared to fixed targets in the latency range +/-50 ms post stimulus offset.

Hemispheric differences were evident with the ACC-N1 of larger amplitude over the hemisphere contralateral to lateralized stimuli, regardless of the ITD or ILD cue available to the listener.

Discussion
Fixed changes in ITD and ILD evoke ACC responses that are congruent with psychoacoustic ratings of laterality, indicating that cortical electrophysiology could be used as a metric for lateralization. Although moving tokens do not evoke ACCs, CAEP offset responses suggest differences in cortical mechanisms underlying spatialized hearing. The concept of stimulus velocity and its relationship to the neural synchrony required to observe a CAEP will be considered.

PS 630

Anticipated ITD Statistics in Human Sound Localization

Rodrigo Pavão[1]; Elyse S. Sussman[2]; Brian Fischer[3]; José L. Peña[2]
[1]Centro de Matemática, Computação e Cognição - Universidade Federal do ABC, SP, Brazil; [2]Dominick P. Purpura Department of Neuroscience - Albert Einstein College of Medicine, NY, USA; [3]Department of Mathematics - Seattle University, WA, USA

The variability of natural scenes places perception in the realm of statistical inference. In this context, perceptual tasks may be optimized if the invariant statistical structure of sensory cues is built into the neural processing. We investigated this question in human sound localization, where interaural time difference (ITD) is a key sensory cue for inferring the direction of acoustic signals in the horizontal plane. ITD statistics were estimated from human head-related transfer functions (HRTFs) and properties of cochlear filters. As previously shown, ITD changed with azimuth following a sigmoid relationship, whose slope was steepest at the center in most frequencies. However, ITD was more variable over time for sounds located in the periphery compared to the center, in a frequency-dependent manner. We tested the hypothesis that these statistics, ITD rate of change with azimuth (ITDrc) and ITD variability (ITDv), are anticipated by the human brain, influencing spatial discriminability and novelty detection. Our results showed that thresholds for discriminating ITD changes could be better predicted by a model relying on both ITDrc and ITDv than on ITDrc alone. In addition, we tested how novelty detection in a spatial oddball paradigm was weighted by anticipated ITD statistics, as indexed by the amplitude of the mismatch negativity (MMN) brain signal, a pre-attentive index of deviance detection. ITDrc and ITDv predicted MMN amplitude, showing a significantly stronger effect of ITD statistics corresponding to repeated (standard) than sporadic (deviants) stimuli. We further show that these statistics could be represented in parameters underlying ITD discriminability postulated by classic neural models. These results show that spatial discriminability thresholds and novelty detection are consistent with a representation of anticipated ITD statistics in the brain, supporting the hypothesis that high-order statistics are built into human perceptual processes biasing behavior.

PS 631

Functional NIRS Investigation of ITD Processing in the Human Cortex

Robert Luke[1]; David McAlpine[2]
[1]Macquarie University, Department of Linguistics; [2]Department of Linguistics, The Australian Hearing Hub, Macquarie University, Sydney, Australia

Human listeners use a variety of binaural cues including interaural time differences (ITDs), the main cue for localising the source of low-frequency sounds. The dominant model of ITD processing, based on psychoacoustic performance, posits an explicit representation of ITD generated by a centrally weighted distribution of coincidence detector neurons innervated with a systematic arrangement of conduction delays. This is followed by a second-level coincidence mechanism that favours ‘straightness’, i.e. consistency of ITD across frequency.

In contrast, neural recordings from a range of small mammals suggest an upper bound of ½ the neural characteristic frequency (CF), the so-called ϖ-limit, to the range of ITDs explicitly coded (McAlpine et. al 2001).

If the ϖ-limit also holds for humans, accurate headphone lateralisation of ITDs beyond this range cannot be based on an explicit neural representation.

Neuroimaging studies have investigated which model is realised in humans for bands of noise centred at 500 Hz (300-700 Hz), and with ITDs of ±500 μs and ±1500 μs. Functional MRI investigation of the human midbrain has demonstrated results consistent with the ϖ-limit model (Thompson et. al 2006). Cortical fMRI results have shown bilateral cortical activation to ±1500 μs ITDs, a result not predicted by either model and presumably caused by a reduction in interaural coherence (IAC) (von Kriegstein et. al 2008).

Using functional near infrared spectroscopy (fNIRS), we assessed cortical activation in 11 listeners to 500-Hz centred bands of noise (300-700 Hz) with ITDs of ±500 μs and ±1500 μs. A critical limitation to fNIRS is the lack of penetration of light through the skull, limiting the depth of sensitivity to the outer cortex. This study exploited that limitation to minimise the influence of changes in IAC, which activates deeper regions of the brain than ITD changes (Hall et. al. 2005).

Significant contralateral activation was observed for sounds with a ±500 μs ITD, and a significant ipsilateral activation for sounds with a ±1500 μs ITD. The data are consistent with Thompson et. al. (2006) and suggest that cortical regions specialised for ITD processing show evidence consistent with a central weighting function for ITD, of which the ϖ-limit is one example, and no evidence for straightness weighting that would account for the perceptual lateralisation of bands of noise with ITDs beyond the ϖ-limit.

McAlpine et. al. (2001). *Nat. Neurosci.*, *4*(4), 396–401.
Thompson et. al. (2006). *Nat. Neurosci*, *9*(9), 1096–1098.

von Kriegstein et. al. (2008). *J Neurophysiol*, *100*(5), 2712–2718.

Hall et. al. (2005). *J Neurophysiol*, *94*(5), 3181-3191.

PS 632

Effects of Age on the Neural Coding and Perception of Binaural Cues

Tess K. Koerner[1]; Ramesh Kumar Muralimanohar[1]; Frederick J. Gallun[2]; Curtis J. Billings[2]
[1]VA RR&D National Center for Rehabilitative Auditory Research (NCRAR); [2]VA RR&D NCRAR

Interaural phase difference (IPD) cues are important for sound source localization and the detection of signals in background noise. Age has been shown to decrease sensitivity to IPDs, which may contribute to impaired temporal processing and increased difficulties understanding speech in adverse listening conditions. This work assessed the effects of age on the neural coding of IPD cues and examined relationships between an electrophysiological measure of IPD sensitivity and behavioral tests that assess binaural hearing abilities. The interaural phase modulation following response (IPM-FR) was recorded in 30 adult participants that varied in age. This passive response was elicited by an ongoing amplitude modulated 500 Hz tone in which the phase of the signals in the right and left ears periodically shift in relation to one another at a depth of ±90˚ and at a rate of 6.8 Hz. The resulting steady state response to the interaural phase modulation rate of the stimulus is thought to reflect neural sensitivity to the temporal fine structure of the signal and has previously been shown to be physiological marker of the effects of age on IPD sensitivity. Participants also completed several behavioral measures, including a binaural frequency modulation detection task and a measure of spatial release from masking using the coordinate response measure sentence corpus. Results from this work will provide more comprehensive knowledge about whether the IPM-FR is predictive of the effects of age on binaural perception. This work has important practical implications regarding the use of the IPM-FR as an objective tool for assessing binaural temporal processing and its effects on speech perception in clinical populations. [Work supported by R01 DC015240 (CJB)]

PS 633

Design of a Chirp Stimulus to Maximize the Binaural Interaction Component (BIC) of the Auditory Brainstem Response (ABR)

Zoe Owrutsky[1]; Daniel J. Tollin[2]
[1]University of Colorado School of Medicine; [2]Department of Physiology & Biophysics, and Department of Otolaryngology, University of Colorado School of Medicine

Chirp stimuli are specifically designed to enhance temporal synchrony in the responses of the auditory nerve and brainstem by taking into account and compensating for the frequency- and level-dependent delays accrued by the traveling wave in the cochlea. When successfully implemented, chirps result in larger amplitude responses in specific waves/peaks of the auditory brainstem response (ABR). Here we test the hypothesis that chirp stimuli can increase the amplitude of the binaural interaction component (BIC) of the ABR. The BIC of the ABR is a potential biomarker for binaural hearing. However, clinical use of the BIC has been limited because it is unreliably measured using

click stimuli in humans. Here we compare different chirp stimulus generation methods to maximize the BIC.

ABR peak latencies were measured in response to tone bursts over a range of stimulus frequencies and intensity levels in three adult chinchillas. Stimuli consisted of 5ms tone bursts presented via sealed and calibrated insert earphones (Etymotic ER-2) at 2000, 4000, 8000, 12000 and 16000 Hz and from ~10 dB below to 50 dB above ABR detection threshold. Latencies of ABR waves I-IV and the BIC DN1 wave (the largest amplitude peak in the BIC) were plotted against frequency and then fit to a power function: β=k*f^(-d), where β is latency in seconds, f is frequency, and k and d are constants. The values of k and d were then used to construct a series of level-specific chirps for three above-threshold stimulus intensity levels based on 1) monaural ABR waves and 2) BIC DN1. Monaural ABR peak latencies decreased systematically with increasing sound frequency as expected from the corresponding latencies due to cochlear delay. Consistent with other studies, our results show that monaural ABR peak amplitudes were enhanced by chirps which compensate for that latency relative to those measured with clicks. Surprisingly though, BIC DN1 peak latencies did not show a similar frequency-dependent latency shift. Rather BIC DN1 latencies appeared to be constant or even showed a small increase with increases in stimulus frequency.

Traditional chirp stimuli designed to optimize monaural ABR peak amplitudes by accounting for frequency-dependent cochlear delays appear ill-suited for eliciting optimal BIC peak amplitudes. Traditional broadband clicks or other non-traditional chirp stimuli may be preferable for eliciting an optimal BIC.

PS 634

Influence of Arousal State and Asymmetries on Objective Neural Measures of ITD Processing in Normal Hearing Adults

Juan Pablo Faúndez; Lindsey N. Van Yper; Jaime A. Undurraga; David McAlpine
Department of Linguistics, The Australian Hearing Hub, Macquarie University, Sydney, Australia

Background
Binaural hearing - particularly interaural timing differences (ITDs) – are important to localise and segregate sounds and to understand speech in noise. To assess neural processing of ITD, electroencephalography (EEG) measures – such as the 'acoustic change complex' (ACC, Ross et al., 2007) and the 'interaural phase modulation – following response' (IPM-FR; Haywood, et al., 2015: Undurraga et al., 2016) have been used. While these responses have been successfully recorded in adults, the question remains whether they can be used in the clinic to evaluate ITD processing in difficult-to-test populations such as children. This study is the first step towards the development of a clinical tool to objectively assess ITD processing. Here, we assess the effects of interaural asymmetries and arousal state on the ACC and IPM-FR in normal-hearing adults. It is important to assess the effects of these potentially confouding factors, not least because clinical audiological tests in children do not always provide exact hearing thresholds (Matkin, 1977; Thompson & Weber, 1974; Wilson & Thompson, 1984; Rance et al., 2006; Van Maanen and Stapells, 2010; Norrix, 2015), and CAEPs and ASSR are affected by arousal state (Dobie and Wilson,1998; Moore, 2002).

Methods
Ten normal-hearing adults participated in our study. ACC and IPM-FR were elicited by periodic changes in ITD. The stimulus comprised of a 500 Hz carrier tone, amplitude modulated at 40 Hz. IPDs were conveyed in the temporal fine structure and periodically switched from + to – 90° at a rate of 0.6 Hz to evoke the ACC and 6.8 Hz to elicit the IPM-FR. Stimuli were presented at 65 and 75 dB(A), and an interaural asymmetry of 0, 5, and 10 dB(A) was introduced. These recordings were obtained during wakefulness. In addition, recordings to the symmetrical condition were conducted during wakefulness and sleep.

Results
ACC and IPM-FR could be obtained in all participants, both during wakefulness and sleep. The amplitude of IPM-FR did not show significant differences between the 0, 5 and 10 dB(A) asymmetry conditions. Further analysis is required for the ACC data.

Conclusions
ACC and IPM-FR represent objective neural measures of ITD processing. Amplitude of IPM-FR is not affected by interaural asymmetries of 5 and 10 dB(A) in awake adults. Hence, IPM-FR is a promising technique to assess ITD processing in children during wakefulness.

PS 635

A Comparison of Two Objective Measures of Binaural Hearing

Won So; Spencer Smith
University of Texas at Austin

Binaural hearing is an integral contributor to speech-in-noise performance. However, because extensive training is required to achieve reliable *psychophysical*measures

of binaural sensitivity, this skill is not commonly assayed in clinical settings. A clinical measure of binaural hearing sensitivity may have multiple applications from evaluating patients complaining of speech-in-noise deficits to fine tuning binaural hearing aids and cochlear implants.

The current study compared two electrophysiologic methods for evaluating binaural sensitivity to interaural phase differences (IPD). In the first method, cortical acoustic change complexes to IPDs (ACCβ) were measured using a combination of different amplitude modulated carrier frequencies (125, 250, and 500 Hz) and IPD step sizes (0, 45, 90, 180°). In this paradigm, stimuli began diotically and an IPD was introduced at the temporal midpoint of each stimulus. ACCβ amplitude and latency were measured as indices of IPD sensitivity. In the second method, cortical steady-state responses to interaural phase modulations (IPM-FR) were measured using stimuli that oscillated periodically between right ear-leading and left ear-leading segments. IPM-FRs were evoked using a combination of different amplitude modulated carrier frequencies (125, 250, and 500 Hz) and IPD step sizes (±0, ±22.5,±45, ±90°). IPD sensitivity was quantified by measuring the spectral amplitude at the IPM-FR frequency (6.9 Hz). ACCβ and IPM-FR were compared on various parameters (e.g., test time, signal-to-noise ratio) to assess which approach is more clinically feasible. Further, relationships between each electrophysiologic measure and behavioral tests of binaural hearing (IPD sensitivity and spatial release from masking) were evaluated to assess which one was more predictive of behavioral performance. This work is an important step toward developing a clinical tool for assessing binaural hearing in a variety of patients such as those with suspected “hidden hearing loss” or hearing aid/cochlear implant users.

(Work supported by NIH K01DC017192)

Hair Cell Regeneration

PS 636

Effects of Dexamethasone–an Enhancer of Hair-Cell Regeneration–on Lateral-Line Innervation and Synapse Formation

Allison L. Saettele[1]; Joseph Kwengwa[2]; Lavinia Sheets[1]
[1]Department of Otolaryngology, Washington University School of Medicine in St. Louis; [2]Washington University in St. Louis

The synthetic glucocorticoid dexamethasone (DEX), an anti-inflammatory reagent, was identified as an enhancer of hair-cell regeneration in a large-scale chemical screen of zebrafish lateral-line neuromasts (Namdaran et al, J Neuroscience, 2012). Conversely, DEX treatment in zebrafish larvae has been shown to inhibit regeneration of mechanically-lesioned motor neurons (Ohnmacht et al, Development, 2016), and it does so by suppressing the inherent immune response.

The effects of DEX and immune suppression on afferent-nerve innervation of regenerating hair cells are still undefined. We therefore wanted to address whether DEX exposure influences afferent innervation and synapse formation in zebrafish lateral-line neuromast hair cells. Free-swimming 5-day-old larvae were briefly exposed to 3 µM copper sulfate ($CuSO_4$), which induces both loss of lateral-line hair cells and considerable retraction of nerve terminals. Both lesioned and control larvae were then exposed to either 10 µM DEX for 48 hours—a dose shown to promote hair-cell regeneration but inhibit immune activity—or carrier alone for 48 hours.

We observed significantly more hair cells per neuromast in both undamaged and $CuSO_4$-lesioned larvae exposed to DEX, further supporting DEX as an enhancer of hair-cell regeneration. Correspondingly, the total length of afferent nerve processes per neuromast in DEX-treated larvae were significantly increased but there was no difference in relative length per hair cell, indicating that innervation of hair cells was not inhibited. Similarly, we observed an increase in the total number of synapses per neuromast but no change in the relative number of synapses per hair cell with DEX treatment. However, our preliminary data suggest, while DEX-treated hair cells form the proper number of synapses, the morphology of pre- and postsynaptic components may be affected.

Taken together, these results show that DEX treatment does not inhibit hair-cell reinnervation or synapse formation, even when the afferent terminals are damaged. Yet changes in synapse morphology suggest DEX treatment may alter hair-cell function. We are currently performing more comprehensive analysis of the effects of DEX treatment on hair-cell synapse morphology and hair-cell function.

PS 637

Single-Cell Transcriptomics of Chick Basilar Papillae in the Process of Hair Cell Regeneration Using an Explant Culture Model

Takayuki Nakagawa[1]; Mami Matsunaga[2]; Tomoko Kita[3]; Hiroe Ohnishi[3]; Norio Yamamoto[1]; Ryosuke Yamamoto[4]; Koichi Omori[1]; Satoko Sakamoto[3]; Akira Watanabe[3]
[1]Dept. Otolaryngology - Head and Neck Surgery, Graduate School of Medicine, Kyoto University; [2]Dept. Otoralyngology - Head and Neck Surgery, Graduate

School of Medicine, Kyoto University; [3]Kyoto University; [4]Kyoto Univ

The limited capacity of mammalian cochleae for hair cell regeneration is closely related to the difficulty in the treatment of sensorineural hearing loss. Recent studies, however, indicated the potential of direct conversion of supporting cells (SCs) to hair cells (HCs) in mammalian cochleae. Those studies also demonstrated that significant hearing recovery through this process is still challenging in mammalian cochleae. In contrast to mammals, the avian basilar papilla has the capacity of HC regeneration leading to complete hearing recovery. In the avian basilar papilla, the direct conversion of SCs is the mainstream of HC regeneration. Aiming to explore novel molecules for promoting SC direct conversion in mammals, the process of HC regeneration through SC direct conversion in the avian basilar papilla was investigated using single-cell RNA sequencing. First, we aimed to establish an explant culture model of chick basilar papillae for HC regeneration via SC direct conversion. Exposure to streptomycin for 2 days caused nearly total HC loss. After the additional culture for 4 days, newly generated HC-like cells, which are trans-differentiating SC-derived cells, appeared in explants. EdU incorporating assay demonstrated that these HC-like cells were not generated through SC proliferation. We then conducted single-cell RNA sequencing of intact and cultured chick basilar papillae with or without exposure to streptomycin using C1 Single-Cell Auto Prep system. Prior to library preparation of the cells, we prepared single-cell suspensions from auditory epithelial cells. Gene expression analysis of cell-type specific markers identified cell clusters, corresponding to SCs and HCs. We also identified the candidate trans-differentiating cells from SCs to HCs. The results provided new insight into the molecular basis of HCl regeneration through SC direct conversion in chick basilar papillae.

PS 638

Early Regenerative Signaling Pathways in the Chicken Basilar Papilla

Nesrine Benkafadar[1]; Amanda Janesick[2]; Mirko Scheibinger[2]; Stefan Heller[2]
[1]Stanford University School of Medicine; [2]Department of Otolaryngology–HNS, Stanford University

Background
Regeneration of sensory hair cells in the mature avian inner ear was first described over 30 years ago. Many other lower vertebrates (fishes, amphibians, reptiles) can spontaneously regrow hair cells, under normal conditions and/or after damage. Regenerated HCs arise from adjacent non-sensory (supporting) cells. HC regeneration happens either when supporting cells (SCs) re-enter the mitotic cycle, forming daughter cells that differentiate into HCs or SCs, or by a direct conversion of SCs into HCs without preceding S-phase re-entry.

The ability of some vertebrates to regenerate hearing suggests the existence of communication between dying HCs and SCs that could be defective in mammals. The long-term goal of this study is to fully characterize the series of events that initiate and execute cochlear HC regeneration in birds after ototoxic damage.

Methods
We established single-dose sisomicin infusion via posterior canalostomy into the P7 chicken inner ear, which leads to rapid and complete HC loss in the basilar papilla. We generated single-cell RNA-seq datasets of basilar papilla sensory epithelia at specific time points post-injection and pre-HC loss. Changes in dying HCs gene expression as well as in SCs were validated with in situ hybridization.

Results
We found TUNEL-positive HCs as early as 12h post-sisomicin injection. All HCs had departed the sensory epithelium at 24h post injection; the most distal HCs disintegrated last. TUNEL-positive SCs were not detected and the SC number was not affected by the aminoglycoside. We observed significant changes in gene expression in HCs after sisomicin treatment that were distinctively different in tall HCs and in short HCs. We also found a group of early responding SCs that is characterized by changes in genes involved in cell-cell junction formation, cytoskeletal remodeling, metabolic changes, epithelial repair, and de-differentiation.

Conclusion
Our results suggest that HCs do not perish quietly, that they display distinct modes of apoptotic death, and that they might signal to surrounding supporting cells. We hypothesize that the SCs initially deal with the massive changes in the sensory epithelium during hair cell departure, followed by a response towards repair and cell regeneration.

PS 639

Balk Transcriptome Analysis for the Initial Process of Hair Cell Regeneration in Chick Basilar Papilla Explant Cultures

Mami Matsunaga[1]; Tomoko Kita[2]; Hiroe Ohnishi[3]; Norio Yamamoto[3]; Koichi Omori[3]; Takayuki Nakagawa[3]
[1]Dept. Otoralyngology - Head and Neck Surgery, Graduate School of Medicine, Kyoto University;

[2]Kyoto University; [3]Dept. Otolaryngology - Head and Neck Surgery, Graduate School of Medicine, Kyoto University

Recent studies reveal that neonatal mammals are capable of hair cell (HC) regeneration through direct conversion of supporting cells (SCs) into HCs, however, that results in limited recovery of hearing. In contrast, the regenerative capacity in the chick basilar papilla (BP) is robust and sufficient to restore both structure and function. Moreover, spontaneous HC regeneration in chick BP occurs throughout the lifetime. To explore the novel strategies for inducing HC regeneration in mammalian cochleae, we investigated transcriptomic profile by bulk RNA-seq analysis of chick BP explant cultures in the initial process of HC regeneration. BP explants dissected from post-hatch day-1 chicks were exposed to streptomycin (SM) for 48 h followed an additional 48-h culture without SM. We counted numbers of SCs labeled with sox2, HCs labeled with myosin VIIa or double-labeled cells (trans-differentiating cells) in frozen sections to estimate the timing for HC loss and appearance new HCs across 9-time points. A total RNA was extracted from 50 BPs for each time point. The transcriptome by bulk RNA-seq was obtained from 4-time points (before, after 24- or 48-h SM exposure and 6-h additional culture after 48-h SM exposure) and mapped to the ensemble GRCg6s / galgal6. The differentially expressed genes were identified by DEseq2, and K-means clustering and gene ontology analysis were performed. As a result, total HC loss was found after the initial 24-h SM exposure. Tras-differentiating cells that were costained with sox2 and myosin VIIa were found 18 h after 48-h SM exposure. Transcriptomic analysis by RNA-seq indicated 807 differentially expressed genes and K-means analysis revealed 9 clusters. Dynamic changes in expressed genes including *Atoh1* were observed between samples obtained before SM exposure and those after 24-h exposure to SM.

PS 640

Single-cell RNA-seq Uncovers Molecular Homology between the Chick and Mammalian Cochlea

Amanda Janesick[1]; Mirko Scheibinger[1]; Daniel C. Ellwanger[2]; Stefan Heller[1]
[1]Department of Otolaryngology–HNS, Stanford University; [2]Department of Otolaryngology–HNS, Stanford University; Genome Analysis Unit, Amgen Research, Amgen Inc.

The fragility of the auditory sensory epithelium is observed across all chordates, however, many non-mammalian species, such as the chicken, have repair and regeneration mechanisms to fully restore hearing after damage. We have developed a robust protocol for bioinformatic analysis of single cell RNA-sequencing and in situ hybridization for validation of differentially expressed genes in the post-hatch day 7 chicken cochlea. This work creates important, “baseline” knowledge of the undamaged chicken cochlea, an organ which previously lacked molecular markers. Hair cells (HCs) and supporting cells (SCs) cluster into neural (“tall”) and abneural (“short”) groups which can now be classified by molecular markers Cxcl14 (tall HC), C14Orf180 (short HC), and Ccdc180 (tall SC). Cxcl14 and C14Orf180 also segregate single murine P28 hair cells into “inners” and “outers” respectively, thus providing new molecular evidence that the chicken cochlea is a homologous organ to the mammalian cochlea. Identification of unique SC populations demonstrate at even at homeostasis (without damage) there is inherent heterogeneity in SCs which could drive disparate regenerative strategies in the chicken cochlea (mitotic division versus phenotypic conversion). Understanding the molecular signature of chicken SCs will allow us to better target the homologous SC type in mammals that would hold the most regenerative potential.

PS 641

Identification of Analogous Sub-types of Hair Cells and Support Cells Across Mammalian and Non-mammalian Species

Brian Herb[1]; Gurmannat Kalra[1]; Nesrine Benkafadar[2]; Amanda Janesick[3]; Beatrice Milon[4]; Kevin Rose[5]; Mirko Scheibinger[3]; Michael Lovett[6]; Tatjana Piotrowski[7]; Stefan Heller[3]; Ronna Hertzano[8]; Neil Segil[9]; Seth Ament[10]; Peter G. Barr-Gillespie[11]; Hearing Restoration Project[12]
[1]University of Maryland, Baltimore; [2]Stanford University School of Medicine; [3]Department of Otolaryngology–HNS, Stanford University; [4]Department of Otorhinolaryngology-Head and Neck Surgery, University of Maryland; [5]University of Maryland School of Medicine; [6]National Heart and Lung Institute, Imperial College London, London, United Kingdom; [7]Stowers Institute for Medical Research, Kansas City, MO; [8]Department of Otorhinolaryngology Head and Neck Surgery, University of Maryland School of Medicine; Institute for Genome Sciences, University of Maryland School of Medicine.; [9]Department of Stem Cell Biology and Regenerative Medicine, Keck School of Medicine of USC, and USC Caruso Department of Otolaryngology – Head and Neck Surgery; [10]University of Maryland School of Medicine Baltimore, Maryland; [11]Oregon Hearing Research Center & Vollum Institute, Oregon Health & Science University; [12]Hearing Health Foundation

Sensory hair cells and their accompanying support cells are a conserved feature of auditory, vestibular and mechanosensory systems across all vertebrate species.

In contrast to mammals, hair cells in non-mammalian vertebrates such as birds and fishes regenerate from sub-populations of support cells. Reprogramming mammalian support cells to mimic support cells from non-mammalian vertebrates and promote hair cell regeneration in humans is a promising strategy to treat hearing loss due to age, noise damage, or ototoxic drug exposure. However, a complicating factor is that the morphology of specific sub-types of hair cells and support cells varies widely across species and sensory organs, and the evolutionary and functional correspondence between these sub-types is unknown. We hypothesized that analogous sub-types of hair cells and support cells across species may share common molecular networks.

To identify these shared networks, we generated single-cell RNA-seq from the mouse cochlea, mouse utricle, chicken cochlea, and chicken utricle, and we compared these data to our previously published single-cell RNA-seq data from the zebrafish lateral line. Within each species and tissue, we identified subtypes of hair cells and support cells and profiled both gene expression and gene regulatory network activity, revealing a unique molecular profile for each cell type. Cross-species comparisons were then made between all cell types, looking for shared networks. These analyses revealed relationships among cell types across mouse, chicken and zebrafish and highlighted both common and divergent molecular signatures. Overall, hair cells, regardless of species or tissue, show the strongest similarities, yet analogous support cells subtypes are also apparent. For example, homogene support cells in the chicken cochlea, greater epithelial ridge support cells in the mouse cochlea, and A/V pole cells in the zebrafish neuromast share a molecular signature with enrichment of pro-growth genes such as Agr2 and Igf2. By identifying cell types in mouse that are most similar to cells in chicken and zebrafish with regeneration potential, we can focus our search for drivers of regeneration as candidate therapeutic targets to promote hair cell regeneration in humans.

PS 642

YAP Signals During Direct Transdifferentiation of Supporting Cells in Cochlear Explant Culture of Chicken and Mouse

Tomoko Kita[1]; Mami Matsunaga[2]; Tomomi Miyatake[1]; Li Gao[3]; Ryosuke Nakamura[4]; Norio Yamamoto[4]; Takayuki Nakagawa[5]; Koichi Omori[4]
[1]Kyoto University; [2]Dept. Otoralyngology - Head and Neck Surgery, Graduate School of Medicine, Kyoto University; [3]Department of Otolaryngology, Head and Neck Surgery, Graduate School of Medicine, Kyoto University; [4]Dept. Otolaryngology - Head and Neck Surgery, Graduate School of Medicine, Kyoto University; [5]Department of Otolaryngology-Head and Neck Surgery, Graduate School of Medicine, Kyoto University

Yes-associated-protein (YAP), a key downstream effector of the Hippo pathway, controls various aspects of development and homeostasis including cell proliferation, migration, survival, differentiation, and regeneration. Regenerating cochlear hair cells (HCs) is a promising strategy to restore hearing after hearing loss in mammals. Recent papers inform us of several transcriptome profiles for HC regeneration using HC damage models of zebrafish, chicken, and mouse. The spontaneous and forced HC regeneration occurs through proliferation and direct transdifferentiation of supporting cells (SCs), which is regulated by several pathways involving Wnt, Notch, FGF, and BMP signaling. Using chick utricle, Lovett's group has already shown that YAP downstream molecules were upregulated after HC damage (Ku et al., J. Neurosci. 2014). In the present study, we inquire whether YAP signals are involved in the direct transdifferentiation of HC regeneration in chicken and mouse cochleae. *Ex vivo* cochlear explant culture methods of P2 mouse and P1 chicken were used as HC damage and/or HC regeneration models. In mouse experiment, we used two models including 1mM neomycin-induced HC damage for ICR mouse and 25 ng/mL diphteria toxin-treated Pou4f3-DTR mouse. In chick experiment, 78 μM streptomycin (SM) was exposed to basilar papilla (BP) for 48 hours, which is already identified as HC regeneration through direct transdifferentiation (Shang et al., JARO 2010). YAP signals were validated by the localization of YAP in the fixed specimens and phosphorylated YAP was detected by western blotting using antibodies. As a result, no expression of YAP was seen in HC of intact cochleae of both mouse and chicken, and whole cells located in inferior and superior edge of BP show higher expression of YAP than SCs located under HCs. After the exposure of SM, YAP expressed in nuclei of SCs mostly located around inferior and superior edge. Western blotting data was almost consistent with the localization of YAP staining. This study suggests that YAP signals are working in the direct transdifferentiation process of SCs in chick BP regeneration model. Most of the known cross-talk occurring between Hippo and Wnt signaling. Therefore, we are now examining the possible involvement of YAP in this HC regeneration process and its relationship with Wnt and BMP signals using chemicals regulating them.

PS 643

YAP-Activating Small Molecules for Inner Ear Regeneration and Beyond

Nathaniel Kastan[1]; Ksenia Gnedeva[2]; AJ Hudspeth[3]
[1]The Rockefeller University, Howard Hughes Medical Institute; [2]Center for Regenerative Medicine and Stem

Cell Research at USC; [3]Howard Hughes Medical Institute and Laboratory of Sensory Neuroscience, The Rockefeller University

Because hair cells of the mammalian inner ear do not regenerate, damage accumulates across a lifetime, often culminating in disabling hearing loss and vestibular dysfunction. Because there is no effective medicinal treatment for hearing loss, treatment focuses on preventative measures, coping strategies, and hearing aids, a cumbersome and often insufficient response to the problem. The goal of this investigation is to identify small molecules that induce proliferation of supporting cells, thus mimicking a key step of the hair cell regeneration observed in non-mammalian vertebrates.

The sensory epithelia of all hearing and vestibular organs share two cell types: supporting cells, which play a homeostatic and architectural role, and mechanosensitive hair cells. In birds the regenerative process involves two phases. Supporting cells adjacent to a site of damage undergo proliferation, yielding daughter cells that can either differentiate into hair cells or remain supporting cells. In the adult mammalian utricle, it has been shown that a modest number of hair cells regenerate after total ablation. However, the new hair cells are predominantly the result of trans-differentiation, and it is unclear whether there is any significant functional recovery. Although this is a meager response, it lies in stark contrast to the total inability of the mammalian cochlea to yield any regenerative response.

Given this backdrop, many researchers have turned to investigating potential avenues of first inducing a proliferative response. Our group identified YAP signaling as requisite for delimiting the size of the developing utricle. This pathway is active during, and necessary for, proliferative regeneration in the neonatal utricle. We therefore performed a drug screen of over 80,000 chemicals to identify those that activate YAP. Having identified and validated six drugs in this system, we have explored these drugs' potentials to induce supporting cell proliferation and subsequent hair cell regeneration in the murine utricle and cochlea. One compound has shown promising results, and we are exploring its mechanism of YAP activation. These drugs may serve as broadly applicable tools with which to perturb and thus further elucidate this signaling pathway or as a basis of therapeutic intervention. Finally, because there are several tissues – such as cardiomyocytes – in which YAP activation induces regeneration, we aim to survey these other non-proliferative tissues as potential therapeutic targets.

PS 644

Dynamic Changes of Surviving Hair Cells of the Damaged Mouse Utricle

Grace Kim; Tian Wang; Zahra N. Sayyid; Alan Cheng
Department of Otolaryngology-Head and Neck Surgery, Stanford University

Background

Sensory hair cells are mechanoreceptors required by the vestibular system to detect head motion. While cochlear hair cell loss results in permanent hearing loss, the mammalian utricle can regenerate lost hair cells. Prior studies examining vestibular stimuli evoked potential (VsEP), a brainstem response as a result of a linear acceleration exerted on the head, have shown a limited recovery after damage concurrent with cell regeneration. However, cellular components contributing to this functional recovery have not been clearly defined. Here, we fate-mapped hair cells prior to hair cell ablation and characterized these "surviving hair cells" in the context of return or absence of VsEP thresholds.

Method

We injected P1 Atoh1-CreERT2; Rosa26tdTomato; Pou4f3-DTR transgenic mice with tamoxifen and diphtheria toxin using Atoh1-CreERT2; Rosa26tdTomato mice as controls. Animals underwent VsEP testing at P15 and P30 prior to tissue harvest at P30. Antibodies against Osteopontin (type I) and AnnexinA4 and MAPT (type II) were used to determine hair cell subtypes, and Tuj1 for identifying neurites. Pre-synaptic (CTBP2) and post-synaptic (Homer) markers were used, and co-labeled synapses per surviving hair cell were quantified. Animals with and without VsEP recovery were separately analyzed.

Results

Approximately 50% of hair cells were fate-mapped at P3, and about 30% of these survived at P30 in the VsEP recovery group and 15% survived in the non-recovery group. In the VsEP recovery group, surviving Atoh1-tdTomato+ hair cells consisted of both type I and II hair cell subtypes (~50% each) in both the extrastriola and striola. In both regions, most fate-mapped type I hair cells lost calyces, but all hair cells still appeared innervated. This contrasts with regenerating hair cells which are primarily type II hair cells, and the few type I hair cells regenerated were devoid of calyces. In comparison to undamaged controls, surviving type I hair cells in the striola and type II hair cells throughout the utricle showed increased number of colocalized pre- and post-synaptic markers. The number of hair cells and therefore the number of each hair cell subtype was significantly lower in the utricles without VsEP recovery. Further evaluation

of non-recovery cohort is ongoing. Future experiments examining bundles of the surviving hair cells are also underway.

Conclusion
Surviving hair cells consist of both type I and II hair cells, a subset of which displayed increased synaptic colocalization. This model should contribute to our understanding of the recovery of vestibular function.

PS 645

Transcriptomic and Epigenetic Regulation of Hair Cell Regeneration in The Mouse Utricle and Its Potentiation by Atoh1

Hsin-I Jen[1]; Matthew Hill[2]; Litao Tao[3]; Kuanwei Sheng[2]; Wenjian Cao[2]; Hongyuan Zhang[2]; Haoze Yu[4]; Juan Llamas[4]; Chenghang Zong[2]; James Martin[5]; Neil Segil[4]; Andrew K. Groves[6]
[1]Program in Developmental Biology, Baylor College of Medicine, Houston, United States; [2]Baylor College of Medicine; [3]University of Southern California; [4]Department of Stem Cell Biology and Regenerative Medicine, Keck School of Medicine of USC, and USC Caruso Department of Otolaryngology – Head and Neck Surgery; [5]Molecular Physiology and Biophysics, Baylor College of Medicine; [6]Department of Neuroscience, Baylor College of Medicine, Houston, United States

The mammalian cochlea loses its ability to regenerate new hair cells prior to the onset of hearing. In contrast, the adult vestibular system can produce new hair cells in response to damage, or by reprogramming of supporting cells with the hair cell transcription factor Atoh1. We used RNA-seq and ATAC-seq to probe the transcriptional and epigenetic responses of utricle supporting cells to damage and Atoh1 transduction. We show that the regenerative response of the utricle correlates with a more accessible chromatin structure in utricle supporting cells compared to their cochlear counterparts. We also find differential expression of chromatin modulators in these two types of supporting cells. In addition, we provide evidence that Atoh1 transduction of supporting cells is able to promote increased transcriptional accessibility of some hair cell genes. Our study offers a possible explanation for regenerative differences between sensory organs of the inner ear, but shows that additional factors to Atoh1 may be required for optimal reprogramming of hair cell fate.

PS 646

Sox2 is Required for Regeneration of Vestibular Hair Cells in Adult Mice

Amanda Ciani[1]; Brandon C. Cox[2]; Jennifer Stone[3]
[1]University of Washington; [2]Departments of Pharmacology & Otolaryngology, Southern Illinois University, School of Medicine; [3]University of Washington School of Medicine

In the vestibular epithelia of adult mammals, supporting cells regenerate a subpopulation of hair cells after hair cells are destroyed. The factors that enable supporting cells to transdifferentiate into hair cells are not well understood. Sox2, a SRY-box transcription factor, is required for specification of inner ear sensory epithelia and for formation of both hair cells and supporting cells during development. Sox2 is expressed in the prosensory progenitor cells that differentiate into both cell types but its expression is downregulated in most hair cells as they develop. However, Sox2 expression is maintained in supporting cells in adulthood. We hypothesized that Sox2 is required in supporting cells for their transdifferentiation into hair cells during regeneration. We tested this hypothesis by conditionally deleting *Sox2* from adult supporting cells using *Pou4f3^{DTR}:Sox9-CreER^{T2}:Rosa^{Tomato}:Sox2$^{f/f}$* mice, in which ~87% of supporting cells have inducible Cre activity. We treated 6 week-old mice with Tamoxifen (Tam) and confirmed loss of Sox2 protein in Tomato-expressing supporting cells within 2 weeks post-injection. We administered diphtheria toxin (DT) to mice at 1 week post-Tam, then waited 3 weeks to determine if hair cell regeneration occurred in mice lacking *Sox2* in supporting cells. *Sox9-CreER^{T2}:Rosa^{Tomato}:Sox2$^{+/+}$* mice were processed in parallel as controls.

We found that hair cell regeneration was severely reduced when *Sox2* was deleted from supporting cells prior to hair cell destruction. In control mice, we counted 225 (±140 SD, n=3) Tomato-positive hair cells per utricle. Tomato labeling indicated that these cells, which were all type II-like, were derived from supporting cells and were therefore regenerated. By contrast, mice with *Sox2* deletion from supporting cells had only 26 (±18.5 SD, n=3) Tomato+ hair cells per utricle, indicating that hair cell regeneration was highly curtailed. In mice with *Sox2* deletion from supporting cells, Tomato-positive cells lacking the hair cell marker Myosin VIIa were sometimes seen in the hair cell layer, suggesting they were supporting cells that had migrated apically, but had not transdifferentiated into hair cells. We are currentlyexamining the identity of these cells and investigating if they are mitotically active. No other obvious differences were seen in supporting cells with *Sox2* deletion at three weeks post-DT. Our findings indicate that Sox2 is required in supporting cells for their transdifferentiation into hair cells in adult mice after hair cell damage.

This work was funded by DC013771 and the Kellogg Family Trust.

PS 647

Atoh1 Enhances Proliferation and Hair Cell Regeneration in the Adult Mouse Utricle

Zahra N. Sayyid[1]; Tian Wang[1]; Leon J. Chen[2]; Sherri M. Jones[3]; Alan Cheng[1]
[1]Department of Otolaryngology-Head and Neck Surgery, Stanford University; [2]George Washington University School of Medicine; [3]University of Nebraska Lincoln

Background
The utricle is a gravity-sensing vestibular organ whose function requires mechanosensory hair cells (HCs). We have previously shown that the damaged, adult mouse utricle regenerates HCs that mature over months, resulting in a limited, unsustained functional recovery. However, the utricle is mitotically quiescent and remains so after damage. Atoh1 is a transcription factor that is necessary for hair cell differentiation. When overexpressed in the neonatal cochlea, Atoh1 induces hair cell formation and proliferation. However, both the number and maturation of ectopic HCs are rather limited. Here, we characterize the regenerating adult mouse utricle after damage and Atoh1 overexpression (Atoh1-OE).

Methods
Postnatal 30-day-old mice (Plp1CreERT/+; R26RtdTomato/+ and Plp1CreERT/+; CAGflox-Atoh1-HA/+; R26RtdTomato/+) received the vestibulotoxin IDPN and tamoxifen. To assess for proliferation early (1 week) and late (1-3 months) after damage, we assayed Ki67 or EdU staining. We also examined markers of HCs, supporting cells, GTTR, and stereociliary bundles. Type I and II HCs were distinguished by the markers Osteopontin and AnnexinA4, respectively. Densities of HCs, supporting cells, and fate-mapped cells were further analyzed for markers up to 180 days after damage.

Results
Tamoxifen induced robust Atoh1-HA expression in supporting cells in the damaged Atoh1-OE utricle. Significantly more regenerated HCs were observed over time, reaching 80% of undamaged, age-matched controls at 180 days. Although HCs regenerated mainly in the extrastriola of damage-only utricles, Atoh1-OE, damaged utricles showed significantly more HCs in both the extrastriola and striola. Atoh1-OE, damaged utricles also showed a gradual and significant increase in traced HA+ HCs over time. At 90 and 180 days after damage, we found significantly more regenerated HCs displaying apical bundles after damage and Atoh1 overexpression as compared to damage only. Myosin7a+/HA+ cells incorporated GTTR, suggesting that Atoh1-OE regenerated hair cells matured and had patent mechanotransduction channels. Whereas type I and type II HCs regenerate in the damaged utricle, Atoh1-OE HCs predominantly (>93%) expressed the type II HC marker AnnexinA4. We detected almost no proliferation in undamaged, Atoh1-overexpressed, or damage-only organs. By contrast, damaged utricles with Atoh1 overexpression had many Ki67+/Sox2+ and EdU+/Sox2+ supporting cells primarily in the striola. A subset of EdU+ cells expressed Myosin7a. Ninety days after damage and Atoh1 overexpression, many EdU+/Sox2+ but no Ki67+/Sox2+ cells were found, suggesting that mitosis was transient.

Conclusions
Atoh1 induces supporting cell proliferation and regeneration of type II HCs in the damaged adult mouse utricle.

PS 648

Viral Expression of Hair Cell-Specific Transcription Factors in Supporting Cells of the Adult Mouse Utricle

Tara Balasubramanian[1]; **Beatrice Mao**[1]; Matthew W. Kelley[2]
[1]Laboratory of Cochlear Development, National Institute on Deafness and Other Communication Disorders; [2]National Institute on Deafness and Other Communication Disorders, NIH

Under normal conditions, the mature mouse utricle has a limited ability to regenerate hair cells through transdifferentiation of supporting cells. However, this spontaneous regeneration does not lead to recovery of function, suggesting that regenerated utricular hair cells may not be fully functional. Previous work has indicated that forced expression of a triad of transcription factors, Atoh1, Pou4f3 and Gfi1, in embryonic stem cells can drive the formation of more mature hair cell types.

To determine whether forced expression of the same three transcription factors can enhance the formation of transdifferentiated hair cells, we conducted *in vitro* experiments on utricles from adult Plp1-Cre/Rosa26-tdtomato transgenic mice. First, we induced genetic marking of supporting cells using 4-hydroxytamoxifen. Endogenous hair cells were then killed using neomycin. Finally, utricles were transfected with an adenoviral vector expressing the hair cell-specific transcription factors *Atoh1, Gfi1,* and *Pou4f3* and a GFP reporter. Cells that were double-labeled for both the supporting cell lineage and viral transfection were then examined for changes in morphology consistent with hair cell formation. These included the appearance of stereocilia-like bundles as well as the expression of utricular cell-

type specific markers including SPP1, OCM (both Type Is) and MAPT (Type IIs). Preliminary results indicate a conversion of supporting cells into hair cells in response to viral transfection and transcriptional expression.

PS 649

Hippo Signaling Regulates Inner Ear Sensory Organ Growth and Restricts Regenerative Responses Through the Yap/Tead complex.

Ksenia Gnedeva[1]; Xizi Wang[2]; Melissa McGovern[3]; Matthew Barton[4]; Juan Llamas[2]; Nathaniel Kastan[5]; Litao Tao[2]; Talon Trecek[2]; Tanner Monroe[6]; Haoze Yu[2]; Welly Makmura[2]; James Martin[6]; A. James Hudspeth[5]; Andrew K. Groves[3]; Mark Warchol[7]; Neil Segil[2]
[1]Center for Regenerative Medicine and Stem Cell Research at USC; [2]Department of Stem Cell Biology and Regenerative Medicine, Keck School of Medicine of USC, and USC Caruso Department of Otolaryngology – Head and Neck Surgery; [3]Department of Neuroscience, Baylor College of Medicine, Houston, United States; [4]Department of Otolaryngology, Washington University School of Medicine in St. Louis; [5]The Rockefeller University, Howard Hughes Medical Institute; [6]Molecular Physiology and Biophysics, Baylor College of Medicine; [7]Washington University School of Medicine

In the developing organ of Corti, the progenitor cells exit the cell cycle in a rapid wave prior to the onset of hair cell differentiation, making it a unique system to dissect the molecular events that control a switch from proliferative growth to terminal differentiation. Using single-cell RNA-sequencing we identified two distinct populations corresponding to the actively cycling and cell-cycle arrested sensory progenitors in E13.5 organ of Corti, and demonstrated that Hippo signaling is activated during this transition. Analysis of the changes in chromatin accessibility (ATAC-seq) demonstrated that within the presumptive regulatory regions, associated with the self-renewal state, the binding motif for Tead transcription factors was highly enriched. Using Chip-seq, we further confirmed that the Yap/Tead complex directly binds to a subset of these presumed regulatory elements and, therefore, likely controls the expression of the associated genes. Consistent with this hypothesis, although we found that Tead transcription factors are continuously expressed in the sensory domain of the cochlear duct, their co-activator, and the target of Hippo signaling - Yap1 - is degraded coinciding spatially and temporally with the characteristic wave of progenitor cell-cycle exit. We further demonstrate that conditional loss of Yap in the inner ear results in great reduction of sensory organ size without largely affecting progenitor cell differentiation, as hair cells and supporting cells are specified normally. We also show that constitutive activation of Yap signaling prevents progenitor cell-cycle exit during development, and results in overgrowth of the sensory epithelia. Finally, we demonstrate a role for Yap/Tead signaling during regeneration in the neonatal inner ear. We show that constitutive activation of Yap/Tead signaling, either through viral over-expression or *via* inactivation of Lats1/2 kinase within the Hippo cascade, results in upregulation of self-renewal gene program and robustly triggers supporting cell proliferation in adult sensory organs. Together, our data suggest that the Yap/Tead transcription factor complex directly controls a self-renewal gene network in the nascent inner ear sensory organs, and that inactivation of the Hippo cascade facilitates regenerative responses in the adult sensory organs after damage.

PS 650

Downstream Targets of Atoh1 during Mammalian Cochlear Hair Cell Differentiation

Dunia Abdul-Aziz[1]; Nicolai Hathiramani[2]; Lauren Phung[3]; Albert Edge[4]
[1]Massachusetts Eye and Ear, Harvard Medical School; [2]Massachusetts Eye and Ear; [3]Massachusetts Eye and Ear, Northeastern University; [4]Harvard

Sensory hair cells mechanotransduce sound in the cochlea, and their loss results in irreversible sensorineural hearing loss in mammals. The transcription factor Atoh1 is essential during hair cell development and for spontaneous hair cell regeneration that occurs in the cochlea and vestibule of nonmammalian vertebrates and mammalian neonates. During this regenerative process, supporting cells upregulate Atoh1 and transdifferentiate into hair cells. Forced overexpression of Atoh1 in newborn mammalian cochlear and adult vestibular systems produces hair cell-like cells. To date, characterization of Atoh1 targets in the cochlea has been limited by the relatively small number of cells in the mammalian cochlea relative to the numbers needed to perform genome-wide studies. Inner ear organoids derived from murine neonatal Lgr5+ cochlear progenitors are capable of differentiating into hair-cell-like cells *in vitro* and provide a robust model to study this differentiation process in response to Atoh1. We present transcriptional and epigenetic changes, in the form of RNA-seq and ATAC-seq, that occur during supporting cell to hair cell differentiation and identify cochlear-specific Atoh1 downstream targets and chromatin changes. We compare the regenerative responses mediated by combined Wnt activation/Notch inhibition to that of Atoh1 overexpression in terms of activation of Atoh1 targets and hair cell genes. We further compare it to other studies which have been performed in the vestibule and cerebellum. Our findings enrich our understanding of the regulatory network underlying hair cell development and the essential factors needed for cellular reprogramming.

PS 651 - WITHDRAWN

PS 652

Comparison of the Proliferative Capacity of Neonatal Supporting Cell Subtypes

Marie Kubota[1]; Mirko Scheibinger[2]; Stefan Heller[2]
[1]Stanford University, School of Medicine, Department of Otolaryngology-HNS; [2]Department of Otolaryngology–HNS, Stanford University

Background
Mammalian hair cells (HCs) are not regenerated after injury, which contributes to the permanence of hearing loss. Recent studies have shown that some supporting cells (SCs) from the neonatal mouse organ of Corti can re-enter the cell cycle and give rise to new HCs. In this project, we quantitatively assessed the ability of different SC subtypes to proliferate and differentiate into HCs.

Methods and Results
Cochlear duct cells obtained from postnatal day 2 mice were cultured for 7 days in media that promoted the formation of floating colonies (spheres). We found spheres with different morphologies such as densely packed (solid type) as well as spheres with large acellular inclusions (hollow type). We cultured the different types of spheres as substrate-attached colonies for additional 14 days. Colonies grown from solid spheres efficiently gave rise to HC marker-expressing cells (hair cell-like cells; HLCs), while HLCs were rarely observed in the hollow sphere-derived colonies. Thus, the culture condition for growing solid spheres was used for subsequent experiments with FACS-sorted SCs. We utilized SOX2-GFP, Lfng-GFP, and Fgfr3-iCreERT2/tdTomato/SOX2-GFP mice to isolate Deiters' cells, inner pillar cells, outer pillar cells, as well as cells from the greater epithelial ridge (GER). Spheres from Deiters' and pillar cells were abundant but relatively small, composed only of a few cells. HLCs were frequently differentiated in the colonies grown from these spheres. In contrast, spheres from GER cells were less abundant and grew extensively in high cell density culture conditions but we observed significantly less growth and possibly cell loss when GER cells were cultured at lower densities. GER cell-derived colonies also gave rise to HLCs. With respect to growth media, we found that certain components that support colony formation had a negative impact on hair bundle formation. We have started profiling the transcriptome of the sorted SC subtypes as well as the cells that are present in spheres.

Conclusions
Cells of the neonatal GER have strong ability to proliferate, especially when cultured at higher densities. The spheres derived from GER cells harbor cell groups that are able to differentiate into new HCs and new SCs. Deiters' and pillar cells are able to form spheres, but the colonies remain small in the conditions used. It is possible that the SCs in such cultures are able to directly differentiate into HLCs. Our ongoing transcriptomic analyses might provide clues about the mechanisms that control neonatal SC proliferation and differentiation.

PS 653

Comparison of Single Versus Combinatorial Strategies for Hair Cell Regeneration in Cochlear Explants

Phillip Uribe[1]; Anne Harrop-Jones[2]; Pranav D. Mathur[2]; Fabrice Piu[1]; Alan C. Foster[3]; Bonnie E. Jacques[1]
[1]Otonomy Inc; [2]Otonomy, Inc.; [3]Otonomy Inc.

Background
Hair cell death is a significant contributor to human hearing loss. While most vertebrates can regenerate hair cells, mammals lack this ability. Research over the last two decades has focused on identifying mechanisms to restore regenerative competence to the mammalian ear. Recent advances have suggested that a therapeutic approach involving a combination of targets may have additive or synergistic effects on hair cell regeneration. To characterize and compare the efficacy of potential therapeutic compounds alone or in combination for hair cell regeneration, we utilized several ex- vivo models: a naïve model without deliberate HC damage as well as moderate and severe models of aminoglycoside-induced hair cell loss. Single or combinations of compounds previously reported in the literature to have regenerative benefit were evaluated in these models in a head-to-head comparison of regenerative efficacy.

Methods
P0-P4 neonatal rat cochlear explants were established and allowed to acclimate overnight. For the damage models, explants were treated the next day with aminoglycoside antibiotics for 12 to 24 hours to induce moderate or severe hair cell damage after which aminoglycoside was removed from the media and test compounds were added for 48-96 hours to determine their dose responsiveness toward hair cell production. For the naïve model, explants were treated the day after acclimation with the same compounds and for the same duration. Cochleae were then fixed and stained for hair cell and support cell markers and the number of both inner and outer hair cells was quantified in 200 µm length segments from the basal, mid and apical regions.

Results
Various experimental conditions were evaluated to mimic or optimize those used in previous ex vivo studies;

variables tested included rodent species, culture media components, vendor/manufacturer of compounds and duration of exposure. In the head-to-head comparisons with either naïve or aminoglycoside-damaged explants, several compounds performed as expected whereas other compounds or combinations failed to perform as reported in the published literature. However, in general, combinations performed better than single compounds in the degree of ectopic hair cell formation.

Conclusions

The use of a naïve model without damage constitutes a simple and rapid method to assess ectopic HC formation potential in cochlear explants. In general, combinations performed better than single compounds in both naïve and damage models. This study highlights the importance of carefully selecting experimental models when screening and ranking compounds for regenerative efficacy.

PS 654

Characterization of Stem Cell Traits amongst Nestin Expressing Cells in the Mammalian Organ of Corti

Hiroki Takeda[1]; Anna Dondzillo[2]; **Samuel P. Gubbels**[2]
[1]Department of Otolaryngology-Head and Neck Surgery, Kumamoto University.; [2]University of Colorado Denver, Anschutz Medical Campus

Disabling hearing loss affects 500 million individuals worldwide, or approximately 7% of the world's population [1]. The majority of cases of hearing loss are due to the loss of the hair cells of the inner ear. While the adult mammalian cochlea has little to no ability to regenerate hair cells, the early postnatal mammalian inner ear appears to have a robust ability to do so.

Research over the last 15 years has characterized a population of postnatal cochlear progenitor cells that express Lgr5 capable of generating both hair and supporting cell phenotypes under specific conditions. This population of cells can proliferate in response to injury and are sensitive to Wnt stimulation and Notch inhibition causing them to generate new supporting and hair cells. Recent evidence from a number of groups suggests however that Lgr5 expressing progenitor cells may not be the only cell population capable of regenerative behavior in the cochlea (2), though the molecular identity of the non-Lgr5 expressing cell population is unclear. Nestin, an intermediate filament protein expressed in multipotent stem cells in the CNS and retina, is expressed in several cell types in the developing and adult cochlea. Our lab has demonstrated that a population of Nestin expressing cells in the cochlea persists long into adulthood and has an expression pattern supporting its role as a marker of progenitor cells in the developing organ of Corti. We examined hallmark features of tissue specific stem cells in the population of Nestin expressing cells in the developing murine organ of Corti in normal and lesioned conditions. We studied the ability of Nestin positive cells to proliferate and differentiate into new hair and supporting cells using three model systems including a Nestin-GFP X Pou4f3$^{+/DTR}$ lesioning *in vivo* mouse model. Our findings indicate that Nestin positive cells in the organ of Corti proliferate and can generate hair and supportive cell immunophenotypes under specific conditions. We also found an expansion of the Nestin expressing cell population after lesioning of the organ of Corti. Taken together, our results suggest that Nestin expressing cells are multipotent, can self-renew and respond to tissue injury supporting their potential role as one type of tissue specific stem cell in the mammalian cochlea.

PS 655

ERBB2 Signaling Promoted Hearing Recovery After Noise in Vivo

Jingyuan Zhang[1]; Daxiang Na[1]; Kenneth S. Henry[2]; Patricia M. White[1]
[1]University of Rochester Medical Center; [2]University of Rochester

Hearing is the ability to detect and perceive sound, an important quality in human activities. Hearing loss follows when cochlear hair cells (HCs) are damaged or lost due to various factors, such as ototoxic insults and exposure to noise. In mammals, HCs are not regenerated once they die, resulting in permanent hearing impairment. Here we report on the effects of expressing constitutively activated ERBB2 receptors (CA-ERBB2) in mouse cochlear SCs. We used a Tet-On transgenic strategy to achieve ERBB2 gain-of-function at different stages. We previously reported that ERBB activation could drive SCs proliferation and ectopic hair cells formation in the neonatal mouse cochlea. To assess the potential therapeutic effects from CA-ERBB2, we exposed mice with a strong noise, consisting of an 8-16 kHz band at 110 dB for two hours. This noise exposure drove temporary thresholds shifts of an average of 30 dB and permanent threshold shifts of 25 dB across all auditory frequencies. Here we report significantly improved auditory thresholds in mice that endured such level of noise, but were treated with CA-ERBB2 expression in their cochlear SCs. Cochlear HCs, as the primary sound transducer, were largely preserved at the high-frequency region in CA-ERBB2 groups. Synapse ribbon numbers from inner hair cells (IHCs) remained the same, however the sizes were different between control and CA-ERBB2 group. We have recently adapted a bullestomy technique for the injection of hydrogels containing small molecules. We aim to activate ERBB2 signaling in the wild type CBA adult mouse cochlea by introducing

WS3, an ERBB2/3 activator. We are investigating if this method can successfully activate ERBB2 signaling in SCs, and if it can promote hearing recovery after noise. Other studies have suggested potential roles for EGF family ligands in promoting inner ear regeneration. Our lab found that overexpression of ERBB signaling correlates with proliferation in cochlear SCs at early stage and improved hearing after noise at young stage. The underlying mechanisms for this improvement will be the focus of future study.

PS 656

Restoration of Cochlear Hair Cell Populations and Hearing Function in Noise-Deafened Guinea Pigs through Administration of Therapeutic siHes1 Nanoparticles

Richard D. Kopke; Matthew B. West; Xiaoping Du; Wei Li; Qunfeng Cai; Ibrahima Youm; Xiangping Huang; Jianzhong Lu; Weihua Cheng; Don Nakmali; Don Ewert; Richard Gammans
Hough Ear Institute

As sensorineural hearing loss (SNHL) imposes a significant barrier to communication and preserved quality of life, the inability of the human cochlea to spontaneously regenerate lost auditory hair cells (HCs) represents a distinct challenge for clinicians to overcome. Our approach to potentially reverse this life-altering condition is achieved through localized injection of small interfering ribonucleic acids (siRNAs) encapsulated within biodegradable poly(lactic-co-glycolic acid) (PLGA) nanoparticles (NPs). This approach induces transient silencing of the Notch pathway effector protein, *Hes1*, and a reciprocal elevation of *Atoh1* expression. This targeted molecular response, in turn, promotes the phenotypic conversion of supporting cells into morphologically-mature HCs.

Through multiple iterations conducted in live-animal models, we have consistently achieved broad, clinically-significant functional recovery that corresponded with wide-spread restoration of both inner HCs (IHCs) and outer HCs (OHCs) throughout the cochlea. Initial experiments involved inducing severe SNHL with a high-level noise exposure in adult guinea pigs followed by a 10-day intracochlear infusion of either placebo NPs or therapeutic *siHes1* NPs. Progressive auditory brainstem response (ABR) threshold recoveries were measured over the entire twelve-week time course of the study, consistent with a continuous and sustainable therapeutic response. Over the course of multiple independent follow-on studies, this pattern of broad, functional recovery has been reproducible and scalable upon reducing the infusion period from ten-days down to 24-hours in noise-deafened guinea pigs. The magnitude of hearing recovery has consistently been greatest in the high frequency basal region of the cochlea, and hearing recovery has progressed until the termination of the experiments. Furthermore, in recent experiments, we have document consistent, treatment-specific restoration of OHC function through recovery of distortion product otoacoustic emissions that correlated with tonotopic OHC regeneration in noise-deafened guinea pigs.

The current aim of this technology is to achieve therapeutic efficacy through intratympanic injection and delivery of *siHes1* NPs through the round window membrane (RWM). PLGA encapsulation has been shown to aid in this active transport process, protecting the siRNA payload during its translocation across the RWM and subsequent distribution throughout the cochlea. Ongoing studies have demonstrated that middle ear (ME) delivery of *siHes1* NPs in a temperature-sensitive hydrogel matrix can achieve adequate levels of drug delivery and target knockdown within the cochlea to induce a therapeutic response. Future studies are aimed at determining if the ME delivery approach can successfully and reproducibly regenerate HCs and restore hearing.

Human Auditory Development

PS 657

Development of Binaural Pitch Fusion and Discrimination in Children with Normal Hearing, Hearing Aids, and Cochlear Implants

Morgan Eddolls[1]; Curtis Hartling[1]; Jennifer Fowler[1]; Germaine Stark[1]; Bess Glickman[1]; Yonghee Oh[2]; Alicia Johnson[1]; Holden Sanders[1]; Lina Reiss[1]
[1]Oregon Health and Science University; [2]University of Florida

Children with hearing loss potentially have central auditory processing abilities that differ from their normal-hearing (NH) peers due to disruption of auditory input and/or abnormal stimulation from hearing devices during development. In addition, central auditory processing abilities may be developing in the age range of 6-12 years old. In this study, we conducted longitudinal measurements of binaural pitch fusion and interaural pitch discrimination in children with NH (n=25), bilateral hearing aids (HA; n=10), bimodal cochlear implants (CI; n=11), and bilateral CIs (n=18). Age at start of testing ranged from 6-9 years old, and measurements were repeated annually for at least 3 years.

For all measurements, stimuli were tones presented through headphones or electric pulse trains presented to individual electrodes, depending on hearing device combination. Binaural pitch fusion was measured

using simultaneous, dichotic presentation of reference and comparison stimuli in opposite ears. The reference ear was stimulated with a fixed frequency (1600 Hz) or electrode (mid-apical in array), while the comparison ear was simultaneously stimulated with varying frequency or electrode. The child was asked if they heard one or two sounds. The fusion range was calculated as the range of comparison stimuli that fused with the reference more than 50% of the time. Interaural pitch discrimination was measured using a fixed reference stimulus with comparison stimuli varied, presented sequentially in a two-interval procedure. The child was asked to choose which stimulus sounded higher in pitch. Interaural pitch discrimination ability was measured as the pitch match range, the range of stimuli ranged higher than the reference stimulus between 25%-75% of the time.

The data collected in the first year showed that all children, except bimodal CI children, had broader binaural fusion compared to their adult cohorts. NH and bimodal CI children also had narrower fusion than bilateral HA children. Similarly for interaural pitch discrimination, NH children had significantly broader pitch match ranges than NH adults and narrower pitch match ranges compared to HA and CI children. No correlation was observed between binaural fusion ranges and interaural pitch match ranges. Initial analyses of the longitudinal data suggest that both binaural fusion and pitch match range become narrower during development, when controlled for group. The findings suggest the importance of device combination and experience with auditory stimulation for central auditory processing abilities in children during development.

PS 658

Developmental Delays Account for Some, but Not All, Aspects of Auditory Processing Impairments in Children with Language-based Learning Problems

Silvia Bonacina; Travis White-Schwoch; Jennifer Krizman; Trent Nicol; Nina Kraus
Northwestern University

One influential hypothesis is that language-based learning problems (LPs), such as dyslexia, specific language impairment, and/or auditory processing disorder, may be characterized as developmental delays in auditory processing (Wright and Zecker, 2004). We tested this hypothesis by comparing frequency-following responses (FFRs) to the speech sound "d" in school-aged children (ages 8-14 years) with and without diagnosed learning problems to developmental trajectories mapped in > 500 listeners ages 3-26 (Krizman, Bonacina, and Kraus, 2019). We focused on three aspects of auditory processing previously implicated in language development: response consistency, spectral encoding (175-750Hz), and timing (Banai et al., 2009; Hornickel et al., 2012; Hornickel and Kraus, 2013; White-Schwoch et al., 2015).

First, we examined the difference in the response of 26 children with LP diagnosis with respect to an age- and sex- matched group of 31 typically developing children (TD). LP children's responses were less consistent, smaller, and later than the control group.

Next, we compared the results for those two groups of school-age children to a normative population of 516 typically developing listeners across three different age groups: early childhood (ages 3-5), adolescence (age 14-15), and young adults (ages 22-26). We mapped LP children onto the typical developmental trajectory to ascertain the extent—and attempt to pinpoint the emergence—of their auditory processing impairments. For response consistency and timing, LP children's responses resembled younger children's responses, whereas TD children's responses were more similar to adolescents' responses—consistent with the predictions of the developmental delay hypothesis. In contrast, for spectral encoding, LP children appeared to have smaller responses than both younger children and adolescents, suggesting either a lack of maturation with a predictable group difference since early childhood, or a precocious decline.

Together, this evidence reveals that the developmental delay hypothesis can account for deficits in certain aspects of neural sound processing (response consistency and timing) but not others (spectral encoding) in children with language disorders.

Supported by: NIH (HD069414) and Knowles Hearing Center

PS 659

The ability to process soft speech and speech in noise is related to language outcomes in children with hearing loss

Monika-Maria Oster[1]; Yoko Ishii[1]; Nicholas Tan[2]; Ashley Moore[1]; Son A Chang[1]
[1]Listen and Talk; [2]Creighton University

Children with hearing loss have greater difficulties processing speech in background noise and at a distance than children with typical hearing. Yet, learning environments are typically noisy and teachers often speak at a distance. To what extent the ability to process speech in noise and soft speech is related to vocabulary and language outcomes in children with

hearing loss, is not fully understood. This question is investigated in a group of 28 3- to 5-year-old children with bilateral mild-to-profound hearing losses (17 hearing aids (HAs), 11 bilateral cochlear implants (CIs)). All children are enrolled in a specialized Listening and Spoken Language preschool program and participate in annual functional assessments of speech perception (NU-CHIPS and PBK-50), vocabulary (R/EOWPVT) and language (CELF). The ability to process speech in noise is evaluated by comparing the percentage of correctly identified words presented at 50dB in quiet and in multitalker babble (+5dB SNR), the ability to process soft speech by comparing percent correct at 50dB HL and 35dB HL in quiet. Preliminary results indicate a significant correlation between age (chronological and listening age) and the ability to process speech in noise and soft levels in both children with HAs and with CIs. However, this relationship appears stronger in children with HAs than CIs. Mean vocabulary and language scores fall within the range expected for typically hearing same-age peers. Children with HAs and CIs of the same listening age do not differ in their vocabulary and language scores, with the exception of receptive language and language structures, which are significantly higher in children with HAs. Overall, the ability to process speech in noise and at soft levels is weakly correlated with vocabulary and language in children with HAs and CIs. However, some age-dependent changes in correlations are observed: At age 3, better processing of speech in noise and at soft levels is correlated with lower vocabulary and language scores. However, by age 4, better perception of speech in noise and at soft levels is correlated with higher vocabulary scores, and by age 5 with higher language scores. In summary, the ability to process speech in noise and at quiet levels improves with age and listening experience, although it seems to improve faster for children with HAs than their CI counterparts. Furthermore, processing speech in noise and at soft levels appears related to changes in vocabulary and language in an age-dependent manner.

PS 660

Average Daily Speech Exposure for Fetuses and Preterm Infants

Brian B. Monson
University of Illinois at Urbana-Champaign

The quality and quantity of speech and language exposure during early childhood is believed to be predictive of language ability during later childhood development. However, the human auditory nervous system comes “online” *in utero,* at least as early as 23 weeks’ gestation. It has been demonstrated that intrauterine fetal experience with extrauterine sounds during this last trimester of gestation is sufficient to impact auditory brain development and neural responses to speech. How and whether fetal exposure to speech affects later childhood language development remain open and difficult questions. To begin to address these questions, we collected and analyzed fetal auditory exposure data for sounds generated in the extrauterine environment using small audio recorders worn by pregnant women during the third trimester of pregnancy. We also collected auditory exposure data for preterm infants staying in the neonatal intensive care unit. Averaged across more than 7000 hours of audio data, daily speech exposure for fetus subjects ranged from 3 to 6 hours, with an average of 4.5 hours, suggesting some newborns may begin extrauterine life with only 50% of the speech and language exposure of their peers. Average daily speech exposure for preterm infants was 3 hours, representing a substantial drop in speech exposure. Whether this variability in exposures is associated with variability in subsequent development remains to be seen and is the subject of follow-up with these participants.

PS 661

Relationship between Stimulus Frequency Ratios and Area of OHCs Contributing Generation of DPOAEs: Simulation using Finite-Element Model of Human Cochlea

Sinyoung Lee; Takuji Koike
Department of Mechanical and Intelligent Systems Engineering, Graduate School of Informatics and Engineering, The University of Electro-Communications, Japan.

Several studies (Moulin, 2000; Knight and Kemp, 2000) showed that the optimum frequency ratio f_2/f_1 of the stimuli varied for each component of DPOAE, e.g. $2f_1$-f_2 and $2f_2$-f_1, and we have also obtained similar measurement results. In this study, the relationship between frequency ratios and the levels of each DPOAE was investigated based on the area where OHCs contribute to the generation of DPOAEs.

DPOAEs were simulated by applying sound pressure composed of frequencies f_1 and f_2 to the stapes head of the finite-element model of human cochlea (Lee and Koike, 2017). The model includes the nonlinear activity of OHC represented by the excitation force as a function of velocity of the basilar membrane (BM). The sound pressure levels of f_1 and f_2 were equally set to be equivalent to 60 dB at the ear canal considering the pressure gain of the middle ear. The excitation force of OHC was obtained with changing f_2/f_1 from 1.1 to 1.3 and f_2 from 1 kHz to 4 kHz. The vibration amplitudes of each component of the stimulus and DPOAE on the BM were also simultaneously obtained.

The area where the OHCs exert enough excitation force to generate DPOAEs (i.e. contribution area) became wider at apical side with increase of f_2/f_1 due to increase of the distance between the CF locations of f_2 and f_1. By contrast, the CF location of each DPOAE moved farther away from the CF locations of the stimuli with increase of f_2/f_1. Thus, the level of lower sideband DPOAE, e.g. $3f_1$-$2f_2$ and $2f_1$-f_2, was decreased with increase of f_2/f_1, because distance between its CF location and the contribution area was increased.

The reason of variation of optimum f_2/f_1 for each DPOAE is considered that both of the width of the contribution area and the CF location of each DPOAE were changed depending on f_2/f_1. Change of f_2 also effected the contribution area and the CF location of each DPOAE.

PS 662

Investigation of Chronological Changes in Dynamic Characteristics of Neonatal Ears Using Sweep Frequency Impedance (SFI) Technique

Nattikan Kanka[1]; Michio Murakoshi[2]; Shinji Hamanishi[3]; Hiroshi Wada[4]
[1]Kagoshima University; [2]Kanazawa University; [3]Tohoku Gakuin University; [4]Tohoku Bunka Gakuen University

Comparing to adults, neonates have apparently smaller and immature ears in structure and function. In terms of its dynamic characteristics, our earlier studies reported that there are two resonance frequencies (RFs) at about 0.3 kHz and 1.1 kHz in neonates, whereas only one RF at about 1.1 kHz in adults (Wada *et al.*, 1998; Murakoshi *et al.*, 2013). Owing to such differences, here we investigated the chronological changes of the outer and middle ear dynamic characteristics in neonates.

Sweep frequency impedance (SFI) meter was designed for middle ear diagnosis. This device measures sound pressure level (SPL) by presenting a sound of sweeping sinusoidal frequency ranging from 0.1 kHz to 2 kHz to the external ear canal at 50-daPa intervals of static pressure ranging from +200 daPa to –200 daPa. The reflected sound is recorded by a microphone and is sent to a personal computer for data analysis. The results obtained from SFI tests are represented by SPL curves, showing the relationship between the input sound frequency and the SPL. In this study, we performed the SFI tests to 2 Japanese healthy neonates from birth to approximately 3 and 5 months of age. The tests were conducted when neonates were in good health condition and were naturally sleeping.

As shown in Fig. 1., with an increase in chronological age, the first variation of SPL curve, i.e., the RF_1 and the changes in SPL (ΔSPL_1), related to the external ear, showed significant changes. The RF_1 increased continuously, whereas the ΔSPL_1 decreased and became unmeasurable by about 5 months after birth. These results suggested that the rigidity of the external ear canal wall increases with chronological age, and the oscillatory behavior of the external ear canal wall tends to disappear by about 5 months of age. In contrast, changes in RF_2 and ΔSPL_2, related to the middle ear, were negligibly small. Our studies are consistent with the results from the previous research findings whereby the chronological age is approximately 5 months of age (Aithal *et al.*, 2017). This tendency may become useful for further neonatal hearing studies.

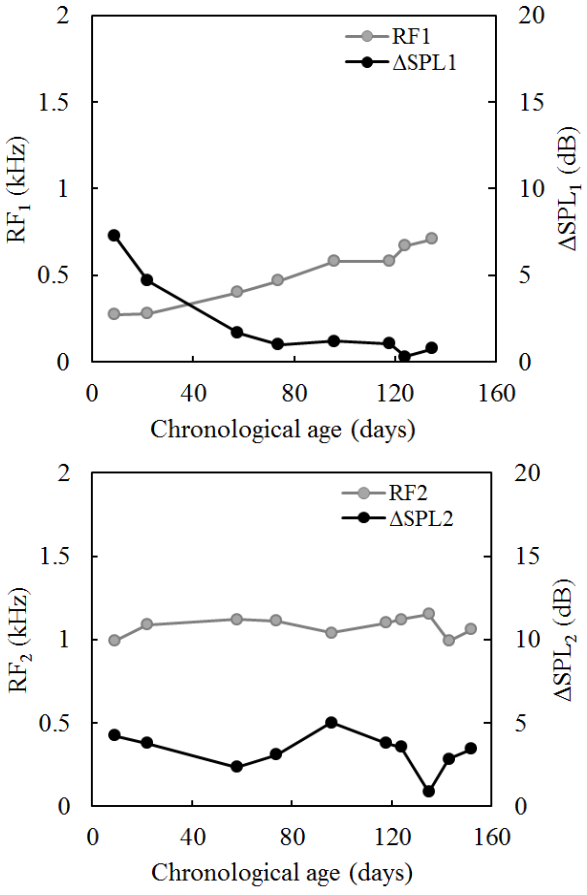

PS 663

Neural Habituation of the Mismatch Response Predicts Pattern Detection and Speech Discrimination in Infants

Kristin Uhler[1]; Phillip Gilley[2]; Sharon Hunter[1]
[1]University of Colorado Anschutz Medical Campus; [2]University of Colorado, Boulder

The development of speech perception, including speech discrimination, depends partially on early exposure to and experience with highly salient and behaviorally relevant acoustic input. Our previous research has highlighted the importance of quality sound access for the development of

speech discrimination in infants as young as one month of age. Specifically, we have demonstrated that the speech-evoked mismatch response (MMR_{SE}) is modulated by discrimination difficulty and may be useful in predicting later behavioral outcomes in infants. However, there is wide variability in discrimination outcomes that may affect the utility of MMR_{SE} as a biomarker; for example, the absence of a response may not be an accurate indicator of discrimination but a reflection of the still developing neural generators for engaging in and completing the task. We examined the MMR_{SE} as a function of the time elapsed from the last deviant stimulus to determine whether the evoked potential magnitudes preceding a deviant trial could predict the identification of a difference response and whether such differences might correlate with later behavioral outcomes. Participants included 49 infants with normal hearing (mean age = 3.34 mo) and 42 infants with hearing loss (mean age =3.47 mo). EEG was recorded from 11 scalp electrodes during sleep and while the experimental stimuli played from a speaker at 70 dBA. Two speech contrasts (/a/-/i/ and /ba/-/da/) were presented in an MMR/oddball paradigm (duration=500 ms; interstimulus interval=1006 ms) with a probability of 0.85 for selecting a standard stimulus (/a/ or /ba/) and a probability of 0.15 for selecting a deviant stimulus (/i/ or /da/). EEG data were transformed using the continuous wavelet transform (CWT; 64 log-spaced scales; 1 to 18 Hz) and then separated into single trials classified as a standard or deviant response. The MMR_{SE} was computed for each contrast and the response magnitudes were treated as predictor variables in a multi-dimensional scaling analysis of scores on a later behavioral task (+4 months) in the same participants using the same speech contrasts (visual reinforcement infant speech discrimination, VRISD). Results from that analysis revealed a significant correlation between the elapsed deviant time and changes in response frequency and magnitude, and a significant correlation between the MMR_{SE} magnitude and later VRISD scores. Taken together, these results suggest that acoustic audibility and salience are both necessary but not sufficient for speech discrimination and that discrimination is dependent on the brain's ability to recognize and habituate to complex stimulus patterns.

PS 664

Relationships Between Newborn Frequency-Following Responses and Follow-up Measures of Language and Cognition in Neonates with Hyperbilirubinemia.

Gabriella Musacchia[1]; Jiong Hu[1]; Qin Hong[2]; Mei-ling Tong[2]; Nikolas Blevins[3]; Natalie Sienko[1]; Matthew B. Fitzgerald[3]
[1]University of the Pacific; [2]Women's Hospital of Nanjing Medical University; [3]Stanford University

Bilirubin-induced neurologic dysfunction (BIND) is a spectrum of central nervous system (CNS) disorders that frequently impacts auditory system development in infants. Bilirubin-related toxicity can have a profound effect on auditory system development, including hearing and language outcomes. Performance on traditional audiologic measures such as the click-evoked auditory brainstem response (ABR) have little relationship to the level of bilirubin in the bloodstream, suggesting that this tool may be suboptimal for identifying infants at risk for transient or sustained neurologic deficits. In contrast, we have demonstrated a negative relationship between transcutaneous bilirubin (TcB) levels and the speech-evoked frequency following response (FFR), such that high TcB level is associated with a poorer frequency-following response (FFR) to speech. This suggests that the FFR could be a tool to predict which children are at greatest risk for transient or sustained neurologic deficits. At present, however, it is unknown whether suboptimal encoding of speech signals (as determined by the FFR) in the first few weeks of life is related to future developmental delays in language and cognition. As a first step towards addressing this question, we collected follow-up sensory, language and cognition behavioral measures consisting of the Griffiths Scales of Child Development and the Gesell Developmental Observation test battery over a two-year post-test period in children diagnosed with hyperbilirubinemia and those without. Our hypothesis is that poor FFRs observed to speech signals in neonates will increase the likelihood of poor language and cognitive outcomes with increasing age. The results of this study will advance our understanding of neurologic deficits associated with preterm birth and exposure to high TB levels, and may help to identify which children are at higher risk for sustained deficits.

Inner Ear: Drug Delivery

PS 665

L-type Voltage-Gated Calcium Channel Agonists Improve Hearing Loss and Modify Ribbon Synapse Morphology in the Zebrafish Model of Usher Syndrome Type 1

Alaa Koleilat[1]; Joseph Dugdale[1]; Trace Chirstensen[1]; Jeffrey Bellah[2]; Aaron Lambert[3]; Mark Masino[3]; Stephen Ekker[1]; Lisa Schimmenti[1]
[1]Mayo Clinic; [2]Columbia University; [3]University of Minnesota, Twin Cities

Usher Syndrome (USH) is the most common cause of deafness and blindness in children and account for 10% of genetic hearing loss. Current treatment options include hearing aids and cochlear implants. In this study we explore developing the first pharmacotherapy for the

treatment of USH Type 1 due to variants in MYO7A. The *mariner* mutant, a zebrafish model of USH1, is deaf and exhibits circular swimming with balance defects. Through transmission electron microscopy and immunohistochemistry techniques we explored the hair cell biology of this model. We discovered that this model has fewer glutamatergic vesicles tethered to the ribbon synapse with a comparable ribbon area. We discovered that the *mariner* mutant has fewer total active hair cells, fewer total CTBP2 puncta and a different distribution of CTBP2 puncta compared to wildtype. We also assessed post-synaptic cell activity by analyzing expression of MAGUK, a kinase family that is involved in anchoring and targeting glutamate receptors. We identified that the mariner mutant has fewer active post-synaptic cells, fewer total MAGUK puncta and a different distribution of MAGUK puncta compared to wildtype. Additionally, we quantified both the circular swimming and the acoustic startle response of wildtype and mutant fish. We identified that *myo7aa*$^{-/-}$ fish have larger turning angles as a function of time and have little to no acoustic startle response compared to wildtype. We then sought to rescue the abnormal phenotypes exhibited by the mutant through the use of L-type voltage-gated calcium channel agonists. We assessed the efficacy of these compounds on changing hair cell morphology and gene expression as well as restoring behavior through our swimming and hearing assessments. Our data support that treatment with L-type voltage-gated calcium channels causes a morphologic change at the ribbon synapse, both in number of tethered vesicles and the distribution of CTBP2 and MAGUK puncta, shifts swimming behavior towards wildtype swimming, and improves startle to sound. This data represents a significant step towards discovering compounds to treat hearing loss caused by human pathogenic variants in *MYO7A*.

PS 666

Drug Delivery into the Cochlea is Influenced by Proximity of the Cochlea Aqueduct to Injection Site

Sara Talaei[1]; Michael Schnee[1]; Ksenia A. Aaron[1]; Anthony Ricci[2]
[1]Stanford University; [2]Department of Otolaryngology and Department of Molecular and Cellular Physiology, Stanford University

Developing drug delivery technologies for reliable and uniform distribution into the cochlea is substantial for inner ear therapeutics. The inner ear is a fluid filled compartment surrounded by bone that is highly mechanosensitive so that access is difficult and the structure is easy to damage. Tracking dye progression through the cochlea injected from different sites will provide information for optimizing drug delivery. We hypothesized that the proximity of cochlea aqueduct to the injection site will influence the distribution of injected compound in the cochlea. We injected a dye into the cochlea from two common injection sites (i.e. round window membrane (RWM) and posterior semicircular canal (PSCC)) and monitored the dye distribution within the cochlea and brain up to 1 hour after injection. We present the injection results from neonatal and adult mice. A computational model was also used to validate our experimental results.

The dye distribution in PSCC injections was more uniform in the cochlea compared to RWM injections. A steep gradient from the base to apex was observed in RWM injections that over time became more uniform, post injection. PSCC injections delivered a higher level of dye into the cochlea while more dye was detected in the brain of RWM injected animals. Dye level in the cochlea of PSCC injected neonates was significantly reduced at one-hour post injection but it remained stable in adults. In our computational model velocity was used as an indicator of the flow within the inner ear perilymphatic space during injection. The velocity distribution patterns for RWM and PSCC injections were similar to our experimental results.

The cochlea aqueduct opening into the perilymphatic space is close to the RWM, prior to the cochlea, while the PSCC injection site is located at the distal end of perilymphatic space with the cochlea between the injection site and the cochlea aqueduct. Our data suggest that the cochlea aqueduct shunts flow prior to reaching the cochlea while PSCC injection enables higher levels of the injected compound flow into the cochlea with a more uniform pattern from base to apex. Therefore, the location of the injection site relative to the cochlea aqueduct is an important parameter influencing drug distribution within the cochlea via direct injections into the inner ear.

Acknowledgements: NIA grant 5PO1 AG051443-01A1, NIDCD RO1 DC009913, Stanford Medicine Dean's Postdoctoral Fellowship and Core support from the Stanford Initiative to Cure Hearing Loss through the Bill and Susan Oberndorf Foundation

PS 667

Alginate as Dexamethasone Eluting System for Treatment of the Inner Ear

Jana Schwieger[1]; Thomas Lenarz[2]; Verena Scheper[1]
[1]Hannover Medical School; [2]Hannover Medical School, Hannover, Germany

Background
Profound sensorineural hearing loss is successfully treatable by implantation of a cochlear implant (CI)

into the scala tympani of the inner ear. The inserted electrode stimulates the spiral ganglion neurons (SGN) electrically to induce an action potential by bypassing the functionless hair cells. One important factor for a reasonable function of the CI is a focused stimulation of small clusters of SGN to achieve a best possible hearing impression. This can be hindered by an excessive foreign body reaction with fibrotic tissue or even bone tissue formation in the inner ear. The grown tissue covers the electrode and isolates it, which leads to a spread of excitation and thereby an unfocussed stimulation of the SGN. Treatment with dexamethasone (Dex) can reduce this tissue encapsulation. A coating of the electrode with alginate can reduce the insertion forces which may additionally reduce the foreign body reaction. We combined both strategies and tested the incorporation of Dex in alginate and the effect of released Dex on spiral ganglion cells (SGC).

Methods

Dex was mixed as pure powder (9β-Fluor-16β-methylprednisolone) or as solution (dexamethasone dihydrogenphosphate-dinatrium, Fortecortin®) with alginate. Pure alginate served as negative control. A small drop of alginate solution was placed in the center of each poly-L-lysine pre-coated well and was subsequently crosslinked with $BaCl_2$-solution for 20 minutes at 37 °C. Afterwards, dissociated SGC were seeded into the wells and incubated with medium including 10 % FCS for 24 and 48 hours, followed by fixation with 4 % PFA and cell staining. The growth behavior of cells was compared between the different groups.

Results

Dex of both formulations was successfully mixed with the alginate and did not hinder the application of the alginate solution to the cell culture plate and a controlled and adherent gelation. The pure Dex powder allowed the addition of a higher concentration than the Dex solution due to limitation by dilution of the alginate. The SGC rarely adhered to the alginate surface in general and the addition of Dex reduced the growth of the cells.

Conclusions

The combination of Dex with alginate is a promising option to reduce the growth of fibrous tissue around the CI-electrode. The alginate prevents an adhesion of cells and the Dex inhibits the cell growth. Further investigations have to focus on the Dex-release kinetics, the coating procedure of the electrode and the long term stability.

PS 668

Mass Spectrometry Imaging shows drug distribution in the cochlea after round window application

Barbara Pinheiro[1]; Monika Kwiatkowska[2]; Marcus Müller[1]; Hubert Löwenheim[1]; Michael Bös[2]
[1]Tübingen Hearing Research Centre, Department of Otolaryngology-Head & Neck Surgery, Eberhard Karls University Tübingen, Germany; [2]Acousia Therapeutics GmbH, Tübingen, Germany

Mass Spectrometry Imaging (MSI) allows label-free imaging to study the distribution of specific drugs in biological samples like tissue sections. The technique is based on matrix-assisted laser desorption ionisation mass spectrometry technology, and was applied the first time to quantify the distribution of drugs and their metabolites in the cochlea after local drug application. Local drug delivery to the inner ear offers valuable benefits for the treatment of hearing loss, it provides better accuracy in dosage and avoids possible side effects related to systemic application. Nevertheless, therapeutic efficacy depends on a plethora of pharmacokinetic parameters culminating in uptake into the targeted cochlear tissue. Several studies have already analysed the principles underlying the entry and distribution of drugs in the inner ear fluid spaces. However, MSI allows to determine the final and functionally relevant spatial and temporal distribution of drugs in the targeted tissue.

We are developing small molecules designed to treat disease-specific mechanisms of sensorineural hearing loss. In the present study these drugs (ACOU063, ACOU085) were administered to the round window niche. MSI was performed on fixed serial frozen sections to collect information about drug specific inner ear tissue distribution. Conventionally stained aligned adjacent sections serve as exact template for cochlear morphology. Besides information about the amount of drug reaching the cochlear tissue, MSI visualises the localization of drugs and their metabolites in specific targeted tissue regions such as the organ of Corti, the spiral ganglion and the stria vascularis. In the guinea pig we were able to trace the drug and a metabolite in the auditory nerve, the spiral ganglion and the stria vascularis. Interestingly, the compounds were traced along the complete tonotopic axis from base to apex of the cochlea. MSI is a valuable analytical tool, providing high spatial distribution and spectral resolution for primary drug compounds as well as their metabolites. This pharmacokinetic knowledge is fundamental to interpret the pharmacodynamic effects of drug candidates and their refinement from early-stage drug discovery to preclinical development and future clinical application.

This work was supported by a grant from the European Union's Seventh Framework Program for research, technological development and demonstration under grant agreement number 603029 (acronym OTOSTEM). We thank Malcolm Clench, Professor of Mass Spectrometry at Sheffield Hallam University, for imaging.

PS 669

Rapid Method for Alzet Pump Implantation for Chronic Drug Delivery into Mouse Cochlea

Frederic Depreux[1]; Claus-Peter Richter[2]; Donna S. Whitlon[1]
[1]Northwestern University; [2]Northwestern University, Dept Otolaryngology

Various techniques have been used to deliver drugs or viral vectors into the cochlea of adult mice. While acute perfusion of scala tympani did not show major challenges, it was more difficult to maintain delivery of compounds over several weeks. Here we describe a method of surgically implanting a mini-osmotic pump for long term drug delivery. For pain management, male CBA/CaJ received a subcutaneous dose of 0.05 mg/kg Buprenex ninety minutes prior to the surgery, followed by a subcutaneous injection of 0.9% sodium chloride solution for hydration thirty minutes later. Anesthesia was induced with 3% isoflurane in oxygen and was maintained by isoflurane 1% to 3%. For the surgery, the animals were placed in a supine position. An incision (approximately 2 cm) was made from the lower mandible towards the right arm. Retracting the skin exposed the submandibular glands, which were separated gently by blunt dissection. Elevation of the posterior belly of the digastric muscle, avoiding manipulation of the facial nerve, provided access to the bulla. A circular hole, approximately 200 µm in diameter, was created with an Oto-laser fiber (Omniguide) connected to a Sharplan CO_2 laser operated in single pulse mode, pulse length 100 ms and radiant power setting at 5 W. This hole was then widened caudally and rostrally with fine forceps until the basal cochlear turn and the stapedial artery were visible. The cochleostomy was created with the CO_2 laser, holding the tip of the laser fiber about 300 µm away from the target area. A single 100 ms – pulse at 7W power setting was sufficient to create the opening into the cochlea. A custom-made catheter consisting of two medical grade tubes (Polyimide, of Microlument, Oldsmar, FL and TYGON®, U.S. Plastic Corp.®, Lima, OH) attached to an ALZET micro-osmotic pump (Model 1004, 0.11 µl/h, 28 days; Durect, Corp. Cupertino, CA) was inserted into the basal turn of the cochlea. The cochleostomy was sealed with the silicone stopper at the catheter and the tubing was secured with dental acrylic at the bulla. The bulla was sealed with the acrylic and the pump was placed on the animals' back. The incision was closed in two layers using 6-0 PDS*II and 6-0 ethilon (Ethicon Inc., Sommerville, NJ). The average duration of the surgery was about 64 min from induction to recovery. The average recovery time for animals was 8 min.

Funded by the Office of Naval Research # N000141812508

PS 670

Gel-Mediated Electrospray Assembly of Silica Supraparticles for Sustained Drug Delivery to the Inner Ear

Yutian Ma[1]; Andrew Wise[2]; Mattias Björnmalm[1]; Christina Cortez-Jugo[1]; Frank Caruso[3]
[1]The University of Melbourne; [2]Bionics Institute; [3]The University of Melbourne, Australia

Supraparticles (SPs), assembled from smaller colloidal nanoparticles, can serve as depots of therapeutic compounds and are of interest for long-term, sustained drug release in biomedical applications. However, current synthesis methods used to achieve high drug loading that involve biocompatible materials are often tedious, thereby limiting the translation of SPs to diverse applications. In this presentation, a simple, effective, and automatable alginate-mediated electrospray technique for the assembly of robust spherical silica SPs (Si-SPs) will be described. Primary silica particles were encapsulated in alginate to form alginate/silica supraparticles (Si-SPsalg) crosslinked with ionic agents. The size and shape of Si-SPs can be tailored by controlling the concentrations of alginate and silica nanoparticles used and key electrospraying parameters such as flow rate, voltage, and collector distance. The electrospray technique also results in robust, spherical SPs with uniform size and requires minimal manual intervention: important properties for quality control, translational into clinical applications, and commercialization. The Si-SPs demonstrate negligible cytotoxicity, good degradability, high drug loading capacity (~7.3 µg of neurotrophins per SPs) and long-term (>4 months) drug delivery behaviour, making them a promising platform for long-term neurotrophin delivery to the inner ear to treat sensorineural hearing loss.

PS 671

Cochlear Pharmacokinetics â€“ Impact of 3D Segmentation using Convolutional Neural Networks

Sanketh S. Moudgalya[1]; Xiaoxia Zhu[2]; Mikalai M. Budzevich[3]; Joseph P. Walton[4]; Nathan D. Cahill[5]; Robert D. Frisina[2]; David A. Borkholder[6]
[1]Rochester Institute of Technology; [2]Medical Engineering Dept., Global Center for Hearing & Speech Research, Univ. South Florida; [3]H. Lee Moffitt Cancer Center &

Research Institute; [4]Department of Communication Sciences & Disorders, University of South Florida, Tampa, FL; Department of Medical Engineering, University of South Florida, Tampa, FL; Global Center for Hearing and Speech Research, University of South Florida, Tampa, FL; [5]School of Mathematical Sciences, Rochester Institute of Technology; [6]Microsystems Engineering, Dept. of Electrical and Microelectronic Engineering, Rochester Institute of Technology

One current approach to cochlear pharmacokinetic modeling empirically measures the spatio-temporal concentration of contrast agents within cochlear scalae, including scala tympani (ST), scala media (SM) and scala vestibule (SV), and then uses these empirical measurements to learn the transfer coefficients within the cochlea [Moudgalya S. et al., 2019]. Computing the concentration from key regions of the mouse cochlea requires accurate segmentation of ST, SM, and SV from a CT scan. Conventionally, segmentation is carried out by deformably registering a high resolution pre-defined template (cochlear atlas) to the CT scan. Although this technique predicts fairly accurate cochlear regions in a scan, it relies on an atlas that is constructed from a single mouse and does not capture anatomical distinctions that are evident across different mice. These variations often cause inconsistencies in the extracted concentration due to accidental inclusion of small boney regions in the segmentation. Moreover, deformable registration techniques are computationally expensive (hours for a typical scan at 16 micron resolution) and are computed for every new scan. Our work focuses on using state-of-the-art, convolutional neural network (CNN) based 3D segmentation algorithms to train a model that predicts scala segments directly from a CT scan. CNNs are known to generalize better than conventional registration and segmentation algorithms, by learning the salient features in every sample across a dataset, and using these features during prediction. CNN models have two stages, training and prediction. The training stage initializes the model with trainable weights, enabling the model to learn to segment after iterating multiple times over scans previously segmented using registration to an atlas. The prediction stage uses these trained weights to segment a new scan into its respective cochlear regions. Although the training stage can be computationally expensive, the prediction stage can accomplish segmentation of a scan in few seconds, achieving significant improvement in processing time. Results on segmentation accuracy are presented and compared to those obtained from atlas-based registration using the Jaccard Index and signal-to-noise ratio (SNR) of extracted concentrations. A key potential advantage of the CNN approach is the learned weights of the model can be transferred and fine-tuned to larger mammals like guinea pig and humans, whose cochleae exhibit similar image features to that of mice. In the future, an end-to-end pharmacokinetics pipeline can be setup wherein segmentation, concentration extraction, and determining transfer coefficients between scalae can all be accomplished using CNNs.

Supported by NIH NIDCD award R01 DC014568.

PS 672

Verification of Therapeutic and Adverse effect of SU02 for Intratympanic Drug Delivery.

Hye Lee[1]; Yu-Jung Hwang[1]; Tae-Soo Noh[2]; Moo Kyun Park[3]; Jun Ho Lee[4]; Seung-Ha Oh[5]; Myung-Whan Suh[5]
[1]Department of Otorhinolaryngology, Seoul National University Hospital, Korea; [2]Department of Otorhinolaryngology-Head and Neck Surgery, Seoul National University College of Medicine, Korea; [3]Seoul National University; [4]Department of Otorhinolaryngology-Head and Neck Surgery, Seoul National University College of Medicine; [5]Department of Otorhinolaryngology-Head and Neck Surgery, Seoul National University College of Medicine, Korea

Objective

Intratympanic (IT) steroid injection is now a mainstream therapy to increase the hearing outcome and reduce adverse effects of systemic steroid administration. But, because the drug/vehicle drains through the Eustachian tube, the treatment effect does not last long and repeated injection are needed in many cases. SU02 was developed to improve the treatment outcome as well as to sustain the therapeutic period with a single injection. In this study we wanted to verify the therapeutic and adverse effect of SU02 in an ototoxic hearing loss animal model.

Methods

Twenty three young male SD rats were used. IT dexamethasone (D, 12mg/ml) was delivered by two different carriers: saline (N=16), SU02 (N=20). Hearing loss animals with no treatment served as a control group (N=10). Rats were treated with IT drug/vehicle injection prior to ototoxic hearing loss. two days later, cisplatin (2 mg/kg), gentamicin (120 mg/kg) and furosemide (90 mg/kg) were intravenously administered for two consecutive days. The auditory brainstem response (ABR) thresholds (8, 16, and 32 kHz) were measured for 1, 4, 8, 12, 21, 30, and 45 days (post hearing loss day, PHD) after hearing loss. Endoscopy of the tympanic membrane (TM) and micro-CT were performed to evaluate how long the drug/vehicle lasted in the middle ear.

Results

When visualized by micro-CT, the drug/vehicle lasted in the middle ear for 43.5±15.6 days in the SU02 group.

This was significantly longer than that of the saline+D group (0.0±0.0 days, $p < 0.001$). There was no ear which developed infection and/or inflammation evaluated by endoscopy (0% in saline+D group and 0% in the SU02 group). The hearing was superior in the SU02 group compared to the saline+D and control group. ABR threshold at 32 kHz in the SU02 group was 39.8±13.6 dB SPL at PHD30 and 38.3±13.1 dB SPL at PHD45. In the saline+D group, it was 60.3±16.8 dB SPL ($p=0.001$) at PHD30 and 63.4±12.5 dB SPL ($p< 0.001$) at PHD45. In the control group, it was 70.5±9.8 dB SPL ($p< 0.001$) at PHD30 and 72.0±5.4 dB SPL ($p< 0.001$) at PHD45.

Conclusions

The treatment outcome in terms of hearing threshold was better when treated by SU02 compared to the conventional treatment (saline+D). The SU02 may be used in patients who developed ototoxic hearing loss. It may also be considered as a preventative therapy for patients who are at high risk of hearing loss due to chemotherapy or anti-tuberculosis therapy.

PS 673

In Vitro Biocompatibility of Engineered Magnetic Nanoparticles in Mouse Organ of Corti Explant Cultures

Nancy J. Zhou[1]; Mukund M. Goyal[2]; Philippe Vincent[1]; Charles C. Della Santina[1]; Elisabeth Glowatzki[3]; Chao Wang[2]; Daniel Q. Sun[1]

[1]Johns Hopkins University School of Medicine; [2]Johns Hopkins University; [3]Johns Hopkins School of Medicine, Baltimore, MD, USA

Background

Composed of an iron oxide nanocore surrounded by a biocompatible coating, magnetic nanoparticles (MNPs) are emerging as promising drug delivery vehicles for the inner ear with the potential of overcoming passive diffusion-related barriers into and within the labyrinth for intratympanically-administered therapeutics. Coating thickness of MNPs is an important design parameter for labyrinthine drug delivery applications, affecting particle transport properties as well as drug loading and elution. Further, coating thickness may play an important role in biocompatibility by shielding the highly oxidative and potentially cytotoxic iron oxide nanocores from delicate inner ear sensory structures. The relationship between coating thickness and cytotoxicity has not been investigated in detail.

Methods

Polyethylene glycol-coated MNPs (PEG-MNPs) were synthesized with 12- and 3000-molecule PEG chains (PEG12 and PEG3000, respectively) and characterized using transmission electron microscopy, dynamic light scattering, and inductively coupled plasma mass spectrometry. The mid-turn of each organ of Corti was microdissected from neonatal (P3-P5) C57BL/6J mouse pups and individually cultured in growth media inoculated with PEG12 MNPs (0.1 or 0.5 mg/ml), PEG3000 MNPs (0.1 or 0.5mg/ml), or neomycin and kainic acid for 72 hours (n=3 for each condition) with and without an external magnetic field gradient (0.3T at surface). Immunohistochemistry was performed using NF200 and MyoVI antibodies for neurite and hair cell labeling, respectively. Images were acquired via confocal microscopy and inner hair cell (IHC), outer hair cell (OHC), and spiral ganglion neurite (SGN) counts were individually quantified using Image J and normalized by distance along the organ of Corti.

Results

Synthesized PEG12 and PEG3000 MNPs were composed of 7nm Fe_3O_4 nanocores with mean overall diameters of 47nm (PDI 0.20) and 150nm (PDI 0.28), respectively. Microscopy revealed particle clusters in close association with cultured explants for each particle and concentration tested. Data indicated that IHC, OHC, and SGNs counts were similar to saline control for both PEG12 and PEG3000 MNPs across the range of concentrations tested, while neomycin/kainic acid resulted in significant depletion of these counts. In addition, an applied external magnet field gradient orthogonal to each tissue explant surface during incubation did not lead to a difference in IHC, OHC, or SGN survival across MNP coating thickness and concentration.

Conclusions

Our results suggest that PEG-MNPs demonstrate histologic biocompatibility in mouse organotypic cultures across a broad range of coating thickness and concentrations, further informing the rational design of MNPs for labyrinthine drug delivery applications.

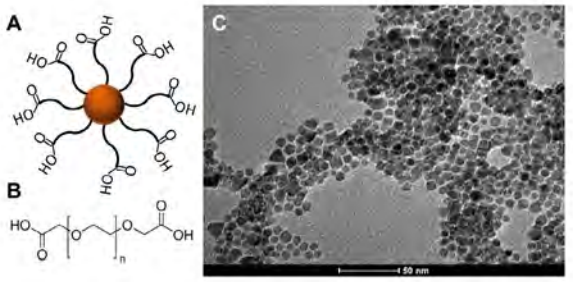

Fig 1: MNPs comprised of PEG chains grafted to an iron oxide core (**A**). Thickness of PEG coating can be controlled by tuning PEG polymer length, with n=12 and 3000 for thin and thick coating, respectively (**B**). Transmission electron microscopy image of synthesized MNPs coated with 3000-molecule PEG dispersed in saline (**C**).

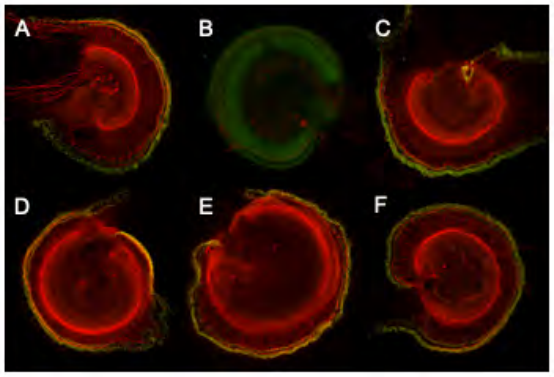

Fig 2: Confocal microscopy with staining for NF200 (red) and MyoVI (green) using Saline (**A**). Neomycin/Kainic Acid (**B**). PEG12 0.1 mg/ml (**C**). PEG12 0.5 mg/ml (**D**). PEG3000 0.1 mg/ml (**E**). PEG3000 0.5 mg/ml (**F**).

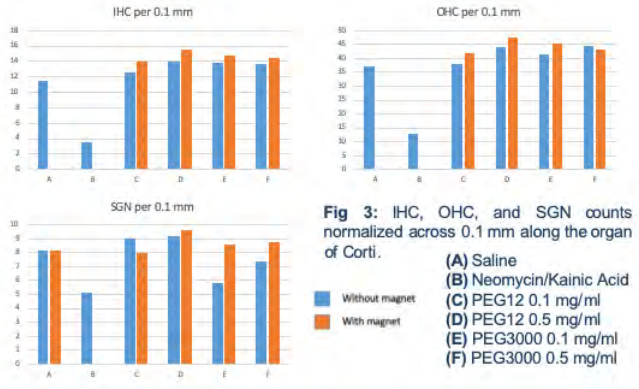

Fig 3: IHC, OHC, and SGN counts normalized across 0.1 mm along the organ of Corti.
(A) Saline
(B) Neomycin/Kainic Acid
(C) PEG12 0.1 mg/ml
(D) PEG12 0.5 mg/ml
(E) PEG3000 0.1 mg/ml
(F) PEG3000 0.5 mg/ml

PS 674

PLGA based implants for intracochlear drug delivery for isolated use or the use in combination with a cochlear implant carrier

Arne Liebau[1]; Eric Lehner[1]; Daniel Gündel[2]; Stefan Plontke[1]; Karsten Mäder[1]
[1]University Halle-Wittenberg; [2]Helmholtz-Centre Dresden-Rossendorf

The effective delivery of drugs to the inner ear is still an unmet medical need. Local controlled drug delivery to the cochlea is challenging due to the hidden location, small volume and high sensitivity of this organ. A local intracochlear delivery of drugs would avoid the problems of intratympanic (extracochlear) and systemic drug application, but is more invasive. The requirements for such a delivery system include a small size, appropriate flexibility and biodegradability. We developed biodegradable dexamethasone loaded PLGA extrudates for the controlled intracochlear release. In order to achieve the desired flexibility, Polyethylene glycol (PEG) was used as a plasticizer. Simulation of the pharmacokinetics of the human inner ear based on the in vitro release profile of the extrudates support the expectation that a constant perilymph drug level is obtained after few hours and retained over several weeks. The drug carrier system was tested for implantation in the human inner ear in 11 human temporal bones. $BaSO_4$-loaded implants of the drug carrier system with different dimensions were implanted into the scala tympani through round window access. An electrode carrier of cochlear implant devices from different manufacturers was first implanted in 6 of the temporal bones and afterwards the extrudate of the drug carrier system in order to test whether it also would be possible to use the drug delivering device in cochlear implant surgery for an accompanying drug therapy. Implanted temporal bones were measured in a high resolution µ-CT to illustrate the position of implanted electrode carriers and the drug carrier system within the inner ear. The µ-CT measurement revealed the feasibility to implant the extrudates into the scala tympani of the human inner ear for either isolated use or the use in combination with a cochlear implant carrier.

PS 675

Blood-Inner Ear Barrier and Cisplatin-Induced Ototoxicity

Rui Ma[1]; Kevin Ig-Izevbekhai[2]; Jianqi Cui[1]; Eunsoo Yoo[3]; Daqing Li[1]
[1]Department of Otolaryngology - Head & Neck Surgery; Perelman School of Medicine, University of Pennsylvania, Philadelphia, PA; [2]Department of Otolaryngology - Head & Neck Surgery; Perelman School of Medicine, University of Pennsylvania, Philadelphia, PA, USA; [3]1Department of Otolaryngology - Head & Neck Surgery; Perelman School of Medicine, University of Pennsylvania, Philadelphia, PA, USA

Cisplatin is a widely-used platinum-based chemotherapeutic agent in the treatment of solid tumors, including squamous cell carcinoma. However, cisplatin-induced toxicity can compromise treatment outcomes and negatively impact quality of life. Ototoxicity causes permanent hearing damage and is not uncommon in clinical otology. In order to understand the role of the blood-inner ear barrier in cisplatin-induced ototoxicity, we used a mouse model with direct inner ear delivery of cisplatin, which bypasses the blood-inner ear barrier. The current study investigates whether there is a threshold of cisplatin in the inner ear fluid associated with hearing loss and inner ear damage.

In this study, a hydrogel inner ear delivery system was used for local cisplatin administration in a mouse model. Auditory function was assessed by auditory brainstem response (ABR) before and after cisplatin administration. Inner ear perilymph was analyzed and inner ear morphology was evaluated following cisplatin treatment at different time points. A correlation was then

drawn between auditory function, inner ear morphology and perilymph platinum concentration.

A total of 60 C57BL/6 mice, aged 4-6 weeks, were used. Mice were divided into 2 groups and treated with either 1µg or 2µg cisplatin. Cisplatin was delivered directly into the cochlea and covered with hydrogel. Auditory thresholds were tested on day 1, day 3, day 7 and day 14. Perilymph was collected and perilymph platinum concentration was measured.

The 1µg cisplatin treatment group showed hearing threshold shifts between 15-30dB in frequency ranges of 16 kHz, 24 kHz and 32 kHz, 7 days after cisplatin treatment. However, hearing thresholds returned to normal on day 14 following treatment. Mice treated with 2µg cisplatin demonstrated hearing threshold shifts between 20-40dB on day 7 as well as day 14 after treatment. Upon histological examination, disorganization and loss of outer hair cells at the apex were most evident on the 3rd and 7th day post-treatment, especially in the 2µg treatment group. Inner hair cells appeared normal. Permanent hearing threshold shifts and inner ear damage were observed in mice with inner ear platinum concentration at or above 2.24µg/ml, while temporary hearing threshold shifts were found below 0.9µg/ml platinum concentration.

This study shows that direct inner ear administration of high-concentration cisplatin, bypassing the blood-inner ear barrier, can result in permanent hearing loss and inner ear damage in a mouse model. Thus, reversal of cisplatin-induced ototoxicity should be focused on lowering the cisplatin concentration below a specific threshold.

PS 676

In Vivo Assessment of Dexamethasone (DXM) Infused and Coated Poly(lactic-co-glycolic acid) (PLGA) Microneedles as an Improved Drug Delivery System for Intracochlear Biodegradable Devices

Devon C. Pawley; Stefania Goncalves; Esperanza Bas; Emre Dikici; Sapna Deo; Sylvia Daunert; Fred Telischi
University of Miami

Inner ear drug delivery techniques are challenging to develop due to the inherent complexity of the cochlear anatomy, which limits molecular transportation. Using a microneedle approach lends the drug infused microneedle the capability to pierce the round window membrane and be placed inside of the cochlea, allowing a consistent dosing of drug to be released over time to the desired area.

Microneedles were prepared by casting a solution of PLGA copolymer and DXM into a custom made mold engineered via photolithography. The FDA approved copolymer PLGA was selected as the polymer degrades over time into lactic acid and glycolic acid, two agents naturally found in the human body, and releases the encapsulated drug to the damaged hair cells. Rhodamine B was used in place of DXM to first study the drug release profile. Ototoxicity assessment for viable hair cell (HC) counts was then performed via fluorescent microscopy by exposing organ of Corti explants dissected from rats to the DXM microneedles in culture. Next, the microneedles were blended with a dye, FM1-43, and were introduced in the scala tympani in adult rats for *in vivo* assessment of the intracochlear drug release. Subsequently, animals were euthanized, cochlea were harvested and analyzed under confocal microscopy to visually assess the distance travelled in the cochlea.

Analysis of the Rhodamine B data demonstrates that DXM begins release from the PLGA in 72 h, with this lag time significantly decreasing after adding extra DXM coating. The ototoxicity assessment of the DXM coated microneedles *in vitro* showed a significant reduction of inner and outer HCs losses when compared to the non-coated prototype and a similar efficacy in protecting from HCs loss when compared to DXM solution. Finally, FM1-43 was shown to release from the microneedles within 3 days after intracochlear placement *in vivo*.

Current *in vivo* investigation involves the implantation of DXM infused microneedles 24 h after the delivery of ototoxic agents to assess the protective affects customized microneedles have against hearing loss in adult rats for ten days. Auditory brainstem response data reveal a reduced hearing threshold for animals having a received DXM infused microneedle. This data demonstrate that biopolymer-based microneedles can release drugs within the perilymph and protect HCs from ototoxicity. Thus, drug infused polymeric microneedles provide a novel method to deliver DXM to the inner ear over a controlled period of time without introducing foreign agents to the cochlea, and thus minimizing hearing loss.

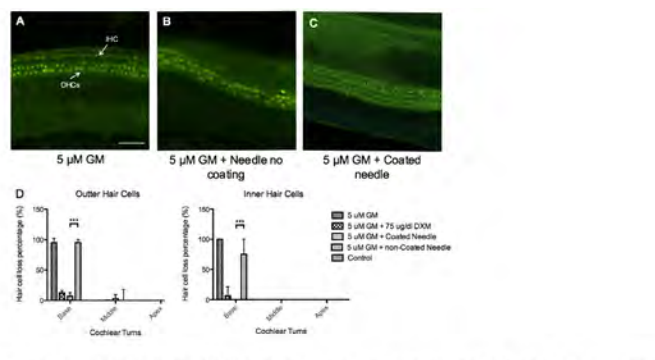

Figure 1: Otoprotective effects of DXM blended microneedles with and without DXM coating. *A-C) Basal turns of organotypic OC exposed to an ototoxic environment (5 uM Gentamicin) and different otoprotective measures - A) Control; B) DXM-blended microneedle; C) DXM-blended and coated microneedle. Gentamicin induced a significant HC loss that was more prominent in the inner hair cells compared to the outer hair cells.*

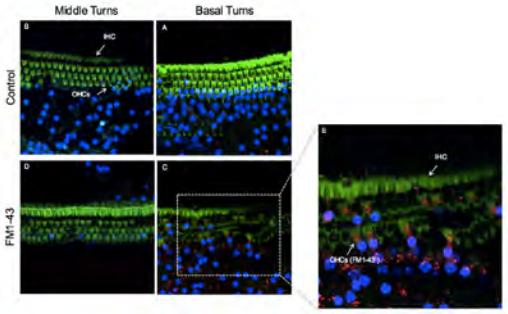

Figure 2. FM1-43 blended microneedles implanted in adult mice for one week to confirm dye release and distribution through the perilymph. *A,B. Control adult mice cochleae; C,D. Mice adult cochleas exposed to a dye blended microneedle. A-D. 40 X images using confocal microscopy; E. 63X magnification of sample. The dye is being slowly released from the microneedles and reaches HCs passing through the mechanotransduction apparatus of the HC, confirming the diffusion of the dye through the perilymph.*

PS 677

An Implantable, Refillable, And Scalable Microsystem For Chronic Murine Inner Ear Drug Delivery

Farzad Forouzandeh[1]; Xiaoxia Zhu[2]; Nuzhet N. Ahamed[3]; Joseph P. Walton[4]; Robert D. Frisina[2]; David A. Borkholder[5]
[1]Microsystems Engineering, Kate Gleason College of Engineering, Rochester Institute of Technology; [2]Medical Engineering Dept., Global Center for Hearing & Speech Research, Univ. South Florida; [3]Microsystems Engineering, Kate Gleason College of Engineering; [4]Department of Communication Sciences & Disorders, University of South Florida, Tampa, FL; Department of Medical Engineering, University of South Florida, Tampa, FL; Global Center for Hearing and Speech Research, University of South Florida, Tampa, FL; [5]Microsystems Engineering, Dept. of Electrical and Microelectronic Engineering, Rochester Institute of Technology

Recent advances in protective and restorative biotherapies have created new opportunities to treat auditory and vestibular disorders with site-directed, programmable drug delivery systems. Advanced microsystems specifically designed to function with nanoliter precision and with sizes and form factors optimized for implantation will enable successful therapy development leveraging the transgenic, knock-in, and knock-out variants of human disease in the mouse model system, and for translational research using larger mammals. Here we present a novel fully implantable microsystem with nanoliter resolution optimized for chronic murine inner ear drug delivery while being inherently scalable to larger animal models and humans. The microsystem consists of a wirelessly controlled micropump and a refillable microreservoir. The micropump is built on the bottom side of a printed circuit board around a catheter microtubing (250 µm OD, 125 µm ID), enabling integration with electronics and a leak-free flow path. Three chambers containing phase-change material along the microtubing enable peristalsis. This pump demonstrated flow rates of 10-100 nL/min in the presence of ±3 °C temperature fluctuation and up to 5 kPa backpressure (10× of physiological backpressure) [1]. The micropump robustness is significantly improved by the enhancement of chamber sealing and deposition accuracy of the phase-change material in the chambers. The robustness is validated by confirming consistent pump rates for chronic operation. The novel microreservoir structure is fabricated using 3D-printing technology, building a surface refill port and a chamber for storing the drug. A pre-compressed silicone septum enables up to ~65000 refills without leakage at up to 100 kPa backpressure (200× of physiological backpressure). The chamber membrane is fabricated with two parylene-C layers using a biocompatible sacrificial material, enabling a long-term biocompatible environment for the drug, and near-zero backflow after drug extraction. The micropump and the microreservoir are integrated into a planar form-factor single-compartment structure, optimized for subcutaneous implantation. *In vivo* results are presented on key pump performance characteristics including microreservoir refilling, wireless communication for micropump reprogramming, and chronic periodic delivery of sodium salicylate to the round window membrane niche. The efficacy of cochlear salicylate infusion was quantified using distortion product otoacoustic emission (DPOAE) thresholds and amplitudes (DPgrams). This low-cost, scalable microsystem enables an advanced level of control for biotherapy development in different animal/human models and for clinical applications.

Supported by NIH NIDCD award R01 DC014568.

[1] Forouzandeh, F. et al., *J. Control. Release* 298, 27–37 (2019).

PS 678

Novel Ionic Liquid Solution for Transtympanic Drug Delivery for Idiopathic Sudden Sensorineural Hearing Loss

Eva Cai[1]; Nicole Black[2]; Eden E.L. Tanner[1]; Samir Mitragotri[1]; Elliott D. Kozin[3]; Aaron K. Remenschneider[4]
[1]Harvard John A. Paulson School of Engineering and Applied Sciences; [2]John A. Paulson School of Engineering and Applied Sciences, Harvard University; [3]Massachusetts Eye and Ear Infirmary- Harvard University; [4]Dept. of Otolaryngology, UMass Memorial Medical Center; Massachusetts Eye and Ear

Background

Idiopathic sudden sensorineural hearing loss (SSNHL) is commonly treated with dexamethasone perfusion of the tympanic space, with the goal of drug diffusion into the inner ear. However, access to intratympanic

(IT) injections is limited and requires evaluation by an otolaryngologist. In an ideal scenario, dexamethasone could be introduced into the external auditory canal and then diffuse through the tympanic membrane and into the inner ear, without need for TM perforation. The trilaminar structure of the TM poses a challenge for middle and inner ear drug delivery. Specifically, the stratum corneum (SC) is a tightly packed brick-and-mortar like structure consisting of corneocytes which are surrounded by lipids, which presents a formidable barrier.

Objective
Ionic liquids (IL) are composed of bulky, asymmetric cations and anions that are liquid below 100°C. ILs have been previously used in transdermal drug delivery applications, successfully enhancing skin permeability and delivering drugs of a range of molecular weights, including large proteins. We hypothesize that ILs could also be employed to deliver dexamethasone into the middle ear space as a novel, noninvasive method to treat patients with SSNHL.

Methods
We formulated solutions of dexamethasone-IL with various drug loading concentrations from 1-50 mg/mL. Solution viscosity is modified via the addition of saline. Dexamethasone concentrations in saline are quantified via UV spectrophotometry. We investigate the delivery of dexamethasone through *ex vivo* human skin and *ex vivo* sheep tympanic membrane. We conducted timed studies of the delivery rate of 1) varying concentrations of dexamethasone in a purely IL solution and 2) dilutions of dexamethasone-IL solutions with saline. These were compared with control groups of IL without dexamethasone, saline, and prescription dexamethasone otic drops.

Results
We successfully created dexamethasone-IL solutions and lowered their viscosity with saline, potentially allowing for better transport through the middle ear space. We show that the dexamethasone-IL solution is able to traverse human epithelium and *ex vivo* TM successfully, resulting in steroid delivery to the middle ear space.

Conclusion
We have developed a novel and noninvasive way to deliver drugs to the middle ear space without requiring IT injection. The usage of ILs in transtympanic drug delivery formulations can be extended to other therapeutic molecules, such as antibiotics or growth factors.

PS 679

analysis of the therapeutic utility of pluronic F127 based nanoparticles in acute hearing loss

Dong-Kee Kim[1]; Keum-Jin Yang[1]; So-Young Jung[1]; Jihye Yoo[2]; Heebeom Koo[2]
[1]Daejeon St. Mary's hospital, college of medicine, The Catholic University of Korea; [2]Department of Medical Lifescience, College of Medicine, The Catholic University of Korea

Objectives
The purpose of this study was to develop a therapeutic drug for acute hearing loss using an antioxidant-containing nanoparticle based on pluronic F127. In our previous study, nanoparticles coated with polyethyleneglycol (PEG) showed an advantage in penetrating the mucosa when delivering medication to inner ear. Pluronic F127 is approved by the FDA for use in the ear and has two PEG blocks.

Materials and Methods
We selected alpha lipoic acid through literature search to be loaded in nanoparticles. The safety of nanoparticle in HEI-OC1 cells, and the protective effect of nanoparticle against aminoglycoside toxicity, were investigated, and to investigate the antioxidant action of nanoparticle, we measured the intracellular levels of ROS in response to kanamycin with or without nanoparticle, as well as levels of antioxidant proteins. For investigating the mechanism of antioxidant activity, we down-regulated NRF2 in HEI-OC1 cell lines by Nrf2 siRNA. In mice, we delivered he nanoparticle by intratympanic injection 4h before ototoxicity induction and analyzed the therapeutic utility of nanoparticles in acute hearing loss.

Results
The size of particles was about 109.1 nm, and in the analysis of drug release, about 28% of the drug was released gradually from nanoparticle for 40 hours at room temperature. In vitro results, nanoparticles showed safety in MTT assay up to 2.5mg/ml and cytoprotective effects at concentrations from 0.25 mg / ml to 2.5 mg / ml. It also showed an increase in antioxidant proteins such as Nrf2, HO-1, SOD-1 and SOD-2. However, this effect was counteracted when Nrf2 siRNA was treated, indicating that the nanoparticles act on the Nrf2 / HO-1 pathway for antioxidant effect. In vivo results, the hearing of animals injected with nanoparticles into the middle ear cavity, was also significantly preserved after ototoxicity induction compared to the control group, and the increase of Nrf2 was also observed in cochlea of these animals, which indicating that the nanoparticle showed the protective effect of hearing through the same antioxidant mechanism.

Conclusion
Pluronic F127 nanoparticles loading alpha lipoic acid showed effective hearing protection in acute hearing loss, which appears to be mediated through the Nrf2 / HO-1 pathway. Considering the known safety and long release times of the nanoparticle, it appears to be a potential new drug for intratympanic injections.

Inner Ear: Gene Therapy

PS 680

The Adeno-associated Viral Anc80 Vector Efficiently Transduces Inner Ear Cells in Olive Baboons (Papio anubis)

Yuan Gao[1]; Shimon P. Francis[1]; Michael J. McKenna[1]; Robert Ng[1]; Enping Qu[1]; Elizabeth Clemmons[2]; Cathy Sung[1]; Yukako Asai[1]; William Sewell[3]; Emmanuel J. Simons[1]; Michelle D. Valero[1]
[1]Akouos, Inc.; [2]Southwest National Primate Research Center; Texas Biomedical Research Institute; [3]Akouos, Inc.; Massachusetts Eye and Ear; Harvard Medical School

Cochlear gene therapy is a promising modality to address genetic and acquired hearing loss. Previous work in genetically deaf transgenic mice demonstrated that the synthetic adeno-associated viral Anc80 (AAVAnc80) vector can rescue cochlear function by delivering healthy gene copies to cochlear hair cells. Intermediary models that are anatomically, developmentally, and immunologically more similar to humans are important for translation to the clinic. Andres-Mateos et al. (2019) and Francis et al. (2019) demonstrated efficient inner hair cell (IHC) transduction with AAVAnc80 in macaques with low pre-existing immunity against AAVAnc80 (*M. mulatta* and *M. fascicularis).* Here, we extend these findings to baboons, which have a cochlea larger than the macaque and may be more similar to humans immunologically. Given that the baboon cranium is substantially larger and thicker than those of cynomolgus and rhesus macaques, the surgical approach was first optimized for baboons using cadaveric specimens. Adult male baboons with normal cochlear function and with low or moderate titers of pre-existing serum neutralizing antibodies (NAbs) were included in the study. We administered AAVAnc80 encoding a green fluorescent protein (GFP) intracochlearly, specifically through the round window membrane of each monkey's left cochlea. Serum, CSF, cochleae, and other organs were collected for analysis following at least a 3-week survival. Efficient transduction of IHCs was observed, regardless of pre-existing serum NAb titers, and evidence for transduction in other cell types was also observed. These data demonstrate efficient delivery and transgene expression in a third NHP species, provide preliminary evidence that moderate serum NAb levels do not inhibit IHC transduction when AAVAnc80 is delivered via this route of administration, and support intracochlear administration of AAVAnc80 as a promising strategy to evaluate in future clinical trials.

PS 681

AAV mediated gene therapy restores auditory sensitivity in mouse models of autosomal recessive non syndromic deafness DFNB31 and Usher syndrome type IID

Hannah Goldberg[1]; Yukako Asai[1]; Bifeng Pan[2]; Kevin Isgrig[3]; Wade Chien[3]; Jun Yang[4]; Gwenaelle S. Geleoc[1]
[1]Boston Children's Hospital & Harvard Medical School; [2]Decibel Therapeutics; [3]National Institute on Deafness and Communication Disorders, NIH, Bethesda; [4]Moran Eye Center, University of Utah, Salt Lake City, UT

The PDZ domain-containing protein whirlin (WHRN), encoded by the WHRN gene is essential for both hearing and vision. WHRN is implicated in the stabilization, elongation and maintenance of the stereociliary bundles of the sensory hair cells in the inner ear. Two major WHRN splice variants have been shown to be expressed in auditory hair cells: the full-length isoform (FL-WHRN) of the protein is located on the tip and shaft of the stereocilia in inner hair cells (IHCs) and the ankle link complex in outer hair cells (OHCs); the short isoform (C-WHRN) is restricted to the tips of the stereocilia in both IHCs and OHCs. Distinct disruptions of one or both of these isoforms lead to a variety of phenotypic configurations including Usher Syndrome type IID (USH2D) and autosomal recessive non- syndromic deafness 31 (DFNB31).

To assess efficacy of novel gene therapy approaches in mouse models of USH2D (*Ush2d*$^{neo/neo}$) and DFNB31 (*Ush2d*$^{wi/wi}$), we used a synthetic viral vector (sAAV) encapsulating gene sequences encoding for FL-WHRN and C-WHRN. Neonatal mutant mice (P1-P2) received one injection of concentrated vectors (~10^12 GC/ml) in the inner ear. Efficacy of the treatment was assessed by comparing uninjected mutants versus injected mutants at the cellular and systems level with analysis of mechanosensitive transduction currents, protein expression, analysis of ABR, DPOAE and balance in the case of the whirler mice.

For USH2D, neonatal *Ush2d*$^{neo/neo}$ mice were injected at P1 with a single synthetic vector driving FL-WHRN expression (sAAV-FL-WHRN). This single injection lead to both improved mechanotransduction in OHCs and IHCs and hair bundle morphology as analyzed with SEM. ABR recovery was variable, down to 50 dB thresholds for the best performer.

For DFNB31, *Ush2d*$^{wi/wi}$ mice received dual vector treatment of sAAV-FL-WHRN and sAAV-C-WHRN at P1. This dual injection lead to significantly improved outcomes including an increase in mechanotransduction currents in OHCs, recovery of protein expression and correct localization of whirlin to the tips and base of the stereocilia. ABR and DPOAE recovery was also significant with best performers responding to ~50 dB sound intensities. Additionally, balance assessments demonstrated minimal full-body rotations and increased rotarod stability in injected *Ush2d*$^{wi/wi}$ mice.

These results provide further validation for viral-mediated gene therapy in the treatment of DFNB31 and Usher Syndrome Type 2D.

PS 682

Small Molecule Based Temporal Control of Protein Expression After AAVAnc80 Mediated Delivery

Niliksha Gunewardene[1]; Danielle R. Lenz[2]; Rachael Richardson[1]; Andrew Wise[1]; Robert Ng[2]
[1]Bionics Institute; [2]Akouos, Inc.

Many genetic mutations that result in hearing loss manifest with complete absence of the mutated protein. Viral vector mediated gene transfer can facilitate the introduction of a fully functional gene back to the inner ear and, as a result, enable hearing restoration. AAVAnc80 has been shown to transduce multiple cell types in the inner ear and is therefore an optimal tool for gene delivery. AAV vector mediated delivery enables long-term expression of the transferred gene; however, in some cases, temporal control of the gene of interest may be required, for example where its constitutive expression can cause cell toxicity. Therefore, we explored a gene regulating system that permits targeted proteasomal degradation based on fusion of a protein of interest to a destabilizing domain. Here, cochlear delivery of AAVAnc80-mScarlet without a destabilizing domain resulted in high expression of mScarlet in cochlear cells in mice. In contrast, mScarlet expression was absent following delivery of AAVAnc80-mScarlet fused to a destabilizing domain due to mScarlet degradation. However, when the cochleae were exposed to a specific small molecule drug that could attach to the destabilizing domain and prevent degradation, robust mScarlet expression was detected in various cells of the cochlea. Upon subsequent removal of the drug, mScarlet was again sent to degradation and expression was eliminated. Substantial hair cell loss was not observed after delivery of the small molecule drug and/or AAVAnc80 vector. To conclude, in the absence of the small molecule drug, transgene expression was fully suppressed, while after the addition of the drug, expression was clearly detected. This method can be applied to temporally and reversibly control the expression of various proteins in the cochlea after AAV vector mediated gene delivery, enabling future gene augmentation with temporally limited transgene expression.

PS 683

Genetic manipulation of inner ear cells through local delivery of adeno-associated viral vectors

Fabian Blanc[1]; Alexis-Pierre Bemelmens[2]; Corentin Affortit[3]; Michel Mondain[1]; Florence François[3]; Charlène Joséphine[2]; Jean-Luc Puel[4]; Jing Wang[4]
[1]INSERM-CHRU Montpellier; [2]CNRS – UMR; [3]INSERM-UMR; [4]Institute for Neurosciences of Montpellier

Genetic manipulation of inner ear cells through local delivery of adeno-associated viral vectors

Fabian Blanc[1,2,3]§, Alexis-Pierre Bemelmens[4], Corentin Affortit[1,2], Michel Mondain[1,2,3], Florence François[1,2], Charlène Joséphine[4], Jean-Luc Puel[1,2], Jing Wang[1,2]

[1]INSERM - UMR 1051, Institut des Neurosciences de Montpellier, 34295 Montpellier, France,
[2]Université de Montpellier, 34090 Montpellier, France,
[3]CHRU Montpellier - Centre Hospitalier Régional Universitaire, 34090 Montpellier, France
[4] CNRS – UMR 9199, Université Paris-Saclay, Molecular Imaging Research Center MIRCen / CEA, 92265 Fontenay-aux-Roses, France

Background - Introduction
Genetic manipulation is a very powerful tool both for studying inner ear pathophysiology involved in failing hearing, and for treating or preventing hearing disorders, by introducing a desired foreign gene or gene-regulatory element, such as RNA interference, into the target cells to replace or fix the defective gene. Different factors, such as vector type, administration method and promoter may have an impact both on the type of inner ear cells targeted, as well as on transgene expression.

Methods
Here we use adeno-associated virus (AAV) vectors to modify gene expression (*e.g.* to introduce a green fluorescence protein (GFP) or to inactivate a gene with shRNA, miRNA) in cochlear cells, both in an *ex vivo* cochlear explant system and *in vivo* in adult mouse cochleae. In addition, efficiency and safety of AAV-mediated gene transfer via both the round window membrane and posterior semicircular canal approaches are evaluated *in vivo* in adult c57BL/6J mice.

Results
We observed marked differences among serotypes in the efficiency of transduction of the different cochlear

cell types. AAV2/9 appears efficient in driving GFP transgene expression in both inner (IHCs) and outer hair cells (OHCs), while AAV2/8 is highly specific for the transduction of the IHCs. In addition, AAV2/Anc80L65 transduces IHCs, OHCs and supporting cells with high efficiency. The AAV2/8 vector containing the CBA promoter driving shRNA- Slc17a8 or miRNA-Slc17a8 to silence vesicular glutamate transporter-3 (Vglut3) is effective via *in vivo* administration of both the round window membrane and posterior semicircular canal approaches. This leads to reduced Vglut3 expression in IHCs together with significant increase of the auditory brainstem response (ABR) thresholds in adult mice. By contrast, control AAV2/8-CBA-GFP delivery affects neither Vglut3 expression nor ABR thresholds until 4 months after injection.

Conclusion

Taken together, our results demonstrate that local delivery of AAV vectors to the inner ear is an efficient and safe means of introducing a desired foreign gene or gene-regulatory elements into the cochlea.

PS 684

Developmental dependent effects of local gene therapy in Usher syndrome type IG

Ghizlene Lahlou[1]; Charlotte Calvet[1]; Vincent Michel[1]; Jacques Boutet de Monvel[1]; Christine Petit[2]; Saaid Safieddine[1]

[1]Génétique et Physiologie de l'Audition, Institut Pasteur, 75015 Paris, France; [2]Institut Pasteur, Paris

Usher syndrome type I (Ush1) is the most frequent genetic cause of deafness-blindness, responsible for congenital profound hearing loss, vestibular areflexia, and progressive visual loss. Promising results were obtained in mouse models for Ush1 in the restoration of balance. Still, in these studies, the viral gene therapy was administered at a neonatal stage, corresponding to foetal development in humans and therefore not adequate for clinical applications. The aim of this study was to explore how extended the temporal window allowing an effective gene therapy administration for Ush1 syndrome actually is.

To this end, *Ush1g*$^{-/-}$mice were used, in which the gene coding for the scaffold protein sans was inactivated. A single delivery of the *sans*cDNA by the AAV2/8 or the Anc80 was performed through the round window at various developmental stages including embryonic (E12-E16), neonatal (P1-P3), and early adult (P12-P30) stages. Viral transduction was assessed by GFP immunolabeling, and efficiency of the treatment was examined by auditory brainstem responses, vestibular behavioral tests, immunostaining analysis, and electron microscopy.

A difference in viral transduction was observed between the different stages. Embryonic administration resulted in a much higher infection rate in outer hair cells (OHC) than in inner hair cells (IHC) [OHCs, 50 ± 23 %, IHCs, 3 ± 5.4 %, p=6.10-11, t-test], while it was predominant in the IHC when administration was performed after birth (IHCs, 62 ± 3% and 88%, OHCs, 33 ± 5% and 0% at neonatal and adult stage, respectively). Similarly, a base-to-apex gradient in GFP expression was noticed at embryonic stage, whereas an apex-to-base gradient was seen at neonatal stage. In vestibular hair cells, transduction was comparable at every stages.

A difference in the phenotypical features was also observed. After neonatal injection, the expression of the protein sans and the morphological defects were fully restored, leading to a complete and durable restoration of vestibular function, and partial rescue of hearing. By contrast, only a partial restoration of the stereocilia morphological aspect and the vestibular function was seen after administration at an adult stage, and no phenotypical rescue was obtained after the neonatal viral delivery.

These results indicate that in the case of a severe morpho-functional developmental pathology like Ush1G, the temporal interval of treatment might have a strong influence on the outcome of gene therapy. These findings are significant for future translational projects building, where optimisation of the stage of delivery will need to be considered.

PS 685

The Adeno-Associated Viral Anc80 Vector Efficiently Transduces Inner Ear Cells in Cynomolgus Macaques (Macaca fascicularis)

Shimon P. Francis[1]; Michael J. McKenna[1]; Yuan Gao[1]; Robert Ng[1]; Enping Qu[1]; Luk H. Vandenberghe[1]; William Sewell[2]; Emmanuel J. Simons[1]; Michelle D. Valero[1]

[1]Akouos, Inc.; [2]Akouos, Inc.; Massachusetts Eye and Ear; Harvard Medical School

Gene therapy is a promising approach to address both genetic and acquired hearing loss, and adeno-associated viral Anc80 (AAVAnc80) vector-mediated gene delivery has successfully recovered cochlear function in mouse models of genetic deafness. An intermediary model system that is anatomically, developmentally, and immunologically more similar to humans is important for translating these findings to the clinic. Previous work

demonstrated broad transduction of non-human primate (NHP) inner hair cells (IHCs) with AAVAnc80 (Andres-Mateos et al., 2019). Here, we extend those findings to demonstrate a dose response of transduction efficiency, as assessed by transgene expression, and preliminary safety of AAVAnc80 in six pre-pubescent monkeys with relatively low levels of pre-existing serum neutralizing antibodies (NAbs) against the vector capsid. Animals were assigned to receive one of three doses of AAVAnc80 vector encoding a green fluorescent protein (GFP) via a single, unilateral intracochlear injection. Three weeks following administration, serum and CSF were collected, and cochleae were harvested. Using hair-cell and anti-GFP immunolabels, we quantified hair-cell survival and the GFP expression in surviving IHCs at nine logarithmically-spaced frequency positions spanning the length of the cochlear spiral. Transduction efficiency was dose-dependent and gradated along the length of the cochlea. Minimal hair cell loss, which was not dose-dependent, was observed in the injected ears, as well as the uninjected control ears. Many prevalent forms of hearing loss are caused by dysfunction of cochlear cell types other than hair cells. Toward the development of potential therapeutics for such forms of hearing loss, it is important to understand the efficiency of transduction within these cell types. Indeed, AAVAnc80 was observed to transduce other cell types in the inner ear. Serum samples collected at necropsy (day 21) showed modest increases in NAb titers when compared with day 0 (date of vector administration) serum samples. The NAb titers in CSF at necropsy were relatively low, even when the serum NAb titer increased. These data, demonstrating efficient transgene expression and preliminary safety in NHPs, support our approach of intracochlear administration of AAVAnc80 as a promising strategy to evaluate in future human clinical trials.

PS 686

Comparison of AAV-GFP vs. AAV-Cre for Studying Transduction Patterns in the Mouse Inner Ear

Moaz Sinan[1]; Kevin Isgrig[1]; Jianliang Zhu[1]; Wade Chien[2]
[1]NIDCD/NIH; [2]National Institute on Deafness and Communication Disorders, NIH, Bethesda

Background
Adeno-associated viruses (AAVs) are popular viral vectors for gene delivery in the inner ear due to their excellent biosafety profiles. Most studies evaluating the transduction patterns and efficiencies of AAVs use AAV-GFP to detect cell types that are transduced by various AAV serotypes. One drawback of this method is that some cell types may be transduced by AAV-GFP at low levels, and the resulting green fluorescence may be too low for easy detection. In this study, we compare using AAV-GFP vs. AAV-Cre for studying transduction patterns in the mouse inner ear.

Methods
Neonatal R26R tdTomato (Ai14) mice were used in this study. AAV2-Cre and AAV2-GFP were injected into mouse inner ear using the posterior semicircular canal approach. Immunohistochemistry was used to assess the infection efficiency. ABR was used to assess auditory function.

Results
AAV2-GFP transduced mostly the inner hair cells (IHCs), as evidenced by GFP expression in these cells. Some outer hair cells (OHCs) were also transduced by AAV2-GFP. In contrast, AAV2-Cre transduced some supporting cells and spiral ganglion cells in addition to IHCs and OHCs, as evidenced by tdTomato expression.

Conclusions
Our study showed that the AAV-Cre system may be more sensitive at detecting the transduction patterns in the mouse inner ear compared to AAV-GFP.

PS 687

Transduction Efficiency of Synthetic and Conventional AAVs for Cochlear Lateral Wall

Kevin Isgrig[1]; Yasuko Ishibashi[1]; Hong Jun Wang[1]; Devin McDougald[2]; Jean Bennett[2]; Wade Chien[3]
[1]NIDCD/NIH; [2]University of Pennsylvania Perelman School of Medicine; [3]National Institute on Deafness and Communication Disorders, NIH, Bethesda

Background
Adeno-associated viruses (AAVs) are popular vector choices for gene delivery in the inner ear due to their excellent biosafety profiles. While most AAV transduction studies in mammalian inner ear focus on the mechanosensory hair cells as well as supporting cells, many inner ear disease processes also affect the cells in the cochlear lateral wall. In this study, we examine the lateral wall transduction patterns of two conventional AAVs (AAV2 and AAV8) and three synthetic AAVs (AAV2.7m8, AAV8BP2, Anc80L65) in the neonatal mouse inner ear.

Methods
Neonatal (P0-P5) CBA/J mice were used in this study. Synthetic AAV-GFPs were injected into mouse inner ear using the posterior semicircular canal approach. Immunohistochemistry was used to assess the infection efficiency. ABR was used to assess auditory function.

Results
AAV8BP2 transduced the marginal cells and intermediate cells with the highest efficiency. Anc80L65, AAV2.7m8, AAV2, and AAV8 transduced the cells in the cochlear lateral wall at lower levels.

Conclusions
Our study showed AAV8BP2 transduced both the marginal cells and intermediate cells at high levels. AAV8BP2 is a useful viral vector for targeting the cochlear lateral wall.

PS 688

A Promising New Type of Self-assembled DNA-based Nanospheres for Drug or Gene Therapy in Inner Ear

Hao Wu; Dehong Yu; Xueling Wang; Yuming Chen; JiaYi Gu
1. Department of Otolaryngology - Head & Neck Surgery, Shanghai Ninth People's Hospital, Shanghai Jiao Tong University School of Medicine; 2. Ear Institute, Shanghai Jiao Tong University School of Medicine; 3. Shanghai Key Laboratory of Translational Medicine on Ear and Nose diseases, Shanghai, China

Background
Ear is a complex organ playing crucial role in maintaining normal hearing and balance function. Since systemic delivery of therapeutics is challenging with blood-labyrinth barrier BLB can significant prevent most drugs from inner ear, Local drug administration, especially, by nanotechnology-based systems had received extensive attention in recent years. Herein, a set of DNA-based nanospheres was synthesized by coordination-driven self-assembly of Fe(II) ions and single-stranded DNA (ssDNA). The synthetic Fe-DNA nanospheres were efficient in internalization by HEI-OC1 cell line. Further research will be working on loading drug or siRNA to inhibit the expression of inflammatory factors and cell apoptosis.

Method
$FeCl_2 \cdot 4H_2O$ (1 mM) was incubated with 25 mM random sequence-ssDNA (1.5mM DNA were labeled by cy5) at 95°C for 2 h. Fe-DNA NPs were washed with double distilled water with centrifugation at 13,000 r.p.m for 5 minutes after incubating. The DNA concentrations were determined by using UV-vis spectrometry at 260 nm, then loading efficiency were calculated by the following formula: Loading efficiency = $((M_t-M_u)/M_t) \times 100$ %. M_u represent the amount of DNA unencapsulated in the NPs and M_t represent the total amount of DNA added. Dynamic light scattering (DLS) and zeta potential were determined by Zetasizer Nano ZS. TEM characterization was detemined Hitachi HF5000 operated at 200 kV. Cell Internalization of of Fe-DNA nanospheres was determined by confocal microscopy.

Result
After centrifugation for 5 minutes, the solid was collected. The loading efficiency of DNA is as high as 86.9%. The average hydrodynamic diameter (HD) of the nanospheres is approximately 439.4 ± 6.7 nm according to DLS analysis. Uniform size of self-assembly spherical nanoparticles were clearly observed by TEM. After 24 h incubation, high florescence intensity in cell cytoplasm indicated that Fe-DNA NPs were efficient in internalization by HEI-OC1 cell line.

Conclusion
In conclusion, a simple DNA-based nanospheres was synthesized with a high loading efficiency of ssDNA. Fe-DNA NPs with high cellular uptake efficiency has the potential of drug/gene therapy in inner ear.

PS 689

Identification and Characterization of POU4F3 Transcriptional Agonists for Hair Cell Regeneration in Mammalian Cochleae

Vikrant Rai[1]; Santanu Hati[1]; Hao Feng[2]; Joe R. Frank[1]; Zhenhang Xu[2]; Sarath Vijayakumar[1]; Douglas Auld[3]; **Jian Zuo**[4]
[1]Creighton University School of Medicine; [2]Biomedical Sciences Department, Medical School, Creighton University; [3]Novartis Institutes for Biomedical Research; [4]Department of Biomedical Science, Creighton University

Cochlear hair cell (HC) death is a primary etiology underlying cisplatin, antibiotics, noise-induced hearing loss and thus regeneration of HCs may provide a promising therapeutic strategy. However, there are no FDA-approved drugs for HC regeneration and hearing restoration. Recent progresses in cochlear HC regeneration in mouse models demonstrate that: 1) activation of transcription factor POU4F3 can convert adult supporting cells (SCs) to HC-like cells; 2) combined activation of ATOH1 and POU4F3 is efficient to convert adult SCs to HC-like cells.

To investigate a POU4F3 agonist, we performed a transcriptional agonist screen of ~45,000 small molecule compounds at Novartis and identified ~86 hits. We validated these hits in the *POU4F3*- or SV40-promoter driven dual reporter Luciferase assays for their activity and cell-titer glow assay for cell viability/toxicity in stably transfected HeLa cells. We got 24 compounds with an increased POU4F3 activity. POU4F3 agonists

#15 and #18, upon transtympanic injection into adult wildtype FVB mice, increased cochlear *Pou4f3* mRNA by 2.5- and 4-fold, respectively. Interestingly, #15 also increased cochlear *Atoh1* mRNA several folds while #18 had no effects.

To improve the efficacy of compound #18, we synthesized 40 analogs of #18 and performed structure-activity relationship (SAR) study on these analogs. 15 out of the 40 analogs had better cell viability and 3-4-fold higher activity in dual reporter luciferase assays in stably transfected HeLa cells than #18. Further, the 15 compounds did not show any toxicity (100nM-10μM) in explant culture.

Our future goal is to test the *in vivo* activity of our top POU4F3 transcriptional agonists for HC regeneration using a mouse model with HC loss and Atoh1 overexpression in SCs. We expect that our POU4F3 agonists are useful in HC regeneration in conjunction with ATOH1 agonists and/or ATOH1 gene therapy in humans.

Supported in part by NIH-R01DC015444, NIH-R01DC015010, USAMRMC-RH170030, ONR-N00014-18-1-2507, MRC-UK-Sub, Bellucci Fund, CURAS and LB692/Creighton.

PS 690

Ex vivo assessment of AAV capsid variant tropism and safety in the rat cochlea

Phillip Uribe[1]; Pranav D. Mathur[2]; Christopher Bartolome[3]; David Jaramillo[3]; Anne Harrop-Jones[2]; Stephanie Szobota[4]; Fabrice Piu[1]; Steven Pennock[3]; Alan C. Foster[4]; Mark Shearman[3]; Bonnie E. Jacques[1]
[1]Otonomy Inc; [2]Otonomy, Inc.; [3]Applied Genetic Technologies Corporation; [4]Otonomy Inc.

Background
Deafness is the most common inherited sensory disorder. Mutations in over 100 genes have been causally associated with varying degrees of hearing loss. Gene therapy is an emerging platform to deliver intact, functioning genes into tissues that lack a functional allele. Adeno-associated viruses (AAVs) have been shown to be safe and effective tools for delivering gene therapies and have a track record of positive clinical outcomes. The AAV capsid represents a critical regulatory element that influences tropism, i.e. those cell types preferentially targeted for infection by a particular capsid. Here, we conducted a head-to-head evaluation of novel and previously described AAV capsid variants in an optimized ex vivo cochlear model to assess organ of Corti tropism.

Methods
P3-P4 Sprague-Dawley rat pups were used for all experiments. Whole organ cochlear explants were established on Day 0, allowed to acclimate overnight, then were treated with AAV either continuously for 120 hours or for 48 hours followed by washout and 72 hours in media without AAV. All AAV variants used CBA promoter to drive expression of a Green Fluorescent Protein (GFP) reporter construct to allow for rapid assessment of tropism. Some of the variables tested included different AAV capsids and titers as well as different concentrations of serum in the media (0%, 2%, 10%). Explants were fixed and stained with phalloidin and anti-GFP. For evaluation of tropism, the organ of Corti was imaged on a confocal microscope and GFP coverage was quantified for each of the different variables assessed. Phalloidin staining was used to assess any cell toxicity resulting from AAV treatment within the organ of Corti.

Results
We found the 120-hour continuous AAV treatment protocol provided the greatest amount of GFP coverage; therefore, all head-to-head capsid evaluations were conducted using this protocol. Our comparative study identified capsids with significant transduction efficiency, including several with greater GFP coverage than previously published preferred variants. Furthermore, differences in tropism were observed depending on the capsid, consistent with in vivo studies. Importantly, none of the AAV capsids tested in this study exhibited signs of toxicity within the organ of Corti.

Conclusions
Here we optimized an ex vivo model for the assessment of AAV tropism within the organ of Corti. We identified several AAV capsids with more favorable tropism profiles than previously published preferred variants in the cochlea. Combined, these experiments represent an important step toward the development of AAV-based gene therapies for hearing loss.

PS 691

Dual Adeno-Associated Viral Anc80 Vector Efficiently Transduces Inner Ear Cells in Non-Human Primates

Yuanzhao Darcy[1]; Shimon P. Francis[1]; Michael J. McKenna[1]; Robert Ng[1]; Enping Qu[1]; Yuan Gao[1]; Cathy Sung[1]; Yukako Asai[1]; William Sewell[2]; Emmanuel J. Simons[1]; Michelle D. Valero[1]
[1]Akouos, Inc.; [2]Akouos, Inc.; Massachusetts Eye and Ear; Harvard Medical School

Restoration of cochlear function has been achieved in mouse models of genetic deafness using viral vector-

mediated gene therapy. Furthermore, our lab and others have demonstrated that the adeno-associated viral Anc80 (AAVAnc80) vector can efficiently transfer genes encoding enhanced green fluorescent protein (eGFP) into the sensory epithelium in non-human primate (NHP) cochleae (Andres-Mateos et al., 2019), and that the transduction efficiency, as assessed by transgene expression, is dose-dependent (Francis et al., 2019; 2020). However, some forms of monogenic deafness are caused by mutations to genes with transcripts that exceed the packaging capacity of AAV vectors. This limitation can be addressed using dual AAV vectors, in which the transgene is divided and packaged into two separate vectors. Reconstitution, recombination, and/or transplicing in cells that are co-transduced will result in the production of full-length cDNA and the target protein. Here, four cynomolgus macaques (*M. fascicularis*) received a one-time administration of dual AAVAnc80 vectors that together encode eGFP; delivery occurred via a unilateral intracochlear injection through the round window membrane. The cochleae were harvested three weeks following administration and immunostained for analysis. Transduction efficiency in inner hair cells, as assessed by eGFP expression (which also requires reconstitution), ranged from ~80-100%, on average; where an eGFP gradient was observed, expression was greatest in the apex. Transduction was also observed in other cell types in the inner ear. These data provide further evidence that dual AAVAnc80 may be an effective tool to restore the function of cochlear proteins with transgenes that exceed the packaging capacity of AAV vectors.

PS 692

Tailored AAV-based Transgene Expression in the Inner Ear with Cell Type-Specific Promoters

Martin Schwander[1]; Xudong Wu[1]; Shu-Lin Liu[1]; Sarah Cancelarich[2]; Xichun Zhang[1]; Gabriela Pregernig[1]; Kathryn Ellis[1]; Fuxin Shi[1]; Kathy So[1]; Leah Sabin[2]; Meghan C. Drummond[2]; Ning Pan[1]; Jonathon Whitton[1]; Joseph C. Burns[1]; Adam T. Palermo[1]
[1]Decibel Therapeutics; [2]Regeneron Pharmaceuticals

Expression of transgenes at the appropriate place and time can be important for the safety and efficacy of gene therapies. Unfortunately, few cochlear cell type-specific promoters have been reported that are small enough to fit within the limited packaging capacity of AAV vectors. In this study, we worked to identify promoters that are both specific to cochlear cells and small enough to fit into AAVs.

We first identified a promoter capable of driving expression of GFP in both inner and outer hair cells. This expression pattern was consistent when AAV was delivered to cochlear explants, mouse cochleae in vivo, and primate cochleae. In the context of gene therapy with TMC1, this hair cell-specific promoter was able to support better recovery than ubiquitous promoters. We hypothesized that this effect could be due to lack of expression in off-target cells, or to more appropriate expression levels in hair cells.

We next designed promoters targeting transgene expression to either inner hair cells or outer hair cells. Here, we combined sequence-driven regulatory region analysis, single-cell RNA sequencing, and single-cell ATACseq data to identify putative expression control elements. With this approach, we were able to identify several outer hair-cell specific promoters and one inner hair cell-specific promoter.

PS 693

Viral-Mediated Gene Delivery to Deafened DTR Mouse Cochlea

Sungsu Lee[1]; Lisa A. Beyer[1]; Diane M. Prieskorn[1]; Xiaobo Ma[2]; Hsin-I Jen[3]; Andrew K. Groves[4]; Yehoash Raphael[2]
[1]Kresge Hearing Research Institute, Department of Otolaryngology - Head and Neck Surgery, Michigan Medicine, Ann Arbor, MI, USA; [2]Kresge Hearing Research Institute, Department of Otolaryngology-Head and Neck Surgery, University of Michigan; [3]Program in Developmental Biology, Baylor College of Medicine, Houston, United States; [4]Department of Neuroscience, Baylor College of Medicine, Houston, United States

Introduction

One way to regenerate hair cells (HCs) in the cochlea is by inducing transdifferentiation of supporting cells (SCs), a process that in mammals occurs spontaneously in vestibular but not auditory epithelia. Gene transfer via adenovirus vectors is currently the most efficient way to manipulate gene expression in these cells. In guinea pigs and rats, injecting adenoviruses into scala media (SM) leads to efficient and specific transgene delivery to the SC. Here we test the outcomes of SM adenovirus injections into adult mouse ears, using both normal and deafened DTR mice.

Methods

Adult Pou4f3-DTR mice (Golub et al. 2012) were deafened by diphtheria toxin (DT) injection between ages of 5-8-weeks. Littermates without DT injection and wild-type mice were used as controls. Adenovirus carrying tdTomato reporter gene was injected into SM at different time points after DT. Hypertonic saline (10%) was mixed with the viral solution to make 1-4% concentration to test

its influence on gene transfer efficiency. Cochleae were harvested 4-7 days after virus injection, and processed for whole-mount immunohistochemistry to visualize tdTomato, Myo7a or Sox2.

Results
SM injection caused acute severe damage to outer HCs. Complete or near-complete HC ablation was seen from 1 week after DT injection. Efficient tdTomato expression in SCs was seen at 4 days after virus inoculation in non-ablated control cochlea. However, in HC-ablated animals, transgene expression was absent or minimal. To overcome the difficulty in expressing transgenes in deafened ears, we injected the adenovirus prior to, or at the same time as, DT. We determined that DT injection on the same day of virus injection resulted in the most efficient tdTomato expression in SCs throughout the cochlea. Injecting DT 4 or 10 days after virus injection resulted in robust tdTomato expression along the entire cochlea with complete HC loss. Hypothesizing that quick cell-junction stabilization after HC damage can hinder adenoviral delivery to SC, we used hypertonic saline to destabilize cell junctions. The 1.5% saline group did not show any tdTomato expression; but 2% to 4% saline increased tdTomato expression throughout the cochlea.

Conclusions
SCs in deafened DTR mice are refractory to adenovirus transduction. Injecting adenovirus prior to DT or at the same time leads to transgene expression throughout the cochlea and does not interfere with ablation of HCs. With this sequence, the DTR mouse can be used for HC regeneration studies using adenovirus gene transfer.

Supported by NIH-NIDCD grant R01-DC014832.

Mechanotransduction

PS 694

Prolonged Depolarization Affects the "Stopping Point" of Adaptation in the Mechanotransducer of Mammalian Auditory Hair Cells

Abigail Dragich[1]; Isabel Aristizábal-Ramírez[1]; Gregory Frolenkov[2]
[1]Dept. Physiology, University of Kentucky; [2]Department of Physiology, University of Kentucky

During step-like deflection of the hair bundle, mammalian auditory hair cells are able to release (adapt) the tension within mechano-electrical transduction (MET) machinery on a sub-millisecond time scale. The extent of this adaptation varies from a nearly complete decrease of MET current at small bundle deflections to almost no adaptation at deflections that saturate MET current. For intermediate deflections, tension in the MET apparatus decreases during adaptation but is never fully released. Instead, the amount of tension released appears to be pre-determined and always approaches a "stopping point", a term used in earlier literature. While the stopping point of adaptation can be seen in virtually all mammalian and non-mammalian hair cells, the mechanism that determines the point at which adaptation stops is unknown.

Here, we studied the changes of MET responses in cochlear outer hair cells after prolonged (>2 s) depolarization. Prolonged depolarization may result in cell signaling events associated with low concentration of Ca^{2+} within stereocilia. Bundle deflection with a piezo-driven rigid probe showed that prolonged depolarization has no effect on the peak current or the time constant of fast adaptation of MET responses; however, we did observe an increase in the extent of adaption. To explore this phenomenon further, we used fluid-jet deflections of the hair bundles which better reveal slow changes of MET current. Even with fluid jet deflection, we were not able to observe any significant slow component of adaptation in the cochlear outer hair cells before depolarization. However, after prolonged depolarization of the cell, we observed a dramatic increase in the extent of adaptation of MET responses evoked by the fluid-jet bundle deflection. Interestingly, these changes in the extent of adaptation resulted from a slow, "creeping"-like, decrease of the MET current during step-like deflection of the bundle and appear to be a different phenomenon than classical slow adaptation. Thus, we concluded that prolonged (>2 s) depolarization reveals a slow process in MET machinery that modifies the stopping point of adaptation. These after-effects of depolarization were observed only with depolarizations longer than 2 seconds and lasted for at least 20 seconds, self-recovering within a minute.

To our best knowledge, this is a first report of stopping point regulation in the MET machinery of hair cells. Potential mechanisms of this phenomenon will be discussed.

Supported by NIDCD/NIH R01DC014658 (to G.I.F.)

PS 695

Calcium and Integrin Binding Protein 2 (CIB2) Is Involved in Fast Adaptation of Mechanotransducer Current in Cochlear Outer Hair Cells

Isabel Aristizábal-Ramírez[1]; Abigail Dragich[1]; Mary Freeman[1]; Arnaud Giese[2]; Zubair Ahmed[2]; Gregory Frolenkov[3]
[1]Dept. Physiology, University of Kentucky; [2]Dept. Otolaryngology Head and Neck Surgery, University of Maryland; [3]Department of Physiology, University of Kentucky

The hallmark of mechano-electrical transduction (MET) in mammalian auditory hair cells is an extremely fast (less than a millisecond) decline of the MET current, known as fast adaptation. This adaptation is too fast to be mediated by a "classical" myosin-dependent adaptation motor. According to one of the models of fast adaptation, Ca^{2+} ions entering the cell through MET channels bind to the so-called tension-release element, thereby reducing the tension in the MET apparatus. Calcium and Integrin Binding protein 2 (CIB2) is an attractive candidate for the tension-release element because CIB2 is essential for hair cell mechanotransduction and binds to TMC1/TMC2 as well as to the cytoskeletal scaffold protein whirlin at the stereocilia tips (Riazuddin et al., 2012; Giese et al., 2017).

Here we explored cochlear function and MET responses in mice heterozygous for the p.F91S variant of CIB2 (*Cib2*$^{+/F91S}$). We have previously reported that homozygous *Cib2*$^{F91S/F91S}$ mice are profoundly deaf and lack "classical" MET responses in the auditory hair cells (Giese et al., 2017). In contrast, heterozygous *Cib2*$^{+/F91S}$ mice have normal hearing but, as we found, are more susceptible to noise exposure compared to their wild type littermates. Using a piezo-driven rigid probe, we quantitatively compared fast adaptation of MET responses in the same outer hair cell (OHC) at negative and positive intracellular potentials, which promote or inhibit Ca^{2+} influx though MET channels, respectively. In correspondence to the previous report (Peng et al., 2013), we've found that fast adaptation in the wild type OHCs is largely unaffected by depolarization. However, we've found significant differences between wild type and *Cib2*$^{+/F91S}$ OHCs in the extent and time constant of adaptation during intermediate bundle deflections at negative (-90mV) but not positive (+90mV) intracellular potentials. This indicates that the effects of CIB2 on fast adaptation may be indeed mediated by Ca^{2+} influx through MET channels. These effects are unlikely to be related to the changes of Ca^{2+} permeability of the MET channels since we didn't observe any changes in the reversal potential of the MET current in *Cib2*$^{+/F91S}$ OHCs. We concluded that a major component of fast adaptation in OHCs does not depend on depolarization or CIB2. However, p.F91S variant of CIB2 does affect the extent and time constant of fast adaptation. Thus, CIB2 is unlikely to be a major tension-release release element responsible for adaptation but it is rather a modulator of adaptation.

Supported by NIDCD/NIH DC012564 (Z.M.A. and G.I.F.)

PS 696

A Novel Method to Visualize Myosin Motor Proteins in Unfixed Cochleae

Itallia Pacentine[1]; Peter G. Barr-Gillespie[2]
[1]Oregon Health & Science University; [2]Oregon Hearing Research Center & Vollum Institute, Oregon Health & Science University

Myosins are motor proteins that are essential for hair-cell development and function. We developed a novel method to visualize myosins in unfixed, permeabilized hair cells. After dissecting mouse cochleae, we permeabilized the tissue with low concentrations of saponin and Triton X-100, then added phalloidin Alexa-488 to visualize stereocilia. We transferred cochleae to a perfusion chamber that was mounted on a microscope, allowing us to image permeabilized hair cells during exposure to reagents. To visualize myosins, we applied EDA-ATP-Cy3 in the presence of vanadate. Vanadate slows dissociation of ADP from myosins, extending the lifetime of myosin-ADP complexes by 1000-fold. Using this method, we consistently visualized a strong signal at the tips of stereocilia, consistent with MYO15A localization. The tip signal persisted during application of latrunculin A, an inhibitor of actin polymerization; remained in *Myo7a*$^{8J/8J}$ mice; and was absent in *Myo15*$^{sh2/sh2}$ mice. Further modification of this technique may reveal different subpopulations of myosins and allow us to study their activity in intact hair cells.

PS 697

The Dynamic Strength of the Hair-Cell Tip-Link Connection

Eric Mulhall[1]; Andrew Ward[1]; Darren Yang[2]; Mounir Koussa[1]; David P. Corey[1]; Wesley Wong[3]
[1]Harvard Medical School; [2]Boston Children's Hospital; [3]Boston Children's Hospital

The tip link is a critical component of the mechanotransduction complex in vertebrate hair cells, which converts vestibular and auditory mechanical stimuli into an electrical signal. The tip link is composed of PCDH15 and CDH23, bonded in *trans* at their N-termini through a unique handshake interface, the structure of which has been resolved by X-ray crystallography (Sotomayor et al., 2012). Electron microscopy and structural studies show that each protein of the tip link likely exists as a parallel dimer (Kachar et al., 2000; Dionne et al., 2018). How strong is the tip link bond? How can just two bonds faithfully maintain the tip link over long times? Could sufficiently loud noise break the bond?

We used single-molecule dynamic force spectroscopy, biochemistry and modeling to describe the force-

dependent kinetics of the tip-link connection. We first used fusion proteins that each contained a single N-terminal binding domain of mouse CDH23 or PCDH15, and found that the single tip-link bond is significantly more resistant to mechanical force and less sensitive to endolymphatic Ca^{2+} than typical classic cadherin bonds.

We then measured the strength of the full length, dimeric tip link, and show how single-strand rebinding enabled by its double-stranded architecture enhances its mechanical strength and lifetime. The dynamic strength of the connection is facilitated by strong cis-dimerization, which keeps unbound N-termini in close proximity. Extracellular Ca^{2+} tunes the strength of the connection by modulating the elasticity of the tip link complex. We also describe the unexpected etiology of a human deafness mutation.

Although previous studies have argued that the tip link is an exceptionally static connection, only labile to Ca^{2+} chelation or to damaging noise stimuli, our data indicate that the lifetime of a double-stranded tip link is about 10 seconds at a resting tension of 10 pN. This suggests that the connection is several thousand times more dynamic than previously thought, challenging current assumptions about tip link stability and turnover rate, and providing insight into how the mechanotransduction complex transforms mechanical information.

PS 698

Discerning multiple novel ER retention signals in TMC1 using an AQP3-GFP based reporter

David Soler[1]; Manikandan Mayakannan[2]; Andrew Sloan[1]; Thomas Mccormick[3]; Ruben Stepanyan[4]
[1]The Department of Neurosurgery & the Brain Tumor and Neuro-Oncology Center, University Hospitals Cleveland Medical Center and the Case Comprehensive Cancer Center; [2]Department of Otolaryngology, University Hospitals Cleveland Medical Center, School of Medicine, Case Western Reserve University; [3]The Department of Dermatology & The Murdough Family Center for Psoriasis, University Hospitals Cleveland Medical Center, School of Medicine, Case Western Reserve University; [4]Department of Otolaryngology, University Hospitals Cleveland Medical Center, and Department of Neurosciences, School of Medicine, Case Western Reserve University

Hair cells provide the central step for sound detection, termed mechanotransduction, where sound-evoked mechanical stimuli are converted into neural impulses, allowing the process of hearing. TMC1, a member of the transmembrane channel-like family, is a key protein of the hair cell mechanotransduction channel complex. TMC1 is a membrane protein and is known to localize to the tips of the shorter rows of hair cell stereocilia, the site of mechanotransduction. However, when expressed in heterologous cell lines, TMC1 fails to localize to the plasma membrane (PM) and instead is retained in the ER. Employing a heterologous system is indispensable for functional and structural studies of sensory transduction channel proteins involved in human deafness such as TMC1. Previously, using an AQP3-GFP Reporter (AGR) system, we recognized that TMC1 N-terminus contains a strong ER retention region, termed omega-1, which precludes any plasma membrane localization in HEK293 cells. Here, we extended the usage of the AGR system to reveal the existence of three additional omegas in the loop regions of TMC1, which completely preclude the AGR system, and presumably TMC1, from reaching the PM in HEK293 cells. Importantly, each omega signal by itself is sufficiently strong to preclude trafficking of the AGR system to the PM. Using alanine/serine mutagenesis within the previously reported omega-1, which is located between amino acids $TMC1^{138\text{-}168}$, we have been able to rescue PM localization of the full N-terminus of TMC1. Further experiments, using this approach to systematically utilize alanine/serine substitutions within each omega signal in conjunction with the AGR system, are needed to achieve TMC1 localization to the PM in heterologous cells.

PS 699

The contribution of TMC1 to hair cell transduction.

Maryline Beurg[1]; Amanda Barlow[2]; **Robert Fettiplace**[2]
[1]University of Wisconsin-Madison; [2]University of Wisconsin-Madison

Cochlear hair cells transduce sound into electrical signals by activation of mechano-electrical transducer (MET) channels thought to be formed at least partly by TMC1. We generated a mouse mutant possessing a single aspartate/asparagine substitution, D569N, in TMC1, which is at a homologous site to a dominant human genetic deafness, DFNA36. In neonatal mouse mutants, MET currents were still present in outer hair cells (OHCs), but the maximal current was smaller at postnatal day(P) 7 and there was no difference between apex and base. In apical OHCs, there was no change in single-channel conductance, but there was up to a three-fold reduction in the MET channel calcium permeability. The permeability of Ca^{2+} relative to Cs^{+} was 4.2 +/-0.5 in wild-type, 2.1 +/-0.5 in heterozygotes and 1.3 +/-0.1 in homozygotes. Reduction in the Ca^{2+} permeability of the channel, even in heterozygotes, may offer an explanation for the semi-dominance of the mutation, such that even with a single mutant copy of the gene, ion conduction through the MET channel is modified. The smaller MET current was attributable

to reduced expression of the channel, which was demonstrated with immunolabeling for TMC1 and for the auxiliary subunit LHFPL5. The stereociliary bundles appeared normal until about P8, by which time the V-shape of OHC bundles became rounded, and there was a reduction in bundle height. After postnatal day 14, there was loss of OHCs proceeding from the base to apex, and by four weeks, the mice were deaf as judged by ABR measurements. Hair cell loss and deafness were seen in heterozygotes, as well as in homozygotes. The mouse mutant accounts for the dominant human deafness and suggests that TMC1, besides forming the MET channel, can regulate its own expression.

PS 700

Physical and Functional Interactions of TMC1 and LHFPL5 in Cochlear Hair Cells

Xiaojie Yu[1]; Qirui Zhao[1]; Xiaofen Li[2]; Wei Xiong[3]; Pingbo Huang[1]
[1]Division of Life Science, Hong Kong Univ. of Science and Technology; [2]Dept of Chemical and Biological Engineering, Hong Kong Univ. of Science and Technology; [3]School of Life Sciences, Tsinghua University

The channel that governs mechanotransduction (MT) by hair cells in the inner ear has been studied intensively for 4 decades, but its molecular identity remains enigmatic. Transmembrane channel–like protein 1 (TMC1) was recently identified as a component of the MT channel, and lipoma HMGIC fusion partner–like5 (LHFPL5) is considered to be part of the MT complex and may functionally couple the tip link to the MT channel. LHFPL5 expression is suggested by a previous study to stabilize TMC1 expression in the MT complex, however, the physical and functional interactions of TMC1 and LHFPL5 remain largely unexplored.

By using yeast two-hybrid assays, we identified a fragment of human TMC1 (aa 462-643, TMC1 F3) as a binding partner of LHFPL5. Further experiments suggested that ectopic full-length TMC1 physically interacted with LHFPL5 in HEK293T cells; more importantly, TMC1 and LHFPL5 functionally interacted and increased each other's protein expression. Because TMC1 F3 harbours several deafness-causing mutations, we examined whether and how the mutations affect the physical and functional interactions of TMC1 and LHFPL5 and thereby impair hearing. Interestingly, D572N/H mutations significantly disrupt the physical and functional interactions of TMC1 and LHFPL5 while W588X/R604X had opposite effects and M486T/P514L/C515R had no effect. By using an ultra-sensitive bead-based pull-down assay developed in our own laboratory, we also examined TMC1-LHFPL5 interaction in vivo. Similarly, endogenous TMC1 and LHFPL5 in the cochleae physically interacted and increased each other's global expression. Moreover, a 20-mer peptide including D572 residue (aa 562-581 of human TMC1) completely disrupted TMC1-LHFPL5 interaction while this disrupting effect was abolished by D572N mutation. These observations further suggested that D572 is essential for TMC1-LHFPL5 interaction and D572N/H mutations disrupt TMC1-LHFPL5 interaction in vivo, which subsequently leads to hearing loss. Our study reveals previously unrecognized physical and functional interactions of TMC1 and LHFPL5 and provides molecular insight into the deafness-causing mutations D572N/H.

The work was supported by Hong Kong RGC GRF16111616 and GRF16102417, NSFC-RGC joint research scheme N_HKUST614/18, and in part by the Innovation and Technology Commission (ITCPD/17-9).

PS 701

Dissection of LHFPL5 Function in Hair Cell Mechanotransduction

Xufeng Qiu; Christopher L. Cunningham; Xiaoping Liang; Guihong Peng; Ulrich Mueller
Johns Hopkins University

We have previously shown that LHFPL5 is an integral component of the ion channel complex at tips of stereocilia that is activated by mechanical force. In addition, LHFPL5 affects the transport of the tip-link protein PCDH15 and one of the ion-channel subunits, TMC1, into stereocilia. Here we show that other members of the LHFP family cannot functionally substitute for the role of LHFPL5 in mechanotransduction. Using chimera between LHFPL5 and other LHFP proteins, we have identified domains in LHFPL5 that are critical for LHFPL5 localization to stereocilia and for mechanotransduction. Using further mutational analysis, we have identified a small domain in LHFPL5 that is critical for mechanotransduction but does not affect the transport of PCDH15 and TMC1 into stereocilia. Mechanotransduction currents are severely reduced in mutant mice that carry the small LHFPL5 mutation. The morphology of stereocilia is not affected in the mutant mice suggesting that the mutation directly affects the function of the mechanotransduction channel in hair cells. This work highlights the specific role of LHFPL5 among its homologs and shows that roles of LHFPL5 in protein transport and mechanotransduction are carried out by different protein domains.

PS 702

Disruption of tmc1/2a/2b Genes in Danio rerio Reveals Hair Cell Subtypes and Partial Overlap of tmc Function in Sensory Patches of the Inner Ear

Eliot Smith[1]; Itallia Pacentine[2]; Anna Shipman[1]; Matthew Hill[2]; Teresa Nicolson[1]
[1]Stanford School of Medicine, Department of Otolaryngology; [2]Oregon Health & Science University

Detection of auditory and vestibular information by the inner ear requires mechanoelectrical transduction (MET) channels at the tips of stereociliary bundles of hair cells. Mechanical deflection of the bundles opens these channels, causing an influx of cations. In mammals, the transmembrane channel-like proteins TMC1 and TMC2 play an indispensable role in the MET complex and substantial evidence implicates the TMCs as pore-forming subunits of the MET channel.

To investigate the role of these proteins in the zebrafish inner ear, we disrupted the orthologs of *TMC1* and *TMC2*. Due to genetic duplication, zebrafish have two *TMC2* paralogs, *tmc2a* and *tmc2b*; consequently, we produced separate zebrafish lines for homozygous *tmc* single, double, and triple mutant combinations. We examined behavioral reflexes, bundle morphology, and localization of other critical components of the MET complex in mutant larvae and their wild-type siblings. We assessed MET channel function both by measuring extracellular microphonic potentials of the inner ear maculae and with FM dyes that only label hair cells with intact MET channels.

The *tmc1*$^{Ex3+1bp}$/*tmc2a*$^{Ex4-23bp}$/*tmc2b*^{sa8817} triple mutant larvae do not react to sound or rotation of the head, lacking acoustic evoked behavioral response (AEBR) and vestibular induced eye movements (VIEM), respectively. The morphology of the stereociliary bundles is grossly normal in the triple mutant. The localization of the MET complex components Protocadherin 15a (Pcdh15a) and Lipoma HMGIC fusion partner-like 5a (Lhfpl5a) is comparable to wild-type siblings, with slightly reduced levels of Transmembrane inner ear (Tmie) proteins. Similar to the functional defects in *Tmc1*$^{(-/-)}$/*2*$^{(-/-)}$ mice, mechanical stimuli elicit no microphonic response and FM label is undetectable in the inner ear of triple mutants. The introduction of a *tmc2b* transgene, Tg(*myo6b:tmc2b-mEGFP*), fully rescues vestibular function, but only partially rescues AEBR and MET function in a subset of hair cells in triple mutant larvae.

FM-labeling in double mutants reveals hair cell subtypes that have two distinct cellular morphologies in the developing cristae. “Teardrop” shaped cells with taller bundles rely on *tmc2a*; however, *tmc2a*-independent “gourd” shaped cells with shorter bundles only require the presence of either *tmc1* or *tmc2b*. Microphonic potentials are reduced in the *tmc2a*$^{Ex4-23bp}$ single mutant and *tmc1*$^{Ex3+1bp}$/*tmc2a*$^{Ex4-23bp}$ double mutant but not in *tmc1*$^{Ex3+1bp}$/*tmc2b*^{sa8817}. The *tmc2a*$^{Ex4-23bp}$/*tmc2b*^{sa8817} double mutants showed large reductions in AEBR, VIEM, and microphonic potentials.

Our findings show a principle role for *tmc2a* in sound and balance detection in larval zebrafish while *tmc2b* restores partial function. The roles of *tmc1* and the hair cell subtypes remain unclear.

PS 703

Entry Rate of Aminoglycoside Antibiotics Varies with Position Along the Neonatal Mouse Cochlea

Virginia N. Mahieu[1]; Peter S. Steyger[2]; Corne J. Kros[1]
[1]University of Sussex; [2]Creighton University

There is evidence for a gradient in single-channel conductance of the mechano-electrical transducer (MET) channels of outer hair cells (OHCs) along the length of the cochlea, with conductance getting larger towards the basal end (Beurg et al 2006 J Neuroscience 26(43):10992-11000, Beurg, Kim & Fettiplace 2014 J Gen Physiol. 144(1):55-69). Support for this notion also comes from evidence for a visible gradient in the passage of large fluorescently labelled peptides through the channels (Desmonds et al 2014 ARO Abs:150), which may indicate a gradient in the pore diameter, increasing from apex to base.

However, a gradient in drug-induced toxicity of OHCs is observed even for smaller molecules such as the aminoglycoside antibiotics (Forge and Schacht 2000 Audiol Neurootol 5:3-22), with apical cells being relatively insensitive compared to basal. This higher sensitivity of basal OHCs may be due to several factors, e.g. a greater number of channels (Beurg et al 2006), smaller cell bodies, as well as a larger entry rate of ototoxic drugs through each channel.

Using whole-cell patch-clamp electrophysiology of OHCs in cultured cochlea from neonatal mice, we recorded MET channel activity while stimulating the hair bundle under various conditions to determine the sensitivity of MET channels of apically- and basally- located OHCs to aminoglycoside antibiotics. For several such antibiotics, including gentamicin and kanamycin, we find there is a difference in the entry rate into the cytoplasm through a single MET channel between apical and basal OHCs of early postnatal mice, which correlates with the gradient in the OHC MET channel conductance. The electrical

profile of the channel also differs between apex and base in a conserved manner between antibiotics, consistent with a narrower pore in the apex than in the base. This suggests that not only does the conductance of the MET channel vary, but so does the diameter and topology of the channel. Furthermore, we present data indicating that the fluorescently conjugated gentamicin-Texas Red (GTTR) binds more strongly to the MET channel, with a ten-fold lower half-blocking concentration than native gentamicin.

Supported by the Sussex Neuroscience 4-year PhD Programme.

Otoacoustic Emissions II

PS 704

High-Frequency Tuning in the Peripheral Auditory System of two Anuran Amphibians

Ariadna Cobo-Cuan[1]; Ulmar Grafe[2]; Fang Zhang[3]; Albert Feng[4]; Peter M. Narins[1]
[1]Department of Integrative Biology & Physiology, UCLA; [2]Faculty of Science & Institute for Biodiversity and Environmental Research; [3]College of Life Sciences, Anhui Normal University; [4]Department of Molecular and Integrative Physiology and Beckman Institute, University of Illinois

Introduction
Despite the prevalence of low-frequency hearing in anuran amphibians, a few frog species have evolved, within certain environmental contexts, high-frequency/ultrasonic communication. The hole-in-the-head frog, *Huia cavitympanum*, and the concave-eared torrent frog, *Odorrana tormota*, are both Asian species that live in unusual environments with high levels of low-frequency noise and have converged on the ability to use a high-frequency communication system. Here, we explore how the peripheral auditory system could contribute to the high-frequency hearing specialization in non-mammalian vertebrates.

Methods
Auditory function in *Huia cavitympanum* (5 males) and *Odorrana tormota* (10 males and 10 females) was assessed by distortion product otoacoustic emission (DPOAE) testing. DPOAE audiograms were measured in a broad frequency range matching the spectrum of the species' calls. Input/output functions were evaluated with f_2 frequencies that elicited large $2f_1$-f_2 emissions in the DPOAE audiograms using a fixed f_2/f_1 ratio of 1.1. In addition, the vibration of the tympanic membrane of *O. tormota* in response to acoustic stimulation with natural calls and pure tones was measured with a scanning laser Doppler vibrometer.

Results
The sensitivity spectrum of the peripheral auditory system in both frog species matches the predominant frequencies in their communication signals. DPOAE audiograms showed a bimodal dependence on frequency with two amplitude maxima that, in other frog species, have been correlated with maximum excitation in either the amphibian papilla or the basilar papilla. Males of *H. cavitympanum* have ears specialized for the detection of frequencies in both the audible and the ultrasonic range, with sensitivity peaks around 10 and 20 kHz. The vibration response of the tympanic membrane in *O. tormota* extends above 30 kHz, but the DPOAE response suggests that amplification mechanisms at the inner ear refine the auditory tuning at frequencies of biological significance. DPOAEs measurements also confirmed a sex-dependent tuning in *O. tormota*, with an upper-frequency limit at 10 kHz in females and 18 kHz in males.

Conclusions
With a communication system that includes energy in a broad spectral range, spanning from low frequencies to ultrasound, the peripheral auditory system in *H. cavitympanum* and *O. tormota* is essential to enhance the sensitivity at the spectral peaks emphasized in the mating call. A peripheral prefiltering shifted to the high-frequency spectrum in these Asian frogs, not only allows extracting the mating signals from the background noise but ensures effective reciprocal communication between males and females.

PS 705

Speech-DPOAEs for Probing Speech Processing in the Inner Ear

Marina Saiz-Alia[1]; Peter Miller[2]; Tobias Reichenbach[3]
[1]Miss; [2]Imperial College London; [3]Department of Bioengineering and Centre for Neurotechnology, Imperial College London

Humans have an exceptional ability to discern individual speakers in complex acoustic environments. We have shown recently that feedback from the auditory cortex to the brainstem through efferent fibers contributes to attending to one of two competing voices [1]. Through the olivocochlear efferent system, the neural feedback extends further down the auditory pathway to the inner ear. In particular, the medial olivocochlear (MOC) fibers synapse on the cochlear outer hair cells and can regulate their activity. However, whether this neural feedback aides the selective attention to a speaker remains unclear.

The effect of MOC fibers on outer hair cell activity can be measured non-invasively through otoacoustic emissions

(OAEs). Previous research has investigated whether OAEs are influenced by selective attention to sound, but found conflicting results. A major limitation in these studies was the simple nature of the sound sources used to evoke the OAEs – and therefore of the sounds that subjects attended to – such as pure tones or tone pips.

Here we sought to develop a method for measuring OAEs related to speech, a complex real-world and ecologically-relevant sound. In particular, we focussed on distortion products otoacoustic emissions (DPOAEs) and sought to relate them to the temporal fine structure of speech (speech-DPOAEs). To this end, we extracted temporal waveforms from a voiced speech signal that corresponded to the activity at different harmonics of the fundamental frequency. Because the fundamental frequency in speech varies over time, these waveforms did have time-varying instantaneous frequencies. We then presented two of these waveforms, corresponding to two nearby harmonics, to a subject and recorded the sound in the ear canal with a microphone. We computed the cross-correlation of the recorded sound with waveforms that corresponded to the upper and lower cubic DPOAEs. We found a significant peak in the cross-correlation at a delay of 2.4 ms, showing the presence of DPOAEs.

Our results demonstrate that non-stationary signals extracted from natural speech and related to the temporal fine structure can be used to effectively elicit and measure DPOAEs in humans. These speech-DPOAEs allow to measure the response latency, and can be recorded from relatively short speech stimuli of one minute in duration. We expect the speech-DPOAEs to serve as a useful tool to probe cochlear mechanisms of speech processing.

[1] A. E. Forte, O. Etard, T. Reichenbach (2017) The human auditory brainstem response to running speech reveals a subcortical mechanism for selective attention, eLife 6:e27203.

PS 706

Phase characteristics of Otoacoustic Emissions Evoked by Amplitude-Modulated Low-Frequency Tone

Toshimasa Ebina[1]; Sho Otsuka[2]; Shigeto Furukawa[3]; Yasuhide Okamoto[4]; Seiji Nakagawa[2]; Takashi Morimoto[1]; Yoh-ichi Fujisaka[1]; Takashi Nonaka[1]; Sho Kanzaki[5]
[1]Rion Co., Ltd.; [2]Chiba University; [3]NTT Communication Science Laboratories; [4]Tokyo Saiseikai Central Hospital / Keio Univercity; [5]Department of Otorhinolaryngology, School of medicine,Keio University

Otoacoustic emission (OAE) tests have gained widespread attention in clinical use as an objective evaluation method for inner ear function. However, the OAE test is not yet employed in the low frequency region because of the influence of low-frequency noise, such as biological noise. For example, it is very difficult to distinguish between the desired signal and the noise, when conducting the distortion product OAE (DPOAE) test in the low-frequency region using the conventional power spectrum analysis method owing to a large power interference of low-frequency noise. Therefore, this study aimed to establish an effective method for assessing the healthy function of cochlear outer hair cells (OHCs) in the low-frequency region. We focused on amplitude-modulated tone-evoked OAE (AMEOAE) as an alternative approach for evaluating low-frequency inner ear function. It is well known that when an AM signal is input into a nonlinear amplifier, the carrier phase is also modulated. It was assumed that the auditory nonlinear system shows the same trend. Otsuka et al. [Proc. Auditory Res. Meeting, ASJ, Vol. 45, No. 7, pp 563-568] reported that the recorded AMEOAE signal shows a carrier phase modulation (PM) at the same rate as the stimulus modulation rate in carrier frequency at 1000Hz. Therefore, we hypothesized that the use of AMEOAEs would offer an improved estimation of the healthy function of OHCs in low-frequency regions from phase information rather than from amplitude information.

Therefore, as a preliminary study, we investigated whether AMEOAE in low-frequency region shows a carrier PM for normal hearing. In addition, the detection rate of AM-induced PM was compared with that of DPOAE.

DPOAE and AMEOAEs were measured in ten subjects with normal hearing, and the measurement frequency was set at 250 Hz. The PMs in AMEOAEs were detected, whereas DPOAEs were not detected, in almost all the subjects. The results suggest that the use of AMEOAEs would offer an improved estimation of the healthy function of OHCs from phase information. This approach using the AM-induced PM in AMEOAEs might especially contribute to the assessment of the functioning of OHCs in the low-frequency region, to distinguish between OHC disorder and the others, such as pseudohypacusis or the feigning of illness, in people with low-tone hearing loss.

PS 707

Medial Olivocochlear Reflexes of Musicians with Various Specialities

Minoru Tsuzaki[1]; Yumi Matsuura[1]; Sho Otsuka[2]; Shigeto Furukawa[3]; Erika Yamamoto[1]
[1]Kyoto City University of Arts; [2]Chiba University; [3]NTT Communication Science Laboratories

The degree of the medial olivocochlear reflex (MOCR) of musicians has been reported to be larger than that of non-musical persons (Brashears et al., 2003). It is unclear whether the difference is related to a certain music-specific effect through intensive musical training or to the accumulated duration of sound exposures at a reasonable level. Even within the genre of classical music, performed sound levels vary among instruments. To gain insights into the underlying mechanisms of MOCR dependence on the musical-experience, we measured the MOCRs of undergraduate/graduate students from the Faculty of Music at Kyoto City University of Arts (KCUA). The specialty courses were a) piano; b) string; c) wind; d) vocal performance; and e) musicology, and the numbers of the participants of each group were 8, 21, 12, 9, and 7, respectively. In addition, eight students from the Faculty of Fine Arts at KCUA participated in the experiment as a control group. The MOCRs were measured for both the left and right ears by calculating the level differences between the click-evoked otoacoustic emissions with and without a broadband noise inducer. The noise inducer was presented contralaterally and ipsilaterally. In the contralateral condition, the noise was presented simultaneously with the clicks. In the ipsilateral condition, the forward suppression paradigm was applied. ANOVAs revealed that the degree of the ipsilateral MOCRs of the left ear varied significantly across specialties, and the effect of this factor on the contralateral MOCRs of the right ear was marginally significant. The mean degree of the MOCR of the string group appeared larger than that of the other groups. The contrast between the string and non-string groups was tested, and significant differences were observed for the results of both ears. This contrast between the string and non-string groups was also significant for the contralateral MOCRs, although the factor of the specialty did not satisfy the significant level in the first phase ANOVA. Among the students in the Faculty of Music, the piano and string players had the longest, comparable experience of musical training and had started at the youngest ages. This implies that the difference in MOCR magnitudes cannot be explained simply by the length of musical training. We observe no significant difference between the musical course groups and the fine arts course.

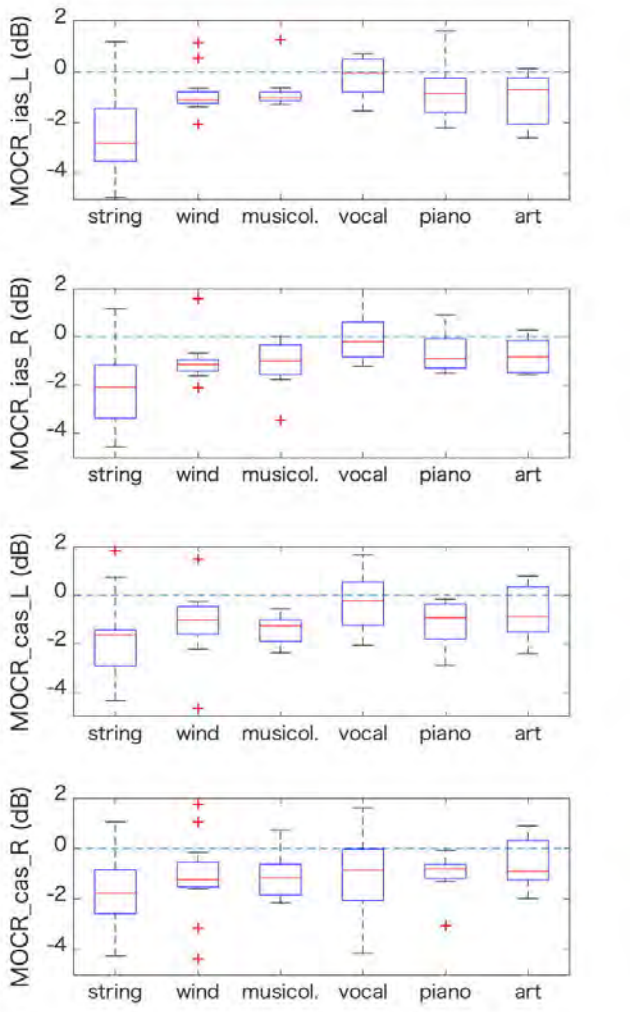

PS 708

Temporal Expectation Modulates Medial Olivocochlear Bundle Reflex

Sho Otsuka[1]; Seiji Nakagawa[1]; Shigeto Furukawa[2]
[1]Chiba University; [2]NTT Communication Science Laboratories

Previous reports indicate that temporal expectation modulates neural activity of cortical and subcortical areas, when sounds occur at predictable moments. However, it is not known if temporal expectation affects processing at auditory periphery. We examined whether temporal expectation modulates the medial olivocochlear reflex (MOCR), a sound-activated feedback response that controls the motility of the outer hair cells (OHCs). The suppression of click-evoked otoacoustic emissions (OAEs) induced by noise presented to the contralateral ear, was used to non-invasively assess the MOCR. The degree of the suppression is thought to reflect the gain reduction of OHCs induced by MOCR. The clicks were presented at the rate of forty clicks per second, and at peak equivalent sound pressure level (SPL) of 55 dB. The noise had a duration of 500 ms and was presented

at 60 dB SPL. In experiment 1, a fixed inter stimulus interval (ISI) was used between the presentation of a visual cue (a cross displayed on a monitor) and the contralateral noise, an elicitor. OAE suppression induced by the elicitor was stronger than OAE suppression without a preceding visual cue. By contrast, when the ISI between the visual cue and elicitor varied, enhancement was not observed; the visual cue did not provide exact information about the timing of the elicitor. These results suggest that the MOCR enhancement reflects increases in preparatory processes with the predictability of timing of the elicitor occurrence; it does not suggest enhanced general readiness of attention induced by the preceding visual cue. In experiment 2, the appearance of a small or big cross cued participants to expect the elicitor after a short interval (250 ms from cue offset) or long interval (1250 ms from cue offset), respectively. We compared OAE suppression induced by the elicitor following a valid and invalid cue. In the latter case, an elicitor appears after the short or long interval although the visual cue predicted the opposite interval. The elicitor occurring after the long interval unexpectedly induces weaker OAE suppression. The elicitor occurring after the short interval unexpectedly induces OAE suppression comparable to the elicitor occurring at an expected moment. The result implies that the MOCR enhancement starts before the expected timing, and disappears after that. In summary, our findings indicate that temporal expectation can modulate MOCR, thereby indirectly influencing OHC motility, based on prior knowledge of timing of occurrence of sounds.

PS 709

Effect of Temporal Regularity of Preceding Sound Sequences on Medial Olivocochlear Reflex

Yuki Ishizaka[1]; Sho Otsuka[2]; Seiji Nakagawa[2]
[1]Student; [2]Chiba University

Medial olivocochlear (MOC) fibers are efferent projections from the superior olivary complex to the outer hair cells (OHCs). The MOC fibers are activated by acoustic stimulation and exert an inhibitory effect on OHC motility; this effect has been termed the medial olivocochlear reflex (MOCR). Our previous studies showed that a preceding sound, regardless of whether it induced an MOCR by itself, expedites MOCR, which suggests that temporal expectation about the timing of stimulus occurrence can modulate MOCR. These investigations were limited to the effect of a single preceding stimulus on MOCR. However, the temporal structure, e.g., regularity and rhythm, of preceding sequences also contains cues for temporal expectation about the timing of upcoming sounds. Here we investigate whether temporal expectation based on the regularities of preceding sound sequences can modulate the MOCR. The MOCR was assessed noninvasively using otoacoustic emissions (OAEs), which are sounds that originate in the cochlea and reflect OHC motility. We measured the suppression of OAEs induced by contralateral noise. The suppression is thought to reflect the MOCR-induced gain reduction of OHCs, which is activated by contralateral acoustic stimulation. OAEs were evoked by clicks, which were presented at the rate of forty clicks per second and at a peak equivalent sound pressure level (SPL) of 70 dB.

One stimulus block for the contralateral ear was composed of a noise and three tone bursts that preceded the noise. The inter-stimulus interval (ISI) among the tone bursts and the noise were varied in two conditions—predictable and unpredictable. In the predictable condition, the ISIs among three tone bursts and one noise were set to 500 ms. In the unpredictable condition, the tone bursts and noise were presented with a variable ISI randomly chosen from 250, 500, and 1000 ms for each presentation. The SPL of the tone bursts and noise was 70 dB. The OAE suppression induced by a noise with ISI of 500 ms after the third tone burst was selected in the unpredictable condition and compared with that in the predictable condition.

The OAE suppression in the predictable condition was stronger than that in the unpredictable condition. The difference in OAE suppression cannot be explained by the effect of a general attention readiness evoked by a single stimulus presented immediately before a noise. This result suggests that MOCR can be modulated by the temporal prediction based on the regularity of the preceding sound sequences.

PS 710

Distortion Product Otoacoustic Emissions Change with Short Lasting Adaption State of Outer Hair Cells

Lukas Rüttiger
University of Tübingen, Department of Otolaryngology, Head and Neck Surgery Tübingen

Introduction and Aim
The sense of hearing embraces a huge dynamic range of environmental sounds from very dim to very loud nature. For the detection and differentiation of dim sound signals, the active movement of outer hair cells is the main contributor to increase the sound induced fluid vibrations to overcome the threshold for activation of sensory inner hair cells (the cochlear amplifier). To meet the actual environmental requirements this active amplification needs to be regulated and modified by adaptation processes that need to take effect below protective responses from middle ear muscle reflex

(MEMR) or activation of the olivo-cochlear efferents (MOC reflex).

Methods
In the rat model, the 2f1-f2 distortion product was evoked over a wide range of stimulus levels (input-output DPOAE growth function with L1 = -10 – 65 dB SPL) before, after moderate sound exposure (3 minutes of about 40 dB SPL), and after stronger sound exposure (3 minutes to about 60 dB SPL) to repetitive, multi frequency tones. The amplitudes of the 2f1-f2 distortion product response was measured before exposure, after exposure, and after recovery times of 10 to 20 minutes. Since middle-ear muscles play an important role for the moderation of acoustic signals reaching the cochlea, the presence of short-term, fast, adaptation of the 2f1-f2 DPOAE signals after stimulus onset was tested in the time domain of the emission signal using primary tone phase variations.

Results
Directly after the 3 x 60 sec-long presentation of the adapting stimulus (60 dB SPL) the 2f1-f2 DPOAE signal response was significantly reduced as compared to the signal response before exposure. This reduction of DPOAE signals from mid-level auditory stimulus responses to moderate continuous sound-exposure of 60 dB SPL was found also in other rodent species (mouse) and was shown to be reversible within a 10-minute recovery time. Phase an amplitude of emission signals follow a close relationship

Conclusions
The short term (minutes) reduction of the 2f1-f2 DPOAE responses to moderate-level stimuli (60 dB SPL) may reflect a slow and reversible short time adaptation of OHC amplification to vivid auditory environments. This adaptation probably presents an intrinsic strategy to regulate OHC contributions for cochlear compression. Therefore, the cochlear amplification adjustment may denote a modification that is independent of MEMR or MOC reflexes that come into play on a much faster time scale but only at high sound levels.

Acknowledgements
Supported by the German Research Council (DFG) grant SPP1608 RU-316/12-1.

PS 711

Understanding the Aging Ear: Distortion and Reflection Otoacoustic Emissions (OAEs) in Younger and Older Ears with Normal Behavioral Thresholds

Courtney S. Glavin[1]; Uzma S. Wilson[1]; Samantha M. Stiepan[1]; Andrea I. Martin[1]; Rachel S. North[1]; Jonathan H. Siegel[2]; Sumitrajit Dhar[1]
[1]Northwestern University; [2]Northwestern University; Dept of Communication Sciences and Disorders

Age-related hearing loss is a growing public health concern. In the United States alone, it is estimated that over 50% of individuals aged 70+ have some degree of hearing impairment; this number is expected to rise due to general population aging (Lin, Niparko, & Ferruci, 2011). Although functional deficits related to aging are generally thought to manifest later in life, recent work indicates that changes in cochlear function may occur as early as the second or third decade (Poling et al., 2014). There is a need to both understand the mechanisms contributing to auditory aging and to detect these age-related changes prior to the onset of functional deficits. Here we explore the relationship between age and cochlear function using two types of otoacoustic emissions (OAEs).

OAEs are low-level sounds generated by active processes within the cochlea and may be a powerful tool to aid in both the detection and elucidation of auditory senescence. It is theorized that there are at least two distinct types of emissions – distortion and reflection – and that each originate from different cochlear processes. Distortion emissions are thought to arise from nonlinear processes related to hair cell transduction, whereas reflection emissions are thought to arise from the backscattering of energy due to irregularities ("roughness") along the cochlea (Zweig & Shera, 1995; Shera & Guinan, 1999). Previous work indicates that distortion and reflection emissions are differentially affected by age, likely due to their differing generation mechanisms (Abdala & Dhar, 2012; Poling et al., 2014; Abdala, Ortmann, & Shera, 2018). Specifically, distortion emissions appear to decline in level at a faster rate than reflection emissions with age (Abdala, Ortmann, & Shera, 2018).

The current study extends this work. We examine the relationship between aging and cochlear function via distortion product otoacoustic emissions (DPOAEs) and stimulus-frequency otoacoustic emissions (SFOAEs) in adults aged 18-61 years with clinically-normal behavioral thresholds. Absolute levels and growth characteristics of DPOAEs and SFOAEs over an extended frequency range will be discussed.

PS 712

Does Aging Effect Cochlear Gain and Tuning?: An Investigation using Stimulus Frequency Otoacoustic Emissions (SFOAEs)

Uzma S. Wilson; Sumitrajit Dhar
Northwestern University

The cochlea is responsible for our exquisite sensitivity to soft sounds, fine frequency selectivity, and large dynamic range (Robles & Ruggero, 2001). These gain, tuning and compression characteristics are a result of the active processes related to outer hair cell activity (Ruggero, 1992). Damage to the cochlea due to aging or toxicity is typically thought to affect all three properties of the cochlea simultaneously (Sellick et al, 1982). However, evidence from auditory nerve tuning curves of cats with various types of induced cochlear insults suggests that gain and tuning may not be affected in the same way (Liberman & Dodds, 1984).

Otoacoustic emissions (OAEs), byproducts of cochlear active processes, are typically used to assay various cochlear processes non-invasively in humans (Kemp, 1978). Here, we examine stimulus frequency otoacoustic emissions (SFOAEs), which are evoked using a single tone or sweep, in order to ask whether cochlear aging has a differential effect on cochlear gain and tuning.

Abdala et al (2018) recently showed that SFOAE levels are reduced in older adults (62-76 years old) compared to young (18-31 years) and middle-aged adults (40-60 years). However, SFOAE phase gradient was steeper in the older two groups compared to the young group, paradoxically indicating sharper tuning in older adults. These findings suggest that cochlear gain and tuning change independently as a function of age. If true, these effects are expected to be more pronounced at high frequencies, which show the earliest change in cochlear status (i.e. > 8 kHz) (Dewey & Dhar, 2018).

Therefore, the goal of this study was to examine the effects of aging on overall SFOAE levels and phase-gradients across a wide range of frequencies. SFOAEs were recorded for f_p = 0.5-20 kHz at multiple stimulus levels (relative to behavioral thresholds) in four different age groups (7-12; 18-25; 30-35; 40-45 years). SFOAE levels and growth characteristics were obtained. The frequency vs phase function was then used to compute the SFOAE phase-gradient delay. Behavioral thresholds and tuning estimates were also obtained and will be compared to various properties of SFOAEs.

PS 713

Dependence of the Nonlinear-Distortion and Coherent-Reflection Components of Cubic Distortion Product Otoacoustic Emissions on Level and Frequency Ratio: Experiment and Model

Vaclav Vencovsky[1]; Ales Vetesnik[1]; Ondrej Klimes[1]; Anthony W. Gummer[2]
[1]Czech Technical University in Prague; [2]University of Tübingen

Stimulation of healthy ears with two pure tones of nearby frequencies generates distortion product otoacoustic emissions (DPOAEs) due to the nonlinear mechano-electrical transducer in the stereocilia of outer hair cells. DPOAEs measured in the ear canal represent interference between two components generated by the wave-fixed (nonlinear distortion or primary) or place-fixed (coherent reflection or secondary) sources. The primary source is located in the region where the evoked traveling waves maximally overlap. The width of this overlapping region depends on the stimulus frequency ratio, f_2/f_1, and their levels, L_1 and L_2. The present work analyses DPOAEs measured in normal hearing subjects using a two-dimensional nonlinear cochlear model. The amplitude and phase of the DPOAE nonlinear-distortion and coherent-reflection components are evaluated as a function of stimulus levels and frequency ratio, with prominent features being explained using simulation results.

DPOAEs were measured with swept sinusoids. The f_2 frequency was swept between 1 and 4 kHz, the level of one of the tones was kept at 50 dB FPL (the OAE probe was calibrated relative to the measured pressure of the forward-going wave) and the level of the other tone was varied: L_2 from 30 to 60 dB FPL or L_1 from 40 to 70 dB FPL. The frequency ratio f_2/f_1 was 1.1, 1.2, and 1.3.

The experimentally measured amplitude of the DPOAE nonlinear-distortion component generally had a bell-like shape when plotted as a function of either L_1 or L_2, with the other tone kept at 50 dB FPL. The largest departure from this bell-like shape was visible at the largest frequency ratio (f_2/f_1 = 1.3). Here, especially at low frequencies (up to about 2.5 kHz), the DPOAE amplitude was largest for L_1 = 70 and L_2 = 50 dB FPL. Usually, this frequency ratio and level yielded larger DPOAE amplitude than the “optimal” ratio of 1.2 customarily used in the experimental literature. The coherent-reflection source caused amplitude fluctuations in the DPOAE amplitude plotted as a function of frequency for constant f_2/f_1. The largest fine structure changes were visible for L_2 = 50 dB FPL, L_1 varied, and f_2/f_1= 1.1. Using the cochlear model, these fine structure changes were identified to be mainly due to basal shift of the primary source on the BM as L_1 increases. These place shifts in the primary source led to phase shift of the nonlinear-distortion component and, therefore, affected DPOAE fine structure.

PS 714

Characterization of an Acute and Cyclic Cisplatin-Induced Hearing Loss in Male Fischer-344 Rats

Trang Nguyen[1]; Lillian Smith[1]; Changsuk Moon[1]; Raja Poda[1]; Jessica Wang[1]; Ning Pan[1]; Lars Becker[1]; Ed Rubel[2]; Inmaculada Silos-Santiago[1]
[1]Decibel Therapeutics; [2]Virginia Merrill Bloedel Hearing Research Center, University of Washington

Cisplatin chemotherapy has significantly increased survival in numerous cancer patient populations for decades. However, cisplatin treatment often results in undesirable side effects, including ototoxicity. Understanding the relationships between cisplatin exposure, the frequency specificity of damage and severity of the progression of hearing loss is critical for determining therapeutic strategies. In this study, we characterize two clinically relevant regimens of cisplatin induce hearing loss in the Fischer-344 (F344) rats.

Protocol 1 – Single dose: Male F344 rats were given a single intraperitoneal injection of 9.75 mg/kg of cisplatin at 9-12 weeks of age. Auditory Brainstem Response (ABR) and Distortion Product Otoacoustic Emissions (DPOAEs) were tested at one week after cisplatin injection. This acute cisplatin regimen resulted in significant DPOAE threshold shifts (between 10-45 dB), ABR threshold shifts (between 15-45 dB), and outer hair cell (OHC) death (between 30-60%) in the basal region of the cochlea (>16 kHz). A single systemic injection of cisplatin has no effect on inner hair cell (IHC) survival. Signs of systemic cisplatin toxicity like weight loss, dry skin, dehydration, delayed gastric emptying and diarrhea were observed and lasted for the duration of the study (one week). Moderate incidence of mortality was observed with high dose cisplatin regimen.

Protocol 2 – Cyclic model: Male F344 rats were administered a single intraperitoneal dose of 3 mg/kg of cisplatin on day 1, 5, 8, 12 and 15 for a total of 5 doses (15 mg/kg). DPOAEs and ABRs were tested on day 18, 37, 75 and 106 after the last cisplatin injection. Cisplatin treated rats have observable DPOAE threshold shifts (up to 45 dB), ABR threshold shifts (up to 50 dB), OHC and IHC loss (up to 100%) in a frequency dependent manner. Signs of systemic cisplatin toxicity like weight loss, dry skin and dehydration were observed. However, the body weight started to increase by day 37. Low mortality rate was observed with the cyclic, cisplatin low dose regimen. Hearing loss in this model is very stable over time, lasting at least 90 days after the last cisplatin injection.

These cisplatin regimens produced ototoxicity, hearing loss patterns and systemic toxicity which can potentially provide platforms for examining mechanisms of cisplatin-induced hearing loss as well as being used to assess therapeutic interventions to protect the hearing of cancer patients receiving cisplatin therapy.

PS 715

Consumption of betel quid is associated with sensorineural hearing loss

Yen-Fu Cheng[1]; Yen-Hui Chan[2]; Chin-Ju Hu[2]; Ying-Chang Lu[3]; Chuan-Jen Hsu[4]; Chen-Chi Wu[5]
[1]Taipei Veterans General Hospital, National Yang-Ming University, Taiwan; [2]National Taiwan University, Taipei, Taiwan; [3]National Yang-Ming University, Taiwan; [4]Taichung Tzu Chi Hospital, Buddhist Tzu Chi Medical Foundation, Taichung, Taiwan; [5]Department of Otolaryngology, National Taiwan University Hospital

Betel quid is among the most widely used psychoactive substances worldwide, along with tobacco, alcohol, and caffeine. Globally, more than 600 million people are estimated to consume betel quid in some form. In addition to the carcinogenicity leading to upper aerodigestive cancers, it also increases the risks of disorders affecting several organs. As betel quid contains several neurotoxic ingredients, we hypothesize that it also possesses ototoxicity and may lead to sensorineural hearing loss (SNHL).

In this study, we investigated the contribution of betel quid consumption to SNHI in a large clinical cohort and explored the pathogenetic mechanisms. We identified a positive correlation between betel quid consumption and hearing loss across different frequencies. We also explored the toxicity of arecoline, the main neuroactive ingredient of betel quid, on murine cochlear expant tissue ex vivo. We found that Arecoline reduced cell activity in the explants. These findings provide insights into underlying mechanism and possible preventive strategies against SNHL caused by Betel quid.

PS 716

Effect of Salicylate on Cochlear Temporal Resolution

Li Li[1]; Xiaopeng Liu[1]; Guang-Di Chen[2]; Richard Salvi[3]
[1]Center for Hearing and Deafness, University at Buffalo; [2]Center for Hearing and Deafness; [3]Center for Hearing and Deafness, 137 Cary Hall University at Buffalo, Buffalo, NY 14214

Background
High-dose sodium salicylate (SS) induces a transient cochlear hearing loss of ~20-30 dB. Besides affecting

outer hair cells, the SS treatment also reduces glutamate receptors on the inner hair cell afferent synapses which could potentially impair neural adaptation and temporal processing. To investigate this issue, we evaluated the temporal response properties of the compound action potential (CAP) pre- and post-salicylate injection.

Methods

The CAP was measured in rats before and 2 hours after treatment with 250 mg/kg SS. We used a double-tone stimulus paradigm to assess temporal resolution. The two tone bursts (5 ms duration with 1 ms rise/fall time) with different inter-tone intervals (2-32 ms) between the offset of the first pulse and the onset of the second pulse were presented at a rate of 10/s at a same frequency and intensity. The amplitude of the CAP to the second tone (CAP_2) was compared to the first tone (CAP_1). The CAP_2/CAP_1 ratio, expressed in percent, was plotted as a function of inter-tone interval.

Results

The ratio of CAP_2/CAP_1 decreased linearly from ~95% (almost no suppression) at 32 ms to ~20% at 2 ms. The decline in the CAP_2/CAP_1 amplitude ratio is believed to be indicative of neural adaptation occurring at the synapse between the inner hair cell and type I auditory nerve fiber. SS treatment caused an increase in CAP threshold of ~20 dB at both 6 kHz and 24 kHz. At 24 kHz, the CAP_2/CAP_1 ratios post-SS were significantly lower than pre-SS at short inter-tone intervals (< 16 ms), but were normal at long inter-tone intervals (32 ms). In response to the double-tone with 16 ms inter-tone interval, the CAP_2/CAP_1 ratio of 72% (±2.4) pre-SS was significantly reduced to 52% (±3.1) post-SS ($p< 0.01$), but in response to the double-tone with 32 ms inter-tone interval, the CAP_2/CAP_1 ratio of 89.6% pre-SS was only slightly reduced to 87.6% post-SS ($p >0.05$). However, we did not observe such effect at 6 kHz. These results suggest that SS disrupted temporal resolution by slowing the recovery from neural adaptation at 24 kHz, but not at 6 kHz.

Summary and Discussion

The 250 mg/kg dose of SS disrupted temporal resolution by depressing CAP_2 amplitudes at short inter-tone intervals possibly due to disruption of the afferent synapse. This change in temporal processing is consistent with the previous behavioral results showing that SS increases gap-detection thresholds.

PS 717

Mechanotransduction Activity Facilitates Hair Cell Toxicity Caused by the Heavy Metal Cadmium

Tamara Stawicki; Isabella Alampi; Caleigh Schmid; Kelly Tarcza; Jay Briggs
Lafayette College

Hair cells are sensitive to many insults including environmental toxins such as heavy metals. Studies have shown links between hearing loss and occupational exposure to or elevated levels of heavy metals in humans. Additionally, hearing loss and hair cell death has been seen in animal models in response to heavy metal exposure. However, the mechanism by which heavy metals cause hearing dysfunction has not been fully elucidated. One open question is how these metals enter hair cells. Some heavy metals are required in cells at trace levels and only toxic at higher levels. These metals usually have designated transporters to enter cells. However, other heavy metals, such as cadmium, have no known function in living organisms and therefore no designated entry mechanism into cells. Instead, cadmium is believed to largely enter cells through ion channels and transporters for other ions such as zinc. To determine how cadmium entered hair cells we tested for reduced cadmium-induced hair cell death in hair cells of the zebrafish lateral line in response to treatments that could potentially block cadmium entry. We attempted to block cadmium entry into hair cells through inhibiting mechanotransduction activity, as this has been shown to protect against other hair cell toxicants, and competing for cadmium with zinc and copper as this has been shown to decrease cadmium uptake in other cell types. We first found that cadmium was able to kill hair cells of 5 days post fertilization (dpf) zebrafish in a dose-dependent manner. We found that blocking hair cell mechanotransduction activity either genetically using a *cdh23* mutant or pharmacologically using the drug benzamil showed significant protection against cadmium-induced hair cell death at a range of cadmium doses. In contrast to this pretreating fish for one hour and then cotreating fish with either zinc or copper showed either modest or no protection respectively. Therefore, we conclude that the mechanotransduction channel and mechanotransduction activity is important for cadmium-induced hair cell death presumably through influencing cadmium entry. With other ion channels such as zinc transporters potentially playing a minor secondary role.

PS 718

Rapid Macrophage Response to Ototoxic Injury of Zebrafish Lateral Line Neuromasts

Mark Warchol; Angela Schrader; Lavinia Sheets
Washington University School of Medicine

The inner ear contains resident macrophages which are recruited to sites of hair cell injury. Similarly, lateral line neuromasts of larval zebrafish typically possess 1-2 nearby macrophages, which migrate into neuromasts after ototoxic injury (Hirose et al., Hearing Res, 2017). The signals that mediate macrophage recruitment toward injured hair cells have not been identified. The optical

clarity of larval zebrafish permits direct imaging of cellular interactions that occur during the hair cell injury, making zebrafish an ideal model for characterizing the interaction between macrophages and hair cells. The present study quantified changes in hair cell structure and in macrophage localization in neuromasts of the zebrafish lateral line in response to treatment with neomycin.

Studies used *Tg*(*mpeg1:ypf*) transgenic fish, which express YFP in macrophages and microglia. At 6-7 dpf, fish were incubated in 100 µM neomycin for 5-30 min, and were either fixed immediately after treatment or were allowed to survive for 1-2 hr. Hair cells were immunolabeled for otoferlin and nuclei were stained with DAPI. All data were collected from neuromast L5 of the posterior lateral line. Results indicate that macrophages respond very quickly to ototoxic injury. Phagocytosis of injured hair cells was first observed at five minutes after the initiation of neomycin treatment. At later time points, macrophage cytoplasm contained both otoferlin-labeled debris and pyknotic nuclei. Active phagocytosis was apparent in 60-80% of neomycin-treated neuromasts. In contrast, no phagocytosis was observed in untreated (control) fish. We also used Annexin V labeling to test for externalization of phosphatidylserine (PtS), a signal that targets a dying hair cell for removal by macrophages. Annexin V labeling of the apical hair cell surface was observed at ~90 sec after the initiation of neomycin treatment, but was not observed in control fish.

A final set of experiments examined whether macrophages stimulate hair cell regeneration. These studies utilized *Tg*(*mpeg1:ntr*) fish, which permit the selective elimination of macrophages by treatment in metronidazole (MTZ). Macrophage-depleted and control fish were exposed to 100 µM neomycin and then allowed to recover for 48 hr. Macrophage numbers in MTZ-treated fish remained very low for this entire period, while control fish contained normal numbers of macrophages. We observed only very minor differences in hair cell recovery in macrophage depleted vs. control fish, suggesting that macrophages are not essential for regeneration of lateral line hair cells.

PS 719

YAP1 Signaling is Involved in The Death of Cochlear Hair Cells

Vikrant Borse[1]; Mark Warchol[2]
[1]Washington University in Saint Louis; [2]Washington University School of Medicine

Background
The YAP1 transcriptional coactivator modulates multiple processes including cell proliferation, differentiation, maturation, survival and death. YAP1 is an effector of the Hippo signaling pathway and is normally confined to the cytoplasm. Inhibition of the Hippo pathway leads to nuclear translocation of YAP1, where it interacts with multiple transcription factors such as TEAD, RUNX, SMADs, p73 to regulate gene expression. Mechanosensation-mediated YAP1 nuclear translocation has been shown in cultures of the mouse utricle (Borse et al., ARO poster PS471, 2019). The present study characterizes the expression pattern of YAP1 in the developing cochlea. Further, it examines the effect of hair cell (HC) damage on YAP1 expression in the inner ear of Pou4f3 hu-DTR mice and the role of HC specific YAP1 overexpression in the inner ear of neonatal mice.

Methods
Immunolabeling was used to characterize the expression of YAP1 in cochleae of developing mice. The Pou4f3-huDTR mice were used to examine the effect of HC loss on YAP1 expression *in vivo*. Single dose of DT 5ng/g (i.m) and 25ng/g (i.p) were administered to P5 and 4-6-week adult Pou4f3-huDTR mice, respectively. We also used YAP KI mice, in which expression of Cre recombinase promote transcription of YAP1 and GFP (Su et al., 2015). YAP KI mice were crossed with Pou4f3CreERT line and Pou4f3CreERT; YAP1 KI mice were generated, to examine the effects of YAP1 overexpression in the inner ear hair cells. Cochleae and utricles were collected and immunolabeling was performed using antibodies against YAP1, GFP, Myosin VIIa, SOX2 and Cleaved Caspase 3 in the whole mount samples. Some specimens were also immunolabeled with phalloidin.

Results
YAP1 expression in the cochlea was mainly confined to supporting cell cytoplasm, although nuclear YAP1 was also observed in Hensen's cells. DT treatment resulted in significant loss of HCs in cochleae and utricles of Pou4f3-huDTR mice. YAP1 expression was observed in dying cochlear HCs, but not vestibular HCs. HCs specific YAP1 overexpression in Pou4f3CreERT-YAP1 KI mice did not affect HC survival in the cochlea or utricle at P7. The recombination efficiency of Pou4f3CreERT line was more than 50% at P7.

Conclusion
YAP1 expression is upregulated by dying cochlear – but not vestibular – hair cells in Pou4f3-huDTR mice.

PS 720

Functional Validation of a Mouse Model for Otovestibular Loss Induced by Allylnitrile

Dorien Verdoodt[1]; Sander Eens[1]; Krystyna Szewczyk[1]; Isabel Pintelon[1]; Debby Van Dam[1]; Peter Ponsaerts[1]; Vincent Van Rompaey[2]

[1]University of Antwerp; [2]University of Antwerp, Antwerp University Hospital

Background

Growing evidence indicates that loss of auditory and vestibular function negatively impacts on cognition. Dependable models for otovestibular loss in mice are a long-standing need to further correlate otovestibular status to cognition. Recently, a viable allylnitrile intoxication mouse model has been established, paving the way for allylnitrile as specific ototoxic tool for induction of otovestibular loss due to degeneration of sensory hair cells (HCs). For hearing evaluation, it is imperative for animals to remain still. Immobilization is often accomplished using the general anesthetics isoflurane or ketamine/xylazine. However, so far, only few studies have directly compared their effects on auditory sensitivity in mice.

Materials and Methods

Adult male CBACa mice were randomly allocated into an allylnitrile (n=8) and a control group (n=6). After baseline audiovestibular measurements, mice were co-administered with a single-dose of allylnitrile peroral at 0 or 1.0 mmol/kg and, to reduce systemic toxicity, three injections of trans-1,2-dichloroethylene (TDCE) intraperitoneally at 0 or 100 mg/kg, 30 min before and 6 and 24 h after allylnitrile. Hearing loss was evaluated by auditory brainstem responses (ABRs) and distortion product otoacoustic emissions (DPOAEs). Behavioural test batteries were used to assess vestibular dysfunction. After testing, temporal bones were dissected for evaluation of HC loss using confocal microscopy. For direct comparison of anesthesia effects on hearing function, baseline ABR and DPOAE measurements were performed in all mice (n=14) under isoflurane and ketamine/xylazine.

Results

Allylnitrile-treated mice lacked detectable ABR thresholds at each frequency tested (2 to 32 kHz), while DPOAE thresholds were significantly elevated in the low-frequency region of the cochlea (5 to 11 kHz) and completely lacking in the mid-to high frequency region (12 to 32 kHz). One-week post-dosing, increased vestibular dysfunction rating (VDR) scores to intermediate values (i.e. 11 to 15) were observed in three out of six allylnitrile-treated mice. Over time, however, VDRs of affected subjects progressively declined to values in the control range (< 3). Gait analysis and stationary beam test performance confirmed the preserved vestibular function 11 weeks post-dosing. Hearing function of mice, as determined by ABRs and DPOAEs, was significantly poorer under isoflurane anesthesia relative to ketamine/xylazine anesthesia.

Conclusion

We present the allylnitrile intoxication CBACa mouse model as a new, reliable and nonsurgical approach for induction of isolated hearing loss. Despite all the advantages that make isoflurane an attractive option as general anesthetic in auditory research, caution should be taken due to its confounding influence on the auditory system.

PS 721

Neomycin inhibits mitophagy and increases auditory hair cell damage

Yuhua Zhang[1]; Renjie Chai[2]
[1]Key Laboratory for Developmental Genes and Human Disease,Institute of Life Sciences,Southeast University,Nanjing ,China; [2]Key Laboratory for Developmental Genes and Human Disease, Ministry of Education, Institute of Life Sciences,Southeast University, NanJing, China

Aminoglycoside is one of the main causes of hearing loss, the reactive oxygen species which released from damaged mitochondria is the key factor for hair cell death. Under normal conditions, damaged mitochondria are degraded by mitochondrial quality control systems such as mitophagy, which maintains mitochondrial mass and ensures normal life of cells. It is unclear whether the mitophagy involved in, and how to regulate the clearance of damaged mitochondria in neomycin-induced hair cell damage. In this study, we used HEI-OC-1 cells as the object of study, the mCherry-Parkin plasmid, EGFP-Parkin plasmid and Flag-Parkin plasmid has been used to examine the translocation of Parkin to mitochondria, we used western blot to detect the expression of mitochondria related protein which can reflect the clearance of damaged mitochondria, in addition, mt-mkeima has been used to test mitophagy level in vitro, we also used EGFP-OPTN plasmid which is a mitophagy receptor to estimating the recruitment of mitopahgy receptor. We first found that PINK1/Parkin-mediated mitophagy which involved in the regulation of damaged mitochondria clearance in the HEI-OC1 cell line, including Parkin recruitment on mitochondria after CCCP treatment, the outer mitochondrial membrane protein TOM20 and the inner mitochondrial memebrane protein COX IV were decreased following the CCCP administration for 24h. We then used neomycin to injury HEI-OC-1 cells and found that mitochondria mass, cell numbers with LC3B on mitochondria and the 561nm signal of mt-mKeima were significantly depressed. Next, we demonstrated that neomycin prevented Parkin which is the key factor of mitophagy recruitment onto the depolarized mitochondria. The colocalization of mitophagy adaptor OPTN with Ubiquitin or LC3B was reduced, we also found that neomycin affected the

transcriptional regulation of PINK1 which is one of the mitophagy initiated factor. After mitophagy dysfunction was partially ameliorated with Parkin activator plasmid which can promote Parkin translocation on mitochondria and we found that the clearance of damaged mitochondria was significantly relieved, and cell death were reduced after neomycin injury. The results in this present research disclose that destroyed mitophagy is an important cause of hair cell damaged by neomycin, PINK1 may be a latent target for restoring hair cell loss following neomycin (aminoglycoside) damage.

PS 722

Intratympanic Lipopolysaccharide Induces Inflammatory Response and Elevates Systemic Gentamicin Uptake in the Cochlea

Yongchuan Chai[1]; Alisa Hetrick[1]; Liana Sargsyan[1]; Hao Wu[2]; Hongzhe Li[1]
[1]VA Loma Linda Healthcare System; [2]Shanghai Jiaotong University School of Medicine

Background
Lipopolysaccharide (LPS), an essential component of the bacterial endotoxin, activates tissue macrophages and triggers the release of inflammatory cytokines. In animal models, intratympanic (*i.t.*) injection of LPS is known to simulate acute otitis media (AOM) and modifies the structure and function of the inner ear. However, whether LPS-induced AOM modulates the uptake of ototoxic aminoglycosides *in vivo* is unclear. In this study, we established an AOM mouse model to investigate the gentamicin uptake in the inner ear and the change of cochlear inflammation for pertaining ototoxicity mechanisms.

Methods
LPS (1 mg/ml) or PBS was injected *i.t.* into the right ear of *C57BL/6* mice to establish the AOM model or sham control. The left ear without treatment was set as an internal control. Fluorescent conjugate, gentamicin-Texas Red (GTTR) was intraperitoneally administered to mice one hour prior to sacrifice, to examine the cochlear uptake of gentamicin at various post-LPS treatment times. Cochlear macrophages were labeled with anti-Iba1 antibody, and inner ear cytokines evaluated by a Mouse Cytokine Array kit, respectively.

Results
In LPS-treated ears: 1) The symptoms of AOM were observed and the ABR threshold was significantly elevated at all tested frequencies; 2) Hair-cell and strial uptake of GTTR was significantly enhanced in LPS-treated ears at 24, 48 and 72 hours, while most prominent in the 48-hour group; 3) The hair-cell GTTR uptake was positively associated with the strial uptake; 4) Overt cochlear infiltration of Iba1-positive macrophages was observed, particularly in the organ of Corti and the spiral ligament; 5) Most detectable cytokines were up-regulated at 48-hour posttreatment. These changes were not observed in the PBS control ears.

Conclusions
LPS-induced AOM switched on the cochlear inflammatory response, including macrophage infiltration and upregulation of pro-inflammation cytokines, and significantly enhanced the cochlear uptake of gentamicin. Potential mechanisms of enhanced drug uptake may include increased strial permeability due to acute middle-ear inflammation, resulting in higher drug concentration in the stria vascularis and the endolymph, and subsequently higher drug uptake by hair cells. Other possible mechanisms, such as the activation of specific candidate channels and endocytosis followed by inflammation, need to be further studied. In sum, this study improves our understanding of drug trafficking in the pathological cochlea, and provides reference for drug treatment of AOM while protecting the inner ear function.

Key words
Acute otitis media, lipopolysaccharide, gentamicin, macrophage, cytokine, drug uptake.

PS 723

Cisplatin-induced Early Ototoxicity Appears in Spiral Ganglion Neurons

Yingying Chen[1]; Eric C. Bielefeld[2]; Jeffrey G. Mellott[3]; Weijie Wang[4]; Amir Mafi[3]; Grace Szatkowsk[3]; Ebenezer N. Yamoah[1]; Jianxin Bao[3]
[1]University of Nevada,Reno; [2]Ohio State University; [3]Northeast Ohio Medical University; [4]Northeast Ohio Medical University, Anhui Medical University

Cisplatin chemotherapy often causes permanent hearing loss, which leads to a multifaceted decrease in quality of life. Identification of early cisplatin-induced cochlear damages would greatly improve clinical diagnosis and provide potential drug targets to prevent this ototoxicity. To study cisplatin-induced early ototoxicity, 4-month CBA/CaJ mice were treated with cisplatin in two cycles, adapted from an established mouse model. Cisplatin was administered by intraperitoneal injection (i.p.) at 4 mg/kg for four days, followed by ten days of recovery. Each animal was exposed to one or two cycles to model clinical treatment regimens. We assessed outer hair cell (OHC) loss, ABR and DPOAE threshold shifts to monitor early and late cochlear damage after cisplatin exposure. We further measured suprathreshold amplitudes,

synapses between IHCs and SGNs, neuregulin-1 (Nrg1) and transcription factors involved in the downstream signaling, integrity of mitochondria and the myelination of the SGNs. Besides loss of outer hair cells and an increase in high-frequency hearing thresholds, a significant latency delay of auditory brainstem response wave 1 was observed even at the middle frequencies area where there were no changes in hearing thresholds in two cycles cisplatin treatment. Subsequently, this delay was confirmed as early cisplatin-induced ototoxicity after only one cycle of cisplatin treatment. In the same mice, mitochondrial loss in SGN axons increased myelination sheets, and changes of Nrg1 signaling were observed. Nrg1 is highly expressed in SGNs, and its signaling is critical for SGN myelination. Thus, we have identified early SGN-associated functional, cellular, and molecular markers after cisplatin treatment. These findings will advance the field of research on early detection of ototoxicity, and future drug development to reduce cisplatin-induced ototoxicity and neurotoxicity.

PS 724

Unfolded Protein Response Activation Correlates with Non-Linear Cisplatin Ototoxicity

Stephanie Rouse; Jiang Li; Ian Matthews; Elliott Sherr; Dylan Chan
UCSF

Cisplatin is a common chemotherapeutic with the dose-limiting side effect of hearing loss. The cellular mechanism underlying cisplatin ototoxicity is poorly understood. Multiple groups have observed a bell-shaped dose response of hair-cell death upon exposure of neonatal cochlear cultures to cisplatin: low cisplatin concentrations induce hair-cell death that increases with increasing cisplatin dose, whereas high cisplatin concentrations give rise to little to no hair-cell loss. Understanding how this non-linear dose-response occurs might shed light into the cellular mechanisms of cisplatin ototoxicity. In particular, understanding how hair cells are protected at high cisplatin concentrations may provide insight into how cisplatin ototoxicity may be prevented at lower, physiological concentrations.

Different mechanisms for this protection have been proposed, including inhibition of cisplatin uptake through copper transporters, and inhibition of protein synthesis, preventing apoptosis. Our previous work, implicating the unfolded protein response (UPR) in noise-induced hearing loss and hair-cell death, led us to investigate whether the UPR, a well-conserved cellular process that affects both protein synthesis and apoptosis, may also play a role in cisplatin ototoxicity.

We treated neonatal cochlear explant cultures and HEK cells with 0-1000 µM cisplatin for up to 48 hours, quantified the expression of UPR marker genes (CHOP (marker of the pro-apoptotic arm), S-XBP1 (pro-homeostatic arm), DR5 (integration of CHOP and S-XBP1)) by qPCR and fluorescence in-situ hybridization, and measured caspase 3/7 activity. The pattern of UPR upregulation varied with cisplatin dose. Expression of CHOP mirrored that of hair-cell death, increasing with cisplatin dose from 0-100 µM. Conversely, S-XBP1 was highly upregulated at high cisplatin concentrations (>250 µM), where hair cells were preserved. Across the entire range of cisplatin doses, the ratio of CHOP/S-XBP1 expression correlated strongly with DR5 expression, caspase 3/7 activity, and hair-cell death. ISRIB, a drug that inhibits the pro-apoptotic arm of the UPR, decreased CHOP expression as well as caspase activity, yet had no effect on S-XBP1. The compound KIRA6, which decreases S-XBP1, had the opposite effect, increasing caspase activity at high doses of cisplatin.

These findings suggest that distinct cisplatin-induced UPR activation patterns are tightly associated with downstream apoptosis, and may underlie this unusual non-linear dose response of cisplatin ototoxicity in cochlear cultures. This raises the possibility that the UPR can be targeted with drugs to prevent cisplatin-induced apoptosis, hair-cell death, and hearing loss, which is supported by our initial findings that ISRIB protects against cisplatin ototoxicity in mice *in vivo*.

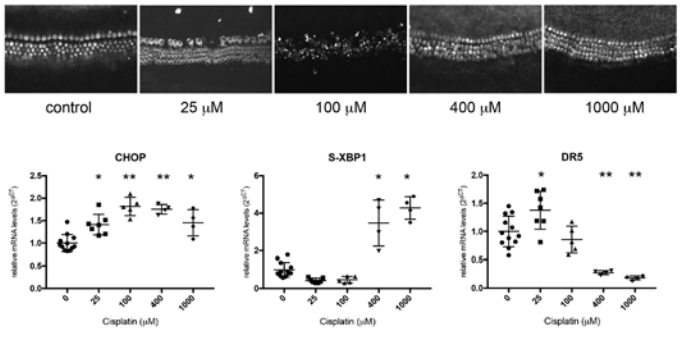

Figure 1. Non-linear cisplatin dose-response of UPR gene expression and hair-cell death in cochlear cultures. A. Cochlear hair-cell death. P3 WT C57BL/6J organotypic cochlear cultures were treated with cisplatin at the doses shown for 24h and stained with Myo7a to detect hair cells. At low concentrations of cisplatin, hair-cell death increases with increasing cisplatin concentration, but above 100 µM, high cisplatin doses are associated with hair-cell survival. **B. UPR expression.** Expression of UPR pathway marker genes was performed in cochlear cultures after 6 hours of cisplatin treatment. CHOP, a marker of the pro-apoptotic arm, and DR5, a downstream integration marker of UPR output indicating progression towards apoptosis, both displayed non-linear dose-dependence similar to that seen for hair-cell death. S-XBP1, a pro-homeostatic marker, showed an inverse non-linear relationship compared to hair cells. Data are $2^{\Delta CT}$ measurements normalized to control, non-treated cultures from the same experimental run, and are presented as means ± SD, with individual data shown as black dots. * = p < 0.05; ** = p < 0.001 by one-way ANOVA followed by pairwise t-test relative to control (0 mM cisplatin) with Dunnett's multiple comparisons test.

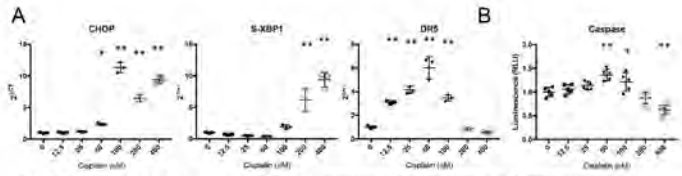

Figure 2. Non-linear cisplatin dose-response of UPR gene expression and apoptosis in HEK cells. A. UPR gene expression. At low concentrations of cisplatin (up to 50 µM), CHOP has increasing expression, and S-XBP1 shows decreasing expression, with increased CP concentration; this is accompanied, as expected, by a linear increase in the expression of DR5. From 50-400 µM cisplatin, however, CHOP continues to be elevated, but S-XBP1 expression also increases dramatically, and DR5 expression decreases. Results shown here are from a single experiment with 3 independent samples for each cisplatin dose; this experiment was replicated three times with identical qualitative trends. **B. Apoptosis.** HEK cells were treated with escalating doses of cisplatin. Caspase 3/7 activity was measured using the Caspase-Glo Assay, demonstrating a non-linear cisplatin dose-dependence of HEK-cell apoptosis that shows a high degree of correlation with DR5 mRNA expression (R^2 = 0.78, p < 0.001 by simple linear regression). Data are means ± SD, with individual data shown as black dots. * = p < 0.05; ** = p < 0.001 by one-way ANOVA followed by pairwise t-test relative to control (0 µM cisplatin) with Dunnett's multiple comparisons test.

PS 725

Histologic and Genetic Characterization of the Flat Cochlear Epithelium

Sydney Sheltz-Kempf; Jeremy S. Duncan
Western Michigan University

Neurosensory hearing loss is one of the most common sensory disorders and its long-term effect is characterized by the flat epithelium present after hair cells have died in the organ of Corti (OC). We sought to establish a model of the flat epithelia resulting from the injection of diphtheria toxin (DTX) in the Pou4f3-DTR mouse line at time points previously uncharacterized in other studies. Previously, the Pou4f3-DTR line has been shown to kill hair cells within the first postnatal week, however, there is some hair cell regeneration soon after. Furthermore, the Pou4f3-DTR line has been shown to kill mature hair cells at P30 and P60, but phalangeal scarring prevents the greater and lesser epithelial ridges from mitotically forming the flat epithelium. By inducing hair cell death in the Pou4f3-DTR line during the late postnatal period, we were able to consistently generate a flat epithelium in the mouse cochlea. By performing immunohistochemistry on whole mounts and frozen sections of cochleas, we were able to histologically characterize the flat epithelium in this model. Furthermore, by performing *in situ hybridization* and qPCR, we were able to better define the genetic expression of these cells. This model provides a consistent flat epithelium phenotype that can be used as a baseline in regeneration studies.

Physiology and Attention in Speech Perception

PS 726

Electroencephalography-based Optimization of Noise Reduction in Hearing Aids

Subong Kim[1]; Yu-Hsiang Wu[1]; Inyong Choi[2]
[1]University of Iowa; [2]Dept of Communication Sciences and Disorders, University of Iowa

Noise reduction (NR) is widely used in modern hearing aids to increase ease and comfort of listening. However, NR not only suppresses the noise but induces inevitable distortion for speech cues, resulting in inconsistent benefits reported in prior studies. It is challenging for audiologists to provide the best configurations for NR since each listener differently reacts to this trade-off between noise suppression and speech-cue distortion. To provide a more systematic approach to selecting NR configurations for each listener, we need to understand individual listeners' differential sensitivity to background noise and speech-cue degradation, and how such individual difference influences the effect of NR. Our central hypothesis is that listeners' speech-unmasking ability predict the benefits of NR, in a way that listeners with poorer speech-unmasking exhibit greater NR benefits. We also hypothesize that the benefits of NR can be measured objectively using electroencephalography, in such way that the optimal NR configuration for a given listener would invoke the cortical processing that the reduced noise level can generate in normal-hearing listeners. In our previous study, we found that the low-level noise (i.e., increased signal-to-noise ratio (SNR)) resulted in increased early (~300 ms after word onset) evoked response in left supramarginal gyrus (SMG), the early point of the dorsal stream pathway in the brain, and decreased late (~700 ms) evoked response in left inferior frontal gyrus (IFG), the late point in the same cortical pathway. These region-latency combinations provide us an "ideal" pattern of the cortical processing observed when spoken-word perception becomes easier in favorable listening conditions. In the present study, we compared cortical evoked responses to consonant-vowel-consonant monosyllabic words in speech-shaped stationary noise between NR and no-NR condition. At the group level, the NR condition, compared to the no-NR condition, invoked stronger early evoked response in left SMG and weaker late evoked response in left IFG. To test our central hypothesis, we also measured each listener's speech-unmasking ability by computing the amplitude ratio of cortical evoked responses to target speech and background noise, henceforth referred to as "internal SNR." Listeners with poor speech-unmasking, indexed by lower internal SNR, exhibited greater NR benefits; they showed an even greater increase of early SMG activity and greater decrease of late IFG activity when NR was on. This study will provide multiple crucial ideas for how to personalize NR settings based on listeners' cortical activity, which will have a substantial clinical impact.

PS 727

Effects of Age and Childhood Hearing Loss on Selective Attention in the Auditory and Visual Domains

Kristina M. Ward; Tina M. Grieco-Calub
Northwestern University

Background
Children have greater difficulty understanding speech in the presence of background noise than adults. We hypothesize that children's poor speech-in-noise perception is, in part, due to their immature selective attention. Specifically, children have greater difficulty selectively attending to a target speech stream while inhibiting their attention to background noise. The ability to selectively attend to a target stream may be further impaired when the fidelity of the auditory input is degraded, such as in children with hearing loss who use hearing aids or cochlear implants. Thus, poor speech

perception in children with hearing loss may not only result from reduced audibility, but also impaired selective attention. The purpose of this study is to quantify how selective attention in the auditory and visual domains changes as a function of age in children and to determine how childhood hearing loss influences this relation.

Methods
Two groups of children 5-to-12 years of age participated in this study: children with normal hearing and children with hearing loss who use hearing aids or cochlear implants. All children completed behavioral change detection tasks to measure selective attention in the auditory and visual domains. During these tasks, children were presented with a target and distractor stream comprised of words (auditory domain) or pictures (visual domain). Children were instructed to press a key when they detected a randomly presented deviant stimulus in the target, but not the distractor, stream. Performance was quantified by children's rate of responses to deviants in the target stream (hits) and distractor stream (false alarms) as well as the reaction time of these responses.

Results
Auditory and visual selective attention improved with age and were poorer in children with hearing loss. Specifically, older children were faster and more accurate at responding to deviants in the target stream than younger children, regardless of hearing status. Children with hearing loss exhibited responses that were slower and less accurate than children with normal hearing across the age range in both the auditory and visual domains.

Conclusions
Selective attention in the auditory and visual domains appears to be affected by age and hearing loss during childhood. We will discuss the results of analyses that test the relations between age, hearing status, and selective attention as well as the implications of these results for children's ability to understand speech in the presence of background noise.

Work supported by NIH NIDCD R56 DC015492 (TGC) and F31 DC017055 (KW).

PS 728

Pilot: Mapping Emotional Prosody Processing in Normal hearing Listeners with fNIRS

Ryssa Moffat[1]; David McAlpine[2]; Deniz Baskent[3]; Robert Luke[4]; Lindsey N. Van Yper[2]
[1]International Doctorate of Experimental Approaches to Language and Brain (IDEALAB); [2]Department of Linguistics, The Australian Hearing Hub, Macquarie University, Sydney, Australia; [3]University Medical Center Groningen; [4]Macquarie University, Department of Linguistics

Recognising emotional prosody is an important element in successful verbal communication. Recipients of cochlear implants (CIs) with good speech recognition perform below normal hearing (NH) peers on emotional prosody recognition tasks. To compensate for the poor transmission of spectral cues by CIs, recipients rely on temporal and intensity cues, as evidenced by behavioural studies. Little is known about the brain mechanisms underlying emotional prosody recognition in CI hearing. We employed the brain-imaging tool functional near-infrared spectroscopy (fNIRS) to examine cortical processing of emotional prosody normal-hearing (NH) listeners, as well as CI recipients.\Twenty NH adults participated in a behavioural forced-choice listening task and a fNIRS passive listening task. Six-syllable sentences with pseudo content words and real function words were used in both tasks (e.g., "the larfle is himber"). Stimuli were recorded with prosodic features adjudged neutral, happy, sad, fearful and angry. To examine each group's reliance on acoustic cues, stimuli were manipulated in four separate ways: 1) pitch cues equalised, 2) pitch and intensity cues equalised, 3) pitch and rate cues equalised, and 4) rate and intensity cues equalised. In the forced-choice listening task, participants identified the emotion conveyed in each stimulus (N=100). During the passive listening fNIRS task, participants heard 10 blocks of each emotion-condition pair (N=20). Comparisons will be made between prosodies, as well as within and between acoustic conditions. Correlations between metabolic and behavioural responses for each prosody-condition pair will be reported. This method offers insight into the relative importance of pitch in emotional prosody recognition and provides the groundwork for understanding emotional prosody processing in CI hearing. This is key for the development of strategies targeting emotional prosody in therapy and classroom settings.

PS 729

Decoding of Selective Attention to Continuous Speech from the Human Auditory Brainstem Response

Mikolaj Kegler[1]; Octave Etard[1]; Antonio Forte[2]; Tobias Reichenbach[1]
[1]Department of Bioengineering and Centre for Neurotechnology, Imperial College London; [2]John A. Paulson School of Engineering and Applied Sciences, Harvard University

Humans are highly skilled at analysing complex acoustic scenes. The segregation of different acoustic streams and

the formation of corresponding neural representations is mostly attributed to the auditory cortex. Decoding of selective attention from neuroimaging has therefore focused on cortical responses to sound. However, the auditory brainstem response to speech is modulated by selective attention as well, as recently shown through measuring the brainstem's response to running speech [1]. Here, we sought to investigate how the attentional modulation of the brainstem response can be employed for efficient decoding of selective attention [2].

To this end, the brainstem response to two competing speakers was measured through high-density electroencephalography (EEG). We furthermore extracted a fundamental waveform from the speech signals, that is, a waveform that oscillated at the fundamental frequency of the voiced parts of speech. We then employed regularized linear regression to map the fundamental waveform to the multichannel EEG signal at different delays. The estimated latency of 9 ms and the topography of the detected brainstem responses were consistent with previous studies that employed short, repeated speech stimuli. To decode attention to one of two competing speakers through the detected brainstem response, we then trained a classifier that was based on the accuracies of the different waveform reconstructions. The decoding performance was computed for subject-specific and population-averaged models, for a few channels of EEG, as well as for a fundamental waveform obtained from simple band-pass filtering which can run in real-time. In all cases, a few seconds of data yielded decoding of selective attention that was significantly better than chance.

Our results show that attention to a speaker can be assessed fast and effectively from the auditory brainstem response to continuous speech as recorded noninvasively from EEG. The accurate classification obtained with only few EEG channels makes the method computationally light and therefore promising for potential applications in mobile devices such as hearing aids.

References

[1] Forte, A. E., Etard, O., & Reichenbach, T. (2017). The human auditory brainstem response to running speech reveals a subcortical mechanism for selective attention. *eLife* 6:e27203.
[2] Etard O., Kegler M., Braiman C., Forte A.E. & Reichenbach T. (2019) Decoding of selective attention to continuous speech from the human auditory brainstem response, *Neuroimage* 200:1.

PS 730

Attentional Modulation of the Neural Representation of Speech: Spectral Profile and Individual Differences

Vibha Viswanathan[1]; Hari Bharadwaj[2]; Barbara Shinn-Cunningham[3]
[1]Weldon School of Biomedical Engineering, Purdue University; [2]Speech, Language, & Hearing Sciences, and Weldon School of Biomedical Engineering, Purdue University; [3]Carnegie Mellon Neuroscience Institute, Carnegie Mellon University

The ability to selectively attend to speech in the presence of other competing talkers is critical for everyday communication; yet the neural mechanisms facilitating this process are poorly understood. Here, we use electroencephalography (EEG) to study how a mixture of speech streams is represented in the brain as subjects attend to one of two sound streams. To characterize the speech-EEG relationships and how they are modulated by attention, we estimate the statistical association between each canonical EEG frequency band (delta, theta, alpha, beta, low-gamma, and high-gamma) and the envelope of each of ten different frequency bands in the input speech. Consistent with previous literature, we find that low-frequency (delta and theta) bands show greater speech-EEG coherence when the speech stream is attended compared to when it is ignored. We also find that the envelope of the gamma band shows a similar attention effect, a result that has previously been reported only in invasive recordings. This is consistent with the theory that neural dynamics in the gamma range are important for attention-dependent routing of information in cortical circuits. In addition, we also find that the greatest attention-dependent increases in speech-EEG coherence are seen in the mid-frequency acoustic bands (0.5—3 kHz) of input speech and the temporal-parietal EEG sensors. Finally, we find individual differences in: (1) the specific set of speech-EEG associations that are the strongest, (2) the overall magnitude of the attentional enhancement of speech-EEG coherence, and (3) the EEG and speech features (i.e., the specific channels and bands) that are most informative about attentional focus. This suggests that for applications such as BCIs that aim to decode auditory attention from EEG, individual-specific customization of features might be necessary to obtain optimal performance.

PS 731

The Effect of Selective Attention Training on Effort during Speech-in-noise Perception

Amy Sarow[1]; Subong Kim[1]; Jason Geller[2]; Inyong Choi[3]
[1]University of Iowa; [2]Department of Psychological & Brain

Sciences, University of Iowa; [3]Dept of Communication Sciences and Disorders, University of Iowa

Understanding speech in noise (SiN) is challenging even for normal-hearing listeners. Engaging top-down selective attention can be a good strategy for SiN, as the attentional modulation on the neural representation of target speech and noise enhances "effective" signal-to-noise ratio (SNR) in the perception domain. In our prior study, we developed a neurofeedback training paradigm based on an auditory attention-driven brain-computer interface, which has been proved to reinforce the strength of attentional modulation. In the current study, we seek to extend the observation of the training effect toward cognitive effort for attention and speech-interpretation processes. Normal hearing subjects completed neurofeedback training with pre- and post-training word-in-noise recognition tests. Both EEG and pupil dilation data were recorded during the pre- and post-training word-in-noise recognition tests. Both pre- and post-training speech-in-noise tasks contained a set of 120 monosyllabic words, spoken by either a female or male speaker, presented two seconds after the noise onset. A speaker-gender auditory cue (male vs. female) was given at the beginning of each trial. Participants completed the post-training speech-in-noise task 24 hours after the pre-test task, to allow for consolidation of the neurofeedback training. During the training, participants completed a two-stream target detection task with a pre-trial (visual) cue indicating which auditory stream ("Up" vs. "Down") to attend to. On each trial, the word "Up" was presented five times, by a female voice, while "Down" was repeated four times by with a male voice. At the end of each trial, participants were given visual feedback regarding which auditory stream they most closely attended to based on a pre-defined template pattern of cortical auditory responses evoked by either the single "up" or "down" auditory stream. Our EEG data for post-training speech-in-noise task showed reduced alpha power obtained at the occipital and frontal channels from the onset of the target word to retention period, suggesting reduced listening effort after the training. Pupillometry data showed that the post-training task-evoked pupillary response is faster and larger during the post-cue pre-target period than the pre-training, which may indicate that training results in increased arousal and attentional focus in the task. With the potential of providing a paradigm for facilitating speech-in-noise perception measured by both EEG and pupillometry, this neurofeedback training study has exciting future implications.

PS 732

Switching Attention and Integration of Binaural Information: Effects of Speech Material and Masker Types on Perception of Alternated and Interrupted Speech in Children

Shiran Koifman; Stuart Rosen
University College London

There is much current interest in Auditory Processing Disorder (APD) in children, not least because of suspicions that APD may lead to poor school performance. Children suspected of APD typically present with difficulties in understanding speech in noisy environments despite a normal audiogram. APD may thus arise from higher-level auditory cognitive deficits. We have been investigating a task that appears to exploit some cognitive aspects of listening not probed by simpler tasks, and assesses a listener's ability to switch attention and integrate short-term auditory information across the two ears.

In this task, target speech is interrupted at a fixed modulation rate (5 Hz), with successive segments of the target being switched from ear to ear. An adaptive procedure varies the duty-cycle (DC), the proportion of time the speech is 'on' in each modulation period, in order to find the proportion required to understand 50% of keywords (the speech reception duty-cycle threshold, SRdT). A masker is interrupted in the same way, and alternated between the two ears out-of-phase with the target speech, resulting in alternated segments of both target and masker signals between the two ears, with only one stimulus present in each ear at any given time. Two types of target sentences were used: 'everyday' sentences like, *'The clown had a funny face'*, and a children's version of the CRM sentences, *'Show the [animal] where the [colour] [digit] is'*. We also varied masker type: unrelated connected speech, spoken in an unfamiliar or familiar language, by talkers from the opposite sex to the target, and a speech-spectrum-shaped-noise modulated with the envelope of the speech maskers. Additionally, the CRM-like sentences were used as maskers with CRM-like targets.

Preliminary data from 7-13 year old children (n=12) suggest poorer performance in the APD group compared to typically developing (TD) controls, particularly when both target and masker originate from the CRM-like corpus. Such a configuration may introduce more informational masking and thus increase the demand on higher-level auditory cognitive function, than in the everyday sentences where semantic similarities between the masker and target are minimal. A larger data set will allow assessment of the extent to which performance in this task is correlated with other tasks, such as a standard speech-in-noise task.

Understanding the involvement of auditory attentional skills and integration of binaural information may be useful in disentangling the reasons why children with APD experience listening difficulties in noisy situations.

PS 733

The Effect of Phoneme-Based Auditory Training on Speech Intelligibility and Listening Effort in Hearing-Aid Users

Aleksandra Koprowska[1]; Jeremy Marozeau[1]; Torsten Dau[2]; Dorothea Wendt[1]; Maja Serman[3]
[1]Hearing Systems Section, Department of Health Technology, Technical University of Denmark; [2]Hearing Systems Section, Technical University of Denmark; [3]Sivantos GmbH

Hearing loss has an adverse effect on speech perception and poses serious problems in everyday communication. Both scientific reports and satisfaction surveys show that even modern hearing aids do not provide a fully satisfactory compensation for the hearing deficits and that many users still experience difficulties in understanding speech and suffer from an increased listening-related effort, especially in challenging acoustic scenarios. Auditory training was proposed as a complementary intervention, which, in combination with hearing aids, can be more successful than hearing aids alone. However, it is still unclear to what extent training-related benefits generalize to untrained speech material and how they influence other aspects of speech perception, e.g., listening effort. In this study, a training strategy targeting phoneme discrimination in the presence of background noise was proposed. The participants with similar hearing profiles and at least six months of experience with hearing aids were enrolled in a two-week training program. The effects of training on phoneme identification, sentence recognition, listening effort, and self-perceived hearing abilities were assessed in relation to the baseline measurements and a control group. The findings of this study indicate that the amount of training-related benefits varies across participants and can be linked to certain characteristics of the individuals, such as age, degree of hearing loss, cognitive skills, etc. Given the variety of the results, more investigation is needed to assess, whether the suggested training paradigm could serve as a successful rehabilitative intervention for hearing-impaired individuals.

PS 734

A Dual-Task Paradigm Sensitive to Listening Effort in a Realistic Scenario

Joaquin T. Valderrama-Valenzuela[1]; Paul Jevelle[1]; Kelly Miles[2]; Elizabeth F. Beach[1]
[1]National Acoustic Laboratories; [2]Macquarie University

Background
People with hearing loss often report that they need to invest a lot of effort when engaging in daily conversations, especially in noise. The dual-task paradigm has been used to quantify the amount of effort invested when listening. Under this paradigm, two tasks are performed concurrently, and performance in the secondary task is interpreted as a proxy of listening effort when the stimuli are presented in the time domain. This research aimed to develop a dual-task test paradigm sensitive to listening effort in a realistic scenario.

Methods
Five normal-hearing adults (3 females, [29-43] years) took part in the study. In the primary task, participants were asked to repeat matrix sentences presented in realistic cafeteria noise. The secondary task consisted of a visual task driven by the auditory stimulus of the primary task. Two vertical rectangles were shown on the screen, and in each trial, a large circle appeared in one of the rectangles at the onset of the auditory stimulus. Participants were instructed to press the arrow pointing towards or away from the circle if the name at the start of the sentence referred to a male or a female, respectively. Accuracy and reaction time were measured. The test was administered over headphones in quiet, -5 dB, and -10 dB SNR. The test was also administered using realistic 3D recordings in a 41-channel Ambisonics speaker array in an anechoic chamber, and these data will also be reported.

Results
For the five participants who completed the test under headphones, the mean accuracy scores in quiet, -5 dB, and -10 dB SNR were 99.6%, 88.4%, and 47.2%, respectively. Accuracy dropped by 11.2% from quiet to -5 dB SNR (p=0.008); and by 41.2% from -5 dB to -10 dB SNR (p=0.0001). The mean reaction times in quiet, -5 dB, and -10 dB SNR were 906 ms, 1083 ms, and 1254 ms, respectively. Reaction times increased 169 ms from quiet to -5 dB SNR (p=0.0035), and 201 ms from -5 dB to -10 dB SNR (p=0.014).

Conclusions
Preliminary results indicate that this dual-task paradigm is sensitive to increased listening effort in a realistic scenario. The observed effects on reaction time may be the result of the relative complexity of the test; the relative depth of cognitive processing required to categorize the gender of the name; and the fact that the primary and secondary tasks compete for the same pool of cognitive resources.

PS 735

Pupil Size Tracks Semantic Ambiguity and Noise

Mason Kadem[1]; Björn Herrmann[2]; Ingrid Johnsrude[3]
[1]The Brain and Mind Institute - Western University; [2]Western University; [3]The Brain and Mind Institute, Western University

Effortful listening is experienced by listeners when speech is hard to understand because it is degraded or masked by environmental noise. Pupillometry (i.e., measure of pupil size) can detect effortful listening: pupil size increases when speech is degraded compared to when it is clear. However, the pupil responds to a broad range of cognitive demands, including linguistic challenges such as syntactic complexity. Here we investigate whether it responds to the need to disambiguate words with more than one meaning, such as 'bark' or 'bank'. Semantic ambiguity is common in English, and previous work indicates that it imposes a processing load. We combine this with an acoustic challenge in a factorial design so the pupil response to these two types of challenge can be directly compared. We found main effects of noise and semantic ambiguity on the peak and mean pupillary area, indicating that pupil dilation can reflect processes associated with semantic disambiguation as well as noise. Pupil size reflect demands imposed by ambiguity both in the acoustic form of words (i.e. due to degradation) and in word meaning.

PS 736

Pupillometry Reveals the Cognitive Cost of Recovering from Errors in Speech Perception

Matthew B. Winn; Katherine H. Teece
University of Minnesota

Speech perception is a gold standard measure of treatment outcomes in audiology. However, speech perception scores are limited by the tendency for listeners to mentally repair or correct mistakes that were made during listening, and thus appear that they heard the speech correctly. Intelligibility scores cannot distinguish a listener who correctly repaired misperceptions from a listener who simply heard the speech clearly and accurately with no need for repair.

Previous work identified situations where this error-correction process might have occurred, and found limitations in perception of ongoing speech, and also greater listening effort. In the current study, the task was designed to explicitly (rather than accidentally) demand error correction using a new test corpus. We introduce a set of sentences where later-occurring words are used to disambiguate early-occurring target words that are masked by noise or intentionally mispronounced to match common perceptual errors made by individuals with hearing loss. In this sentence recognition task, participants reported what they thought was spoken. Cognitive repair of speech was verified when listeners heard a masked/mispronounced word but restored to its likely target to report a full well-formed sentence. For example, for "The woman xxxxx her candle with a match", a listener who correctly inserts the word "lit" has demonstrated cognitive repair.

The cognitive cost of repairing missing words in perception was measured using pupillometry. Increased magnitude and latency of pupil dilation served to identify extra cognitive load associated with the repair process. In addition to full details of the validation of the stimulus set, preliminary data using this new paradigm will be presented, using listeners with cochlear implants and with normal hearing. Results thus far indicate that listeners with cochlear implants show less of a marked change when words are missing or mispronounced, possibly indicating that the "intact" speech was already being misperceived and corrected quite often, in a way that was not detected by intelligibility scores.

PS 737

Autonomic Nervous System Correlates of Speech Categorization Revealed Through Pupillometry

Gwyneth Lewis; Gavin Bidelman
University of Memphis

Human perception requires the many-to-one mapping between continuous elements of a physical structure and discrete sets of categorical representations. This "downsampling" operation plays a critical role in speech perception because acoustic cues do not share constant relations with perceptualphonetic representations. Categorical perception (CP) of speech is thought to mitigate perceptual variance by emphasizing between- rather than within-category contrasts. Beyond this benefit, CP might generate additional perceptual constancy needed to extract auditory percepts of speech from interfering sound sources (i.e., noise). Here, we used psychophysiological (pupillometry) measures to determine the degree to which noise interference impacts cognitive load and the perceptual identification of phonetic vs. non-phonetic speech features during categorization. Listeners classified a synthetic five-step acoustic-phonetic continuum of speech tokens ranging from /u/ to /a/ presented in various signal-to-noise ratios (SNRs [clear, 0 dB, -5 dB]). Continuous recordings of pupil dilation served as a measure of processing effort, with larger and later dilations reflecting increased listening demand.

Critical comparisons were between time-locked changes in eye data in response to sound tokens with a clear phonetic identity (i.e. continuum endpoints, Tk1/5) vs. those without a clear phonetic identity (i.e., continuum midpoint, Tk3). Listeners' behavioral data indicated that clear speech elicited sharper psychometric functions and faster responses which steadily declined in noise. As for listeners' pupillary responses, results showed that noise increased pupil dilation across stimulus conditions, but not straightforwardly. Peak pupil size was modulated solely by SNR, being larger for degraded relative to clean speech (i.e., [0 dB and -5 dB] > clean). In contrast, peak dilation latency varied with both token and SNR. Interestingly, unambiguous tokens (Tk1/5) elicited earlier, more pronounced increases in pupil dilation relative to phonetically ambiguous speech (Tk3). Recent work has observed that pupil diameter increases for sounds participants consider more salient, vigorous, or loud, which could reflect greater listening demand or arousal. The differences in pupillary responses observed here suggest that listeners rely on perceptual categorization to reconstruct auditory percepts under challenging real-world listening conditions.

PS 738

Subcortical Coding of Neuro-acoustic and Neuro-categorical Information in Speech

Erika Skoe; Emily Myers
University of Connecticut

A fundamental property of speech perception is that speech sounds are perceived categorically. Categorical responses to speech stimuli have been uncovered at multiple levels of the cortical processing stream; however, questions remain as to whether sensory areas even earlier in the neural processing stream inherit the ability to code speech categories via top-down feedback from cortex. Studies using a continuum of vowel stimuli suggest that subcortical responses to speech, as measured by the frequency-following response (FFR), reflect purely a neuro-acoustic code, with no evidence that they code the abstract the speech category perceived by the listeners (i.e., neuro-categorical coding) (Bidelman et al., 2015; 2016). Yet, vowels are among the least categorically perceived speech sound contrasts, leaving open the question of whether stimuli that evoke a more categorical perceptual pattern (i.e., stop-contrasts: b/d) might show traces of neuro-categorical coding in the FFR. Indeed, recent work has hinted at the possibility that the speech-evoked FFR is sensitive to speech-sound category information (Maggu et al., 2016; Zhao et al., 2018), lending further motivation to undertake the present study. Here, as part of a pilot study to a larger planned investigation of individual differences in categorical perception, we recorded speech-evoked FFRs using a 7-point stop (ba/da) consonant continuum in a sample of young adults with normal hearing thresholds (n=12). Consistent with previous work, we find that the FFR codes the stimulus continuum in a graded fashion, with the correlation between responses to different stimuli dropping linearly as the acoustic distance increases between stimuli. As a companion to this neuro-acoustic coding, we also find features of categorical coding when other analysis approaches are applied to the FFR. Specifically, in the power spectrum, we find that stimuli that span the perceptual category boundary are more different than those within the same category, even though the extent of the acoustic change is the same for both comparisons. These findings suggest that categorical coding can be observed in subcortical auditory areas, although they cannot address the timeline under which it first emerges. We assert that categorical coding in the FFR provides some of the strongest evidence for top-down influence on early stages of speech processing given that category membership is a learned feature that is not carried by the acoustic signal itself.

Plasticity in the Central Auditory Pathway

PS 739

Practice Makes Transfer Imperfect – Evidence from Auditory Learning

Yael Zaltz, PhD[1]; Liat Kishon-Rabin[2]; Avi Karni, MD[3]; Daphne Ari-Even Roth, PhD[1]
[1]Communication Disorders Dept, Steyer School of Health Professions, Sackler Faculty of Medicine, Tel-Aviv University; [2]Department of Communication Disorders, Steyer School of Health Professions, Sackler Faculty of Medicine, Tel-Aviv University; [3]The Sagol Department of Neurobiology, Faculty of Natural Sciences & The E.J. Safra Brain Research Center for the Study of Learning & Learning Disabilities, Faculty of Education, University of Haifa, Israel. Division of Diagnostic Radiology, The Chaim Sheba Medical Center, Tel Hashomer, Israel

Evidence from motor and visual studies suggests that the ability to generalize learning-gains to untrained conditions decreases as the training progresses. This decrease in generalization was suggested to reflect a shift from higher to lower levels of neuronal representations of the task following prolonged training. In the auditory modality, however, the few studies that tested the influence of prolonged training on generalization ability using simple, non-linguistic stimuli showed no decrease (and sometimes even an increase) in generalization. These studies used pre- and post-training testing of the untrained conditions in order to assess the amount of generalization. This repeated testing may have

confounded the evaluation of the effect of training per-se on the extent of generalization. Therefore, the present study aimed to test the impact of extended training in a basic psychoacoustic task, on the ability to generalize the learning-gains to untrained conditions, without exposing the participants to those untrained conditions before or during training. To this end, 82 young-adults participated in two experiments that differed in the specific training regimen: Forty-eight of them were trained and 34 served as naïve participants in control groups. In both experiments, training was conducted using an auditory difference limen for frequency (DLF) task with an adaptive forced-choice procedure, in a single or nine sessions of training. Following training, generalization to the untrained ear and to an untrained frequency was assessed. Results of both experiments showed that: (a) training induced significant learning (i.e., smaller DLF) following a single session of training, and more so following nine training sessions; (b) the ability to generalize the learning-gains to the untrained conditions was more limited after the extended DLF training, independent of training regimen; (c) larger improvements in the trained condition, resulted in smaller generalization to the untrained conditions. These findings of increased specificity with training in the auditory modality support the notion that basic skill learning may be subserved by similar neural mechanisms and proceed under similar neuro-behavioral constraints across modalities. One such constraint may include a qualitative shift in the memory subserving the performance of a well-trained task as the training is prolonged. The notion that training makes imperfect generalization in the auditory modality should be considered in protocols of auditory training and further established in different populations such as hearing impaired.

PS 740

The Role of Correlations and Rate Codes for Natural Sound Texture Recognition and Discrimination

Xiu Zhai[1]; Mina Sedeghi[1]; Fatemeh Khatami[2]; Heather Read[1]; Ian Stevenson[1]; Monty Escabi[1]
[1]University of Connecticut; [2]University of the Pacific

The perception of natural sound textures - a class of natural sounds with homogenous statistical structure such as crackling fire, wind, and rain – has been proposed to arise through time-averaged summary statistics of the auditory periphery. How and where the auditory system constructs such summary statistics and the neural codes that contribute to texture recognition and discrimination are unknown. Here we recorded neural activity in the inferior colliculus (IC) of unanesthetized rabbits and perform accompanying studies in humans listening to natural textures and synthetic variants with perturbed statistics. We demonstrate that sound texture statistics modulate the correlated firing of frequency organized neural ensembles in the IC and such neural correlations converge veridically on those of the original sounds. Using a naïve Bayes classifier implemented neural decoder, we then show that spectral and temporal neural correlations in the IC provide a strong signal that enables single-trial texture identification with evidence accumulation times lasting ~ 1 sec. The neural classifier performance as well as the time required to accumulate evidence about the specific sound increase upon adding sound statistics. By comparison, response spectrum-based rate codes provide a fast (tens of ms) neural signal for performing classification tasks regardless of the sound statistics. Furthermore, when the spectrum cues are removed from the stimulus (by equalizing their spectrum), rate code classifier performance drops to chance. In contrast, neural correlation based classifiers still perform well, indicating that the diverse structures of neural correlations reflect informative sound related structure that is relevant for identification. Accompanying studies in human listeners reveal homologous trends: regardless of the stimulus duration, the sound spectrum serves a strong discrimination cue that is not informative of the texture identity. However, statistical cues beyond the spectrum are critical to the texture identification and recognition performance improve upon increasing the sound duration and adding such cues in synthetic variants. Thus, sound spectrum-based cues and the accompanying neural responses are inconsistent with and appear to contribute little to the recognition of natural sound textures. Neural correlation statistics in the IC, by comparison, provide a faithful signal that is consistent with listeners recognition performance and reflect informative statistical structures in texture sounds. (supported by NIDCD R01DC015138).

PS 741

Experience Based Changes to Auditory Corticostriatal E/I Receptor Function Gates LTP and Permits Auditory Associative Learning

Nihaad Paraouty; Jessica Sharan; Todd M. Mowery
New York University

Associative learning relies on the activation of cortical excitatory inputs in the sensorimotor striatum. When salient stimuli are repeatedly paired with positive or negative rewards, the desired behavioral response becomes extremely reliable as learning occurs. While LTP is the most likely neural mechanism governing this process, the experience-based changes to synaptic properties along the corticostriatal circuit driving LTP remain unclear. Here we use an appetitive reinforcement operant conditioning procedure to train gerbils on a discrimination task. Behavioral performance

is assessed daily as well as experience-based changes to E/I synaptic properties in a corticostriatal slice preparation. Our primary aim was to determine how the changes in striatal cellular properties gate LTP and task acquisition. Mongolian gerbils were trained on a Go-Nogo task. Following trial initiation, animals were exposed to either a 12-Hz amplitude-modulated noise stimulus, which indicated the availability of food reward, or a 4-Hz stimulus, which indicated no reward and a time-out punishment in case of false alarms. Following each training session, a sensitivity measure, d-prime, was computed and a corticostriatal brain slice was obtained. Inhibitory $GABA_B$ or excitatory NMDA synaptic properties were recorded from medium spiny neurons in the auditory striatum or Layer 5 pyramidal neurons. Theta burst stimulation of auditory cortex L5 pyramidal neurons was used to assess the probability of LTP induction in the striatum. Our data indicate that as the animals learn the task, $GABA_B$ inhibitory receptor strength is reduced, while NMDA receptor strength is increased. Following task acquisition (when animals are performing with a d-prime >1.5 and false alarm rate < 30%), both $GABA_B$ and NMDA receptor strengths return to baseline values, i.e., pre-task acquisition. In addition, LTP probability increases in the striatum during task acquisition before returning to baseline values. Together these results suggest that a reduction in $GABA_B$ receptor strength may facilitate NMDA receptor activation leading to cortically-induced LTP expression in the striatum. The results suggest that the short time window during which E/I receptor function is altered permits learning to occur by allowing stimuli-evoked responses to briefly have a greater potentiation effect.

PS 742

A New Type of Activity Dependent Plasticity in the Inferior Colliculus

Alice L. Burghard; Chris M. Lee; Douglas L. Oliver
University of Connecticut - UCONN Health

Neurons with long-lasting sound-evoked afterdischarges (LSA) in the inferior colliculus (IC; Ono et al. 2016) respond to long-duration sounds (> 30 seconds) with an increased spike rate that persists for seconds to minutes after the sound offset. However, the function of this plasticity in a subpopulation of IC neurons is still unknown. To study the response properties of LSA neurons, we presented narrowband sounds lasting 30-90 seconds from a front-facing speaker in an open field environment and recorded spontaneous multiunit activity from multichannel electrodes in the right IC of anesthetized mice before, during, and after the presentation of the sound. Spikes were sorted with KiloSort2 (Pachitariu et al., 2016). We found that 152 of 754 (20%) of neurons were able to produce LSA. Some neurons showed LSA to multiple repetitions of the same stimulus. We have observed that the same neuron may produce LSA in response to long-duration sounds of different levels, center frequencies, or modulation depths. The magnitude of the LSA was positively correlated with the average firing rate during the sound stimulation and the level of the sound.

We also compared the responses to tone pips presented before and after the presentation of a long-duration sound. We sometimes observed a higher rate of firing between the tone-pip driven responses similar to the increase in the spontaneous activity described above. In some neurons, we found an increase in spectral power of the tone-pip driven response after the long-duration sound presentation. This effect was most prevalent in the first 5s after the offset of the long-duration sound but could last for the whole duration of 20s post-long-duration sound testing. While the effect was shorter in duration than the long-term potentiation found in IC neurons, it may be related to the post-tetanic potentiation observed in IC slice recordings (Wu et al., 2002).

This work was supported by a grant from DOD | United States Army |MEDCOM | Congressionally Directed Medical Research Programs - W81XWH-18-1-0135

PS 743

Vivarium Noise and Ultrasonic Noise as a "Silent" Confounding Variable in Auditory (and Non-Auditory) Research Using Animal Models

Jeremy Turner
Illinois College

The typical modern biomedical research laboratory and animal vivarium facility are filled with equipment that produces noise and ultrasonic noise. Examples include ventilated caging motors, procedure and cage changing hoods, fluorescent lighting, computers and monitors, motion-activated light controllers, and even the equipment used to measure behavioral or physiological responses. This presentation reviews the many sources of noise and ultrasonic noise in the modern research laboratory and vivarium, their typical spectral and level outputs, and variability both within and between biomedical research facilities. We suggest this variability, which is typically not measured nor reported in hearing research studies, serves as a source of error variability in our research studies, complicating our attempts to replicate studies over time and across labs. In addition to serving as a source of variability for auditory scientists, noise and ultrasonic noise can also serve as stressors for research animals, and by activating stress pathways can therefore serve to confound virtually every area of biomedical and behavioral research. We suggest some strategies for

measuring, controlling, managing, and even reporting on the noise and ultrasonic noise in our vivarium and research laboratory settings. Such steps will help us in auditory science better interpret the research findings in studies and aid in cross-lab replications where the acoustic background in the vivarium or research lab might have dramatic impacts on our model systems.

PS 744

Vagal Nerve Afferents Influence Animal Behavior: A Gut-Brain Connection.

Diana C. Peterson
High Point University

Numerous studies show that intestinal microflora can influence brain activity and psychosis. Whether the influence is caused by direct neuronal circuitry or systemic influences is unknown. The current study attempts to identify whether vagal afferents directly influence brain activity and animal behavior by reversibly deactivating vagal afferent projections from the jejunum.

Methods
C57BL6 mouse behavior was recorded for a period of two weeks during several behavioral tests (i.e., elevated plus maze, open-field, and forced swim). Once control data was obtained, 3-5 injections of either an optogenetic vector (AAV-CaMKIIa-eNpHR3.0-EYFP) or saline control (0.01-0.03 ml) were placed into the mesenteric wall of the jejunum. During the surgery, a fiber optic ferrule was implanted over the cervical vagus on one side to allow illumination of the vagus nerve. After surgical recovery, behavioral tests were initiated for 2 weeks to assess variations in behavior from the initial control that may be caused by the surgery. These tests were then utilized as the control behavioral activity for each animal. Four weeks post-surgery, behavioral experiments were initiated in which vagal afferents to the injected regions of the jejunum were deactivated with light stimulation of the vagus. Results were compared between vector injected animals and saline injected animals. Results for each animal were also compared between the light-on (vagus deactivated state) and no-light (vagus non-deactivated state).

Results
No differences in mice activity was observed across pre-surgical control, post-surgical control, and post-surgical non-deactivated vagal state behavioral tests. In the saline condition, animals with light activation of the vagus showed no variation in their behavioral activity from that of the non-light control state. In the optogenetic vagus deactivation condition, animals showed a freezing behavior for the extent of time that the vagus was deactivated. The freezing behavior caused animals to sink in the forced swim test, requiring multiple rescues during each session.

Conclusions
Optogenetic deactivation of the vagus had dramatic and immediate influences on animal behavior. We hypothesize that the freezing behavior was caused by incongruous signaling between the right and left sides of the brain. Whether this hypothesis is correct or not, the experiment shows that vagal afferent projections provide a pathway by which the enteric system can influence brain activity and behavior.

PS 745

Brain-derived neurotrophic factor (BDNF) in the auditory periphery controls central learning mechanisms and social behavior

Philipp Eckert[1]; Philine Marchetta[1]; Marie Manthey[2]; Michael H. Walter[3]; Wibke Singer[1]; Michele Jacob[2]; Lukas Rüttiger[1]; Thomas Schimmang[4]; Peter K. Pilz[3]; Marlies Knipper[5]
[1]University of Tübingen, Department of Otolaryngology, Head and Neck Surgery Tübingen; [2]Tufts University School of Medicine, Department of Neuroscience; [3]University of Tübingen, Department of Animal Physiology; [4]Instituto de Biologica Genetica Molecular, Universidad der Valladolid; [5]University of Tübingen, Department of Otolaryngology, Head and Neck Surgery Tuebingen

Brain-derived neurotrophic factor (BDNF), a key modulator of synaptic plasticity is predicted to locally control cortical receptive field maturation and memory with sensory experience. BDNF`s main function for the adult central nervous system performance starts with sensory experience when local cortical BDNF is assumed to regulate the excitability of cortical circuits (Hong et al., 2008), a process leading to enhanced cortical auditory resolution. In the auditory system BDNF become gradually upregulated in cochlear neurons or glial cells and the ascending auditory path between P4 and P14 (Singer et al., 2014). Aiming to get a first insight in BDNF`s function from hearing onset onwards, *Bdnf* was deleted in lower level brain regions under the promoter of the paired-box transcription factor Pax2 (Zuccotti et al., 2012; Chumak et al., 2016). A striking novel role of BDNF in Pax2-expressing cells in the auditory periphery is identified that points to BDNF as trigger for rapid auditory processing, executive memory-linked functions, and normal social behavior.

This work was supported by the Deutsche Forschungsgemeinschaft FOR 2060 project RU 713/3-

2; GRK 2381; SPP 1608 RU 316/12-1 and KN 316/12-1; BFU2013-40944; NIH NIMH 1R01MH106623.

PS 746

Graded control of neuromodulatory brain state using parametric stimulation of the Vagus Nerve

Zakir Mridha[1]; Jan Willem de Gee[1]; Yanchen Shi[1]; Rayan Alkashgari[2]; Justin Williams[2]; Aaron Suminski[2]; Matt Ward[3]; Wenhan Zhang[1]; **Matthew J. McGinley**[4]
[1]Baylor College of Medicine, Department of Neuroscience; [2]University of Wisconsin, Department of Bioengineering; [3]Purdue University, Department of Bioengineering; [4]Department of Neuroscience, Baylor College of Medicine

The vagus nerve relays information about brain state to the body. Vagus nerve stimulation (VNS) is thought to 'back fire' neuromodulatory centers (such as LC), releasing neuromodulators throughout the brain. The neuromodulatory effects of VNS are thought to mediate its clinical benefits, in for example the treatment for refractory epilepsy, tinnitus, or depression. Furthermore, VNS enhances auditory learning in healthy individuals, which is thought to boost cortical plasticity via the same neuromodulators (Engineer et al., 2015). A major challenge in using VNS, for therapeutic purposes or auditory enhancement, is that there is no known readout of nerve engagement or its subsequent neuromodulatory impact. As a result, stimulation parameters are chosen and optimized, largely through trial-and-error and feedback from patients about symptoms and side effects. We have previously shown that pupil size tracks neuromodulatory brain state and its influence on auditory physiology and behavior (McGinley et al., 2015; Reimer et al., 2016).

Here, we developed a VNS preparation for awake, head-fixed mice and tested if pupil dilation is a biosensor of VNS-triggered cortical neuromodulation. We adapted an implanted cuff design from prior work in rats (Ward et al., 2015). Stimulation via our cuff is well-tolerated by mice for up to several months. We performed an extensive search across a VNS parameter space of 4 pulse widths (0.1-0.8 ms), 5 amplitudes (0.1-0.9 mA), and 3 rates (5-20 Hz; 10 s trains), while monitoring pupil size and other eye movements. We found consistent pupil dilation that parametrically increased with increasing pulse width, amplitudes or rate. Experiments with promiximal (or proximal and distal) cut of the nerve confirm that the pupil dilation results from selective activation of the vagus nerve. Using two-photon imaging of neuromodulatory axons in auditory cortex, we observed that cortical neuromodulation was phasically boosted during VNS, and then decayed back to a stable baseline. We also found that care with grounding and current spread is necessary to avoid major off-target effects such as small phase-locked eye movements and further pupil dilation. Taken together, our results provide a foundation for carefully controlled VNS, and pupil dilation as its readout, for the enhancement of auditory learning and other applications requiring closed-loop, graded control of brain state.

References: McGinley et al. (2015), Neuron, 87. Reimer, McGinley, et. al. (2016), Nature communications, 7. Engineer et al. (2015), Brain Stimulation, 8. Ward et al. (2015), IEEE Trans Neural Syst Rehabil Eng, 23.

Speech Perception Methodology

PS 747

The McGurk illusion effect is not attributed to audiovisual fusion

Mariel Gonzales[1]; Kristina Backer[1]; Brenna Mandujano[2]; Antoine Shahin[1]
[1]University of California-Merced; [2]Fresno State University

The classical McGurk illusion occurs when an audio of a speaker uttering the phoneme /ba/ combined with the video of the speaker uttering /ga/, leads to hearing 'da' or 'ta. The perception of a third phoneme has been touted as evidence for audiovisual (AV) fusion. Moreover, the McGurk illusion has been distinguished from the visual dominance illusion in which auditory perception is biased toward the visual utterance (e.g., audio /ba/, video /fa/, heard 'fa'). This study provides evidence that the McGurk illusion is due to visual dominance. Subjects were presented with silent videos of a talker uttering the consonant-vowel syllables /da/, /ga/, /ha/, /ka/, /la/, /na/, /sa/, and /ya/ (V-only), those same videos merged with audios of /ba/ (AV), and superimposed audio pairs: /ba//ba/, /ba/da/, /ba/ga/, /ba/la/, /da/ga/ (A-only). Subjects were instructed to type the syllable they saw (V-only trials) or heard (AV and A-only trials). We show that: 1) In the V-only condition, subjects largely saw 'da'/'ta' in response to /ga/, /ka/, and several other consonant-vowel syllables. When the illusion was experienced in the AV condition, 'da'/'ta' was heard regardless of the syllable presented. Thus, 'da'/ta' becomes a default percept when the place of articulation is indiscernible. 2) The frequency of the illusion was inversely correlated to the frequency of the perception of 'ba'/'pa' in the A-only condition (/ba/ba/ trials). The latter finding suggests that the strength of /ba/ encoding is inversely related to the susceptibility to the McGurk illusion. Cumulatively, these results suggest that audiovisual integration occurs via visual modification of phonetic representations rather than fusion of AV percepts.

PS 748

How Representative of Everyday Speech Signals are Clinical Speech Test Materials?

Timothy Beechey[1]; Jorg Buchholz[2]; Peggy Nelson[1]
[1]University of Minnesota; [2]Macquarie University

Speech perception tests are important tools for determining the impact of hearing impairment on a person's functioning (as defined by the World Health Organization's International Classification of Functioning and Disability) and quality of life, as well as for measuring the impacts of any interventions.

The uses of speech tests for hearing assessment fall into two broad categories: site-of-lesion diagnosis; and quantification of speech perception performance in different listening conditions. While these uses are distinct, the particular speech tests employed for these two purposes are designed according to the same principles, and, often, are the very same tests. The fundamental design criterion which underlies standard speech tests is the Performance-Intensity (PI) function. Speech tests are designed to ensure steep PI functions in order to achieve test sensitivity.

Although high test sensitivity is an important diagnostic property, it does not contribute to—and may be detrimental to—the ability of a speech test to predict speech perception performance outside the clinic. Because steep PI functions are achieved, in part, by removing as much variation from the speech signal as possible, changes in performance measured by a speech test are unlikely to reflect changes in functioning outside the clinic, when people are confronted with natural speech signals. The usefulness of speech tests as predictors of functioning and disability depends largely on how representative the demands of a speech perception test are to the demands of speech perception in everyday life. As a consequence, standard speech tests may not be the ideal tools for understanding how hearing impairment, and our interventions, affect everyday speech perception.

There is a need to better understand the extent to which standard speech test signals do, and do not, represent the types of speech signals encountered by people with hearing impairment during daily communication. This study provides a comparison of the acoustic characteristics of speech signals from a widely used clinical speech intelligibility test, the BKB sentence test, with recordings of conversational speech produced by the same BKB sentences talker, within dyadic conversations with a hearing-impaired conversation partner, in a range of realistic acoustic environments. Speech signals are compared in terms of spectral, temporal, and intensity characteristics, segmental reductions and deletions, and prosody. In particular, this study seeks to highlight the importance of natural variation in speech which is an integral part of natural speech perception, but which is generally absent from standard speech test signals.

PS 749

Speech Error-Detection Thresholds in Cochlear Implant and Normal Hearing Listeners

Sarah Bakst; Caroline A. Niziolek; Ruth Y. Litovsky
University of Wisconsin–Madison

In normal hearing speakers, the speech production system detects errors and updates motor plans while talking by accessing auditory feedback. Cochlear implants (CIs) degrade the incoming acoustic signal, which may result in sub-optimal comparison between the auditory feedback and intended speech target, thereby possibly diminishing the ability to correct nascent errors. Automatic error-detection is important for producing intelligible speech and successful communication. This experiment investigates whether CI users can detect variability in their own productions, an important first step in understanding the extent to which auditory information from the implant aids in acquiring and maintaining intelligible speech.

This experiment estimates the auditory threshold at which listeners can detect differences in their own speech, specifically in the first and second formants (F1/F2), spectral peaks which are important for distinguishing vowel height (e.g. "he" vs. "hey") and backness ("he" vs. "who"). We hypothesized that CI users may not be able to detect sub-phonemic differences in their own speech, especially if those differences remain within electrode bands in their frequency allocation tables.

Participants were recorded speaking the words "Ed" and "oh" sixty times each. A single token of each word was selected as a base for stimuli generation. Using Audapter (Cai et al. 2008, Tourville et al. 2013), the F1 of "Ed" and the F2 of "oh" were increased and decreased in increments of 1 Hz to create stimuli for discrimination testing. For normal hearing (NH) listeners, the resulting stimuli were passed through a 16-channel, sine-wave vocoder (no frequency shift) to approximate the spectral degradation of a CI.

Speakers heard their own altered speech while partaking in a four-interval, two-alternative-forced-choice adaptive discrimination design (3-up-1-down, AABA or ABAA presentation). The experiment ended after 21 reversals (change from correct to incorrect or vice versa). The

intervals from the final six reversals were averaged to approximate the threshold.

Preliminary data (CI n=5, NH n=4) show variable sensitivity. For two CI users, all thresholds crossed electrode boundaries, but three CI and all NH listeners had within-frequency band sensitivity for at least one formant, suggesting that electrode boundaries may not be the limiting factor in sensitivity to fine-grained acoustic variation and that real-time error-detection may be possible. Planned acoustic analyses, including evidence from electrodograms, will consider the cues that listeners use to hear fine distinctions in their own speech. Future experiments will test whether CI listeners use their auditory feedback to correct their speech in real time.

PS 750

A Cautionary Note on the Effects of Gender and Speaker Variability in a Two-Talker Separation Task

Lorenza Zaira Curetti[1]; Rebecca Millman[2]; Patrick Gaydecki[3]; Michael Stone[2]
[1]NIHR Manchester Biomedical Research Centre, Manchester Academic Health Science Centre, Manchester University NHS Foundation Trust; [2]Manchester Centre for Audiology and Deafness, School of Health Sciences, University of Manchester; [3]School of Electrical and Electronic Engineering, University of Manchester

Concurrent speech segregation can be facilitated by differences in gender between target and masker talkers (e.g. fundamental frequency and formants). These cues can increase speech intelligibility and reduce listening effort in a variety of speech-on-speech listening tasks (Rennies et al., 2019). Here, middle-aged, normal-hearing listeners (< 25 dB HL, 125 Hz - 6 kHz) were required to identify a set of keywords from two simultaneously presented sentences drawn from the "York" Coordinate Response Measure (CRM; Kitterick et al., 2010), while performing a secondary two-level visual working memory task. Two sentences spoken by different-gender talkers (male/female), mixed at a signal-to-noise ratio (SNR) of 0 dB, were presented concurrently. Sentences were subjected to three different degrees of dynamic range compression (none, moderate, severe), applied either before, or after, mixing the two sentences together. Contrary to expectations, gender and speaker variability swamped the effects of the processing conditions. While gender differences facilitated source segregation, the male and female speakers, each used here both as a target and a masker, resulted in unequal masking. Speech intelligibility models (Speech Intelligibility Index [SII; ANSI S3.5-1997] and the multi-resolution speech-based envelope power spectrum model [mr-sEPSM; Jørgensen et al., 2013]) were employed to assess the origin of these discrepant results. The SII operates on frequency-band-specific SNRs while the mr-sEPSM operates on modulation-band-specific SNRs to generate its output measure SNRenv. A 120-s speech signal was generated for each talker (4 males, 4 females) by concatenating randomly selected CRM sentences, each signal being normalised to an input level of 62 dB SPL. SII model outputs revealed small but negligible differences between the gender combinations. Conversely, the mr-sEPSM model predicted significant differences in relative SNRenv dominated by the target gender. Investigation of additional speech material (American-English CRM [Bolia et al., 2000]; speech recordings used in Moore et al., 2008) showed similar patterns of results. Furthermore, all speech corpora tested demonstrated that within-gender speaker differences can introduce significant variability in the predicted masking effects. In summary, even when an SNR of 0 dB is used, the envelopes of the target and masker waveforms can confound signal processing effects in multi-talker scenarios. Speech corpora with a small number of speakers may not be representative of real-world performance unless some form of speaker pairing is used to reduce the unwanted variability.

PS 751

A Non-intrusive Measure of Speech Quality using the Bispectral Features of an Auditory Neurogram and Support Vector Regression

Md E. Hossain[1]; **Muhammad S. Zilany**[2]
[1]University of Sydney; [2]Texas A&M University at Qatar

Measurement of speech quality is essential for monitoring and maintenance of the quality of service at different nodes of the network in modern telecommunication systems as well as for the development of speech coding and enhancement techniques. However, the subjective evaluation of speech quality using listeners is more complex and time-consuming. Also, it is difficult to predict human perception due to the complex and nonlinear nature of processing in the human auditory system. In this work, we propose a reference-free objective measure of speech quality using appropriate features from the simulated neural responses and subsequently map them into a quality rating using support vector regression. The 2D neurograms were constructed from the simulated responses of the auditory-nerve fibers with a wide range of characteristic frequencies to speech signals. The features of the neurograms were extracted using third-order statistics referred to as the bispectrum. The speech quality scores predicted by the proposed method were compared to the subjective scores for normal listeners using two standard speech corpora (NOIZEUS and ITU-T P.Sup. 23 database) under diverse

degraded conditions. The estimated results using the proposed method were also compared with those of several existing metrics such as perceptual evaluation of speech quality (PESQ), ITU-T Recommendation P.563, and virtual speech quality objective listener (ViSQOL). Preliminary result suggested that the proposed method outperformed most of the traditional existing metrics under the test conditions. This objective measure could also be extended to evaluate the speech quality for listeners with hearing loss.

PS 752

Assessing the Reliability and Validity of the Iowa Test of Consonant Confusion

Ann Holmes[1]; Jason Geller[1]; Adam Schwalje[2]; Inyong Choi[3]; Bob McMurray[1]
[1]Department of Psychological & Brain Sciences, University of Iowa; [2]Department of Otolaryngology -- Head and Neck Surgery, University of Iowa Hospitals and Clinics; [3]Dept of Communication Sciences and Disorders, University of Iowa

Background
Consonant discrimination, especially in background noise, is a critical problem for hearing impaired listeners' speech perception. The Iowa Test of Consonant Confusion (ITCC) was developed as a phonemically balanced word recognition task designed to capture confusions in the initial consonant of monosyllabic consonant-vowel-consonant (CVC) words when the target word is given with four choices of minimum pair words. This study sought to evaluate the psychometric properties of ITCC by examining reliability (test-retest), convergent validity (ISNT vs. CNC), and divergent validity (ISNT vs. AzBio).

Method
The ITCC stimuli consisted of 120 phonetically balanced CVC words that were recorded from four different talkers, two male and two female. Twenty-four normal-hearing listeners (mean age = 25.3 years, SD = 6.90; pure tone thresholds < 25 dB HL from 250 to 8000 Hz) were recruited for two sessions of testing where they completed ITCC with all four talkers across both sessions, 20 AzBio sentences, and 100 CNC words presented in multi-talker babble. For ITCC, after listening to a target word in background noise, participants were asked to choose an answer from a list of four choices comprised of phonemically confusable sets of minimal pairs. For AzBio and CNC, participants were required to respond verbally.

Results
Test-retest reliability between session one and session two was high (r= 0.81, p < 0.001, $CI_{95\%}$[0.61, 0.92]), ITCC correlated with CNC performance (r= 0.40,p=0.05, $CI_{95\%}$[0.00, 0.69]), but it did not correlate with AzBio performance (r = 0.19, p= 0.368, $CI_{95\%}$[-0.23, 0.55]).

Conclusion
ITCC was developed to address the weaknesses of other speech-in-noise tasks and to provide an extended test for diagnosing consonant confusions in background noise. The results from this study suggest that ITCC can be used as a valid speech-in-noise task both experimentally and clinically. At the University of Iowa, ITCC will be used with cochlear implant users to address their speech-in-noise abilities longitudinally.

PS 753

Statistical learning in rooms under transcranial magnetic stimulation

Heivet Hernandez-Perez[1]; David McAlpine[2]; Jessica Monaghan[1]
[1]Macquarie University; [2]Department of Linguistics, The Australian Hearing Hub, Macquarie University, Sydney, Australia

In the auditory system, adaptation to sound intensity can operate over multiple time scales and contributes to statistical learning (Dean et al., 2005, 2008; Simpson et al., 2014). Moreover, efferent feedback from the cortex to the inferior colliculus has been directly linked to learning the longer-term statistical structure of sound environments so that this information can be used when a familiar environment is re-encountered (Robinson et al., 2016). Brandewie and Zahorik (2010) described a psychoacoustic task that demonstrated speech perception advantages of re-exposure to familiar environments. They found that prior exposure to room statistics (Reverberation Times; RTs) in the form of a "carrier phrase" spoken in a simulated room significantly improved participants' masked speech understanding for speech spoken in the same room. Here, we aimed to understand: 1) how real room RTs contribute to the statistical learning of room acoustics and 2) how this learning may be affected when the inferior frontal gyrus (IFG), involved in the expression of auditory statistical learning (Karuza et al., 2013), is temporarily impaired using repetitive transcranial magnetic stimulation (rTMS). Following the methods of Bradewie & Zahorik (2010; 2013), phrases from the Coordinated Response Measurement (CRM) corpus were presented in noise to ten participants with normal hearing. The CRM phrases had different durations: 0, 0.2357, 0.5715 and 0.8485 s (e.g., "Green Five now", "Go to Green Five Now", "Baron Go to Green Five now" and "Ready Baron Go to Green Five now", respectively). Carrier phrases were convolved with impulse responses from 3 real rooms (Room 1:

RT_{60} = 0.46 s; Room 2: RT_{60} = 0.96 s; Room 3: RT_{60} = 2.42 s) and presented in free sound-field conditions in an anechoic chamber using a ring of 41 loudspeakers. Similar to Brandewie & Zahorik (2013) participants perceived target phrases e.g., ''Green Eight", more accurately when the carrier phrases had longer duration (containing more statistical information from the rooms presented). It was also observed that rTMS disrupts this learning across all carrier phrases and rooms tested ($p < 0.05$). In addition, we found that the carrier length effect is only observed when Room 1 is presented in the mixture of rooms. Our results revealed that IFG is involved in learning room statistics, which may reflect adaptation through feedback mechanisms from IFG to the auditory pathway. Moreover, our data suggest that ecologically relevant RTs such as that of Room 1 enable a perceptual anchoring that allows learning room statistics in less commonly encountered environments.

PS 754

Emotional Vocalizations in Mice Evoke Distinct Patterns of Dopamine and Acetylcholine Release in the Amygdala after Brief Mating and Restraint Experiences

Zahra Ghasemahmad[1]; Rishitha Panditi[2]; Bhavya Sharma[2]; Drishna Karthric Perumal[2]; Jeffrey J. Wenstrup[1]
[1]Northeast Ohio Medical university, Kent State University; [2]Northeast Ohio Medical university

Social vocalizations, reflecting the internal state of a sender, can change the internal state and behavior of listeners. These listener responses are mediated in part by the basolateral amygdala (BLA). The BLA receives information related to vocalizations from auditory cortex and thalamus, compares this information with previous experience, then shapes reactions to vocal stimuli. We hypothesized that behavioral reactions are shaped by inputs from neuromodulatory centers into the BLA. Here, we examine how emotion-laden vocalizations evoke patterns of neurochemical release in the mouse BLA.

A liquid chromatography/mass spectrometry (LC/MS) technique allowed simultaneous detection of non-electroactive chemicals (GABA, Glutamate, and acetylcholine (ACh)) and catecholamines in the same microdialysis samples, and the concentration of neurochemicals were related to playback of emotional vocalizations. To identify these highly emotion-laden vocalizations of CBA/CaJ mice, we characterized vocal sequences unique to restraint (aversive) and an intense stage of mating (appetitive). Mice were tested in 3 groups: males-mating, males-restraint, and females-mating (w/estrous monitoring). Groups were based on previous results showing distinct sex-based behavioral responses to mating vocalizations but similar responses to restraint calls. After a single, one-hour experience of each behavior (mating and restraint) on consecutive days, mice were implanted with a guide cannula above BLA. Four days later, a microdialysis probe was inserted on the day of the playback experiment. CSF samples were collected from BLA before, during, and after vocalization playback in 10-minute intervals. Probe location in BLA was histologically confirmed.

Here we report on ACh and dopamine (DA) release following single exposures to mating and restraint behaviors. In response to 20-minute playback of mating vocalizations, DA increased in both male and female (proestrus) mice and remained elevated after playback for 1 hour, while ACh concentration decreased during playback and returned to background after playback stopped. Females in estrous showed both ACh and DA increases in response to playback of mating vocalizations. In contrast, playback of restraint vocalizations decreased DA during and after playback, while ACh showed increased release during playback and returned to the background level after playback stopped.

Our findings suggest patterns of ACh and DA release in the BLA that may contribute to distinct behavioral responses to appetitive and aversive vocal sequences. These results support previous studies suggesting involvement of dopaminergic pathways in reward processing and emitting positively valenced vocalizations in rats. Further, our data support work showing that the cholinergic system is involved in fear condition responses and emitting alarm calls.

PS 755

Cochlear-Implant Users Benefit from Voice-Feature Continuity at the Cocktail Party

Jens Kreitewolf[1]; Daniela Hollfelder[2]; Martin Orf[1]; Julia Erb[1]; Samuel R. Mathias[3]; Karl-Ludwig Bruchhage[2]; Barbara Wollenberg[2]; Jonas Obleser[1]
[1]Department of Psychology, University of Lübeck; [2]University Hospital Schleswig Holstein, Campus Lübeck, Clinic for Otorhinolaryngology - Head and Neck Surgery; [3]Department of Psychiatry, Boston Children's Hospital, Harvard Medical School

Most of our everyday listening happens under adverse conditions largely because natural auditory scenes often comprise a multitude of sounds heard at once. These "cocktail-party"-like situations pose a difficult problem for normal-hearing (NH) listeners, and are particularly challenging for cochlear-implant (CI) users. We have previously shown (Kreitewolf et al., 2018) that NH

listeners are better at comprehending target speech when they can group sounds based on continuity in two prominent voice features: glottal-pulse rate (GPR) and vocal-tract length (VTL). Unlike NH listeners, CI users do not seem to benefit from voice cues. For example, recent work (El Boghdady et al., 2019) suggests that CI users do not exploit differences in GPR and VTL to segregate target from masker speech.

Here, we took a different approach to investigate the use of GPR and VTL for cocktail-party listening in *N* = 11 NH listeners and *N* = 11 CI users. Listeners heard a stream of spoken digits embedded in multi-speaker babble and were asked to report each digit immediately after its presentation. To explore the contributions of GPR and VTL to cocktail-party listening, we manipulated continuity in GPR and/or VTL across consecutive digits. Additionally, we assessed listeners' sensitivity to GPR and VTL differences.

Our results showed that both NH listeners and CI users benefited from voice-feature continuity. For both groups of listeners, we observed the largest benefits when both GPR and VTL were continuous across consecutive target digits. To assess listeners' abilities to track consecutive digits in the target stream, we calculated the so-called previous-digit-correct benefit (PDCB). Interestingly, CI users yielded greater PDCBs when they could rely on VTL versus GPR continuity. NH listeners, however, seemed to benefit equally from GPR and VTL continuity. The benefits from voice-feature continuity were not correlated with GPR or VTL sensitivity.

These findings provide first evidence that CI users exploit continuity in voice features to improve listening at the cocktail party. Unlike NH listeners, CI users seem to rely more on VTL than GPR continuity for perceptual grouping of target sounds. VTL is effectively fixed within natural talkers and might be particularly useful for perceptual grouping in everyday cocktail-party listening. The stronger reliance on VTL than GPR continuity may therefore contribute to CI users' residual abilities to solve the cocktail-party problem in natural settings.

References

El Boghdady et al., *J Acoust Soc Am* (2019).

Kreitewolf et al., *J Acoust Soc Am* (2018).

PS 756

Identifying Listeners Whose Speech Intelligibility Depends on an Extra Moment to Repair Perceptual Mistakes

Steven P. Gianakas[1]; Matthew B. Fitzgerald[2]; Matthew B. Winn[1]

[1]University of Minnesota; [2]Stanford University

The short time period after a sentence is spoken may be crucial for listeners with hearing loss to mentally repair or correct mistakes that were made during listening. They can thus present with good intelligibility scores despite utilizing higher level processing to correct for poorer bottom-up information. The current audiologic test battery cannot distinguish a listener who correctly repaired a misperception from a listener who heard the speech accurately with no need for repair. It is important for audiologists to make this distinction because one listener could be working harder than the other, and potentially susceptible to falling behind in ongoing conversation where there isn't silent time to repair mistakes.

In this study, we presented recipients of cochlear implants with both high and low-context sentences followed by silence (to allow mental repair), or noise (which should disrupt the repair process). For virtually every listener with a cochlear implant, speech recognition scores were lower when test sentences were followed by noise, with variable amount of susceptibility across listeners. With an extra moment of silence after a sentence, some listeners were able to improve their scores by as much as 50 percentage points, suggesting potentially immense influence of cognitive repair that is not captured in conventional testing. Specifically, the noise interfered most with high-context sentences, suggesting that the extra time is used by listeners to benefit from semantic context when possible. In contrast, listeners did not benefit from that extra time after the sentence when there was minimal or no contextual information available.

The process of using an "extra moment" to repair misperceived speech seems very common among people with hearing loss, for whom it is likely to contribute to elevated listening effort. Identifying listeners susceptible to relying on an extra moment will enable audiologists and speech-language-pathologists to provide high quality patient-centered aural rehabilitation to listeners with hearing loss.

PS 757

Neural Correlates of Context-Dependent Lexical Bias (Ganong effect) on Categorical Speech Perception

Gwyneth Lewis; Claire Pearson; Ashleigh Harrison; Gavin Bidelman
University of Memphis

Objective

The "Ganong effect" is a perceptual phenomenon whereby lexical context constrains a listener's categorical perception (CP) of the phonetic boundary of word-nonword speech continua. Results from fMRI suggest that this effect reflects direct linguistic influences on perceptual processes, as well as post-perceptual effects on executive processes such as decision. Here, we conducted an EEG experiment with more temporally sensitive measures of neural activation to shed light on the time-course of these context-related influences on CP and their influence on perceptual vs. decision-related speech mechanisms.

Method

Behavioral and neuroelectric brain responses (ERPs) were acquired from participants as they categorized speech stimuli from 8-step word-nonword (gift-kift) and nonword-word (giss-kiss) continuua. Behavioral analyses compared relative differences in response times (RTs) and classification performance on identical tokens from the two continua (e.g., midpoint token of giss-kiss vs. midpoint of the gift-kift continuum). Source space analyses focused on activity in the superior temporal gyrus (STG) and the inferior frontal gyrus (IFG). If lexical status constrains early CP, placement of the phonetic category boundary should modulate early STG activity.

Results

Behavioral data revealed a slowing in RTs for tokens near the category boundary and a lexically biased shift in the perceived category boundary toward the lexical anchor of the continuum (e.g., bias toward "g" responses for gift-kift; "k" bias for giss-kiss). At the neural level, STG and IFG activity simultaneously showed stronger amplitudes for more ambiguous gift-kift tokens (Tk3). Boundary giss-kiss tokens (Tk3) enhanced STG at ~200 ms followed by IFG activity at ~300 ms.

Conclusion

Results suggest early lexical influences on CP of speech whereby the perceived category boundary of speech phonemes shifts toward lexical items. Neurally, more ambiguous tokens from the lexical continuum (gift-kift 3) modulated STG and IFG activity early on in recognition (~100 ms), while non-lexical boundary items (giss-kiss 3) modulated activity during later time windows (STG: ~200 ms; IFG: ~300 ms). Although it was predicted that lexically shifted boundary items (i.e., gift-kift 4) would modulate STG activation, individual variability among participants' perceived category boundary (e.g., between gift-kift 3 and gift-kift 4) may have obscured this effect. Tentatively, early differences in STG modulation observed here challenge the view that the Ganong effect solely reflects post-perceptual decision-stage processes.

PS 758

Can Auditory-Nerve and Inferior Colliculus Models Explain Perceptual Confusions for Fricatives?

Yasmeen Hamza; Afagh Farhadi; Douglas Schwarz; Joyce McDonough; Laurel H. Carney
University of Rochester

Fricatives are a common class of phonemes, produced by forcing air through a constriction along the vocal tract, resulting in a characteristically high-energy noise. The place of the constriction (articulation) and the presence/absence of vocal-fold vibration (voicing) produce different fricatives. Some fricatives (e.g., stridents; Arpabet: /S, Z, SH, ZH/) have relatively higher energy than others (non-stridents; Arpabet: /F, V, TH, DH, H/). Much phonetic work has focused on the articulation and acoustics of fricatives; however, a lack of agreement remains on important features for perception. In the current study, we model auditory-nerve (AN) and midbrain (central nucleus of inferior colliculus, ICC) responses to fricatives to test the hypothesis that response profiles across populations of neurons provide robust correlates to perception.

Intervocalic (vowel-consonant-vowel) English-language fricatives (3 repetitions) spoken by 10 speakers were scaled so that the level of the initial mid-vowel section (60 ms) was 65 dB SPL. AN and ICC responses were simulated using computational models. ICC neurons can be excited (band-enhanced) or suppressed (band-suppressed) by amplitude modulations, as described by modulation transfer functions. Both types of ICC responses were modeled. Average rates in response to the mid-fricative stimuli (60 ms) were plotted as a function of model characteristic frequency (CF). A neural-phonetic framework described fricative profiles in terms of voicing and the CF of the response peak. Sibilant fricatives had consistent and unique profiles. Non-sibilant fricatives, apart from /H/, had profiles that varied across utterances. Furthermore, similar profiles were observed across fricatives for non-sibilants with the same voicing cue: /F/ and /TH/, and /V/ and /DH/. A classifier analysis used to build confusion matrices based on spectral or neural model responses showed similar confusions to the ones described above.

We are currently evaluating correlations between the classifier-generated confusion matrices based on AN or ICC model responses and published perceptual confusion matrices. We hypothesize that perceptual confusions of fricatives are explained accurately and consistently by modeled neural response profiles. Future electrophysiological recordings from the IC of awake rabbits will be used to further test this hypothesis. Additionally, simulating neural responses of the impaired ear to fricatives could guide the development of processing strategies aimed at reaching the normal-hearing neural targets.

Supported by NIH-R01-DC010813.

Stem Cells

PS 759

Matrigel Coated Mammalian Embryonic Stem Cells Survival in Artificial Endolymph

Irem Gul Sancak[1]; Karunya Kandimalla[2]; Daihyun Song[3]; Rafael da Costa Monsanto[4]; Mio Uchiyama[5]; Grace Park[6]; Michael, Mauro Paparella[7]; Sebahattin Cureoglu[6]
[1]Department of Surgery, Ankara University Faculty of Veterinary Medicine, Ankara, Turkey; [2]Department of Pharmaceutics, College of Pharmacy, University of Minnesota, Minneapolis, USA; [3]Department of Biochemistry, Molecular Biology and Biophysics, University of Minnesota, Minneapolis, USA; [4]Department of Otolaryngology, Universidade Federal de São Paulo/Escola Paulista de Medicina (UNIFESP/EPM) – São Paulo, SP, Brazil; [5]Department of Otolaryngology, Showa University, Tokyo, Japan; [6]Department of Otolaryngology, Head and Neck Surgery, University of Minnesota – Minneapolis, Minnesota, USA; [7]Paparella Ear Head and Neck Institute – Minneapolis, Minnesota, USA

Background
Marmoset cells are known to be the closest cell line to human originated cells. Transplantation of stem cells into the inner are is challenging due to the special characteristics of the environment. High potassium levels in the scala media immediately reduce the number of cells transplanted. Co-culturing the cells and introducing them to the new environment and coating them to protect from high potassium is our goal in this study.

Methods
Marmoset cells are grown into 3rdpassage using E8 medium with 10% FBS in a humidified chamber with 5% CO^2at 37 °C. Marmoset cells are stained with PKH-26 for a red fluorescence and seeded into the 12 well plates with 1:1 mixture of matrigel and cell suspension. Cells are divided into four groups: a control group with no treatment, endolymph like solution treated group, perilymph like solution treated and 50:50 mixture of endolymph and perilymph solution treated group. Duration of the treatment was 30 minutes in each group. Cells are examined using a fluorescence microscope with deconvolution microscopy. To follow and compare the cell fate flow cytometry was also used.

Results
Matrigel-coated ESCs survival in different potassium level environments compared and matrigel coating is found to be useful in ESCs survival. The best results were observed in the 50:50 group.

Conclusion
Co culturing the cells with 50:50 endolymph solution is advised before transplanting them into the inner ear.

Key Words
Stem cell, Matrigel, Coating

PS 760

Translatome Analysis of Damage-Activated Hidden Progenitor Cells in the Mouse Cochlea

Patrick Atkinson[1]; Beatrice Milon[2]; Tomokatsu Udagawa[1]; Yang Song[3]; Elvis Huarcaya Najarro[1]; Ronna Hertzano[4]; Alan Cheng[1]
[1]Department of Otolaryngology-Head and Neck Surgery, Stanford University; [2]Department of Otorhinolaryngology-Head and Neck Surgery, University of Maryland; [3]Institute for Genome Sciences, University of Maryland; [4]Department of Otorhinolaryngology Head and Neck Surgery, University of Maryland School of Medicine; Institute for Genome Sciences, University of Maryland School of Medicine.

The greater epithelial ridge (GER) is a poorly characterized, mitotically quiescent organ adjacent to the organ of Corti. We have recently established a novel supporting cell ablation model using the $Lgr5^{DTR/+}$ mouse line. We found that after the selective ablation of Lgr5+ supporting cells in the neonatal mouse cochlea, cells of the GER robustly proliferate along the whole length of the organ. These cells then migrate and replenish lost inner phalangeal supporting cells, indicating the presence of a damage-activated progenitor cell population within the GER. To assess the molecular signatures of these progenitor cells of the GER at rest and after supporting cell loss, RiboTag-sequencing was performed using the $Rpl22^{HA/+}$, $GLAST^{CreERT/+}$ and $Lgr5^{DTR/+}$ mouse lines. GLAST-Cre was used as it is expressed by cells residing within the GER and the inner phalangeal cell region.

The RiboTag model allows for the immunoprecipitation of ribosomes from Cre^{+} cells, thereby allowing cell-type-specific detection of actively translated mRNAs (translatomes). Control (Rpl22$^{HA/+}$, GLAST$^{CreERT/+}$) and DTR (Rpl22$^{HA/+}$, GLAST$^{CreERT/+}$, Lgr5$^{DTR/+}$) mice were injected with DT and tamoxifen at P1, which caused selective ablation of Lgr5^{+} supporting cells and Cre-recombination, respectively. Cochleae were harvested at P4. RNA was extracted from both whole sensory epithelia (input) and immunoprecipitated samples (IP) to enrich for translatomes of GLAST-Cre^{+} cells.

Unsupervised clustering analysis identified stark translatomic differences between sample types (IP vs Input) and treatment groups (Control vs Damaged). In the control cochleae, we identified 147 genes that were highly enriched in the Glast Cre^{+} cells (log2 fold change ≥ 2). Many of these genes represent novel makers for the GER, which were further validated using NanoString and in situ hybridization, and in particular our newly identified stem-cell niche. To delineate damage-activated genes we compared expression between control IP and damaged IP samples and identified 603 differentially expressed genes. These genes were enriched for biological processes highly associated with cell division. Using NanoString we validated 14 of the top 19 differentially expressed genes, including known regulators of cell cycle. Moreover, qPCR found increased Mki67 mRNA levels after damage, all consistent with the observed damaged-induced proliferation.

Collectively these findings identify dramatic molecular changes in GLAST-Cre^{+} GER cells after ablation of cochlear supporting cells. These damage-activated genes are candidate mediators of regeneration by the mammalian GER.

PS 761

Mouse Embryonic Stem Cells Survive After Transplantation into Scala Media

Yozo Inagaki[1]; Diane M. Prieskorn[2]; Lisa A. Beyer[2]; Liqian Liu[1]; Yehoash Raphael[1]; R. Keith Duncan[1]
[1]Kresge Hearing Research Institute, Department of Otolaryngology-Head and Neck Surgery, University of Michigan; [2]Kresge Hearing Research Institute, Department of Otolaryngology - Head and Neck Surgery, Michigan Medicine, Ann Arbor, MI, USA

Introduction

In cochleae devoid of hair cells, the organ of Corti is reduced to flat epithelium, which does not respond to current transdifferentiation approaches for hair cell regeneration. Transplantation of stem cells followed by stepwise differentiation into new hair cells is a potential avenue for therapy in the flat epithelium. We have previously shown that HeLa cells (Park at al., 2014) and a human embryonic stem cell line (Lee at al., 2017) fail to survive when injected into endolymph, but "conditioning" the scala media by transiently reducing the levels of potassium facilitated survival of implanted cells. Here we tested the hypothesis that mouse embryonic stem cells (mESCs) are robust enough to survive in scala media without the conditioning protocol.

Methods

Eight pigmented guinea pigs were deafened with neomycin. Five days later, mESCs with a constitutive mCherry nuclear reporter were injected into scala media (4 µl suspension of about 80,000 dissociated cells infused into the 2nd turn using a syringe pump) with (N=4) or without conditioning with furosemide and sodium caprate (N=4). Because the first few hours in endolymph are critical, we assayed outcome after one day. Cochleae were harvested, fixed, and mCherry fluorescence augmented with an antibody. Stria vascularis and auditory epithelium were whole-mounted on slides for analysis by epi-fluorescence.

Results

Post-surgical recovery was faster without the conditioning. The transplanted cochleae of all 8 animals, with or without conditioning, exhibited a large number of mCherry-positive cells, mostly near the stria vascularis in the 2nd turn of the cochlea near the injection site. The organ of Corti region also contained positive cells. The cells appeared viable and many of them were in mitosis. The cells were injected as dissociated cells but once in the cochlea they tended to form aggregates, adhering to each other. Qualitative observations did not reveal differences between the two experimental groups.

Conclusions

mESCs survived in the scala media of deafened guinea pig with or without conditioning, demonstrating the conditioning is unnecessary for this type of cell. mESCs were found in the largest numbers close to the site of injection, mostly in the stria vascularis region. Multiple mitotic figures observed in the population of surviving mESCs attest to their viability. Animals that did not receive furosemide and sodium caprate recovered faster from surgery. These findings facilitate the next steps for inducing differentiation of the stem cells into desired phenotypes in the cochlea.

Support: NIDCD Grant R21-DC-016171

PS 762

Generation of Multi-ciliated Airway Cell Sheet Derived from Pluripotent Stem Cells for Middle Ear Regeneration on Temperature-responsive Polymer

Takeshi Tada[1]; Hiroe Ohnishi[2]; Fumihiko Kuwata[2]; Koichi Omori[2]; Tsunetaro Morino[3]; Yoshiyuki Kasai[3]; Hiromi Kojima[3]; Norio Yamamoto[2]
[1]Department of Otolaryngology-Head and Neck Surgery Graduate School of Medicine, Kyoto University; [2]Dept. Otolaryngology - Head and Neck Surgery, Graduate School of Medicine, Kyoto University; [3]Department of Otorhinolaryngology, Jikei University School of Medicine

Background
Middle ear mucosa is one of airway epithelium with ciliated cells. Because of its function to aerate the middle ear cavity, mucosa defect after the middle ear surgery causes postoperative complications, including cholesteatoma recurrence. Our previous report showed the effectiveness of transplanting autologous tissue-derived “nasal mucosal cell sheet” which is a different type of airway epithelium, into the middle ear to achieve early postoperative mucosal regeneration (Yamamoto K et al., 2015).

Nasal mucosal cell sheet requires the excision of nasal mucosa. To reduce this kind of burden, we plan to use human-induced pluripotent stem cell (hiPSC)- derived multi-ciliated airway cells (MCACs) instead of the autologous nasal mucosal cell sheet because iPSCs are available from any tissues in the body.

For successful transplantation of induced mucosa, it is necessary to collect the cell sheet with preserved structure. As scaffolds to achieve its stable collection, we tried induction of MCACs on culture inserts with temperature-responsive polymer, which were used for nasal mucosal cell sheet. The temperature-responsive polymer changes its structure depending on the temperature and enables the cells cultured on it to detach without destroying their structure.

In this study, we examined if this scaffold can induce MCACs efficiently by comparing with polyethylene terephthalate (PET) membranes, which showed stable differentiation efficiency of hiPSCs into MCACs (Konishi et al., 2015).

Methods
hiPSC was induced into airway epithelial cell (AEC) spheroids as previously reported (Konishi et al., 2015). The spheroids were dissociated into a single-cell suspension by enzyme treatment, seeded on temperature-responsive culture inserts or PET membrane, and performed air-liquid interface culture to generate MCAC sheets. We examined the morphology of the MCAC sheets by immunofluorescent staining and electron microscopy.

Results
Immunofluorescence staining revealed that MCAC sheets contained acetylated β-tubulin and E-cadherin positive cells in both temperature-responsive culture inserts and PET membrane groups. There was no statistically significant difference in the induction efficiencies of ciliated cells, but PET membrane group showed less variation between experiments. In the scanning electron microscopy, ciliated cells were observed in both groups. Transmission electron microscopy (TEM) showed a “9 + 2” structure, which is a specific structure in cilia, on both groups. TEM also showed no remarkable difference in basal structures of the sheets on both groups.

Conclusions
Temperature-responsive culture inserts were suitable scaffolds for hiPSC-MCACs induction. However, the induction efficiency of the PET membrane was relatively stable.

PS 763

Optimizing the Differentiation Efficacy of Multiple Human-induced Pluripotent Stem Cell Lines into Multi-ciliated Airway Cells

Yasuyuki Hayashi[1]; Hiroe Ohnishi[1]; Hideaki Okuyama[1]; Yo Kishimoto[1]; Masayoshi Yoshimatsu[1]; Fumihiko Kuwata[1]; Ryosuke Nakamura[1]; Tatsuo Nakamura[2]; Shimpei Gotoh[3]; Toshiaki Takezawa[4]; Koichi Omori[1]
[1]Dept. Otolaryngology - Head and Neck Surgery, Graduate School of Medicine, Kyoto University; [2]Institute for Frontier Life and Medical Sciences, Kyoto University; [3]Dept. Drug Discovery for Lung Diseases, Graduate School of Medicine, Kyoto University; [4]Institute of Agrobiological Sciences, National Agriculture and Food Research Organization

Background
Airway epithelial cells play important roles in respiratory immunity via muco-ciliary clearance organized by multi-ciliated airway cells (MCACs) and secretory cells, and the lack of MCACs can cause infection, inflammation and mucous plugging in the airway. We have developed an artificial graft and used it for clinical tracheal reconstruction after tracheal resection. However, it takes a long time for the complete epithelialization of the luminal surface of the grafts. The delayed epithelialization can raise the risk of post-operative

infection. Therefore, the quick epithelialization of the grafts is essential to reduce post-operative complications. Recently, we have confirmed the successful engraftments of human-induced pluripotent stem cell derived MCACs (hiPSC-MCACs) utilizing atelocollagen vitrigel membrane and artificial trachea into the tracheal defects of immuno-deficient rats. That has suggested hiPSC-MCACs might be useful candidates to promote the quick epithelialization of the grafts. However, a great number of hiPSC lines have been generated, and each cell lines have their own propensities to preferentially differentiate towards specific phenotypes. Understanding characteristics of cell lines will be immensely valuable in the selection of the appropriate cell line for clinical application.

Objective
The aim of this study was to show the differentiation capacity of various hiPSC lines into MCACs, and to optimize the differentiation protocols.

Method
To optimize MCACs induction method for each hiPSC line, hiPSCs were supplemented with different concentration of retinoic acid (RA) and glycogen synthase kinase 3β (GSK3β) inhibitor. The induction efficiency into the ventralized anterior foregut endoderm cells (VAFECs), which are progenitor cells of MCACs, was quantified by counting the number of NKX2-1 expressing cells. Further, the histological and morphological features of induced MCACs were investigated.

Result
The optimal concentrations of RA and GSK3β inhibitor were determined for three hiPSC lines. The induced MCACs expressed the airway cell markers and showed the cilia-like structures in their apical surface.

Conclusion
We succeeded in inducing the MCACs from multiple hiPSC lines, and also established the optimal induction protocols for each hiPSC.

PS 764

Examination of high expression conditions of Connexin 26 in 3D culture of ES cells for generation of inner ear cells

Ichiro Fukunaga[1]; Cheng Chen[2]; keiko kanayama[2]; yoko oe[2]; Sayaka Ohta[2]; Katsuhisa Ikeda[3]; Kazusaku Kamiya[4]
[1]Juntendo university; [2]Department of Otorhinolaryngology, Juntendo University Faculty of Medicine,; [3]Juntendo University Faculty of Medicine; [4]Department of Otolaryngology, Juntendo University School of Medicine

Introduction
Mutation of the Gap Junction Beta 2 gene (GJB2) encoding connexin 26 (CX26) is the most frequent cause of hereditary deafness worldwide. We have recently reported that induced pluripotent stem cells (iPSCs)-derived functional CX26-GJP-forming cells (CX26GJCs), as found in the cochlear supporting cells, using 3D and 2D culture combination (Fukunaga et al., Stem Cell Reports, 2016). Furthermore, we previously suggested that CX26 expressing vesicles formed in day 7 aggregate are the origin of CX26-GJP-forming cells in the 2D culture. However, to use these cells as a disease model for drug screening or other large-scale assays, the cell culture system must be improved to increase the number of cells available at a single time. In this study, we examined the conditions for producing a large amount of CX26GJCs.

Method
We examined conditions to induce CX26-GJP forming cells from ESCs using our previous protocol (Fukunaga et al., 2016).

Results
Under a specific inhibitor treatment in 3D culture, mRNA expression levels of CX26 (*GJB2*)/CX30 (*GJB6*) and the number of CX26 positive vesicles were increased compared with previous study. Furthermore, we found that CX26 positive vesicles which is the origin of CX26GJCs were increased by the inhibitor supplementation in a dose-dependent manner. After transferring the CX26+ vesicles onto cochlear feeder cells, the lengths of the GJPs of the proliferated CX26-expressing cells were increased and the GJPs were observed to contain CX26/CX30. In addition, the number of colonies containing CX26GJCs increased in the 2D culture due to the dose-dependent increase in CX26 small vesicles in the 3D culture. By controlling the 3D culture conditions, large-scale production of highly purified CX26GJCs suitable for high-throughput drug screening or regenerative therapy for GJB2-related deafness may be possible.

PS 765

Selective and super-selective induction of cochlear hair cells from human iPS cells

Tsubasa Saeki[1]; Makoto Hosoya[2]; Masato Fujioka[3]; Kaoru Ogawa[3]; Hideyuki Okano[1]
[1]Department of Physiology, School of Medicine, Keio University; [2]Department of Otolaryngology-Head and Neck Surgery, School of Medicine, Keio University; [3]Department of Otolaryngology, Head and Neck Surgery, School of Medicine, Keio University

Loss of hair cells in mammalian cochlea is irreversible once injured and results in permanent sensorineural

hearing loss. Induction of hair cells from human induced pluripotent stem cells (hiPSCs) may provide platforms for disease modeling, eventually to therapeutics by drug screenings. Since reliable and robust induction method is indispensable for the biomedical application, improving method for better induction efficiency and maturity of the induced hair cells is of great value. In this study, we developed a novel strategy for differentiation of hiPSCs into cochlear hair cell linage by using several candidate compounds.

Firstly, we differentiated hiPSCs to otic progenitor cells with high efficiency using a previously reported method (Hosoya et al., 2017). Immunocytochemistry and qRT-PCR showed that otic progenitor cells expressed early otic progenitor markers, including PAX2, PAX8 and SOX2. When we treated the induced otic progenitor cells with two liquid factors, we observed upregulation of otic progenitor markers, *PAX2, PAX8* and prosensory domain marker,*LGR5*. Next, we examined the effects of compounds whether these can facilitate the induction of cochlear inner or outer hair cells from hiPSCs derived otic progenitors. Treatment of cells with compound A promoted upregulation of various hair cell markers including *ATOH1, MYO7A, MYO15A* by qRT-PCR analysis. Immunocytochemistry revealed that the induced hair cell-like cells expressed hair cell markers, MYO7A and BRN3C. Moreover, compound G significantly upregulated the expression levels of cochlear outer hair cell marker, *PRESTIN*. On the other hand, we did not detect increased expression of cochlear inner hair cell marker, *vGLUT3* by compound treatment.

We found novel drugs that promote differentiation of hiPSCs derived otic progenitor cells into cochlear hair cell linage. We will further refine induction protocol in its efficacy in hair cell differentiation and examine culture conditions to differentiate into mature cochlear hair cells.

Acknowledgement
This study was supported by Kyowa Hakko Kirin Co., Ltd.

PS 766

Identification of Mouse Auditory Cortex-Derived Neural Stem Cells

Zhengqing Hu; Li Tao
Wayne State University

Auditory signals are transmitted from the cochlea to the central nervous system. Development of stem cell biology generates the opportunity to identify neural stem cells (NSCs) in the auditory system. We have reported the existence of NSCs in postnatal day 3 (P3) mouse auditory cortex (AC). However, it is unclear whether NSCs exist in late postnatal and adult stages when the brain becomes mature. The aim of this study is to determine whether NSCs exist in adult mouse brain AC.

P3, P14, and 2-month-old mouse AC tissues were cryosectioned and immunostained with NSC markers. Additionally, AC tissues were identified and dissociated into singular cells and small cell clumps, which were cultured in the suspension culture medium to observe neurosphere formation. The spheres were examined by immunofluorescence to determine the expression of NSC proteins.

The results show that the AC tissues of P3, P14, and 2-month-old mice are immunostained by NSC markers SOX2 and NESTIN. In the quantitative study, the number of SOX2/NESTIN double-expressing cells is significantly reduced during maturation, from approximately 12% at P3, 7% at P14, and less than 2% at 2-month-old, suggesting that the number of NSCs decreases with age. In the cell culture, P3 and P14 AC tissues can proliferate to form neurospheres for at least three passages, whereas 2-month-old mouse AC cells rarely form neurospheres. EdU incorporation study shows that approximately 32% of cells of the P3 group incorporate EdU, whereas the number becomes ~9% in the P14 group. The neurospheres express multiple NSC proteins, including SOX2 and NESTIN. The number of SOX2/NESTIN double-expressing cells decreases with age, approximately 82% in the P3 group and ~41% in the P14 group.

These results suggest that AC-NSCs exist in the mouse AC area in the postnatal mouse. The number and the proliferation ability of AC-NSCs reduce with age. Identifying AC-NSCs will be important for auditory research and other central nervous systems.

Tinnitus

PS 767

Safety and Efficacy of Combined Sound and Trigeminal Nerve (Tongue) Stimulation to Treat Tinnitus: Effects of Different Stimulation Settings over Time

Hubert H. Lim[1]; Caroline Hamilton[2]; Stephen Hughes[2]; Emma Meade[3]; Martin Schecklmann[4]; Thavakumar Subramaniam[5]; Sven Vanneste[6]; Deborah Hall[7]; Berthold Langguth[4]; Brendan Conlon[8]
[1]University of Minnesota, Minneapolis, USA; [2]Neuromod Devices Limited; [3]Neuormod Devices Limited; [4]University of Regensburg; [5]St. James's Hospital/Trinity College Dublin; [6]The University of Texas at Dallas, and Trinity College Dublin; [7]University

of Nottingham; [8]St. James's Hospital/Trinity College Dublin, and Neuromod Devices Limited

Tinnitus affects 10-15% of the population. Unfortunately, there are limited treatment options. Recent animal and pilot human research has demonstrated the ability to drive extensive auditory plasticity and potentially treat tinnitus by pairing sound with trigeminal or somatosensory nerve activation, such as with tongue stimulation. A non-invasive device (Lenire) using auditory and tongue (bimodal) stimulation was evaluated in two large randomized and blinded clinical trials in over 500 participants with tinnitus in Ireland and Germany. The first study (TENT-A1) investigated three stimulation settings (PS1, PS2, PS3) presented for 12 weeks (60 minutes recommended per day) and evaluated during treatment and up to 12 months post-treatment (326 enrolled participants). Primary outcome measures included the Tinnitus Handicap Inventory (THI) and Tinnitus Functional Index (TFI). The second study (TENT-A2) investigated different stimulation settings over time across four treatment arms (191 enrolled participants). The first treatment arm consisted of the most effective stimulation setting from TENT-A1 during the first 6-weeks (PS1) followed by a new bimodal stimulation setting during the second 6-weeks (PS4). The second and third arms consisted of different bimodal settings than the first arm, while the fourth arm consisted of an acoustic only condition during the first 6-weeks followed by a bimodal condition during the second 6-weeks. All three stimulation settings in TENT-A1 resulted in statistically significant improvements in tinnitus for THI ($p < 0.0001$) and TFI ($p < 0.0001$) that were also clinically significant (>7 THI points, >13 TFI points). Post-treatment, PS1 resulted in persistent improvements lasting 12 months after treatment ceased ($p < 0.0001$). The treatment was safe and well-tolerated with a high compliance rate (84%; >36 hours of usage). The largest therapeutic effects occurred within the first 6-weeks. In TENT-A2, similar results were observed for PS1 during the first 6-weeks as in TENT-A1. Changing the stimulation setting from PS1 to PS4 led to a greater improvement ($p < 0.001$) than observed in TENT-A1 that also persisted for 12 months post-treatment, as well as reaching a higher compliance rate of 91%. Post-hoc analyses showed that different bimodal stimulation settings over time could be as effective as the PS1-to-PS4 condition and that specific bimodal stimuli consistently outperformed the acoustic only condition for both THI and TFI. Overall, these findings demonstrate that the Lenire treatment provides safe, fast-acting (within 6 weeks) and reproducible therapeutic effects that can last at least 12 months. Furthermore, adjusting the stimulation settings over time can drive greater therapeutic effects.

PS 768

Context-Dependent Auditory Processing in Individuals with Tinnitus

Nike Gnanateja Gurindapalli[1]; Bharath Chandrasekaran[2]
[1]Department of Communication Sciences and Disorders, University of Pittsburgh; [2]Department of Communication Sciences and Disorders, School of Health and Rehabilitation Sciences, University of Pittsburgh

In the current study, we evaluated the context-dependent auditory processing in individuals with tinnitus having normal audiograms (T-NA). Tinnitus is a condition associated with an imbalance between the sub-cortical and cortical processing mechanisms. Even though there is a vast amount of literature on tinnitus, only a few studies have explored the sub-cortical auditory processing deficits in individuals with tinnitus and normal audiograms (T-NA). The observed sub-cortical deficits could be present due to a peripheral or a central deficit. However, the findings across studies are equivocal. Human auditory processing is highly context-dependent, and this has been extensively researched at the cortical level. Context-dependent effects have been evidenced even at the brainstem using frequency-following responses (FFRs). The predictive-tuning framework (Chandrasekaran et al., 2014) suggests that repetitive stimulus presentation invokes corticofugal activity, which fine-tunes sub-cortical encoding based on ongoing stimulus statistics and context. We speculate that in studies showing normal sub-cortical auditory processing using conventional FFRs, there might be an increased contextual effect due to aberrant homeostatic plasticity, which in turn obscured underlying sub-cortical processing deficits. Using an innovative approach and application of the predictive-tuning framework, we aim to disentangle sensory and context-dependent encoding in T-NA. We expected to observe increased contextual effect and an underlying sub-cortical processing deficit in T-NA. We used the context-dependent FFRs to evaluate sub-cortical auditory processing in T-NA and in a control group without tinnitus (NA). We recorded FFRs to a harmonic complex (26-50th harmonics) with a fundamental frequency (F0) of 128 Hz. The FFRs to this stimulus were recorded with the same stimulus presented repetitively (repetitive paradigm), and in the context of harmonic complexes (variable paradigm) that varied in pitch and presented at an occurrence ratio of 1(target):4(context). Additionally, in a separate analysis, we also used a large battery of sensitive tests of peripheral auditory processing to supplement the results. The repetitive paradigm resulted in higher FFR amplitudes at F0 in the repetitive than the variable paradigm in both the groups. The FFR amplitudes at F0 were comparable between both the groups in the repetitive paradigm. However, in

the variable paradigm, T-NA showed smaller amplitudes than NA. Consequently, the contextual effect (Repetitive-Variable) was higher in the T-NA than in NA. This finding results in two important inferences; 1) sensory encoding at the brainstem (contextual paradigm) is affected in T-NA, 2) increased context effect presumably reflects the homeostatic compensatory plasticity in T-NA.

PS 769

A Study of the Pan-European Prevalence of Tinnitus and Hearing Difficulty using a Standardized Set of Questions

Roshni Biswas[1]; Alessandra Lugo[2]; Deborah A. Hall[3]; Michael Akeroyd[4]; Xiaoqiu Liu[2]; Winfried Schlee[5]; Silvano Gallus[2]
[1]University of Nottingham, UK / IRCCS- Istituto di Ricerche Farmacologiche "Mario Negri", Italy; [2]IRCCS-Istituto di Ricerche Farmacologiche "Mario Negri", Italy; [3]University of Nottingham Malaysia; [4]University of Nottingham; [5]University of Regensburg, Germany

Epidemiological studies on tinnitus report large variability. Prevalence estimates range between 5% and 43% for any tinnitus, and between 1% and 40% for severe tinnitus. Although hearing difficulty is known to be the most important risk factor for tinnitus, little information is available on the comorbidity. Our objective was to estimate the Pan-European prevalence of any and severe tinnitus, assess tinnitus-related healthcare resource use, and explore the relationship between tinnitus and hearing difficulty.

Between 2017-2018, a computer assisted personal interview survey was conducted in 12 European Union Member States (Bulgaria, England, France, Germany, Greece, Ireland, Italy, Latvia, Poland, Portugal, Romania and Spain). For this, a set of questions and response options from existing tinnitus survey questionnaires in English were adapted and translated to 11 European languages. Care was taken to ensure that the translations matched. For each country, around 1000 adults (aged ≥18 years) were recruited, representative of the general population in terms of sex, age, socio-economic characteristics and habitat. In total, 11427 subjects (5404 men and 6023 women) were enrolled.

Overall prevalence of any tinnitus was 14.7% (ranging from 8.7% in Ireland to 28.3% in Bulgaria), with similar results in men (14.1%) and women (15.2%; p=0.086). Severe tinnitus was found in 1% participants (ranging from 0.6% in Ireland to 4.2% in Romania), with higher prevalence in women (1.4%) compared to men (1.0%; p=0.034). The overall percentage of individuals reporting at least one clinical visit for tinnitus was 6.8%, with 5.7% in men and 7.5% in women (p< 0.001). Prevalence of hearing difficulty was 19.9% overall with 19.2% in men and 19.7% in women (p=0.351). Prevalence of tinnitus significantly increased with increase in age (p for tends < 0.001), and worsening of hearing status (p for trends < 0.001).

Our study is the first multinational report of Pan-European tinnitus prevalence using standardized questions. The overall prevalence numbers refine previous estimates, though we did observe widespread heterogeneity across countries. From the variability in estimates of "any", "bothersome", and "severe" tinnitus, we can conclude that the actual phrasing of questions and response options are important contributors to the prevalence estimates. Once generalized to the overall European Union population, our results indicate that 75 million, that is more than 1 in 7 adults suffer from tinnitus.

Acknowledgements
This project has received funding from the European Union's Horizon 2020 research and innovation program under the Marie Sklodowska-Curie grant agreement number 722046.

PS 770

Identification of functional biomarkers of tinnitus and tinnitus/hyperacusis in patients

Benedikt Hofmeier[1]; Fatma Refat[2]; Pauline Hinrichs[1]; Marlies Knipper[3]; Lukas Rüttiger[4]; Uwe Klose[5]; Stephan Wolpert[1]
[1]Tübingen University, Department of Otolaryngology, Head and Neck Surgery; [2]Minia University Department of ENT, Audiovestibular Unit; [3]University of Tübingen, Department of Otolaryngology, Head and Neck Surgery Tuebingen; [4]University of Tübingen, Department of Otolaryngology, Head and Neck Surgery Tübingen; [5]Tübingen University, Department of Diagnostic and Interventional Neuroradiology

Tinnitus is as a symptomatic malfunction of our hearing system, where phantom sounds are perceived without acoustic stimulation.

In recent years, we have developed a fingerprint for tinnitus and recently hyperacusis using a combination of behavior animal models for tinnitus/hyperacusis and electrophysiological as well as molecular approaches for the characterization of the peripheral and central auditory system. The characteristic features that distinguished equally hearing impaired animals with and without tinnitus or hyperacusis are described (Möhrle et al., 2019, Hofmeier et al., 2018, Knipper et al 2013; Rüttiger et al 2013, Singer et al 2013). Here, we aimed

to test our hypotheses for patients with tinnitus only and patients with tinnitus and co-occurrence of hyperacusis.

We present a clinical pilot study in hearing-impaired subjects. We use questionnaires, audiometric measurements, the analysis of body fluids, and functional magnetic resonance tomography (fMRI) analyzing evoked BOLD fMRI and resting state r-fcMRI.

The results in defined patient groups are discussed in the context of previous findings gained in animals.

This work was supported by the Deutsche Forschungsgemeinschaft DFG KN 316/10-1; RU 713/3-2 (FOR 2060; RU 316/12-1, KN 316/12-1 (SPP 1608); KN 316/13-1; KL1093/12-1.

PS 771

Mapping the Cortical Tinnitus Network Using Acoustically- and Electrically-induced Suppression

Phillip Gander[1]; William Sedley[2]; Sukhbinder Kumar[2]; Hiroyuki Oya[1]; Christopher Kovach[1]; Kirill Nourski[1]; Hiroto Kawasaki[1]; Matthew Howard[1]; Timothy Griffiths[2]
[1]University of Iowa; [2]Newcastle University

Tinnitus occurs when peripheral hearing damage leads to secondary changes in ongoing brain activity. These central mechanisms are poorly-understood, partly because relevant experimental evidence is almost entirely indirect, meaning it does not reflect the real-time perception of tinnitus, and/or it does not provide a direct measure of neural activity.

Previously we reported on a test of this hypothesis in a human neurosurgical subject, who had an extensive array of electrocorticography and depth electrodes placed for the localization of epilepsy. Tinnitus loudness was modulated with residual inhibition using noise, and quantified with real-time ratings. Here we report an experimental replication in a second neurosurgical subject with broadly comparable tinnitus and intracranial recording.

Similar findings in both subjects were obtained: 1) Suppression of tinnitus correlated with widespread reductions in delta (1-4 Hz) oscillatory power throughout most of auditory cortex, and large parts of non-auditory cortex in temporal, parietal, limbic and motor areas. These areas also showed changes in inter-regional delta phase coherence with tinnitus suppression. 2) Theta (4-8 Hz), alpha (8-12 Hz), and high beta (20-28 Hz) power was similarly suppressed in most of these areas. 3) Gamma (28-144 Hz) power increased, during tinnitus suppression, throughout auditory cortex and in posterior temporal, inferior parietal, sensorimotor and parahippocampal cortex. In the second subject electrical stimulation of Heschl's gyrus elicited reductions in tinnitus loudness comparable to that induced by sound. The change in tinnitus perception from stimulation occurred without alteration to other external auditory perception.

These findings support the definition of the brain networks critically involved in tinnitus perception which will be necessary to create effective treatments and possible cures.

PS 772

Random Forest Classification to Predict Response to High-Definition Transcranial Direct Current Stimulation Therapy for Tinnitus

Emilie Cardon; Laure Jacquemin; Griet Mertens; Paul Van de Heyning; Olivier M. Vanderveken; Vedat Topsakal; Vincent Van Rompaey; Annick Gilles
University of Antwerp, Antwerp University Hospital

Tinnitus, the perception of sound in the absence of an external sound source, has a worldwide prevalence of 10-20%. Noninvasive brain stimulation techniques such as transcranial direct current stimulation (tDCS) are hypothesized to reduce tinnitus severity by modifying cortical hyperactivity in brain regions associated with tinnitus perception. However, the response to tDCS treatment in individual tinnitus patients has proven to be extremely variable, with a significant number of patients reporting a lack of tinnitus improvement after treatment. We employed random forest (RF) classification, a supervised machine learning approach, to predict individual treatment response in a large cohort of chronic subjective tinnitus patients.

Ninety-nine tinnitus patients received six biweekly sessions of high-definition transcranial direct current stimulation (HD-tDCS) of the right dorsolateral prefrontal cortex. Before treatment and at a three-month follow-up time point, patients were asked to fill in a set of questionnaires, including the Tinnitus Functional Index (TFI), a Visual Analogue Scale (VAS) to assess tinnitus loudness, and the Hospital Anxiety and Depression Scale (HADS). The Edinburgh Handedness Inventory (EHI) was used to assess handedness. Positive response to treatment was defined as a reduction of at least 10 points on the TFI. RF classification with five-fold cross-validation was applied to predict whether an individual responded positively to the treatment. The RF classifier was based on questionnaire scores at the pre-treatment visit. Additional validation was performed on an external dataset from an independent tinnitus treatment center.

Thirty out of 99 patients responded successfully to the HD-tDCS treatment. The RF classifier predicted treatment response with a balanced accuracy of 87.05% and an area under the curve of 0.864 in patients that were new to the model. This corresponded to a sensitivity of 76.54% and a specificity of 92.99%. Feature importance analysis revealed that patients with higher TFI, VAS and HADS depression scores and negative EHI scores, corresponding to left-handedness, were more likely to respond positively to HD-tDCS treatment.

In conclusion, individual response to HD-tDCS treatment may be accurately predicted using easily obtainable questionnaire data. Patients with higher tinnitus burden, concurrent depressive symptoms and/or a preference of the left over the right hand may respond more positively to HD-tDCS of the right dorsolateral prefrontal cortex. Although larger studies are necessary to validate the proposed random forest classifier, our results might provide the basis for better and more personalized guidance towards the right treatment for chronic tinnitus patients.

PS 773

Tinnitus Does Not Impair Auditory Perception

Fan-Gang Zeng[1]; Matthew L Richardson[2]; Katie Turner[1]
[1]University of California Irvine; [2]University of California

Despite extensive research in tinnitus characterization and masking, few have studied perceptual consequences of tinnitus, resulting in unsubstantiated claims such as tinnitus filling in the gap or impairing speech perception. Here we present systematic psychophysical results from gap detection to discrimination of intensity and frequency as well as tone-in-noise detection, temporal modulation detection and speech perception in noise. A unique feature of the present study was that the stimulus intensity and frequency were matched to tinnitus loudness and pitch on an individual basis in the gap detection, frequency and intensity discrimination experiments. We also controlled the hearing loss factor by presenting stimuli either at a frequency where hearing threshold was normal or at an equal sensation level or the most comfortable level at frequencies where the threshold was elevated. Finally, we compared the performance by a heterogenous group of tinnitus subjects (n=31) against the gold standard from a homogenous group of young, normal-hearing, non-tinnitus subjects (n=17). Surprisingly, tinnitus subjects produced equal, or sometimes even slightly better performance than the gold control under these tightly controlled conditions. We propose that different from the bottom-up auditory perception of external sounds, tinnitus reflects a top-down perceptual filling-in process. These different perceptual processes are responsible for the present negative effect of tinnitus on external sounds. The present result further suggests that the hearing difficulty in tinnitus sufferers is not due to tinnitus per se, but rather due to their co-morbid conditions and secondary effects.

PS 774

Hearing Protection Use, Noise Exposure, and Tinnitus in US Adolescents and Adults: A Nationally Representative Study

Janet S. Choi; Joni K. Doherty
University of Southern California

Background
Despite the known negative impact of noise exposure on hearing health and the diversification of noise exposure sources in the US, hearing protection use has not been well-promoted. We investigated the rates of regular hearing protection use in relation to noise exposure, tinnitus, and audiometry-measured hearing loss in US. Factors associated with regular hearing protection use were explored in this first comprehensive analysis of regular hearing protection use in a nationally representative sample.

Methods
We analyzed data from the 2007-2012 National Health and Nutritional Examination Survey during which participants aged ≥12 years completed a questionnaire on hearing protection use and noise exposure (n=10,405). Regular hearing protection use was defined as reporting hearing protection device use at least about half the time, usually or always in the past 12 months. A full audiometric evaluation was available in a subgroup of participants (n=9,108). High-frequency hearing loss was defined as pure-tone average (PTA) ≥25dB in worse hearing ear at 3, 4, 6, and 8 kHz. Logistic regression was used to examine the association between hearing protection use and relevant factors. Analysis incorporated sampling weights to yield results that are generalizable to the US population.

Results
Overall, the rates of regular hearing protection use were 23.9% [95% CI: 21.0-26.7%] in US: rates were lower among adolescent aged 12-18 years at 15.6% [95% CI: 12.7-18.4%] and among older adults aged ≥65 years at 14.7% [95% CI: 11.7-17.6%]. The rates were 37.6% [95%CI: 32.4-42.8%] and 24.6% [95% CI: 20.3-29.0%] among adults reporting significant work-related noise exposure and off-work noise exposure, respectively. Adults who reported having tinnitus in the past year was more likely to report regular hearing protection use

(OR: 1.2 [95% CI: 1.05-1.35]). There was no significant association between hearing protection use and audiometry-measured high-frequency hearing loss. In a multivariate model, regular hearing protection use was significantly associated with a younger age, being male, being white, and having a higher socioeconomic status.

Conclusion

The rates of regular hearing protection use remain low in the US, especially among adolescents and older adults. Despite the Occupational Safety and Health Administration requirement, the regular hearing protection use is less than 50% among those with significant occupational noise exposure. Our findings warrant future studies to understand the barriers to hearing protection use and explore ways to promote hearing protection use in occupational and recreational settings.

Vestibular Orientation

PS 775

Timing Effects on Visual-Vestibular Heading Perception in Normal Subjects

Raul Rodriguez
University of Rochester

Persistent dizziness symptoms result from conflicting visual and inertial sensory stimuli. The mismatch between visual and inertial stimuli has been studied with respect to angular differences, but not in regards to timing conflicts. This study explores the effects of asynchronous presentations of visual and inertial stimuli on inertial heading perception. Experiments were conducted with varying offsets between visual and inertial heading stimuli. The experiments were initially divided into nine blocks, each block corresponding to a visual stimulus timing delay, each inertial and visual stimulus combination was presented twice. The timing delays tested were: -500, -250, -150, -100, 0, 100, 150, 250, 500 ms (e.g., at -500 ms, the visual stimulus was presented first, then 500 ms later, the inertial stimulus was presented). The range of inertial heading directions was ±140° in 35° increments and a visual stimulus range of ±120° in 30° increments relative to inertial heading. Inertial headings were reported by orienting a dial in the perceived direction. Four subjects have completed the initial set of conditions. The decrease in visual influence before and after the zero millisecond delay led to adding -50, -25, 25, and 50 ms, and the increased variability at 500ms led to adding the 1000 and 2000 ms conditions. Two of the subjects that have completed the initial conditions have also completed the additional conditions. Visual offsets at opposite angle were reflected and combined (e.g. -30° was combined with 30° visual offset). As the offsets become larger, the difference between the zero millisecond response and the surrounding timing delays become statistically significant. At 0° and 30° offsets, there is no statistical difference between a zero millisecond delay and a 150 millisecond delay. However, at 60°, 90°, and 120° offsets, there is a statistically significant difference ($p < 0.05$; ANOVA; Bonferroni). A similar effect was found between the zero millisecond delay and the 25 ms delay at those offsets (i.e. 0°, 30° not statistically significant $p < 0.05$; ANOVA; Bonferroni; and 60° and 90° being statistically significantly different $p < 0.05$; ANOVA; Bonferroni). Timing appears to have an effect the strength of the visual stimulus influence on inertial heading perception.

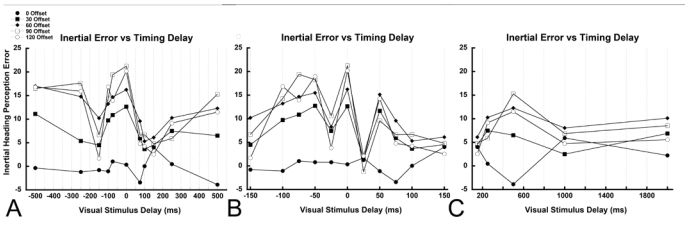

PS 776

Comparison of Spatial Navigation in Real-World vs. Virtual Reality Environments in Healthy Adults

Elliott Rebello[1]; Eric Wei[1]; Dara Bakar[2]; Qiliang He[3]; Timothy McNamara[3]; Yuri Agrawal[1]
[1]Johns Hopkins University School of Medicine; [2]Warren Alpert Medical School of Brown University; [3]Vanderbilt University

Background

Spatial navigation is a complex behavior that is critical for survival. Spatial navigation is thought to occur via place-based (allocentric) navigation, whereby individuals navigate based on a mental representation of the environment that is separate from the individual or route-based (egocentric) navigation, whereby individuals navigate via a learned sequence of movements. In this study, we compared allocentric versus egocentric navigation in real-world and virtual reality environments.

Methods

20 healthy adults were recruited. Subjects were shown a route in a real-world environment and a virtual rendering of that environment. Subjects were then tasked with both reproducing the route and navigating to the endpoint via the shortest possible path. For these tasks, the efficiency and accuracy of navigated paths were determined by the number of turns taken and distance travelled. The accuracy of subjects' cognitive maps was further evaluated by Judgment of Relative Direction (JRD). The Santa Barbara Sense of Direction (SBSOD), a 15-item questionnaire assessing subjective spatial navigation ability was also administered.

Results

The average age of the participants was 23.7 (1.1) and 13 were female. The average SBSOD score was 4.6 (1.1). Participants made significantly fewer mean turns on the place-based task (Real 1.3, SD 0.1; VR 1.4, SD 0.8) than the route-based task (Real 3.6, SD 1.4; VR 3.3, SD 0.6). No significant difference was found between distance ratios for either navigation task in either environment. Moreover, mean JRD errors were significantly greater in the VR setting (66°) than in the real world setting (50°; p = 0.0091). Real-world JRD performance was significantly associated with mean SBSOD score (-10.7°; p=0.004) and with SBSOD Question #4, "My sense of direction is very good" (-7.5°; p=0.003).

Conclusions

In this study of healthy adults, we found that participants performed significantly better on the real-world JRD task compared to the VR JRD, suggesting that the availability of body-based cues from self-motion in the real world may play a critical role in navigation performance. Moreover, the association between the real-world JRD and the SBSOD suggests that the real-world JRD task may most closely resemble allocentric navigation tasks that are faced in daily life, and as such may better reflect an individual's perception and experience of their navigation ability than VR settings. These data provide a foundation for comparing navigation ability in real-world vs. VR environments in other populations including older individuals and those with vestibular loss.

Table 1: Summary of experiments

Real world	Virtual reality
Route-based navigation (*Route 1, 2*)	Route-based navigation (*Route 1, 2*)
Place-based navigation (*Route 1, 2*)	Place-based navigation (*Route 1, 2*)
Judgments of relative direction (*Routes 1 & 2*)	Judgments of relative direction (*Routes 1 & 2*)

Table 2: Subjective and objective measures of spatial navigation ability by gender

	Males (N=7)	Females (N=13)	p-value
SBSOD	4.3 (2.5, 5.6)	4.6 (3.0, 6.3)	0.5654
JRD			
Real world	55 (23, 88)	47 (21, 76)	0.3856
Virtual reality	63 (23, 89)	67 (42, 98)	0.5769
Place-based			
# turns			
Real world	2.0 (2.0, 2.0)	2.7 (2.0, 5.0)	0.0966
Virtual reality	2.4 (2.0, 5.0)	3.0 (2.0, 7.0)	0.4543
Route-based			
# turns			
Real world	6.4 (6.0, 9.0)	7.5 (6.0, 18)	0.4476
Virtual reality	6.4 (6.0, 9.0)	6.7 (6.0, 9.0)	0.6601

Table 3: Comparison of performance on route-based vs place-based navigation

	Route-based	Place-based	p-value
# turns			
Real world	7.1 (6.0,18)	2.5 (2.0,5.0)	<0.0001
Virtual reality	6.6 (6.0,9.0)	2.8 (2.0,7.0)	<0.0001

Table 4: Comparison of performance on real-world vs virtual reality-based navigation

	Real-world	VR	p-value
JRD error (°)	50 (21,88)	66 (23,98)	0.0091
# turns			
Route-based	7.1 (6.0,18)	6.6 (6.0,9.0)	0.4703
Place-based	2.5 (2.0,5.0)	2.8 (2.0,7.0)	0.3922

Table 5: SBSOD as a predictor of spatial navigation performance: multivariate regression analysis

	SBSOD	
	β-coefficient	p-value
JRD		
Real world	-10.7	0.004
Virtual reality	-1.1	0.775
Place-based		
# turns		
Real world	0.1065	0.245
Virtual reality	-0.2089	-0.227
Route-based		
# turns		
Real world	-0.1539	0.624
Virtual reality	-0.0752	0.589

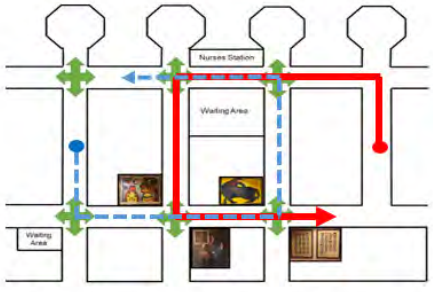

Figure 1. Otolaryngology Clinic real-world environment. Green arrows depict 4-way intersections, pictures are example hallway landmarks. The two routes (Route 1, 2) are shown in red (solid line) and blue (dotted line), with the circles denoting the starting point of each route.

Figure 2. Screenshot of virtual reality environment, with sample landmarks on the walls.

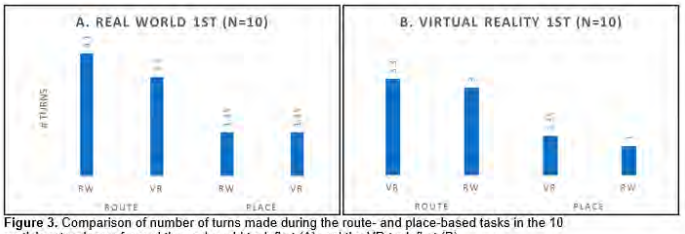

Figure 3. Comparison of number of turns made during the route- and place-based tasks in the 10 participants who performed the real-world task first (A) and the VR task first (B).

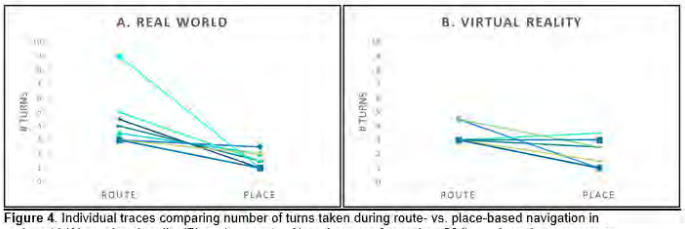

Figure 4. Individual traces comparing number of turns taken during route- vs. place-based navigation in real-world (A) vs. virtual reality (B) environments. Note there are fewer than 20 lines given that numerous individuals had the same trace.

PS 777

Impaired Spatial Cognition in Bilateral Vestibulopathy is related to Hearing Loss.

Bieke Dobbels[1]; Griet Mertens[2]; Annick Gilles[2]; Julie Moyaert[3]; Raymond Van de Berg[4]; Erik Fransen[1]; Paul Van de Heyning[2]; **Vincent Van Rompaey**[2]
[1]University of Antwerp; [2]University of Antwerp, Antwerp University Hospital; [3]Antwerp University Hospital; [4]Maastricht University Medical Center, Tomsk State University

Background
Previous studies have demonstrated spatial cognitive deficits in patients with bilateral vestibulopathy (BVP). However, BVP patients frequently present with a concomitant sensorineural hearing loss, which is a well-established risk factor of cognitive impairment and incident dementia. Nonetheless, previous research on spatial cognitive deficits in BVP patients have not taken hearing status into account. The objective of this study was to compare spatial cognition in BVP patients to healthy controls, with analyses adjusting for hearing status.

Methods
Spatial cognition was assessed in 64 BVP patients and 46 healthy controls (HC) by use of the Virtual Morris Water Task (VMWT). All statistical analyses were adjusted for hearing (dys)function, sex, age, education and computer use.

Results
Overall, patients with BVP performed worse on all outcome measures of the VMWT. However, these differences between BVP patients and healthy controls were not statistically significant. Nonetheless, a statistically significant correlation between sensorineural hearing loss and spatial cognition was observed. The worse the hearing, the longer subjects took to reach the hidden platform in the VMWT. Furthermore, the worse the hearing, less time was spent by the subjects in the correct platform quadrant during the probe trial of the VMWT.

Conclusion
In this study, no difference was found in spatial cognition between BVP patients and healthy controls. However, a statistically significant correlation was observed between sensorineural hearing loss and spatial cognition.

PS 778

Effect of Visual Target Ambiguity on the Semicircular Ocular Reflex

Yumiko 0. Kato[1]; Koshi Mikami[1]; Shuichi Sakamoto[2]; Izumi Koizuka[1]
[1]St. Marianna University School of Medicine; [2]Research Institute of Electrical Communication, Tohoku University

To estimate the effect of multi-modal vestibular rehabilitation, we are attempting to integrate modalities in location perception using the semicircular ocular reflex (ScOR).

Seven healthy adults participated in the present study. Horizontal eye movements were recorded by video-oculography under three conditions (Fig. 1). In the earth fixed (EF) condition, the absolute position of the visual target was fixed. In the head fixed (HF) condition, the visual target was rotated in same direction to head rotation. In the pursuit (P) condition, the visual target was rotated sinusoidally without head rotation. We used a six-pattern visual target with three levels of blurriness and two levels of brightness (Fig. 2). The chair the participants were sitting on was rotated on the yaw-axis sinusoidally at 0.32 Hz at an amplitude of 20 degrees. For the control, we observed the ScOR in complete darkness at the same frequency and amplitude. The ScOR gain under the EF and HF conditions and the pursuit gain under the P condition were analyzed by the Steel-Dwass test, in which the significant level was 0.05.

For the brighter targets, under the EF condition, visual ScOR (VScOR) gains were larger than those in the control (ScOR). Under the HF condition, VScOR gains were smaller than those in the control (ScOR). The gain differences among the targets' blurriness were not significant. For the darker targets, under the EF condition, VScOR gains with any target were larger than those in the control (ScOR). Under the HF condition, VScOR gains with the spot and with the 20-degree blurred circle were smaller than those in the control (ScOR), however,

the VScOR gain with the 40-degree blurred circle was not different to those in the control (ScOR). Under the EF condition, there was no VScOR difference among blurriness. Under the HF condition, the VScOR with the spot was smaller than that with the most blurred target (Fig.3).

For the brighter target, under the EF and HF conditions, targets enhanced and inhibited ScOR, respectively. On the other hand, under the EF condition, all darker targets, enhanced ScOR, indicating that even ambiguous position information can improve the accuracy of eye movement with a well-established neural system. Under the HF condition, the targets' blurriness effected ScOR, which suggests that the amount of information affects eye movement. Using the HF condition, it may be possible to estimate the amount of information of stimuli in location perception throughout plural modalities.

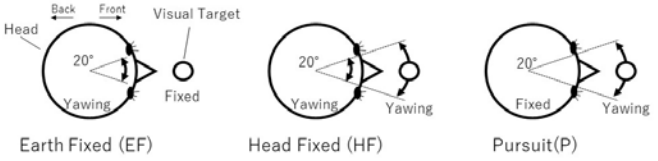

Fig. 1. Three experimental conditions. Subject's head and visual target are illustrated in the vertex view. Arrows show the motion of the head and target.

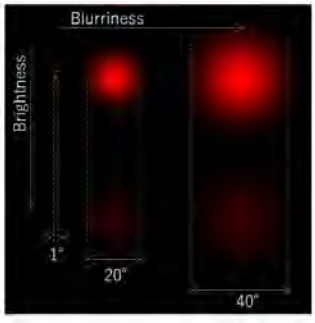

Fig. 2. Blurriness and brightness of each stimulus. Upper circles are brighter targets, lower circles are darker targets. The brighter targets were 10 Lx and the darker targets were 0.4 Lx at the center of circles. Left is a sharp-edged spot with a one-degree angle of vision. Middle and right are Gaussian filtered circles with a blurred edge and about a 20-degree and 40-degree angle of vision, respectively. Numbers show the angle of vision of each target.

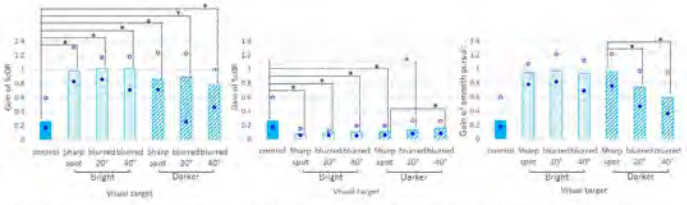

Fig. 3. Gain of eye movement to stimulus. Left: under earth fixed condition. Middle: under head fixed condition. Right: under pursuit condition. Bars show the median of the gain. Solid bars show the control, dotted bars show brighter targets, and striped bars show darker targets. Solid circles show minimum value and open circles show maximum value under each condition and target. *: Significant difference $p < 0.05$.

PS 779

Effect of Visual Field Size on Common Causation Perception During Visual-inertial Heading Estimation.

Benjamin T. Crane[1]; Raul Rodriguez[2]
[1]University of Rochester; [2]University of Rochester, Department of Bioengineering

Visual and inertial cues are the sensory modalities for heading determination. The visual cue is ambiguous as it can represent either self-motion through a fixed environment or environmental motion. When there are differences in visual and inertial direction, it is only appropriate to integrate them when they are both due to motion through a fixed environment, a situation known as common causation. Difference is heading direction is one factor that makes common causation less likely to be perceived, although surprisingly large differences can be perceived as similar. This project tests the hypothesis that visual field size is a factor significant factor in determining common causation. Previous experiments used 141° of the horizontal visual field and 115° of the vertical visual field. The current experiments look at the potential for visual field size to influence common causation by limiting the visual field to 17° in both directions, thus effectively cutting the screen down to 11% of the original size.

Both inertial and visual stimuli consisted of 2s of synchronized motion. The visual stimulus consisted of a 70% coherence star field. Trial blocks included 12 possible visual and inertial headings which covered the full 360° range in the horizontal plane in 30° increments. Every heading combination was presented in random order with 144 stimuli in each block. During each block a mechanical dial was sued to report the perceived direction of the visual (V_p) or inertial (I_p) heading and buttons to report if the headings were the same or different. Six trial blocks were performed in each subject, in 3 blocks inertial heading was reported and in the other 3 visual heading was reported. In all 6 blocks subjects reported if headings were the same or different.

Greatly diminishing the visual field size and removing peripheral vision had a surprisingly small effect on visual direction determination or common causation perception. The lateral component of non-cardinal visual headings (e.g. 30°, 60°) was over estimated by about 20°. Perception of common causation was also very similar to a full visual field with common causation highest when stimuli were aligned in cardinal directions and very low when stimuli were separated by 90° or more. When offset, visual headings continued to have a large influence on inertial heading perception – 10° with

a 30° offset, 8° with 60-90° offsets, and 3° with a 120-150° offset. These were smaller than the offsets see with the full visual field (13° with a 30° offset, and 13-19° with 60-120° offsets. The initial stimulus influence on the visual stimulus was small 1-2° in both conditions.

Support: R01 DC013580

PS 780

Bilateral vestibulopathy decreases self-motion perception

Raymond Van de Berg[1]; Lisa van stiphout[2]; Floor Lucieer[3]; Maksim Pleshkov[4]; Vincent Van Rompaey[5]; Josine Widdershoven[6]; Angélica Perez-Fornos[7]; Nils Guinand[8]; Herman Kingma[9]
[1]Maastricht University Medical Center, Tomsk State University; [2]Faculty of Health, Medicine and life Sciences; [3]Division of Balance Disorders, Department of Otorhinolaryngology and Head and Neck Surgery, Maastricht University Medical Centre, Maastricht, Netherlands.; [4]Division of Balance Disorders, Department of Otorhinolaryngology and Head and Neck Surgery, Maastricht University Medical Centre, Maastricht, Netherlands; [5]University of Antwerp, Antwerp University Hospital; [6]Faculty of Health, Medicine and life Sciences, University of Maastricht, Maastricht, Netherlands; [7]Department of Clinical Neurosciences, University of Geneva; [8]Geneva University Hospital; [9]Professor of Clinical Vestibulology, Maastricht University Medical Centre+

Objective
The vestibular implant is able to (partially) restore the vestibulo-ocular reflex and vestibulo-collic reflex in patients with bilateral vestibulopathy (BV). However, perception is not routinely used as an outcome measure of vestibular implantation. This results from the fact that the clinical value of perceptual self-motion thresholds in this specific population is not yet fully determined. Therefore, objectives of this study were 1) t0.2 ino compare perceptual self-motion thresholds between BV patients and healthy subjects, and 2) to evaluate the association of perceptual self-motion thresholds with the outcomes of tests of vestibular reflexes, in BV patients.

Methods
Thirty-seven BV patients and 34 healthy subjects were included in this study. Perceptual self-motion thresholds were measured in both groups using a CAREN platform (Motek Medical BV, Amsterdam, The Netherlands). The caloric test, torsion swing test, video head impulse test of all semicircular canals, and cervical and ocular vestibular evoked myogenic potentials were measured in BV patients only. Differences in thresholds between both groups were analysed. Hierarchical cluster analysis was performed to visualize patterns between vestibular perception and vestibular function within the group of BV patients.

Results
Perceptual self-motion thresholds were significantly higher in BV patients compared to healthy subjects, regarding nearly all rotations and translations (depending on the age group) ($p \leq 0.001$). Cluster analysis showed that within the group of BV patients, higher perceptual self-motion thresholds were generally associated with lower vestibular test results (significant for yaw rotation, caloric test, torsion swing test and video head impulse test ($p \leq 0.001$).

Conclusion
Self-motion perception is significantly decreased in BV patients compared to healthy subjects regarding nearly all rotations and translations. Furthermore, decreased self-motion perception is generally associated with lower residual vestibular function in BV patients. It is advised to consider self-motion perception as a functional outcome measure for vestibular rehabilitation (including the vestibular implant), and possibly clinical practice in the future.

PS 781

Vestibular Contributions to Place-Based and Route-Based Navigation Strategies

Eric Wei[1]; **Elliott Rebello**[1]; Qiliang He[2]; Timothy McNamara[2]; Yuri Agrawal[1]
[1]Johns Hopkins University School of Medicine; [2]Vanderbilt University

Background
An emerging body of evidence suggests that vestibular function in critical for spatial navigation. It is unclear however how vestibular function contributes to the two types of navigation strategies (i.e. place-based versus route-based) and whether the vestibular system affects every day functional measures of spatial navigation.

Methods
In this study, we aim to recruit 20 patients with vestibular loss and 20 controls. Participants completed tests of route-based and place-based navigation in a real-world environment and analogous navigation tests in a virtual-reality (VR) setting. The accuracy of participants' mental map was assessed using the Judgment of Relative Direction (JRD), a measure of allocentric spatial memory whereby participants had to point to one landmark in the environment relative to an imagined standing location and facing direction in that environment. The number of

turns and the path length were also measured for each task. Additionally, participants' subjective navigational ability was evaluated using the 15-item Santa Barbara Sense of Direction (SBSOD) scale.

Results

Thirteen vestibular patients have been recruited thus far from the Johns Hopkins Otology-Neurotology Clinic, including patients with Meniere's disease, vestibular migraine, bilateral vestibular hypofunction, BPPV, and other etiologies. Twenty healthy young adults were also recruited as controls. Compared to controls, vestibular patients had a greater mean JRD error in both the real-world (65° versus 50°, p = 0.03) and virtual reality navigation tasks (81° versus 66°, p = 0.01). There were no significant differences between the two groups in the mean number of turns made on the real-world route-based and virtual-reality place-based navigation tasks, but vestibular patients made significantly more turns on the VR route-based (4.6 versus 3.3, p = 0.01) and the real-world placed-based (2.0 versus 1.2, p = 0.01) tasks relative to controls. Similarly, there were no significant differences in the path ratio on the real-world route-based task, but vestibular patients had significantly higher path lengths on the VR route-based (1.3 versus 1.1, p = 0.02), real-world placed-based (2.3 versus 1.2, p = 0.002), and VR place-based (3.2 versus 1.3, p = 0.03) tasks relative to controls. There were no significant difference in mean SBSOD scores between the two groups.

Conclusions

Enrollment is currently ongoing. However, these preliminary data suggest that vestibular function is critical to performance on both route-based and place-based navigation tasks. Moreover, the virtual-reality setting may be a more challenging test of route-based navigation performance and more appropriate in differentiating vestibular patients from healthy adults.

PS 782

Treatment of Gravitational Pull Sensation in Patients With Mal de Debarquement Syndrome (MdDS).

Sergei Yakushin; Viviana Mucci; Bernard Cohen
Icahn School of Medicine at Mount Sinai

MdDS is a debilitating neurological condition, characterised by a sensation of self-motion (e.g. rocking, swaying and bobbing) as well as migraine and other psychosomatic symptoms. In most cases symptoms occur after disembarking from a vehicle (motion triggered, MT), however, MdDS can have spontaneous onset (SO) (Cha, 2009). MdDS is poorly understood and has limited experimental treatments (Mucci et al, 2018). One treatment involved the re-adaptation of the eigenvector of the velocity storage (Dai et al, 2014). In this study we aimed to analyze more closely the presence of the gravitation pool sensation recorded in 444 patients (74%) from the 600 patients examined (81%MT) while performing the re-adaptation treatment from 2014. The most common direction of the gravitational pull was backward (55%) and sideways (34%), while pull forward (14%), up (3%) and down (6%) were less frequent. Among these 600 patients, 50 patients (8%) had solely a sensation of gravitational pull but no sensation of self-motion. It remained unclear whether re-adaptation treatment would be appropriate to treat this sensation, since it could potentially induce additional oscillatory sensations. Thus, in this study the management of the gravitation pool sensation was considered along side with the use of the re-adaptation treatment.

Optokinetic stimuli (OKN) with head stationary upright at 5-10°/s was used to treat the gravitational pulls of these 50 patients (82% female). Pull backward and up was successfully treated by OKN going up. Forward and downward pulls were reduced by OKN doing down. Lateral pull was treated by OKN going in direction opposite to pull. Treatment was considered successful if after the treatment 11-point self-scored severity scale (0-no, 10-maximal symptoms) was reduced ≥50%. Scores were obtained before and after 4 days of treatment. The treatment was successful in 73% MT and 71% SO MdDS patients.

The spatial orientation of the velocity storage is codes by gravity sensitive VO neurons (Yakushin et al., 2017). It has been previously hypothesized that MdDS may be coded by the vestibular-only (VO) neurons (Cohen at al., 2018), which have adaptable direction of the gravity polarization vector (Eron et al., 2008). Considering the high success rate recorded in this study, we speculate that OKN can influence polarization vector of the VO neurons and altering patient's perception of gravitational pull. Thus, this therapy may be safely used for abating the gravitation pool sensation in MdDS patients.

Exploring the Structure and Function of Hair-Cell Ribbon Synapses

Chairs: Christian Vogl & Katie Kindt

SYMP 72

Cochlear Excitability and Excitotoxicity

Mark Rutherford
Department of Otolaryngology-Head & Neck Surgery, Washington University

Mammalian cochlear ribbon synapses evolved to transmit auditory information continuously at high rates.

Each auditory nerve fiber (ANF) has a single spike generator activated by a single inner hair cell (IHC) ribbon-type active zone. To overcome refractoriness, excitatory postsynaptic potentials (EPSPs) in ANFs are generally much larger than threshold for spike generation measured at lower rates. Large suprathreshold EPSPs ensure precise spike timing with respect to the stimulus. They also render the compact ANF postsynaptic terminal vulnerable to glutamatergic excitotoxicity. This talk explores specializations supporting high rates of information transfer and mechanisms influencing ANF resilience or vulnerability to noise-induced trauma

SYMP 73

Understanding Sound Encoding: Functional, Anatomical and Molecular Correlation of Response Properties of Cochlear Inner Hair Cell Synapses

Lina Maria Jaime; Tobias Moser
Synaptic Nanophysiology Group, Max Planck Institute for Biophysical Chemistry Goettingen, Institute for Auditory Neuroscience & InnerEarLab, University Medical Center Göttingen

Sound encoding relies on ribbon synapses between cochlear inner hair cells and spiral ganglion neurons. These specialized synapses exhibit differences in spontaneous activity, spike rate adaptation and operating range. Despite efforts to dissect the underlying mechanisms of these distinct properties, the prevalent techniques only provide information about one side of the synapse. Here, we used pre- and postsynaptic patch-clamp recordings in near physiological conditions to gather information about the single synapse active zone. We combined this electrophysiological information with post patch-clamp immunohistochemical analysis to correlate anatomical and molecular features underlying the functional diversity of cochlear ribbon synapses.

SYMP 74

Using Optical Approaches in the Zebrafish Lateral-line to Understand Ribbon Synapses

Qiuxiang Zhang; Katie Kindt
National Institute on Deafness and other Communication Disorders

In order to study hair-cell ribbon synapses, our work utilizes the zebrafish lateral-line system. Using this system, we have created an optical toolkit to visualize the transfer of information from hair cells to afferent neurons in vivo. Currently we are using a custom built light-sheet microscope to image evoked activity in all cell bodies within the afferent ganglion simultaneously. We are using this approach to create a functional map that connects all hair-cells in the lateral-line to afferent cell bodies within the ganglion. We plan to use this approach to investigate the level of redundancy within the ganglion and its resiliency to loss of hair cells and synapses.

SYMP 75

Elucidating Morphological Changes of Hair Cell Ribbon Synapses Upon Maturation

Susann Michanski[1]; Timo Henneck[1]; Tina Pangršiβ Vilfan[2]; Anna Maria Steyer[3]; Wiebke Möbius[3]; Carolin Wichmann[1]
[1]1 Molecular Architecture of Synapses Group, Institute for Auditory Neuroscience & InnerEarLab, University Medical Center Göttingen; [2]4 Department for Otolaryngology, Institute for Auditory Neuroscience & InnerEarLab University Medical Center Göttingen; [3]University Medical Center Göttingen Electron Microscopy Core Unit, Department of Neurogenetics, Max Planck Institute of Experimental Medicine Göttingen

Hearing and balance rely on hair cell (HC) ribbon synapses that transmit sensory information by precise and sustained neurotransmitter release. Despite intensive research on these synapses, the underlying mechanisms of ribbon formation, assembly and maturation in vestibular and cochlear HCs are still not well understood. We combine several high-resolution imaging techniques such as transmission electron microscopy, electron tomography and focused ion beam-scanning electron microscopy to gain a detailed characterization of morphological changes of different HC ribbon synapses upon maturation. Furthermore, we investigate different active zone parameters depending on their topographic localization within the murine HCs.

SYMP 76

Mechanism Underlying DFNA25

Yuvraj Joshi[1]; Stéphanie Miot[2]; Jérôme Bourien[2]; Marie Guillet[2]; Gaston Sendin[2]; Jing Wang[2]; Salah El Mestikawy[2]; Jean-Luc Puel[2]; Regis Nouvian[1]
[1]Institut des Neurosciences de Montpellier; [2]Institute for Neurosciences of Montpellier

DFNA25 is a non-syndromic deafness caused by the mutations in the SLC17A8 gene, encoding the vesicular glutamate transporter 3, VGLUT3. The VGLUT3 knock-out mouse presents a congenital hearing loss, because of the lack of glutamate release at the hair cell ribbon synapse. However, DFNA25 is variable in terms of onset and rate of progression, with an age-dependent penetrance resembling an early-onset presbycusis. Therefore, the Vglut3 KO is of limited use to understand DFNA25. By using a knock-in mouse, which harbors a human mutation, we aim at deciphering the mechanism underlying DFNA25 from system down to molecular level.

SYMP 77

Active Zone Assembly and Protein Turnover in Cochlear Inner Hair Cells

Christian Vogl[1]; Roos Voorn[1]; Cristian Setz[2]; Silvio Rizzoli[3]
[1]Pre-synaptogenesis in Hair Cells Group, Institute for Auditory Neuroscience & InnerEarLab, University Medical Center Göttingen; [2]Dept. of Otolaryngology, University Medical Center Göttingen; [3]Department of Neuro- and Sensory Physiology, University Medical Center Göttingen

Ribbon-type presynaptic active zones of cochlear inner hair cells (IHCs) are sophisticated nano-machineries that enable ultrafast, indefatigable as well as temporally precise synaptic vesicle (SV) release and efficient SV replenishment. While many of the molecular key players have been identified over recent years, the temporal sequence of presynapse assembly and structural refinement prior to hearing onset still remain enigmatic. Moreover, important aspects such as sub-structural protein turnover rates and lifetimes of membrane-anchored ribbons at mammalian IHC active zones are yet to be determined. To address these issues, we combined super-resolution STED microscopy with isotopic imaging and live-cell analysis

SYMP 78

Imaging Cochlea In Vivo: First Step Towards Watching Hair Cells in Action

Jinkyung Kim[1]; Anthony Ricci[2]
[1]Department of Otolaryngology, Stanford University School of Medicine; [2]Department of Otolaryngology and Department of Molecular and Cellular Physiology, Stanford University

In vivo imaging with cellular resolution enables us to identify and characterize how sensory cells interact in generating a signal to the central nervous system. However, cochlear in vivo imaging remains challenging, owing to not only its deep location but also bony structure filled with fluids that when disrupted lead to hearing loss. Here we demonstrate a method to resolve individual cochlear hair cells while maintaining hearing function in live mice. Results from the surgical approach report auditory threshold elevations of approximately 10 dB, that remains stable for up to 2 hours post-surgery. Two-photon in vivo imaging allows observation of outer and inner hair cells at around the 8-10 kHz region of the cochlea through the imaging window. Calcium signals of inner hair cells in GCaMP6s mouse are significantly increased in response to an 8 kHz pure tone sound stimulation, a signal that is markedly decreased at higher frequencies. Our in vivo imaging strategy will allow for investigation how hair cells are recruited across frequencies and intensities as well as how inner and outer hair cells are interacting.

Infection and Inflammation from Middle Ear to Inner Ear-Effects on Hearing

Chairs: Allen F. Ryan & Qing Zheng

SYMP 79

Single-cell RNASeq and selective deletion define the roles of middle ear cell types during otitis media

Allen F Ryan[1]; Arwa Kurabi[2]
[1]Department of Surgery/Otolaryngology, UCSD School of Medicine; [2]UC San Diego

The middle ear (ME) lining is a unique structure in that it transitions from a simple monolayer of squamous epithelium with a minimal stroma to a highly structured, multilayer, secretory mucosa in response to infection. In addition, large numbers of leukocytes are attracted to the mucosa and ME lumen. In acute otitis media (OM), the ME clears and the mucosa reverts to its resting state within days. The responses of mucosal cells and leukocytes contribute to both pathogenesis of, and recovery from, OM.

The transformation of the ME requires the coordinated responses of many distinct cell types. In order to identify the contributions of each ME cell category, we performed single-cell RNASeq during the entire course of an episode of acute OM induced by inoculation with non-typeable Haemophilus influenzae (NTHi). We focused on genes that were differentially expressed by the various cell types of the ME. In addition, we evaluated innate immune genes since acute OM resolves too rapidly for cognate immunity to be significantly engaged.

In the normal ME, we identified more than 20 distinct cell types based on significant differences in gene expression. These included multiple epithelial, stromal, endothelial and resident leukocyte cell identities, as well as pericytes and melanocytes. While many of these cells corresponded to cells previously identified via morphology or immunohistochemistry, several cell types were observed that had not been detected previously in the ME. NTHi infection added two additional cell types: neutrophils and red blood cells.

Differential gene expression revealed a number of unexpected functions of ME cells, including apparent interactions between different cell types. In addition, innate immune genes were differentially expressed by all ME cell types both before and during OM, indicating

distinct cellular responses to ME pathogens. While macrophages expressed the largest number of innate immune genes, it was clear that the response to infection is distributed across all cell types in the ME. Deletion of macrophages from the ME during OM increased pathogenesis and delayed recovery, underscoring the importance of this cell type.

The results illuminate ME cellular and molecular responses during OM, and can be used to design cell-specific treatments to reduce pathogenesis, while preserving infection control, during OM.

SYMP 80

Targeting the biofilm to develop novel approaches to treat and prevent otitis media due to nontypeable Haemophilus influenzae

Lauren Bakaletz[1]; Steven Goodman[2]
[1]The Abigail Wexner Research Institute at Nationwide Children's Hospital and The Ohio State University College of Medicine; [2]Nationwide Children's Hospital

Biofilms formed by the three predominant otopathogens are central to the chronicity, recurrence and recalcitrance of both otitis media and otorrhea. The biofilm matrix provides a formidable shield against host immune effectors and antimicrobials, thereby protecting resident bacteria. We've characterized a lattice of extracellular bacterial DNA (eDNA) and associated DNABII proteins that serves as a critical structural component of biofilms. This discovery has guided our design, development and pre-clinical testing of several therapeutic and preventative strategies for both otitis media and otorrhea. These novel biofilm-targeted strategies are showing great promise and lead candidates are poised for entry into clinical evaluation.

SYMP 81

Otitis Media Susceptibility and Changes in the Head and Neck Microbiome due to Genetic Variants

Regie Lyn Santos-Cortez
University of Colorado School of Medicine

This talk will summarize findings from our collaborative work on the identification of human genetic variants that confer susceptibility to otitis media and induce changes in the microbiome of the head and neck, including the middle ear, nasopharynx and oral cavity. Our studies involve exome and Sanger sequencing, linkage and association analyses, RNA-sequencing and microarray studies, 16S rRNA sequencing for different head and neck sites, and immunolocalization and flow cytometry studies in epithelial cells. We found that both common and rare variants play a role in otitis media by affecting epithelial expression and shaping the head and neck microbiome.

SYMP 82

Role of Eustachian Tube Dysfunction in Otitis Media

Cuneyt Alper
University of Pittsburgh School of Medicine

Otitis media (OM) is a common disease in the pediatric population that also occurs in older children, adolescents and adults. Disease is characterized by inflammation of middle ear (ME) mucosa and the presence of effusion in the usually air-filled ME. ME effusion reduces the movement of the tympanic membrane (TM) which impairs the sound transfer to the inner ear causing hearing loss. There is a large body of research showing that the Eustachian tube (ET) plays a major role in the pathogenesis of chronic OM with effusion and TM retraction/retraction pocket. Role of ET dysfunction and its management is discussed.

SYMP 83

Development of a New Humanized Mouse Model to Study Otitis Media

Arwa Kurabi
UC San Diego

Otitis media (OM) is a large public health problem. Animal models of OM have been developed to study different disease factors in vivo and ex vivo. Much has been discovered about the basic immune, inflammatory and mechanisms of OM using animal models. In recent years, "Humanized mice" have become a valuable tool with which to study the human immune system in a mouse system. These animal models have a number of potential uses in OM studies, including incorporating OM patients stem-cells to develop the chimeric animals to study the role of human immune response during the course of OM.

SYMP 84

Exploring the genetic landscape of chronic Otitis Media: towards new therapies for glue ear

Steve Brown
MRC Harwell Institute, Harwell, UK

The mouse is a formidable tool for identifying and dissecting the genes involved with hearing loss. Otitis media with effusion (OME) is the commonest cause of hearing impairment in children and the commonest reason for surgery in children. Evidence from studies of the human population suggests that there is a significant

genetic component predisposing to the development of chronic OME (COME), however the underlying genes conferring susceptibility are largely unknown. A number of mouse models of COME have been identified and are illuminating the genes and pathways involved, elaborating the molecular pathological mechanisms and identifying novel targets for intervention.

SYMP 85

Infection and Inflammation from Middle Ear to Inner Ear, Effects on Hearing in mouse models for Usher and Down syndromes

Qing Zheng
Case Western Reserve University

Early detection of childhood hearing loss and prompt management are essential for preventing language delays and psychosocial/intellectual developmental problems. The major cause of hearing loss in children is otitis media, particularly true in Down syndrome, and inflammation can spread from the middle to the inner ear. The sustained activation of resident brain macrophages (microglia) and other immune cells has been demonstrated to exacerbate the pathogenesis of neurodegenerative disorders. In this symposium, we provide an overview of inflammation and macrophage-related signaling mechanisms that have been implicated in hearing loss in mouse models for both Usher syndrome and Down syndrome.

Recent Advances in Age-Related Hearing Loss

PD 73

Structural and Functional Changes in Hair Cells and Auditory Neurons in Aged Mouse Models with a Hearing Phenotype Similar to Humans

Jeong Han Lee[1]; Maria Cristina Perez-Flores[2]; Seojin Park[2]; Mincheol Kang[3]; Michael Anne Gratton[4]; Guy Perkins[5]; Ebenezer N. Yamoah[1]
[1]University of Nevada,Reno; [2]University of Nevada, Reno; [3]University of Nevada Reno; [4]Washington University School of Medicine, St. Louis, MO, USA; [5]University of California, San Diego

Age-related hearing loss (ARHL), also known as presbycusis, is prevalent in mammalian aging and is the most common sensory disorder in the elderly and as such is a major social and health challenge. Currently, there is no treatment for ARHL. One of the problems is that auditory neurons do not regenerate in mammals, and the loss of these long-lived neurons leads to permanent hearing impairment. We investigated auditory neuron structure and function in aged CBA/CaJ mice, whose age of onset of ARHL has been evaluated and is comparable to an equivalent human age. We discovered systematic and profound changes in hair cells and auditory neuron structure and functions. We used conventionally in vivo recordings, electrophysiological, and imaging methods in this study. We investigated mitochondrial structure and function in aged OHCs using three-dimensional electron microscopy (3DEM) supported by key functional assays in CBA/CaJ mice. We found that aging increased the auditory brainstem response (ABR) and distortion product otoacoustic emissions (DPOAE) thresholds indicating OHC malfunction, which correlated to clear-cut pathology. We discovered that mitochondria were depolarized in 24-month OHCs and had altered size and number, which led us to determine that the number of dynamin-related protein (Drp1) RNA molecules (mitochondrial fission), but not optic atrophy 1 (Opa1) RNA molecules (mitochondrial fusion) was significantly reduced in old compared to young OHCs indicating a down-regularization of mitochondrial fission. Interesting, mitochondria were found to be tethered to the subsurface cisternae (SSC) by short, thin filaments and both cristae and crista junctions were polarized towards the SSC at all ages. The crista and crista junction densities were lower, yet the crista junction polarization had increased in aged mitochondria. These findings suggest that mitochondria close to the SSC may calibrate their ATP-generating capacity by efficiently sensing increased calcium levels due to their cristae and crista junction polarization. SSC stress and lowered modeled mitochondrial energy production in aged OHCs may contribute to functional cellular stress and the observed death of OHCs in CBA/CaJ mice. Additionally, there were profound changes in auditory neuron myelination and functional properties along the tonotopic axis of the cochlea. We will describe in detail, the morphological and functional changes in auditory neurons, and propose functional alterations that may retard the progression of ARHL.

Funded by the NIDCD and NIA (DC016099; DC015135; DC006685 AG060504; AG051443).

PD 74

Characterization of Hearing Function in APP/PS1 Alzheimer's Disease Mice

Yang Liu; Shu Fang; Li-Man Liu; Yan Zhu; **Hong-Bo Zhao**
Dept. of Otlaryngology, University of Kentucky Medical Center

Background
Alzheimer's disease (AD) is a neurodegenerative disease characterized by a progressive loss of memory and cognitive decline. The main AD pathological changes include amyloid-β (Aβ) plaque deposition, neurofibrillary

tangles (NFT), tau protein aggregation, and neuronal loss. Over the last decade, increasing evidence from epidemiological studies suggests that defects in sensory systems are highly associated with AD. AD pathology can even appear in sensory associated areas before appearing in regions involving memory. Hearing is an important neural-sensory input for central neural system and cognition. However, little is known about hearing functional changes in AD. In this study, we investigated the functional change in the auditory system in AD mice.

Methods
APP/PS1 AD mice (Jackson Lab: Stack No. 004462) are double transgenic mice expressing a chimeric mouse/human amyloid precursor protein (Mo/HuAPP695swe) and a mutant human presenilin 1 (PS1-dE9), and usually develop Aβ-deposits in brain and appear typical AD phenotypes by 6-7 months of age. In this study, the APP/PS1 mice were used. ABR, DPOAE, and cochlear microphonics (CM) at different ages were recorded. Wild-type (WT) littermates were used as control.

Results
In young ages (~ 2 months old), APP/PS1 AD mice measured as ABR threshold had no significant difference from WT mice. As age increased, APP/PS1 AD mice demonstrated accelerated hearing loss. At 3-4 months old, APP/PS1 AD mice had significant hearing loss in comparison with WT littermate controls. Moreover, ABR wave IV and V disappeared, indicating that the upper auditory centers in the brainstem were involved. DPOAE was also reduced. However, CM appeared normal in APP/PS1 mice at the measure age of 6-month old.

Conclusions
APP/PS1 AD mice have significant hearing loss at 3-month old, indicating that the AD pathology could appear in the auditory brainstem and cochlea at the early stage. These data also suggest that hearing function testing could provide an early, non-invasive biomarker for assessing AD development and lesion identification.

Supported by NIH R01 DC 017025 and DC 017025-01S1

PD 75

The Role of Complement Signaling in Cochlear Function and Age-Related Hearing Loss

Kenyaria V. Noble[1]; Gang Li[1]; LaShardai Brown[2]; Jeremy Barth[3]; Carl Atkinson[4]; Baerbal Rohrer[5]; Hainan Lang[6]
[1]Department of Pathology and Laboratory Medicine, Medical University of South Carolina, Charleston, South Carolina 29425, United States; [2]Department of Biology, Winthrop University, Rock Hill, South Carolina 29733, United States; [3]Deparment of Regenerative Medicine and Cell Biology, Medical University of South Carolina, Charleston, South Carolina 29425, United States; [4]Deparment of Microbiology and Immunology, Medical University of South Carolina, Charleston, South Carolina 29425, United States; [5]Deparment of Ophthalmology, Medical University of South Carolina, Charleston, South Carolina 29425, United States; [6]Medical University of South Carolina

Neural and strial presbyacusis are two common forms of hearing loss that may be associated with neural cell degeneration in the auditory nerve (AN) and impaired metabolic activity in the cells of the cochlear lateral wall (LW). Complement molecules are key mediators of inflammation and dysregulation of their expression contributes to the progression of several neurodegenerative diseases. The alternative axis of the complement signaling pathway (AP) is involved in the activation of innate immune cells via biological effector molecules generated in the common terminal pathway (CTP). Our project aims to address the role of complement signaling in auditory function and the extent to which dysfunction of key complement molecules is associated with age-related pathophysiological alterations in the AN and LW.

Young adult and aged C3-KO (CTP) and FactorB-KO (AP) mice and their wild type controls (WTs; C57 BL/6J mice), as well as CBA/CaJ mice, were used. Auditory brainstem response (ABR) was used to assess auditory function. To determine transcriptomic alterations in complement activation, RNA-sequencing analysis was conducted on the cochlear LW and AN tissues from young and aged CBA/CaJ mice, as well as young adult FactorB-KO mice and WTs. Pathological alterations of the cells in the AN and cochlear LW were examined via quantitative immunohistochemistry and confocal imaging.

Immune response genes were transcriptionally regulated in aged mouse LW and AN, with FactorB expression upregulated nearly 2-fold in AN, suggesting region-dependent effects on the complement pathway. In AN of young adult FactorB-KO mice, there was a significant effect on the receptor-mediated signaling pathway (p-adj = 0.04), including reductions in expression of C5aR1/2, which encodes the complement receptors typically expressed by macrophages. ABR thresholds in young adult C3-KO mice were comparable to controls while FactorB-KO mice exhibited about 20 dB threshold elevation. Near one year of age, FactorB-KO mice showed near-complete loss of hearing while C3 deficiency only resulted in a mild loss of hearing sensitivity. Our data also revealed strain-dependent and neuron subtype-dependent neuronal cell loss. The cellular architecture

of macrophages in areas of severe SGN degeneration was consistent with activation, displaying rounding and reduced cellular projections. Together, these results suggest that the complement pathway, specifically the alternative axis (FactorB), plays an essential role in the maintenance of normal cochlear function and perturbed signaling contributes to age-related cochlear tissue degeneration and auditory function declines.

PD 76

Structural and Functional Changes in the Stria Vascularis of the Aging CBA/CaJ Mouse.

Michael Anne Gratton[1]; Jared J. Hartsock[1]; Ruth Gill[1]; Grady Phllips[1]; Brianna Dufek[2]; Dominic Cosgrove[2]
[1]Washington University School of Medicine, St. Louis, MO, USA; [2]Boys Town National Research Hospital, Omaha, NE, USA

Presbycusis or age-related hearing loss (ARHL) is the most common sensory loss in people aged ≥ 65 years. Metabolic presbycusis, presumably based upon strial pathology, is estimated to factor prominently in approximately 25% of presbycusis, while a mixture of metabolic and sensory dysfunction forms the basis for mixed presbycusis. The present work details the age-related changes in the cochlear lateral wall of the CBA/CaJ mouse which lead to a diminished endocochlear potential that coincides or precedes altered function of the cochlear sensory epithelium. Comparative analysis of stria vascularis from 3 month to 21-month-old female CBA/CaJ mice showed a reduction in the overall thickness of the strial tissue with reduced diameter of the strial vessels associated with the migration of the vessels towards the luminal surface. Immunofluorescence analysis showed increased expression of type IV collagen β1/β2 and laminin 211 in the strial capillary basement membranes (SCBMs). This was associated with significant thickening of the SCBMs as measured by transmission electron microscopy. Kir4.1 immunostaining revealed a reduction in the complexity of infoldings of marginal and intermediate cells in the aged CBA/CaJ mice compared to the 3-month-old stria. These structural and molecular changes in the strial compartment were associated ABR measures that were elevated across all frequencies tested (8-32 kHz) compared to the 3-month-old mice. This hearing loss was associated with a progressive reduction of in the magnitude of the endocochlear potential, indicating compromised function of the stria vascularis. Collectively, this data suggests that the CBA/CaJ mouse might be a suitable model for the study of the mechanisms underlying mixed presbycusis, the most prevalent form of ARHL.

PD 77

ATP-Purinergic Receptor P2x2 Deficiency Induced Aging-Related Hearing Loss

Hong-Bo Zhao[1]; Shu Fang[1]; Yang Liu[1]; Li-Man Liu[1]; Ling Mei[2]; Yan Zhu[1]
[1]Dept. of Otlaryngology, University of Kentucky Medical Center; [2]Dept. of Otolaryngology, University of Kentucky Medical Center

Background
Recent studies in our laboratory and other laboratories reveal that ATP-purinergic signaling can activate ATP-gated P2X receptors to regulate sound transduction, outer hair cell electromotility, gap junctional coupling, K^+-sinking and recycling, and endocochlear potential (EP) generation. Moreover, P2X2 mutations can lead to hearing loss (DFNA41) and increase susceptibility to noise. Also, P2X2 mutation seems associated with aging-related hearing loss. However, detailed information is unclear. In this study, we used P2X2 knockout (KO) mice to investigate whether P2X2 deficiency can induce or accelerate/exacerbate age-related hearing loss.

Methods
P2X2 KO mice (Stack No: 004603) were purchased from Jackson laboratory. Wild-type (WT) littermates were used as control. ABR threshold, DPOAE, and cochlear microphonics (CM) were recorded to assess cochlear and hearing function.

Results
Under normal condition, hearing function in P2X2 KO mice measured as ABR threshold showed no significant difference in comparison with WT mice until ~2-month old. Afterward, ABR thresholds in P2X2 KO mice were progressively increased, and appeared significant hearing loss at 5-month old. Hearing loss started at high-frequency region and then extended to middle and low frequency regions. DPOAE and CM also have changes.

Conclusions
The data suggest that ATP-purinergic signaling may play an important role in age-related hearing loss, and that P2X2 deficiency can induce age-related hearing loss

Supported by NIH R01 DC 017025 and DC 017025-01S1

PD 78

G6PD Overexpression Protects from Oxidative Stress and Retard Age-related Hearing Loss Progression

Jose M. Bermúdez-Muñoz[1]; Adelaida M. Celaya[1]; Sara Hijazo-Pechero[2]; Manuel Serrano[3]; Jing Wang[4]; Isabel Varela-Nieto[5]
[1]"Alberto Sols" Biomedical Research Institute (CSIC-UAM); CIBERER Unit 761, CIBER, Institute of Health Carlos III, Madrid, Spain; [2]"Alberto Sols" Biomedical Research Institute (CSIC-UAM), Madrid, Spain; [3]Institute for Research in Biomedicine (IRB), Barcelona, Spain.; [4]Institute for Neurosciences of Montpellier; [5]"Alberto Sols" Biomedical Research Institute (CSIC-UAM); CIBERER Unit 761, CIBER, Institute of Health Carlos III; IdiPAZ, La Paz Hospital Institute for Health Research, Madrid, Spain

Ageing of the auditory system is associated with the incremental production of reactive oxygen species (ROS) and the accumulation of oxidative-derived damage in macromolecules, which contribute to cellular malfunction, compromise cell viability and, finally, causes functional decline. The cellular detoxification power partially relies in NADPH production, which is a cofactor for major cellular antioxidant enzymes. NADPH is mainly produced by glucose-6-phosphate dehydrogenase (G6PD), an enzyme that catalyzes the rate-limiting step in the pentose phosphate pathway.

We show here that the transgenic mouse *G6PD*-Tg, which shows enhanced NADPH production along life, maintains lower auditory thresholds than wild type mice during ageing. *G6PD* overexpression preserved inner (IHC) and outer hair cells (OHC), OHC innervation and number of synapses per IHC. Transcripts for antioxidant enzymes were increased whereas levels of pro-apoptotic proteins were reduced in 3-month-old *G6PD*-Tg. Consequently, nitration of proteins, mitochondrial damage and $TUNEL^+$ apoptotic cells were reduced in 9-month-old *G6PD*-Tg compared to wild type mice. Unexpectedly, *G6PD* overexpression triggered low grade inflammation that was effectively resolved in young mice, as shown by the absence of cochlear cellular damage and macrophages infiltration.

In conclusion, we propose here that NADPH overproduction from an early stage is an efficient mechanism to maintain the balance between the generation of ROS and the cell detoxification power along ageing and, therefore to prevent hearing loss progression.

This work has been founded by Spanish MINECO/FEDER SAF2017-86107-R to IVN. JMBM was supported by contracts from MINECO/FEDER SAF2014-AGEAR and MINECO/FEDER SAF2017-86107-R

PD 79

Autophagy regulates the degeneration of the auditory cortex through the AMPK-mTOR-ULK1 signaling pathway

Jie Yuan[1]; baoai han[2]; Haiying Sun[1]
[1]Departments of Otorhinolaryngology, Union Hospital, Tongji Medical College, Huazhong University of Science and Technology, Wuhan 430022, China.; [2]Public Laboratory, Key Laboratory of Breast Cancer Prevention and Therapy, Ministry of Education, Tianjin Medical University Cancer Institute and Hospital, National Clinical Research Center for Cancer, Tianjin Medical University, Tianjin 30000, China.

Presbycusis is the most common sensory impairment associated with aging; however, the underlying molecular mechanism remains unclear. Autophagy has been demonstrated to serve a key role in diverse diseases; however, no studies have examined its function in central presbycusis. The aim of the present study was to investigate the changes of autophagy in the physiological processes of the auditory cortex and its role in the degeneration of the auditory cortex, as well as the related mechanisms using naturally aging rats and a D-galactose (D-gal)-induced mimetic rat model of aging. The present study demonstrated that autophagy increased from 3 months to 15 months in the normal saline (NS) control group, while it decreased in the D-gal group. Compared with the age-matched NS group, the D-gal group demonstrated significantly increased levels of the autophagy-related proteins, LC3 and Beclin 1 (BECN1) and the anti-apoptotic proteins B-cell lymphoma (BCL)2 and BCL-extra large (BCL-xL) at 3 months, with no obvious changes in cell apoptosis level and neuron ultrastructural morphology. However, LC3, BECN1, BCL2 and BCL-xL were decreased at 15 months in the D-gal group, with cell apoptosis significantly increased and substantial neuron degeneration. Additionally, 5' AMP-activated protein kinase (AMPK) activity was enhanced, and mechanistic target of rapamycin (mTOR) and ULK1 phosphorylation (Ser 757) activities were inhibited at 3 months compared with those of the NS group, while the opposite was observed at 9 and 15 months. The present results suggested that autophagy increases from young to adult and decreases at old age in the physiological processes of the auditory cortex, and has anti-apoptotic as well as anti-aging functions in the degeneration of the auditory cortex. Additionally, autophagy was regulated through AMPK activation and mTOR suppression, and impairment of autophagy may serve a key role in the degeneration of the auditory cortex, even in the pathogenesis of central presbycusis.

PD 80

Evidence for "Central Gain" in the Auditory System of Older Adults

Kelly C. Harris; James W. Dias; Carolyn M. McClaskey
Medical University of South Carolina

Plasticity is a fundamental property of the brain and is the primary means by which the adult brain adapts to changing environments and enables new behavior. Aging is thought to reduce neural plasticity in the cortex, restricting the aging brain's response to change and adaptation. Neural presbycusis, or an age-related loss or inactivity of auditory nerve (AN) fibers, may compound these effects by reducing input to the higher auditory centers, including the cortex, and may or may not increase hearing thresholds. The extent to which age-related changes propagate from peripheral (cochlear/AN) deficits and/or arise from changes at the cortex remains unclear. These complexities warrant a neuroimaging approach that can identify where and when deficits initially occur and the extent to which that initial insult is propagated through the auditory system. We used the compound action potential (CAP) as a measure of AN function to assess age-related and individual differences in auditory input to the cortex. In the same subjects, patterns of cortical reorganization were identified using cortical evoked potentials. AN and cortical activity were assessed in 48 older and 35 younger adults with a range of hearing thresholds. Despite robust and significant deficits in AN function, cortical activity was relatively well preserved in older adults. These results are consistent with reports in animal models of 'central gain' and are thought to reflect homeostatic mechanisms that strive to maintain stable levels of cortical activity despite changes in peripheral input. Changes in the neurochemical environment, particularly excitatory (glutamate) and inhibitory (GABA) neurotransmitters, are thought to underlie some of these homeostatic changes in plasticity. In concurrence with changes in neurotransmission, age-related reductions of auditory input (as reflected by increased pure-tone thresholds) may lead to increased auditory cortex atrophy. A subset of our participants underwent magnetic resonance imaging to assess associations between AN and cortical function and measures of glutamate and GABA, and cortical microstructure. Our results suggest that changes in AN synchrony may alter the balance of excitatory and inhibitory neurotransmission and that stronger synchrony is associated with greater gray matter volume in auditory cortex. In contrast, measures of cortical function were not associated with glutamate/GABA balance or cortical microstructure. A significant advancement in our understanding of plastic changes that occur in response to older adults' gradual loss of hearing is needed, so that plastic processes can be leveraged to support maximal benefit during rehabilitation. Work supported (in part) by grants from NIH/NIDCD.

The Current Status of Inner Ear Neurons: Development, Death, and Stem Cell-Based Transplantation Therapies

Chairs: Aleta Steevens & Peter Santi

SYMP 86

Generating Exogenic Cells for Transplantation in Gene Edited Animals via Blastocyst Complementation

Walter C. Low
University of Minnesota

Current approaches for generating cells for transplantation utilize induced pluripotent stem cells (iPSCS) that are derived from somatic cells. The resulting differentiated cells approximate the structure and function of the targeted somatic cells but are not exact replicas. This is due in part to the incomplete reprogramming of the iPSCs into cells of interest. To address this issue a novel approach utilizing gene-edited embryos has emerged to create a developmental niche in which donor iPSCs can occupy to generate the desired cell phenotype. The prospect of generating exogenic neural cells for transplantation and repair of the nervous system is now under investigation.

SYMP 87

Genetic Pathways Involved in Otic Neuroblast Specification

Amy E. Kiernan
University of Rochester

Otic neurons innervate the hair cells of the auditory and vestibular system and are the earliest differentiating cell type in the inner ear, arising at otic cup/otocyst stages. A cascade of gene expression involving transcription factors and proneural genes has been identified as essential for the generation of the otic neuronal population. This talk will discuss the genetic factors involved in neuroblast selection from the otic progenitor pool, as well as how neuronal and sensory cell formation may be balanced, as both cell types are generated from the same neurosensory region of the otocyst.

SYMP 88

Inner Ear Neuron Development and Auditory Circuit Wiring

Lisa Goodrich
Harvard

Spiral ganglion neurons (SGNs) communicate sound information from the cochlea to the brainstem. Within the cochlea, Type I SGNs extend radial processes that are organized into bundles along the tonotopic axis, with each process synapsing with one inner hair cell (IHC). Type II SGN processes grow past the IHCs and spiral along the length of the cochlea, forming en passant synapses with multiple outer hair cells. This talk will summarize the cellular and molecular mechanisms that ensure proper cochlear wiring, with emphasis on time-lapse imaging studies that suggest a surprisingly active role for glia during early neurite outgrowth.

SYMP 89

Primary Neural Degeneration in the Inner Ear: Mechanisms, Prevalence, and Diagnosis

M. Charles Liberman
Harvard

Temporal bone histopathology shows that primary neural degeneration, i.e. loss of spiral ganglion cells (SGCs) without loss of hair cells, occurs in 1) several types of genetic deafness, 2) some cases of acquired sensorineural hearing loss, and 3) a subset of presbycusic ears. Animal and human work shows that peripheral axons can degenerate long before SGCs, even if most hair cells survive. Audiological testing reveals patients with auditory neuropathy, i.e. persistence of otoacoustic emissions without an ABR, however, this phenotype can arise from inner hair cell dysfunction or neural degeneration. Animal work has revealed the signaling pathways required for neuronal survival in the adult cochlea. This talk will review these findings with an eye towards summarizing what can be inferred about SGC survival in living subjects.

SYMP 90

Inner Ear Stem Cells for Auditory Neuron Repair

Albert Edge
Harvard

Glial cells can act as progenitors for neurons in the neurosphere assay, in which cells from the newborn spiral ganglion expand in number in vitro. These Sox2-positive cells differentiate spontaneously into cells expressing neural markers. We can increase the number of cells differentiating into neurons by overexpressing Lin28 or Ascl1. The neurons that differentiate from glial cells make synapses with hair cells in the deafferented newborn cochlea. We use the newborn cochlea after disruption of afferent synapses as a model to assess the effects of neurotrophins and axonal guidance molecules on synaptogenesis between neurons and hair cells.

SYMP 91

Generating Inner Ear Neurons using Blastocyst Complementation

Aleta Steevens; Walter C. Low; Peter Santi
University of Minnesota

A novel approach for generating inner ear neurons is Blastocyst Complementation (BC). In BC, the deletion of the required gene for the development of a tissue type creates a vacant niche that can be complemented at blastocyst stage by stem cells that carry wild-type copies of the missing gene and generate the target tissue type. Neurogenin1 (Neurog1) is the required gene for inner ear neurogenesis and its deletion would create an appropriate niche for stem cell complementation. This talk will describe preliminary results that demonstrate blastocyst complementation of Neurog1 deficiency is a potential method for generating stem cell-derived otic neurons.

SYMP 92

Stem Cell Transplantation to the Inner Ear

Hainan Lang
Medical University of South Carolina

The development of feasible procedures for cell transplantation in the inner ear is challenging due to the inaccessibility and complexity of cochlear structure. How pathophysiological conditions impact homing and survival of the transplanted cells is an important consideration. Using an animal model of primary auditory-neuropathy, we found that there is an optimal time window for engraftment and survival of transplanted cells that occurs in the early post-injury period. Our findings that gene expression profiles in the acutely-injured auditory nerve recapitulate aspects of postnatal development and glial cells as a resource for promoting the outcome of cell-based therapy also will be discussed.

SYMP 93

Diagnosis and Treatment of Human Spiral Ganglion Dysfunction

Hinrich Staecker[1]; Adam Mellot[2]; Athanasia Warnecke[3]
[1]University of Kansas Medical Center, Kansas City, KS, USA; [2]University of Kansas School of Medicine; [3]Hannover Medical School, Hannover, Germany

Experimental strategies for improving the function of the spiral ganglion include transplantation of stem cells or induction of endogenous cells to replace missing spiral ganglion cells and a variety of strategies to deliver neurotrophic growth factors. Critical to clinical implementation of these findings are a means for evaluating the underlying function of the human inner ear and developing delivery strategies for both cellular and molecular therapeutics. Analysis of human perilymph for expression of miRNAs and proteins can aid in understanding the pathologic state of the cochlear and guide intervention in the future

Auditory Brainstem: Beyond Hearing Detection

PD 81

Relationships between perception, the frequency following response and acoustic features of speech and music stimuli

Steven Losorelli[1]; Gabriella Musacchia[2]; Vivian Lou[1]; Blair Kaneshiro[1]; Nikolas Blevins[1]; Matthew B. Fitzgerald[1]
[1]Stanford University; [2]University of the Pacific

Sound identification is a central feature of human communication. To successfully identify and assign appropriate labels to different sounds, individuals must be able to distinguish between them, based on their spectro-temporal acoustic characteristics. This process is largely automatic for individuals with normal hearing, but can be a significant challenge for individuals with hearing loss who receive acoustic input via cochlear implants. For these people, an objective measure of the neural representation is of considerable interest for both clinicians and researchers. Previous results from our laboratory suggest that the frequency-following response (FFR) has the potential to accurately predict vowel identification or recognition of musical instruments at an 70-90% accuracy ($p < 0.001$). However, the neural response components that underlie classification are not clear, nor is the relationship between the classifier and the neural response in individual participants. To address this gap, we quantified the relationship between stimulus and response on an individual basis using cross-correlations between a set of speech and music stimuli and the resulting FFRs. Correlations were calculated for normal-hearing individuals across two experiments. In the first experiment, responses to three consonant-vowel phonemes and three musical instruments were examined. In the second experiment, responses to six vowels processed through an acoustic simulation of a cochlear implant were examined. In both experiments, individuals also completed a perceptual-identification task which examined the accuracy at identifying these stimuli. Our preliminary results show a strong, but imperfect relationship between the classifier predictions and the neural response. This relationship suggests that classification of FFR responses may be a promising approach for the objective assessment of auditory perception. One caveat to this conclusion is that the difference in performance between the classifier and the behavioral task suggest that the classifier may not compute a neural proximity space that best approximates the perceptual space. Thus, correlation–as well as non-classification approaches that find optimal weightings and combinations of stimulus and response features, respectively, may maximize their correlation in the similarity space.

PD 82

Auditory Brainstem Detection Thresholds

George S. Liu[1]; Noor-E-Seher Ali[1]; Daibhid O Maoileidigh[2]
[1]Department of Otolaryngology, Stanford University; [2]Department of Otolaryngology - Head & Neck Surgery, Stanford University

The auditory brainstem response (ABR) is an objective measure of the auditory system's neural performance. Because averaging responses over stimulus repetitions reduces the background noise, the average ABR is used to diagnose hearing deficits in the auditory pathway. The ABR threshold is the lowest sound pressure level at which the average ABR evidences that a series of stimuli was detected. This is analogous to defining threshold by asking a subject to decide only after a set of stimuli was presented whether they heard the stimuli on average. In contrast, psychophysical thresholds are based on a subject deciding whether they hear each individual stimulus before the next stimulus is presented. We show how to find a psychophysics-like threshold from ABRs to individual stimulus presentations, which we call the auditory brainstem detection (ABD) threshold. Independent of how an ABR is quantified, we hypothesize that the ABD threshold is higher than the ABR threshold.

We record 512 individual ABR traces in 5 Sprague Dawley rats evoked by tone pip stimuli at 16kHz with 5 dB steps from 0-80 dB SPL. To objectively quantify individual responses, we employ two summary features: (1) the difference between the voltages measured at two specific times after stimulus onset and (2) the inner product between individual responses and their average. The voltage difference quantifies the amplitude of individual ABRs whereas the inner product quantifies the similarity between individual ABRs.

ABR thresholds based on the average value of either summary feature are close to each other. If the average

feature value corresponding to an ABR threshold is used to classify individual responses, however, more than a quarter of the individual responses are false positives created by the background noise. Guided by psychophysics, we introduce a detection cutoff for a feature such that the false positive rate is 0.05 and define the ABD threshold as the lowest sound pressure level for which half of the individual responses exceed the cutoff, i.e. the true positive rate equals 0.5 at the ABD threshold. In agreement with our hypothesis, the ABD thresholds based on either feature are larger than the ABR thresholds by 50 dB SPL and 20 dB SPL respectively for the voltage difference and the inner product. To determine which feature is better for detecting individual ABRs, we analyze their receiver operator characteristic curves. We find that the inner product outperforms the voltage difference at stimulus levels exceeding 30 dB SPL.

PD 83

Membrane Filters Influence Sensitivity to Interaural Delay in the Envelope of High-Frequency Sound

Andrew Brughera[1]; Jessica J. M. Monaghan[2]; David McAlpine[3]

[1]Boston University; [2]Macquarie University; [3]Department of Linguistics, The Australian Hearing Hub, Macquarie University, Sydney, Australia

Many human listeners detect interaural time differences (ITDs) in the intensity envelope of high-frequency sound, with sensitivity at amplitude modulation (AM) rates up to 256 or 512 Hz for 4 and 6-kHz carrier frequencies, and up to 128 or 256 Hz for 10-kHz carriers (Bernstein & Trahiotis, 2002). For top listeners, sensitivity to this envelope-ITD extends to AM at 800 Hz for 4-kHz carriers, and 600 Hz for 6 and 10-kHz carriers (Monaghan et al., 2015). Neural sensitivity to envelope-ITD in the lateral superior olive (LSO) of cats reflects the modulation frequency range of top listeners: sensitivity remains strong for high carrier frequencies at 500-Hz modulation, and persists at 750-Hz modulation (Joris, 1996). The rat LSO reflects the sensitivity of typical listeners, becoming increasingly lowpass at higher characteristic frequency (CF): the low-frequency region features a majority of neurons with membrane cut-off frequencies from 80 to 360 Hz; the mid-frequency region includes membrane cut-offs up to 260 Hz; and the high-frequency region has membrane cut-offs strictly below 80 Hz (Remme et al., 2014).

Hypothesizing that membrane filters influence envelope-ITD sensitivity, we applied transposed tone stimuli to model auditory nerve fibers (Zilany et al., 2014) providing independent inputs (40 excitatory ipsilateral, 8 inhibitory contralateral) to each model LSO neuron (Gjoni et al., 2018; Rothman & Manis, 2003; Wang & Colburn, 2012). Each population of 24 model LSO neurons has distinct membrane filtering, yielding its distinct membrane speed from slow to very fast. We calculated neural just-noticeable-differences (JNDs) (Brown and Tollin, 2016) in envelope-ITD for each population. For each stimulus condition, the best performing population had a JND similar to the best human ITD-discrimination threshold. For carrier frequencies from 4 to 10 kHz, as modulation rate increased from 32 to 256-Hz, a transition from relatively slow to faster model membranes tracked the best human performance. At 512-Hz modulation, fast model neurons at 6 kHz, and very fast model neurons at 4 to 10 kHz, all supported measurable JNDs. For 800-Hz modulation at 4 kHz, a measurable JND was achieved by off-frequency listening in very fast model neurons at CF 4.43 kHz, closer to the modulation sideband. Overall, our results suggest that in envelope-ITD sensitivity, mediocre listeners perform as if consistently relying on slow LSO neurons, and top listeners perform as if selectively monitoring sensitive LSO neurons according to membrane speed and acoustic stimulus.

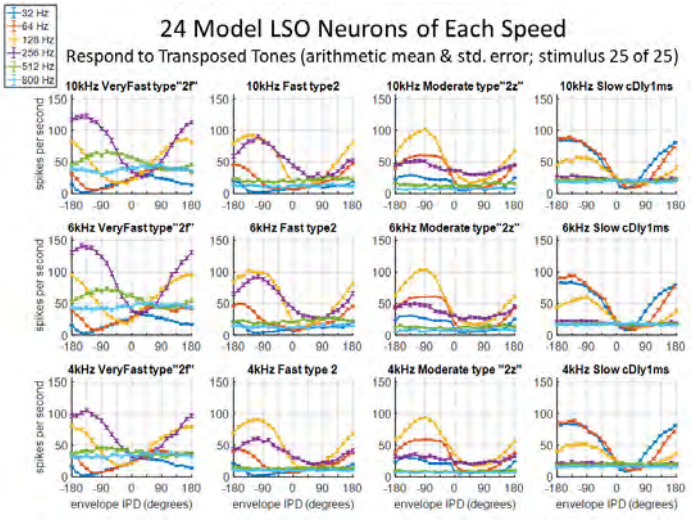

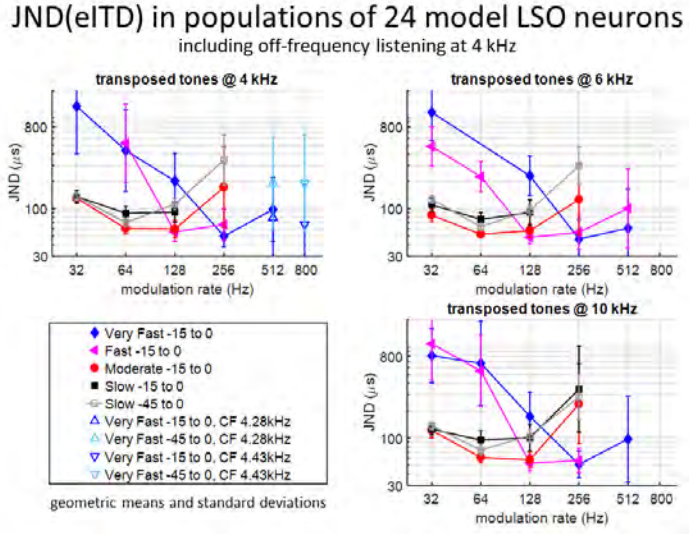

PD 84

Subcortical Responses to Continuous Music in Human Listeners

Tong Shan; Ross K. Maddox
University of Rochester

Music is an art form that has acoustically rich signals and the power to evoke strong emotions. However, how music is processed in the human brain and how it is coded in the early pathway of auditory system remain largely a mystery. To measure the brain response to sound signals, event-related potentials, and Auditory Brainstem Responses (ABR) specifically, have been widely used, but these typically rely on short and repeated stimuli. Recently, it was shown that the subcortical response to natural continuous speech can also be derived using deconvolution approach. This approach should also be generalizable to the response to any auditory stimuli such as music. Here, we used the methods developed for the speech-derived ABR to assess the response to naturally performed music.

Instrumental pieces that contained no vocal parts comprised our musical stimuli. To adjust for long-term changes in the overall amplitude of the pieces, we divided each piece by its slow (< 0.1 Hz) envelope. We also truncated silent gaps to a maximum of 1 s. Each subject was presented with the music stimuli continuously at 60 dB SPL for approximately two hours. EEG electrodes were placed at FCz and both earlobes, with a ground at FPz. We derived the response as in our previous work with speech: by deconvolution, treating the EEG signal as the output and the rectified audio signal as input.

We found robust responses to music over a wide range of latencies, indicating that we can assess both subcortical and cortical activity in response to arbitrarily chosen music. Early results also indicate that the music response component may be later than the wave V of the speech response. These initial results pave the way for studies of brain responses, potentially as they relate to higher order factors such as musical aptitude and taste in genre. They will also allow us to study potential differences in the processing of music versus speech in general and across subject populations.

PD 85

An Efficient and Robust Approach to Detect Auditory Evoked Responses using Adaptive Averaging

Yunfeng Hua; Haoyu Wang; Bei Li; Xu Ding; Xueling Wang; Zhiwu Huang; Hao Wu
1. Department of Otolaryngology - Head & Neck Surgery, Shanghai Ninth People's Hospital, Shanghai Jiao Tong University School of Medicine; 2. Ear Institute, Shanghai Jiao Tong University School of Medicine; 3. Shanghai Key Laboratory of Translational Medicine on Ear and Nose diseases, Shanghai, China

Auditory brainstem response (ABR) is widely employed to evaluate hearing function of test subjects for both clinical and research purposes. Currently, hearing threshold estimation still relies on trained professionals to assess the ABR audiograms, resulting in the largest cost component of the test. Here we report a novel approach to detect the threshold objectively and reliably using adaptive averaging. From single-sweep ABR recordings of mice or human participants, pairs of group averages were generated for testing the minimum sweep number that is required for time-locked evoked responses being detected using cross-correlation function. At near-threshold sound levels the required sweep number increases exponentially, allowing objective and precise threshold estimation. The autodetected results were highly consistent with the expert-assessed ground truth. Moreover, up to 69 % sweeps at suprathreshold sound levels were found redundant for the threshold estimation and could be avoided by stopping on-going averaging to improve test efficiency. Thereby, implementation of the approach in commercial recording devices will automate the hearing test in a more reliable and cost-effective way.

PD 86

Simultaneous Investigation of Subcortical and Cortical Sensitivity to Temporal Information

Sonia Varma[1]; Sangamanatha Veeranna[2]; David Purcell[3]; Ingrid Johnsrude[4]; Björn Herrmann[2]
[1]University of Western Ontario; [2]Western University; [3]University of Western Ontario, School of Communications and Sciences and Disorders; [4]The Brain and Mind Institute, Western University

Age- and noise exposure-related hearing loss is associated with changes at the peripheral, subcortical, and cortical stages of the auditory pathway. Many of these changes are not detectable using pure tone audiometry, but may still contribute to suprathreshold symptoms of hearing impairments such as tinnitus, hyperacusis, and impaired perception of speech in noise. Research often focuses on individual stages of the auditory system, but given the cascading effects of peripheral damage on central processing and the extensive feedforward and feedback connections among different stages of processing, research approaches that focus on the entire auditory system to understand auditory pathology are critically needed. Here, we explore a novel stimulus paradigm with electroencephalography (EEG) in younger, normal-hearing adults (N=29, 17-34 years) to

assess neural function at multiple stages of the auditory pathway simultaneously. We employ click trains that continuously accelerate then decelerate (3.5 Hz FM) with inter-click-intervals ranging from 4 to 40 ms. Peripheral and subcortical activity can be assessed in response to the individual clicks while concurrently assessing neural phase-locking in the auditory cortex, and sustained activity, likely originating from higher-level cortices, to the 3.5-Hz temporal regularity. We recorded EEG data while participants passively listened to the frequency-modulated click-train stimulus and an unmodulated (isochronous with 40 ms inter-click-interval) control stimulus. We observed that the latencies of Waves III and V of the ABR were sensitive to temporal information represented in the inter-click-interval. Longer latencies were observed when intervals between clicks were shorter. Si/=We found no correlations between subcortical ABR latency shifts, reflecting adaptation, and cortical sensitivity to temporal regularity. This suggests that sensitivity to temporal information (inter-click-interval) at subcortical levels, and cortical processing of temporal regularities, may be at least partially independent, or that their relationship is non-linear. By recording neural responses from different stages of the auditory system simultaneously, our research opens the door to new assessment tools that characterize relationships in responses across levels of processing, potentially enhancing sensitivity to abnormality.

PD 87

Frequency Following Responses to Voice Pitch in Newborn Infants: Effect of Phototherapy

Jiong Hu[1]; Gabriella Musacchia[1]; Qin Hong[1]; Matthew B. Fitzgerald[2]
[1]University of the Pacific; [2]Stanford University

Objective: Using frequency following response (FFR) to monitor auditory neurophysiological status in neonates with progressive moderate hyperbilirubinemia, measured by transcutaneous levels (TcB) and total serum bilirubin levels (TSB).

Method
A group of 21 newborns with moderate hyperbilirubinemia who were prescribed with phototherapy were recruited in this study. Both click-ABR and FFR, which was elicited by a recorded natural voice pitch, were recorded via one channel montage. TSB levels, TcB levels, click-ABR latencies and FFR amplitudes at the F0 (110-185 Hz) and F1 (280-320 Hz) frequency ranges were measured at the time of pre- and post-phototherapy. Pair-wised t-tests were carried out to examine the effect of phototherapy on click-ABR and FFR assessments.

Results
No significant differences were found in the wave V latencies of click-ABR in all sessions (pre- and post-phototherapies). Paired t-tests showed a significant difference for FFR amplitude in the F0 range, such that F0 amplitude increased after phototherapy. F1 amplitudes in the post-phototherapy group were also significantly higher than the pre- group. There was a negative correlation between TSB and FFR amplitude in the F0 frequency range, such that lower bilirubin level was associated with greater FFR amplitude in the F0 range. Correlations between FFR amplitude at F1 region were not significantly correlated with TSB levels. Further, the TcB levels did not correlate well with FFR amplitude in the F0 range nor the F1 range. In all, the data suggest that FFR amplitudes reflected the changes affected by the phototherapy. Also, some bilirubin measurements, such as the TSB levels, show correlation with FFR.

Conclusion
Voice pitch elicited FFR shows promise in monitoring and evaluating the dynamic change in the status of newborns' auditory neural system, especially those who were at risk of neurotoxic damages, such as hyperbilirubinemia.

PD 88

Effects of speech enhancement on brainstem coding of consonants in normal-hearing listeners

Jayaganesh Swaminathan[1]; Rupa Balachandran[1]; Gabriella Musacchia[1]; Virginia Best[2]; Kevin Ng[1]; Justin Cha[1]
[1]University of the Pacific; [2]Boston University

The scalp recorded human frequency following response (FFR) represents sustained phase-locked neural activity among a population of neurons in the rostral brainstem. The present study used FFRs to examine the effects of a speech enhancement strategy on the neural coding of consonants in normal-hearing listeners. FFRs were recorded from normal-hearing listeners in response to voiced stop consonant-vowel syllables (/ba/, /da/ and /ga/) presented with and without speech enhancement and background noise (5 dB signal-to-noise ratio; speech shaped noise). The speech enhancement approach enhanced the energy and the onset slope of the word initial consonants.

Preliminary results indicate a systematic effect of speech enhancement on onset response latencies and sustained phase locked responses that are largely predictable from the variations introduced to the acoustic cues that are critical for distinguishing these voiced consonant-vowel syllables. Possible implications of applying such

speech enhancement approach to ameliorate temporal processing disorders in clinical populations will be discussed.

Middle-Ear Bonanza

PD 89

Changes in Saccade-Related Eardrum Oscillations After Surgical Denervation of the Stapedius Muscle

Stephanie Schlebusch[1]; Matthew Cooper[2]; David Kaylie[2]; Cynthia King[2]; David Murphy[2]; Christopher A. Shera[3]; Jennifer Groh[2]
[1]Duke Univeristy; [2]Duke University; [3]University of Southern California

The connection between the visual and auditory systems plays an important, integrative role in perceiving surrounding stimuli correctly. We have recently reported an oscillation of the eardrum time-locked with the onset of a saccade and in the absence of incoming sound that suggests this connection may begin as early as the auditory periphery. These eye movement-related eardrum oscillations (EMREOs) covary in phase and amplitude with the direction and magnitude of a synchronous saccade (Gruters, Murphy et al. PNAS 2018). However, the acting anatomical features and their joint contributions to this eardrum oscillation- possibly including the stapedius, tensor tympani, and outer hair cells - are still unknown. We first sought to determine the interactions between the stapedius muscle and the eardrum during saccade activity, an important initial step towards understanding both the mechanisms within the middle and inner ear that cause the EMREO and the function of the EMREO.

We provide here an update on our findings before and after denervating and transecting the stapedius muscle in rhesus monkeys. To date, one monkey has undergone the surgical procedure and pre-surgical baseline assessment is presently under way in another. EMREOs are assessed using microphones placed in the ear canals while the head-restrained monkeys make spontaneous eye movements that are tracked with a video eye tracker (1000 Hz sampling rate).

Pre-surgically, we can see a well-characterized, highly reproducible EMREO in both ears of both monkeys, with a strong contribution from the horizontal component of saccades, as expected from previous work. After stapedius denervation and transection in one ear of one monkey, the EMREO signal was altered, with a significant reduction in the sensitivity to the horizontal component of saccades. Together with observations from clinical patients (King et al. ARO 2020), the emerging picture is that there are multiple contributors to the EMREO, and that the stapedius muscle contributes to the amplitude of this signal.

PD 90

Frequency Dependence of Stapes Displacement and Intracochlear Pressure in Response to Very High Level, High Frequency Sounds

Nathaniel T. Greene[1]; Mohamed Alhussaini[2]; James Easter[3]; Daniel J. Tollin[4]; Theodore Argo[5]; Tim Walilko[5]
[1]Department of Otolaryngology, University of Colorado School of Medicine; [2]Assiut University; [3]Cochlear Boulder, LLC; [4]Department of Physiology & Biophysics, and Department of Otolaryngology, University of Colorado School of Medicine; [5]Applied Research Associates, Inc.

Transmission of high-level sounds through the middle ear is limited by motion of the ossicular chain, which restricts the total peak-to-peak displacement of the stapes. Previous studies in small animals have suggested that intracochlear pressure (P_{IC}), a proxy for sound transduction by the basilar membrane, increases proportionally with stapes displacement (D_{Stap}) in response to moderate (< 130 dB SPL) sound pressure levels (SPLs). This relationship, if true for higher SPLs, suggests that cochlear exposures will saturate at high SPLs. Models (e.g. the Auditory Hazard Assessment Algorithm for Humans, AHAAH), thus predict that exposures will be limited and the predicted injury lower than expected (relative to a linear increase) for high SPL exposures.

We recently reported that, for low frequency sounds (< 1 kHz), both stapes displacement and intracochlear pressures increase linearly with exposure level for moderate exposure levels (< 130 dB SPL), and saturate for high exposure levels (>130 dB SPL), but that the relationship between these measures, and thus the cochlear input impedance, remains constant and independent of level. However, the magnitudes of each response were frequency dependent, thus this constant relationship may not hold for high frequency stimuli where ossicular motion can be more complex.

In order to examine the relationship between D_{Stap} and P_{IC} to very high-level sounds, measurements of D_{Stap} and P_{IC} were made in cadaveric human temporal bones prepared by mastoidectomy and extended facial recess to expose the ossicular chain. Measurements of P_{IC} were made in scala vestibuli (P_{SV}) and scala tympani (P_{ST}), with simultaneous measurement of SPL in the external auditory canal (P_{EAC}) and laser Doppler vibrometry (LDV) measurements of stapes velocity (V_{Stap}). Stimuli were 1 second duration tone pips with frequencies between 10

Hz and 10 kHz in ¼ octave steps, presented between 125 to >160 dB SPL. Both D_{Stap} and P_{SV} increased proportionally with sound pressure level in the ear canal up to a frequency-dependent saturation point, above which both D_{Stap} and P_{SV} magnitudes saturate and acoustic transfer function magnitudes begin to decrease. However, D_{Stap} and P_{SV} responses show more complex response patterns at high levels, including substantial energy at harmonic frequencies, suggesting cochlear exposures continue to increase beyond this saturation point. Models predicting cochlear exposures that assume a firm saturation will thus underestimate cochlear exposures to high SPL stimuli.

PD 91

Examining the Efficacy of Forward-Pressure-Calibrated Activators on Wideband Measures of the Middle-Ear Muscle Reflex.

Jordan A. Beim[1]; Chhayakant Patro[1]; Magdalena Wojtczak[2]
[1]University of Minnesota; [2]Department of Psychology, University of Minnesota

The middle ear muscle reflex (MEMR) has been demonstrated to be a promising candidate in potential diagnosis of cochlear synaptopathy, the loss of connection between the inner hair cells of the cochlea and the auditory nerve fibers. MEMR strength is typically assessed by measuring changes in the middle ear response to a probe with and without a reflex activator. Wideband assays of the MEMR are preferable use when attempting to establish the link between MEMR strength and cochlear synaptopathy as they have been shown to be more sensitive than standard clinical tests that use only a single frequency probe. There is considerable variability in human MEMR measurements that may limit their diagnostic power. Some of this variability could arise from differences in the intensity of the (often broadband) MEMR activator at high frequencies due the interference caused by standing waves generated by the forward and backward reflections of sound between the tympanic membrane and the insert coupler used in the measurement of MEMR. Forward-pressure level (FPL) calibration has been shown to be an effective method in equalizing the intensity of sound presented to the cochlea across listeners. In this experiment we compare measurements of MEMR activation with and without FPL calibration in the same listeners to examine the effects this calibration may have on estimates of MEMR strength.

Measurements of wideband acoustic reflectance were made using MEMR activators that were calibrated with conventional (SPL-based) method as well as with FPL calibration in the same listener. Trains of clicks with flat spectra from 250 - 12,000 Hz were presented at 90 dB pSPL in the presence and absence of a contralateral broadband (0.5-10 kHz) MEMR activator noise. Noise levels ranged from 70-85 dB SPL/FPL. Ear canal pressure recorded during the measurements was used to estimate the change in absorbed sound power owing to the presence of the MEMR activator at each activator level.

Preliminary results indicate that the FPL calibrated MEMR activators produced greater change in absorbed power at the same stimulus level. Between-subject variability was lower when FPL calibration was used. Test-retest reliability was also examined.

The results of this study suggest that FPL calibration should be used in wideband measures of MEMR strength. Improvements to the reliability and sensitivity of the measure will benefit measurements used for group comparisons such as those in studies of cochlear synaptopathy.

Work Supported by NIH grant R01 DC015987.

PD 92

Comparison of Two Ear-Canal-Reflectance Measurement Principles in Adult Ears

Kren Monrad Nørgaard[1]; Efren Fernandez-Grande[1]; Constanze Schmuck[2]; Søren Laugesen[3]
[1]Technical University of Denmark; [2]Interacoustics A/S; [3]Interacoustics Research Unit

Applications of ear-canal reflectance have been researched extensively in recent literature. Evidence supports its use for diagnosing conductive hearing disorders and compensating for the ear-canal acoustics in non-invasive measurements of the auditory system. Existing ear-canal-reflectance measurement methods using insert ear probes are affected by multiple sources of error. One such principal error is the oblique insertion of the ear probe, that is, a misalignment relative to the ear-canal walls, and consequential errors in estimating the ear-canal cross-sectional area. Due to the lack of a reference measurement principle, the accuracy associated with current ear-canal reflectance measurements is largely unknown.

In this presentation, we compare ear-canal reflectance measurements conducted in 54 adult ear canals based on two fundamentally different measurement principles: the traditional insert ear probe and a miniature sound-intensity probe. For the traditional ear probe, we characterize the obliqueness of the various ear

insertions using a probe-fit indicator derived from the ear-probe measurements. The (p-p) sound-intensity probe is based on two microphones and the cross-spectral method for estimating the particle velocity. The sound-intensity probe is fundamentally distinguished from the ear probe by measuring sound intensity rather than sound power. Consequently, estimation of the ear-canal cross-sectional area is not needed to calculate the ear-canal reflectance from the measured quantities.

Our results across the population of test subjects generally show a reasonable agreement between the two measurement principles. However, the measurements using the sound-intensity probe appear to be affected by non-negligible errors that in many cases inundates the expected variation using the ear probe. Although our results suggest that oblique ear-probe insertions are not prevalent for typical insertions into adult ear canals, they are certainly encountered. In the seven most severe cases, identifying and compensating for the oblique insertion is crucial and results in improved agreement between ear-canal reflectances using the two measurement principles. Substantial errors when neither detecting nor compensating for these oblique insertions would otherwise go unnoticed.

PD 93

In Vitro Sound-Induced Motion of Biomimetic 3D-Printed Tympanic Membrane Grafts

Marta Pawluczuk[1]; Nicole Black[2]; Elliott D. Kozin[3]; Aaron K. Remenschneider[4]; Jeffrey Cheng[5]
[1]Undergraduate Research Assistant; [2]John A. Paulson School of Engineering and Applied Sciences, Harvard University; [3]Massachusetts Eye and Ear Infirmary-Harvard University; [4]Dept. of Otolaryngology, UMass Memorial Medical Center; Massachusetts Eye and Ear; [5]Eaton-Peabody Laboratory, Massachusetts Eye and Ear Infirmary,Department of Otolaryngology – Head and Neck Surgery, Harvard Medical School

Background
The tympanic membrane (TM) contains circular and radial collagen fibers in the lamina propria that have been shown to be crucial for sound conduction at both low and high frequencies. Unfortunately, both autologous and non-autologous TM graft materials do not remodel into a circular and radial architecture after TM reconstruction surgery. A TM graft with optimized architecture to mimic the native TM fiber arrangement may result in improved low and high frequency hearing.

Methods
TM grafts were 3D-printed with a novel Bio-ink developed by our group in the following architectures: 50 circular lines (50C), 50 circular and 25 radial lines (50C/25R), and 50 circular and 50 radial lines (50C/50R). Porcine submucosa (Biodesign® Otologic Repair Graft) was used as a control material. Six of each experimental and control grafts were tested. Sound-induced motion of grafts between 25 and 25,000 Hz was determined using digital opto-electronic holography (DOEH) and laser Doppler vibrometry (LDV).

Results:
Digital Opto-Electronic Holography: All graft types show a progression of motion patterns from simple to complex as frequency increases. Biodesign® grafts tend to vibrate more at low frequencies (< 3000 Hz) but do not vibrate consistently, while the 50C grafts tend to vibrate the least at most frequencies among all graft types. The 50C/25R and 50C/50R grafts show similar simple motion patterns below 3000 Hz, but different complex motion patterns at high frequencies. The 50C/50R grafts show overall larger displacement normalized by sound pressure at most measured frequencies.

Laser Doppler Vibrometry: Biodesign®, 50C, and 50C/25R grafts showed relatively similar normalized velocity with multiple resonance peaks in the range of 1,000-5,000Hz. The 50C/50R grafts vibrated at significantly higher velocities, particularly at high frequencies (>10,000 Hz), and had one main resonance peak around 2,000 Hz.

Conclusion
By mimicking the circular and radial architecture of the native TM, we observed different sound-induced vibration patterns of the grafts. Our results suggest the 50C/50R structure produces the most vibration across both low (via the grafts vibrating with a single mode as a “soft” sheet) and high frequencies (via the grafts exhibiting multiple complex motion patterns as a reinforced, “stiff” sheet), consistent with the native TM fiber arrangement plays a role for sound conduction across a broad frequency. Analysis of the acoustic properties of *in vivo* grafts is currently underway.

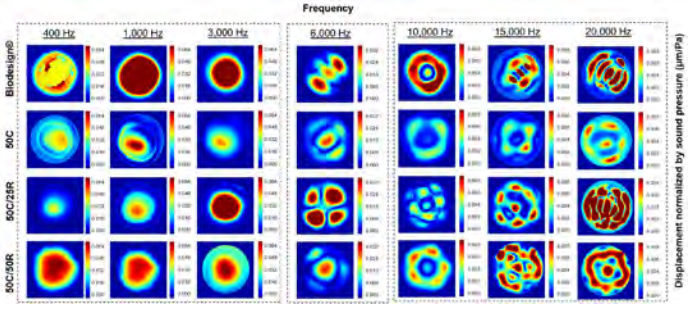

PD 94

Otopathologic Changes of the Incudomalleolar Joint in Patients with Rheumatoid Arthritis

Melissa Castillo-Bustamante[1]; Marc Polanik[2]; Dhrumi Gandhi[1]; Elliott D. Kozin[1]; Aaron K. Remenschneider[3]
[1]Massachusetts Eye and Ear Infirmary- Harvard University; [2]Massachusetts Eye and Ear Infirmary-Harvard University; [3]Dept. of Otolaryngology, UMass Memorial Medical Center; Massachusetts Eye and Ear

Objective
Rheumatoid arthritis (RA) is an autoimmune condition that results in chronic inflammation of synovial joints. Conductive hearing loss is commonly observed early in the disease; however, little is known about why this occurs or whether the small synovial incudomalleolar joint (IMJ) is affected by rheumatic change. Herein, we otopathologically analyze the IMJ and calculate the 3-dimensional joint volume in patients with RA, comparing findings to age-matched controls.

Study design
Otopathologic analysis of human specimens from a temporal bone repository

Method
The National Temporal Bone Database was reviewed for cases with RA during life. Specimens were examined under light microscopy, histopathologically described, and volumetric measurements of the IMJ synovial space were obtained after three-dimensional reconstruction. Available audiometric data was reviewed.

Results
Twenty ears with RA and 10 non-pathologic control ears were identified. Mean age was not significantly different between groups: 65.3 for RA, and 69.3 for controls, (p=0.441). Females comprised 75% of RA patients, while normal controls were 80% female. Histologic findings in patients with RA included: chronic synovial inflammation, diminished ossicular blood supply, demineralization of the incus and malleus at the IMJ articulation and fibrillation of the articular cartilage. None of these findings were present in normal controls. In patients with RA, the mean synovial space volume in RA was 0.030 mL (range 0.001 -0.043; SD 0.008, median 0.032). Control specimens demonstrated a mean synovial space volume of 0.074 mL (range 0.026 -0.371, SD 0.105, median 0.039). A trend towards smaller synovial space in RA was observed (p=0.0730). Nine RA patients had audiograms, eight of them with symmetric bilateral moderate to severe sensorineural hearing loss (SNHL), affecting high frequencies. One patient had bilateral conductive hearing loss. Five control ears had audiograms, all of them demonstrated normal thresholds.

Conclusions
Patients with RA have clear evidence of chronic inflammation within the IMJ. The synovial space of the RA group demonstrated a trend towards being smaller than controls. Further study using immunohistochemistry is needed to better understand the extent and type of synovial inflammation. Clinical correlation is necessary to determine the functional impact of IMJ inflammation.

PD 95

Middle-Ear Sound Transmission under Static Pressure Change in Humans

Birthe Warnholtz[1]; Ivo Dobrev[2]; Benjamin Sackmann[3]; Michael Lauxmann[4]; Alexander Huber[2]; Jae Hoon Sim[2]
[1]University Hospital Zurich; [2]Department of Otorhinolaryngology, Head and Neck Surgery, University Hospital Zurich, Zurich, Switzerland; University of Zurich, Zurich, Switzerland; [3]Hochschule Reutlingen / Universität Stuttgart; [4]Hochschule Reutlingen

Unique anatomical features of the human middle ear, such as the flexible incudomalleal joint, contribute to adaptation to circumferential static pressure change and thus protection of the inner ear. Therefore, there have been efforts to mimic such adaptive and protective functions in surgical reconstructions with middle-ear prostheses. However, while position change of the middle-ear ossicular chain under static pressure change was examined in previous studies, it has not been revealed clearly how the unique anatomical features of the human middle ear react to the static pressure change during middle-ear sound transmission. This study aims to investigate middle-ear sound transmission in humans, which is directly related to hearing perception, under static pressure change.

Experiments were carried out in human cadaveric temporal bones, using a custom-made static pressure system. Static pressure in the range of +/- 4 kPa was applied to the tympanic membrane over an artificial ear canal via a pump and closely controlled by a manometer. Then, acoustical stimulation in the frequency range of 0.25-10 kHz was applied via a loudspeaker and the dynamic motion of the stapes footplate was measured using a 3D-Laser Doppler vibrometer. Subsequently, the incudomalleal joint was immobilized with glue and dental cement, and the measurement was repeated.

The results showed that the middle-ear sound transmission decreased at low frequencies below 2 kHz. The degradation of the middle-ear sound transmission was larger for negative static pressures. Significant phase shifts with static pressure changes were not observed for both mobile and immobile incudomalleal

joint. With immobilization of the incudomalleal joint, similar trends were observed but the magnitude of the degradation became smaller.

Considering the results, the anatomical feature of the human middle ear are presumed to minimize change of middle-ear sound transmission as well as static position change of the middle-ear ossicular chain under circumferential static pressure change. Further investigation is expected to integrate such adaptive functions of the human middle ear into surgical reconstructions.

PD 96

Vibration measurements of the gerbil eardrum under pressure sweeps

Orhun Kose; W. Robert J. Funnell; Sam J. Daniel
McGill University

Tympanometry is a relatively simple non-invasive test of the status of the middle ear. An important step toward understanding the mechanics of the middle ear during tympanometry is to make vibration measurements on the eardrum under tympanometric pressures. Our previous studies included post-mortem and in-vivo vibration measurements at several points on the gerbil eardrum, showing the frequency response and the effects of quasi-static pressure steps.

In this study, we measured vibration responses under both pressure steps and pressure sweeps. Vibrations were recorded using a single-point laser Doppler vibrometer with five glass-coated reflective beads (diameter ~40 μm) as targets placed at points on the manubrium, pars tensa and pars flaccida. Vibration magnitudes and peak frequencies are compared between the step cycles and sweep cycles. The repeatability of consecutive pressure sweep cycles is presented, as well as interspecimen variability. The results of this study provide insight into the mechanics of the gerbil middle ear under tympanometric pressures.

Neuroplasticity and Tinnitus - In Memory of Dr. Larry E. Roberts

Chairs: Susan E. Shore & Victoria M. Bajo

SYMP 94
Introduction and Tribute to Larry Roberts

Richard Salvi
Center for Hearing and Deafness, 137 Cary Hall
University at Buffalo, Buffalo, NY 14214

Larry Roberts had a long and distinguished career in auditory neuroscience that he pursued with a passion until his passing at age 81. His research during the past two decades focused on the neural correlates of tinnitus and the role of neuroplasticity. Although he was an emeritus professor at McMaster University, he maintained an active research lab, continued to mentor Ph.D. and post-docs, and recently co-edited a special Issue in Neuroscience on tinnitus, hyperacusis, central gain and hidden hearing loss. He will be remembered for collaborative, kind and supportive spirit and his enthusiasm for science.

SYMP 95

Homeostatic and Timing-Dependent Plasticity following Cochlear Damage and their Association with Tinnitus in Animal Models

Susan E. Shore
University of Michigan

Fusiform cells of the dorsal cochlear nucleus (DCN), integrate cochlear inputs with multiple multimodal pathways. Following noise exposure, fusiform cells in animals with behavioural evidence of tinnitus show best-frequency-specific increases in spontaneous firing and synchronization. Conversely, animals without evidence of tinnitus do not show these physiological signatures in spite of equivalent cochlear damage. These data suggest that hearing loss, whether visible or 'hidden', is insufficient by itself to produce a tinnitus phenotype. Changes in cochlear output after noise exposure require accompanying neuro-plastic changes in recipient neurons in the cochlear nucleus to result in physiological and behavioural signatures of tinnitus.

SYMP 96

Neural plasticity following Restricted Cochlear Deafferentation and Optogenetic Silencing of the Auditory Cortex.

Victoria Bajo
University of Oxford

To investigate cortical plasticity after peripheral lesions, recordings were performed in the auditory cortex bilaterally in ferrets with unilateral, restricted spiral ganglion lesions. Gap-in-noise operant behaviour showed lesion-induced hetereogeneous outcomes with some ferrets displaying temporal processing impairments compatible with tinnitus and others showing post-lesion adaptation. Analysis of cortical cells showed evidence for lesion-related central neuroplasticity that correlated with each animal's behavioural phenotype. Optogenetic silencing of contra-lesioned auditory cortex neurons reverted specific behavioural changes. Our results suggest that primary auditory cortex plays an important role in mediating deafferentation-related neuroplasticity, suggesting possible strategies for remediation of the maladaptive processing potentially underpinning tinnitus.

SYMP 97

Auditory Thalamus and Tinnitus

Don M. Caspary
Southen Illinois University School of Medicine

Tinnitus, defined as a phantom sound, severely impacts the quality of life in a subset of the general population with tinnitus. Noise exposure is the most common cause of tinnitus resulting in partial peripheral deafferentation and numerous maladaptive plastic changes of the central auditory pathway. We examined two neurotransmitter systems important in the pathophysiology of tinnitus in auditory thalamus and auditory cortex. Complex, tinnitus-related changes in inhibitory GABA neurotransmission in established animal models support a role for GABA in maladaptive gain control. Synaptic pharmacologic changes in cholinergic neurotransmission may underpin attentional changes observed in tinnitus models and human sufferers.

SYMP 98

Measures of Tinnitus-Related Plasticity in Humans

Brandon T. Paul
Sunnybrook Research Institute

Tinnitus is believed to arise from forms of neural plasticity occurring in the auditory system following deafferentation due to noise exposure, aging, or ototoxic drugs. One of Larry Roberts' many contributions was to investigate neuroplastic changes in humans with tinnitus using sound-evoked potentials. I will summarize our work describing how evoked potentials in tinnitus differ from non-tinnitus controls, and depend on attention, auditory training, forward masking (residual inhibition), and the frequency region in which potentials are evoked. Findings overall suggest that disinhibition of cortical networks plays a role in these changes and possibly contributes to tinnitus perception.

SYMP 99

Residual Inhibition and Tinnitus in Animal Models

Alex Galazyuk
Northeast Ohio Medical University

Tinnitus can be briefly reduced by a sound, the phenomenon known as "residual inhibition" (RI). Although RI was first described more than 100 years ago (Spaulding, 1903) the underlying mechanisms remain unknown. Sounds suppress spontaneous firing in auditory neurons. Hyperactivity, or elevated spontaneous firing in the auditory system has been linked to tinnitus. Therefore, suppression of this activity by a sound can explain RI. Metabotropic glutamate receptors (mGluRs) play a key role in the suppression of spontaneous firing. An mGluR-targeted drug applied systemically suppresses both spontaneous activity in auditory neurons for several hours and also reduces tinnitus in mice.

SYMP 100

Reconciling Animal Studies with Tinnitus in Humans

Jos Eggermont
University of Calgary

Animal research in tinnitus has made great strides, and so have results obtained in humans. However, where animal studies typically cover the afferent pathway up to auditory cortex, human neuroimaging rarely covers subcortical activity. Important differences are that animal studies favour inducing TTS, and study tinnitus free of hearing loss confounds. In humans, the majority of cases have PTS and comorbidities confound the picture. Yet, in early tinnitus neural connectivity studies point to activity in auditory cortex, likely reflecting subcortical generators, whereas in long-standing tinnitus, changes in the parahippocampal area are consistently found. There is definitely room for convergence.

The Newborn Hearing Screen - Its History -Where We Are-and Where We Should Be Going

Chairs: Jun Shen & Richard Smith

SYMP 101

Lessons Learned from 30 Years of Universal Newborn Hearing Screening

Karl White
Utah State University

The benefits of identifying childhood hearing loss during the first few months of life have been recognized since the 1940's. It was not until the 1990's that technology evolved to the point that universal newborn hearing screening became practical and had reasonable outcomes. However, a number of challenges and opportunities for improvement remain. This presentation will summarize the history of newborn hearing screening, describe the current status around the world (with particular emphasis on the United States), and discuss the most important challenges and emerging issues that could be addressed to further improve early identification of childhood hearing loss.

SYMP 102

National Coordination Center Newborn Hearing Screening Work Group Consensus and Plan to Implement Genetic Screening in the United States

Richard Smith
University of Iowa

Early intervention for newborns born deaf or hard-of-hearing leads to improved language, communication and social-emotional outcomes. To identify these babies, universal physiologic hearing screening has been implemented in many countries. Its use has been very successful in identifying hearing-impaired babies however the incorporation of genetic and congenital cytomegalovirus screening into the testing algorithm improves detection of at-risk babies. We present a framework for integrating genetic testing and cytomegalovirus screening into the current newborn hearing screening and highlight challenges that will be faced as more comprehensive screening strategies are adopted.

SYMP 103

Nationwide Population Genetic Screening Improves Outcomes of Newborn Screening for Hearing Loss in China

Jun Shen
Harvard Medical School

Over 1.2 million newborns in China were screened for 20 hearing-loss-related genetic variants from 2012 to 2017. Genetic results were categorized as positive, at-risk, inconclusive, or negative. Hearing screening results, risk factors, and up-to-date hearing status were followed up via phone interviews. Follow up of 12,778 babies with non-negative results revealed that incorporating genetic screening improves the effectiveness of newborn hearing screening programs by elucidating etiologies, discerning high-risk subgroups for vigilant management, identifying additional children who may benefit from early intervention, and informing at-risk newborns and their maternal relatives of increased susceptibility to ototoxicity.

SYMP 104

Concurrent Hearing and Genetic Screening of 180,469 Neonates with Follow-up in Beijing, China

Pu Dai
PLA General Hospital

Concurrent hearing and genetic screening of newborns is expected to play important roles not only in early detection and diagnosis of congenital deafness, triggering intervention, but also in predicting late-onset and progressive hearing loss and identifying individuals who are at risk of drug-induced hearing loss. Concurrent hearing and genetic screening in the whole newborn population in Beijing was launched in January 2012. This study included 180,469 infants born in Beijing between April 2013 and March 2014, with last follow-up on February 24, 2018. Hearing screening was performed using TEOAE and AABR. For genetic testing, dried blood spots were collected and nine variants in four genes, GJB2, SLC26A4, mtDNA 12S rRNA and GJB3, were screened using a DNA microarray platform. Of the 180,469 infants, 1,915 (1.06%) were referred bilaterally or unilaterally for hearing screening; 8,136 (4.508%) were positive for genetic screening (heterozygote/homozygote/compound heterozygote and mtDNA homoplasmy/heteroplasmy), among whom 7,896 (4.375%) passed hearing screening. Forty (0.022%) infants carried two variants in GJB2 or SLC26A4 (homozygote or compound heterozygote), 10 of whom passed newborn hearing screening. In total, 409 (0.227%) infants carried the mtDNA 12S rRNA variant (m.1555A>G or m.1494C>T), and 405 of them passed newborn hearing screening. In this cohort study, 25% of infants with pathogenic combinations of GJB2 or SLC26A4 variants, and 99% of infants with an m.1555A>G or m.1494C>T variant, passed routine newborn hearing screening, indicating that concurrent screening provides a more comprehensive approach for management of congenital deafness and prevention of ototoxicity.

SYMP 105

The Value of Genetic Screening: Lessons Learned in CMV Positive Screening and Followed by Genetic Testing

Joseph Peterson
University of Iowa

Based on physiologic hearing screen results, reflexive deafness-targeted congenital cytomegalovirus (CMV) testing has become more prevalent in an effort for earlier diagnosis. Current treatment for congenital CMV with hearing loss is an extended course of antiviral medication with a significant risk of neutropenia. We present illustrative examples of deaf children screened for CMV who also underwent genetic testing. One child, initially diagnosed with CMV-related hearing loss and started on antiviral treatment, was diagnosed with GJB2-related hearing loss. His antiviral treatment was subsequently discontinued. Another child diagnosed with CMV was found to have a pathogenic variant in CDH23, a gene often implicated in Usher syndrome. For a child with bilateral congenital deafness, genetic testing is four times more likely than CMV screening to yield a positive result. In children who have a genetic cause of hearing loss, antiviral treatment caries risk with minimal treatment benefit. We calculate based on prevalence

data that ~2% of CMV-positive hearing loss patients have a genetic etiology. A sub-cohort of CMV-positive patients with symmetric mild-to-moderate bilateral hearing loss will have a >7% chance of having genetic hearing loss. After an initial physiologic newborn hearing screen, a combination of targeted CMV and genetic hearing screening would provide higher diagnostic yield, better prognostic information, allow for meaningful genetic counseling and avoid of unnecessary treatment.

SYMP 106

Sequencing a Baby for an Optimal Outcome: A Genomic Future for Newborn Screening

Anne Giersch
Brigham and Women's Hospital, Harvard Medical School

SEQaBOO (SEQuencing a Baby for an Optimal Outcome) is a research project integrating high-throughput genomic approaches into routine newborn screening. In this project, we are testing the hypothesis that rapid discovery of the etiology of a newborn's hearing impairment via whole genome sequencing will benefit clinical management of an infant with congenital hearing loss.

The SEQaBOO project will enroll approximately 500 newborns who do not pass their newborn hearing screen along with their biological parent(s) (trios) from three Boston hospitals: Brigham and Women's Hospital, Boston Children's Hospital, and Massachusetts Eye and Ear. Active enrollment began in July 2018, and to date over 100 families have been enrolled. Genetic information pertinent to the infant's hearing will be returned to the child's otolaryngologist. Annual surveys will ascertain general health, including speech and language development, in addition to hearing status, and parental attitudes toward genomic sequencing. Parents may choose to participate in the annual surveys only, and not receive genomic sequencing. In addition, parents will be offered the option of receiving for themselves results from the American College of Medical Genetics and Genomics recommended list of genes (ACMG59) with potential high medical importance. Positive results from the ACMG59 list will be communicated to the individual's primary care physician. All negative results are communicated to the parents via telephone.

Approximately 70% of families approached to date have agreed to participate in the study. Turn-around time is approximately one month for genomic sequencing and variant analysis of a list of several hundred hearing loss related genes and the ACMG59 genes (if the parents opted in). Currently, only sequence variants are being assessed, but we are working to integrate protocols for copy number variant calls and infectious agent detection such as CMV.

In summary, SEQaBOO aims to analyze and assemble genomic datasets, perform clinical genomic research of hearing impairment identifiable through newborn screening, and explore implications of integration of genomic sequencing into newborn screening. The goal is to identify barriers to adopting genome sequencing and to establish best practices for integrating genome sequencing into routine newborn care in the future.

Regeneration

PD 97

High Resolution Characterization of Transcriptional Responses during Zebrafish Hair Cell Regeneration

Sungmin Baek; Daniel Diaz; **Tatjana Piotrowski**
Stowers Institute for Medical Research, Kansas City, MO

Non-mammalian organisms such as fish and frogs regenerate hair cells in the inner ear and the sensory lateral line throughout life. In zebrafish the regenerative response is particularly fast and relatively synchronized. To begin to elucidate how hair cell regeneration is triggered and characterize the gene regulatory network underlying zebrafish hair cell regeneration we performed single cell RNASeq analyses of lateral line cells. We recently published a scRNASeq analysis of homeostatic neuromasts which identified six different support and hair cell populations in a sensory organ (Lush, Diaz et. al 2019). Here we characterize the transcriptional responses of different cell types to hair cell death at 0min, 30min, 1h, 3hs, 5hs and 10hs after hair cell loss. The 0min – 1h time points are markedly different from the 3hs – 10hs time points and the 0min time point is distinct from the 30min and 1h time points. These time points revealed when the transcriptional responses switch from an injury response to regeneration and hair cell differentiation responses. As we know the identity of all cell types we were also able to determine which cell types are likely communicating with each other and which transcriptional responses are cell type specific versus a more systemic response. The speed and synchronization of hair cell regeneration in the zebrafish allowed us to characterize the transcriptional changes in unprecedented temporal and cellular detail, which will help the field to interrogate which of these responses also occur in mammals and which ones fail to be triggered.

PD 98

Ototoxic Damage Induces Interferon Signaling in Chicken Cochlear Epithelial Supporting Cells

Amanda Janesick[1]; Mirko Scheibinger[1]; Nesrine Benkafadar[2]; Stefan Heller[1]
[1]Department of Otolaryngology–HNS, Stanford University; [2]Stanford University School of Medicine

The fragility of the auditory sensory epithelium is observed across all chordates, however, many non-mammalian species, such as the chicken, have repair and regeneration mechanisms to fully restore hearing after damage. We have established a reliable, in vivo damage model in the post-hatch day 7 chicken by infusing a single dose of sisomicin via the posterior semi-circular canal. Hair cell extrusion and death occurs quickly within 1 day across the entire tonotopic axis of the chicken cochlea. Proliferation in the supporting cell layer exhibits a sharp peak within the first 36-48 hours of regeneration, occurring predominantly on the neural, afferent side of the epithelium. Here we report results from bulk RNA-seq at 48 hours, and single cell RNA-seq at 30, 38, 48, and 96 hours post-sisomicin, in vivo. Bioinformatic analysis and validation by in situ hybridization has identified interferon and cytokine signaling as a unique pathway that has never before been implicated in hair cell regeneration. Interferon inducible and regulator factors typically control immune responses and are almost always expressed in macrophages. However, we do not find evidence of macrophage infiltration, rather, that interferon-inducible genes are up-regulated in proliferating supporting cells. We have concluded that these epithelial supporting cells are behaving as non-professional, macrophages, hijacking immune genes for the purpose of regeneration. Uncovering the mechanism underlying regeneration in birds will bring us closer to the goal of identifying and unearthing rudimentary parts of the regenerative machinery in mammals.

PD 99

Cross-Species Analysis of Gene Regulatory Networks Underlying Hair Cell Regeneration

Gurmannat Kalra[1]; Brian Herb[1]; Nesrine Benkafadar[2]; Amanda Janesick[3]; Beatrice Milon[4]; Kevin Rose[5]; Mirko Scheibinger[3]; Michael Lovett[6]; Tatjana Piotrowski[7]; Stefan Heller[3]; Ronna Hertzano[8]; Neil Segil[9]; Seth Ament[10]; Peter G. Barr-Gillespie[11]; Hearing Restoration Project[12]
[1]University of Maryland, Baltimore; [2]Stanford University School of Medicine; [3]Department of Otolaryngology–HNS, Stanford University; [4]Department of Otorhinolaryngology-Head and Neck Surgery, University of Maryland; [5]University of Maryland School of Medicine; [6]National Heart and Lung Institute, Imperial College London, London, United Kingdom; [7]Stowers Institute for Medical Research, Kansas City, MO; [8]Department of Otorhinolaryngology Head and Neck Surgery, University of Maryland School of Medicine; Institute for Genome Sciences, University of Maryland School of Medicine.; [9]Department of Stem Cell Biology and Regenerative Medicine, Keck School of Medicine of USC, and USC Caruso Department of Otolaryngology – Head and Neck Surgery; [10]University of Maryland School of Medicine Baltimore, Maryland; [11]Oregon Hearing Research Center & Vollum Institute, Oregon Health & Science University; [12]Hearing Health Foundation

A therapeutic approach to restoration of hearing in those who have lost this ability due to age, noise damage, or ototoxic drug exposure requires regeneration of missing hair cells from cells remaining in the cochlea. Hair-cell regeneration is well known to be robust in non-mammalian vertebrates, including birds and fishes. By contrast, spontaneous regeneration in mammals—including mice and humans—does not occur, except for limited numbers of hair cells appearing after certain experimental manipulations. The Hearing Restoration Project (HRP), funded by the Hearing Health Foundation, aims to develop methods to regenerate hair cells in mammals. As part of this strategy, here we present an integrated analysis of transcriptomic and epigenomic data -- including multiple newly generated datasets -- comparing the damage responses of sensory epithelial cells in hearing organs that show regeneration (chick, zebrafish) to those that do not (mouse). We reconstructed gene regulatory networks active in the hearing organs of chick, zebrafish, and mouse based on single-cell transcriptomics data from each species, and we validated these models using ATAC-seq and ChIP-seq from sorted mouse sensory epithelial cells. We then explored transcriptional network dynamics during naturally occurring damage-induced hair-cell regeneration in chicken cochlea, chicken utricle, and zebrafish lateral line, and DAPT-induced trans-differentiation of dissociated supporting cells from the mouse cochlea into hair cells. In addition, we characterized transcriptional networks that are active specifically in subsets of cochlear supporting cells from neonatal mice, which have a limited capacity for trans-differentiation to hair cells. Our analyses revealed numerous transcription factors that are activated specifically in conditions associated with hair-cell regeneration. Identifying gene regulatory networks that respond to damage in species with hair-cell regeneration but that do not respond in those lacking regeneration will assist in targeting key pathways regulating regeneration.

PD 100

LATS, YAP, and TEAD Control of Proliferation in the Ear

Mark A. Rudolf[1]; Mikolaj M. Kozlowski[2]; Jeffrey T. Corwin[1]
[1]University of Virginia; [2]Washington University in St. Louis

Background
An emerging paradigm in epithelial repair specifies that upon damage, YAP is dephosphorylated and accumulates in nuclei of stretched cells, where it promotes proliferation with TEAD transcription factors. We investigated whether this principle governs supporting cell (SC) proliferation during the regenerative replacement of hair cells (HCs) in non-mammalian vertebrates. We also tested whether inhibitory phosphorylation of YAP by the Hippo kinase cascade (MST1/2 and LATS1/2) restricts proliferation of SCs in mammals.

Methods
To test whether HC loss or disruption of the Hippo pathway modifies the nuclear accumulation of YAP in SCs, we cultured utricles from chickens and neonatal mice with streptomycin or the MST1/2 inhibitor XMU-MP-1 and measured the nuclear:cytoplasmic intensity ratio of YAP immunostaining. To circumvent the inhibitory phosphorylation of YAP, we generated *Yap-S127A$^{+/-}$;Sox10$^{rtTA/+}$* mice and administered doxycycline intraperitoneally to overexpress the phosphorylation-insensitive YAP-S127A *in vivo*. The inducing injection was given at P1, P3, P5, or P9, with EdU administered for three days after induction and fixation one day later. Additionally, we cultured utricles from P1 and P30 *Lats1$^{flox/flox}$; Lats2$^{flox/flox}$* mice and used adenovirus to transduce SCs with mCherry or mCherry-T2A-Cre.

Results
In chicken utricles, HC loss significantly increased the nuclear:cytoplasmic intensity ratio of YAP in SCs (0.94±0.05 vs 0.77±0.02 in undamaged controls, p< 0.0001). The nuclear:cytoplasmic ratio of YAP also increased after MST1/2 inhibition (1.14±0.10 vs 0.83±0.07, p=0.0006). The small molecule YAP-TEAD inhibitor CA3 attenuated regenerative proliferation in a dose-dependent manner (p=0.0010, ANOVA). However, neither HC loss (0.89±0.11 vs 0.89±0.10, p=0.9818) nor MST1/2 inhibition (0.90±0.04 vs 0.90±0.11, p=0.9858) appeared to affect YAP localization in P1 mouse utricles.

In vivo overexpression of YAP-S127A in P1 mouse utricles increased proliferation 35-fold over littermate controls (97±54 EdU+ cells/10,000 μm^2 vs 3±2, p< 0.0001). When YAP-S127A overexpression was induced at P3, P5, and P9, the EdU+ SCs declined to 57±11, 26±22, and 3±2 cells/10,000 μm^2, respectively. Conditional knockout of LATS1/2 in cultured mouse utricles reduced phospho-YAP (S127) levels in SCs and increased proliferation over littermate controls by 40-fold at P1 (240±145 EdU+ cells/utricle vs 6±3, p=0.0180) and 9-fold at P30 (17±21 vs 2±3, p=0.0393), with most EdU+ SCs located in the striola.

Conclusions
In the chicken utricle, nuclear accumulation of YAP is regulated by the canonical MST1/2-LATS1/2 kinase cascade. In the mouse utricle, MST1/2-independent, LATS1/2-mediated phosphorylation of YAP is required for SC quiescence, even in adults. However, proliferation is restricted by additional age-related changes that occur downstream or in parallel.

PD 101

Ablation of Lgr5+ Cochlear Supporting Cells Induces Mitotic Regeneration by the Greater Epithelial Ridge

Tomokatsu Udagawa[1]; Beatrice Milon[2]; Patrick Atkinson[3]; Yang Song[4]; Elvis Huarcaya Najarro[3]; Mirko Scheibinger[5]; Ronna Hertzano[6]; Alan Cheng[3]
[1]Stanford University; [2]Department of Otorhinolaryngology-Head and Neck Surgery, University of Maryland; [3]Department of Otolaryngology-Head and Neck Surgery, Stanford University; [4]Institute for Genome Sciences, University of Maryland; [5]Department of Otolaryngology–HNS, Stanford University; [6]Department of Otorhinolaryngology Head and Neck Surgery, University of Maryland School of Medicine; Institute for Genome Sciences, University of Maryland School of Medicine.

Background
Supporting cells are glial-like cells essential for cochlear maturation and function. Marked by the Wnt target gene Lgr5, supporting cell subtypes in the neonatal cochlea can serve as hair cell progenitors. Prior studies in the neonatal cochlea show that supporting cell subtypes are also spontaneously regenerated. This suggests the presence of a pool of progenitor cells for supporting cells, of which the identity and characteristics have not been clearly defined. Here we have established a model of supporting cell ablation using the Lgr5$^{DTR-EGFP/+}$ mice and used fate-mapping approaches to delineate the source of regeneration.

Methods
Lgr5$^{DTR-EGFP/+}$ mice were injected with diphtheria toxin (DT) at P1 to selectively delete Lgr5$^+$ cochlear supporting cells and EdU at P3-5 or P7-9 to detect proliferation. Cochleae were harvested for histological analysis at

P3-21. Immunostaining and in situ hybridization were performed for various markers of supporting cells. Lgr5$^{DTR\text{-}EGFP/+}$; Pax2-Cre mice were crossed with Atoh1-mCherry; Rosa26R$^{GCaMP3/+}$ mice for calcium imaging. For fate-mapping, Lgr5$^{DTR\text{-}EGFP/+}$; Rosa26R$^{tdTomato/+}$ mice were crossed with Plp1$^{CreER/+}$, GLAST$^{CreER/+}$, or Sox2$^{CreERT2/+}$ mice. To induce Cre recombination, tamoxifen was administered at P1.

Results

After DT injection at P1, P4 Lgr5$^{DTR\text{-}EGFP/+}$ cochleae showed markedly reduced Lgr5-EGFP expression and degeneration of supporting cell subtypes: inner phalangeal cells (IPhCs), pillar cells (PCs) and Deiters' cells (DCs). There was also robust proliferation as marked by EdU^{+} Sox2^{+} cells in the lateral greater epithelial ridge (GER). Between P7-21, PCs and DCs remained degenerated, whereas IPhCs were completely replenished and many were EdU-labeled, indicating mitotic regeneration. P7 regenerated cochleae showed spontaneous calcium activity spanning the IPhC and GER regions, suggesting coordination among regenerated cells. At P14 and P21, regenerated IPhCs expressed GLAST and Na/K-ATPase-β1 indicating maturation. To determine the source of regenerated IPhCs, we fate-mapped the various supporting cell subtypes of the cochlea: IPhCs, PCs, DCs, and GER cells after ablation of Lgr5^{+} supporting cells. We first labeled IPhCs using Plp1-tdTomato mice and found that marked IPhCs completely disappeared with no replenishment, suggesting that Plp1^{+} IPhCs do not self-regenerate. In contrast, both Sox2-tdTomato^{+} (IPhCs, PCs, DCs and GER) and GLAST-tdTomato^{+} (IPhCs and GER) cells were EdU-labeled and replaced lost IPhCs at P7 and P14, suggesting that GER cells proliferate in response to supporting cell loss and migrate to replenish IPhCs.

Conclusions

Collectively these findings demonstrate that the GER contains a population of damage-activated supporting cell progenitors.

Funding

California Initiative in Regenerative Medicine RN3-06529; NIH/NIDCD RO1DC013910; R01DC013817; Akiko Yamazaki and Jerry Yang Faculty Scholarship, Department of Defense MR130316.

PD 102

Conditional Inactivation of LSD1 Promotes Atoh1-mediated Hair Cell Conversion in Mouse Cochleae

Yan Zhang[1]; Huizhan Liu[2]; Sarath Vijayakumar[2]; Cassidy Nguyen[3]; David Z. He[2]; **Jian Zuo**[4]
[1]Creighton University School of Meidicne; [2]Creighton University School of Medicine; [3]Creighton University; [4]Department of Biomedical Science, Creighton University

Overexpression of Atoh1 in non-sensory supporting cells (SCs) in mouse cochleae induced SC conversion to hair cells (HCs) in vivo. However, the conversion efficiency is low and declines with age; the converted HCs remain immature. To increase the efficiency and completion of Atoh1-mediated HC conversion, we conditionally inactivated Lysine Specific Demethylase 1 (LSD1), a cofactor of nucleosome remodeling demethylase (NuRD) which is commonly associated with gene repression and involved in regulating cell lineage fate. In cochlear SCs we first activated the CreER recombinase by tamoxifen at P0/P1 to delete one or both copies of the LSD1 gene in the Lgr5CreER; LSD1flox; Atoh1-HA mouse line. The HC conversion efficiency was analyzed at P35 to P60 by immunofluorescent staining of the organs of Corti for Atoh1-HA and Myosin VIIA. Within those newly converted HCs (cHCs), ~50% expressed vGlut3, otoferlin, and Slc7a14 (a transporter protein that specifically express in postnatal inner HCs). cHCs also displayed outward currents and stereocilia under scanning electron microscopy (SEM). Single cell RNA seq was performed to identify LSD1-Atoh1 downstream genes that can promote conversion and maturation of cHCs in vivo. Our results demonstrated that the loss of LSD1 gene together with ectopic expression of Atoh1 increased HC conversion efficiency and maturation.

Supported in part by NIHR01DC015010, NIHR01DC015444, ONR-N00014-18-1-2507, USAMRMC-RH170030, and LB692/Creighton.

PD 103

LIN28B Controls the Regenerative Capacity of Cochlear Supporting Cells

Xiaojun Li[1]; Angelika Doetzlhofer[2]
[1]Johns Hopkins University School of Medicince; [2]Johns Hopkins University

Mechano-sensory hair cell located within the inner ear cochlea are critical for our ability to detect sound. In humans and other mammals, cochlear hair cells are only produced once during embryonic development and hair cell loss due to aging, disease or trauma is a leading cause for hearing impairment and deafness. Remarkably, non-mammalian vertebrates such as fish, amphibians and birds are capable of regenerating hair cells throughout their life-time. These newly generated hair cells are produced by neighboring supporting cells through both mitotic and non-mitotic mechanisms. Interestingly, cochlear supporting cells in newborn mice

are capable of regenerating hair cells in response to regenerative cues (e.g. hair cell damage, Notch inhibition). However, such regenerative capacity (plasticity) sharply declines within the first postnatal week and little to no hair cell regeneration is observed in cochlear tissue of postnatal day 5 (P5) pups. What causes the sharp drop in supporting cell plasticity during the first postnatal week is currently unknown. Here we demonstrate a causal link between the cochlear supporting cell plasticity and LIN28B-mTOR activity. The RNA binding protein LIN28B is a well-known activator of stemness and its re-expression has been recently shown to enhance hair cell regeneration in neonatal cochlear tissue. Employing cochlear organoid and explant cultures, we show that re-expression of LIN28B restores the regenerative capacity of stage P5 supporting cells. Conversely, we find that conditional ablation of Lin28a/b accelerates the decline in regenerative capacity, rendering P2 supporting cells unresponsive to mitotic and regenerative stimuli. Finally, we provide evidence that LIN28B promotes supporting cell plasticity, at least in part, through enhancing mTOR signaling. In particular, we show that treatment with rapamycin, a selective mTOR inhibitor, abolished the LIN28B-mediated gain in hair cell regeneration in P5 organoid and cochlear explants. Future studies will examine whether reactivation of LIN28B-mTOR signaling is sufficient to restore supporting cell plasticity in the mature cochlea.

PD 104

RGMa Inhibition Promotes Synaptic Regeneration between Spiral Ganglion Neurons and Inner Hair Cells.

Jerome NEVOUX[1]; Mihaela ALEXANDRU[1]; Thomas BELLOCQ[1]; Lei TANAKA-OUYANG[1]; Kohsuke TANI[2]; Albert Edge[3]
[1]CHU Bicetre, AP-HP, Université Paris Saclay; [2]MEEI, Harvard Medical School; [3]Harvard

Background: Auditory synapses between hair cells and spiral ganglion neurons are damaged by noise trauma, before degeneration of neurons. The auditory brainstem response (ABR) and distortion product otoacoustic emission (DPOAE) show a temporary threshold shift (TTS) but return to normal after 1-3 weeks. The amplitude of wave 1 of the ABR decreases at high frequencies, 32 kHz being the most damaged part of the cochlea. We studied the effect of blocking repulsive guidance molecule a (RGMa) in the cochlea, with a specific antibody, in vitro using kainic acid (KA), a glutamate agonist which reproduces an excitotoxic trauma, and in vivo using noise-exposed mice. Methods: Post-natal day 3 to 5 cochleae from CD1 mice were dissected for the in vitro experiments. After 24 hours in culture, we exposed the explants to a solution of 0.5 mM KA for 2 hours, followed by treatment for 24 hours with a solution containing anti-RGMa antibody at 10 g/mL. The in vivo experiments used CBA/CaJ mice at 8 weeks of age, exposed to a calibrated noise band for 2 hours at 98 dB. TTS was assayed 24 hours later. Anti-RGMa antibody was applied to the round window of the right ear one week later, under general anesthesia, and compared to polyclonal rabbit IgG to the left ear. Results: After treatment with anti-RGMa antibody in vitro, there was a significantly higher synaptic regeneration compared to the explants treated with either KA only or polyclonal IgG ($p< 0.05$). Two weeks after surgery, thresholds of the ABR and DPOAE recovered, but the amplitude of the suprathreshold wave 1 of the ABR, which reflects cochlear synaptic function did not recover. There was a positive effect of the anti-RGMa antibody on wave 1 amplitude, correlated with an increased number of synapses per inner hair cell in the 32 kHz region ($p< 0.05$); in contrast, there was no difference at 11 kHz. Conclusion: Our study showed increased synaptic regeneration between inner hair cells and spiral ganglion neurons both in vitro and in vivo using anti-RGMa antibody. Increasing the number of synapses by drug therapy thus has an effect on synaptopathy associated with noise overexposure and, given that synapse loss occurs before hair cell and neural loss. may prevent hearing loss associated with higher levels of noise exposure and with age.

Age-Related Changes in Animal Models

PS 783

Preventing Presbycusis in Mice with Enhanced Medial Olivocochlear Feedback

Gonzalo B. Terreros[1]; Luis E. Boero[2]; Valeria C. Castagna[2]; Sebastian Silva[3]; Marcelo J. Moglie[4]; Juan Maass[3]; Paul Fuchs[5]; Paul Delano[6]; A. Belén Elgoyhen[4]; **M. Eugenia Gómez-Casati**[2]
[1]Instituto de Ciencias de la Salud, Universidad de O'Higgins, Rancagua, Chile.; [2]Instituto de Farmacología, Facultad de Medicina, Universidad de Buenos Aires; [3]Programa Interdisciplinario de Fisiología y Biofísica, Instituto de Ciencias Biomédicas (ICBM), Facultad de Medicina. Universidad de Chile; [4]INGEBI - CONICET; [5]the Center for Hearing and Balance, Johns Hopkins University School of Medicine; [6]1. Neuroscience Department, Faculty of Medicine, University of Chile. 2. Otolaryngology Department, Clinical Hospital of the University of Chile. 3. Biomedical Neuroscience Institute, BNI. Facultad de Medicina. Universidad de Chile, Santiago, Chile. 4. Centro Avanzado de Ingeniería Eléctrica y Electrónica, AC3E, Universidad Técnica Federico Santa María, Valparaíso, Chile.

'Growing old' is the most common cause of hearing loss. Age-related hearing loss first affects the ability

to understand speech in background noise, even when auditory thresholds in quiet are normal. It has been suggested that cochlear synaptopathy is an early contributor to age-related auditory decline. We characterized age-related cochlear synaptic degeneration and hair cell loss in mice with enhanced β9β10 cholinergic nicotinic receptors (β9KI mice) that mediate inhibitory medial olivocochlear (MOC) feedback. Auditory brainstem responses (ABR) were recorded to evaluate cochlear function at 6 months and 1 year of age in WT and β9KI mice. ABR thresholds were significantly elevated by 5-20 dB SPL in aged compared to young WT mice at all frequencies (Friedman test, $p< 0.001$). However, no differences in ABR thresholds were found between young and aged β9KI with enhanced MOC feedback (Friedman test, $p >0.05$). Distortion product otoacoustic emissions (DPOAE) responses in aged WT ears were elevated by 5-30 dB SPL at all the frequencies (Friedman test, $p< 0.01$). In contrast, no alteration in DPOAE thresholds was observed in 1 year-old β9KI mice (Friedman test, $p >0.05$), indicating that OHC function is not degraded in aged mice with enhanced MOC inhibition. Suprathreshold ABR peak 1 amplitudes was not altered in young β9KI compared to the same age WT mice (Mann-Whitney test, $p >0.05$). However, at 1 year there was a reduction in amplitudes in WT ears that was significant at high frequencies when compared to mutant mice (Mann-Whitney test, $p< 0.01$ at 22.65, 32 and 45.25 kHz). IHC-afferent synapses were identified by immunostaining with antibodies against CtBP2-Ribeye and GluA2 AMPA-type glutamate receptors. The numbers of colocalized synaptic puncta per IHC were not different in β9KI compared to WT mice at 6 months of age. Notably, at 1 year of age the number of synaptic markers per IHC were higher in mice with enhanced MOC function at all the cochlear locations (Mann-Whitney test, $p< 0.0001$), suggesting that the strength of the olivocochlear reflex restrains cochlear synaptopathy. Quantification of hair cells showed that in aged WT there was some loss of OHCs compared to β9KI ears that was significant at the apical and basal cochlear region (Mann-Whitney test, $p< 0.01$), indicating that the enhanced strength of the MOC system provides the protective effect against OHC damage. Thus, the present study provides the first proof-of-principle supporting enhancement of the MOC system as a viable approach for prevention of auditory function decline during aging.

PS 784

Exposure to a Temporally Modulated Augmented Acoustic Environment Alters Tonotopic Organization and Improves Gap Detection in IC Neurons in Old CBA/CaJ Mice

Luis Franco-Waite[1]; Ryan Longenecker[2]; terrance Jones[1]; Rachal Love[1]; Timothy Fawcett[1]; Joseph P. Walton[3]

[1]Univ South Florida; [2]Univ. South Florida; [3]Department of Communication Sciences & Disorders, University of South Florida, Tampa, FL; Department of Medical Engineering, University of South Florida, Tampa, FL; Global Center for Hearing and Speech Research, University of South Florida, Tampa, FL

Background

It is well established that exposure to augmented acoustic environments (AAEs) during early development can have profound effects on auditory midbrain and cortex tonotopic organization. The developmental plasticity that drives tonotopic reorganization has been reported in many species, including mice, however there is a paucity of research that has investigated the effects of AAE in aged animal models. In the current study old mice were exposed to various spectral and temporal AAE stimuli in order to assess the effects on complex sound neural processing.

Method

CBA/CaJ mice (22-24 months old) were exposed for 2 months for 12 hours per day to an AAE. The first cohort of mice was exposed to an AAE comprised narrowband, noise bursts having a center frequency of 8 kHz (AAE-8) with silent gaps of 2-16 msec duration randomly embedded in each noise burst. The second cohort of mice was exposed to an AAE with a center frequency of 20 kHz (AAE-20) and 100% amplitude modulated with alternating modulation frequencies of 40 Hz and 100 Hz which switched every 2 seconds. To assess the effects on central auditory processing, neural activity was recorded from a 16-channel electrode in the inferior colliculus (IC). Frequency response maps were measured from 4 to 64 kHz and from 0 to 80 dB SPL, from which each units' best frequency, threshold, and tuning sharpness were derived. To assess temporal processing, neural coding of gap-in-noise stimuli were measured to determine the minimum gap threshold (MGT) and neurometric gap functions from IC neurons.

Results/Conclusions

Excitatory Frequency Response Areas (eFRA) showed a systemic shift toward the AAE frequencies in both cohorts, with neurons from the AAE-8 cohort remapping towards 8 kHz and neurons from AAE-20 remapping

towards 20 kHz. Neural metrics derived from the eFRAs also differed among cohorts with Q values of neurons from AAE-20 having sharper bandwidths compared to neurons from AAE-8 when the neurons BF was < 15 kHz. In contrast to this, neurons from AAE-20 mice had broader Qs when the BF was >15 kHz. Minimum thresholds (MT) for neurons from AAE-20 mice had significantly lower thresholds than those from AAE-8 mice. The distribution of minimum gap thresholds (MGTs) were shorter for neurons from AAE-8 mice, as compared to AAE-20. Several key conclusions can be drawn these results; i) the aged auditory midbrain shows remarkable plasticity after 2 mons of exposure to AAE, ii) IC neurons respond differently to AAE which is spectrally shaped to low and high frequencies, and iii) neural correlates of temporal gap encoding can be improved by AAEs.

Work supported by NIH-NIA grant AG09524.

PS 785

Gene Expression and SVK-1 Cell Treatment Analyses of Connexin 30 and 43 in Relation to Age-Related Hearing Loss

Jennifer Pineros; Xiaoxia Zhu; Bo Ding; Robert D. Frisina
Medical Engineering Dept., Global Center for Hearing & Speech Research, Univ. South Florida

Introduction
Connexin proteins (Cx) are essential for intercellular communication. Mutations in Cx genes have been linked to human syndromic and nonsyndromic deafness. Previous work has shown *Cx30* downregulating with age in the stria vascularis (SV), but other Cx's involvement in age-related hearing loss (ARHL), as well as where Cx isoforms are in the cochlea are still to be determined.

Materials and Methods
CBA/CaJ mice (N=8) were classified into two groups according to age: young adult (3 mon, n=4) and old (30 mon, n=4) to test aging trends in the gene expression of *Cx30* and *Cx43* using SV and organ of Corti (OC) samples. The results were analyzed with t-tests and linear regression. Auditory brainstem response (ABR) and distortion product otoacoustic emissions (DPOAE) were recorded to measure hearing changes. *In vitro* cell treatments using SV-K1 cells are being conducted using different chemicals – hydrogen peroxide (H_2O_2), cisplatin (CIS), and aldosterone (ALD), for *Cx30*. These were separated into two different experimental paradigms: dose-dependent and time-course.

Results and Discussion
For the *in vitro* SV-K1 cells, only *Cx30* was detected using RT-qPCR, but not *Cx43*. Additionally, for *in vitro* HEI-OC1, both *Cx43* and *Cx30* were detected. Comparison between the young adult and old cochlear samples using RT-qPCR confirmed downregulation of both genes in the OC and downregulation of *Cx30* in the SV. The dose-dependent treatments of H_2O_2, CIS and ALD, showed all three chemicals *decreasing Cx30* gene expression, suggesting complications developing among Cx isoforms in the cochlea when facing age-related stress. Next, we are going to screen potential treatments utilizing insulin-like growth factor (IGF-1) and anti-inflammatories. Time-course experiments are underway for validation, for *Cx43* using HEI-OC1 cells. Additionally, immunohistochemistry and *in situ* hybridization will be carried out for further investigation of co-localization of cochlear Cxs isoforms.

Summary
Our study suggests a trend of down-regulation of *Cx30* in the SV and OC with aging. *Cx43* did not appear in the SV but showed in the OC. The *in vitro* cell treatments currently appear to be good options to investigate interactions among Cxs and may result in a possible treatment that will hopefully reverse ARHL. Time-course experiments on *Cx30* and similar studies on *Cx43* are ongoing. The long-term goal is to determine how aging affects the connexin family in different regions of the cochlea, and the impact of potential treatment options for ARHL.

Supported by: NIH grant P01 AG009524.

PS 786

Investigation of Mechanisms and Prevention of Age-Related Decline of Outer Hair Cell Function in Aging CBA/CaJ Mice: Ibuprofen Treatments

Parveen Bazard[1]; Bo Ding[1]; Xiaoxia Zhu[1]; Thomas Parks[2]; Parmvir Bahia[2]; Thomas T. Clark[2]; Robert D. Frisina[1]
[1]Medical Engineering Dept., Global Center for Hearing & Speech Research, Univ. South Florida; [2]Molecular Pharmacology & Physiology Dept., Morsani College of Medicine, Univ. South Florida

Introduction
Ibuprofen is a well-known drug, available over the counter. It is used to treat various conditions including headache, muscle aches, arthritis, inflammations and minor injury. There are no studies about ibuprofen effects on hearing. Here, we have investigated the effects of ibuprofen on hearing of aging mice and underlying molecular mechanisms.

Methods

In-vivo Electrophysiology Experiments: 19 month old CBA/CaJ female mice were fed chow containing 375 ppm ibuprofen for six months. Auditory Brainstem Responses (ABRs) and Distortion Product Otoacoustic Emissions (DPOAEs) were measured every second month. *In vitro Cell Fractions Isolation:* HEI-OC1 cells were treated with different ibuprofen doses. A Cell Signaling protein fractional kit (#9038) was used to separate different cell fractions: nuclear, membrane and cytoplasmic fractions. *Western Blotting:* Western blot analysis was performed with total lysate and subcellular fractions for prestin protein expressions. *In-vitro Electrophysiology: In-vitro* whole-cell voltage-clamp experiments were performed to study the effects of ibuprofen on prestin activity.

Results

During six months of treatments, there was a steady decline in DPOAE amplitudes and threshold elevations for the control group (normal mouse chow). Whereas, DPOAEs (both- amplitudes and thresholds) were stable for the ibuprofen group, especially, at high frequencies. However, both groups showed similar ABR thresholds elevations, indicating that treatment benefited DPOAEs prominently. Based upon this, we explored the effects of ibuprofen treatment on prestin –the motor protein expressed in outer hairs cells, with *in-vitro* experiments. Western blotting showed that there was an increase in total prestin protein levels but not statistically significant. Subcellular protein fractions: nuclear, membrane and cytoplasmic fractions were also analyzed using western blot techniques. Membrane prestin expression was low compared to the nucleus and cytoplasmic fractions; whereas nucleus fractions showed high levels of protein, indicating that prestin is mostly located inside nucleus for HEI-OC1 cells. There was an increase in cytoplasmic and membrane prestin levels with ibuprofen treatments. β-actin, a loading control structural protein was not observed in membrane samples. Preliminary, voltage patch clamp experiments showed that there was a change in voltage-dependent non-linear membrane capacitance – an electronic signature of prestin, especially with higher doses of ibuprofen. Further dose-dependent experiments are underway. Future molecular biology and physiology experiments will be done to understand the cellular mechanisms involved anti-inflammatory actions on hair cells.

Summary

This work demonstrates ibuprofen therapeutic potential in treatment of certain aspects of presbycusis in mice.

Work supported by NIH grant P01-AG009524 from the National Institute on Aging.

PS 787

Age-Related Hearing Loss in Zebrafish: Surprising Senescence in an Animal with Continuous Hair Cell Turnover

Allison Coffin[1]; Riuyu Zeng[2]; Coty Jasper[3]; Phillip Uribe[4]; Bonnie E. Jacques[4]; Joseph Sisneros[2]
[1]Washington State University, Vancouver; [2]University of Washington; [3]Washington State University Vancouver; [4]Otonomy Inc

Age-related hearing loss (ARHL) impacts over 50% of the population, leading to social isolation and reduced quality of life. ARHL is caused by several factors in concert, including loss of hair cells. Surprisingly, zebrafish also exhibit ARHL, despite the ability to produce new hair cells throughout life. Prior research demonstrates reduced hair cell density and elevated auditory thresholds in aged animals, suggesting changes in hair cell turnover. The present study examines cellular and genetic correlates of ARHL in a zebrafish model. Aged zebrafish show significant decreases in cell proliferation in the undamaged saccule and lagena (primary and secondary auditory organs), indicating an age-related decline in hair cell turnover. Interestingly, the utricle, which is the primary vestibular organ, does not show age-related changes in cell division, suggesting epithelium-specific regulation of tissue senescence. Using RNA-Seq, we found that aging is also associated with a striking change in gene expression. Inner ears of young adult animals show significant upregulation of genes important for cell division, cellular maturation, and axon guidance, hallmarks of an actively developing tissue. By contrast, ears from aged animals over-express pro-inflammatory genes, suggesting a role for immune modulation of auditory function. Inflammation is also a feature of aging in the mammalian cochlea, evidence that ARHL shares conserved attributes across vertebrates. Our ongoing studies use pharmacologic and genetic manipulation to understand the relative contribution of inflammation in the aging auditory periphery and to identify potential drug targets.

PS 788

Age-Related Hearing Loss in CBA/CaJ Mice: Inflammatory Induced TNFÎ± Changes in the Mouse Cochlea

Cody D. Spence[1]; Bo Ding[2]; Xiaoxia Zhu[2]; Mark A. Bauer[2]; Robert D. Frisina[2]
[1]Medical Engineering Dept., Morsani College of Medicine, Global Center for Hearing & Speech Research, Univ. South Florida; [2]Medical Engineering Dept., Global Center for Hearing & Speech Research, Univ. South Florida

Introduction

Age-related hearing loss (ARHL) is a highly prevalent condition of the elderly that is commonly treated with hearing aids. However, hearing aids are under-utilized, with patients citing discomfort and high cost. A drug that prevents or treats ARHL could alleviate some of these shortcomings and improve quality of life. To find a potential drug target for ARHL, we examined cochlear mechanisms of ARHL.

Materials and Methods

Auditory Brainstem Response (ABR) audiograms and Distortion Product Otoacoustic Emissions (DPOAE) were measured with a TDT Biosig system (Alachua, FL) on young adult (2-4 months, n=6) and old (30-32 months, n=4) CBA/CaJ mice. In vivo tissue samples were harvested from the organ of Corti and stria vascularis of young adult (n=4) and old (n=4) mice. Complementary in vitro studies with SVK-1 cells from the mouse stria vascularis and HEI-OC1 cells from the mouse organ of Corti were also performed. H2O2 was used in varying durations (0-24 hours at 150μM) to simulate oxidative stress associated with aging. RT-qPCR was used to measure gene expression of TNFβ, an inflammatory cytokine, normalized to GAPDH. For in vitro studies, TNFβ expression was compared to control cells (no treatment). 1-way ANOVA, 2-way ANOVA with multiple comparisons, and unequal variance t-tests were performed using GraphPad Prism 8.1.2 (La Jolla, CA).

Results and Discussion

DPOAE amplitudes decreased and ABR and DPOAE thresholds increased in older mice compared to young adults ($p < 0.0001$), indicating ARHL had occurred. Organ of Corti tissue from old mice had higher TNFβ expression than in young adult mice ($p=0.016$). SVK-1 cells had peak TNFβ expression after 1 hour of treatment with 150 μM H2O2 ($p < 0.0001$). While TNFβ gene expression in HEI-OC1 cells did not significantly deviate from controls after treatment with 150 μM H2O2, a similar expression profile was observed as in SVK-1 cells. Since gene expression was not a linear increase over time, a negative feedback mechanism regulating TNFβ expression may be involved. SVK-1 cells also had a higher gene expression of TNFβ than HEI-OC1 cells at the peak time of 1 hour ($p=0.007$), potentially due to the stria being more vascularized than the organ of Corti. Future directions include examining expression of other inflammatory-related genes to justify exploring the use of anti-inflammatory agents in the prevention or treatment of ARHL.

Acknowledgements

We would like to acknowledge Parveen Bazard, PhD, for his help. Work supported by NIH-NIA P01 AG009524.

PS 789

Expression Level Changes of Inflammatory and Apoptotic Biomarkers under Hydrogen Peroxide Stress in HEI-OC1 Cochlear Cells

Mark A. Bauer; Bo Ding; Xiaoxia Zhu; Robert D. Frisina

Medical Engineering Dept., Global Center for Hearing & Speech Research, Univ. South Florida

Introduction

The auditory hair cell line, HEI-OC1, is a popular model for the investigation of drug treatments as well as the molecular bases of hearing loss and dysfunction, including age-related hearing loss (ARHL-presbycusis). We hypothesize that inflammation plays a significant role in ARHL, and we model key aspects of ARHL *in vitro* utilizing hydrogen peroxide (H_2O_2) as our stimulant. A battery of both inflammatory and apoptotic markers were chosen to analyze to uncover cellular mechanisms of action that may contribute to cochlear ARHL.

Methods

In vitro assays were performed on HEI-OC1 cells using increasing hydrogen peroxide doses over a period of 24 hours. Western Blot analysis was then performed on the processed cell lysate using antibodies against the inflammatory proteins Akt, NFkB, and IL-1B, as well as antibodies against the apoptotic biomarkers Bax, Bcl-2, caspase-3, and caspase-9.

Results

Initial results show a positive increasing trend of Akt and NFkB expression levels to increase as hydrogen peroxide concentrations are increased, relative to control protein expression levels. Additionally, slight changes in the apoptotic markers and IL-1B were observed. These data suggest that the feedback mechanisms with the hair cell line seem to favor Akt as a prominent biomarker in the cell's survival through the inactivation of signaling pathways that induce apoptosis. Previous investigations reported in the literature, using other non-hearing-related cell lines, also confirm the present findings. In the presence of hydrogen peroxide then, inflammation, as indicated by an NFkB increase, seems to be a key response mechanism in the HEI-OC1 cell line to stressful stimuli, which could play an important role in the biological mechanisms of ARHL.

Conclusions and Future Work

Our initial findings suggest that the HEI-OC1 cell line when treated with hydrogen peroxide may be an effective model for studying effects of inflammation in hair cells. This allows for future studies to develop therapeutic interventions that utilize anti-inflammatory

drugs, for example, for the prevention and treatment of presbycusis. Further experiments are underway to confirm our preliminary findings concerning the interactions of these inflammatory cytokines with the apoptotic pathway proteins using both the HEI-OC1 and SV-K1/stria vascularis cell lines.

Supported by: NIH grant P01 AG009524 from the Nat. Inst. on Aging.

PS 790

Mechanisms of Protection from Premature Hearing Loss in Transgenic TFB1 Mice via Down-regulation the ROS-dependent Activation of AMPK Signaling

Jingjing Zhao[1]; Gen Li[2]; Nuno Raimundo[3]; Hao Wu[2]; Lei Song[2]
[1]1.Department of Otolaryngology - Head & Neck Surgery, Shanghai Ninth People's Hospital, Shanghai Jiao Tong University School of Medicine; 2.Ear Institute, Shanghai Jiao Tong University School of Medicine; 3.Shanghai Key Laboratory of Translational Medicine on Ear and Nose diseases, Shanghai, China; [2]1. Department of Otolaryngology - Head & Neck Surgery, Shanghai Ninth People's Hospital, Shanghai Jiao Tong University School of Medicine; 2. Ear Institute, Shanghai Jiao Tong University School of Medicine; 3. Shanghai Key Laboratory of Translational Medicine on Ear and Nose diseases, Shanghai, China; [3]Institute of Cellular Biochemistry, University Medical Center Goettingen, Germany

AMP-activated protein kinase (AMPK) activation occurs in response to cellular energy decline and mitochondrial dysfunction triggered by reactive oxygen species (ROS). In this study, we explored the specific pathology and rescue of a previously reported mitochondrial deafness mouse model, which overexpressed 12S ribosomal RNA methyltransferase mtTFB1(Tg-mtTFB1M) and exhibited non-syndromic hearing loss, similar to human maternally-inherited deafness caused by the mtDNA mutation A1555G. The hearing loss, measured by auditory brainstem response (ABR) in 10-12 mon old mice, are accompanied with cochlear pathology including reduced endocochlear potential (EP), loss of spiral ganglion neurons (SGN), inner hair cell (IHC) synapses and outer hair cells (OHC). Accumulated ROS and increased apoptosis signaling were detected in cochlear tissues of Tg-mtTFB1 mice by western blot (WB) analysis, accompanied with aberrant activation of AMPK in the spiral ganglion neurons (SGN), stria vascularis (SV) and organ of Corti (OC) that were confirmedby immunohistochemistry. To further explore the underlying mechanism of the auditory phenotype in relevance to AMPK signaling, we genetically knocked out AMPKβ1 as rescue to mtTFB1. We observed rescues of hearing phenotypes in Tg-mtTFB1 mice: improved ABR wave I, EP and IHC function, as well as SGNs, IHC synapses, and OHC survivals. We also found decreased level of ROS, reduced pro-apoptotic signaling (Bax) and increased anti-apoptotic signaling (Bcl-2) in the cochlea tissues of AMPK KO mice, indicating reduced AMPK level attenuated apoptosis via ROS-AMPK-Bcl2 pathway in cochleae. To conclude, AMPK hyperactivation causes accelerated presbycusis in Tg-mtTFB1 mice by redox imbalance and dysregulation of apoptosis pathway. The effects of AMPK downregulation on pro-survival function and oxidative stress reduction indicate AMPK as a target to rescue or relieve mitochondrial hearing loss due to the ROS-dependent cell apoptosis and death.

Acknowledgements
Supported by the National Natural Science Foundation of China (NSFC) grant to L.S. (81770995) and European Research Council Starting Grant to NR (337327 MitoPexLyso).

PS 791

Metformin modulated lipid metabolism and attenuated AHL through activation of AMPK

Yanlin Xiao[1]; Hanqing Lin[2]
[1]School of Medicine, Southern University of Science & Technology; [2]Department of Otolaryngology, Sun Yat-sen Memorial Hospital, Sun Yat-sen University

Background
Diet-induced obesity has long term effect on hearing degeneration. High-fat diet is considered as a risk of age-related hearing loss. Metformin improves chronic lipidic toxicity by regulating lipid metabolism and was recently found to mediates protective effect in neurodegeneration diseases. Our research aims at the effect of metformin and its role in hearing loss.

Methods
C57BL/6 mice were fed a high-fat diet for 36 weeks. Mice were receiving metformin administration at the last 12 weeks before development of significant hearing loss. Mice were assessed for weight gain, glucose and cholesterol metabolism, and adiposity. In addition, cochlea tissue was analyzed by liquid chromatography with tandem mass spectrometry.

Results
In this study, we found that mice with high-fat diet developed progressive haring loss at the age of 15 month. Cochlear metabolomics data revealed that metformin reduced of metabolite of triglyceride. Metformin activated AMPK under oxidative stress derived from

lipidic toxicity and suppressed caspase signaling. Mice developed moderate ABR threshold shifts with metformin administration than progressive shifts with in high-fat diet group.

Conclusions

These results indicate that disruption of lipid metabolism and lipidic toxicity impaired cochlear function and metformin may be protective against lipidic oxidative stress.

PS 792

RNA-seq Analysis of Potential lncRNAs for Age-Related Hearing Loss in a Mouse Model

Tong Zhao[1]; Xiuzhen Liu[2]; Zehua Sun[3]; Jinjin Zhang[3]; Xiaolin Zhang[4]; Chaoyun Wang[3]; Bo Li[1]; Tihua Zheng[5]; Qingyin Zheng[6]

[1]Hearing and Speech Rehabilitation Institute,College of Special Education, Binzhou Medical University, Yantai, China,; [2]Clinical Medicine Laboratory, Binzhou Medical University Hospital; [3]Hearing and Speech Rehabilitation Institute; [4]Department of Otolaryngology-Head & Neck Surgery, Binzhou Medical University Hospital; [5]Hearing and Speech Rehabilitation Institute, College of Special Education, Binzhou Medical University, Yantai, China; [6]Department of Otolaryngology- Head & Neck Surgery, Case Western Reserve University

Age-related hearing loss (AHL) is an important health problem in the elderly population. There is no treatment for AHL, and its molecular mechanisms are partly unknown. In this study, we assayed the different expressional lncRNAs in six-week-old and one-year-old C57BL/6J mice through RNA-seq analysis. We found 69,711 co-expression lncRNAs in these two groups. Of these, 289 lncRNAs were up-regulated and 449 lncRNAs were down-regulated in one-year-old mice compared to six-week-old mice (corrected $P < 0.05$). Gene ontology- biological process (GO-BP) analysis showed 29 mRNAs were enriched on sensory perception of sound (GO:0007605). We chose the intersection of popular genes associated with hearing loss, different expressed genes in RNA-seq, and genes enriched in sensory perception of sound (GO:0007605). There were 34 mRNAs in this intersection. We selected the lncRNAs regulating the 34 mRNAs and measured the expression level of the selected lncRNAs in animal and cellular models of AHL by qRT-PCR. Among them, four lncRNA were significantly different in both animal and cellular models of AHL, and lncRNA NONMMUT010961.2 was the most marked. Our results suggested lncRNAs may be associated with AHL and, thus, may lead to a new treatment for AHL.

PS 793

Degradation and Modification of Cochlear Gap Junction Proteins in Early Development of Age-related Hearing Loss

Shori Tajima[1]; Katsuhisa Ikeda[2]; Kazusaku Kamiya[1]

[1]Department of Otolaryngology, Juntendo University School of Medicine; [2]Juntendo University Faculty of Medicine

AHL(Age-related hearing loss) is defined as a progressive, bilateral, high-frequency hearing loss in elderly people. Connexin(CX)26 is one of the major protein subunits to form gap junctions in the cochlea. Mutations in CX26 are one of the most common causes of inherited nonsyndromic deafness. The relationships between CX26 and AHL are not fully understood. Here, we investigated the CX26 quantitative change and molecular pathology of AHL.

C57BL/6J mice were used as a representative model of AHL. The hearing levels were evaluated by ABR (auditory brainstem responses). We investigated the formation of gap junction plaques in cochlear inner sulcus cells and hair cell morphology by confocal microscopy and the cochlear gap junction proteins such as CX26 and CX30 by western blotting and compared 4- and 32-week mice. Moreover, we used a biochemical approach to separate the hydrophobic and hydrophilic microdomains of cochlear membrane proteins and then quantified CX26 and CX30 in these fractions by western blotting to investigate the relationship between connexins and lipid rafts.

ABR thresholds gradually increased to 32 weeks and rapidly elevated at 36 weeks. It was suggested that the pathological progression of hearing loss in early stage accelerated between 32 weeks and 36 weeks. Therefore, 32-week-old mice were investigated as initial stage model of AHL. In immunohistochemical analysis of the cochlea in 4-week-old mice, gap junctions showed linear plaques along the cell-cell junction sites with adjacent cells. In contrast, gap junction plaques in 32-week-old mice did not show the normal linear structure but instead formed small spots around the cell-cell junction sites and gap junction lengths were significantly shorter than in 4-week-old mice. Hair cell loss were also compared between 4- and 32-week-old mice. However, their differences were not significant. In western blotting, CX26 and CX30 protein level were significantly decreased in 32-week-old mice compared with 4-week-old mice. Moreover, CX26 was more significantly enriched in the hydrophilic fraction at 4 weeks but was more significantly enriched in the hydrophobic fraction at 32 weeks, indicating an age-related conversion of this biochemical property.

These results indicated that the disruption of GJPs and hydrophobic conversion of CX26 were crucial pathogenesis of AHL occurring before the hair cell degenerations. Moreover, disruption of the gap junction plaques and decreased gap junction proteins might contribute to the onset and progression of AHL. Furthermore, the treatment targeting CX26 such as GJB2 gene therapy may be effective for AHL.

Auditory Brainstem II: Normal Hearing & Hearing Impairment

PS 794

Intrinsic Properties of Mouse MNTB Principal Neurons are Heterogeneous

Mackenna Wollet[1]; Jun Hee Kim[2]
[1]University of Texas Health Science Center San Antonio; [2]University of Texas Health Sciences San Antonio

Principal neurons of the medial nucleus of the trapezoid body (MNTB) in the auditory brainstem receive glutamatergic inputs from the contralateral cochlear nucleus, and in turn project glycinergic input to the medial and lateral superior olive (MSO and LSO). The synaptic structure of the calyx of Held onto MNTB principal neurons shows diverse morphologies, indicating heterogeneity in the synaptic communication. A previous study suggests that the synaptic input on each MNTB principal neuron is organized as a structural and functional continuum and could serve as a filter for regulating the inhibition delivered to superior olive neurons during sound localization (Grande and Wang, 2011). However, it remains unclear whether the counter parts of the calyx terminal, MNTB neurons, also have heterogeneity in their morphology and intrinsic properties. Within the auditory brainstem, nuclei such as the MNTB, are organized tonotopically. To examine how intrinsic properties of MNTB neurons differentiate along the tonotopic map, we recorded action potentials (APs) from high-frequency sound responding neurons (HF neurons) in the medial MNTB and low-frequency responding neurons (LF neurons) in the lateral MNTB, which were evoked by step-current injections in whole-cell recording. HF neurons displayed smaller APs with amplitudes of 94.1 ± 2.66 mV (n=10), while APs from LF neurons had larger amplitudes of 102.8 ± 1.12 mV (n=7, p=0.0250, Mann-Whitney U test) without difference in the threshold and half-width of APs. Interestingly, we found that intrinsic properties of HF neurons within the medial MNTB are not homogeneous. There are distinct two groups of HF MNTB neurons based on their spiking pattern. In the group I, 12 of 24 HF neurons display a single spike with a fast AHF followed by strong adaptation. In the group II, 12 of 24 HF neurons display intermittent AHP and a longer inter-spike interval between 1st and 2nd spikes, and have high spiking frequency (~102 Hz) in response to long-depolarizing current injection (200 pA, 200 ms). Group I HF neurons generate AP with smaller amplitude and a peak potential of 25.3 ± 2.5 mV (n=12), whereas the peak of AP in group II HF neurons reaches 41.9 ± 1.4 mV (n=12). There is no difference in the threshold of AP (-44.2 ± 2.2 mV vs -42.7± 0.7 mV, respectively). Our preliminary results demonstrate that mouse MNTB neurons have heterogeneous intrinsic properties.

PS 795

Effect of Inhibitory Synapses from the Medial Nucleus of the Trapezoid Body onto Medial Olivocochlear Efferent Neurons

Lester Torres Cadenas[1]; Matthew Fischl[1]; Catherine Weisz[2]
[1]NIDCD/NIH; [2]National Institute on Deafness and Other Communication Disorders

Synaptic inputs onto medial olivocochlear (MOC) efferent neurons in the brainstem are poorly understood. Excitatory, glutamatergic inputs originate in the cochlear nucleus, but the source, strength, or identity of neurotransmitters at putative inhibitory synaptic inputs have not been characterized. We performed whole-cell voltage-clamp electrophysiological recordings from MOC neurons to investigate inhibitory synaptic inputs. MOC neurons in the ventral nucleus of the trapezoid body (VNTB) were identified for recordings in brainstem slices from P12-P23 mice using ChAT-IRES-cre mice crossed with a tdTomato reporter mouse line to label cholinergic neurons. MOC identity was confirmed by co-labeling tdTomato positive neurons with an antibody against choline acetyltransferase (ChAT), by confirming co-labeling of tdTomato with a retrograde tracer applied to the cochlea, and by filling the neurons with biocytin during the recording followed by DAB staining to confirm characteristic MOC neuron morphology. During voltage-clamp recordings, spontaneous post-synaptic currents (PSC) were partially sensitive to gabazine and to strychnine, demonstrating GABAergic and glycinergic synaptic transmission. To determine the source of inhibitory inputs to MOC neurons, focal glutamate uncaging to activate MNTB somata was performed while recording from MOC neurons. MNTB activation via glutamate uncaging evoked PSCs in the MOC neuron, confirming the MNTB as the source of inhibitory synaptic inputs. To assess synaptic plasticity, MNTB axons were electrically stimulated with pairs or trains of pulses at different inter-stimulus intervals (ISI) while recording MOC responses. Evoked PSCs exhibited synaptic depression with repeat stimulation, suggesting that the MNTB effect on MOC neurons decreases over the course

of a sustained stimulus. We next assessed the inhibitory effect of the MNTB on MOC neurons. In current-clamp recordings, MOC neurons in brainstem slices have spontaneous action potentials at resting membrane potential. Electrical stimulation of MNTB axons to evoke neurotransmitter release was applied individually, or in trains of 20 pulses at 10, 50, and 100 Hz, resulting in hyperpolarizing, inhibitory synaptic responses in the MOC neuron. Inhibition by the MNTB suppressed action potentials in MOC neurons by causing a delay, but not complete inhibition, of MOC spiking activity. The delay of action potentials by IPSPs suggests that MNTB neurons can inhibit MOC activity, which would in turn delay MOC synaptic inhibition of cochlear outer hair cells.

PS 796

Investigation of Inhibitory Input and Synaptic Integration in Medial Olivocochlear Neurons using Novel Approaches - In Vitro

Matthew Fischl[1]; Catherine Weisz[2]
[1]NIDCD/NIH; [2]National Institute on Deafness and Other Communication Disorders

Olivocochlear efferent neurons provide feedback to the cochlea to modulate cochlear responses to sound. Medial olivocochlear (MOC) neurons reside in the ventral nucleus of the trapezoid body and project back to the cochlea, terminating on outer hair cells (OHC). MOC cholinergic signaling decreases OHC electromotility via a calcium activated potassium conductance which hyperpolarizes OHCs. Though the properties of MOC synapses onto OHCs are well documented, the intrinsic and synaptic physiology of MOC neurons themselves have not been thoroughly explored. Our lab recently showed that the MOC neurons receive inhibitory input from ipsilateral neurons of the medial nucleus of the trapezoid body (MNTB). This result indicates that both excitation (likely from T-stellate neurons in the contralateral cochlear nucleus) and inhibition (from the MNTB which is innervated by contralateral globular bushy cells in the cochlear nucleus) to MOC neurons is likely driven by the contralateral ear. In an effort to understand how MOC neurons integrate multiple sources of sound-evoked input, we developed a novel slice preparation which preserves presynaptic circuitry while facilitating patch clamp electrophysiology. We first used neuron tracing and immunohistochemical techniques to visualize cochlear nucleus axonal projection patterns to preserve circuit connectivity. Our preparation, a wedge-shaped slice, contains an intact auditory nerve root and cochlear nucleus on the thicker side (~1-1.5 mm thick) and then tapers to the thinner side (300-500 um) where MOC neurons can be accessed for whole-cell patch-clamp recordings more easily for detailed study of synaptic inputs. With this preparation we can stimulate the auditory nerve directly, preserving the approximate timing of inputs as they enter the auditory brainstem and allowing for synaptic plasticity to occur at synapses upstream of MOC cells. Our preliminary data suggest that both excitatory and inhibitory inputs to MOC cells can be activated via auditory nerve stimulation, with excitation and inhibition arriving with distinct latencies. Measuring the resulting inputs to MOC neurons will allow us to determine the combined influence of excitation and inhibition to the MOC, and how each affects MOC output and in turn, cochlear modulation.

PS 797

Plasticity of Ascending and Descending Inputs onto Medial Olivocochlear Efferent Neurons

Gabriel E. Romero[1]; Laurence Trussell[2]
[1]Physiology & Pharmacology Graduate Program, Oregon Health & Science University; [2]Oregon Hearing Research Center and Vollum Institute, Oregon Health and Science University, Portland, Oregon

The medial olivocochlear (MOC) reflex improves detection of salient sounds in noise and protects the auditory system from noise-induced hearing loss. While the MOC reflex has been studied extensively at the level of the cochlea, the central brainstem circuitry underlying its function is less well understood. This lack of knowledge hinders our understanding of the MOC system's protective role in regard to hearing loss, and its function during normal hearing, where it is dynamically active in response to a diverse auditory environment. This research aims to enhance our understanding of normal MOC reflex function by investigating the central circuitry underlying the MOC reflex. Here we report an analysis of ascending and descending excitatory synaptic inputs onto MOC neurons from the ventral cochlear nucleus (VCN) and inferior colliculus (IC), respectively. A choline acetyltransferase(ChAT)-cre mouse line was crossed to a tdTomato reporter to generate mice (ChAT-tdTomato) with tdTomato in cholinergic cells. In histological sections, tdTomato labeled neurons were observed in the lateral superior olive and ventral nucleus of the trapezoid body (VNTB), where the somata of lateral and medial olivocochlear neurons reside, respectively. A retrograde tract-tracer was pressure injected into the membranous labyrinth of the inner ear and a majority of cre-positive neurons in the contralateral VNTB were labeled, confirming they were indeed MOC efferents. To enable optical excitation of ascending or descending terminals onto MOC neurons, the VCN or IC of ChAT-tdTomato mice were unilaterally infected with AAV2-CAG-ChR2-Venus-WPRE-SV40. To determine how MOC neurons integrate and convey synaptic information, we conducted patch-clamp recordings on cre-positive VNTB neurons in acute

brain slices from P30-P48 ChAT-tdTomato mice while optically exciting ascending or descending presynaptic inputs. Optogenetic activation of either input was found to evoke excitatory postsynaptic currents (EPSCs) in MOC neurons. These light-evoked EPSCs were due to inwardly-rectifying, fast-gating Ca^{2+}-permeable AMPA receptors. While postsynaptic AMPAR-mediated responses were similar between VCN and IC input, they differed dramatically in presynaptic short-term plasticity. Amplitudes of VCN originating light-evoked EPSCs regularly depressed at low (5 Hz) to high (50 Hz) rates of stimulation, whereas IC originating EPSCs often facilitated. At high rates of stimulation, IC input exhibited presynaptic augmentation, as the recovery from facilitation was on the order of seconds (β = 4.7 seconds). These results suggest that ascending VCN input to MOC efferent neurons may best convey low rates or short bursts of action potentials, whereas descending IC input becomes stronger and more reliable at higher rates.

PS 798

Fast Endocytosis and Dynamin Block at Auditory Brainstem Synapses

Andre Dagostin; Henrique von Gersdorff
Vollum Institute

The rapid cycling of vesicles in the presynaptic terminal is required for continuous and proper synaptic function. One important path for membrane reuptake after vesicle fusion is clathrin-independent and clathrin-mediated endocytosis. Both forms of endocytosis rely on dynamin for the final step of membrane fission and vesicle reformation. Not only membrane recycling but also active zone clearance depends on membrane reuptake, making dynamin a key player in neurotransmission, especially in high frequency firing neurons. To study the disruption of the endocytic function through dynamin blockade, we recorded currents from neurons of the medial nucleus of the trapezoid body (MNTB) or the lateral superior olive (LSO) in brainstem slices from postnatal day 20-25 mice (C57BL/6J). We evoked postsynaptic currents by electrically stimulating the afferent fibers of each nucleus at 300 Hz, at 33-35°C and in low $[Ca^{2+}]_e$(1.2 mM).To block dynamin, we used Dyngo 4A, and to ensure proper drug delivery, we sonicated the solution and incubated the slices in it for at least 20 minutes prior to recording.

The first striking effect of Dyngo on MNTB synapses is the increase in the frequency of the spontaneous mEPSCs (3.4±0.7 Hz to 38.6±6.8 Hz), which is a good indication that the drug acting on the presynaptic terminal. On the other hand, we observed a reduction in the evoked EPSC amplitude (~40%), sometimes leading to failures at the end of the stimulation protocol, which may be explained by a great reduction in vesicle pool size (readily releasable pool – RRP). In consonance with this observation, membrane capacitance recordings from mature calyces display a fast form of endocytosis and this capacitance decay was slower after depolarization once dynamin is blocked by Dyngo 4A.

We also observed a reduction on glycinergic evoked currents in the LSO (~70%). But differently from the MNTB synapses, failures were not observed at 300 Hz stimulation. Moreover, the paired-pulse ratio increased and a dip seen in some IPSCs trains in controls, was absent with Dyngo. Interestingly, calcium imaging on LSO boutons showed a lower calcium influx into the terminals after incubation with Dyngo 4A. These preliminary results suggest that intact Dynamin function is necessary to maintain the RRP size during prolonged stimulation.

Proper dynamin function appears to be required for reliable transmission in MNTB synapses during high-frequency activity. In LSO principal cell synapses, dynamin activity not only regulates RRP size, but also shapes STP, which ultimately regulates information coding in the postsynaptic neuron. Importantly, we emphasize that caution should be exercised in interpreting the effects of Dyngo 4A due to non-specific effects that may disrupt the calcium handling dynamics of nerve terminals.

PS 799

Modulations of Neural Action Potential Rates Can Influence Electrical Properties of Oligodendrocytes and Myelination of Individual Trapezoid Body Axons

Mihai Stancu[1]; Ezhilarasan Rajaram[1]; Hilde Wohlfrom[1]; Tejbeer Kaur[2]; Mark Warchol[3]; Edwin W. Rubel[4]; Conny Kopp-Scheinpflug[1]
[1]LMU Munich; [2]Creighton University; [3]Washington University School of Medicine; [4]University of Washington

Our previous work shows that myelination of auditory brainstem fibers regulates axonal conduction to match the system's need for speed and precision (Seidl et al, 2014; Sinclair et al., 2017). We demonstrated that binaural sensory deprivation induced by earplugs significantly reduced sound-evoked activity, but had no impact on spontaneous firing rates. While we observed a reduction in myelin thickness following bilateral earplugs, axon diameter was unaltered by this procedure. This suggests that axon diameter is either genetically encoded rather than modulated by activity, or

that spontaneous activity alone is sufficient to maintain axon diameter. To test this hypothesis, we induced varying degrees of sensory deprivation ranging from 1) absence of spontaneous and sound-evoked activity following pharmacogenetic deletion of auditory hair cells; via 2) absence of all sound-evoked activity while maintaining spontaneous firing (binaural earplugs) to 3) a halving of sound-evoked activity while maintaining spontaneous firing (monaural earplugs).

Sensory deprivation was induced either by raising mice of both sexes with monaural or binaural earplugs for 10 days or by intraperitoneal injections of diphtheria toxin into Pou4f3-huDTR mice (Tong et al., 2015). Earplug effectiveness was tested with auditory brainstem response recordings. For the monaural deprivation paradigm, neurotracers were injected into the ventral cochlear nucleus to identify fibers originating from the plugged ear in subsequent histological experiments. Axon diameter and myelin thickness were measured in trapezoid body (TB) fibers using immunohistochemical labeling for neurofilament and myelin basic protein. Patch-clamp recordings in coronal brainstem slices *in vitro* were performed to assess possible routes of communication between myelinating oligodendrocytes and axons.

All 3 deprivation paradigms caused significant reductions in myelin thickness of TB fibers, but only the lack of both spontaneous and sound-evoked activity caused significant reductions in axon diameter. This suggests that in the auditory system spontaneous activity is sufficient to maintain axon diameter, while additional sound-evoked activity is required to regulate myelin thickness. To test for a local communication signal between active axons and myelinating oligodendrocytes, passive and active properties of oligodendrocytes were assessed by patch-clamp recordings before and after high-frequency (1000Hz) electrical stimulation of TB axons. In response to this stimulation, 40% of the oligodendrocytes exhibited increased potassium currents.

We conclude that neuronal activity levels are locally communicated to the oligodendrocytes so that myelination can be regulated for individual active fibers within the TB fiber tract. In contrast to the regulation of myelin, axon diameter seems to only require spontaneous firing activity.

PS 800

Urocortin 3 Provides Strength and Endurance to Calyces of Held tuned to Low Sound Frequencies within the Medial Nucleus of the Trapezoid Body (MNTB).

Sara Pagella[1]; Ian D. Forsythe[2]; Conny Kopp-Scheinpflug[1]
[1]LMU Munich; [2]University of Leicester

Synapses involved in preserving temporal precision operate at extreme steady-state levels at which minuscule environmental perturbations such as energy restrictions can corrupt normal transmission. Additionally, context-related challenging natural stimuli may require fast adaptation. The flexibility required to fulfill such tasks is provided by an abundance of highly intertwined modulators and feedback systems. The Calyx of Held synapse is a prime example of these ultrafast, efficient systems and is known to be extensively modulated by many protein kinases and second messengers downstream of G-protein coupled receptor (GPCR) mediated signaling pathways. However, only few GPCR ligands have proven functional after hearing onset, rendering the identity and origin of potent and resilient initiators in the mature system unknown.

Patch-clamp recordings were performed on coronal brainstem slices of C57Bl6 mice at 36±1°C. Only calyces and cells located laterally within the MNTB were selected. Afferent fibers were activated by midline stimulation. Internal solutions contained fluorescent dyes to confirm calyceal recordings. Postsynaptic data were collected from P14-P30. Presynaptic data were recorded from P9-P12 (young) and from P13-P25 (mature). Single-unit MNTB recordings in vivo were obtained from mature C57Bl6 mice under MMF anesthesia.

Application of a specific Ucn3 receptor inhibitor (K41498) suggests a tonic presynaptic release of Ucn3 which then acts on the presynaptic terminal itself. Ucn3 application increases eEPSCs amplitudes and potentiates synaptic transmission during afferent fiber stimulation. Ucn3 application also caused faster recovery from depression after 100Hz stimulation trains, while the inhibitor had an opposite effect. Our data support an increase in the readily releasable pool (RRP) rather than a change in release probability as a mechanism underlying the potentiation and the preservation of temporal precision.

Preliminary MNTB recordings from Ucn3 KO mice in vivo revealed narrower presynaptic (calyceal) action potentials (APs) exclusively in laterally located, low-frequency cells. The positive correlation between presynaptic AP duration and latency of the postsynaptic

response observed in the wild type seems restricted to very short synaptic delays in Ucn3 KO mice. Direct presynaptic recordings from the calyx in vitro confirmed the change in presynaptic AP waveform. Application of Ucn3 prolonged presynaptic AP duration from 0.22ms to 0.28ms (n=8; paired t-test: P=0.029).

Ucn3, a stress-related neuropeptide, found solely in lateral calyces of the MNTB provides feedback and potentiates the synapse, making it resistant to exhaustion well after hearing onset. Ucn3 is fundamental to maintain high-frequency firing and preserves optimal calyx reactivity during bouts of high stress on the system.

PS 801

Effects of NLX-101, a 5-HT1A Serotonin Receptor Agonist, on the Auditory Brainstem Response of CBA/J Mice

Mackenzie Mills; Nikita Kumar; Robert Withnell; Laura M. Hurley
Indiana University

Serotonin 5-HT1A receptors are distributed throughout auditory nuclei with especially high concentration in the inferior colliculus. In mice, the inferior colliculus primarily contributes to waves IV and V of the auditory brainstem response. 5-HT1A receptor activation reduces the amplitude and latency of auditory brainstem response waves IV and V evoked by 8 kHz and 16 kHz tone burst stimuli. This study investigated the effects of NLX-101 (Neurolixis) on the auditory system in mice. NLX-101 (F15599) is a biased post-synaptic 5-hydroxytryptamine 1A (5-HT1A) serotonin receptor agonist which has been investigated as a treatment for disorders such as schizophrenia, depression, Parkinson's, and Rett syndrome. However, the effects of NLX-101 on the auditory system have not been examined.

In this study, male CBA/J mice were injected subcutaneously with NLX-101 (0.024-2.5 mg/kg; n=5) or saline (n=5). Auditory brainstem responses were recorded for 60 minutes pre-injection and 90 minutes post-injection. Responses were recorded using needle electrodes inserted at the left bulla (reference), vertex (active), and in the back (ground). Acoustic stimuli included broadband clicks and 21 kHz pure-tone bursts presented at the midline. Auditory brainstem response thresholds were also monitored throughout the experiment. Amplitude and latency of suprathreshold auditory brainstem response peaks I, IV, V, and P0 were analyzed using custom peak detection software in Matlab.

Results showed that group averages for the amplitude of auditory brainstem response waves I, IV, and P0 decreased over the duration of the experiment in both experimental and control groups, however, the experimental group showed amplitude decreases that were greater on average compared to the saline group. The detectability of wave V showed high variability in all animals and was often unidentifiable. There was no change in average wave latency following injection in either group. One mouse injected with the largest dose of NLX-101 (2.5 mg/kg) showed the greatest change in the ABR waveform with wave I, IV, and P0 amplitudes maximally decreasing 30 minutes post-injection and slowly recovering thereafter. Click evoked thresholds were relatively stable over the course of the experiment and did not change more than 10 dB SPL in any animals. This work informs the use of NLX-101 as a pharmaceutical treatment for a variety of central nervous system disorders, however, experiments with additional mice and stimulus levels are needed to fully understand the effects of this drug on the auditory system and to account for changes in wave amplitude and latency related to anesthesia.

PS 802

Hyperreactivity to Loud Noise and Increased Anxiety-like Behaviors in Serotonin Transporter (SERT) Knockout (KO) Mice After Noise Exposure

Ye-Hyun Kim[1]; James H. Engel[1]; Mark Scotto Di Vetta[2]; Amanda M. Lauer[1]
[1]Johns Hopkins School of Medicine; [2]Johns Hopkins University

Background
Patients with hearing loss or chronic tinnitus often report symptoms of anxiety or depression and its negative impact on social engagement. In cases of tinnitus, the perceived severity of tinnitus is often correlated with patient's stress level. The prevalence of emotional distress in hearing impaired patients suggests a possible link between stress/anxiety and hearing dysfunction. Recent studies have indicated the serotonergic system as a neuromodulator in the auditory pathways. Serotonin not only plays an important role in stress-related mood disorders, but also has been shown to modulate the excitability of auditory neurons in the auditory brain regions. To better understand the role of the serotonergic system in emotional distress resulting from hearing dysfunction, we investigated anxiety-like behaviors and noise-induced hearing loss in serotonin transporter (SERT) KO mice, in which deletion of SERT results in global dysregulation of serotonin and predisposition for a stress phenotype. SERT polymorphisms are associated with anxiety-related traits in humans, and SERT-positive neurons are expressed in regions of the auditory pathway implicated in tinnitus and hyperacusis, including dorsal cochlear nucleus and inferior colliculus.

Methods
SERT Knock-out (KO) (*Slc6a4* -/-), SERT Heterozygote (HET) (*Slc6a4* +/-), and control (C57BL/6J) mice were unilaterally noise exposed at 6 weeks-old. Unanesthetized mice were exposed to 116 dB, 16 kHz center frequency, 1 kHz band-pass filtered noise for 1 hour. Auditory brainstem response (ABR) and acoustic startle response (ASR) were tested before and after noise exposure to assess changes in hearing sensitivity and behavioral reactivity to loud noise, respectively. Open field and social interaction tests were also performed to investigate the effect of noise exposure on anxiety and social interaction behaviors.

Results
Unilateral noise exposure resulted in prominent high frequency hearing loss in the exposed ears in SERT KO, SERT HET, and control mice as measured by ABRs. Following noise exposure, SERT KOs displayed significantly larger ASR amplitudes compared to SERT HETs and controls, suggesting heightened reactivity to loud noise. Furthermore, SERT KOs exhibited significantly increased freezing time in an open field test and significantly reduced interaction time during a social interaction test after the noise exposure, indicating increased anxiety-like behaviors.

Conclusions
Our findings demonstrate that serotonergic system dysfunction affects behavioral reactivity to loud noise and increases anxiety-like behaviors following noise exposure. These results provide new insights into serotonin dysregulation and its relationship between emotional distress and hearing loss and identify a possible risk factor for negative psychological responses to hearing dysfunction.

PS 803

Synaptic NMDA currents and Short-Term Plasticity influence Spike Generation in Neurons of the Ventral Nucleus of the Lateral Lemniscus

Linda Fischer[1]; Michael Rebhan[2]; Nikolaos Kladisios[1]; Christian Leibold[2]; Felix Felmy[1]
[1]University of Veterinary Medicine; [2]Ludwig-Maximilians-University Munich

Neurons in the ventral part of the ventral nucleus of the lateral lemniscus (VNLL) receive large glutamatergic, somatic synapses that underlie the temporal precise generation of action potentials (APs). It remains unclear which synaptic components contribute to the precision and output generation during resting states as well as during ongoing activity. To determine the different synaptic contributions to the generation of APs, we recorded from VNLL neurons in acute brain slices from gerbils aged between postnatal day 19 and 30. We found that fast glutamatergic synaptic transmission in VNLL neurons was based exclusively on AMPA and NMDA receptor currents. The small NMDA component increased the EPSC time course at potentials close to rest. During synaptic 20-pulse stimulation trains, EPSCs exhibited short-term plasticity with paired pulse facilitation at initial pulses for stimulus frequencies above 50 Hz, and a subsequent frequency-dependent depression. Using dynamic clamp recordings, the effects of NMDA currents and short-term plasticity on AP generation were decomposed. During more than 6 seconds of simulated ongoing activity with random frequencies, short-term depression reduced AP generation and prevented a single synapse to become permanently supra-threshold. The depression effectively low-pass filtered the input and only permitted reliable onset APs to input transients presented at frequencies below 50 Hz. Above 100 Hz stimulation, frequency ongoing generation of APs was supported by the NMDA component. Thus, interplay of short-term plasticity and NMDA currents form the physiological basis for prominent onset response to simulated activity transients and ongoing action potential generation during high frequency input stimulations.

PS 804

Synaptic activity at the MNTB is disrupted in a mouse model with enhanced efferent olivocochlear system

Mariano N. Di Guilmi[1]; Luis E. Boero[2]; Valeria C. Castagna[2]; Adrián Rodríguez-Contreras[3]; Carolina Wedemeyer[1]; M. Eugenia Gómez-Casati[2]; A. Belén Elgoyhen[1]
[1]INGEBI - CONICET; [2]Instituto de Farmacología, Facultad de Medicina, Universidad de Buenos Aires; [3]The City University of New York, City College, Biology Department

The auditory system in many mammals is immature at birth but precisely organized in adults. Spontaneous activity in the inner ear plays a critical role in guiding this process. This is shaped by an efferent pathway that descends from the brainstem and makes transient direct synaptic contacts with inner hair cells (IHCs). In this work, we used an β9 cholinergic receptor knock-in mouse model with enhanced medial efferent activity (*Chrna9L9'T*, *L9'T*) to understand the role of the olivocochlear system in the correct establishment of auditory circuits. Wave III amplitudes of auditory brainstem responses (which represent synchronized activity of synapses within the superior olivary complex) were smaller in *L9'T* mice, suggesting a central dysfunction. The mechanism underlying this functional alteration was analyzed in brain slices containing

the medial nucleus of the trapezoid body (MNTB), where neurons are topographically organized along a medio-lateral axis. Electrophysiological recordings evidenced MNTB synaptic alterations. Spontaneous synaptic response (mEPSCs) displayed no changes in its amplitude among genotypes, while mEPSCs mean frequency displayed a significant increase in the *L9'T* lateral region (M: 2.52±0.56 Hz; L: 345 7.17±1.94 Hz; Mann-Whitney test, Z: -2.11, p=0.035). Moreover, evoked synaptic transmission was altered in the transgenic mice. While no significant differences in the unitary medial and lateral EPSC amplitudes were recorded in WT mice (M: 7.59±1.12 nA, n=9, 7 animals; L: 7.35±0.95 nA, n=10, 8 animals, ANOVA, F:0.027, p=0.87), evoked synaptic currents in the lateral side (5.07±0.87 nA, n=12, 11 animals) of *L9'T* mice were smaller compared to those of the medial side (8.05±1.37 nA, n=11, 11 animals; ANOVA, F:5.07, p=0.0357). These abnormalities were further supported by morphological alterations. Rhodamine-dextran labeling evidenced multiple innervation in *L9'T* MNTB principal cells suggesting an impairment during development. At the i*n-vivo* level, multielectrode recordings showed that the overall level of MNTB activity was reduced in the *L9'T*. The average multi-unit activity in WT (11.49±3.58 Hz, n=6 animals) was larger than in *L9'T* mice (2.53-±0.43 Hz, n=8 animals; Mann-Whitney U Test, Z=2.19, 806 p=0.028). The present results suggest that the transient cochlear efferent innervation to IHCs during the critical period before the onset of hearing is involved in the refinement of topographic maps as well as in setting the correct synaptic transmission at central auditory nuclei.

PS 805

Arrangement of Contact Sites from Single Excitatory Fibers on Medial Superior Olive Dendrites

Alexander R. Callan[1]; Martin Heß[1]; Christian Leibold[1]; **Felix Felmy**[2]
[1]Ludwig-Maximilians-University Munich; [2]University of Veterinary Medicine

Neurons in the medial superior olive (MSO) detect interaural time differences (ITD) in the microsecond time range. The temporal precision of the underlying cellular integration process for this coincidence detection is based on pre- and postsynaptic and morphological specializations. Thick bipolar dendrites with large potassium conductances accelerate the EPSP time course while still introducing a propagation time for distal EPSPs towards the soma, which is at least in the same range as physiologically relevant ITDs. Therefore, the arrangement of synaptic contacts of an input fiber may also be crucial to the size of the binaural coincidence time window.

To quantify the morphological arrangement of excitatory inputs on dendrites of MSO neurons and its impact on coincidence detection we combined axonal tracing, quantitative morphometry and computational modelling. Labelled axons terminating on MSO neurons followed closely the dendritic structure from distal sites to the terminal bouton with very little branching. Contact sites of labelled axons were identified as swellings adjacent to MAP2 labelled dendrites, a morphological feature that was VGlut positive. Single axons carried usually more than one swelling. Axonal swellings tended to cluster along the dendrite and the majority of terminal boutons were close to the soma. A single contact site harbors more than one active zone. Thus, a single fiber exerts strong excitation to the MSO dendrite along its whole extent. The influence of the distributions of axonal contact sites and travel times were examined in multi-compartmental models of an MSO neuron with conduction velocities known from either myelinated or un-myelinated axons. Distributed contact sites along the dendrite produced shorter EPSP peak latencies, normalized the EPSP time course and lead to larger summed EPSPs when compared to the same synaptic drive applied at a single site. Distributed synaptic sites also improved ITD sensitivity by sharpening the coincidence detection window, but sharpening only occurred when active low threshold potassium channels were present in the model. In a passive membrane model, distributed synapses actually widened the coincidence detection window, as predicted by cable theory. Thus, the arrangement of excitatory inputs of single fibers generally strongly affects the neuron's ability to transfer information about ITDs. Simulations also showed that, as expected, myelination further shortened EPSP peak latencies, but, interestingly, had no effect on coincidence window and EPSP amplitude, and hence did not facilitate ITD encoding.

PS 806

Cochlear protection after noise exposure requires 5-HT3A receptor via efferent feedback system

Kazuya Ohata[1]; Makoto Kondo[2]; Yukiko Hanada[3]; Yoshiyuki Ozono[1]; Takashi Sato[1]; Hidenori Inohara[4]; Shoichi Shimada[2]
[1]Department of Otorhinolaryngology-Head and Neck Surgery, Graduate School of Medicine, Osaka University; [2]Department of Neuroscience and Cell Biology, Graduate School of Medicine, Osaka University; [3]Department of Otorhinolaryngology, National Hospital Organization Osaka National Hospital; [4]Department of Otolaryngology - Head and Neck Surgery, Graduate School of Medicine, Osaka University

The cochlear efferent feedback system plays important roles during auditory processing, including the regulation of the dynamic range of hearing, and provides protective

effects against acoustic trauma. These effects are exerted through medial olivocochlear (MOC) neurons; however, the precise mechanisms remain unclear. Here, we show that the serotonin type 3A (5-HT3A) receptor is expressed in MOC neurons that innervate outer hair cells. Analyses of *Htr3a*$^{-/-}$ mice revealed that the 5-HT3A receptor is significantly involved in the activation of MOC neurons after noise exposure. 5-HT3A receptor knockout resulted in decreased MOC function, as measured by distortion product otoacoustic emissions, and in increased loss of ribbon synapses following noise exposure. 5-HT3A receptor agonist treatment reversed the noise-induced loss of ribbon synapses, enhancing the protective effects against acoustic trauma. These findings demonstrate that the 5-HT3A receptor is essential for cochlear protection after noise exposure via the MOC feedback system. This novel 5-HT3A receptor-mediated mechanism represents a new protective and therapeutic target for various hearing dysfunctions.

Auditory Brainstem: Functional Measurements

PS 807

Toward Improved Methods for Bone Conduction Auditory Brainstem Response Measurement

Andrew D. Brown[1]; Aoi A. Hunsaker[2]; Nathaniel T. Greene[3]
[1]Department of Speech & Hearing Sciences, University of Washington; [2]Department of Speech and Hearing Sciences, University of Washington; [3]Department of Otolaryngology, University of Colorado School of Medicine

The auditory brainstem response (ABR) indexes the functional status of the early auditory pathway, and is a good predictor of behavioral hearing thresholds. In cases of suspected conductive hearing pathology, and in selected research settings, it is necessary to assess hearing function via both the air conduction (AC) and bone conduction (BC) pathways. Whereas the ABR waveform elicited via AC stimulation is generally well-defined and informative, comprised of canonical 'waves' that can be ascribed to semi-discrete stages of the auditory pathway, the morphology of typical BC ABR waveforms is comparatively poor, often characterized by a single broad peak. Several peripheral factors may limit the fidelity of the BC ABR waveform, including transducer performance (insufficient gain or calibration), stimulus artifact, temporal dispersion of the stimulus during transmission through the bones and soft tissues of the head, and superposition of ipsilateral and contralateral responses. The objective of the present effort is to elicit improved BC ABR waveforms via modifications to BC transducers and stimuli, toward improved (more informative) BC ABR measurements. In an initial experiment intended to improve transducer performance, clinical BC transducers (Radioear B81) were electromagnetically shielded and fitted with high-density foam pads on the mastoid-contacting plate. An artificial mastoid was used to quantify acoustic effects of these manipulations. A series of BC ABR measurements was then completed in human subjects to quantify resultant changes in the ABR waveform (including reduction of stimulus artifact). In a second, parallel set of experiments intended to measure temporal dispersion of BC stimuli, broadband transients were delivered via a clinical BC transducer (Radioear B81) to fresh-frozen whole cadaveric heads while intracochlear pressures were measured using fiber optic pressure probes (FISO). The transient recorded in these intracochlear pressures was used to compute the BC-elicited impulse response, and subsequently to generate, using minimum-phase filtering, modified transient BC stimuli yielding temporally 'corrected' intracochlear pressure waveforms. That is, new BC stimuli were derived to offset the temporal dispersion observed using conventional BC stimuli. Finally, in an ongoing set of measurements, these derived BC stimuli are presented to human subjects using modified (shielded/padded) transducers in an otherwise standard ABR paradigm. Further work in this vein will elucidate basic aspects of BC sound transmission and hearing, and may yield improved BC ABR measurement protocols for diagnostic and research purposes.

PS 808

Effects of Aging and Language Background in Pitch Processing at the Brainstem Level

Jiong Hu[1]; Jennifer Henderson Sabes[2]; Shuo Wang[3]; Dongxin Liu[3]
[1]University of the Pacific; [2]University of the Pacific and University of California San Francisco; [3]Beijing Institute of Otolaryngology

Background
It has been well established that younger adults have stronger brainstem responses compared to older adults. Recent studies have also demonstrated that for people who speak tonal languages, their brainstems' pitch coding ability appear to be more robust and precise than those who do not. It has been proposed that such discrepancies may be due to the degradation in temporal processing due to aging, and the neural plasticity at the brainstem level resulted from long time auditory input from tonal language, respectively. However, no study to date has looked at the combined effect of aging and long term auditory input on listeners' pitch coding ability. The purpose of this study is to examine the voice pitch elicited brainstem responses, in listeners who are in different age and language back grounds.

Method
Four groups of participants were evaluated in this study: Mandarin speaking young adults, Mandarin speaking older adults, English speaking young adults and English speaking older adults. They all had normal audiometric test results as well as normal suprathreshold click-evoked ABR timing. Two Mandarin Chinese syllables with different fundamental frequency pitch contours were used to elicit brainstem responses. All stimulus tokens were controlled by Intelligent Hearing System and presented monaurally at 70 dB SPL. EEG signals were collected using standard one-channel montage. Fundamental frequencies (f0) of both the stimulus and the responses were digitally extracted and compared to individual brainstem responses. Spectral energies at the F0 and first formant (F1) ranges were also calculated. Several indices were used to examine different aspects of pitch processing ability at the brainstem level: Pitch Strength, Pitch Correlation, Response Robustness, and the F0 and F1 spectral energies. Responses elicited by different tones were also compared across and within the elderly and young adult groups, as well as different language groups.

Results
Results obtained from the younger listeners' group were more robust than their older counterparts, in both language backgrounds. Similarly, listeners with tonal language backgrounds had stronger pitch coding ability than those who speak non-tonal languages, in different age groups.

Conclusion
Results of this study suggest that aging plays an important role in listeners' pitch coding capacity, regardless of their language backgrounds. Results also re-established that long-term auditory inputs, such as tonal languages, certainly help enhancing the efficiency in processing ability in our auditory system.

PS 809

A Proposal for Objective Measurement of Gap Detection Threshold by Auditory Steady-State Response

Takashi Morimoto[1]; Toshimasa Ebina[1]; Yoh-ichi Fujisaka[1]; Takashi Nonaka[1]; Hidehiko Okamoto[2]
[1]Rion Co., Ltd.; [2]International University of Health and Welfare

This study aimed to establish a method for objective measurement of temporal resolution in the auditory system. Auditory temporal processing appears to play an important role in speech recognition and have been intensively studied. Gap detection threshold (GDT) is one of the proposed indices of auditory temporal resolution. However, existing implementations, such as the proposed laborious and subjective assessment methods, suffer from major flaws. For example, the experimenter's alertness, progressive and conservative characters, and language recognition ability may affect his/ her GDT. In problematic cases, the measurement may be time-consuming and may be discontinued since many trials are required to estimate his or her true threshold.

An appropriate objective measure is essential to overcome the above-mentioned issues. Therefore, we propose an objective method to measure GDT using auditory steady-state response (ASSR) elicited by silent intervals at a rate of 40 Hz embedded within pink noise (this stimulus is termed "gap in noise"). Furthermore, Fobel and Dau [JASA, 116 (4), pp. 2213–2222, 2004.] reported that rising-frequency chirp signals, compensated by the cochlear delay characteristics, enhance the amplitude of wave-V of the auditory brainstem response. Thus, we conducted an additional experiment to investigate the effects of a stimulus that had rising-frequency silent interval, i.e., the location of the interval differs slightly with each frequency band (this stimulus is termed "rising-frequency gap in noise"), on the ASSR. Herein, the delay characteristic reported by Neely et al. [JASA, 83 (2), pp. 652-656, 1988] was used to compose "rising-frequency gap in noise".

Ten subjects with normal hearing without otological and psychological histories participated in this study. The results obtained show that 1) the amplitudes of ASSR tend to increase as the duration of silent interval increases, 2) the silent interval detectable by ASSR corresponds well to the GDT, and 3) the amplitudes of ASSR elicited by "rising-frequency gap in noise" are larger than those elicited by "gap in noise."

These results suggest that GDT could be objectively estimated from ASSR elicited by silent intervals embedded within noise. Particularly, the ASSR elicited by "rising-frequency gap in noise" can be used as an indicator of the temporal resolution in the auditory system. Our new approach using ASSR elicited by the "rising-frequency gap in noise" will especially contribute for objective measures of auditory temporal resolution in elderly people, infants, and individuals with cognitive impairments and/ or language retardations, who cannot perform GDT measurements.

PS 810

Sex Differences in Auditory Brainstem Response Audiograms from Vasopressin-Deficient and Wild-type Long-Evans Rats

Payton E. Charlton; Kelcie C. Schatz; Kali Burke; Matthew J. Paul; Micheal L. Dent
University at Buffalo, SUNY

Rats are highly social creatures that produce ultrasonic vocalizations (USVs) during social interactions. Brattleboro rats, a Long-Evans derived laboratory rat that lacks vasopressin (AVP) due to a mutation in the *Avp* gene, produce fewer USVs with altered spectrotemporal characteristics during social interactions. It is unclear why Brattleboro rats produce atypical USVs, but one factor could be differences in auditory acuity between wild-type and Brattleboro Long-Evans rats. Previous studies have suggested a link between auditory processing and increased levels of AVP. Additionally, few studies have investigated sex differences in auditory processing by Long-Evans rats. Sex differences in auditory acuity have been demonstrated in many different species throughout the animal kingdom, but have not yet been determined in rats. This study aimed to measure auditory brainstem response (ABR) derived audiograms for frequencies ranging from 1 to 64 kHz in adolescent male and female homozygous Brattleboro rats (Homs), heterozygous Brattleboro rats (Hets), and wild-type Long-Evans rats, to better understand the role of AVP and sex differences in auditory processing. There were no differences in the ABR audiograms between Hom, Het, and wild-type Long-Evans rats, indicating that the chronic differences in levels of AVP do not appear to alter auditory processing. Interestingly, males and females across the three genotypes did vary in their ABR thresholds with males exhibiting higher thresholds compared to females. These are the first known sex differences to be demonstrated in rat ABR audiograms. The sex differences in ABR thresholds were most significant at the lowest and highest frequencies, which could possibly affect the perception of USVs. This study was supported by NSF IOS-1754878 to MJP and NIH DC012302 and DC016641 to MLD.

PS 811

Broadband and Frequency-Specific Auditory Brainstem Responses to Ongoing Naturalistic Speech

Melissa J. Polonenko[1]; Ross K. Maddox[2]
[1]University of Rochester Medical Center, Rochester NY USA; [2]University of Rochester, Departments of Neuroscience and Biomedical Engineering, Del Monte Institute for Neuroscience

Background
The auditory brainstem plays a pivotal role in processing sound, including salient speech signals. However, out of necessity most human brainstem studies have focused on brief stimuli such as clicks, tonebursts, or speech syllables. Recently, Maddox and Lee (2018) described a method for measuring auditory brainstem responses (ABRs) to ongoing natural speech, and found responses with a characteristic but temporally broad wave V.

Objectives
We extended this work by re-synthesizing natural speech to create “peaky” speech, with the objectives of 1) evoking additional waves of the ABR reflecting other neural generators, and 2) measuring responses across different frequency bands.

Methods
Peaky speech was created by first determining glottal pulse times during voiced segments of continuously-uttered stories. Harmonics were then re-synthesized so that their phases all crossed zero at the time of each pulse. Experiments comprised three parts: 1) proof of concept comparing responses to three kinds of diotic male-uttered speech: unaltered, peaky broadband, and peaky multi-band; 2) comparison of responses to male- and female-uttered peaky speech; and 3) exploration of dichotic peaky multi-band speech for audiological use. Multi-band speech comprised octave bands with center frequencies of 707, 1414, 2828, 5656 Hz for parts 1 and 2, and 500, 1000, 2000, 4000, 8000 Hz for part 3. All three experiments lasted 128 minutes, with 64-second segments of each condition interleaved. Two-channel responses were measured in adults with normal hearing, and waveforms derived using deconvolution.

Results
ABRs to original and peaky broadband male speech had wave V’s with similar mean latency. Wave I and sometimes wave III were identifiable in peaky speech responses, particularly for higher frequency bands and broadband speech. For multi-band speech, wave V latency characteristically decreased with increased frequency. Ten clear frequency-specific ABRs were simultaneously obtained to five audiological bands in each ear for each subject. Female peaky speech evoked smaller and later responses than male peaky speech. Responses to male speech reached good signal-to-noise ratios (SNR) faster than female speech, with 75% of subjects reaching 0 dB SNR within only 3 minutes for broadband and 20 minutes for multi-band male speech.

Conclusions
Re-synthesized naturalistic speech elicits canonical ABRs with standard component waves. Applications

include understanding the link between cortical and subcortical processes and objectively assessing frequency-specific hearing function using narrated stories. The technique also holds promise as a tool for speech-in-noise testing and amplification verification.

PS 812

Modeling Place Specificity in the Parallel Auditory Brainstem Response

Thomas J. Stoll; Ross K. Maddox
University of Rochester

The frequency-specific auditory brainstem response (ABR) is a valuable and widely used tool in both the clinic and in research labs, yet it is not without its shortcomings. In clinical use, the ABR tests one frequency and one ear at a time, leading to long overall test times. To address this, we recently developed the parallel ABR (pABR), which utilizes randomized stimulus timing to measure the responses to multiple frequencies in both ears all at once. The pABR produces similar results to the standard ABR in shorter times.

Another potential benefit of the pABR is an improvement in cochlear place specificity. At high stimulus intensities, cochlear excitation spreads asymmetrically towards the base, leading to low-frequency responses that include sometimes substantial contributions from higher-frequency parts of the cochlea. For the standard ABR, place specificity can be improved by using notched noise maskers, which block time-locked toneburst responses in the off-frequency regions. However, adding masking slows the collection of responses even further, and is rarely done in practice. Here we sought to model whether the pABR benefits from the same principle, with off-frequency responses to each toneburst frequency being masked by the set of other-frequency tonebursts.

We employed a commonly used model of the auditory periphery and nerve to examine the excitation of the inner hair cells (IHC) and auditory nerve (AN). Responses were simulated over a range of stimulus intensities and presentation rates for frequency-specific tonebursts in isolation and in parallel with all other frequencies. At low intensities, for both the IHC and AN, we found place-specific responses for both serial and parallel presentation. However, at high intensities, the pABR offered improved place specificity. This effect became more pronounced at higher presentation rates.

In this initial modeling study, we demonstrate that the pABR can improve place specificity for stimulus configurations in which the standard ABR shows significant cochlear spread. These modeling results align with our previously observed experimental results: at lower frequencies, pABR waveforms are smaller and have longer latencies than their serially recorded counterparts. These differences may stem from the fact that the off-frequency parts of the response have been masked. Thus, the pABR may provide responses that are not only faster than the standard ABR but that also more directly link stimulus frequency and cochlear place.

PS 813

Sub-cortical Responses to Continuous Musical Pieces and Selective Auditory Attention

Octave Etard[1]; Rémy Ben Messaoud[2]; Gabriel Gaugain[2]; Tobias Reichenbach[1]
[1]Department of Bioengineering and Centre for Neurotechnology, Imperial College London; [2]Imperial College London

Background
Humans excel at analysing complex acoustic scenes. Whilst the segregation of independent acoustic streams is mostly attributed to the auditory cortex, we recently showed that sub-cortical responses at the fundamental frequency of speech were modulated by selective attention as well [1,2]. Music is another important real-world sound that is characterized by pitch. Here we therefore investigated how sub-cortical responses to naturalistic musical stimuli can be measured and whether they are modulated by selective attention.

Methods
Normal hearing volunteers were presented diotically with continuous musical pieces consisting of either one single melodic lines, played by either a piano or a guitar, or consisting of two melodic lines, one played by a piano and the other by a guitar. For the stimuli with two melodic lines the volunteers were asked to selectively listen to one of the two instruments while ignoring the other. Vibratos were inserted into both melodic lines, and the volunteers were tasked with detecting those corresponding to the attended instrument. Neural activity was measured throughout the experiment from EEG.

We then used regularised linear forward and backward models to relate the recorded neural activity to different features of the music stimuli, including the broadband stimulus waveform, the temporal fine structure, and note onsets. The neural responses to each instrument were compared when they were attended versus when they were ignored. We then also related an index of neural modulation by attention to the behavioural performances of the different subjects.

Results
We found neural responses to the temporal fine structure of the musical stimuli. The latency (8 ms) and frequency content (above 100 Hz) of the responses indicated a sub-cortical origin. When analysing the responses to the two concurrent melodic lines, we found the responses to the attended instrument to be stronger than those to the ignored instrument, demonstrating a neural modulation of these sub-cortical responses.

References
[1] Forte, A. E., Etard, O., & Reichenbach, T. (2017). The human auditory brainstem response to running speech reveals a subcortical mechanism for selective attention. eLife 6:e27203. [2] Etard O., Kegler M., Braiman C., Forte A.E. & Reichenbach T. (2019) Decoding of selective attention to continuous speech from the human auditory brainstem response, Neuroimage 200:1.

PS 814

Subcortical Synchrony Drives Speech-in-noise Perception: Evidence from Multiple Cases of Auditory Neuropathy

Travis White-Schwoch[1]; Samira Anderson[2]; Jennifer Krizman[1]; Silvia Bonacina[1]; Trent Nicol[1]; Nina Kraus[1]
[1]Northwestern University; [2]Department of Hearing and Speech Sciences, University of Maryland, College Park, MD, USA

The hypothesis that subcortical synchrony is important for speech-in-noise perception is supported by three lines of evidence: (*i*) correlations between speech-in-noise performance and measures of subcortical synchrony; (*ii*) evidence that populations who struggle with speech-in-noise perception, such as older adults and children with learning disabilities, also exhibit poor subcortical synchrony; and (*iii*) evidence that multiple forms of auditory-cognitive training lead to gains in both speech-in-noise perception and subcortical synchrony. Still, this hypothesis remains debated, in part because these lines of research are essentially correlational. Causal support for this hypothesis could come from demonstrating a lack of subcortical synchrony in patients with extreme difficulties understanding speech in noise.

We pursued this question in 12 patients with auditory neuropathy, clinically defined as an absent auditory brainstem response (ABR) despite present otoacoustic emissions (OAEs) (Kraus et al., 1984, *Laryngoscope*; Starr et al., 1996, *Brain*). Of these, 8 were old enough to provide detailed reports on their listening skills. The remaining 4 underwent detailed electrophysiological testing on ABRs and frequency-following responses (FFR, a more sensitive measure of subcortical synchrony).

The 8 older patients reported significant difficulty with auditory tasks that require listening in noise, including speech-in-noise perception, following directions in classrooms or at work, and difficulty understanding competing talkers. Despite a range of hearing thresholds, ABRs were absent in the entire cohort.

We performed detailed speech perception and electrophysiological testing on IT, a patient with profound auditory neuropathy despite normal hearing thresholds. Speech perception in quiet was normal. On multiple measures of sentence perception in noise, however, she performed below the 1st percentile. Consistent with her absent ABR, we could not elicit frequency-following responses (FFRs) to multiple stimuli, rates, and listening conditions.

Several pathophysiological profiles can cause the auditory neuropathy phenotype, including pre-and post-synaptic insults, raising the question of whether IT's case generalizes. To this end, we tested ABRs and FFRs in children with auditory neuropathy (3 due to hyperbilirubinemia and 1 due to a novel variant of a genetic syndrome). None of the patients had ABRs or FFRs. One patient, AA, has a unilateral neuropathy; he had no ABRs or FFR in the affected ear but a detectable ABR and FFR in the unaffected ear.

The co-occurrence between an absent ABR/FFR and profound deficits in speech-in-noise perception reinforces the hypothesis that subcortical synchrony underlies successful perception of speech in noise.

Supported by the Knowles Hearing Center.

PS 815

Human Discrimination of Binaural Cues in High-Frequency Complex Sounds Simulated with a Two-Channel Count Comparison Model.

Jonas Klug; Jörg Encke; Go Ashida; Mathias Dietz
University of Oldenburg

The human auditory system uses various binaural cues to localize sound sources. Sounds originating from off-midline directions are received with an interaural time difference (ITD) and an interaural level difference (ILD). Most previous models simulating binaural perception extracted ITDs using a cross-correlation of bilateral excitatory inputs that resembles the function of so-called delay lines. However, mammals, probably including humans, are likely to extract ITD information without long delay lines. Furthermore, in contrast to the prevailing model concept, neurons wich are sensitive to envelope ITDs usually operate with an excitatory-inhibitory mechanism.

In this study, we combine the well-established auditory periphery model by Bruce et al. (Hearing Research 2018) with a coincidence counting model of the LSO (Ashida et al. PLOS Comput. Biol., 2016). A previous version of this model quantitatively accounted for a wide range of psychoacoustic lateralization data (Klug et al. ARO 2019).

Here we show predictions for psychoacoustic ITD and ILD discrimination data for various high-frequency complex sounds such as amplitude modulated tones and narrow band noise. Due to the relatively high stimulus intensity (~70 dB SPL), on-frequency phase-locking to the stimulus envelope was low so that the model extracted the relevant temporal information mainly from off-frequency neurons. Consequently, the model was tested with spectrally flanking noise, limiting off-frequency extraction and thus decreasing sensitivity.

However, the spectrally flanking noise effectively improved phase-locking of on-frequency model neurons which resulted only in a moderate decline of ITD sensitivity which is in line with psychoacoustic data. Furthermore, we expanded our back-end for making decisions in discrimination tasks and improved the fitting strategy for the model parameters in order to optimize the predictive performance of the model.

PS 816

Non-neural Artifact and Electrode Impedance Minimally Influence FFR Components

Jennifer Krizman; Silvia Bonacina; Travis White-Schwoch; Trent Nicol; Nina Kraus
Northwestern University

The frequency-following response, or FFR, captures the neurophysiologic response to sound's acoustic ingredients with remarkable precision. For this reason, the FFR provides considerable detail about sound processing in the brain. Though unique in its ability to capture myriad aspects of sound processing, like any other evoked response, the FFR is susceptible to contamination from non-neural sources during data collection. Two potential sources of non-neural noise are myogenic artifact and high electrode impedance. However, the extent to which they influence an FFR and whether their impact differs across FFR components is unknown. We compared FFRs of 464 university athletes and 416 of their non-athlete peers, aged 17-24 years. We chose these groups because previously student-athletes were found to have lower levels of non-stimulus activity, as measured by the amplitude of activity during the prestimulus region. This region is susceptible to both neural noise and non-neural noise; therefore, it is possible that the groups could differ on the quality of the recording, rather than on neurophysiological noise levels. To determine whether non-neural noise sources impact FFR recordings, and therefore account for these group differences, we correlated artifact rejection count and electrode impedance to individual FFR components, including pre-stimulus amplitude, and ran regressions to determine how much variance of each component can be explained by non-neural noise. We found that non-neural noise did not significantly correlate with individual response components, such as peak timing or magnitude of specific frequencies, and that it contributed minimally to broadband response magnitude. As expected, the largest contribution of artifact and impedance was to non-stimulus activity; however, covarying for these non-neural noise sources actually strengthened the group difference. Together these results suggest that individual differences in *neural* noise can be captured by activity over the prestimulus region, despite the influence of *non-neural* noise contributions to that region.

Supported by: NIH (NS102500) and the Knowles Hearing Center

PS 817

Auditory brainstem response estimates of hearing in deer mice (genus Peromyscus)

Laurel A. Screven; Madison M. Weinberg; Amanda M. Lauer
Johns Hopkins School of Medicine

Mouse models have become ubiquitous models used in both behavioral and electrophysiological measures of auditory function. Inbred laboratory mice (*Mus musculus*) have several limitations in their relevance as a model for human hearing, including their short lifespan, genetic homogeneity, high frequency range of hearing, and increased susceptibility to noise compared to humans. Deer mice (genus *Peromyscus*) have been used as an alternative laboratory model for linking natural variation in behavior with genetic and epigenetic factors. *Peromyscus* species may model the human condition more closely because of their longer lifespan (6-8 years) compared to *Mus* (2-3 years). Additionally, midbrain recordings suggest that *Peromyscus* species have increased sensitivity to lower frequencies (Ralls, 1967; Brown, 1973). The goal of the present experiment was to investigate the hearing ability in *Peromyscus*. Threshold sensitivity was estimated using auditory brainstem response audiometry (ABRs) for clicks and tone frequencies ranging from 250 to 32000 Hz. Mice were tested at multiple age points to characterize maintenance of hearing sensitivity. ABRs were further evaluated by quantifying wave amplitudes and latencies for suprathreshold intensities. Cochleas

were collected from some animals for histological analysis. Our results show that hearing sensitivity of *Peromyscus* is similar to *Mus* as estimated using the ABR. Despite their outbred status, ABR thresholds in *Peromyscus* showed low variability across individuals. The amplitude of the supreathreshold ABR waveforms appeared larger in *Peromyscus* than *Mus*, suggesting there may be differences in the ascending auditory pathway between the different species. Although hearing sensitivity may be similar between *Peromyscus* and *Mus*, there may be advantages of using *Peromyscus* in investigating more complex aspects of hearing due to their range of well-documented natural history, their tractability in laboratory housing environments, longevity, and usefulness in population genetics and transcriptomics studies. *Peromyscus* species have successfully been used in modeling epilepsy, aging, development, and eye disease.

[This work was supported by R01-DC016641 and R01-DC017620 (AML), NIH T32-DC000023 (LAS), and the David M. Rubenstein Fund for Hearing Research.]

PS 818

Effect of Anesthetic Type and Concentration on Auditory Brainstem Response Parameters

Noor-E-Seher Ali[1]; Anthony Ricci[2]
[1]*Department of Otolaryngology, Stanford University;*
[2]*Department of Otolaryngology and Department of Molecular and Cellular Physiology, Stanford University*

Background: Auditory brainstem responses (ABRs) are non-invasive hearing test used to physiologically assess the auditory pathway and peripheral function. To perform ABRs on animals, common anesthetics used are isoflurane and the combination of ketamine and xylazine (KX). The objective of this study is to determine the effects of KX and different concentrations of isoflurane on threshold, wave 1 amplitude, wave 1 latency, and RMS.

Methods: Fifteen Sprague Dawley rats approximately 20 days old were used for this experiment. Eight rats were anesthetized by administering 100mg/kg ketamine and 16 mg/kg xylazine intraperitoneally. Seven rats were inducted with 3% isoflurane and then maintained on 1.5% isoflurane for ten minutes. ABR recording was performed at 16 kHz from 0-80 dB intensity. For the isoflurane group, additional anesthetic concentrations were tested at ten-minute intervals at 2% and 3% isoflurane. Threshold was defined as the lowest intensity where a signal within the first 4 ms was 3 standard deviations above RMS of 0 DB trace. Wave 1 amplitude was defined as peak to trough (P1N1). Latency was defined as time from onset of stimulus to P1.

Results: We found average threshold with KX (27.5 ± 4.6 dB) was similar to threshold with 1.5% isoflurane (28.5 ± 6.9 dB), P = 0.3. Threshold with 2% isoflurane (37.1 ± 4.8 dB) and 3% isoflurane (38.5 ± 6.9 dB) was significantly higher, P = .009. Comparing three concentrations of isoflurane at 80 dB, as isoflurane concentration increased amplitude significantly decreased (P = 6.8E-05) and latency significantly increased (P = 7.35E-10). RMS of 0 dB trace decreased inversely to isoflurane concentration. Analysis of amplitude vs. intensity revealed at lower intensities such as 50 dB, amplitude was not significantly different between 1.5% isoflurane (612 ± 148 nV) and 2% isoflurane (513nv ± 150), P = 0.2, whereas at 80 dB, amplitude at 1.5% isoflurane (1719 ± 226 nV) and 2% isoflurane (1404 ± 214 nV) were significantly different, P = .0001)

Discussion: ABRs are commonly used to test hearing sensitivity and peripheral function; it is important to understand the effects of anesthesia on ABR parameters. Our data suggests that animals are more deeply anesthetized with increasing concentration of isoflurane which is reflected by the increase in threshold, decrease in amplitude, and increase in latency. It also suggests that the isoflurane may be anesthetizing fibers selectively as shown by the disproportionate difference in amplitude at high intensities compared to low intensities

Acknowledgements: This work was supported by NIH-NIDCD grant RO1 5P01AG051443 and NIH-NIDCD core grant DC010363. The Stanford OHNS core facilities is supported by the Stanford Initiative to Cure Hearing Loss through the Bill and Susan Oberndorf foundation.

Auditory Brainstem: Molecules & Function

PS 819

Comparison of Cochlear and Brainstem/Cortical Following Responses Evoked by Amplitude-modulated Tones in Normal-hearing Adults

Jessica Chen; Skyler G. Jennings
University of Utah

Background
Studies in laboratory animals show that the upper frequency limit of phase locking is lower in central neurons compared to auditory nerve fibers. In humans, phase locking can be indirectly assessed by measuring evoked potentials in response to amplitude-modulated (AM) tones. The analysis of these potentials can emphasize phase locking to the envelope (i.e. envelope following response [EFR]), or to the fine structure (i.e. frequency following response [FFR]). The EFR and FFR are dominated by electrical activity from neural generators close to the recording electrode. For the traditional high-

forehead (Fpz) recording montage, generators originate from the brainstem and cortex. This study compares EFRs and FFRs measured from a tympanic membrane (TM) electrode (EFR_{TM}, FFR_{TM}) with those measured from a high-forehead electrode (EFR_{FPZ}, FFR_{FPZ}). Since the generators for the TM electrode originate from the cochlea and auditory nerve, we hypothesize that the upper frequency limit for the EFR_{TM} and FFR_{TM} will exceed that of the EFR_{FPZ} and FFR_{FPZ}.

Methods

Auditory evoked potentials were measured in response to AM tones using a two-channel recording montage, to emphasize brainstem/cortical (Fpz electrode), or cochlear (TM electrode) generators. Stimuli with alternating polarity were used to extract the compound action potential and cochlear microphonic from measurements with a TM electrode. The modulation frequencies (fm) applied to 1000 or 3000 Hz carriers ranged from 20 to 1000 Hz.

Results

The modulation frequency with the largest amplitude was higher for EFR_{TM} compared to EFR_{FPZ}. This was true for both 1000 and 3000 Hz carriers. Robust $FFRs_{TM}$ were obtained for 1000 and 3000 Hz carriers. FFR_{FPZ} was present for the 1000 Hz carrier but not the 3000 Hz carrier.

Conclusions

The amplitudes of EFRs recorded from the forehead peaked at fm=40 Hz and were small or in the noise floor for fm=1000 Hz. Our results suggest that generators contributing to the EFR_{TM}, such as the auditory nerve, are able to follow higher modulation frequencies compared to brainstem/cortical generators. Pre-neural generators that contribute to the FFR_{TM}, such as cochlear hair cells, follow individual cycles of the carrier frequency beyond that observed from neural brainstem/cortical generators. These findings suggest that the upper limit of phase locking decreases from auditory nerve fibers to brainstem/cortical neurons in humans, consistent with single-unit recordings in laboratory animals.

PS 820

Molecular Characterization of the Olivocochlear Efferent System

Michelle Frank[1]; Austen Sitko[1]; Lisa Goodrich[2]
[1]Dept. of Neurobiology, Harvard Medical School; [2]Harvard

The sense of hearing relies on numerous cell types to transduce sound, process acoustic information, and guide behaviors. Many early auditory computations occur in the superior olivary complex (SOC), where specialized circuits aggregate sensory information from both ears to mediate sound localization. The SOC also houses auditory feedback cells that project back into the cochlea to target both hair cells and spiral ganglion neurons (SGNs). These olivocochlear efferent neurons (OCNs) are known to play numerous roles in the auditory system, including protecting the cochlea from acoustic injury and aiding in speech-in-noise detection. Mammalian OCNs are typically classified into two major categories based on their anatomical projections: medial olivocochlear neurons (MOCs) project to outer hair cells, whereas lateral olivocochlear neurons (LOCs) project to type I SGNs. Little is known, however, about the molecular or genetic factors that distinguish these major subsets of OCNs from each other or from other brainstem neurons. As such, no markers exist to identify or manipulate subsets of OCNs, and virtually nothing is known about any heterogeneity within these major OCN subtypes.

To address this gap, we've used a high-throughput, single-cell sequencing approach to profile the transcriptome of individual OCNs. Because OCNs are essentially all cholinergic, we used Chat-Cre to drive expression of the nuclear-localized reporter allele Sun1-GFP and FAC-sorted dissociated nuclei to collect a pool of single, cholinergic nuclei. We then used the 10x Genomics platform to capture RNA from these individual nuclei. Our dataset encompasses a total of about 43,600 nuclei from mice at P1, P5, and P26-28 and includes 1,674 OCNs, as well as a number of motor neuron subtypes, several other neuronal populations, and a small number of non-neuronal cells. At each time point, we've identified clusters corresponding to MOC and LOC neurons. Differential gene expression analysis has identified novel markers for both MOC and LOC neurons, as well as factors that distinguish OCNs from the nearby facial motor neurons and other brainstem cholinergic cell types. Many of these markers are present neonatally and persist into adulthood. We've also identified several previously unreported receptors and guidance molecules that are differentially expressed between MOCs and LOCs, which may offer new insights for the development and function of OCN circuitry.

PS 821

A model with efferent gain control explains the time-varying responses of inferior colliculus neurons to amplitude-modulated stimuli

Afagh Farhadi[1]; Skyler G. Jennings[2]; Elizabeth A. Strickland[3]; Laurel H. Carney[1]
[1]University of Rochester; [2]University of Utah; [3]Purdue University

The medial olivocochlear (MOC) efferent system has been hypothesized to account for psychoacoustic phenomena, such as the effect of a precursor on detection and discrimination thresholds. However, a time-varying gain control efferent system that simulates ascending and descending neural pathways has not been implemented in previous models. The MOC efferent system receives excitatory projections from both the central nucleus of the inferior colliculus (ICC) and from the small cell-cap (SCC) in the anteroventral cochlear nucleus. High-spontaneous-rate (HSR) auditory-nerve (AN) fibers, which have saturated average rates at mid-to-high sound levels but have fluctuating instantaneous rate patterns that vary across frequency channels, initiate the ascending path to the ICC. Low- and medium-spontaneous-rate fibers, which encode sound level in their average rates, project to the SCC, which in turn projects to the MOC. In this work, phenomenological models of AN fibers and midbrain neurons included the two projections to the MOC, which controlled cochlear gain. The response rates of ICC neurons in awake rabbit to AM stimuli at several modulation depths change over a long time course (hundreds of msec). These responses were used to adjust the time constant of the efferent activity. The hypothesis tested in this modeling study was that a model with efferent control could explain the time course of the increase in discharge rate observed for IC cells with band-enhanced (BE) modulation transfer functions (MTF). In the proposed model, lower cochlear gain reduces inner-hair-cell saturation and thus increases fluctuations in responses of HSR ANs, leading to increased rates of BE IC cells and increased MOC activity. This process provides positive feedback that increases ICC rates over time in response to AM stimuli. Supporting the hypothesis, most IC BE cells had rates that increased over time in response to AM stimuli, especially for stimuli with lower modulation depths. BE ICC cells were the focus of this preliminary study because the increase in their rate over time cannot be confused with rate adaptation. The impact of modulation depth, modulation frequency and sound level on the time course of ICC responses was studied. This information was employed to adjust the parameters of the MOC efferent system in the proposed model for subcortical processing. This research has been supported supported by NIH-DC010813.

PS 822

Low-Level Noise Increases Auditory Loudness and Temporal Processing

Lin Shi[1]; Katie Palmer[2]; Yuying Liu[3]; Haolin Wang[1]; **Wei Sun**[2]
[1]The First Affiliated Hospital of Dalian Medical University; [2]State University of New York at Buffalo; [3]Shanghai First People's Hospital, Shanghai Jiao Tong University

Although low level noise is typically considered to be safe to our ear, recent studies suggested that long term exposure to a "safe" noise may still impair cochlear synapses and induce hearing disorders. However, effects of low-level noise on the central auditory system (CAS) and auditory processing are still not clear. Here we studied effects of two weeks of noise exposure (83 dB SPL) on auditory loudness and temporal processing using CBA mice. The loudness change was evaluated using acoustic startle response (ASR) and the auditory temporal processing was evaluated using gap-induced prepulse inhibition. C-Fos staining of the central auditory system was used to detect the neural activity changes induced by the noise exposure. Consistent with previous studies, no permanent hearing threshold shift was detected after the low-level noise exposure evaluated by auditory brainstem response test (ABR). However, the amplitude of ASR increased significantly after the noise exposure and lasted several days before it returned to the previous level. The gap detection induced by brief silent signals (1-100 ms) also improved significantly right after the noise exposure. These data suggests that low level noise exposure can cause an increase of loudness and temporally improve auditory temporal processing. Noise exposure caused an increase of C-Fos stainings in the caudal pontine reticular nucleus (PNC) and dorsal cochlear nucleus (DCN), but not in the higher levels of auditory system (the inferior colliculus, the medial geniculate body, the pedunculopontine tegmental nucleus and the auditory cortex). Our results revealed that low level noise exposure can increase auditory loudness and temporal processing by increase the excitability of the low-level auditory pathways. These phenomena may be related to noise induced tinnitus and hyperacusis which are related to auditory loudness perception changes.

PS 823

Evidence for Two Octopus Cell Subtypes: an in vivo Single-Cell Recording and Labeling Study

Hsin-Wei Lu[1]; Philip Smith[2]; Philip Joris[1]
[1]KU Leuven; [2]University of Wisconsin, Madison

Octopus neurons are remarkable but little studied projection neurons of the cochlear nucleus. Their name (Osen, 1969) refers to their unique dendritic orientations. Their somas occupy the octopus cell area (OCA) of the posteroventral cochlear nucleus (PVCN), and their axons project through the intermediate acoustic stria (IAS) to the contralateral brainstem. In vitro, these neurons have very leaky membranes and small action potentials (Golding and Oertel, 1995), which may explain the paucity of in vivo data. Extracellular recordings in the OCA revealed two types of onset responses to short pure tones (Godfrey et al., 1975): pure onset (Oi), and

onset with a low rate of sustained spiking (OL). Both groups showed remarkable temporal precision and entrainment to clicks. Of four studies that achieved direct in vivo recording and labeling, two found that octopus cell axons project into the trapezoid body (TB) rather than into the IAS. Thus, the function-structure relations of octopus cells and the significance of OL vs. Oi responses remain unclear. We report more than 30 Oi and 8 OL units using in vivo single-cell (sharp or whole-cell) recordings in the Mongolian gerbil PVCN. Thirteen Oi and 4 OL cells could be morphologically reconstructed by biocytin staining. OL cells showed distinct membrane properties compared to Oi cells: they have larger (30-40 mV in OL vs 10-20 mV in Oi) and broader (>1 ms halfwidth in OL vs ~0.5 ms halfwidth in Oi) spikes with a prominent afterhyperpolarization. OL units had narrower frequency tuning and lower pure-tone thresholds (40-50 dB SPL in OL vs 65-80 dB in Oi). Although both subtypes show entrainment to click trains, Oi units overall could follow clicks at a higher rate (> 300 Hz) compared to OL units. Oi but not OL units show tuning to monaural phase of Schroeder harmonic complexes. Both groups show large cell bodies within the OCA and dendrites oriented towards one side. However, OL axons headed ventrally into TB, whereas Oi axons headed into the IAS. Preliminary data also suggest projectional differences between the two types. In summary, our results imply that Oi and OL responses derive from two distinct cell populations. They share some key features of octopus cells but also differ in membrane properties, frequency tuning, temporal responses, and axonal projection patterns. We suggest that the OL neurons form a newly discovered class of projection neuron.

PS 824

Investigating Potential Mechanisms for Enhancement of Synchronization in Bushy Cells of the Ventral Cochlear Nucleus

Melih Yayli; Ian C. Bruce
McMaster University

Auditory nerve fibers (ANFs) show synchronous firing to a specific half cycle of the incoming sinusoidal stimuli. This synchronous firing behavior is further enhanced in the bushy cell populations within the ventral cochlear nucleus (VCN; Joris et al., J. Neurophys. 1994; Joris and Smith, Neurosci. 2008). These cells receive excitatory inputs from ANFs and inhibitory inputs from other cochlear nucleus cell populations such as D-stellate (DS) and tuberculoventral (TV) cells. Anatomical studies have also shown evidence for gap junctions (electrical synapses) between busy cells in both rat (Gómez-Nieto and Rubio, J. Comp. Neurol. 2009) and rhesus monkey (Gómez-Nieto and Rubio, Neurosci. 2011). For globular bushy cells (GBC), their enhancement in synchronous firing can be explained by GBC's receiving large numbers of subthreshold ANF inputs and acting as a coincidence detector (Joris and Smith, Neurosci. 2008). For spherical bushy cells (SBC), which have only small numbers of ANF inputs, the mechanism for synchrony enhancement is still unclear. In this study, biophysically detailed neural network models for GBC and SBC microcircuits have been developed based on the model of Manis and Campagnola (Hear. Res. 2018). The model receives ANF inputs from the phenomenological auditory periphery model of Bruce et al. (Hear. Res. 2018). We will extend this model to include gap junctions between populations of bushy cells.

Potential mechanisms for synchrony enhancement, including the roles of inhibition (broadband and narrowband inhibition provided by DS and TV cells respectively) and gap junctions, will be inspected by using our GBC and SBC microcircuit models. The results of this study will provide insight into the mechanisms behind the enhanced synchronization and entrainment properties of bushy cells, which are important for subsequent binaural processing within the superior olivary complex.

[Funded by NSERC Discovery Grant #RGPIN-2018-05778.]

PS 825

Bushy Neurons of the Anteroventral Cochlear Nucleus in Mice Show Different Response Types In Vitro to Auditory Nerve Stimulation

Meijian Wang; **Ruili Xie**
Department of Otolaryngology, Ohio State University

Bushy neurons of the anteroventral cochlear nucleus are known to process auditory temporal information. These neurons are innervated by giant Endbulb of Held synapses from the auditory nerve and are widely studied as a model for auditory processing. While most in vitro studies considered bushy neurons as a homogeneous group, it remains unclear how diverse bushy neurons behave in brain slices to sustained auditory nerve inputs. Here, we investigated how bushy cells respond to auditory nerve stimulation in acute brain slices from mature CBA/CaJ mice. Whole-cell current clamp recording was made from target bushy neurons while the auditory nerve was activated with electric train stimulations at 100 and 400 Hz. We found three subtypes of firing patterns in bushy neurons based on their responses, which included onset, transient and sustained firing patterns. Bushy neurons with onset firing pattern fired only a few spikes to the onset of the train stimulation, followed by evoked EPSPs

that failed to trigger any action potentials. Bushy neurons with transient firing pattern showed robust spikes at the beginning of the stimulation, followed by gradually decreased spike rate until they stopped firing toward the end of the stimulus train. Finally, bushy neurons with sustained firing pattern showed robust firing at the beginning, followed by reduced but stable firing rate, which lasted throughout the duration of the stimulus trains. The results indicate that bushy neurons show diverse response patterns in vitro to auditory nerve stimulation, and these different subtypes of bushy cells could have different roles in processing auditory information.

PS 826

Temporary Treatment With a Colony Stimulating Factor 1 Receptor Inhibitor Early in Development Affects Auditory Brainstem Response in Young Adult Mice

Giedre Milinkeviciute; Sima M. Chokr; Jasmine T. Lu; Aaron Gudmundson; Karina S. Cramer
Department of Neurobiology and Behavior, UC Irvine

Communication between neurons and glia is required for the establishment of functional neural circuits. Microglia promote neural wiring through regulated apoptosis, neurogenesis, synaptogenesis, as well as synaptic pruning. We are investigating the role of microglia in auditory brainstem circuit formation during development. Previously, we described a method for the depletion of microglia early in development using an inhibitor of colony stimulating factor 1 receptor (CSF1R), which is essential for microglial survival. We focused on the formation and pruning of the calyx of Held in the medial nucleus of the trapezoid body (MNTB). We showed that expression of glial fibrillary acidic protein (GFAP) is significantly decreased and monoinnervation of MNTB neurons is significantly disrupted in microglia-depleted mice at postnatal day (P) 13. Here, we investigated whether microglia return after the treatment is stopped, and if so, how long it takes for these cells to fully repopulate MNTB. Most importantly, we describe the effects that temporary microglial depletion during early postnatal development has on the auditory function in young adult mice. Microglia were pharmacologically depleted by a series of subcutaneous injections. Treatment was terminated at P10. Brainstems of mice were examined at P13-14 and P27-28. Brains were processed using standard histologic methods for visualization of GFAP and ABRs were recorded at P28. Microglia slowly repopulate the brainstem after the treatment is stopped. The first cells appear in the lateral extremities of the brainstem and are seen in the cochlear nucleus and lateral superior olive at P21. Later, microglia infiltrate the rest of the brainstem by gradually moving towards the midline. MNTB becomes fully repopulated by P27. The expression of GFAP is significantly decreased in microglia-depleted mice at P13-14; however, the expression is restored to the control levels by P27-28. Auditory thresholds in response to clicks, low and high frequencies are significantly increased in mice that underwent microglia depletion early in development. Our results indicate that the temporary absence of microglia before hearing onset leads to lasting effects on the auditory function despite complete repopulation of microglia and restored GFAP expression level. These findings highlight the significance of microglia in the formation of auditory neural circuits early in development. These results suggest peripheral and central changes that result from early postnatal CSF1R inhibition.

Auditory Cortex: Neural Mechanisms

PS 827

Functional Connectivity of Interneuron Subtypes in Layer 1 of the Mouse Primary Auditory Cortex

Lucas G. Vattino[1]; Carolyn G. Sweeney[1]; Ana C. Castro[2]; Benjamin M. Glickman[2]; Anne E. Takesian[1]
[1]Department of Otolaryngology–Head and Neck Surgery, Harvard Medical School; Eaton-Peabody Laboratory, Massachusetts Eye and Ear; [2]Eaton-Peabody Laboratory, Massachusetts Eye and Ear

Inhibitory interneurons in layer 1 of the primary auditory cortex (A1) convey behaviorally-relevant information by integrating sensory-driven inputs with neuromodulatory signals. It has been proposed that these interneurons have the capacity to regulate moment-to-moment A1 activity and therefore the encoding of the sensory environment in a context-dependent manner. We and others have shown that these interneurons are heterogenous and can be subdivided into two major classes defined by expression of either neuron-derived neurotrophic factor (NDNF) or vasoactive intestinal peptide (VIP). However, it remains unknown if these subtypes receive differential excitatory and inhibitory inputs. Using fluorescence-guided whole-cell electrophysiology in mouse thalamocortical slices to record from NDNF or VIP interneurons during thalamic electrical stimulation, we found that both subtypes receive monosynaptic thalamic excitatory inputs. Moreover, two-photon GCaMP6s calcium imaging in A1 of awake mice revealed that all layer 1 interneurons respond to noise burst stimuli, but VIP interneurons are less responsive than those not expressing VIP (non-VIP). These results were supported by immunolabeling of glutamate vesicular transporter 2 (VGluT2), a marker of thalamocortical boutons. Puncta expressing VGluT2 were distributed onto the somato-dendritic compartments of all layer 1 interneurons. However, VIP interneurons showed a reduced number of VGluT2 positive puncta

as compared to non-VIP interneurons. Together, our results suggest that layer 1 interneuron subtypes are differentially recruited by sound stimuli, arising from differences in their thalamic inputs. To study the putative circuitry between these interneuron subtypes, we obtained recordings in layer 1 interneurons while selectively light-activating channelrhodopsin (ChR2)-expressing VIP or NDNF cells. We revealed $GABA_A$-mediated synaptic connections within networks of NDNF or VIP interneurons. By understanding the layer 1 microcircuits, our results may shed light on the function of the distinct layer 1 interneurons in sound perception.

PS 828

Noise-Induced Neuroinflammation Contributes to Central Auditory Processing Disorder

Weihua Wang[1]; Samer Masri[1]; Nakayla Chan[1]; Tyler Marsh[1]; David Schaub[1]; Li Zhang[1]; Jinsheng Zhang[2]; **Shaowen Bao**[1]
[1]University of Arizona; [2]Wayne State University

Hearing loss is a major risk factor for tinnitus, hyperacusis and other central auditory processing disorders. Although recent studies indicate that hearing loss causes neuroinflammation in the auditory pathway, its potential contribution to hearing loss-related pathologies are still poorly understood. We examined neuroinflammatory responses and changes in cytoarchitecture in the auditory cortex following noise-induced hearing loss and their involvement in central auditory processing disorder. Our results indicate that noise-induced neuroinflammation is required for changes in specific auditory cortical circuits. Blockade of those changes with anti-inflammatory drugs or reversing those changes with optogenetic or chemogenetic methods alleviate noise-induced central auditory processing disorder. These results implicate neuroinflammation as a therapeutic target for hearing loss-related central auditory processing disorders.

PS 829

Synaptic Zinc Shapes the Sound-Evoked Responses of Corticocollicular Neurons in the Auditory Cortex

Mason McCollum; Philip Bender; Charles T. Anderson
WVU School of Medicine

Many auditory neurons are sensitive to acoustic context, m0.2 ineaning that their responses to sounds are influenced by other sounds in the environment. This contributes to stimulus-specific adaptation – neuronal responses to frequently heard sounds are suppressed while responses to rarely heard sounds are maintained – which is hypothesized to enhance acoustic novelty detection. In humans, a similar phenomenon is observed with mismatch negativity, an event-related potential recorded from the scalp that is sensitive to sounds that deviate from a sequence of repeated sounds. Schizophrenia is associated both with deficits in mismatch negativity and with altered processing in the primary auditory cortex. Since many people with schizophrenia have deficits in detecting acoustic novelty, this suggests that cortical acoustic context sensitivity is important for normal cortical processing and contributes to the etiology of this disorder.

The auditory cortex is highly enriched with synaptic zinc. Zinc (as Zn^{2+}) is loaded into glutamatergic vesicles by the zinc transporter ZnT3 and coreleased with glutamate. Synaptic zinc shapes the sound-encoding properties of neurons in mice. In human populations, schizophrenia is linked with reduced levels of ZnT3 mRNA and protein; and ZnT3 knockout mice, which lack synaptic zinc, have severe auditory discrimination deficits. Therefore, it is of great interest to understand how synaptic zinc shapes acoustic context sensitivity in the auditory cortex.

Corticocollicular neurons in the auditory cortex receive input from a wide array of presynaptic neurons and send descending axons to multiple subcortical auditory processing structures. These neurons are tuned to a broad range of sounds and have long and variable latencies in their sound-evoked responses. Because of these features, corticocollicular neurons are well-suited to integrate recent acoustic experience and demonstrate sensitivity to acoustic context.

Here, we use 2-photon calcium imaging in awake mice while presenting a variety of sound stimuli. We find that synaptic zinc signaling shapes the tonal receptive field structure of corticocollicular neurons as well as their sensitivity to specific speeds and directions of frequency-modulated sweeps – stimuli that present the same spectral information in different acoustic contexts. We also combine whole-cell patch-clamp recordings from identified corticocollicular neurons in acute brain slices with optogenetic stimulation to measure how synaptic zinc shapes inputs from specific classes of presynaptic neurons. Together, these experiments allow us to dissect how synaptic zinc shapes the synaptic inputs and the spiking output of corticocollicular neurons and hence understand cortical mechanisms contributing to acoustic context sensitivity.

PS 830

Long-Range Projecting Inhibitory Neurons in Primary Auditory Cortex

Christine Junhui Liu[1]; Benjamin M. Glickman[2]; Lucas G. Vattino[3]; Ana C. Castro[2]; Anne E. Takesian[3]
[1]Speech and Hearing Bioscience and Technology, Division of Medical Sciences, Harvard Medical School; Eaton-Peabody Laboratory, Massachusetts Eye and Ear; [2]Eaton-Peabody Laboratory, Massachusetts Eye and Ear; [3]Department of Otolaryngology–Head and Neck Surgery, Harvard Medical School; Eaton-Peabody Laboratory, Massachusetts Eye and Ear

Cortical circuits remodel throughout life to adapt to changes in experience and the surrounding environment. Identifying neural targets that control central auditory plasticity will have far-reaching impact, offering potential ways to restructure neural circuitry. Our work and that of others previously identified a group of superficial inhibitory neurons, characterized by selective serotonergic 5-HT_{3A} receptor expression (5-HT_{3A}R neurons), as a key convergent site for sensory and neuromodulatory inputs that gates plasticity in auditory cortex. However, little is known about the anatomical and functional connectivity of these neurons. Previous studies have focused on short-range, local outputs of 5-HT_{3A}R neurons. Here, we report long-range projections from 5-HT_{3A}R neurons that extend vertically into deep layers of the cortical column, horizontally into neighboring columns, and to subcortical regions. To survey the columnar and laminar organization of the long-range projecting 5-HT_{3A}R neurons, we employed the AAV-Brainbow technology, a genetic strategy using Cre-loxP recombination for stochastic combinatorial expression of fluorescent proteins. This technique allowed us to individually label 5-HT_{3A}R neuron subtypes with distinct colors and examine their axonal projections and postsynaptic targets. Parallel studies using retrograde viral tracers and immunohistochemistry classified the presynaptic identity of the 5-HT_{3A}R neurons that project to distal subcortical targets. Together, these experiments reveal that several subtypes of 5-HT_{3A}R neurons expressing vasoactive intestinal peptide (VIP), gamma-synuclein (SNCG), and neuropeptide Y (NPY) send long-range projections to distant cortical and subcortical regions. Ongoing electrophysiological studies aim to evaluate the intrinsic and synaptic properties of these long-range projecting 5-HT_{3A}R neurons. These results will guide future *in vivo* studies to determine the effects of these neurons in promoting plasticity in auditory cortical circuits. Together, the characterization of these long-range projecting 5-HT_{3A}R neurons offers a key first step to uncover mechanisms regulating auditory plasticity, providing potential novel therapeutic targets for recovery from peripheral hearing loss.

PS 831 - WITHDRAWN

PS 832

Cellular and synaptic signaling mechanisms underlying increased cortical gain after noise-induced hearing loss in mice

Manoj Kumar[1]; Thanos Tzounopoulos[2]
[1]Pittsburgh Hearing Research Center, Department of Otolaryngology, University of Pittsburgh; [2]University of Pittsburgh, Otolaryngology and Neurobiology

Noise-induced hearing loss (NIHL) reduces auditory sensory inputs relayed from the cochlea to the auditory cortex (AC). To compensate for the loss of peripheral inputs, excitatory neurons in AC increase their response gain, the slope of sound level against the neuronal response. Importantly, this increased gain may even result in hyperacusis and tinnitus. Despite the established role of changes in cortical excitation-inhibition balance in AC after NIHL, the precise synaptic signaling mechanisms and time-specific plasticity in excitatory principal neurons (PNs) and inhibitory, parvalbumin- (PV) and somatostatin-expressing (SOM) neurons remains unknown. Employing *in vivo* wide-field Ca2+ imaging in awake mice, we found that the sound-evoked responses of PNs and PVs are reduced 1 day after NIHL but surpassed baseline responses 10 days after NIHL. On the contrary, SOM response is reduced 1 day after NIHL and remained reduced for 10 days. These results suggest that a cell- and time-dependent plasticity in PNs, PVs, and SOMs contribute to increased AC gain after NIHL. Next, we found that chronic cortical elimination of synaptic-zinc, a cell-specific neuromodulator of cortical gain, eliminated the NIHL-induced gain increase in AC principal neurons, suggesting that synaptic zinc is required for the increased cortical gain after NIHL. Supported by NIDCD, R-01 DC007905 award to TT

PS 833

Histological Cortical Depth Profiles for Microstructural Analysis of Feline Auditory Cotrex

Kwame S. Kutten[1]; Lea Sollmann[2]; Peter Hubka[2]; Jenny Trieu[1]; Daniel J. Tward[1]; Laurent Younes[1]; Andrej Kral[3]; J. Tilak Ratnanather[1]
[1]Johns Hopkins University; [2]Hannover Medical School; [3]Dept. of Experimental Otology, Hannover Medical School, Germany; DFG Cluster of Excellence "Hearing 4 All"

Hearing loss causes both structural and functional changes in the auditory cortex. Previous work in cats demonstrated that congenital deafness alters the thickness of deeper cortical layers V and VI (Berger *et al.* 2017). Abnormal responsiveness to visual stimuli in the

higher order auditory cortex have also been observed (Land *et al.* 2016). Thus to explore structural and functional alterations of cortical topology due to hearing-loss, three-dimensional cortical depth profiles were constructed from SMI-32 histology. This histological staining primarily labels dendrites and cell bodies of a subgroup of pyramidal cells enabling the identification of cortical layers III and V. After volumetric reconstruction of histological data, inner and outer surfaces were defined at the gray-white boundary and pia mater of the feline auditory cortex. Curved paths which approximate the columnar structure of the cortex were identified through deformable registration. Points in these curves were reparametrized on a domain from 0.0 (at pia matter) to 1.0 (at white matter) to adhere to the equivolumetric topology of the cortex. Staining intensities were interpolated along twenty points within each curve of the equivolumetric domain. These depth profiles could be used to characterize cortical areas and could delineate boundaries between primary and higher-order areas of the cortex (Schleicher *et al.* 1998). Future work may combine these profiles with electrophysiological data to correlate functional and structural parameters of cortical columns.

Funding
This work was supported by National Institutes of Health (NIH) grant R01-DC016784, Germany Federal Ministry of Education and Research (BMBF) grant 01GQ1703 and the Kavli Neuroscience Discovery Institute

PS 834

Inactivating Parvalbumin Interneurons in Auditory Cortex Alters Cortical Oscillation Patterns

Mawaheb Kassir
University of California, Riverside

Cortical brain activity exhibits an oscillatory nature that has been observed in neuronal circuits and across neuronal populations (Cardin, 2018). These characteristic rhythmic oscillations have been shown to be regulated by inhibitory action elicited via GABAergic interneurons onto pyramidal cells (Whittington et al., 1995; Sanchez-Vives & McCormick, 2000). It is suspected that interneurons differentially modulate circuit and cortical oscillatory activity. For instance, in the mouse visual cortex, parvalbumin (PV) interneurons were found to promote 20-80 Hz oscillations and restrict field potential synchronization, while somatostatin interneurons promoted 5-30 Hz oscillations (Chen et al., 2017). In the auditory cortex, the particular contribution of PV interneuron activity in regulating population activity has not yet been investigated, though it is a critical step towards understanding human pathologies that simultaneously involve central auditory deficits and disruptions in PV interneurons. In this study, I tested how silencing PV neurons in auditory cortex alters rhythmic population activity during the presentation of sounds.

Auditory cortex of PV-Cre mice was stereotaxically injected with a PV-targeting adeno-associated virus carrying a silencing DREADD (i.e., designer receptor exclusively activated by designer drugs), and mice were subsequently implanted with recording electrodes. We previously developed a three-electrode electrocorticogram that provides temporal precision and translational potential to human studies (Lovelace et al., 2018). A recording electrode was surgically implanted onto each hemisphere of auditory cortex, and a third electrode was implanted onto the occipital lobe to serve as reference. Three weeks post-surgery, mice were intraperitoneally injected either with vehicle or with the DREADD ligand, clozapine-*n*-oxide (CNO), which temporarily elicits the inactivation of DREADD-infected PV neurons. During this time window of CNO or vehicle exposure, auditory cortical activity was recorded as mice were awake and freely moving in a dark arena and sound stimuli were presented to them.

Results showed that baseline levels of low and high frequency oscillations in auditory cortex increased and decreased, respectively, following CNO injections compared to vehicle. Evoked-response potential (ERP) amplitudes, particularly the P1 and N1 amplitudes, significantly increased following CNO injections compared to vehicle. The results suggest that silencing PV neurons more strongly synchronizes auditory population responses at lower oscillatory frequencies and strengthens their response to sound stimuli, similar to that previously seen in the visual cortex (Chen et al., 2017). In conclusion, PV interneurons may play a role in weakening synchronized responses to sounds and promoting high frequency oscillations in baseline circuit dynamics.

PS 835

Auditory Hypersensitivity and Circuit Disruptions in a Rat Model of Fragile X Syndrome

Benjamin D. Auerbach[1]; Kelly Radziwon[1]; Olivia Kozody[1]; Richard Salvi[2]
[1]Center for Hearing and Deafness, University at Buffalo; [2]Center for Hearing and Deafness, 137 Cary Hall University at Buffalo, Buffalo, NY 14214

Abnormal sensory processing is a hallmark of autism spectrum disorders (ASD) and related neurodevelopmental disorders like Fragile X syndrome (FX), most notably manifesting as extreme sensitivity to sound (i.e. hyperacusis). Auditory hypersensitivity is not

only a pressing clinical problem in FX and ASD, but it also likely reflects fundamental circuit defects that extend to more complex but less accessible features of the disorders, such as impaired communication and language development. We have combined novel behavioral assays with high-density *in vivo* electrophysiological recordings from multiple points along the auditory pathway to identify the pathophysiological changes associated with auditory hypersensitivity in a *Fmr1* KO rat model of FX. We found evidence for excessive loudness perception and decreased tolerance in *Fmr1* KO rats that coincided with sound-evoked hyperactivity and hyperconnectivity in the auditory cortex despite unaltered subcortical drive. This novel symptoms-to-circuit approach has the potential to uncover fundamental deficits at the core of FX and ASD pathophysiology while also having direct clinical implications for one of the most disruptive features of these disorders.

PS 836

Comparing the Superficial Vasculature of the Central Nervous System and temporal bone in Six Laboratory Animals

YooYeon Kim[1]; Janet Ren Chao[2]; Chulho Kim[3]; tae-cheon kang[4]; Jun Gyo Suh[5]; **Jun Ho Lee**[6]
[1]Laboratory of Brain and Cognitive Sciences for Convergence Medicine, Hallym University College of Medicine; [2]Division of Otolaryngology, Department of Surgery, Yale School of Medicine; [3]Department of Neurology, Chucheon Sacred Heart Hospital, Hallym University; [4]department of anatomy and neurobiology, college of medicine, hallym university; [5]Department of Medical Genetics, College of Medicine, Hallym University; [6]Department of Otorhinolaryngology-Head and Neck Surgery, College of Medicine, Hallym University

The purpose of the present study was to define the applicability of tissue clearing to the field of otology. We provide images of the entire central nervous system vasculature, and compare the anatomical findings in six different laboratory animals. And, we combined tissue clearing with vital staining perfusion via a pumping system to examine the vascular anatomy of temporal bones in laboratory animals. We used six different types of species including Korean wild mouse, mouse, Mongolian gerbil, hamsters and Guinea pigs. A mixture of Alcian blue reagent and 4% paraformaldehyde was circulated throughout the entire circulatory system of the animal via a perfusion pump system. Transparency images were obtained from the temporal bones according to the protocol of the SunHyun 3D Imaging Kit. In examining the inner surface of the tympanic membrane, flaccid part (pars flaccida) was positioned along the entire marginal area in Guinea pig. In the Guinea pig, unlike the other species, the cortical bone of the mastoid (bullae) was easily removed using cold instruments, allowing a direct approach to the enclosed structures. The distribution and pattern of cochlea melanocytes were compared among the species. “Mobius strip” like accumulated melanocytes in vestibules were shown in both the Korean wild mouse and mouse. The collateral blood supply to the cochlea in six different species was checked in various pattern. And, we successfully mapped the brain vascular system in six different species of animals.Combining dye infusion with tissue clearing techniques, we documented the middle ear and transparent inner ear structures in six different species. The information and associated images will help other researchers to develop hypotheses and design experimental investigations.

PS 837

Noise Exposure Induced Cortical Auditory Receptive Field Plasticity and Improved Signal-in-Noise Performance Dependent on the Sound Statistics

Natsumi Homma; Craig Atencio; Patrick Hullett; Christoph Schreiner
University of California San Francisco

Receptive fields (RFs) and neural circuits develop and can be altered to optimally process relevant stimuli and adapt to the sensory environment. In humans, the developmental stage is essential for acquiring language. It has been shown that sound exposure during a critical period dynamically altered the RF properties in the auditory cortex such as frequency tuning, tuning bandwidth, or temporal resolution (de Villers-Sadani and Merzenich, 2011). Similarly, sound exposure during adulthood can alter some RF structures (Eggermont, 2017). However, the relationship between the altered neural coding and perceptual abilities is yet largely unknown. In this study, we tested the hypothesis that exposure to moderate levels of structured background noise enhances the ability of animals to process vocalization in noise. We raised rat pups in moderate noises (~60 dB SPL) of different spectro-temporal statistics throughout the course of their auditory critical period (P6-45) and into adulthood. Once these animals reached adulthood (P45), we trained them, as well as an unexposed control group, to detect vocalizations presented in these noises using a go/no-go behavioral paradigm. Based on signal detection theory, the sensitivity index (*d'*) was obtained for several signal-to-noise ratios. Noise exposure enhanced the behavioral performance of detecting rat vocalizations in background noise. Improvement depended on the stimulus statistics of the exposure noise. In addition, we estimated neural discriminability of rat vocalizations in noise using Euclidean distance-based spike train classifiers and obtained spectro-

temporal RFs based on the spike-triggered average. We found that cortical signal encoding of vocalizations was improved in noise-exposed animals accompanied by specific shifts in RF properties compared to unexposed animals. To capture additional aspects of altered neural coding, we used a two-filter linear-nonlinear approach (Sharpee et al., 2004) and estimated RFs in the primary auditory cortex (A1) and ventral auditory field (VAF). The filter analysis showed that noise exposure i) increased mutual information captured by the first filter, which is thought to act as a feature detector, ii) modulated synergy between the first and weaker, secondary filters, and iii) the RF shifts of the second filter were in accordance with the first filter, mainly showing the suppression of exposure sound statistics. These findings support the idea that noise exposure can alter cortical RF properties to enhance information extraction in noisy environment, thus reducing the impact of background noise masking and helping the animals to perceptually segregate signals from noise background.

PS 838

Two-Photon Activity Imaging of Corticocollicular Neurons in Layer 5 of the Auditory Cortex

Tatjana T. Schmitt; Simon L. Wadle; Jan J. Hirtz
Physiology of Neuronal Networks, Department of Biology, University of Kaiserslautern

The auditory cortex (AC) modulates the activity of upstream pathways in the auditory brainstem via descending (corticofugal) projections. This feedback system plays an important role in the plasticity of the auditory system by shaping response properties of neurons in many subcortical nuclei. Around half of layer 5 (L5) neurons are corticofugal, the majority of them project to the inferior colliculus (IC). This pathway is involved in processing of complex sounds, auditory-related learning and defense behavior. Partly due to their location in deep cortical layers (500 – 800 µm), population activity patterns of corticofugal neurons within neuronal ensembles of the AC remain poorly understood. We employed two-photon imaging to record the activity of hundreds of L5 neurons simultaneously in anesthetized mice (postnatal day 50-70). To focus on corticocollicular neurons, we injected rAAV2-retro (Tervo et al. 2016. A Designer AAV Variant Permits Efficient Retrograde Access to Projection Neurons. Neuron. 92: 372–382) into the mouse IC. Using this approach, we expressed GCaMP7f exclusively in corticocollicular neurons. Pure tones and amplitude modulated tones were used to determine tonotopy and tuning bandwidth. Complex acoustic stimulations, like natural sounds and vocalizations, were used to study network ensemble activity. In addition, we mapped the AC using widefield imaging to distinguish between different subfields containing corticocollicular neurons. In a further set of experiments, we expressed GCaMP7f in the AC indiscriminately of neuron subtype and additionally injected rAAV2-retro-tdTomato into the IC. Hence, we could image activity of L5 neurons in general, but were also able to identify the subpopulation of corticocollicular neurons and analyze their specific response properties. By observing corticocollicular neuronal ensemble activity during different sound stimulation protocols, our work contributes to the understanding of the physiology and function of the auditory corticofugal system.

PS 839

Effects of Noise-Induced Hearing Loss on Matrix Metalloproteinase-9 and Auditory Cortex Activity

Jamiela Kokash[1]; Iryna M. Ethell[2]; Khaleel A. Razak[3]
[1]Neuroscience Graduate Program, University of California, Riverside; [2]Department of Biomedical Sciences and Neuroscience Program, University of California, Riverside; [3]Department of Psychology and Neuroscience Program, University of California, Riverside

Background

Noise-induced hearing loss (NIHL) is a major cause of hearing impairment and is a prevalent deficit due recreational and occupational hazards. We hypothesize that NIHL contributes to central molecular deficits, which may lead to compensating cortical gain in the auditory cortex. The altered cortical activity may be due to an increase in the activity of a particular protease, matrix metalloproteinase-9 (MMP-9), that cleaves extracellular matrix proteins and may be responsible for changes in perineuronal net (PNN) intensity and composition. PNNs are aggregates of extracellular matrix proteins that form primarily around GABAergic inhibitory interneurons, such as parvalbumin positive (PV+) interneurons. PNNs are essential in critical period plasticity and enhance the excitability of PV+ cells. This upregulation of MMP-9 after NIHL may contribute to increased degradation of PNNs and altered excitatory-inhibitory balance.

Methods

To test the first part of our hypothesis, we used Fluorogenic Dye-quenched (DQ)™-gelatin to quantify proteolytic activity of MMP-9 in the auditory cortex of noise exposed mice. Tissue samples were collected from C57/BL6 mice (P50-80) that were either exposed to 3 hours of 125dB SPL 6-12kHz narrowband noise or three hours of silence. Samples were taken at various time points: 12 hours or 1, 5, 10, and 30 days post-exposure. Once the fluorescence intensity of MMP-9 was measured, the relative activity was estimated based on the known specific activity of MMP-9 recombinase.

We tested cortical activity by analyzing recordings from EEG implants in the auditory and frontal cortices of mice. The recordings were taken before noise exposure compared to immediately after and 1, 3, and 10 days after. This allowed us to examine frequency specific power differences in baseline EEG caused by NIHL.

Results

MMP-9 activity in auditory cortex increased 1 day after noise exposure. However, there was no difference at 12 hours and 5, 10, or 30 days post-exposure. This is consistent with what a previous study from our lab has shown – NIHL is associated with reduced PNN intensity in the CNS starting from 1 day after noise exposure. The EEG recordings show differences between the exposed and unexposed mice within the gamma range (30-100Hz) and high frequency oscillations (100-250Hz) at various time points after exposure.

Conclusions

We found that there are time specific changes to MMP-9 activity within the central nervous system following noise-induced hearing loss. These changes may lead to altered network balance within the auditory cortex that may result in pathological activity.

PS 840

Synaptic Zinc Contributes to Contrast Adaptation in Mouse Auditory Cortex

Patrick A. Cody[1]; Thanos Tzounopoulos[2]
[1]University of Pittsburgh, Bioengineering; [2]University of Pittsburgh, Otolaryngology and Neurobiology

Phenomena of sensory adaptation have been extensively described but understanding of the underlying synaptic mechanisms trails behind. A common function of sensory adaptation is to maintain a signal percept amid changing contexts. This is, at least in part, accomplished via contrast gain control, a process in which instantaneous firing-rate gain compensates for changes in background stimulus contrast, or variance. In auditory cortex, this process modulates the sensory evoked response to the sound level contrast within which a signal is presented: the signal response amplitude increases with decreasing variance in sound level of background noise. We assayed this phenomenon with 2-photon calcium imaging in layer (L) 2/3 of mouse primary auditory cortex (A1) to investigate the biological mechanisms involved in this specific form of sensory adaptation termed contrast gain control. Consistent with previous studies, A1 L2/3 principal neurons adapt their sound evoked responses to the sound level contrast and duration of the background noise preceding the signal. We found that pure-tone responses within 1 octave of cell best frequency (BF) are significantly modulated by contrast regardless of their location within the background bandwidth. Adaptation following tones outside 1 octave of cell BF and outside the background bandwidth is less reliable. Because synaptic zinc has emerged as a cell-specific modulator of response gain and tuning in A1 L2/3 neurons, we tested whether it contributes to contrast adaptation. We found that upon zinc chelation, responses were no longer greater in low contrast relative to high contrast; high contrast responses increased while low contrast responses remained consistent. Synaptic zinc thus contributes to elevated low contrast responses via inhibition of responses in high contrast. Our findings highlight synaptic zinc signaling as a contributor to contrast adaptation in auditory cortex.

PS 841

Optimization of structural imaging in auditory pathway on Chinchilla Lanigera as a pre-clinical model of Blast TBI.

Vijaya Prakash Krishnan Muthaiah[1]; Kathiravan Kaliyappan[2]; Ferdinand Schweser[3]; Marilena Preda[4]
[1]Department of Rehabilitation Sciences, University at Buffalo; [2]Postdoctoral Research Associate; [3]University at Buffalo; [4]Senior Research Support Specialist

Background

Post-blast concussive symptoms reported by troops post-deployment varies based on the intensity, sequential repetitions and spacing between repetitions of the blast over-pressure (BOP). The mechanism(s) of BOP-induced injury has been studied in different animal models such as rats, mouse (Elder et al., 2014), pig (Chen et al., 2017), chinchilla (Hickman et al., 2018; Chen et al., 2017) and monkey (Lu et al., 2012). However, gaps remain in generalizing the pathophysiology arising from animal injury to humans. Adhering to the guidelines for using animal models in blast research (Watts et al., 2019), in the present study, we characterize the pre- and post-blast neuroimaging in chinchilla lanigera as an experimental animal model of BOP trauma. **Scientific Rationale:** In chinchilla, blast-induced cochlear synaptopathy (Hickman et al., 2018) has been investigated. However, there are no reports available on MRI post-blast characterization to identify injury end-points in chinchilla being an ideal animal model for auditory research.

Methods

Towards identifying BOP-induced injury end-points for various level of severity of damage, in present study, we are reporting pre- and post-blast MRI characterization in chinchilla with a focus on auditory pathway, such as cochlear nucleus (CN), inferior colliculus (IC) and auditory

cortex (AC). MRI scanning is conducted at Center for Biomedical imaging, UB which is equipped with 200mm horizontal-bore 9.4T magnet (Bruker Biospin, Biospec 94/20 USR) and a 440 mT/m imaging gradient system and a dual-element transceiver coil placed over the head of the anesthetized chinchilla. A series of gradient spin echo images were attempted to acquire T1/T2/ diffusion weighted images. Echo time, repetition time, flip angle, bandwidth, voxel size is being optimized using the animals that are being dedicated for impulse noise titration. We attempted focusing on parameters such as T1/T2 relaxation time, volume, diffusion and fractional anisotropy in our ROI (CN, IC and AC).

Results

The obtained T1/T2/DW images and the determined parameters serve as a baseline for future cohorts from which injury severity will be determined post-BOP for various repetitions at ~170 dB pSPL.

Conclusion

This is the first study to characterize the structural imaging of chinchilla as a platform to establish a robust pre-clinical model of Blast TBI. Outcomes of the present baseline characterization helps to validate post-BOP structural changes such as axonal distintegrity, cortical thinning using T1/T2/Diffusion weighted neuroimaging in the chinchilla. This will help to reliably demonstrate clinically-relevant end-points and recapitulate neurological sequelae in blast induced TBI.

Auditory Cortex: Neural Responses

PS 842

Mice Like It Rough

Olivier Postal[1]; Typhaine Dupont[1]; **Warren M. Bakay**[1]; Noémi Dominique[1]; Christine Petit[2]; Nicolas Michalski[1]; Boris Gourévitch[1]
[1]Institut Pasteur; [2]Institut Pasteur, Paris

According to a recent and intriguing hypothesis (Arnal et al, 2015, 2019), roughness, i.e. temporal envelope modulations in the range of 30-150 Hz, should be present in natural alarm signals as well as in artificial alarms from humans, thus boosting the detection of these alarms in various tasks. In particular, aversion to dissonant chords in humans would build upon the high level of roughness present in such sounds. However, it is not clear whether this hypothesis also applies to other species, such as rodents. We observed that, when using a two-alternative forced choice to go drink, mice did not show any preference for consonant chords. In fact, we showed, unexpectedly, that mice seemed more comfortable with rough sounds than with sounds having slower or faster amplitude modulations, i.e. less roughness. This preference correlates with the phase locking abilities of midbrain and thalamic auditory neurons but not with those of auditory cortical neurons. Altogether, these results suggest that some emotional features carried by the acoustic temporal envelope might be species-specific.

PS 843

Coding of Azimuthal Sound Position Across Primary and Secondary Regions of Ferret Auditory Cortex

Jonatan Nordmark[1]; Agnes Landemard[1]; Celian Bimbard[1]; Yves Boubenec[2]; Shihab Shamma[1]
[1]École Normale Supérieure; [2]Laboratoire des Systèmes Perceptifs, CNRS UMR 8248

Auditory cortex is necessary for accurate sound localization (Wood et al., 2017); nevertheless, the neural mechanisms for space processing as well as its cortical functional specialization are still debated. Previous studies have suggested carnivore auditory cortex is divided into two distinct functional pathways; a dorsal stream devoted to space encoding and a ventral stream dedicated to object recognition (Lomber & Malhotra, 2008). This view has been challenged by the idea that azimuth position is indiscriminately encoded across auditory fields at the single-neuron level (Bizley et al., 2009). Here, by using functional ultrasound imaging (fUS) (Bimbard et al., 2018), we performed large-scale comparisons of azimuth encoding in primary and secondary auditory fields of awake ferrets.\We imaged high-resolution hemodynamic brain responses to noise bursts coming from spatially separated azimuthal locations. We report spatial tuning to the contra-lateral hemifield in distinct regions across auditory cortex, both in primary and secondary regions, but with sharper tuning in secondary dorsal region. Interestingly, these space encoding regions were found consistently across animals in dorsal auditory cortex, but not in primary and ventral auditory cortices. Ongoing investigations aim at combining fUS and spike population analysis to decode different timescales of cortical spatial processing.

References

Bizley, J.K.,Walker, K.M.M., Silverman, B.W., King, A.J., Schnupp, J.W.H. (2009). Interdependent Encoding of Pitch, Timbre, and Spatial Location in Auditory Cortex. Journal of Neuroscience, 29(7), 2064-2075.

Lomber, S.G., & Malhotra, S. (2008). Double dissociation of “what” and “where” processing in auditory cortex. Nature Neuroscience, 11(5), 609–616.

Wood, K.C., Town, S.M., Atilgan, H., Jones, G.P., & Bizley, J.K. (2017). Acute Inactivation of Primary

Auditory Cortex Causes a Sound Localisation Deficit in Ferrets. PLOS ONE, 12(1), e0170264.

Bimbard C., Demene C., Girard C., Radtke-Schuller S., Shamma S., Tanter M., Boubenec Y. (2018). Multi-scale mapping along the auditory hierarchy using high-resolution functional UltraSound in the awake ferret. Elife, eLife 2018;7:e35028 DOI: 10.7554/eLife.35028

PS 844

Encoding of Acoustical and Behavioural Information by Auditory Cortical Neurons

Amy Hammond-Kenny; Victoria M Bajo; Andrew J King; **Fernando R Nodal**
University of Oxford

The role of auditory cortex in sensory processing from detection to identification of sounds, as well as in perceptual learning, is well established. However, it is still a matter of discussion whether its neural activity is driven exclusively by the acoustical properties of the stimulus or how other non-sensory, but behaviourally-related information might modulate it.

To investigate this, ferrets were trained by positive operant conditioning in two different audio-visual tasks. In one task (detection), animals had to detect a stimulus (auditory, visual or audio-visual) and approach its location in order to obtain a water reward. In the other task (categorization), animals had to respond differently according to the spatial congruency of the auditory and the visual components of the stimuli to obtain the reward. For spatially-congruent auditory and visual cues, they had to approach their common location, whereas for spatially-incongruent cues, they had to respond to a stimulus-independent location.

Once initial behavioural data had been obtained, bilateral arrays of tungsten electrodes were implanted over the primary auditory cortex to record single-unit activity during the execution of both tasks. We explored whether the neural activity recorded correlated with the auditory stimulus characteristics and/or other contextual information, including correct detection, categorization or task identity. From five animals, a total of 509 single units that exhibited excitatory responses to auditory and/or visual stimuli were identified and later confirmed, by histological analysis, to reside within the middle ectosylvian gyrus, where the primary auditory cortex is located. Units were classified as auditory (84%) if they responded exclusively to sound and bimodal (16%) if auditory responses were enhanced or suppressed by visual stimulation.

The activity of all recorded units was modulated by the physical properties of the auditory stimuli: location and level. On the other hand, it was independent of the correctness of the animal's response and of the identity of the trial for each task. However, when identical trials (audio-visual congruent trials) across both tasks were compared, the same units showed significantly lower activity for the categorization than for the detection task. These findings were corroborated, using a population decoding analysis.

Our results demonstrate that, in addition to encoding acoustical information, primary auditory cortical activity contains behavioural contextual information related to the task in question, but not to the behavioural outcome.

PS 845

Context-dependent Encoding of Sounds in Primary Auditory Cortex

Rémi Proville[1]; Mehdi Rousset[2]; Chris Rodgers[3]; **Yves Boubenec**[2]
[1]Tailored Data Solutions; [2]École Normale Supérieure; [3]Columbia University

Any sensory stimulus consists of a superposition of myriad different features. Context-relevant features determine how stimuli are grouped into behaviorally-relevant classes. Importantly, stimuli can switch class depending on context. How do neural circuits achieve such flexible categorization? According to the classical picture, sensory cortices predominantly represent stimulus sensory features, but little is known about how primary sensory cortices contribute to flexible categorization. Here we show that primary auditory cortex engages context-specialized neuronal populations to assign identical stimuli to different behavioral classes in a context-dependent manner.

Recent work revealed how ferret primary auditory cortex (A1) flexibly encodes sound behavioral meaning upon task engagement at the population level (Bagur et al, 2018). This shift from sensory-driven to behavioral coding relies on changes in baseline activity at the population level. Strikingly, other work in the rat showed that baseline activity of A1 neurons exhibited context-preference during flexible categorization (Rodgers & DeWeese, 2014). Here we re-analyzed this dataset to disentangle how context-preferring neurons encode stimuli depending on the task rule at play (called 'context' hereafter).

Consistent with previous findings, population-level decoding technique showed that task-specific baseline activity induced enhanced representations of task-relevant target stimuli. This confirms that task-specific patterns of

spontaneous activity at the population level can have a functional role in stimulus coding. Context-specialized neuronal pools specifically enhanced target stimuli in their preferred context. Non-context preferring neurons showed no target enhancement. Decoding of error trials showed a reversed behavior, with reduced target responses, and enhanced responses to other stimuli. All together, these findings suggest that different pools of A1 neurons are selectively engaged in a context-dependent fashion. The specific activation of those functional circuits relies on task-relevant changes in spontaneous activity and may be the basis of flexible categorization.

PS 846

Non-invasive Measures of Temporal Pitch Processing in an Animal Model using the Acoustic Change Complex (ACC) and Frequency Following Response (FFR)

Matthew L Richardson[1]; Francois Guerit[2]; Andrew J. Harland[2]; Robin Gransier[3]; Jan Wouters[3]; Robert P. Carlyon[2]; John C. Middlebrooks[1]
[1]University of California; [2]University of Cambridge; [3]KU Leuven

Cochlear implant users have limited pitch perception, in part because of poor transmission of temporal fine structure through auditory pathways activated by electric stimulation. To address the problem, we are developing objective EEG measures of temporal coding and discrimination in a cat model. Here we use filtered acoustic pulse trains to simulate electric stimulation of a single cochlear electrode. The Acoustic Change Complex (ACC) response is used to measure cortical sensitivity to changes in pulse rate while the Frequency Following Response (FFR) measures neural phase-locking at the brainstem level.

Stimuli consisted of pulse trains produced by harmonic complexes that were bandpass filtered to focus stimulation on the basal cochlear regions activated by a cochlear implant and to remove place-of-excitation cues arising from resolved harmonics. The filtered complexes were centered at 8 kHz and pink noise was added to mask distortion products. The pulse trains alternated every 1 second between a baseline pulse rate and rates that were 35 or 65% higher. During the electrophysiological procedure cats were sedated with ketamine and acepromazine and scalp potentials were recorded with clinical sub-dermal electrodes. The ACC amplitude was measured for a N1-P2 complex elicited by a temporal change “ascending” or “descending” in pulse rate, whereas the FFR was measured as the spectral amplitude in response to the pulse rate during the steady-state portions of the stimuli.

ACC and FFR responses were initially characterized for baseline pulse rates varying from 94-560 pulses-per-second (pps). For the ACC, significant N1-P2 responses were observed for all cats at one or more pulse rates. ACCs were most prominent for ascending pulse rates and the larger pulse rate change (+65%). ACC amplitudes generally were absent at 94 pps, increased to a maximum between 280-360 pps and gradually diminished for higher pulse rates. For the FFR, spectral peaks were measurable for rates above 94 pps, maintained maximal amplitudes until approximately 560 pps, and gradually decreased at higher pulse rates.

These preliminary results demonstrate the feasibility of recording the ACC and FFR simultaneously for studying temporal processing at the cortical and brainstem level in the cat. The results will be compared to parallel experiments in humans and, eventually, to single-unit recordings only possible in non-human species. The aim is to obtain a combined physiological and psychophysical understanding of temporal acuity limitations in cochlear implant stimulation.

Funded by Wellcome Trust Collaborative Science Award RG91976,NIH NIDCD R01 DC017182,and NIDCD Training Grant T32 DC010775-09.

PS 847

Multisensory Responses in Primary Auditory Cortex of the Cat

Catherine Boucher[1]; Xiaohan Bao[1]; Yaser Merrikhi[1]; M. Alex Meredith[2]; Stephen G. Lomber[1]
[1]Department of Physiology, McGill University; [2]Dept. of Anatomy and Neurobiology, Virginia Commonwealth University

Core auditory cortex of the cat is comprised of primary auditory cortex (A1) and the anterior auditory field (AAF). Neurons in both fields respond strongly to acoustic stimuli and are tonotopically organized. In hearing animals, a small number of cells in AAF respond to tactile stimulation. Following early-onset hearing loss, a much larger proportion of neurons in AAF become responsive to tactile and/or visual stimulation, indicating that crossmodal sensory reorganization is robust in this core auditory area. Unfortunately, results from similar studies conducted in A1 of the cat are not as clear. In hearing cats, most studies do not show multisensory responses in A1 (Stewart & Starr, 1970; Rebillard et al., 1977; Kral et al., 2003). Furthermore, only one study has documented crossmodal plasticity in A1 following perinatal hearing loss (Rebillard et al., 1977), while others have not (Stewart & Starr, 1970; Kral et al., 2003). A methodological consideration of these studies involves

the type of anesthetic used. In this study, hearing animals were lightly anesthetized with ketamine. We recorded audiovisual responses from A1 (i.e., unisensory auditory, unisensory visual, subthreshold multisensory or bimodal) and we examined the visual characteristics to which A1 maximally responds. Multisensory stimuli were developed by pairing a pure tone stimulus with a flash stimulus at various stimulus onset asynchronies, and the visual stimuli presented include gratings, flashes, dots, and checkerboards. A linear multielectrode array recorded multi-unit activity and local field potentials across cortical layers. Contrary to previous work using other anesthetics, we identified unisensory auditory, unisensory visual, bimodal, and subthreshold multisensory multi-unit activity in A1. We also found neurons where auditory-visual interactions either suppressed or enhanced neuronal activity. Additionally, visual stimulation can modulate the neural response to auditory inputs depending on the stimulus onset asynchrony. Taken together, it is possible to identify visually responsive neurons in A1 of the cat. These results will serve as baseline data for a future study, examining the degree to which this cortical area undergoes crossmodal plasticity following early-onset hearing loss.

PS 848

Tones Masked by Noise Bands in an Animal Model: Psychophysics and EEG

John C. Middlebrooks[1]; Matthew L Richardson[2]; Francois Guerit[3]; Robert P. Carlyon[3]
[1]UC Irvine; [2]University of California; [3]University of Cambridge

We are exploring the spread of electrical excitation by various cochlear-implant configurations in humans and cats. As a first step in that work, we are using acoustical stimulation in normal-hearing cats to develop psychophysical and electrophysiological procedures for evaluating tonotopic spread of excitation. We present pure tones in the presence of 1/8-octave or 1-octave noise bands centered logarithmically on 8 kHz.

In the psychophysical procedure, cats were trained to press and hold a pedal, which started a continuous 1/8-octave or 1-octave noise band. After a variable time, the probe sound was turned on. The cat was rewarded if it released the pedal within a criterion time after noise onset. Early or late releases were punished with a time out. Both 1/8-octave and 1-octave noise bands produced substantial elevation of thresholds ("masking") for detection of an 8-kHz probe tone. Probes ½-oct below (5.6 kHz) or above (11.3 kHz) 8 kHz demonstrated reduction of masking by about 40 dB in the presence of the 1/8-oct noise band. In contrast, masking of 5.6 and 11.3 kHz was reduced only by about 10 dB in the presence of the 1-oct noise band.

In the electrophysiology procedure, cats were sedated with ketamine and acepromazine. We recorded event-related potentials with needle electrodes placed over the contralateral hemisphere, the ipsilateral mastoid, and on the back. A clear P1-N1 complex was elicited by the onset of a probe tone. For each of the 2 noise bandwidths, we presented the noise band continuously and added 50-ms probe tones at 1-second intervals. We adjusted the levels of the noise bands to suppress onset responses to 8-kHz tones by about 60%. In the presence of the 1/8-oct masker, that suppression was substantially reduced at probe frequencies of 5.6 and 11.3 kHz, whereas the 1-oct noise band produced a largely constant degree of suppression across a 5.6-to-11.3 kHz range of probe frequencies.

These results support the feasibility of these psychophysical and non-invasive electrophysiological measures for study of tonotopic spread of activation in a cat model. Parallels with our ongoing experiments in normal-hearing humans (Carlyon *et al.*, ARO midwinter meeting, 2019) permit direct inter-species comparison of measures of spread of excitation. This will allow us to combine the more-sophisticated psychophysics obtainable in humans with planned invasive neural measures in cats.

Funded by Wellcome Trust Collaborative Science Award RG91976 and NIH NIDCD R01 DC017182 and T32 DC010775-09

PS 849

Comparisons of Responses to Broadband Noise Sounds Between the Core and Parabelt Regions in Macaques

John Orczyk[1]; Troy A. Hackett[2]; Charles E. Schroeder[3]; Yoshinao Kajikawa[1]
[1]Nathan Kline Institute; [2]Vanderbilt University; [3]Columbia University

The auditory parabelt region is the third tier of auditory cortical processing in primates. Compared to lower tier regions, studies of the parabelt are still scarce, but recent studies have started to uncover basic neuronal properties. For example, while onset latency of auditory responses is longer in the parabelt than other regions, spectral tuning is sharper than previously thought. Tonotopic gradients of its subdivisions are organized in an orderly fashion. One class of information still missing is response types. For example, chopper responses to pure tones described in auditory brainstem nuclei do not appear in

auditory cortex after several relay stations. Comparable transformation of auditory coding may also be expected between low and high tiers of auditory cortex. Because response latencies are long, deterioration of temporal following to rapid repetitive sounds is expected in parabelt. However, how responses to static sounds differ between regions is uncertain. We compared responses to brief static broadband noise sounds (BBN) between core and parabelt regions. Five macaque monkeys were implanted with recording chambers targeting either the core or parabelt regions. During passive listening, 100 ms BBN were delivered at calibrated sound levels. Field potentials and multiunit activity (MUA), recorded using linear array microelectrodes, were profiled to identify cortical layers. Response patterns were obtained by averaging >40 trials. Robust responses to BBN (60 dB SPL or 0 dB attenuation) were observed in both core and parabelt regions. They occurred with phasic excitatory onset peaks followed by variable response patterns including, inhibitory pause, rebound increase or sustained responses. Onset and peak latencies were delayed in parabelt relative to the core. In both regions, response patterns to soft BBN (40 dB attenuation) were different from responses to loud sounds. They occurred without phasic onset peaks, but had slowly rising and decaying patterns. Parabelt responses followed core responses with greater onset and peak delays. Thus, parabelt responses to BBN appeared to mirror the patterns in core responses. These observations are consistent with the position of the parabelt at a later stage of auditory processing that follows the core. However, comparable changes in response patterns between sound levels occurred between parabelt and core. Thus, response transformations between those regions may be limited to temporal slowing.

PS 850

Selective Spatial Tuning of Neurons in Auditory Cortex during a Freely Moving Sound Source Localization Task

Diana Amaro[1]; Michael Pecka[2]
[1]Division of Neurobiology, Ludwig-Maximilians-University Munich; [2]Biocenter, Section of Neurobiology, Department Biology II, Ludwig-Maximilians-Universitaet Munich

Foraging for food or escaping a predator are crucial actions for evolutionary success. The continuous locomotion and head-movements that are associated with these behaviors require the brain to analyze a constantly changing sensory environment. For most animals, the auditory sense – especially the ability to localize a sound source – is essential during such behaviors. To this end, our brain uses egocentric cues (interaural time differences – ITDs – and/or interaural level differences – ILDs) for the computation of the sound source location. Traditionally, experiments to study these computations are performed by evaluating neuronal responses to ITDs/ILDs in anesthetized animals. However, these paradigms lack self-motion, which continuously modulates the egocentric cues. Thus, these cues are inadequate to define a sound source position in absolute space (allocentrically), which is ultimately the relevant information to obtain during a naturalistic behavior, e.g. escaping a predator. Moreover, identification of a particular sound source critically depends on its current behavioral significance, which typically is also absent in experimental settings.

To investigate spatial coding of behaviorally relevant sound sources during active locomotion, we developed a goal-oriented sound localization task. Mongolian gerbils freely navigate in a circular arena and forage for an auditory target. During a trial, the position of the animal is continuously tracked and the acoustic stimulation is altered accordingly in real-time: either a distractor loudspeaker or one diametrically opposed to it – the target loudspeaker – is active. After trial initiation by the animal, short harmonic complexes are presented by the distractor loudspeaker while the animal navigates through the arena. If the animal enters a specific area ('target island'), the stimulation switches to the target loudspeaker. The absolute location of the 'target island' in the arena is randomized across trials and therefore is *a priori* unknown. By rewarding the animal when it correctly identifies the correct loudspeaker (by remaining in the target island), we introduce differential behavioral meaning to each sound source.

Animals are chronically implanted in primary auditory cortex with a tetrode bundle, allowing to determine the spatial tuning of individual neurons to either sound source during task performance. We find that in a sub-population of neurons, spatial tuning is modulated by behavioral relevance in this task and exhibits an allocentric representation component. This novel finding is crucial for our understanding of how cortical circuits represent the environment under ethologically relevant conditions, specifically the selective tracking of a sound source while moving.

PS 851

Spatiotemporal Activation Patterns of the Auditory Cortex of the Free-Tailed Bat Provide a Mechanism for Ensemble Coding of Vocal Repertoire.

Silvio Macias; Kushal Bakshi; Michael Smotherman
Texas A&M University

In the present study, we addressed the question of whether coding of communication calls from conspecifics

rely on the selective responses of single neurons or in the population response of multiple neurons in the auditory cortex. We used the Mexican free-tailed bat, Tadarida brasiliensis, which uses a complex highly elaborate vocal repertoire. Spike discharges and temporal properties of local field potentials (LFP) were studied in 810 recording sites in five bats using ten types of communication calls and two types of sonar pulses as auditory stimuli. In response to the different types of calls, neurons in the primary auditory cortex of the free-tailed bat showed a shorter (~20 ms) and a longer latency (>200 ms) response component. Both components exhibited a diverse selectivity to communication calls with neurons responding to the twelve call types and neurons responding to only one or two calls. Spectrotemporal receptive fields (STRFs) calculated from naturalistic stimuli could help to understand the response selectivity. Neuronal selectivity exhibited a columnar organization. The temporal course of spike PSTHs and LFP responses were inadequate for discerning different call types. Using the topographical localization of each recorded neuron and its response magnitude, we calculated the maps of activations of the entire primary auditory cortex in response to each of the calls. Each call produced responses in a spatially distinct population of neurons differing in degrees of activation, leaving a distinctive footprint (or "callprint"). We propose that these different spatiotemporal activation patterns provide a mechanism for ensemble coding of the vocal repertoire and complex acoustic stimuli in general.

PS 852

The Sound of Silence: Responses to Omitted Tones in the Auditory System.

Ana B. Lao-Rodríguez; David Pérez-González; Gloria G. Parras; Manuel S. Malmierca
University of Salamanca

Mismatch negativity (MMN) was first recorded in the 70s using EEG in the context of the oddball paradigm and is currently interpreted in terms of predictive coding. According to this framework, the brain does not respond passively to incoming inputs but it extracts the inputs regularities and uses them to actively predict what should happen next. Using a similar experimental approach, previous studies have demonstrated that neurons in the auditory system adapt to repeating sounds and resume their firing to new, unexpected sounds. This phenomenon seen at the neuronal level is referred to as stimulus-specific adaptation (SSA) and has been suggested to be the neuronal correlate of MMN. However, MMN has been demonstrated not only with pure tones but also with more complex patterns of sound stimulation. Moreover, MMN has also been found to occur using an omission deviant. SSA in animals has been mostly tested using pure tones under the oddball paradigm and to date neuronal responses to stimulus omissions have been elusive. We recorded single neurons from the inferior colliculus (IC) and auditory cortex (AC) in anesthetized rats using an oddball paradigm in which the deviant tone was replaced by an omission deviant. These omitted tones occurred in periodic and randomized sequences, to study the influence of expectancy. We presented the tones with different ISIs (125ms, 250ms and 500ms) which allowed to observe non-overlapping responses. Finally, if omission responses were found we also presented oddball sequences and compared the responses to the deviant tones with the omission responses. Our results demonstrate that a subset of neurons of the auditory pathway show responses to omitted tones. Omission responses shown by AC neurons are stronger than those from IC, showing a higher probability of occurrence with shorter ISIs. AC neurons not only show a significant increase in their activity during an omitted stimulus but also show a significant decrease in their response when the stimulation effect is suppressive unlike the IC neurons. In a predictive coding model, the omission response reflects solely a predictive component and not a prediction error per se. Thus, the finding of omission responses confirms that the auditory system does not need an external stimulus trigger to detect a deviation from expectations (Bendixen, et al 2012) and provides an empirical demonstration to support that the rat brain can generate predictions.

Financial support was provided by the Spanish MINECO (Grant # SAF2016-75803-P) to MSM

PS 853

Spectrotemporal Response Properties of Primary Auditory Cortex in the Free-tailed Bat, Tadarida brasiliensis.

Silvio Macias[1]; Kushal Bakshi[1]; Todd Troyer[2]; **Michael Smotherman**[1]
[1]Texas A&M University; [2]University of Texas at San Antonio

Echolocating bats rapidly build an internal representation of their local acoustic scene from fine acoustic cues extracted from a discontinuous stream of brief, faint echoes. Biosonar performance requires both high spectral acuity and fast temporal resolution, two parameters that tend to be inversely related throughout the auditory system. There is evidence that in free-tailed bats the auditory midbrain accommodates higher spectral and temporal modulation rates than has been found in other mammals, but whether this capacity is transferred up to the cortex is unknown. We measured the topographical and intralaminar distribution of spectrotemporal response properties throughout the primary auditory cortex (AC)

of the Mexican free-tailed bat, *Tadarida brasiliensis*, using intracortical microelectrode arrays and a series of tonal, FM sweep, and dynamically modulated ripple (DMR) stimuli. A caudal low-frequency to rostral high frequency tonotopy was confirmed with characteristic frequencies (CF) ranging from 15 to 70 kHz. Half of the units had CFs between 20 and 30 kHz, reflecting a topographical overrepresentation of the predominant sonar pulse bandwidth. Lowest thresholds were found at 20-25 kHz. Frequency response areas (FRA) and spectrotemporal receptive fields (STRFs) obtained from spike-sorted multiunit activity revealed a diverse range of FRA shapes and complex STRFs, sometimes with multiple excitatory and inhibitory fields. CF and tuning parameters were similar across lamina within columns. Response latencies were shortest (< 10 ms) between 500-600 mm, corresponding to thalamocortical input layer IV. CSD profiles calculated in response to the CF showed a current sink located at approximately deep layer IV. Frequencies below FRA did not evoke a current sink in layer IV, while frequencies above the FRA evoked shorter latency sinks at layer IV, potentially revealing integration of spectral information during processing of the downward FM echo. Majority of units showed stronger responses to downward FM sweeps, with directional selectivity indices (DSI) higher than 0.4. The primary mechanism for FM sweep selectivity appeared consistent with previously identified lateral inhibitory interactions, which were indirectly evident in FRAs obtained from LFPs. These data support the hypothesis that in *Tadarida brasiliensis* the entire primary auditory cortex is preferentially wired to rapidly process spectral information contained in downward FM sweeps.

PS 854

Cortical Consequences of Cochlear Implant Insertion: an Electrophysiological Study in The Primary Auditory Cortex of Guinea Pig.

Elie Partouche[1]; Victor Adenis[1]; Dan Gnansia[2]; Pierre Stahl[2]; Jean-Marc Edeline[1]
[1]Neuro-PSI, UMR CNRS 9197; [2]Oticon Medical

In human, cochlear implant (CI) is particularly successful to restore hearing in cases of profound deafness. However, several patients with residual hearing are now using electro-acoustic stimulation (EAS devices) and it is crucial to preserve their remaining hearing abilities. We examined here, in an animal model, to what extent inserting a cochlear implant in the tympanic ramp significantly altered auditory evoked responses in the primary auditory cortex. Experiments were performed in anesthetized guinea pigs (6-18months old) with normal hearing. The tonotopic gradient of the primary auditory cortex (AI) was established by inserting an array of 16 cortical electrodes (2 rows of 8 electrodes separated by 1mm and 350µm within a row). Multiunit activity (MUA) was collected while delivering pure tones at 75dB. The cortical depth was adjusted to optimize the detection of the tonotopic gradient. The Frequency Response Area (FRA) was also tested from 0.14kHz to 36kHz from 75 to 5dB. A set of stimulating electrodes (300µm) was then inserted in the cochlea via a cochleostomy (400µm in diameter) performed at 1.5mm from the round window (5 electrodes inserted in the 1st basal turn) and its connector was secured on the skull. The cortical electrodes were placed back in auditory cortex at the same location as before the CI insertion. The frequency tuning at 75dB and the FRA were re-determined with the same set of stimuli. On control animals, the frequency tuning and the FRA were determined before and 30min after removing and putting back the cortical array without opening the bulla and inserting electrodes in the cochlea. The data obtained in 21 animals indicated that inserting CI in the tympanic ramp led to increase the cortical threshold (by 10-15dB) in the high (18-36kHz) and, to a lesser extent (5-10dB) in the mid-frequencies (9-18kHz). The thresholds were slightly improved (by about 5dB) in the low frequencies (0.14-3.8kHz). The evoked firing rate (FR) was modified in the opposite direction: the increases in threshold were accompanied by decreases in FR and the decreases in threshold were accompanied by slight increases in FR. These effects were not observed in controls animals. These data suggest that in our conditions CI insertion can impair residual hearing in the high and mid-frequencies, but the cortical responses to low frequencies seem to be unaffected.

PS 855

Responses of Auditory and Frontal Cortices during Sound Source Segregation

Neha H. Joshi[1]; Daniel Duque[2]; Jonathan B. Fritz[3]; Andrew J. Oxenham[4]; Shihab A. Shamma[5]
[1]University of Maryland; [2]Institut d'Investigacions Biomèdiques August Pi i Sunyer; [3]Institute for Systems Research, University of Maryland, College Park; Now at Center for Neural Science, New York University; [4]University of Minnesota, Minneapolis; [5]Institute for Systems Research, University of Maryland, College Park

This study concerns the neural mechanisms involved in the perceptual segregation of sound sources, a process that appears effortless in humans and animals despite its complexity. Since the ferret frequency range of hearing encompasses the human range, and their auditory cortex is complex enough to encode well various English phonemes (Mesgarani et al., 2008), ferrets are an excellent animal model for phoneme discrimination. They can be behaviorally trained to differentiate "target" words (trisyllabic sequences) from various alternative

"reference" words. In this study, ferrets learned, using a conditioned avoidance Go/No-Go behavioral paradigm, to attend to a unique target speaker's voice and to respond to a specific trisyllabic sequence target (speech-like "word") only when uttered by a specific target speaker. Ferrets successfully performed this word recognition task (in the presence of other non-target trisyllabic words) in the 1-speaker context, and also demonstrated speech segregation by learning to reliably detect the same target word uttered by speaker 1, in a complex 2-speaker scene with overlapping words (including the target trisyllabic sequence) uttered by the second speaker. We recorded neuronal activity in the primary and secondary auditory cortices (AC, n = 154 neurons), and also in the dorsal frontal cortex (dFC, n = 54 neurons) of quietly listening and task-engaged ferrets in the 1-speaker and 2-speaker contexts.

Neurophysiological evidence from our recordings in AC suggests that there is differential processing in the frequency domain of the target speaker compared to the unattended speaker during active task engagement. We observed complete suppression of neural responses to the interfering speaker during task performance, but not in the passively listening animal. Responses in dFC also showed attention-modulated differential processing, where responses to the target word spoken by the attended speaker became considerably enhanced relative to responses to the same trisyllabic sequence spoken by the interfering speaker. In dFC, the suppression of responses to the interfering syllables occurred rapidly and only upon deviation from the target syllable sequence. These results demonstrate that neurons in the auditory and frontal cortices encode words selectively depending on learning and attentional context, indicating that in this task, the animal does not simply suppress target syllables based on their syllabic sequence identity but rather based on their vocal source. These results help us better understand the role of attention and underlying neural mechanisms in stream segregation in multi-speaker environments, and provide valuable insight into pre-processing of speech during auditory scene analysis.

PS 856

Effects of Arousal on Population Coding of Natural Sounds in Primary Auditory Cortex

Charles Heller; Daniela Saderi; Zachary Schwartz; Stephen V. David
Oregon Health and Science University

Behavioral state variables such as arousal and task-engagement have been found to increase the gain and reliability of sensory responses and to decrease the strength of stimulus-independent correlations between neurons in primary auditory cortex (A1). These state-dependent changes are thought to increase the signal to noise ratio of the neural response and enhance the faithful encoding of sensory stimuli. However, the representation of an auditory stimulus is likely to be distributed across more than just one or two neurons. Therefore, understanding how state-dependent modulations impact sensory coding in neural populations larger than n = 2 remains an area of active research. To investigate this question, we presented awake, passive ferrets with natural sound stimuli while recording neural activity from local A1 populations using a linear 64-channel silicon probe. We simultaneously measured the animal's level of arousal via pupillometry. This approach provided access to the activity of several (10 – 30) closely spaced units across a range of arousal states and acoustic contexts. In order to determine the effect of arousal on auditory representation, we split all natural sound segments into 250 ms segments and trained an optimal linear decoder to use activity of simultaneously recorded units to discriminate between each pair of stimuli during high versus low arousal states. We found that natural sounds were more easily discriminated during high arousal states, suggesting that the population-level representation of sound is state-dependent. To determine if this result was primarily due to changes in the gain and reliability of single cells or due to changes in high-order interactions between neurons, we retrained our decoder on each neuron in the population individually. We then developed a method to combine single neuron decoding performances into a single metric for the population. This procedure effectively removed all higher order interactions between neurons, such as pairwise correlations, and provided a measure of single cell decoding performance that could be directly compared with population decoding performance. Single cell decoding performance also increased during high arousal, suggesting that gain and reliability changes contribute to enhanced auditory encoding at the population level. Additionally, we discovered that removing higher order interactions improved decoding performance relative to that of the actual population, but the relative benefit was weaker in the high arousal state. Thus, we find that arousal-dependent modulation of both single units and higher order circuit interactions between units improve auditory encoding in A1.

PS 857

A Distributed Network of Noise-Resistant Neurons in the Central Auditory System

Samira Souffi; Chloé Huetz; Christian Lorenzi;Jean-Marc Edeline
Neuro-PSI UMR CNRS 9197

In daily life, background noise strongly penalizes auditory perception of target stimuli such as speech in humans or vocalizations in animals. Despite this, auditory neurons successfully detect and discriminate behaviorally salient sounds even when the signal to noise ratio (SNR) is quite low. Several recent studies showed that cortical neurons are robust to noise addition and develop strategies to adapt to the noise statistics. For example, in a recent study (Ni et al., 2017), it was reported that auditory cortex neurons can be assigned to categories depending upon their robustness to noise. More precisely, by testing the responses to conspecifique vocalizations in different SNRs, this study has described four types of responses classes (robust, balanced, insensitive and brittle) in the marmoset primary auditory cortex, and has pointed out that depending upon the background noise the same neuron can exhibit different response classes (Ni et al., 2017). However, no study has systematically evaluated the robustness to noise at each level of the auditory system. Here, we recorded neurons from the cochlear nucleus up to the secondary auditory cortex in response to a set of four vocalizations presented either in a stationary noise or in a chorus noise at three SNRs.

We used exactly the same methodology as in Ni and colleagues (2017) to assign the neurons to a response class. The Extraction Index (EI, defined by Schneider and Woolley, 2013) was computed at the three SNR levels and a clustering approach (based on k-means algorithm) was implemented to reveal groups of EI profile. This approach led to classify auditory neurons in categories revealing five distinct neuronal behaviors in the auditory system. We provide evidence that neurons robust to noise can be found at all levels of the auditory system with a considerable fraction of them in the inferior colliculus and thalamus. In addition, from one background noise to the other, the neurons behavior can change at all stages of the auditory system, revealing that the context-dependence of auditory processing is a general property of the whole auditory system. We propose here that the noise-robustness observed in many studies at the cortical level stems, at least partially, from subcortical mechanisms, thus allowing the cortical networks to focus on higher-level processing such as classifying the target stimuli into phonetic or linguistic features.

Binaural Hearing: Psychoacoustics, Modeling, and Multisensory

PS 858

Resolving Front-Back Reversals in Sound-Source Localization

M. Torben Pastore; **William Yost**
Arizona State University

Cone of Confusion “errors (front-back and up-down reversals)” occur when stationary listeners attempt to localize the sources of sounds using only interaural differences of time (ITDs) and level (ILDs). This paper addresses only front-back reversals (FBRs) in the azimuth plane. It has been well established that FBRs rarely occur when listeners rotate their heads and/or when sounds from sources contain high-frequency spectral cues for sound-source localization. We investigated four other ways in which FBRs may be reduced: 1) When a cue was provided indicating if a sound source might be in the front or back hemifield, 2) When listeners were provided an expectation as to which hemifield (front or back) a sound source might be located, 3) When there was a spatial pattern as to how sound sources might be presented over trials, and 4) When listeners were provided trial-by-trial feedback about their spatial location judgments. FBRs were reduced in all cases, suggesting that the auditory spatial system is able to take advantage of many different variables in order to reduce FBRs and provide for veridical sound source localization perception. [Funding from NIH (NIDCD: R01DC015214 to WAY & F32DC016808 to MTP) and Facebook Reality Laboratories]

PS 859

Listeners Exhibiting "Slight" Hearing Loss and Binaural Deficits Also Exhibit Higher Levels of Stimulus-Independent Internal Noise

Leslie R. Bernstein; Constantine Trahiotis
University of Connecticut Health Center

Background
The results of recent experiments in our laboratory have demonstrated consistently that listeners classified via pure-tone audiometry as having no more than “slight” hearing loss may exhibit substantial deficits when tested in a binaural detection task. Analyses indicate that those deficits stem from increased levels of stimulus-dependent, additive internal noise. This study assessed whether, when tested with suitably low-level stimuli, such listeners would also exhibit increased levels of low-level, stimulus-independent, additive internal noise. The results at all three center frequencies tested (250 Hz, 500 Hz, and 4 kHz) indicate that they do.

Methods
We measured detection thresholds for tonal signals: 1) in the NoSϖ configuration as a function of masker level; 2) in the NρSϖ configuration as a function of masker interaural correlation (ρ); 3) in "the quiet" for So and Sϖ. Those measures were combined suitably to yield estimates of stimulus-independent, additive internal noise. Bands of Gaussian noise 100-Hz-wide served as maskers. Testing was performed separately at 250 Hz and 500 Hz, (where the fine-structures of the stimuli convey changes in binaural temporal information) and at 4 kHz (where the envelopes of the stimuli convey changes in binaural temporal information). As in our previous experiments, in order to maximize sensitivity to envelope-based ITDs, the stimuli centered at 4 kHz were the transposed counterparts of tones and 100-Hz-wide Gaussian noises centered at 125 Hz.

Results and conclusions
The NoSϖ binaural detection thresholds replicated the outcomes of our earlier studies [e.g., Bernstein and Trahiotis, J. Acoust. Soc. Am. 144, 292-307 (2018)]. That is, once again, we found that detection thresholds were elevated for listeners having pure-tone thresholds at 4 kHz > 7.5 dB HL as compared to listeners having pure-tone thresholds at 4 kHz < = 7.5 dB HL. The important new finding is that listeners having pure-tone thresholds at 4 kHz > 7.5 dB HL also exhibit elevated levels of stimulus-independent, additive internal noise. Specifically, for those listeners, estimated levels of stimulus-independent internal noise were found to be elevated by about 5 dB at 250 and 500 Hz and by about 9 dB at 4 kHz. Taken together with our previous findings, it appears that listeners such as those in our >7.5 dB (no more than "slight" hearing loss) group have higher levels of both stimulus-dependent and stimulus-independent internal noise.

Research supported by the Office of Naval Research (ONR Award No. N00014-18-1-2437)

PS 860

Audiovisual Training Rapidly Improves Sound Localization With Earplugs

David J. Audet[1]; William O. Gray[1]; Andrew D. Brown[2]
[1]Department of Speech and Hearing Sciences, University of Washington, Seattle, WA; [2]Department of Speech & Hearing Sciences, University of Washington

Hearing protection devices (HPDs) offer to protect users from noise-induced hearing loss. However, reduced situational awareness, including degraded sound localization caused by marked changes to the natural head-related transfer function (HRTF), is a common and potentially serious side effect of HPD use. For some user groups (e.g., military personnel), preservation of situational awareness may supersede concern for hearing protection, limiting HPD usage even when devices are readily available. Here we considered the feasibility of localization training to improve hearing-protected sound localization performance. Twelve normal-hearing young adults participated in the study. Subjects completed a battery of baseline localization tests with open ears and while wearing a passive HPD. Responses were measured for 24 loudspeakers (0˚-345˚, 15˚ increments in azimuth) using a head tracking paradigm. Subjects then returned for 45 minutes of localization training once per week for eight weeks. During these sessions, stimuli were presented from a subset of 12 loudspeakers (0˚-330˚, 30˚ increments in azimuth). Half of subjects (n=6, randomly assigned) were given robust audiovisual feedback during training; the remainder of subjects (n=6, control) were given no feedback. Results demonstrated a rapid reduction in the rate of putative front-back (≥ 45˚) errors in the group receiving audiovisual feedback, while more gradual improvement was observed in the control group. Performance was similar across the two groups by the final week of training, although the feedback group continued to outperform the control group on average. Importantly, post-training testing (no feedback provided for either group) across the original set of 24 loudspeakers demonstrated generalization of localization training to the 12 untrained locations for both groups. Data are in line with previous reports of listeners' adaptation to chronically altered spectral shape cues but demonstrate that training is effective even with (1) very intermittent exposure to distorted cues and (2) relatively severe cue distortions caused by occluding HPDs. Results suggest that audiovisual training could provide a means to rapidly improve situational awareness for regular users of HPDs and other HRTF-altering hearing devices.

PS 861

The perceived lateralization of binaural beats: Estimating Onset Dominance and the Perceptual Weighting of Interaural Time Difference Cues

Nicholas Haywood[1]; David McAlpine[2]
[1]Macquarie University, Department of Linguistics; [2]Department of Linguistics, The Australian Hearing Hub, Macquarie University, Sydney, Australia

For lateralization judgments concerning low-frequency stimuli, interaural time/phase differences (ITD/IPDs) cues near stimulus onset are afforded greater perceptual weight than those following. For binaural-beat stimuli, perceived lateralization will correspond to those carrier IPDs present during stimuli segments containing (diotic) amplitude rises (e.g., after onset, during on-going amplitude modulation (AM); Dietz et al., 2013). These experiments aimed to further define the window during which listeners are most sensitive to carrier IPD properties during modulated sound.

Stimuli comprised a 125-ms tone modulated with an 8 Hz sinusoidal envelope. A 4 Hz binaural-beat was evoked from dichotic carrier tones (498 and 502 Hz) – so, the carrier transitioned 180° of IPD between onset/offset. Ten starting IPDs where tested, and the beat direction was also controlled. Subjects heard four identical stimuli cycles, and reported whether the stimuli were heard to the left/right (2AFC, n=12). Interpolation suggested that a perceptually centred image would be heard when the beat transitioned from left- to right-leading (or vice versa) 22-ms after stimulus onset.

To better estimate the time-point within the beat cycles where IPD corresponded to overall reported lateralization, reference data concerning the perceived lateralization of static IPDs were used. From these data, the lateralization percept for each discrete IPD present within the beat cycle was estimated. Observed lateralization across all binaural beat conditions, showed a close match to estimated lateralization 25-ms after stimulus onset (comparison: minimum mean square error). As it is unlikely that listeners are sensitive to IPD at a single time-point only, the reference data were also converted into estimates for 'read-out' windows of varying length. Equally-weighted windows continued to prove a good match to the observed data, provided that they were temporally centred around 25-ms after onset, and did not extend to include IPDs present at the modulation peak (i.e., a maximum duration of 50-ms). Overall, the analysis provides evidence that IPDs occurring near to onset strongly influence lateralization, and IPDs around AM peak have little-to-no influence. Estimates from static IPD data also correspond well with observed lateralization for beating stimuli with abrupt onset/offset ramps (20-ms).

On-going experiments that are further estimating the parameters of the IPD 'read out' window by varying either the binaural beat rate or the sinusoidal AM rate will be presented. From such manipulations, it will be possible to further infer the time periods during which listeners are most sensitive to carrier IPD cues.

PS 862

Using Background Noise to Improve Sound Localization Following Simulated Unilateral Hearing Loss

Lindsey Ryan-Warden; Eva Ng; **Peter Keating**
University College London

Many listening abilities become more difficult in noisy environments, particularly following hearing loss. In particular, sound localization can be disrupted even if target sounds are clearly audible and distinct from background noise. Since subjects locate sounds by comparing the input to the two ears, sound localization is also considerably impaired by unilateral hearing loss. It is less clear, however, whether the effects of unilateral hearing loss are worsened by background noise. To address this, we measured sound localization abilities in the front hemifield, either in the presence or absence of broadband background noise. Adult human subjects were tested with normal hearing or with a simulated conductive hearing loss in one ear (earplug). To isolate the role of binaural processing, we tested subjects with narrowband target sounds. Surprisingly, we found that continuous background noise improved narrowband sound localization following simulated unilateral hearing loss. By contrast, we found the opposite effect under normal hearing conditions, with background noise producing illusory shifts in sound localization. Overall, our results suggest that continuous background noise may be used to improve sound localization under certain circumstances. This may have important implications for real-world hearing, both in normal-hearing subjects and the hearing-impaired.

PS 863

Time Course of Stimulus-History Dependent Adaptation and its Effect on Spatial Resolution

Andrea Lingner[1]; Michael Pecka[2]; Benedikt Grothe[1]
[1]Division of Neurobiology, Ludwig-Maximilians-University Munich; [2]Biocenter, Section of Neurobiology, Department Biology II, Ludwig-Maximilians-Universitaet Munich

Traditionally, the auditory system is thought to serve reliable sound localization. Electrophysiological evidence however indicates that specific feedback systems in the early binaural pathway cause the subjectively perceived location of sounds to be strongly influenced by immediately preceding spectrally similar or overlapping stimuli, hence by the acoustic context. These findings contradict the canonical concept of sound localization and raise questions about the functional significance of these feedback loops.

Here we present data from human psychoacoustical experiments investigating the nature and time course of context-dependent spatial sensitivity and its effect on sound source segregation. In accordance with previous human psychophysical studies (e.g. Phillips and Hall, Hear Res. 2005 Apr; 202(1-2):188-99), we found pronounced shifts in the spatial perception of sounds away from a prior presented adapter sound, corresponding to a substantial miss-judgement of absolute sound source positions in the range of tens of degrees of auditory space. For short time courses (a few hundreds of milliseconds after a previous sound)

these localization errors are confined to locations close to spatial position of the adapter. Consequentially, human listeners also reported a focal increase in spatial resolution near the adapter location on the expense of locations further away (Lingner et al., Sci Rep. 2018 May 29; 8(1):8335). These perceptional shifts can last up to several seconds and moreover expand to the hemisphere contralateral to the adapter position. Recently, we discovered that even for these rather long periods of time human listeners report a focal increase in spatial resolution near the adapter location.

Our findings support the notion that spatial hearing in mammals serves relative separation rather than absolute sound localization.

PS 864

A Virtual Reality Approach to test Biases in Human Sound Localization

Roland Ferger[1]; Miguel Vivar[2]; José L. Peña[1]
[1]Dominick P. Purpura Department of Neuroscience - Albert Einstein College of Medicine, NY, USA; [2]The Bronx High School of Science

This projects aims to contribute elucidating how the brain selects relevant features of the environment to encode information efficiently. Recent findings point toward representations of prior information leading to adaptive biases in sound localization. These biases can be explained as anticipating statistics of sound signals arriving at the ears, determined by physical attributes of ear canal and surrounding structures, as described by head-related transfer functions (HRTF). To investigate these biases in human sound localization, we have started a project to leverage the power of modern virtual reality (VR) technologies to advance research in this field. Our approach combines visual VR technology with virtual acoustic stimuli generated from generic and/or individualized HRTFs. An HTC Vive VR head mounted display (HMD) and headphones are used to generate a controlled audiovisual virtual space. Participants are asked to localize virtual sound sources by turning their head towards the perceived origin of the sound. Head position and direction can be readily read out from the VR headset throughout the experiment at the visual frame rate (approximately 90 Hz). Visual objects facilitate the interaction with the VR and provide feedback that can be enabled, disabled or manipulated according to the needs of each experiment. This method allows control over positions of visual and auditory elements of the experiment as well as the participant's head. From recorded head tracking data, we can extract measures such as response latency, accuracy and precision. This approach allows the easy implementation of stimulus paradigms that directly test our hypotheses. Future plans include the implementation of eye-tracking and a combination with EEG recordings from participants performing tasks in our audiovisual virtual space.

PS 865

Spectral Weighting for Sound Localization in the Free Field: Effects of Spectral Intensity Profile

Monica L. Folkerts[1]; G. Christopher Stecker[2]
[1]Department of Hearing and Speech Sciences, Vanderbilt University; [2]Boys Town National Research Hospital

The ability to localize a complex tone in a free-field relies upon binaural cues (interaural-time-differences [ITDs] and interaural-level-differences [ILDs]) distributed across frequencies. The duplex theory of sound proposes that low frequencies are localized based on ITDs and high frequencies are localized based on ILDs [Strutt 1907, Philos Mag 13:214- 32; Macpherson & Middlebrooks 2002, J Acoust Soc Am 111:2219-36]. Low-frequency ITDs have been indicated as the cue predominantly used during localization of broadband sounds [Wightman & Kistler 1992, J Acoust Soc Am 91:1648-61]. In order to further understand the frequencies utilized during sound localization, Folkerts and Stecker [2018, ARO 42:413] quantified spatial-cue weights across frequency in the form of spectral weighting functions (SWFs) for sound localization. The measurement technique was adapted from Stecker [2001, ARO Abs 24:258], which measured temporal weighting functions (TWFs). Results closely aligned with a frequency "dominance region" around 750-Hz [Bilsen & Raatgever 1973, Acustica 28:131-132] rather than an overall utilization of low frequencies. The current study extends this work to measure the effect of component intensity on SWFs. In one condition, components were presented at equal loudness to determine if the "dominance region" was due to the effect of the loudest component. Other conditions introduced intensity variation across components in the form of spectral slopes to further disambiguate the effects of spectral "dominance region" and any potential "level dominance" [Berg, 1990, J Acoust Soc Am 88:149-158; Lutfi & Jesteadt, 2006, J Acoust Soc Am, 120: 3853-3860]. Stimuli were similar to those used previously to measure SWFs except for the sound levels. Listeners were asked to localize 100-ms complex tones containing seven tonal or noise-band components. In the equal loudness condition, components increased or decreased in sound level based on the frequency of each component following the equal-loudness contour ISO 226 [2003, IOS, Geneva] for 80 phons. In the spectral-slope conditions, component intensity either increased or decreased with frequency, by 6 dB per component. Each trial presented individual components with random azimuth variation of 0°, ±5, 6.25°, or ±11. 25° around

a “base” azimuth selected for that trial. Base azimuths varied within a ±56. 25° range across trials. Multiple linear regression of the rank-transformed azimuthal response estimated the SWFs weights. Presenting components at equal loudness reduced but did not eliminate emphasis of the spectral “dominance region”. The spectral-slope condition resulted in increased weights for the loudest components. [Supported by NIH R01-DC016643]

PS 866

Modeling "Straightness" Versus "Briefness:" Do Adapting Neural Models Account for Temporal Weighting and Bandwidth Effects on Binaural Sensitivity?

G Christopher Stecker
Boys Town National Research Hospital

Recent years have seen major progress in understanding and modeling the detailed physiology of binaural neurons and their peripheral inputs, providing clearer views of how signals are transformed through the auditory system. Yet out understanding of many psychoacoustical phenomena continues to benefit from simpler mathematical models that abstract key properties and avoid treating complex nonlinearities. A particularly fruitful example is that of binaural cross-correlation, an idea that emerged with Jeffress’ (1948; J Comp Physiol Psych 41:35-39) *Place Theory of Sound Localization*by arrays of coincidence-detecting neurons that receive delayed input from each ear. Assuming an appropriate distribution of internal delays, that operation is mathematically equivalent to cross-correlating the peripherally transformed left and right-ear waveforms. Binaural cross-correlation models thus consist of two major components: a peripheral input transformer and a central cross-correlation computer. Most studies have modeled the periphery as a bank of bandpass filters to capture frequency selectivity along the basilar membrane, followed by a nonlinear transform that captures rectification and compression by inner hair cells. Some models have additionally considered the spike-generation process in the auditory nerve. Few have considered the nonlinear adaptive properties of the nerve, bushy cells, and related synapses which further transform the signal prior to binaural interaction. In this modeling study, we replaced the traditional peripheral transformer with an adapting neural model of the auditory nerve (Bruce, Erfani, & Zilany 2018; Hear Res 360:40-54) and bushy cell (Ashida, Heinermann, & Kretzberg 2019; github.com/pinkbox-models/GBC2019 v. 0.99). Binaural cross-correlation of averaged spiking output was used to investigate the effects of stimulus bandwidth and the temporal distribution of binaural information (“temporal weighting”). Of note, the transient-adapting neural response exaggerates positive envelope fluctuations and reduces binaural sensitivity except during brief temporal windows around such events. That is, unlike linear filters, auditory neurons maintain sensitivity to the rapid changes inherent in broadband sounds despite a high degree of frequency selectivity. That phenomenon (“briefness”) may plausibly account for the effects of stimulus band-widening, which reduces ambiguities inherent in the cross-correlation of narrowband inputs (Shear 1987; PhD Dissertation, CMU) without resorting to summation across frequency channels (“straightness”). [Supported by NIH R01 DC016643]

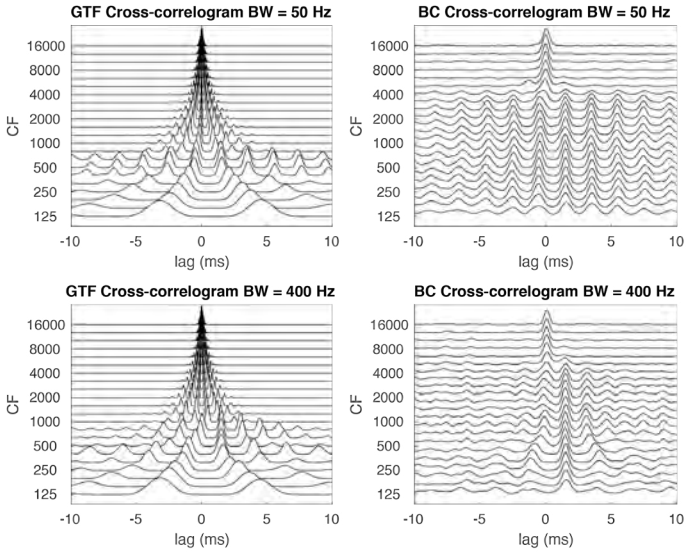

Binaural cross-correlograms for narrow (50 Hz, top) and wide (400 Hz, bottom) bands of noise centered at 500 Hz and with an imposed ITD of +1500 µs. GTF (left): band-by-band cross correlation of left and right ear signals after gammatone filtering, halfwave rectification and power-law expansion (Shear 1987). BC (right): cross-correlation of modeled bushy cell outputs for the two ears (Ashida et al. 2019). Although periodic “slipped cycle” peaks remain in the GTF cross-correlation function, increasing the bandwidth improves across-frequency alignment of peaks near the true ITD around 300-700 Hz CF. The true delay could be recovered by subsequent cross-frequency integration (“straightness”). In comparison, increasing bandwidth dramatically attenuates slipped-cycle peaks of the BC cross-correlation peaks in all frequency channels. The true delay can be extracted directly from the cross-correlation function of even a single frequency channel.

PS 867

Going Beyond ILD-Vector (Interaural Level Difference) Processing For Localization To Also Solve Multiple Source Separation And Source Streaming; The Needed Biology

Mark S. Riggle
Causal Aspects, LLC

Processing the ILD as a vector of frequencies (ILD-V) provides complete localization (azimuth, elevation, and distance); additionally, that localization is simple biologically to implement. That biologic implementation is also consistent with the evolutionary origin of hearing where there could not originally have been anything tonotopic nor any specialized neural structures for hearing. A strong selective pressure for further evolving hearing is understanding the natural environment where multiple sources are simultaneously active. We show how the mathematics of ILD-V localization can also

be applied to separating multiple sources and then to stream a selected source. While an implementation to perform those tasks is more specialized than for single source localization, the biological implementation is still straightforward and those needed specialization can be found in the ascending auditory pathway. Separating multiple sound sources first requires detecting when the ILD (or the IPD) in a frequency-time slot (T-F slot) modulates (which indicates multiple sources active in that T-F slot) and then allocating the remaining T-F slots (without ILD/IPD modulation) to locations. After that, streaming a particular source then requires just passing those T-F slots that have an ILD matching that source's location -- this is creating the binary mask of T-F slots for a selected source. We detail this theory and review the widespread data supporting the biological implementation of these processes (in both mammals and owls). Interestingly, the theory suggests that the complexity of the ascending auditory pathway evolved not for localization but rather for the multiple source separation and streaming problem. Furthermore, it suggests that the auditory localization space maps are probably not encoded in the ascending pathway nor in the forebrain but rather by the cerebellum.

PS 868

Deep Neural Networks as Models of Real-World Human Sound Localization

Andrew Francl[1]; Martha Gahl[2]; Josh H. McDermott[1]
[1]Department of Brain and Cognitive Sciences, MIT; [2]MIT Brain and Cognitive Sciences

The ability to localize a sound source by listening is a core component of audition, and has been a focus of hearing research for over a century. Sound localization has traditionally been studied using simple sounds and listening conditions, such as single noise bursts or tones in anechoic environments. However, in everyday life we localize sounds in environments with multiple sound sources, background noise, and room reverberation. At present we lack models that can explain these everyday abilities.

Recent engineering advances have led to artificial neural network models that perform at human levels for many perceptual tasks. Such network models are optimized to extract cues from the input that best support performance of the trained task. As a result, a trained model can reveal characteristics of near-optimal performance, and can provide hypotheses for biological systems that solve the same task. We utilized this approach to build a model that localizes sound sources in noisy reverberant environments from binaural audio. Following optimization, the model accurately localized sounds recorded in real rooms that had significant background noise and reverberation. We then simulated a large set of classic psychoacoustic experiments on the model. Despite having no previous exposure to the tone and noise stimuli nor the anechoic environment used in the experiments, the model qualitatively replicated a number of classic behavioral effects, including the frequency-dependent use of interaural time differences (ITDs), increased localization errors away from the midline, and better localization with increasing stimulus bandwidth. Contrary to the textbook account of binaural hearing but consistent with recent human data, the model was sensitive to interaural level differences (ILDs) at both low and high frequencies. Lastly, the model replicated the precedence effect, a behavioral phenomenon in humans hypothesized to be a result of echo suppression. The results suggest that many human sound localization behaviors may be understood simply as a consequence of optimization for real-world localization.

PS 869

Eye Movement Decoded from Eardrum Motion: The Decipherable EMREO

David Murphy[1]; Cynthia King[1]; Rachel Landrum[1]; Stephanie Schlebusch[2]; Christopher Shera[3]; Jennifer Groh[1]
[1]Duke University; [2]Duke Univeristy; [3]University of Southern California

After every eye movement, the brain must realign the visual and auditory reference frames in order to co-locate sights and sounds. Exactly where, when, and how such visual-auditory spatial integrations occur is not fully understood. We recently discovered that the eardrum oscillates beginning a few milliseconds before saccades and continuing until well into ensuing periods of fixation (Gruters, Murphy et al PNAS 2018). Information about at least the horizontal direction and length of saccades appear to be reflected in the phase and magnitude of these eye movement-related eardrum oscillations (EMREO).

Here, we investigated two questions concerning this signal: 1) Can independent estimations of vertical and horizontal saccade parameter contributions be linearly combined to predict EMREO waveforms for saccades in all directions (a fundamental assumption of current analyses)? 2) What are the frequency component(s) of this signal and how do they vary as a function of time and saccade parameters?

We found that EMREOs depend on both horizontal and vertical saccade components, varying predominantly with eye displacement, but are modulated by absolute

(initial or final) position as well. From time-series regression analyses, EMREO appear to represent combinations of these saccade parameters such that any saccade corresponds to a specific eardrum oscillation that contains a near-linear combination of the vertical and horizontal saccade parameters.

Time-frequency analyses showed multiple frequency components in the waveform evolving across time and varying with saccade parameters. Like the time-series analysis results, the timecourse of these frequency components vary somewhat between subjects, suggesting that new analyses are needed to compare data across subjects.

These results demonstrate that detailed information about the relationship between visual and auditory reference frames is present in the earliest stage of the auditory pathway. They also demonstrate that this information is approximately mapped as linear combination of saccade parameters and can therefore be recovered with a small set of basis components. Future work delving into the relationship between EMREO and the transduction of incoming sounds will be needed to ascertain their effects on the processing of auditory spatial locations in relation to the visual scene.

PS 870

Relationship Between Saccade-related Eardrum Oscillations and Hearing Loss

Cindy King[1]; David Murphy[1]; Stephanie Schlebusch[1]; Rachel Landrum[1]; David Kaylie[1]; Christopher A. Shera[2]; Jennifer Groh[1]
[1]Duke University; [2]University of Southern California

Integration of auditory and visual information is necessary in order to make sense of the world around us. How and where this integration occurs within the brain is not known. Our laboratory has identified a phenomenon where, in the absence of auditory stimuli, both eardrums begin synchronous, low-frequency oscillations just prior to saccadic eye movements. These eye movement-related eardrum oscillations (EMREO) change in amplitude and phase with changes in saccade magnitude and direction. This discovery suggests that connections between the visual and auditory systems likely begin as early as the auditory periphery (Gruters, Murphy et al, PNAS 2018). Ongoing work in non-human primates can provide insights into potential anatomical mechanisms (Schlebusch et al, Advances and Perspectives in Auditory Neuroscience conference 2019; Schlebusch et al, Society for Neuroscience conference, 2019; Schlebusch et al, Association for Research in Otolaryngology conference 2020) and examining the response in different human clinical populations can also further our understanding of the underlying mechanisms and potential utility of these oscillations.

Human subjects participated in visual tracking tasks, divided into one-hour sessions across several days. Subjects were seated, facing a monitor, and stable head position was maintained using a chinrest. Microphones placed in both ear canals recorded the oscillations. Eye movements were tracked with a video eye tracker. Analysis shows a reliably recorded EMREO could be obtained in approximately 5 minutes of recording time. The impact of hearing loss on the response is examined, comparing responses from individuals with different hearing losses to population data from normal hearing subjects. The effect of altered visual input is also examined by measuring EMREOs before and after a prism adaptation task.

PS 871

Reaction Times in Multisensory Spatial Localization in Front and Rear Space

Colton Clayton; Yi Zhou
Arizona State University

Visual signals influence auditory perception in a wide range of tasks including sound source localization. The addition of a visual stimulus could either facilitate or hinder the accuracy and reaction time of auditory localization depending on spatial congruence between auditory and visual stimuli (Schroger & Widmann, 1998; Ragot, Cave & Fano, 1988). The past studies, however, typically focus on auditory-visual interactions within the central field of vision (+/- 20 degrees) according to the spatial rule of proximity. Little is known about the spatial extent of visual influence when a sound may come from either frontal or rear space, typical of real-world listening environments. Our recent study shows that frontal visual stimulation led to a frontal bias in localizing a rear sound source (Montague & Zhou, 2018). The present study extends this research and investigates the effects of visual stimulation on reaction times. Experiments are designed to survey two types of reaction time (RT) simultaneously in a dual-response task: (1) saccade RT by listeners shifting their gaze to indicate the lateral direction of a perceived sound source and immediately after (2) choice RT for pushing a button to indicate the perceived front or back location of a sound. For all but one listener, RTs of both types to the rear auditory-only (AO) targets were either longer or not significantly different than those to the frontal targets, suggesting longer processing/response time for rear auditory targets. Results also showed that additional visual cues could either speed up or slow down both

types of RTs relative to AO responses, depending on the strength and direction of the visual-effect domain. For listeners experiencing strong visual capture, the visual-effect domain appears to cover the frontal hemifield and visual signals led to strong frontal bias and sped up RTs relative to AO responses. For listeners experiencing little visual capture, the visual-effect domain appears to cover the lateral hemifield and visual signals delayed RTs to auditory targets in the opposing lateral hemifield. Overall, our results show that vision has a significant influence on the speed of auditory decision making, even when sound sources originate from locations behind the head, providing further evidence that audio-visual interactions are not limited by the spatial rule of proximity.

Collicular/Midbrain Function

PS 872

Stimulus-Specific Information on Sound Azimuth Conveyed by Gerbil Collicular Neurons

Shigeto Furukawa[1]; Katuhiro Maki[2]
[1]NTT Communication Science Laboratories; [2]Aichi Shukutoku University

Auditory neurons often exhibit some degree of tuning to sound-source location. A typical tuning curve, a plot of spike discharge rate versus sound location, consists of a peak around a certain sound location with flanking slopes. The significance of the peaks and slopes in auditory space coding in brainstem nuclei have been debated in earlier studies (Grothe et al., Physiol. Rev., 2010). We approached this issue by examining stimulus-specific information (SSI; Butts and Goldman, Plos Biol., 2006) derived for an individual single units.

We recorded single-unit responses from the central and external nuclei of the inferior colliculus (collectively referred to as IC) and the superior colliculus (SC) of anesthetized gerbils. Stimuli were broadband noise bursts presented from a sound source that varied in azimuth on the horizontal plane in virtual auditory space. The stimulus level was varied at 15, 30, and 45 dB relative to the unit's response threshold. For each unit, azimuth-wise SSI was derived from the spike counts within a certain time window after stimulus presentation. SSI function was computed for each stimulus level or for pooled trials across multiple levels. In the context of the present study, SSI is a measure that represents the amount of azimuth-related information conveyed by the unit response at each azimuth. A higher SSI value indicates a greater significance of the response at the azimuth.

Trial-to-trial response variability was generally lower in the units in IC than those in SC. Butts and Goldman (2006) indicated theoretically that when trial-to-trial variability of the responses is high, the maximal SSI is conveyed for the stimulus at the tuning-curve peak, and as the variability decreases, the maximal SSI shifts to the region with the steep slopes. The majority of units exhibited higher SSI values at the tuning-curve peak than at the slope region, regardless of whether they were in IC or SC. The dominance of the peak was more apparent when the SSI were derived for pooled stimulus levels, in which the level variation was regarded as an additional cause of response variability. The results indicate that, at least at the single-neuronal level and for broadband stimuli, the maximal information is conveyed by responses to azimuth at the peak region of the tuning curve in both IC and SC.

PS 873

The role of group II mGluRs in spontaneous and sound-evoked firing modulation in the mouse IC

Inga Kristaponyte[1]; Nichole L. Beebe[1]; Jesse Young[1]; Brett R. Schofield[2]; Alexander V. Galazyuk[2]
[1]Northeast Ohio Medical University; [2]Northeast Ohio Medical University; Kent State University

Metabotropic glutamate receptors (mGluRs) are thoroughly researched because ligands targeting them have a potential for clinical development in several psychiatric and neurological disorders (Yang et al., 2017; Chaki, 2017; Li et al., 2015; Nicoletti et al., 2015). These receptors are also expressed throughout the auditory system (reviewed in Lu, 2014), although our knowledge regarding their roles is limited. It is possible that mGluRs in the auditory system might be important targets for pharmacological treatment of hearing disorders.

MGluRs are classified into three distinct groups: group I includes receptor subtypes 1 and 5, group II – subtypes 2 and 3, and group III – subtypes 4, 6, 7, and 8. The objective of this project is to characterize how group II mGluRs (mGluRs2/3) modulate spontaneous and sound-evoked firing in the mouse inferior colliculus (IC). This interest in group II mGluRs arises from recent results showing that behavioral signs of tinnitus in mice were suppressed by intraperitoneal administration of mGluR2/3 agonist LY354740 (Galazyuk et al., 2019). This study demonstrated that intravenous LY354740 injection reduced spontaneous activity in the IC of both noise-overexposed and control animals. It is possible tinnitus was suppressed because mGluR2/3 activation reduced spontaneous hyperactivity in one or more auditory brain regions.

To test the role of group II mGluRs specifically in the IC, extracellular single cell recordings were made from the IC in VGAT-ChR2-EYFP mice. In these animals, all

inhibitory neurons (GABAergic and glycinergic) express channelrhodopsin-2. Laser light pulses above the IC surface were used to activate inhibitory cells, allowing us to distinguish GABAergic from glutamatergic IC cell types optogenetically. The same neuron was recorded before and after iontophoretic or topical LY354740 application to pharmacologically activate mGluRs2/3. All recording sites were marked and immunostaining for GAD and the glycine transporter GlyT2 was performed to identify IC subdivisions. The results suggest that mGluR2/3 activation enhances sound-evoked firing in the central nucleus of IC in both GABAergic and non-GABAergic neurons. Preliminary data show that spontaneous firing might be affected. These data provide a rationale to further investigate group II mGluRs for possible pharmacological treatment of hearing disorders. Supported by NIH R01 DC016918 (to AG) and R01 DC004391 (to BRS).

PS 874

Sound Processing by VIP Neurons in the Mouse Inferior Colliculus

David Goyer[1]; Marina A. Silveira[1]; Alexander P. George[1]; Nichole L. Beebe[2]; Brett R. Schofield[3]; Michael T. Roberts[4]
[1]Kresge Hearing Research Institute, Dept. of Otolaryngology - Head and Neck Surgery, University of Michigan; [2]Northeast Ohio Medical University; [3]Northeast Ohio Medical University; Kent State University; [4]University of Michigan - Ann Arbor - Department of Otolaryngology-Head and Neck Surgery - Kresge Hearing Research Institute

The central nucleus of the inferior colliculus (ICc) is the hub of the ascending auditory system, as it is a nearly obligatory processing center for the output of the auditory brainstem. To better understand how sounds are processed in the ICc, it is important to identify the classes of neurons that make up the ICc and determine how they function within neural circuits. By using a combination of genetic, anatomical, and physiological methods, we recently identified a novel class of ICc stellate cells that are labeled in Vasoactive Intestinal Peptide (VIP)-IRES-Cre mice. VIP neurons in the ICc are glutamatergic, have a sustained firing pattern, have a stellate morphology, represent ~ 20% of stellate cells in the ICc, and 94% have spiny dendrites. Via axonal tract tracing studies, we found that VIP neurons project to auditory thalamus, auditory brainstem, the periaqueductal gray, and superior colliculus. Using Channelrhodopsin assisted circuit mapping (CRACM), we found that VIP neurons receive excitatory and inhibitory input from the contralateral IC and excitatory input from the contralateral DCN. EPSPs evoked by optical stimulation of DCN afferents were surprisingly slow (halfwidth: 15.8 ± 9.8 ms), but activation of DCN afferents also elicited feedforward inhibition (FFI), which limited EPSP duration. Having identified VIP neurons as a distinct neuron type in the IC, we are now probing their functional role in sound processing. Our initial data from in vivo, optogenetically-targeted extracellular recordings suggest that VIP neurons exhibit narrow tuning curves with relatively high tone thresholds and are only weakly driven by sinusoidal-amplitude modulated (SAM) tones. Yet, VIP neurons responded well to broadband and SAM noise, indicating that VIP neurons are more strongly driven when integrating inputs over a range of sound frequencies. These results are consistent with the stellate morphology of VIP neurons in which their dendrites cross two or more isofrequency laminae. Using patterned illumination with CRACM in vitro, we also are working to determine if inputs from the DCN and contralateral IC synapse onto different subcellular regions of VIP neurons. These experiments represent a critical step toward determining how defined neural circuits influence sound processing in the ICc.

PS 875

The Role of the Auditory Cortico-collicular Pathway in Deviance Detection in the Inferior Colliculus of Awake Mice

Alexandria Lesicko; Maria Geffen
University of Pennsylvania

Neurons in multiple structures along the auditory pathway exhibit sensitivity to the statistical context of sound stimuli, firing minimally to repeated tone presentations, but exhibiting an enhanced response to uncommon or “deviant” tones. This process, known as stimulus specific adaptation (SSA), is enriched in regions of the subcortical auditory system that receive descending cortical input, such as shell regions of the inferior colliculus. To determine whether the inferior colliculus inherits SSA from the auditory cortex, we selectively inhibited the auditory cortico-collicular pathway while recording from units in the inferior colliculus. Bilateral injections of a retro AAV-Cre construct were made in the inferior colliculus, while an AAV-Flex-ArchT construct was injected and cannulas were implanted bilaterally in the auditory cortex. Extracellular recordings were performed in multiple subregions of the inferior colliculus in awake mice while oddball stimuli, consisting of 90% repeated, or “standard” tones, and 10% deviant tones, were played to the contralateral ear. A green laser was used to inhibit cortico-collicular cells on a fraction of trials, and differences in deviance detection were quantified for laser on and off conditions by computing a frequency-specific SSA index. Additional tone sequences, including a cascade and many-standards sequence, were presented to further decompose the SSA index into two

additional metrics: an index of repetition suppression and an index of prediction error. Preliminary data suggest that units in the awake inferior colliculus exhibit complex receptive fields, with pure tones separated by 0.5 octaves commonly eliciting contrasting response profiles. A large fraction of units were also inhibited by acoustic stimuli. Baseline levels of SSA in the awake inferior colliculus were found to be lower than previous reports in anesthetized preparations, and cortico-collicular inactivation led to heterogeneous effects on metrics of deviance detection. Combined our data demonstrate that cortical feedback can both increase and decrease adaptation in subcortical structures.

PS 876

A Leading Sound Affects the Local-Field Potential Elicited by a Trailing Sound in the Rat's Inferior Colliculus in a Direction-Dependent Manner

Syed Anam Asim; Sarah Tran; Pamela Stark; **Huiming Zhang**
Department of Biomedical Sciences, University of Windsor

The perception of a sound can be affected by another sound in an environment, with the effect being dependent on the temporal and spatial relationship between the sounds. To understand neural mechanisms underlying this perceptual phenomenon, we recorded sound-driven local-field potential from the rat's midbrain auditory structure, the inferior colliculus (IC). The IC receives major excitatory inputs driven by the contralateral ear and inhibitory inputs driven by the ipsilateral ear. Simultaneous stimulation of the two ears using a pair of earphone (i.e., dichotic stimulation) produces strong action potential discharges in individual collicular neurons when the stimulation favors the contralateral ear. Discharges are reduced when the stimulation favors the ipsilateral ear. In addition to excitatory inputs, stimulation of the contralateral ear can produce lagging GABAergic inhibitory inputs to the IC through the superior paraolivary nucleus. Integration among excitatory/inhibitory inputs renders neurons in the IC special abilities to process temporal/directional acoustic information.

The specific purpose of this study is to find how a leading sound affects neural responses to a trailing sound in the IC and whether such an effect is dependent on the spatial relationship between two sounds. Local-field potentials were elicited by a pair of leading-trailing tone bursts presented from two loudspeakers (i.e., free-field stimulation). The two sounds were either colocalized at the ear contralateral to the site of recording or spatially separated with the trailing sound at the contralateral ear while the leading sound at another azimuth. The interval and angle of separation between the two sounds were systematically varied. We found that the response to a trailing sound was suppressed by a leading sound no matter whether the leading sound was colocalized with or separated from the trailing sound. The suppressive effect was larger and lasted longer when the leading sound was presented at the contralateral rather than the ipsilateral ear. The $GABA_A$ receptor antagonist bicuculine did not completely eliminate the difference between the suppressive effects produced by the leading sound at contralateral and ipsilateral locations. Thus, GABAerigic inputs from the superior paraolivary nucleus are not likely the sole factor responsible for the relatively large suppressive effect produced by a contralaterally presented leading sound. Our results have provided a new insight into the binaural processing in the auditory midbrain.

Research supported by NSERC and University of Windsor

PS 877

Gamma Oscillations Across the Barn Owl's Midbrain Auditory Space Map

Andrea J. Bae; Keanu Shadron; Roland Ferger; José L. Peña
Dominick P. Purpura Department of Neuroscience - Albert Einstein College of Medicine, NY, USA

Brain oscillations evoked by sensory stimuli are fluctuations in field potentials reflecting the combined activity of neural populations driven by a given stimulus. These oscillations have been described in many species from invertebrates to primates. However, their contribution to coding remains elusive.

Barn owls are specialists in sound localization studied for several decades. Their well described midbrain stimulus selection network provides a unique opportunity to evaluate the role of brain oscillations in coding. Previous in vivo recordings in the owl's optic tectum (OT) have shown that gamma oscillations (25-140 Hz) are spatially tuned to both visual and auditory information. Subsequent in vitro recordings in other avian models have described the circuit mechanisms underlying these oscillations between OT and other tegmental nuclei, the nucleus isthmi pars parvocellularis (Ipc) and the nucleus isthmi pars magnocellularis (Imc). Given that these previous studies were conducted with single electrodes, the full range with which these oscillations occur at a given time across the midbrain space map is not known, though it is inferred to be tightly associated with the tuning properties of the nearby neurons. To this end,

we performed multielectrode array recordings across the owl's OT to evaluate the spatial extent of gamma oscillations. Electrodes were positioned to cover a range of neurons tuned to different sound source locations.

Initial analyses show notable coherence in the local field potential in the absence of sound stimulation, which is stronger between electrodes placed near similarly tuned neurons. However, while sound stimulation with the preferred direction increases power within the gamma range, as previously shown by single electrode recordings, this enhancement appears less correlated across nearby electrodes than in spontaneous responses. Not surprisingly, decreasing the signal to noise ratio by manipulating binaural correlation leads to a lesser increase in gamma power than binaurally correlated stimuli.

Our preliminary results indicate that sound from a given direction increases gamma power at single locations of the map tuned to that direction. In the absence of sound, local field potentials within the gamma range are more coherent across the midbrain map than during sound stimulation. These results suggest a differential effect of sound stimulation on gamma power coherence between single and population levels, which may have implications for coding.

PS 878

Cholinergic Signaling Modulates the Excitability of VIP Neurons in the Mouse Inferior Colliculus via Nicotinic Acetylcholine Receptor-Dependent Mechanisms

Luis M. Rivera-Perez[1]; Kevin O. Cruz-Colon[2]; Michael T. Roberts[3]
[1]University of Michigan - Ann Arbor - Kresge Hearing Research Institute; [2]University of Puerto Rico - Ponce - Department of Biology; [3]University of Michigan - Ann Arbor - Department of Otolaryngology-Head and Neck Surgery - Kresge Hearing Research Institute

How our brains identify and respond to speech and other auditory cues remains unclear. Neurons in the inferior colliculus (IC), a hub for auditory processing located in the midbrain, exhibit selective responses to the spectral and temporal features of speech and other complex sounds. Previous findings suggest that acetylcholine (ACh), a neuromodulator associated with attention and synaptic plasticity, may provide an attention-based mechanism to alter auditory processing in the IC. Furthermore, neurons in the IC express different combinations of nicotinic acetylcholine receptor (nAChR) subunits. However, the cellular mechanisms underlying cholinergic modulation in the IC remain unknown. We recently found that brief pulses of ACh drive prolonged periods of firing in Vasoactive Intestinal Polypeptide (VIP) neurons in the IC. We hypothesized that ACh modulates the intrinsic excitability of VIP neurons through a signaling pathway that begins with the activation of specific nAChRs, requires calcium influx, and leads to increased synaptic release onto downstream targets. To address this, we are using brain slice electrophysiology and pharmacology to determine the mechanisms that govern the modulatory effects of ACh on VIP neurons. Our results show that the prolonged firing of VIP neurons elicited by brief pulses of ACh depends on activation of β4β2 nAChRs. Furthermore, we found that this effect is not abolished by blocking glutamatergic, GABAergic, and glycinergic synaptic transmission, suggesting that ACh acts by activating β4β2 nAChRs expressed on VIP neurons themselves and not through activation of a neuron presynaptic to VIP neurons. In current experiments, we are testing whether intracellular calcium plays a role in the prolonged excitatory response to ACh application. In future experiments, we will determine how cholinergic modulation of VIP neurons affects synaptic release onto postsynaptic targets in the auditory thalamus by using optogenetics and brief ACh pulses to stimulate presynaptic VIP terminals in the medial geniculate (MG). Our results will provide a better understanding of how cholinergic modulation shapes sound processing and provide a foundation for determining how cholinergic modulation can be used to promote adaptive plasticity in people with hearing loss.

PS 879

Responses to Tones Masked by Gaussian or Low-Noise Noise in the Inferior Colliculus of Awake Rabbits

Langchen Fan; Kenneth S. Henry; Laurel H. Carney
University of Rochester

Energy has been hypothesized to explain human detection performance for more than eighty years. For example, in tone-in-noise (TIN) detection tasks, a tone is typically assumed to be detected based on the energy at the output of an auditory filter. However, when stimulus energy is made less reliable, i.e. in the roving-level paradigm, human thresholds are elevated less than predicted by the energy model. Envelope cues have been proposed to serve as a cue in these conditions, and envelope-based models can outperform the energy model. Encoding of envelope-related cues for TIN tasks has not been studied in the central auditory system. The envelope is encoded in the slow fluctuations in the responses of auditory-nerve (AN) fibers; the amplitudes of these fluctuations are affected by both the stimulus envelope and by saturation of inner-hair-cell (IHC) transduction. Response rates in

the inferior colliculus (IC) are hypothesized to change with the fluctuation amplitudes elicited by TIN stimuli, based on IC sensitivity to amplitude modulations, as described by modulation transfer functions (MTFs). Here, neural responses to TIN stimuli were examined in the IC of awake rabbits. Adding a tone to narrowband gaussian noise (GN) flattens the stimulus envelope and additionally flattens AN response fluctuations due to IHC saturation. In contrast, adding a tone near threshold to low-noise noise (LNN) predominantly increases the amplitude of stimulus fluctuations. Neurons with band-enhanced MTFs were expected to have responses that were positively correlated to the fluctuation amplitudes elicited by these two types of TIN stimuli, while band-suppressed neurons were expected to have response rates that were inversely correlated to fluctuation amplitudes. Results show that most neurons with band-enhanced MTFs had decreasing rates with increasing tone level for GN maskers and increasing rate for LNN maskers. Most neurons with band-suppressed MTFs had increasing rate with increasing tone level for GN maskers and decreasing rate for LNN maskers. Both results are consistent with the hypothesis based on envelope-related cues, pointing towards an envelope-based encoding strategy for TIN in the IC. Neural thresholds were also calculated for comparison with human and rabbit detection thresholds. The best rate-based thresholds were similar to behavioral thresholds, whereas the best timing-based thresholds were more sensitive. This work was supported by NIH-DC010813.

PS 880

NPY neurons and NPY signaling in the mouse inferior colliculus

Marina A. Silveira[1]; Justin Anair[1]; Nichole L. Beebe[2]; Brett R. Schofield[3]; Michael T. Roberts[4]
[1]University of Michigan; [2]Northeast Ohio Medical University; [3]Northeast Ohio Medical University; Kent State University; [4]University of Michigan - Ann Arbor - Department of Otolaryngology-Head and Neck Surgery - Kresge Hearing Research Institute

Located in the midbrain, the inferior colliculus (IC) integrates information from numerous auditory nuclei and is an important hub for sound processing. Despite its importance, little is known about the function and molecular identity of neurons in the IC. Using a multi-faceted approach, we have identified Neuropeptide Y (NPY) as a marker for a distinct neuron class in the IC. In the NPY-hrGFP mouse line, hrGFP-positive neurons are distributed throughout the IC, and hrGFP selectively-labels IC neurons that express NPY. Immunostaining showed that NPY neurons in the IC are exclusively GABAergic (98.5% of hrGFP-positive neurons co-label with an antibody against GAD67; total NPY neurons counted: 2673). Using design-based stereology, we found that NPY neurons represent ~25% of the GABAergic neurons in the IC. To examine the physiology of NPY neurons, we targeted whole cell patch clamp recordings to hrGFP-expressing neurons in acute brain slices. These recordings demonstrated that the majority of NPY neurons exhibit a sustained firing pattern (spike frequency adaptation ratio < 2), express little *Ih* (*sag ratio* at -80mV = 0.88±0.09) and have a propensity to spontaneously fire, suggesting they might tonically release NPY in the IC. In post hoc reconstructions of recorded neurons, we found that NPY neurons have a stellate morphology and extend their dendrites across multiple isofrequency laminae in the IC (n=45). Because NPY is an important neuromodulator in many brain regions, we next investigated the functional role of NPY signaling in the IC. Using immunostaining, we found that the NPY Y1 receptor (Y1R) is widely expressed in the IC. We then turned to the Y1R-Cre mouse line to identify Y1R-expressing neurons. When crossed with Ai14 reporter mice, expression of the fluorescent protein tdTomato in Cre-expressing neurons revealed that Y1R neurons are distributed throughout the rostral-caudal extent of the IC. Next, we targeted whole-cell current clamp recordings to Y1R-expressing neurons and found that application of [Leu^{31},Pro^{34}] NPY, a high affinity Y1R agonist, leads to hyperpolarization of Y1R neurons in the IC. Thus, our data show that NPY neurons represent a distinct class of GABAergic neurons in the IC and that NPY signaling can regulate neuronal excitability in the IC. Future experiments will be aimed at determining how NPY neurons and NPY signaling contribute to auditory processing.

PS 881

Characterization of The Lateral Cortex of The Mouse Inferior Colliculus Using A Combination of Optogenetic Circuit Mapping and In Vivo Two-Photon Imaging

Baher A. Ibrahim[1]; Yoshitaka Shinagawa[1]; Alexander R. Asilador[1]; Daniel A. Llano[2]
[1]Beckman Institute for Advanced Science and Technology, University of Illinois at Urbana-Champaign, IL, USA; [2]Department of Molecular and Integrative Physiology, University of Illinois at Urbana-Champaign, IL, USA

The inferior colliculus (IC) is a critical midbrain structure for the processing of auditory stimuli. The IC is a hub that permits widespread convergence of both bottom-up and top-down projections involving auditory, somatosensory, visual, motor and arousal-related brain regions. One of the non-lemniscal divisions of the IC, the lateral cortex (LC), contains periodic modules of GABAergic cells and terminals which stain strongly for a range of metabolic

markers. Anatomically, the auditory inputs from the auditory cortex or central nucleus of the IC strongly avoid these inhibitory modules and instead form dense projections to the matrix areas that surround the modules. In contrast, these modules receive direct inputs from the somatosensory brain regions. *In vivo* two-photon imaging was used here to characterize the functional activity of the GABAergic and non-GABAergic cells inside and outside the modules. Both GABAergic and non-GABAergic cells outside the modules showed a tonotopic mapping of low to high frequencies (5-40 kHz) extending from rostromedial to caudolateral aspects of the lateral IC. In addition, while the cells in the modules showed no excitatory responses to sound, only the GABAergic cells in the modules showed inhibitory responses at high-frequency tones. Interestingly, the responsive cells to the broadband noise sound were only located outside the modules and mostly tuned to 5 kHz pure tone. Using laser-assisted mapping, the AC terminals were found to make monosynaptic connections mostly with all the cells of the lateral cortex of the IC with the exception of GABAergic cells in the modules that receive the lowest percentage of these monosynaptic connections, which could suggest that module/matrix organization of the lateral cortex has the capacity to process auditory stimuli while being modulated by auditory cortical projections.

PS 882

Neural Coding of Pitch Cues in the Auditory Midbrain of Unanesthetized Rabbits

Yaqing Su[1]; **Bertrand Delgutte**[2]
[1]University of Geneva; [2]Harvard Medical School, Dept. of Otolaryngology

Pitch is an important attribute of auditory perception that conveys key features in speech and music, and helps listeners extract meaning in complex auditory environments. Pitch can be produced either by a set of harmonically-related components that are individually resolved by frequency analysis in the cochlea, or by periodic envelope fluctuations resulting from the beating between neighboring unresolved harmonics. Although pitch perception has been extensively studied, the underlying neural mechanisms are still poorly understood. Here we investigated the coding of pitch in the inferior colliculus (IC) which receives ascending inputs from most brainstem auditory nuclei and where neural firing rates are sensitive to amplitude modulation.

To explore the role of IC in the neural processing of pitch, we recorded single-unit activity of 298 neurons in the IC of five normal hearing, unanesthetized rabbits in response to harmonic complex tones and sinusoidally modulated noise with a wide range of spectral and temporal properties. We identified three neural codes for pitch cues: (1) a temporal code via phase locking to the stimulus envelope repetition rate (ERR) below 900 Hz, (2) a band-selective (bandpass or band-reject) rate tuning to the ERR for frequencies between 60 and 1600 Hz, and (3) a rate-place code for resolved harmonics that was mainly available for fundamental frequencies above 800 Hz. About 40% of the neurons demonstrated more than one of the three codes. All three codes were fairly robust across a 40-dB range of sound level.

While the temporal code and the rate-place code are inherited from the auditory periphery, band-selective rate tuning to ERR has rarely been observed at processing stages prior to the IC. Using a phenomenological model (Nelson and Carney, JASA 116: 2173-2186), we show that bandpass rate tuning to ERR can arise via interaction of excitatory and inhibitory synaptic inputs, and thus the IC performs a temporal-to-rate code transformation of pitch cues. We also used spectral receptive field models to show that the rate-place code may be enhanced by inhibition along the auditory pathway.

Together, these three codes provide cues for the pitch of stimuli over the entire range of fundamental frequencies and for stimuli with both resolved and unresolved harmonics. However, additional neural mechanisms are needed to extract pitch from these neural codes.

Supported by NIH grant R01 DC002258

PS 883

Dopamine Gates Prediction Errors in the Auditory Midbrain

Guillermo V. Carbajal; Catalina Valdés-Baizabal; David Pérez-González; Manuel S. Malmierca
University of Salamanca

To remain responsive to important input from an ever-changing acoustic landscape, perceptual systems have evolved mechanisms to detect deviations from regular patterns in the stream of sensory information. Since neuromodulation strongly impacts sensory processing, we explored the role of dopamine in the stimulus-specific adaptation (SSA) exhibited by neurons in the inferior colliculus.

We recorded auditory responses of single units to an oddball stimulus paradigm while applying dopamine or eticlopride (a D_2-like receptor antagonist) via microiontophoresis. Our results showed dopaminergic modulation of the SSA in most inferior colliculus neurons. If the SSA index was augmented by application of dopamine, it decreased with application of eticlopride, and

vice versa. We also recorded inferior colliculus neurons using a cascade control sequence, where tones were arranged in a predictable succession of increasing or decreasing frequency, thereby offering a proper control for the repetition effects generated by the standard stimulus of the oddball paradigm. Hence, response comparisons between the oddball and cascade sequences allowed us to dissociate the relative contribution of prediction error effects from those purely due to repetition suppression in the SSA index, as well as to study how dopamine application affected both components differentially. We observed a direct relationship between the changes of SSA and repetition suppression indices elicited by dopaminergic manipulation, but that relationship did not prevail when analyzing the component of prediction error. Whenever dopamine produced a significant change in the SSA index (increase or decrease), the index of repetition suppression tended to change in that same direction. Conversely, the index of prediction error tended to decrease when the application of dopamine altered the SSA index, regardless of the direction of that change.

As in other previous works from our lab, this further confirms that there is a component of prediction error present in auditory midbrain SSA that cannot be accounted for by repetition suppression effects. But most importantly, this provides a novel demonstration that prediction error and repetition suppression are independently neuromodulated by dopamine, reassuring the dissociation between both components of SSA from a neurochemical standpoint. Furthermore, our results suggest that dopaminergic circuits could be encoding the precision of prediction errors at the inferior colliculus level, thus regulating the inflow of prediction error up the auditory hierarchy.

This work has been funded by Spanish MINECO (SAF2016-75803-P). CVB held a fellowship from Mexican CONACyT (216652). GVC held a fellowship from the Spanish MICINN (BES-2017-080030).

PS 884

Temporal coding deficits of AM tones in IC neurons of mice lacking the a2d3 Ca2+ channel subunit

Katrin Hegmann[1]; Gerhard Bracic[2]; Jutta Engel[2]; **Simone Kurt**[3]
[1]Humpis-School Ravensburg; [2]Saarland University, Department of Biophysics and CIPMM, Homburg, Germany; [3]Saarland University, Department of Biophysics and CIPMM, Homburg

Although many forms of human hearing impairment and deafness result from deficits in the auditory periphery, particularly the cochlea, hearing disorders exist that reside in the central auditory system, which is responsible for transferring, processing and finally perceiving auditory information. Mice lacking the auxiliary a_2d3 subunit of voltage-gated Ca^{2+} channels, which have almost normal hearing thresholds, show distorted ABR waveforms pointing to an auditory processing disorder. a_2d3 is widely expressed in the brain, especially in neurons of the auditory brainstem and the spiral ganglion neurons. The a_2d3 subunit is essential for normal P/Q currents in spiral ganglion neurons in culture (Stephani et al., Front Cell Neurosci 2019) and for normal morphology and function of auditory nerve fiber terminals, the endbulbs of Held. Behavioral experiments revealed auditory discrimination learning deficits in the temporal domain as previously shown (Pirone*, Kurt* et al., J Neurosci 2014).

To determine the role of a_2d3 for central auditory processing, we performed *in vivo* electrophysiological recordings from neurons of the inferior colicullus (IC) from $a_2d3^{+/+}$ and $a_2d3^{-/-}$ mice. We characterized neural responses to amplitude-modulated tones to examine the impact of endbulb of Held synapse malfunction for temporal coding.

Neurons of the IC of $a_2d3^{-/-}$ mice showed prolonged response latencies. Evoked rates were decreased whereas spontaneous rates were increased in $a_2d3^{-/-}$ mice compared to the wildtype. Mice lacking a_2d3 showed a reduced ability to phase-lock in response to stimulation with amplitude-modulated tones.

Taken together, our results demonstrate a potential link between the function of specific (endbulb of Held) synapses at the junction between the peripheral and central auditory system and impaired central processing and perception, which might underlie auditory processing disorders.

This study was supported by DFG PP1608/2.

PS 885

Growth and cellular patterning during fetal human inner ear development studied by a correlative imaging approach

Lejo Johnson Chacko[1]; David Wertjanz[2]; Consolato Sergi[3]; Joszef Dudas[2]; Natalie Fischer[2]; Theresa Eberharter[2]; Romed Hoermann[2]; Rudolf Glueckert[4]; Helga Fritsch[2]; Helge Rask-Andersen[5]; **Anneliese Schrott-Fischer**[2]; Stephan Handschuh[6]
[1]Anichstrasse 35; [2]Medical University of Innsbruck; [3]University of Alberta; [4]Inner Ear Laboratory, Medical University Innsbruck, Innsbruck, Austria; [5]Uppsala University; [6]Veterinary University of Vienna

Background
Progressive transformation of the otic placode into the functional inner ear during gestational development in humans leads to the acquisition of hearing perception via the cochlea and balance and spatial orientation via the vestibular organ.

Results
Using a correlative approach involving micro-computerized tomography (micro-CT), transmission electron microscopy and histological techniques we were able to examine both the morphological and cellular changes associated with human inner ear development. Such an evaluation allowed for the examination of 3D geometry with high spatial and temporal resolution. In concert with gestational progression and growth of the cochlear duct, an increase in the distance between some of the Crista ampullaris is evident in all the specimens examined from GW12 to GW36. A parallel increase in the distances between the macular organs - fetal utricle and saccule - is also evident across the gestational stages examined. The distances between both the utricle and saccule to the three cristae ampullares also increased across the stages examined. A gradient in hair cell differentiation is apparent from apex to base of the fetal cochlea even at GW14.

Conclusion
We present structural information on human inner ear development across multiple levels of biological organization, including gross-morphology of the inner ear, cellular and subcellular details of hearing and vestibular organs, as well as ultrastructural details in the developing sensory epithelia. This enabled the gathering of detailed information regarding morphometric changes as well in realizing the complex developmental patterns of the human inner ear. We were able to quantify the volumetric and linear aspects of selected gestational inner ear specimens enabling a better understanding of the cellular changes across the fetal gestational timeline. Moreover, these data could serve as a reference for better understanding disorders that arise during inner ear development.

PS 886

Early appearance of key transcription factors influence the spatio-temporal development of the human inner ear

Lejo Johnson Chacko[1]; Consolato Sergi[2]; Theresa Eberharter[3]; Joszef Dudas[3]; Helge Rask-Andersen[4]; Romed Hoermann[3]; Helga Fritsch[3]; Natalie Fischer[3]; Rudolf Glueckert[5]; Anneliese Schrott-Fischer[3]
[1]Anichstrasse 35; [2]University of Alberta; [3]Medical University of Innsbruck; [4]Uppsala University; [5]Inner Ear Laboratory, Medical University Innsbruck, Innsbruck, Austria

Expression patterns of transcription factors Leucine-rich repeat-containing G-protein coupled receptor 5 (LGR5), Transforming growth factor-β-activated kinase-1 (TAK1), SRY (sex determining region Y)-box 2 (SOX2), GATA binding protein 3 (GATA3) in the developing human fetal inner ear was studied between the gestation weeks 9 to 12. Further development of cochlear apex between gestational weeks 11 through 16 (GW11 to GW16) was examined using transmission electron microscopy.

LGR5 was evident in the apical poles of the sensory epithelium of the cochlear duct and the vestibular end organs at GW11. Immunostaining limited to hair cells of organ of Corti by GW12. TAK1 immune positive in inner hair cells of the organ of Corti by GW12 and colocalized with p75 neurotrophic receptor expression. Expression for SOX2 confined primarily to the supporting cells of utricle at the earliest stage examined at GW9. Intense expression for GATA3 presented in the cochlear sensory epithelium and spiral ganglia at GW9. Expression of GATA3 was present along the midline of both the utricle and saccule in the zone corresponding to the striolar reversal zone where the hair cell phenotype switches from type I to type II. The spatiotemporal gradient of the development of the organ of Corti was also evident with the apex of the cochlea forming by GW16.

It seems that highly specific staining patterns of several transcriptions factors are critical in guiding the genesis of the inner ear over development. Our findings suggest that the spatio-temporal gradient in cochlear development extends at least until gestational week 16.

PS 887

Identifying Parallels in the Mechanisms of Hearing and Deafness Between the Fruit Fly, Drosophila melanogaster, and Humans

Daniel Sutton[1]; Jonathan Andrews[2]; Shinya Yamamoto[3]; Andrew K. Groves[4]
[1]Baylor College of Medicine; [2]Jan and Dan Duncan Neurological Research Institute; [3]Jan and Dan Duncan Neurological Research Institute, Baylor College of Medicine; [4]Department of Neuroscience, Baylor College of Medicine, Houston, United States

Over 60% of all human disease genes have orthologs in the fruit fly and all major signaling pathways are conserved. The auditory system of the fly, Johnston's organ (JO), is located within the second segment of each antenna and is comprised of around 200 stretch receptor units called scolopidia. Scolopidia contain mechanosensitive neurons that respond to gravity and sound from vibrations of the outermost antennal segment. Although JO is morphologically different from the cochlea, the function of orthologs of some human deafness genes are known to be conserved. A previous screen of protein localization and gene expression in the *Drosophila* Johnston's organ of orthologous mammalian deafness genes identified considerable conservation between flies and mammals. We are performing behavioral screenings and electrophysiological recordings in Johnston's organ to identify which of these genes are functionally significant

Orthologous genes with a previously characterized null viable phenotype were given priority for behavioral testing. We isolated homozygous female flies and paired them in isolated chambers with a Canton-S (wild type) male fly. To test the mutant female's response to the male's courtship song, we used a high-speed camera to record the time until copulation. For electrophysiological testing, we isolated homozygous mutant flies and exposed them to a stimulatory pulse song to deflect the antenna. Sound-evoked electrical responses were recorded from the antennal segment.

Data from the behavioral screen from 3 orthologous mutant fly lines showed a statistically significant delay in time to copulation. Orthologs of Sun1 and Nesprin 4, which form the LINC complex in mammals and are necessary for outer hair cell health and hearing function, and the ortholog of Pcdh15, which is a member of the tip complex in mammals and causes deafness and Usher syndrome, all showed compromised mating behavior. We will perform electrophysiological recordings of these mutants to confirm that these observations are due to defects in JO.

The finding from our previous work showed that roughly 80% of the genes tested had orthologs in the fruit fly with conserved expression/localization in Johnston's organ. Of the 3 orthologs that we have tested through courtship behavior, all 3 have a significant increase in time to copulation. This provides evidence that gene expression and protein localization within Johnston's organ is an indicator of functional involvement. This conservation of molecular mechanisms within JO shows that *Drosophila* genetics can be utilized to quickly and efficiently study conserved mammalian deafness genes.

PS 888

Cochlear development of a Non-Human primate model animal, Common Marmoset

Makoto Hosoya[1]; Masato Fujioka[2]; Kaoru Ogawa[2]
[1]Department of Otolaryngology-Head and Neck Surgery, School of Medicine, Keio University; [2]Department of Otolaryngology, Head and Neck Surgery, School of Medicine, Keio University

Considering regenerative therapy, understanding of organ development and tissue generation is important, because re-track developmental steps are one of the promising ways for regeneration. Moreover, recently pluripotent stem cell based cell therapy has been developed and expected to be a feasible therapeutic way by replacing damaged cells to new targeted cells induced from pluripotent stem cell including embryonic stem cells or induced pluripotent stem cells (iPS cells). Detailed developmental information about the targeting organ or cells are required for inducing well differentiated cells efficiently.

Much of the understanding of the cochlear development has been derived from rodent model. These knowledges from mouse model are useful for understanding basic our human cochlear development and would be beneficial for realizing hearing regenerative therapy. However, there are several gap for applying rodent model to human. First, it is known that some mouse model fail to reproduce human congenital hearing loss model. This means that the factor involving the cochlear development have different rules between the rodent and human at least in some cases. Secondly, it was known that for inducing cochlear hair cells from embryonic stem cells or iPS cells, there was no bipotent induction method and we have to choose different ways for mouse cell or human cells. This fact suggests that there might be some different factors involving each developmental steps. Therefore, it is important for understanding human cochlear development. However, there are more limited information about human cochlear development, especially from the molecular biology view point, because of rarity of chance to assess human fetal sample or ethical hardness in some country. Moreover if

human fetal samples were available, it would be suitable for only anatomical or histopathological analysis and not to be used for molecular biological analysis for tissue preparation problems.

Therefore, we used non-human primates to investigate the development of hearing organs. In particular, we were interested in a small New World monkey species, the common marmoset (Callithrix jacchus), which has been investigated for hereditary hearing loss research in this field. Moreover, now genetic modification is possible in the common marmoset we can use this species as a non-human primate model for the developmental analysis.

Here, we report comprehensive analyses of gene expressions in the developing primate cochlea of common marmoset and comparing the developmental stages between the common marmosets, mice and human for basic analyses toward inner ear regeneration in human.

PS 889

The gEAR Porta – Inner Ear scRNA-seq & Epigenetic Data Made Accessible

Joshua Orvis[1]; Brian Gottfried[1]; Jayaram Kancherla[2]; Kevin Rose[1]; Yang Song[3]; Amiel A. Dror[4]; Beatrice Milon[5]; Hector C. Bravo[2]; Anup A. Mahurkar[1]; Ronna Hertzano[6]
[1]University of Maryland School of Medicine; [2]University of Maryland-College Park; [3]Institute for Genome Sciences, University of Maryland; [4]Galilee Medical Center, Israel; [5]Department of Otorhinolaryngology-Head and Neck Surgery, University of Maryland; [6]Department of Otorhinolaryngology Head and Neck Surgery, University of Maryland School of Medicine; Institute for Genome Sciences, University of Maryland School of Medicine.

The gEAR portal (gene Expression Analysis Resource, umgear.org) is an online tool for multi-omic and multi-species data visualization, sharing, and analysis with a focus on datasets relevant to auditory and vestibular research. The gEAR is a continually-updating resource that can be utilized to answer simple questions such as 'where is this gene expressed in the ear or central auditory pathways' or 'how does this gene change with age, mutations, during regeneration and after damage', to more complex analysis of existing datasets for differential gene expression, and identification of tissue and cell type-specific marker genes. For those actively generating gene expression datasets, the gEAR provides the ability to upload for private usage and share their data with collaborators prior to publication, visualize and analyze their data in the context of other datasets including single cell RNA-seq and prepare their data presentation format for sharing via a permalink that can be used for data dissemination in publications. Additionally, the gEAR portal provides direct links to a variety of other resources for each gene query, species-specific annotation, and a note-tool for keeping track of ideas/results obtained during browsing. Since ARO 2019, the gEAR underwent many upgrades with a new user-friendly front page, a user manual, an improved compare tool with integrated significance tests, a 'gene cart' manager allowing users to also generate custom gene-lists for queries, an ability to generate custom user-defined displays for any dataset, a new and improved dataset uploader, and a greatly improved single-cell RNA-Seq workbench containing numerous new features. The latter is of importance as scRNA-seq has matured as a commonly used technique for measuring gene expression across tissues with the addition of numerous relevant datasets in our field. This presentation functions as a step-by-step introduction to the gEAR portal and its many upgrades as it became a mainstream multi-omic data source for the ear research community.

PS 890

In silico Analysis of the Otocyst Development using Published Single Cell RNA-sequencing Data

Ryosuke Yamamoto[1]; Hiroe Ohnishi[2]; Takayuki Nakagawa[2]; Koichi Omori[2]; Norio Yamamoto[2]
[1]Kyoto Univ; [2]Dept. Otolaryngology - Head and Neck Surgery, Graduate School of Medicine, Kyoto University

Background
The inner ear comprises four epithelial domains: cochlea, otolith organ, semicircular canals, and endolymphatic duct. The otocyst harbors progenitors for most cell types of the mature inner ear; however, the four anatomical structures are still unclear at embryonic days 10.5 (E10.5). Durruthy-Durruthy et al. investigated the mouse otocyst and early neuroblast lineage at single-cell resolution using quantitative RT-PCR (Durruthy-Durruthy et al., Cell, 2014). They subdivided the otocyst into distinct octants and established a 3D otocyst model based on 96 genes expression. However, the heterogeneity of the otocyst at transcriptome level is still unknown, and time-course changes of gene expression in the otocyst are not also clarified. In this study, we attempted to elucidate the mechanism of the otocyst fate determination using published data obtained by single-cell RNA sequencing (RNA-seq).

Methods
In February 2019, Cao et al. published the transcriptome data of 2 million whole-body cells collected from E9.5-13.5 mice (Nature, 2019). They subjected the single-cell transcriptomes to Louvain clustering and Uniform Manifold Approximation and Projection (UMAP)

visualization and identified 56 developmental trajectories, including otic epithelial trajectory. We downloaded single-cell transcriptomic data of the 5000 otic epithelial lineage cells. We mainly used Monocle 3 to analyze the data by Louvain clustering and UMAP visualization.

Results

We projected 5,000 cells onto a two-dimensional space encoding transcriptional state using UMAP so that the distances between cells with similar transcriptome patterns were close. E9.5 cells were distributed in the center, and the other cells at later stages constitute four major cell populations, suggesting that otic progenitors differentiate into four kinds of tissues. We annotated four each cell population using known genes that characterize the four different tissues in the inner ear and identified them as the cochlea, vestibule, semicircular canals, and endolymphatic duct. Additionally, we identified the prosensory epithelium cells in the cochlea and semicircular canal clusters. We found cluster-specific genes. We are also performing pseudo-time analysis to build unsupervised, diffusion-based developmental trajectories.

Conclusions

We visualized the 5,000 single-cell transcriptomes on 2D space. In the figure, cells at later than E9.5 formed four clusters which corresponded to the four components of the inner ear: cochlea, otolith organ, semicircular canals, and endolymphatic duct. The ongoing analysis may provide insights regarding the molecular pathways that drive the development of the four epithelial components of the inner ear.

PS 891

Comprehensive Single Cell RNAseq Analysis of the Neonatal Murine Utricle

Taha Jan[1]; Yasmin Eltawil[1]; Daniel Ellwanger[2]; Stefan Heller[2]; Alan Cheng[3]
[1]Stanford University; [2]Department of Otolaryngology–HNS, Stanford University; [3]Department of Otolaryngology-Head and Neck Surgery, Stanford University

The murine utricle undergoes dynamic cellular maturation after birth. Previous histological studies have demonstrated an increase in the number of hair cells from postnatal day 0 to 8 and show that hair cell subtypes mature at least during the first month. Thymidine analog studies have demonstrated a decrease in proliferative cells in the utricular sensory epithelium and the presence of proliferative cells on the periphery. We asked whether the postnatal utricle contains transcriptionally unique cell subtypes and how they may relate to one another. To probe the postnatal mouse utricular sensory epithelium in an unbiased manner, we performed single cell RNA sequencing at three different age groups (P2, P4, and P6) using the Smartseq2 protocol, which allows for comprehensive "deep" sequence assessment of expressed transcripts. We profiled approximately 1000 cells with a median read count of 515,842 per cell and median gene count of 3,485 detected genes per cell. Clustering analysis revealed four hair cell states, two supporting cell states (striolar and extrastriolar), and two transitional cell states. We validated marker genes for the various identified cell states with immunofluorescence and in situ hybrididzation. Multiplex fluorescent in situ hybridization identified over a dozen novel markers. In summary, we have generated a deep sequenced single cell RNAseq profile of the developing murine utricular sensory epithelium with validation of novel markers and delineation of the previously poorly characterized transitional epithelium.

PS 892

Optimized Clustering and Dichotomous Testing of scRNA-Seq Data for Analysis of Human Inner Ear Organoids

Daniel R. Romano; Takashi Nakamura; Eri Hashino
Indiana University School of Medicine

Computational analysis of single-cell RNA-sequencing (scRNA-seq) data involves the steps of quality control, dimension reduction, clustering, and differential expression analysis (DEA). Faithful assignment of cell types and/or subtypes depends on high-yield DEA and, in turn, substantive clustering. Clustering optimization is a well-recognized problem in machine learning but is arguably underappreciated in scRNA-seq analysis. Instead, researchers often employ heuristics such as manual merging of 'overclustered' data based on the expression of well-characterized marker genes. While these approaches may be appropriate for scRNA-seq data from predictable cell populations, they are not suitable for stem cell-derived organoids, which represent heterogeneous – and sometimes unexpected – cell populations at various developmental stages. To address this issue, we have devised a novel approach for optimizing the clustering of organoid scRNA-seq data using the Calinski-Harabasz (CH) index. We then capitalized on this optimization to develop a clustering-sensitive, likelihood ratio-inspired (LRI) test for DEA. Human embryonic stem cells were differentiated into inner ear organoids, and after 60 days, aggregates were dissociated into single cells, which were then FACS-sorted for EPCAM. The 10x Genomics Chromium Platform was used for cell lysis and cDNA library construction, and the Illumina NovaSeq 6000 was used for sequencing. The resulting data were then mapped onto the human genome and analyzed in R using both Seurat and custom code. We compared the top 10 genes returned by DEA of optimally- and overclustered data, as well as those returned by the Wilcoxon and LRI tests. We

found that clustering optimization reduced the percentage of mitochondrial, ribosomal, and housekeeping genes returned by DEA. This suggests that when scRNA-seq data is not optimally clustered, DEA is lower yield and, in turn, cell type assignment is more challenging. Furthermore, manual merging of overclustered data failed to restore the CH index, emphasizing the fact that overclustering is more nuanced than simple subdivision of substantive clusters. After clustering optimization, the Wilcoxon and LRI tests returned just 25% of the same genes. Several clusters shared no genes, including a cluster of presumptive hair cells, for which the LRI test returned a greater number of hair cell-enriched genes than did the Wilcoxon test. These results demonstrate the importance of clustering optimization in the scRNA-seq analysis of organoid cells. In addition, the LRI test appears to be superior to the Wilcoxon test in returning cell type-enriched genes for optimally clustered data.

PS 893

Sensory Cells of Amniote Cochleas are susceptible to Zika Virus Infection

Vidhya Munnamalai[1]; Nabilah Sammudin[2]; Caryl Young[1]; Ankita Thawani[3]; Richard Kuhn[2]; Donna Fekete[4]
[1]The Jackson Laboratory; [2]Purdue; [3]Baylor College of Medicine; [4]Purdue University

Congenital Zika Syndrome in humans is caused by vertical transmission of Zika virus (ZIKV) to the gestating fetus, often resulting in microcephaly and ventriculomegaly. Previous research has demonstrated that ZIKV preferentially infects neural progenitor cells and causes increased cell death and reduced proliferation of infected cells. More recently, it has been reported that ~6% of ZIKV-associated microcephalic newborns show diminished otoacoustic emissions and auditory brainstem responses, suggesting at least some pathogenesis may originate within the cochlea. This supposition is supported by our unpublished results from chicken embryos infected *in ovo*. ZIKV (~10^8 pfu/ml) is delivered into the fluid cavity of the otocyst at embryonic day (E)2 to 5. Antibody against double-stranded RNA is used to detect infection. Sensory and non-sensory otic epithelium, the statoacoustic ganglion, and periotic mesenchyme are infected 2-8 days post injection. Although infection of the auditory organ is seen at all time points, it is most robust following injections at later ages and/or at later stages of harvest (up to E13). These data suggest that there is a critical time window for ZIKV to infect (and perhaps spread) in the embryonic cochlea.

To further address the time course of susceptibility to ZIKV, we studied cultured mouse cochleas at either pre- or post-mitotic stages. Mouse cochleas are explanted on E12.5, E15.5 and postnatal day 2 (P2) and ZIKV (5-10 x 10^5 pfu) is added for the first 24 hours. Samples are analysed after 3-6 days in vitro. At all 3 ages, ZIKV infects hair cells, supporting cells and periotic mesenchyme. On E12.5, the prosensory domain is still proliferating, confirming that ZIKV infects sensory progenitors in the cochlea. By E15.5, the organ of Corti has exited the cell cycle, providing evidence that post-mitotic progenitors are also susceptible to infection. By P2, hair cell differentiation is underway and under damaging conditions the organ shows less plasticity to return to a proliferative state; nonetheless, the sensory cells can be infected. In fact, more hair cells were infected at P2 than at earlier ages. The inner hair cells were also found to be more susceptible to infection than outer hair cells. Finally, we performed virus neutralization experiments where cochlear cultures are preincubated with the ZIKV-117 antibody against the viral envelope protein for 6 hours and then ZIKV is added. Infection is completely blocked under these conditions. When the antibody is washed out prior to ZIKV infection, ZIKV infection prevailed.

PS 894

Caspase-3 Cleaves Extracellular Vesicle Proteins During Auditory Brainstem Development

Forrest Weghorst[1]; Yeva Mirzakhanyan[2]; Kian Samimi[1]; Mehron Dhillon[1]; Melanie Barzik[3]; Lisa L. Cunningham[3]; Paul D. Gershon[2]; Karina S. Cramer[1]
[1]Department of Neurobiology and Behavior, UC Irvine; [2]Department of Molecular Biology and Biochemistry, UC Irvine; [3]Laboratory of Sensory Cell Biology, NIDCD, NIH

Sound localization in vertebrates relies on extremely precise auditory brainstem circuits, which can detect minute differences in sound intensities and arrival times between the ears. The molecular mechanisms of axon guidance and synapse formation in the development of these specialized pathways are incompletely understood. We previously demonstrated that accurate development of the interaural time difference circuit in the chick auditory brainstem requires activity of the apoptotic protease caspase-3. During embryonic development, the active form of caspase-3 is serially expressed in the neurites of the ascending auditory brainstem: first in auditory nerve axons on embryonic day (E)6-7; then in the axons of their target, *n. magnocellularis* (NM), on E8-10; and finally in the dendrites of NM's target, *n. laminaris* (NL) on E11-12. Pharmacological inhibition of caspase-3 from E8 to E10 results in NM axonal targeting errors and morphological disruption of NL. Because caspase-3 acts by cleaving proteins, we sought to determine the proteolytic targets of caspase-3 relevant to circuit development in the chick auditory brainstem. Embryos were treated with caspase-3 inhibitor or vehicle solution on E9-10, and their auditory brainstem proteomes were sequenced using

nanoLC-MS/MS. Proteins with peptides bearing the mark of caspase-3 proteolysis (a cleavage site following an aspartate or glutamate residue) that were present in vehicle-injected brainstems but absent in caspase-3-inhibited brainstems were considered likely targets of caspase-3. These proteins were submitted to GO term analysis using the DAVID Bioinformatics Resource, which revealed that caspase-3 targets were enriched for proteins associated with extracellular vesicles (EVs; membrane-bound nanoparticles with important functions in intercellular signaling and macromolecule transport). Other metrics, such as the number of EV proteomic datasets on the database EVpedia that contain each caspase-3 target and non-target protein, suggested that caspase-3 targets are found in EVs much more often than the average protein. To determine whether chick auditory brainstem EVs actually contain caspase-3 targets, EVs were purified from E10 auditory brainstem tissue using size exclusion chromatography. The E10 EV proteome was sequenced and found to contain significantly more caspase-3 target proteins than expected by chance, indicating that caspase-3 targets are enriched in auditory brainstem EVs. Additionally, nanoparticle tracking analysis showed that the majority of these EVs are around 100 nm in diameter, consistent with classically defined exosomes. These data suggest a novel developmental mechanism by which caspase-3 influences auditory brainstem circuit formation through the proteolytic cleavage of extracellular vesicle proteins.

PS 895

Roles of Tubby in the Formation of Stereociliary Links and Hearing Function

Jeong-Oh Shin[1]; Woongsu Han[1]; Ji-Hyun Ma[1]; Hyehyun Min[1]; Jinsei Jung[1]; Jinu Lee[1]; Un-Kyung Kim[2]; Jae Young Choi[1]; Seok Jun Moon[1]; Dae Won Moon[3]; Chul Hoon Kim[1]; Jinwoong Bok[1]
[1]Yonsei University; [2]Kyungpook National University; [3]DGIST

The tubby mouse with a null mutation in the Tub gene arose spontaneously at the Jackson Laboratory four decades ago. Tubby mice show obesity, retinal degeneration, and hearing loss. Several tubby functions have been proposed, including transcription factor, GPCR mediator, and postsynaptic regulator. However, none of these directly explain the defects of tubby mice. The pathological mechanism of hearing loss in tubby mice is more ambiguous due to the early onset several months before hair cell degeneration. To elucidate the in vivo function of tubby required for normal hearing, we analyzed cochlear structures and hearing function of tubby mice. Tubby mice showed a significant increase in auditory brainstem response (ABR) thresholds at all frequencies examined. The amplitudes of distortion product otoacoustic emissions (DPOAEs) were also greatly reduced, suggesting dysfunction of outer hair cells (OHCs). Consistent with these results, tubby proteins are specifically localized at the tips of OHC stereocilia and the loss of tubby leads to the loss of two extracellular stereociliary links: 1) the horizontal top connectors (HTCs) that link adjacent stereocilia and 2) the tectorial membrane (TM)-attachment crowns (TM-ACs) that connect the tips of tallest stereocilia to the TM. These structural and functional defects of tubby mice closely resemble those of stereocilin (Strc) knockout mice. We observed that stereocilin, which is normally localized at the tips of OHC stereocilia, is lost in tubby mice, suggesting an important role of tubby in stereocilin localization, which is essential for the formation of HTCs and TM-ACs. We further examined tubby mice in AKR inbred strain (tubby-AKR), which was reported to carry a modifier allele known as “modifier of tubby hearing 1” and to rescue the hearing loss of tubby mice that originally arose in C57BL/6 strain (tubby-B6). Indeed, ABR thresholds are significantly reduced and DPOAE amplitudes were increased significantly in tubby-AKR. Interestingly, the rescue of hearing in tubby-AKR is due to the selective restoration of TM-ACs, but not HTCs. Finally, although HTCs do not seem essential for acquiring hearing function, they play an essential role in providing resilience to acoustic trauma, thus reducing the impact of noise-induced hearing loss. In summary, our study reveals the mechanism underlying the hearing loss of tubby mice. The unexpected cellular localization and function of tubby in the OHCs provides novel insights into how stereociliary links contribute to the structural integrity essential for normal hearing.

PS 896

ADF and Cofilin Link Mechanotransduction to Actin Remodeling in Developing Stereocilia

Jamis McGrath[1]; Chun-Yu Tung[2]; Inna A. Belyantseva[3]; Pallabi Roy[2]; Melanie Barzik[4]; Bo Zhao[5]; Thomas B. Friedman[3]; Benjamin Perrin[1]
[1]Indiana University - Purdue University Indianapolis; [2]Indiana University-Purdue University Indianapolis; [3]Laboratory of Molecular Genetics, National Institute on Deafness and Other Communication Disorders, NIH, Bethesda, Maryland, USA; [4]Laboratory of Sensory Cell Biology, NIDCD, NIH; [5]Department of Otolaryngology-Head and Neck Surgery, Indiana University School of Medicine

Stereocilia lengths and widths change dramatically during early postnatal mouse development as bundles remodel their actin cores to acquire functional staircase morphologies. Mechanotransduction is required for this process, but the mechanisms connecting it to actin regulation are largely unknown. A key event in stereocilia bundle patterning is to distinguish row 1 stereocilia, which

are the tallest, from those of row 2, which are shorter and have mechanotransduction channels. By following actin-GFP incorporation and turnover in developing bundles, we found that row 2 stereocilia actin turns over more rapidly, but is less stably incorporated, than in row 1 stereocilia. Correspondingly, from birth to postnatal day 6, row 2 stereocilia tips had increasing amounts of free barbed ends, where monomers can be added or lost, as compared to row 1 tips. In parallel with increasing levels of barbed ends, we found the actin severing proteins ADF and cofilin-1 (Cfl1) were also selectively enriched in row 2 stereocilia tips. Loss of ADF/Cfl1 or mechanotransduction prevented the enrichment of free barbed ends and altered the morphology of stereocilia in the shorter rows. Thus, mechanotransduction is required to localize ADF/Cfl1 to row 2 stereocilia tips, where these proteins remodel the actin cores, presumably by severing actin filaments. Through this process, the dimensions of mechanotransducing stereocilia are refined to help generate the trademark staircase morphology of the hair cell bundle.

PS 897

Stereociliary Bundle Reorientation in the Absence of PCP Signaling and Proper Tectorial Membrane Development

Justin Nemelka[1]; Sungjin Park[1]; **Michael Deans**[2]
[1]University of Utah; [2]Dept. of Surgery, Div. of Otolaryngology, Dept. of Neurobiology and Anatomy

The core PCP proteins function to coordinate the orientation of stereociliary bundles between neighboring hair cells. These include the Wnt receptors Frizzled3 and Frizzled6, and the transmembrane proteins Vangl1 and Vangl2. Research from our lab and others has shown that Vangl1 and Vangl2 contribute to the intercellular exchange of polarity information, and that their loss results in adjacent hair cells with polarized bundles that are misoriented relative to each other. Thus, is was unexpected to find that auditory hair cells allowed to undergo postnatal development in *Vangl2* CKO mice reoriented their misaligned stereociliary bundles such that they became properly oriented relative to the short axis of the cochlea. We demonstrate that this phenomenon is not restricted to *Vangl2* mutants and that stereociliary bundle reorientation also occurs in the absence of *Frizzled3* and *Frizzled6*. Moreover, this is not due to compensation by redundant PCP signaling factors because reorientation still occurs following the simultaneous deletion of both *Vangl* genes in mouse (*Vangl1* and *Vangl2)*.

It has been suggested from studies in the developing chick basilar papillae that that the overlying tectorial membrane could physically realign stereociliary bundles so that they are properly oriented within the sensory epithelia. We tested this hypothesis using *TectA* CRISPR mutant mice in which tectorial membrane development is severely disrupted. In *TectA; Vangl2* compound mutants the severity of the initial PCP phenotype and extent of reorientation remains comparable between *Pax2*-Cre; *Vangl2* CKOs and *TectA*; *Pax2*-Cre *Vangl2* CKOs at all developmental stages. Thus, the reorientation of misaligned stereociliary bundles can occur in the absence of physical manipulation. Since bundle reorientation occurs in a gradient along the length of the cochlea, by examining reorienting cells at different cochlear positions we can infer the movement of the kinocilium during the reorientation process. These morphometric analyses reveal that during reorientation the kinocilium and its associated basal body always travel along the cell periphery in a clockwise or counterclockwise direction, and never pass directly across the apical cell surface. Altogether these observations suggest the activity of an as yet unidentified planar polarity cue that realigns stereociliary bundles so that they are properly oriented along the short axis of the cochlea through a mechanism that does not require intercellular PCP signaling.

PS 898

Short Stature Homeobox 2 Contributes to a Subpopulation of Zebrafish Statoacoustic Ganglion

Alejandra Laureano; Kathleen Flaherty; Anna-Maria Hinman; Kelvin Y. Kwan
Rutgers University

Introduction

The Short Stature Homeobox 2 gene (*SHOX2*) was identified as a candidate transcription factor involved in early auditory neuron development. Zebrafish, like humans possess both orthologues of the *SHOX* gene family (*SHOX* and *SHOX2*), whereas mice only possess *SHOX2*. To better understand and recapitulate the role of *SHOX2* in human inner ear development, zebrafish was chosen as a model organism.

Results

Zebrafish *shox2* has not been implicated in inner ear development. We showed that *shox2* transcript is dynamically expressed in the inner ear by *in situ* hybridzation and is present at key timepoints in developing statoacoustic ganglion (SAG). *In toto* imaging of live fish harboring both *shox2 (Tg*(*shox2:Gal4,UAS:mCherry*)) and pan-inner ear (*Tg(pax2a:GFP*)) fluorescent reporters revealed the presence of *shox2* in the otic neurogenic region at 18hpf where progenitors reside.

To assess if *shox2* cells contribute to the developing SAG, lineage labeling at 24hpf was done. Different fluorescent *shox2 (Tg(shox2:Gal4,UAS:XFP))* reporters were mated to either neuronal progenitor *(TgBAC(neurog1:dsRed))*

or transit amplifying neuroblast *(TgBAC(neurod1:EGFP))* reporters. Dual fluorescent fish show overlap of reporter signal and implicate shox2 expression in a subpopulation of developing SAG. Co-localization of the shox2 reporter signal with Islet 1/2 immunostaining suggests Shox2 expression in a subset of post-mitotic neurons. Together, the lineage labeling implicate shox2 expression in a subpopulation of developing SAG neurons.

To determine the function of *shox2* in the developing inner ear, anti-sense morpholinos were used to reduce *shox2* transcript levels. Three-day old *shox2* morphants displayed behaviors suggestive of inner ear and neurological dysfunction compared to controls. Abnormal behaviors observed include circling, lack of avoidance behavior and spasms. For stable deletion of *shox2*, a null mutation was generated using CRISPR/Cas9. Absence of *shox2* alters the population of mature SAG neurons and hair cells in the anterior maculae of larval zebrafish inner ear.

Discussion

The results suggest a role of *shox2* in neurosensory development. We propose that *shox2* is essential for the development of a subpopulation of SAG neurons.

PS 899

CAMSAP3 is Required for Mucus Clearance in the Middle Ear

Jing Zheng[1]; Alan Robinson[2]; Yingjie Zhou[3]; Mary Ann Cheatham[3]
[1]Feinberg School of Medicine Northwestern University; [2]Northwestern University, Dept. Otolaryngology; [3]Northwestern University

Otitis media is one of the most common diseases among children and if untreated, can lead to hearing loss and even fatality. Motile cilia on multiciliated cells (MCCs) within the middle ear are the first line of defense against pathogens in order to prevent otitis media. Unlike most non-motile sensory cilia, motile cilia are composed of microtubules (MTs) in a '9+2' configuration: 2 central singlet MTs surrounded by 9 doublet MTs. The central MT pair within the axoneme is critical for MCCs to generate a coordinated, directional flow, allowing for mucus clearance, and thereby protecting the middle ear from infection. One of the long-standing questions concerning multiciliogenesis is how the central MT pair is assembled. In contrast to the 9 MT doublets, the central pair is not continuous with MT triplets in the basal body. Hence, we hypothesize that CAMSAP3, a microtubule minus-end regulator, is involved in building the central MT pair as CAMSAP3-coated MTs are stable and capable of acting as seeds for MT elongation. Therefore, we investigated a global CAMSAP3 knockdown mouse model, *Camsap3*^{tm1a}, created by the "knockout-first" conditional allele targeting strategy. We confirmed that *Camsap3* transcripts are indeed decreased in *Camsap3*^{tm1a} homozygous mice but are not completely absent as reported other *tm1a* alleles using the same strategy. In addition, *Camsap3*^{tm1a} homozygous mice exhibit multiple pathological phenotypes including otitis media and hearing loss. Since many of these symptoms are linked to Primary Ciliary Dyskinesia (PCD), a condition caused by motile ciliary defects, we further examined MCC function in three different tissues, including the tympanic cavity. Our data show defects in the synchronized ciliary motion of MCCs in *Camsap3*^{tm1a} homozygous mice. Anatomical examination further revealed that CAMSAP3 localizes to the transition zone of motile cilia, where the central MT pairs are initiated. In *Camsap3*^{tm1a} homozygotes, MCCs lack CAMSAP3 at the transition zone, central MT pairs are missing in a majority of the cilia, and the polarity of basal bodies is disorganized. Taken together, our data suggest that CAMSAP3 is required for normal motile cilia formation and function, both of which play crucial roles in preventing otitis media and hearing loss. (Work supported by grants from the NIDCD (DC011813) and the Knowles Hearing Center).

PS 900

Extracellular ATP Promotes Embryonic Spiral Ganglion Neuron Branch Dynamics via P2X3 Receptors

Zhirong Wang[1]; Travis Babola[2]; Johnny Jung[1]; Katherine Rangoussis[1]; Talya Inbar[1]; Christian Faaborg-Andersen[1]; Dwight E. Bergles[2]; Thomas Coate[1]
[1]Georgetown University; [2]Johns Hopkins University

The mammalian cochlea undergoes a highly dynamic process of growth and innervation during development. This process includes spiral ganglion neuron (SGN) branch refinement, a process whereby SGNs undergo a phase of "debranching" prior to forming unramified synaptic contacts with sensory hair cells. P2X3 is an ionotropic ATP receptor with high calcium permeability and is expressed by SGNs during hair cell innervation. Using genetic single-neuron labeling and calcium imaging approaches in mouse models, we have found that P2X3 normally controls SGN branch dynamics and activity patterns during development. In particular, *P2rx3* null mouse show more complex branching patterns at SGN peripheral terminals and around the SGN cell bodies. In addition, the P2X3 specific agonist, a,ß,me-ATP, potentiates calcium events in developing SGNs, whereas SGN calcium transients are dysregulated in both *P2rx3* null cochleae and cochleae treated with the P2X3 inhibitor NF110. We conclude that SGN branch refinement requires P2X3-mediated extracellular ATP signaling and intracellular calcium signaling.

PS 901

Molecular and Physiological Profiles of Spiking Oligodendrocytes in the Developing Auditory Brainstem

Elizabeth Gould; Jun Hee Kim
University of Texas Health Sciences San Antonio

The rapid processing of auditory information critically depends on myelination. Myelin structure controls the speed of conduction to regulate auditory transmission. It is hypothesized sound-evoked activity regulates oligodendroglial development and myelination. During development, oligodendrocyte lineage cells (OL) exhibit distinct physiological characteristics, indicating OL exhibit different physiological responses to neuronal input. Our recent study demonstrates that a subpopulation of OL conducts functional $Na_v1.2$ currents sufficient to evoke spikes and displays a distinct response to glutamatergic input in the auditory brainstem (Berret et al., 2017). The differential functions of OL with distinct physiological characteristics are unknown. In this study, we utilized physiological characteristics paired with transcriptional profiling to determine the genetic logic that determines specific physiological features to identify the specific roles of unique OL populations in the auditory brainstem. Using single-cell qPCR combined with whole-cell recording, we found that *Scn2a*, the gene that encodes for the alpha subunit of $Na_v1.2$ channel, is restricted to spiking OL. Spiking OLs express a significant number of *Scn2a* mRNAs, but there was no detectable *Scn2a* mRNAs in non-spiking OL (n = 11 spiking OLs vs 25 non-spiking OLs, t-test, $p< 0.01$). In the OL-specific *Scn2a* conditional knockout (cKO), all OL recorded could not generate a spike in response to depolarizing current injection (n= 19 OLs from 4 cKO mice). The genetic deletion of *Scn2a* in OLs eliminated spiking properties in OL. Single-cell transcriptomics revealed that cell-cycle genes are enriched in *Scn2a*-expressing OLs. *Mk167*, a marker of cells that have exited G0, was significantly higher in spiking OLs than non-spiking OL (2760 ± 762 mRNAs, n = 11 spiking OL vs 501 ± 436 mRNAs from 22 non-spiking OL, t-test, $p< 0.01$). The results suggest spiking OL have a capability to proliferate and likely control OL density. In support of this hypothesis, labeling with the thymidine analog, EDU (n = 4 mice), showed that about half of the actively dividing OL in the auditory brainstem express $Na_v1.2$ channel. Interestingly, auditory stimulation (16 KHz at 80 dB for 2 hours, 7 days) significantly increased OL proliferation in the auditory brainstem (sound stimulated: 10% EDU+Olig2+/Olig2+ cells; control 4.6% EDU+Olig2+/Olig2+ cells, t-test, $p = 0.029$). Increased neuronal activity may trigger spiking OL to promote OL proliferation and maturation. In summary, this study suggests that *Scn2a*-expressing OLs are a unique subpopulation of oligodendrocytes that respond to auditory stimulation, and contribute to the development of the auditory brainstem.

PS 902

Microglia and Fractalkine Signaling in Multimodal Midbrain Circuit Assembly

Cooper A. Brett; Mark L. Gabriele
James Madison University

Microglial cells (MGCs) are highly dynamic and have been implicated in shaping discrete neural maps in several systems. MGCs respond to numerous cues in their microenvironment, including a neuronally-expressed chemokine, CX3CL1 (fractalkine). The present study examines MGC and CX3CL1 patterns with regard to the emerging modular-extramodular framework within the lateral cortex of the inferior colliculus (LCIC). A reliable modular marker, glutamic acid decarboxylase (GAD), together with an extramodular marker, calretinin (CR), enable visualization of modular-extramodular domains in the nascent mouse LCIC. Major multimodal afferent and efferent systems of the LCIC appear to interface with its neurochemically-defined patch-matrix-like organization. Here we utilize Iba-1 (a microglial marker) and CX3CL1 labeling to explore the potential involvement of MGCs and fractalkine signaling in establishing LCIC functional compartments. A developmental series of postnatal (P0, P4, P8, P12, P20) GAD67-GFP and CX3CR1-GFP mice were utilized. GABAergic neurons are specifically labeled in GAD67-GFP knock-ins, highlighting LCIC modular fields. MCGs are labeled in both heterozygous and homozygous CX3CR1-GFP mice. In $CX3CR1^{GFP/GFP}$, fractalkine signaling is compromised due to a nonfunctional CX3CL1 receptor (CX3CR1). Brains were sectioned at 50µm on a sliding freezing microtome prior to immunocytochemistry protocols for Iba-1 (1:1000, Wako Chemicals), and/or CX3CL1 (1:100, R&D Systems), or GAD67 (1:100, Millipore). Appropriate biotinylated secondary antibodies and streptavidin fluorescent conjugates were utilized for unequivocal visualization of the different markers. A Nikon C1si TE2000 microscope was used for all widefield and confocal image acquisition. GAD- and CR-positive LCIC compartments emerge shortly after birth and exhibit increasingly complementary patterns over the first two postnatal weeks. Iba-1 staining shows MGCs occupy the neonatal LCIC, with spatial heterogeneities and morphological appearances that change as the modular-extramodular framework and its segregated multimodal afferent patterns are shaped. MGCs are present throughout the IC at birth, before concentrating in the LCIC by P4. MGCs at P8 conspicuously border modular-extramodular boundaries prior to invading modular confines by P12. CX3CL1 labeling is clearly modular at P12, in keeping with the notion of fractalkine-mediated recruitment of microglia

to modular centers. Preliminary results in CX3CR1$^{GFP/GFP}$ mice suggest microglial movement into modules is delayed with compromised fractalkine signaling. The present study characterizes MGC and CX3CL1 patterns with respect to neurochemically-defined LCIC modular-extramodular zones. Ongoing studies utilizing CX3CR1-GFP mice aim to identify mechanisms whereby fractalkine influences MGC-mediated refinement of multimodal LCIC connections.

PS 903

FMRP expression in the auditory ganglion regulates the development of auditory nerve projections within the cochlear nucleus

Xiaoyu Wang; Diego Zorio; Yuan Wang
Florida State University

Fragile X mental retardation protein (FMRP) is an RNA-binding protein that regulates the synthesis of many synaptic proteins. In the auditory system, FMRP deficiency leads to aberrant synaptic connectivity and auditory processing deficits. While FMRP function is extensively studied in the brain, whether FMRP is expressed in sensory periphery and whether this expression influences the development of central nerve systems remain unknown.

We first examined FMRP expression in the cochlea of two rodent species, FVB mice and Mongolian gerbils, using immunocytochemistry. Mice are typical high frequency listeners, while gerbils are sensitive to low frequency sounds as humans. In both species, the majority, if not all, neurons in the auditory ganglion (AG) exhibit high levels of FMRP immunoreactivity. No obvious variation is detected along the tonotopic axis. FMRP expression is detected in both developing (P6) and mature (P56) animals, implicating an importance of FMRP in AG development and/or function. We further confirmed a similar expression in the chicken AG during development (embryonic day 6 (E6), E9, and E15) and after mature (E19 and postnatal day 4 (P4)). Quantitative analyses of western blot on samples specifically collected from AG reveal a significant reduction from E19 to P4. Together, these protein analyses identify an evolutionally conserved expression of FMRP in developing AG neurons.

We next determined whether FMRP expression in AG is important for the development of their central projections to the brain via the auditory nerve fibers (ANFs). To achieve this goal, we genetically knocked down FMRP expression in a subset of AG neurons of chicken embryos and examined their axon pattern within the nucleus magnocellularis (NM), the avian analogues of spherical bushy cells (SBCs) in the mammalian anteroventral cochlear nucleus. In mature systems, NM and SBC neurons are innervated by ANFs via the endbulb of Held synapses. Following FMRP knockdown, transfected ANFs extend and penetrated into NM at E9, similar to nontransfected wildtype axons. In the next a few days, however, a considerable number of transfected ANFs failed to terminate on NM neurons. Instead, these fibers continued to grow, passing through the NM laterally or ventrally, suggesting defective axonal targeting and/or terminal stabilization. A small number of ANFs did terminate on NM neurons with endbulb-like terminals. 3D reconstructions of individual terminals at E15 and E19 did not reveal a significant difference in terminal morphology or size between transfected and nontransfected endbulbs. On the other hand, immunocytochemistry demonstrated a reduction in the terminal level of synaptotagmin 2, a calcium sensor responsible for triggering synaptic vesicle exocytosis, suggesting possible impairment of synaptic transmission. Taken together, these data demonstrate that periphery FMRP expression is important for the formation of synaptic connectivity in the auditory brainstem.

Grant Support: NIH/NIDCD R01DC13074

PS 904

Role of GABA Co-transmission in the Developmental Refinement of the MNTB-LSO Pathway

Jongwon Lee; Brian Brockway; Karl Kandler
University of Pittsburgh School of Medicine

During development, glycinergic synapses in the sound localization pathway from the medial nucleus of the trapezoid body (MNTB) to the lateral superior olive (LSO) co-release GABA. This GABA co-transmission is most prominent before hearing onset when the MNTB-LSO pathway undergoes activity-dependent refinement, raising the possibility that GABA plays a role in the developmental elimination or strengthening of immature MNTB-LSO connections.

To test this hypothesis, we investigated the developing MNTB-LSO pathway in region-specific knockout mice, in which GABA release from MNTB neurons is impeded by genetic deletion of the GABA synthesizing enzyme GAD67 (Vglut3-Cre x GAD67$^{flox/flox}$). Immunohistochemistry confirmed a significant decrease of GAD67 antibody staining in MNTB neurons and in axonal fibers in the LSO in KO mice compared to control mice. Whole-cell patch clamp recordings of MNTB-elicited postsynaptic currents in LSO neurons in slices (postnatal day 2-4) confirmed a significant decrease of pharmacologically isolated (CNQX + strychnine) GABA mediated responses in KO mice (n=6) compared to control mice (n=7). Deletion of GAD67 had no effect on membrane capacitance (n=44), input resistance (n=43), or hyperpolarization-activated currents (I_H) (n=44) in LSO neurons.

To examine whether disruption of GABA transmission impairs the refinement of functional connectivity in the MNTB-LSO pathway, we measured MNTB-elicited synaptic response amplitudes to increasing stimulation intensities in slices from P10-12 animals and used statistical analysis with a Gaussian mixture model with Bayesian information criteria to estimate the number and strength of MNTB fibers converging on individual LSO neurons. We found no difference between KO and control mice in the number of MNTB fibers converging on single LSO neurons (median ± interquartile range: Control: 4 ± 2 fibers, n=22, KO: 5 ± 2 fibers, n=20). However, in KO mice, individual fiber strength was significantly increased compared to control mice (mean ± SD: Control: 833 ± 392 pA, n=22; KO: 1277 ± 719 pA, n=20). Consequently, maximum postsynaptic currents elicited by stimulation of all converging MNTB inputs were significantly increased in KO mice (Control: 3692 ± 1660 pA, n=23; KO: 5901 ± 2981 pA, n=21).

Our results indicate that GABA co-transmission in the developing MNTB-LSO pathway is important for the precise adjustment of input strength but not for the functional pruning of inputs before hearing onset.

Acknowledgements
We thank Dr. Srivatsun Sadagopan for providing valuable input for statistical cluster analysis. This study was supported by the NIDCD (5R01DC004199).

PS 905

Anatomical Characterization of Developing Olivocochlear Efferent Neurons

Austen Sitko[1]; Michelle Frank[1]; Lisa Goodrich[2]
[1]Dept. of Neurobiology, Harvard Medical School; [2]Harvard

The mammalian cochlea receives direct efferent input from cholinergic olivocochlear neurons (OCNs), which reside in the superior olivary complex in the ventral brainstem. Medial olivocochlear neurons (MOCs) innervate outer hair cells (OHCs) and are reported to transiently innervate inner hair cells (IHCs) prior to hearing onset. Lateral olivocochlear neurons (LOCs) innervate peripheral processes of Type I spiral ganglion neurons (SGNs) just below the base of IHCs. OCNs protect against loud sounds and modulate afferent activity and auditory processing. Moreover, the timing of OCN arrival and innervation in the cochlea coincides with important periods of axon guidance and synapse formation of SGNs. Indeed, developmental interactions between afferents and efferents are crucial for establishing appropriate wiring of both populations, which in turn underlies appropriate auditory circuit function. However, many details of both the mature function of OCNs in the cochlea and how they interact with and influence SGN wiring and synaptic development remain unclear.

Our understanding of the development and function of OCNs has been limited by an inability to selectively label or manipulate MOCs and LOCs independently of one another. Knowledge of OCN morphology and wiring patterns in the cochlea largely come from studies in the mature system, which can distinguish MOCs and LOCs based on their connectivity patterns. As such, very little is known about the morphological development of MOCs and LOCs, which could provide valuable insight into the role of OCNs in the development and refinement of cochlear neural circuitry. Single-cell RNA sequencing studies in our lab revealed new markers of OCNs, which we have leveraged here to assess the anatomical development of MOCs and LOCs. After identifying *Ret* as a marker of OCNs, we utilized a Ret-CreER mouse line to drive expression of a fluorescent reporter at different embryonic ages beginning at E9.5, when OCNs start to differentiate from neighboring facial branchial motor neurons. We found that recombination of Ret-CreER at E11.5 selectively labels MOCs, while recombination at E12.5 and later labels both MOCs and LOCs. With this genetic access to MOCs, we are tracking the early morphological development of MOC efferent fibers in the cochlea, assessing their trajectory, emergence and diversity of branching patterns, and details of their transient innervation of IHCs. This work, in combination with ongoing studies of the molecular identity of MOCs and LOCs, will advance our understanding of the development of the olivocochlear efferent system and its relationship with developing afferent circuitry.

PS 906

Robust Development of Auditory Brainstem Responses in Pups from Different Maternal Backgrounds Suggest Intrinsic Developmental Programs Control Hearing Onset in Wistar Rats.

Preethi Singh[1]; Jingyun Qiu[1]; Geng Pan[1]; Annalisa De Paolis[2]; Frances Champagne[3]; Jia Liu[4]; Luis Cardoso[2]; **Adrián Rodríguez-Contreras**[1]
[1]The City University of New York, City College, Biology Department; [2]The City University of New York, City College, Biomedical Engineering Department; [3]The University of Texas at Austin, Psychology Department; [4]The City University of New York, Advanced Science and Research Center, Neuroscience Initiative

In several mammalian species, including humans, maternal care is the main source of nutritional, social, and sensory stimulation that is important for survival and has the potential to impact the neurologic development of the offspring. In this study, we used a maternal selection

approach to test the hypothesis that differences in maternal care during the first week of life are associated with differences in the timing of hearing onset in Wistar rat pups. If the frequency of maternal LG correlates with the timing of hearing onset in the offspring, then pups within a litter would have an early or delayed hearing onset that correlates with the low-LG or high-LG phenotype of their mother. To test the possible association between maternal LG and sensory development in the progeny, we performed different tests, including auditory brainstem responses (ABRs), micro-CT X-ray tomography (micro-CT), and real time polymerase chain reaction (RT-PCR) to monitor neurodevelopmental changes in the progeny of low-LG and high-LG dams. Our results show that extreme LG phenotypes are not overtly associated with the timing of hearing onset in Wistar rat pups, or the expression of genes involved in neuronal, glial cell and vascular development in auditory brainstem and sensory cortex, challenging the hypothesis that differences in maternal care are involved in timing hearing onset and more generally in early pup development. However, the data confirms the existence of early and delayed auditory development that occurs within a two-day window in different litters. Furthermore, timing of hearing onset is correlated with increased variability in the timing of EO, which occurs during a two-day window after hearing onset. We propose that there is a within litter bias that is responsible for setting the limits of hearing onset and allows flexibility for regulation of other developmental landmarks such as eye opening which are associated with plasticity in the auditory cortex (Mowery et al. 2016. The onset of visual experience gates auditory cortex critical periods. Nat Commun 7, 10416).

PS 907

Spiral Ganglion Neurons with Distinct Preferred Frequency Response Employ Different Strategies to Innervate the Cochlear Nucleus

Chloe Borcean; Samiha Mohammed; Annie Parng; Hyun-Ju Yoon; Jennifer Scheffel; Darwin Gutierrez; Wei-Ming Yu
Department of Biology, Loyola University Chicago

To allow animals to separate a complex sound into its frequency components, the auditory system is organized in tonotopy; neurons at various levels of the auditory pathway are topographically arranged by their responses to different sound frequencies. Disruption of tonotopy often results in auditory processing disorders and language learning disabilities. Despite its importance in auditory functions and clinical implications, almost nothing is known about how the tonotopic map is established during development. In this study, we use genetic approaches to label spiral ganglion neurons (SGNs) and their auditory nerve fibers with different characteristic frequencies respectively. We found that functionally distinct SGN populations employ different cellular strategies to target and innervate neurons in the cochlear nucleus during tonotopic map formation. Auditory nerve fibers with high characteristic frequencies (high-CF fibers) initially overshoot and sample a large area of different targets before refining their connections to correct targets, while fibers with low characteristic frequencies (low-CF fibers) are more accurate in initial targeting and undergo minimal target sampling. Additionally, compared to the high-CF fibers, a higher proportion of low-CF fibers terminate on bushy cells with multiple branching and smaller Endbulb of Held synapses. These observations reveal the diversity of cellular mechanisms that functionally distinct auditory neurons use to pick their targets during tonotopic map formation.

PS 908

Complement Receptor Expression with Respect to Emerging Modular-Extramodular Framework of the Lateral Cortex of the Inferior Colliculus

Julianne B. Carroll; Jacob M. Weakly; Mark L. Gabriele
James Madison University

The lateral cortex of the inferior colliculus (LCIC) is a multimodal shell nucleus of the auditory midbrain which receives segregated somatosensory and auditory afferents. Its characteristic modular-extramodular organization develops during an early postnatal critical period, with somatosensory inputs targeting glutamic acid decarboxylase (GAD)-specific modules and auditory inputs surrounding calretinin (CR)-positive extramodular zones by postnatal day 12 (P12). Microglial cells (MGCs) have been implicated in the development and refinement of analogous discretely organized maps in a variety of other unimodal systems. One pathway implicated for initiating neuronal-glial interactions whereby exuberant or underutilized synapses are selectively tagged for elimination is the classical complement cascade. The present study examines the potential role of complement signaling in the developing LCIC, focusing on MGC-specific expression of the complement receptor, CR3. Immunostaining for CR3/CD11b was performed in GAD67-GFP and CX3CR1-GFP mice during a defined critical period for LCIC development (birth to P12). CD11b is a member of the integrin family necessary for forming the CR3 heterodimer. GAD67$^{+/GFP}$ mice facilitate easy visualization of emerging LCIC modular fields, while CX3CR1$^{+/GFP}$ mice highlight microglia expressing the fractalkine receptor (a known MGC marker). CR staining was also employed as a marker for LCIC extramodular domains. Z-stacks of coronal sections throughout the extent of the LCIC were acquired and analyzed using a Nikon Eclipse imaging system and

associated Nikon Elements software package. CD11b expression appears diffusely homogeneous throughout the LCIC at birth and up to P4. However, by P8 and P12, as LCIC compartments sharpen and multimodal afferent streams fully segregate, CD11b expression becomes concentrated to layer 2 modular fields. In CX3CR1$^{+/GFP}$ mice, CD11b labeling does not colocalize with GFP-labeled MGCs, suggesting that perhaps unique subsets of microglia exist in the nascent LCIC with different molecular signatures and responsibilities. Changing CR3/CD11b patterns in the developing LCIC hint towards complement signaling involvement in refining early LCIC multimodal connections. Ongoing experiments aim to correlate the temporal and spatial expression of upstream complement components, namely C1q and C3, with the described CR3 patterns during an early LCIC critical period.

Hair Cell Synaptic Transmission

PS 909

Using Spike-Triggered Average to Investigate the Response of Afferent Neurons in the Lateral Line System of Zebrafish

James C. Liao[1]; Otar Akanyeti[2]
[1]University of Florida, Whitney Lab for Marine Bioscience; [2]Aberystwyth University

We used spike-triggered average (STA) to estimate the linear receptive field of afferent neurons to a random, complex mechanical stimulus applied to neuromasts of the lateral line system in 5-7 dpf larval zebrafish. To compute the STA, the stimulus in the time window preceding each spike was extracted, and the resulting (spike-triggered) stimuli were averaged. This provided an unbiased estimate of a neuron's receptive field to our white-noise stimulus. Applying this approach to hair cells *in vivo* has been challenging, but we have now developed the ability for high-speed motion tracking of deflected kinocilia. Previous work has typically assumed that the motion commands to a stimulus would result in the same motion in the kinocilia, but this depends critically on the distance of the stimulator to the hair cell. We calculated the spike-triggered averages for several hundred trials and found a consistent response to our stimuli. Our work reveals new information about which mechanical deflection parameters of hair cell stimuli (position, velocity and acceleration) trigger afferent spiking.

PS 910

Modified Cochlear Surface Preparation in the Adult Mouse

Qiaojun Fang; **Shan Xu**; Fan Wu; Su-Hua Sha
Medical University of South Carolina

Background
Cochlear surface preparations, in combination with immunolabeling techniques and confocal imagery, are a very useful tool for the investigation of cochlear pathologies, including losses of ribbon synapses and sensory hair cells, changes in protein levels in hair cells and supporting cells, hair cell regeneration, and determination of report gene expression (i.e., GFP) for verification of successful transduction and identification of transduced cell types. However, the adult mouse cochlea is miniscule and the cochlear epithelium is encapsulated in a bony labyrinth, making microdissection difficult. Although dissection techniques have been developed and used in many laboratories, we have modified these techniques of microdissection of adult mouse cochlear surface preparations using cell and tissue adhesive to make the methods easier and more convenient.

Method
The inner ear of adult mice at any age can be used following fixation and decalcification. Before beginning dissection, check if the cochleae are decalcified by touching the bony vestibular portion with forceps to assess for elasticity. If the bone is elastic rather than firm, the cochlea is decalcified. Alternatively, cut a small piece from the edge of the vestibular portion. If this results in crushed bone, the cochlea is not decalcified. After the cochlea is decalcified, dissect the entire cochlear epithelium into four pieces (apex, middle, base, and hook regions) and then adhere them to a 10-mm round coverslip for immunolabeling or immunohistochemistry in a four-well dish.

Results
With this technique, in combination with immunolabeling for CtBP2 (a marker for presynaptic ribbons) and GluA2 (a marker for post synaptic terminals), it is possible to count IHC/auditory nerve synapses using confocal images under Z projections with 0.25-µm intervals, based on the size of mouse ribbon synapses. This is consistent with published results. By immunolabeling surface preparations with different antibodies, assessment of molecular signaling and structure in sensory hair cells is possible. There was no difference in immunoreactions or uniformity with and without the cell and tissue adhesive. Using different fixatives, surface preparations have provided the basis for scanning electron microscopy (SEM) images for visualization of cochlear stereocilia.

Conclusion
Cochlear microdissection of whole-mount surface preparations in combination with immunolabeling provides a basic tool for investigation of inner ear pathologies and molecular mechanisms. This modified adult mouse cochlear dissection method using cell and tissue adhesive facilitates immunohistochemical labeling while avoiding tissue loss during the multiple washing steps.

Acknowledgements
The research project described was supported by the grant R01 DC009222 from the National Institute on Deafness and Other Communication Disorders, National Institutes of Health.

PS 911

Restoration of Hearing and Synapses in Tmc Mutant Mice Using Virally Mediated Gene Therapy

John Lee[1]; Carl Nist-Lund[1]; Gwenaelle S. Geleoc[1]; Jeffrey R. Holt[2]
[1]Boston Children's Hospital & Harvard Medical School; [2]Department of Otolaryngology, F.M. Kirby Neurobiology Center, Boston Children's Hospital and Harvard Medical School

TMC1 and TMC2 form sensory transduction channels in auditory and vestibular hair cells. Mice with targeted deletion of *Tmc1 (Tmc1Δ)* are deaf, while those without *Tmc2 (Tmc2Δ)* are phenotypically normal. Mice lacking both *(Tmc1Δ;Tmc2Δ)* lack sensory transduction, and exhibit deafness and vestibular dysfunction. While hair bundle function and hair cell survival have been assessed in *Tmc* mutant mice, consequences of absent and/or impaired sensory transduction on ribbon synapses have not been examined. We found *Tmc1Δ* and *Tmc1Δ;Tmc2Δ* mice have abnormal synapse counts relative to WT mice, suggesting a role for sensory transduction in the development and maintenance of synapses.

Exogenous expression of *Tmc1* via AAV-mediated gene therapy has been utilized as a biologic strategy for restoring sensory transduction, promoting hair cell survival, and improving auditory function (i.e. improved ABR thresholds) in *Tmc1Δ* mice. However, consequences of gene therapy on ribbon synapses have not been assessed.

The purpose of this study was to determine if synaptic recovery is evident in *Tmc1Δ* mice following gene therapy. Characterizing synaptic consequences of restoring sensory transduction via gene therapy will enhance our understanding of mechanisms underlying synapse maintenance and inform continued development of gene therapy strategies for hearing loss

Cochlea from wild-type, *Tmc1Δ, Tmc2Δ, Tmc1Δ;Tmc2Δ*, and *Tmc1Δ* mice injected with AAV-*Tmc*1 were harvested at various time points (P7, P10, P14, P21, P28) and immunostained with antibodies to C-terminal binding protein 2, glutamate receptor GluA2, and myosin7a. Each cochlea was microdissected and frequency maps were generated using apex-to-base length measurements. Confocal z-stacks of the 8.0, 11.3, 16.0, 22.6, and 32.0kHz cochlear regions were obtained. Imaris imaging software was used to generate 3-D projections, count average synapse numbers, and estimate synapse volumes. *Tmc1Δ* mice were injected intracochlearly at P1 with PhPB-CMV-Tmc1 and ABR thresholds to 8, 11.3, 16, 22.6, and 32kHz pure tone stimuli were obtained at P28.

Injected *Tmc1Δ* mice demonstrated increased synapse counts and ABR threshold recovery relative to noninjected mice. The degree of ABR threshold recovery correlated with synapse recovery. Injected *Tmc1Δ* mice with significant ABR recovery had more synapses than mice with mild ABR recovery.

Differences in IHC ribbon synapses observed in *Tmc* mutant mice suggest sensory transduction is required for development and maintenance of cochlear synapses. *Tmc1Δ* mice injected with viral vectors demonstrated recovery of both hearing sensitivity and synapse numbers.

PS 912

In Vestibular Type I Hair Cells, Permeation Through the Basolateral Potassium Conductance, GK(LV), is Regulated by Interactions Between the Selectivity Filter and External Monovalent and Divalent Ions

Donatella Contini[1]; Gay R. Holstein[2]; **Jonathan Art**[1]
[1]University of Illinois College of Medicine; [2]Icahn School of Medicine at Mount Sinai

Traditionally, permeation through ion channels has been understood in terms of gating and selectivity of the channel pore region. In the standard model, allosteric coupling between mechanical or electrical forces, and/or ligand binding to the channel protein gates the channel, allowing ions to pass between the intracellular and extracellular spaces. In such a model, selectivity is imparted at the external aspect of the pore by steric hindrance at points where shells of hydration are stripped from the ion and transit is permitted by the sequential interaction of the ion with carbonyl oxygens lining the pore. Internal block of permeation by divalent ions or amino acids can result in inward or anomalous rectification, with inward current that relieves the block flowing unimpeded, while outward current may increase the block in a voltage-dependent manner. Similarly, permeation can be blocked by actions at the N- and C-termini of the channel. Specifically, in

many potassium channels motion of the free amino terminus partially occludes the channel and gives rise to N-type inactivation, while interactions distorting the external mouth of the pore generate C-type inactivation that is sensitive to external monovalent and divalent cations, with Ca^{2+} increasing and K^+ slowing the rate of inactivation or deactivation.

We have used simultaneous dual recordings from type I hair cells and their calyx afferents in the central region of the turtle semicircular canal crista to examine the effects of ion accumulation in the synaptic cleft on the major basolateral hair cell conductance, $G_{K(LV)}$. Comparison of the available conductance from holding potentials of -100 mV and -70 mV suggests that as much as 75% of the total $G_{K(LV)}$ may be inactivated at the more depolarized potential. Moreover, elevation of $[K^+]_o$ slows the inactivation and deactivation of the conductance, decreasing the steady-state rectification of the I-V curve, while chelation of $[Ca^{2+}]_o$ linearizes the curve depolarized from -100 mV. These results are consistent with a model in which the $G_{K(LV)}$ is largely open when depolarized to -100 mV, and inactivated by external divalent binding near the selectivity filter. This inactivation can be relieved by elevation of $[K^+]_o$, suggesting that the amount of $G_{K(LV)}$ available near the resting potential is a dynamic property of ion accumulation associated with hair cell depolarization and vesicle fusion. In this model, the majority of outward rectification is imparted by the balance of $[K^+]_o$ and $[Ca^{2+}]_o$ in the synaptic cleft.

PS 913

Synaptic Transmission Between Type I Hair Cells and Calyx Afferents is Multiplexed on Three Time Scales by Ion Accumulation, Quanta, and Resistive Coupling

Donatella Contini[1]; Gay R. Holstein[2]; Jonathan Art[1]
[1]University of Illinois College of Medicine; [2]Icahn School of Medicine at Mount Sinai

Due to the large apposition between type I hair cells and their calyx afferents, glutamatergic quantal transmission between them in the central region of turtle vestibular semicircular canal cristae is augmented and multiplexed on three time scales. The slowest mode of transmission is potassium ion accumulation in the cleft. This serves as a bidirectional mechanism by which both hair cell and afferent are depolarized to potentials that allow rapid vesicle fusion and the potential for large excitatory postsynaptic potentials to trigger action potentials, APs. Given the volume of the cleft, we estimate that changes in ion concentration occur over tens of milliseconds and reflect a relatively low-pass filtering of recent activity. The second and more intermediate speed of transmission, with millisecond packets of transmitter, is the conventional glutamatergic quantal transmission that was observed in all cases where the hair cell was depolarized to potentials necessary for calcium influx and vesicle fusion. With the afferent resting at potentials slightly hyperpolarized to that necessary for AP generation, information would be rapidly and faithfully communicated across the synapse if the first quantum released by depolarization generates an AP in the afferent. The unexpected third form of synaptic transmission is the most rapid, and results from the large potassium-sensitive basolateral hair cell conductances and the inner-face calyx conductances that are present at their resting potentials. Like ion accumulation, this is bidirectional transmission, and a current flowing out of either hair cell or afferent at the synapse will divide between a fraction flowing in the intercellular cleft and out into the bath, and a fraction flowing across the cleft into its cellular partner, without the need for permanent electrical coupling via conventional gap junctions. This mode of transmission may potentially occur within tens to hundreds of microseconds since current division requires no changes in cellular potential. Moreover, the amplitude of the dynamic coupling between the hair cell low-voltage potassium conductance, $G_{K(LV)}$, and the mixed afferent conductance, G_{HCN}, would be greatest under conditions in which the potassium concentration in the cleft, $[K^+]_{cleft}$, is elevated the most.

PS 914

Modeling Non-Quantal Transmission at the Calyceal Synapse Between Type I Hair Cells and Vestibular Afferents

Aravind Chenrayan Govindaraju[1]; Imran Quraishi[2]; Anna Lysakowski[3]; Ruth Anne Eatock[4]; Robert M. Raphael[1]
[1]Rice University; [2]Yale University; [3]University of Illinois at Chicago; [4]University of Chicago

In vestibular sensory epithelia of amniotes, afferent neurons form large cup-shaped synaptic terminals (calyces) on type I hair cells and small bouton terminals on type II hair cells. Type I hair cells transmit to calyces by both **quantal (Q)** release of glutamate from vesicles and **non-quantal (NQ)** flow of ions from the hair cell into the synaptic cleft and the postsynaptic calyx. Details of this complex transmission remain unknown, and the relevant compartments (cells and synaptic cleft) are hard to access, hindering the measurement of ion concentrations and electric potentials. As a complementary approach, **we are developing a mathematical model of the vestibular hair cell-calyx synapse (VHCC model) with the goal of predicting and accounting for both Q and NQ transmission modes and their interactions.**

The VHCC model is implemented as a 2D axisymmetric parametric surface in COMSOL with dimensions of hair cell and calyx geometry taken from electron micrographs. It incorporates ion channels (MET, HCN, KV, CaV, NaV; based on immunocytochemical and whole-cell recording results) and ion pumps (Na-K ATPase, KCC) at appropriate locations and surface densities on hair cell and calyx membranes. The model uses measured or estimated values for membrane capacitance and properties of ion channels, including two types critical for NQ transmission: the distinctive low-voltage-activated channels of type I hair cells (gK,L) and postsynaptic HCN channels (Contini et al. J Physiol 595:777, 2017). The input to the model is a step or sinusoidal deflection of the hair bundle. To model the dynamic behavior of the system, the VHCC model uses expressions for K+ and Na+ electrodiffusion in the cleft, simplified Hodgkin-Huxley-style ion currents based on whole-cell recordings, stochastic vesicle release, and the cable equation for voltage change along the hair cell membrane and the afferent fiber. The VHCC model can mimic firing patterns found in experimental voltage and current recordings. Model simulations confirm that removing either HCN channels or gK,L blocks NQ transmission and predict spatio-temporal gradients in K+ and Na+ within the synaptic cleft and a voltage gradient from the apex to base of the hair cell. Manipulations that increase maximal KCC-mediated K+ flow out of the synaptic cleft or reduce the calyx to the size of bouton terminals reduce cleft K+ accumulation, NQ transmission, and afferent spike rate. Thus, the VHCC model supports findings and hypotheses implicating gK,L and gHCN, K+ accumulation in the cleft, and calyx morphology as factors in NQ transmission.

NIH-NIDCD-R01DC012347

PS 915

STORM Imaging Reveals Calcium Nanodomains in Proximity to BK Channels in Hair Cells of the Mouse and Chick

Na Xue[1]; Omolara Lawal[1]; Junping Bai[1]; Joseph Santos-Sacchi[2]; Dhasakumar Navaratnam[3]
[1]Yale University; [2]Surgery (Otolaryngology), Yale; [3]Neurology, Yale

BK channels are found in hair cells of vertebrates where they serve many roles. These channels are unusual in that their voltage of activation is significantly shifted in a hyperpolarizing direction by a rise in intracellular calcium. In mammalian inner hair cells (IHC), BK channels contribute the most to its outward current and are critical for determining its resting membrane potential. In outer hair cells (OHCs), these channels serve a similar role and lie in proximity to nicotinic receptors at the base of the cell near efferent synapses. In chick hair cells, BK channels interact with closeby voltage-gated calcium channels and cause electrical resonance.

In mammalian IHCs, there is conflicting data on the role of calcium in BK channel activation. Using superresolution microscopy, we determine that calcium-induced calcium release (CICR) likely plays a role in activation of these channels. We determine that BK channels at the base of IHCs are in close proximity to IP3 and ryanodine receptors. BK channels that lie at the neck of IHCs in a ring like pattern have a differential association with IP3 and ryanodine receptors depending on its neural or abneural location. Channels at the neural side of the cell, like thos at the base of the cell, are associated with IP3 and ryanodine receptos. In contrast, BK channels at the abneural side of the cell are not associated with either IP3 or ryanodine receptors.

In mammalian OHCs, clusters of BK channels at its base are located in close proximity to IP3 and ryanodine receptors. These data confirm the role of the synaptic cistern in OHCs, and serve to activate these channels likely through CICR.

In chicken hair cells prior data have shown the close approximation of BK channels with voltage-gated calcium channels. We determine that both IP3 and ryanodine receptors to be expressed in proximity to BK channels at the base of these cells. Together, these data implicate CICR as playing an important role in these hair cells function. We present electrophysiological data, supporting STORM data, that BK channels are affected by CICR.

In conclusion, our findings support the role of CICR in hair cell function. We show proximate expression of both IP3 and ryanodine receptors with BK channels. We also provide electrophysiological evidence for CICR in BK channel function in chicken hair cells. Given its localization at the base of hair cells our data would implicate CICR in synaptic vesicle release.

PS 916

Cell-specific Quantification of Ion Channel Transcription upon Cochlea-Specific Ablation of Cav1.3 Calcium Channels

Stephanie Eckrich; Friederike Stephani; Jutta Engel
Saarland University, Department of Biophysics and CIPMM, Homburg, Germany

$Ca_v1.3$ voltage-gated Ca^{2+} channels are crucial for the function of inner hair cells (IHCs). In mature IHCs, stimulus-induced Ca^{2+} currents elicit transmitter release.

In pre-mature IHCs, Ca^{2+} action potentials relying on $Ca_v1.3$ channels drive their terminal differentiation, including expression of BK potassium channels, which mark the onset of hearing around postnatal day 12 in mice. In IHCs of deaf systemic $Ca_v1.3\beta^{/}\beta$ mice, BK channels are missing in the apical[1,2] and are sparsely expressed in the basal cochlear turn[3]. Real-time PCR of whole $Ca_v1.3\beta^{/}\beta$ cochleae revealed reduced levels of *Kcnma1* mRNA, encoding BK[2]. In Pax2::Cre;$Ca_v1.3^{flex/}\beta$ mice, the cochlea-specific embryonic ablation of $Ca_v1.3$ channels produces a $Ca_v1.3\beta^{/}\beta$-like phenotype including lack of BK channel expression in around 90% of their IHCs[3]. Recombination of *loxP* sites fails in the remaining 10% of IHCs, which are therefore $Ca_v1.3$-positive but flanked by $Ca_v1.3$-deficient IHCs. Notably, these IHCs show impaired BK channel expression compared to $Ca_v1.3^{flex/}\beta$ controls (i.e. without Cre)[3], suggesting that BK channel up-regulation requires not only the expression of $Ca_v1.3$ in the IHC itself but also in neighboring IHCs. *In situ* labeling of mRNA transcripts by RNAscope allows quantitative analysis of multiple genes on a cellular basis. Here, we used probes detecting *Kcnma1* and *Cacna1d*, encoding $Ca_v1.3$ channels, on apical cochlear turns of 4 week-old Pax2::Cre;$Ca_v1.3^{flex/}\beta$ mice (conditional knockout; cko-$Ca_v1.3^{flex/}\beta$) and littermate $Ca_v1.3^{flex/}\beta$ controls. *Cacna1d*-probes recognized both, the intact transcript of the *Cacna1d-flex* construct in control as well as its truncated form in cko-IHCs. The amount of *Cacna1d-flex* mRNA did not differ between cko- and control IHCs. In cko-$Ca_v1.3^{flex/}\beta$ mice, a subset of the truncated *Cacna1d* mRNA clustered in the nuclei of IHCs. However, the abundance of *Kcnma1* mRNA was reduced by a third in cko-IHCs. Further analysis will be performed to shed light on the reduction of BK channel expression in individual $Ca_v1.3$-expressing IHCs present in the otherwise $Ca_v1.3$-deficient cochlea of cko-$Ca_v1.3^{flex/}\beta$ mice. Additionally, wildtype and systemic $Ca_v1.3\beta^{/}\beta$ mice will be used to elucidate *i)* if the intact *Cacna1d-flex* construct affects the abundance of *Cacna1d* mRNA and *ii)* the cause of the accumulation of *Cacna1d-flex* mRNA in IHC nuclei. Funded by CRC894, DFG-project EC488/1-1 (to S.E.) and Saarland University.

References

[1]Brandt et al. (2003) J Neurosci [2]Nemzou et al. (2006) Neurosci [3]Eckrich et al. (2019) Front Cell Neurosci

PS 917

High Extracellular K+ Causes Ribbon Synapse Degeneration in the Inner Hair Cells

Hong-Bo Zhao; Yan Zhu; Li-Man Liu
Dept. of Otlaryngology, University of Kentucky Medical Center

Background

Recent studies demonstrated that ribbon synapses between inner hair cells (IHCs) and auditory nerves (ANs) can be damaged by noise and other factors leading to hidden hearing loss (HHL). However, the underlying mechanism remains unclear. It has been hypothesized that the cochlear synaptopathy may result from excitotoxicity of glutamate, which is a major neurotransmitter of the ribbon synapse between IHCs and ANs. However, despite substantial terminal swelling following perfusion of glutamate receptor (GluR) agonists, the presynaptic and postsynaptic components remained intact, indicating other mechanisms may play a critical role in the ribbon synapse degeneration. Noise exposure can cause hair cell and spiral ganglion neuron excessive excitation releasing more K^+ to increase extracellular K^+ concentration. In this study, we examined whether high extracellular K^+ can cause ribbon synapse degeneration.

Methods

Mouse cochlea was incubated with high-K^+ (5-50 mM) extracellular solutions for 2 hr and another cochlea was simultaneously incubated in normal extracellular solution as control. Ribbon synapses were examined by immunofluorescent staining for CtBP2. The ribbon synapses under IHCs and outer hair cells (OHCs) were quantified under confocal microscopy.

Results

Elevation of extracellular K^+ could cause IHC ribbon swelling and degeneration in a dose-dependent manner, similar to noise-induced ribbon synapse degeneration. The ribbon degeneration was increased as K^+ concentration was increased. The ribbon degeneration could be attenuated by K^+ or Ca^{2+} channel blockers. However, glutamate GluR agonists could cause ribbon swelling but not degeneration. Application of GluR antagonist CNQX also had no effect on ribbon degeneration. Finally, similar to noise-induced ribbon degeneration in the cochlea, K^+ only caused IHC ribbon degeneration but not outer hair cell ribbon degeneration.

Conclusions

These data indicate that K^+ rather glutamate excitotoxicity cause ribbon synapse degeneration in noise-induced cochlear synaptopathy in HHL.

Supported by NIH R01 DC 017025

PS 918

Age-Related Structural and Functional Changes at Auditory Hair Cell Ribbon Synapses

Thibault Peineau[1]; Séverin BELLEUDY[1]; Yohan Bouleau[1]; Didier Dulon[2]
[1]Bordeaux University; [2]INSERM

Hearing relies on faithful synaptic transmission at the afferent ribbon synapses contacting the cochlear inner hair cells (IHCs). At these glutamatergic synapses, IHCs have a unique presynaptic organelle, the synaptic ribbon, which is essential for aggregating synaptic vesicles and organizing Ca^{2+} channels at the active zone. The morphological and functional changes occurring in the IHC synaptic ribbons during aging are not fully understood. Here, we characterized the age-related changes in the IHC synaptic ribbons of C57BL/6J mice, a strain which is known to carry a cadherin23 mutation and experiences early hearing loss with age. In these mice, we found a progressive decrease in the number of ribbons and afferent fibers per IHCs with aging, starting at postnatal day 30 (P30) and reaching up to 50 % loss in middle age mice at P365. The size of the ribbons became larger to reach a nearly three-fold volume increase at P360 while IHCs' size displayed a 30% reduction with a decrease in BK-channel expression. Whole-cell patch-clamp recordings of old P365 IHCs indicated an increase in Ca^{2+}-channel density and a stronger exocytosis per ribbon, which may explain recruitment (hyperacousis) in humans with aging.

A deletion of the *Otof* gene, encoding otoferlin, a hair cell specific excytotic Ca^{2+} sensor, produced an accelerated loss of IHC ribbons with aging in C57BL/6/6J mice, with a 50 % loss by P60. The ribbons also become larger with aging, but with the particularity to have a compact spatial distribution at the IHC synaptic basal plasma membrane, where F-actin was found disrupted. Taken together, these results suggested that cadherin23 and otoferlin are important for the maintenance of the synaptic ribbons, in particular for the small ones which are known to be associated with the postsynaptic afferent auditory nerve fibers having high spontaneous firing rate and encoding low-threshold sound intensity.

Acknowledgments
Fondation pour l'Audition and Entendre SAS

PS 919

Effects of Acoustic Trauma on Neurotransmitter Release by Inner Hair Cells

Luis E. Boero[1]; Shelby Payne[2]; **Eugenia Gómez-Casati**[1]; Mark Rutherford[3]; Juan Goutman[4]
[1]Instituto de Farmacología, Facultad de Medicina, Universidad de Buenos Aires; [2]Department of Otolaryngology - Head & Neck Surgery, Washington University School of Medicine; [3]Department of Otolaryngology-Head & Neck Surgery, Washington University; [4]INGEBI - CONICET

Noise exposure has gained relevance as one of the most important sources of hearing loss. The underlying causes of this condition have been investigated over years at histological and morphological levels, with much less progress in the physiological aspects. It has been demonstrated that acoustic trauma (AT) produces long-term structural damages to the inner ear, such as a reduction in the number synapses between inner hair cells (IHCs) and afferent neurons. Here we intend to address if the capacity of IHCs to release neurotransmitter is altered after noise exposure.

Mice of either sex at ages P15-P16 (C57BL/6J *VGluT3* KO or WT) were exposed to 1-12 kHz noise at 120 dB SPL, for 1 hour in a reverberant acoustic chamber. Hearing function was assessed before, one day after and two weeks after noise exposure through auditory brainstem responses (ABRs) and distortion product otoacoustic emissions (DPOAE). Ca^{2+} currents and changes in membrane capacitance (ΔCm) were recorded in whole-cell patch clamp configuration from IHCs one day after exposure. Post-exposure afferent synaptopathy was quantified by whole-mount immunostaining for CtBP2 –the major component of the synaptic ribbon-, GluA3 –a postsynaptic AMPA receptor subunit- and CaV1.3, to see the synaptic coupling to calcium entry.

IHCs from either exposed (1 day after trauma) or unexposed mice were recorded, and the voltage dependence of release was investigated with short depolarizing pulses. Larger ΔCm jumps were observed in exposed IHC compared to controls (20.2±3.2 fF and 12.4±1.8 fF, respectively at -30 mV pulse). However, Ca^{2+} currents did not show any difference between exposed and control mice at these voltages. In addition, exposed IHC showed augmented ΔCm specially with pulses above 100 ms (for 1s pulse: 104.5±7.1 fF for control, 167.7±22.6 fF for exposed). No differences in calcium entry between exposed and control cells were observed for any duration of depolarization. During AT protocol, IHC suffers a big Ca^{2+} influx and also releases large amounts of glutamate (which could act retrogradely). To determine which of these two is responsible for the potentiated release, we made use of the vesicular glutamate transporter *vGluT3* knock-out (KO) mouse. In contrast to what was observed in WT mice, exposed KO showed reduced ΔCm compared to controls.

These results suggest that noise exposure potentiated vesicle release in IHC, possibly by accelerating vesicle

recruitment, and this phenomenon would be dependent upon the intense glutamate release produced during AT.

PS 920

Characterization Of HA-Tagged Î±9 And Î±10 nAChRs In The Mouse Cochlea

Pankhuri Vyas[1]; Adam Goldring[1]; Megan B. Wood[2]; Yuan-Yuan Zhang[1]; Paul Fuchs[3]; Hakim Hiel[1]
[1]Johns Hopkins University School of Medicine; [2]Johns Hopkins University School of Medicine; [3]the Center for Hearing and Balance, Johns Hopkins University School of Medicine

Neurons of the medial olivary complex (MOC) inhibit cochlear hair cells through the activation of β9β10-containing nAChRs. Efforts to study the localization of these proteins have been hampered by the absence of reliable antibodies. Thus, a CRISPR-Cas9 approach was used to attach a hemagglutinin tag (HA) to the C-terminus of mouse β9 and β10 proteins. Immunodetection of the HA tag in the adult organ of Corti of these β9HA mice revealed strong immunolabeling clustered at the synaptic pole of OHCs. The clustered HA signal was juxtaposed with choline acetyltransferase immunolabeling of the medial olivocochlear efferent terminals. This immunolabeling pattern was observed in both homozygous (mt/mt) and heterozygous (mt/wt) β9HA mice. The wild type organ of Corti (wt/wt) showed no immuno-signal for HA. The expression of β9HA was examined in both pre-hearing (P7) and hearing (P25-45) mice. As previously established by *in situ* hybridization studies, β9-containing AChRs are expressed by IHCs of prehearing mice (P7). Immunopuncta of β9HA were smaller in size and confined to the synaptic pole of IHCs. In hearing mice (P30-45) β9HA immunolabeling was limited to the efferent contact area of OHCs but IHCs showed no β9HA labeling. It is worth noting that in addition to the a9HA synaptic clusters OHCs showed a light diffuse signal throughout their cytoplasm. Both heterozygous and homozygous β9HA mice had auditory brainstem responses (ABRs) not significantly different from those of wildtype littermates. Application of ACh evoked membrane current in hair cells in cochlear explants from homozygous and heterozygous β9HA mice.

Similarly, β10HA immunolabeling was restricted to the efferent contact area of OHCs in mature knock-in mice (P25-P45) and absent from wildtype mice. The present work describes animal models that will facilitate efforts to study the role of the β9β10 nAChR in cochlear development, aging and after acoustic trauma.

Acknowledgements: Supported by NIDCD R01 DC001508 and R01 DC015309, the David M. Rubenstein Fund for Hearing Research and the John E. Bordley Professorship.

Hair Cells

PS 921

Deletion of Mtu1 (Trmu) in zebrafish revealed the essential role of tRNA modification in mitochondrial biogenesis and hearing function.

Qinghai Zhang[1]; **Min-Xin Guan**[2]
[1]Zhejiang University; [2]Zhejiang Unviersity

Mtu1(Trmu) is a highly conserved tRNA modifying enzyme responsible for the biosynthesis of βm5s2U at the wobble position of tRNAGln, tRNAGlu and tRNALys. Our previous investigations showed that MTU1 mutation modulated the phenotypic manifestation of deafness-associated mitochondrial 12S rRNA mutation. However, the pathophysiology of MTU1 deficiency remains poorly understood. Using the mtu1 knock-out zebrafish generated by CRISPR/Cas9 system, we demonstrated the abolished 2-thiouridine modification of U34 of mitochondrial tRNALys, tRNAGlu and tRNAGln in the mtu1 knock-out zebrafish. The elimination of this post-transcriptional modification mediated mitochondrial tRNA metabolisms, causing the global decreases in the levels of mitochondrial tRNAs. The aberrant mitochondrial tRNA metabolisms led to the impairment of mitochondrial translation, respiratory deficiencies and reductions of mitochondrial ATP production. These mitochondria dysfunctions caused the defects in hearing organs. Strikingly, mtu1-/- mutant zebrafish displayed the abnormal startle response and swimming behaviors, significant decreases in the sizes of saccular otolith and numbers of hair cells in the auditory and vestibular organs. Furthermore, mtu1-/- mutant zebrafish exhibited the significant reductions in the hair bundle densities in utricle, saccule and lagena. Therefore, our findings may provide new insights into the pathophysiology of deafness, which was manifested by the deficient modifications at wobble position of mitochondrial tRNAs.

PS 922

SBF-SEM Reveals a Unique, Networked Mitochondrial Phenotype in Hair Cells of the Zebrafish Lateral Line

Andrea L. McQuate; David W. Raible
University of Washington

Mitochondria are implicated in many types of hearing impairments, including those brought on by age, noise exposure, and heritable disorders. In hair cells of the inner ear, mitochondria produce the bulk of the ATP used by the cell, and buffer calcium during

mechanotransduction. Yet little is known about hair cell mitochondrial morphology, or whether disruption of that morphology is detrimental to hair cells and can result in hearing loss. We use the zebrafish lateral line as a model for inner ear hair cells. Using serial block-face scanning electron microscopy (SBF-SEM), we have found that neuromast hair cells have a stereotyped number of mitochondria. The largest mitochondrion in hair cells is highly networked, on average 5 standard deviations from the mean mitochondrial volume, and roughly 20% of the total mitochondrial volume. In contrast, supporting cell mitochondria are relatively homogenous and do not contain networks. This suggests the networked mitochondrial morphology is hair cell specific. To determine the role of mitochondrial fusion in hair cell mitochondrial network formation, we generated a mutant for the gene *opa1*, implicated in both hearing loss and blindness, and involved in the fusion of the inner mitochondrial membrane. Hair cells from *opa1* mutants demonstrate a fragmented mitochondrial phenotype. SBF-SEM reveals that *opa1* mutant hair cells have similar total mitochondrial volume to WT hair cells. However, these cells demonstrate reduced mitochondrial membrane potential, disrupted mitochondrial-ER contacts, and abnormal calcium handling during mechanotransduction. These results suggest the networked mitochondrial morphology of hair cells might play a distinct role in their function.

PS 923

Using Zebrafish to Understand the Role and Subcellular Localization of Gap Junctions In Vivo

Alisha Beirl; Katie Kindt
National Institute on Deafness and other Communication Disorders

Background

For proper hearing and balance, sensory hair cells are critical for the detection of sensory information. Glia-like supporting cells surround hair cells and are thought to be important for hair-cell development, function and maintenance. Within hair-cell epithelia supporting cells are electrically-coupled via gap junctions. Gap junctions are made up of connexin subunits that form intercellular channels that facilitate the bidirectional passage of ions and small molecules between cells. In mammals, several gap junctions have been implicated in hearing loss including: CX26 *(GJB6)*, Cx30 (*GJB6*), Cx29 (*GJC3*), Cx31 (*GJB3*), and Cx43 (*GJA1*). In certain human populations mutations in CX26 are responsible for up to 50% of non-syndromic hearing loss. Currently the roles gap junctions play in hearing and balance are not fully understood. Our work seeks to use zebrafish to develop an in vivo model to understand the role gap junctions play in hearing and balance.

Methods

For our studies we are using CRISPR-Cas9 methods to generate mutants in: *cx27.5, cx30.3, cx35.4 and cx43.4*. We assess inner-ear function using a startle assay. To visualize the subcellular localization of connexins we have created transgenic zebrafish that express a GFP-tagged Cx35.4 fusion protein in supporting cells. Using a similar approach, we created a transgenic line that expresses a dominant negative version of cx35.4 (R75W) in supporting cells. This mutation has been shown to cause hearing loss in humans and mice.

Results and Conclusion

Previous work and homology data suggest zebrafish Cx27.5, Cx30.3 and Cx35.4 are the closest homologues to mammalian CX26 and CX30 (Chang-Chien et al., 2014). We have found that triple homozygous mutants with lesions in *cx27.5, cx30.3* and *cx35.4* exhibit a startle response that is indistinguishable from wildtype larvae. Immunohistochemistry analysis reveals that synapse and hair-cell number and morphology are unaffected in triple mutants. A recent transcriptomic profiling study using RNA-Seq revealed just two connexins: Cx35.4and Cx43.4 are highly expressed in supporting cells of the zebrafish lateral line (Lush et al., 2019). Based on this work we are creating double mutants deficient in *cx35.4* and *cx43.4*. In addition, we have examined the localization of a Cx35.4-GFP fusion protein in supporting cells. Cx35.4-GFP fusion localizes to junctions between supporting cells of the zebrafish lateral line. Currently we are testing what effect a dominant negative version of Cx35.4 (R75W) has when expressed in supporting cells. Overall this work will generate a new in vivo model to investigate the role gap junctions play in hearing and balance.

PS 924

Characterization & gene therapy of the hearing impairment for 2 clarin genes variably affecting the auditory hair cells

Aziz El-Amraoui[1]; Lucy A DUNBAR[2]; Pranav Patni[1]; Sedigheh Delmaghani[1]; Carlos Aguilar[2]; Sandrine VITRY[1]; Andrew Parker[2]; Maureen WENTLING[1]; Sylvie Nouaille[1]; Andrea Lelli[1]; Christine Petit[1]; Sally Dawson*[3]; Walter Marcotti[4]; Steve Brown[5]; Michael Bowl[6]
*[1]Institut Pasteur, Paris; [2]MRC Harwell; [3]University College London; *equal contribution; [4]University of Sheffield, UK; [5]MRC Harwell Institute, Harwell, UK; [6]Mammalian Genetics Unit, MRC Harwell Institute*

Characterization & gene therapy of the hearing impairment for 2 clarin genes variably affecting the auditory hair cells

Aziz El-Amraoui[1], Lucy A Dunbar[2], Pranav Patni[1], Sedigheh Delmaghani[1], Carlos Aguilar[2], Sandrine

Vitry[1], Andrew Parker[2], Maureen Wentling[1], Sylvie Nouaille[1], Andrea Lelli[3], Christine Petit[3], Sally Dawson[4], Walter Marcotti[5], Steve DM Brown[2], Michael R Bowl[2]
[1]*Progressif Sensory Disorders, Institut Pasteur, INSERM UMRS1120, Sorbonne Universités, 25 rue Dr Roux, Paris 75015, France*
[2]*Mammalian Genetics Unit, MRC Harwell Institute, Harwell Campus, OX11 0RD, UK*
[3]*Génétique et Physiologie de l'Audition, Institut Pasteur, INSERM UMRS1120, Collège de France.*
[4]*UCL Ear Institute, University College London, UK*
[5]*Department of Biomedical Science, University of Sheffield, UK*

Background & Aim
While tremendous progress has been made regarding the mechanisms of congenital and early-onset hearing loss, we currently know very little about the key hearing pathways critical in progressive and late-onset hearing impairments. Recently, we have been investigating the role of clarin-1 in the auditory system, a tetraspan-like glycoprotein that is essential for post-lingual hearing and sight in humans. Clarin-1 belong to the clarin protein family consisting of three paralogous proteins sharing the same modular organization (4 transmembrane domains and a C-terminal class-II PDZ binding motif). In a recent mutagenesis screen undertaken at MRC Harwell, *Clrn2* was identified as a novel deafness gene with mutant mice exhibiting hearing loss due to a truncating mutation within the encoded clarin-2 protein (Trp4Stop), the line was named *Clrn2*^{clarinet}.

Methods
Utilizing *Clrn1*$^{-}$, *Clrn2*^{clarinet} & additional clarin mouse models, we bring together a wide spectrum of molecular and cellular, imaging, and physiological studies to elucidate the requirement of this protein family for the functioning of the inner ear, along with assessing the potential of viral-mediated *Clrn* gene expression to prevent and/or correct hearing deterioration.

Results
Our studies show that, similar to clarin-1, clarin-2 is targeted to the hair-bundle stereocilia. Longitudinal functional studies show that lack of clarin-2 leads to a rapid progressive moderate-to-profound hearing loss. Utilizing UK biobank, an association is found between *CLRN2* variants and adult hearing difficulties in humans. While absence of clarin-2 does not affect the normal formation, patterning or shaping of the auditory hair bundles, the shorter 'mechanotransducing' stereocilia later progressively regress at terminal differentiation stages. Recordings of mechanoelectrical transduction (MET) responses in *Clrn1*$^{-/-}$ and *Clrn2*$^{clarinet/clarinet}$ mice at postnatal day 7 reveals that lack of either protein results in a similar reduction in maximal MET currents. However, unlike *Clrn1*$^{-/-}$ mice, which display a 30% loss of spiral ganglion neurons, clarin-2 have a normal complement of neurons.

Conclusion
Together, our findings support a model where clarin-1 & clarin-2 both play key, but non-redundant, roles in the hair bundle, mediating mechanoelectrical transduction. Furthermore, our findings suggest that clarin-1, but not clarin-2, plays an essential organizer role at the hair cell synaptic region. Using viral-mediated gene therapy approaches followed by audiometric tests and detailed morpho-molecular analyses we show that many of these abnormalities can be prevented, thereby restoring hearing abilities in clarin-deficient mice.

PS 925

Isolation of USH1F Protein Complexes from Purified Hair Cell Stereocilia

Clive P. Morgan[1]; Jocelyn F. Krey[2]; Peter G. Barr-Gillespie[3]
[1]*Oregon Health & Science University;* [2]*Oregon Hearing Research Center & Vollum Institute, Oregon Health & Science University, Portland, Oregon, USA;* [3]*Oregon Hearing Research Center & Vollum Institute, Oregon Health & Science University*

Usher syndrome (USH) is an autosomal recessive disorder, characterized by sensorineural hearing loss, retinitis pigmentosa, and variable vestibular dysfunction. Usher syndrome type I (USH1) is the most severe form of the disease. Most USH1 genes have been identified, including USH1B (myosin VIIA), USH1C (harmonin), USH1D (cadherin 23), USH1F (protocadherin 15), USH1G (SANS), and USH1J (calcium and integrin binding family member 2). Mutations in *PCDH15*are one of the leading causes of USH1. Mice lacking PCDH15 are profoundly deaf and have severe vestibular defects. In both mouse and chick, PCDH15 is an integral part of links between stereocilia including the tip-link, which is believed to operate the mechanosensitive (MET) channel directly.

We have developed a new hair-bundle isolation strategy that allows us to isolate and identify protein complexes in the bundle. Starting with thousands of inner ears stored at -80°C after initial dissection, we then isolate bundles from mechanically disrupted tissue using a combination of density centrifugation and monoclonal antibody affinity purification with magnetic-bead separation. We previously described the isolation of several MYO7A (USH1B) protein complexes exploiting these bundle-membrane preparations.

We have also coupled affinity isolation with an anti-PCDH15 antibody (G19), peptide elution, followed by secondary capture using other antibodies against MET components. By removing excess antibody and reducing non-specific background, we have increased detection of low abundance proteins. In particular, using both shotgun and targeted mass spectrometry, we have detected TMC1 and TMIE in PCDH15-containing protein complexes in the chick inner ear. These methods will allow us to identify additional proteins present in PCDH15 complexes, as well as to quantify molecular ratios of each protein in the complexes.

PS 926

USH2A and ADGRV1 Expression in Mammalian Cells and Their in vitro Interaction

Dongmei Yu[1]; **Jun Yang**[2]
[1]University of Utah; [2]Moran Eye Center, University of Utah, Salt Lake City, UT

Background
Mutations in *USH2A* and *ADGRV1* lead to the most common genetic form of deaf-blindness, Usher syndrome. Currently, the molecular mechanism underlying this disease is unclear, and no cure is available. Proteins encoded by the *USH2A* and *ADGRV1* genes are very large transmembrane proteins. Their short intracellular region interacts with PDZ domain-containing scaffold proteins and form a multiprotein complex in inner ear hair cells and retinal photoreceptors. However, the majority (more than 95%) of USH2A and ADGRV1 proteins is the extracellular region, which hosts hundreds of pathogenic missense mutations and has not been well studied. In this project, we tested the conditions to express recombinant USH2A and ADGRV1 extracellular fragments in mammalian cultured cells and investigated their interaction.

Methods
Mouse USH2A and ADGRV1 full-length and fragment cDNAs were fused with different signal peptide sequences and cloned into mammalian expression plasmids. Recombinant proteins were expressed in several 293 mammalian cell lines using serum-free medium. The secretion of proteins was examined by immunoblotting analysis of cell lysates and conditioned medium. Proteins were purified by affinity, gel filtration, and/or ion exchange chromatography.

Results
USH2A C-terminal half ectodomain was secreted into the medium significantly, while USH2A full-length and N-terminal half ectodomain proteins were not. Negative stain electron microscopy showed that the N-terminal half of USH2A ectodomain adopted a folded conformation. Different ADGRV1 ectodomain fragments also exhibited different secretion ability in transfected mammalian cells. One of them was shown to be a bar-like conformation using negative stain electron microscopy. Recombinant USH2A and ADGRV1 ectodomain fragments were able to interact in vitro.

Conclusions
USH2A and ADGRV1 ectodomains interact with each other, although their intracellular regions have been shown not to interact directly. More studies are needed to optimize the secretion of USH2A and ADGRV1 ectodomain proteins from mammalian cultured cells in order to study their conformation and high-resolution three-dimensional structure.

Acknowledgements
This study was supported by the Knights Templar Eye Foundation Career Grant to Dongmei Yu and the University of Utah Neuroscience Initiative Grant to Jun Yang.

PS 927

Characterizing the Role of the Mouse Deafness Gene Baiap2l2 in Hair Bundle Development

Julia Halford[1]; Paroma Chatterjee[2]; Sherri M. Jones[3]; Matthew R. Avenarius[4]; Peter G. Barr-Gillespie[1]
[1]Oregon Hearing Research Center & Vollum Institute, Oregon Health & Science University; [2]Oregon Hearing Research Center & Vollum Institute, Oregon Health & Science University, Portland, Oregon, USA; [3]University of Nebraska Lincoln; [4]Oregon Health & Science University

A more complete understanding of the molecular foundation of hearing is needed to further develop therapeutic interventions for deafness and hearing loss, which affect nearly 5% of the global population. We are investigating the role of the mouse deafness gene *Brain-specific angiogenesis inhibitor 1-associated protein 2-like protein 2 (Baiap2l2)* in hair bundle development and function, and thereby contributing to a molecular understanding of hearing. The protein product of *Baiap2l2* belongs to the Bin-amphiphysin-Rvs (BAR) family of proteins, which act as links between the plasma membrane and the actin cytoskeleton. BAIAP2L2 contains an inverse-BAR (I-BAR) domain, which selectively associates with negatively curved membranes, such as those at the tips of stereocilia, and can cluster the membrane phospholipid $PI(4,5)P_2$. BAIAP2L2 shares structural similarity with the related cytoskeletal effectors BAIAP2 and BAIAP2L1, which suggests that BAIAP2L2 may also be involved in the growth of cytoskeletal structures such as the actin core

of stereocilia. Immunolocalization places BAIAP2L2 at stereocilia tips and demonstrates BAIAP2L2 enrichment in stereocilia tips that contain the transduction apparatus.

Baiap2l2 ablation using CRISPR/Cas9 resulted in severe hearing loss, indicated by elevated auditory brainstem response thresholds, and reduced outer hair cell function, shown by reduced distortion product otoacoustic emissions. FM1-43 uptake was used as a preliminary test of transduction. *Baiap2l2*-null hair cells demonstrated significantly reduced levels of dye labeling, with insensitivity of dye labeling to tip-link breakage with BAPTA Ca^{2+}-chelation. Despite clear deficits in hair cell function, bundle morphology in *Baiap2l2*-null hair cells appears grossly normal. Significant, albeit slight, changes in stereocilia dimensions were nonetheless determined. BAIAP2L2 protein-protein interactions were also examined *in vitro*. The functional domains of BAIAP2L2 were tested against a panel of actin-regulatory, hair-cell enriched proteins in pulldown assays. BAIAP2L2 interacted with the actin-binding stereocilia proteins EPS8 and ESPNL, as well as the small Rho GTPases CDC42 and RAC1. These results indicate that *Baiap2l2* contributes specifically to hair-cell function within the bundle compartment but does not exert a large effect on the growth and development of stereocilia actin cores. Determining the molecular role of BAIAP2L2 will require further investigation.

PS 928

Transcription Co-Factor LBH Is Necessary for Maintenance of Stereocilia Bundles and Survival of Cochlear Hair Cells

Yi Li[1]; Kimberlee Giffen[2]; Huizhan Liu[2]; Grati M'Hamed[3]; Xuezhong Liu[4]; Karoline Briegel[3]; David Z. He[5]
[1]Beijing Tongren Hospital; [2]Creighton University School of Medicine; [3]University of Miami School of Medicine; [4]University of Miami; [5]Creighton University

Progressive hearing loss affects 15% of American adults. Most sensorineural hearing loss is caused by progressive loss of hair cells, the sensory receptor cells in the cochlea. The underlying molecular basis of hair cell maintenance and loss is largely unknown. Our previous cell type-specific RNA-seq transcriptomic analysis of hair cells showed that *Lbh*, a transcription co-factor important for development of the limb bud and heart, is expressed in hair cells with preferential expression in outer hair cells (OHCs). In the present study we used *Lbh*-null mice to examine the role of LBH in cochlear hair cells. Nascent hair cells from the knockout mice had normal-looking stereocilia bundles when examined with scanning electron microscopy. Whole-cell recording showed that the stereocilia bundle was mechanosensitive and OHCs exhibited the characteristic electromotility, suggesting that LBH is not critical for hair cell differentiation. However, *Lbh*-null mice displayed progressive loss of hearing and otoacoustic emissions with degenerating stereocilia bundles and hair cell loss, especially OHCs, after hearing onset. Cell-specific RNA-seq and bioinformatic analyses identified *Spp1, Six2, Gps2, Ercc6, Snx6* as well as *Plscr1, Rarb, Per2, Gmnn* and *Map3k5* among the top five transcription factors up- and down-regulated in the *Lbh*-null OHCs. Significant gene enrichment in *Lbh*-null OHCs was associated with biological processes related to transcription, cell cycle, DNA damage/repair, autophagy, Wnt signaling and Notch signaling. Our study implicates, for the first time, the loss of transcription co-factor LBH in progressive hearing loss, and demonstrates a critical requirement of LBH in promoting hair cell survival (Supported by NIH/NIDCD grant R01 004696 and Bellucci Depaoli Family Foundation).

PS 929

GIPC3 is Essential For Normal Development of Hair Bundles and Cuticular Plates of Cochlear Hair Cell Stereocilia

Paroma Chatterjee[1]; Connor Benson[2]; Clive P. Morgan[2]; Peter G. Barr-Gillespie[3]
[1]Oregon Hearing Research Center & Vollum Institute, Oregon Health & Science University, Portland, Oregon, USA; [2]Oregon Health & Science University; [3]Oregon Hearing Research Center & Vollum Institute, Oregon Health & Science University

Immunoprecipitation experiments from extracts of partially purified chicken stereocilia reproducibly demonstrated that GIPC3 is in a complex with MYO7A. GIPC3 belongs to the family of GIPC proteins, which are characterized by the presence of a PDZ domain, a module that often plays a pivotal role in signal transduction, as well as two domains shared by the GIPC family. The paralog GIPC1 binds to MYO6, and we demonstrated that GIPC3 also interacts with MYO6. A previous study showed that mice carrying a missense mutation in the PDZ domain of *Gipc3* has progressive sensorineural hearing loss and audiogenic seizures in mice; moreover, pathogenic mutations cause autosomal recessive deafness in humans. Transgenic *Gipc3* expression in the mutant mice rescued the hearing loss phenotype, demonstrating the importance of this gene in normal hearing. We utilized a *Gipc3* allele generated by the International Mouse Phenotyping Consortium that is likely to be null. Preliminary auditory brainstem response recordings from *Gipc3* null mice showed complete hearing loss in KO mice compared to littermate controls. Immunofluorescence localization using a specific monoclonal antibody showed punctate

GIPC3 labeling in stereocilia and broad expression throughout the cuticular plate. The fluorescence signal was reduced substantially in both these regions in *Gipc3* KO mice. We used confocal microscopy to characterize morphological changes in the hair bundles and cuticular plate throughout development of the cochlea. Hair bundles of *Gipc3* KO inner and outer hair cells acquired a structure different from that of wild-type cells. By P8.5, the cuticular plate of *Gipc3* KO mice was reduced in area compared to that of wild-type mice. In addition, hair bundles lost of the V-shaped bundle arrangement of stereocilia. Furthermore, the immunofluorescence signal for MYO7A was substantially reduced in the *Gipc3* KO mice compared to littermate controls. We suggest that GIPC3 interacts with both MYO6 and MYO7A and assists in building the hair bundle and maintaining the cuticular plate structure, both of which are required for normal mechanotransduction.

PS 930

Dynamin 3 Is Necessary for Maintaining the Dynamic Structure and Mechanics of Stereocilia Bundles of Cochlear Outer Hair Cells

Huizhan Liu[1]; **David Z. He**[2]
[1]Creighton University School of Medicine; [2]Creighton University

Stereocilia are specialized membrane protrusions with actin cores on the apical surface of the hair cells of the inner ear. Stereocilia play a key role in the process of mechanical to electrical transduction. Little is known about the mechanism and trafficking machinery involved to transport proteins to the stereocilia bundle to maintain the stereocilia morphology and dynamics. It is also not clear whether the protein components of stereocilia bundles and the molecular mechanisms underlying stereocilia maintenance are different between inner and outer hair cells (IHCs and OHCs). Using cell-type specific transcriptome analyses, we showed that *Dnm3* is preferentially expressed in adult OHCs. *Dnm3,* encoding dynamin-3, is a member of a family of GTP-binding proteins that are associated with microtubules and involved in the membrane recycle, vesicular trafficking, and regulating actin assembly and organization. Using immunostaining and confocal microscopy, we showed that DNM3 was strongly expressed in the adult OHC stereocilia bundle with no expression in the cytosol. DNM3 was not detected in the OHC stereocilia bundles before postnatal day 4 (P4). DNM3 expression was also not detected in the adult IHC and vestibular hair cell stereocilia bundles. Auditory brainstem response (ABR) and distortion product otoacoustic emission (DPOAE) as well as mechanotransduction and bundle mechanics were examined from *Dnm3*-null mice to determine the role of DNM3 in maintaining dynamics and mechanical property of OHC stereocilia. ABR and DPOAE thresholds were both elevated by 20 and 40 dB at P21. Scanning electron microscopy showed stereocilia bundles of OHCs appeared to be normal at P5. However, significant degeneration and loss of OHC stereocilia bundles were observed at P21 while IHC stereocilia appeared to be normal. The stereocilia bundles of *Dnm3*-null OHCs were mechanosensitive, although bundle stiffness and the magnitude of mechanotransduction currents were significantly reduced. Our study showed that OHCs have a distinct molecular mechanism to maintain their stereocilia dynamics and mechanical property (supported by R01 DC016807/NIDCD and the Bellucci Depaoli Family Foundation).

PS 931

Constitutive activation of Dia1 induces hair cell vulnerability via attenuated integrity of apical junctional complexes and stereocilia

Yuzuru Ninoyu[1]; Hirofumi Sakaguchi[2]; Chen Lin[3]; Hiroaki Mohri[3]; Naoaki Saito[3]; Takehiko Ueyama[3]
[1]Lab. of Molecular Pharmacology, Biosignal research center, Kobe university/ Kyoto prefectural University of Medicine, Dep. of Otoralyngology-Head and Neck Surgery; [2]Kyoto prefectural University of Medicine, Otolaryngology-Head and Neck Surgery; [3]Lab. of Molecular Pharmacology, Biosignal research center, Kobe University

Dia1 is one of the diaphanous-related formin (DRF) family memmbers, which has pivotal role for many cellular processes through straight actin elongation activity. *DIA1* is the causative gene of the first type of non-syndromic, autosomal dominant sensorineural hearing loss (DFNA1),. Recently, a novel mutation of *DIA1* related to hearing loss with macrothrombocitopenia has been reported among European and Japanese deafness families. The mutation, *DIA1(R1213X)*(or *DIA1(R1204X)*) in the diaphanous autoregulatory domain (DAD), makes DIA1 constitutively active due to disruption of intramolecular autoinhibition via the C-terminal truncation. Our group has reported the gain-of-function mechanism in the mutant and succeeded to generate the disease specific mouse model ($DIA1^{Tg(FLAG\text{-}DIA1\_R1204X)}$). However, subcellular localization and physiological/pathological function of DIA1/DIA1(R1213X/R1204X) remains unknown. In the present study, we demonstrate the localizaiton of Dia1 and the constitutively active DIA1 mutant in cochleae using mice expressing the FLAG- or AcGFP-tagged DIA1 mutant. Dia1/DIA1 mutant was regionally expressed in the organ of Corti from early post-neonatal days. In accordance with cochlear maturation, Dia1/DIA1 mutatnt became localized at apical junctional complexes (AJCs) in outer and inner hair cells (HCs). In $DIA1^{Tg/Tg}$ mice, impairment

in AJCs and stereocilia accompanied with HC loss was observed at 6 months. We established a stable cell line, MDCK$^{AcGFP\text{-}DIA1(R1213X)}$, which expresses AcGFP-DIA1(R1213X). In MDCK$^{AcGFP\text{-}DIA1(R1213X)}$ cells, the tight junction immunostained by ZO1 was ruffled, and the mutant markedly localized at the apical surface of cells and microvilli. In addition, localization at the stereocilia tip of AcGFP-DIA1(R1213X) was obserced iin mice. To further investigate HC vulnerability in DIA1$^{Tg/Tg}$ mice, we exposed 4-week-old mice to intense noise with 105 dB SPL for 1h, which induced temporary threshold shift in WT and DIA$^{Tg/Tg}$ mice. The number of residual HCs after noise exposure (NE) was not significantly decreased in DIA1$^{Tg/Tg}$ mice compared with that in WT mice, which was verified by DPOAE measurement. However, cochlear synaptopathy evaluated by CtBP2 immunostaining as well as ultrastructural changes in HCs were observed at the basal turn in DIA1$^{Tg/Tg}$ mice. These data suggested that Dia1 plays important roles for maintenance of AJCs and stereocilia, which secures cochlear and HC integrity. In summary, we revealed the subcellular localization and physiological/pathological function of Dia1 and the constitutively active DIA1 mutant in mice cochleae, especially HCs. The constitutively active mutant of DIA1 attenuates integrity of HCs, resulting in cochlear synaptopathy after mild noise NE. This subclinical/latent vulnerability of HCs may be the cause of progressive hearing loss in DFNA1 patients.

PS 932

Molecular Predictions for a CNGA3/CNGB1a Channel and its Membrane Guanylyl Cyclase Pathway Targeting Rhodopsin in Hair Cells

Marian J. Drescher[1]; Neeliyath A. Ramakrishnan[2]; Dennis G. Drescher[1]
[1]Wayne State University School of Medicine; [2]Wayne State University School of Medicin

Background
Previously (IEB Abstr. 52:011, 2015), we identified CNGA3/CNGB1a subunits in hair cells, which combined in a heteromeric CNG channel has high sensitivity to cis-diltiazem, and unusually, cAMP (Zhong, Lai, and Yau, 2003). This channel would be relatively insensitive to pseudechetoxin, a pharmacological inhibitor of CNG channels (Farris et al., 2003), due to the inclusion of CNGA3 and separately, CNGB1a. CNGB1a blocks pseudechetoxin inhibition of photoreceptor CNGA1 and olfactory CNGA2 and CNGA4 (Brown et al., 2003), the latter cAMP-gated CNG subunits also expressed in cochlear hair cells (Drescher et al., 2002). A membrane guanylyl cyclase (GC) pathway regulating cGMP has been elucidated, with splice variant transcripts for 14 pathway proteins published in GenBank.

Methods
Predicted co-localization of rod/cone phototransduction proteins in cochlear hair cells was examined with Z-stack confocal microscopy. Yeast two-hybrid (Y2H) analysis of tip-link protein protocadherin 15CD3 protein-protein interactions (PPI) would inform of a relationship between the rhodopsin/GC pathway and mechanotransduction.

Results
(1)CNGA3 immunofluorescence was localized to subcuticular plate regions and stereocilia where it formed specific layered patterns for OHC and IHC with partial CNGB1 co-localization. (2)Rhodopsin was immunolocalized to OHC subcuticular plate sites, a position targeted in UV light stimulation of hair cell mechanotransduction (Azimzadeh et al., 2018). (3) Tetraspan flippase ABCA4 mediating transport of photoreceptor chromophore, **11-cis-retinylidene,** co-localized with CNGB1a and rhodopsin. (4)CNGB1a and ABCA4 immunofluorescence was traced to tracks crossing the cuticular plate to the apical surface of hair cells. (5)Y2H identified direct PPI for protocadherin 15CD3 with GRK6b (which directly binds rhodopsin and recoverin), EMILIN1, ACTG1 and RYR2.

Conclusions
(1)Transcript and protein analysis support the hypothesis that a CNG channel with specific subunits CNGA3/CNGB1a and molecular pathways for synthesis and degradation of cGMP exists in vestibular and cochlear hair cells, teleost and mammalian. (2)A hair cell CNGA3/CNGB1a channel would have PIP2-binding motifs, required for mechanotransduction (Effertz et al., 2017). A homomeric CNGA3 channel would be gated by cGMP and inhibited by PIP2, the latter observed for baseline current. A heteromeric CNGA3/CNGB1a channel is sensitive to cis-diltiazem ($K_{1/2}$=23.6μM), with 5-fold enhancement in activation by cAMP compared with homomeric channel (Zhong et al., 2003), increased by PIP2, lacking sensitivity to pseudechetoxin. (3)Rhodopsin is required for hearing and localized to sites similar to those required for UV-light-enhanced mechanotransduction. (4)Co-localization of ABCA4 with CNGB1 and rhodopsin is consistent with phototransduction PPI. (5)GRK6b would couple rhodopsin to tip-link protein protocadherin 15CD3 and actin-binding filamin A whose PPI are mechanosensitive.

PS 933

Effects of Chloroquine on Hair Cells: Implications for Ototoxicity Monitoring

Samantha N. Davis; Patricia Wu; Esra D. Camci; Edwin W. Rubel; David W. Raible
University of Washington

Hearing and balance deficits are often reported during and following treatment with antimalarial drugs. For example, these adverse side effects have been the subject of many case studies of chloroquine treatment for the prevention and treatment of malaria. However, we are unable to locate experimental work examining the direct actions of chloroquine on hair cells in common experimental models. This study aims provides dose-response analyses on the effects of chloroquine on hair cells using the zebrafish lateral line as well as cochlear cultures from neonatal mice.

Zebrafish larvae (5 dpf) were exposed to concentrations of chloroquine phosphate ranging from 0–1600 µM for 1 hr or 24 hr, fixed and then stained with anti-parvalbumin antibody. Hair cell numbers were counted in 4 predetermined neuromasts and compared to numbers from untreated controls to create dose-response functions for each exposure duration. A significant, dose-dependent reduction in the surviving hair cells was seen across conditions. However, the amount of loss approached an apparent asymptote at about 60% by 400 µM. We found no significant difference in the dose-response functions between the two exposure durations.

Cochleae from P2 neonatal mice were cultured on collagen-coated coverslips for 24 hours prior to drug exposure. Cultures were then exposed to varying concentrations (0 to 400 µM) of chloroquine phosphate for 48 hours, fixed and stained with β-Myosin VIIa, DAPI, and phalloidin. The number of inner and outer hair cells were counted in apical and basal regions and compared to control cultures. Again, a large dose-dependent decrease in surviving hair cells was observed. Unexpectedly and in contrast to results in zebrafish, there was no plateau effect seen in the percentage of surviving hair cells, resulting in near total hair cell loss at 400 µM.

In summary, chloroquine exposure caused significant hair cell death in both zebrafish lateral line and neonatal murine cochlea cultures. While there is much more to be learned about the effects of chloroquine and other anti-malarial drugs on hair cells and other inner ear structures, these data provide a useful baseline to work with. They also suggest a need for future studies employing hearing and balance monitoring during exposure to chloroquine and other anti-malarial drugs.

Inner Ear Therapeutics II

PS 934

Morphologic changes of stem cells transplanted into scala media induced by photobiomodulation

So-Young Chang[1]; Nathaniel Carpena[2]; Jae Yun Jung[3]; Hosup Shim[4]; Ji Eun Choi[5]; Phil-Sang Chung[3]; Min Young Lee[6]
[1]Dankook University; [2]Beckman Laser Institute Korea, College of Medicine, Dankook University, Cheonan, South Korea; [3]Beckman Laser Institute Korea, Dankook University, Dankook University Hospital; [4]Department of Nanobiomedical Science and BK21 PLUS NBM Global Research Center for Regenerative Medicine, Dankook University; [5]Dankook University Hospital; [6]Beckman Laser Institute Korea, Dankook University Hospital, Dankook University

Background
Stem cell (SC) therapy is one of the potential candidate to revive the hearing function since hair cells in cochlear does not regenerate once damaged. Recently, methodological technique to increase the SC survival within the scala media has been reported. But, delivering the factors to alter the differential status of the SC is not feasible due to the several anatomical and structural characteristics of cochlea. Cochlear hair cells lie within the bony capsule of cochlea. Round window which could serve as route for delivery exists but disruption of this structure leads to the alteration of cochlear homeostasis and further damage of the cells within. Photobiomodulation (PBM) is terminology for the technique which induces desired change of biological target using the light energy with various parameter. Increased differentiation of several SCs into target cells using this non-invasive PBM has been reported.

Objective
In this study, we confirmed the hair cell damage by ototoxic agent and optimal drug concentration and combination for hair cell damage, then assessed the survival of the SC using previously reported technique. Lastly, morphologic changes of the SCs transplanted into the scala media by PBM application was analyzed.

Materials and Methods
Pigmented guinea pigs and a GFP-tagged mouse embryonic SCs were used. Two different amount, 5 and 10 microliters, of neomycin was used to induce hair cell damage with or without furosemide. To check the hearing function, ABR was evaluated before and after neomycin. Before SC transplantation, scala media (SM) was flushed with sodium caprate to temporarily disturb the condition of SM. Three µL of SC (2 X 10^4 cells/µL) was injected into SM after 7days neomycin injection. The

animals, which transplanted ESCs, were irradiated with 808 nm diode laser at intensity of 250 mW for 90 min and then sacrificed at 3 h after the transplantation surgery. Epifluorescences of GFP, MyosinVIIa & Phalloidin were analyzed. GFP positive area was measured using the image J program.

Results

Both amount of neomycin showed loss of hair cells compared to the control group. Furosemide was not necessary to induce the total hair cell damage. Transplanted SC survived and attached to membranous labyrinth with the previously reported protocol. We confirmed the survival of these attached cell 3 hours after transplantation. Application of PBM after SC transplantation did not increase the number of surviving attached SCs. But with epifluorescence analysis of GFP positive cells, GFP positive cells were merged and formed aggregated GFP positive structures. Averaged GFP positive area per each GFP positive structure was statistically larger with PBM compared to no PBM.

Conclusions

Using the prior conditioning protocol, SCs survived after transplantation into scala media, PBM did not increase the survival or attachment of SCs but increased the aggregation process leading the bigger GFP positive structure. This result suggests that PBM is inducing the cellular activity which may lead to further differentiation, but to confirm this theory further analysis is necessary.

PS 935

Cool Otoprotective Outer ear Lavage (COOL) Therapy for Cisplatin Induced Hearing Loss

James Stanford[1]; **Drew Morgan**[2]; Nicholas Bosworth[2]; Punam Thapa[2]; Tianwen Chen[1]; Georgio Proctor[1]; Bradley J. Walters[2]; Douglas E. Vetter[3]; Robert Black[4]; Lesco Rogers[4]; Christopher Spankovich[1]

[1]Department of Otolaryngology University of Mississippi Medical Center; [2]University of Mississippi Medical Center; [3]Department of Neurobiology and Anatomical Sciences, University of Mississippi Medical Center; [4]Scion Neurostim, LLC

Introduction

Ototoxicity from cisplatin remains a significant concern; it is estimated that 70-100% of patients undergoing cisplatin treatment incur ototoxic adverse events including hearing loss, tinnitus, and dizziness. Currently, a number of investigators are exploring pharmacological otoprotectant strategies for cisplatin induced hearing loss. The overarching concern for pharmacological therapies is potential for decrease in the anti-tumor efficacy of the cisplatin and/or a need for invasive (transtympanic or intracochlear) methods of administration. Previous research has demonstrated that systematic or localized hypothermia can protect against noise and iatrogenic damage from cochlear implant surgery. Based on this literature, we hypothesized that localized thermoregulation may mediate cisplatin ototoxicity. In a proof of concept study, we previously demonstrated significant protection from hearing loss using cool water ear canal irrigation, while warm water exacerbated damage. However, that study was limited to a single bolus injection of cisplatin and acute time period. Here we examined application of localized cooling of the ear canal during repeated doses of cisplatin, over an expanded period of time, and using two methods of cooling.

Methods

Twenty-four guinea pigs (12 male and 12 female) underwent auditory physiological testing (auditory brainstem response and distortion product otoacoustic emissions at 8-32 kHz) pre and post administration of cisplatin. Cisplatin (4 mg/kg ip) was administered in 3 weekly single injections for a total of 12 mg/kg. The left ear of the guinea pigs was exposed to either cool water (20°C; ICS Water Caloric Irrigator) or a cool ear bar (15°C, cooled by a Peltier device; TNM™, Scion NeuroStim) before, during, and after cisplatin administration (total time 30 minutes) while anesthetized. Control animals received same dosing, but underwent a sham treatment. The animals were tested 3 days post each dosage and 1 month post the final dose. At the end of the experiment animals were euthanized for histological evaluation.

Results

Auditory testing at 3 days revealed significantly less hearing loss in animals that received the COOL Therapy compared to cisplatin-only control animals. No significant difference was observed between the two methods of cooling. Protection was still observed at 1 month post final dose with no further progression in hearing loss noted.

Conclusions

Localized cooling of the ear during administration of cisplatin mitigated loss of auditory function and loss of hair cells. These findings suggest a novel, localized, and minimally invasive otoprotective strategy. We are currently examining mechanisms of the observed otoprotection and exploring translation to human populations.

PS 936

Transient Application of a Potent and Specific KCNQ2/3 Activator, RL_81, Protects Against Noise-Induced Hearing Loss, but Not Against Age-Related Hearing Loss (AHL)

Laura Marinos[1]; Bryce Hambach[2]; Thanos Tzounopoulos[3]
[1]Pittsburgh Hearing Research Center, Department of Otolaryngology, University of Pittsburgh; [2]Pittsburgh Hearing Research Center, Department of Otolarynogology, University of Pittsburgh; [3]University of Pittsburgh, Otolaryngology and Neurobiology

Tinnitus and hearing loss are two common consequences of exposure to loud noise, and often individuals express high levels of comorbidity with these disorders. One major mechanism leading to tinnitus is hyperactivity of auditory brainstem neurons, due to decreased Kv7.2/3 (KCNQ2/3) potassium currents (Li et al., 2013; 2015). To develop a drug to activate KCNQ channels for potential tinnitus treatment, we developed RL_81. RL_81 targets KCNQ2/3 channels specifically and potently, unlike its predecessor, retigabine, which targets a range of KCNQ channels (Kumar et al., 2016; Liu et al., 2019). With tinnitus and hearing loss displaying such high levels of comorbidity, we wanted to first investigate RL_81's effect on hearing loss. After verifying that brief (1 day) application of RL_81 sped up ABR threshold recovery when administered directly after noise exposure, we wanted to investigate whether 5-day RL_81 application one week after noise exposure protects against noise-induced hearing loss. To do this, mice were exposed to 16 kHz, 116 dB bandwidth noise for one hour, and one week following exposure, were given RL_81 every twelve hours for five days. ABR thresholds and DPOAE's were taken prior to the noise exposure, as well as three and twelve weeks post noise exposure. We found that when hearing was tested three weeks post exposure transient RL_81 application provided protection against ABR threshold shifts. When examining hearing 12 weeks post noise exposure, we found that RL_81 still provided protection at lower frequencies, but no longer in the higher frequencies. Since we also found that the higher frequencies were affected in the sham group, regardless if treated with RL_81, we conclude that this timing and dosage given of RL_81 application protects against long-term noise-induced hearing loss, but not against age-dependent hearing loss. We found that this protection is mediated, at least in part, from protection of outer hair cell (OHC) function, since RL_81 conserved the distortion product after noise exposure. We conclude that specific and potent KCNQ2/3 activators, such as RL_81, represent a novel pharmaceutical path for treatment of noise-induced hearing loss.

This research was funded by the DOD award W81XWH1810623 (to TT).

PS 937

Development of Dual-Action Topical Therapeutics for Cytomegalovirus-Induced Hearing Loss

Elizabeth Arrigali[1]; Monica Serban[2]
[1]Department of Biomedical and Pharmaceutical Sciences, University of Montana; [2]Department of Biomedical and Pharmaceutical Sciences and Department of Chemistry and Biochemistry, University of Montana

Cytomegalovirus (CMV) infection among the leading nongenetic cause of hearing loss in children in the US. The cost associated with its diagnosis and treatment has been estimated at $4 billion/year. Currently, only infants with symptomatic CMV infections are clinically treated for hearing loss prevention with antivirals. However, these antivirals show modest short-term improvements and have uncertain long-term outcomes. In this context, there is a lack of treatment options for asymptomatic CMV infected children with initial normal hearing who develop hearing loss later in life. With the above considerations, there is an urgent need to develop alternative therapeutics that will provide better treatment options to both symptomatic and asymptomatic CMV-infected patients. Our approach is to use a hyaluronic acid (HA) based therapeutic, which was shown to have intrinsic anti-inflammatory properties and to enhance drug transmembrane permeation, as a carrier for antioxidants into the inner ear.

HA was conjugated with antioxidants via carbodiimide chemistry. The conjugates were purified by dialysis and chemically characterized via ^{1}H-NMR. The cytocompatibility of the conjugates was assessed with House Ear Institute-Organ of Corti 1 (HEI-OC1) and Immortalized Stria Vascularis (SV-k1) cells with an methyltetrazolium salt (MTS) colorimetric assay and CyQUANT assay that assesses metabolic activity and proliferation respectively. The oxidative protection abilities of the conjugates were assessed using a fluorescent (CM-H2DCFDA) reagent. Cells were kindly provided by Dr. Kalinec's lab from UCLA.

Hyaluronan-antioxidant conjugates (HACs) were successfully synthesized as confirmed by ^{1}H-NMR analyses of chemical structures and purities. The conjugates showed a 15-20% degree of HA substitution with no traces of unreacted antioxidants. Previously published data by the Serban lab demonstrated that functionalized HAs with antioxidant substituents in the 15-20% range were protective against oxidative damage in

primary cells. When evaluated for cytocompatibility with HEI-OC1 and SV-k1 cells, the HACs maintained excellent cellular viability, increased cellular metabolic activity with minimal effects on cellular proliferation as compared to the antioxidant or HA alone (Figures 1-4). We are currently in the process of evaluating the antioxidant effects of HACs on HEI-OC1 and SV-k1 cell lines.

Our data so far highlights the practicality of chemically conjugating HA with antioxidants while preserving the protective function of the selected antioxidant. We anticipate that our ongoing experiments will support our hypothesis that HA conjugation with antioxidants can protect inner ear cells by synergistically reducing inflammation, oxidative stress, and by enhancing the drug's permeability across the round window membrane.

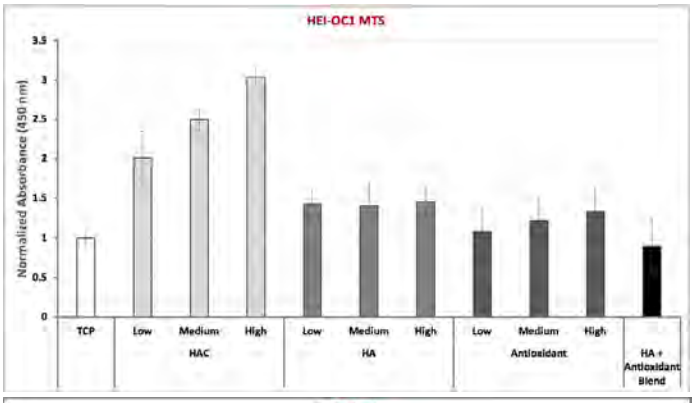

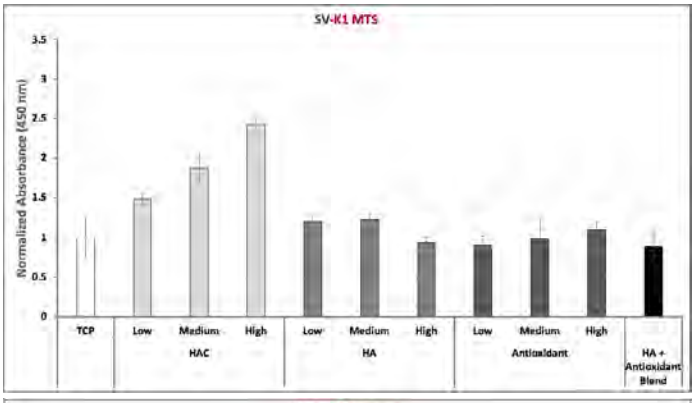

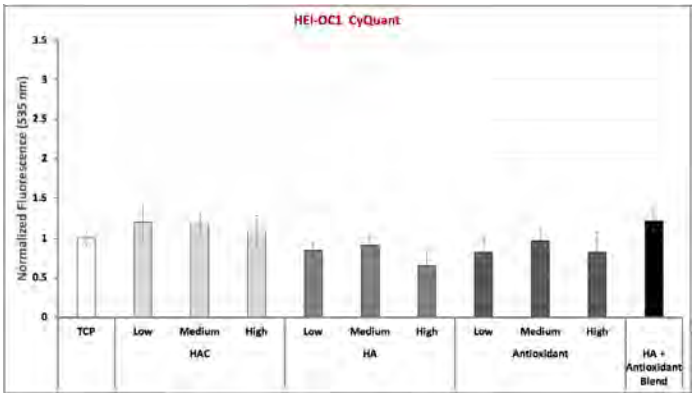

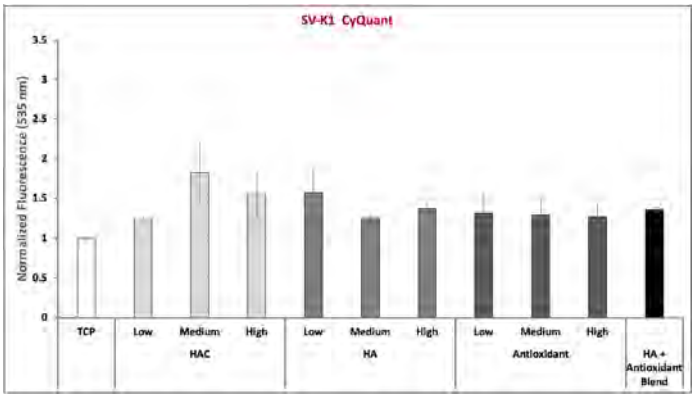

PS 938

Protective properties of Pre- and Post-treatment of Dexamethasone Against Kanamycin Induced Ototoxicity in the mouse: ex vivo model.

Jeong Eun Park[1]; Young Joon Seo[2]; **Sung Kyun Kim**[1]
[1]Hallym University Dongtan Sacred Heart Hospital;
[2]Yonsei University Wonju College of Medicine

Introduction

Glucocorticoids are known to have anti-inflammatory and immune suppression effects, and have otoprotective effect by binding to glucocorticoid receptors in the inner ear. Herein, we hypothesized that dexamethasone can facilitate to protect against the aminoglycoside induced ototoxicity as ex vivo model.

Methods

The cultured explant cochlea of ICR mouse (P3) were incubated in kanamycin (0.4 mM) for 24 hrs and dexamethasone (100ug/ml) was restored before or after incubation of kanamycin for 48 hrs. The morphological changes in the hair cells (HCs) were evaluated by immunostaining of primary antibodies for Myosin 7a (1:100). Alexa 488-conjugated secondary antibodies and alexa 647-conjugated phalloidine were used for detection, and Fluoroshield was used to label the nuclei. The entire cochlea was divided into five pieces of equal length designated the basal (2/5), middle (2/5), and apical (1/5) turn of the cochlea. Three 100 μm regions in each turn were counted for ototoxic damage in HCs.

Result

There were no significant differences in HCs counts between control explants and explants treated with dexamethasone. Loss of HCs to kanamycin was higher in mid and basal turns than in apical turn. The number of HCs were most in the basal and apical turn of pretreatment group.

Conclusion

The results indicated that dexamethasone attenuates kanamycin ototoxicity in both pretreatment and posttreatment. The otoprotective properties of dexamethasone against kanamycin was effective pretreatment than rescue treatment.

PS 939

Chemokine Receptors, CXCR1/2, Serve as Novel Targets for Treating Cisplatin Ototoxicity

Raheem Al Aameri[1]; Asmita Dhukhwa[1]; Sandeep Sheth[2]; Debashree Mukherjea[1]; Leonard Rybak[1]; Vickram Ramkumar[1]

[1]SIU School of Medicine; [2]Larkin University College of Pharmacy

Cisplatin (cis-diamminedichloroplatinum II) is a major chemotherapeutic agent used to treat different solid tumors such as head, neck and ovarian cancer. However, cisplatin chemotherapy produces significant ototoxicity which derives from damage or loss of the cells in the organ of Corti, stria vascularis and spiral ganglia, mediated in part by generation of reactive oxygen species (ROS). ROS produce lipid peroxidation, inflammation, DNA damage, and apoptosis or necrosis of cells in the cochlea. Previous studies indicate the involvement of CXC chemokine/chemokine receptors in cisplatin ototoxicity. In this study, we focused on the CXCR1 and CXCR2 receptors in mediating cisplatin-induced hearing loss. Both of these receptors are expressed in the rat organ of Corti, with strong labeling in the stria vascularis, spiral ligament, spiral ganglion neurons and organ of Corti and are induced by cisplatin in a time-dependent manner. Inhibition of CXCR1/2 by trans-tympanic administration of the chemical inhibitor (SB225002) abrogated cisplatin-induced hearing loss, protected against loss of outer hair cells and reduced the loss of inner hair cell ribbon synapses. Similar findings were obtained following knockdown of CXCR2 by trans-tympanic administration of CXCR2 siRNA. Both SB225002 and CXCR2 siRNA suppressed the expression of inflammatory genes in the cochlea, including *CXCL1*, *NOX3*, *iNOS*, *TNF-α*, *IL-6* and *COX-2*, which are induced by cisplatin. These results support the conclusion that CXCR1/2 are relevant targets for treating cisplatin ototoxicity, presumably by suppressing cochlear inflammation.

PS 940

The Combinatorial Otoprotective Approach to Cisplatin Ototoxicity

Nicole Febles[1]; Robert D. Frisina[1]; Bo Ding[1]; Nathan D. Gallant[2]

[1]Medical Engineering Dept., Global Center for Hearing & Speech Research, Univ. South Florida; [2]Mechanical Engineering Dept., College of Engineering, Univ. South Florida

Introduction

Sensorineural hearing loss (SNHL) is an irreversible, incurable, degenerative condition, resulting in the permanent damage/loss of cochlear cellular tissue. Cisplatin, a highly favorable chemotherapy agent, is one of the predominant drugs found to cause ototoxicity resulting in SNHL. Currently, *no FDA-approved drugs to prevent and/or treat any type of SNHL* exist, resulting in a necessity for hearing and cancer research advancements. Therefore, we hypothesize a combinatorial otoprotective approach can successfully protect against the multifaceted cisplatin ototoxicity. The following initial study investigated the prevention of cisplatin ototoxic affects, in a recognized auditory hair cell line, HEI-OC1 cells, by employing a combinatorial pretreatment of an antioxidant, caspase-inhibitor and neurotrophin, prior to Cisplatin treatment. Western Blotting (WB), DNA fragmentation and cellular viability assays were utilized in analyzing the protective effects of our approach.

Methods

HEI-OC1 cells were grown in permissive conditions and seeded in 96 well plates and 100 mm dishes for 24-hours as previously described. On Day2, experimental pretreatment conditions or IFN-β-free growth media were added. On Day3 respective wells were incubated with Cisplatin for 24-hours. DNA fragmentation, cell viability and WBs were performed and evaluated on Day4 via Invitrogen Click-iT TUNEL Alexa Flour Imaging and ATTC Cell Proliferation MTT Assay and XCell SureLock Mini-Cell System with Cell Signaling Primary and Secondary Antibodies. All statistical analysis was done with a 1-way ANOVA and Holm-Sidak all pairwise multiple comparison procedure using Sigma Plot (See Table 1 and 2).

Results

Our initial TUNEL and MTT assays revealed HEI-OC1 cells incubated with a high concentration (≥200 μM) of Cisplatin for 24-hours, resulted in significant DNA fragmentation and cellular death, when compared to control 24-hours. Conversely, HEI-OC1 cells pretreated with our cocktail of otoprotective agents for 24-hours prior to Cisplatin incubation revealed significant

protection against DNA fragmentation and cellular death, when compared to Cisplatin only 24-hour conditions. Additionally, WB results revealed our otoprotective agents protected against apoptosis when compared to Cisplatin only for 10- and 16-hour, represented by the absence of cleaved Caspase-3 bands.

Conclusion

Our results suggest Cisplatin induces cellular death via apoptosis in an HEI-OC1 cellular model, as seen with our MTT assay, WB cleaved apoptotic bands, and TUNEL imaging results. Our results also support a promising inhibition to this apoptotic activity and reduced cellular death via our combinatorial pretreatment of agents prior to Cisplatin administration. Optimization and further characterization of protection will be investigated in future studies.

Supported by Univ. South Florida.

PS 941

Harnessing the Power of Exosomes to Mediate Sensory Hair Cell Protection in the Inner Ear

Melanie Barzik[1]; Andrew M Breglio[2]; Lindsey A. May[2]; Nora C. Welsh[2]; Shimon P. Francis[3]; Tucker Q Costain[2]; Lizhen Wang[2]; D. Eric Anderson[4]; Ronald S. Petralia[5]; Ya-Xian Wang[2]; Thomas B. Friedman[6]; Matthew JA Wood[7]; Lisa L. Cunningham[1]

[1]Laboratory of Sensory Cell Biology, NIDCD, NIH; [2]NIDCD, National Institutes of Health; [3]Akouos, Inc.; [4]NIDDK, National Institutes of Health; [5]Advanced Imaging Core, National Institute on Deafness and Other Communication Disorders, NIH, Bethesda, Maryland, USA; [6]Laboratory of Molecular Genetics, National Institute on Deafness and Other Communication Disorders, NIH, Bethesda, Maryland, USA; [7]University of Oxford

Introduction

Hair cell death and consequent hearing loss caused by ototoxic drugs are reduced by non-cell-autonomous induction of heat shock proteins (HSPs), particularly HSP70 (May et al., 2013; Baker et al., 2015, Francis et al., 2017). Here we investigated the roles of exosomes, nanometer-sized endosomally-derived secretory vesicles, as mediators of this non-autonomous protective signaling in the inner ear. Exosomes promote intercellular communication by delivering protein, lipid, and nucleic acid cargo. Unique surface molecules allow exosomes to interact with target cells either by internalization or by signaling through cell surface receptors. Delivery of exosome cargo can alter target cell function and fate.

Methods

Whole-organ cultures of utricles from adult mice were heat shocked, and extracellular exosomes were purified from conditioned media. Exosomes were quantified using nanoparticle tracking analysis. Isolated exosomes were applied to naïve utricle cultures in the presence or absence of neomycin. Hair cell viability was assessed by determining hair cell counts on fixed utricles labeled with the hair cell marker Myosin 7a. Exosome biogenesis was inhibited using spiroepoxide, an inhibitor of neutral sphingomyelinase 2. Tandem mass spectrometry was used to analyze exosome cargo. The HSP70-TLR4 signaling axis was investigated using a hair cell specific conditional TLR4 knock out mouse model and a proximity ligation assay.

Results

Heat shocked utricles release exosomes that carry a variety of classical exosome markers including HSP70, as well as many other proteins. Purified exosomes were sufficient to improve the survival of hair cells exposed to neomycin, while depletion of exosomes from the extracellular environment or inhibition of exosome biogenesis abolished this protective effect. Application of a function-blocking antibody against HSP70 in the presence of ototoxic drugs interfered with the pro-survival activity of exosomes. Expression of the known receptor for HSP70, Toll-like receptor 4 (TLR4), on sensory hair cells was necessary for the protective effect of exosomes, and a proximity ligation assay showed that exosomal HSP70 interacted with TLR4 on hair cells.

Conclusions

Our results reveal a previously-undescribed mechanism of pro-survival intercellular communication in the inner ear and show that exosomes mediate non-autonomous hair cell survival under ototoxic conditions. These exosomes may hold potential as a new class of therapeutics for hearing loss. We are currently in the process of leveraging their inherent immune-silent characteristics to generate precision-engineered exosomes that target pro-survival pathways in the inner ear.

PS 942

High-Throughput in silico Screening Identified JAK Inhibitors in Preventing Gentamicin Induced Hearing Loss

Zhuo Li[1]; Hao Feng[2]; Marisa Zallocchi[3]; Kan Lin[1]; Jonathan Fleegel[1]; Jian Zuo[4]

[1]Creighton University; [2]Biomedical Sciences Department, Medical School, Creighton University; [3]Creighton University School of Medicine; [4]Department of Biomedical Science, Creighton University

Aminoglycosides (AG) are a class of antibiotics with high potency against gram-negative bacteria. However, one fifth of patients receiving AG treatment suffer from hearing loss and renal failure. Despite their toxic effects, AG are still frequently used because of fast bactericidal effect and low cost. In this study, we employed the Connectivity Map (CMap) to identify drugs that can provide oto-protection against gentamicin. This unbiased *in silico* method explores a broad chemical space and millions of existing transcriptome profiles on pharmaco-genetic perturbations.

CMap is a genomic drug discovery method introduced by Lamb in 2006. It correlates the disease-associated gene signatures to the transcriptomic responses of small molecular perturbations. Tao and Segil recently published the transcriptome signature of neonatal mouse organ of Corti induced by gentamicin (Front. Cell. Neurosci., 9:190, 2015). We therefore focused on 62 differential expressed genes (DEGs), which are also differentially expressed in kidney, they reported to identify small molecules that can induce reverse transcriptome responses from the L1000 platform with the L1000CDS^2 search engine. 50 signatures (23 compounds) constitute our primary hit list for the experimental validation.

We have tested the protective effect of nine compounds (24 signatures) with P3 FVB mouse cochlear explants. Treating explants with 50 µg/mL gentamicin for 24 hours will cause around 50 % hair cell loss of the middle and high frequency regions in the cochlea. The low frequency region of the cochlea is not significantly affected by gentamicin. Eight out of nine tested compounds show protection against gentamicin at various effective concentrations while doxorubicin is toxic to the hair cell. JZ101, a JAK1/2 inhibitor, shows full protection at 40 nM with no detected toxicity up to 200 µM. It also protects zebrafish neuromasts at 165 nM. We also studied the mechanism of action of JAK1 and JAK2 in protecting gentamicin induced hair cell loss with explants, which is not well-characterized before. Because of the excellent therapeutic index, we are studying JZ101 in preventing gentamicin induced hearing loss with 4-week old C57Bl/6 mice.

PS 943

Evaluation of the Otoprotective Properties of Dexamethasone and Sodium Thiosulfate in Response to Cisplatin Treatment of Lateral-Line Neuromasts in Larval Zebrafish

Angela Schrader; Allison Saettele; Mark Warchol; **Lavinia Sheets**
Washington University School of Medicine

Permanent hearing loss occurs in the majority of patients who receive cisplatin chemotherapy. Prior studies have suggested that cisplatin ototoxicity can be reduced by co-treatment with anti-inflammatory glucocorticoids, but it was not clear whether glucocorticoids act directly on hair cells, inflammatory cells, or other cell types within the ear. Additionally, recent clinical data indicate treatment with sodium thiosulfate (STS) protects hearing when administered after cisplatin treatment. In order to identify the efficacy and cellular targets of these protective drugs, we used larval zebrafish to determine whether pre- and co-treatment with dexamethasone (DEX) or post-treatment with STS could reduce hair cell injury and afferent neuron pathology following cisplatin exposure.

Initial experiments characterized the dose- and time-response patterns of cisplatin-induced hair cell death. Fish were treated for 2 hr in 50-1,000 µM cisplatin and allowed to survive in embryo medium for either 2 or 24 hr. At 2 hr survival times, significant hair cell loss was observed only in fish treated with 500 or 1,000 µM cisplatin. Lesioned neuromasts also possessed a robust inflammatory response, as determined by macrophage recruitment. However, fish that survived for 24 hr after cisplatin showed considerable injury in all dosage groups. These data suggest that exposure to relatively low doses of cisplatin can kill hair cells, but that they require ~24 hr for cell death to occur.

We next tested whether treatment with DEX or STS can reduce cisplatin-induced hair-cell death and lateral-line neurite damage. For DEX treatment, zebrafish were exposed to 10 µM DEX for 24 hr, followed by 250 µM or 1,000 µM cisplatin for 2 hr, and then allowed to recover for 24 hr. Counts of immunolabeled hair cells revealed no protective effect of DEX for either dose of cisplatin. The effects of STS were studied by treating fish in 50 µM STS for 24 hr after cisplatin treatment. We observed modest protection against hair-cell loss from 250 µM cisplatin. Moreover, STS treatment following 1,000 µM cisplatin exposure appeared to preserve afferent neurite morphology despite profound hair-cell loss.

These data indicate that cisplatin treatment evokes inflammation, but that co-treatment with dexamethasone does not reduce hair-cell death or neurite damage. STS treatment following cisplatin may provide some protection against hair cell death and preserve innervation. We are currently performing further analysis of STS to determine to what extent STS provides protection from cisplatin-induced lateral-line injury and whether STS acts directly on hair cells and neurons.

PS 944

Small Molecule B-Raf inhibitors Protect Cochlear Hair Cells from Cisplatin Toxicity

Lauryn E. Caster[1]; Matthew A. Ingersoll[2]; Eva M. Holland[2]; **Emma A. Malloy**[2]; Duane Currier[3]; Jaeki Min[3]; Taosheng Chen[3]; Jian Zuo[4]; Tal Teitz[5]
[1]Department of Pharmacology and Neuroscience, Creighton University; [2]Pharmacology and Neuroscience Department, Medical School, Creighton University; [3]Department of Chemical Biology and Therapeutics, St Jude Children's Research Hospital; [4]Department of Biomedical Science, Creighton University; [5]Deaprtment of Pharmacology and Neuroscience

Question
Hearing loss due to cisplatin toxicity, a chemotherapeutic drug, affects an estimated 40-60% of patients, while there is no FDA-approved compound available for treatment. The loss of hearing is caused by damage to the hair cells, spiral ganglia, and stria vascularis in the inner ear. In order to identify compounds that protect hair cells from cisplatin-induced death, screening was conducted using HEI-OC1 cells and a caspase 3/7 activity assay. Cell-based compound screening of 187 specific kinase inhibitors revealed B-Raf as a potential therapeutic target to protect against cisplatin ototoxicity. While initially tested B-Raf inhibitor dabrafenib exhibited a protective effect in the cell line screen and in mouse cochlear explants, additional B-Raf inhibitors from the screen, PLX-4720 and RAF265, were tested to strengthen the protein's potential role in cisplatin toxic insult.

Methods
B-Raf inhibitors PLX-4720 and RAF265 were tested in mouse cochlear explants against cisplatin toxicity. Experiments were done in FVB P3 cochlear explants as described in our previous publication (Teitz et al, JEM 2018).

Results
PLX-4720 and RAF265 showed significant protection from cisplatin in mouse cochlear explants at low concentrations (IC50 ~200 nM and ~30 nM respectively). The inhibitors tested did not show toxicity when explants were treated with the compounds alone (concentrations of 60 μM to 3 μM, therapeutic indexes ~ 300 – 2000 respectively).

Conclusions
B-Raf is a viable target for hearing protection ex vivo in cochlear explants. Ongoing experiments in our lab are designed at testing the protection of the top B-Raf inhibitors against cisplatin- and noise- induced hearing loss in mouse models.

Funding
This work was supported in part by Dr. and Mrs. Randolph Ferlic Summer Undergraduate Research Fellowship to L. Caster and LB692/Creighton and Bellucci Translational Hearing Grants to T. Teitz.

PS 945

Effect of L-N-acetylcysteine and Dexamethasone in an in vitro Model of Inner Ear Trauma

Rahul Mittal[1]; David Shahal[1]; Viraj Shah[1]; Dibyanshi Mishra[1]; Camron Davies[1]; Rahul Sinha[2]; Carolyn Garnham[3]; Jeenu Mittal[1]; Adrien A. Eshraghi[1]
[1]Department of Otolaryngology, University of Miami Miller School of Medicine; [2]University of Miami Miller School of Medicine; [3]MED-EL Hearing Implants, Innsbruck, Austria

Background
The inner ear trauma caused by cochlear implant electrode insertion trauma (EIT) initiates multiple molecular mechanisms in hair cells or support cells resulting in initiation of programmed cell death within the damaged tissues of the cochlea which leads to loss of residual hearing. In earlier studies L-N-acetylcysteine (L-NAC) (an antioxidant), and dexamethasone (Dex) (a steroid) have been shown independently to protect the HCs loss against different types of inner ear trauma. Dexamethasone is a glucocorticoid with anti-inflammatory and anti-apoptotic characteristics. L-NAC is a free radical scavenger, as well as a precursor to the antioxidant glutathione. Glutathione is an important step in the clearance of reactive oxygen species. These molecules have different otoprotective effects. The goal of this study is to test the efficacy of a combination of these molecules to enhance the otoprotection against EIT and determine appropriate dosages.

Methods
OC explants were dissected from P-3 rats and placed in serum-free media. Explants were divided into control and experimental groups. Control group: 1) untreated controls 2) EIT. Experimental groups: 1) EIT+ L-NAC (different concentrations) 2) EIT+ Dex (different concentrations) 3) EIT+ L-NAC+ Dex. In EIT Groups, a 0.28-mm diameter monofilament fishing line was introduced through the small cochleostomy located next to the round window area, allowing for an insertion of between 110° and 150°. After EIT was caused, explants were cultured in media containing L-NAC alone, or Dex alone at decreasing concentrations. Concentrations of L-NAC and Dex that showed 50 percent protection of hair cell loss individually were used as a combination in the experimental group 3. After incubation, the explants were fixed and stained with FITC-phalloidin, imaged by fluorescence microscopy, and viable HCs were counted.

Results
There was decrease of total hair cell count in the EIT explants compared with control group. We identified the dosage of L-NAC, and Dex together for survival of at least 50% protection of hair cells *in vitro*. This combination therapy may be beneficial in other type of inner ear trauma that can result in hair cell loss.

Conclusion
EIT involves oxidative stress and lipid peroxidation early on after the implantation. L-NAC, and Dex are effective alone in protecting the sensory cells *in vitro* at high doses. A combination containing L-NAC, and Dex at much lower doses of each compound, is effective in protecting sensory cells. These compounds can be combined with synergistic effect allowing a decrease of potential side effects of each compound and providing significant otoprotection for EIT.

PS 946

Does Overexpression of the Transcription Factor Pou4f3 Protect Against Noise-induced Hearing Loss?

Jarnail Singh[1]; Michelle R. Randle[1]; Chantz A. Pinder[1]; Luyi Zhou[1]; Brandon C. Cox[2]
[1]Southern Illinois University, School of Medicine; [2]Departments of Pharmacology & Otolaryngology, Southern Illinois University, School of Medicine

Sensory hair cells are killed by multiple insults including exposure to excessive noise, ototoxic drugs, and ageing. The irreversible loss of hair cells in the mammalian cochlea results in permanent sensory neural hearing loss. Recent studies have shown that overexpression of *Atoh1, Islet1, HSP70,* and neurotrophin genes protects or restores hearing function, hair cells, and/or synapses in the adult cochlea. Here, we investigated the possible role of *Pou4f3* to protect hearing and hair cells from noise exposure. We used tamoxifen inducible *Prestin^{CreERT2}:CAG loxP-stop-loxP-Pou4f3-IRES-mCherry* mice to overexpress *Pou4f3* in outer hair cells (OHCs) at 4 weeks of age. Baseline auditory brainstem responses (ABRs) were performed one day prior to noise exposure (8-16 kHz broadband noise at 105 dB SPL for 1 hour), which was given at 5 weeks of age. Hearing function was then evaluated by ABR at either 1 or 2 weeks after noise exposure, followed by temporal bone collection for assessment of hair cell death. OHCs were manually quantified from confocal images of whole-mount cochlear turns immunostained with an anti-myosin VIIa antibody, and Cre-negative littermates were used as controls. Preliminary ABR results at 1 and 2 weeks post-noise exposure show some protection in mice with *Pou4f3* overexpression at 12 kHz, but not at other frequencies tested. Interestingly, there appears to be increased numbers of OHCs in mice with *Pou4f3* overexpression in all turns of the cochlea at 1 week post-noise exposure compared to controls. However, at 2 weeks after noise exposure, there are no differences in the number of OHCs between controls and mice with *Pou4f3* overexpression. While these preliminary data suggest that overexpression of *Pou4f3* might have limited otoprotective effects, there was variable responses among samples and across genders that needs further investigation. In addition, it is well known that inner hair cells (IHCs) are more resistant to multiple insults as compared to OHCs, and studies have shown that *Pou4f3* is expressed at a higher level in IHCs. Therefore, we are also investigating whether reduced *Pou4f3* expression in IHCs makes them more vulnerable to noise exposure.

Funding: NIH/NIDCD R01 DC014441

PS 947

Quinoxaline, its Derivatives, and Application in Otoprotection

Sonia Rocha-Sanchez[1]; Umesh Pyakurel[1]; Shikha Tarang[1]; Santanu Hati[2]; Hazel Taylor[3]; David Z. He[2]; Huizhan Liu[2]; Jian Zuo[4]; Marisa Zallocchi[2]
[1]Creighton University School of Dentistry; [2]Creighton University School of Medicine; [3]Creighton University; [4]Department of Biomedical Science, Creighton University

As society becomes more technologically advanced, the source of noise pollution and availability of ototoxic are rapidly increasing, posing a threat to our hearing health. Although the underlying mechanism by which these compounds affect auditory function varies, they share common intracellular byproducts, particularly the generation of reactive oxygen species (ROS). This knowledge added to recent advancements in our understanding of oxidative stress and its role in hair cell death has led to the rise of a host of antioxidants as potential therapeutic targets. However, to this date, none of these agents are FDA-approved for otoprotection use. Likewise, the spectrum of otoprotective activity of these agents is unknown. Previous studies support the chemoprotective and therapeutic potential of quinoxaline (Qx), a non-steroidal anti-inflammatory compound, to prevent and treat ototoxin-induced hair cell death. Previous in vitro and zebrafish studies supports Qx's variable chemoprotective effect several against several aminoglycoside antibiotics and full protection against cisplatin. To assess Qx's impact in vivo in a mammalian system, we conducted histological and physiological assessments in wild type (WT) C57BL/6J mice treated

with a single intraperitoneal dose of Qx 24 hours followed or not by cisplatin treatment. Consistent with its otoprotective effect and contrasting with the cochleae of animals treated with cisplatin-only, no changes on HC integrity nor decrease in cell numbers were observed in the cochleae of animals treated with Qx alone or pre-treated with Qx followed by cisplatin injections. Likewise, the auditory function of all animals treated only with Qx, or the Qx/Cisplatin combined treatment was preserved as compared to the significant threshold elevation observed in animals treated with cisplatin alone. Next, given Qx' variability against aminoglycosides, we used medicinal chemistry to synthesize a new series of Qx analogs. A total of 37 Qx derivatives were tested in zebrafish. Several of these new compounds performed better than the originally tested Qx, suggesting that modifications of the structure-activity relationship of the quinoline core may be enough to improve protection and specificity against the ototoxic effects of different aminoglycosides. Altogether, these results raise our enthusiasm for the optimization of Qx analogs that can be used to treat and protect hearing in different scenarios.

Support: 1R21OD019745-01A1 (SMRS);
5R01DC015010-04 (JZ)

PS 948

Ebselen Attenuates Amikacin-Induced Ototoxicity in Mice

Rende Gu; Ryan Longenecker; Jennifer Homan; Jonathan Kil
Sound Pharmaceuticals, Inc

Background
Aminoglycosides (AG) such as amikacin are commonly used in CF patients with recurrent pulmonary infections and those infected with multi-drug resistant TB and atypical TB infections. AGs are highly ototoxic, resulting in auditory dysfunction including hearing loss and tinnitus. Prior studies have shown that ebselen can prevent and treat sensorineural hearing loss in animals and humans. While auditory brainstem response (ABR) has been used to assess hearing loss, behavioral models to assess tinnitus and auditory dysfunction have yet to be established. The Acoustic Startle Reflex (ASR) can assess hearing loss, hyperacusis, and tinnitus making it a powerful tool to assess auditory dysfunction. The goal for this study is to establish an ASR methodology for examining the effect of amikacin on auditory dysfunction and the efficacy of ebselen in reducing amikacin-induced ototoxicity in a clinically translatable mouse model.

Methods
CBA/CaJ mice three months of age were divided into two groups which both received amikacin (500 mg/kg/s.c.) daily for 14 continuous days: Group A received injections of ebselen (20 mg/kg/i.p.). Group B received injections of vehicle (DMSO/saline/i.p.). ABRs were performed at baseline, 1 day, 4 and 8 weeks after the end of injections. ASRs were collected at baseline, and 7, 14, 21, 45, and 75 days from the start of injections. ASR tests included input/output functions to assess general hearing and hyperacusis, PPI (Prepulse Inhibition) Audiometry to assess hearing deficits, and GPIAS (Gap-induced Prepulse Inhibition of the Acoustic Startle) to assess tinnitus. Following ASR, hair cell counts were obtained via cochlear histologic analysis.

Results
Following 14 days of amikacin injections, ABR thresholds increased from baseline over the 8-week recovery period with evidence of fluctuations. Input/output ASRs revealed hyperacusis in response to low level stimulation, which was significantly ameliorated by ebselen treatment. Frequency specific PPI deficits were also observed. Gap detection deficits, representing tinnitus, were observed in a smaller subset of animals. Cochlear histology did not reveal significant changes in hair cell counts.

Conclusions
A behavioral model of AG-induced ototoxicity has been developed and offers a new tool to study ototoxicity and otoprotection involving three forms of auditory dysfunction. We show that a 14-day course of amikacin treatment can cause hearing loss, hyperacusis, and to a lesser extent, tinnitus. Ebselen was able to ameliorate amikacin-induced hearing loss and hyperacusis. These data support the clinical testing of ebselen as a potential treatment for the hearing loss, tinnitus, and hyperacusis in patients receiving amikacin.

PS 949

Histological, Physiological, and Behavioral Evidence of Ebselen Mediated Otoprotection in a Mouse Model of Noise-Induced Hearing Loss

Ryan Longenecker; Jennifer Homan; Rende Gu; Jonathan Kil
Sound Pharmaceuticals, Inc

Background
Noise-induced hearing loss (NIHL) is the leading occupational disease in the United States, especially in military populations. Previous works by several labs has shown that ebselen prevents NIHL in mice, rats and guinea pigs, in both acute and chronic periods. To further develop ebselen as an otoprotectant, the acoustic

startle reflex (ASR) mouse model was used to advance our understandings in a behavioral model. Additionally, we wanted to investigate the connection between noise-exposure and biological sex, which has been suggested as important factor in NIHL sensitivity. Ultimately, the goal of this study was to evaluate ebselen-mediated otoprotection using electrophysiological, behavioral, and histological methodologies.

Methods

Three groups (n=10/per group) of awake and unrestrained CBA/CaJ mice were exposed to an octave band noise centered at 8 kHz and presented for 4 hours at 113 dB SPL. Prior to noise, Group 1 received ebselen once po (10 mg/kg/qd), and Group 2 received ebselen twice po (5 mg/kg/bid). The control groups received the same volume of saline/dmso (vehicle). This dosing occurred the day before, the day of, and the day after noise exposure. Hearing was assessed with auditory brainstem response (ABRs) tested at 4,8,16, and 32 kHz, input/output functions, and prepulse inhibition (PPI) plus gap detection assays tested at 4, 8, 12.5, 16, and 20 kHz. These assays were collected before, 1 day, and 2 months after noise exposure. Following hearing assessments, mice cochleae were prepared for hair cell and spiral ganglion analyses.

Results

QD ebselen dosing was more effective at mitigating temporary and permanent threshold shifts than BID or vehicle dosing schedules. Male mice demonstrated greater hearing deficits when assessed with ABR, ASR, and cochlear hair cell counts. These hearing deficits were mostly seen at and above the center of the noise exposure (8-20 kHz) and was also observed with PPI Audiometry, a methodology developed to quickly assess behaviorally hearing sensitivity (Longenecker et al., 2016). Tinnitus was observed in a subset of noise exposed animals, although not as many as in previous studies utilizing a unilateral exposure.

Conclusions

The noise exposure parameters used in this study resulted in significant damage to the cochlea, especially in male mice. QD dosing was more effective at protecting against acute NIHL, especially in female mice. Future studies will examine exposure duration and exposure laterality to test the effectiveness of ebselen as an otoprotectant.

Inner Ear: Fluids & Vasculature

PS 950

Absence of Endolymphatic Sac Ion Transport Proteins in Large Vestibular Aqueduct Syndrome

Andreas H. Eckhard[1]; David Bächinger[1]; MengYu Zhu[2]; Jennifer T. O'Malley[3]; Diane Jones[2]; Barbara J. Burgess[2]; Joseph B. Nadol[4]

[1]Department of Otorhinolaryngology, Head and Neck Surgery, University Hospital Zurich, Zurich, Switzerland; [2]Massachusetts Eye and Ear Infirmary; [3]1) Otopathology Laboratory, Department of Otolaryngology, Massachusetts Eye and Ear; [4]1) Otopathology Laboratory, Department of Otolaryngology, Massachusetts Eye and Ear 2) Department of Otolaryngology, Harvard Medical School

Background

Large vestibular aqueduct syndrome (LVAS), a congenital inner ear disorder, is defined by the pathognomonic features of a widened bony vestibular aqueduct (VA) and an enlarged endolymphatic sac (ES). The pathophysiology of its cochleo-vestibular symptoms remains unknown. Although, the loss of the ion transporters pendrin (anion transporter) and the epithelial sodium channel (ENaC) in the ES was identified as critical for the development of a LVAS phenotype in mouse models. However, human temporal bone studies that translate the findings from these animal studies in the human condition are missing. Here, we investigated the epithelial morphology and epithelial ion transport protein expression in the enlarged ES from archival temporal bone cases with a clinical history of LVAS.

Materials and methods

Formalin-fixed, decalcified, celloidin-embedded tissue sections (CE sections) from two cases from the human temporal bone collection at the Massachusetts Eye and Ear Infirmary were selected, based on the complete preservation of the ES (including the extraosseous ES portion) without signs of artefactual damage. In hematoxylin/eosin-stained sections the epithelial cell morphology of the enlarged ES was investigated and compared to that of the normal extraosseous ES portion. Consecutive tissue sections were immunolabeled for the alpha, beta, and gamma subunits of ENaC, as well as for the macrophage marker ionized calcium binding adaptor molecule 1 (Iba1).

Results

In both cases, (i) the epithelium in the enlarged ES appeared atypically differentiated based on its uncommon squamous-like cell morphology, and its complete lack of ENaC immunolabeling, (ii) a rudimentary extraosseous ES portion with normal cuboidal epithelial cell morphology

and normal ENaC immunolabeling was present, and (iii) the lumen and the perisaccular dural tissue of the enlarged ES exhibited a massive infiltration of immune cells. A large number of those were identified as macrophages, based on positive Iba1 immunolabeling.

Conclusion
The present findings substantiate the hypothesis of a dysfunctional epithelial ion transport in the human enlarged ES as a causal factor in the development of endolymphatic fluid disturbances and inner ear symptoms in LVAS. The absence of ENaC in the human enlarged ES epithelium, in particular, is in line with observed abnormal changes in ENaC expression and endolymphatic sodium transport in mouse models for LVAS. Thus, this study makes important contributions in linking the human condition of LVAS to animal models, and in validating their clinical relevance.

PS 951

Identification of Proteins that Interact with Slc26a4 in Endolymphatic Sac Epithelium

Hyun Jae Lee[1]; Juleh Eide[2]; Cristina Fenollar-Ferrer[3]; Andrew Griffith[4]; Isabelle Roux[2]
[1]Molecular Biology and Genetics Section, National Institute on Deafness and Other Communication Disorders, National Institutes of HealthBethesda, MD 20892, USA.; [2]Molecular Biology and Genetics Section, National Institute on Deafness and Other Communication Disorders, National Institutes of Health, Bethesda, MD 20892, USA.; [3]Molecular Biology and Genetics Section, National Institute on Deafness and Other Communication Disorders, National Institutes of Health, Bethesda, MD 20892, USA., Laboratory of Molecular Genetics, National Institute on Deafness and Other Communication Disorders, NIH, Bethesda, Maryland, USA; [4]Otolaryngology Branch, National Institute on Deafness and Other Communication Disorders, National Institutes of Health

Pendrin, the transmembrane protein encoded by the *SLC26A4* gene, is an anion exchanger highly expressed in epithelial cells of the endolymphatic sac, as well as the stria vascularis and spiral prominence of the lateral wall of the cochlear duct. It is also expressed in the kidney and thyroid. Mutations in *SLC26A4* are a common cause of hearing loss associated with enlargement of the vestibular aqueduct (EVA). In a previous study, we provided direct evidence that fluid absorption occurs in a Slc26a4-dependent manner in the developing mouse endolymphatic sac (Honda *et al. Elife.* 2017). However, the molecular mechanisms mediating Na^+, Cl^-, and water absorption remain unclear. To understand the function and regulation of this pathway, we sought to identify proteins that interact with pendrin in the endolymphatic sac epithelium.

First, we tested whether known partners of other Slc26 family members that mediate Cl^-/HCO_3^- exchange can also interact with pendrin. Two candidates were the Na^+/H^+ exchanger regulatory factor proteins, Nherf1 and Nherf3, that mediate the formation of multiprotein complexes interacting with the carboxy-terminal PDZ motifs of Slc26a3 and Slc26a6. Slc26a3 and Slc26a6 are co-expressed with pendrin in mitochondria-rich cells of the endolymphatic sac (Honda *et al. Elife,* 2017). Although we could confirm their known interactions with Slc26a3 and Slc26a6, Nherf1 and Nherf3 did not show a significant interaction with pendrin in nanoscale pulldown assays (Bird *et al. Mol Biol Cell,* 2017).

Second, we performed yeast two-hybrid screening to agnostically identify proteins interacting with pendrin. We used the intracellular amino- and carboxyl-terminal regions of mouse pendrin as baits to screen an E16.5 mouse endolymphatic sac prey nanolibrary and an adult mouse kidney (age 8-10 weeks) prey library (collaboration with Hybrigenics). One-hundred-eighty-nine potential interacting proteins were identified in these screens. We prioritized candidates with transcripts detected in the same cells expressing *Slc26a4* transcripts using our published endolymphatic sac single-cell transcriptomes (Honda *et al. Elife*, 2017). Candidate interactions were further tested using 1-by-1 assays in yeast (Hybrigenics). We performed the nanoscale pulldown assay to confirm potential pendrin-partner interactions.

We are currently optimizing conventional pulldown procedures for kidney and endolymphatic sac tissues, followed by mass spectrometric analysis, as a complementary approach to identify and confirm pendrin-interacting proteins. We plan future studies to functionally dissect the pendrin interactome, including how it influences pendrin activity and endolymphatic fluid reabsorption in the developing mouse inner ear.

PS 952

Pericytes are vital for mature vascular stability and hearing

Jinhui Zhang[1]; Xiaohan Wang[2]; Zhiqiang Hou[1]; Lingling Neng[1]; Han Jiang[1]; George W. Burwood[1]; Junha Song[3]; Manfred Auer[3]; **Xiaorui Shi**[1]
[1]Oregon Health & Science University; [2]Harvard University; [3]Lawrence Berkeley National Laboratory

Pericytes richly populate small vessels in the adult ear, yet little is known of their function. Using an inducible pericyte depletion mouse model (Pdgfrβ-CreERT2/iDTR),

we demonstrate pericytes are critical for the stability of mature vessel beds and hearing. Pericyte loss causes marked changes in vascular architecture, and parallel loss of hair cells. Most interestingly, we found that pericytes, not pre-existing endothelial cells, converted to tip cells, leads angiogenesis. Pericyte-to-tip cell conversion is strongly dependent on VEGF-A_{165} signaling. Blockage of the VEGF-A_{165} receptor dramatically arrests pericyte conversion and angiogenesis, while upregulation of VEGF-A_{165} production by targeting pericytes with a cre-dependent inversion genetic vector promotes the conversion and angiogenesis. Correspondingly, delivery of an AAV1-VEGF-A_{165} viral vector to pericyte-depleted animals significantly improves vascular function and hearing by promoting pericyte survival and regeneration. This study provides the first clear-cut evidence of the critical role pericytes play in adult ear vascular stability, angiogenesis, and hearing.

Pericytes richly populate small vessels in the adult ear, yet little is known of their function. Using an inducible pericyte depletion mouse model (Pdgfrβ-CreERT2/iDTR), we demonstrate pericytes are critical for the stability of mature vessel beds and hearing. Pericyte loss causes marked changes in vascular architecture, and parallel loss of hair cells. Most interestingly, we found that pericytes, not pre-existing endothelial cells, converted to tip cells, leads angiogenesis. Pericyte-to-tip cell conversion is strongly dependent on VEGF-A_{165} signaling. Blockage of the VEGF-A_{165} receptor dramatically arrests pericyte conversion and angiogenesis, while upregulation of VEGF-A_{165} production by targeting pericytes with a cre-dependent inversion genetic vector promotes the conversion and angiogenesis. Correspondingly, delivery of an AAV1-VEGF-A_{165} viral vector to pericyte-depleted animals significantly improves vascular function and hearing by promoting pericyte survival and regeneration. This study provides the first clear-cut evidence of the critical role pericytes play in adult ear vascular stability, angiogenesis, and hearing.

Acknowledgments
This research was supported by NIH/NIDCD R21 DC016157 (X.Shi), NIH/NIDCD R01 DC015781 (X.Shi), NIH P30-DC005983 (Peter Barr-Gillespie), Medical Research Foundation from Oregon Health and Science University (OHSU) (X.Shi), and P01GM051487-20 (Manfred Auer).

PS 953

Acoustic trauma causes strial vascular degeneration and regional pericyte transition: exogenous pericyte transplantation attenuates the vascular decline

Zhiqiang Hou[1]; Lingling Neng[1]; Jinhui Zhang[1]; Jing Cai[1]; Xiaohan Wang[2]; Ivan Lopez[3]; **Xiaorui Shi**[1]
[1]Oregon Health & Science University; [2]Harvard University; [3]University of California-Los Angeles

Capillary damage and regression after loud sound trauma has long been observed, but the mechanism underlying the pathology has not been understood. In this study, using both *in vivo* animal based and *in vitro* primary cell line based models, we found a small proportion of strial pericytes (PCs) phenotypically convert *(*PC β-*SMA*$^{-}$ to PC β-*SMA*$^{+}$*) b*eginning at approximately 1 week after loud sound stimulation. The number converting slightly increases by 2 weeks. The transition is associated with noise-induced up-regulation of transforming growth factor beta 1 (TGF-β1). The pericyte-myofibroblast transition was suppressed when up-regulation of TGF-β1 was blocked with the TGF-β1 receptor blocker, SB431542. With an *in vitro* primary pericyte cell line model, we demonstrated that increased TGF-β1 robustly induced β-SMA expression in cochlear PCs. Furthermore, with an *in vitro* three-dimensional cell-based EC-PC co-culture model, we demonstrated PCs are essential for maintaining the stability of vascular architecture. The vascular architecture in the model becomes markedly thicker, with less finely articulated branches, when ECs are co-cultured with transformed PCs. With acoustic trauma, reduced capillary density, increased basement membrane protein (collagen IV and laminin) expression, and PC phenotype changes are seen. Moreover, when VEGF-A165 pre-transfected PCs are transplanted to the cochlea 2 weeks following loud sound damage, we found that blood vessel loss was significantly attenuated. These findings provide strong evidence that loud sound triggers regional emergence of myofibroblast-like PCs, which may be one of causes of capillary wall thickening and regression. New pericyte transplantation effectively rehabilitates the vascular defects of loud sound-induced strial vascular degeneration.

Acknowledgments
This research was supported by NIH/NIDCD R21 DC016157 (X.Shi), NIH/NIDCD R01 DC015781 (X.Shi), NIH/NIDCD R01-DC010844 (X.Shi), NIH P30-DC005983 (Peter Barr-Gillespie), Medical Research Foundation from Oregon Health and Science University (OHSU) (X.Shi).

PS 954

Hearing Loss in Congenital CMV Infection: Endocochlear Potential and Lateral Wall Function are Preserved Despite Rampant Inflammation

Keiko Hirose[1]; Song-Zhe Li[1]; Jared J. Hartsock[2]
[1]Washington University School of Medicine; [2]Washington University School of Medicine, St. Louis, MO, USA

Congenital cytomegalovirus (cCMV) is a common cause of hearing loss in newborns and is responsible for morbidity and mortality of infants worldwide. The clinical outcomes of infants with cCMV are highly varied and what determines the severity of illness is not well understood. Many children who are born healthy develop hearing loss over time, and currently there are limited treatments to halt progression of hearing loss in infants known to have cCMV. We have used a mouse model of CMV to explore the mechanism of hearing loss associated with infection during early auditory development.

We have demonstrated a robust cochlear inflammatory response in all infected mice and hearing loss in approximately 50% of mice infected with systemic CMV. Virus is cleared by 21 days after infection, although hearing loss continues to progress well after viral clearance. Hair cells and supporting cells are well preserved in infected animals with hearing loss. Reduction of spiral ganglion density and reduction of inner hair cell synapses have been observed, but it is uncertain if these changes account for threshold shift observed in these animals. We tested the endocochlear potential (EP) in mature mice infected with CMV at birth. We found no significant difference in EP between normal hearing infected mice and those with hearing loss; none of the EPs in CMV infected animals were outside the range of normal. Despite considerable pathology of the cochlear lateral wall, including some disrupted tight junctions and abundant inflammatory cells, the EP is well maintained in animals with CMV associated threshold shift. Thus, the mechanism of virally-induced hearing loss cannot be directly attributed to a deficit in ion recycling or breakdown of the endolymph/perilymph barrier as a result of congenital CMV infection.

PS 955

Suppression of connexin 43 leads to strial vascular hyper-permeability, endocochlear potential drop, and hearing loss

Jinhui Zhang[1]; Xiaohan Wang[2]; Zhiqiang Hou[1]; Lingling Neng[1]; Jing Cai[1]; Han Jiang[1]; **Xiaorui Shi**[1]
[1]Oregon Health & Science University; [2]Harvard University

Connexin 43 (Cx43) is a protein constituent of gap junctions in some barrier cells, especially astrocytes and microglia of the blood-brain-barrier (BBB), where it plays an important role in intercellular communication and barrier regulation. Despite the importance of Cx43 in other blood barriers, not much attention has been paid to expression and function of Cx43 in the blood-labyrinth-barrier (BLB) of the stria vascularis in the cochlea. Using immunocytochemical techniques, we accidentally found Cx43 expressed in capillary endothelial cells (ECs) and perivascular resident macrophages (PVMs) in adult C57BL/6 mouse cochlea. In particular, we found the Cx43 expression in foot processes of PVMs at points of contact with endthelium. Consistent with Cx43 expression *in vivo*, we also found Cx43 expressed in EC-EC and EC-PVM interfaces in a co-cultured cell line model. Using a patch-clamp dye loading technique, we demonstrated that Alexa Fluor® 568 dye injected into PVMs diffuses to connected neighboring ECs. The dye diffusion between the PVMs and ECs can be blocked when the Cx43 channel was blocked by a selective Cx43 blocker, 18β-glycyrrhetinic acid (18βGA). Suppression of Cx43 with small interfering RNA (siRNA) *in vivo* significantly elevated hearing threshold, and caused the endocochlear potential (EP) to drop and the blood barrier to become more permeable. In further study using *in vitro* primary EC cell line models, we identified that suppression of Cx43 disrupts intercellular tight junctions in the EC monolayer and increases endothelial monolayer permeability. Taken together, these findings underscore the importance of Cx43 expression in the normal ear for maintaining BLB integrity, normal EP, and hearing function.

Acknowledgments
This research was supported by NIH/NIDCD R21 DC016157 (X.Shi), NIH/NIDCD R01 DC015781 (X.Shi), NIH/NIDCD R01-DC010844 (X.Shi), NIH P30-DC005983 (Peter Barr-Gillespie), Medical Research Foundation from Oregon Health and Science University (OHSU) (X.Shi).

PS 956

In-depth Proteome of Perilymph in Guinea Pig Model

Yu-Jung Hwang[1]; Jung-Hun Lee[2]; Hye Lee[1]; Dohyun Han[2]; Myung-Whan Suh[3]; Seung-Ha Oh[3]
[1]Department of Otorhinolaryngology, Seoul National University Hospital, Korea; [2]Proteomics Core Facility, Biomedical Research Institute, Seoul National University Hospital, Korea; [3]Department of Otorhinolaryngology-Head and Neck Surgery, Seoul National University College of Medicine, Korea

Introduction
Perilymph fluid is an essential factor to hearing. Damaged sensory cells, supporting cells, or stria vascularis cells in the ST and SV cause sensorineural hearing loss (SNHL). Currently, perilymph proteomics studies have been performed in clinical models. But human serum was not a nice model for studying SNHL, as its protein list did not match well with perilymph proteins. In this study, we investigated perilymph fluid proteome in guinea pig model. Those proteins were Gene ontology (GO) enriched in three categories like above and network model among them were constructed.

Methods
Albino Hartley guinea pigs weighing 300g - 350g with normal hearing were used. Perilymph was collected twice, 2 µl each with a time interval of approximately 30 sec. Purity of perilymph was subjectively estimated from grade 1 to grade 4, based on the color of the sample. Collected perilymph samples were separated by high-pH reversed liquid chromatography. The prepared peptide samples were analyzed by Quadrupole Orbitrap mass spectrometry. MS raw files were processed by MaxQuant software with the Andromeda search engine The gene ontology (GO) enrichment was performed using the DAVID bioinformatics tool. For network analysis, protein-protein interactions (PPIs) of DEPs were interrogated from STRING Database.

Results
1,500 proteins were detected and 1,413 were identified. By its 'add annotation' function and Uniprot search, 1,328 proteins were characterized. GO enrichment was analyzed in three categories; bioprocess, cellular component and molecular. It was followed by 'Regulation of Biological Quality', 'Protein Folding', 'Catabolic Process' and 'Negative Regulation of Hemostasis'. In terms of cellular component, 'Extracellular Region Part', 'Extracellular Region', 'Organelle', 'Cell Junction' and 'Macromolecular Complex' related proteins were observed as highest order of –log(p-value). Perilymph protein counts collected from left and right side of ears were 1,275 and 1,317 respectively. When we compare both left and right groups, no significant difference were found. And the percentage of proteins which both the firstly and secondly collected were sharing was 93.2 %, 1,238 counts.

Discussion
We observed whether there is any different expression of proteins, when the proteome groups are divided into their collection side base, left and right sides, and their collection order base, firstly and secondly collected samples. With our deeper understanding of the perilymphatic protein profiles, we may be able to distinguish specific causes of hearing loss in the future, leading to personalized medicine.

PS 957

Time Course of Blood-Labyrinth Barrier Compromise Following Cochlear Implantation

Alec N. Salt[1]; Daniel Smyth[2]; Jared J. Hartsock[3]
[1]Washington University in St. Louis; [2]Cochlear Limited; [3]Washington University School of Medicine, St. Louis, MO, USA

We have previously reported that intracochlearly-applied fluorescent dextran marker was lost more rapidly from perilymph of animals 24 hrs and 7 days after cochlear implantation than measured immediately (2 hrs) after the procedure. These results suggested that the blood-labyrinth barrier (BLB) could become leakier with time after cochlear implantation. Alteration of BLB permeability is likely to influence drug pharmacokinetics in the ear with either local or systemic applications. In the present study we assessed BLB permeability in guinea pigs by giving a 2-hour intravenous infusion of fluorescein after which perilymph was sampled from both implanted and non-implanted ears. Sequential sampling, taking 10 x 1 µL samples from the cochlear apex of each ear, allowed variations along scala tympani to be demonstrated. Implants were placed through a cochleostomy into the basal turn of scala tympani. Fluorescein levels were compared for perilymph from implanted and non-implanted ears and from ears of non-implanted control animals. When perilymph was taken immediately after implantation (2 hrs) fluorescein levels were not elevated in implanted ears relative to non-implanted ears. This indicates that "insertion trauma" did not cause significant impairment of the BLB. At longer times after cochlear implantation (24 hrs – 14 days), perilymph levels of fluorescein in the implanted ears were consistently higher than non-implanted ears (up to 5x). The spatial distribution of fluorescein along scala tympani was consistent with a distributed entry rather than focal entry near the cochleostomy site. By 28 days the difference between the two ears was reduced, closer to normal. These data demonstrate that the BLB permeability increase following cochlear implantation develops slowly over a few days after implantation. There was a low correlation between BLB permeability increase and hearing loss ($R^2$0.28) but no correlation between hearing loss and time after implantation ($R^2$0.02). In one animal measured 14 days after implantation, perilymph samples from the implanted ear appeared contaminated with erythrocytes, possibly indicating infection, and showed very high fluorescein levels (22x the non-implanted ear and reaching 30% of plasma concentration). Although indicating that under some conditions barrier compromise may be extreme, this animal was atypical and was excluded from the present

analysis. Changes in BLB properties after cochlear implantation may play a factor in drug pharmacokinetics and contribute to post-operative physiological changes affecting outcomes such as electrode impedances, dizziness and possibly loss of residual hearing.

This study was supported by Cochlear Limited.

PS 958

Complehensive analysis of N-glycan in the epithelial-like tissue of the mammalian cochlea

Yoriko Nonomura
Department of Otorhinolaryngology Head and Neck Surgery, Niigata University School of Medicine

Hearing is an essential sensation in animals including human. The cochlea of the inner ear contains an extracellular fluid, endolymph, which exhibits a highly positive potential of +80 mV and a high [K^+] of 150 mM. The electrochemical properties in the endolymph, which are essential for hearing, are maintained by a network of numerous membrane proteins in the stria vascularis. In the stria, we previously detected approximately 1800 kinds of membrane proteins involved in the homeostasis of the endolymph (Eur J Neurosci, 2015).

In general, glycosylation occurs on Asn residue (N-linked) or alternatively on Ser/Thr residue (O-linked) of the proteins. N-linked glycans play pivotal roles in protein folding, trafficking and the modulation of the activities of the membrane proteins. Recent studies have reported the congenital hearing loss caused by the deficiency of the enzymes in N-glycan synthesis. However, little is known about the glycosylation of the proteins in the cochlea. We previously performed the proteomic analysis of the stria and detected 16 enzymes for N-glycan synthesis. In this study, we comprehensively analyzed the profile of the N-linked glycans in the stria vascularis by using a combination of three different HPLCs. Seventy-nine N-linked glycans were identified in the rat stria vascularis. Among these, in 55 glycans, the complete structures were determined; in the other 24 species, partial glycosidic linkage patterns and full profiles of the monosaccharide composition were identified. In the process of characterisation, several sialylated glycans were subjected sequentially to two different alkylamidation reactions; this derivatisation helped to distinguish β2,3-linkage and β2,6-linkage sialyl isomers with mass spectrometry. These resources will be useful to further understand molecular mechanisms underlying the audition and deafness.

PS 959

The organization of the vasculature in the normal and pathological inner ear: Healthy vasculature is important for a healthy hearing

Ivan A. Lopez[1]; Gail P. Ishiyama[2]; Dora Acuna[3]; Xiaorui Shi[4]; Akira Ishiyama[1]
[1]Deparment of Head and Neck Surgery, David Geffen School of Medicine; [2]Department of Neurology, UCLA School of Medicine; [3]Department of Head and Neck Surgery, UCLA School of Medicine; [4]Oregon Health & Science University

Background
We aimed to investigate whether the loss of vasculature in the human cochlea from normal and Meniere's disease specimens is related to the loss of neurons in the spiral ganglia, loss of stria vascularis and general atrophy. We used for this purpose celloidin embedded H&S stained serial sections of the human temporal bone. The normal organization of the arteries and veins has been described as follow (Schuknecht H, Pathology of the inner ear 2010): The arteries that irrigate the stria vascularis come from the external radiating arteriole, the arteries that irrigate the spiral ganglia come from the internal radiating arteriole. The bifurcation come from the primary branch from the main cochlear artery. The posterior spiral vein arrives at the base of the spiral ganglia and bifurcate towards the mid-modiolus and the spiral limbus. It also provides a branch that arrive to the spiral ligament and spiral prominence. Recent studies in the mouse vasculature suggest that aging affects the stria vascularis and the basal portion of the spiral ganglia (Neng L et al., Cell Tissue Res 361:685-96, 2015, Han J, et al, Hearing Res, 371:105-116,2019). In Meniere's disease the utricle vasculature shows pathological changes (Ishiyama et al., Sci Reports 7(1):253, 2017, Frontiers Physiol,9:1068, 2018).

Methods
We examined the vasculature (*arteries and veins*) in serial celloidin embedded sections of 3 normal young age (40-years old (yo) male, 50-yo female, 55-yo male), 3 normal old age (80-yo female, 85-yo male, 89-yo female) and 26 Meniere's disease (unilateral) specimens (ages ranging from 51-95-yo, average 74-yo, 12 female, 14 male). Cochlea images in the mid-modiolus were acquired using a Leica SP8 microscope equipped with a high-resolution camera (Leica DFC7000T). These images allowed to identify changes in the whole cochlea and zooming-in to identify fine morphological details. All images were analyzed blindly by two independent observers, comparisons were made between the normal and Meniere's affected side (hydrops) and contralateral side (non-hydrops).

Results
In all the normal young and old age specimens the vasculature was always present in the normal lateral wall, spiral limbus and spiral ganglia. The organ of Corti shows a normal complement of inner and outer hair cells and supporting cells. In normal old aged cochlea, there was a loss of vasculature in the spiral ganglia neurons (sgns) at the base of the cochlea, the loss of neurons correlates with loss of cells in the organ of Corti. In Meniere's specimens with hydrops there were two types of pathological findings: Group 1 (n=21), loss of spiral ganglia neurons (sgns) and stria vascularis (sv) and group 2: Loss of sgns mainly (n=5). The contralateral non-hydrops side: group 3 (n=13), loss of sgns and sv, group 4 loss of sgns mainly (n=7), and group 5 (n=6), normal sgns and sv. The loss of sgns and/or sv correlated with loss of blood vessels in group 1 to 4, group 5 showed normal vasculature.

Discussion and conclusion
Normal young and old aged specimen's showed healthy structures in organ of Corti, stria vascularis, spiral ligament, spiral prominence, and spiral ganglia neurons. The vasculature (arteries and veins) is well organized in both cases. In Meniere's disease the loss of several structures in the cochlea correlated to the loss of vasculature. These results suggest that healthy vasculature is very important to healthy hearing.

Supported by: NIDCD grant 1U24DC015910-01.

PS 960

Further Application of Light Sheet Microscopy of the Gerbil Cochlea

Kendall A. Hutson; Stephen H. Pulver; Douglas C. Fitzpatrick
Univ. of NC at Chapel Hill

We previously showed our use of light sheet imaged material for counting hair cells and generating a 3-dimensional frequency map on the basilar membrane. Here we show additional applications of light sheet imaging for: cochlear implants, vasculature and that material prepared for the light sheet microscope can be re-hydrated and prepared as a whole mount. All cochleae were decalcified, dehydrated through a series of alcohols and cleared in Spalteholz solution. Specimens were mounted on an acrylic stand and imaged with a LaVison Ultramicroscope II.

Implant Imaging
Fixed gerbil cochleae were implanted with animal electrode arrays. Electrodes were advanced through the round window until resistance was felt, the free end sutured to a vestibular canal and the remainder trimmed away. From the light sheet images, a 3-dimensional view of the electrode path -- as it ascended from the round window through the scala tympani of the first cochlear turn -- could be investigated. We found that the apical lead edge of the electrode's silastic insulation could be located and inspected for translocation into the scala vestibule; and the entire trajectory of the implanted electrode could be examined for possible structural damage caused during insertion.

Vascular Imaging
In immersion fixed material, imaged with a 488 nm laser, many details of the cochlear vasculature can be seen. In 3-dimensional space, the course and relations of the spiral modiolar artery and vein are quite vivid as these vascular structures traverse across each cochlear turn. The intricate anastomoses within the stria vascularis, radiating arterioles, collecting venules and vascular elements of the osseous spiral lamina can all be visualized.

Rehydration and Dissection for Confocal Microscopy
For light sheet imaging, hair cells are immunostained after decalcification, and then enter the dehydration and clearing regimen for the light sheet microscope. We have found that by re-hydrating this material back to buffer, that the basilar membrane can still be dissected out and processed as a whole mount for imaging on the confocal microscope. There was little, if any, degradation of the intensity of immunolabeling. At high magnification, both the hair cell soma and nucleus membranes were intact. Stereocilia of both inner and outer hair cells were readily visible. Thus, the 3-dimensional organization of the cochlea can be studied at the cellular level with the light sheet microscope, and this same material can be taken to the confocal microscope for examination at the subcellular level.

PS 961

In vivo live image of mouse cochlear using two photon microscopy

Seong Hoon Bae[1]; Sang Hyun Kwak[1]; Jinsei Jung[2]
[1]Yonsei university college of medicine; [2]Yonsei University

Objectives
We tried the first in vivo live image of mouse cochlear using two photon microscopy.

Methods
LysM or CXCR1 - GFP transgenic mouse cochlear was exposed by surgical dissection. Two photon laser

scanning microscopy (LSM7MP, Zeiss, Germany) was applied. Movie clip and image of in vivo cochlear was obtained using x20 object lens.

Results

Live image can visualize three different types of cochlear capillary, according to location and morphology. Stria vascularis, Spiral ligament, and cortical vessels. CX3CR1-GFP mouse could show perivascular macrophages in the spiral ligament successfully. LysM-GFP mouse showed rolling neutrophils in the cochlear capillaries after bacterial endotoxin injection with some extravasated neutrophils in spiral ligament.

Conclusion

Using two photon microscopy, we could successfully visualize immune cells and vascular structures of cochlear of living mouse.

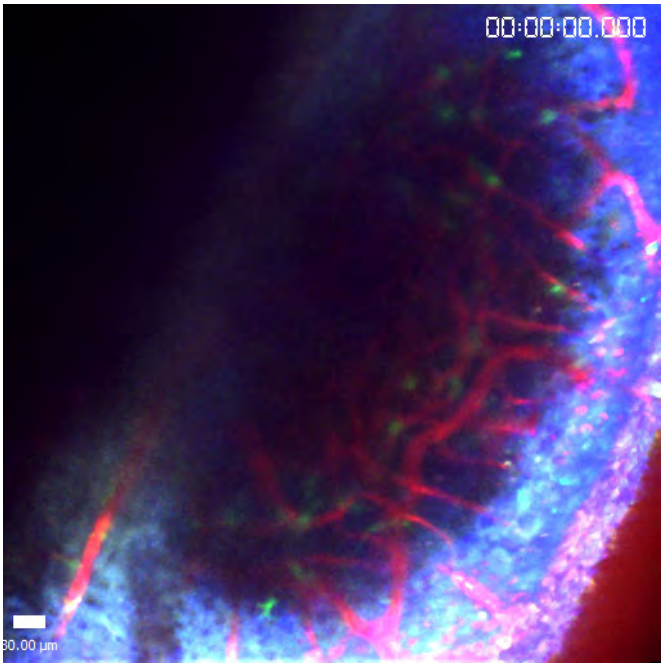

PS 962

A Novel 3D-Printed Head Holder for Guinea Pig Ear Surgery

Chris Valentini[1]; Young Jae Ryu[2]; Betsy Szeto[3]; Michelle Yu[3]; Jeffrey W. Kysar[3]; Anil K. Lalwani[4]
[1]Columbia University Vagelos College of Physicians & Surgeons; [2]Columbia University, Fu Foundation School of Engineering and Applied Science; [3]Columbia University in the City of New York; [4]NewYork-Presbyterian / Columbia University in the City of New York

Background

Many otologic surgeries require fine manipulation of tissues such as the round window membrane (RWM) with a high level of precision such that small head movements from respiration need to be eliminated. Currently, commercially available stereotaxic frames for animal surgery are expensive and rely on ear bars or mouthpieces to secure the head, preventing certain surgical field set ups. We present an economical and effective solution for guinea pig head stabilization during ear surgery that enables the use of a nose cone for anesthesia administration while allowing unimpeded access to the ear. The technical specifications for this 3D-printed photopolymer resin head holder are readily available to any researcher with access to a 3D printer.

Methods

Prototypes were designed using the Solidworks 2019 software and printed using Formlabs Form 2 Printers with photopolymer resin. The head holder consists of a C-shaped brace with adjustable radial inserts of ¼-20 UNC standard screws with shaved tips. Screws can be tightened or loosened anterior to the ear to provide head fixation to animals of various sizes. The C-shaped brace is attached to a rod that can be secured to a commercially available micromanipulator. The head holder design was tested during *in vivo* guinea pig experiments involving insertion of a microneedle into the RWM for one minute while under isoflurane anesthesia administered via nose cone. Head motion with and without the head holder was evaluated visually through stereotactic microscope at 2.4x magnification. Degree of RWM tearing during microneedle insertion served as an additional measure of head holder efficacy in minimizing motion. Confocal microscopy was used to evaluate the potential tears in the RWM.

Results

The head holder design was easy to use and allowed for both nose cone administration of anesthesia and access to the ear for intraoperative auditory testing. Functionally, the head holder successfully minimized head movement during surgery: visual inspection of the guinea pig head under stereotactic microscope confirmed less head motion with the head holder than without. Furthermore, harvested RWMs evaluated at 72 hours following surgery showed smaller resulting perforations in experiments that used the head holder.

Conclusion

Our novel 3D-printed head holder enables simultaneous access for nose cone administration of anesthesia and audiologic testing. Moreover, it provides a modular, intuitive, and economical alternative to commercial stereotaxic devices for minimizing head motion during small animal surgery.

PS 963

Biophysical Model of ATP Dependency of Ion Transport by Marginal and Vestibular Dark Cells

Julia Lasater[1]; **Robert M. Raphael**[2]
[1]University of Pennsylvania; [2]Rice University

The maintenance of a sustained potassium current into the cochlear and vestibular endolymph is an energy intensive process carried out by marginal cells in the stria vascularis and vestibular dark cells at the base of each crista ampullaris and around the utricle. These cells have extensive basolateral infoldings rich in mitochondria and possess a high density of the Na^+-K^+-ATPase pump and function to maintain a high potassium concentration (~150 mm) in the endolymph. The biophysics of marginal/dark cell ion transport processes is not fully understood. To advance this research, we modified a previously developed integrated mathematical model of ion transport across the marginal/dark cells (Qurashi, et al. *Am. J. Phys*. 2007) to include ATP concentration as a new variable, implementing a 15-state Post-Albers model of the Na^+-K^+-ATPase (Oka et al. *J Theor. Biol*. 2010). This model includes explicit affinities for Na^+ and K+ on both sides of the membrane as well as voltage dependence of dissociation constants. The model was implemented in Matlab and contains mathematical expressions for known ion transporters at the basal and apical faces of the marginal/dark cell. This extended model allows us to simulate the effects of energetic depletion by studying how potassium transport across the epithelium depends on ATP concentration. The results indicate that the current carried by the Na^+-K^+-ATPase ($i_{K,pump}$), the K^+ carried by the Na^+-K^+-Cl^- cotransporter (NKCC1) ($i_{K,NKCC}$) and the net K^+ current across the epithelium (i_K^{te}) all begin to decline when the ATP concentration on the basolateral side falls below 1 mM. Of particular physiological significance is that the model predicts that i_K^{te} reverses direction as ATP levels fall, meaning that potassium will be transported out of the endolymph. The model permits analysis of the effects of NKCC1 density, maximal K^+ permeability in the apical membrane, Na^+ permeability in the apical membrane, and basolateral Cl^- conductance on epithelial function. The influences of extracellular K^+ and Cl^- on the transepithelial K^+ current and the effects of genetic mutations in channels such as KCNQ1/KCNE1 that give rise to deafness and noise-induced hearing can also be simulated. Overall, the inclusion of ATP as a variable in the computational model advances our understanding of the function and dysfunction of ion transport in the inner ear.

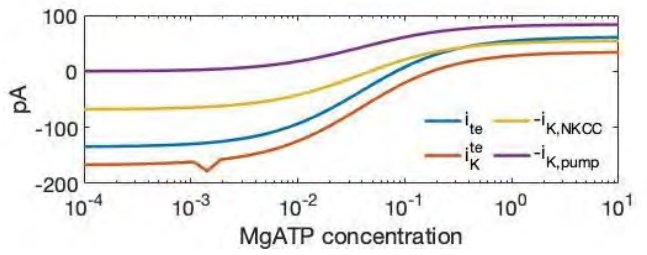

PS 964

Novel 3D-Printed Hollow Microneedles Can Facilitate Safe and Reliable Aspiration of Perilymph for Proteomic Analysis

Betsy Szeto[1]; Chris Valentini[2]; Aykut Aksit[1]; Michelle Yu[1]; Emily G. Werth[1]; Lewis M. Brown[1]; Elizabeth Olson[3]; Jeffrey W. Kysar[1]; Anil K. Lalwani[4]
[1]Columbia University in the City of New York; [2]Columbia University Vagelos College of Physicians & Surgeons; [3]Columbia University; [4]NewYork-Presbyterian / Columbia University in the City of New York

Background

Inner ear diagnostics is limited by the inability to atraumatically obtain samples of cochlear fluid. The round window membrane (RWM) is an attractive portal for accessing perilymph samples as it has been shown to heal within 1 week after the introduction of microperforations. A 1 ul volume of perilymph is adequate for proteomic analysis, yet the total volume of perilymph within the scala tympani of the guinea pig is limited to less than 5 ul. This study investigates the safety and reliability of a novel hollow microneedle device in aspirating perilymph samples sufficient for proteomic analysis.

Methods

The guinea pig RWM was accessed via a postauricular surgical approach. 3D-printed hollow microneedles with an outer diameter of 100 um and an inner diameter of 35 um were used to perforate the RWM and aspirate 1 ul of perilymph. Perilymph samples were analyzed by liquid chromatography-mass spectrometry-based quantitative proteomics. Hearing was assessed before and after aspiration using compound action potential and distortion product otoacoustic emissions. RWMs were harvested 72 hours after aspiration and evaluated for healing using confocal microscopy.

Results

Over 400 proteins were detected per 1 ul sample of perilymph. The inner ear protein cochlin, widely recognized as a perilymph marker, was detected in both samples tested to date. There was no permanent damage to hearing, and perforations healed completely by 72 hours.

Conclusion
Hollow microneedles can facilitate aspiration of perilymph across the RWM at volumes adequate for proteomic analyses without causing permanent anatomic or physiologic dysfunction. The ability of microneedles to mediate safe and effective intracochlear sampling in the guinea pig suggests great promise for their potential application in inner ear diagnostics in humans.

Inner Ear: Synapses & Auditory Nerve

PS 965

Probing the Role of Neuroligins 1 and 3 among the Cochlear Synapses

Miguel A. Ramirez; Jeffrey N. Savas
Northwestern University Feinberg School of Medicine

Neuroligins (Nlgn) are trans-synaptic adhesion proteins that physically link pre and postsynaptic membranes, in addition to aiding in synaptic specification. Interestingly, Nlgn 1 and 3 single knockouts (KOs) have been shown to alter glutamatergic synaptic transmission among central nervous system synapses. Additionally, both Nlgn1 and 3 have been shown to have synaptogenic properties. However, despite their key roles as regulators of synaptic activity, and involvement in synaptic development, Nlgns have gone largely uncharacterized among the cochlear ribbon synapses. Thus, we aim to determine how Nlgns 1 and 3 contribute to hearing and potentially increase our understanding of possible mechanisms underlying temporary hearing loss.

Immunofluorescence (IF) experiments were conducted that aimed to determine potential localization patterns for Nlgns 1 and 3 throughout the 8-24 kHz regions of the mouse cochlea. The resulting puncta were then analyzed using AMIRA 3-D reconstruction and quantitated using MATLAB. Auditory brainstem response recordings (ABR) and distortion product otoacoustic emissions (DPOAE) were conducted to verify the functionality of the inner and outer hair cells, respectively. From ABRs, we collected data from click and tone stimuli to determine if there were deviations in threshold levels, latency, and Wave I amplitudes in Nlgn 1 or 3 KOs compared to WT littermate controls.

Nlgn 1 and 3 co-localization with ribbon synapse markers was verified by IF and provided preliminary measures for Nlgn protein levels throughout the cochlea. Wave I amplitudes obtained by ABR tone and click were both significantly reduced in Nlgn3 KOs compared to WT littermates. This reduction in ABR activity was not a result of decreased outer hair cell function as DPOAEs were unaltered. Future experiments will explore how Nlgns 1 and 3 contribute to cochlear synaptogenesis, synaptic transmission, and cochlear synaptopathy. Given the role for Nlgns throughout development, obtaining information regarding Nlgn abundance at ages correlated with major developmental time points, such as the onset of hearing, are necessary. However, given the challenges in measuring low abundance proteins within the cochlea by western blot or mass spectrometry (MS). We are designing a two-step method pairing in-gel purification and parallel reaction monitoring (PRM) via tandem MS/MS. Which would significantly increase our ability to detect low abundance proteins within the cochlea. Together, these experiments provide a necessary first step towards the characterization of Nlgns 1 and 3 within ribbon synapse physiology and are likely to reveal previously underappreciated roles for Nlgns in hearing.

PS 966

The Role of CaBP1 and 2 in Hair Cell Synaptic Function

David Oestreicher[1]; Vladan Rankoviβ[2]; Tina Pangršiβ[3]
[1]Experimental Otology Group, Department for Otolaryngology and Institute for Auditory Neuroscience and InnerEarLab, University Medical Center, Göttingen, Germany; [2]AuditoryGerman Primate Center, Leibniz Institute for Primate Research, Göttingen, Germany, 3Institute for Auditory Neuroscience and InnerEarLab, University Medical Center, Göttingen, Germany, 4Collaborative Research Center 889 "Cellular Mechanisms of Sensory Processing", Göttingen, Germany; [3]Experimental Otology Group, Department for Otolaryngology and Institute for Auditory Neuroscience and InnerEarLab, University Medical Center, Göttingen, Germany, Collaborative Research Center 889 "Cellular Mechanisms of Sensory Processing", Göttingen, Germany

Voltage-gated Calcium channels $Ca_V1.3$ are driving presynaptic calcium influx in mammalian inner hair cells (IHCs) and thus are essential for stimulus secretion coupling. The $Ca_V1.3$ channels in IHCs show remarkably little inactivation, which is important for the signaling of ongoing sound stimulation. Hereby, CaBPs might play an important role for $Ca_V1.3$ modulation, as they shape presynaptic calcium signals by binding to voltage-gated calcium channels and reducing their inactivation upon cell depolarization. Four members of the CaBP family are co-expressed in IHCs: CaBP 1, 2, 4 and 5. So far, only mutations in CaBP2 were found to lead to hearing impairment in humans (DFNB93), which is characterized by moderate to severe low- to mid-frequency hearing loss. It was proposed that the lack of functional CaBP2 through pronounced inactivation of $Ca_V1.3$ reduces the availability of Ca^{2+} channels for triggering neurotransmitter release upon arrival of sound stimulus, degrading the temporal precision of sound encoding and

thus leading to hearing impairment. It is however not understood, how the different CaBPs work together in regulating the IHC Ca^{2+} currents and supporting hearing.

Using systems physiology (auditory brainstem response (ABR)), immunohistochemistry and *in vitro* IHC patch-clamp, we are investigating the role of different CaBPs at IHC synapses of Cabp1, Cabp2 and double Cabp1 and 2 knockout (KO) mice. Moreover, we are aiming to develop a novel gene delivery-based therapy approach for DFNB93.

We analyzed presynaptic function of IHCs through patch-clamp measurements of calcium and barium currents and monitored exocytosis by measuring changes in membrane capacitance. These measurements demonstrate pronounced VDI and CDI of Ca^{2+} currents in IHCs of CaBP1/2 double knockout (DKO) mice, which significantly reduces exocytosis, while isolated deletion of CaBP1 leaves IHC synaptic function unperturbed.

We further attempted to rescue IHC presynaptic function and hearing in Cabp2 knock-out mice by AAV2/1-mediated gene transfer of Cabp2 into IHCs. Auditory brainstem recordings show a partial improvement of hearing in approx. 60% of injected animals, which may be due to decreased inactivation of calcium channels.

We conclude that the functions of CaBP1 and CaBP2 are partially redundant: the loss of CaBP1 on its own does not affect IHC Ca^{2+} currents, but concomitant loss of CaBP2 significantly enhances the Ca^{2+} current inactivation. CaBP2 modulates both, VDI and CDI of IHC $Ca_V1.3$ channels, however its effects on CDI are obscured in the single CaBP2 KOs due to compensation by other CaBPs. Intracochlear delivery of CaBP2-encoding AAVs robustly targets postnatal IHC in vivo and leads to a significant improvement of hearing performance in a mouse model for DFNB93, thereby implicating CaBP2 as a clinically-relevant gene therapy target.

PS 967

Hearing function and ribbon synapses in mice lacking Slack channels after mild to moderate noise trauma

Pauline Schepsky[1]; Kerstin Blum[1]; katharina Sorg[2]; Dietmar Hecker[2]; Robert Lukowski[3]; Bernhard Schick[2]; Peter Ruth[3]; Simone Kurt[4]; Jutta Engel[1]
[1]Saarland University, Department of Biophysics and CIPMM, Homburg, Germany; [2]Saarland University, Department of Otorhinolaryngology, Homburg, Germany; [3]University of Tübingen, Department Clinical Pharmacy,Tübingen, Germany; [4]Saarland University, Department of Biophysics and CIPMM, Homburg

Slack (Slo2.2, gene *Kcnt1*) is a Na^+- and voltage-activated potassium channel that reduces neuronal excitability in response to neuronal activation and Na^+ influx. Slack mRNA and Slack currents have been described in spiral ganglion neurons (SGN), and mice deficient for both Slack ($^{-/-}$) and Slick (Slo2.1, gene *Kcnt2*) showed reduced ABR wave I amplitudes at 6 weeks of age despite normal thresholds (Reijntjes et al., Scientific Reports 2019).

The function of Slack channels expressed in spiral ganglion neurons for hearing is unknown. $Slack^{-/-}$ mice showed normal ABR thresholds and normal DPOAE amplitudes at 14 weeks of age. To test whether Slack channels are required for reliable signal transmission under conditions when the auditory system is challenged by a mild or a moderate acoustic trauma, $Slack^{-/-}$ and $Slack^{+/+}$ mice on C57BL6/N background were subjected to 100 or 106 dB SPL band noise (8 – 16 kHz) for two hours. The shift in hearing thresholds was assessed directly after the trauma and between one and 28 days after trauma. Thereafter, inner hair cells were analyzed for numbers and for the pairing of presynaptic ribbons (CtBP2) and postsynaptic protein (HOMER1) clusters along the cochlear length. While the ABR thresholds and recovery performance of wild type and knockout mice after the mild trauma barely differ, recovery from noise trauma, ABR wave I amplitudes and the fate of ribbons in $Slack^{-/-}$ mice and $Slack^{+/+}$ controls under the higher trauma conditions are currently being analyzed.

Supported by IRTG 1830/2

PS 968

Na+ Accumulation in Dendritic Projections Occur in the Absence of Na+- Activated K+ Channels and Reduce Action Potential Conduction Velocity

Seojin Park[1]; Maria Cristina Perez-Flores[1]; Jeong Han Lee[2]; Mincheol Kang[3]; Xiao-Dong Zhang[4]; Hannah A Ledford[4]; Nipavan Chiamvimonvat[4]; Victor Matveev[5]; Ebenezer N. Yamoah[2]
[1]University of Nevada, Reno; [2]University of Nevada,Reno; [3]University of Nevada Reno; [4]University of California Davis; [5]New Jersey Institute of Technology

The source of Na+ for KNa channel activation can have an immense impact in neurons. Unlike Ca2+ in which the extracellular and intracellular concentration difference is ~104-fold, that of Na+ is only 10-fold. The binding constant of the KNa channel for Na+ is ~20-30 mM, suggesting that the safety factor for channel activation is narrow. The constrains of Na+ sources and diffusion, the mechanisms by which intracellular Na+ concentrations rise to activate KNa channels under physiological conditions remain unexplained and controversial. The

major source for Na+ entry is through voltage-gated Na+ channels (Nav). For Na+ concentration to rise upon entry to levels expected to activate KNa channels, substantially, several conditions should be met; 1) The Na+ source should be sustained as would be expected from persistent and resurgent Na+ current. 2) The neuron may be endowed with Na+ buffers with diverse capacity. 3) In a restricted Na+ diffusion domain such as dendrites, it is conceivable that Na+ concentration may rise faster than its clearance to reach KNa activation levels. Paradoxically, in rat dorsal root ganglion, small-diameter neurons, KNa current stabilizes the resting membrane potential but does not participate in shaping single action potential (AP) profile, while in medium-diameter neurons, the current contribute towards the depolarizing after potential of single APs. These contrasting results raise the possibility that multiple and competing factors control Na+ regulation and availability to activate KNa. We found distinct localization of KNa and Nav1.6 mRNA and protein expression, but not Nav1.2 channels, in postsynaptic axons/dendrites of spiral ganglion neurons (SGNs). We report a unique specificity of physical coupling, such that KNa and Nav1.6 are < 20 nm apart. Indeed, the spatial association between KNa and Nav1.6 establishes Na+ domain at the afferent axonal terminals, which regulate AP firing, shown experimentally and in silico. These findings were confirmed using FRET and biochemical analyses. The physical and functional selective coupling between KNa and Nav1.6 channels in SGN afferent type I axons yield well-timed AP conduction, such that null deletion of Kcnt1/2 increased jitters in conducted APs. Next, reduction or elimination of KNa currents resulted in increased dendritic Na+ concentration enough to reduced Na+ current driving force and conduction velocity. These findings are among the first evidence to show local coupling between KNa and Nav channels and illustrate the functional importance of privileged submembrane Na+ domain.

Funded by the NIDCD and NIA (DC016099; DC015135; DC006685; AG060504; AG051443).

PS 969

The Differential Firing Pattern of Type II Spiral Ganglion Neurons

Maria Cristina Perez-Flores[1]; Jeong Han Lee[2]; Seojin Park[3]; Mincheol Kang[1]; Yingying Chen[2]; Ebenezer N. Yamoah[2]
[1]University of Nevada Reno; [2]University of Nevada,Reno; [3]University of Nevada, Reno

The mature mammalian cochlea exhibits segregated innervation of its two populations of sensory hair cells by the spiral ganglion neurons (SGNs), the primary auditory neurons. SGNs comprises of two distinct population. Myelinated type I SGNs represent ~95% of the afferent neuron population and extend one peripheral process which forms a single synapse with one inner hair cell (IHC). The type II SGNs are unmyelinated and constitute only 5-7% of the afferent neuron population, and they receive synaptic inputs from ~9 outer hair cells (OHCs). Type I neurons have been extensively characterized because they outnumber type II neurons (~20-fold). In contrast, type II neurons have small-size and thin-axons, making them difficult for in vivo recording.

Type I and II SGNs consist of molecularly distinct cell populations. Type I neurons are classified into three molecular subtypes with additional variations existing across the tonotopic axis. In type II neurons an average of 6,320 genes/cell were detected. Even if such a molecular profile can be used for subtype classification, further functional characterization remains unknown. Recent studies in type II fibers suggest that they may mediate the sensation of auditory pain. However, their very extensive neurite projection from the soma is not amenable for adequate current and voltage-clamp characterization. In this work we have identified strategies to record from the bonafide type II neurons, we have benefited from the fact that; a) the neurons are unmyelinated which is an advantage to use patch-clamp strategies; b) as type II is peripherin positive, we could potentially use EGFP-positive transgenic mouse model to isolate type II SGNs and identify them accurately. In this work, we took advantage of the transgenic mouse model to provide evidence that; 1) all peripheral neurons express peripherin at early stages, and this expression is time-dependent. 2) In 3-5 weeks old mice, peripherin expression remains specifically in type II neurons. Myelination of type I neurons suppresses peripherin expression. 3) In culture, after 24 hr the number of peripherin-positive neurons increased in a time-dependent manner, as myelin detached from type I neurons. Thus, removal of myelin may trigger EGFP expression in the transgenic mouse model. For this reason, we only recorded from peripherin-positive neurons maintained in culture for less than 12 hr. 4) type II neurons expressed heterogeneous firing properties, from fast, moderate adapting and a group of small-size neurons which displayed spontaneous firing activity. These results revealed new insights into the functional significance of type II SGNs.

This work was supported by the NIDCD and NIA (1R01 DC016099; 1R01DC015135; AG060504).

PS 970

Distribution of Inner Hair Cell Efferent Synapses in the Murine Cochlea Across the Life Span

Anna Dondzillo[1]; Hiroki Takeda[2]; Samuel P. Gubbels[1]
[1]University of Colorado Denver, Anschutz Medical Campus; [2]Department of Otolaryngology-Head and Neck Surgery, Kumamoto University.

Presbycusis or age-related hearing loss (ARHL) is characterized by progressive worsening of hearing abilites and difficulties in understanding speech in the presence of noise. Presbycusis affects one in four people of the US population aged 60-69(1). Growing anatomical and physiological evidence suggests that at least one aspect of presbycusis, speech understanding in noise, might be caused by hair cell synaptic rearrangements.

The outer hair cells (OHCs) receive axosomatic input from contralateral Medial Olivocochlear (MOC) neurons. The inner hair cells (IHC) do not receive direct input, but rather their afferents, receive inhibitory input from the ipsilateral Lateral Olivocochlear (LOC) neurons. In contrast, in young mammals, inner hair cells receive temporary, inhibitory cholinergic input from the contralateral MOC neurons, which deactivates at around hearing onset in mice. In the last decade, pivotal studies using electron microscopy and whole-cell patch-clamp electrophysiology have shown that cholinergic inhibitory synapses re-appear on IHCs in the aged cochlea(2,3). These findings open the possibility of a novel mechanism of IHC modulation in the aging cochlea. However, the findings are based on the apical, low-frequency region of the cochlea, and therefore are not amenable to generalization about the entire cochlear duct. Furthermore, any hypothesis as to the potential function of the efferents in hearing is hard to formulate until we understand the scale of this phenomenon in the entire cochlea. Here we aim to find out whether a similar increase in the number of efferent synapses occurs across the entire cochlea.

We examined inner hair cells and their efferent synapses in apical, middle, and basal cochlear turns in C57BL/6 mice at three age groups. Using antibodies to presynaptic SV2 protein to label efferent presynaptic compartments and anti-Myosin 7a antibody to identify hair cells we studied this efferent synapse using laser confocal microscopy and a machine learning algorithm. We found that the number of efferents differs between cochlear turns, with the highest number in the old cochlea in the basal turn. Our preliminary data suggests that using a machine learning approach to identify fluorescently labeled cells and clusters of anti-synaptic antibody is a helpful tool in large scale confocal data analysis.

PS 971

Neurotrophin 3 (NT3) Expression by Cochlear Supporting Cells Modulates Gap Detection and Neuronal Activity in the Dorsal Cochlear Nucleus

Lingchao Ji[1]; Calvin Wu[1]; David T. Martel[2]; M. Charles Liberman[3]; Susan Shore[1]; Gabriel Corfas[1]
[1]University of Michigan; [2]University of Michigan, Ann Arbor; [3]Harvard

We previously showed that Neurotrophin 3 (NT3) derived from cochlear supporting cells regulates the formation of synapses between inner hair cells (IHCs) and type I spiral ganglion neurons (Wan et al., eLife 2014). Specifically, NT3 over-expression increases IHC synapse numbers and enhances ABR peak 1 amplitudes; whereas, decreased NT3 levels reduces the number of IHC synapses and peak 1 amplitude. These results suggested that NT3 levels could influence auditory processing. To explore this, we tested the behavioral and physiological phenotypes of these transgenics, focusing on pre-pulse inhibition (PPI) or gap inhibition of the startle response, as well as spontaneous and sound-evoked neural activity in the dorsal cochlear nucleus (DCN).

Mutant and control mice were injected with tamoxifen daily from P1–P7. At 8 weeks, ABRs and DPOAEs were measured, along with startle responses, to assess stimulus detectability, sensory gating and temporal processing. Single-unit recordings from DCN were analyzed for response gain, spontaneous rate, and cross-unit synchrony. Finally, NT3 mRNA levels in the cochlea were measured by real-time quantitative RT-PCR.

As shown previously, postnatal NT3 knockdown or overexpression from supporting cells respectively reduces or enhances suprathreshold ABR without changing ABR or DPOAE thresholds. Remarkably, mice with reduced NT3 showed reduced gap inhibition, but only when the gap immediately preceded the startle. Correspondingly, NT3 overexpression enhanced gap inhibition, suggestive of enhanced auditory acuity. Importantly, NT3 levels did not influence either the amplitude or threshold of the startle reflex or PPI of the startle response. While NT3 levels did not affect sound-driven activity in DCN, spontaneous firing rates and cross-unit synchrony was significantly increased in the NT3 overexpressing mice but only those with enhanced gap detection (50%). A smaller proportion of NT3 knockdown mice also showed increased neural synchrony, but the increase was less extensive than that in NT3 over-expressers and did not correlate with altered gap detection. Real-time quantitative RT-PCR

verified the changes in NT3 expression in both mutant lines. Importantly, relative NT3 expression levels correlated with ABR P1 amplitude and the magnitude of gap inhibition and DCN spontaneous activity. Together, these results indicate that changes in ABR1 peak 1 amplitudes caused by supporting cell NT3 knockdown or over-expression lead to altered sound coding in DCN, which could contribute to the gap-detection deficiency or enhancement.

Research supported by grants from NIDCD (R01 DC004820 and R01 DC017119) and the American Tinnitus Association

PS 972

Position Dependence of Synaptic Volume in the Organ of Corti under Different Conditions

Jay A. Gantz[1]; Jason Carlquist[1]; Babak V-Ghaffari[1]; Mark Rutherford[2]
[1]Department of Otolaryngology - Head & Neck Surgery, Washington University School of Medicine; [2]Department of Otolaryngology-Head & Neck Surgery, Washington University

The ways in which synaptic activity regulates the morphology and function of the afferent connections between cochlear inner hair cells (IHCs) and auditory nerve fibers (ANFs) is unclear. We examined how synaptic activity affects synapse morphology before and after noise exposure using vesicular glutamate transporter-3 (Vglut3) knockout mice, with attention to synapse size and position on the IHC.

Methods
Cochlea from WT or Vglut3 KO mice were imaged either before, one day, or two weeks after two hours of 100 dB, 8–16 kHz noise exposure. We developed a reproducible and robust workflow to measure and compare the 3D morphology of presynaptic ribbons (anti-CtBP2) and postsynaptic AMPA receptors (AMPARs, anti-GluA3) across experimental groups using confocal immunohistofluorescence microscopy. We used Imaris image processing software to define synapses as surface objects, and a custom Matlab procedure to pair presynaptic ribbons with postsynaptic AMPARs, as well as to remove unpaired or erroneously paired objects. Synapse position on the modiolar-pillar and habenular-cuticular axes was measured, and synapses were assigned to one of four quadrants.
Results
In general, we observed that when IHCs have fewer synapses, the synapses tend to be larger in volume. Tonotopically, WT ribbons were fewer and larger in the cochlear apex than mid-cochlear region. KO ribbons, which are similar in number between apex and mid-cochlea, did not show consistent tonotopic difference in volume. GluA3 did not consistently differ in volume tonotopically, except for enlargement in the modiolarβcuticular quadrant of apical WT IHCs. By genotype, ribbons and GluA3 clusters were significantly fewer and larger in KO than WT in all cases: in the apical and mid-cochlea, in unexposed mice, and also 1-day and 2-weeks after noise exposure. Noise exposure resulted in fewer, larger ribbons in the WT midcochlea at 2-weeks after exposure for all IHC quadrants; while WT apical ribbons increased in volume only in the modiolar quadrants. WT AMPAR volumes did not show such changes. Enlargement of KO ribbons by 2-weeks after noise was less than WT, and only seen in the modiolar quadrants. AMPARs of the KO increased in volume by 2-weeks after noise only in the modiolarβcuticular quadrant. Ribbons and AMPARs were bigger on the modiolar than the pillar side of the IHC in WT but not KO. In the apical cochlea of WT, ribbons and AMPARs displayed an inverse gradient along the habenular-cuticular axis, where GluA3 was larger on the cuticular side and ribbons were larger on the habenular side. After noise, these spatial gradients were diminished.

Conclusions
Overall, synapse number and size tended to be inversely correlated at the hair cell level (comparing tonotopic location, WT vs. KO, and pre- vs. post-noise exposure). When comparing quadrants within cells we observed the opposite: the modiolarβhabenular quadrant had both the largest number of ribbons and the largest ribbon volumes. Some differences in synapse morphology can be attributed to glutamate activity (global genotypic differences in synapse size and number, subcellular spatial trends seen in WT only), while others appear independent of glutamatergic transmission (KO ribbon and AMPAR size changes after noise exposure).

PS 973

Three-dimensional electron microscopy of inner hair cell synapse and afferent morphology from hearing onset to maturation

Shelby Payne[1]; Natalie Skigen[1]; Jason Carlquist[1]; Sonali Gattani[1]; Guhan Iyer[1]; Bethany Davis[1]; Honey Patel[1]; Allison Schwed[1]; Heather Chung[1]; Matt Nester[1]; Atri Bhattacharyya[1]; Mark Rutherford[2]
[1]Department of Otolaryngology - Head & Neck Surgery, Washington University School of Medicine; [2]Department of Otolaryngology-Head & Neck Surgery, Washington University

The inner spiral plexus is a complex neuropil where synapse morphology changes during postnatal

development. Serial electron microscopy (EM) sections of the cat cochlea showed morphological differences among ribbon synapses and auditory nerve fibers (ANFs), supporting a widely accepted classification scheme where ANFs on either side of the IHC have different morphologies, sound-response thresholds, and spontaneous rates (Liberman 1978, 1980). In mouse, the correlation between sound-response properties and synapse/ANF morphology is not established and serial EM reconstruction of the inner spiral plexus has not been performed. To study the position-dependence of synaptic properties, we mapped 3D coordinates of inner hair cell (IHC) afferent synapses in spatial dimensions aligned relative to the IHC axes, or, aligned relative to the organ of Corti axes. Modiolar side synapses of one IHC can occupy the same relative position in the modiolar-pillar axis of the organ of Corti as pillar side synapses of a neighboring IHC.

Using a serial block face technique (focused ion beam scanning electron microscopy, FIB-SEM), we acquired ~(30 μm)^3 regions of the IHC-ANF synapses, ½ turn from the apex, at a characteristic frequency of ~11 kHz from C57BL/6J mice at p17, when synapse and spike-generator structure and function are not entirely mature (Wong et al., 2014, Kim and Rutherford, 2016), and at p34, when the cochlea is functionally and anatomically mature. With 7 nm isotropic voxels (X, Y, and Z), we segmented structures with AMIRA, created reconstructions, and designed custom tools to measure the presynaptic ribbon, presynaptic and postsynaptic densities, and afferent and efferent neurons.

At p17 we did not observe a significant difference in ribbon volumes between modiolar- and pillar-side synapses at the 11 kHz tonotopic location, consistent with measurements of ribbon volume based on confocal immunofluorescence of CtBP2 from the 11 kHz location in p18 CBA/CaJ mice (Liberman and Liberman, 2016). We measured the distances between the outermost edges of the ribbon body to the synaptic cleft as an unbiased measurement of synapse shape and size. Pillar-side synapses (335 ± 160 nm) had greater average ribbon-cleft distances than modiolar-side synapses (256 ± 106 nm), using the IHC reference frame. Ribbons near the base of the IHC at p17 have the shortest nearest neighbor distances (2.67 ± 0.35 μm), smaller afferent fiber diameters, and smaller median distances between the ribbon and cleft compared to ribbon synapses elsewhere.

Measuring the diameters of each fiber of an IHC at p17 in the IHC reference frame: fibers synapsing onto the base of the IHC have smaller diameters (1706 ± 155 nm) than those synapsing nearer to the nucleus, and modiolar-side fibers were smaller in diameter (1852 ± 162 nm) than pillar-side fibers (2087 ± 154 nm). Comparing presynaptic ribbon, presynaptic and postsynaptic density, and afferent morphology between p17 and p34, we will further quantify the afferent synapses using the IHC reference frame and the Organ of Corti reference frame.

PS 974

Electrophysiological Markers of Cochlear Nerve Function Correlate with Hearing-In-Noise Performance among Audiometrically Normal Subjects.

Kelsie J. Grant[1]; Anita M. Mepani[1]; Kenneth E. Hancock[2]; M. Charles Liberman[3]; **Stéphane F. Maison**[2]
[1]Eaton-Peabody Laboratories, Mass Eye & Ear; [2]Eaton-Peabody Laboratories, Mass Eye & Ear; Department of Otolaryngology Head & Neck Surgery, Harvard Medical School; [3]Harvard

Hearing loss after noise exposure or ototoxic drugs and in aging results from loss of sensory cells, as reflected in audiometric threshold elevation. Recent studies from animal models and human temporal bones show that OHC loss can be preceded by loss of synaptic connections between the sensory cells and a subset of auditory-nerve fibers. The silencing of these neurons with high thresholds and low spontaneous rates degrades auditory processing and likely translates into a variety of perceptual abnormalities whether or not sensory cell function is compromised. While this condition, known as cochlear synaptopathy, can be diagnosed in mice by a reduction of auditory-nerve suprathreshold responses, its diagnosis in humans remain a challenge.

To look for evidence of cochlear synaptopathy in humans, we recruited 124 normal-hearing subjects (≤ 25 dB HL from 0.25 – 8 kHz) from 18 – 63 yrs, with no history of ear or hearing problems. All subjects were native English speakers and passed the Montreal Cognitive Assessment test. Word recognition was assessed at 55 dB HL in quiet and in difficult listening situations using the NU-6 corpus (with competing white noise at 0 SNR or with a 45% or 65% compression with 0.3 sec reverberation). Performance on a modified QuickSIN was also measured. OHC function was assessed using DPOAEs from 0.5 kHz to 16 kHz, while cochlear nerve function was assessed by electrocochleography (ECochG) in response to 100-ms clicks at either 9.1/sec or 40.1 per second, delivered in alternate polarity at 125 dB pSPL, in the absence or presence of a 90-msec forward masker (8-16 kHz noise) at 15 dB SL. The total noise dose for all ECochG measurements was well within OSHA and NIOSH standards.

Results show that several electrocochleographic markers of peripheral neural deficits including SP and AP are correlated with word-recognition scores, whereas measures of OHC function are not, consistent with selective neural damage. Furthermore, addition of the forward masker or increasing the click rate suppressed the neural responses to a greater extent in subjects with the poorest word scores compared to those with the best scores, consistent with greater neural fatigability in poor performers. These results support the idea that some of the differences in word recognition scores among listeners with normal audiometric threshold may arise from cochlear neuropathy.

Research supported by a grant from the NIDCD (P50 DC015857)

PS 975

Speech Evoked Electrocochleography- Preliminary Findings in Humans

William J. Riggs; Meghan M. Hiss; Varun Varadarajan; Jameson K. Mattingly; Edward Dodson; Aaron C. Moberly; Oliver F. Adunka
The Ohio State University

Clinical audiometric testing relies on behavioral measurements of thresholds to quantify auditory function/impairment. However, histologic evaluations of human temporal bones have demonstrated that the gold standard of diagnostic hearing evaluations, the behavioral audiogram, remains a poor indicator for determining the amount of sensory loss of the cochlea (Landegger et al. 2016). Thus, otoacoustic emission testing often accompanies audiologic assessments for evaluating hair cell function. However, peripheral encoding of sound has historically been studied using simple stimuli (i.e. pure tones, tone bursts, broadband clicks, or chirp stimuli). However, the basis of human communication is devised of complex acoustic harmonic interactions that are generated from the human vocal tract. Theoretically, these intricacies may require auditory encoding processes that are not engaged when encoding traditionally employed stimuli. Thus, the aim of this study is to explore both pre-neural and neural encoding processing of human speech using electrocochleography (ECochG) to identify its utility in assessing auditory function.

Currently, seven adult subjects (≥18 years) undergoing various otologic surgeries have participated in this study. ECochG was carried out with the active electrode at the round window. Acoustic stimulation consisted of synthetic phonemes (40 & 80 ms in duration) and tone bursts presented in alternating polarity at suprathreshold levels. Difference and sum curves were created to assess pre-neural formant encoding and amplitude and latencies of neural peaks. Preliminary analyses reveal a robust ability to quantify pre-neural encoding of the fundamental, second and third harmonic structures as well as identify auditory nerve activation patterns associated with the speech stimulus. These findings suggest that speech evoked potentials could likely be used as a tool to better assess peripheral auditory function especially when teasing out peripheral vs. central deficits in conjunction with traditional audiologic assessment.

PS 976

Probable Cochlear Synaptopathy in Cochlear Implant Subjects

Douglas C. Fitzpatrick
Univ. of NC at Chapel Hill

Electrocochleography (ECochG) can be used to assess the residual cochlear function in cochlear implant (CI) subjects. The summed magnitude of the ECochG responses to tones of different frequencies shows a high degree of correlation with word score outcomes in adults (r=0.67) and older children (r=0.60) (*Fontenot et al, 2019, Ear Hear 40: 577-59*). Our hypothesis is that these correlations are due to hair cell rather than neural activity, because the neural activity should reflect the audiometric results which are not predictive of outcomes with implants, while hair cell activity could be new information about cochlear health. The phenomenon would be indicative of ‘cochlear synaptopathy’, which has not been identified with objective measures in human subjects.

The stimuli were a series of tone bursts from 0.25-4 kHz at 90 dB nHL, a level series of tones at 500 Hz, and a level series of clicks. Recordings were collected intraoperatively from the round window of adult subjects (n=166). Recordings were analyzed to identify instances of hair cell activity with no corresponding neural activity, in the form of either a CAP or ANN. In addition, measurements of the CM, CAP and ANN were used to determine the proportions of nerve and hair cell components.

In 90 of 373 recordings (24%), where neural activity should be observed if present (i.e., where the CM were relatively large, taken as >0.5 μV and extending to nearly 100 μV), there was no evidence of either a CAP or ANN. For the ANN, the determination was made by analysis of the ‘average cycle’ or average of cycles from the ongoing part of the response, which is highly sensitive to the presence of neural contributions. To high frequencies, in addition to an absent CAP in many cases there were also cases with large CMs and small CAP.

Similarly, to low frequencies there were many cases of a small ANN component in large ongoing responses.

Evidence for cochlear synaptopathy, seen as large hair cell responses with small or absent neural contributions, is found in cochlear implant subjects. Thus, the hypothesis that functional hair cells not revealed in the audiogram can indicate neural survival that is available for electrical stimulation is supported.

Ototoxicity II

PS 977

TLR4 and MyD88 Activation of TRPV1 Modulates Cellular Uptake of Aminoglycosides

Farshid Taghizadeh[1]; Meiyan Jiang[1]; William B. Meier[1]; Peter S. Steyger[2]
[1]Oregon Health & Science University; [2]Creighton University

Background
Clinically-essential aminoglycoside antibiotics, particularly gentamicin, can induce permanent loss of cochlear sensory cells, leading to life-long hearing loss. Previously, we demonstrated that the pore of the capsaicin receptor/channel TRPV1 is permeant to gentamicin. Experimental induction of inflammation increases cochlear expression of TRPV1, increases cochlear uptake of gentamicin, and enhances cochleotoxicity in wildtype mice. Inflammation-enhanced cochleotoxicity is not seen in *Trpv1*$^{-/-}$, *Tlr4*$^{-/-}$ or *Myd88*$^{-/-}$ mice treated in a similar manner.

Aim
We hypothesized that MyD88, TLR4 and TRPV1 directly interact with each other to regulate the inflammatory response to lipopolysaccharides (LPS) and potentiate uptake of gentamicin after LPS-induced inflammation.

Methods
Immunofluorescence (IF) experiments and Proximity Ligation Assays (PLA) were utilized to investigate co-localization of these three proteins in MDCT cell lines. Inflammation was induced using 1 µg/mL of LPS. siRNA was used to knock-down the expression of MyD88 and TLR4. Drug uptake was determined via the intracellular fluorescence of Texas Red conjugated to gentamicin (GTTR).

Results
TLR4 and TRPV1 were consistently co-localized in MDCT cells in IF and PLA experiments, as did MyD88 and TRPV1. Co-localization of MyD88 and TRPV1 was maximal 5 minutes after immunogenic stimulation with LPS *in vitro*, and was mostly intracellular. Co-localization of TLR4 and TRPV1 was maximal 30 minutes after stimulation with LPS. Knock-down of MyD88 expression attenuated uptake of GTTR, but not the expression of TRPV1. Knock-down of TLR4 expression did not affect uptake of GTTR, despite reducing cellular expression of TRPV1, and this lower expression of TRPV1 was further reduced after stimulation with capsaicin.

Conclusion
These data indicate that TRPV1 is a major facilitator of gentamicin uptake in cell lines, and this uptake is potentiated by LPS-induced inflammation. TRPV1 directly interacts with the two major players of LPS-induced inflammatory pathway: TLR4, and MyD88. Interaction of TRPV1 with MyD88 prevents desensitization of TRPV1 in early stages of LPS stimulation. Interaction of TRPV1 with TLR4 maintains baseline expression of TRPV1 and prevents its degradation after stimulation.

Supported by the OHSU Medical Student Fellowship in Otolaryngology, the Everts-Smith Educational Endowment (FT) and NIDCD R01 DC004555 (PSS).

PS 978

Using Zebrafish to Correlate Hair-Cell Presynaptic Activity and Ototoxin Resistance

Daria Lukasz[1]; Katie Kindt[2]
[1]Johns Hopkins University; NIDCD; [2]National Institute on Deafness and other Communication Disorders

Aminoglycoside antibiotics are used to treat life-threatening bacterial infections but can also damage sensory hair cells. Hair-cell death causes irreversible and often isolating hearing loss. Within hair-cell organs of various species, including the zebrafish lateral line, differential susceptibility to aminoglycosides has been reported among particular subpopulations. Why some cells are spared while others are not is unclear. One possible explanation is functional differences among hair cells within a population. For example, differences in functional calcium signals could impact aminoglycoside susceptibility, as calcium signals are an integral part of cell health and apoptosis.

To study functional calcium signals, we conducted calcium imaging in zebrafish larvae expressing membrane-localized genetically encoded calcium indicators (GCaMPs) in external lateral-line hair cells. *In vivo* GCaMP imaging enables us to measure evoked presynaptic calcium signals within hair cells in real time. After collecting functional measurements, we applied the aminoglycoside neomycin to larvae and tracked cell survival. This approach allows us to monitor individual cells and draw correlations between resistance and

activity. We further assessed the role of calcium signaling acutely by pharmacologically blocking presynaptic $Ca_v1.3$ channels with the antagonist isradipine or chronically by examining *$ca_v1.3^{-/-}$* mutant fish. We also examined *$otofb^{-/-}$* mutants, which lack the calcium sensor required for the coupling of synaptic vesicle fusion to presynaptic calcium influx.

Previous work indicates that strong evoked presynaptic activity is only detectable in a subset (~30%) of lateral-line hair cells (Zhang et al., 2018). We assessed whether this snapshot of activity underlies previously reported differential susceptibility. We found that the subset of 'active' cells are more resistant to aminoglycosides. Fate mapping indicates that 'active' cells, although functionally mature, are cumulatively younger than 'inactive' cells. As previously demonstrated (Pickett et al., 2018), our work suggests that cell age is an important determinant of aminoglycoside susceptibility. In support of this idea, isradipine treatment during aminoglycoside incubation did not alter the resistance of 'active' cells. Examination of *$ca_v1.3^{-/-}$* mutants, however, revealed augmented hair-cell survival in these fish. Similar results were obtained in *$otofb^{-/-}$* mutants. This suggests that presynaptic activity may damage hair cells over time, making them more susceptible to aminoglycosides. Overall, whether aminoglycoside resistance in *$ca_v1.3^{-/-}$* and *$otofb^{-/-}$* mutants is determined by: differences in reactive oxygen species production, aminoglycoside uptake or clearance kinetics, or cell-death mechanisms is still unclear. Ultimately, this work increases our understanding of how activity-dependent signals modulate ototoxin susceptibility and is critical to the development of otoprotective therapies.

PS 979

Studying Cisplatin Toxicity Using a Fluorescently Tagged Platinum Compound in Zebrafish and Mouse Hair Cells

Patricia Wu[1]; Esra D. Camci[1]; Roberto Ogelman[1]; Matthew Hall[2]; Lisa L. Cunningham[3]; Julian A. Simon[4]; Edwin W. Rubel[1]; David W. Raible[1]
[1]University of Washington; [2]NCATS Chemical Genomics Center (NCGC); [3]Laboratory of Sensory Cell Biology, NIDCD, NIH; [4]Fred Hutchinson Cancer Research Center

Cisplatin is a platinum-based chemotherapeutic used to treat solid cancers. Drugs of this class are known to be ototoxic and cause the loss of sensory hair cells in the inner ear. We use a fluorescently tagged platinum compound (Bodipy-Pt), to measure uptake into hair cells in the zebrafish lateral line and in neonatal mouse cochlear cultures. We find that Bodipy-Pt shows similar dose-dependent killing of zebrafish hair cells when compared to cisplatin alone, suggesting that bodipy labeling has not altered toxicity. In the lateral line, we observe dose-dependent accumulation of Bodipy-Pt into hair cells. In addition, hair cell entry of Bodipy-Pt is dependent on mechanotransduction, as evidenced by the lack of hair cell uptake in zebrafish mutants for *cadherin 23*, and reduced uptake after treatment with the mechanotransduction channel blocker, Benzamil. ORC-13661, identified in a large-scale screen as a compound that blocks aminoglycoside toxicity, also effectively blocks cisplatin toxicity (Kitcher et al., 2019). We find that ORC-13661 blocks Bodipy-Pt uptake in zebrafish hair cells. Bodipy-Pt also allows us to follow cisplatin dynamics after uptake. Following Bodipy-Pt incubation and washout, we observe a reduction in fluorescence signal, suggesting that some cisplatin may be cleared from hair cells over time, well before hair cell death occurs. Remaining Bodipy-Pt is retained in puncta. In neonatal mouse cochlear cultures, we find Bodipy-Pt to be preferentially taken up in outer hair cells. In summary, Bodipy-Pt is a useful tool to study cisplatin kinetics and trafficking in multiple systems, furthering our understanding of the underlying mechanisms of cisplatin ototoxicity.

PS 980

The interaction of TRL7 with TRPA1 drives hyperexcitability cell death modulated by miRNA let-7b in auditory cells

Ken Hayashi[1]; Yuna Suzuki[2]; Akihiro Kishino[3]; Fumiyuki Goto[4]; Kaoru Ogawa[5]
[1]Kamio Memorial Hospital; [2]Department of Biochemistry, Nihon University School of Medicine; [3]Institute of Development, Aging and Cancer, Tohoku University School of Medicine; [4]Department of Otorhinolaryngology, Tokai University of School of Medicine; [5]Department of Otolaryngology, Head and Neck Surgery, School of Medicine, Keio University

Objective
The microRNAs (miRNAs) in cell-released exosomes can circulate with the associated vehicles to reach neighboring cells and distant cells. MiRNA let-7b play a major role to regulate cell death through the interaction with Toll-like Receptor 7 (TLR7) on cell membrane or in intracellular endosome. MiRNA let-7b play a major role to regulate cell death through the interaction with TLR7 and control the cell excitation through TRPA1. Our objective is to clarify the molecular mechanism of hyperexcitability-induced cell death in auditory cells, identifyingthe role of the interaction of TLR7 with TRPA1.

Materials and Methods
HEI-OC1 has been used as an auditory cell line.MiRNA and si-RNA were transfected into cells by lipofection.

The cell viability was determined by cell viability assays. Western blot analysis was performed for detecting molecular signaling pathways. The ultrastructure of cells was observed under transmission electron microscope (TEM).

Results

Early endosomes and late endosomes were confirmed in the cytoplasm of miRNA let-7b-transfected cells. Not only early endosomes and late endosomes but also autophagosome were found in the cytoplasm of miRNA let-7b-exposed cells. The structure of plasma membrane showed the endocytosis in miRNA let-7b-exposed cells. The cell viability after direct exposure of miRNA let-7b or TLR7 agonist was decreased in time-dependent manner, while the number of apoptotic cells were significantly increased. The expression of TLR7 and TRPA1, cleaved-caspase-3 (apoptosis induction maker), LC3-II, Atg-7 and Beclin-1 (autophagy induction maker) and p-ERK (cell excitation maker) were increased in miRNA let-7b-exposured cells. Interestingly, the cell viability wasn't decreased, and the number of apoptotic cells wasn't increased in miRNA let-7b-exposured TLR7 knock down (KD) cells. TRPA1 agonist increased the expression of TRPA1 and p-ERK. The expression of TLR7 was decreased in TRPA1 KD cells, correlating with TRPA1. These results indicate that TRL7 and TRPA1 form a complex, enhanced in response to miRNA let-7b. The biochemical interaction between TLR7 and TRPA1 might function as a gatekeeper of auditory cell excitation. These results indicate that endosomal miRNA let-7b acts as potentially novel TLR7 endogenous ligands, and induced TLR7-mediated cell death and the hyperexcitability via TLR7/TRPA1 binding in auditory cell. Namely, the biochemical interaction of TLR7/TRPA1 was enhanced in response to exosomal miRNA let-7b in auditory cells.

Conclusion

Our results reveal that exosomal miRNA let-7b modulates the interaction between TLR7 and TRPA1, and induce hyperexcitability-induced cell death in auditory cell, serving as a novel biomarker of the hyperexcitability of auditory cell.

PS 981

Cisplatin-Induced Loss of Hair Cells in Zebrafish Neuromasts is Accompanied by Nitration and Degradation of LMO4

Monazza Shahab; Rita Rosati; Samson Jamesdaniel
Wayne State University

Generation of reactive oxygen species, a critical factor in cisplatin ototoxicity, can lead to the formation of peroxynitrite and consequent nitration of proteins. LMO4, a transcriptional regulator, was found to be the most abundantly nitrated cochlear protein after cisplatin treatment. LMO4 protein levels were significantly decreased after cisplatin treatment in rodent cochlea. In recent years, zebrafish has emerged as an invaluable model for screening ototoxic drugs and otoprotective compounds. Zebrafish have sensory organs called neuromasts composed of mechanosensory hair cells that run along the lateral line. The lateral line and the inner ear, share many features, which include the types of cells, their origin, and their central projection in the hindbrain. Therefore, we hypothesized that cisplatin treatment would induce nitration of LMO4 in zebrafish hair cells and thereby facilitate hair cell loss. To test this hypothesis, zebrafish larvae (5-day post-fertilization stage) were treated with 1000 μM cisplatin. A count of the hair cells that were immunostained with parvalbumin, a hair cell biomarker, indicated a significant decrease in the number of hair cells after cisplatin treatment ($p< 0.005$, $n=6$). Quantification of the staining intensity of LMO4 and nitrotyrosine by immunohistochemistry analysis indicated that cisplatin treatment induced a significant decrease in the levels of LMO4 ($p< 0.01$) and a significant increase in levels of nitrotyrosine ($p< 0.001$), in zebrafish hair cells. More importantly, the cisplatin-induced decrease in LMO4 levels correlated with the loss of hair cells ($R=0.727$) implying a possible link between the levels of LMO4 and cisplatin-induced hair cell loss. In addition, the negative correlation ($R=-0.349$) between LMO4 and caspase-3 levels, which was significantly increased by cisplatin treatment ($p< 0.005$ for $n=3$), suggested a potential link between LMO4 levels and cisplatin-induced apoptosis in zebrafish hair cells. We conclude that nitrative stress as well as decrease in the protein levels of LMO4 are important factors in cisplatin-induced the loss of zebrafish hair cells. These findings suggest that zebrafish can be used as a model to screen otoprotective compounds that inhibit protein nitration and study the role of LMO4 signaling in cisplatin ototoxicity.

PS 982

The Response of Cochlear Microglia-Like Cells to Ototoxic Challenge in Different Strains of Wildtype Mice

Liana Sargsyan; Alisa Hetrick; Yongchuan Chai; Hongzhe Li
VA Loma Linda Healthcare System

Background

Resident microglia-like cells (MLCs) are present in the mammalian cochlea and their activation and recruitment to the lesioned cochlea have been reported after noise damage, ototoxic medication and treatment. The present study tested different strains of wildtype mice

(CBA/CaJ and C57BL/6) to determine whether the damage to cochlear synaptic ribbons was a significant pathological factor for recruiting macrophages or MLCs to the sensory epithelium after ototoxic challenge using either single consecutive doses of gentamicin and furosemide, or a single intratympanic injection of lipopolysaccharide (LPS).

Methods

Six-week-old C57BL/6 and CBA/CaJ mice were recruited. The first experimental group of mice were injected with a single dose of gentamicin (100 or 400 mg/kg) followed by 200 mg/kg furosemide after 30 min, both intraperitonially. The temporal bones were collected 3 or 7 days after the treatment. The second experimental group received intratympanic LPS in the right ear and cochlea were collected after 48 hours. The left cochlea of this group mice was served as controls. Collected cochleae were micro-dissected and hair cell nuclei with ribbon synapses were identified using anti-CtBP2 immunolabeling. Phalloidin and anti-Iba1 were used to determine the integrity of outer hair cells (OHC) and MLC identification at various frequency locations, by confocal microscopy.

Results

Three and seven days after low-dose combined gentamicin treatment, C57BL/6 mice presented with an increased number of resident MLCs with intact inner hair cells (IHCs), OHCs, and ribbon synapses in the sensory epithelium, low-to-middle frequency locations. After high-dose combined gentamicin injection, an increased number of resident MLCs was also observed at the aforementioned frequency locations, followed by the observation of synaptopathy and OHC loss, but intact IHCs in C57BL/6 mice. Neither synaptopathy, nor OHC loss occurred in CBA/CaJ mice after treatments. Intratympanic LPS injection increased MLCs numbers in the sensory epithelium across all frequency locations but synaptopathy was only observed at higher frequency locations with intact OHCs and IHCs in C57BL/6 mice. No LPS-induced synaptopathy was seen in CBA/CaJ mice, or in control groups.

Conclusions

CBA/CaJ mice appeared more resistant to ototoxic challenge, across all tested cochlea frequency locations, regardless ototoxic reagent or treatment route. In general, the number of MLCs increased before synaptopathy or OHC loss, whichever ototoxic reagent. The fact that MLC-proliferation or recruitment proceeds any observable morphological damage is suggestive of the neuroprotective feature in these immune cells. This observation warrants detailed phenotypical characterization of these MLCs in upcoming research.

PS 983

Reformulating Gentamicin to Reduce Ototoxicity and Maintain Antimicrobial Activity

Mary E. O'Sullivan[1]; Randy Lin[1]; Robert Greenhouse[1]; Alan Cheng[1]; Anthony Ricci[2]
[1]Department of Otolaryngology-Head and Neck Surgery, Stanford University; [2]Department of Otolaryngology and Department of Molecular and Cellular Physiology, Stanford University

Introduction

Gentamicin is an aminoglycoside antibiotic associated with ototoxicity. It is a mixture of C-subtypes (Gent C1, C1a, C2, C2a, C2b) and impurities (GentA, X, B, G418, Sisomicin). Gentamicin's are products of a Micromonospora species fermentation reaction, and the mixture produced is FDA-regulated. Regulations allow for specific ranges of C-subtypes and impurities(< 10%), however, toxicity and efficacy of individual components is not known.

Method

In vitro antimicrobial activity was examined in *E. coli, K. pneumoniae, P. aeruginosa*, and *S. aureus*. Minimum inhibitory concentrations (MICs) were established by the Clinical Microbiology Institute. Antimicrobial breadth was determined by counting the number of strains with a MIC ≤4µg/ml. Ototoxicity was examined using organotypic cultures of P5 rat cochleae. Following a 1hr-drug incubation, cochleae were cultured for 48hrs, mid-apical outer hair cells were counted following Dapi, Phalloidin and MyoVIIa labeling. Ototoxicity EC50±SE values were established from ≥6-point dose response curves fitted with logistic functions. We prepared a gentamicin mixture, containing C-subtypes only, to serve as a reference point for mixture vs. individual subtype comparisons. This mixture contained 54%C1, 23%C1a, 15%C2, 6%C2a and 2%C2b - a mixture that meets current regulatory requirements.

Results

Relative to the mixture of gentamicin subtypes we prepared, there was no significant loss in breadth for C1a, C2, C2a, C2b, however, C1 was active against fewer species. There was a decrease in potency for C1, C2, C2a, C2b but not for C1a. For the impurities, GentB, A, X, and G418 show a decrease in breadth and potency relative to the mixture we prepared, while Sisomicin has maintained breadth and potency. For ototoxicity, GentB and C2b were less ototoxic than the gentamicin mixture, and GentC2 and Sisomicin were more ototoxic. GentC1, C1a, and C2a have comparable ototoxicities to the mixture. GentC2b is the only subtype that has maintained antimicrobial breadth and has

reduced ototoxicity (2-fold decrease). To make a safer mixture, we removed C1 (least antimicrobial) and C2 (most ototoxic) from our reference mixture and replaced them with C2b (least ototoxic). The reformulation has comparable ototoxicity to C2b (2-fold decrease), has similar antimicrobial breadth but is more potent than C2b alone.

Conclusion

We propose C2b and the novel reformulation should move forward for additional testing to determine if the current formulations should be replaced with a single compound or a mixture. *In vivo* studies are also required to understand if the differences in antimicrobial potency detected are important for clinical translation.

PS 984

Identification of a Cyclodextrin Effective for Treating Niemann-Pick type C Disease Without the Ototoxicity of Currently Used 2-Hydroxypropyl-beta-cyclodextrin.

Anna M. Taylor[1]; Karen S. Pawlowski[2]; **Joyce J. Repa**[3]
[1]UT Dallas; [2]University of Texas at Dallas; [3]UT Southwestern Medical Center

Niemann-Pick type C disease is a rare autosomal recessive disorder in which mutations in either *NPC1* or *NPC2* genes result in aberrant intracellular transport of cholesterol from the late endosome/lysosome and massive lipid accumulation within this compartment in all cells. NPC disease presents as hepatic dysfunction, splenomegaly, pulmonary disease and neurodegeneration resulting in premature death. The *Npc1-/-* mouse recapitulates this disease phenotype and serves as a valuable model organism to test novel therapies.

In 2009, we and others first reported that 2-hydroxypropyl-beta-cyclodextrin (CYCLO) promotes the egress of lysosomal cholesterol in cells and tissues of the *Npc1-/-* mouse. A single injection of CYCLO to a young *Npc1-/-* mouse reduces lipid accumulation, relieves liver disease, delays neurodegeneration and significantly extends lifespan. However, CYCLO therapy results in sudden, irreversible hearing loss, as occurred in humans participating in a recently reported clinical trial for NPC, and was found associated with outer hair cell damage in NPC cats and mice.

Cyclodextrins are cyclic oligosaccharides that have a distinctive barrel configuration with a hydrophilic exterior promoting water solubility, and a hydrophobic interior accommodating small lipophilic molecules. Based on our previous studies of mechanisms of action for CYCLO in NPC, we proposed a more complex cyclodextrin may retain favorable therapeutic lysosomal functions, yet exhibit limited cholesterol adsorption/solubilization likely to impact hair cell integrity. Thus we tested 7-sulfobutylether-beta-cyclodextrin (SBE), as follows:

Ototoxicity-testing: Balb/c mice were given a single subcutaneous injection of CYCLO (8000 mg/kg), equimolar SBE (12350 mg/kg), or vehicle (saline). Auditory Brainstem Response thresholds (ABRs) were recorded at 4, 16, and 32 kHz before and 3-weeks after treatment. Inner ear tissue was microdissected to perform cytocochleograms. Hearing loss was evident in the CYCLO-treated mice with threshold shifts of 28 dB (4kHz), 32 dB (16 kHz), and 15 dB (32 kHz). No hearing loss was observed in either the saline- or SBE-treated mice. Hearing changes were consistent with the outer hair cell loss observed only in the CYCLO-treated mice (60% OHC loss (apex); 28-35% loss (mid); and 60% loss (base)).

NPC therapeutic efficacy: 7-day old *Npc1-/-* mice and wildtype littermates were injected with 4000 mg/kg CYCLO, equimolar SBE, or saline. Following injection only *Npc1-/-* mice showed changes in cholesterol balance, gene expression, and inflammation and these changes were roughly equivalent for SBE and CYCLO. Most importantly, lifespan extension was observed for both cyclodextrins tested. Thus SBE may be a safer, non-ototoxic drug for NPC therapy.

PS 985

Major differences in 2-hydroxypropyl-beta-cyclodextrin ototoxicity in adult and postnatal rats

Dalian Ding[1]; Senthilvelan Manohar[2]; Haiyan Jiang[1]; Richard Salvi[3]
[1]Center for Hearing and Deafness; [2]Center for Hearing and Deafness,University at Buffalo; [3]Center for Hearing and Deafness, 137 Cary Hall University at Buffalo, Buffalo, NY 14214

2-hydroxypropyl-β-cyclodextrin (HP-β-CD), a complexing vehicle used in hydrophobic drug delivery, is a cholesterol chelator recently used to treat Niemann-Pick C1 (NPC1) lysosomal storage disease. However, the high doses of HP-β-CD used to treat NPC1 causes hearing loss in in human, cats, guinea pigs, and mice by damaging outer hair cells. To gain insights on it effects, HP-β-CD ototoxicity was evaluated in adult rat and in P3 rat cochlear organotypic cultures. Adult rats were treated with 4000 mg/kg (s.c.) of HP-β-CD. Three days after HP-β-CD administration, distortion product otoacoustic emissions (DPOAE) were largely abolished and auditory brainstem response (ABR) thresholds

were elevated significantly at low frequencies and were almost undetectable at high frequencies. Cochlear OHC were completely destroyed except in the extreme apex. In contrast, inner hair cells (IHC), vestibular sensory hair cells and cochlear and vestibular ganglion neurons were intact. Thus, HP-β-CD only destroys OHC in vivo. P3 rat cochlear and vestibular cultures were treated with 0%, 0.25%, 0.5%, 1%, or 2% HP-β-CD in culture medium for 24 h or 48 h. Interestingly, HP-β-CD destroyed both OHC and IHC as well as both type I and type II vestibular hair cells. The earliest damage appeared near the tips of the stereocilia of cochlear and vestibular hair cells; these results suggest that the stereocilia may be the most vulnerable structures in P3 cultures. Importantly, In addition, HP-β-CD also severely damaged cochlear and vestibular peripheral ganglion neurons. Thus, HP-β-CD is toxic to all type of cochlear and vestibular hair cells and neurons in postnatal rats in vitro whereas HP-β-CD only appears to damage the OHC in adult rats in vivo.

PS 986

Ototoxicity Profile of Platinum-based Chemotherapy Drugs in Mice

Benjamin K. Gersten[1]; Katharine Fernandez[2]; Tracy S. Fitzgerald[3]; Lisa L. Cunningham[2]
[1]National Institute on Deafness and Other Communication Disorders; [2]Laboratory of Sensory Cell Biology, NIDCD, NIH; [3]Mouse Auditory Testing Core Facility, National Institute on Deafness and Other Communication Disorders, NIH, Bethesda, Maryland, USA

Introduction
Although cisplatin is a widely-used chemotherapeutic agent that targets a variety of cancers, it is highly ototoxic and causes hearing loss in as many as 80% of treated patients (Frisina, 2016). The related platinum-based chemotherapeutic drugs oxaliplatin and carboplatin are reportedly less ototoxic by comparison (Yuce, 2014; Fetoni, 2016). The mechanisms underlying this differential ototoxicity remain to be determined. Using an in vivo cyclic drug administration protocol that mimics the delivery of these drugs to cancer patients (Fernandez, 2019), we examined pharmacokinetics of these three drugs as well as hearing loss caused by each drug.

Methods
Adult CBA/CaJ mice were used. Baseline auditory function was assessed using the auditory brainstem response (8-40 kHz) and distortion product otoacoustic emissions (f_2: 4-40 kHz). Cisplatin, carboplatin, oxaliplatin or saline was delivered via IP injection using a cyclic drug administration protocol. Each cycle consisted of a 4-day period of drug administration followed by a 10-day recovery period. Mice were exposed to three full cycles. After the last cycle, auditory function was reassessed. This procedure was used for two experiments. In one cohort of mice, drug doses contained equimolar concentrations of platinum. In a second cohort, drug doses were proportional to clinical doses used to treat cancer. Cochlear morphology was examined using immunofluorescence. Platinum uptake was measured using inductively-coupled plasma mass spectrometry. An acute pharmacokinetic experiment was performed in which platinum levels were measured at 1 hour or 24 hours after a single bolus containing the equivalent of one 4-day cycle's drug dose at equimolar concentrations.

Results
When cisplatin, carboplatin, and oxaliplatin were administered in equimolar concentrations, cisplatin caused outer hair cell (OHC) dysfunction, OHC death, frequency-dependent changes in auditory sensitivity, and increased cochlear platinum levels. At this dose, neither carboplatin nor oxaliplatin caused functional changes; however, oxaliplatin-treated mice showed significant cochlear uptake of platinum. The effect of drugs administered in clinically proportional doses is currently being examined. Data from the acute pharmacokinetic experiment suggest that platinum levels increase in the inner ear within one hour of platinum-drug exposure, and that platinum is not readily cleared from the inner ear.

Discussion
Our data suggest that cisplatin pharmacokinetics contribute to the differential ototoxicity of platinum-containing anti-cancer drugs.

PS 987

Deletion of LMO4 in Mouse Inner Ear Enhances Susceptibility to Cisplatin-Induced Ototoxicity

Rita Rosati; Monazza Shahab; **Samson Jamesdaniel**
Wayne State University

Cisplatin, a potent chemotherapeutic drug, induces cell death by apoptosis. Its side effects, which include ototoxicity, nephrotoxicity, and neurotoxicity, limit the clinical utility of this life-saving drug. Cisplatin-induced protein nitration, particularly, nitration of LIM domain-only 4 (LMO4), a transcriptional regulator, has emerged as a critical factor in facilitating cochlear apoptosis. Our studies indicated that cisplatin-induced nitration and degradation of cochlear LMO4 could compromise STAT3-mediated anti-apoptotic signaling to induce ototoxicity. Furthermore, CRISPR/Cas9 knockout of LMO4 enhanced the susceptibility of organ of Corti cell cultures to cisplatin-induced cytotoxicity while overexpression of LMO4 mitigated the cytotoxic effects

of cisplatin. To verify this protective role of LMO4 in cisplatin-induced ototoxicity, we generated a LMO4 conditional knockout mice ($LMO4^{lox/lox}$; $Gfi1^{Cre/+}$) by breeding $LMO4^{lox}$ and $Gfi1^{Cre}$ heterozygotes. Unlike the LMO4 knockouts generated using $Foxg1^{Cre}$, which have a shortened cochlea (because $Foxg1^{Cre}$ targets otocyst), specific deletion of LMO4 in hair cells, using $Gfi1^{Cre}$, did not alter the cochlear morphology. The structure and organization of hair cells assessed using confocal microscopy of organ of Corti stained with fluorescein-conjugated phalloidin and DAPI nuclear stain indicated that the length of cochlea as well as the appearance of the hair cells were similar to that of the wild-type littermates. Moreover, the auditory brainstem responses (ABR) and distortion product otoacoustic emissions (DPOAE) of 6-week old knockout mice indicated that they have good hearing and their hearing thresholds were similar to that of wild-type littermates. However, treatment of LMO4 knockout mice with 3 mg/kg dose of cisplatin for 5 days induced a 22-32 dB shift in ABR thresholds on day 8, whereas, the shift in cisplatin-treated wild-type littermates was only 12-20 dB, suggesting enhanced susceptibility of the knockout mice to cisplatin-induced ototoxicity. Auditory brainstem responses recorded from the left ear of 3 mice were analyzed and the results are expressed as mean ± standard deviation. Together, these findings imply that in the absence of apoptotic stimuli LMO4 is a nonfactor for the survival and function of hair cells. However, when challenged with an adverse stimulus such as cisplatin, the absence of LMO4 makes them highly susceptible to ototoxicity, probably, because of the defunct LMO4/STAT3 cellular defense mechanism. Thus, the complexity of LMO4 signaling in cisplatin-induced hearing loss is characterized by its critical role as a protector against cellular apoptosis, which when compromised by cisplatin facilitates ototoxicity.

PS 988

Correlating Growth Inhibitory Effects of Sisomicin Analogs to their Uptake into Gram-Negative Bacteria

Randy Lin[1]; Mary E. O'Sullivan[1]; Hasan DeMirci[2]; Alan Cheng[1]; Anthony Ricci[3]
[1]Department of Otolaryngology-Head and Neck Surgery, Stanford University; [2]Stanford University, PULSE Institute; [3]Department of Otolaryngology and Department of Molecular and Cellular Physiology, Stanford University

Our drug synthesis strategy aimed to lower aminoglycoside ototoxicity by reducing drug entry through hair cell mechanoelectrical transducer channels. Analogs of sisomicin with structural modification had reduced ototoxicity *in vitro*, although some lost antimicrobial potency against gram-negative bacteria species in spite of their ability to bind the bacterial ribosome. Our goal here is to investigate the influence of aminoglycoside inward uptake on their toxicity against gram-negative bacteria.

We determined the minimum inhibitory concentration of four parent compounds and four synthetic analogs against *E. coli* and *P. aeruginosa*. Ribosome-binding was examined using cryogenic X-ray crystallography. Ribosome-binding compounds with reduced antimicrobial activity were further tested in a growth inhibition assay to establish a single-drug dose-response curve in complex medium, where we tracked cell density spectrophotometrically between 30min and 24hr. Growth inhibition was used as an indirect measure of aminoglycoside uptake. To directly study how drug uptake relates to antimicrobial activity, we applied a membrane permeabilizing compound, polymyxin B nonapeptide (PMBN), as a pre-treatment in our assay.

For compounds that bind the bacterial ribosome (sisomicin, streptomycin, neomycin A, paromomycin and sisomicin analogs), our dose-response data showed a time-dependent increase in antimicrobial efficacy.

In *E. coli*, sisomicin and two different sisomicin analogs (N1MS, N1PyrS), but not N1TFMS, were bactericidal, although they were all ribosome-binding. After PMBN pre-treatment, MICs of sisomicin, N1MS, and N1PyrS decreased, suggesting their uptake is limited by the outer membrane in *E. coli*. N1TFMS produced significant growth inhibition in the presence of PMBN, whereas N1,3"Bz, which is non-ribosomal binding, remained non-antimicrobial with PMBN pretreatment. As control, PMBN alone was not bactericidal at doses tested.

In *P. aeruginosa*, sisomicin and N1MS, but not N1PyrS, were bactericidal, although they were all ribosome-binding. As in *E. coli*, PMBN pre-treatment significantly increased growth inhibition by sisomicin, N1MS and N1PyrS, suggesting uptake of these compounds is significantly limited by the outer membrane.

PMBN-mediated growth inhibition was observed in both early and late time points for *P. aeruginosa* but only at the late time point for *E. coli*, suggesting a difference in membrane dependence between species.

Our data directly demonstrates that both ribosome binding and transport mechanisms dependent on the outer membrane are required for aminoglycoside antimicrobial activity.

PS 989

Vesicle Traffic in Outer Hair Cells

Csaba Harasztosi; Entcho Klenske; Anthony W. Gummer
University of Tübingen

Different types of endocytic vesicles have been demonstrated in the infranuclear region of outer hair cells (OHCs) using electron microscopy (Nadol, 1983) and horseradish peroxidase staining (Siegel & Brownell, 1986). Applying the styrylpyridinium dye FM1-43, it was shown that membrane particles are intensively endocytosed at the apical pole of OHCs and transcytosed to the basolateral plasma membrane and along a central strand down to the nucleus (Griesinger *et al.*, 2004; Kaneko et al., 2006). Using a double-barrel local-perfusion system (Harasztosi *et al*., 2018), we demonstrated more intense endocytic activity in the synaptic region and faster vesicle trafficking towards the apex (Harasztosi and Gummer, 2019). Investigating apicobasal and basoapical trafficking, we have demonstrated that myosin-VI is responsible for carrying vesicles in both the apicobasal and basoapical directions, and that kinesin participates only in basoapical trafficking (Harasztosi *et al.*, ARO 2018, PD34). The aim of the current study was to reveal a possible dynein contribution to vesicle trafficking along microtubules in OHCs and to identify trafficking mechanism(s) transporting vesicles from the central strand to the subsurface cisternae (SSC).

FM1-43 was applied locally to OHCs isolated from the guinea-pig cochlea. The presence of dynein-dependent transcytosis was tested by applying ciliobrevin-D (cili-D). To investigate trafficking to the SSC, the kinesin inhibitor monastrol and the myosin-VI inhibitor 2,4,6-triiodophenol (TIP) were applied to the cell. Trafficking speed was determined from the fluorescence signal onset-delays measured at different intracellular locations. A relative-delay parameter was used to elucidate trafficking from the cell centre to the SSC.

Ciliobrevin-D had no effect on the slope parameter of apicobasal trafficking (control: 0.13±0.01 µm/s, n=15; cili-D: 0.12±0.01 µm/s, n=11), but significantly reduced the speed of basoapical traffic (control: 0.20±0.02 µm/s (n=7); cili-D: 0.06±0.01 µm/s, n=6). Investigating trafficking to SSC, TIP significantly increased the relative-delay parameter at the infra-middle (control: 1.27±0.22, n=5; TIP: 2.04±0.37), supranuclear (control: 1.29±0.22, n=5; TIP: 1.66±0.07, n=4), apical (control: 1.28±0.20, n=5; TIP: 1.50±0.14, n=4), and infracuticular (control: 1.15±0.04, n=4; TIP: 1.57±0.21, n=5) locations. However, monastrol application significantly increased the relative-delay parameter only in the infracuticular region (control: 1.15±0.04, n=4; mon: 1.42±0.25, n=4).

The data demonstrate that dynein participates only in the basoapical trafficking of OHCs. The data also show that myosin-VI is responsible for vesicle traffic from the central strand to the SSC; however, in the infracuticular region kinesin also contributes to that trafficking.

PS 990

Oncomodulin Alters the Time Course of Transient Calcium Signaling in Cochlear Outer Hair Cells

Yang Yang; Kaitlin Murtha; Leslie Climer; Dwayne D. Simmons
Baylor University

Oncomodulin (OCM, β-parvalbumin), an EF-hand calcium binding protein (CaBP), is expressed predominantly by outer hair cells (OHCs) in the adult mammalian cochlea. Oncomodulin shares over 50% sequence homology with β-parvalbumin (βPV), which is expressed in immature and young adult OHCs. Developmentally in mice, βPV expression occurs as early as embryonic day 18, whereas OCM expression occurs postnatally. OCM is the only known CaBP for which targeted deletion causes progressive hearing loss. We hypothesize that the absence of OCM alters Ca^{2+} signaling in OHCs.

We investigated the effect of OCM on induced Ca^{2+} transients in two ways. First, we tested differences between OHCs expressing OCM and those lacking OCM expression. Wildtype and OCM KO mice with a targeted knock-in of a Ca^{2+} sensor (GCaMP6s) were analyzed before and after the onset of endogenous OCM expression. Following dissection of cochlear spirals, the change in Ca^{2+} concentration in OHCs was probed by the fractional change in fluorescence ($\Delta f/f0$) signal after depolarization with KCl (37mM). Second, in order to understand potential differences between OCM and βPV, we also measured Ca^{2+} transients in cultured mammalian cell lines transfected with OCM and βPV plasmids. After transfection with either OCM or βPV plasmids, HeLa cells were incubated in the Ca^{2+} indicator dye Fluo-4, treated with ATP to induce Ca^{2+} transients, and the $\Delta f/f0$ plotted.

In P0 GCaMP6s mice, both WT and Ocm KO hair cells lack OCM expression. Depolarizing OHCs showed no significant differences in their $\Delta f/f0$ rise-time and recovery-time contants. At P0, all three OHC rows as well as inner hair cells had similar time constants. However, at the onset of OCM expression around P2, OHCs from OCM WT GCaMP6s mice showed significantly increased time contants compared to OHCs from OCM KO OHCs. The

faster time constants in the OCM KO at P2 suggests that OCM is capable of altering Ca^{2+} transients in OHCs. In transfected HeLa cells, both OCM and βPV plasmids significantly altered the rise time (time constant) of transient Ca^{2+} signaling after stimulating with ATP. βPV also seemed to decrease the recovery time compared to controls.

Results from these studies on Ocm KO OHCs and transfected HeLa cells strongly indicate OCM plays a significant role as a Ca^{2+} buffer. In both instances, the presence of OCM lengthens the duration of the rising phase of Ca^{2+} signals, suggesting that its absence shortens the rising phase of Ca^{2+} transients.

PS 991

Macro-Patch Studies on Outer Hair Cell Nonlinear Capacitance

Joseph Santos-Sacchi[1]; Winston Tan[2]
[1]Surgery (Otolaryngology), Yale; [2]Department of Surgery (Otolaryngology), Yale School of Medicine

Prestin (SLC26a5) underlies outer hair cell (OHC) mechanical activity (electromotility, eM). The protein's voltage-dependent conformational changes couple into length changes of the cell. These conformational changes are measurable as an electrical correlate of eM, i.e., nonlinear capacitance (NLC), which is maximal at V_h, the voltage where prestin charge is distributed equally across the OHC lateral membrane.

We have recently shown that NLC and eM display low pass behavior that counters current dogma. NLC and eM exhibit multi-exponential or stretched exponential components, and the frequency response is dependent on holding voltage relative to V_h; that is, it is voltage-dependent (Santos-Sacchi and Tan, JNeuro, 2018). Furthermore, we have shown that NLC is not stationary in time following voltage steps (Santos-Sacchi et al., JPhysiol, 1998). Most of these studies have been done on whole cell preparations. Whole cell behavior can be influenced by internal and external mechanical impediments, and since prestin is mechanically sensitive its response characteristics conceivably could be altered to provide an inaccurate picture of intrinsic prestin kinetics. Here we evaluate NLC in membrane macro-patches to reduce extraneous (though likely physiologically important) influences to confirm the low pass, stretched-exponential nature of prestin kinetics.

We utilized macro-patches (~4 mm inner pipette tip diameter; seal > 5 GΩ, on-cell and excised) of guinea pig OHC lateral membrane under voltage clamp, where voltage control is excellent. Voltage chirp arrays (32 contiguous chirps, 4096 pts each at 10 μs sampling; 10 mV peak) were summed with 20 mV step offsets from -160 to +160 mV), for total step durations of about 1.5 s. Stray and linear capacitive currents were removed by subtracting the AC response at +160 mV, where NLC is absent. The resulting nonlinear capacitive currents were used to solve for membrane capacitance with dual-sine and single-sine techniques (Santos-Sacchi, JBiophys, 2004) at frequencies from 390 to 20000 Hz.

We find that NLC extends beyond our highest measurement frequency, but exhibits continuous low pass behavior that can be fit either with multi-Lorentzian or power functions, confirming our whole-cell observations on eM and NLC. Additionally, the voltage and frequency dependence of NLC changes over the course of step durations. Notably, a low frequency component of NLC diminishes over time, and V_h shifts positively across all frequencies, but is fairly stable across frequency. Importantly, our data illustrate that experimental approaches that average eM, NLC, or possibly even in vivo electrophysiological correlates of OHC activity in order to enhance signal-to-noise may miss important aspects of OHC performance.

Key words: Outer hair cell, prestin, capacitance

(Supported by NIH-NIDCD R01 DC016318 and R01 DC008130.)

PS 992

Synaptic Calcium Signals in Cochlear Outer Hair Cells

Marcelo J. Moglie; Ana Belén Elgoyhen; Juan Goutman
INGEBI - CONICET

Ca^{2+} regulation seems as a fundamental prerequisite for the normal operation of cochlear outer hair cells (OHCs). The existence of multiple cellular specializations, such as large amounts of cytoplasmic Ca^{2+} binding proteins, cisterns and pumps involved in Ca^{2+} extrusion mechanisms, points in that way. The main Ca^{2+} source is influx through mechanotransducer channels, but influx through voltage-gated Ca^{2+} channels (VGCCs) and the nicotinic β9β10 receptors has been also found. While VGCCs may be involved in synaptic transmission with type II afferent fibers, the highly Ca^{2+} permeable β9β10 receptors mediate the cholinergic synapse with efferent fibers from the medial olivocochlear complex in the brainstem. Ca^{2+} influx through nicotinic receptors is coupled to the activation of Ca^{2+}-dependent K^+ (SK) channels within a very narrow domain limited by a near-membrane postsynaptic cistern. Thus, efferent

cholinergic synapse exerts inhibition over OHCs' functions: it hyperpolarizes the OHCs and reduces cochlear amplification. We aimed to determine the magnitude and spread of synaptic Ca^{2+} signals and the specific role of the efferent postsynaptic cisterns during synaptic activity using simultaneous electrophysiological recordings and Ca^{2+} imaging techniques.

Electrical stimulation of cholinergic axons revealed single efferent Ca^{2+} entry sites. The signal was spatially restricted and its amplitude (2.7 ± 0.3 $\%\Delta F/F_0$) correlated with the size of evoked inhibitory postsynaptic currents. Trains of stimuli gave rise to larger Ca^{2+} signals and their amplitude was dependent on stimulation frequency (20 Hz: 8.1 ± 2.6 $\%\Delta F/F_0$; 40 Hz: 13.0 ± 3.1 $\%\Delta F/F_0$; 80 Hz: 21.2 ± 2.7 $\%\Delta F/F_0$). Additionally, pharmacological blockade of Ca^{2+} uptake during efferent stimulation suggests a role in efferent Ca^{2+} signal decay. Finally, depolarization protocols used to activate VGCCs, allowed detection of afferent Ca^{2+} entry sites. These were closely positioned to efferent ones. Interestingly, the maximal amplitude reached during depolarizations (7.8 ± 1.3 $\%\Delta F/F_0$) was smaller than that attained by the cholinergic input. This result is consistent with previous reports showing limited voltage-gated Ca^{2+} currents in mature OHC. The larger size of efferent Ca^{2+} signals compared to afferent influx and their close proximity, suggests that afferent activation evoked by spilled-over efferent Ca^{2+} is a possibility.

PS 993

Microtubule-Associated Protein 1S (MAP1S) is Required for Normal OHC Electromotility and Hearing

Winston Tan[1]; Jun-Ping Bai[2]; Alexei Surguchev[3]; Joseph Santos-Sacchi[4]; Dhasakumar Navaratnam[5]
[1]Department of Surgery (Otolaryngology), Yale School of Medicine; [2]Yale Department of Neurology; [3]Yale Department of Surgery; [4]Surgery (Otolaryngology), Yale; [5]Neurology, Yale

Prestin (SLC26a5) is a motor protein within the lateral membrane of outer hair cells (OHCs). Changes in OHC membrane voltage drives molecular conformational changes in prestin that couple into robust cell length changes termed electromotility (eM), a key element for mammalian cochlear amplification.

Earlier studies by our group showed that prestin interacts with microtubule-associated protein 1S (MAP1S), a protein that also binds actin and tubulin. We also demonstrated expression of MAP1S in OHCs. Furthermore, coexpression of MAP1S with prestin enhanced the surface expression of prestin as confirmed by biochemical and electrophysiological means. Using super resolution imaging (dSTORM), we find MAP1S in close proximity to prestin at the OHC lateral membrane. These data led us to hypothesize that MAP1S links prestin to the underlying cytoskeleton in OHCs and modulates prestin activity. To study the role of MAP1S in OHC and hearing function, we used a MAP1S knockout (MAP1S KO) mouse model. By measuring auditory brainstem responses (ABRs) and distortion product otoacoustic emissions (DPOAEs) we showed that both young (2 months) and old (8 months) MAP1S KO mice had significantly reduced hearing sensitivity and OHC function respectively compared with wild-type (WT) mice of the same age. Surprisingly, nonlinear capacitance (NLC), an electrical correlate of eM, was preserved in both young and old KO mice. These results indicated that the hearing loss is associated with OHC dysfunction but is not related to changes in NLC.

To investigate the underlying basis of the hearing phenotype, we measured OHC eM. Single isolated OHCs were whole-cell voltage clamped and stimulated with a hyperpolarising voltage ramp (100 to -120 mV), superimposed with summed AC voltages at harmonically related frequencies from 195.3 to 6250 Hz. The ramp-induced eM was recorded with a fast video camera (Phantom 310, Vision Research) at a frame rate of 25 kHz and measured by tracking the cuticular plate of the OHC using a shape tracking algorithm that provides sub-pixel resolution of movements. Our results showed that eM was significantly decreased in both young and old MAP1S KO mice by 30% and 50% respectively relative to age-matched WT controls. Interestingly, there was no age-dependent change of eM in WT mice, whereas there was a 30% decrease of eM with age in KO mice. The frequency response characteristics of eM are under analysis.

In conclusion, our findings suggest that MAP1S, through its interactions with prestin and the underlying cytoskeleton, plays a key role in modulating the active mechanical properties of the OHC, and that this is critically important for normal hearing. These data for the first time implicate the cytoskeleton in eM that was thought to be primarily a membrane-based phenomenon.

(Supported by NIH-NIDCD R01 DC000273, R01 DC016318 and R01 DC008130).

PS 994

Nonlinear Capacitance in Voltage-Clamp and Temperature-Clamp

Richard D. Rabbitt
University of Utah

Introduction

All cell membranes exhibit nonlinear electrical capacitance arising from physical properties of the lipid bilayer, ionic double layers, and membrane associated proteins. In general, capacitance is a function of voltage, temperature, and stress, with changes in capacitance or charge quantified by *effective*constitutive properties of the membrane including permittivity, electrostriction, piezoelectricity and pyroelectricity. It is well established in outer hair cells that nonlinear capacitance (capacitance voltage susceptibility) arises primarily from prestin-dependent piezoelectricity (*1, 2*), but it's not as clear specifically how capacitance temperature and stress susceptibilities arise in other hair cell types (*3*)or outer hair cells (*4*). The present work examines the thermodynamic origins of capacitance susceptibilities with a focus on voltage-clamp and temperature-clamp in hair cells.

Methods

Starting with the Gibbs free energy for a general thermo-piezoelectric composite, the charge displacement across a thin control volume encompassing the membrane can be quantified in terms of the voltage across the membrane, spontaneous structural polarization, temperature perturbation and stress (*5*). Expressions for the capacitance susceptibilities to voltage, temperature and stress were derived from equilibrium thermodynamics and compared to voltage-clamp and temperature-clamp data from model membranes, vestibular hair cells, and cochlear outer hair cells.

Results

Results demonstrate that capacitance voltage susceptibility arises in lipid membranes and passive cells primarily from electrostriction. Results further demonstrate that capacitance temperature susceptibility arises in lipid membranes and passive cells primarily form an increase in area and thinning of the membrane, with asymmetry in the double layers underlying a polarization offset. Hair cells are more complex, requiring voltage-dependent constitutive parameters to describe capacitance voltage and temperature susceptibilities.

Conclusion

Thermodynamics of thin thermo-piezoelectric membranes clarifies origins and provides means to interpret experimental measurements of permittivity, electrostriction, piezoelectricity and pyroelectricity under voltage-clamp, temperature-clamp, and stress-clamp conditions.

Funding

NIDCD R01-DC006685

References

1) J. Santos-Sacchi, W. Tan, *J Neurosci***38**, 5495-5506 (2018). 2) D. C. Mountain, A. E. Hubbard, *J Acoust Soc Am***95**, 350-354 (1994). 3) R. D. Rabbitt*et al.*, *J Neurophysiol***116**, 825-843 (2016). 4) O. Okunade, J. Santos-Sacchi, *Biophys J***105**, 1822-1828 (2013). 5) J. S. Yang, R. C. Batra, *J Appl Phys***76**, 5411-5417 (1994).

PS 995

Kv7.4 Channel Exhibits Electromechanical Properties in Cochlear Outer Hair Cells

Maria Cristina Perez-Flores[1]; Jeong Han Lee[2]; Seojin Park[3]; Mincheol Kang[1]; Xiao-Dong Zhang[4]; Choong-Ryoul Sihn[1]; Hannah A Ledford[4]; Wenying Wang[1]; Nipavan Chiamvimonvat[4]; Richard D Rabbitt[5]; Ebenezer N. Yamoah[2]

[1]University of Nevada Reno; [2]University of Nevada,Reno; [3]University of Nevada, Reno; [4]University of California Davis; [5]University of Utah

Background

Outer hair cell (OHCs) are unique in their ability to generate voltage-driven somatic length changes and cycle-by-cycle force. The somatic motor mechanism draws power from voltage-driven charge displacement and to function requires the expression of the protein Prestin in the cell membrane. The first stage of transduction is achieved through the direct mechanical gating of mechano-electrical transduction (MET) channels in the stereocilia, which modulate the input transduction current at auditory frequencies. When cationic current enters the cell, the membrane depolarizes, driving a piezoelectric-like shortening of the cell and converting electrical input into mechanical output. The shortening of OHCs in response to MET currents is nearly constant for low-frequency stimuli but begins to decline for frequencies above the electro-mechanical corner frequency of the cell - a frequency set in part by the capacitance and conductance of the OHC at the resting membrane potential. The corner frequency is unusually high in OHCs relative to most excitable cells, primarily due to the expression of the K^+ channel $K_v7.4$ which introduces a large conductance, and concomitant current (I_{Kn}), at the cell resting potential. Although the contribution of $K_v7.4$ channels to the tonic conductance and corner frequency is clear, it is not known if the channels also contribute to OHC function at auditory frequencies on a cycle-by-cycle basis.

Methods

OHCs from male and female C57Bl/6J mice (ages postnatal (P) 4-48-days) (Jackson Laboratory) were used in acutely dissected organ of Corti. The tissue was mounted under an insect pin glued to a coverslip for electrophysiological recordings. HEK 293 cells were

transfected with CRY2olig-mCherry and CIBN-K_v7.4-EGFP using Lipofectamine 2000 (Life Technologies, Carlsbad, CA). Live cells were imaged using a 63X oil objective on a Zeiss LSM 700 confocal laser scanning microscope. All cells were selected without exposure to blue light. Baseline images were taken with rapid exposure times (less than 4 seconds per frame) to measure baseline intensity and limit excitation before the experiment. For FRAP experiments, cells were excited with blue light; mCherry and EGFP emissions were collected over time. Imaging and analyses were performed using Zen 2009, ImageJ, and Imaris software. All analyses were performed in a blinded fashion.

Results

We report ultrafast electro-mechanical gating of the K^+ channel K_v7.4 in OHCs that develops in parallel with clustering of the channels at the base of the OHCs and with the onset of mature cochlear function. Increases in kinetics and sensitivity result from cooperativity among densely packed channels, revealed in the present work using optogenetics to artificially induce clustering in a model cell line and using voltage-clamp recordings in OHCs during hearing maturation. Upon clustering, the half-activation voltage shifted negative, and the speed of activation increased relative to solitary channels. Clustering also rendered K_v7.4 channels mechanically sensitive, an emergent property not detected in solitary channels. Data from murine cochlear OHCs confirmed that endogenous K_v7.4 channels cluster at the base of OHCs and provide mature cells with ultrafast electro-mechanical K^+ channel gating, varying in magnitude and speed with the tonotopic location in the cochlea. Results in silico further suggest that ultrafast K_v7.4 electro-mechanical gating provides OHCs with a feedback mechanism that enables the cochlea to overcome viscous drag and resolve sounds with incredible sensitivity, frequency selectivity, and bandwidth.

This work was supported by the funding the NIDCD and NIA (DC016099; DC015135; DC006685; AG060504; AG051443).

PS 996

Local electrostatics control electromotile conformational transitions of Prestin/SLC26A5

Dominik Lenz; Julia Hartmann; **Dominik Oliver**
Philipps University Marburg

SLC26 comprises a family of multifunctional anion transporters that mediate passive or coupled transport of small anions. SLC26A5 (prestin) stands out by functioning as a voltage-driven mechanical actuator in sensory outer hair cells. The quasi-piezoelectric function of prestin depends on binding of intracellular anions, suggesting that the underlying dynamics may be derived from an ancestral anion transport mechanism. We previously identified the structural architecture of prestin as a 7 transmembrane domain inverted repeat architecture, a layout shared with SLC4 (e.g., AE1) and SLC23 transporters. To address the molecular mode of action of anions in electromechanical function, we conducted a glutamate scan of the putative anion binding site. While introduction of glutamate at most positions probed was disruptive for protein function, glutamate at a central position (S396E) was tolerated. Moreover, S396E rendered prestin anion-independent and insensitive to competitive anionic blockers. We conclude that S396E reveals location and coordination of substrate anions. We obtained a similar phenotype, i.e. retained functionality in the absence of monovalent substrate anions, when we alternatively neutralized a single positively charged arginine, that is likely involved in coordinating the substrate anion. Thus, the net local electrostatic field around the substrate binding site seems to govern the voltage-dependent conformational transition.

To gain insights into the conformational dynamics underlying electromechanical activity we performed cysteine accessibility scanning mutagenesis of transmembrane segments 3 and 10, which mainly form the binding site as defined by glutamate substitution. Accessibility was essentially restricted to intracellular reagents. However, a position within TM3 near the substrate binding site was accessible both from the inside and from the outside - contrary to the crystal structure of the bacterial homolog SLC26Dg predicting inaccessibility to extracellular solutes in the inside-open conformation. Two-sided accessibility thus indicates movement of the rigid TM bundle comprising TMs 3 and 10 towards the extracellular side, possibly in an elevator-like movement. We speculate that this partial movement constitutes the conformational transition underlying prestin's electromechanical activity.

PS 997

Frequency dependence of prestin: intrinsic transition rates and viscoelastic relaxation

Kuni H. Iwasa
NIH

The biological function of outer hair cells (OHCs) is thought to convert the electrical energy available to those cells into mechanical energy based on piezoelectricity and to contribute to the sound-elicited vibration in the cochlea. This activity is critical to the sensitivity, sharp frequency selectivity, and wide dynamic range of the mammalian ear.

The fast motile activity of OHCs is based on conformational transitions (gating) of prestin, the molecule with mechanoelectric coupling. The motile response is elicited by the receptor potential, where movement of charge across the membrane is coupled with changes of membrane area. The charge movement results in extra membrane capacitance (nonlinear capacitance) and area changes in the axial displacement of the cell. The frequency dependence of conformational changes has been described by two approaches: one is based on stochastic equations [1] analogous to those used for transporters [2] without accounting for mechanical factors; another is based on the equation of motion [3] similar to piezoelectric material, assuming intrinsic transition rates infinitely fast.

Here, stochastic equations and equation of motion are combined to account for both finite intrinsic transition rates and mechanical load. In general, the frequency dependences of length changes and nonlinear capacitance depend on the holding voltage. This voltage dependence becomes clearer as the intrinsic transition rates dominate as viscoelastic relaxation becomes faster.

The motile response and nonlinear capacitance of these cells are attenuated by the low-pass filtering due to the intrinsic transition rates. The direct effect of attenuating the motile response at high frequencies on power output for a given level of receptor potential is quite obvious. Less obvious is the effect on the receptor potential, which drives the motile response, through nonlinear capacitance: A reduction of nonlinear capacitance by slow gating of the motile element reduces attenuation of the receptor potential. This effect is countered by reduced effectiveness of elastic load in reducing the membrane capacitance [3]. However, the reduction in the receptor potential by slow gating is obvious in systems with inertial load, where negative nonlinear capacitance can [4] eliminate the net membrane capacitance near their resonance frequencies in the absence of slow gating.

[1] Iwasa KH (1997) Biophys J, 73: 2965-2971.
[2] Kolb HA, Läuger P (1978) J Membr Biol 41:167-187.
[3] Iwasa KH (2016) Biophys J, 111: 2500-2011.
[4] Iwasa KH (2017) Sci Rep, 7:12118.

PS 998

A mouse model for studying regulation of cochlear amplification by chloride

Vijay Renigunta[1]; Dominik Lenz[1]; Julia Hartmann[1]; Michael G. Leitner[2]; **Dominik Oliver**[1]
[1]Philipps University Marburg; [2]Medical University of Innsbruck

Prestin's electromechanical activity is dependent on the interaction with intracellular anions (*1*). Given the typical physiological concentrations, chloride is expected to be the most relevant anion. The affinity for chloride has been estimated at about several millimolar (*1, 2*). Hence, even moderate changes outer hair cell (OHC) chloride levels may affect the activity of prestin, and consequently OHC electromotility and cochlear amplification. Moreover, patch-clamp recordings on isolated OHCs (in vitro) revealed a chloride conductance that is colocalized in the lateral membrane with prestin and is activated by membrane stretch (*3*). This conductance may function as a chloride influx pathway to modify intracellular chloride concentration in OHCs. Thus, it has been speculated that mechanically activated chloride influx into OHCs may dynamically regulate prestin's activity – maybe even at acoustic frequencies, thereby driving electromotility directly without a need for fast voltage oscillation (*2, 3*). Alternatively, slow variations in intracellular chloride might regulate prestin's electromechanical activity thereby adjusting the gain of cochlear amplification. However, whether such dynamic control by chloride is a relevant physiological process has remained unknown.

We have previously identified a central binding site for chloride in prestin (*4*). Recently, we found that inserting a fixed negative charge precisely at this site by site-directed mutagenesis (S396E) renders prestin entirely insensitive to anions while retaining full functionality. To address the role of chloride in regulating OHC electromotility we used Crispr/Cas technology to generate a mouse model carrying the single S396E mutation. OHCs in homozygote mutant mice were morphologically normal and the prestin mutant was targeted correctly to the lateral membrane. Patch-clamp recordings from mutant OHCs showed large NLC signals, that were unchanged when intracellular chloride was replaced by inert anions such as aspartate. NLC in mutant mice was also insensitive to salicylate, a competitive inhibitor of prestin's electromotile activity.

In conclusion, we have generated a mouse carrying a anion-insensitive prestin variant, which can now be used to study electromotility in the absence of chloride binding and the associated kinetics. Moreover, by measuring cochlear sensitivity we will probe for changes in cochlear amplification that would be expected if chloride concentration were involved in controlling prestin's activity under physiological conditions.

1. D. Oliver *et al.*, *Science* **292**, 2340-2343. (2001).
2. J. Santos-Sacchi, L. Song, J. Zheng, A. L. Nuttall, *J. Neurosci.* **26**, 3992-3998 (2006).

3. V. Rybalchenko, J. Santos-Sacchi, *J Physiol* **547**, 873-891 (2003).
4. D. Gorbunov *et al.*, *Nat Commun* **5**, 3622 (2014).

PS 999

Progress in SLC26A6 (A6) Structural Studies by Cryo-EM

Alexei Surguchev[1]; Alberto Rivetta[2]; Jun-Ping Bai[3]; Frederick Sigworth[2]; Dhasakumar Navaratnam[4]; Joseph Santos-Sacchi[5]
[1]Yale Department of Surgery; [2]Cellular and Molecular Physiology, Yale; [3]Yale Department of Neurology; [4]Neurology, Yale; [5]Surgery (Otolaryngology), Yale

Introduction
SLC26A6 (A6) a member of the SLC26 family of anion transporters, is responsible for transporting oxalate, chloride, and bicarbonate. A6 is an anion-exchanger/transporter expressed in the apical membrane of kidney proximal tubule cells. The molecular mechanism which allows it to transport anions is currently unclear. The current 7+7 inverted repeat model is based on homology modeling of three distant family members SLC26Dg, UraA, and AE1; however, better structural information is long overdue in order to clarify our understanding on how it functions as a transporter on a molecular level. Here we discuss our continuous efforts in optimizing expression, purification, and ultimately interrogating the feasibility of using SLC26A6 for EM studies by negative staining and Cryo-EM. *Methods:* SF9 insect cells infected with A6-GFP baculovirus were used for expression. Membranes were extracted and A6-GFP was subjected to a two-step purification procedure of affinity and SEC chromatography in the presence of the non-ionic detergent DDM. SEC peak fractions were analyzed by negative staining (NS) EM. A6-GFP from the peak fractions were loaded on grids, vitrified by Vitrobot, and imaged on a FEI Glacios Cryo-EM microscope. *Results:* A6-GFP eluted as two peaks. The first one, at 670kDa, is close to the expected size of A6 tetramer in DDM. It looks monodisperse. The second one, at about 300 kDA is close to the size of dimer in DDM. Negative staining micrographs of A6-GFP confirmed the monodispersity and reveals the presence of donut-like particles. About 250 particles were picked up for 2D class average generation. Currently, we are screening for the most suitable conditions for protein adsorption to cryo grids. Following this optimization, we plan to proceed to data collection. Additionally, we are probing the functionality of baculovirus produced A6 by measuring currents by patch clamp. *Conclusions:* A6-GFP was purified from virus-infected SF9 cells. After SEC, A6-GFP eluted as two peaks in DDM: a monodisperse tetramer at 670kDa, and a 300 kDA dimer. The negative staining of A6-GFP revealed the presence of donut-like particles which were used to produce 2D class averages. Cryo-EM sample preparation and grid sample loading needs optimization before attempting data collection.

(Supported by NIH-NIDCD R01 DC000273, R01 DC016318, R01 DC008130, and YD000220).

Plasticity After Hearing Loss or Restoration

PS 1000

Four Historical Pediatric Case Reports Which Resulted in Major Advances in the Understanding and Care of Communication Disorders

Robert J. Ruben
Albert EinsteinCollege of Medicine

Throughout history the 'case report' has resulted in significant advances for the understanding of communication disorders. These four children, from the 17th to 19th centuries, were selected because each of these cases resulted in important new insights in scientific understanding and major new approaches to the care of communication disorders.

1. **Luís de Velasco** (1610 --?), the product of a consanguine marriage, was born deaf. His care resulted in the 1620 publication of the first book describing the techniques of deaf education which heretofore had been kept secret. Luís's deafness resulted in making available to all the techniques used for successful deaf education. The English ambassador the Spanish court described Luis at age 13 as: "Young Lord able to speak as distinctly as any man whosoever; and to understand so perfectly what others said that he would not lose a word in a whole day's conversation."

2. **James Mitchell** (ca. 1799 – ca. 1815) was born blind and deaf, probably due to congenital rubella. Tears shed by James at his father's funeral were seen as evidence that he had emotions and that, although he lacked sight, hearing and recognizable language, he was nevertheless a complete and moral human being. This case was central to nineteenth-century inquiries into the nature of intelligence, a broader view of cognition, and the development of language.

3. "**Victor"** (ca.1788 –1828) experienced profound language deprivation at an early age because he was left to run wild. His inability to develop language despite normal hearing initiated

the concepts of a critical period for language acquisition and of the the measurement of non-linguistically, innate, intelligence.

4. **Laura Dewey Bridgman** (1829 – 1889) became deaf and blind from meningitis at age 18 months. On her behalf, Samuel Howe developed the first tactile language program to enable the development of language in a person who could neither see nor hear. This allowed Laura to acquire expressive and receptive language. Her experience was the model for all others similarly challenged, including Helen Keller.

Medical advances usually come about from rigorous hypothesis leading to controlled research. The “case report” has been another path toward scientific and medical development. The illnesses of these four children, through innovation--Luís de Velasco and Laura Dewey Bridgman--or detailed observation--James Mitchell and Victor—led to enduring advances in the scientific understanding and care of communication disorders.

PS 1001

Central Gain in the Human Auditory System: Investigations in "Normal Hearing" and in Tinnitus

Kelsey Dougherty; Alexandra Mai; Anna Hagedorn; Hari Bharadwaj
Purdue University

The nervous system is known to adapt in many ways to changes in the statistics of the inputs it receives. An example of such plasticity observed in animal models is that central auditory neurons tend to retain their driven firing rate outputs despite reductions in peripheral input due to hearing loss. This “central gain” has been demonstrated to occur even when the peripheral loss is not accompanied by audiometric threshold shifts, i.e., following noise-induced or age-related loss of afferent synapses and nerve terminals innervating the cochlea (cochlear synaptopathy) despite intact sensory hair cells. Down-regulation of inhibitory neurotransmission is thought to contribute to such plasticity. Pathological versions of such central gain are thought to underlie disorders such as tinnitus and hyperacusis.

Here, we studied two human cohorts that are at risk for peripheral deafferentation by virtue of above-average noise exposure or age. Consistent with cochlear synaptopathy, suprathreshold auditory brainstem response (ABR) wave I amplitudes and the middle-ear muscle reflex (MEMR) were simultaneously attenuated in both high-risk groups despite audiograms and otoacoustic emissions (OAEs) matched to young controls. For the same subjects, we then examined whether there was evidence of central gain accompanying the reduced auditory nerve responses. To this end, we designed an electroencephalogram (EEG)-based paradigm that concurrently elicits separable responses from different levels of the auditory pathway. We find that (i) for a moderate-high stimulus intensity, individual differences in response amplitudes that are as large as 20 dB at the auditory nerve level were reduced to less than 2 dB at the cortical level, (ii) individual differences in the rate of response amplitude growth as a function of stimulus intensity were progressively smaller as we ascend the auditory pathway from the nerve to the cortex, and (iii) a central gain metric defined as the size of the cortical response relative to the size of the auditory nerve response monotonically increased with age despite normal audiograms.

Together, these findings suggest that peripheral deafferentation and consequent central gain are ubiquitous in the human auditory system. To examine the behavioral consequences of reduced inhibition associated with this central gain, we measured individual comodulation masking release (CMR) which is thought to be mediated in part by inhibitory action. Finally, we applied the same battery of physiological measures in individuals with self-reported tinnitus. This presentation will describe these results and discuss the clinical implications.

PS 1002

Auditory Processing Remains Vulnerable to Prolonged Developmental Hearing Loss After the Critical Period

Kelsey L. Anbuhl; Todd M. Mowery; Dan H. Sanes
New York University

Experimental studies of developmental hearing loss (HL) typically focus on a critical period during which sensory deprivation can permanently disrupt neural function. However, childhood HL often emerges progressively after birth and extends through adolescence, leading to significant perceptual deficits. Furthermore, the magnitude of these deficits increases with longer periods of undetected HL. This suggests that the auditory central nervous system remains vulnerable to HL after a critical period has ended, and implicates HL duration as a key independent variable. Here, we examined the effect of prolonged transient HL (using reversible earplugs) in gerbils, beginning after the auditory cortex (ACx) critical period closes at postnatal day (P)23, and extending through adolescence (P102). After earplug removal and restoration of normal audiometric thresholds, animals were trained and tested psychometrically on an amplitude modulation (AM) detection task using an aversive Go/Nogo procedure. AM depth detection thresholds were

measured 3 weeks after earplug removal from HL-reared gerbils (n=14) and compared to control littermates that received similar handling (n=12). Auditory brainstem responses were collected to determine whether the HL induced changes to the auditory periphery or brainstem. Following behavioral testing, ACx brain slices were obtained from a subset of behaviorally-tested animals (control: n=6; HL: n=6) to assess synaptic and intrinsic firing properties in layer 2/3 pyramidal neurons.

Auditory task acquisition did not differ for control and HL animals, with both groups requiring comparable number of trials to reach criterion performance (i.e., d' >1.5 for 100% AM depth). However, HL-reared animals displayed significantly poorer AM detection thresholds on the first day of testing (HL: -11 dB; Control: -8 dB re: 100% AM), and this deficit persisted through 10 consecutive testing days. An analysis of covariance (ANCOVA) revealed the effect of HL alone to be highly significant ($p < 0.0001$). Whole-cell recordings from ACx pyramidal neurons revealed that excitatory postsynaptic potential amplitudes were elevated in HL animals, whereas inhibitory postsynaptic potential (IPSP) amplitudes were unchanged. Furthermore, the threshold current required to evoke an action potential was significantly lower in HL cells, suggesting that ACx cells were more excitable. This phenotype differs dramatically from that observed following critical period HL which induces a significant reduction of IPSP amplitude and decreases excitability. Taken together, these results reveal that transient HL beginning after the ACx critical period closes can induce significant perceptual deficits when it extends through adolescence. However, the associated ACx cellular changes are distinct from critical period HL.

Support: F32-DC018195-02, T32-MH019524, R01-DC014656

PS 1003

Neural Mechanisms underlying Speech Level Processing in Hearing Loss

Chengjie G. Huang; Nicholas A. Lesica
UCL Ear Institute

Noise-induced hearing loss is a widespread global problem. Hearing loss is known to cause distortions in the neural code, which leads to misinterpreted signals as sound information ascends the auditory pathway. As a result, the perception of complex sounds such as speech is compromised. This problem is further complicated by the fact that the intensity level of the speech varies in natural settings. Therefore, we set out to investigate how speech sounds heard at different intensity levels are processed in the inferior colliculus (IC) using an established noise-induced hearing loss model in the Mongolian Gerbil, *Meriones Unguiculatus*. Due to the similarity in low-frequency hearing gerbils share with humans, they provide a unique opportunity to investigate this problem under the context of speech with English language consonant/vowel combinations. We used multichannel single-unit recordings in freely-moving gerbils to study how neural coding was affected after noise-induced hearing loss. We recorded in the central nucleus of the IC and assessed neural responses using a variety of information quantification techniques. We found that responses to several consonant/vowel combinations changed drastically after noise-induced hearing loss and were more affected at lower intensity levels than high intensity levels. In addition, when speech was played in noise, the effects of hearing loss were prominent at lower intensity levels but diminished at higher intensity levels. These results are promising as they mirror those results found in speech recognition psychophysics studies and therefore are a potential neural correlate of perception. Further analysis of these data should allow us to develop a novel understanding of how hearing loss distorts the neural code and processing of speech, as well as how background noise further impacts perception. Through improved understanding of the neural mechanisms that contribute to impaired perception with noise-induced hearing loss, we may be able to identify new directions for potential therapeutic treatments.

PS 1004

Accelerated Hippocampal Neurodegeneration in a Mice Model of Noise-induced Hearing Loss is Associated with Microglial Alterations

Hong Zhuang[1]; Jing Yang[2]; Zhihui Huang[2]; Hongyu Zhang[2]; Haiqing Liu[2]; Xiaobo Li[2]; Jian Wang[3]; Richard Salvi[4]; Gaojun Teng[5]; Lijie Liu[1]
[1]Medical College, Southeast University; [2]Institute of Life Sciences, Southeast University; [3]Dalhousie University; [4]Center for Hearing and Deafness, 137 Cary Hall University at Buffalo, Buffalo, NY 14214; [5]Zhongda Hospital, Southeast University

Background
Hearing loss (HL) and dementia have become serious public health problems worldwide. Epidemiological surveys suggest that HL is a risk factor in the development of dementia. In our previous study, we found that mice with noise-induced HL (NIHL) exhibited impaired hippocampus-related cognitive function that was associated with a decline in hippocampal neurogenesis and dendritic complexity. Microglial cells are resident immune cells of the central nervous system and play essential roles not only in brain homeostasis, but also in neurodegenerative diseases. In view of recent work demonstrating microglial activation in the cochlear

nucleus following damage to the inner ear (cochlear ablation or intense noise exposure) and the abundant anatomical and functional connections between the auditory pathway and hippocampus, we hypothesized that microglia activation might occur in hippocampus following NIHL.

Methods
Male CBA/J mice, 6-8 weeks old, were exposed to 123 dB SPL broadband noise for 2 h. They were sacrificed in subgroup at 1, 3, 6, or 12 months post the noise exposure (1MPN, 3MPN, 6MPN, and 12MPN), together with matched subgroups of unexposed mice. HL was determined by ABR at 1MPN. Hippocampal neurogenesis and the microglia status in both auditory pathway and hippocampus were assessed by immunofluorescence labeling.

Results
(1) Severe HL were seen in ABR in the NIHL group at 1MPN. (2) NIHL mice exhibited significantly accelerated hippocampal neurodegeneration. (3) NIHL mice showed varied, but a significant increase in microglial activation across multiple auditory nuclei at each tested time point, while microglial dystrophy was observed in the DG region.

Conclusions
Our results show that severe NIHL can result in alterations in microglial activation in the auditory pathway and hippocampus from 1 to 12 months following the noise exposure. Chronic microglia activation could be indicative of ongoing neuroinflammation and/or the contribution of microglia to synaptic remodeling. The potential involvement of microglia in chronic inflammation could serve as a new therapeutic target to protect the central auditory system and reduce the risk of dementia.

PS 1005

Characterization of Alterations in Nociceptive Sensitivity Following Noise Exposure in Mice

Lorraine Horwitz; Susan E. Shore; Bo Duan
University of Michigan

Introduction
Noise exposure can result in cochlear damage, contributing to hearing loss, fullness in the ear, tinnitus, and hyperacusis. Hyperacusis is a debilitating auditory hypersensitivity disorder which is characterized by decreased tolerance to environmental sounds. This disease can be further classified as loudness hyperacusis (moderate-intensity sounds are perceived as too loud), avoidance hyperacusis (negative emotional reaction to sounds) and pain hyperacusis (sound-induced pain) (Baguley et al., 2011). Pain is a distressing feeling often caused by intense or damaging stimuli which motivates the individual to withdraw from a dangerous situation, protect a damaged body part while it heals, and/or to avoid similar experiences in the future. Pain hyperacusis can be particularly traumatic as pain within and/or surrounding the ear and parts of the face can begin almost immediately after moderate-intensity noise exposure or develop slowly over several hours (Hayes et al., 2014). Furthermore, patients with hyperacusis report widespread skin hypersensitivity (Fioretti et al., 2016). How pain sensitivity is altered following noise exposure is not well understood. This study examines changes in nociceptive sensitivity following acute noise exposure in mice.

Methods
Awake mixed C57B16 x 129 mice of both sexes were administered binaural noise (8-16 kHz, 100 dB SPL, 1 hour) producing temporary threshold shifts (TTS). Age- and gender matched sham-noise exposed controls were used. For all behavioral experiments, described previously (Bourane et al., 2015, Cheng et al., 2017, Duan et al., 2014), after three 'habituation' sessions (30 min per day) in the behavioral testing apparatus, acute somatosensory measures were recorded on two consecutive days in the given order: rotarod, von Frey, Hargreaves test, hot plate, and cold plate. The interval between different tests was at least 2 h.

Results
Noise exposure leading to TTS in mice results in mechanical pain hypersensitivity without alterations to thermal (hot/cold) pain measurements or changes in locomotor ability.

Conclusions
Mechanical and thermal nociceptive information are transmitted through distinct neuronal pathways (Todd, 2010). This study may be useful in understanding skin hypersensitivity seen in hyperacusis patients. Future studies are necessary to determine the precise neuronal mechanism linking auditory stimuli to somatosensory dysregulation.

PS 1006

Mice Exposed to Unilateral Acoustic Trauma Respond to Negatively Valenced Social Vocalizations

Kayleigh Hood[1]; Laurel Screven[2]; Madison M. Weinberg[2]; Amanda M. Lauer[2]; Laura M. Hurley[1]
[1]Indiana University; [2]Johns Hopkins School of Medicine

Affective brain systems may contribute to auditory disorders such as tinnitus. To assess the importance of

affect to perception following hearing loss, assays for responses to affectively weighted social vocalizations in animal models are instructive. Here, we measure the responses of CBA/CaJ mice to broadband vocalizations (BBVs, or 'squeaks') following acoustic trauma. BBVs are produced by mice in distress and by females as they reject males. We played back a sequence of BBVs to males and used ultrasonic vocalizations (USVs) as an output measure. To generate high rates of USVs, males were separated from live females by a Plexiglas barrier. Because of the lack of physical contact, females did not produce their own BBVs in this paradigm, but males were highly motivated to produce USVs. During 5 minutes of BBV playback, males that had previously been unilaterally exposed to noise (116 dB 1kHz band centered at 16kHz for one hour) reduced the numbers of USVs that they produced relative to preceding and following periods of no playback, similar to untraumatized animals. In contrast, animals with severe bilateral hearing loss showed steady declines in calling over time, similar to mice paired with anesthetized females or no females. Baseline calling rates varied widely among males from hundreds to thousands, but the absolute decrease in call number did not correspond to baseline rate, resulting in larger proportional effects of BBVs with lower call rates. These findings suggest that the production of USVs during BBV playback is a measure that can capture responses to a negatively valenced vocal signal, even in mice that have been unilaterally deafened.

PS 1007

Cortical Neural Synchrony Predicts Stimulus-Level-Dependent Increases in Auditory Evoked Potentials in Younger and Older Adults

Carolyn M. McClaskey; James W. Dias; Kelly C. Harris
Medical University of South Carolina

Compared to young normal-hearing adults, older adults often exhibit deficits in auditory nerve function that include decreased neural response amplitudes and poorer neural synchrony. Despite diminished auditory nerve activity, cortical response amplitudes in older adults are often equivalent to or exceed those of younger adults, and this is often attributed to age-related changes in inhibition at the level of the cortex. In contrast, limited evidence suggests that age-related deficits in neural synchrony may persist or even become more pronounced at the cortex. The enhanced cortical responses of older adults may therefore arise more from the recruitment of additional cortical neurons that occur with changes in inhibition and less so from neural synchrony. To investigate the relative contribution of these two mechanisms in the cortical responses of older adults, the current study investigated the extent to which increased cortical response amplitudes with increasing stimulus level were associated with stimulus-level-dependent increases in neural synchrony, and assessed how changes in neural synchrony differed between older and younger adults. Across groups, we hypothesized that stronger neural synchrony with increasing intensity level would predict steeper cortical evoked response amplitude growth. We also predicted that, for older adults, increases in response amplitudes would not be fully explained by increases in neural synchrony, reflecting both poorer neural synchrony and diminished inhibition in these listeners. Cortical auditory-evoked responses were measured from younger (18-30 years) and older (55+ years) adults in response to brief tone bursts presented at 80, 90, and 100 dB SPL. Tones had stimulus frequencies of 1 kHz and 4 kHz, corresponding to frequency regions in which older listeners had varying levels of hearing impairment. Response amplitude was quantified as N1 peak amplitude and neural synchrony was quantified as phase-locking value (PLV) in the theta frequency range (4-8 Hz). As expected, N1 amplitudes increased with increasing stimulus level, but did not differ between groups. PLV also increased with increasing stimulus level and was higher for 1 kHz tones than for 4 kHz tones. PLV did not differ between older and younger adults, but instead varied with the degree of listeners' hearing loss. Consistent with our hypothesis, changes in PLV mediated changes in N1 amplitude. Results suggest that increases in neural synchrony underlie stimulus-level-dependent increases in cortical response strength, but that the strength of the predictive relationship between them depends on the age and hearing health of the listener. Work supported (in part) by NIH/NIDCD.

PS 1008

Deep Neural Network Model of Speech Intelligibility for a Digit in Noise Task

Stephanie Haro[1]; Gregory Ciccarelli[2]; Thomas Quatieri[2]; Christopher Smalt[3]
[1]Speech and Hearing Biosciences and Technology, Harvard Medical School; [2]Human Health & Performance Systems, MIT Lincoln Laboratory; [3]Human Health & Performance Systems, MIT Lincoln Laboratory,

Speech intelligibility (SI) for individuals with noise-induced hearing loss is not often assessed in the clinic by use of speech-in-noise test across signal to noise ratios (SNRs) and when it is measured, the assessment is not comprehensive. Given a patient's SI score, it is unknown what combination of peripheral and central processing lead to the patient's behavioral results. The use of a computational model can account for the complex interactions between different hearing loss damage mechanisms and potentially bridge the gap

between noise induced low spontaneous rate (LSR) auditory nerve synapse loss in animal studies and understanding synaptopathy that occurs humans. We use a biologically plausible computational model that permits simulating synaptopathy to investigate upstream effects of SI due to synaptopathy.

Single digit utterances from a 220 subject audio database were input a cochlear auditory nerve model to produce neurogram, spectrogram-like stimuli representations. The peripheral model is capable of modeling various degrees of degradation, i.e. we compared populations of auditory nerve fibers with and without low spontaneous rate fibers to simulate cochlear synaptopathy across a wide range of SNRs.

The peripheral cochlear model was cascaded with a deep neural network (DNN) classifier, the latter of which acts as our forward model of central auditory processing. This two stage model aims to mimic the upstream process of identifying which of the 10 possible single digits it receives from the neurogram. To train the classifier, we used simulated healthy neurograms at an SNR of 30 dB or greater. The result was a sigmoidal function of SNR, similar to human behavioral performance.

Using 10-fold cross validation, synaptopathic neurograms emulated the healthy neurogram performance drop at very high and very low SNRs (0.17 % difference at 70 dB and 0.22% difference at -30 dB SNR). However, between 10 and 30 dB SNR, the synaptopathic neurograms had a mean performance drop of 19.53 % relative to the healthy model. The modeled low SNR performance losses illustrate that complete destruction of a system's LSR fibers causes a performance drop of about 2 misheard words per 10 digits presented. Ultimately, such a model could be matched to individual behavioral responses and SI performance. Derived peripheral and central model parameters could then potentially inform underlying damage mechanisms and treatment options.

Speech Psychophysics

PS 1009

Asymmetrical Forward and Backward Auditory Context Effects in Listeners with Normal Hearing and with Cochlear Implants

Matthew B. Winn
University of Minnesota

The auditory system generally codes information as change relative to ongoing stable properties. This principle extends to speech as well; differences between spectral properties of a target phoneme and its surrounding speech become perceptually magnified to create context effects. Put simply, the same sound is perceived differently depending on its acoustic context. Previous studies in this topic have primarily identified forward context effects where precursor sounds affect perception of later sounds. A smaller number of studies have identified backward effects where perception of a phoneme is affected by information that immediately follows. These two sets of studies have used very different stimuli, both in terms of context and target sounds. In the current study, we used the same target phoneme contrast ("sh" – "s"), expressed as a graduated synthetic continuum to control spectral properties, and the same phonetic contextual environment (the vowel in "shell"). The context could go either forward ("mesh" / "mess") or reverse ("shell" / "sell"). The contexts (vowels) were spliced from female or male talkers. The outcome measure was the impact of the direction and talker's gender on the perceived phonetic boundary between "sh" and "s", which is shifted to a lower frequency in the context of a man's voice compared to a woman's voice. Participants included 12 listeners with cochlear implants (CIs) as well as 15 listeners with normal hearing (NH). Stimuli were identified in a single-interval 4-alternative forced choice task where each step of the continuum was repeated 6 times for each direction, for each talker. Effects of context were individualized (centered) to each participant's perceptual boundary so that intercept effects did not diminish the target context effects.

Results revealed asymmetries in effect direction for NH listeners as well as a reversal of this asymmetry in CI listeners. For NH listeners, backward context effects were stronger than forward effects; for CI listeners, forward context effects were stronger. Results are in conflict with forward / backward masking accounts of phonetic context effects, and suggest that backwards effects likely emerge from different mechanisms than the forward effects commonly described in the literature. Additionally, context effects in CI listeners appear to be qualitatively different than those obtained in NH listeners.

PS 1010

Perceptual Weighting of Voice Onset Time and Fundamental Frequency Cues in Noise

Mishaela DiNino[1]; Yunan Charles Wu[1]; Lillian Behm[2]; Timothy P. Nolan[3]; Barbara G. Shinn-Cunningham[3]; Lori L. Holt[1]
[1]Carnegie Mellon University Department of Psychology; [2]Hamilton College; [3]Carnegie Mellon University Neuroscience Institute

Multiple acoustic dimensions contribute to categorization of speech, and some dimensions more robustly signal category identity than others. Studies of this 'perceptual

cue weighting' have been conducted extensively in both healthy listeners and those with traditional hearing impairments. Such studies could help us understand why some listeners with normal hearing thresholds (NHTs) have difficulty perceiving speech in noise Examination of /b/-/p/ categorization may be particularly valuable for this line of research: the primary cue signaling these sounds can shift across quiet and noisy conditions. In quiet, voice onset time (VOT; time between the consonant burst and voicing) is most diagnostic of category membership. In noise, fundamental frequency (F0) sometimes becomes the principle acoustic dimensions among young adults with NHTs, although this effect has not been observed consistently. The goal of this study was to determine the optimal masking parameters of noise to achieve a switch from primary reliance on VOT to F0.

Adults aged 18-32 with NHTs participated in a series of perceptual cue-weighting experiments. Naturally-spoken "beer" and "pier" sounds were manipulated to create a two-dimensional acoustic space across VOT and F0, and presented at 75 dB SPL in quiet and in noise at various signal-to-noise ratios (SNRs). All participants relied primarily on VOT to categorize sounds in quiet. When stimuli were presented at -3 dB SNR in speech-shaped noise based on the long-term average spectrum (LTAS) of the speech stimuli, listeners did not shift to rely primarily on F0 - likely because the vowel sound in the stimuli was louder than /b/ and /p/ and this noise masked all phonetic cues too greatly. Broadband noise that was instead based on the LTAS of conversational speech *did* shift cue reliance to F0 at -3 and +0 dB SNR, but not in the easier condition of +3 dB SNR. Setting the amplitude of this noise relative to the vowel onset instead of the entire stimulus (to control for intensity differences among stimuli with varying VOT lengths) produced the most consistent perceptual shifts, as these methods resulted in a switch to F0 from VOT reliance at -3, 0, and +3 dB SNR levels relative to quiet. Substantial variability in raw cue weight coefficients in noise was observed in all experiments, demonstrating that weighting of these acoustic cues varies even among young adults with NHTs. This experimental paradigm could thus provide a better understanding of the perceptual mechanisms that impact speech communication.

PS 1011

The Role of Fundamental Frequency in Competing-Talker Scenarios

Paolo A. Mesiano[1]; Johannes Zaar[1]; Lars Bramsløw[2]; Niels H. Pontoppidan[2]; Torsten Dau[1]
[1]Hearing Systems Section, Technical University of Denmark; [2]Eriksholm Research Centre

In competing-talker scenarios it is essential to perceptually disentangle the target speech from the interfering speech. Binaural cues are known to be very useful for segregating spatially separated sound sources in many listening situations. However, even in situations where only monaural cues are available, normal-hearing (NH) listeners exhibit exceptional abilities in terms of identifying and understanding the target speech while hearing-impaired listeners often experience difficulties. The investigation of monaural cues is therefore essential for developing hearing-aid compensation strategies that aim to restore the ability to exploit such cues. Previous studies with NH listeners showed that differences in fundamental frequency (F_0) between the target talker and an interfering talker can help segregate the speech signals. However, most of these studies used speech materials consisting of time-aligned closed-set sentences with a pre-defined structure that are far from everyday speech. Furthermore, F_0 was either defined by talker sex or measured as a talker-specific average, thus ignoring the significant F_0 variability across same-sex talkers and across sentences spoken by a given talker, respectively. In contrast, the present study used everyday-speech type sentences without a constrained time-alignment and employed a more accurate method for assessing the impact of F_0 separation on intelligibility. Pairs of sentences from the Danish Hearing in Noise Test (HINT) spoken by the same talker were processed to obtain a desired median-F_0 difference and presented to 15 NH listeners in a target-masker paradigm with first-keyword visual cueing. The sentence pairs were taken from a corpus of 6 male and 6 female talkers. F_0 separations of 0, 3, 6 and 12 semitones were presented at target-to-masker level ratios (TMR) ranging from -12 to 4 dB. An effect of F_0 separation was found, but the effect size was substantially smaller than in previous studies. It is hypothesized that the high level of sentence synchrony employed in the previous studies led to strong energetic masking, potentially amplifying the effect of F_0 separation beyond its real-life importance. The analysis of the current data set demonstrates that the benefit induced by F_0 separation is only significant when the degree of overlap between F_0 contours of paired sentences is high, and negligible otherwise. Furthermore, F_0 separation and TMR are not sufficient to explain the variability in the data, indicating that a more detailed analysis of the F_0 information in the paired sentences is required to better understand its impact on the intelligibility of target speech in competing-talker scenarios.

PS 1012

Neural Correlates of Speech Categorization in Auditory and Visual Modalities

Gwyneth Lewis; Claire Pearson; Ashleigh Harrison; Gavin Bidelman
University of Memphis

Objective

We tested whether neural mechanisms of categorical perception (CP) are specific to speech sounds or can also generalize to graphemes (i.e., visual letters) of the same phonemes. Given that linguistic experience shapes CP, and that letter-speech sound integration plays a crucial role during early reading acquisition, we hypothesized that CP might also be involved in the visual perception of written graphemes.

Method

Behavioral and neuroelectric brain responses (ERPs) were acquired from participants as they categorized stimuli from sound (phoneme) and letter (grapheme) continua (da-ga). Behavioral analyses compared relative differences in response times (RTs) and classification performance. Source space analyses focused on category-level activity in bilateral primary auditory (A1) and visual (V1) brain regions. If CP allocates attention to visual features that distinguish letters prior to grapheme-to-phoneme conversion and acoustic-to-phoneme conversion, neural activity should distinguish ambiguous letters (continuum midpoint) from more prototypical letters (continuum endpoints). We also examined cross-modal effects, i.e., whether patterns of V1 activity to visual tokens resemble A1 responses to corresponding auditory tokens.

Results

Despite the continuous nature of the tokens, participants heard or saw a clear perceptual shift in the sounds or letters, respectively, indicating CP in both modalities. Visual tokens elicited slower RTs near the category boundary (Tk3). Auditory tokens did not elicit this effect, likely because stop consonants (unlike vowels) are perceived more discretely and are therefore not ambiguous enough to slow RTs. At the neural level, A1 showed stronger amplitudes for categories compared to ambiguous tokens [i.e., (Tk1, Tk5) > Tk3], both in the auditory modality beginning at ~100 ms and in the visual modality at ~300 ms. Interestingly, auditory tokens elicited similar effects on V1 and A1 activity (weaker for Tk3). While bilateral V1 activity did not strongly distinguish categories, analysis of V1 activity by hemisphere revealed that ambiguous visual tokens strongly enhanced left V1 activity at ~300 ms.

Conclusion

Our preliminary results show that both auditory and visual tokens elicit CP. Moreover, neural data suggest speech representations in auditory and visual cortex are influenced cross-modally by category level processing.

PS 1013

Musicians Show Improved Speech Segregation In A Competitive, Multitalker Cocktail Party Scenario

Gavin Bidelman; Jessica Yoo
University of Memphis

"Cocktail party" speech perception requires parsing and recognizing multiple concurrent sound streams, a skill that also draws upon general cognitive faculties (e.g., memory, attention). Several studies have suggested that musical training enhances the brain's ability to perceive speech in noise (SIN), though this effect remains controversial. Equivocal findings might stem from the fact that SIN benefits are assessed in simple figure-ground tasks rather than true multi-talker scenarios which offer spatial cues for segregation and engage binaural processing. Here, we investigated whether musicians show perceptual advantages in cocktail party speech segregation in a competitive, multi-talker environment. We used Coordinate Response Measure (CRM) sentences to measure musician' and nonmusicians' speech recognition and localization performance in a 3D cocktail party environment conducted in an anechoic chamber with a 16-channel speaker array. Participants were asked to report the color-number combination (recognition task) and perceived azimuth (localization task) spoken by a target talker presented among competing CRM talkers. We manipulated task difficulty by parametrically varying the number of competing masking streams presented at other spatial locations in the speaker array (0-1-2-3-4-6-8 multitalker conditions). Musicians achieved more accurate and faster speech recognition accuracy than their nonmusician peers, showing less noise-related decrement in performance from 0 to 8 competing talkers. Localization accuracy for targets was within two speakers (~40°) for both groups. Musicians also showed superior performance on cognitive measures of fluid IQ and working memory. Correlational analyses revealed positive associations between individuals' years of musical training and (i) working memory and (ii) speech recognition performance in the CRM task, and (iii) performance on the normative QuickSIN test. Our findings confirm superior cocktail party speech perception and auditory streaming in musicians but also suggest this speech advantage is related to superior cognitive abilities.

PS 1014

Performance Intensity Function of Speech in Noise- the Effects of Linguistic Redundancy and Hearing Loss

Indira CP[1]; Sandeep M[2]
[1]Research Fellow; [2]Associate Professor

Speech perception in noise (SPIN) is extensively used in audiology clinics for diagnostic as well as rehabilitative purposes. However, there is a lack of uniformity in the speech material used across the clinics/labs and the stimulus intensity used to estimate SPIN. Monosyllables, words and sentences are used as stimuli. Owing to linguistic redundancy, one can expect SPIN to be different across these stimulus types, and accordingly influence its threshold measure (SNR-50) as well as speech identification scores (SIS). Hence, the study aimed to assess the effect of stimulus type on the performance-intensity function of SPIN, in normal hearing individuals and individuals with SNHL.

Twenty-five normal hearing adults (NHgroup, 18 to 29 years) and 5 adults with mild to moderate cochlear hearing loss (SNHL group, 55-64 years) participated in the study. They were monaurally tested for their SNR-50 and SIS using monosyllables, words and sentences (standardized lists in Kannada) in the presence of correlated speech shaped noise. These measures were obtained at five levels (10 to 50 dB SL in 10 dB steps w.r.t. their speech detection threshold). SNR-50 was determined for monosyllables and words by two down-one up adaptive procedure, and for sentences, linear regression was used.

rmANOVA and post-hoc analysis of the SIS-noise and SNR-50 scores in the NHgroup (Fig.1) showed significant difference across monosyllables, words and sentences at all the five levels, except between monosyllables and words at any of the levels (Tables-1, 2). rmANOVA and post-hoc comparisons across levels showed that SIS-noise and SNR-50 increased with increase in presentation level for all the speech material, but in different patterns. SIS-noise for monosyllables increased with presentation level till 50dBSL, whereas for words and sentences, it reached asymptote by 30dBSL. SNR-50 achieved asymptote at lower sensation levels for monosyllables and sentences (Tables-3, 4).

In SNHLgroup, Friedman's test and post hoc analyses revealed significant main effect of material on SIS-noise in all the SLs except for 10dB (Fig.2, Tables-5, 6). Contrary to the findings in the NHgroup, the maximum performance in SIS-noise as well as SNR-50 was achieved at 10dBSL and it decreased at higher SLs. Significant differences between scores at different presentation levels existed only for sentence stimuli.

To conclude, the level of presentation and the type of the stimulus have significant influence on SPIN, and the pattern of influence is different in individuals with hearing loss. The findings call for stimulus-specific protocols and inferences in SPIN test.

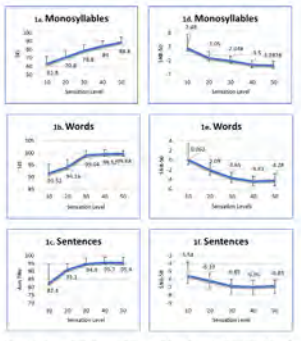

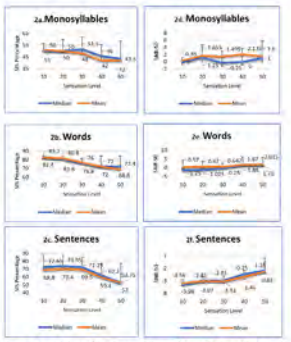

Table 1: Results of rmANOVA across monosyllables, words and sentences at different SLs for SISnoise and SNR50 in NHgroup.

dBSLs	SISNoise		SNR50	
	$F_{4,24}$	p	$F_{4,24}$	p
10	81.05	<0.001	48.46	<0.001
20	157.3	<0.001	72.35	<0.001
30	105.7	<0.001	109.1	<0.001
40	85.65	<0.001	65.18	<0.001
50	41.32	<0.001	54.59	<0.001

Table 2: Result of post-hoc comparisons that revealed presence of significant difference between the different speech material used for NHgroup

dBSLs	SISNoise (t)			SNR50 (t)		
	MS-Words	MS-Sent	Words-Sent	MS-Words	MS-Sent	Words-Sent
10	-14.245**	-8.284**	3.639*	2.473	8.298**	12.340**
20	-13.571**	-13.097**	3.459*	2.063	10.257**	12.492**
30	-12.859**	-9.229**	4.208**	4.033**	16.521**	10.939**
40	-10.982**	-8.285**	4.974**	2.533	11.898**	9.147**
50	-4.382**	-8.502**	-6.333**	9.537**	1.354	-10.613 **

*Note: * = p</=0.05, **p<=0.001*

Table 3: Results of one-way rmANOVA across SLs for monosyllables, words and sentences at in the NHgroup

Stimulus type	SISNoise		SNR50	
	$F_{4,24}$	p	$F_{4,24}$	p
Monosyllables	166.9	<0.001	31.91	<0.001
Words	89.06	<0.001	40.48	<0.001
Sentences	27.34	<0.001	11.55	<0.001

Table 4: Result of post-hoc comparisons that revealed presence of significant difference of scores across presentation levels in NHgroup, for MS, words and sentences

dBSLs	SISNoise (t)			SNR50 (t)		
	MS	Words	Sentences	MS	Words	Sentences
10-20	-9.238 **	-4.694 **	-4.229 *	3.707 *	4.169 *	2.138
10-30	-10.667 **	-10.136 **	-5.976 **	5.165 **	6.116 **	3.796 *
10-40	-14.061 **	-10.954 **	-5.808 **	6.816 **	6.913 **	5.177 **
10-50	-18.013 **	-11.476 **	-5.651 **	6.926 **	7.176 **	3.802 *
20-30	-7.155 **	-8.439 **	-5.055 **	3.259 *	5.947 **	2.975
20-40	-11.475 **	-8.817 **	-6.170 **	6.041 **	8.111 **	6.296 **
20-50	-16.665 **	-9.702 **	-4.930 **	5.373 **	9.755 **	2.697
30-40	-7.695 **	-1.809 **	-0.915	5.682 **	4.075 *	0.595
30-50	-10.445 **	-2.138	-0.516	5.991**	2.744	-0.100
40-50	-7.103 **	-1.000	0.461	1.077	-0.689	-0.706

*Note: * = p</=0.05, **p<=0.001*

Table 5: Results of Friedman's test across monosyllables, words and sentences at different SLs for SISnoise and SNR50 in SNHLgroup.

dBSLs	SISNoise		SNR50	
	Chi-square (4)	p	Chi-square (4)	p
10	5.558	*0.056*	37.62	*0.022*
20	8.40	*0.015*	8.40	*0.01*
30	7.60	*0.022*	57.684	*0.021*
40	10	*0.007*	5.2	*0.074*
50	10	*0.007*	1.2	*0.549*

Table-6: Result of post-hoc comparisons that revealed presence of significant difference between the different speech material used (SNHLgroup).

	SISnoise (T-stat)			SNR-50 (T-stat)		
	MS-Words	MS-Sent	Words-sent	MS-Words	MS-Sent	Words-sent
10	3.212*	2.294	0.918	0.577	4.619 *	4.041 *
20	6.364 **	4.243*	2.121	2.121	6.364 **	4.243 *
30	4.619 *	4.041 *	0.577	2.111	5.126 **	3.015 *
40	inf**	inf **	inf **	0.816	2.858	2.041
50	inf **	inf **	inf **	0.000	0.905	0.905

*Note: * = p</=0.05, **p<=0.001*

PS 1015

Individual Differences in Frontal-Occipital Fasciculus Microstructure Predict Visual Enhancement of Auditory Speech Identification

James W. Dias; Carolyn M. McClaskey; Kelly C. Harris
Medical University of South Carolina

Frontal cortical structures involved in speech articulation, attention, and memory have been implicated in auditory, visual, and audiovisual speech perception. Previous work has found correlations between frontal and occipital cortical activity when perceivers passively watch and listen to visual and audiovisual speech. These frontal-occipital relationships may be facilitated by their anatomical connectivity via the inferior frontal-occipital fasciculus (IFOF). The current investigation examined the extent to which individual differences in IFOF microstructure predicted auditory (AO), visual (lipreading) (VO), and audiovisual (AV) speech identification. Sixteen younger adults with normal hearing and normal (or corrected-to-normal) sight participated. Following diffusion-weighted magnetic resonance imaging (DW-MRI), each participant's whole-brain, left IFOF, and right IFOF white matter tracts were mapped using the Automatic Fiber Quantification (AFQ) and mrDiffusion packages for MATLAB. The left IFOF and right IFOF constituted those tracts connecting frontal and occipital cortices in the left and right hemispheres, respectively. Scalars for white-matter microstructure, including fractional anisotropy (FA), mean diffusivity (MD), radial diffusivity (RD), and axial diffusivity, were extracted from the whole-brain and IFOF tracts. Generally, robust white-matter microstructure is characterized as having higher FA and lower MD, RD, and AD. Individual differences in IFOF FA and diffusivity (MD, RD, and AD) failed to predict AO, VO, or AV speech identification on their own. However, lower IFOF diffusivity (left and right) did predict better AV speech identification after accounting for AO speech identification, even after accounting for whole-brain white matter diffusivity, suggesting the IFOF may facilitate AV speech identification by modulating visual speech input. To explore this possibility, psychometrics for the contributions of auditory and visual speech to the bimodal auditory-visual benefit when identifying AV speech (i.e., audiovisual gain) were computed. Individual differences in IFOF diffusivity (left and right) accounted for variability in the visual contribution, but not the auditory contribution, to audiovisual gain. Lower IFOF diffusivity predicted more visual speech contribution to audiovisual gain. The results suggest that individual differences in IFOF microstructure may modulate the role of visual speech in audiovisual speech identification. The results also support theoretical accounts suggesting frontal cortical mechanisms modulate visual speech processing and the role of visual speech in audiovisual speech perception.

This research was supported (in part) by grants from the NIH/NIDCD (R01 DC014467, R01 DC017619, P50 DC00422, and T32 DC014435).

PS 1016

Talker Variability and Audiovisual Speech Augments Word Learning in Adult CI Listeners

Jasenia Hartman[1]; Jenny Saffran[1]; Ruth Y. Litovsky[2]
[1]University of Wisconsin-Madison; [2]The University of Wisconsin–Madison

For many deaf people, cochlear implants (CIs) facilitate spoken word acquisition. Yet, despite this achievement, CI listeners vary in how well they acquire spoken words relative to their normal-hearing (NH) peers. Previous studies have found that CI listeners face challenges in phonetic perception which may attribute to their poor word-learning abilities. Several studies have found that learning from multiple talkers improves word-learning outcomes for NH listeners. In the presence of variation, listeners are able to tune into the acoustic dimension that is relatively invariant between talkers, allowing for robust representation of the word form. Similarly, audiovisual information in the form of a talking face also improves speech perception for NH listeners. Specifically, the mouth region permits listeners to extract relevant linguistic information. Little is known about whether talker variability improves learning for adult CI listeners and whether CI listeners fixate to the mouth of a talker than NH listeners when learning new words.

In this word-learning study, adult CI listeners and NH listeners were taught novel word-object pairings spoken by either a single talker or by multiple talkers (6 different talkers). Participants were then tested on their ability to learn the words using a novel talker in a two-alternative forced choice task (2-AFC). The test phase consisted of “easy” and “hard” trials (word choices differed by either several, or a single phonetic feature, respectively). Listeners received an audiovisual presentation of the talker in both the learning and test phase to facilitate phonetic processing. An eye tracker (SR Eyelink 1000Hz) was used to assess eye movements to the target and to the mouth over time.

Overall, CI listeners learned words spoken by multiple talkers better than words spoken by a single talker, and they performed better on the “easy” compared to “hard” trials. Learning from multiple talkers improved performance by 30% for “easy” trials and 18% for “hard” trials. These findings suggest that talker variability may be more beneficial for helping CI listeners learn words that differ by a several phonetic features. Finally, listeners spent 80% of the time fixating to the mouth, suggesting that they rely heavily on the visual cues to extract linguistic information. We expect a larger benefit of talker variability for NH listeners compared to their age-matched CI peers. We also predict that NH participants will fixate less on the mouth of a talker.

Funding: NIH-NIDCD (R01DC003083 to RYL) and NSF-GRFP-DGE-1256259

PS 1017

Predicting Masked Sentence Recognition in Children with and without Hearing Loss: Noise and Two-Talker Maskers

Kaylah Lalonde[1]; Ryan McCreery[1]; Elizabeth Walker[2]
[1]Boys Town National Research Hospital; [2]University of Iowa

Masked speech recognition requires coordination of a complex set of perceptual, cognitive, and linguistic skills. Individual differences in any of these domains could contribute to the large individual variability in masked speech recognition skills among children with normal hearing (CNH) and children who are hard of hearing (CHH). The purpose of this study was to examine hearing-related differences in the relationship between masked speech recognition and age, vocabulary, working memory, and selective attention. Six-to twelve-year-old CHH (with mild to severe bilateral sensorineural hearing loss) and CNH completed an adaptive sentence recognition test in a two-talker masker and in a spectrally-matched noise masker. Testing in each masker included two adaptive tracks that converged on the 25% and 75% correct points on the psychometric function, respectively. After 40 trials in each masker, data were fitted to psychometric functions, and the slope and 50% threshold SNR were calculated. CHH wore their devices throughout testing. Each child also completed standardized measures of receptive vocabulary, visuospatial working memory, selective attention, and hearing sensitivity. Aided and unaided audibility were quantified based on the Speech Intelligibility Index. Data collection is ongoing. Mixed linear modeling will be used to examine the contributions of the audibility, cognitive, and linguistic variables to individual differences in sentence recognition thresholds in each masker. Preliminary analyses indicate that CHH have poorer masked sentence recognition than CNH, and that children in both groups have poorer masked sentence recognition in the two-talker masker than in the noise masker. In both groups, sentence recognition in the noise masker is predicted by vocabulary. In the two-talker masker, CHH’s sentence recognition is predicted by age, and CNH’s sentence recognition is predicted by selective attention. Thus far, results suggest that the factors supporting children’s sentence recognition in a two-talker masker may differ depending on a child’s hearing status.

[Funded by NIH-NIDCD R01 DC013591 and supported by NIH-NIGMS P20 GM109023]

PS 1018

The Relationship Between Response Time and Presentation Level in Infant Speech Discrimination: A Methodological Study

Kristin Uhler[1]; Nathaniel T. Greene[2]; Kerry Walker[3]; Melinda Anderson[4]
[1]University of Colorado Anschutz Medical Campus; [2]Department of Otolaryngology, University of Colorado School of Medicine; [3]University of Colorado Anschutz; [4]University of Colorado School of Medicine

Performance on speech discrimination tasks improves with increased presentation level (PL) in infants and adults, although infants with normal hearing (NH) require greater PLs to discriminate speech compared to adults. It is unknown if this relationship between PL and speech discrimination performance is the same for infants with hearing loss (HL), and if this varies by type of speech sound contrast assessed. We examined feasibility of using a commercially available software package to compare response times to two speech contrasts in this pilot study. Specifically, we assessed speech discrimination for two speech sound contrasts (/a-i/ versus /ba-da/), in infants with NH and with HL, at three PLs (50, 60, and 70 dB SPL).

Pilot data were collected from 23 participants (females: 6 with HL and 4 with NH; males: 7 with HL and 6 with NH), ranging in age from 7-20 months. Degree of HL ranged from mild to severe, and all 11 infants with HL used bilateral hearing aids. A conditioned head turn paradigm, visual reinforcement infant speech discrimination (VRISD), was used to examine speech discrimination. Testing of speech contrasts was counterbalanced across subjects and either began with /a-i/ or /ba-da/. Following conditioning to the task, testing was always initiated at 50 dB SPL. If the child reached criteria percent correct (≥.73 p(c) max) then testing was completed, but if they did not reach criteria, testing was completed at 70 and then 60 dB SPL. Response time was calculated for all head turns (hits and false positives) and provided as the time between a button press to initiate a trial until a button was pressed to indicate a head turn.

There was great variability in response time across infants. Mean response time was examined in relationship to the PL and for each contrast. Correct head turn responses (hits) were 500 ms faster at 50 dB SPL and 60 dB SPL than incorrect (false positives) head turn responses.

The results of this pilot study suggest a more sensitive measure of response time is needed. Additionally, due to the variability in response time, a larger sample size is required. Data collection is ongoing and additional results will be presented in the context of the impact that change in recoding response methodology has on the measured relationship to presentation level.

PS 1019

Development of the Binaural Intelligibility Level Difference (BILD) in a Two-Talker Masker

Lori Leibold[1]; Jenna Browning[2]; Emily Buss[3]
[1]Boys Town National Research Hospital; [2]Medel; [3]UNC

Introduction

Masked SRTs in a diotic masker are lower for adults when target speech is presented out-of-phase to one ear (N0Sϖ) relative to when target speech is presented in-phase across the two ears (N0S0). This effect, called the binaural intelligibility level difference (BILD), is 5-8 dB for adults with normal hearing when target words are presented in broadband noise (e.g., Licklider, 1948; Goverts and Houtgast, 2010). Few studies have evaluated the BILD in children. Moreover, the magnitude of the BILD in a speech masker has not been well characterized at any age.

Methods

Listeners were 109 children (5.3-17.6 years) and 60 adults (19-37 years) with normal hearing. Target speech was the revised Bamford-Kowal-Bench sentence corpus (BKB; Bench et al., 1979) spoken by a female talker. The masker was continuous two-female-talker speech, presented diotically via headphones at a fixed level of 65 dB SPL. An adaptive threshold procedure was used to estimate the signal-to-noise ratio (SNR) corresponding to 50% keyword recognition in two conditions: (1) N0S0 and (2) N0Sϖ. The BILD was computed as the difference in SRT between these two conditions.

Results

For adults, SRTs were higher for the N0S0 relative to the N0Sϖ presentation, with mean SRTs of -5.9 and -13.2 dB SPL, respectively. The BILD was >3 dB for all but two adults, with a mean BILD of 7.3 dB across all adults (range = -0.6 to 13.3 dB). Consistent with the adult data, children's SRTs were higher for the N0S0 (mean SRT = -1.4 dB SPL) relative to the N0Sϖ presentation (-7.7 dB SPL). A BILD >3 dB was observed for 107/109 children, with a mean BILD of 6.3 dB (range = -3.3 to 10.4 dB). An examination of the child data indicates that the BILD improves with the logarithm of child age (r = 0.40; p < 0.001).

Conclusions

As previously demonstrated for speech recognition in a steady noise masker (e.g., Goverts and Houtgast, 2010),

adults capitalize on a difference in interaural phase in the context of speech recognition in a masker composed of two streams of speech. The BILD appears to be larger for speech-in-speech relative to speech-in-noise recognition, consistent with the idea that the introduction of the binaural difference facilitates segregation of target from masker speech. While all but two children demonstrated a robust BILD in the context of speech-in-speech recognition, age effects in the magnitude of this benefit were observed.

PS 1020

Speech Recognition in Quiet and Noise in Patients with Conductive, Mixed, and Sensorineural Hearing Losses

Michael Smith[1]; Z. Jason Qian[2]; Emma Tran[3]; Nikolas Blevins[1]; Matthew B. Fitzgerald[1]
[1]Stanford University; [2]Department of Otolaryngology-Head & Neck Surgery, Stanford University School of Medicine; [3]Stanford University School of Medicine

A primary complaint of patients with hearing loss is struggling to understand speech in noise (SIN). This has led many clinicians and scientists to recommend that measures of SIN should be routinely assessed in audiologic practice. However, little to no information is available as to the abilities of patients with conductive (CHL) or mixed (MHL) hearing losses to understand SIN. A general consensus among audiologists and physicians is that once the signal is sufficiently audible, then speech recognition abilities in patients with CHL should be equivalent to individuals with normal hearing (NH). By this logic, when audibility is maximized, individuals with MHL would be predicted to have speech recognition abilities equivalent to those observed in patients with sensorineural hearing loss (SNHL) with equivalent bone-conduction thresholds. Here, we test these predictions by examining speech recognition abilities measured in quiet and in background noise in patients diagnosed with varying degrees of CHL, MHL, and SNHL. We report data from over 4000 patients who, as part of their audiologic assessment, completed pure-tone audiometry, word-recognition in quiet (WRQ), and the QuickSIN. The QuickSIN determines the signal-to-noise ratio needed to repeat 50% of key words in low-context sentences and is often used in clinical environments when SIN abilities are assessed. Presentation levels were the same for both testing in quiet and in noise. We defined a conductive component as having occurred when there was a > 10 dB difference between the mean pure-tone average (PTA: 0.5-2 kHz) for air- and bone-conduction thresholds. We then compared performance on WRQ and QuickSIN measures in patients with NH, CHL, MHL, and SNHL as a function of the degree of hearing loss determined by their air-conduction thresholds. Our preliminary results suggest that both WRQ and QuickSIN scores in patients with CHL are largely equivalent to those of individuals with NH. In contrast, individuals with MHL showed performance on both WRQ and QuickSIN that more closely approximated their air-conduction thresholds than their bone-conduction thresholds. The mechanism behind these results remain unclear but likely reflect in part the reduced audibility in some patients with MHL. Taken together, these results provide crucial information regarding measurement in speech understanding abilities in quiet and noise for patients undergoing medical management for auditory pathology. In addition, they provide key information for clinicians and scientists necessary for SIN to become the default test of speech perception in the routine audiogram.

PS 1021

Effects of age and hearing loss on speech understanding in quiet and noise in clinical populations.

Matthew B. Fitzgerald[1]; Michael Smith[1]; Nikolas Blevins[1]; Z. Jason Qian[2]
[1]Stanford University; [2]Department of Otolaryngology-Head & Neck Surgery, Stanford University School of Medicine

Audiologic assessment is crucial in managing patients with hearing loss across the lifespan. In routine audiologic assessment, monosyllabic word-recognition in quiet (WRQ) has been the default test of speech perception for over 60 years. The continued use of WRQ scores is noteworthy in part because difficulties understanding speech in noise (SIN) is perhaps the most common complaint of individuals with hearing loss. Such complaints have led to increasing awareness that audiologic assessment should include measures of the ability of patients to understand speech in noise. Recent work from our lab indicates that SIN abilities 1) can largely predict categories of excellent vs. poor WRQ scores, 2) are more accurate at flagging the presence of vestibular schwannomas than WRQ scores, and 3) are more likely to predict deficits on questionnaires of perceived patient handicap than WRQ scores. Taken together, these data provide support for the idea that SIN measures can replace WRQ in the routine audiologic test battery. To make such changes, however, audiologists and physicians need a better understanding of how SIN performance is influenced by other key demographic variables, such as age. It is widely assumed by clinicians and researchers that performance on both WRQ and SIN both decrease with age. However, the effect of age can vary widely depending on the assessment tools and the degree of hearing loss.

Here we report data from over 4000 patients who as part of their audiologic assessment completed pure-tone audiometry, WRQ, the QuickSIN, and the SSQ12. PTA and WRQ are staples of the standard audiologic test battery. The QuickSIN determines the signal-to-noise ratio needed to repeat 50% of key words in low-context sentences, and is often used in clinical environments when SIN abilities are assessed. Our preliminary results suggest that WRQ scores decrease with advancing age, but only when individuals have moderate or greater hearing losses. Individuals with normal or mild hearing losses show little effects of age when measuring WRQ. In contrast, QuickSIN scores decrease with advancing age for all ranges of hearing from normal to severe. The effect of age seems to be larger with increasing amounts of hearing loss. We speculate the differing effects of age on WRQ and QuickSIN scores stem at least in part from the low-context sentences used in the QuickSIN. Accurate identification of these sentences likely requires increasing amounts of working memory, and this capacity is thought to decline with advancing age.

PS 1022

Objective and Behavioral Markers of Low- and High-Frequency Processing and their Contribution to Speech Intelligibility in Healthy and Impaired Ears

Markus Garrett[1]; Viacheslav Vasilkov[2]; Manfred Mauermann[1]; **Sarah Verhulst**[2]
[1]Oldenburg University; [2]Ghent University

Suprathreshold hearing abilities are important for communication, especially in challenging listening environments. Despite having normal audiometric thresholds, many people suffer from degraded suprathreshold hearing as a consequence of aging or noise exposure. However, the underlying mechanisms (e.g., hair cell damage, synaptopathy) are not well understood. This study investigates the particular roles of low- and high-frequency processing for speech recognition using a range of behavioural and objective electrophysiological markers of near and suprathreshold hearing in listener groups with different ages and audiometric hearing status. Specifically, groups (N=15) of young normal-hearing (yNH, 24 y/o), elderly normal-hearing (oNH, 64 y/o), and elderly listeners with sloping high-frequency audiograms (oHI, 65 y/o) were considered.

To characterize individual hearing deficits, we report routine diagnostics (pure-tone audiogram and distortion-product otoacoustic emission) and complement these with brainstem EEG measures which aim to quantify synaptopathy. Additionally, we assessed psychoacoustic temporal fine-structure (TFS1 test) and temporal envelope coding (AM detection) performance and compared these metrics to the speech reception thresholds using the German matrix test. The speech material was filtered to only contain signal frequencies which were also present in either the temporal fine-structure or envelope tasks, and/or brainstem EEG measures.

While the low-frequency relationships between speech intelligibility, temporal coding and brainstem EEG measures were complex, the high-frequency relationships did show an emerging pattern. A brainstem EEG metric sensitive to synaptopathy predicted the individual high-pass filtered speech intelligibility well across listeners, and suggests that both oNH and oHI suffer from synaptopathy, in line with post-mortem temporal bone studies. Including DPOAE thresholds in the regression model to control for outer hair cell damage still yielded significant contributions from the synaptopathy metric. The results of this study are important as they allow non-invasively assessment of synaptopathy while showing that this form of hearing deficit has measureable consequences for speech recognition in noise. The interplay between markers provides a better understanding of how individual aspects of supra-threshold hearing ability impact speech encoding.

PS 1023

Effects of Low Frequency Acoustic Hearing on Spectral Resolution and Speech Perception

Emily R. Spitzer; David M. Landsberger; David R. Friedmann
NYU School of Medicine

Background
Cochlear implant (CI) recipients who are able to utilize residual acoustic hearing for electric-acoustic stimulation (EAS) are reported to have better outcomes for speech perception in noise, localization, and music perception compared to traditional CI users. However, not all patients see these benefits and the degree of improvement is variable and unrelated to simple audiometric thresholds. It is unclear the extent to which the usability of residual hearing is determined by audibility, bandwidth and other distortions due to hearing loss. To isolate these factors, we compared performance on measures of spectral resolution and speech perception between normal hearing listeners (presumably no distortions) and hearing impaired listeners.

Methods
Normal hearing (NH, n=12) and hearing impaired (HI, n=23) listeners with steeply sloping audiograms participated. Spectral resolution was measured with the Spectral-temporal Modulated Ripple Test (SMRT) and

speech perception was measured with AzBio sentences in quiet and noise. NH listeners heard stimuli through low pass filters designed to mimic steeply sloping hearing losses and at two levels (40 and 60 dBA) to simulate low and high audibility. HI listeners heard stimuli unaided at their most comfortable listening level.

Results

For NH listeners, speech perception performance degraded with increasing filter stopband frequency and an interaction was found between level and the introduction of noise. SMRT was not affected by level and decreased only slightly with increasing filter stopband frequency. For HI listeners, SMRT performance was correlated with speech perception and duration of deafness. Mid-frequency thresholds (750-1000Hz) were most predictive of SMRT and speech perception scores. Performance on SMRT was much poorer than predicted by even the most restrictive NH simulation; scores were also worse than previously published data for CI users listening electric-only. The ranges for speech perception scores were similar between NH simulations and HI listeners.

Conclusions

NH simulations provide a "best-case" scenario for spectral resolution and speech perception with residual hearing. The degree of deviation from these simulations seen for SMRT may be a measure of the quality of the residual hearing. Because SMRT correlated well with speech perception, this test can be used as a quick, non-linguistic measure to predict performance. The typical thresholds used for determining hearing preservation and EAS eligibility were not correlated with speech perception, suggesting that SMRT may be a better tool for predicting EAS benefit.

PS 1024

Extended High Frequencies Provide both Spectral and Temporal Information to Improve Speech-in-Speech Listening

Allison Trine; Brian B. Monson
University of Illinois at Urbana-Champaign

Recent studies from our lab and others have investigated the utility of extended high frequencies (EHF, defined as frequencies ≥ 8 kHz) for speech perception. Many studies examining speech-in-speech listening (*i.e.*, the cocktail party problem) simulate an unnatural scenario where the target talker and maskers are all facing the listener. We analyzed listeners' performance in a more realistic listening scenario with a target talker facing the listener, and co-located maskers having head orientations facing away from the listener. By comparing full-band and bandlimited (low-pass filtered at 8 kHz) conditions, we previously found that access to EHF information under our more ecological listening conditions provided an advantage to listeners for speech-in-speech recognition. We questioned whether temporal information or spectral detail extracted from EHFs provided this advantage. Thus, we assessed performance when listeners were only given the EHF-band temporal envelope in the full-band condition. Results indicate that access to temporal cues alone are sufficient to improve speech-in-speech recognition performance, but access to spectral detail provides additional gains. Our results indicate that spectral structure at the EHFs, not just temporal envelope, is utilized by young, normal-hearing listeners.

Therapeutics for the Prevention of Age-Related Hearing Loss

PS 1025

Reduced Cochlear Connexin26 Caused by Oxidative Stress is Involved in Age-Related Hearing Loss

Kai Xu; Sen Chen; Xiaozhou Liu; Xue Bai; Le Xie; Yuan Jin; Yu Sun; Weijia Kong
Huazhong University of Science and Technology

Connexin26(Cx26) is one of the major protein subunits forming intercellular channels in inner ear. These channels allow ions, second messengers, microRNAs, and other small molecules to pass through and maintain normal hearing. Previous studies showed that partial loss of cochlear Cx26 in neonatal mouse causes age-related hearing loss (ARHL) in adult. However, the roles of cochlear Cx26 in hearing function of aged animals remain unclear. In this study, the expression levels of cochlear Cx26 were quantified at different ages of C57/B6 mice. As the age increases, the expression level of cochlear Cx26 continues to decline, accompanied with ROS accumulation. In supporting cells of aged mice, the gap junction plaques showed drastically fragmented, resulting in a reduced total plaque area. Further in BXPC3 cells, ROS accumulation induced by glucose oxidase (GO) or hydrogen peroxide can cause a significant decrease in the amount of Cx26 expression. Based on these observations, the Cx26 of fgfr3-positive or sox2-postitive SCs were knocked out in juvenile mice before the natural decline of cochlear Cx26. These two lines showed specific high frequency hearing loss and hair cell death in basal turn, which is similar to the phenotype of ARHL. These results indicated that ROS accumulation during the aging process can cause a decrease in cochlear Cx26 expression. Reduced Cx26 expression in organ of Corti leads to accelerate the process of ARHL.

PS 1026

Overexpression and Knockdown of Claudin 9 Levels Induce Hearing Loss

Yingying Chen[1]; Jeong Han Lee[1]; Seojin Park[2]; Maria Cristina Perez-Flores[2]; Braulio Peguero[3]; Bruce Tempel[3]; Ebenezer N. Yamoah[1]
[1]University of Nevada,Reno; [2]University of Nevada, Reno; [3]University of Washington Seattle

The tight junctions (TJs) between supporting cells and hair cells (HCs) "insulate" the contents of the endolymph (high K^+) from the perilymph (low K^+). The claudins are a family of transmembrane proteins that are an essential part of the TJ forming barriers in epithelial and endothelial tissues. In the cochlea, Claudin 9 (Cldn9) is highly expressed in the organ of Corti, where separation of the high K^+ concentration in the endolymph from the perilymph fluid is necessary for protection of HCs. Our laboratory has used the 129S6/SvEvTac (129S6) mouse as a model of early-onset age-related hearing loss (ARHL). We mapped five quantitative trait loci (QTL), and the QTL on the proximal 30Mb of chromosome 17 contains Cldn9. We propose this locus harbors at least one of the genes that affect ARHL in the 129S6 mouse. To study the effect of Cldn9, doxycycline-tet-OFF-Cldn9 transgenic heterozygous mice (C57BL/6 and CBA/CaJ background) were used. Two different concentrations of doxycycline water (0.25 mg/ml and 1.0 mg/ml) were fed to Cldn9 mice and their wildtype littermates. ABR and DPOAE were tested at different ages (1-3 months old). Immunostaining of myo7a for HCs and CtBP2 and PSD95 as pre- and post-synaptic markers was carried out to assess HCs and synaptic functions. Cldn9 and other TJs, which included Cldn6 and ILDR1, were co-labeled with myo7a and sox2 to identify the location and expression levels. The ABR and DPOAE experiments demonstrate that changing the concentration of doxycycline in the drinking water changes the hearing phenotype of Cldn9-TetOFF mice by 1-month of age. This change is limited to mice with the Cldn9-TetOFF promoter and not wildtype (+/+) littermate. Heterozygous mice (+/-) with a regulatable Cldn9 promoter exhibit a range of hearing phenotypes similar to various degrees of ARHL. A low-frequency hearing loss is observed with 0.25 mg/ml of doxycycline. A profound hearing loss is observed when Cldn9 is overexpressed with 0 mg/ml of doxycycline or knockdown with 1.0 mg/ml of doxycycline in the drinking water. The expression pattern of Cldn6 and ILDR1 in Cldn9 mice were altered. Homozygous mutant mice (-/-) with two copies of the Cldn9-TetOFF allele have profound hearing loss regardless of the concentration of doxycycline used. Cldn9 expression in the cochlea is tightly regulated with other TJ proteins to control the sensory epithelium integrity and hearing function.

Funded by the NIDCD and NIA (DC016099; DC015135; DC006685; AG060504; AG051443).

PS 1027

Presbycusis is Associated with Age-related Autophagy Flux Blocking in CBA/CaJ Mice

Bo Ding[1]; Lauren Paganella[2]; Xiaoxia Zhu[1]; McKenzie Watson[3]; Robert D. Frisina[1]
[1]Medical Engineering Dept., Global Center for Hearing & Speech Research, Univ. South Florida; [2]Medical Engineering Dept., Global Center of Hearing and Speech Research, University of South Florida; [3]1. Department of Medical Engineering, Global Center for Hearing & Speech Research, University of South Florida

Introduction

Autophagy, a highly conserved cellular mechanism, plays a critique role in the pathology of some neurodegenerative diseases. Whether or not autophagy is involved in cochlear aging processes is not clear. Therefore, we used cochlear cell lines and aging CBA/CaJ mice to gain insights into the role of autophagic mechanisms in inner ear hearing changes with age.

Methods

The cochlear cell line SV-K1 was used as an *in vitro* model. Treatments, such as Bafilomycin, Chloroquine and Arsenic Trioxide were used for both *in vivo* and *in vitro* experiments. In addition, CBA/CaJ mice were divided into three groups: young adult at 3-months old, middle age at 12 months and old age at 28- months. These animals underwent measurement of auditory brainstem responses (ABRs) and otoacoustic emissions before sacrifice.

Results

414 genes out of 500 candidates of interest are included in the Affymetrix Mouse GeneChip database. 37 autophagy candidates showed significant gene expression changes with age. A one-way ANOVA showed that most of them (34 out of 37) presented nonmonotonic changes with age. Three genes, *DRAM1, Hsp90ab1* and *Sec23a*, showed monotonic changes with age in the cochlea. *Dram1, HSP90 ab1* and *Sec23A* are all associated with activation of the autophagy modulator, mTOR. To investigate this further, we examined protein expressions for *in vivo* cochlear samples. All 3 protein expressions presented down-regulation with aging in the cochlea, suggesting that mTOR activity may increase with age. Since the phosphorylation of p70S6K at threonine 389 and 4E-BP at serine 65 have been used as hallmarks of mTOR activation and correlated with autophagy in various systems, we examined downstream members of the mTOR pathway: S6K1 and 4E-BP1 showed increased

phosphorylation in the aged cochlea compared with the young adult cochlea, demonstrating that mTOR activity increases with age. Autophagy biomarkers, LC3II and P62, were increased in the old cochlea compared to young adult cochlea, similar to the results of our *in vitro* experiment with the autophagy inhibitor CH treatment in SV-K1. However, the middle age cochlea showed that LC3 was decreased, but with P62 increasing compared with the young adult cochlea. This suggests that an increased LC3II is not always indicative of autophagy induction or a blockade of autophagy.

Conclusion
Age-related hearing loss is associated with autophagy blocking in the aging cochlea, which may affect mTOR activity and the fusion between autophagosomes and autolysosomes.

Work Supported by NIH grant P01 AG009524 from the Nat. Inst. on Aging.

PS 1028

Autophagy Flux Modulation Induced by Estrogen Inhibition Affects Hearing in Female Mice

Xiaoxia Zhu[1]; Bo Ding[1]; McKenzie Watson[2]; Tanika T. Williamson[2]; Tian Liu[3]; Jung-A A. Woo[3]; David E. Kang[3]; Robert D. Frisina[1]
[1]Medical Engineering Dept., Global Center for Hearing & Speech Research, Univ. South Florida; [2]1. Department of Medical Engineering, Global Center for Hearing & Speech Research, University of South Florida; [3]Byrd Institute & Alzheimer's Center, USF Health Morsani College of Medicine, Univ. South Florida

Introduction
We previously demonstrated roles for female hormones in age-related hearing loss (ARHL) in both human and mouse. Yet, the cellular mechanisms remain elusive. Autophagy is a highly conserved catabolic process essential for embryonic development and adult cellular homeostasis. Evidence has linked compromised autophagic processes to age-related neurodegenerative disorders, such as Parkinson's and Alzheimer's diseases. In light of this, our research team determined the roles estrogen may play in regulating autophagy, and its possible involvement in cochlear aging and ARHL.

Methods
Cochlea cell lines, SV-K1 and HEI-OC1 were used as *in vitro*models. Tamoxifen (TAX) and 17-βestradiol were administered to both cell lines. For *in vivo*studies, two month (mon) old young adult CBA/CaJ mice (N= 18) were divided into three groups: females with ovariectomy (OVX) at 2 mon old, intact females, and male controls. These groups were treated with TAX (20mg/kg/day, intraperitoneal [IP] for 2 weeks) starting at 12 months old. Hearing was measured with auditory brainstem responses (ABRs) and distortion product otoacustic emissions (DPOAEs).

Results
ABR thresholds were elevated at 10 months in the OVX group relative to the intact females and male controls of the same age. In addition; the ABRs thresholds for the intact females were elevated compared to the OVX and male groups between 12 and 16 months. DPOAE amplitudes were decreased in the OVX group at middle and high frequencies before and after TAX treatment compared to their 2 month old baseline. There were significant DPOAE amplitude declines in the intact female and male groups after TAX treatment at high frequencies. The pattern of LC3II expression in the aged cochlea was different from the young adult expression, suggestive of autophagy inhibition with aging. In old females with or without OVX, the estradiol levels were decreased and similar to the males. 17β-Estradiol treatment *in vitro* decreased expression levels of the autophagy markers LC3II and p62 compared to control treatment. However, TAX blocked these LC3II and p62 expression changes induced by 17β-Estradiol. We also observed that TAX alone did not change the LC3II and p62 expression patterns compared with control treatment. Under laser scanning confocal microscopy, we observed that estradiol promoted the autophagy flux by the fusion of autophagosomes with autolysosomes.

Conclusion
Estrogen influences auditory function changes through cochlear age-related autophagic modulation.

Work Supported by NIH grant P01 AG009524 from the Nat. Inst. on Aging.

PS 1029

Deregulation of mitophagy plays an important role in the process of age-related hearing loss

Yeon Ju Kim; Oak Sung Choo; Jin-Sol Lee; Hantai Kim; Jeong Hun Jang; Yun-Hoon Choung
Department of Otolaryngology, Ajou University School of Medicine

Background
Mitophagy is a degradation process of damaged, dysfunctional, and superfluous mitochondria to maintain cellular homeostasis. Recent evidences suggest that defective mitophagy is associated with age-related disease. Auditory cells are non-proliferating cells and

mainly rely on mitochondrial oxidative phosphorylation to acquire energy, therefore, mitochondrial function is important for auditory cell survival. The purpose of this study was to identify the role of mitophagy in age-related hearing loss.

Methods
C57/BL6J mice with ages of 7, 14, 32, and 44 weeks were used. At each time interval, hair cells and spiral ganglion cells were investigated by transmission electron microscopy (TEM), RNA sequencing, and immunohistochemistry for co-localization of TOMM20 and LC3B as representative markers of mitophagy function.

Results
TEM of aged specimens revealed apparent deterioration of mitochondria and an increase in lysosomes, but mitophagy was not detected in auditory cells. Moreover, most transcripts associated with mitophagy were downregulated in an age-dependent manner. We identified one significant differentially expressed gene associated with mitophagy, BNIP3L/NIX. The protein level of BNIP3L/NIX was decreased in aged whole cochlear cells compared with young cochlea. Consistent with the in vivo results, an oxidative stress-induced auditory senescent cell line also showed decreased levels of BNIP3L/NIX. Mitophagy-inhibited cells with BNIP3L/NIX knockdown showed hyperresponsiveness to oxidative stress resulting in cell senescence with increased levels of TOMM20 and LC3B. Overexpression of BNIP3L/NIX promotes the degradation of TOMM20 and LC3B during premature cell senescence.

Conclusions
Mitophagy pathway might play an important role in maintaining cochlear cell homeostasis during the aging process of hearing.

PS 1030

Senescent miR34a inhibited DRP-1-dependent mitophagy and exacerbated AHL

Hanqing Lin; Hao Xiong; Zhongwu Su; Jiaqi Pang; Yiqing Zheng
Department of Otolaryngology, Sun Yat-sen Memorial Hospital, Sun Yat-sen University

Background
Age-related hearing loss is a major unresolved public health problem. Previous study revealed that miR34a disrupted autophagy flux and was associated of cochlear aging. Evidence implied that miR34a might also alter mitochondrial function in aging process but the mechanism remains unclear. Here we investigated the role of miR34a in mitochondrial dysfunction and whether it would regulate the process of AHL.

Methods
Cellular senescence induced by hydrogen peroxide (H_2O_2) and aged cochlea were evaluated by senescence associated β-galactosidase stainning. HEI-OC1 cells were transfected with a miR34a mimic or inhibitor. Mitophagy levels were evaluated by fluorescence image of co-localization of mitotracker and lysotracker and western blotting of LC3II and P62. Mitochondrial function was assessed by ATP assay, mtDNA assay.

Results
In this study, we found that DRP-1 decreased during aging. MiR34a mimic downregulated DRP-1 expression and induced cellular senescence in HEI-OC1 cells. Cells transfected with miR34a inhibitor displayed increased DRP-1 expression and mitophagy level with better mitochondrial function.

Conclusions
Altogether, these results indicate that mitophagy eliminated dysfunction mitochondria and DRP-1 may be protective against oxidative stress-induced senescence. Aged-related miR34a might be the key factor that disrupt DRP-1 and mitochondrial function thus lead to cochlear senescence.

PS 1031

Comparison of Cochlear Mitochondrial Function in Adult and Aged C57BL/6J Mice

Min Jung Park[1]; Ah-Ra Lyu[1]; Tae-Hwan Kim[2]; Sun-Ae Shin[1]; Seong-Hun Jeong[1]; Yong-Ho Park[1]
[1]Chungnam National University; [2]Chungnam National University Hospital

Hearing loss with advanced age is a well-known fact of life. Mitochondrial dysfunction is associated with the etiologies of sensory-neural hearing loss, including age-related hearing loss (ARHL), noise- and ototoxic drug-induced hearing loss. We used C57BL/6J mice as an ARHL model to determine a possible association between ARHL and mitochondrial dysfunction. Male 2-month-old adult and 20-month-old aged C57BL/6J mice were used to examine auditory brainstem response (ABR), hair cell loss, synaptopathy, cochlear blood flow, morphological changes of mitochondria, and mechanisms involved in oxidative stress responses, cell death and mitochondrial dynamics. The elevation of ABR was significant in 20-month-old aged mice as compared to 2-month-old adult animals. Aged mice presented a significant inner and outer hair cell loss, spiral ganglion neuron (SGN) damage and CtBP2 decline as compared

to adult mice.Transmission electron microscopy (TEM) images revealed a substantial impairment in mitochondrial structure in the inner and outer hair cells as well as SGNs, indicating morphological changes of cochlear mitochondria may be a critical contributing factor to ARHL. To evaluate the underlying mechanisms of aged cochlear mitochondria, antioxidant enzymatic scavengers were quantified in the cochlea using RT-PCR. Aged animals expressed significantly increased levels of antioxidant enzymatic scavengers such as superoxide dismutase (SOD), catalase and glutathione S-transferase (GST) as compared to adult mice, indicating aging cochlea produces excessive superoxide radicals requiring increased ROS detoxification by the antioxidant enzymatic scavengers. Next, we examined genes involved in mitochondrial dynamics including fusion and fission, an important constituent of cellular quality control. Aging cochlea showed a significantly increased expression of fission (Drp1 and Fis1) and fusion (Mrf1 and OPA1) genes. The fusion and fission are known to facilitate the elimination of damaged mitochondria by autophagy. Our result showed that the genes related to autophagy (ATG5, Beclin, and LC3) were significantly increased in aging cochlea. Furthermore, as mitochondrial division is reported as an important step in cellular death, we tested cell death pathways, such as apoptosis and necroptosis. Aging cochlea showed significantly increased necroptotic (RIPK1, RIPK3, and MLKL) and apoptotic (Caspases and Bax) genes as compared to adult animals. Taken together, these data suggest that aging cochlea presents a higher oxidative stress response, damaged mitochondria, and increased expression of genes related to fusion, fission, autophagy, and cell death pathway compared to adult cochlea.

PS 1032

Long Non-coding RNA EPHB1 Promotes Mimetic Aging Hair Cell Survival through Activation of Autophagy Pathway

Xia Wu[1]; Weijia Kong[2]
[1]Department of Otorhinolaryngology, Union Hospital of Tongji Medical College, Huazhong University of Science and Technology; [2]Huazhong University of Science and Technology

Long Non-coding RNA EPHB1 Promotes Mimetic Aging Hair Cell Survival through Activation of Autophagy Pathway

Xia Wu, Wei-jia Kong
Department of Otorhinolaryngology, Union Hospital, Tongji Medical College, Huazhong University of Science and Technology, Wuhan, Hubei, 430022, China.

Background
Long-non-coding RNA plays an important role in cell growth and development, maintaining cell homeostasis and apoptosis, but the regulation mechanism of lncRNA in the study of auditory system degeneration process has not been fully elucidated. Change in lncRNA expression can cause a wide range of epigenetic changes. Therefore, lncRNA may be involved in the regulation of the occurrence and development of auditory degeneration.

Methods
The organ of Corti (include cochlear and spiral ganglion) was dissected from C57 mice at the age of 15 months and 2 months. RNA was extracted for lncRNA sequencing analysis. Then, we verified the expression changes of lncEPHB1 in natural aging mouse and D-gal–induced aging animal model and cells model (neurons-like ht-22 cell) by qPCR. The small interfering RNA against lncEPHB1 was used in ht-22 cells to assess if it is involved in the regulation of the D-gal induced mimetic aging process. Flow cytometry and immunolabeling with TNUEL staining were used to identify the changes in apoptosis levels in the D-gal induced aging ht-22 cells after inhibition of lncEPHB1 expression. The ht-22 cells were transfected with the mRFP-GFP-LC3 plasmid, to detect changes in autophagic flux after lncEPHB1 knock-down.

Results
The gene differential expression analysis showed that the expression of lncEPHB1 decreased significantly in the organ of Corti of aging mice compared with 2-month mice. Interestingly, we found that the expression of lncEPHB1 was reduced more obvious in spiral ganglion and auditory centers (hippocampus and auditory cortex) than in the cochlear. In addition, we found that the expression of lncEPHB1 also decreased significantly in D-gal-induced aging animals and cell models compared with control. After inhibition of lncEPHB1 expression by siRNA, the ROS and apoptosis levels of ht-22 cells increased significantly after D-gal treatment. Furthermore, we found that inhibition of lncEPHB1 expression reduces autophagy pathway in ht-22 cells.

Conclusion
These results indicate that lncEPHB1 may affect the survival of spiral ganglion during aging by regulating the autophagy pathway.

Acknowledgements
The research project described was supported by the grant 81500795 from the National Natural Science Foundation of China.

PS 1033

Age-Related Hearing Loss due to Apoptosis of Spiral Ganglion Neurons in Atherosclerosis: In Vivo and Population-Based Study

YooYeon Kim[1]; Janet Ren Chao[2]; Chulho Kim[3]; Harry Jung[4]; Boyoung Kim[5]; Phuong Nguyen Thi Thanh[5]; Junghwa Bahng[6]; Jiwon Chang[7]; Jun Gyo Suh[5]; Jun Ho Lee[7]

[1]Laboratory of Brain and Cognitive Sciences for Convergence Medicine, Hallym University College of Medicine; [2]Division of Otolaryngology, Department of Surgery, Yale School of Medicine; [3]Department of Neurology, Chucheon Sacred Heart Hospital, Hallym University; [4]Institute of New Frontier Research, Hallym University College of Medicine; [5]Department of Medical Genetics, College of Medicine, Hallym University; [6]Department of Audiology, Hallym University of Graduate Studies; [7]Department of Otorhinolaryngology-Head and Neck Surgery, College of Medicine, Hallym University

It has been reported that metabolic disease/ atherosclerosis associated with hearing loss. Atherosclerosis is classified as an aging disorder that affects neuroinflammatory and neural damage. Apolipoprotein E knockout (ApoE KO) mouse, an animal model for hyperlipidemia and atherosclerosis, causes hearing loss and neuroinflammation. S100 calcium-binding protein B (S100B), one of the neural damage biomarkers, induces neuronal death through apoptosis at high extracellular concentration. It has not been known that relation between neural hearing loss and increased S100B expression in ApoE KO mice of diet-induced atherosclerosis. This study hypothesized that up-regulated S100B expression causes apoptosis of SGNs in ApoE KO mice of diet-induced atherosclerosis, resulting in neural hearing loss. Additionally, we evaluated whether the degree of high frequency hearing loss, a hallmark of age-related hearing loss (ARHL), differ according to the atherosclerotic cardiovascular disease (ASCVD) risk in general population. We performed the hearing assessment and pathological analysis of the cochlea in ApoE KO male mice fed a western diet for 16 weeks. To prove the results of experimental study, ASCVD risk score and audiogram in national population study were analyzed. Hyperlipidemia, atherosclerosis, and hearing loss developed over time in the ApoE KO mice fed a western diet. Hearing loss correlated with a higher percentage of atherosclerotic lesions in the aorta. S100B expressions in the plasma and SGNs were increased in ApoE KO mice of diet-induced atherosclerosis. Apoptosis of the SGNs were observed in ApoE KO of diet-induced atherosclerosis by TUNEL staining. In population-based study, age and sex were the significant predictors for ARHL in multivariate logistic model. In addition, middle and high-frequency hearing loss were positively associated with the increasing of the ASCVD risk score. Taken together, in ApoE KO mice of diet-induced atherosclerosis, increased expression of S100B may produce apoptosis of SGNs, resulting in neural hearing loss. In ARHL patients, the degree of hearing loss was positively correlated with ASCVD risk in middle and high frequency sound. These results suggest that the middle-aged patients with early hearing loss might need to be evaluated and treated for an underlying metabolic condition. Furthermore, early-ARHL might be a marker for underlying atherosclerosis of the cardiac and cerebral vasculature and indicate the need for evaluation and treatment.

PS 1034

Establishment of oxidative-induced premature senescence model in auditory cells

Yuna Suzuki[1]; Ken Hayashi[2]; Takeshi Oshima[3]; Makoto Makishima[1]

[1]Department of Biochemistry, Nihon University School of Medicine; [2]Department of Otorhinolaryngology, Kamio Memorial Hospital; [3]Department of Otorhinolaryngology, Nihon University School of Medicine

Objectives

Age-related hearing loss (ARHL) is one of the most common disorder affecting older adults. The attention to ARHL has been growing not only from the aspect of health conditions but also the point of the association with cognitive decline. In addition to physiological aging process, current studies reported that oxidative stress causes cellular senescence in auditory cells and plays a crucial role in ARHL. Recent study reported that prolonged senescent cells showed the increased level of the secretion of pro-inflammatory cytokines having harmful effects on their microenvironment. These findings indicate that senescent cells can contribute to organismal aging and age-related disease, however, the regulatory mechanism in ARHL remain unclear. Here, we estimated whether oxidative stress induces premature senescence in auditory cells and subsequent inflammation response, termed senescence-associated secretory phenotype (SASP) for shed light on ARHL.

Materials and Methods

HEI-OC1 has been used as an auditory cell line. HEI-OC1 cells were exposed with 500μM Arsenic Sodium (AS), as a typical oxidative agent and well-known environmental stress. The cell viability and the population doubling rate were measured under these conditions. SA-βgal positive cells and enzymatic activity were measured for detecting senescence. β-H2AX staining was for detecting DNA damage. RT-qPCR analysis was performed to evaluate the mRNA level of senescence-associated genes.

Results
The population doubling rate was significantly decreased after treatment of AS in HEI-OC1 cells, while these had no effect on cell viability. The enzymatic activity and the number of SA-βgal positive cells significantly increased 72hours after AS treatment. This result means that AS treatment cells ceased their proliferation without apoptosis and displayed characteristic feature of senescence. β-H2AX staining showed increasing the number of nuclear foci in AS-treated cells. This suggest that Arsenic exposure resulted in DNA double-strand breaks in auditory cells. The expression of p21 mRNA level was significantly elevated at the peak of 24hours after AS treatment in AS-treated cells. This result indicated that that AS causes cell cycle arrest. The pro-inflammatory cytokines, IL-6, IL-1β and TNF-β related to SASP in mRNA levels were also elevated at the same peak. Collectively, these data suggest that arsenic exposure induces premature senescence and inflammation mediated by DNA damage response pathway in auditory cells.

Conclusion
We established the model of arsenic-induced premature senescence in auditory cells. This data indicates that the regulatory of SASP factors in ARHL could be assessed by our model.

PS 1035

Long-lasting Functional and Structural Damages on the Inner Ear Cells Induced by P-type Ca2+-ATPase Mutations

Osamu Minowa[1]; Takashi Daiho[2]; Kazuo Yamasaki[3]; Hiroshi Suzuki[3]; Toshihiko Shiroishi[4]; Atsushi Yoshiki[4]; Tetsuo Noda[5]; Nagomi Kurebayashi[6]; Takashi Murayama[6]; Kazusaku Kamiya[7]; Yasushi Okazaki[1]; Katsuhisa Ikeda[8]
[1]Juntendo University, Graduate School of Medicine, Diagnostics and Therapeutics of intractable Diseases; [2]Department of Biochemistry, Asahikawa Medical University; [3]Department of Biochemistry, Asahikawa Medical University,; [4]Riken BioResource Center (BRC); [5]Cancer Institute, The Japanese Foundation for Cancer Research; [6]Department of Pharmacology, Juntendo University School of Medicine; [7]Department of Otolaryngology, Juntendo University School of Medicine; [8]Juntendo University Faculty of Medicine

Using forward genetics approach, we have isolated 4 mouse lines of Pmca2 mutant, each of which has a different missense mutation and shows quite diverse phenotype; there exists a large difference in age-dependent ascending rate of ABR thresholds or period of hair cells/SG cells disappearance. F1 genetic background of C57BL/6J and C3H/HeJ augmented these phenotypic differences from weeks period of onset to years.

It remains elusive what precise mechanism underlies human age- dependent hearing loss or presbyacusis onset and development. It also raises controversy that rodent model of age-dependent hearing loss can be applied to human.

The clear differences in phenotype among the above mutants appear to result from the differences between Ca2+-pump activities of P-type Ca2+-ATPase, the product of mutated Pmca2 genes. Assuming that a biomolecular pathway towards the age-dependent emergence of phenotypes is divided into two axes (functional impairment and survival odds) and clarifying these axes may facilitate discovery of appropriate model of human progressive hearing loss. Ca2+ ion is generally thought to act as a second messenger in multiple signal pathways in very short time range, however it might also act in as-yet-unknown pathway for a life-long period.

To investigate these pathway axes in vitro, we have established cultured cell system in which each mutated protein expression is controlled to give equal amount and proper localization. Molecular analysis of this system is expected to reveal latent bases of the mutant's long-range effects.

PS 1036

Impact of Mitochondria Function on Endbulb of Held Synaptic Transmission during Age-related Hearing Loss

Yong Wang[1]; Ruili Xie[2]
[1]The Ohio State University; [2]Department of Otolaryngology, Ohio State University

Synaptic transmission at the first central auditory synapse, the Endbulb of Held, can sustain high levels of activity that require continuous supply of ATP and efficient clearance of calcium accumulation at the synaptic terminal. Mitochondria are one of the most prominent organelles at the Endbulb of Held terminal that support both functions. Our previous studies showed that synaptic transmission at the Endbulb of Held deteriorates during age-related hearing loss. It remains unclear how mitochondria function change during the process. In this study, we evaluated the endbulb synaptic function in young (2-5 months) and aged (27-31 months) CBA/CaJ mice by performing whole-cell patch clamp recording from bushy neurons in parasagittal slices of cochlear nucleus, while electrically stimulating the auditory nerve to activate the Endbulb synapses. We used a variety of pharmacological compounds that selectively disrupt

different aspects of mitochondria function and monitored the effects of drugs. In general, endbulb synapses from young, normal hearing animals showed stronger resistance to drug induced mitochondrial disruption than those from old hearing impaired mouse. The results suggest that mitochondria function is compromised during aging at the Endbulb of Held synapse, which may add another layer of detrimental effect to hearing impairment in the central auditory pathway.

Supported by NIDCD grants R03DC013396 and R01DC016037 to RX.

PS 1037

nAChR Modulation of Auditory Cortical Signaling: Aging

Madan Ghimire[1]; Rui Cai[1]; Troy Hackett[2]; Lynne Ling[1]; Donald Caspary[1]
[1]Southern Illinois University School of Medicine; [2]Vanderbilt University Medical Center

Background
Age-related loss of speech understanding (Presbycusis) is one of the most common human maladies affecting one third individuals between ages of 65-74 and well over half the population older than 75. Aging studies suggest that the elderly can, to some extent, maintain speech understanding as they age despite degraded ascending temporal information by using attentional and cognitive resources. Animal and human studies have shown the importance of cortical cholinergic systems in cognition and attentional modulation, implicating a possible role for cortical nicotinic cholinergic receptor (nAChR) in age-related loss of speech understanding. Sottile et al. (2017) found age-related declines in pre- and post-synaptic nAChRs responses and potential subunit changes in auditory thalamus. The present study focused on how aging might impact the basal forebrain cholinergic modulation of primary auditory cortical (AI) projection neurons (layer 5), potentially altering top-down processing.

Methods
All experiments used young adult 3-4 month and Aged 28 month old FBN. In situ hybridization and western blot studies were used to quantify transcript and protein levels for nAChRs subunits. Excitatory post-synaptic currents were obtained from whole cell in vitro recordings from LV pyramidal cells in response to acetylcholine (ACh) in the presence of muscarinic blocker atropine.

Results
Preliminary in vitro patch-clamp recordings from LV-AI neurons showed significant age-related reductions in peak amplitude of nAChR mediated post-synaptic currents evoked by puffing ACh. Signs of nAChR desensitization was observed at higher ACh dosages in recordings from AI neurons in aged animals. The selective alpha7 nAChR subunit antagonist methyllycaconitine (MLA) showed significantly greater blockade of cholinergic mediated responses in AI neurons from aged rats than in AI neurons from young rats. Blockage of beta-2 subunit containing nAChR showed no age-group differences between patched AI neurons. These findings are consistent with our previous (Presented ARO 2019) findings of age-related declines in the number of binding sites (Bmax) with changes in dissociation constant (kd) for beta-2 subunit containing nAChRs in radioligand binding studies. The electrophysiological and binding data are also supported by in situ studies by Hackett lab (Presented ARO 2019) also showing significant age-related decreases in nAChR subunit transcript. However, preliminary western blot analysis of alpha7, beta2 and vesicular acetylcholine transporter in primary auditory cortex remained relatively unchanged in aged animals.

Conclusion
These studies show an age-related functional decrease in cholinergic responses, and neurochemical findings in support of altered nAChR affinity and/or mutation to different nAChR subtypes in aging cortex.

PS 1038

Age-associated decline in Nrf2 signaling and associated mtDNA damage may be involved in the degeneration of the auditory cortex: Implications for central presbycusis

yongqin li[1]; Baoai Han[2]; Haiying Sun[3]
[1]Huazhong University of Science and Technology; [2]1Public Laboratory, Key Laboratory of Breast Cancer Prevention and Therapy, Ministry of Education, Tianjin Medical University Cancer Institute and Hospital, National Clinical Research Center for Cancer, Tianjin Medical University, Tianjin 30000, China; [3]Departments of Otorhinolaryngology, Union Hospital, Tongji Medical College, Huazhong University of Science and Technology, Wuhan 430022, China.

Central presbycusis is the most common sensory disorder in the elderly population. However, the underlying molecular mechanism remains unclear. The NF-E2-related factor 2 (Nrf2) is a key transcription factor in the cellular response to oxidative stress, but the role of Nrf2 in central presbycusis remains to be elucidated. The aim of the present study was to investigate the pathogenesis of central presbycusis using a mimetic aging model induced by D-galactose (D-gal) *in vivo* and *in vitro*. The

levels of nuclear Nrf2, as well as the mRNA levels of Nrf2-regulated antioxidant genes, were downregulated in the auditory cortex of aging rats, which was accompanied by an increase in 8-hydroxy-2'-deoxyguanosine formation, accumulation of mitochondrial DNA 4,834-base pair common deletion and neuron degeneration. In addition, oltipraz, a typical Nrf2 activator, was found to protect cells against D-gal-induced mtDNA damage and mitochondrial dysfunction by activating Nrf2 target genes *in vitro*. Interestingly, it was also observed that activating Nrf2 with oltipraz inhibited cell apoptosis and delayed senescence. Taken together, the data of the present study suggested that the age-associated decline in Nrf2 signaling activity and the associated mtDNA damage in the auditory cortex may be implicated in the degeneration of the auditory cortex. Therefore, restoration of Nrf2 signaling activity may represent a potential therapeutic strategy for central presbycusis.

Auditory Prostheses: Factors and Mechanisms Shaping Outcomes

PD 105

Novel Variants in Syndromic Hearing Impairment Genes and Associations with Audiometric Thresholds in a Multi-ethnic Cohort of US Patients with Cochlear Implants

Angelo Augusto M. Sumalde[1]; Patricia J. Yoon[2]; Dylan C. Ray[3]; Stephen Newton[2]; Stephen P. Cass[3]; Kenny H. Chan[2]; Regie Lyn P. Santos-Cortez[3]
[1]Department of Otolaryngology, University of Colorado School of Medicine; University of the Philippines Manila College of Medicine; [2]Department of Otolaryngology, University of Colorado School of Medicine; Department of Pediatric Otolaryngology, Children's Hospital Colorado; [3]Department of Otolaryngology, University of Colorado School of Medicine

Up to 50% of hearing loss has a genetic etiology. New variants continue to be discovered, with certain variants being more prevalent or unique to certain ethnicities. Different variants are also believed to result in different prognoses or clinical outcomes post-intervention, particularly cochlear implantation (CI). Additionally, a number of clinical variables have been suggested to contribute to post-CI outcomes. This study aimed to investigate genetic and clinical factors in CI patients of multiple ethnicities. Medical and genetic testing records of patients who underwent CI at the Children's Hospital Colorado and University of Colorado Hospital from January 2008 to December 2016 were reviewed. Variables for study included age at CI surgery, age at audiometric testing post-surgery, sex, genetic test results, temporal bone findings from CT imaging or MRI, implant type, co-morbid conditions, duration of implant use, and pre- and post-CI audiometric thresholds. Minor allele frequencies (MAF) of variants were obtained from the genome Aggregation Database (gnomAD) and classified using the Deafness Variation Database (DVD) v8.2, MutationTaster, Polyphen-2, or SIFT/PROVEAN where appropriate. Statistical analysis was done using Fisher exact, Wilcoxon rank sum and Spearman correlation tests. Out of 32 CI patients with genetic test results, eighteen (56.2%) patients had pathogenic gene variants. Six had autosomal recessive variants within GJB2. Other known pathogenic variants were identified in the genes CDH23, MYO15A, POU4F3, SLC26A4, STRC, TECTA and TMPRSS3. Four novel pathogenic variants were identified, namely CHD7 c.5720C >G(p.Ser1907*), ADGRV1/GPR98 c.[12535C >T(p.Arg4179*)];[13911delC(Pro4638Glnfs*49)], and ARID1B c.4640C >A(p.Pro1547Gln), with the latter three found in Hispanic patients. In addition, a patient with dysmorphic cochleae had a 3p25.3 deletion. Carriage of genetic variants was associated with better pre-CI audiometric thresholds at 2000 Hz (p=0.048), while the occurrence of clinical co-morbidities was related to worse pre-CI audiometric thresholds at 4000 Hz (p=0.04). Post-CI thresholds were significantly worse in patients with inner ear malformations, particularly in patients with cochlear nerve hypoplasia or aplasia. In conclusion, four novel pathogenic variants were identified, which contributes to knowledge of the allelic spectrum for hearing loss, particularly in the Hispanic population. These findings on novel variants and associations with pre- and post-CI audiometric thresholds will be useful in genetic counseling and prognostication of hearing outcomes in CI patients.

PD 106

Effects of Pulse Phase Duration on the Electrically-Evoked Compound Action Potential in Children with Cochlear Nerve Deficiency and Children with Normal-Sized Cochlear Nerves

Shuman He[1]; Jeffrey Skidmore[2]; Lei Xu[3]; William J. Riggs[2]; Chloe Vaughan[4]; Xiuhua Chao[3]; Michelle Shannon[5]; Cynthia Warner[5]
[1]The Ohio State University; Nationwide Children's Hospital; [2]The Ohio State University; [3]Department of Auditory Implantation, Shandong Provincial ENT Hospital Affiliated to Shandong University; [4]The Ohio State University, Eye and Ear Institute; [5]Nationwide Children's Hospital

Background
Prolonged pulse phase durations (PPDs) are often used as a mapping parameter for implanted children with cochlear nerve deficiency (CND). This clinical practice leads to reduced CI battery life due to high power consumption and increased risks of tissue and electrode damage (Loucks et al., 1939; MacIntyre et al.,

1957). Therefore, it is clinically important to investigate whether prolonged PPDs actually provide the benefit of enhancing CN responsiveness for implanted children with CND. Neural responsiveness of the CN can be evaluated using the electrically-evoked compound action potential (eCAP). This study compared the effect of increasing the PPD on three eCAP parameters reflecting CN responsiveness: threshold, maximum amplitude and slope of the Input/Output (I/O) function between children with CND and children with normal-sized CNs.

Methods
Study participants included 30 children with CND and 30 children with normal-sized CNs. All subjects were implanted with a Cochlear™ Nucleus® device in the test ear. The eCAP I/O function evoked by a single biphasic pulse was measured at three electrode locations across the electrode array for each subject. PPDs tested in this study ranged from 50 to 88 microsecond. For each subject, the maximum charge level tested for all PPDs was held constant at each electrode location. Generalized Linear Mixed effect Models (GLMMs) with subject group, electrode location and PPD duration as the fixed effects and subject as the random effect were used to compare the eCAP amplitude, the eCAP threshold and the slope of the eCAP I/O function.

Results
Children with CND had smaller maximum eCAP amplitudes, higher eCAP threshold and flatter slopes of eCAP I/O function than children with normal-sized CNs. When the upper limit of the total electrial charge was held constant, increasing the PPD had no statistically significant effect on the eCAP in both study groups.

Conclusions
For the same amount of electrical charge, increasing the PPD from 50 to 88 microsecond did not significantly affect CN responsiveness to electrical stimulation in human CI users.

Acknowledgments
This work was supported by the R01 grant from NIDCD (R01DC017846) and the R01 grant from NIDCD and NIGMS (R01DC016038).

PD 107

Enhancement of Interaural Level Differences and Binaural Band Selection Improves Sound Localization in Bilateral Cochlear Implant Users

Tom Gajęcki[1]; Waldo Nogueira[2]
[1]Hannover Medical School; [2]Hannover Medical School, Hannover, Germany; Cluster of Excellence, Hearing4all, Germany

Introduction
Bilateral cochlear implant (BiCI) users have difficulties localizing sounds, mainly due to the distortion of interaural differences in level and in time (ILD and ITD). In this work, we aim at emphasizing ILD cues to improve sound source localization in BiCIs.

Due to the nature of electrical stimulation used in current CI devices, sound coding strategies have to limit the dynamic range of the sound to be transmitted to the listener. This decrease in the dynamic range directly affects the ability of BiCI users to exploit ILD cues. However, these cues are not distorted only due to the limited available electric dynamic range; frequency distribution differences across ears also play an important role. In N-of-M type sound coding strategies, where the N most energetic frequency bands are selected for stimulation, these frequency distribution differences arise when different bands are selected in each of the devices, leading to interaural spectral decorrelation.

Methods
Motivated by the narrow dynamic range and the presence of interaural spectral decorrelation, an ILD enhancement method that emphasizes interaural differences in level to exploit the available electric dynamic range, and binaural band selection to keep coherent stimulating bands across ears are investigated to help BiCI listeners to exploit ILD information while maintaining consistent spectral content in both listening sides. Horizontal plane sound-source localization performance of five BiCI listeners was evaluated in a virtual sound field, under direct computer control of bilaterally synchronized stimulation. Subjects were asked to identify the direction of arrival of broadband noise bursts at four different azimuths.

Results
The results indicate that the participants were able to discriminate the direction of arrival more accurately for narrow azimuths when the ILD enhancement was applied, compared to the natural ILD and independently of binaural band selection. On the other hand, localization abilities improved for wider azimuths when using binaural band selection compared to independent band selection, regardless of whether ILD enhancement was applied or not.

Conclusions
The outcomes of this work show that the proposed ILD enhancement method, besides binaural band selection, improves the localization of sound sources in the front horizontal plane.

This work was funded by the Deutsche Forschungsgemeinschaft (DFG, German Research

Foundation) under Germany's Excellence Strategy – EXC 2177/1 (Project Number: 390895286)

PD 108

An objective measure of binaural sensitivity in cochlear implant recipients with bilateral acoustic hearing

René Gifford[1]; Virginia Richards[2]; Chris Stecker[3]; Linsey Sunderhaus[1]; Spencer Smith[4]
[1]Vanderbilt University Medical Center; [2]University of California, Irvine; [3]Boys Town National Research Hospital; [4]University of Texas at Austin

Cochlear implant (CI) users with bilateral acoustic hearing demonstrate significant benefit from combined electric and acoustic stimulation (EAS), with which they demonstrate better speech recognition in diffuse noise and improved spatial hearing. Even so, the utilization of bilateral acoustic amplification among EAS candidates remains low–possibly because EAS benefit varies across patients and environments, and is not reliably related to objective clinical measures such as audiometric thresholds. We have demonstrated a significant correlation between EAS benefit (improved speech in noise, spatial discrimination and motion discrimination) and EAS listeners' sensitivity to interaural time differences (ITDs) acoustic hearing domain. Though the relationship between ITD thresholds and EAS benefit is robust (r = 0.6 to 0.8), psychophysical estimation of binaural cue sensitivity is extremely time consuming–making it infeasible for clinical use and thus unavailable for a large proportion of CI users. Therefore, the purpose of this study was to investigate the applicability of using a cortical auditory evoked potential (CAEP)—the acoustic change complex (ACC)—to estimate sensitivity to interaural phase differences (IPDs) in adult EAS listeners. Our hypothesis was that the magnitude of the IPD-evoked ACC would correlate with 1) behavioral ITD thresholds for a 100-800 Hz stimulus, 2) degree of EAS benefit observed for speech recognition in diffuse noise, and 3) spatial discrimination. We tested 5 adult EAS listeners on measures of behavioral ITD sensitivity, speech understanding in diffuse noise, spatial hearing (freefield minimum audible angle, MAA), and CAEPs via the ACC. To validate test protocols and verify feasibility, CAEPs were also obtained for a group of 7 young and 3 middle-aged listeners with normal hearing. Stimuli applied sinusoidal amplitude modulation (SAM) to a 1.6-second, 250-Hz tone at 90 dB SPL. The 10- or 40-Hz SAM tone was presented either diotically for the entire 1.6-second duration or had a 180-degree IPD applied at 0.8 second (in one ear) to elicit the ACC. Preliminary data demonstrate: 1) the IPD ACC was measurable in all controls and for 4 of 5 EAS listeners, and 2) there was a trending correlation between IPD ACC magnitude and behavioral ITDs, as well as EAS speech recognition in diffuse noise, and EAS MAA. These preliminary data suggest that the use of the IPD ACC could help identify CI users with bilateral acoustic hearing who might benefit from EAS.

PD 109

Melodic Interval Perception by Unilaterally Deaf Cochlear Implant Listeners

Emily R. Spitzer[1]; John J. Galvin[2]; David R. Friedmann[1]; David M. Landsberger[1]
[1]NYU School of Medicine; [2]House Ear Institute

Two notes sounded sequentially form a melodic interval, one of the building blocks of melody. Relative to normal hearing (NH) listeners, cochlear implant (CI) users may have distorted melodic interval perception due to the limited number and spacing of electrodes. It is unknown how this distortion varies across individuals or different CI devices. For patients with single-sided deafness (SSD) or good contralateral hearing (bimodal), melodic interval perception can be precisely compared between acoustic and electric listening, which may reveal differences between individuals. Based on estimates of spiral ganglia location relative to typical electrode locations, we hypothesize that larger spaced intervals will be required for electric hearing to match an acoustic reference interval.

10 CI users participated (5 SSD and 5 bimodal). The magnitude of an electric probe interval (pure tones ranging from 4-36 semitones) was compared to the magnitude of an acoustic reference interval (4, 8 or 12 semitones). Acoustic intervals were delivered via headphones; electric intervals were delivered via direct audio input (DAI) to the clinical processor. Ears were informally loudness balanced prior to the task. The low notes were either B3 (246.9 Hz) or C4 (261.6 Hz) and randomized across ears and trials to avoid entrainment. During testing, participants heard a reference and a probe interval and indicated which was larger. Ten comparisons for each reference-probe combination were presented randomly. Psychometric functions were fit to the data to determine the electrical interval size needed to match an acoustic interval.

Most SSD and bimodal CI users required larger intervals to the CI ear to match the reference intervals. There was variability across participants; for example, the matching electric interval for an 8-semitone reference ranged from 8-27 semitones. There was also variability across participants in the degree of distortion across the three reference intervals. While some participants showed similar degrees of distortion for all references,

others showed more distortion for larger intervals. No differences in the patterns of results were observed between SSD and bimodal CI users.

Consistent with our hypothesis, larger electric intervals were needed to match the magnitude of an acoustic reference interval. This is likely due to the limited spectral resolution of a CI, resulting in compression of the melodic pitch range of electric hearing. Because clinical processors were used, it is unclear whether the differences in degree of distortion is due to variations in frequency allocation or the electrode-neural interface within and across subjects.

PD 110

Free-Field Simultaneous Speech Recognition Reveals Asymmetric Hearing Only in Hard-Listening Conditions

Milagros J. Fumero; Maria Romo-Castillo; Almudena Eustaquio-Martin; Enrique A. Lopez-Poveda
University of Salamanca

The aim of the present study was to assess the ability of cochlear-implant (CI) users to follow two simultaneous conversations when listening with two functionally independent devices (the standard clinical approach) compared to listening with binaurally coupled devices inspired by the medial olivocochlear reflex (the MOC strategy; Lopez-Poveda et al., 2016, Ear Hear 37(3):e138-e148). Listeners with normal hearing were presented with two simultaneous, time-centered sentences and were asked to recognize and repeat as many key words as possible from the two sentences. One of the sentences was uttered by a woman (W) located to the left of listener while the other sentence was uttered by a man (M) located to the right of the listener. Free-field listening was simulated by convolving monophonic sentence recordings with KEMAR head-related impulse responses. The task was conducted for three different spatial configurations of the talkers relative to the listener (W-15M+15, W-45M+45 and W-90M+90). The test was conducted for unprocessed stimuli and for stimuli vocoded through the STD and MOC strategies. We hypothesized that performance would be better with the MOC than with the STD strategy because the MOC strategy provides better segregated stimuli to each ear, hence allowing listeners to divide their attention to either ear. Contrary to our hypothesis, performance was not statistically different for the two strategies. Incidentally, however, in the vocoded conditions, listeners recognized significantly more words uttered by the male than the female talker. This was not the case for unprocessed stimuli, where recognition was statistically similar for the two talkers. The experimental design did not allow elucidating if this is because listeners focused on the right-ear stimulus (to benefit from the 'right-ear advantage') or because they focused on the male talker. Whatever the reason, these results demonstrate that asymmetric listening occurs in (simulated) free-field listening only in difficult listening conditions, such as with vocoded stimuli. [Work funded by MED-EL and the Spanish MINECO (ref. BFU2015-65376-P)].

PD 111

Evaluating the Effect of Increased Spread of Excitation on Speech-in-Noise Perception by Cochlear Implant Listeners

Tobias Goehring[1]; Julie G. Arenberg[2]; Robert P. Carlyon[1]
[1]University of Cambridge; [2]Massachusetts Eye and Ear Infirmary, Harvard Medical School

Cochlear implant (CI) listeners struggle to understand speech in background noise. Interactions between electrode channels due to current spread increase the masking of speech by noise and reduce the effective number of channels. Therefore, strategies to reduce channel interaction have the potential to improve speech-in-noise perception by CI listeners. We investigated the effects of channel interaction on speech-in-noise perception by CI users by imposing spectral "blurring" as a simulation of increased spread of excitation. Research questions were: (1) does blurring affect CI users' speech-in-noise perception when either all or only a subset of channels are blurred? (2) are listeners with better spectro-temporal acuity more affected by blurring? (3) does this depend on whether blurring is applied at the input (analysis filter bank) or at the output (electrode level) stage of the CI?

Experiment 1 produced blurring by adjusting the spectral overlap of the analysis filters, while controlling for loudness. Its effects were measured on speech-in-noise reception as a function of the amount of blurring applied to either all, or 5-of-15, electrode channels. Large amounts of blurring applied to all channels significantly increased speech reception thresholds (SRTs). SRTs for each listener were constant up to some blurring knee point, above which they increased. We argue that the blurring knee point may provide a method for evaluating the effects of spectro-temporal acuity on speech perception that is largely independent of cognitive influences. Indeed, higher knee points were significantly associated with better performance on a non-speech spectro-temporal task ("STRIPES", Archer-Boyd *et al,* 2018). Surprisingly, even extreme amounts of blurring applied to 5-of-15 channels did not affect SRTs.

Experiment 2 applied blurring at the electrode level to simulate a wider spread of information across

the cochlea – similar to a wide current spread - by simultaneously stimulating a set of adjacent electrodes (rather than just one) for each channel. T- and M-levels were adjusted to account for changes in loudness due to the wider excitation profiles. Interestingly, results were similar to Experiment 1 and there was again no effect of blurring applied to 5-of-15 channels even when using 8 electrodes per channel.

This is important because channel deselection strategies typically turn off a small number of "bad" electrodes to enhance speech perception and our results show that when 5 evenly spaced electrodes convey strongly degraded spectral information there is no effect on SRTs. We will determine whether this finding generalises to different noise types.

PD 112

Vowel Confusions and Threshold Profiles of Bilaterally Implanted Children

Kevin Franck[1]; Kelly Jahn[1]; **Julie G. Arenberg**[2]
[1]Massachusetts Eye and Ear, Harvard Medical School; [2]Massachusetts Eye and Ear Infirmary, Harvard Medical School

The purpose of this study is to better understand the variability in performance among children with cochlear implants. By studying bilaterally implanted children, we can compare peripheral measures of threshold and vowel perception between ears and across populations. Children who have learned how to listen with a cochlear implant may rely more on the input from the periphery than adults who are attempting to match an acoustic template. Therefore, we seek to determine the degree to which peripheral variability contributes to vowel confusion errors, or if there may be a central component. Thirteen children, ten, bilaterally implanted, ages 11.5 to 17.7 years participated. All children received their first implant between the ages 1 and 4.3 years (mean =2.6). All were implanted with the Advanced Bionics, HiRes90k device. Medial vowel identification was measured in the /hVd/ context, presented at 60 dB SPL in quiet and with a +10 SNR of 4-talker babble, if performance in quiet was at least 70% correct. Monopolar (MP) and steered quadrupolar (sQP) thresholds were obtained for 14 electrodes in each ear of each child using a sweep procedure. Perceptual distance was used to compare the confusion matrices for medial vowels and compared within (i.e., left and right ear) and across children to determine the contributions of the peripheral signal versus central decision making. Threshold profiles were assessed in a similar manner to determine the degree of correlation of threshold profiles within and across children. Only two of ten children had smaller perceptual distances between ears than compared to other children, suggesting that most children's confusion patterns reflect differences in the periphery. Threshold profiles were classified by shape. Of the 23 ears tested, 22 were linear for MP and of those 64% were flat and 6 of the 10 bilaterally implanted children had the same shape in both ears. With the sQP configuration, 17 ears had a linear profile and 41% of those were flat, and 3 of the 10 bilateral children had the same shape in both ears. These profile results suggests the periphery is as different between ears of bilaterally implanted children as it is across children, especially when sQP is used. The relationship between these profiles and vowel confusions will be discussed. If these relationships are consistent across ears and children, this could inform methods to optimize programs for individual implant listeners.

Clinical Otolaryngology and Pathology

PD 113

Rapid Detection of Circulating Inner Ear Biomarkers using an Electrochemical Immuno-biosensor.

Sahar Sadat Mahshid[1]; Alain Dabdoub[2]
[1]Biological Sciences, Sunnybrook Research Institute; [2]Biological Sciences, Sunnybrook Research Institute; Department of Otolaryngology-Head & Neck Surgery, University of Toronto

Permanent damage to cochlear or vestibular cells leads to hearing and balance disorders, respectively. There is no diagnostic test available to identify these disorders with the exact location of cellular damage in the inner ear. Thus, there is a need for new diagnostic approaches that are based on the detection of inner ear biomarkers circulating in the blood, through a rapid biosensor platform. These approaches require the knowledge of effective blood biomarkers, the development of highly sensitive and specific recognition strategies for these biomarkers, and the design of biosensor platforms that can be used at the point-of-need. We developed techniques for the identification and quantification of inner ear biomarkers using approaches from immunohistochemistry, synthetic biology, materials innovation, and electrochemical devices.

Here, we present the first biosensor platform for the rapid one-step detection of otolin-1, a blood circulating protein specifically expressed in the utricle and saccule in the inner ear. Our biosensor was combined with a DNA-based immunoassay on nanostructured electrodes for sensitive electrochemical detection of otolin-1. We first designed an assay that employed nucleic acid sequences re-engineered to undergo a large-scale surface hybridization. Upon hybridization, the target

protein, as well as redox reporter moieties, are brought to the electrode surface, which results in the generation of a specific electrochemical output. The electrode surface was then engineered by employing high-curvature nanostructured materials to enable sensitive sample analysis at low detection limits, close to the desired range, and in small (finger prick) volumes. We show that our electrochemical immuno-biosensor is capable of detecting otolin-1 at low picomolar concentrations with a three-fold quantitative range in a 10 µL sample in under 30 minutes.

Ultimately, more accurate diagnostics will help identify the sites of lesion in the inner ear – sensory hair cell types, auditory neurons, synapses, stria vascularis or central auditory pathway, and will provide the ability to rapidly detect and closely monitor the occurrence and progression of inner ear disorders as well as the efficacy of any treatment.

PD 114

Connexin 26 targeted assay on a miniaturized microarray for assessment of hemichannel function

Athanasia Warnecke[1]; Hongling Wang[2]; Frank Stahl[3]; Steffens Melanie[2]; Carsten Zeilinger[4]
[1]Hannover Medical School, Hannover, Germany; [2]Hannover Medical School; [3]Gottfried-Wilhelm-Leibniz University of Hannover, Institut für Technische Chemie; [4]Gottfried-Wilhelm-Leibniz University of Hannover, BMWZ

Hearing loss due to connexin mutations shows different phenotypes despite the same genotype. Means to assess the function of connexins are not available hitherto but would be of interest to predict the course of disease in connexin mutations. In the present study, we investigated if human Connexin 26 (hCx26 or Cx26WT) hemichannel opening can be triggered by temperature and by compensation of the Ca2+blockade with EDTA. Point mutations within Cx26 were therefore analysed by a novel optical microarray-based Lucifer Yellow uptake assay or by two electrode voltage clamp (TEVC) on frog oocytes to monitor simultaneous activities of channel proteins. The temperature-dependent activity of the hemichannels was influenced by the point mutations L90P, F161S, R184P or K188N drastically. Several of the mutations (e.g., Cx26K188N) blocked trafficking. Therefore, the temperature-dependent activity of the recombinant synthesized and purified wild-type Cx26WT and Cx26K188N hemichannel was tested by liposome flux assay (LFA) and on a microarray-based Lucifer Yellow uptake assay under warm conditions (>30 °C). The data from TEVC measurements and dye flux experiments showed that the mutations gave no or only a weak activity at increased temperature (>30 °C). We conclude that the position K188 in the Cx26WT forms a temperature-sensitive salt bridge with E47 whereas the exchange to K188N destabilizes the network loop- gating filter, which was recently identified as a part of the flexible Ca2+binding site. We assume that the temperature sensitivity of Cx26 is required to protect cells from uncontrolled release or uptake activities through Cx26 hemichannels. Whether and how these findings can be used for diagnosis or treatment of connexion-related hearing loss needs further investigation. We expect to use this miniaturized microarray system for the simultaneous screening of channel mutations in hearing disorders.

PD 115

Revisiting the etiologies and hearing features of pediatric auditory neuropathy: an integrative approach

Chen-Chi Wu[1]; Pei-Hsuan Lin[1]; Chuan-Jen Hsu[2]; Tien-Chen Liu[3]
[1]Department of Otolaryngology, National Taiwan University Hospital; [2]Taichung Tzu Chi Hospital, Buddhist Tzu Chi Medical Foundation, Taichung, Taiwan; [3]National Taiwan University College of Medicine

Background
Auditory neuropathy is an important entity in childhood sensorineural hearing loss. The management of auditory neuropathy is challenging due to heterogeneity in the etiologies and the diversity of clinical features. The aim of this study was to analyze the etiologies and hearing features of pediatric auditory neuropathy using an integrative audiologic, genetic, and imaging approach.

Methods
From 1997 to 2018, patients diagnosed with pediatric-onset auditory neuropathy were enrolled and divided into four groups based on the following etiologies: acquired, genetic, cochlear nerve deficiency-related, and indefinite auditory neuropathy. Medical and family histories, genetic results, and imaging findings were ascertained to determine the etiologies. The results of a battery of audiologic tests, including behavioral audiometry, distortion product otoacoustic emissions, auditory brainstem responses, and auditory steady-state responses were analyzed in the patients in the four groups.

Results
Of the 101 patients enrolled, 48 (47.5%), 16 (15.8%), 11 (10.9%), and 26 (25.7%) were determined to have acquired, genetic, cochlear nerve deficiency-related, and indefinite auditory neuropathy, respectively. Prematurity

and OTOF mutations were the leading causes of acquired and genetic auditory neuropathy, respectively. Patients with distinct etiologies had pathologies at different sites and exhibited different audiologic findings. Specifically, the onset of hearing loss was earlier in patients with acquired auditory neuropathy (odds ratio, 10.2; 95% confidence interval, 2.2-47.4), whereas the presence rate of distortion product otoacoustic emissions was higher in patients with genetic auditory neuropathy than in those in the other three groups (odds ratio, 10.7; 95% confidence interval, 1.3-85.4). Moderate to strong correlations (Pearson's r = 0.51 to 0.83) between behavioral thresholds and auditory steady-state response thresholds were observed in patients with different etiologies or sites of pathology.

Conclusions
The etiology was determined in approximately 75% of the children with auditory neuropathy using comprehensive history-taking, genetic examinations, and imaging studies. Different etiologies are associated with different audiologic features, and auditory steady-state responses might serve as an objective measure for estimating behavioral thresholds after correction.

PD 116

Phase 2b Randomized Double Blind Placebo-Controlled Trial of SPI-1005 for Meniere's Disease

Jonathan Kil[1]; Shaun A. Nguyen[2]; E. Emily Harruff[3]; Thomas Willcox[4]; Michael Hoa[5]; Hinrich Staecker[6]; Sujana Chandrasekhar[7]; Jeffrey D. Sharon[8]; J. Walter Kutz[9]; Michael Hoffer[10]; May Huang[11]; Gorden McMurry[12]; Paul R. Lambert[2]
[1]Sound Pharmaceuticals, Inc; [2]MUSC; [3]Sound Pharmaceuticals; [4]Thomas Jefferson University; [5]Georgetown University Medical Center; [6]University of Kansas Medical Center, Kansas City, KS, USA; [7]ENT&Allergy Associates; [8]UCSF; [9]UTSouthwestern Medical Center; [10]University of Miami; [11]Northwest Ear; [12]Advanced ENT&Allergy

Background
Glutathione peroxidase (GPx) is a critical cytoprotective enzyme in the brain, eye, ear, lung, and kidney. GPx1 is the dominant isoform in the inner ear and is highly expressed within the organ of Corti, spiral ganglia and stria vascularis of the cochlea. Ebselen is a selenorganic compound that mimics and induces GPx1 and has been shown to prevent and treat sensorineural hearing loss in animals (Kil et al., Hear Res 2007). SPI-1005 is an investigational new drug that contains ebselen and was shown to prevent acute noise-induced hearing loss in a Phase2 randomized controlled trial (RCT) (Kil et al., Lancet, 2017) and to treat newly diagnosed Meniere's Disease (MD) in a Phase1b RCT (Kil et al., ARO, 2018). We now report the Phase2b RCT data in active MD where hearing loss, tinnitus, and vertigo are documented and/or patient-reported.

Methods
149 adults with active MD, including hearing loss of ≥30 dB in one of three low frequencies at baseline, were consented, screened, and randomized (1:1:1) to receive either placebo, 200, or 400 mg SPI-1005, twice daily po for 28 days, with follow-ups at 4 and 8 weeks after the start of treatment. The pre-specified endpoints were to determine if SPI-1005 could improve hearing by a clinically relevant difference vs placebo, using pure-tone audiometry (PTA). Additional measures of efficacy included the Words-in-Noise test (WINT), and the patient-reported Tinnitus Functional Index (TFI) and Vertigo Symptoms Scale (VSS).

Results
124 adults (mean age 55 years: range 22-73 years) were in the Intent-to-Treat (ITT) analysis. The primary audiometric endpoint (≥10 dB gain from baseline in at least one low frequency) showed a significant improvement in the 400 mg vs placebo (61% vs 37%, $p < 0.023$), a 65% relative improvement at 8 weeks. The WINT showed significant improvements (≥4 words improvement from baseline) in the 400 mg vs placebo (60% vs 34%, $p < 0.017$), a 76% relative improvement at 8 weeks. Secondary endpoints showed improvements in tinnitus loudness (TFI) in the 400 mg vs placebo (1.4 vs 0.7, $p < 0.02$) at 8 weeks. No significant improvements in VSS were observed at either 4 or 8 weeks. No SAEs were reported and no negative impact on safety were observed.

Conclusions
SPI-1005 was well tolerated and effective in improving hearing loss and tinnitus in active Meniere's Disease using PTA, WINT and TFI (ITT analysis). These findings support the advancement of SPI-1005 to Phase3 pivotal RCTs in MD.

PD 117

Audiovestibular Dysfunction in Infratentorial (Classical) Superficial Siderosis: Retrospective Cross-Sectional Study

Natallia Kharytaniuk[1]; Duncan Wilson[2]; Gargi Banerjee[2]; Simon F. Farmer[3]; Peter Cowley[4]; David J. Werring[5]; Doris E. Bamiou[6]
[1]The Ear Institute, University College London; Department of Neuro-otology, University College London Hospitals; NIHR UCLH BRC Deafness and Hearing Problems Theme, London, UK; [2]Department of Neurology, National Hospital for Neurology and

Neurosurgery, London, and Department of Brain Repair and Rehabilitation, Stroke Research Centre, Institute of Neurology, Russell Square, University College London, UK; [3]Department of Neurology, National Hospital for Neurology and Neurosurgery, London, UK; [4]Lysholm Department of Neuroradiology, National Hospital for Neurology and Neurosurgery, London, UK; [5]Department of Neuro-otology, University College London Hospitals; Department of Neurology, National Hospital for Neurology and Neurosurgery, London; Department of Brain Repair and Rehabilitation, Stroke Research Centre, Institute of Neurology, Russell Square, University College London, UK;; [6]The Ear Institute, University College London; Department of Neuro-otology, University College London Hospitals; NIHR UCLH BRC Deafness and Hearing Problems Theme, London, UK;

Infratentorial superficial siderosis (iSS) is characterised by deposits of haemosiderin over the subpial surfaces of the central nervous system structures. It invariably involves cerebellum and vestibulocochlear nerves, resulting in hearing and balance impairment. Small case-series report the audiovestibular dysfunction in iSS to be of both central (brainstem and above) and peripheral (vestibular end-organ and nerve) origin, but there are few large systematic studies using standardised tests. The precise localisation of the involved part of the audiovestibular pathway might be useful to guide management and optimise patient outcomes.

The aim of this retrospective cross-sectional study was to identify from a prospectively-collected specialist database of iSS patients (defined using standardised radiological criteria) who were seen in the Neuro-otology, Otolaryngology or Audiovestibular Medicine services with the view to identify the most likely site of lesion. We reviewed the tests performed, their findings, and proposed management strategies.

We included 56 patients, 34(61%) males, mean age 59.3 years(SD±14.4, range 19-82). The initial symptom was: hearing difficulties 29(52%), imbalance 11(20%), and both 9(16%); two(4%) patients were asymptomatic, one(2%) patient reported anosmia. Hearing assessment records were available on 18(32%) patients; of these, 17(94%) had at least one abnormal test result, including pure tone audiometry (PTA), otoacoustic emissions (OAE), impedance and reflex testing, auditory brainstem responses (ABR) and speech tests. PTA identified mainly high-frequency asymmetrical variable degree (mild-to-profound) sensorineural hearing loss. ABR were recorded in ten(18%) patients, of which eight(80%) were abnormal, with absent or poor morphology of wave I being the most common finding consistent with retrocochlear impairment. One patient with near-normal PTA thresholds had unilateral absent ABR waves I-V, with normal OAEs. Overall, twenty-two patients(39%) were recorded to have received hearing aids, seven(12.5%) received cochlear implants (unilateral/bilateral). One patient received hearing therapy only. Vestibular assessments records were available on 12(21%) patients and were abnormal in 11(92%). The most common finding was of mixed bilateral peripheral and central dysfunction (six(10%) patients). Three patients underwent physiotherapy.

We found impairments in audiovestibular function in over 90% of iSS patients who were tested, with abnormal ABR in 80%, confirming predominantly retrocochlear auditory and mixed vestibular impairment. It is important that all patients with iSS have a timely and comprehensive audiovestibular assessment. This would ensure accurate identification of the site of lesion (central versus peripheral involvement, or both), initiation of treatment and rehabilitative measures specific to patients' needs, and to aid monitoring of disease progression.

*DJW and DEB share senior authorship.

PD 118

High Risk of Sudden Sensorineural Hearing Loss in Several Autoimmune Diseases According to a Population-Based National Sample Cohort Study

Junhui Jeong[1]; Hyunsun Lim[2]; Kyuin Lee[1]; Chang Eui Hong[1]; Hyun Seung Choi[1]
[1]Department of Otorhinolaryngology, National Health Insurance Service Ilsan Hospital; [2]Departments of Policy Research Affairs, National Health Insurance Service Ilsan Hospital

Objective
We investigated the risk of sudden sensorineural hearing loss (SSNHL) in patients with autoimmune diseases compared with a control group in a population-based study using a National Health Insurance Service National Sample Cohort data from Korea. Methods: We enrolled autoimmune-disease patients who were ≥ 20 years old in 2006 into the autoimmune-disease group, and we selected a control group that had similar demographic characteristics as the autoimmune group. We tracked the two groups from 2006 to 2015 and compared the proportion of patients who developed SSNHL between them. Results: Among the 13,250 in the autoimmune-disease group, 145 experienced an SSNHL event (1.09%). Among the 66,250 in the control group, 484 experienced an SSNHL event (0.73%). The SSNHL risk was significantly higher in the autoimmune-disease group than in the control group. SSNHL incidence was significantly higher among patients with antiphospholipid

syndrome (APS), multiple sclerosis (MS), rheumatoid arthritis (RA), and connective tissue diseases including Sjögren syndrome and Behçet's disease compared to the control group. In detailed stratified analyses using reinforced additional diagnostic codes, only RA patients had significantly higher SSNHL incidence than the control group.

Conclusion

The association of several autoimmune diseases with SSNHL was evaluated in this large-scale, population-based, big data study. The risk of SSNHL was significantly higher in patients with APS, MS, RA, and connective tissue diseases including Sjögren syndrome and Behçet's disease compared with patients without autoimmune diseases. In particular, SSNHL was significantly associated with RA according to detailed analyses using reinforced additional diagnostic codes.

Table 1. Demographic characteristics of the autoimmune-disease group and the control group

	Autoimmune-disease group (N = 13,250)	Control group (N = 66,250)	*p*-value
SSNHL			<0.001
No events	13,105 (98.91)	65,766 (99.27)	
Events	145 (1.09)	484 (0.73)	
Age range (years)			1.000
20–29	1,452 (10.96)	7,260 (10.96)	
30–39	2,315 (17.47)	11,575 (17.47)	
40–49	2,849 (21.50)	14,245 (21.50)	
50–59	2,715 (20.49)	13,575 (20.49)	
60–69	2,161 (16.31)	10,805 (16.31)	
70–79	1,468 (11.08)	7,340 (11.08)	
80–	290 (2.19)	1,450 (2.19)	
Sex			1.000
Male	4,419 (33.35)	22,095 (33.35)	
Female	8,831 (66.65)	44,155 (66.65)	
Residence			1.000
Seoul (capital)	2,725 (20.57)	13,625 (20.57)	
Metropolitan	3,288 (24.80)	16,430 (24.80)	
City (small and medium sized)	5,549 (42.63)	28,245 (42.63)	
County	1,590 (12.00)	7,950 (12.00)	
Income level			1.000
1st (lowermost) quintile	2,116 (15.98)	10,580 (15.98)	
2nd quintile	2,217 (16.73)	11,085 (16.73)	
3rd quintile	2,916 (22.01)	14,580 (22.01)	
4th quintile	2,238 (16.87)	11,175 (16.87)	
5th (uppermost) quintile	3,766 (28.42)	18,830 (28.42)	

SSNHL = sudden sensorineural hearing loss. Figures in parentheses are percentages.

Table 2. Risk of sudden sensorineural hearing loss in individual autoimmune diseases based on diagnostic code compared with the control group.

Individual autoimmune disease	Total number	Number of SSNHL	HR (CI)	*p*-value
Autoimmune-disease group	13,250[1]	151		
Antiphospholipid syndrome	4	0	19.916 (1.22–325.062)	0.0358*
Sarcoidosis	33	0	2.25 (0.139–36.319)	0.5676
Multiple sclerosis	52	3	13.335 (4.646–38.277)	<0.0001*
Rheumatoid arthritis	8,233	98	1.519 (1.204–1.917)	0.0004*
Polyarteritis nodosa	10	0	7.146 (0.451–113.133)	0.1629
Wegener's granulomatosis	47	0	1.24 (0.077–19.962)	0.8794
Systemic lupus erythematosus	279	4	1.538 (0.534–4.43)	0.4254
Dermatopolymyositis	46	0	1.51 (0.094–24.316)	0.7712
Systemic sclerosis	37	0	1.856 (0.116–29.593)	0.6615
Connective tissue diseases including Sjögren syndrome and Behçet's disease	890	11	1.878 (1.044–3.378)	0.0354*
Ankylosing spondylitis	1,417	11	1.132 (0.594–2.157)	0.7066
Psoriasis	2,876	24	1.307 (0.852–2.005)	0.2205
Control group	66,250	484	1	

SSNHL = sudden sensorineural hearing loss; HR = hazard ratio; CI = confidence interval. *p-value < 0.05.

[1]Total number in autoimmune-disease group (13,250) is less than the sum of patients with each autoimmune disease (13,924) because some patients had more than two autoimmune diseases.

Table 3. Risk of sudden sensorineural hearing loss in individual autoimmune diseases based on 'Special Exception of Assessment' codes compared with the control group.

Individual autoimmune disease	Total number of each disease (Total number in matched control group)	Number of SSNHL for each disease (Number of SSNHL in matched control group)	HR (CI)	*p*-value
Autoimmune-disease group				
Multiple sclerosis	26	1	4.12 (0.256–66.213)	0.3177
	(130)	(2)	1	
Rheumatoid arthritis	1112	19	2.229 (1.297–3.829)	0.0037*
	(5560)	(46)	1	
Systemic lupus erythematosus	229	4	2.843 (0.696–11.617)	0.1458
	(1145)	(13)	1	
Connective tissue disease including Sjögren syndrome and Behçet's disease	394	5	2.328 (0.815–6.647)	0.1144
	(1970)	(13)	1	
Ankylosing spondylitis	367	5	1.767 (0.582–5.367)	0.3153
	(1835)	(14)	1	
Psoriasis	37	0	1.543 (0.031–76.415)	0.8275
	(185)	(2)	1	

SSNHL = sudden sensorineural hearing loss; HR = hazard ratio; CI = confidence interval. *p-value < 0.05.

PD 119

Pericyte Activation is at the Root of Alport Disease Initiation in both the Renal Glomerulus and the Stria Vascularis of the Inner Ear.

Dominic Cosgrove[1]; Brianna Dufek[1]; Daniel Meehan[1]; Duane Delimont[1]; Gina Samuelson[2]; Xiaorui Shi[3]; Zhiqiang Hou[3]; Grady Phllips[4]; Michael Anne Gratton[4]
[1]Boys Town National Research Hospital, Omaha, NE, USA; [2]Boys Town National Research Hospital; [3]Oregon Health & Science University; [4]Washington University School of Medicine, St. Louis, MO, USA

Alport syndrome results from mutations in any of the type IV basement membrane collagen genes COL4A3, COL4A4, and COL4A5 that lead to glomerular disease associated with hearing loss. The pathology in both the kidney and cochlea has a delayed onset and progressive nature. In earlier work, we demonstrated that initiation of Alport glomerular disease involved up-regulation of endothelin-1 (ET-1) which activates glomerular pericytes (mesangial cells) via endothelin A receptor (ET_AR) signaling. This activation results in actin cytoskeletal rearrangements resulting in the invasion of glomerular capillaries by mesangial filopodia. The mesangial proteins deposited in the glomerular basement membranes (GBM) activate the inflammatory process that ultimately culminates in kidney fibrosis. In the inner ear, Alport mice show progressive thickening of the strial capillary basement membranes (SCBM) with accumulation of the same ECM molecules that accumulate in the GBM. These pathological changes to the stria can be blocked by treating mice with ET_AR inhibitors. The SCBM changes are also associated with reduced vascular permeability, hearing loss, reduced endocochlear potentials and an elevated sensitivity to noise-induced hearing loss. Pericytes are detaching and migrating into the interstitium of the stria vascularis before SCBM thickening is observed, and prior to hearing loss via ABR measures. When cultured primary strial pericytes are stimulated with ET-1, they undergo actin cytoskeletal rearrangement as determined by immunofluorescence analysis and biochemical analysis of filamentous to globular (F/G) actin ratios. F/G actin ratios are significantly higher in ET-1-treated cells relative to untreated control cells. This same effect is observed when cultured primary glomerular pericytes are treated with ET-1. Collectively, these studies suggest that the ET-1 stimulation of glomerular and strial pericytes is a key event in disease initiation in both organs. Supported by R01DC015385

PD 120

Healing and Hearing Outcomes of Chinchilla Tympanoplasty Procedures with Novel Biodegradable, Biomimetic 3D-Printed Tympanic Membrane Grafts

Nicole Black[1]; Dhrumi Gandhi[2]; Jennifer S. Zhu[1]; Marta Pawluczuk[3]; Elliott D. Kozin[2]; Jeffrey Cheng[4]; Jennifer Lewis[5]; Aaron K. Remenschneider[6]
[1]John A. Paulson School of Engineering and Applied Sciences, Harvard University; [2]Massachusetts Eye and Ear Infirmary- Harvard University; [3]Undergraduate Research Assistant; [4]Eaton-Peabody Laboratory, Massachusetts Eye and Ear Infirmary,Department of Otolaryngology – Head and Neck Surgery, Harvard Medical School; [5]Harvard John A. Paulson School of Engineering and Applied Sciences; [6]Dept. of Otolaryngology, UMass Memorial Medical Center; Massachusetts Eye and Ear

Background

Tympanoplasty aims to close a chronic tympanic membrane (TM) perforation and restore proper sound conduction to the ossicular chain. Commonly used graft materials, such as temporalis fascia and cartilage, do not degrade nor remodel after implantation. Reconstructed

TMs do not possess the native lamina propria's circular and radial collagenous architecture and are inefficient at sound conduction at high frequencies.

Methods

Our team has developed a novel biodegradable ink made from poly(ester urethane urea) (PEUU) with fugitive poly(ethylene glycol) (PEG). We 3-dimensionally (3D)-print grafts from the PEUU + 25wt% PEG at 8mm in diameter and approximately 100μm in thickness with 50 circular and 50 radial lines to recapitulate the native TM fiber arrangement. Following PEG leaching, plasma treatment, and ultraviolet sterilization, we soak the porous PEUU grafts in a saline solution. Lanigera chinchillas undergo baseline auditory brainstem response (ABR) testing at 1, 2, 4, 8, and 16kHz. A thermal myringotomy loop is used to create a perforation in the intact TM. After 4 weeks, the chronic perforation is repaired with 3D-printed PEUU grafts or control autologous temporalis fascia grafts. After 3 months, ABR testing is performed again, the chinchillas are sacrificed, and temporal bones are fixed and embedded. Remodeled TMs are stained with hematoxylin & eosin to measure thickness changes and visualize protein deposition.

Results

3D-printed PEUU and temporalis fascia grafts close chronic chinchilla TM perforations. While fascia grafts appear to retain their original structure and thickness, histological results show that PEUU grafts degrade to approximately 30-40% of their original thickness after 3 months, and they exhibit native cellular ingrowth on the lateral and medial sides of the graft. ABR threshold changes between 3 months and initial hearing are more favorable for the 3D-printed P-PEUU grafts than the fascia grafts, suggesting less hearing loss from baseline. Importantly, ABR threshold shifts at 16kHz average 8dB for TMs healed with the 3D-printed P-PEUU grafts (n=6), in contrast to approximately 19dB for the fascia grafts (n=5).

Conclusion

We have developed a novel material and manufacturing process for creating biodegradable and biomimetic circular/radial TM grafts. These grafts demonstrate surgical ease of placement, closure of chronic TM perforations, and superior high frequency audiometric outcomes compared to fascia grafts.

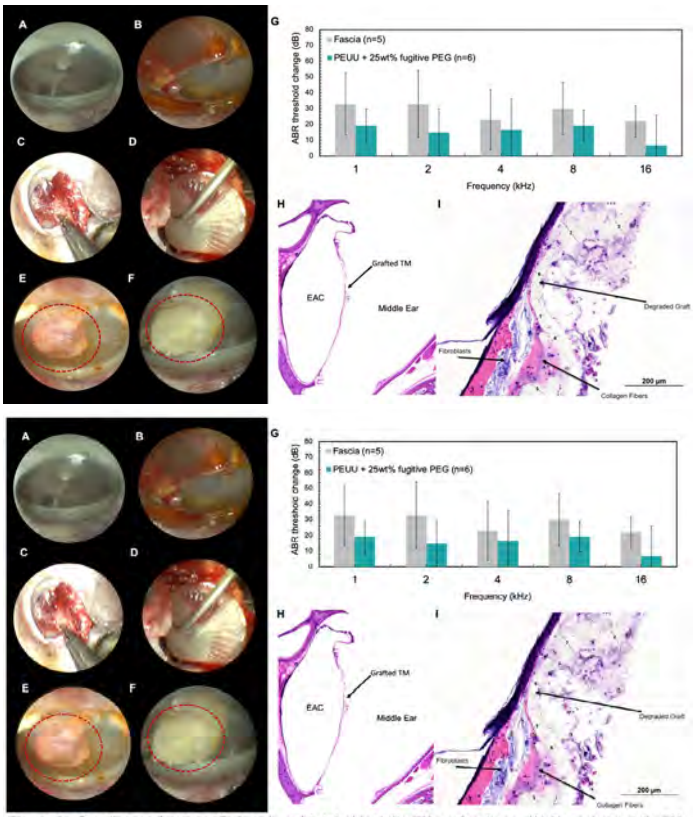

Figure 1. Creation and repair of chronic subtotal chinchilla TM perforations. (A) Normal chinchilla TM. (B) Chronic perforation that persists for 1 month without healing. Underlay tympanoplasty with (C) autologous fascia and (D) 3D-printed P-PEUU graft. Healed TMs 3 months post-implantation are endoscopically viewed with (E) autologous fascia and (F) 3D-printed P-PEUU grafts. (G) ABR results similar or improved hearing threshold changes before and 3 months post-implantation with P-PEUU grafts compared to fascia, suggesting a lack of ototoxicity of P-PEUU material and its degradation products. (K,L) Histological sections with H&E staining demonstrates perforation closure and partial degradation of P-PEUU graft material with native tissue ingrowth on both the medial and lateral sides of the graft.

Generally Genetics

PD 121

Cx26 (GJB2) Mutation Heterozygous Carriers are Vulnerable to Noise

Shu Fang; Yang Liu; Li-Man Liu; Yan Zhu; **Hong-Bo Zhao**

Dept. of Otlaryngology, University of Kentucky Medical Center

Background

Cx26 (*GJB2*) mutations cause most of autosomal recessive deafness (DFNB1) and affect as many as 3 of every 1,000 babies. The frequency of heterozygous-mutation carriers is even higher. These heterozygous-mutation carriers usually show normal hearing. We previously found that active cochlear amplification in the Cx26 heterozygous knockout (KO) mice is increased rather than decreased. In this study, we further examined the susceptibility of Cx26 heterozygous KO mice to noise.

Methods

Cx26 heterozygous conditional KO mice, which were created by a Cre-FloxP technique, were used. One

group of Cx26 heterozygous KO mice were exposed to white noise (95 dB SPL) for 2 hours, one time. Another group of Cx26 heterozygous KO mice without noise exposure serviced as control. ABR, DPOAE, and cochlear microphonics (CM) were recorded to assess cochlear and hearing function.

Results & Discussion

Cx26 heterozygous KO mice demonstrated normal hearing as measured by ABR threshold, similar to normal hearing of Cx26 mutation heterozygous carriers observed in the clinic. However, after noise exposure, Cx26 heterozygous KO mice demonstrated significant hearing loss in comparison with control. We further found that DPOAE in Cx26 heterozygous KO mice was increased rather decreased. Cochlear microphonics (CM) in Cx26 heterozygous KO mice was also increased. Thus, "over-increased" gain of the active cochlear amplification in Cx26 heterozygous KO mice may increase susceptibility to noise.

Conclusions

These data indicate that Cx26 mutation heterozygous carriers are susceptible to noise and should avoid exposing to noise.

Supported by NIH R56 DC 015019 and R01 DC 017025

PD 122

Drug Screening and AAV Gene Therapy for GJB2 Related Hearing Loss with iPS cells

Kazusaku Kamiya[1]; Ichiro Fukunaga[2]; Osamu Minowa[3]; Katsuhisa Ikeda[4]
[1]Department of Otolaryngology, Juntendo University School of Medicine; [2]Juntendo university; [3]Juntendo University, Graduate School of Medicine, Diagnostics and Therapeutics of intractable Diseases; [4]Juntendo University Faculty of Medicine

Mutation of the Gap Junction Beta 2 gene (GJB2) is the most frequent cause of hereditary deafness worldwide and accounts for up to 50% of non-syndromic sensorineural hearing loss cases in some populations. GJB2 encodes connexin (CX) 26, a component in cochlear gap junction. We have demonstrated that the degradation of gap junction plaque (GJP) macromolecular complex composed of CX26 and CX30 are critical pathogenesis starting at the embryonic days (Kamiya, *J Clin Invest*, 124(4):1598–1607, 2014). Cochlear CX26-gap junction plaque (GJP)-forming cells such as cochlear supporting cells are thought to be an important therapeutic target for the treatment of hereditary deafness. As one of the therapeutic strategy, we demonstrated that the cochlear delivery of Gjb2 using AAV significantly improved the GJPs and auditory responses of Cx26 deficient mice (Iizuka, Hum Mol Genet, 2015, 24(13):3651-61). As several AAV serotypes has different cell tropism to cochlear cell types such as hair cells without gap junction and supporting cells with gap junctions, we examined some appropriate AAV serotypes to develop the effective gene therapy for GJB2 related hearing loss.

For the disease modeling, we developed a novel strategy to differentiate induced pluripotent stem (iPS) cells into functional CX26-GJP-forming cells that exhibit physiological properties typical of the developing cochlea. Furthermore, these disease model cells from CX26-deficient mice recapitulated the drastic disruption of GJPs, the primary pathology of GJB2-related hearing loss (Fukunaga, *Stem Cell Reports*, 7(6), 1023-1036, 2016). To establish the disease model cells from the patients with GJB2 related hearing loss, we developed human iPS cells from the patients with Japanese and East Asian typical GJB2 mutations, GJB2 V37I, G45E/Y136X and 235delC. As the patients with these three homozygous mutations shows different hearing levels (mild, severe, and profound hearing loss respectively), the disease model cells from these patient derived iPS cells can be used to analyze different degree of GJB2 related hearing loss among most typical GJB2 mutations in East Asia. By using disease model cells, we established a GJP based screening system with high throughput imaging cytometer and screened some molecules to enhance the gap junction function of the model cells.

PD 123

Burden of Rare Missense Variants in OTOG Gene in Familial Meniere's Disease

Pablo Roman-Naranjo[1]; Alvaro Gallego-Martinez[1]; **Jose Antonio Lopez Escamez**[2]
[1]Otology & Neurotology Group CTS495, Department of Genomic Medicine, GENYO - Centre for Genomics and Oncological Research – Pfizer/University of Granada/ Junta de Andalucía, Spain; [2]Centre for Genomics and Oncology GENYO

Background

Familial Meniere's disease (MD) has been reported in 6-9% of sporadic cases, and few genes (*FAM136A, DTNA, PRKCB, SEMA3D* and *DPT*) have been involved in single families with autosomal dominant inheritance and incomplete penetrance, suggesting genetic heterogeneity; however, no gene has been found to be associated with MD in different families. The aim of this study was to identify rare variants and relevant genes for sensorineural hearing loss (SNHL) in familial MD by using exome sequencing.

Methods
We recruited 109 individuals with MD (73 cases from 46 different families and 36 early-onset sporadic patients) from 11 hospitals, according to the diagnostic criteria defined by the Barany Society in 2015. A case-control study was designed to search for rare variants in SNHL genes. Exome sequencing data from 46 MD families were analyzed. After quality checks, functional annotation, filtering and prioritization, minor allelic frequencies (MAF) of rare variants in 116 SNHL genes were calculated. Next, we conducted a single rare variant analysis (SRVA, MAF< 0.001 and CADD score >15), and a gene burden analysis (GBA, MAF< 0.05) by selecting one patient from each family. Allelic frequencies from Non-Finnish European (NFE) from Exome Aggregation Consortium (ExAC) and Collaborative Spanish Variant Server reference datasets were used as controls.

Results
A total of 5136 single nucleotide variants in hearing loss genes were considered for SRVA in familial MD cases, but only one heterozygous variant in the *OTOG* gene (rs552304627) was found in two unrelated families. The GBA found an enrichment of rare missense variants in the OTOG gene in 14/46 families (30%) against either NFE population from ExAC (OR= 4.3(2.6-7.0), p= 4.1x10-8) or Spanish population (OR= 3.6(2.1-5.9), p= 7.1x10-6). Nine different rare missense variants were found in *OTOG* gene in 14/46 non-related families, and 6 families had 2 or more shared variants. However, sporadic patients with early onset MD did not show an excess of rare variants when they were compared to NFE population (OR=2.1(1.2-3.7), p=0.11) or Spanish population (OR=2(1.1-3.5), p=0.20)

Conclusions
We have found an enrichment of multiplex rare missense variants in the *OTOG* gene in familial MD. This finding supports *OTOG* as a relevant gene in familial MD and set the groundwork for genetic testing in MD.

Funding
JALE is partially funded by INT18/00031 from ISCIII. This study was funded by the Luxembourg National Research Fund INTER/Mobility/17/11772209 Grant and EF-0247-2017 from Andalusian Health Government to JALE.

PD 124

Protective Genetic Variants for Usher I Syndrome and Hearing Loss

Qingyin Zheng[1]; Zehua Sun[2]; Aizhen Zhang[1]; Fuyi Xu[3]; Weinan Du[1]; Robert Williams[3]; Lu Lu[4]
[1]Department of Otolaryngology- Head & Neck Surgery, Case Western Reserve University, Cleveland, Ohio, USA; [2]Hearing and Speech Rehabilitation Institute; [3]University of Tennessee Health Science Center; [4]University of Tennessee Health Science Center (UTHSC)

More than 28 million Americans and 360 million people worldwide have hearing loss (HL). Most HL is caused by damaged cochlear hair cells (HCs) that do not regenerate in mammals after damage. Mutations in cadherin 23 (*CDH23*) are involved in many forms of HL, including Usher syndrome, Type 1D autosomal recessive deafness 12 (DFNB12), and some age-related hearing loss (AHL). There are striking homologies in humans and mouse models in genetic variants and disease mechanisms. Of interest, higher CpG methylation levels in *CDH23* can also be associated with AHL[1]. We and others have demonstrated that the DBA/2J (D2) strain of mouse exhibits early-onset progressive hearing loss (PHL) and is deaf by three months-of-age[3-9]. In contrast, the widely used C57BL/6J (B6) strain develops high frequency HL starting at three months and this progresses to a profound loss after one year[7-18]. By using backcrosses and recombinant inbred (RI) strains, including the family of BXD lines that are progeny of crosses of B6 and D2, we have mapped several quantitative trait loci—*ahl, ahl2*, *ahl4,* etc.—and have identified mutations in *cadherin 23* and *fascin2*. Both murine mutants have contributed to our understanding of inner ear biology and HL. The BXD family has now been greatly expanded and has key advantages for the study of HL. We have a total of ~150 full inbred BXD strains (Ashbrook et al., bioRxiv, 2019), all of which have been sequenced at ~38X. We have identified over 6 million segregating SNPs and now have excellent genetic maps and deep phenomics data. As expected, differences in hearing (EPs) among the BXD lines are much greater than those between parental strains. We have identified significant genetic locus on chromosome 16 that modulates ABR thresholds at 8, 16, and 32 kHz using BXD family, and have uncovered 5 BXD strains that have remarkably intact hearing (20 dB) even at two years—an age at which both parents and most common inbred strains are deaf. In this study, we further examined morphology of strains with good hearing and strains with deafness at one year old through H&E staining, and cochleae gene expression of B6 and D2 mice at young (6 weeks) and old age (12 months) through RT-PCR and RNA-seq method. The result of H&E staining showed that the inner (IHC) and outer (OHC) hair cells lost significantly and the density of spiral ganglion cells decreased significantly in the strains with deafness comparing to the strains with good hearing. The result of RNA-Seq of cochleae showed that relative gene expression levels of heat shock protein genes, the candidate genes, are more highly

expressed than other known hearing loss causal genes (*Ush1c, Fscn2*) in both old and young BXD parental mice, suggesting that they are most like the protective genes. The qRT-PCR result showed that the expression of heat shock protein genes has significant expression difference between DBA/2J and C57BL/6J. Currently we are collecting gene expression of cochleae from BXD strains and will finally define the candidate genes that modulate hearing variance among BXD mice. Our goal is to use this family to uncover new HL variants and mechanisms and also to develop improved models with which to study long-lasting protective variants. Grant support: R01DC015111(QYZ)

1, Bouzid, A. *et al.* CDH23 Methylation Status and Presbycusis Risk in Elderly Women. *Front Aging Neurosci* **10**, 241,
2, Kim, B. J. *et al.* Discovery of CDH23 as a Significant Contributor to Progressive Postlingual Sensorineural Hearing Loss in Koreans. *PLoS One* **11**,
3, Wang, Q. *et al.* Otoprotective effects of mouse nerve growth factor in DBA/2J mice with early-onset progressive hearing loss. *J Neurosci Res* **95**, 1937-1950,
4, Johnson, K. R., Longo-Guess, C., Gagnon, L. H., Yu, H. & Zheng, Q. Y. A locus on distal chromosome 11 (ahl8) and its interaction with Cdh23 ahl underlie the early onset, age-related hearing loss of DBA/2J mice. *Genomics* **92**, 219-225,
5, Jones, S. M. *et al.* A comparison of vestibular and auditory phenotypes in inbred mouse strains. *Brain Res* **1091**, 40-46,
6 , Zheng, Q. Y. & Johnson, K. R. Hearing loss associated with the modifier of deaf waddler (mdfw) locus corresponds with age-related hearing loss in 12 inbred strains of mice. *Hear Res* **154**, 45-53,
7, Johnson, K. R., Zheng, Q. Y. & Erway, L. C. A major gene affecting age-related hearing loss is common to at least ten inbred strains of mice. *Genomics* **70**, 171-180,
8, Zheng, Q. Y., Johnson, K. R. & Erway, L. C. Assessment of hearing in 80 inbred strains of mice by ABR threshold analyses. *Hear Res* **130**, 94-107,
9, Noben-Trauth, K., Zheng, Q. Y., Johnson, K. R. & Nishina, P. M. mdfw: a deafness susceptibility locus that interacts with deaf waddler (dfw). *Genomics* **44**, 266-272,
10, Zheng, Q. Y. *et al.* Digenic inheritance of deafness caused by 8J allele of myosin-VIIA and mutations in other Usher I genes. *Hum Mol Genet* **21**, 2588-2598,
11, Han, F. *et al.* A new mouse mutant of the Cdh23 gene with early-onset hearing loss facilitates evaluation of otoprotection drugs. *Pharmacogenomics J* **12**, 30-44,
12, Zheng, Q. Y. *et al.* A new spontaneous mutation in the mouse protocadherin 15 gene. *Hear Res* **219**, 110-120,
13, Zheng, Q. Y. *et al.* Digenic inheritance of deafness caused by mutations in genes encoding cadherin 23 and protocadherin 15 in mice and humans. *Hum Mol Genet* **14**, 103-111,
14, Keithley, E. M., Canto, C., Zheng, Q. Y., Fischel-Ghodsian, N. & Johnson, K. R. Age-related hearing loss and the ahl locus in mice. *Hear Res* **188**, 21-28,
15 , Noben-Trauth, K., Zheng, Q. Y. & Johnson, K. R. Association of cadherin 23 with polygenic inheritance and genetic modification of sensorineural hearing loss. *Nat Genet* **35**, 21-23,
16, Staecker, H., Zheng, Q. Y. & Van De Water, T. R. Oxidative stress in aging in the C57B16/J mouse cochlea. *Acta Otolaryngol* **121**, 666-672 (2001).
17, Ikeda, A. *et al.* Genetic modification of hearing in tubby mice: evidence for the existence of a major gene (moth1) which protects tubby mice from hearing loss. *Hum Mol Genet* **8**, 1761-1767,
18, Johnson, K. R., Erway, L. C., Cook, S. A., Willott, J. F. & Zheng, Q. Y. A major gene affecting age-related hearing loss in C57BL/6J mice. *Hear Res* **114**, 83-92 (1997).

PD 125

Mutations of MAP1B, encoding the microtubule-associated phosphoprotein, cause sensorineural hearing loss

Limei Cui[1]; **Min-Xin Guan**[2]; Ye Chen[1]
[1]Zhejiang University; [2]Zhejiang Unviersity

We have identified three novel heterozygous mutations (c.4198A >G, p.1400S >G; c.2768T >C, p.923I >T; c.5512T >C, p.1838F >L) in the MAP1B, cosegregating with autosomal dominant inheritance of nonsyndromic hearing loss in three unrelated Chinese families. MAP1B gene encoded a microtubule-associated phosphoprotein involved in the microtubule dynamics of growing axons and growth cones, however, its function in the auditory system is unknown. Here, we showed that Map1b is highly expressed in the spiral ganglion neurons in the mice cochlea. Using otic sensory neuron-like cells, generated by pluripotent stem cells from patients carrying the MAP1B mutation and controls, we demonstrated that the p.1400S >G mutation caused the reduced levels and deficient phosphorylation of MAP1B, which are involved in the microtubule stability and dynamics. Strikingly, otic sensory neuron-like cells exhibited disturbing dynamics of microtubule, axonal elongation, and defects in electrophysiological properties. Dysfunctions of these derived otic sensory neuron-like cells were rescued by genetically correcting MAP1B mutation using CRISPR/Cas9 technology. Involvement of MAP1B in hearing was confirmed by audiometric evaluation of Map1b knock-out mice. These mutant mice displayed late-onset progressive sensorineural hearing loss that was more

pronounced in the high frequencies. The spiral ganglion neurons isolated from Mab1p mutant mice exhibited the deficient phosphorylation and disturbing dynamics of microtubule. Map1b deficiency yielded defects in the morphology and electrophysiology of spiral ganglion neurons, but did not affect the morphologies of cochlea in mice. Our data demonstrated that dysfunctions of spiral ganglion neurons caused by Map1b deficiency led to hearing loss. Our findings provided the new insights into pathophysiology of hearing loss.

PD 126

Acsl4 mutation leads to early and fast progressive hearing loss affecting the inflammatory response within the inner ear.

Elisa Martelletti[1]; Neil Ingham[2]; Romain Colas[3]; Jesmond Dalli[3]; Karen Steel[2]
[1]King's College London. Wolfson Centre for Age-Related Diseases.; [2]King's College London and Wellcome Trust Sanger Institute; [3]Queen Mary University of London

Acsl4 (Acyl-CoA synthetase long-chain family member 4) transfers a coenzyme A molecule to free fatty acids in order to activate the metabolic processing of the lipids. It has a high affinity to arachidonic and eicosapentaenoic acids as substrates, and it is a critical enzyme in preventing the production of eicosanoids. This project is focused on elucidating the effect of *Acsl4* mutation and lipid metabolism on auditory function.

ABR measurements in response to click stimuli and tone pips ranging from 3-42kHz were performed at different ages to determine the onset of the hearing impairment. *Acsl4* mutant mice had normal hearing sensitivity at 2 weeks old, but only one week later they dramatically lost hearing sensitivity starting from the high frequencies and by 4 weeks old the thresholds at all frequencies are severely impaired. Further analysis at 3 weeks old revealed that *Acsl4* mutant mice had increased DPOAE thresholds, but normal endocochlear potential. They also showed degeneration of hair cell stereocilia and loss of hair cell nuclei in the basal and middle turns of the cochlea, with a reduction in the number of ribbon synapses in the surviving hair cells. Acsl4 did not appear to regulate the transcription of key enzymes of eicosanoid production in the arachidonic acid cascade. However, lipidomics analysis of pro-inflammatory and pro-resolving lipids revealed *Acsl4* mutant mice have a distinct lipid mediator profile at 2 (normal hearing) and 3 (impaired hearing) weeks old in comparison with littermate controls. Moreover, upon flow cytometry analysis, our preliminary results show a trend of increased numbers of immune cells in *Acsl4* mutants. Overall, our findings suggest that *Acsl4* mutation causes an early and fast progressive hearing loss affecting the inflammatory response within the inner ear.

PD 127

An In-Frame Deletion in RIPOR2 is an Important Cause of Adult-Onset Hearing Impairment

Suzanne E. de Bruijn[1]; Jeroen J. Smits[1]; Chang Liu[2]; Cornelis P. Lanting[1]; Andy J. Beynon[1]; Joëlle Blankevoort[1]; Jaap Oostrik[1]; Wouter Koole[1]; Erik de Vrieze[1]; Cor W.R.J. Cremers[1]; Frans P.M. Cremers[1]; Susanne Roosing[1]; Helger G. Yntema[1]; Henricus P.M. Kunst[1]; Bo Zhao[3]; Ronald J.E. Pennings[1]; Hannie Kremer[1]
[1]Radboud University Medical Center; [2]Indiana University School of Medicine; [3]Department of Otolaryngology-Head and Neck Surgery, Indiana University School of Medicine

Hearing impairment (HI) is one of the most prevalent disabilities worldwide. Congenital and childhood-onset HI can often be explained by monogenic defects, whereas age-related HI is a complex disorder caused by an interplay between environmental and genetic risk factors. The diagnostic yield of genetic testing decreases with an increasing onset age, and is estimated to be only ~10% for cases with an onset of HI in the 4th decade of life.

To obtain more insight in the causes of (predominantly) adult-onset HI, families with this type of HI were collected. In one of these families, previous research revealed a 12.4-Mb locus (*DFNA21*) but the pathogenic variant remained elusive. In the present study, we identified an in-frame deletion in *RIPOR2* (NM_014722.3; c.1696_1707del) to underlie autosomal dominant nonsyndromic HI in this family and in eleven additional (large) families of Dutch origin. *RIPOR2* has previously been associated with recessively inherited early-onset HI. Haplotype analysis indicated the in-frame deletion to be a founder variant, present in one per 1,275 individuals of a cohort from the South-East of the Netherlands (22,952 presumably unaffected individuals).

Clinical examinations revealed that the c.1696_1707del variant is associated with a variable audiometric phenotype and predominantly adult age of onset; the penetrance at the age of 50 years was 89%. *Ex vivo* functional studies were performed to investigate the pathogenicity of the *RIPOR2* variant and demonstrated an aberrant localization of the mutant RIPOR2 in the stereocilia of murine cochlear hair cells whereas wildtype protein was concentrated at the stereocilia base. Moreover, mutant RIPOR2 failed to rescue the morphological defects observed in RIPOR2-deficient hair cells, in contrast to the wildtype protein.

These results suggest that the in-frame deletion is the most important cause of monogenic HI in the Netherlands, and possibly Western Europe. Studies of larger and unselected cohorts of individuals from Western European countries are needed to get an unbiased insight in the penetrance and to determine the allele frequency of the c.1696_1707del variant outside of the Netherlands. This study emphasizes the importance of monogenic causes in adult-onset HI, and that seemingly 'mild' variants in genes associated with early-onset HI need to be scrutinized in medical genetic testing for cases with an adult-onset type of the condition. The progress that is being made on genetic therapies for hearing disorders, underlines the importance of genetic diagnoses for subjects with HI to become eligible for such therapies.

PD 128

Treatment of Monogenic and Digenic Dominant Mutations by CRISPR/Cas9 Ribonucleoprotein Delivery In Vivo

Veronica Lamas[1]; Yong Tao[1]; Yiran Li[1]; Xue Gao[2]; Corena Loeb[1]; Mingqian Huang[1]; Yujuan Hu[1]; Weijia Kong[3]; Xuezhong Liu[4]; David Liu[5]; Zheng-Yi Chen[1]
[1]Massachusetts Eye and Ear/Harvard Medical School; [2]Harvard University; [3]Huazhong University of Science and Technology; [4]University of Miami; [5]Merkin Institute of Transformative Technologies in Healthcare, Broad Institute of Harvard and MIT/ Department of Chemistry and Chemical Biology, Harvard University/ Howard Hughes Medical Institute

Introduction
Lipid-mediated delivery of CRISPR/Cas9 ribonucleoprotein (RNP) complexes has been successfully used to rescue hearing loss in a mouse model of dominant mutation of hair cell origin, the *Beethoven* (*Bth*) mouse. However, the functional improvement observed in the *Bth* model after RNP treatment was restricted to the inner hair cells. To expand the delivery paradigm to hearing loss of outer hair cell origin, we studied hearing rescue in a genetic mouse model carrying a dominant mutation, *Oblivion (Obl),* in the *Pmca2* gene. We further study if RNP-mediated delivery of editing agents can simultaneously target dominant mutations of two genes, *Tmc1* and *Pmca2*, to rescue hearing due to di-genic mutations.

Methods
Allele specific gRNAs targeting the *Oblivion* mutation were complexed with Cas9 protein and delivered in the inner ear of *Oblivion* neonatal mouse by liposomes. Control gRNAs were similarly injected. Hearing and behavioral studies were performed at one, two, three and four months after injection, with tissues harvested for characterization. Indels were determined by PCR of amplicons of varying sizes followed by NGS. To study the efficiency of the RNP strategy targeting multiple genes, we performed liposome-mediated delivery of Cas9 combined with specific gRNAs targeting the *Obl* and *Bth* mutations into the inner ear of neonatal mice carrying both mutations.

Results
RNP delivery of Cas9/gRNA by liposome targeting the *Oblivion* mutation significantly improved the ABR and DPOAE thresholds across most of the frequencies. It also increased the survival of the auditory hair cells and improved the startle reflex amplitudes. The hearing rescue effect is gRNA specific and depends on Cas9 cleavage activity. High-throughput sequencing demonstrated genome editing effects by the presence of deletions of over 1 kb around the mutation site. Delivery of lipid complexes of Cas9/gRNA targeting both *Obl* and *Bth* mutations significantly improved ABRs of the double mutant mice, whereas injection of single *Obl* or *Bth* gRNA failed to rescue hearing.

Conclusion
The study demonstrates that RNP delivery of CRISPR/Cas9/gRNA complex is sufficient to rescue hearing in dominant genetic mouse model with outer hair cell deficit. Combined with our previous work, our approach can be applied to rescue hearing in dominant hearing loss models of both inner and outer hair cell origins. We further demonstrate that our system can be applied to rescue hearing in mice carrying mutations in two genes, opening a new avenue to target genetic hearing loss of multi-gene origin.

Auditory Nerve Function

PD 129

Degradation of Speech-In-Noise Coding in Auditory-Nerve Fibers Following Cochlear Hearing Loss: Insights from Spectro-Temporal and Information-Theoretic Approaches

Satyabrata Parida; Michael G. Heinz
Purdue University

Benefits of studying neural coding of speech include a better understanding of how the normal auditory system encodes speech, as well as how this neural representation is degraded following hearing impairment. Ultimately, this knowledge can serve as a guide to optimize clinical interventions prescribed to patients. To this end, we collected extra-axonal spike trains from single auditory-nerve fibers of normal-hearing and noise-exposed chinchillas. Responses were collected to a natural speech sentence in quiet as well as in noisy

backgrounds, including spectrally-matched speech-shaped stationary and fluctuating noises, at perceptually important signal-to-noise ratios. Our approach focused on neurophysiological evaluations of two psychophysically inspired speech-coding hypotheses, namely the multiresolution envelope power spectrum model and the efficient-coding framework. We found that noise-exposed fibers had response envelopes to noisy-speech that were more like noise responses and less like speech responses than control fibers; this effect was particularly severe for fluctuating backgrounds. Thus, our data support the merit of temporal envelope coding as a neural basis for why hearing-impaired listeners show a lack of masking release in fluctuating backgrounds. As a proxy for channel capacity in the auditory nerve, we estimated the average Victor-Purpura distance between spike trains from pairs of neurons in response to speech for normal-hearing and noise-exposed animals; interneuron distance was significantly lower for the hearing-impaired fibers, suggesting a reduction in overall channel capacity of the auditory nerve. Response entropy was also estimated by first constructing probability density functions by binning spike trains across trials and then computing the cumulative f-divergence based distance between density functions of adjacent bins for individual neurons. We found significantly higher entropy for noise-exposed fibers, consistent with enhanced envelope coding in quiet; however, it will be important to estimate entropy in background noise to establish whether enhanced envelope coding is actually detrimental in the presence of competing maskers. Overall, our results highlight the importance of considering the deleterious effects of enhanced inherent noise-response fluctuations following cochlear hearing loss, in addition to degradations in speech-coding fidelity, for predicting speech intelligibility. In addition, our data support the importance of accounting for across-channel interactions in efforts to improve outcomes of hearing-aids and devising neurally based speech-intelligibility models, especially for individuals with hearing impairment.

PD 130

Signal Processing for Remediation of Threshold-Independent Hearing Disorder

Daniel Rasetshwane; Aryn Kamerer; Judy G. Kopun; Sara E. Fultz; Stephen Neely
Boys Town National Research Hospital

Background

Sensorineural hearing loss that does not elevate quiet thresholds, and therefore would be missed by standard pure-tone audiometry, is sometimes referred to as “hidden hearing loss” or “hidden hearing disorder”. Evidence from animal studies suggests that the underlying mechanism associated with this type of threshold-independent hearing disorder (TIHD) is cochlear synaptopathy, a reduction in the number of functional fibers in the auditory nerve, which consequently degrades temporal-coding abilities. The goal of this project is to determine the efficacy of remediating hidden hearing disorder through a signal-processing algorithm that enhances temporal cues of speech.

Signal Processing

We have developed a signal-processing algorithm that automatically identifies and amplifies spectro-temporal cues contained in speech signals. These cues include speech transients associated with consonants, transitions between consonants and vowels, and transitions within some vowels.

Behavioral Tests

Thirteen adults were tested. Five of the participants had TIHD based on performance on recognition of NU-6 time-compressed words that could not be explained by their hearing sensitivity. Participants listened to speech stimuli processed with the temporal-cue enhancement algorithm. Tasks included recognition of consonants, nonwords and sentences. Consonants were presented in the presence of speech-shaped noise (SSN) at -6 and 0 dB signal-to-noise ratio (SNR). Nonwords were presented in the presence of SSN, with an adaptive-tracking procedure used to determine the SNR required to obtain 29% and 71% correct. Sentences were presented in the presence of SSN and babble, both at -3 dB SNR. Recognition of unprocessed stimuli served as baseline performance.

Results

Average improvement of 5% and 10.1% were observed for consonant recognition, with 11 and 13 participants demonstrating improved performance at -6 and 0 dB SNR, respectively. Average improvements of 0.8 dB and 4.8 dB were observed for nonword recognition, with 7 and 9 participants demonstrating improved performance for 29% and 71% correct, respectively. On average, listeners with TIHD demonstrated greater improvement in performance for the most difficult condition (29% correct recognition of nonwords). However, recognition for sentences was poorer for enhanced speech compared to baseline.

Conclusions

The temporal-cue enhancement algorithm improved speech recognition for consonants and nonword stimuli, but not for sentences. Efforts are ongoing to optimize algorithm parameters and to individualize the algorithm to participant characteristics such as degree of hearing loss and tolerance for processing artifacts. Our innovative approach to the remediation of TIHD complements

ongoing efforts by several other research groups aimed at developing drug treatments for cochlear synaptopathy.

Funding
This study was funded by a grant from NIH NIDCD.

PD 131

Neural Presbycusis: Age-Related Deficits in Auditory-Nerve Function and Differential Effects on Functional Abilities

Kelly C. Harris; Carolyn M. McClaskey; James W. Dias; Jayne B. Ahlstrom; Judy R. Dubno
Medical University of South Carolina

There is increasing evidence that aging results in a loss or dysfunction of auditory-nerve fibers (neural presbycusis), which may contribute to age-related deficits in functional abilities, such as temporal processing and speech recognition. Auditory-nerve function in humans can be assessed using the compound action potential (CAP), a measure of summated auditory-nerve activity. With increasing age, shallower growth of the CAP with increasing signal level is observed, which results in smaller CAP amplitudes at higher levels in older than younger adults. Two primary factors contribute to larger peak amplitudes at higher levels and steep CAP amplitude-intensity functions: (1) more auditory-nerve fibers respond as the signal level increases, and/or (2) these same neurons respond but respond more synchronously as signal level increases. In the first case, a larger number of neurons may respond at higher levels because of level-dependent broadening of tuning curves, and/or recruitment of higher threshold (lower spontaneous rate) fibers. In the second case, increased neural synchrony is reflected by increasingly similar (reduced variance of) onset latencies across trials with increasing signal level, the narrower the standard deviation becomes the higher the synchronization. We hypothesized that decreases in recruitment of auditory neurons and/or neural dyssynchrony varies with age-related neural pathology, which in turn results in differential patterns of change across CAP metrics with increasing signal level and age. To assess age-related changes in auditory-nerve function, we measured the CAP as a function of signal level in 50 older and 35 younger adults and computed several new CAP metrics, which included novel measures of intertrial phase locking (PLV). As expected, CAP amplitudes were smaller in older than younger adults, but only at higher signal levels. Moreover, smaller CAP amplitudes for older adults were driven, in part, by age-related reductions in neural synchrony (PLV) and not by increases in pure-tone thresholds. To assess the effects of deficits in auditory-nerve function on functional abilities, we also measured frequency modulation detection, spatial selective attention, and recognition of time-compressed speech and speech in noise in a subset of participants. Discussion will focus on associations between age-related deficits in auditory-nerve function and auditory function. Work supported (in part) by grants from NIH/NIDCD.

PD 132

A Gaussian Model of the Auditory Brainstem Response: Proof of Concept and Validity

Aryn Kamerer; Stephen Neely; Daniel Rasetshwane
Boys Town National Research Hospital

Early auditory evoked potentials, though not part of the standard diagnostic battery of hearing, have received a great deal of attention in recent years. The standard of extracting data from the auditory brainstem response (ABR) and electrocochleogram is visual determination of peaks and troughs to calculate latencies and amplitudes. Automation of this process, by finding local maxima and minima, is fairly simple and is used my many researchers. Nonetheless, both automation and visual-determination perform poorly in noisy data and can over- or underestimate amplitudes when waves overlap in time, e.g. the summating and action potentials, or waves V and VI. One solution may be a statistical approach of fitting a series of Gaussian functions to the response waveform.

A model was created to estimate the summating potential and action potential, i.e. wave I, of the ABR. Feasibility of the model was tested by estimating ABR waves recorded from 32 adults using least-squares nonlinear regression. Model fit was determined by 1) correlation of the model to recorded waveforms and 2) absolute agreement between visually-determined and model-estimated metrics of latency and amplitude. Validity of the model was tested in a parameter recovery experiment in which ABR data were simulated.

Correlation of the Gaussian model to the recorded waveforms was excellent. Estimated amplitudes of wave I were in good agreement with visual-determination, but estimated SP amplitudes were in poor agreement with visual-determination. Consistent differences between the model and visual determination were noted. The model was better able to recover amplitude and latency parameters of simulated ABR data than visual determination by two experts.

The Gaussian model of waveform morphology is a promising method of extracting data from evoked potentials. The Gaussian model can easily be implemented into existing practice as it is simple, reliable, and metrics are calculated instantly. Another

benefit of a model approach over automated peak-picking is the addition of metrics such as wave width that may be a proxy measure of neural synchrony, and first-spike latency that may classify the responding fibers by spontaneous rate.

PD 133

Assessing Auditory Nerve Integrity with Acoustic Reflex Growth Functions

Joseph Pinkl; Lamiia Abdelrehim; Brian Earl
University of Cincinnati Department of Communication Sciences & Disorders

Noise exposure is a common cause of hearing loss with classical studies indicating outer hair cell damage as the underlying pathology. Recent animal studies have identified primary degeneration of high-threshold auditory nerve fibers following noise-induced temporary threshold shifts. The consequences of this degeneration is not believed to be reduced hearing sensitivity, but reduced intensity discrimination abilities necessary for listening in noise. This cochlear synaptopathy is hypothesized to occur in humans, although there are currently no standard diagnostic criteria in use. The acoustic reflex is mediated by the auditory nerve and activates in response to high intensity sounds. Acoustic reflex growth functions (ARGF) measure the change in contraction strength as a function of stimulus intensity. ARGFs may be sensitive to degradation of high-threshold auditory nerve fibers and thus could provide a tool for diagnose of cochlear synaptopathy in humans.

Adult participants (n=14) with normal hearing thresholds and middle ear function underwent standard audiometry, speech-in-noise testing (QuickSIN) and ipsilateral ARGFs using high-band noise (HBN), low-band noise (LBN), and broadband noise (BBN). Stimulus intensity was increased in 5 dB steps from 50 to 90 dB HL. ARGFs were plotted as a function of the change in acoustic compliance across stimulus intensity. The growth functions were categorized into 3 types: linear, nonlinear, and plateau. Participants were divided into two groups: normal ears (less than or equal to 3 dB signal-to-noise ratio [SNR] loss) and abnormal ears (greater than 3dB SNR loss) as indicated by QuickSIN performance. The ARGF data were fit with linear and nonlinear models and the maximum change in acoustic compliance within a 5dB increment was also measured.

Seven of the 28 tested ears fell within the abnormal speech perception group. The ARGFs recorded from this group included eight ARGFs categorized as nonlinear growth and the remainder categorized as linear growth. Unpaired two-tailed t-tests were computed to compare the slope of the ARGF and the maximum change in acoustic compliance between the two groups. There were no statistically significant differences between groups pertaining to these measures for any of the three stimuli.

While no significant relationship between ARGFs and speech-in-noise performance, unusual spikes of compliance changes exceeding 0.1 ml within a 5dB increment were observed. This occurred in ears yielding normal and abnormal SNR scores. A larger sample size while controlling for confounding factors such as caudal efferent activity and noise-exposure history is warranted.

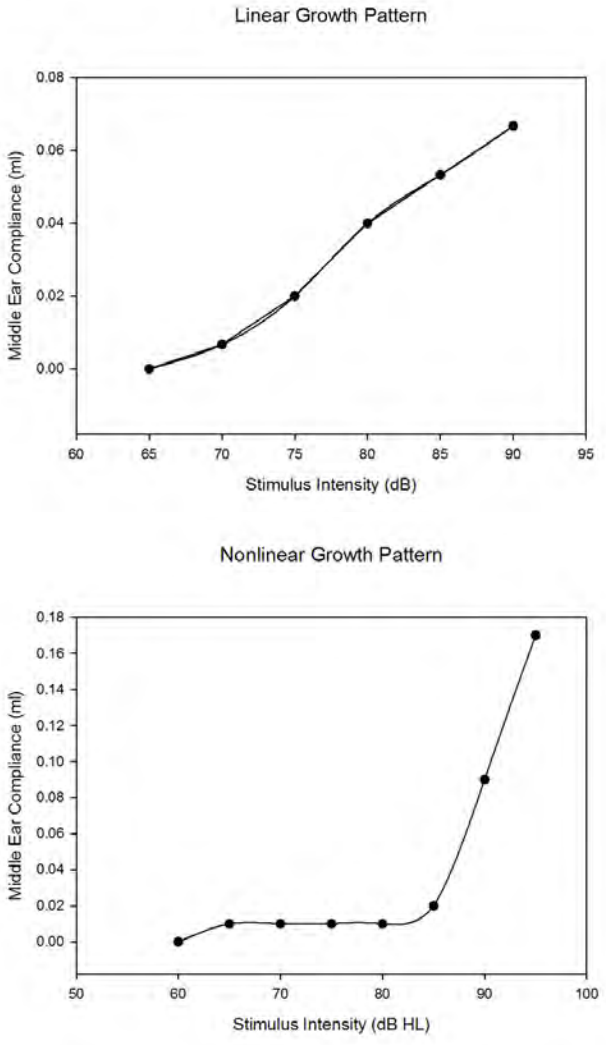

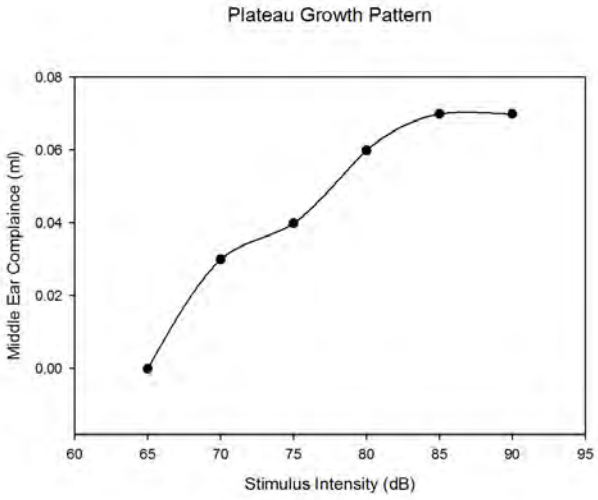

PD 134

Simulating the Effects of KLT, HCN and M-current Channels in Auditory Nerve Fibers

Ian C. Bruce[1]; Daniel Shields[1]; Laura Green[1]; Babak V-Ghaffari[2]; Mark Rutherford[3]
[1]McMaster University; [2]Department of Otolaryngology - Head & Neck Surgery, Washington University School of Medicine; [3]Department of Otolaryngology-Head & Neck Surgery, Washington University

Having an accurate description of the patterns of action potentials (APs) generated in auditory nerve fibers (ANFs) by either synaptic inputs from inner hair cells or direct electrical stimulation from cochlear implants is important for understanding neural coding in acoustic and electric hearing. Biophysical computational models are a powerful tool for capturing what is known about the electrochemical dynamics and ion-channel gating mechanisms underlying neural excitability.

Previous computational models of an ANF node of Ranvier suggest that low-threshold potassium (KLT) and hyperpolarization-activated cyclic nucleotide-gated cation (HCN) channels affect an ANF's absolute and relative refractory periods and produce adaptation/accommodation to high-rate pulse trains (Negm & Bruce, IEEE TBME 2014; Boulet & Bruce, JARO 2017). In this study we explore the effects of another type of potassium channel that has recently been identified in mammalian ANFs, M-current potassium channels formed by Kv7.2 and Kv7.3 ion channel proteins (Kim & Rutherford, J Neurosci 2016). Like the KLT and HCN channels, the M current is active at the resting membrane potential of ANFs and has slower opening/closing dynamics than the AP-generating sodium and potassium channels. Thus, the M current is expected to also have an influence over the refractory, facilitation, accommodation and adaptation behavior of ANFs.

We have incorporated an M-current model used in other cell types (Lawrence et al, J Neurosci 2006) into the previous ANF model of Boulet & Bruce (JARO 2017). As a first step of evaluating this new model, we have compared simulation results to the room-temperature ANF patch-clamp data of Rutherford et al (J Neurosci 2012). In response to long current step stimuli, the sag in hyperpolarization and the occurrence of rebound spikes in response to some negative current amplitudes are controlled primarily by the HCN and KLT currents, while the M current has an influence on the positive current amplitude at which spiking begins and the magnitude of the sustained depolarization following an onset spike. For ramp current stimuli, the HCN and KLT currents mainly determine the ramp duration at which spiking begins, but the M current is a major factor in the amount of jitter that is observed in the spike latency. Overall, this new model incorporating the M current better predicts these patch-clamp data. Further refinement of free parameters in the model is ongoing.

[Funded by NSERC Discovery Grant #RGPIN-2018-05778 (ICB), NIH/NIDCD R01DC014712 (MAR), and a Hearing Health Foundation Fellowship (BV-G).]

PD 135

Characterizing Auditory Nerve Function in Mice Using A Multi-Metric Approach That Quantifies Neural Synchrony in the Auditory Brainstem Response

Carolyn M. McClaskey[1]; Clarisse H. Panganiban[2]; Kenyaria V. Noble[3]; Hainan Lang[1]; Kelly C. Harris[1]
[1]Medical University of South Carolina; [2]Wolfson Centre for Age-Related Diseases, King's College London; [3]Department of Pathology and Laboratory Medicine, Medical University of South Carolina, Charleston, South Carolina 29425, United States

The auditory brainstem response (ABR) is a ubiquitous and valuable tool used to noninvasively characterize auditory nerve (AN) and brainstem function in human and animal models. Traditional ABR methods primarily rely on ABR threshold and peak amplitudes and latencies when characterizing auditory function. Recent work in our group has developed a multi-metric approach that incorporates measures of neural synchrony to comprehensively and noninvasively characterize AN function in humans. This approach analyzes both the trial-averaged ABR waveform and single-trial-level data with a focus on suprathreshold processing. The present study evaluates the feasibility of these tools for characterizing AN function in adult mice. Tone-evoked ABRs were collected from

young adult CBA/CaJ mice between 2.5 and 3.5 months of age. Stimuli were 11.3 kHz tone pips presented at sound intensity levels that progressively decreased from 90 dB SPL to 5 dB SPL in 5-dB steps. Suprathreshold AN function was quantified from Wave I at stimulus levels from 55 to 90 dB SPL. Wave I peak amplitude, area, peak latency, onset latency, and half-width were measured from the trial-averaged ABR response. Inter-trial phase coherence (phase-locking value, PLV), was quantified by time-frequency decomposition of the trial-by-trial responses and is a metric of neural synchrony of AN fibers across trials. As expected, Wave I peak amplitude, area, and PLV increased with increasing stimulus level and Wave I peak and onset latency decreased with increasing stimulus level. At higher but not lower stimulus levels, Wave I amplitudes were correlated with PLV, peak latency, and area, but not with half-width or onset latency. Differing associations across metrics at different stimulus levels suggest the need for techniques that incorporate more than peak amplitudes and latencies in assessments of AN function. Taken together, these results demonstrate the feasibility of a multi-metric approach that incorporates suprathreshold processing and neural synchrony in the study of AN function in animals. Changes in neural synchrony at the level of the peripheral AN may contribute to behavioral changes in numerous pathological conditions such as age and noise exposure. A method that quantifies neural synchrony *in vivo* and integrates this with additional ABR metrics beyond threshold and peak amplitude/latency may be better able to assess changes in AN function in a variety of animal models. Work supported (in part) by grants from the NIH/NIDCD.

PD 136

Behavioral Discrimination of Masked Vowel-Like Sounds in an Avian Animal Model of Auditory-Nerve Loss

Kenneth S. Henry; Kristina Abrams
University of Rochester

Progressive loss of auditory-nerve synapses within the cochlea occurs with increasing age and as a possible consequence of overexposure to loud sound. Auditory-nerve loss appears undetectable with a clinical audiogram and has been proposed to adversely impact perception of complex signals in noise, known as hidden hearing loss. However, evidence of hidden hearing deficits due to auditory-nerve loss is presently mixed. Here, we used operant-conditioning procedures in the budgerigar, an avian species with human-like behavioral sensitivity to many simple and complex sounds, to assess the impact of moderate-to-severe auditory-nerve damage on discrimination of synthesized vowel-like sounds in quiet and in noise. Auditory-nerve damage was induced using bilateral infusions of the glutamate analog kainic acid, which reduced wave-I amplitude of the auditory brainstem response by 40-70% while leaving otoacoustic emissions unaffected. Two-down, one-up, adaptive tracking procedures were used to quantify behavioral discrimination of vowel-like sounds as a function of signal level in quiet and in noise. Signals were 'single-formant' harmonic tone complexes with a fundamental frequency of 200 Hz and a triangular spectral envelope peaking at either 2000 or 2100 Hz. Noise was 75 dB SPL, simultaneously gated with the signal, and either steady state or square-wave modulated at frequencies of 16, 45, or 128 Hz. Behavioral performance was similar between control and kainic-acid exposed animals in noise (n=5 animals each), with both groups showing the same degree of masking release with decreasing square-wave modulation frequency. Performance in quiet was also similar between groups, though two exposed animals with the greatest auditory-nerve loss (~70% loss as inferred from auditory brainstem responses) showed mild-to-moderate perceptual impairment. These results raise the possibility that discrimination of low-level stimuli can be adversely impacted by auditory-nerve loss whereas discrimination of louder sounds remains unaffected, potentially due to the substantial spread of excitation commonly observed at moderate-to-high sensation levels. This new finding would challenge the prevailing view that suprathreshold processing is most impacted by auditory-nerve loss.

Brain Imaging of Auditory Function - Human Studies

PD 137

The Neural Processing of Sound at 3 Months

Bonnie K. Lau; Samu Taulu; Patricia K. Kuhl; Adrian KC Lee
University of Washington

Although infants already show sophisticated auditory skills at birth, the human central auditory system undergoes extensive development throughout infancy. Early auditory abilities play a pivotal role in infants' ability to acquire language, appreciate music, and navigate the complex acoustic environments around them. However, the neural mechanisms that support infant sound processing are not well understood. This study used magnetoencephalography (MEG) with recent advancements in movement compensation to obtain functional measures of auditory processing in awake infants. MEG responses were recorded in 3-month-old infants to an English bi-syllabic word and an amplitude-modulated complex tone as a non-speech but spectro-temporally complex control stimulus. MEG recordings were made with an Elekta Neuromag®

whole-head 306-channel MEG system equipped with 102 magnetometers and 204 gradiometers (Elekta Neuromag®, Helsinki, Finland). Infants were fitted with a close-fitting fabric cap containing five head-position indicator (HPI) coils for continuous head position tracking and two electrocardiography electrodes on the chest to record cardiac signals. Each subject's cardinal landmarks, the location of the five HPI coils, and 200 extra points were digitized prior to recording. The raw MEG data were filtered using the temporally extended signal space separation (tSSS) method to remove artifacts originating outside the head. Along with rejecting artifacts using tSSS, a movement compensation algorithm was applied to correct for head movement during the recording. Following automatic cardiac artifact suppression with signal space projection, data were then epoched from -100 to +2000 ms with respect to the onset of the stimulus. The neural generators of the MEG signals were determined using an equivalent current dipole (ECD) model. ECD modeling is a well-defined and robust source localization technique that requires a minimum number of assumptions making it suitable for use with infants. High quality MEG data with good signal-to-noise ratios were recorded in infants as young as 3 months of age in both conditions. ECD field maps showed focal sources in the brain confirming the ECD model is a robust source localization approach that can fit auditory sources in infants. Dipole modeling of MEG signals in combination with advanced movement compensation offers a temporally precise method of investigating the neural processing of sound in infants.

PD 138

Dissociating Spectral Envelope and Fundamental Frequency in Tonotopic Representations within Human Auditory Cortex

Emily J. Allen[1]; Juraj Mesik[1]; Kendrick N. Kay[1]; Andrew J. Oxenham[2]
[1]University of Minnesota; [2]Department of Psychology, Center for Applied and Translational Sensory Sciences, UMNTC

Traditional tonotopic mapping uses stimuli in which there is perfect co-variation between increases in fundamental frequency (F0), the acoustic attribute most closely related to our perception of pitch, and increases in spectral centroid, the acoustic attribute associated with our perception of timbral "brightness." As such, it is unknown whether tonotopic maps reflect pitch per se or merely spectral content. We sought to dissociate the representations of these auditory dimensions by using harmonic complex tones that systematically vary in either F0 or spectral centroid. Using 7T fMRI, we measured BOLD responses in 10 right-handed, normal-hearing participants as they actively listened to pseudo-randomly ordered blocks of pure tones, complex tones spanning a broad range of F0s with a fixed spectral centroid, and complex tones spanning a broad range of spectral centroids with a fixed F0. BOLD responses were used to generate basic "winner-take-all" maps and were also subjected to more sophisticated models of voxel tuning properties. In these models, we separately fit each voxel with a Gaussian population receptive field function describing its preference and tuning width for both F0 and spectral centroid. We then compared maps of these tuning preferences to those estimated with the pure-tone data.

Modeling of the pure tones revealed robust, orderly, high-low-high tonotopic gradient reversals around Heschl's gyrus, in line with previous studies. The spectral centroid representations showed a very similar high-low-high pattern in this same region. In contrast, variations in F0 did not produce the same large-scale tonotopic representations.

Using appropriate design of complex tones, our study resolves the F0-centroid ambiguity inherent in traditional tonotopic mapping. We show that traditional tonotopy is a reflection of the spectral content of sound, and it remains unclear whether systematic F0 or pitch topography exists in primary auditory cortex. Further analyses will investigate whether voxel activity patterns can be fully explained on the basis of sound spectra alone, or whether there are some voxel populations in which F0 can explain additional variance.

Supported by National Institutes of Health (NIH) Grant No. R01 DC005216.

PD 139

Auditory Cortex Tracks Acoustic Onsets of Ignored Speech: A Potential Mechanism in Stream Segregation

Christian Brodbeck[1]; L Elliot Hong[2]; Jonathan Z. Simon[1]
[1]University of Maryland, College Park; [2]University of Maryland, School of Medicine

Humans are remarkably skilled at listening to one speaker in an acoustic mixture of multiple speech sources, even in the absence of binaural cues. Previous research on the neural representations underlying this ability suggests that the auditory cortex primarily represents the acoustic mixture at low response latencies (starting ~50 ms), and selectively processes the attended signal at longer latencies (starting ~100 ms). It is not known, however,

exactly how the attended source signal is segregated from the mixture, including to what degree ignored sources may or may not also be segregated. One possibility is that separate acoustic sources are segregated pre-attentively into different streams, with attention merely selecting among those representations. At the other endpoint of a spectrum of possibilities, pre-attentive processing could be restricted to features of the mixture, with selective processing only of features belonging to the attended source. In order to distinguish between these possibilities, we analyzed human magnetoencephalographic (MEG) responses to a two-talker mixture. Participants listened to a mixture of a male and a female voice, each reading an audiobook segment, while attending to one speaker and ignoring the other. MEG responses in the auditory cortex were modeled as linearly additive responses to acoustic envelope features and also to acoustic onset features, extracted with a neurally-based acoustic edge detector model. Onsets were included separately because concurrent acoustic onset in multiple frequency bands is a grouping cue for bottom-up source separation that is particularly prominent in speech, for example, at the onsets of the multiple harmonics of voiced segments. MEG responses were modeled additively with predictors computed from the two source speech signals as well as from the acoustic mixture. Results show a new neural representation of acoustic onsets in the ignored speech source, over and above onsets of the mixture and the attended source. The auditory cortex tracked onsets in the acoustic mixture with a lower latency (~70 ms) than recovered, speaker-specific onsets (~100 ms). These results suggest that the auditory cortex initially reconstructs acoustic onsets that could belong to any speech source, even when those onsets are acoustically obscured by another source. Since these onsets precede sustained source-specific information in the acoustic spectrogram, these representations of onsets could provide important cues for a subsequent processing stage, at which features of the attended source are analyzed more selectively.

PD 140

Plasticity in Auditory Categorization Is Supported by Differential Engagement of The Auditory-Linguistic Network

Gavin Bidelman; Breya walker
University of Memphis

To construct our perceptual world, the brain categorizes variable sensory cues into behaviorally-relevant groupings. Categorical representations are apparent within a distributed fronto-temporo-parietal brain network but how this neural circuitry is shaped by experience remains undefined. Here, we asked whether speech and music categories might be formed within different auditory-linguistic brain regions depending on listeners' auditory expertise. We recorded EEG in highly skilled (musicians) vs. less experienced (nonmusicians) perceivers as they rapidly categorized speech and musical sounds. Musicians showed perceptual enhancements across domains, yet source EEG data revealed a double dissociation in the neurobiological mechanisms supporting categorization between groups. Whereas musicians coded categories in primary auditory cortex (PAC), nonmusicians recruited non-auditory regions (e.g., inferior frontal gyrus, IFG) to generate category-level information. Functional connectivity confirmed nonmusicians' increased left IFG involvement reflects stronger routing of signal from PAC directed to IFG, presumably because sensory coding is insufficient to construct categories in less experienced listeners. Our findings establish auditory experience modulates specific engagement and inter-regional communication in the auditory-linguistic network supporting categorical perception. Whereas early canonical PAC representations are sufficient to generate categories in highly trained ears, less experienced perceivers broadcast information downstream to higher-order linguistic brain areas (IFG) to construct abstract sound labels.

PD 141

Neural Responses to Statistical Change across Multiple Acoustic Dimensions

Benjamin Skerritt-Davis; Mounya Elhilali
Johns Hopkins University

To make sense of our auditory surroundings, the brain tracks sound sources as they evolve through the scene, collecting and combining relevant information across perceptual features such as pitch, timbre, and spatial location to create a unified auditory object. Previous work using both invasive and non-invasive brain imaging techniques provides evidence that each feature is represented independently in the brain at early stages of processing, however behavioral evidence and everyday experience clearly point toward a joint object representation at later stages of processing for effectively parsing a scene. The intermediate stage when feature combination occurs is unknown. In this work, we use electroencephalography and a multi-feature change detection paradigm to investigate the computational mechanisms behind feature combination, and we use a computational model for predictive processing to determine when this feature combination occurs. To better simulate multi-feature processing in natural listening environments, we used stochastic melodies based on random fractals varying along two perceptual features simultaneously. In two separate experiments with both spectral and spatial manipulations, we found two distinct brain responses to our stimuli: an early deviance response to local deviations from the

preceding context, and a late prolonged response to task-relevant changes in the statistics of the melody. The early response occurred independently of which feature was changing, while the late response was modulated by whether one or multiple features was changing. We use the computational model to infer the underlying mechanisms behind this feature combination.

PD 142

Tone-Sequence Awareness under Informational Masking Probed with Pre- and Post-Stimulus Cues: A Magnetoencephalography Study in Human Listeners

Kai Gärtner; **Alexander Gutschalk**
Department of Neurology, University of Heidelberg

Previous studies suggested that a long-latency negativity in auditory cortex is closely coupled to perceptual awareness of tones under informational masking. An alternative interpretation of this activity in auditory cortex is that it reflects enhanced processing subsequent to the identification of the target stream. Here, we present two MEG experiments in which the target can only be identified based on a cue presented before or after the multi-tone scenes.

In Experiment 1, scenes comprising 9 different, non-synchronous tones, each repeated 5 times with random inter-tone intervals, were presented to 20 participants. The target tone was indicated by a cue that was either placed before or after the scene, and participants were asked to indicate if the tone was part of the scene or not. Hit rates were significantly higher (96% vs 76%) and false-alarm rates lower (4% vs 16%) for pre- compared to post-stimulus cues. MEG showed no difference between hit and miss trials for the post-stimulus cues, but strong enhancement of negative source activity in auditory cortex for hit trials in the pre-stimulus cue condition (75-275 ms).

In Experiment 2, to ensure that listeners perceived the whole target stream, random tone sequences were presented in the presence of a random multi-tone masker to 14 participants. Participants were required to indicate if the post-stimulus cue (a repetition of the target sequence or another random tone sequence) was present in the masker interval, or not (hits: 47%, false alarms: 7%). MEG results in Experiment 2 showed stronger negative source activity in auditory cortex for hit compared to miss trials, despite the post-stimulus cue used.

These results suggest that the long-latency negativity in auditory cortex may be related to the perception of auditory streams in the presence of a multi-tone masker, but make it unlikely that it is related to the perceptual awareness of the single tones. Possibly, attention is generally required to perceive auditory streams in this setting.

PD 143

Oscillatory Correlates of Auditory Working Memory in Human Intracranial EEG

Joel Berger[1]; Phillip Gander[1]; Sukhbinder Kumar[2]; Kirill Nourski[1]; Matthew Banks[3]; Hiroyuki Oya[1]; Hiroto Kawasaki[1]; Matthew Howard[1]; Timothy Griffiths[4]
[1]University of Iowa; [2]Newcastle University; [3]University of Wisconsin; [4]Institute of Neuroscience, Newcastle University

Working memory is the capacity to hold and manipulate behaviorally relevant information in mind in the absence of ongoing sensory input. Here we explored the hypothesis that working memory for tones requires a network of oscillatory activity in auditory cortex, frontal cortex, and hippocampus, and examined the form of such activity in neuronal ensembles.

We recorded local field potentials from six human subjects undergoing invasive monitoring for presurgical localization of epileptic foci. The subjects were implanted with depth electrodes along the axis of Heschl's gyrus (HG) containing primary cortex in its posteromedial portion, subdural electrodes over temporal and frontal cortex, and depth electrodes targeting hippocampus. Following a visual alert, subjects were presented with a pair of tones belonging to two different categories. A visual cue informed the subjects which tone to keep in mind. A 3 s retention period was followed by a tone which could be the same or different from the tone held in mind. The subjects made a same/different judgement. A total of 160 trials (80 each of 'Low' and 'High' tone retention) were presented. We measured averaged event-related potentials and carried out time-frequency analysis using wavelet transforms.

During retention, a sustained increase (compared to rest period) in power in the beta band (15-20 Hz) was observed in the lateral part of HG. Increase in power in the gamma band (60-100 Hz) was observed in the posterior portion of superior temporal gyrus and in inferior frontal gyrus. In the hippocampus, power increase in low frequencies (less than 10 Hz) in the retention period was observed.

The data demonstrate a network of brain regions during auditory working memory that includes auditory, frontal, and hippocampal cortex and is consistent with the network shown in our previous fMRI study (Kumar et al, J Neurosci 2016 36:4492-4505). The findings serve as a foundation for analyses of effective connectivity to test

the hypothesis that the auditory cortex activity during retention is driven by the activity in inferior frontal gyrus or hippocampus.

PD 144

Neural Alpha and Beta Oscillations are Differentially Modulated in a Challenging Visual Compared to Auditory Task

Vanessa C. Irsik[1]; Ingrid Johnsrude[2]; Björn Herrmann[3]
[1]University of Western Ontario; [2]The Brain and Mind Institute, Western University; [3]Western University

Neural oscillations in the alpha (~8-12 Hz) and beta (~13-20 Hz) frequency bands provide a window into cognitive processes such as attention. Most research on alpha oscillations has been conducted in the visual domain, leading to the dominant "functional inhibition" framework, in which lower alpha power is associated with functional gain (e.g., better processing), and high alpha power is associated with functional inhibition. Conversely, increased power in the beta frequency band is associated with successful detection of visual targets (Donner et al., 2007; Gross et al., 2004). Data from other modalities are not always consistent with the visual domain. For example, alpha power increases during challenging listening compared to passive listening, suggesting that high alpha power is associated with better auditory processing (Henry et al., 2017), whereas decreased beta power is generally observed during difficult listening tasks (Weiss & Mueller, 2012). Visual and auditory paradigms often differ substantially, leaving unanswered whether patterns of alpha and beta power are similar across modalities, indicating that they may serve similar functions. In the current electroencephalography (EEG; 64-channel) study, we investigate whether alpha and beta power differ between modalities when participants (N=15, Sex: 7 females and 8 males; Mean age: 25.4 years) perform a challenging auditory compared to a visual task. In the auditory task, participants were asked to detect a near-threshold target (gap) in an 8.5-s stream of auditory white noise. In the visual task, participants were asked to detect a near-threshold target (contrast change) in an 8.5-s stream of visual white noise. Behavioral performance was titrated for each individual such that it was similar for the auditory and visual tasks (~70 % hit rate). In the auditory task, alpha power at parietal electrodes increased after noise onset until target onset, while no effect on power in the beta band was observed. Conversely in the visual task, no effect in the alpha-frequency band was observed, whereas power in the beta band decreased at occipital electrodes from noise onset until target onset. These data demonstrate fundamental differences in the way neural oscillations are engaged during perceptually challenging detection tasks in the visual compared to the auditory domain, challenging the view of functional inhibition as a modality-independent mechanism.

Inner Ear Therapeutics

PD 145

Statins reduce cisplatin-induced hearing loss in humans

Katharine Fernandez[1]; Paul Allen[2]; Maura Campbell[2]; Thomas Townes[3]; Brandi Page[4]; Chuan-Ming Li[5]; Jaylon Harkness[4]; Marcia Mulquin[6]; Anna Clements[6]; Candice Ortiz[3]; Carmen Brewer[6]; Nicole Schmitt[6]; Shawn Newlands[2]; Lisa L. Cunningham[1]
[1]Laboratory of Sensory Cell Biology, NIDCD, NIH; [2]University of Rochester Medical Center; [3]Walter Reed National Military Medical Center; [4]Johns Hopkins University; [5]Epidemiology and Statistics Program, National Institute on Deafness and Other Communication Disorders (NIDCD), National Institutes of Health (NIH); [6]National Institute on Deafness and Other Communication Disorders

Introduction

Induction of heme oxygenase-1 (HO-1) reduces cisplatin-induced hair cell death in mice. The cholesterol-lowering drugs collectively known as statins are inducers of HO-1. Recent animal studies indicate that statins inhibit cochlear injury and reduce hearing loss induced by noise trauma or aminoglycosides. We have evidence in mice that lovastatin reduces hearing loss caused by cisplatin. Here we have examined a cohort of patients treated with cisplatin for head and neck cancer to determine if statins reduce the incidence and/or severity of ototoxicity.

Methods

We analyzed audiometric data collected before and after cisplatin treatment from 290 subjects (241M, 49F). Changes in hearing were calculated relative to pre-treatment audiograms, and the presence of hearing loss was identified according to modified American Speech-Language-Hearing-Association (ASHA), Common Terminology Criteria for Adverse Events (CTCAE) and TUNE ototoxicity grading scales. Audiometric data from statin users were compared to those of non-statin users to evaluate the effects of statin use on cisplatin ototoxicity. Parameters of interest in addition to hearing loss included effects of age, sex, cisplatin dose, statin type/dose, and radiation co-therapy. Multivariable logistic regression was used to calculate odds ratios (OR) and 95% confidence interval (CI)

Results
Statins were protective against cisplatin-induced hearing loss as defined by each of the three ototoxicity scales (ASHA, TUNE, CTCAE, ChiSq, $p < 0.05$). Based on the TUNE Grading Scale criteria, controlling for age, sex, cumulative cisplatin dose, radiation and the presence of a pre-existing hearing loss, the odds of a statin user acquiring a clinically significant hearing loss was 32% less than that of a non-statin user (OR 0.68, 95% CI: 0.47-0.99). All analyses were conducted using both right and left ears independently for each subject, as 23% of our subjects had asymmetrical hearing losses, possibly due to asymmetry of baseline hearing, tumor location and/or radiation to the cochlea.

Conclusions
Our data indicate that statins reduce cisplatin ototoxicity in patients with head and neck cancer. Statins have good safety profiles in decades of clinical use. Importantly, statins do not interfere with the therapeutic effects of platinum-based chemotherapy and have recently been described as effective adjunctive anti-cancer drugs in patients with head and neck cancers. Concurrent use of statin therapy offers a low-risk therapy to protect the hearing of patients undergoing cisplatin-based chemotherapy. Current studies are aimed at determining which statin is most otoprotective.

This work was supported by the NIDCD Division of Intramural Research

PD 146

Repurposing an FDA approved Drug Dabrafenib for Protection from Noise- and Cisplatin- Induced Hearing Loss

Matthew A. Ingersoll[1]; Lauryn E. Caster[2]; Eva M. Holland[1]; Emma A. Malloy[1]; Zhenhang Xu[3]; Hao Feng[3]; Duane Currier[4]; Jaeki Min[4]; Taosheng Chen[4]; Jian Zuo[5]; Tal Teitz[6]
[1]Pharmacology and Neuroscience Department, Medical School, Creighton University; [2]Department of Pharmacology and Neuroscience, Creighton University; [3]Biomedical Sciences Department, Medical School, Creighton University; [4]Department of Chemical Biology and Therapeutics, St Jude Children's Research Hospital; [5]Department of Biomedical Science, Creighton University; [6]Deaprtment of Pharmacology and Neuroscience

Question
Hearing loss caused by chemotherapy, noise, and aging is a major medical need in our society and, to date, no drugs have been approved by the FDA for this purpose.

Methods
Protein kinases are particularly attractive therapeutic targets as they regulate critical cellular functions, and many have been approved for human treatment. We recently conducted high-throughput screens of 187 specific kinase inhibitors in dose response mode for cisplatin-induced cell-death protection in an inner ear cell line and identified dabrafenib (TAFINLAR) as a top hit.

Results
Dabrafenib is a potent selective small molecule inhibitor of B-Raf kinase that is orally bioavailable and FDA-approved for treating advanced melanoma and non-small cell lung carcinoma. The screen identified multiple hits from the B-Raf kinase family and the top hit dabrafenib fully protected the hair cells against cisplatin toxicity in mouse cochlear explants with IC_{50} of 30 nM and therapeutic index >2,000. Importantly, dabrafenib significantly protected against noise- and cisplatin- induced hearing loss in mouse models (15-22 dB protection at 8,16 and 32 kHz frequencies) when delivered orally for three days at doses of 100 mg/kg daily. The dabrafenib dose is within the daily range approved for long-term human treatment (6-12 months). We are currently testing dabrafenib in tumor cell lines to verify it does not interfere with cisplatin's tumor killing activity while also optimizing treatment regimens in mouse models for protection for both noise- and cisplatin- induced hearing loss. Finally, the activity of dabrafenib was enhanced in combination with specific inhibitors of cyclin-dependent kinase 2 which we recently identified as conferring protection against cisplatin- and noise- induced hearing loss (Teitz et al, JEM 2018; Hazlitt et al, J. Med. Chem 2018).

Conclusions
Our studies will hopefully provide one of the first FDA Approved drugs repurposed specifically for protection from noise- and cisplatin- induced hearing loss.

PD 147

Extracellular Vesicles derived from Mesenchymal Stromal Cells as New Cell-free but Cell-based Therapeutic for the Inner Ear

Jennifer Schulze[1]; Mario Gimona[2]; Eva Rohde[2]; Hinrich Staecker[3]; Thomas Lenarz[1]; Athanasia Warnecke[1]
[1]Hannover Medical School, Hannover, Germany; [2]Paracelsus Medical University, Salzburg, Austria; [3]University of Kansas Medical Center, Kansas City, KS, USA

Background
The application of extracellular vesicles (EVs) is very promising for immune-modulatory and regenerative therapies. A variety of cell types secrets EVs which

contain cell-specific cocktails of bioactive molecules including proteins (enzymes, growth factors and cytokines), lipids and RNAs of their cell of origin. Since MSC were already used for cell therapies, MSC-EVs may be employed for novel regenerative therapies within the inner ear. In this investigation we used EVs derived from bone-marrow and umbilical cord MSC and analyzed their effect on dissociated rat SGN (*in vitro*) and hair cells after noise trauma (*in vivo*).

Methods

EVs were isolated from human bone marrow and human umbilical cord MSC. The SGN were isolated from neonatal (P3-5) Sprague Dawley rats and were enzymatically and mechanically dissociated. The SGN were cultured in the presence of EVs at different concentrations. After 48h of cultivation, the SGNs were fixed, stained and the neuronal survival rate, neurite length and morphology were determined. Five week old C57Bl/6 mice (female, Jackson Labs) were used and the initial hearing ability was checked via auditory brainstem response (ABR). Mice received noise trauma at 118 dB 16 kHz for 3 hours. The posterior semicircular canal was opened with a microdrill and 1 ml of EVs or artificial perilymph was injected. After4 weeks recovery time, the ABR measurement was repeated.

Results

Our *in vitro*data showed that EVs increased the survival rate as well as the neurite length of SGN. Moreover, the percentage of monopolar and bipolar neurons was significantly increased and the percentage of SGN without neurites was significantly decreased. Our *in vivo*data indicate that EVs attenuate threshold shifts and protect hair cells. Depending on the manufacturing process, we could harness different types of EVs with varying efficacy.

Conclusion

The observed enhanced neuronal survival and protection of hair cells against noise trauma is a promising first step in the evaluation of the suitability of EVs as a novel therapeutic for the inner ear to reduce inflammation, scar formation and to protect the residual hearing of patients after cochlear implantation. Most importantly, with the generation of EVs with varying potency, we have a set-up for future investigations on their potential mode of action.

This work was funded by the Deutsche Forschungsgemeinschaft (DFG, German Research Foundation) under Germany's Excellence Strategy – EXC 2177/1 - Project ID 390895286 and by the European Regional Development Fund Interreg V-A Italia–Austria 2014–2020 (Project"EXOTHERA IT-AT 1036") and the Project "ExtraNeu"from the State of Salzburg.

PD 148

Attenuating the Pathophysiologies of Noise Induced Hearing Loss by pre-Treatment with Near-Infrared-Light

Moritz Gröschel[1]; Ira Strübing[1]; Dan Jiang[2]; Patrick Boyle[3]; Arne Ernst[1]; Dietmar Basta[1]
[1]Dept. Of Otolaryngology at UKB, University of Berlin, Germany; [2]Dept. Of Otolaryngology, Guy's and St Thomas' NHS Foundation Trust, London, UK; [3]Advanced Bionics European Research Center, Hannover, Germany

Noise induced hearing loss (NIHL) is accompanied by several pathologies, e.g. an increased auditory threshold, fundamental changes in suprathreshold auditory processing, reduction of cochlear hair cells, spiral ganglion neurons and synaptic transmission. Different approaches are applied to prevent NIHL and physical intervention is one technique currently under investigation. Specific wavelengths within the near-infrared light (NIR)-spectrum are known to influence cytochrome-c-oxidase activity which leads in turn to an increased ATP production and decreased pathologies (e.g. apoptosis). It has been shown recently that NIR can decrease auditory threshold shift significantly if applied daily after a noise exposure. Since an enhanced ATP-level is known to have a pre-conditioning effect for the prevention of excitotoxicity, the present study aimed at investigating the efficacy of a single NIR-pre-treatment in attenuating the structural and functional pathophysiologies of NIHL. The cochleae of adult NMRI-mice were pre-treated with NIR-light for 5; 10; 20; 30; 40 minutes via the external ear canal. All animals were noised exposed immediately after the pre-treatment by broad band noise (5 – 20 kHz) for 30 minutes at 115 dB SPL. One group was noise exposed only and served as control. Frequency specific ABR-recordings for determination of auditory threshold shift and suprathreshold analysis were carried out before all treatments and two weeks after the noise exposure. Cochlear pathologies (hair cell/synaptic loss) were determined by immunostaining. Two weeks after noise exposure, ABR threshold shifts of NIR-treated animals were significantly lower ($p < 0.05$) at three frequencies in the 5-minute pre-treatment group and for the entire frequency range in all other treatment groups compared to controls. Moreover, reduced excitability (decreased ABR wave IV slopes after noise exposure) was present in noise-exposed animals, whereas it remained unchanged in response to NIR-pre-treatment. As hair cell loss did not differ between the groups, subcellular alterations might contribute to the present results. In conclusion, we were able to show that a single and short-term NIR-pre-treatment is able to reduce hearing loss and pathophysiologies by effective protection

of auditory structures. This study was supported by Advanced Bionics GmbH, Hannover, Germany.

PD 149

SENS-401 Significantly Reduces Lasting Hearing Loss from Chronic Noise Exposure in a Rat Model

Mathieu Petremann; Charlotte Romanet; Christophe Tran Van Ba; Viviana Delgado-Betancourt; Vincent Descossy; Pauline Liaudet; **Jonas Dyhrfjeld-Johnsen**
Sensorion

An estimated 12% of the global population (~924 million people) is considered to be at risk for hearing loss from noise exposure (Le et al., 2017). Chronic workplace or recreational noise exposure (WHO, 2018) are considered the cause of 50% the cases of hearing loss worldwide (Daniel, 2007). Currently no effective pharmacological treatment is approved for reducing or treating noise-induced hearing loss (NIHL), in cases where protective equipment or regulations do not sufficiently reduce exposure. We here report a significant reduction of lasting hearing loss in a rat model of chronic noise exposure by oral administration of the clinical stage otoprotectant SENS-401 (arazasetron), already demonstrated to significantly reduce hearing loss from severe acoustic trauma (Petremann et al, 2019).

Following baseline audiometry (ABR 8/16/24/32 kHz, DPOAE 4/8/16/24/32 kHz), 7 week old male Wistar rats were exposed to 100 dB SPL, 3-12 kHz noise for 2 hours daily for 14 days followed by audiometry on D15. Animals were randomized into treatment groups (n=8 per group) receiving placebo vehicle, 6.6 mg/kg or 13.2 mg/kg SENS-401 treatments p.o. all twice daily for 28 days starting ahead of noise exposure on the first day. On day 29, audiometry was repeated to determine effects of chronic noise exposure and treatment regimen.

At the end of chronic noise exposure on D15, animals exhibited ABR threshold shifts of 2.19-26.25 dB across frequencies with no statistically significant difference between groups and only minor changes in DPOAE amplitudes (mean amplitude loss of 0.4-2.0 dB across group). On D29, all treatment groups showed minimal changes in DPOAE amplitudes (-6.2 to 5.5 dB across frequencies and groups, mean amplitude changes of -0.4 to 1.6 dB across groups) with no statistically significant inter-group differences. Conversely, the placebo treated group showed ABR threshold shifts of 6.3-12.8 dB across frequencies on D29 (mean shift of 8.7 dB), statistically significantly reduced in SENS-401 treated groups (mean shifts of 3.2 and 4.2 dB, p=0.03 and p=0.14). There was no statistically significant difference between SENS-401 doses, which respectively lead to mean ABR threshold shift reductions of 63% and 51%.

These results demonstrate for the first time the potential of SENS-401 to significantly reduce lasting hearing impairment in a model of mild NIHL from chronic noise exposure. Further studies will explore additional noise exposure and treatment regimens. SENS-401 is currently being investigated for the treatment of sudden sensorineural hearing loss (SSNHL) in an international, multi-centric clinical trial (AUDIBLE-S, NCT03603314).

PD 150

Modulation of NAD+ Biosynthsis Improves Mitochondrial Function and Resist Cisplatin-induced Ototoxicity

Ting Zhan[1]; Hao Xiong[2]; Jiaqi Pang[1]; Hanqing Lin[1]; Haidi Yang[2]
[1]Department of Otolaryngology, Sun Yat-sen Memorial Hospital, Sun Yat-sen University; [2]Sun Yat-sen Memorial Hospital, Sun Yat-sen University

As an extensively used chemotherapeutic agent, cisplatin (*cis*-diaminedichloroplatinum-II)-induced toxicity were found in patients more than ever. One of its most adverse effects is ototoxicity. However, the precise mechanism underlying cisplatin-associated ototoxicity is still unclear. Nicotinamide adenine dinucleotide(NAD^+), a co-substrate for the sirtuin family and PARP1, has emerged as a potent theropeutic molecular target in various diseases. In our investigates, we observed that NAD^+ level was decreased in the cochlea explant of mice treated with cisplatin. Supplementation of NAD^+ precusor (NMN) of NAD^+ salvage synthsis pathway could increase its level and thus protected hair cells from cisplatin-mediated death.Meanwhile, the use of specific inhibitors(TES-991,TES-1025) of β-amino- β-carboxymuconate-β-semialdehyde decarboxylase (ACMSD), a rate-limiting enzyme of the de novo NAD^+ synthesis pathway, had shown similar results by increasing the content of ATP, increasing SIRT1 activity and weakening PARP1 activation. *In vivo* experiments confirmed the hearing protection of NAD^+ in cisplatin treated mice model.In conclusion, we demonstrated that modulation of NAD^+ biosynthsis via the de novo pathway or salvage pathway could both prevent ototoxicity of cisplatin in mice by improving mitochondrial function, increasing SIRT1 activity and weakening PARP1 activation. These results suggest that direct modulation of cellular NAD^+ levels could be a promising therapeutic approach for protection from cisplatin-induced ototoxicity.

PD 151

Insulin-like Growth Factor 1 Protects Cochlear Outer Hair Cells against Cisplatin

Norio Yamamoto[1]; Kohei Yamahara[2]; Takayuki Nakagawa[1]; Koichi Omori[1]; Juichi Ito[3]
[1]Dept. Otolaryngology - Head and Neck Surgery, Graduate School of Medicine, Kyoto University; [2]Shizuoka City Shizuoka Hospital; [3]Shiga Medical Center Research Institute

Cisplatin is a potent anti-cancer drug widely used in both pediatric and adult therapeutic regimens for many kinds of malignant tumors, including head and neck cancer. However, cisplatin has several adverse effects, including renal damage and ototoxicity. Ototoxicity by cisplatin is caused by the damage to hair cells (HCs), spiral ganglion cells, and stria vascularis. It is usually irreversible and, currently, no definitive therapy exists. The histological lesions in the cochlea after cisplatin administration are reported to be most prominent in outer hair cells in the organ of Corti. Due to these adverse effects, the dose of cisplatin is sometimes reduced, resulting in the decreased effectiveness against malignant tumors. Therefore, to obtain the maximum outcome of cisplatin without ototoxicity, it is necessary to develop a treatment against the ototoxicity that does not interfere with anti-cancer effects. We previously reported that insulin-like growth factor 1 (IGF1) protects cochlear HCs against several kinds of damage to the cochlea, including noise exposure, ischemia, and aminoglycoside exposure, resulting in hearing recovery. However, the effect of IGF1 against cisplatin ototoxicity remains unclear because cell-death mechanisms by cisplatin are different in some points from other ototoxic materials such as aminoglycoside. In the present study, we investigated the efficacy of IGF1 as a protectant for cochlear outer HCs against cisplatin by using cochlear explant culture systems of postnatal day 2 mice. Administration of IGF1 to the explants grown in the medium containing cisplatin protects outer HCs effectively from damage by cisplatin. Pharmacological inhibition of IGF1 receptor (IGF1R) using an IGF1R antagonist, JB1, markedly attenuated the protective activity of IGF1. This result indicates that IGF1 exerts its effects through its canonical receptor, IGF1R. We found that IGF1 maintained outer HC numbers by inhibiting apoptosis of OHCs. However, induction of supporting cell proliferation, which is involved in the HC protection against aminoglycoside, was not observed in the cisplatin treatment. Immunohistochemistry data demonstrated that IGF1R is expressed in the adult sensory epithelium and spiral ganglion cells, suggesting the possibility of IGF1 protective effect on HCs of adult mammals against cisplatin. In conclusion, IGF1 could be an efficient and safe approach to treat cisplatin-induced ototoxicity.

PD 152

Long-term Efficacy and Safety of Non-invasive Therapeutic Hypothermia Treatment in a Preclinical Noise-Induced Hearing Loss Model

Samantha Rincon Sabatino[1]; Rachele Sangaletti[2]; Andrea Rivero[1]; Curtis King[3]; Suhurd M. Rajguru[4]
[1]University of Miami; [2]Dept. of Otolaryngology, University of Miami; [3]Lucent Medical Systems, Seattle,WA; [4]Dept. of Biomedical Engineering and Otolaryngology, University of Miami

Noise-induced hearing loss (NIHL) is an acquired form of sensorineural hearing loss associated with irreversible cochlear trauma in response to acoustic over-stimulation. NIHL is associated with neuropathy or synaptopathy depending on severity of acoustic trauma in the animal model. Oxidative stress, glutamate excitotoxicity, inflammation and strial swelling and atrophy have been observed in temporary-threshold inducing noise-exposures. Induction of therapeutic hypothermia has been proposed as an alternative or additive to pharmacological intervention to provide protection to cochlear structures following acute noise exposure. Here, we present efficacy, safety and mechanistic studies of non-invasive and local mild therapeutic hypothermia (mTH) as a treatment for preservation of residual hearing following noise exposure. Male and female Brown Norway rats aged 15-20 weeks old and with normal baseline hearing (auditory brainstem response thresholds ≤30dB) were randomly placed into 4 groups: (1) NIHL, (2) NIHL with mTH-treatment, (3) mTH-treatment alone, and (4) non-exposed controls. Noise exposure consisted of a continuous 4-8 kHz narrowband noise at 105 dB for two hours. mTH-treatment was induced at 15 minutes post-exposure to achieve desired cooling of inner ear at 31-33 ºC for two hours. ABR thresholds shifts from baseline were obtained at several timepoints up to 9 months post-exposure for pure tone stimuli ranging from 2-32 kHz and click broadband stimulus. ABR threshold shifts were compared between groups and between male and female subjects within each group. We also examined progression of age-related hearing loss in NIHL and mTH-treated groups with respect to non-NIHL and non-treated control animals. In a separate set of short-term experiments, cochleae from different groups were harvested at 24 hours to detail the biological processes involved in mTH neuroprotection using genome-wide expression studies. Male and female animals in non-NIHL mTH-treatment groups showed no change in ABR hearing thresholds or behavior and health assessments post-treatment. Both NIHL groups showed significant temporary threshold shifts compared to non-exposed controls with lower threshold shifts observed in mTH-treatment animals at 24 hours post-exposure. At 28 days post-exposure,

average ABR thresholds and wave I amplitudes were recovered to baseline in mTH-treated animals, whereas normothermic animals showed elevated threshold shifts and decreased wave I amplitudes at 8 and 16 kHz pure tone frequencies. Male and female rats had comparable variances in post-exposure threshold shifts between all groups. Our results collectively suggest a promising non-pharmaceutical application of mTH that is a safe and effective neuroprotective intervention following acoustic over-exposure.

Supported by 1R01DC013798 and F31DC018212

Auditory Circuits for Sound Processing and Perception

PD 153

A Non-canonical Cortico-Amygdala Inhibitory Loop.

Hector Zurita; Paul LC Feyen; Alice Bertero; Alfonso junior Apicella
University of Texas at San Antonio

Discriminating between auditory signals of different affective value is critical for the survival and success of social interaction of an individual. Anatomical, electrophysiological, imaging, and optogenetics approaches have established that the auditory cortex (AC) by providing auditory information to the lateral amygdala (LA) via long-range excitatory glutamatergic projections has an impact on sound-driven aversive/fear behavior. Here we test the hypothesis that the LA also receives GABAergic projections from the cortex. We addressed this fundamental question by taking advantage of optogenetics, anatomical, and electrophysiology approaches and directly examining the functional effects of cortical GABAergic inputs to LA neurons of the mouse auditory cortex. We found that the cortex, via cortico-lateral-amygdala somatostatin neurons (CLA-SOM), has a direct inhibitory influence on the output of the LA principal neurons. Our results define a cortico-lateral-amygdala long-range inhibitory circuit (CLA-SOM inhibitory projections β LA principal neurons) underlying the control of spike timing/generation in LA and LA-AC projecting neurons, and attributes a specific function to a genetically defined type of cortical long-range GABAergic neurons in cortico-lateral-amygdala communication. In this study, we describe a cellular basis for direct inhibitory communication from the AC to the LA, suggesting that the two opposing forces in the mammalian cerebral cortex, excitation and inhibition, can dynamically affect the output of the LA providing a general mechanism for auditory driven aversive/fear behavior.

PD 154

Auditory Representation in Cortex During Perceptual Learning

Robert C. Froemke[1]; **Kathleen A. Martin**[2]
[1]NYU School of Medicine; [2]New York University

During perceptual learning, animals improve their ability to discriminate between sensory stimuli. This behavioral improvement occurs at variable rates across animals. Previous work in the auditory system showed that perceptual learning reliably enhances cortical representations of task-relevant stimuli in trained animals. These neural changes have predominantly been observed outside of the behavioral context and regardless of learning rate. However, our lab recently found that engagement in behavior alters auditory cortical responses. Neural and behavior discrimination over perceptual learning are correlated. How do sensory representations change over auditory perceptual learning?

To address this question, we assessed neural dynamics over learning during behavior within each mouse. We developed an appetitive, head-fixed auditory perceptual learning two-alternative forced-choice task for mice. Animals learned to lick a left lick port for tones of a chosen frequency (usually 11 or 13 kHz) and right for tones of any other frequency to obtain water rewards. This allowed us to probe both auditory acuity and categorical responses over perceptual learning. Animals improved their discrimination between center and surround frequencies at variable rates (between 9-21 days), but continued to make errors at frequencies close to the center frequency (n=20 animals). Bilateral muscimol infusions in auditory cortex of trained mice substantially reduced behavioral performance (n=7 animals, $p < 0.05$). We performed two-photon calcium imaging of excitatory and inhibitory neurons in auditory cortex throughout learning, to assess neural activity both during this behavior and passive listening. Over learning, passive receptive field tuning of individual neurons did not significantly change. However, in the behavioral context, many excitatory neurons exhibited a categorical response to the auditory stimuli, not simply encoding the frequency of the stimulus, but rather the behavioral meaning (n=5 animals). This categorical response was present early in behavioral learning, but was broader, mirroring the behavioral performance. We believe local inhibition may shape the categorical response seen in excitatory neurons.

PD 155

Midbrain and Cortical Responses to Natural Sound Textures

Fei Peng[1]; Ambika Mishra[1]; Nicol harper[2]; Jan Schnupp[1]
[1]City University of Hong Kong; [2]University of Oxford

Previous psychophysical studies have identified a hierarchy of statistical parameters which determine the identity of auditory textures, such as running water, buzzing bees, or multispeaker babble (McDermott, J. H., 2011). By imposing these statistics on noise, realistic sounding textures can be synthesized. Presumably neurons in the auditory pathway must be sensitive to such statistical parameters to facilitate texture discrimination, and sensitivity to higher-order statistical parameters may emerge gradually as one ascends the auditory pathway. We analysed a database of over 200 natural textures to find 13 sound textures which span the space of parameters observed in nature. For each texture, we generated sounds, which, step-by-step, introduce statistical parameters of an increasingly higher order, so as to morph noise gradually to natural textures. That is, we start with a synthesized texture with only its power in each cochlear channel matched to the natural sound. Then, after each 1.5 seconds, the following measured statistics were added to the synthesized texture; the variance in each cochlear channel, then the skew and kurtosis, then the correlations between cochlear channels, then the modulation power, then all other measured statistics including modulation correlations, finally ending with the full natural texture. Multi-unit activity (MUA) in response to this stimulus was recorded from the inferior colliculus (IC) and the auditory cortex (AC) of anesthetized rats using multi-channel silicon probe. The neural activity at each probe channel was evaluated using the analog multi-unit activity (AMUA, Schnupp, J. W., 2015), and the onset (0-150 ms) and ongoing (150-500ms) responses after each statistics transition were compared to the response during the 500 ms span before the transition, to assess changes in the response over the transition. Changes in neural response were measured as the median change in AMUA over all textures and probe channels. Patterns of response change dependence were complex, however some general observations were apparent. We observed that the onset and ongoing activity of IC neurons was increased after the power to variance transition, but decreased with each subsequent higher-order statistical transition. The onset and ongoing activity of AC neurons was less consistent over transitions, but both did show an increase at the transition from the cochlear-channel correlations to the modulation power. Ongoing analyses will reveal the extent to which the observed responses are predicted by spectro-temporal receptive field (STRF) models.

PD 156

Sensory Responses in Mouse Auditory Cortex are Influenced by Behavior and Expectation

Nicholas Audette; **David M. Schneider**
New York University

Hearing is not simply about detecting sounds. To benefit from hearing, animals must perceive and respond to sounds in a way that is sensitive to behavioral context by integrating acoustic input with variables including environmental features, prior associations, and ongoing movement plans. Recent experiments have shown that movement, reward-relevance, and predictability can independently affect neuronal activity at the earliest stage of cortical processing. However, it remains unclear how these contextual variables interact with one another to influence sensory responses at the single neuron and population levels in the primary auditory cortex. To investigate this question, we developed a simple lever-press behavioral paradigm in which mice learn to make highly-stereotyped, reward-driven forelimb movements accompanied by auditory feedback. The relationships among movement, sound, and reward can be experimentally controlled to produce a variety of contexts and associations. Trained mice altered their behavior in response to tones that were omitted or presented at unexpected times, indicating that they learned the expected relationship between movement and sound. We then used dense multi-unit array recordings in performing mice to measure neural population activity in response to sensory stimuli that were either self-generated or presented passively. We find that average sound-evoked neural responses in primary auditory cortex are suppressed when sounds are self-generated compared to passive listening. Movement-based suppression was strongest for predictable tones while tones that deviated from an expected frequency evoked relatively larger neural responses. Surprisingly, strong neural suppression was present even when predictable tones were tightly linked with rewarded outcomes. Despite this population-level suppression, single-neuron analysis revealed that a subset of neurons was preferentially activated by expected tones, raising the possibility that predictability might sparsen - rather than dampen - neural responses to expected sounds. This closed-loop, lever-based behavior provides an experimental platform for studying how internal and external variables augment auditory processing, behavior, and perception.

PD 157 WITHDRAWN

Functional Connectivity Between Cortical and Subcortical Auditory Regions During Rest and Movie Viewing

Chad Buckland[1]; Mark O'Reilly[1]; Ingrid Johnsrude[2]
[1]Western; [2]The Brain and Mind Institute, Western University

Functional connectivity (FC) analyses have been used to examine the functional organization of spatially distinct brain regions in a variety of functional magnetic resonance studies, including task-based and task-free rest. Movie watching during scanning has provided a tool for overcoming the limitations presented by the unconstrained nature of resting-state studies, including pragmatic concerns over movement. However, the movie paradigm may also present advantages when examining connectivity in sensory regions, particularly in the auditory network. We examined connectivity between four auditory seed regions in the cortex, (primary auditory cortex, medial belt, lateral belt, and parabelt) and three subcortical seed regions (inferior colliculus (IC), medial geniculate body (MGB), and caudate) in healthy adults (n=80), using the Human Connectome Project (HCP) dataset (15 min resting state; 15 min rest). Regions were defined using the Glasser parcellation (Glasser et al., 2016), Freesurfer's subcortical segmentation, and manually defined spherical seeds for IC and MGB. Connectivity values between cortical auditory seed regions, specifically in primary auditory cortex and belt areas, were significantly higher (p's < .05) during movie watching than during rest. Additionally, given their role in auditory processing, FC to the inferior colliculus and medial geniculate body from the four auditory seed regions in the cortex was examined. Movie watching appears to generate significantly higher connectivity values (p's < .05) between cortical seed regions and subcortical regions (IC and MGB) than does the resting state. The amplitude and range of blood oxygenation level dependent (BOLD) signal in these areas was also examined due to these measures potentially affecting FC estimates. In order to examine FC in another sensory seed region, primary visual cortex connectivity was also examined and shows similarly elevated connectivity values to auditory seed regions during movie watching when compared to rest. However, increased FC values are not universal across all regions, particularly in subcortical regions excluded from the initial analysis. A qualitative analysis of these connectivity profiles may provide further avenues for future research. Analysis of connectivity differences between conditions suggests interindividual variability may drive differences in connectivity values, providing a possible explanation for robust movie FC in sensory regions given the time-locked nature of the stimulus provided. Movie-driven fMRI is suggested as a tool for future studies of sensory network organization.

PD 158

Convergence of Top-down and Bottom-up Inputs to Marmoset Auditory Cortex during Vocalization

Joji Tsunada; **Steven J. Eliades**
University of Pennsylvania

Speech is a sensory-motor process in which auditory self-monitoring is used to control vocal production and ensure accurate communication. Monitoring vocal feedback allows rapid speech adjustments to compensate for perceived changes in vocal output, a behavioral ability shared with many animal species. The auditory cortex has been implicated in this self-monitoring process based upon previous studies showing both a vocalization-induced suppression as well as sensitivity to changes in vocal feedback. However, the mechanisms of vocal suppression and integration of feedback in auditory cortex remain poorly studied. We recorded neural activity from both auditory and frontal cortex of marmoset monkeys during vocal production, examining both spiking activity and local field potentials. We found that previously-demonstrated vocal suppression in spiking activity is associated with a pre-vocal increase in low-frequency theta-band activity in both frontal and auditory cortex. We further show that, for many neurons, the magnitudes of these pre-vocal signals correlate with the acoustics of the subsequent vocalization. These findings suggest that this input to auditory cortex, presumably a top-down signal from frontal cortex, contains predictions of the expected sound of a vocalization, consistent with current models of sensory-motor processing. Additionally, we found that gamma-band oscillations increase during vocalization, in contrast to suppression in spiking unit output. This dissociation between spiking activity and local field potentials further implicates local processing within the auditory cortex as a possible mechanism of vocalization-induced suppression and sensory-motor integration.

This work was supported by NIH/NIDCD Grant K08-DC014299.

PD 159

An Auditory Long-Range Inhibitory Projection onto Striatal Cholinergic Neurons

Alice Bertero; Alfonso Junior Apicella
University of Texas at San Antonio

Integration of sensory information is fundamental for the survival of an individual, and discrimination of auditory

signal value is critical for decision making. In particular, auditory decisions require the engagement of the dorsal-posterior striatum with a stable representation of sounds during an auditory tasks and a strengthening of the cortico-striatal synapses associated with learning. The excitatory projections connecting the auditory cortex and the auditory striatum have been extensively investigated, but recently the existence of a long-range somatostatin inhibitory pathway had shed new light on the complex control exerted by the auditory cortex on the spiny projection neurons of the striatum. Although the spiny projection neurons are the major neuronal component of the basal ganglia, striatal cholinergic interneurons also have a relevant role in procedural learning since their rhythmic firing is paused during the presentation of sensory stimuli that have acquired a value/meaning. This phenomenon, referred as *Pause Response*, is believed to play a critical role in shaping striatal output, dopamine signals and learning, but the underpinning mechanisms are still not completely understood and potentially involve a still unknown GABAergic input. Here, by using optogenetics, anatomical and in vivo electrophysiology approaches, we demonstrate for the first time the existence of long-range parvalbumin and somatostatin inhibitory projections from the auditory cortex to striatal cholinergic neurons. We also behaviorally determine that the long-range cortical GABAergic input, by varying the length of the cholinergic pause, can optimize the accuracy and flexibility of learning across different contexts. Taken together, our study pave the way for a better understanding of the sensory control of striatal cholinergic neurons, and the contribution to auditory cortex long-range inhibitory projections to *Pause Response*.

PD 160

Neuromodulatory- and Prefrontal- Sensory Cortical Interactions Underlying Motivated Shifts in Attentional (Listening) Effort

Jan Willem de Gee[1]; Zakir Mridha[1]; Yanchen Shi[1]; Anton Banta[1]; Wenhan Zhang[1]; **Matthew J. McGinley**[2]
[1]Baylor College of Medicine, Department of Neuroscience; [2]Department of Neuroscience, Baylor College of Medicine

Humans and other animals constantly adapt their allocation of cognitive resources to changes in the environment. In the auditory domain, the brain is capable of enhancing the processing of difficult-to-perceive sounds when they are important (Kahneman, 1973). In the context of perceptual decision-making, this is referred to as attentional effort (Sarter et al., 2006), and are a component of listening effort. In contrast to the extensive study of e.g. the *selective* aspect of attention (Desimone and Duncan, 1995), the neural circuit mechanisms of attentional effort are poorly understood. Key candidate mechanisms are direct neuromodulation of sensory cortex (Aston-Jones & Cohen, 2005), and bi-directional interactions of sensory and frontal cortical regions (Miller & Cohen, 2001).

Here, we seek to determine the neural circuit basis of attentional effort. We developed an auditory attentional effort (AE) task for head-fixed mice. In the AE task, mice lick for sugar-water reward to report detection of the unpredictable emergence of temporal coherence in an ongoing tone cloud, analogous to coherent motion in common visual attention tasks. Perceptual difficulty is parametrically and unpredictably varied, trial-by-trail, through partial degradation of the coherence. To manipulate attentional effort, we alternate between a large and small reward volume in blocks of 60 trials. Thus, mice are motivated to expend more attentional effort in blocks with large rewards.

Increased attentional effort in high-reward blocks manifested as increased sensitivity (d' from SDT) to detect coherence in noise (2-way rmANOVA $F_{1,21}$ = 38.5; $p < 0.0001$; N=22 mice), particularly for weak-coherence targets (interaction $F_{2,42}$ = 11.7; $p < 0.0001$). Mice exhibited >5 effort shifts within each session, tightly time-locked to block changes. In addition, contrary to the trivial prediction that high reward increases global neuromodulator levels (arousal), mice *decreased* their arousal in high reward blocks, apparent in baseline pupil size ($p = 0.002$). Thus global neuromodulation doesn't account for attentional effort. Finally, feedback pupil responses exhibited multiple signals reflecting flexible AE regulation, including: correctness, reward context, and prediction errors. In ongoing 2-photon GCaMP imaging, we are determining the roles of frontal-sensory and neuromodulatory signals in mediating these shifts in overt behavior.

References: Kahneman (1973), Prentice-Hall. Aston-Jones & Cohen (2005), Annu. Rev. Neurosci., 28, 403-450. Desimone & Duncan (1995), Annu. Rev. Neurosci, 18(1), 193-222. Sarter, Gehring, & Kozak (2006), Brain Res. Rev., 51(2), 145-160. Miller & Cohen (2001), Annu. Rev. Neurosci., 24(1), 167-202.

PD 161

Neural Specific Roles for the Chromatin Remodeler CHD7 in the Developing Cochlear Epithelium

Vinodh Balendran[1]; Jennifer M. Skidmore[1]; Lisa A. Beyer[2]; Jelka Cimerman[1]; Elizabeth A. Hurd[3]; Yehoash Raphael[4]; **Donna M. Martin**[5]
[1]Department of Pediatrics; University of Michigan; [2]Kresge Hearing Research Institute, Department of Otolaryngology - Head and Neck Surgery, Michigan Medicine, Ann Arbor, MI, USA; [3]University of Edinburgh; [4]Kresge Hearing Research Institute, Department of Otolaryngology-Head and Neck Surgery, University of Michigan; [5]Department of Pediatrics; Department of Human Genetics; University of Michigan

Mammalian cochlear development depends upon highly orchestrated and dynamic patterns of gene expression that are regulated by epigenetic modifiers. Previous studies have implicated the chromatin remodeler CHD7 and the transcription factor SOX2 in differentiation of cochleovestibular ganglia and sensory epithelia. In mouse embryonic forebrain neural stem cells, CHD7 and SOX2 have been shown to directly interact, and in the developing inner ear, *Sox2* expression is reduced with *Chd7* loss. These observations suggest cell type specific, reciprocal, and/or complementary mechanisms for SOX2 and CHD7 contributions to neural and sensory cell development. Here we report an analysis of CHD7 and SOX2 localization in the developing mouse inner ear, with a focus on their relative contributions to neural vs cochlear epithelial components. We also present results of a detailed phenotypic analysis of conditional knockout (cko) mice with pan-otic (*Foxg1Cre, Pax2Cre*), hair cell (*Atoh1Cre*) or ganglion cell (*Neurog1Cre*, *ShhCre*) targeted *Chd7* deletions. We find that in the Embryonic day (E)10.5 otocyst, *Chd7* is more broadly and abundantly expressed than *Sox2*, and that both genes are highly expressed in the ventral proneurosensory domain. Notably, *Chd7* and *Sox2* expression in the wild-type ganglion declines gradually from E10.5 to E18.5 with growth of the ganglion and organ of Corti. Distinct populations of ganglion cells with single or co-expression of *Chd7* and *Sox2* emerge between E10.5 and E12.5, and while CHD7-positive cells are distributed throughout the ganglion, SOX2-positive cells are restricted to the periphery. Pan-otic (*Foxg1Cre, Pax2Cre*) deletion of *Chd7* results in severely hypoplastic cochleae with disorganized, ectopic, and supernumerary hair cells and aberrant axonal looping and innervation. In contrast, *Atoh1Cre;cko* mice exhibit normal cochlear epithelia at postnatal day 1 (P1) while *Neurog1Cre;cko* mice have smaller ganglia as early as E10.5. Axonal bundles and hair cell innervation appear intact at P1 in both *Neurog1Cre;cko* and *ShhCre;cko* mice. Together, these data suggest early requirements for both *Chd7* and *Sox2* in neurogenesis and differentiation, with ganglion cell-specific functions for *Chd7*. *Chd7* is not required in a cell-autonomous manner for proper hair cell formation but does have non cell-autonomous effects on cochlear epithelial formation and organization. These studies should help uncover why individuals with CHARGE syndrome due to heterozygous *CHD7* loss exhibit sensorineural hearing loss and assist with development of targeted or regenerative therapies for other forms of deafness and vestibular disorders.

Supported by NIH R01 DC009410
A. Alfred Taubman Research Scholar
Donita B. Sullivan M.D. Research professorship in Pediatrics

PD 162

A Single-Cell Atlas of Ear Development Reveals Molecular Foundations of Sensory Patches, Semicircular Canals, and the Endolymphatic Duct and Sac

Ian Swinburne; Sean Megason
Harvard Medical School

The inner ear amazes as it continuously detects both sound waves for hearing and body acceleration for balance. Antennae shaped hair cells—at the tips of which are mechanically gated ion channels—convert physical inputs into bioelectrical signals during a process called mechanotransduction. The remainder of the inner ear serves the hair cells by providing a stable endolymph, extracellular structures that enhance the transmission of mechanical inputs, sculpted chambers that direct three-dimensional movement to distinct sets of hair cells, and neuronal partners for the relay of signals. Zebrafish mutants that lack the Lmx1bb transcription factor develop abnormally with extra hair cells, incomplete morphogenesis of semicircular canals, and an endolymphatic sac that cannot relieve excess luminal pressure. Because the inner ear has many cell-types next to one another, we used single-cell RNAseq to generate an atlas of developing wild-type and *lmx1bb* mutants that includes the cell-types and gene lists that distinguish their behavior. We found the molecular states that distinguish the cells of the otic sensory patches from those of the neuromasts, as well as gene expression differences that may contribute to the extra hair cells of the *lmx1bb* mutant. In the semicircular canals, we found molecular states that distinguish their cells from those of the dorsal otic epithelium, as well as differences in gene expression in the mutant that likely contribute to abnormal morphogenesis. In addition, the

identification of genes enriched in nascent canal cells should lead to better characterization of “canal genesis zones”. Recently, we found a tissue-scale relief valve activity in the ear’s endolymphatic sac. Quantitative live imaging revealed cycles of slow pressure-driven inflation of the endolymphatic sac’s tissue followed by rapid deflation every 0.3-4.5 hours. Absence of these cycles in *lmx1bb* mutants leads to distended ear tissue that resembles pathologies associated with hearing and balance disorders such as Mèniére’s disease. Using serial-section electron microscopy, we found that thin lamellar projections underlie the relief valve function as the ultimate barrier to pressure release. Lattice light-sheet microscopy with adaptive optics revealed a lively and bubbling tissue where the overlapping lamellae are dynamically extending and retracting over one-another until they open under pressure. Single-cell RNAseq identified differences between endolymphatic duct and sac cells that provide an entry point for questions related to valve formation and function. Together, we anticipate that the atlas will be a valuable resource for answering fundamental questions of inner ear patterning, morphogenesis, and physiology.

PD 163

Single Cell Chromatin Accessibility Delineates Cellular Identities of the Neonatal Organ of Corti

Shuze Wang; Mary Lee; Jie Liu; **Joerg Waldhaus**
University of Michigan

The organ of Corti is formed by a variety of sensory hair cells and supporting cells arranged in rows spanning from the apical tip to the base within the cochlea. Given their stereotypic arrangement, the different cell types were identified based on their anatomical position along the medial to lateral axis. Recent studies using microfluidic devices and droplet-based technology have shown that each of the cell types are characterized by a unique transcriptional signature. Ultimately, small differences in individual transcript concentrations along the apex to base axis were sufficient to reconstruct the organ’s two-dimensional architecture from single-cell RNA-based data.

The aim of this study is to test if differences in the chromatin landscape can be utilized to identify the individual cell types of the organ of Corti. To achieve this goal, we generated single cell Assay for Transposase-Accessible Chromatin-Sequencing (ATAC-seq) libraries from postnatal day 2 organ of Corti preparations divided into apical and basal compartments. Fluorescence activated cell sorting in combination with Fgfr3-iCre/Ai14 and Atoh1-GFP alleles were used to enrich for pillar cells, Deiters’ cells, and hair cells. The chromatin accessibility was determined, and we clustered the data after initial quality control. In an effort to develop an unsupervised approach to assign cell type identity to the ATAC-seq clusters the data were integrated with an age matched single-cell RNA-Sequencing dataset, also generated from the Fgfr3-iCre/Ai14/Atoh1-GFP mouse line. Overlapping clusters in ATAC-seq and RNA-seq datasets were revealed by pairwise comparison of differentially accessible gene regions and differentially expressed transcripts, respectively. This approach allowed for successful identification of pillar cell, Deiters’ cell, and hair cell clusters. Furthermore, exclusion of off-target cell clusters was performed.

The results of this study will add to our understanding of how the epigenome and transcriptome interact to define individual cell types within the organ of Corti. Further studies will investigate the developmental regulation of chromatin accessibility, its impact on gene expression and will contribute to the development of novel strategies in hair cell regeneration.

PD 164

Single-cell Proteomics Reveals Downregulation of TMSB4X to Drive Actin Release for Stereocilia Assembly

Mirko Scheibinger[1]; Ying Zhu[2]; Daniel C. Ellwanger[3]; Jocelyn F. Krey[4]; Dongseok Choi[5]; Ryan Kelly[6]; Stefan Heller[1]; Peter G. Barr-Gillespie[7]
[1]Department of Otolaryngology–HNS, Stanford University; [2]Environmental Molecular Sciences Laboratory, Pacific Northwest National Laboratory; [3]Department of Otolaryngology–HNS, Stanford University; Genome Analysis Unit, Amgen Research, Amgen Inc.; [4]Oregon Hearing Research Center & Vollum Institute, Oregon Health & Science University, Portland, Oregon, USA; [5]OHSU-PSU School of Public Health, Oregon Health & Science University, Portland, Oregon, USA; Graduate School of Dentistry, Kyung Hee University, Seoul, Korea; [6]Environmental Molecular Sciences Laboratory, Pacific Northwest National Laboratory; Department of Chemistry and Biochemistry, Brigham Young University; [7]Oregon Hearing Research Center & Vollum Institute, Oregon Health & Science University

Hearing and balance rely on small sensory hair cells that reside in the inner ear. To explore dynamic changes in the abundant proteins present in differentiating hair cells, we used a highly sensitive single-cell proteomics approach—nanoliter-scale shotgun mass spectrometry—for cells isolated from the E15 chick utricle. We sought to understand how supporting cells, with their modest F-actin cytoskeletons, could transform

rapidly into stereocilia-endowed hair cells without significant upregulation of actin gene transcription. We found that hair cells were readily distinguished from supporting cells based on only 50-75 proteins identified in each. Notably, the actin monomer binding protein thymosin β4 (TMSB4X) was abundant in supporting cells but not in hair cells; trajectory analysis based on the proteomics data showed that its expression decreased as progenitors developed into hair cells. Single-cell RNA-seq analysis showed that *TMSB4X* transcripts are downregulated when transcription of *ATOH1*, a key regulator of hair cell differentiation, is activated. Thus, we propose that most actin is sequestered by TMSB4X in progenitor cells, but upon differentiation to hair cells, actin is released to build the sensory hair bundle.

PD 165

SoxC Transcription Factors are Crucial Regulators of Sensory Progenitor Differentiation in the Organ of Corti

Xizi Wang[1]; Ksenia Gnedeva[2]; Litao Tao[1]; Juan Llamas[1]; Haoze Yu[1]; Talon Trecek[1]; Welly Makmura[1]; Neil Segil[3]
[1]Department of Stem Cell Biology and Regenerative Medicine, Keck School of Medicine of USC, and USC Caruso Department of Otolaryngology – Head and Neck Surgery; [2]Center for Regenerative Medicine and Stem Cell Research at USC; [3]Keck Medical School of the University of Southern California

All vertebrates use sensory organs containing mechanosensitive hair cells to perceive sound and motion. These sensory receptors are few in number and cannot be regenerated after damage, thus leading to permanent hearing loss and balance disorders. During embryonic development, cells that give rise to the organ of Corti in the mammalian inner ear first exit the cell cycle to form a well-defined prosensory domain, and subsequently initiate a process of differentiation that gives rise to a stereotyped mosaic of hair cells and supporting cells. The mechanisms governing fate commitment within the forming prosensory domain remain poorly understood, yet understanding the transition from proliferative progenitor to committed precursor is important for a full understanding of the failure of regeneration in this system.

Transgenic mice expressing either Sox2-GFP or $p27^{kip1}$-GFP reporters provided a means to FACS-purify proliferating vs. post-mitotic progenitor cells from the developing (E12.5 - E13.5) organ of Corti, respectively. Using RNA- and ATAC- sequencing, we observe that a group of potential gene regulatory elements associated with hair cell fate-commitment emerge during the transition to post-mitotic progenitor cells, and these distal elements are enriched for Sox transcription factor binding motifs. Based on this observation, we explored the role of two members of the *SoxC* gene family, *Sox4* and *Sox11*, whose transient expression in the sensory epithelia during embryonic development is limited to the period just prior to hair cell differentiation.

It has been shown that homozygous conditional mutation of SoxC genes blocks progenitor cell differentiation in the hair cell lineage. Our comparative analysis of chromatin structure in WT and SoxC CKO organ of Corti progenitors demonstrated that the accessibility of the regulatory elements associated with early sensory cell fate-commitment is dependent on SoxC gene expression, while ChIP-seq analysis confirmed direct binding of SoxC to these potential regulatory elements. Single-cell RNA sequencing further confirmed that conditional loss of SoxC genes leads to downregulation of the predicted prosensory gene targets in the progenitor cells. Consistent with this observation, overexpression of SoxC prior to cell fate determination enhances sensory differentiation. Also, re-introducing SoxC genes using Anc80-AAV gene delivery vector after hair cell loss leads to trans-differentiation of postnatal utricular supporting cells in vivo.

Our results reveal that SoxC transcription factor expression correlates with changes in chromatin structure and gene expression that are crucial for sensory cell differentiation and subsequent hair cell-specific gene expression in the progenitor population of the organ of Corti.

PD 166

Molecular Regulation of Sensory Epithelial Cell Patterning in the Mammalian Inner Ear

Chandrakala Puligilla[1]; Atul Pandey[2]; Daisy Haque[2]; Kristen Phlegar[2]; Bradley Schulte[2]; Vilhelm Bohr[3]
[1]NIH/NIA; [2]Medical University of South Carolina; [3]NIA/NIH

The mammalian cochlea establishes distinct cellular-level medial and lateral domains within the organ of Corti with no overlap occurring between neighboring hair cells and supporting cells. The medial domain contains inner hair cells and associated supporting cells, while the lateral domain contains outer hair cells and their associated supporting cells, Deiters' cells. This precise arrangement of heterogenous cell types into specific domains is essential for normal auditory function as its disruption leads to complete loss of hearing. Moreover, it is well established that hair cell damage resulting from aging, noise exposure or aminoglycoside toxicity

causes disruption of cellular patterning in the cochlea. Therefore, the knowledge of the precise sequence of molecular events regulating normal cellular pattern formation is crucial not only to drive the correct spatial positioning and alignment of regenerated hair cells but also to develop therapeutic strategies to restore organized hair cell patterning after injury. Despite its significance, molecular factors that regulate precise patterning of sensory hair cells are unclear. Our data shows that conditional deletion of E-cadherin in mice leads to significant disruption in cellular patterning of outer hair cells and Deiters' cells. The precision of cell patterning is completely lost throughout the cochlear duct and instead of aligning in organized rows, both outer hair cells and Deiters' cells become aberrantly attached to form patches leading to a cluster-like arrangement, instead of rows. In addition, outer hair cell-Deiters' cell clusters in E-cadherin mutants migrate away from their lateral domain. On the other hand, loss of E-cadherin had no effect on spatial positioning or organization of inner hair cells and their supporting cells. These results suggest that E-cadherin functions to drive correct alignment of outer hair cells-Deiters' cells and that E-cadherin acts to prevent cells from crossing borders of its expression domain, which thereby confines their position within the sensory epithelium. However, the molecular mechanisms whereby E-cadherin functions to generate exquisite cellular pattern remain unclear. We have observed that loss of E-cadherin function leads to overexpression of β-catenin-mediated Wnt signaling suggesting that E-cadherin possibly regulates patterned organization of sensory cells via modulating β-catenin activity. Accordingly, inhibition of Wnt/β-catenin-mediated transcription is sufficient to rescue E-cadherin mutant phenotype. Taken together, these data imply that physiological levels of E-cadherin expression are necessary for precise cellular alignment and that Wnt/β-catenin activity must be maintained at a level for E-cadherin to promote precise positioning and patterning of sensory epithelial cells.

PD 167

Dynamic changes in cis-regulatory occupancy by Six1 drive progressive differentiation to establish cell identity and hair-cell-bundle polarity in auditory sensory epithelium

Jun Li[1]; Ting Zhang[1]; Aarthi Ramakrishnan[1]; Bernd Fritzsch[2]; Jinshu Xu[1]; Li Shen[1]; **Pin-Xian Xu**[1]
[1]Icahn School of Medicine at Mount Sinai; [2]University of Iowa, Dept. of Biology and Dept. of Otolaryngology

The transcription factor Six1 in cooperation with Eya1-Sox2 induces a hair-cell-like phenotype in cochlear explants. However, whether Six1 plays a subsequent role in establishing hair-bundles or activates distinct programs to create cell diversity in auditory sensory-epithelium remains unknown. Here, we show that Six1-binding to *cis*-regulatory elements changes dramatically at cell-state transitions. Intriguingly, Six1 pre-occupies enhancers of cell-type-specific regulators and effectors before their expression. We demonstrate cell-type-specific activity of Six1-bound novel enhancers of *Fgf8*, *Dusp6*, *Vangl2*, the hair-cell master regulator *Atoh1* and a cascade of *Atoh1*'s downstream factors, all of which physically interact with Six1. Six1-binding sites carry consensus-sequences for RFX/X-box, and Six1-Rfx1/3 cooperatively regulate gene expression through binding to SIX:RFX-motifs. Late *Six1* deletion disrupts hair-bundle polarity and Six1 targets a wide range of hair-bundle regulators, of which 83 are deafness-associated genes. This study provides a mechanistic understanding of how Six1 acts in feedforward loops to progressively establish sensory cell identity.

PD 168

Brg1-Eya1/Six1-dependent regulation of the Sox2 transcriptional landscape establishes proneurosensory lineage in the mouse inner ear

Jinshu Xu[1]; **Jun Li**[1]; Aarthi Ramakrishnan[1]; Huihui Jiang[1]; Ting Zhang[1]; Bernd Fritzsch[2]; Li Shen[1]; Pin-Xian Xu[1]
[1]Icahn School of Medicine at Mount Sinai; [2]The University of Iowa

During inner ear development, $Sox2^+$ proneurosensory progenitors differentiate into sensory cells and spiral ganglion neurons for hearing, which requires the combined activities of Eya1/Six1. However, how these key regulators interact with epigenetic networks to activate *Sox2* to specify $Sox2^+$ progenitors remains to be determined. Here we show that Brg1-based SWI/SNF chromatin-remodeling complexes act at multiple steps during neurosensory lineage development. Brg1 regulates the expression of *Eya1*/*Six1*, both of which are required for *Sox2* activation in otic ectoderm. Chromatin-immunoprecipitation-sequencing reveals Brg1-binding at the loci of *Eya1*, *Six1* and *Sox2*. Brg1 and Eya1-Six1 form protein complexes and show overlapping occupancy to three distal 3' *Sox2* enhancer elements that direct overlapping expression in neurosensory cells. Eya1/Six1 also selectively interact with BAF60a/c and not BAF60b. These findings uncover essential functions of how neurosensory-lineage-specific factors Eya1/Six1 interact with Brg1-BAFs to precisely establish the transcriptional program of *Sox2* for promoting proneurosensory fate.

PD 169

Evaluating Estrogen's Multi-Modal Modulatory Potential: A Framework for Understanding Protection from Noise-Induced Hearing Loss

Benjamin Shuster[1]; Ryan Casserly[2]; Shaun Viechweg[2]; Erika Lipford[1]; Kanisa Davidson[2]; Rafal Olszewski[3]; Jennifer Enoch[2]; Mark McMurray[1]; Beatrice Milon[4]; Mark Rutherford[5]; Kevin Ohlemiller[6]; Michael Hoa[3]; Didier Depireux[2]; Jessica Mong[2]; Ronna Hertzano[7]
[1]Department of Otorhinolaryngology-Head and Neck Surgery, University of Maryland; [2]University of Maryland School of Medicine; [3]Auditory Development and Restoration, National Institute on Deafness and Other Communication Disorders, NIH; [4]Department of Otorhinolaryngology-Head and Neck Surgery, University of Maryland; [5]Department of Otolaryngology-Head & Neck Surgery, Washington University; [6]Washington University School of Medicine; [7]Department of Otorhinolaryngology Head and Neck Surgery, University of Maryland School of Medicine; Institute for Genome Sciences, University of Maryland School of Medicine.

Debilitating hearing loss afflicts both men and women. Importantly, sex differences in hearing physiology and susceptibility to age-related hearing loss (ARHL) and noise-induced hearing loss (NIHL) are documented in animal models and in the human population. NIHL, in particular, is a burgeoning global health concern. The World Health Organization estimates that 1.1 billion individuals worldwide are at risk for developing NIHL.

An increasing body of literature demonstrates that estrogen modulates hearing and may account for differences in auditory physiology and susceptibility to NIHL between the sexes. Previous studies from our laboratory demonstrate that female mice are protected from a permanent threshold shift (PTS)-inducing noise exposure in comparison to male mice, and that estrogen confers this protection. Additional data from our laboratory demonstrate that auditory brainstem response (ABR) wave-I amplitudes are larger in female mice at baseline and after noise trauma, which is indicative of greater synchronous activity at the level of the spiral ganglion.

Hearing loss after noise trauma could result from changes or damage to one or more of the cell types or structures in the inner ear as well as in the cochlear nucleus. An understanding of how estrogen confers protection from NIHL in female mice requires knowledge of the effects of estrogen on these cell types and structures. Utilizing an ovariectomy model to control circulating levels of estrogen, our lab is exploring the multi-modal modulatory potential of estrogen in the inner ear and cochlear nucleus. Using a combination of physiologic, histologic, and transcriptomic approaches, we demonstrate that exogenous estrogen supplementation in female B6CBAF1/J mice is sufficient to modulate inner ear physiology (including ABR wave-I amplitude) and transcriptome. Additionally, we are investigating histologic changes in the cochlear nucleus resulting from exogenous estrogen supplementation. Taken together, these data demonstrate estrogen's multi-modal modulatory potential on peripheral and central auditory physiology and may begin to provide a framework for understanding estrogen's protective effects from NIHL.

PD 170

Preservation of Pre-Hearing Spontaneous Activity in a Mouse Model of Gjb2-Mediated Deafness

Calvin J. Kersbergen; Travis Babola; Dwight E. Bergles
Johns Hopkins University

Spontaneous bursts of neural activity generated in the developing cochlea propagate through central auditory circuits prior to hearing onset, inducing correlated firing among neurons that will eventually encode similar frequencies of sound. Burst firing is initiated when ATP is released by inner supporting cells (ISCs), triggering a cascade of events that culminates in potassium efflux and subsequent excitation of nearby inner hair cells (IHCs). ISCs are extensively coupled through gap junctions, and mutations in *Gjb2*, which encodes gap junction protein connexin 26 (Cx26) that is highly expressed by ISCs, are the most frequent genetic cause of congenital sensorineural hearing loss. Although disruption of spontaneous activity can alter the survival and maturation of auditory neurons, the consequences of Cx26 deficiency for early patterned activity during this critical phase of development are unknown.

To define how the absence of Cx26 influences spontaneous events in the cochlea and central auditory centers prior to hearing onset, we used a novel knock-in Cre recombinase mouse line (*Tecta-Cre*) to delete Cx26 from ISCs within the cochlea (Cx26 cKO). Unexpectedly, ISCs adjacent to IHCs in cKO postnatal day 7 (P7) cochleae continued to exhibit a low membrane resistance and extensive gap junctional coupling. In contrast, ISCs closer to the spiral limbus exhibited high input resistances and were uncoupled from the supporting cell syncytium, indicating a differential dependence on Cx26 among supporting cells. ISCs in Cx26 cKO mice continued to exhibit spontaneous calcium waves and

cellular crenations, but events were reduced in size and restricted to the ISC-IHC border. IHCs in Cx26 cKO cochleae continued to experience ATP-dependent spontaneous inward currents and calcium transients, with a frequency and mean amplitude similar to control mice, indicating that nearby ISCs remain capable of driving coordinated spontaneous activity in IHCs in the absence of Cx26. *In vivo* imaging of neuronal calcium transients in the inferior colliculus of unanesthetized P7 Cx26 cKO mice revealed a modest reduction in spontaneous event frequency, but mean amplitude, event duration, and bilateral representation of neural activity were unchanged. Moreover, spontaneous activity was present until hearing onset, indicating that robust, correlated firing of auditory neurons within isofrequency zones persists despite the inability of these mice to detect sound after ear canal opening. This preservation of cochlea-induced, patterned neural activity in the absence of Cx26 may initiate proper development of auditory pathways prior to hearing onset, thereby enhancing the performance of therapies designed to restore hearing.

PD 171

Tac1-expressing Type II Afferent Neurons in the Cochlea Respond to ATP after Acute Damage

Megan B. Wood[1]; Nathaniel J. Nowak[1]; Paul Fuchs[2]
[1]Johns Hopkins University School of Medicine; [2]the Center for Hearing and Balance, Johns Hopkins University School of Medicine

Tac1 encodes a precursor protein, Protachykinin-1, that can be cleaved into several neuropeptides including substance P and Neurokinin A. Substance P and CGRPβ are secreted by peptidergic nociceptors of the somatosensory system after painful stimuli. When Tac1-Cre was crossed with the Ai9 reporter mouse line, tdTomato was expressed in a subset of neurons in the dorsal root ganglion. These *Tac1*+ neurons were co-labeled with substance P and CGRPβ in the proportions previously reported. RNA-sequencing data available in the UMGear database shows that *Tac1* is expressed by type II afferent neurons and a subset of type I neurons. We then used the Tac1-Cre::Ai9 reporter mice to confirm the expression pattern of *Tac1* in the cochlea. Type II afferent neurons were clearly labeled in the basal turn. In a gradient from the middle to apical turns, additional cell types in the organ of Corti and surrounding tissue express the reporter along with the type II afferent neurons until almost every cell is labeled. This gradient did not extend to the spiral ganglion where the number of neurons labeled is consistent from base to apex. The number of spiral ganglion cells labeled in the *Tac1* reporter mouse supports the RNA-sequencing results. Tac1-Cre was then used to drive GCaMP6f expression in the cochlea. In the basal turn, this creates a specific model to study the response of type II afferent neurons to acute tissue damage caused by laser ablation. In the middle and apical turns, GCaMP6f expression also reveals calcium signaling in supporting cells after damage. The activity of supporting cells and type II afferent neurons is reduced in the presence of the purinergic signaling blocker PPADS. This shows that ATP is an important activator of those cell types after acute damage. The Tac1-Cre animal is a useful tool to study type II afferent neurons in the base of the cochlea. However, the expression of both *Calca* (encodes CGRPβ) and *Tac1* by type II afferent neurons provides additional evidence that these neurons share characteristics with nociceptors beyond morphology and response to tissue damage.

PD 172

The role of the calcium-sensing receptor in regulating intracellular calcium dynamics in the mammalian cochlea

Snezana Levic[1]; Ebenezer N. Yamoah[2]
[1]Brighton and Sussex Medical School; [2]University of Nevada,Reno

Background

Calcium ions (Ca^{2+}) play fundamental roles in sensory processing in vertebrate hair cells (HCs). These include mechano-transduction, synaptic release, and frequency selectivity. The remarkable capability of HCs as mechanoelectrical signal transducers relies on tightly regulated intra- and extra-cellular Ca^{2+}microdomains. Extracellular Ca^{2+}($[Ca^{2+}]_{ext}$) levels could play important roles at the apical domain in regulating mechanosensory adaptation and at the basal domain for controlling synaptic transmission, and spontaneous electrical activity during development. We have recently reported the expression of calcium-sensing receptor (CaSR) in the mammalian organ of Corti. The present study investigated if CaSR alters the intracellular calcium ($[Ca^{2+}]_i$) handling in the sensory epithelium, and the potential mechanisms of CaSR action.

Method

We used functional microscopic techniques. Freshly isolated mouse cochleae were used, and pharmacological manipulations were employed to address relevant physiological questions.

Results

Using immunocytochemical methods, we demonstrate robust expression of the CaSR in the cochlear epithelium. Positive immune-reactivity was detected in hair cells as well as supporting cell in the mouse inner ear. To determine the functional roles of the

CaSR, we used pharmacological activators to increase the intracellular calcium in supporting and sensory epithelium. Additionally, we used known inhbitors of the CaSR to suppress receptor activation. Moreover, both external and internal calcium sources were manipulated to interrogate the function activity of the receptor protein. We demonstrate that the CaSR in the cochlear epithelia play a role in regulating intracellular Ca^{2+}dynamics. This report provides the first evidence of the involvement of CaSR in differentially regulating the Ca^{2+}_i dynamics in developing and mature sensory and supporting cells of the Organ of Corti.

PD 173

In-Vivo and Postmortem Gerbil Organ of Corti Fluid Space Morphology Using 3D Volume Optical Coherence Tomography (OCT)

NamHyun Cho[1]; Haobing Wang[2]; Mike E. Ravicz[3]; Sunil Puria[4]
[1]Department of Otolaryngology Head and Neck Surgery, Harvard Medical School; Eaton-Peabody Laboratories, Massachusetts Eye and Ear; [2]Eaton-Peabody Laboratories, Mass. Eye and Ear; [3]Eaton-Peabody Lab., Mass. Eye & Ear; Department of Otolaryngology, Harvard Medical School; [4]Department of Otolaryngology Head and Neck Surgery, Harvard Medical School; Eaton-Peabody Laboratories Massachusetts Eye and Ear

Introduction

Much of our knowledge about cochlear anatomy comes from measurements on fixed, dehydrated, resin-embedded histological preparations; sputter-coated scanning and transmission electron microscopy; or fluorescent dye-labeled two-photon and confocal imaging of postmortem tissue. While these methods have been the gold standard, their shortcomings include known preparation-related distortions of cochlear fluid spaces and surrounding cellular and extracellular structures and an uncertain relationship to the in-vivo anatomy. In this study, we used high-resolution OCT through the intact round window membrane (RWM) to assess the morphology of the fluid spaces of the gerbil basal Organ of Corti (OoC) in three dimensions in-vivo and postmortem.

Methods

We used a Thorlabs Ganymede-III-HR 905-nm center wavelength OCT system with a 100-kHz camera (axial and lateral resolutions ~1.33 µm and ~2 µm, respectively, in water) and LabVIEW-based custom VibOCT software. Cochlear health was monitored by compound action potentials. Cochlear volume was obtained, by concatenating multiple depth volume scans, in-vivo and 30, 60, 90 mins postmortem. The starting point of the volume scans ranged from 0–200 µm from the basal end of the cochlea (~48-28 kHz, Müller, 1996) and spanned a distance of approximately 1 mm towards the apex. The inner spiral sulcus (ISS), inner and outer tunnels of Corti (ITC/OTC), and space of Nuel (SN) volumes were segmented using Simpleware (Synopsis). Each tube-like fluid space was fit with a centerline, and orthogonal cross-sectional areas were fit with ellipses and their major and minor diameters measured as a function of basal to apical position.

Results

OCT provides sufficient resolution for visualizing OoC fluid spaces and cellular and extracellular structures. In vivo, the RWM and Reissner's membrane (RM) are convex. From the basal to apical extent, all of the OoC fluid spaces generally decrease in area. RWM and RM start to flatten postmortem, indicating a decrease in scala tympani and scala media volume, respectively. ISS volume generally decreases and OTC volume decreases 30 mins postmortem. This loss of ISS volume postmortem indicates a loss of ISS pressure, suggesting that, in-vivo, this volume may play a role in maintaining the gap in subtectorial space. SN volume increases 30 mins postmortem, persists to 60 mins, and then decreases slightly. These OCT images of the intact cochlea in-vivo and postmortem provide an opportunity to reassess previously published morphology measurements. [Work approved by the ACC at MEE and supported by R01-DC007910 from the NIDCD.]

PD 174

A Novel Microneedle Device for Controlled and Reliable Liquid Biopsy of the Human Inner Ear

Samuel Early[1]; In Seok Moon[2]; Krishna Bommakanti[1]; Ian Hunter[3]; Konstantina M. Stankovic[4]
[1]Massachusetts Eye and Ear Infirmary; [2]Yonsei University; [3]Massachusetts Institute of Technology; [4]Eaton Peabody Laboratories, Department of Otolaryngology, Massachusetts Eye and Ear

Sensorineural hearing loss is the most common sensory deficit worldwide, yet our understanding of the underlying pathophysiology is limited by the challenges of access to the inner ear in a safe and reliable manner. We present a novel microneedle device for trans-round window membrane liquid biopsy, which utilizes controlled depth of perforation and microliter aspiration control to safely biopsy fluids of the inner ear. Of eleven devices tested in fresh frozen human temporal bones, seven demonstrated alignment between electrical, visual and tactile detection of round window membrane perforation, and nine were successful in aspiration of meaningful diagnostic samples

from the perilymphatic space. Purity of the average perilymph sample was 69% for a 5 µL sample volume, equivalent to 3.5 µL attributable to perilymph.

Diagnostic success was shown both by transmastoid facial recess and transcanal tympanotomy approach. This device can enable new advances in the understanding of inner ear pathology, and brings us one step closer to liquid biopsy of the inner ear becoming a routine part of clinical care.

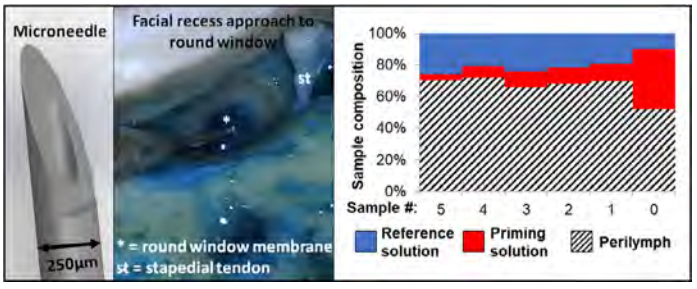

PD 175

Electrically-Evoked Olivocochlear Efferent Suppression in the Peripherin Knockout Mouse Supports Outer Hair Cell - Based Control of the Cochlear Amplifier

Jennie M. Cederholm[1]; Chamini Perera[1]; Georg von Jonquieres[1]; Jeremy L. Pinyon[1]; Kristina E. Parley[1]; Jean-Pierre Julien[2]; Allen Ryan[3]; **Gary D. Housley**[1]
[1]UNSW Sydney; [2]Laval University; [3]University of California, San Diego

Peripherin is a type III intermediate filament protein that is prominent in peripheral sensory neurons, including cochlear type II spiral ganglion neurons (SGN). In the peripherin knockout (PrphKO) mouse model, small unmyelinated dorsal root ganglion neurons are lost (Lariviere et al. J. Neurochem. 2002). Our original study of the cochlear innervation of these mice revealed a pronounced disruption of the type II SGN (outer spiral bundle) innervation of the outer hair cells (OHCs) (Froud et al. Nature Comms. 2015). Associated with this was a loss of contralateral suppression (transient reduction in quadratic DPOAE when noise is presented to the opposite ear), despite hypertrophy of the olivocochlear efferent synaptic boutons on the OHCs. On this basis, we proposed that sensory coding by the OHCs, transmitted via the type II SGN, likely provides the primary input for the olivocochlear efferent reflex control of the 'cochlear amplifier'. This is counter to the broadly adopted perspective that the type I SGN innervating the inner hair cells provides this drive. The PrphKO mice were subsequently studied by a group who were unable to verify disruption of the outer spiral bundle, but confirmed the absence of contralateral suppression (Maison et al. eNeuro 2016). This group undertook electrical stimulation of the olivocochlear efferent bundle on the floor of the fourth ventricle in two PrphKO mice, and found a slowly developing increase in cubic DPOAE during stimulation, rather than classic rapid and adapting suppression of the DPOAE evident in wildtype controls. They concluded that the loss of contralateral suppression in the PrphKO mice most likely arose from an undetermined impact on olivocochlear efferent firing properties, rather OHC sensory disconnection. Given the controversy, we re-evaluated the PrphKO mouse phenotype. Immunohistochemical analysis (neurofilament 200, TUJI1, parvalbumin, CtBP2, VAChT) resolved a progressive disruption of the outer spiral bundles, from moderate in the base to severe at the apex, while the type I SGN and efferent innervation were unaffected. Further, viability of olivocochlear efferent suppression was confirmed in PrphKO mice by electrical stimulation in the fourth ventricle, showing rapid and adapting electrically-evoked suppression of the cubic DPOAE (2f1-f2, about 16 kHz; n = 3), similar to that seen in wildtype (n = 2). These findings consolidate support for the postulate of OHC-based sound transduction control of the cochlear amplifier. Undertaken with UNSW Sydney ACEC ethics approval; funding from NHMRC grant refs. APP1052463, APP1089838; Research Service of the U.S. Veterans Administration BX001205, RX000977.

PD 176 **WITHDRAWN**

Descending Modulation of Afferent Activity by Hindbrain Efferent Neurons in the Zebrafish Lateral Line System

Elias Lunsford; Dimitri Skandalis; James C. Liao
University of Florida, Whitney Lab for Marine Bioscience

Accurate sensory processing during movement requires the animal to distinguish between external and self-generated stimuli to maintain sensitivity to biologically relevant cues. Descending modulatory inputs from efferent neurons are thought to filter sensory reafference in the periphery via corollary discharge during muscle activation. We examine this in the zebrafish lateral line system, which consists of mechanosensory organs that are stimulated by fluid movement during swimming. We employed simultaneous electrophysiological recordings to reveal the modulation of afferent neuron activity by hindbrain efferent neurons during motor activity. Because direct recordings of efferent neurons remains challenging, to do this we first monitored calcium activity with Tg(elav13:GCaMP6s) fish to verify synchronous activity between putative cholinergic efferent neurons and motor neurons We found that lateral line afferent activity was reduced during fictive swimming but was not always completely inhibited. We examined correlates

of motor activity to determine which may best predict the attenuation of afferent activity and, therefore, what temporal components of the motor signal may be reflected in the efferent corollary discharge. Afferent activity remained reduced even after the offset of motor activity, revealing that inhibitory control is not confined to the duration of the swim. This reduction in spike rate was substantial and only returned to intrinsic spontaneous spike rates after a well-defined refractory period. We quantified the anticipated influence the refractory period would have during the glide phase of the natural burst-and-glide behavior of swimming zebrafish. The duration of the glide that experiences reduced afferent activity scaled with parameters of the preceding swim bout. We suggest that the lateral line adaptively filters self-generated flow stimuli during both active and passive phases of locomotion, and that fast, short swimming bouts minimizes lateral line desensitization during the glide period. Our results caution against interpreting afferent activity in octavolateralis systems in which motor activity is not simultaneously monitored.

SAVE THE DATES

FEBRUARY 20-24, 2021

44th Annual MidWinter Meeting
Renaissance SeaWorld
Orlando, Florida

FEBRUARY 5-9, 2022

45th Annual MidWinter Meeting
San Jose Convention Center
San Jose, California

FEBRUARY 11-15, 2023

46th Annual MidWinter Meeting
Renaissance SeaWorld
Orlando, Florida

Association for Research in Otolaryngology
19 Mantua Road
Mt. Royal, NJ 08061
www.aro.org